AD-A261 253

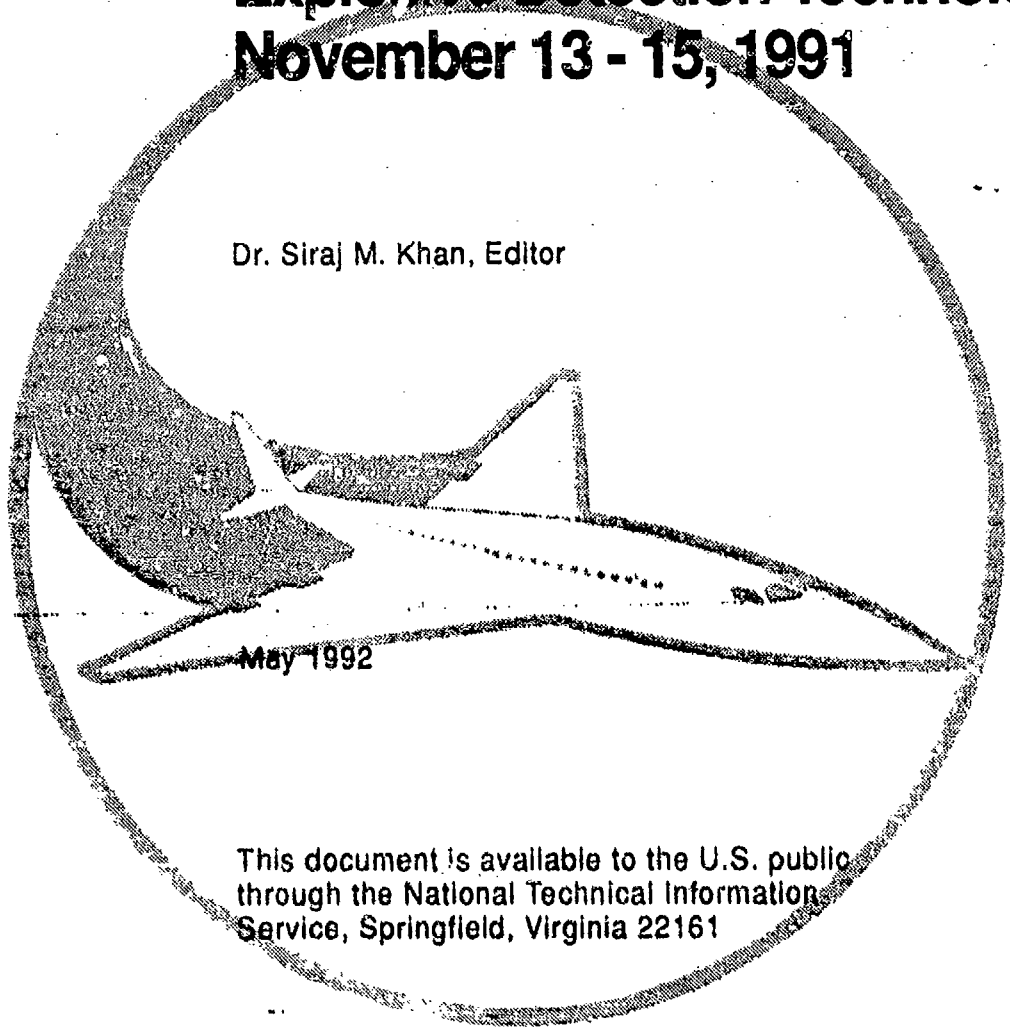
DTIC
ELECTE
FEB 1 8 1993
S C D

DOT/FAA/CT-92/11

FAA Technical Center
Atlantic City International Airport
N.J. 08405

Proceedings of the First International Symposium on Explosive Detection Technology November 13 - 15, 1991

Dr. Siraj M. Khan, Editor



May 1992

This document is available to the U.S. public through the National Technical Information Service, Springfield, Virginia 22161

U.S. Department of Transportation
Federal Aviation Administration

93 2 16 046

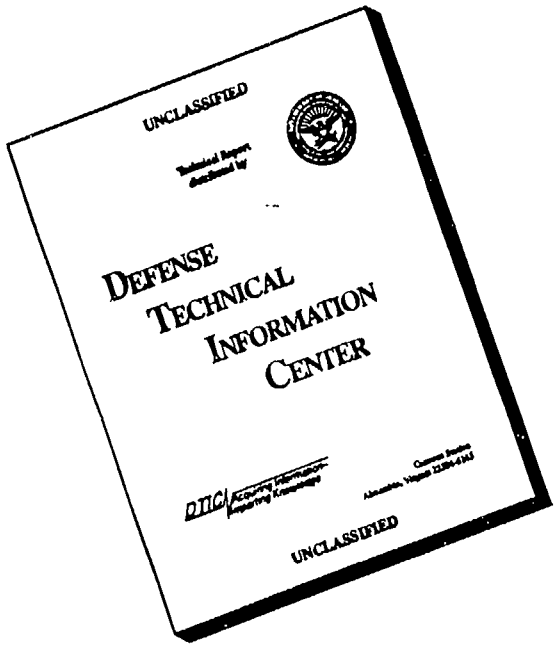
93-02958
968 p

NOTICE

This document is disseminated under the sponsorship of the U.S. Department of Transportation in the interest of information exchange. The United States Government assumes no liability for the contents or use thereof.

The United States Government does not endorse products or manufacturers. Trade or manufacturers' names appear herein solely because they are considered essential to the objective of this report.

DISCLAIMER NOTICE



THIS DOCUMENT IS BEST QUALITY AVAILABLE. THE COPY FURNISHED TO DTIC CONTAINED A SIGNIFICANT NUMBER OF PAGES WHICH DO NOT REPRODUCE LEGIBLY.

Technical Report Documentation Page

1. Report No.	2. Government Accession No.	3. Recipient's Catalog No.
DOT/FAA/CT-92/11		

4. Title and Subtitle	5. Report Date
Proceedings of the First International Symposium on Explosive Detection Technology - November 13-15, 1991	May, 1992
	6. Performing Organization Code: ACA-600
7. Author(s): Dr. Siraj M. Khan, Editor	8. Performing Organization Report No.: DOT/FAA/CT-92/11
9. Performing Organization Name and Address: U.S. Department of Transportation, Federal Aviation Administration, Technical Center, Atlantic City International Airport, NJ 08405	10. Work Unit No. (TRAIS): M183NC
	11. Contract or Grant No.
12. Sponsoring Agency Name and Address: U.S. Department of Transportation, Federal Aviation Administration, Technical Center, Atlantic City International Airport, NJ 08405	13. Type of Report and Period Covered: Final Report, November, 1991
	14. Sponsoring Agency Code

15. Supplementary Notes

16. Abstract

This report contains opening remarks, kickoff address and keynote address, and 89 papers presented at the First International Symposium on Explosive Detection Technology held November 13-15, 1991, in Atlantic City, New Jersey. The general papers deal with the outlook of civil aviation security policy makers in the United States, the United Kingdom, and France, and a general introduction to the subject of explosive detection technology. These are followed by papers on physical techniques for explosive detection (nuclear, X-ray and electromagnetic techniques and combinations thereof), chemical and biological techniques for explosive vapor detection, tagging, signal processing and simulation, and testing and field experience. This compendium of useful and practical information has been prepared for program managers, scientists, and engineers engaged in research, development, test, and evaluation (RDT&E) in the critical area of global aviation security.

17. Key Words	18. Distribution Statement
Bulk detection, Vapor detection, X-ray scanners, Tagging of explosives, Biosensors, Systems integration	This document is available to the U.S. public through the National Technical Information Service, Springfield, VA 22161

19. Security Classif. (of this report)	20. Security Classif. (of this page)	21. No. of Pages	22. Price
Unclassified	Unclassified	976	

Form DOT F 1700.7 (8-72) Reproduction of completed page authorized

FOREWORD

The proceedings of the First International Symposium on Explosive Detection Technology has been compiled and edited for the purpose of providing a much needed collection of essential information and procedures for the detection of explosives at airports and has been prepared for program managers, scientists and engineers employed in the area of civil aviation security. The deliberations at the symposium focused on further development and improvement and future deployment of promising biological, chemical and physical explosive detection systems (EDS) for luggage and personnel screening. An important goal of the symposium was to facilitate technology transfer and to allow networking opportunities for organizations and individuals involved in civil aviation security throughout the world.

DTIC QUALITY INSPECTED 3

Accesion For
NTIS CRA&I
DTIC TAB
Unannounced
Justification
By
Distribution /
Availability Codes
Dist | Avail and / or Special
A-1

ACKNOWLEDGEMENTS

It is a great pleasure to acknowledge the enthusiastic support of Harvey Safeer, Director, FAA Technical Center; Paul Polski, Director, Aviation Security R&D Service; and Albert Yost, Manager, Systems Development Division. The assistance provided by Dave Nesterok of the Technology Transfer Office was also invaluable to the success of the symposium. Finally, the help of Dr. Fred Snyder and William Curby in reviewing the technical papers on vapor technology is sincerely appreciated.

EXECUTIVE SUMMARY

This Proceedings contains papers presented at the First International Symposium on Explosive Detection Technology held on November 13-15, 1991 at Atlantic City, New Jersey. These papers have been arranged in various sections for convenience in accessing the relevant information.

The papers in the General section address policy matters such as the existence and nature of the terrorist threat to civil aviation and ways and means available to counter that threat. In particular, the paper by Vice Admiral Robbins offers a proposed solution to this threat to global civil aviation. His proposal consists of adopting a plan, approach, or strategy which will have a long-range goal, embedded in which are some short-range goals. He strongly emphasizes the need to get a workable explosive detection sensor or system (EDS) into the field at the earliest possible time.

The papers in the section on Nuclear Techniques describe the numerous methods used in this area of explosive detection technology. The only fieldable nuclear-based system at the present time is the thermal neutron analysis (TNA) EDS. This EDS is essentially a nitrogen detector. Other nuclear methods (e.g., pulsed fast neutron analysis (PFNA)) can detect and measure the rations of carbon, nitrogen and oxygen in the explosive, thereby achieving greater specificity. These techniques are, however, still at the developmental stage. Since most of the nuclear techniques depend on a source of neutrons or other particles, a section on accelerators of charged particles is also included.

The section on X-ray and Gamma-ray Techniques describes some innovative approaches to screening of luggage and personnel. These include dual energy, back-scatter, 3-dimensional, computed tomography, and gamma resonance absorption. Developmental work using combinations of nuclear, X-rays and other techniques is also presented in the next section. The fusion of nuclear (TNA, positron emission tomography (PET)) and the different X-ray technologies appears to a have lot of promise.

The section on Testing and Field Experience includes a very important paper on the testing protocol for bulk detection. Other papers describe the practical issues faced by developers and the approaches they have adopted to handle these issues when it was time to field an EDS at an airport.

The section on Electromagnetic Techniques includes a description of the methods of explosive detection using the physical phenomena of nuclear magnetic resonance (NMR) and nuclear quadrupole resonance (NQR). Whereas NMR depends on a constant applied magnetic field, NQR does not require the existence of such a field. This imparts to the NQR method an advantage over the NMR method, since it not only simplifies the system but the problem of erasure of magnetic media by the applied magnetic field is also eliminated.

The papers on vapor detection technology are grouped into three sections. The Vapor Detection: General section includes papers dealing with the preprocessing of the vapor (extraction, preconcentration, transportation and ionization) before it is actually detected by a suitable detector. This is followed by a section on Mass and Ion-mobility Spectroscopy. These two detection techniques appear to be the most favored for the accurate and rapid detection of explosive vapors. Finally, the section on Gas Chromatography, which is a separation technique, contains two papers. The first paper uses chemiluminescence and the second paper uses electron capture for detection.

The section on Tagging has in it papers which describe the program to tag military plastic and sheet explosives, the preparation and characterization of explosives contain a taggant, and the techniques for the detection of the taggants.

The section on Biosensors describes the various biochemical techniques for the detection of explosives. It also contains a paper on canines since the olfactory response in a dog is a biochemical phenomenon.

The section on Signal Processing and Simulation has papers describing the different approaches used for the identification of a bomb in a suitcase. These include discriminant analysis, artificial neural systems, design optimization and performance prediction. Computer simulation for the purpose of EDS performance improvement is also discussed.

The section on Systems Integration contains papers which contribute to our understanding of the application of the systems approach to the explosive detection problem.

TABLE OF CONTENTS

PAGE

Foreword iii
Acknowledgements v
Executive Summary vii

GENERAL

1. "Introduction"
   Dr. Siraj M. Khan 1

2. "Opening Remarks"
   Harvey Safeer 3

3. "Kickoff Address"
   Paul A. Polski 5

4. "Keynote Address"
   Vice Admiral Clyde E. Robbins 9

5. "Role of Advanced Technology in the Security of Surface Transportation"
   Bernard B. Boubli 13

6. "The UK Perspective on Aviation Security"
   Richard H. Doney 19

7. "Insights into U.S. Domestic Aviation"
   Richard Redman 21

8. "Role of Advanced Technology Within a Broad Security Approach"
   Pascal Morvan 23

NUCLEAR TECHNIQUES

9. "Principles of Nuclear-Based Explosive Detection Systems"
   T. Gozani 27

10. "A Review of the Development of a Luggage Explosive Detection System"
    J. Bartko and F. H. Ruddy 56

11. "A Transportable Luggage Examination System Based on Neutron Interrogation"
    D. B. Syme and G. D. James 66

12. "An Approach to Improving TNA EDS"
    S. Buchsbaum, D. Knize, L. Feinstein,
    J. Bendahan, and P. Shea 70

13. "PFNA Technique for the Detection of Explosives"
    Z. P. Sawa and T. Gozani 82

14. "A Pulsed Fast-Thermal Neutron Interrogation System"
    G. Vourvopoulos, F. J. Schultz, and J. Kehayias 104

15. "The Nitrogen Camera: A New Explosive Detector"
    W. P. Trower 116

TABLE OF CONTENTS (CONTINUED)

16. "Neutron Elastic Scatter (NES) for Explosives Detection Systems (EDS)"
H. J. Gomberg and B. G. Kushner 123

17. "Detector Selection for Nuclear-Based Explosive Detection System"
W. Lee, J. Bendahan, P. Ryge, and T. Gozani 140

18. "Explosive Detection System Based on Electronic Neutron Generator (ENG)"
W. Lee, D. B. Mahood, P. Ryge, J. Bendahan, and T. Gozani 151

19. "Associated Particle Imaging"
A. Beyerle, R. Durkee, G. Headley, J. P. Hurley,
and L. Tunnell 160

ACCELERATORS

20. "The RFQ Linac: A High-Current Compact Ion Accelerator for Explosive Detection"
R. W. Hamm 175

21. "Design of a High Current Proton Accelerator"
A. M. Todd, C. C. Paulson, J. W. Rathke, M. F. Reusch,
O. A. Anderson, and K. N. Leung 184

22. "An H⁻Ion Source for Resonant Gamma Production"
P. W. Schmor and L. Buchmann 197

X-RAY AND GAMMA-RAY TECHNIQUES

23. "Photons In - Photons Out: Non-Destructive Inspection of Containers Using
X-Ray and Gamma Ray Techniques"
L. Grodzins 201

24. "Three Dimensional X-Ray Systems and Image Enhancement Techniques"
M. Robinson and P. Evans 232

25. "An Explosive Detection System for Screening Luggage with
High Energy X-Rays"
J. R. Clifford, R. B. Miller, W. F. McCullough, and K. W. Habiger 237

26. "Explosives Detection Limitations Using Dual-Energy
Radiography and Computed Tomography"
K. W. Dolan, R. W. Ryon, D. J. Schneberk, H. E. Martz, Jr.,
and R. D. Rikard 252

27. "Detection of Objects Concealed Under Persons' Clothing
Using the 'Secure' System"
S. W. Smith 261

28. "New X-Ray Technology for the Detection of Explosives"
D. Schafer, M. Annis, and M. Hacker 269

29. "Advanced Dual Energy X-Ray for Explosives Detection"
K. D. Krug and J. A. Stein 282

TABLE OF CONTENTS (CONTINUED)

30. "3-Dimensional X-Ray Imaging for the Detection of Contraband"
D. C. Shreve, R. Schirato, R. Polichar, and V. Orphan 285

31. "The Evolution of Computed Tomography (CT) as an Explosives Detection Modality"
F. L. Roder 297

COMBINATIONS OF X-RAY, NUCLEAR, AND OTHER TECHNIQUES

32. "Explosive Detection Using X-Rays and Thermal Neutron Activation"
T. R. Wang, P. J. Bjorkholm, R. Scarlet, and S. Goldberg 309

33. "Fusion of the Nuclear and Different X-Ray Technologies for Explosives Detection"
V. Leung, P. Shea, F. Liu, and M. Sivakumar 311

34. "Explosive Detection for Checked Luggage by DETEX, a Combined X-Ray and Positron-Tomograph System"
H. W. Pongratz 319

35. "Selective Gamma Ray Resonant Absorption for Explosives Detection"
C. Nicholls, J. D. King, and F. McDaniel 333

TESTING AND FIELD EXPERIENCE

36. "A General Protocol for Operational Testing and Evaluation of Bulk Explosive Detection Systems"
J. A. Navarro, D. A. Becker, B. T. Kenna, and C. F. Kossack 347

37. "Performance Testing of Explosives and Weapons Detection Systems"
T. G. Sheldon, R. J. Lacey, N. C. Murray, and G. M. Smith 368

38. "A Framework for the Objective Test and Evaluation of Explosive Detection Technology"
D. R. Greenlee 376

39. "Validation of Simulated Explosives for Testing TNA Explosives Detection Systems"
M. J. Hurwitz and W. P. Noronha 381

40. "Airport Testing of a New Thermal Neutron Analysis Explosives Detection System"
M. J. Hurwitz, W. P. Noronha, and T. A. Atwell 388

41. "Radiological Safety Aspects of TNA Deployment"
I. M. Bar-Nir and P. Ryge 396

42. "Radiological Safety Regulation and Licensing of Nuclear-Based Explosive Detection Systems"
P. Ryge and I. M. Bar-Nir 409

43. "Experience with Explosive Detection Systems in Airports"
I. M. Bar-Nir, R. L. Cole, and D. Sumi 415

TABLE OF CONTENTS (CONTINUED)

44. "Sampling Explosives on Airline Passengers"
E. K. Achter, G. Miskolczy, F. W. Fraim, E. Hainsworth, and J. R. Hobbs 427

ELECTROMAGNETIC TECHNIQUES

45. "Explosives Detection by Pure ^{14}N NQR"
A. N. Garroway, J. B. Miller, and M. L. Buess 435

46. "Explosive Detection Using Dielectrometry"
D. C. Seward and T. Yuki 441

47. "Liquid Explosives Screening System"
D. R. McKay, C. R. Moeller, E. E. Magnuson, and L. J. Burnett 454

48. "Improved NMR Signatures of Explosives"
L. J. Burnett and J. P. Sanders 465

49. "Application of Magnetic Resonance to Explosives Detection"
J. D. King, A. D. Santos, C. I. Nicholls, and W. L. Rollwitz 478

50. "Explosive Detection Using Microwave Imaging"
D. G. Falconer and D. G. Watters 486

51. "Consideration of Untried Magnetic Resonance Techniques for Possible Baggage Analysis"
E. H. Poindexter, H. A. Leupold, R. H. Wittstruck, and G. J. Gerardi 493

VAPOR DETECTION: GENERAL

52. "Dichotomous Key Approach for High Confidence Level Identification of Selected Explosive Vapors"
D. H. Fine, D. P. Rounbehler, and W. A. Curby 505

53. "Explosive Vapor Emission"
B. T. Keana, F. J. Conrad, and D. W. Hannum 510

54. "A Thermodynamic Study of the Vapor Pressures of C-4 and Pure RDX"
W. McGann, A. Jenkins, and K. Ribeiro 518

55. "Extraction, Transportation, and Processing of Explosives Vapors in Detection Systems"
A. Jenkins, W. McGann, and K. Ribeiro 532

56. "Vapor Sampling Using Controlled Heating"
E. A. Bromberg, A. L. Carroll, F. W. Fraim, and D. P. Lieb 552

57. "Efficient Collection of Explosive Vapors, Particles, and Aerosols"
F. W. Fraim, E. K. Achter, A. L. Carroll, and E. Hainsworth 559

58. "Negative-Ion Formation in the Explosives RDX, PETN, and TNT Using the Reversal Electron Attachment Detection (READ) Technique"
A. Chutjian, S. Boumsellek, and S. H. Alajajian 571

TABLE OF CONTENTS (CONTINUED)

59. "Calibration Methods for Explosives Detectors"
S. J. MacDonald and D. P. Rounbehler 584

60. "Vapor Detection Using SAW Sensors"
G. Watson, W. Horton, and E. Staples 589

61. "Fourier-Transform Infrared Spectroscopy Applied to Explosive Vapor Detection"
D. O. Henderson, E. Silberman, and F. W. Snyder 604

MASS AND ION MOBILITY SPECTROSCOPY

62. "Atmospheric Pressure Ionization Time-of-Flight Mass Spectrometer for Real-Time Explosives Vapor Detection"
H. G. Lee, E. D. Lee, and M. L. Lee 619

63. "Real-Time Explosives/Narcotics Vapor Enhancement and Collection Systems for Use with the Atmospheric Pressure Ionization Time-of-Flight Mass Spectrometer"
M. M. Hintze, B. L. Hansen, and R. L. Heath 634

64. "Detection of Explosives Material on Single Microparticles"
W. B. Whitten, J. M. Dale, and J. M. Ramsey 637

65. "Tandem Mass Spectrometry for Explosives Vapor Detection"
G. L. Glish, S. A. McLuckey, B. C. Grant, and H. S. McKown 642

66. "Modifications to the Ionization Process to Enhance the Detection of Explosives by API/MS/MS"
W. R. Davidson, B. A. Thompson, T. Sakuma, W. R. Stott, A. K. Akery, and R. Sleeman 653

67. "The Role of Mass Spectrometry in the Detection of Explosives"
W. R. Davidson, W. R. Stott, A. K. Akery, and R. Sleeman 663

68. "Modifications to the Ionization Process to Enhance the Detection of Explosives by IMS"
L. L. Danylewych-May 572

69. "Fourier Transform Ion-Cyclotron Resonance (FT-ICR) Mass Spectrometry of RDX, PETN, and Other Explosives"
C. S. Giam, M. S. Ahmed, R. R. Weller, and j. Derrickson 687

70. Detection of Trace Explosive Evidence by Ion Mobility Spectrometry"
D. D. Fetterolf and T. D. Clark 689

GAS CHROMATOGRAPHY

71. "Analysis of Explosives Using High Speed Gas Chromatography with Chemiluminescent Detection"
D. P. Rounbehler, S. J. MacDonald, D. P. Lieb, and D. H. Fine 703

72. "A GC/ECD Approach for the Detection of Explosives and Taggants"
S. Nacson, B. Mitchner, O. Legrady, T. Siu, and S. Nargolwalla 714

TABLE OF CONTENTS (CONTINUED)

TAGGING

73. "Marking of German Plastic Explosive for the Enhancement of Vapor Detection"
P. Kolla 723

74. "Program to Tag Military Plastic/Sheet Explosives"
S. Eng, J. A. Lannon, and C. Westerdahl 734

75. "An Improved Vapor Taggant Detector"
T. H. Chen 737

76. "Plant Laboratory Scale Preparation and Complete Characterization of Modified Composition C-4 Containing a Taggant"
T. H. Chen, C. Campbell, R. Reed, W. F. Ark, J. Autera, D. A. Wiegand, and M. S. Kirshenbaum 739

77. "Detection of Taggant in Modified Composition C-4 Tagged with a Taggant"
T. H. Chen, C. Campbell, and R. A. Reed 741

BIOSENSORS

78. "Dry Immunochemical Sensor for the Detection of PETN Vapor"
H. R. Lukens 753

79. "The Challenge of Biodetection for Screening Persons Carrying Explosives"
C. Weinstein, S. Weinstein, and R. Drozdenko 759

80. "The Flow Immunosensor: An Antibody-Based System for Explosives Detection"
A. W. Kusterbeck, F. S. Ligler, and J. P. Whelan 770

81. "Explosives Search Dogs"
S. Lovett 774

SIGNAL PROCESSING AND SIMULATION

82. "Bomb/No Bomb: From Multivariate Analysis to Artificial Neural Systems"
P. Shea, F. Liu, and B. Yedidia 777

83. "A Novel Approach to Design Optimization of Nuclear-Based Explosive Detection Systems"
E. Greenspan, J. Bendahan, and T. Gozani 787

84. "Assessing the Operational Impacts of Checked Luggage Screening"
S. Wolff 810

85. "Fast Nuclear Spectroscopy for Explosive Detection Systems"
P. Ryge, R. Benetti, A. Patel, and E. Chou 825

86. "Computer Simulations and Performance Predictions for Explosive Detection Systems"
J. Bendahan, E. Elias, Z. Shayer, J. Pierre, E. Altschuler, and T. Gozani 840

87. "Recognition of Partially Occluded Threat Objects Based on Hybrid Hopfield Neural Network"
J. H. Kim, E. H. Park, C. Ntuen, and S. Cheung 850

88. "Segmentation of X-Ray Images Using Probabilistic Relaxation Labeling"
T. Q. Thai 860

SYSTEMS INTEGRATION

89. "Robotics Systems for Deployment of Explosive Detection Sensors and Instruments"
M. W. Siegel, A. M. Guzman, and W. M. Kaufman 873

90. "A Systems Approach to the Explosive Detection Problem"
M. C. Smith and R. L. Hoopengardner 880

91. "Integration of the Human, Canine, Machine Interface for Explosives Detection"
J. W. Ternes and A. M. Prestrude 891

92. "Logistics and the 'ilities' Requirements for Explosive Detection Systems"
R. L. Cole and G. V. Brown 903

93. "Impact on the Air Carrier of Explosive Detection Systems"
D. Hsiung, P. Shea, and M. Sivakumar 911

APPENDIXES

Appendix A: List of Attendees at the First International Symposium on Explosive Detection Technology 921

Appendix B: List of Acronyms Used in Explosive Detection Technology 943

Appendix C: Bibliography of Explosive Detection Technology 949

Appendix D: Author Index 959

INTRODUCTION

Dr. Siraj M. Khan
FAA Technical Center
Atlantic City, NJ

The urgent and critical need to detect explosives in airline passenger luggage was very clearly demonstrated by the unfortunate and terrible incident involving Pan Am Flight 103. As a result the FAA has scaled up its efforts to prevent future events of this type from occurring The First International Symposium on Explosive Detection Technology which was held on November 13 - 15, 1991 at Sands Hotel in Atlantic City, NJ was a step in that direction. Its purpose was two-fold: first, to provide a forum for the exchange of ideas, information and technology among program managers, scientists and engineers working in the area of civil aviation security for U.S. and foreign government agencies, defense contractors, national and defense laboratories, and the universities; and, second, to determine the direction of research and development in the critical area of global civil aviation security.

The symposium was very well attended. A total of 430 civil aviation security experts from U.S. and abroad participated (See Appendix A: List of Attendees) and over 100 papers, most of them of a technical nature, were presented. The activities consisted of oral, poster and informal discussion sessions. Arrangements were also made for break-out sessions. A total of fifteen foreign governments including France, Germany and the UK and a large number of U.S. government agencies such as FBI, DOD and DOE were represented. Technical papers on various topics in detection technology were presented at the symposium by scientist and engineers from nineteen universities, fourteen national and defense laboratories and equivalent organizations from Canada, France, Germany and the UK.

The highlights of the symposium included the opening remarks by Harvey Safeer, Director, FAA Technical Center; a briefing on aviation security R&D at the Technical Center by Paul Polski, Director, Aviation Security R&D Service; the keynote address by Vice-Admiral Clyde E. Robbins, Director, Office of Intelligence and Security, U.S. Department of Transportation; and the banquet speech by John Burt, Executive Director of Systems Development, FAA.

The technical sessions at the symposium fell into five general categories: (1) bulk detection (nuclear, x-ray and electromagnetic techniques), 42 papers; (2) vapor detection (gas chromatography, mass spectrometry and ion-mobility spectroscopy), 35 papers; (3) testing and field experience, 9 papers; (4) signal processing and simulation, 6 papers; and (5) systems integration, 8 papers.

This symposium also provided an opportunity to put forth a proposal to embark on the following activities in an attempt to enhance the art and science of civil aviation security in particular and transportation security in general:

1. organize a professional association of experts in the field of transportation security;

2. publish a technical journal which will contain refereed scientific and technical papers in the area of transportation security; and

3. establish working groups and sub-groups on various topics of interest to increase coordination among the technical experts.

This proposal generated great interest among the audience and some of them even came forward with constructive and helpful suggestions.

The stated purpose of the symposium was clearly met. This event provided a singular opportunity for technology transfer and networking among various organizations and individuals who participated. The speeches by Vice-Admiral Robbins and John Burt provided the direction which the R&D should take in this critical task. The message is clear and a lot remains to be done to ensure and maintain the safety and security of international airline passengers.

A survey conducted near the end of the symposium showed that the attendees liked the arrangements and the presentations. A majority of those responding to the questionnaire thought that the content, variety and length of the presentations was in the excellent-to-good category. An overwhelming majority (91%) felt that the symposium met their expectations. Most

of the responses in the questionnaire contained constructive and useful comments which will be utilized to make the future symposia even better. Overall, everyone was very satisfied with the organization of the symposium and it was judged to be a great success.

All the presenters were asked to submit their papers for inclusion in these proceedings when they arrived for the symposium. Despite an extension of several weeks in the deadline only about 90 written papers out of more than 100 papers presented at the symposium were received and these papers have been re-arranged in various categories for ease in access to information covered at the symposium. A few of the presenters sent us only hard copies of the view-graphs and these have not been included because a decision was made early on to publish only written papers.

A list of acronyms used in explosive detection technology (Appendix B) is included to assist new comers in this field. Appendix C contains a bibliography of explosive detection technology which contains a listing of reports and other documents published since 1971 and available in the open literature. This list was obtained from the National Technical Information Service (NTIS). Finally, an author index is presented in Appendix D.

OPENING REMARKS

Harvey Safeer, Director
FAA Technical Center
Atlantic City International Airport, New Jersey

I would like to take this opportunity to welcome you to the First International Symposium on Explosive Detection Technology.

This symposium has attracted some of the finest talent in the industry. Based on its success thus far, we can safely say that we are going to start planning our second symposium next Monday.

This symposium is the first of its kind. Other symposia on explosives detection have directed themselves to parts of the problem. This is the first time we've brought people together from all over the world, making this a truly international symposium.

We have more than 60 participants from foreign countries, including 15 speakers from Canada, France, Germany, and the United Kingdom. We also have technical experts from the United States, representing 19 universities, 15 national and defense laboratories, and defense contractors, in addition to the FAA.

Many of you may be aware that the federal government is engaged in a massive effort aimed at "technology transfer." Taxpayers have invested significant amounts of money in federal laboratories, and this money in turn has been used to fund contracts in the private sector, universities, and other government facilities.

It is now the desire of the federal government to get information that has been generated through these expenditures of taxpayers' funds back into the hands of industry so that industry can benefit and we can produce the products that we need. In particular, what is needed in aviation is a safe, secure, and efficient air transportation system. So this can be viewed as part of our technology transfer effort. We're bringing together the experts to talk to each other about what's happening in explosive detection.

In order to bring together as many people as possible, you'll note that briefings have been rather short. Fifteen minutes is allotted for each presenter. But we will be publishing the proceedings, which will be made available to all of you. There will be enough information at each of these presentations to whet your appetite so that you can go down your shopping list and see who is doing something of interest to you and something that you can benefit from. There could be another company that has a complementary technology, a university that is working on a process or product that can feed into your needs, or contacts that are important in sharing the technology.

This symposium is not accidental. It coincides with the enhanced efforts of the Technical Center to expand our program in aviation security research, engineering, and development.

For those of you who have the time to come out and visit our facility this week, you'll see that there is a lot of construction going on. We have two laboratories under construction. One, which will be involved in the air traffic control systems, will house the computers for the next generation of air traffic control. The other building is of more importance to you because it will house our aviation security research, engineering, and development effort.

We will be building a laboratory facility that will be available to all of you in industry, academia, and other government agencies. Just as we share facilities that are owned and operated by the Defense Department, our facility will become available for use by other agencies and by the private sector.

We haven't configured fully the inside of that facility because we are still talking to many of you about ideas for how to best use this facility to complement, rather than duplicate, what already exists.

If you have an opportunity to speak with Paul Polski during the course of these few days, either tell him what your ideas are or make arrangements to get back in touch with him.

It's almost, and I say almost, a clean slate. While we have not yet configured the laboratories, they are

already designed. We have the space, and we know which lab is going to have positive pressure control, which lab will be reinforced so it can handle TNA type devices, and which labs will be constructed metal-free so that we can look at devices that rely on magnetic or electrical energy without interference. The walls are up now, and we are looking for the best use of the insides.

I have some good news and some bad news. The bad news is that even though you will be sitting here for your dinner, the dancing girls won't be up here. The good news is that you won't have to listen to me again because we were advised this morning that John Burt, the FAA's Executive Director for System Development and my new boss, will be the keynote speaker at our banquet. John has been on the road and just got back into Washington yesterday. Paul spoke to him and he called back this morning to say: "It is important. I'll be there."

So the bottom line is: We at the FAA are committed to pursuing an aggressive research, engineering, and development program. We fully understand that the solution to our problem stands in advancing the state of the art several orders of magnitude beyond what it is today. We fully understand that many of you have devices that have been developed which you believe can do the job. We're going to make our facilities and our program available to you to field test, laboratory test -- or whatever kind of test is practical -- those devices.

We are looking for technology breakthroughs, which means we know there are going to be failures. We are ready to expect failure, but, most importantly, we are not ready to give up. Congress has given us the resources, and we have a long-range plan which will provide the guidelines for how we proceed. The technology is out there. We must try to serve as a catalyst to bring it together and truly make this endeavor a partnership between government, industry, and academia.

I wish you the best of luck in this symposium. I look forward to hearing as many of the sessions as I can, and I certainly look forward to reading the proceedings.

Thank you for coming.

KICKOFF ADDRESS

Paul A. Polski
Director, Aviation Security
Research and Development Service
FAA Technical Center
Atlantic City International Airport, New Jersey

1. WELCOME

I welcome all of you to this important symposium. Looking at the audience this morning, I am truly amazed with the diversity of disciplines, agencies, and countries that are represented at the First International Symposium on Explosive Detection Technology.

There are people here from the medical professions. For years, they have been using detection equipment to examine the human anatomy, thus helping that profession do its job better. There are people here from quality control offices, who have been using detection equipment to examine the inside of products to ensure that they have been assembled correctly. There are people here who have been using devices to study the properties of coal and other materials. There are others from a broad spectrum of industry and government organizations concerned with explosive detection technology.

I think diversity represents the key ingredient of a good meeting. I know that a lot of productive networking and interfacing will happen in the next few days. This will surely help advance the state-of-the-art in explosive detection technology.

In these brief "kickoff" remarks, I want to address the following subjects relevant to explosive detection technology: challenge, systems, community, documentation, test and evaluation, the FAA's new security laboratory, and symposium discipline.

2. CHALLENGE

As Director of Security Research and Development at the FAA Technical Center, I have one of the most challenging, and indeed most rewarding, jobs in the government.

Our Secretary of Transportation has told us that we need to be more proactive in our approach to the detection of explosives. Unfortunately, in the security business, we sometimes tend to be reactive; problems happen and then we get out there to solve them after the fact. Certainly, being proactive -- preparing ahead of time for the threat -- has got to be one of our major objectives.

The FAA Administrator is insistent upon getting improved equipment into operation. This is also a major thrust of various security groups, including the victims of Pan Am 103. We have a tremendous challenge here and we will meet it.

You are going to hear from John Burt [FAA Executive Director for System Development] on Thursday evening. I want to tell you that he is a manager and a leader who has embodied quality, acquisition improvement, and a better way of doing business for the FAA and our great country. I am sure that you will find his remarks very stimulating. He is going to help us improve the standards and speed of our progress.

3. SYSTEMS APPROACH

My boss, Harvey Safeer, has been a major guidance and inspiration to me. He has aided me in accomplishing the things I need to do and has helped us to fight for the resources that we need.

Historically, in the systems approach to the explosive detection business, we have looked primarily at the probability of detection, which is paramount, and secondarily at the probability of false alarm. We have also been interested in the spread, or difference, between these two probabilities.

In the last year or two, increasing emphasis has been placed on other probabilities: probability that the equipment will run day in and day out; probability that it will run well; probability that it can be

supplied, maintained, and supported; probability that it fits well in the airport environment; and probability that it is affordable. Thus, we who work on this very critical research need to seriously scrutinize not only the probabilities of detection and false alarm, but also of all other aspects of explosive detection equipment. We must make sure that we are putting together sound systems that will work effectively in an operational airport.

I'm challenged by our customers. They include the flying public, the airlines, the airports, and others in the FAA. They want to make sure that we spend our money wisely. Our explosive detection equipment absolutely has to be acceptable to the efficient operation of the airlines and certainly to the equipment operators.

So, in summary on this point, we must work together to ensure the best use of existing resources so that we will achieve even more effective explosive detection systems as quickly as possible.

4. SECURITY COMMUNITY

Development of new technologies in the defense community has become a routinized ritual. Every couple of years, a new tank, ship, or plane is developed to meet the increasing threat. That type of acquisition in our country, and most countries for that matter, tends to generate a lot of associations, publications, and meetings. This understanding results in organizations working together better. To be candid, I don't think we've come together that well yet. We need to put aside nonproductive pursuits and get down to the real technical work at hand.

This is one of the key reasons that we've established a stronger independent test and evaluation program. Through it, we can objectively assess just exactly what are the best technologies to develop and deploy.

5. MULTIPLE TECHNOLOGIES

There is another good thing about getting together as a community. Our search for the Silver Bullet, i.e., a single machine that will find all major threat explosives, is probably going to take some time. Quite possibly, the equipment that we have on the street today, or nearly on the street, may best be put together in a collective fashion. I'm talking about an architectural approach that may involve two or three or more technologies together. This is ultimately going to be the near term answer to our explosive detection solutions.

Our Congress, the National Academy of Sciences, OTA, and others are indicating that we need a combination of technologies to best satisfy detection requirements in the near term. So here I see x-ray, vapor, nuclear devices, and a number of other technologies coming together. We need to expand ourselves from a vertical orientation to one which looks at what the industry next door has. I certainly hope that in the next couple of days, we all will benefit from looking at different combinations of technologies to detect explosives.

6. DOCUMENTATION

My next point is that I think we need better documentation. I'm not a documentation freak. You can overdo that. I came out of the Defense Department and they do that fairly well over there. But, in our field, I see a paucity of things in writing, records, plans, and solid descriptions of the testing and evaluation we do.

We put together, and some of you will be seeing it soon, a program plan -- a real, good, solid, detailed plan -- which details who we are, where we are, where we are going, and how long we think it is going to take to get there. It's primarily a technology book and a road map to achieve success using the best we can get from our existing capabilities.

This program plan will help our six program managers to better develop program management plans, and to determine in what direction they will go in their various disciplines. It will give us better doctrine and protocols for test and evaluation. We need that documentation very badly, and we're working very quickly to develop it.

7. TEST AND EVALUATION

I mentioned test and evaluation earlier. Let us take a look at the Service that I run right now.

We have a Test Director, who is preciously independent from the program managers. They need to satisfy him in readying their projects for tests. Our test approach is very objective: we ask all the bad questions and tell the truth, which is exactly what I want to see happen in my service.

8. SECURITY R&D LABORATORY

Harvey mentioned the security laboratory. One fear that I have is that we will open the door and nobody will come. Therefore, we're putting together a utilization plan for the laboratory. I invite all of you on a "knock and enter" basis to come and use our laboratory, talk to us, and work with us.

What a tremendous facility it will be. This is the first time that a building will be erected from the ground up, solely for the purpose of research, development, test, and evaluation on security. It certainly is going to have a lot of utility.

Along that line, I would like to mention some other areas that we need to be aware of: airport design, human factors, training, integration of systems, and aircraft hardening.

9. SYMPOSIUM DISCIPLINE

I want to mention something about the conduct of our symposium. We are very concerned about the tight schedule of our symposium. We could easily lose control of this program if we don't maintain a tight schedule and good discipline. There are three particular groups of participants that I need to address these remarks to: the briefers, the session chairpersons, and those asking questions.

We took a hard look at how we wanted to run this symposium and at what we wanted to achieve. Certainly, we want a lot of good dialogue. We want to increase awareness, and we want to see the surfacing of new thoughts on detection technologies. We hope to open up minds and get good back and forth discussions to identify better ways of detecting explosives.

But we also need good symposium discipline. Primarily to the briefers: when your schedule says fifteen minutes, please keep your delivery to fifteen minutes. Secondarily, to the chairpersons: I don't think we've set any flashing lights or anything, but I need the chairpersons to take charge of their segments, to be dynamic, and, if you have to, give people the hook. Stand up, turn off the mike, or whatever, but I don't want to see this conference going on two or three hours into evening overtime. This will disrupt people's schedules and this really hurts. But, most importantly, we all must watch the time as we ask questions.

Maybe there is a hot question that you would like to get some visibility for or articulate. If you can't because there's no time, see that person later. We're all going to be here for the next three days. Get the speaker's card, talk to him or her, and work it that way. I hope you all ask challenging questions, push these people, try to find the optimum technology, and discuss how we can put it all together.

In closing, I want to plug some other symposiums that will be coming up next year. They are as follows:

1) National Energetic Materials Workshop
   - Golden Inn Hotel: Avalon, New Jersey
   - April 14-17, 1992

2) Internal Blast & Aircraft Container Hardening Workshop
   - FAA Technical Center
   - April 29-30, 1992

3) Industry Day
   - FAA Technical Center
   - June 1992

4) Physics & Engineering of Advanced Detectors and Collection Focusing Systems
   - San Diego, California
   - July 19-24, 1992

5) Aircraft Hardening Symposium
   - Atlantic City, New Jersey
   - August 1992

6) Second Annual Symposium on Explosive Detection Technology
   - Atlantic City, New Jersey
   - November 1992 or 1993

7) Technical Symposium, OPTCON '92: "Applications of Signal and Image Processing in Explosive Detection Systems"
   - Boston, Massachusetts
   - November 15-20, 1992

I intend to be here for the next three days, day and night. I want you to come and ask me questions. And if you don't get an opportunity to do so, or you think of something later, please give me a call.

At this time, I would like to thank you all for attending. I am looking forward to a very fruitful two and a half days work. Thank you.

KEYNOTE ADDRESS

Vice Admiral Clyde E. Robbins, Director
Office of Intelligence and Security
United States Department of Transportation
Washington, DC

Good morning. I'm delighted to be here. I'm always a little reluctant to hand out my biography because it is somewhat misleading. What it really says is that I can't hold a job.

I have moved around a number of times. The experiences I had in Alaska with the Exxon Valdez were very educational, and then the earthquake that followed led to an interesting sequence of events.

While I worked for six months at the Exxon Valdez oil spill site as the on-scene coordinator, I had many visitors. Some were repeaters, and one of those repeaters was Vice President Dan Quayle. He was up there twice, and I briefed him both times. Then we went out and looked at the shorelines, at the oil, at the birds, and at one thing or another. I got to know him a little bit and thought that he would probably forget me rather quickly. In some ways, I was hoping he would because of what was going on up there.

I went back to San Francisco in October. I had been there about three weeks when the earthquake hit, and I became the Federal Emergency Transportation Coordinator. Of course, the Vice President came to visit me again. We met again, and were waiting for Secretary Skinner to arrive when he took me aside. He looked around to make sure there weren't any live microphones and said, "Doesn't anything good happen where you are?"

I had been in this job for just over a month when Saddam Hussein marched into Kuwait, so I do not think good things happen where I am. Therefore, if you want to leave now, it's OK. I understand.

After Saddam, I think things have cooled down a bit, and I am honored to be here today as your speaker. This is a distinguished group, and it is one that is extremely important. In many ways, you and your colleagues hold my future in your hands.

Pan Am 103 has done a number of things, not only for this nation, but for other nations as well. Perhaps most importantly, it let us know how vulnerable we all are. It brought a shocking revelation home to many families in the United States -- the world we live in is pretty dangerous.

The location and magnitude of the disaster focused the attention of the world on terrorism as no other event ever had.

Sometimes I think that when the United States finally gets involved, things will begin to happen. Otherwise, they don't seem to. It's pretty easy to put those events aside when they happen in a desert in Africa, the Indian Ocean, or places like that.

But I stand here before you today because of the indiscriminate killing of people on Pan Am 103. My office was formed as a result of the Pan Am 103 incident and the impact it has had on the international transportation system. There was a perception, and probably rightfully so, that the Department of Transportation had not put enough emphasis on security. The President, the Secretary, and the Congress knew that it was time for something to be done.

I don't think for a minute, and I hope that no one else does, that when they appointed me to this job, I would solve the problem of terrorism or eliminate the threat to the transportation system. Merely assigning new people or new positions isn't going to make the problem go away. If it was so easy, it would have been done before.

Fortunately, strikes against the airlines and other transportation systems have been isolated events since Pan Am 103. As a matter of fact, there have been no attacks against U.S. airlines since then. Only incidents in ticket offices and an occasional incident in a parking lot have occurred. Folks, I'm here to tell you that isn't going to last.

That is the way I have to plan. I have to plan as if this is not going to last because the chances are that I'm correct. I think we need to expect a terrorist action any time, anywhere, and we must be prepared.

Terrorists have us at a great disadvantage. They can sit back. They can watch. They can wait. And they can do that very well. They can study our systems. It doesn't matter how confidential or secret we make them. They can find our weak spots and attack, or they can develop new equipment that will thwart the methods that we have in place.

Explosives are, of course, their weapon of choice at this point. They can plant them, and they can be gone, and that is what they want to be -- gone.

They don't want to be caught. They aren't heroes. They are criminals. I consider the development of explosive detection devices [EDDs] crucial. It really is urgent. But if it is so urgent, why has progress been so slow?

Before I try to answer that question, let me give you a scenario that will, I hope, get EDDs into the field faster.

I think a detection system has to be just that -- a system. It has to be a group of detectors. Some of it may be equipment and some of it may be people, but it has to be a system that we put together. We're playing catch-up ball, of course, but that is not a reason not to move.

I would not like to concentrate on the past other than what we can learn from it. Rather, let us take the time we have together to see if we can improve the future.

I know that the Department of Transportation and the FAA are ready to listen. You are the experts. You can help us solve the problem. I hope it will be the kind of cooperative arrangement that was mentioned earlier; we help you and you help us solve the problem.

In terms of the development of EDDs and why they are so urgent, I want to talk a little bit about our shortcomings. I will keep it general because I am not sure how secure this facility is and I would not like to publicize all of our weak spots. Nevertheless, I have to tell you that the explosive detection equipment that we have out there today leaves a lot to be desired.

Now, that's a blinding flash of the obvious to most of you. I think that things like X-rays, as we have them today, are very limited. Furthermore, some operators aren't very well trained.

I was recently in a foreign country and visited one of the airports where there had been a problem. The barriers around the airport were not very good, and they were not keeping people out. There had been a lot of construction, so there weren't any good fences and the patrolling was not very good. I had promised that I would get over there in a couple of months to look at it because they were working with rear ends and elbows trying to get it fixed.

I went over there a few weeks ago and saw a vast difference from what I had seen before. They had put the fences back up, and they had more than tripled the number of people responsible for security. It really looked good. I thought that this airport had really gotten its act together.

The next day, I was getting ready to leave the city and go to another one, and I, like most of you, had to wait in the airport. I don't know what you do when you're in an airport, but I watch to see how the security system looks from the passenger's standpoint.

They had all of the screening people there, and they had two areas where they were screening passengers. There were only a few passengers, however. While there were a few passengers dribbling in, you only saw two or three screeners actually doing things. The other three or four screeners were standing around goofing off. They were telling stories, and pretty soon all five or six of them were goofing off and telling stories.

As we were going through the screening point, I saw a guy go through with a briefcase, set off the alarm, and keep right on walking. No one said a word to him. They had a great physical security system completely short-circuited by inattentive screeners standing the watches.

Interestingly, that system got much better shortly after that when more passengers began to come through. They opened both screening points and divided the screeners in half. There were half as many screeners to goof off, and they suddenly got interested in what they were doing and began doing a pretty good job.

That is the kind of thing we are faced with. The whole system must work if we are going to be successful. What we're trying to do isn't really like finding a needle in a haystack; it is more like finding a needle in the Pacific Ocean because there is a large volume of material and people that pass through airline terminals that aren't carrying bombs.

Let's face it, if we had to rely on the current state-of- the-art EDDs, I would not sleep very much. What we have to rely on is a number of measures, not the least of which is profiling, to protect the transportation system from would-be bombers.

Perhaps, for just a second, I should talk about the threat. I would like to talk about the threat in the right circumstances because I think everyone should realize that there is a threat out there.

We haven't done a great deal to lower that threat. Yes, perhaps it is a lot better than it was before the Gulf War because there has been a lot of activity in countries to take action against would-be terrorists. State sponsors of terrorism are standing aside, waiting to see what is going to happen in the world situation. Unfortunately, terrorism is the voice of the downtrodden, so we have to be prepared. It could happen, as I said earlier, at any time. That is why I think the development of EDDs is so important and so urgent.

The development of EDDs is a tough problem to deal with. I don't need to tell you that. In addition, we haven't put much money into security in past years, though we have increased it significantly in the last two years. I am hoping that the 1993 budget will be very good for R&D and, of course, that much of that money goes to the FAA Technical Center.

One of the things that we haven't done very well is let the industry know exactly what the future holds. No one is eager to spend money developing equipment and concepts if they don't think that there is any money there. Companies are not in business as an altruistic adventure, as you well know. They are in it for the money. If we don't provide the right atmosphere for the development of the equipment and the arrangements for getting it in place -- and I hasten to say that foreign countries have done better than we have in this regard -- then we can't expect too much out of the industry worldwide.

Over the last year, I've seen that situation change to some extent. The development of explosive detection devices has become a growth industry. We probably haven't matched that growth with a clear signal as to what is going to happen with that equipment. We need to change that, and we will.

I think either Harvey or Paul said, "In this business, there is no silver bullet." You all know that. There will not be one piece of equipment that we can put into the field that will solve all of our problems. That should be encouragement for everybody in the field to work on equipment that they think will do part of the job.

When I talk about a system, then, I am talking about a number of pieces of equipment. Again, we are faced with a question: What criteria must the components meet in order to be approved by the FAA for use?

There are those among you who have said to me that your equipment would be useful if FAA would only approve it. Airlines are saying that they are not going to buy equipment until it is approved or until the FAA signals what the future holds for them. The FAA has been reluctant to approve equipment which may be obsolete next year or two years from now or to approve equipment that is only partially successful.

So where are we going with this? I met recently with the victims of Pan Am 103. One of the points they made was that they felt my job is to get something out into the field as quickly as possible. Whether it works 100 percent, or maybe only 50 or 25 percent, it might be better than what we have today.

We don't have to wait for the perfect piece of equipment. Admiral Gorshkov of the Russian Navy once said that "better" is the enemy of "good enough," and he was absolutely right. We have to get some equipment out there and get it in operation soon. And we have to do it in a way that won't discourage industry from continuing to develop better equipment. That's a tall order.

I don't propose forcing specific equipment on airlines. I want to leave them some flexibility. I know they are eager to get better equipment themselves. The last thing that they want to have is a bombing on one of their airplanes.

What I propose is that we have a long-range goal. Perhaps embedded in that are some short-range goals

that will help you do the job better. That kind of approach led to the development of the airplane. Just suppose the Wright Brothers waited until the plane they built was big enough to fly across the Atlantic before they undertook their first flight. We would probably still be searching for something that would fly.

We have to walk before we can run. We need to put in place an approval process so that equipment, which may not do everything for everybody, will be significantly better than what we have right now.

As significantly better equipment is developed, we must have a system that can accept it without causing a great economic impact. Phase in. Phase out. Grandfathering. There are a number of ways we can do that.

To lay out this scenario a little bit more carefully, we will make an assumption. There is no silver bullet. There is no one solution to security. Security then will be based on performance standards. Flexibility will have to prevail.

I will urge the FAA to set up a system of approval for specific pieces of equipment or procedures. Each airline or airport could then use different pieces of equipment for its security system. Using the performance standards, the plans for using equipment and procedures to meet standards would be submitted to the FAA for approval.

Following the approval, the equipment would be bought and installed. As experience was gained, modifications to plans would be submitted to the FAA for approval as well.

There are certainly some downsides to such a flexible approach. We would have what some would describe as a "hodgepodge" of equipment and methods at the airport that would be difficult for the FAA to monitor.

But, to be successful, the FAA must have a flexible approach, and I think they will. My discussions with General Steele [FAA Assistant Administrator for Civil Aviation Security] certainly indicated that he recognizes that.

I am delighted that the Technical Center and the FAA are holding this symposium. I think it is a good first step. I can't stress to you enough the importance of finding a solution to this problem. I hope we all come away with a better understanding of the problem and at least a peek at the solution.

We can't afford to fail. We must not succumb to the criminal element that terrorizes the public in an attempt to force us to submit to its terms. They are criminals. They are not heroes. They are the scum of the earth, and we need to track them down and bring them to justice in one way or another. President Reagan stated it very well when he said, "They can run, but they can't hide." I think most nations are now pulling together to try to track down these terrorists. If all nations get on board, solving the terrorism problem will be a lot easier.

In the meantime, developing detection equipment is urgent. Let's work together, and I think we will find the solution. Thank you very much.

ROLE OF ADVANCED TECHNOLOGY IN THE SECURITY OF SURFACE TRANSPORTATION

Bernard B. Boubli
Head of Security
Eurotunnel

1. PREAMBLE

First of all, let me set the stage. Privileged with the honor of addressing this very learned assembly is a man who was ensconced in the United Nations system, wrapped in a dignified international civil servant robe and quite content with the prudent rhythm of progress of world affairs. For the past two years I have been thrust into the roller-coaster of the industrial arena, somewhat naked, but with the same resolve to serve security in its broadest confines. I have thus taken the plunge from 40.000 feet to somewhere around 100 feet below the sea bed and much to my surprise and relief have found the security equation to be broadly the same in its basic principles.

2. SECURITY -- THE UNINVITED GUEST

Like taxes and death, security is unavoidable in any transportation enterprise. It is often spoken of in the awed tones usually reserved for religious experiences and natural disasters, and the question of its implementation is a financial porcupine which bristles with difficulties as soon as it is touched.

The measure of its success is when a few years down the road, top management concludes that considerable amounts of money have been spent needlessly as nothing has happened after all.

Security costs money and has little to show for it. It intrudes and irritates by rearing its unwelcome head at the least opportune moments bringing along the need for that extra capital outlay, from a quester often suspected of mild paranoia.

It is perceived as abusive, cutting across boundaries, ruffling the neatly patterned feathers of well thought out organizational charts, treading on sensitive political toes and shamelessly trespassing.

All this is conventional wisdom.

In reality, security, like the medical discipline, concerns itself with prevention and protection of one and all, calling upon the use of similar equipment through diagnosis, prophylactic measures, containment and healing. In the process it intrudes in an otherwise perfectly happy life, censuring the petty vices, meddling in routine habits, and confining the patients to unwelcome enforced patterns.

Not heeding medical advice entails personal risk. Not heeding security advice entails collective risk.

This moderately long introduction was somewhat subliminal in nature, as it conveyed to the sub-surface the main components of this presentation, namely:

- The Threat Assessment
- The Regulatory Framework
- The Technological Dimension
- The Human Factor
- The Financial Hurdles

Before embarking on brief dissertations on these points, let me say how difficult it has been to write anything down which would not fall within the realm of plagiarism, in the light of the U.S. Office of Technology Assessment (OTA) report "Technology Against Terrorism: the Federal Effort". It is a superb document which steals the thunder from any presentation and makes one wonder why he is here, monopolizing the floor time so generously awarded by the organizers of this symposium. I therefore retreated to the international arena, an arena I know well. In spite of a few hidden skeletons in closets, one or two of which I was instrumental in concealing, I still believe it is the avenue that will ultimately lead to an enduring solution to the problems at hand through international cooperation which will foment the indispensable political will.

3. ROOTS OF THE EUROPEAN TERRORIST THREAT

Terrorism has ancient roots, with precedents in written history going back at least to Roman times when religious and nationalist groups used directed random acts of violence to oppose Roman domination. The OTA's "Technology Against Terrorism" report notes that:

> "There are, across the world, persistent conflicting political, social, and economic claims. Moreover, there will probably always exist frustrated and unstable individuals, delighted to devise an ideological or theological excuse to commit unconscionable acts."

Unfortunately, Europe has a long history of being a staging ground for such individuals.

The end of the cold war east-west conflict will not end or even reduce terrorism in Europe. The breakup of the Soviet Union and the end of its domination over Eastern Europe is likely to make terrorist acts even more dangerous and unpredictable. Competing nationalist, ethnic, and religious groups are likely to renew old rivalries.

These problems are not likely to remain in check within the territorial borders controlled by competing factions, but will almost certainly result in terrorist acts in Europe and other parts of the world.

The movement of refugees from struggling Eastern European countries to more prosperous Western European countries including Britain and France will create stresses. There will be high unemployment among the refugees until they can be settled, and there are likely to be right-wing nationalist backlash movements in those countries where the refugees threaten to displace existing workers from their jobs. The refugee movements across European national boundaries will provide a cover for terrorists posing as refugees.

3.1 The Nuclear Threat

Up to this point we have implicitly assumed that a terrorist threat would be conventional explosives or armaments. We cannot ignore a nuclear threat. Grave damage could be done without detonating a nuclear weapon within the target. Successfully positioning an artifact and holding the facility and people in it hostage would give terrorists the means to force their will upon us. The threat of the release or dispersal of radioactive materials including radioactive medical isotopes or nuclear waste, is also a threat which cannot be ignored.

How real is the nuclear threat? The "Technology Against Terrorism" report chillingly states that:

> "The spectre of nuclear terrorism, such as the theft or detonation of a nuclear bomb, the use of fissionable material or intensely radioactive waste as a radioactive poison, or the seizure or sabotage of nuclear facilities, is seen by many experts as plausible and by others as inevitable."

At this point, a thought comes to mind: even though illicit narcotic substances do not create a hazard with the same degree of immediacy as that of an explosion, they nevertheless cause profound damage to the very fabric of society and may be considered as the ultimate, most sophisticated and enduring form of terrorism ever devised.

3.2 Inadvertent Threats

Security must also take into account inadvertent threats to the security of an installation. Inadvertent threats are those where the driver of a truck or other vehicle may unbeknownst to him be carrying substances which constitute a threat.

In many instances, the driver is not even aware of the nature of the cargo or of the potential danger when transporting items that are corrosive, toxic, or potentially explosive in a high speed transportation, variable pressure environment.

4. THE REGULATORY FRAMEWORK

In 1988, during a revision of Annex 17 to the Chicago Convention, the International Civil Aviation Organization (ICAO) introduced two new recommendations which for the first time alluded to research and development (R&D) and technology in an international instrument.

These recommendations dealt with the need at the national level to promote R&D of new security equipment, and at the international level to encourage cooperation through the pool of efforts in this field in recognition that the answer to curb acts of unlawful interference would be tributary to technological advances.

"Each Contracting State should promote whenever possible research and development of new security equipment which will better satisfy international civil aviation security."

"Each Contracting State should cooperate with other states in pooling their efforts in the field of research and development of new security equipment which will better satisfy international civil aviation security objectives."

This little noticed amendment to Annex 17 marks a quantum leap in the progress of the security discipline, recognizing that beyond law making, directives, procedures and international agreements, the reliance on advanced technology had finally been acknowledged by the international community.

Unfortunately, no such formal international law making exists for other modes of transport, such as surface/maritime where the size of the containers to be examined dwarfs the airlines passengers' hand or checked baggage and even the freight pallets.

Before exiting this very brief foray in the regulatory framework I wish to leave you with a thought about the battle we are facing: while a full fledged international instrument has recently been adopted dealing with the marking of explosives to enhance their detectability, plastic weapons are being developed unabated and marketed by legitimate firms to defeat the technology deployed to detect them. Indeed, food for thought about our modern society.

5. THE TECHNOLOGICAL DIMENSION

This field is plagued by a proliferation of vocabulary where "existing" technology is assumed to be "proven" technology or where "shelf" technology is assumed to be "mature", not forgetting "down scaling" mistaken for "downgrading".

Wholesale judgments are often uttered about such or other technology as colored by the vendor's more or less successful pitches.

An exchange of information on evaluation methodologies on national and international levels would save much time and effort to all concerned.

a) It would facilitate the exchange of meaningful test results yielding knowledge on how an equipment performs because the test procedures were known.

b) Individual testing methodologies would improve and the best test method would emerge (from the combination of many).

c) It would influence the setting and revision of standards in a constructive manner.

d) It will prevent sterile duplication of work with allocation of funds to other pressing tasks.

Different test methodologies will exist for different types of equipment. Some are easier and more straightforward to define (archway metal detectors), others much more taxing (explosives vapor detectors).

One thing is certain however: it is far easier to define a testing evaluation methodology than it is to define a standard (in case of vapor detectors, probably impossible). Furthermore, testing equipment to a methodology gives more information than checking performance against a standard.

The former puts competing equipment in rank order and allows the choice of the best equipment to be made for the specific problem encounter. The latter only gives the information that the equipment in question meets a minimum performance level which may or may not be relevant to the problem to solve.

This brings us to the very heart of this symposium. There is no such thing as good or bad technology. There is equipment better or worse suited to solve a specific equation, regardless of the intrinsic excellence or flaws of its technological foundation. The "Technology Against Terrorism" report notes that no single phenomenology can presently provide a high probability of detection of explosive devices and other hazardous material. A combination of sensors using different phenomenologies can provide the degree of security required in any particular case.

"....with today's or next year's technology a more effective and imposing system can be devised by combining several different ways of doing the same thing rather than relying on only one technique. In combining technologies the strength of some {....}

could compensate for the weaknesses of others. Such a systems approach, combining different technologies .... would be difficult to test and would introduce great additional uncertainty for the terrorist".

"Uncertainty to the terrorist"; here are a few words worth pausing to reflect on.

The randomness of terrorist attacks gives the illusion of their infinite ingenuity and our boundless vulnerability, discouraging many parties into immobilism. Turning the randomness factor against the perpetrators is probably the single most powerful weapon at our disposal and can be achieved through increased security awareness, but above all, by keeping the terrorists, as much as possible, with the uncertainty of the limitations of the technology deployed: nuclear interrogation methods handsomely fit the bill.

The optimum approach to implementing a high-technology security system employing different complementary sensor phenomenologies is an Open Architecture combined with centralized information processing and control.

The Open Architecture philosophy allows system capabilities to be increased or decreased as examination priorities change with changes in the perceived threat. The Open Architecture philosophy allows the configuration to be modified with advances as they become cost-effective and operationally mature. The information, processing and control capability should allow integration of sensor and data inputs centrally allowing interaction and co-ordination with Government Authorities and Law Enforcement Agencies whose efforts are concentrated at border crossing or other sensitive points.

The relevance of the equipment to the problem encountered is the single most important issue in any selection decision and is mainly governed by three interdependent parameters:

a) Weight (amounts to be detected)

b) Throughput (time allocated)

c) Reliability (false alarming)

It is clear that for an aircraft at 35,000 feet, *the amount* to be detected must be as small as possible because of the consequential phenomena which create greater hazard than the explosion itself. *Time* is also of the essence if commercially tenable throughput is to be maintained. *Reliability*, directly affected by amount/time, becomes problematic.

It is precisely these three factors at the levels required that have caused the technological hurdle to the development of the ideal equipment for aviation security.

For surface transportation, the *critical amount* to be discovered is considerably higher, thus easing the pressure on the two other factors exponentially.

Military or customs anti-terrorist activity is of course less dependent on any of the three factors: any *amount* will do if it can be discovered, *time* will be taken as necessary, which increases dramatically *reliability*.

5.1 Basic Assumptions

- The main objectives of terrorist organizations are to publicize their cause or to undermine the authority of the Governments.
- To achieve both objectives, it is necessary to perpetrate their attack while the target is newsworthy and a headline maker.
- For the press, the glory of success or the aftermath of a tragedy are equally material for sensational headlines that sell copy.
- However a modest amount of explosive would be sufficient to cause damage, a major fire, a derailment, or a sequence of incidents resulting in tragedy.
- A high incidence of anonymous threats entailing mass evacuation would have profound negative impact on the public, similar to that resulting from an actual explosion.
- For this reason, while it is imperative to prevent the introduction of an explosive device, it is equally imperative to be in a position to manage the flow of anonymous threats and avoid unnecessary panic mass movements.

- To do so, it is necessary to have in place a reliable security system which affords the possibility to identify, within certain boundaries, those few anonymous calls that ought to be taken seriously, thus avoiding repeated disruption of traffic flows and maintaining a smooth operation pattern.

- There is no such thing as 100% security. The time factor in any commercial venture is incompatible with acceptable flows and attempts to implement exhaustive measures could grind the system to a halt or slow it down to commercially untenable levels, with the same negative impact a physical assault on the structure would have.

- It is therefore necessary to seek a balance threat/reliability which a happy marriage between technology and creative procedures could bring about.

- A particular technology, tailored to suit the specific equation, would go a long way towards ensuring maximum security. However, the resources necessary may reach a threshold beyond which reasonable compromise becomes necessary.

6. THE HUMAN FACTOR

The security system must be designed to provide an examination capability to protect the facility against terrorist threats and against the intentional or inadvertent transport of corrosive, toxic, or explosive materials. The options are the use of human inspectors to physically examine selected vehicles, or high technology systems using sensors and information processing systems providing data to trained analysts.

It must be capable of providing an inspector with the information required to detect and identify explosive and toxic, corrosive materials carried in a vehicle. The system must be highly reliable. The system must be capable of providing consistent results under all environmental conditions encountered. The system must be capable of a high throughput without being an intrusion and a nuisance.

The performance of human inspectors is highly dependent on alertness and motivation. Hot or cold temperatures in the inspection area, illness or emotional distress, and a range of other factors impact inspectors' effectiveness.

Unlike high technology sensors, a human cannot detect bombs or other dangerous materials purposely or inadvertently hidden inside a vehicle or its contents. Because of the inherent physical limitations of the human senses, an unacceptably high level of intrusiveness would be required to provide an acceptable assurance that hidden bombs will be detected. The only method of reliably detecting hidden explosives in a vehicle, using human inspectors, is to laboriously and intrusively dismantle suspected vehicles. Such a system is obviously not consistent with high throughput requirements.

7. THE FINANCIAL HURDLE

Security should transcend borders, nationalities, interest groups and commercial considerations. Terrorists belonging to opposing factions have routinely united to perpetuate their nefarious deeds.

Our divisiveness, micro-ambitions, shortsighted interests and lack of global vision is their best and cheapest weapon.

The financial factor is a flagrant display of our shortsightedness. The security investment is always dwarfed by the human, commercial and legal consequences of an occurrence.

The awesome scientific potential, material, and know-how gathered at this meeting is like a priceless mosaic waiting to be put together by a magic wand into a universal solution to the problem at hand.

This, of course, is a dream, dissipated by otherwise very legitimate preoccupations such as, for the private sector, funding, competitiveness, patents, market share, confidentiality, return on investment, and contractual wizardry; and at the Governmental level, the need for transparency, equal opportunity, equitable distribution, elaborate administration, political mood, public opinion pressures, etc.

You will forgive me for dreaming of an elusive philanthropist unencumbered by all these legitimate constraints, taking the plunge to harness the R&D in progress, guiding it towards the universal system which would put the terrorists, and ourselves, out of business!

Ladies and Gentlemen, a speech is like a love affair. Any fool can start it, but to end, it requires considerable skill.

Let me close on the findings of a corporate audit of A.C.M.E.'s Symphonic Orchestra.

> "During considerable periods, the four Oboe players had nothing to do. Their number could well be reduced and the work distributed more evenly throughout the entire concert, thus precluding idle time."
>
> "All of the 12 Violins were playing identical notes. This seems to be unnecessary duplication. The staff of this section could be drastically cut. If more sound were required, it could be boosted by electronics."
>
> "Much effort was observed in the playing of demi-semi-quavers, this appears to be an unnecessary produce refinement. It is recommended that we merely round off all notes to the nearest semi-quaver to make use of trainees and lower classification operators."
>
> "There also seems to be too much repetition of certain musical passages... no useful purpose can be served by repeating on the Horns something which has already been handled by the Strings.. concert time of two hours could be reduced to 20 minutes."
>
> "Finally, further investigation could be made into obsolescent equipment. The lead violinist's instrument was centuries old... if normal depreciation schedules had been applied, this instrument's value would be zero and the purchase of more modern equipment could have been considered."

REFERENCES

1. Office of Technology Assessment, "Technology Against Terrorism". The Federal Effort, OTA-ISC-481 US Government Printing Office, July 1991.

2. International Civil Aviation Organization Annex 17 to the Convention of International Civil Aviation. "Security, Safeguarding International Civil Aviation Against Acts of Unlawful Interference".

THE UK PERSPECTIVE ON AVIATION SECURITY

Richard H. Doney
Principal Scientific Officer, Transport Security Division
Department of Transport
United Kingdom

1. INTRODUCTION

This presentation summary is divided into two parts. The first sets out the views of the UK government on aviation security in general and identifies the major thrusts of its policy. The second part describes how that perspective affects our attitude toward technology. It discusses a number of questions which will have to be satisfactorily answered before we can come to place reliance on explosive detection systems.

2. UK SECURITY VIEWS AND ACTIONS

The UK has for a long time been at the center of world affairs. It has direct experience of security problems in many areas. It is a major player in civil aviation.

2.1 Role of the Department of Transport

The Department of Transport has an interest and responsibility in all modes of transport. It is the lead department in ensuring that the UK meets its international transport security obligations. In the aviation and maritime security fields, it has extensive powers under two Acts of Parliament to introduce and enforce security measures.

2.2 Events over the Last Decade

Substantial attacks over the last decade fall into three groups: hijackings, bombings, and airport attacks. Although there has been an international response to these attacks, its implementation has not been consistent. The type of any future attack remains difficult to predict.

2.3 Reaction of the Public

Attacks have raised public expectations about aviation security. But reaction is variable, seemingly depending on 'how close to home' the event is. Perhaps the public expects more from aviation security than can be realistically delivered.

2.4 The Future

An extensive realignment in world order is taking place. The impact on international terrorism is uncertain. How will this affect aviation security?

2.5 Threat and Risk

Many states have based their regimes on having a capability to intensify security in response to a change in the threat. The UK has questioned this approach. Being aware of changes in threat in time to respond is difficult if not impossible.

2.6 Host State Responsibility

This is a principal concept of Annex 17, but its interpretation is dependent on the attitude of individual states. Differences in interpretation can lead to difficulties for governments and carriers. Less developed countries often perceive terrorism as a problem of the industrialized states, not theirs. They may have other priorities due to scarce resources.

2.7 UK Action

The UK seeks to improve aviation security. Measures which will ensure that every person and article carried on board an aircraft is "safe" are being introduced progressively.

3. UK PERSPECTIVE ON SECURITY TECHNOLOGY

3.1 The Operational Requirement for Screening

The requirement for screening - for example, bags - can be simply stated as a question: "Is this bag safe to fly - yes or no?" Screening systems are required to operate in an environment which shares many of the

characteristics of a production line. The process is akin to quality control where a 'defect' is the inclusion in a bag of a prohibited item. People and their possessions have to be processed at high rates. What effect does this have on the nature of the equipment required? Can systems be constructed which meet this operational requirement?

3.2 Perceptions and Limitations

Those involved in science and technology have a long history of overselling their products. As a result, optimistic claims about the abilities of smart new machines are often accepted by a naive public as the truth. This faith in the ability of machines to detect explosive devices poses a problem for those trying to design effective screening systems.

The usefulness of a screening machine is often determined by what it cannot do rather than what it can do. Manufacturers' brochures rarely point out the limitations of equipment. This is the task of those who trial (test) equipment for governments and users.

3.3 Automated Systems

Automated decision making is often given as a key goal by people searching for effective explosive detection systems. It is held to be somehow 'better' than human decision making. Is there a real advantage? Will there be no role left for people?

3.4 Development Paths

It is a big step from knowing that a particular technology will meet the operational requirement to having machines rolling off a production line. Many technologies are currently at the prototype stage: realistically, few can survive in the competition of the marketplace. What options exist for creating an orderly market which manufacturers can afford to invest in? Is the 'EDS specification/certification' route appropriate?

3.5 Trialing (Testing)

Trialing (testing) under realistic conditions is the key to understanding how a particular technology can be integrated into a composite security system. Results can often be interpreted in a variety of ways according to particular tastes and prejudices. Many new technologies rely on complex algorithms to distinguish a bag with anomalous characteristics from its safe companions. Bag characteristics vary from country to country, destination to destination. How do we trial (test) and operate machines whose performance had to be optimized according to 'local rules'?

3.6 UK R&D Programme

The R&D programme is structured under three headings: equipment, human factors and system studies. This structure recognizes the fact that an effective security system is dependent on a balance of technology and procedures. It is unlikely that technology alone will ever provide a total solution.

INSIGHTS INTO U.S. DOMESTIC AVIATION

Richard Redman
FBI Bomb Data Center
FBI Academy

During the past decade it has been statistically and violently established throughout the world, that the terrorists main weapon of choice is the bomb! Use of a bomb does not require the presence of the terrorist at the time the violence is perpetrated and its ugly devastation seizes the attention of the media and consequently, the public. What could be more satisfying for a terrorist than to wreak destruction and gain widespread attention at the same time by using a relatively safe and simple act.

Too many U.S. Airline executives reason that because since 1949 only 143 people have been killed in the United States by bombs exploding aboard aircraft, that statistic should be the crucial indicator in evaluating the potential threat. Such a view, "It hasn't happened yet, so why think it will?" is so short sighted and unwise in the present world's climate, and is oblivious to the considerations of motivation and opportunity.

A lot about how and why terrorists choose their targets is known. I myself have been trained in target analysis and am well aware of how open this country is to terrorist attack. Concerning the possibility of domestic attack, all but one of the necessary conditions are already present--the terrorists' resolve to commit them.

Domestic aviation targets are as viable as other conventional domestic targets, i.e. power grids, ports, POL (petroleum, oil lubrication), etc. As international aviation security tightens, U.S. domestic aviation becomes a more inviting target to terrorists groups bent on hitting U.S. symbols.

Although only 143 people have been killed since 1949 in the U.S., 2,152 people were killed by bombs exploding aboard aircraft abroad in the same time period. Many terrorists groups do perceive commercial aviation as an extremely attractive target, and will continue to do so. Also, there isn't any reason to believe that future aviation attacks will be only against aircraft in flight. Attacks at airports are very possible, and have happened before.

Does our present use of screening machine technology provide an adequate defense at our nation's airports? In the 1970's the aviation security considerations were geared to prevent the rash of skyjackings that were taking place. The advent of metal detectors, x-ray machines, and the human screeners, were intended to prevent guns and knife weapons from getting aboard aircraft. Because skyjacking decreased significantly in the succeeding years, many people in the aviation industry believed that these preventive measures were directly responsible for the successful results. Such believers are dangerous obstacles to establishing a really excellent aviation security system, for they believe their own hype and that real security can be accomplished at relatively little cost and effort. They believe that people who think otherwise are alarmists. One need only look at the screening test failures of undetected firearms and simulated bombs to realize the tragic potential had those been actual guns and bombs. Furthermore, the FAA test guns and bombs are unrealistic and are displayed in an unrealistic fashion, almost as if intended to be easily discovered by screeners.

As a member of the FBI/FAA Airport Vulnerability Survey Team, I assessed airport bombing security considerations from the areas of perimeters, parking, airport concourse, screening points, AOA's, and bomb squad/canine capabilities. My assessment is based on known capabilities of terrorist groups (from past terrorist operations of fact) and reasonable expectations of increased capabilities based on my knowledge of, technology and training easily obtainable by not only a determined dedicated terrorist group, but also by the public. My question was simply, could a determined and reasonably equipped person or persons penetrate the aviation/airport security and place and

detonate an explosive device? The answer was equally simple-Yes! My conclusions were that even the unsophisticated attacker could achieve success to an extent that I cannot specify further in this paper.

In the U.S., aviation and airport security is focusing too much on the commercial passengers and their carry-on baggage. Since for years now the aviation terrorists have demonstrated that their current modus operandi is in the use of baggage-hold bombs, I must conclude that we are not even fashionably reactive in our aviation security effort! Aviation security can only be as strong as its weakest area, and domestically we are neglecting whole areas of concern.

Technology will, and should, play a large role in accomplishing an effective security for our aviation industry and the U.S. public. It is crucial to public safety that effective explosive detection systems are developed and implemented.

ROLE OF ADVANCED TECHNOLOGY WITHIN A BROAD SECURITY APPROACH

Pascal Morvan
Air France
1, Square Max Hymans
75015 Paris
France

1. INTRODUCTION

When I first participated in the Symposium on Explosives Detection in Mannheim in July 1989, my experience in that field was limited to two years of responsibility for bomb squad personnel (1983-1985). I was very impressed by the technological advances made during the prior four years, as well as the enthusiasm of the speakers.

Only two years later we can say that this great enthusiasm was justly founded. The political pressure which precipitated the effective development of equipment and the more restrictive regulations which require implicitly the use of EDS equipment have created the present climate for use of EDS. Nevertheless, in reality the practical solutions are yet to be found for several reasons:

1) Economic considerations (cost);

2) Difficulty in integrating the new EDS equipment in an existing airport environment;

3) Uncertainty in defining and quantifying the threat; and

4) To be convinced to enter into the process of implementation.

2. TYPES OF THREAT

I would like to elaborate on detection methods based on the types of threat. Knowledge of the threat is essential and should define the choice of explosive detection technique to be deployed. Let's consider three cases.

- The first is the search for and **detection of residue or vapor.** The state of the art of this technology is such that if there is even one molecule of explosive collected in the detection chamber it can be detected by some methods (biotechnology, laser detector). However, two questions arise:

1) Is the ability to collect the sample as good as the ability to detect it (I'm afraid the answer is no)?

2) Is there any vapor in the ambient to detect (at least one molecule)?

I have a partially negative answer to this second question. Last year in French Biscaye separatists from ETA successfully concealed bombs in steam pressure cookers to avoid detection by dogs. Similarly, terrorists have also used a data sheet explosive to defeat x-ray systems. All terrorists adapt remarkably well.

They have knowledge of detection procedures especially if used systematically, and they have knowledge of performances of technologies such as vapor or residue detection. All attempts made to conceal explosives - for example, with polypropilene sheets - have been successful. This consideration appeals to a non-systematic, complementary use of this technique.

- Secondly, is the **detection of bulk explosive.** This technology has been most effective because, unlike vapor detectors, small amounts of residue that pose no real threat - for example, on clothing - will not alarm the system. However, the presence of a critical amount of explosive, which is a real threat, will be detected by a bulk explosive detection.

The nature of the explosives to be detected is no longer a question. Even if you are exhaustive and include liquid explosives, such as ammonium nitrates, etc., the list should not exceed more than 100 different compositions.

The amount of explosive that must be detected, on the other hand is the most controversial and difficult problem. This should be the first issue addressed before selecting EDS equipment. A 20% difference

in the minimum quantity of explosive to be detected makes a huge difference in terms of the technology. The false alarm rate, the time of examination and cost are issues - especially when you reach the limits of detection. This has been illustrated by the difficulties of the first convincing industrial product available, the TNA.

For many years the assessment of the minimum quantity has been based on empirical knowledge and the result of accidents. The critical quantity was alleged to be around one kilo. Discussions have been reopened for recent accidents - in particular PA103.

The only certain fact is that the problem of detection of bulk explosives is made difficult by variables, such as size of the plane, location of explosives, and environmental conditions.

Serious studies on these parameters have been started. These studies require new theoretical knowledge; for example, to determine the rupture criteria of light plane structures to the fast shock wave produced by explosions or the role of vibration phenomena in the rupture process. For that reason, the first results will probably not be available for a few years.

Facing the limitations in detecting small quantities of bulk explosives, the natural response is to harden the airplane - even though the largest uncertainty is in determining the weak point of the plane and the best method of hardening. However, it will be much more difficult to reach a uniform hardening throughout - especially on existing planes. Furthermore, it should never require transforming the planes into battle tanks. The emergence of future planes containing 600 to 1000 passengers could be the opportunity to introduce a requirement (the exact figures need to be determined) which can facilitate the desired hardening criteria.

- Thirdly is the **detection of ignition components.** Ignition components are detonators, batteries and electronic circuits. So many components in passenger bags contain batteries and electronic circuits which give very high false alarm rates, as is the case with classical x-ray. Nevertheless, that is the only method - combined with hand search - that can be used today on a large scale. The recent improvements in the field of x-ray are very encouraging, because they are more specific to the threat, and because they facilitate the human decision.

The search of detonators is very interesting given the fact that all commercial or military detonators contain heavy metals (mercury, lead) and that their shape is supposed to be well-known. For the terrorists who have knowledge of what detects these detonators - since it is written in every aviation newspaper - it will be necessary to modify the shape of existing detonators. This is not easy and could be dangerous. Another option is the use of chemical components but they are more difficult to handle and less efficient than classical detonators.

Whatever the method is, explosive detection technology has made some notable progress for checked-in baggage for which equipment will be available in the very short term.

The solutions for bulk explosives, for example, are TNA or better TNX whose performances can still be improved. Progress has also been made with tomography scanners. Vapor detectors, eventually associated with x-ray, can be a valuable solution but only as an alternative or additional measure for the reasons which I mentioned before. However, these systems and even detonator detection techniques remain costly in terms of manpower.

Furthermore, the performance of PFNA, PFNX and gamma ray resonance absorption show exciting potential for future solutions (PFNA for example will probably be able to check an entire container of baggage at one time). This could simplify the costly manpower and handling problems. For these systems to be effective, the false alarm rate must be minimized.

Generally, the problem of false alarms becomes more critical when the EDS system is operated far from the passenger check-in area. However, if inspection is performed at the check-in counter, it causes long lines and delays which inconvenience passengers and requires a large inspection area. Then the path to secure between the controls and the plane is very long, which increases the risk of pollution of the supposed controlled baggage during the transfer. The shortened flow path decreases the ability of the terrorist to place a bomb. Therefore, we need to focus on the subject of secured zones and access control. Although these are not really the topics of this session, they are necessary complements to explosive detection strategy. It would be useless to spend millions of dollars for detection equipment and at the same time permit holes in the security shield

by failing to consider secured zones access control and other basic measures like matching the passenger and the baggage.

All the components of access control systems are now well known and operational (CCTV, locks with badges for personnel and cars, remote control computer system, etc.). But I don't know of any airport where the problem is satisfactorily solved. It is very difficult to control the movement of tens of thousands of airport personnel who have good reasons for moving throughout the airport. This problem is compounded when you have a great percentage of temporary manpower. The future security solutions must be found on restricted zones and the need for persons to pass from one zone to another with as little hinderance as possible.

Additionally, other traffic such as mail and express freight, must be considered. The solution developed for controlling baggage must be easily applied to this traffic. More progress must be made, but large x-ray systems and more efficient methods like PFNA will offer some valuable solutions.

One difficulty observed with the introduction of the large x-ray equipment is the treatment of suspect items, because it is necessary to have a nearby, safe, well equipped area to deal with alarms in order to avoid blocking the system. If this is not the case, the operators will bypass the system after a few false alarms.

As you can see, it is easy to do an intellectual exercise on security given the availability of equipment.

We must not forget that planes leaving high-tech airports return from countries with smaller airports that are not in a position to finance such systems. In those airports the airlines must develop complementary measures. More portable, easy to use equipment is required and there are too few new ideas in that field. I would like to emphasize the necessity for progress noting that very often the least equipped countries are those where the risks are the highest.

3. CONCLUSION

- EDS solution is not unique, they have to adapt to each airport with minor modifications. There is not an ultimate system, but one system for every airport. This diversity will also be a deterrent for the terrorists.

- Security should obviously take into account the economical aspects. This is especially important in relative peace and recession times. I'm convinced it is possible to advance future technologies in a cost effective way, both in terms of capital cost and associated manpower. The security solution should provide safety and ease of movement for passengers, baggage and other traffic.

- The knowledge of the threat, in terms of quantity of explosive is solvable, it requires only enough money and time.

Finally, I would like to remind you of a terrible French experience. We should not build another Maginot line. We must be flexible and not focus on only one solution.

As a complement to development of innovative technology for detection, we must continue to develop a global approach to security problems and an international security blueprint in order to coordinate between all security measures. With these conditions we will be better armed to solve a problem which can be compared to an open Fort Knox, with visits of tens of thousands of people per day, and the capability to detect in that flow, 24 hours a day, a needle in a haystack.

NUCLEAR TECHNIQUES

PRINCIPLES OF NUCLEAR-BASED EXPLOSIVE DETECTION SYSTEMS

Tsahi Gozani
Science Applications International Corporation
2950 Patrick Henry Drive
Santa Clara, CA 95054

1. INTRODUCTION

During the last decade, and in particular since 1985, great strides were made in research, development, design, construction, and deployment of nuclear-based detection of bulk explosives. Nuclear techniques are shown to provide the only feasible approach for meeting the demanding requirements of operation in the security arena in general, and at airports in particular.

In the past decade, plastic explosives became the weapon of choice for terrorists, most spectacularly demonstrated in mid-air explosions of airliners with disastrous loss of life and property. This has motivated the development of rapid and effective explosive detection systems (EDS). Though during the last year there has been an apparent lull in successful airline sabotage, there is no reason to believe that this situation will continue through the decade of the 90's. Terrorism -- national and international, whether motivated by political, narcotic or any other cause -- is still very much with us. In fact, the change in world order manifested by the massive breakdown of political entities is a great source of instability and tends to further exacerbate the situation.

This paper briefly reviews the wide tapestry of possible nuclear techniques for explosive detection. From this wide selection, some feasible and a few practical techniques, which can comply with the tough operational requirements, are emerging.

The paper describes the requirements for explosive detection sensors and the reasons why nuclear techniques are uniquely responsive to these requirements. The "nuclear" (i.e., elemental) signatures of explosives, available nuclear reactions, and other nuclear scientific considerations are discussed and demonstrated with the aid of results from sensors or systems which are in advanced stages of R&D or fully deployed.

2. SYSTEM ENGINEERING OF EDS

The development of a functional EDS, esoteric as it may be, has to follow the rational life cycle of the system engineering discipline (Figure 1). This generic life cycle states the obvious (which is unfortunately sometimes lost in the sea of enthusiasm of the inventive mind). Once the need for the development, in our case, of an explosive detection system, has been identified, the customer (i.e., FAA, airline, etc.) has to define and specify, preferably in consultation with the potential developers, the requirements of the system in order to fulfill its mission. The developer needs to analyze and fully understand these requirements and the system's specifications. He then proceeds to the stage, defined in the diagram as "Conceptual Design". In our developmental sequence it may entail:

- identify possible solutions;
- identify possible technologies;
- establish and understand the scientific basis for the technologies;
- select the proper technology that is most responsive to the requirements;
- develop a notional concept;
- iterate the above process;
- finalize a conceptual design with sufficient details for the ensuing engineering design of the system.

We will follow below some of the most important steps mentioned above.

3. GENERIC SYSTEM REQUIREMENTS

EDS requirements can be divided into three basic categories: performance, operational and safety as listed below.

3.1 EDS Requirements

Performance Goals

- Positive detection of presence or establishing the absence of explosives;
- Sensitive to all known civilian and military explosives;
- Insensitive to explosive configuration or concealment method;
- Sensitivity threshold at minimum amounts of explosives needed to cause fatal damage;
- Fully automated operation and decision making, though the decision as to the final disposition of suspected objects is obviously done by a high-level human operator.

Operational Goals

- Non-intrusive;
- Throughput rate which does not adversely affect airport routine;
- Relisble and easy to maintain;
- Simple to operate ("user friendly") (should not require too high a level of personnel to operate);
- Reasonable price and running costs;
- Reasonable space and site requirements.

Safety

- No significant radiation risks to personnel or passengers;
- Non-hazardous to inspected items;
- Does not fog film; does not damage magnetic media.

4. POSSIBLE SOLUTION

Once the system's requirements are identified and understood, the developer needs to survey for possible solutions for explosive detection. There are several techniques, methods, or procedures that are purported to "detect" explosives. These techniques/procedures fall into five groups:

- Profiling/intelligence
- Hand search
- X-Ray techniques
- Vapor detection and canine
- Biological
- Magnetic
- Active nuclear techniques.

While each technique and procedure is valuable, except for the last category, none is truly an explosive technique, failing one or more important parts of the EDS requirements. The role of the first four categories in a total security system is very important. This role would not be obfuscated, but enhanced further once an efficient, rapid and automated EDS is deployed.

5. GENERIC FEATURES OF CONTRABAND

Nuclear techniques using highly penetrating radiations, as probes and induced ones, i.e., neutrons and gamma rays, are inherently non-intrusive and amenable to automation--two important requirements of any effective EDS. However, the most unique capability of nuclear-based EDS is probably its ability to directly, and generally unambiguously, detect fundamental features of contraband. Nuclear techniques can detect elements (actually isotopic nuclei) via their unique nuclear structures. However, unless contrabands possess unique chemical and, hence, elemental signatures that distinguish them well from benign materials, the potential of nuclear techniques would not be realized. Fortunately, explosives and narcotics are well-separated in one or more elemental features from most common materials. Generically, most military and some commercial explosives are denser than benign materials and are richer in oxygen and nitrogen and relatively poorer in carbon and hydrogen. Narcotics, on the other hand, are about as dense as most common household goods. They are relatively richer in carbon and hydrogen and poorer in oxygen (and nitrogen). Table 1 shows a list of 50 materials--explosives, narcotics, and common materials that may

be carried in passenger luggage or shipped. The composition (covering all the major elements, i.e., H, C, N, O) of these materials is given in units of elemental density (g/cc). A graphic presentation of these compositions is shown in Figures 2, 3, and 4. These are three-dimensional plots, with the different elements along each axis. These plots and their two-dimensional projections show the degree of separation of explosives and drugs from benign materials. The more features used, the better the separation. In addition to one, two, or three-dimensional features, i.e., explosive may be distinguished by detecting high O-density, high N-density, and low C-density simultaneously, one can also develop non-linear signatures. A good example of this is the ratio of carbon to oxygen densities (see Figure 5). It is unusually low for explosives and unusually high for narcotics. Many more signatures are possible. The selection of the most effective ones depends on the specific nuclear techniques used, its design, and implementation. The basic elemental signatures, important as they are, define only a theoretical discrimination capability between contraband and benign materials. It assumes a perfect measurement and observation of the pure (unmixed) materials, e.g., either contraband or explosive. In reality, the measurements are far from perfect and the observations are made over volumes larger (or even much larger) than the ones occupied by the pure materials. This fact causes blurring of the separation between contraband and common materials. The loss of separation increases the probability of false detection and mis-detection. It underlines the importance of selecting techniques and methods of implementation that provide information as directly as possible, on as small a volume elements as possible. Different nuclear techniques offer that capability to different degrees.

6. SELECTION PROCESS OF NUCLEAR TECHNIQUES

Once the requirements of EDS have been defined and understood, the rather laborious selection process of the proper nuclear technique and its ensuing development commences. All nuclear-based EDS can be described by a very simple block diagram (Figure 6). All EDS have neutron or gamma-ray sources. These sources can be either radioisotopic or accelerator-based. The probing radiation has to be "processed"--namely gamma rays and fast neutrons, are usually collimated and/or modified, e.g., high energy neutrons are slowed down to thermal energies. The probing radiation interacts with the material's content of the luggage. The interactions may create unique signatures of the specific elemental constituents present in the probed object. The resulting signals from the interactions with the various elemental constituents can be one or more of the following:

1) Specific change in the intensity of the probing radiation (n, or γ) from a resonance absorption and/or scattering. This change is superimposed on the overall attenuation of the probing radiation which, in this context, is considered as background.

2) Specific energy loss for the probing fast neutrons via elastic scattering.

3) Inducing emission of specific gamma rays, promptly or as a result of delayed activation, as a result of neutron capture or inelastic scattering.

The induced (or modified probing) radiations are detected by an array of appropriate detectors located in the vicinity of the probed object. The detector signals are usually processed firstly via analog electronic processing and then digitally. The information from all detectors is analyzed by a main computer which, based on prior calibration and information can make the decision to clear the object or to alarm. The various components of the EDS raise a lot of technical issues. The most important ones are listed below.

- Nuclear reactions, e.g., (n,γ), (n,n) $(n,x\gamma)$, (γ,γ); (γ,n), (γ,p), (γ,xn)
- Cross-sections, branching ratios, angular distributions
- Sources of radiation - radioisotopes, accelerators, steady state or pulsed (fast or slow)
- Detectors - type, size, efficiency, energy resolution, time resolution, sensitivity to probing radiation, stability
- Electronics/Data Acquisition (hardware and software) - count rate and data rate, miniaturization
- Structural and shielding materials

- Decision Analysis (hardware and software) - image reconstruction, feature analysis, classical, and/or advanced decision techniques (e.g., ANS)

A flow chart for the development of a system based on a nuclear technique is shown in Figure 7. It shows the complex interrelation between the myriad of factors and issues affecting the design of the system. Proper considerations of these items in the design and construction will ensure (at least technologically) a successful EDS.

7. SELECTION OF NUCLEAR REACTION(S)

Critical to successful development of responsive EDS is the selection of the proper nuclear reactions. Though many nuclear reactions involving the nuclear constituents of contrabands are accessible, only few lead to the responsive EDS. The list of accessible nuclear reactions is given in Table 2. The table lists the isotope being probed, the probing radiations (i.e., n or γ and their energy range), the nuclear reaction of interest and its measurable products, the name of the technique or system (developed or being researched) which uses the specific nuclear reaction, and finally a comment which qualitatively identifies the main strength and weakness of the reaction. Specificity indicates how positively that isotope indicates the presence of explosive. Sensitivity indicates the strength of the measured signal. This is a qualitative assessment based on the magnitude of the cross-section for the nuclear reaction, the ease and precision with which the reaction products can be detected, signal-to-noise ratio, strength of the signal given the needed source intensity, etc. Even a superficial look at the table will reveal that some nuclear reactions are wholly inappropriate for EDS as they do not fulfill several of the most important system requirements.

8. REACTION CROSS-SECTIONS

The selection of the most appropriate nuclear reaction(s) for the EDS requires the study of the reaction cross-sections ($\sigma(E, E', \Omega)$). This entails the variation of the cross-section as a function of the probing neutron (or gamma-ray) energy (E), angular (Ω) and energy (E') distributions of the scattered and induced radiations. The exact behavior of all these qualities is important in assessing, via modeling and simulation, system performance. Many reactions are well studied and their cross-sections are well known. This statement is particularly correct for neutron capture (n,γ) process, where the cross-section for thermal and epithermal neutrons are well known along with the branching ratio of the resulting gamma rays.[1] The main parameter for the thermal neutron analysis (TNA) technique is the (n,γ) reaction in ^{14}N. The production cross-section of the key gamma ray (10.8 MeV) in TNA is 10.6 mb. Other very important physics parameters are the total absorption thermal neutron cross-sections in the common elements encountered, for example, in passenger bags: N - 1.9 b, H - 0.33 b, Cl - 33.2 b. Similarly the gamma ray scattering and absorption in all energies of interest are well known and the cross-section values are reliable. The cross-sections for elastic scattering of fast neutrons in the energy range of 0.5 to 14 MeV are important to all techniques that use these neutrons as the probing radiations (i.e., fast neutron analysis - FNA, pulsed fast neutron analysis - PFNA, neutron elastic scattering - NES, neutron resonance attenuation - NRA). The value of these cross-sections (energy and angular dependence) are well known for most elements of interest in explosive contraband detection. Figures 8a, 8b, 8c, and 8d show the neutron elastic scattering cross-sections of H, C, O, and N. The main feature of these cross-sections is the resonance structure in the energy range of 0.5 to 6 MeV in the C, N and O. The baseline (without the sharp structure) cross-sections in all of these elements, including hydrogen, have the same basic shape. In fact above 7 MeV, with few exceptions, the cross-section is almost constant at about 1 barn value. Thus the neutron penetrability, which is dominated by the cross-section for elastic scattering (and to a lesser extent, by their angular dependence) decreases rapidly as the neutron energy is lowered.

The resonance structure in the neutron scattering was used by Overley[2] to determine the H, C, N, and O content in relative small samples of bulk materials (e.g., grains). Since each element has unique resonances and other features superimposed on the baseline shape, the attenuated neutron flux through the probed object should reflect the structure, showing depleted flux at the specific resonance. This technique called neutron resonance attenuation (NRA) requires varying (sweeping) the neutron energy or using pulsed wide (e.g., "white") neutron spectrum, and time of flight (TOF) technique. By solving as many (or more) equations as the number of elements present, one can, in principle, get a two dimensional projection, along the neutron beam line, of the elemental content of the object. Unfortunately when

the probed object is large the neutron multiple scattering tends to "fill-in" the depleted area greatly debasing (lowering the signal to noise) the information. Beyond a certain thickness, depending on the elemental content and density, very little useful information, with the possible exception of information on the average physical density, can be obtained. A related technique to NRA is neutron elastic scattering (NES) technique proposed by Pennetron Inc.[3] It is based on the small difference between the fast neutron energy loss in elastic collision with carbon, nitrogen and oxygen. For example, the maximum energy loss for backscattered neutrons is 28.4% in C, 24.9% in N and 22.1% in O. However, detecting small energy changes with good accuracy is difficult. The discrimination between the various elements can be enhanced by using the structure in cross-sections mentioned above. Again, the multiple scattering occurring in bulk samples is detrimental.

The situation in regard to the cross-section for neutron inelastic scattering, the production of gamma rays from these reactions, and their angular distribution is not as good as that of the elastic scattering cross-sections. While the basic phenomena and the approximate value of these parameters are well known, a detailed look shows larger uncertainties than desirable. An example to this situation is given in Figure 9. This figure shows the cross-section for the production of 6.13 MeV gamma ray in the neutron inelastic scattering on ^{16}O. Three evaluations are shown. These evaluations slightly differ in the location of the peak energy of the resonances but greatly differ in the absolute value of the cross-section. It is interesting to notice that even the cross-section with the lowest value for this reaction in oxygen, and for that matter, in carbon and nitrogen (see Figure 10) is still higher than the (n,γ) cross-section in nitrogen, which is the basis for TNA. The cross-sections shown in Figure 10 are fundamental to the Fast Neutron Analysis (FNA) and Pulsed Fast Neutron Analysis (PFNA) techniques.[4] In these techniques one particle goes in and a different one comes out: "neutron in - gamma out." The induced radiation is uniquely characteristic of the nuclei that created it. Its intensity however, is determined mainly by the probing radiation (neutrons) penetrability and the value of the cross-section for the specific interaction. The former is mostly determined by the cross-section for neutron elastic scattering discussed above. The latter is shown in Figure 10, indicating that the relative sensitivity will be the highest to carbon followed by oxygen and then nitrogen.

9. DETECTORS AND DETECTIONS

Successful design of a nuclear based explosive detection system requires the use of appropriate nuclear detectors. When using "neutron in - neutron out" techniques (i.e., NRA, NES), efficient neutron detectors are required. These techniques require not only the detection of the neutrons but also the determination of their energy. Thus neutron spectrometers with high efficiency and good energy resolution are needed. Such detectors are not readily available. Organic (plastic or liquid) scintillators do provide some energy information, through the proton recoil mechanism, but the unfolded pulse height distribution would not have the energy resolution required of the NRA and NES techniques. However these detectors are very useful, because of their relative high efficiency and excellent time resolution, when the neutron energy is determined by time of flight (TOF) technique. Indeed this is the technique used in the application of the NRA technique to determine the protein content of various grains.[2] Unfortunately TOF neutron spectrometry is very inefficient and requires a very strong pulsed neutron source and long measurement time.

All techniques that require gamma ray spectrometry have a wider range of detectors to choose from (see e.g., reference 5). The choice of a gamma ray detector depends on the specific technique and is influenced by: efficiency, energy resolution, the ability to handle high count rate, time resolution, stability, sensitivity to the probing radiation (e.g., 14 MeV neutrons), geometrical constraints, cost, availability, etc. The most commonly studied and used gamma ray detectors for "neutron in/gamma out" techniques are (in decreasing order): NaI(Tl), BGO, BaF_2. The various considerations in using these detectors are discussed in reference 5. Some examples are shown below. The first is a pulse height spectrum of an NaI(Tl) detector in a TNA system measuring a typical heavy passenger luggage containing an explosive simulant (Figure 11). This spectrum illuminates, in capsule, many of the strengths and weaknesses of TNA. It shows the weak but unique and well separated peak of nitrogen. The very intense lower energy background underlines the importance of reducing pulse pile up. It also shows that by proper choice of detector size, shape and the special electronics, one can get very good gamma ray spectroscopy even at the very high count

rate required for TNA to be a practical high throughput explosive detection system.

In a practical FNA technique the probing radiation is a collimated beam of 14 MeV neutrons. These neutrons create a significant background in most gamma ray detectors. The ability to protect the gamma ray detectors from the direct beam and scattered neutrons is crucial for this application. Figures 12 through 14 show the quality of spectra that can be obtained from pure samples. Figures 12 and 13 are for graphite and oxygen (in D_2O) using NaI detectors and Figure 14 shows graphite spectra measured with a BGO detector. All spectra show the high background ("sample out spectrum") inherent to this technique. It also shows that the difference spectrum ("net spectrum") is of high quality and is usable. The ultimate spectroscopical quality can be obtained in the PFNA method using the same detectors. This is achievable because in the pulsed FNA the signal gamma rays can be separated by the time of flight (TOF) of the neutrons from the background events. A sample of PFNA spectra is given in Figures 15 through 20. All these spectra were measured in the time window when the neutrons interact with the sample. The time uncorrelated events (e.g., created by thermal neutrons interacting in the room or detector) have been subtracted.

10. PUTTING IT TOGETHER

Nuclear based explosive detection techniques can be qualitatively assessed by studying the strength of their signal for the most distinctive elemental signatures. Though such assessment is incomplete since it does not take other factors into account, it does provide a beneficial oversight. A sample comparison of the most studied techniques is given in Table 3. The stronger the nuclear signal of an element, which is most abundant in contraband, the better. The case of oxygen and nitrogen in explosive for FNA/PFNA and GRA respectively is a good example. However other cases, where low density of particular elements in contraband is the unique feature, are quite important if the nuclear signal is strong enough. This is the case of carbon in FNA/PFNA. In general the more signatures one can measure the better is the system performance: namely, low mis-detection and false alarm probabilities.

11. IMAGING CAPABILITIES AND DECISION ANALYSIS

The composition of contraband, though different from benign materials, when measured with any device will occasionally be classified as benign and vice versa. The ability to separate between the benign and the non-benign materials is determined by the number of relevant quantities (e.g., oxygen, carbon and nitrogen densities) that can be measured and the accuracy of their determination. This is shown in Table 3 for the three most studied explosive detection techniques. However, since the elements present in explosives and other contrabands are present in almost all materials commonly used, their presence is far from a conclusive evidence that an alarm should be sounded. The unmistaken presence of proper concentrations of these elements in amounts and proportions that are characteristic of contraband is a definite cause for an alarm. The more localized the information given by a technique, the more credible the decision to alarm. The ability to get localized signal is related to the imaging capability of the technique. Some techniques are inherently imaging techniques and are built as such. An example of this is the x-ray computerized axial tomography (CAT) system. Such a system can provide the physical density averaged over a small volume element (voxel) of several cubic mm. Among the nuclear based techniques, it is the PFNA that can, in principle, directly provide all key elemental components in as small voxels as 100 cm^3. The amount of explosives that can be packed in such a volume is very small (< 200 grams), thus offering very high sensitivities. Whether or not it is practical to screen every object to that small a detail (the number of such small voxels even in an object such as a suitcase is a couple of thousand) depends on the design of the system and the required throughput. Other techniques can provide spatial information on one or more of the elemental concentrations through straightforward image reconstruction techniques (e.g., TNA and FNA) or by very complicated mechanical means to provide tomographical information (e.g., multiple irradiation GRA). The rest of the nuclear techniques, in principle, provide only two dimensional projections of elemental concentrations (e.g., GRA for nitrogen, NRA for C, N, O) similar (but with poorer resolution) to x-ray images of projected physical density. Table 4 summarizes the current imaging capabilities of the nuclear based detection techniques. It should be recalled that the objective of an EDS is to detect a small but finite size explosive or contraband. The quality of the required elemental

image is not the same as for a standard x-ray, where a human operator tries to discern from the projected image whether a gun or knife is present. The automated decision algorithm of EDS uses the (generally crude) image as one, though very important, of several features to clear the screened object or alarm on it. Many of the features, e.g., contiguous detectors with the highest count rate, do contain information with a lot of spatial content. Thus, even without a full fledged image reconstruction, an EDS can make a reliable decision, as long as the technique has inherently the 3-D spatial content.

12. CONCLUSION

The obstacle course of developing a responsive nuclear based explosive detection system has been covered in this paper. It is recognized that rarely will all the steps that were described be followed. But total disregard of those steps by the developers (pursuing the approach of a "solution" looking for a problem) or by the potential users who need the development (vainly pursuing the magic "silver-bullet"), is a recipe for failure.

It is shown that properly conceived and developed nuclear based techniques can and do provide the means to detect explosives and contraband concealed in objects of all sizes in a manner compatible with the well-established requirements.

REFERENCES

1. "Prompt Gamma Rays from Thermal Neutron Capture," M. A. Lone, R. A. Leavitt and D. A. Harrison, Atomic Data and Nuclear Data Table, 26, 511-559 (1981).

2. "Determination of H, C, N, O Content of bulk Materials from Neutron-Attenuation Measurements," J. C. Overley, Int. J. Appl. Radiat. Isot., Vol 36, No. 3, 185-191 (1985).

3. "Neutron Elastic Scattering (NES) for Explosive Detection Systems (EDS) " H. J. Gomberg and B. G. Kushner, see this Proceedings.

4. "PFNA Technique for the Detection of Explosives," Z. P. Sawa and T. Gozani, see this Proceedings.

5. "Detector Selection for Nuclear-Based Explosive Detection System," W. Lee, J. Bendahan, P. Ryge and T. Gozani, see this Proceedings.

6. "An Explosive Detection System for Screening Luggage with High Energy X-Ray," J. Clifford, K. Habiger, R. Miller and W. McCullough, and "Explosive Detection for Checked Luggage by DETEX, A Combined X-ray and Positron-Tomograph System," H. W. Pongratz, see this Proceedings.3

Table 1
Elemental Densities (g/cc) of Contraband and Various Common Materials

	1 MATERIAL	2 H	3 C	4 N	5 O
1	NITROGLY	0.0352	0.2544	0.2960	1.0144
2	EGDN	0.0355	0.3256	0.2531	0.8658
3	AMNIT	0.0850	0.0000	0.5950	0.9860
4	BLPOWDER	0.0000	0.4026	0.1830	0.6588
5	NCEL	0.0384	0.3888	0.2256	0.9472
6	PETN	0.0422	0.3344	0.3115	1.0683
7	DETASHEET	0.0636	0.4647	0.1806	0.7711
8	TNT	0.0359	0.6031	0.3016	0.6895
9	COMP-B	0.0462	0.4172	0.5216	0.7302
10	PBSTY	0.0211	0.4651	0.2718	0.9302
11	TETRYL	0.0299	0.4864	0.4050	0.7404
12	DYN	0.0500	0.1750	0.2188	0.7375
13	HMX	0.0532	0.3078	0.7182	0.8208
14	C3	0.0464	0.3648	0.5248	0.6656
15	C4	0.0594	0.3614	0.5693	0.6633
16	PICRIC	0.0229	0.5526	0.3221	0.8606
17	PBAZ	0.0000	0.0000	1.2947	0.0000
18	TRIAC	0.1164	0.4644	0.0000	0.6192
19	HEXA	0.0906	0.5432	0.2120	0.7253
20	WOOL	0.0071	0.0563	0.0329	0.0377
21	SILK	0.0080	0.0593	0.0432	0.0395
22	DACR	0.0063	0.0938	0.0000	0.0500
23	ORLON	0.0086	0.1019	0.0396	0.0000
24	NYLON	0.1106	0.7262	0.1414	0.1619
25	POLYES	0.0056	0.1001	0.0000	0.0444
26	COTTON	0.0090	0.0720	0.0000	0.0690
27	RAYON	0.0093	0.0660	0.0000	0.0740
28	POLYET	0.1344	0.8056	0.0000	0.0000
29	POLYPR	0.1316	0.7884	0.0000	0.0000
30	PVC	0.0638	0.5107	0.0000	0.0000
31	SARAN	0.0419	0.4050	0.0000	0.0000
32	LUCITE	0.1056	0.6334	0.0000	0.4222
33	NEOPR	0.0550	0.8000	0.0000	0.0000
34	PAPER	0.0434	0.3080	0.0000	0.3451
35	ALCOH	0.1048	0.4168	0.0000	0.2720
36	SUGAR	0.1040	0.6720	0.0000	0.8240
37	OIL	0.0960	0.6160	0.0000	0.0880
38	BARLEY	0.0685	0.4320	0.0100	0.4700
39	SOYBE	0.0750	0.4900	0.0844	0.3510
40	WOOD	0.0441	0.3808	0.0000	0.2744
41	WATER	0.1110	0.0000	0.0000	0.8890
42	POLYUR	0.0869	0.5775	0.3058	0.1342
43	MELAM	0.0768	0.4576	1.0656	0.0000
44	HEROIN	0.0628	0.6820	0.0379	0.2166
45	HHCL	0.0569	0.6214	0.0345	0.1971
46	COCAI	0.0692	0.6730	0.0461	0.2110
47	COCL	0.0653	0.6003	0.0412	0.1883
48	MORPH	0.0067	0.7156	0.0491	0.1682
49	PCP	0.0104	0.8587	0.0576	0.0000
50	LSD	0.0078	0.7427	0.1299	0.0495

Table 2
Assessment of Accessible Nuclear Reactions for
Neutrons or High-Energy Photon Interrogation

No	Isotope	Probe (and its energy)	Used in the Listed Technique/System	Reaction	Comments
1	^{1}H	n_{th}	TNA	$^{1}H(n_{th},\gamma)^{2}H$	Low specificity, high sensitivity
2	^{1}H	n (slowing down spectrum)	TNA FNA/PFNA	Attenuation, thermalization, absorption	Low specificity, med-high sensitivity
3	^{2}H	γ(>2.2 MeV)		$^{2}H(\gamma,n)^{1}H$	Low specificity, very low sensitivity
4	^{2}H	n(14 MeV)		$^{2}H(n,2N)^{1}H$	Low specificity, very low sensitivity
5	^{12}C	n_{th}		$^{12}C(n_{th},\gamma)^{13}C$	Medium specificity, low sensitivity
6	^{12}C	n(>5 MeV)	FNA/PFNA	$^{12}C(n,n'\gamma)^{12}C$	Medium specificity very high sensitivity
7	^{12}C	n(>7 MeV)	FNA/PFNA	$^{12}C(n,np)^{12}B^{*}$	Medium specificity low sensitivity
8	^{12}C	n(>7 MeV)	FNA/PFNA	$^{12}C(n,\alpha)^{9}Be^{*}$	Medium specificity low sensitivity, high background
9	^{12}C	n(0.4 - 10 MeV)	FNA/PFNA NES/NRA	$^{12}C(n,n)^{12}C$	Medium specificity and sensitivity
10	^{12}C	γ(>19 MeV)		$^{12}C(\gamma,N)^{11}C$	Medium specificity, low sensitivity, extremely high (γ and n) dose rate, requires hi-E electron accel
11	^{13}C	n_{th}		$^{13}C(n_{th},\gamma)^{13}C$	Medium specificity, very low sensitivity
12	^{13}C	γ(>5 MeV)		$^{13}C(\gamma,n)^{12}C$	Medium specificity, very low sensitivity, very high dose rate
13	^{14}N	n_{th}	TNA	$^{14}N(n_{th},\gamma)^{15}N$	High specificity, low sensitivity, basis for TNA, to date most practical

No	Isotope	Probe (and its energy)	Used in the Listed Technique/System	Reaction	Comments
14	^{14}N	γ(9.172 MeV)	GRA	$^{14}N(\gamma,p)^{13}C$ 95% $^{14}N(\gamma,\gamma)^{14}N$ 5%	High specificity, low-med. sensitivity, basis for GRA, requires very intense proton accelerator
15	^{14}N	γ(11 MeV)	DETEX (MIDEP)	$^{14}N(\gamma,n)^{13}N^*$	High specificity, low sensitivity, very high (γ and n) dose rate
		γ(30 MeV)	"Nitrogen Camera"	$^{14}N(\gamma,2n)^{12}N^*$ $^{14}N(\gamma,zp)^{12}B^*$	High specificity, low sensitivity, very high (γ and n) dose rate, very high background, requires very hi-E electron accelerator
16	^{14}N	n(>3 MeV)	FNA/PFNA	$^{14}N(n,n'\gamma)^{14}N$	High specificity, med. sensitivity, high (14)/low (3 MeV) background
17	^{14}N	n(>7 MeV)	FNA/PFNA	$^{14}N(n,\alpha\gamma)^{11}B$	High specificity, low to med. sensitivity, high (14)/low (7 MeV) background
18	^{14}N	n(>7 MeV)	FNA/PFNA	$^{14}N(n,p\gamma)^{14}C$	High specificity, low sensitivity, high (14)/low (7 MeV) background
19	^{14}N	n(>7 MeV)	FNA/PFNA	$^{14}N(n,d\gamma)^{13}C$	High specificity, low sensitivity, high (14)/low (7 MeV) background
20	^{14}N	n(14 MeV)	FNA/PFNA	$^{14}N(n,2n)^{13}N$	High specificity, low sensitivity, high (14) background
21	^{14}N	n(0.4 - 10 MeV)	FNA/PFNA NES/NRA	$^{14}N(n,n)^{14}N$	High specificity, low sensitivity
22	^{16}O	n(>7 MeV)	FNA/PFNA	$^{6}O(n,n'\gamma)^{16}O$	High specificity, high sensitivity
23	^{16}O	n(>7 MeV)	FNA/PFNA	$^{16}O(n,p)^{16}N$	High specificity, low sensitivity

No	Isotope	Probe (and its energy)	Used in the Listed Technique/System	Reaction	Comments
24	^{16}O	n(>7 MeV)	FNA/PFNA	$^{16}O(n,\alpha)^{13}C$	High specificity, low E signatures, low sensitivity
25	^{16}O	n(0.4 - 10 MeV)	FNA/PFNA NES/NRA	$^{16}O(n,n)^{16}O$	High specificity, low sensitivity
26	^{16}O	γ(16 MeV)		$^{16}O(\gamma,n)^{16}O$	High specificity, low sensitivity, very high (γ and n) dose rate, high neut. background, require hi-E electron accel.
27	Cl	n_{th}	TNA	$^{35}Cl(n,\gamma)^{36}Cl$	High specificity, very high sensitivity (where applicable)
28	Cl	n(>3 MeV)	FNA/PFNA NES/NRA	$^{35}Cl(n,n'\gamma)^{35}Cl$ $^{35}Cl(n,np)^{34}S$	High specificity, high sensitivity (where applicable), high (14)/low (3 MeV) background

TNA - Thermal Neutron Analysis
FNA - Fast Neutron Analysis
PFNA - Pulsed Fast Neutron Analysis
GRA - Gamma Ray Resonance Attenuation
NRA - Neutron Resonance Attenuation
NES - Neutron Elastic Scattering
DETEX (MIDEP) - See Ref. 6.
"Nitrogen Camera" - Proposed by P. Trower

Table 3
Elemental Signatures of Contraband
And Their Strengths in Some Nuclear-Based EDS

Characteristic Feature	Explosives		Drugs		Nuclear Signal Strength		
	Level	Specificity	Level	Specificity	TNA	GRA	FNA/PFNA
Elemental Density							
N (Nitrogen)	High to V. High	High to V. High	Low	High	Low	High	Medium
O (Oxygen)	Very High	Very High	Low	High	0	0	High
C (Carbon)	Medium	Medium	High	High	Very Low	0	V. High
H (Hydrogen)	Low to Medium	Medium	High	Medium	Very High	0	High
Cl (Chlorine)	Medium in Percholate	High	Medium	V. High	Very High	0	High
Some Elemental Density Correlation							
O/C	High to V. High	High to V. High	Low	High to V. High	N/A	N/A	High to V. High
Cl/O	Low to Medium	High	V. High	V. High	N/A	N/A	High
O vs. N,	High/High,	Very High,	Low/Med.	High	N/A	N/A	High/Medium
O vs. C	High/Low	High	Low/High	V. High	N/A	N/A	High/V. High
Total Density	High	Low-Medium	Med.-Low	Low	High	Very High	High
Application					Suit-case Size	Suit-case Size	FNA - suitcase size / PFNA - from suitcase to shipping container

"Level" - Value of the elemental density in the explosives or drugs
"Specificity - How specific is the value of the signature (i.e., elemental density or some function of it) to the explosives or drugs
"Nuclear Signal Strength" - How strong the detected signal from the elemental signature. It is related to the nuclear cross section, means of detection, estimate of S/N, etc.
TNA - Thermal Neutron Analysis
GRA - Gamma-ray Resonance Absorption
FNA - Fast Neutron Analysis
PFNA - Pulsed Fast Neutron Analysis

Table 4
Imaging Capabilities of Nuclear Based Detection Techniques

Name of Technique	Primary Signatures	Secondary Signature	Imaging Capabilities	Comments
TNA	N	Cl, H	3-D, "Emission Tomography"	Limited view detectors improve spatial resolution, requires stronger source
FNA	O, C, N	H, Cl	3-D, "Emission Tomography"	"
PFNA	O, C, N, Cl, Others	Metals, Si, Others	3-D, Direct	Imaging methods improve S/N for the direct imaging, provides also H-imaging
GRA	N	-	2-D, Projection	
GRA	N	-	Pseudo 3-D, Multiple angle irradiation	Mechanically complex, longer measurement time
NRA	O, N, C	H	2-D	Poor S/N
NES	O, N, C	H	(3-D)	Poor S/N, complex, uncertain
DETEX[1] (MIDEP)	N	-	(3-D) (Direct imaging)	Requires extremely high dose rate, self absorption of signal (.511 MeV) gamma-rays, low efficiency, slow

[1]See Reference 6.

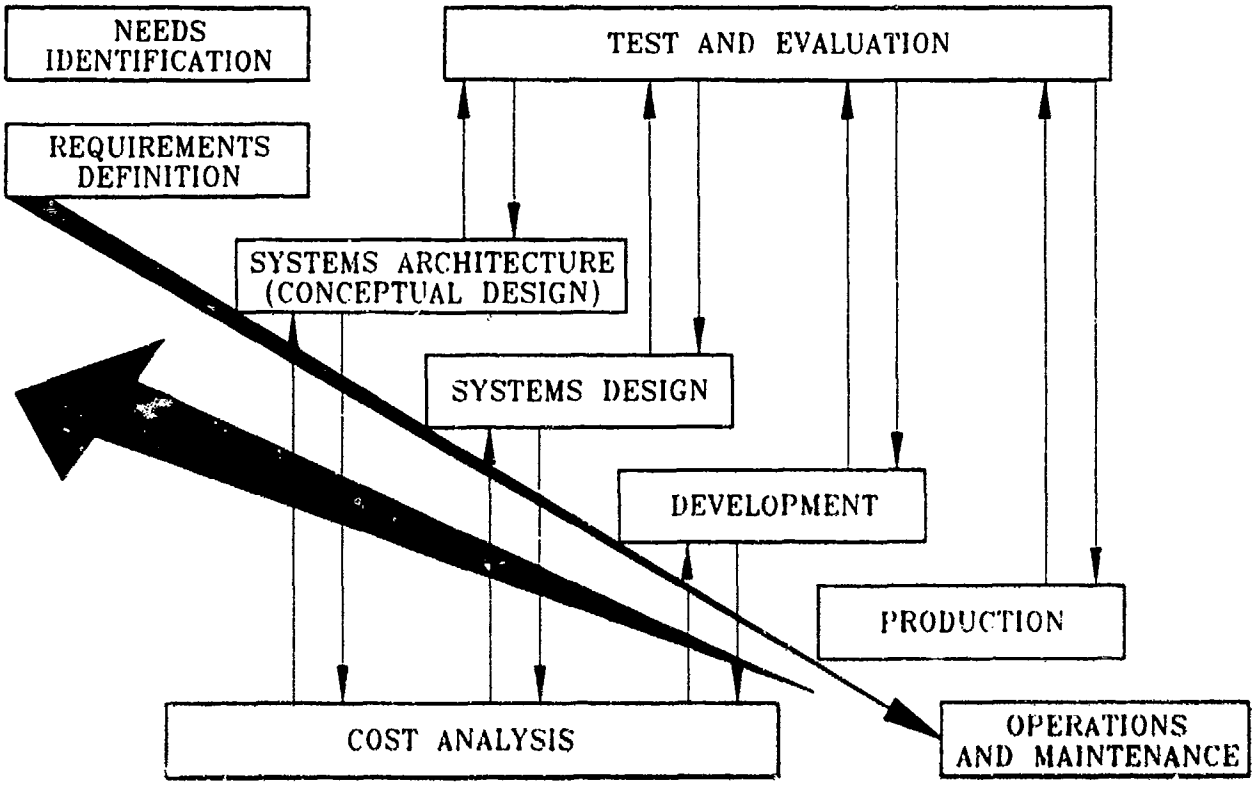


Figure 1 System Engineering Life Cycle

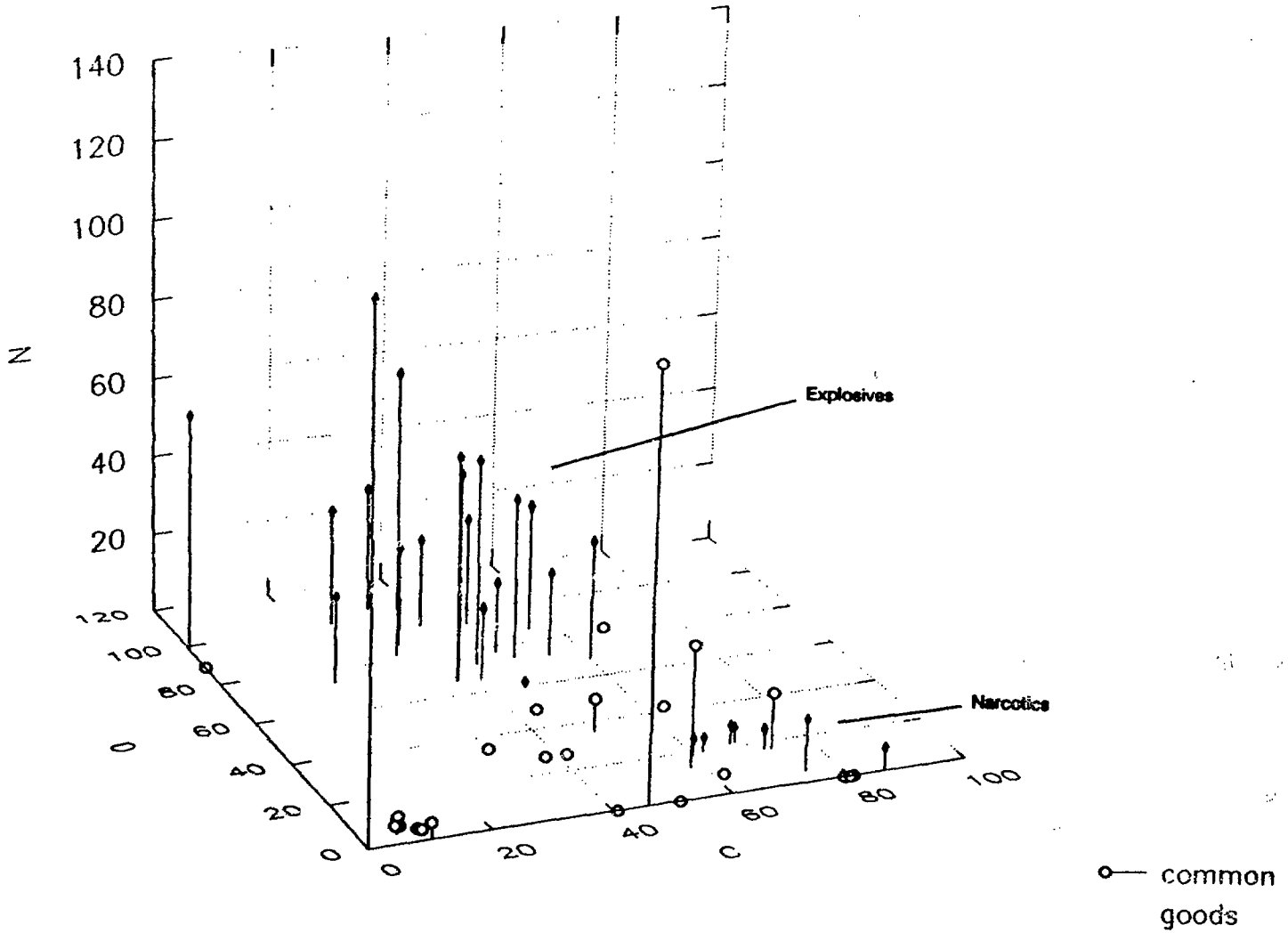


Figure 2 3-Dimensional (N,C,O) Representation of Elemental Compositions of Various Materials.

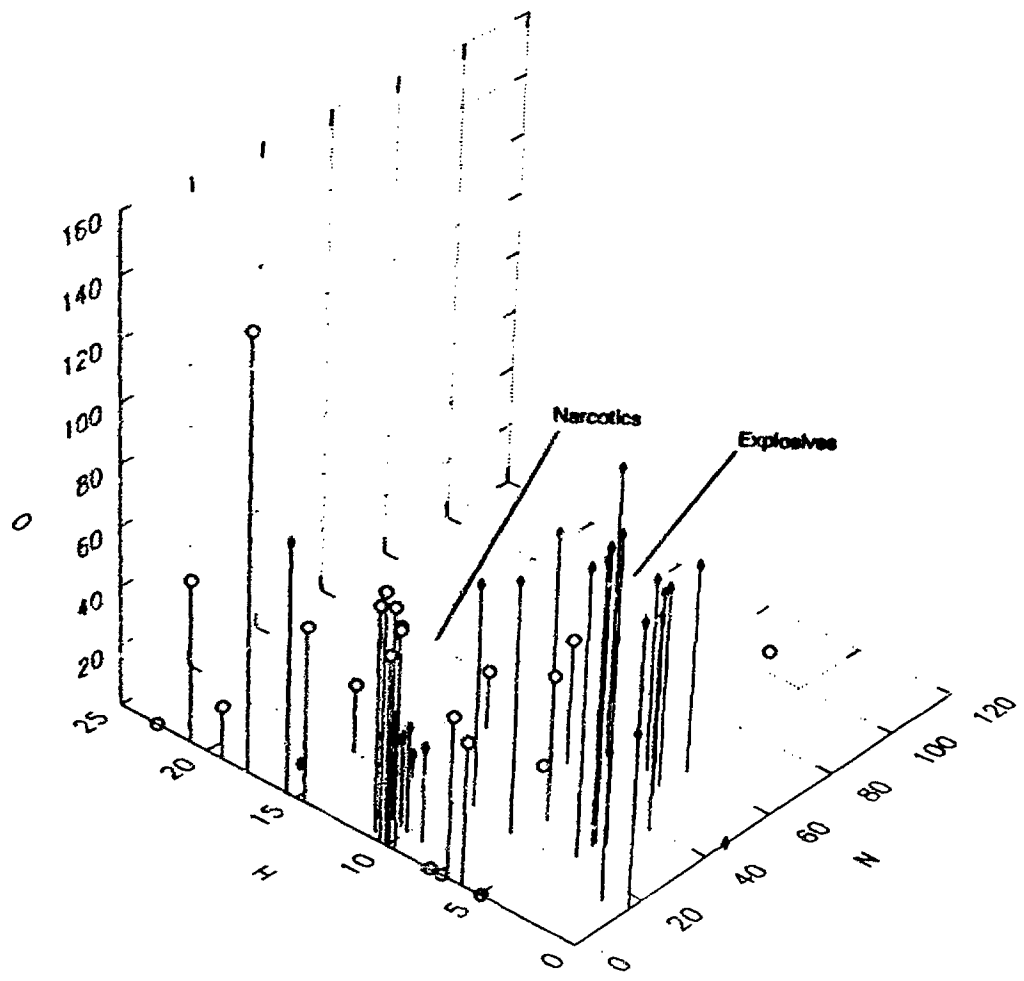


Figure 3 3-Dimensional (H,N,O) Representation of Elemental Compositions of Various Materials.

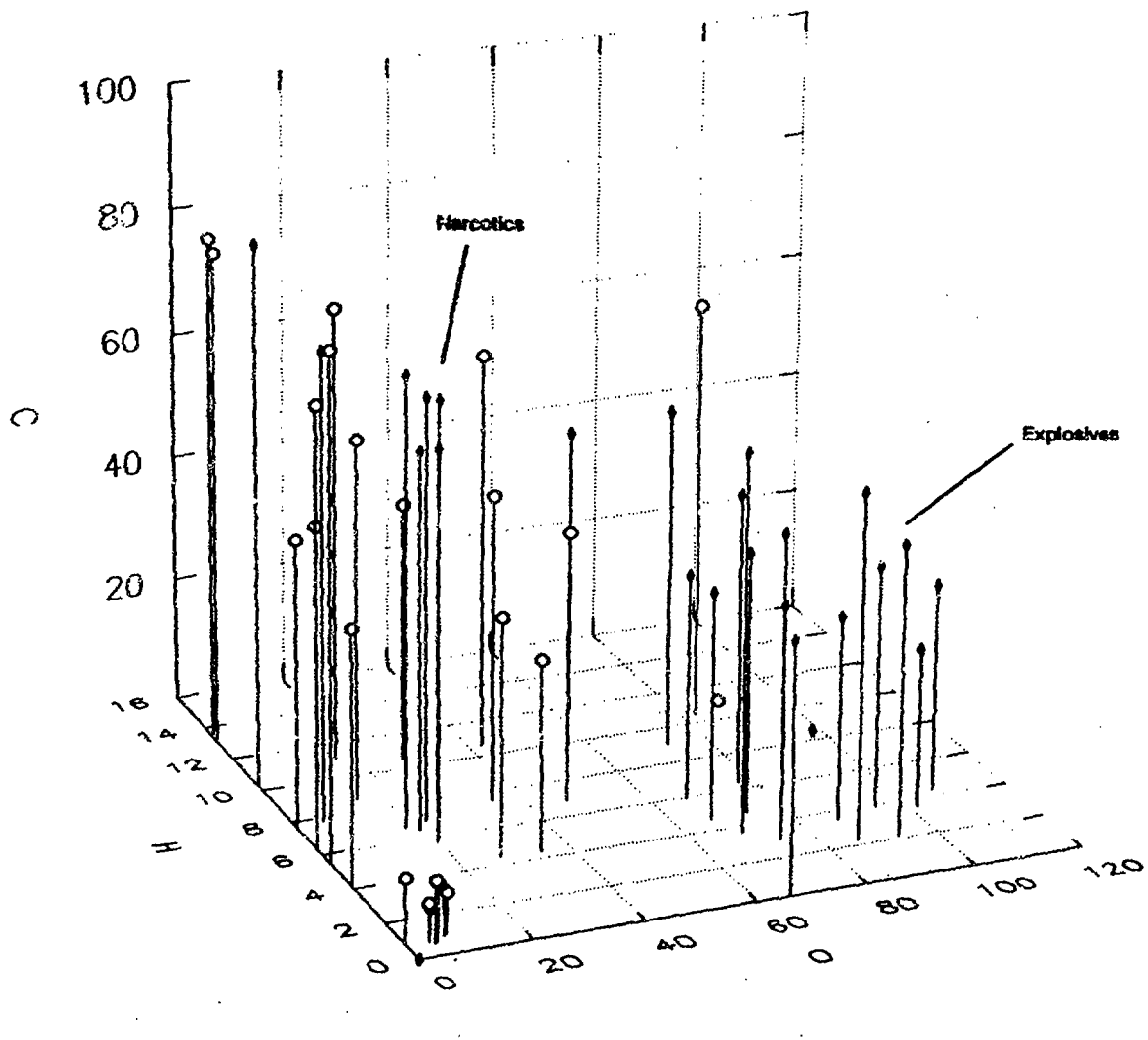


Figure 4 3-Dimensional (H,C,O) Representation of Elemental Compositions of Various Materials.

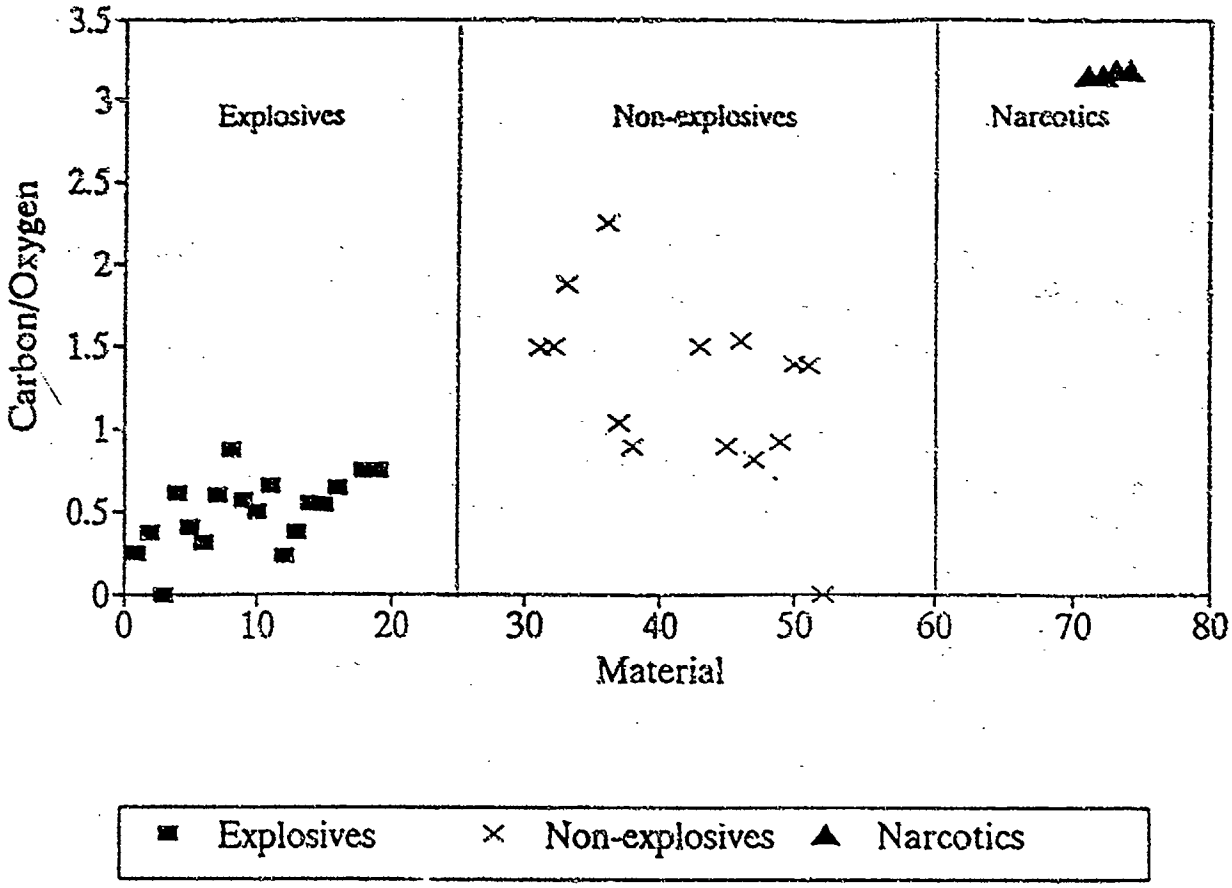


Figure 5 Ratio of Carbon to Oxygen Densities as a Signature for Contraband.

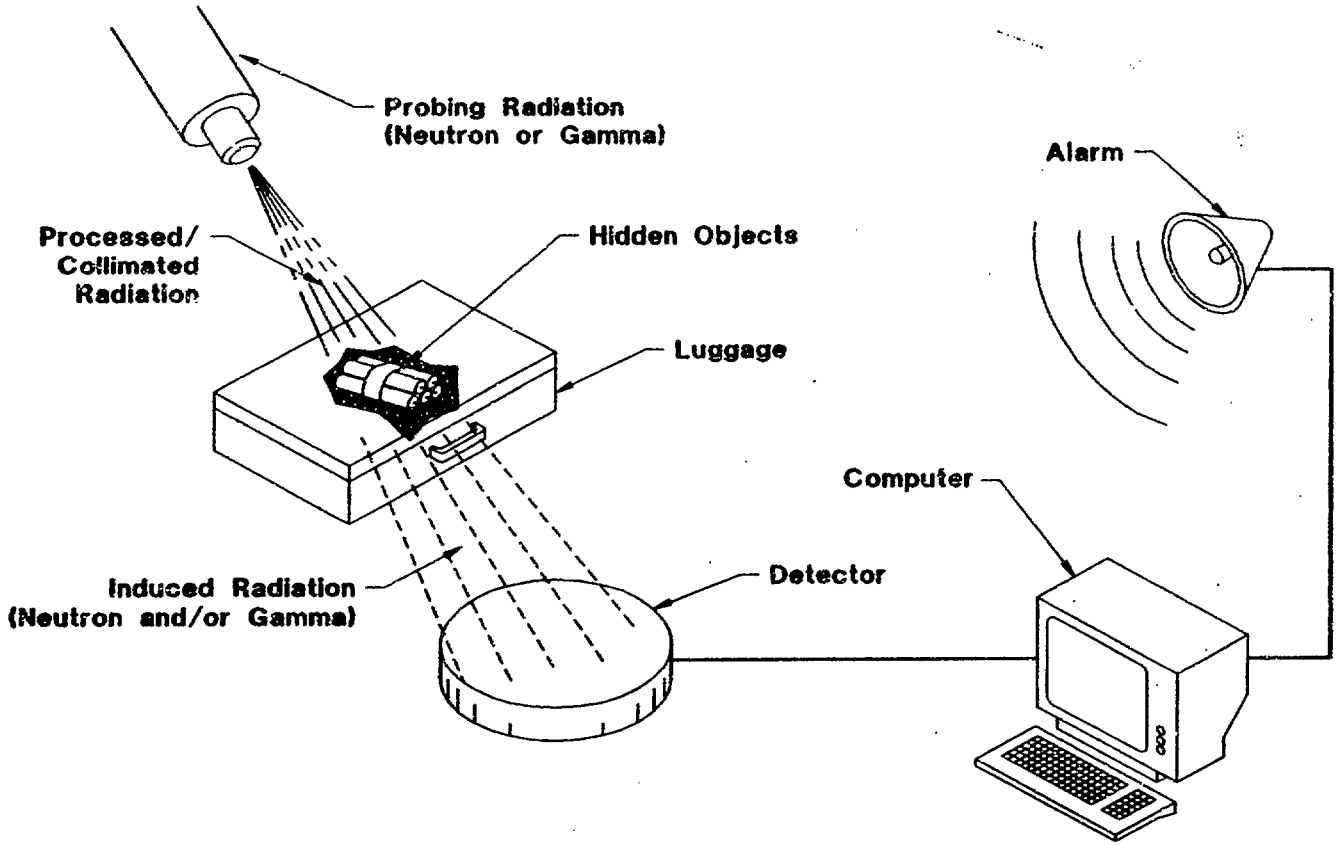


Figure 6 Basic Descriptive Diagram of a Generic Active Nuclear Based Explosive Detection System.

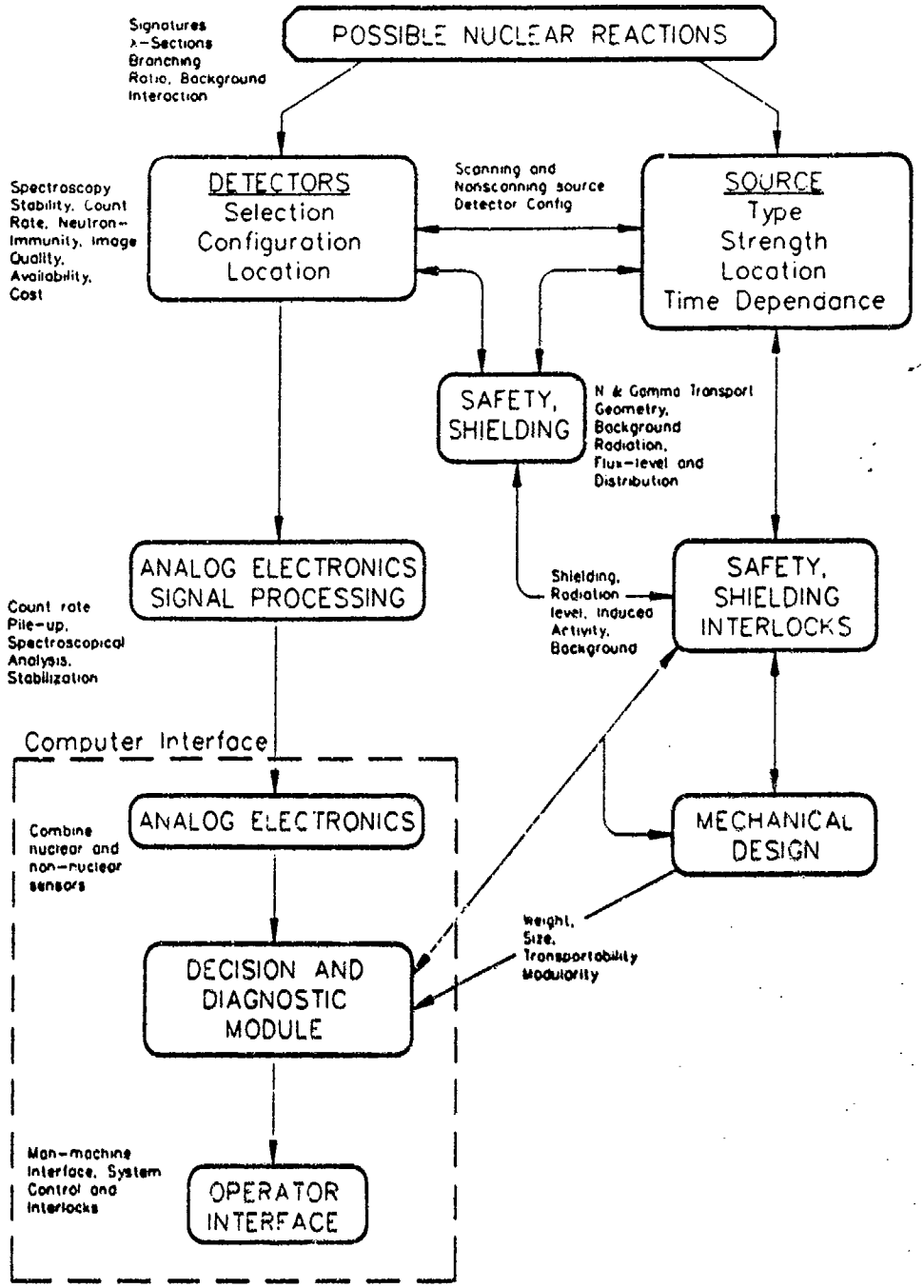


Figure 7 Flow Chart of Development of Nuclear Based Techniques

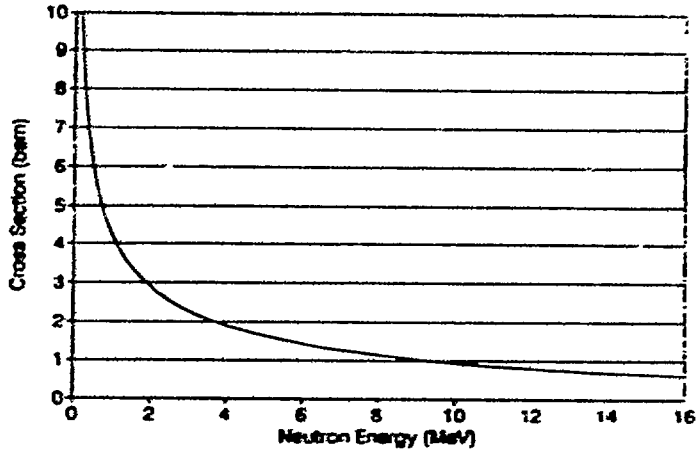


Figure 8a H Elastic Scattering Cross Section

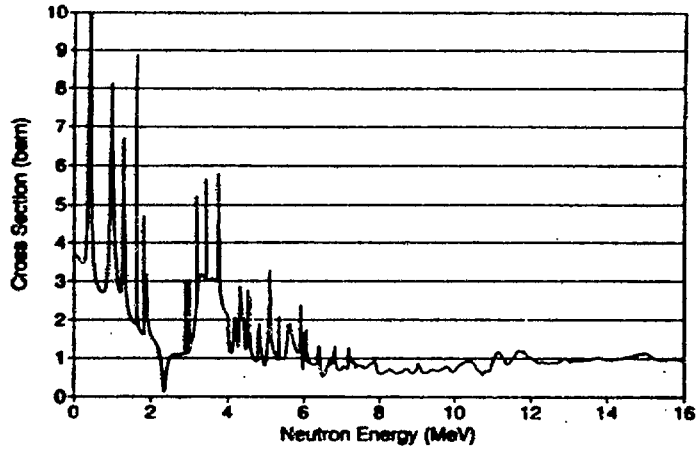


Figure 8c Oxygen Elastic Scattering Cross Section

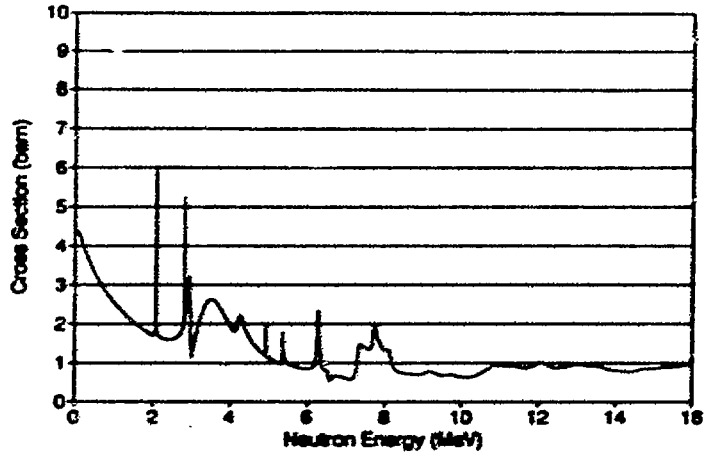


Figure 8b Carbon Elastic Scattering Cross Section

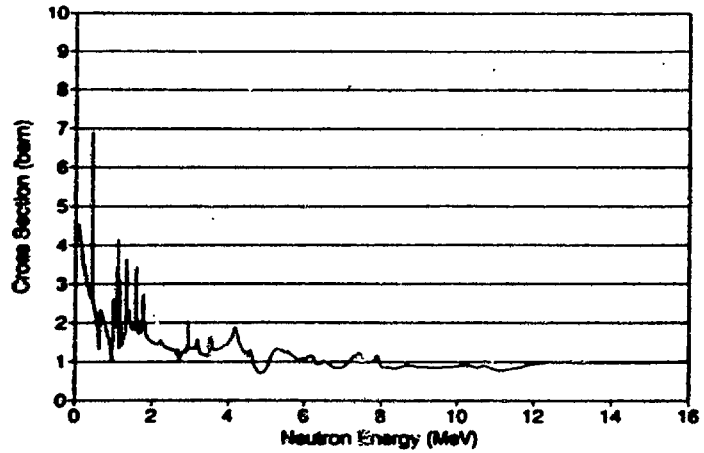


Figure 8d Nitrogen Elastic Scattering X-Section

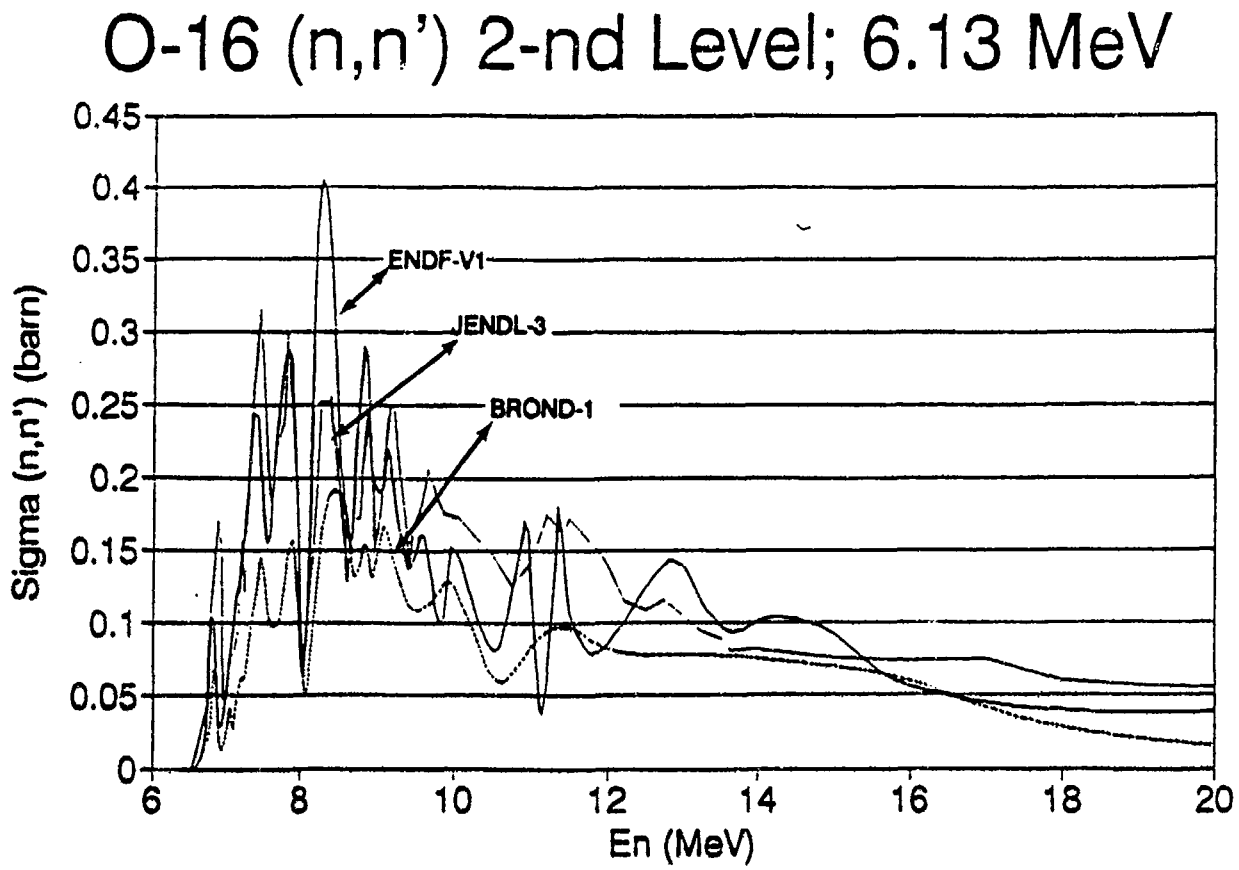


Figure 9 Oxygen (n,n,γ) Cross-Section - Different Evaluation/Computations

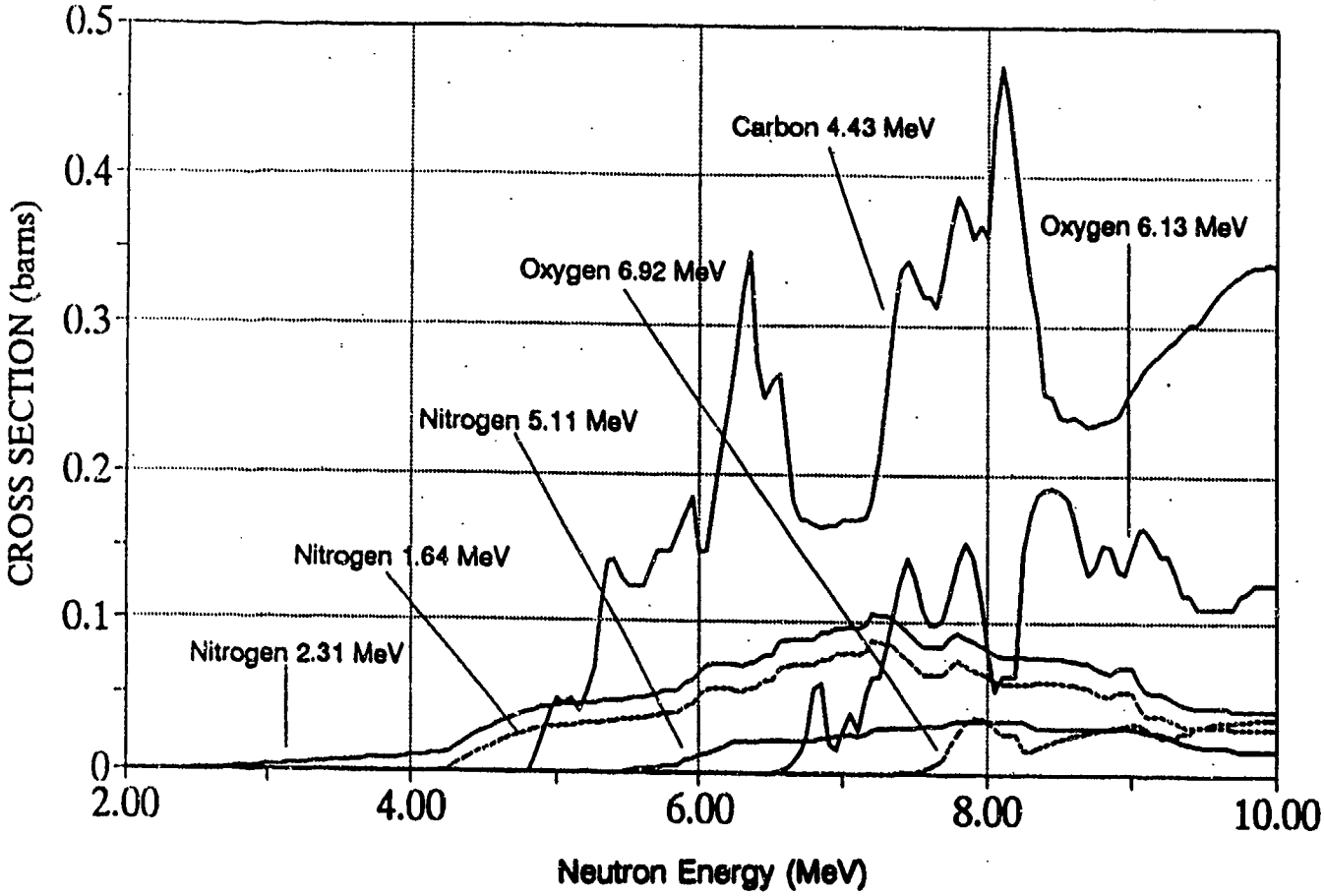


Figure 10 Gamma-Ray Production Cross-Sections Relevant to PFNA for Oxygen, Nitrogen and Carbon.

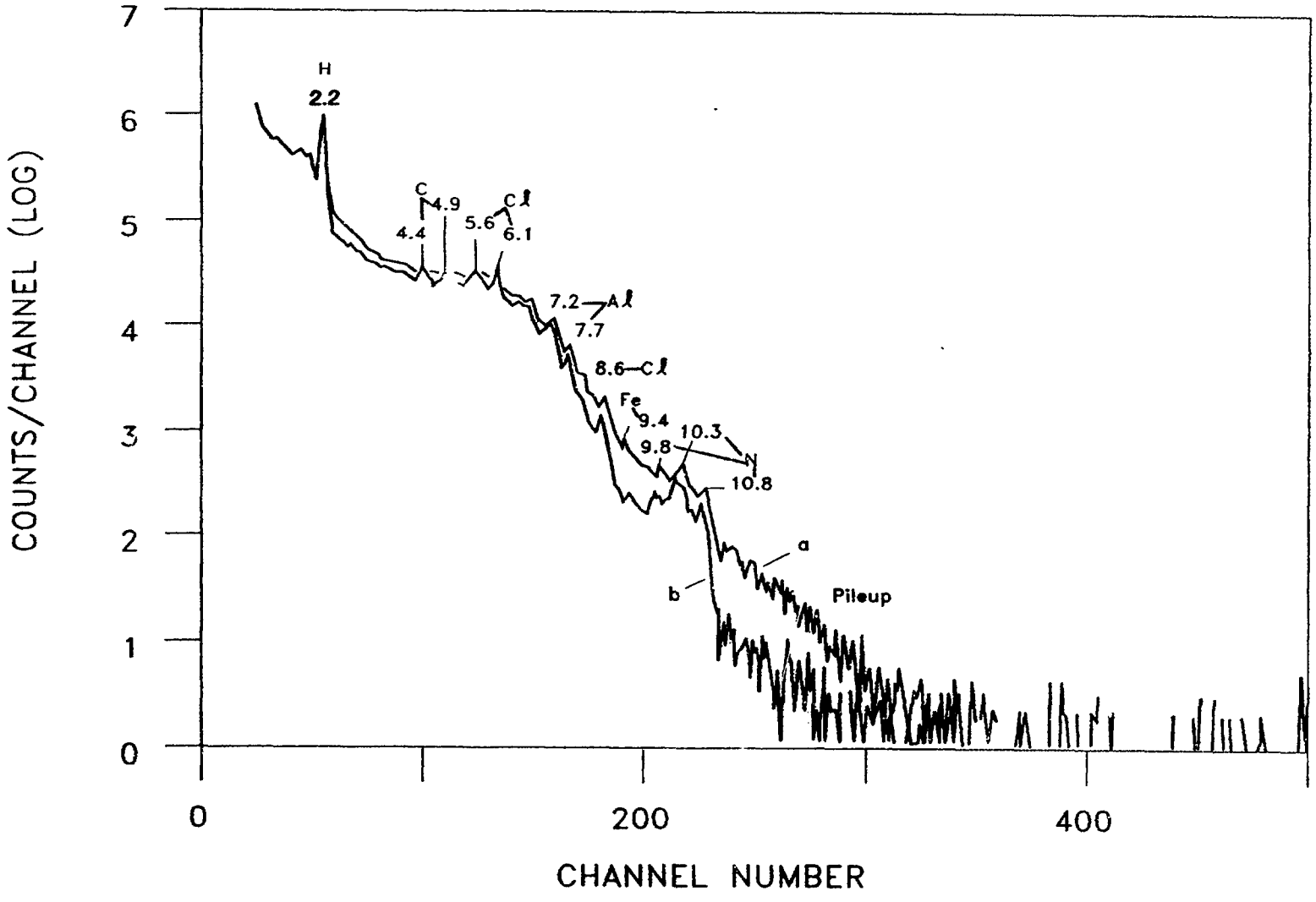


Figure 11 **Pulse Height Distribution in Single NaI Detection in SAIC TNA-EDS**
a) Fast Commercial Spectroscopical Amplifier
b) SAIC Analogy Signal Processor

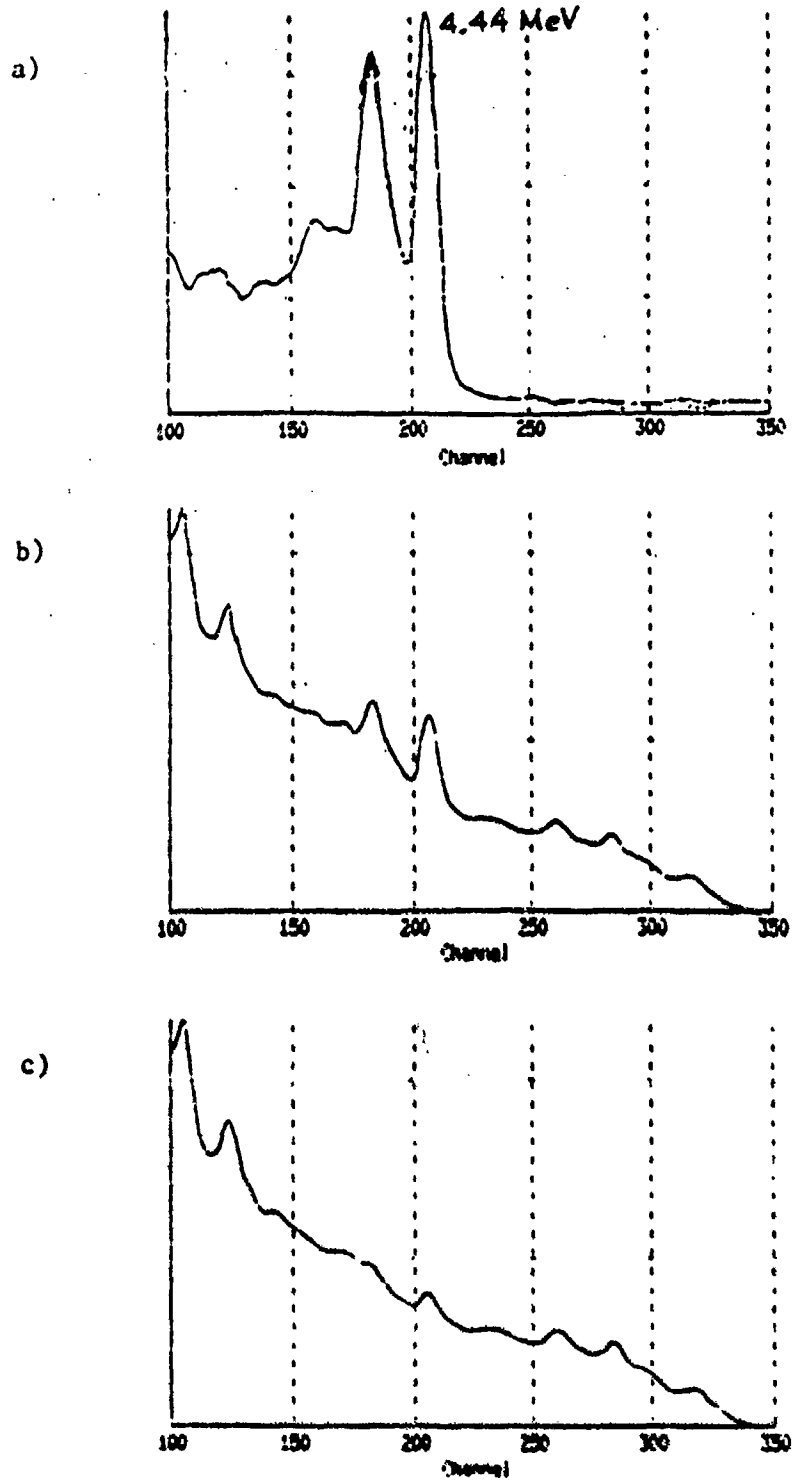


Figure 12 FNA System (Collimated Configuration).
Graphite Sample Measured with NaI(Tl) Detector.
a) Net Spectrum
b) Sample-In Spectrum
c) Sample-Out Spectrum

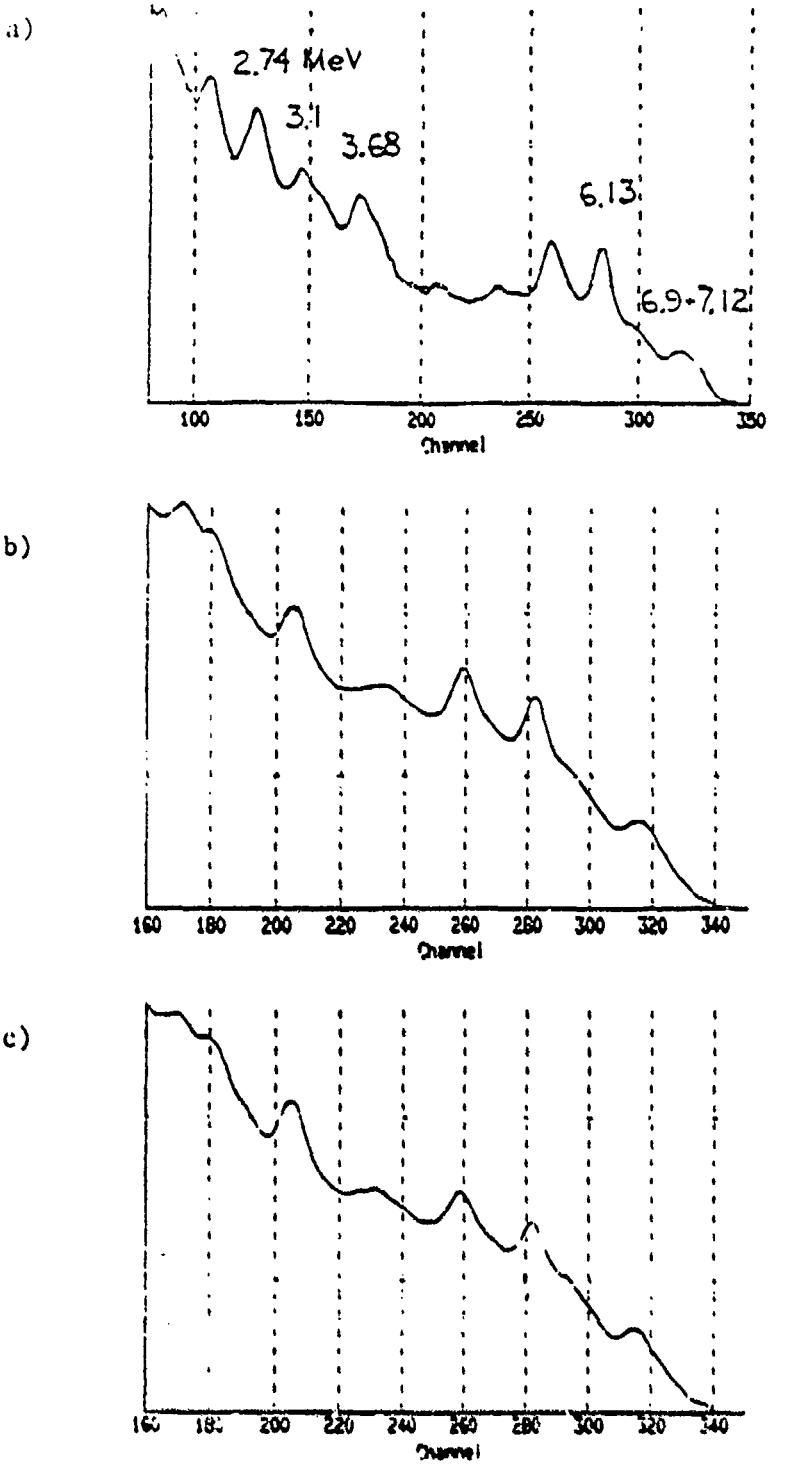


Figure 13 FNA System (Collimated Configuration).
Oxygen (D_2O) Sample Measured with NaI(Tl) Detector.
a) Net Spectrum
b) Sample-In Spectrum
c) Sample-Out Spectrum

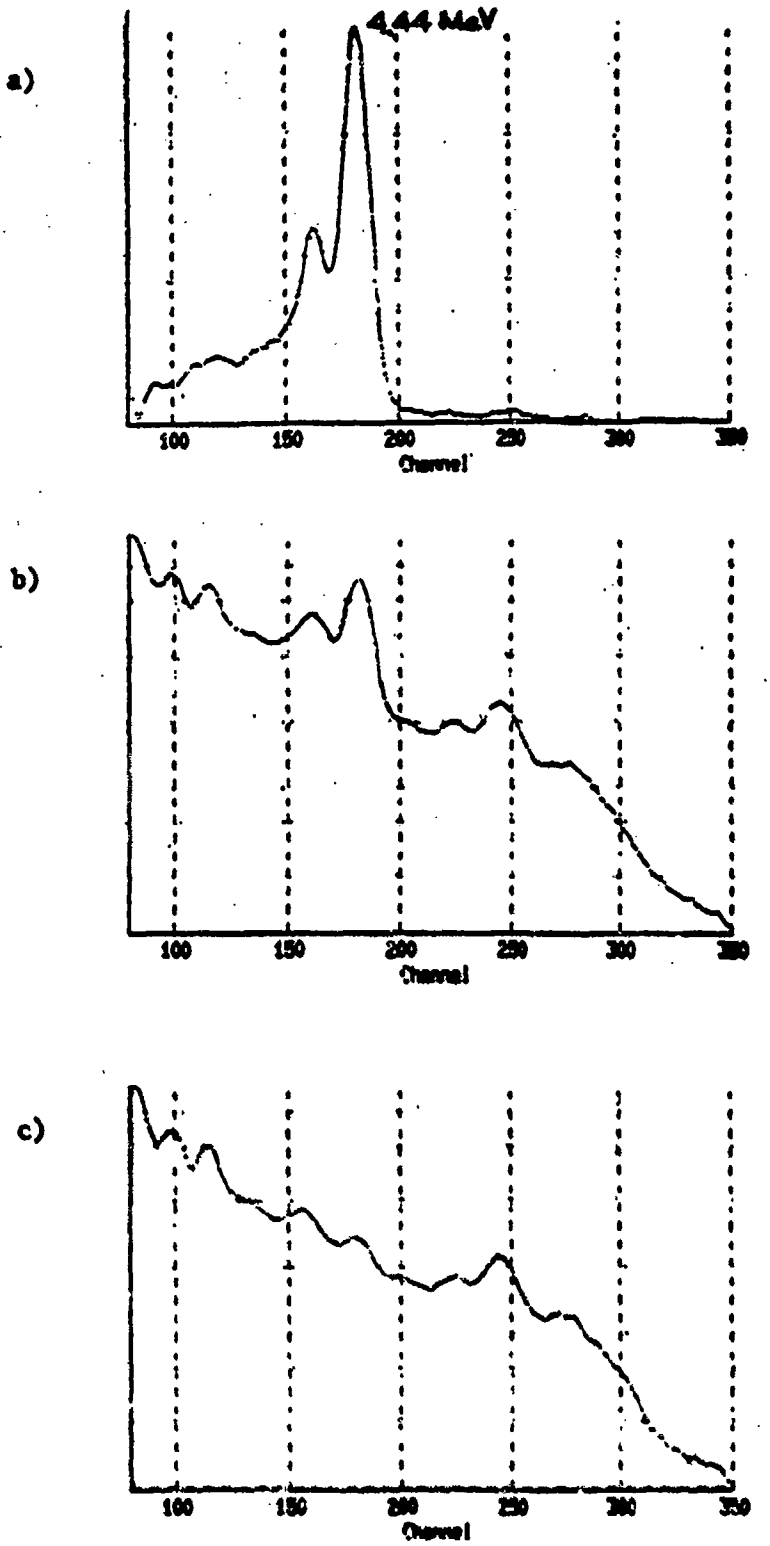


Figure 14 FNA System (Collimated Configuration).
Graphite Sample Measured with BGO Detector.
a) Net Spectrum
b) Sample-In Spectrum
c) Sample-Out Spectrum

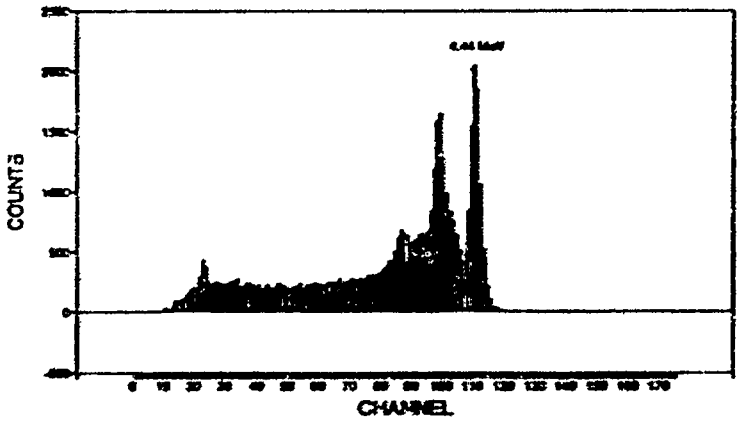


Figure 15 Gamma-Ray Spectrum of Carbon Measured in PFNA Laboratory System (3"x3" NaI(Tl)).

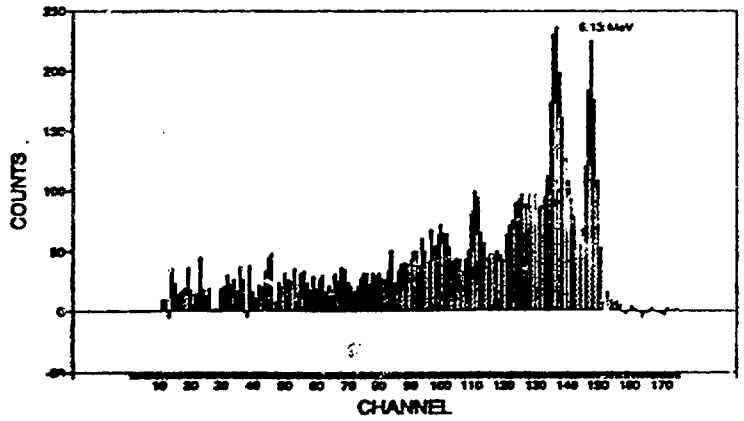


Figure 17 Gamma-Ray Spectrum of Oxygen (H_2O in an Acrylic Box) Measured in PFNA Laboratory System (3"x3" NaI(Tl)).

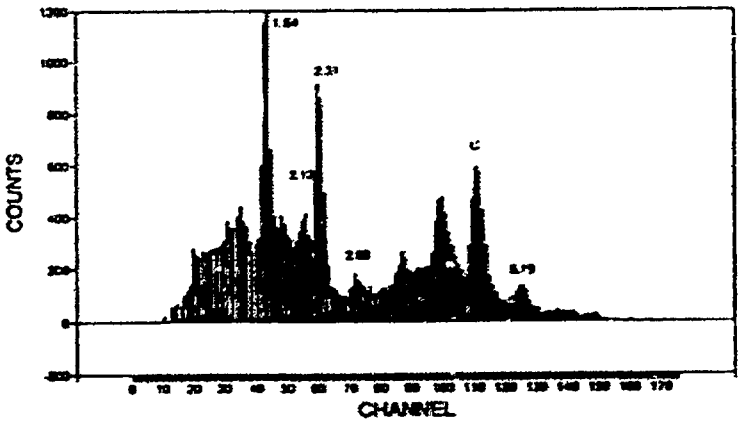


Figure 16 Gamma-Ray Spectrum of Melamine ($C_3H_6N_6$) Measured in PFNA Laboratory System (3"x3" NaI(Tl)).

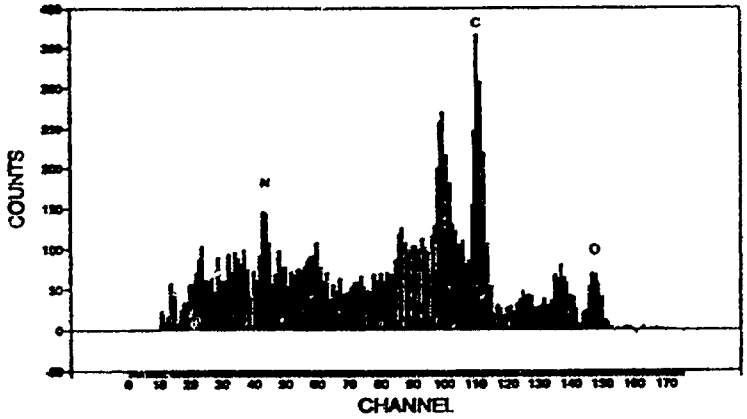


Figure 18 Gamma-Ray Spectrum of Dry Leather Measured in PFNA Laboratory System (3"x3" NaI(Tl)).

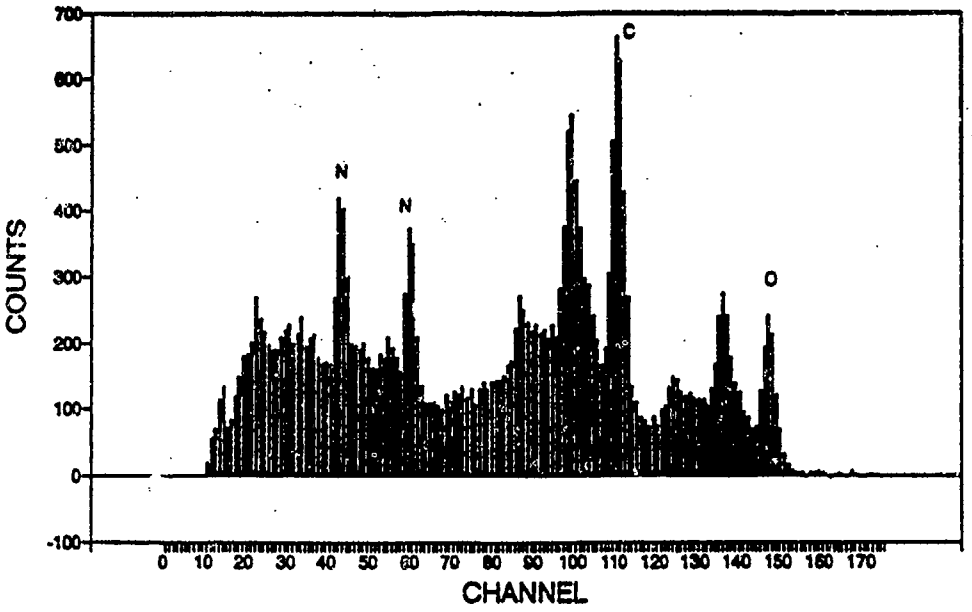


Figure 19 Gamma-Ray Spectrum of DETA Simulant Measured in PFNA Laboratory System (3"x3" NaI(Tl)).

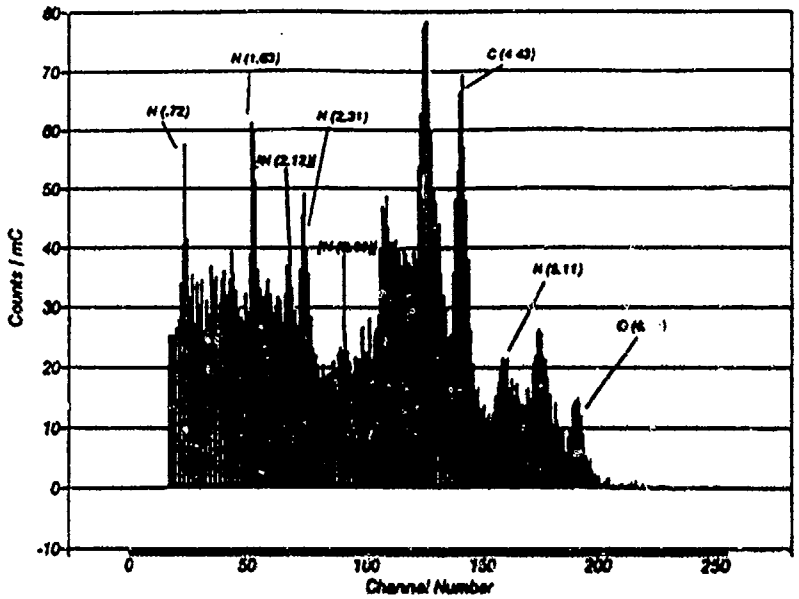


Figure 20 The Gamma-Ray Energy Spectrum Measured with a 3"x3" NaI(Tl) Detector in PFNA Laboratory System for a Small Sample of C-4 Explosive Simulant. The Fingerprint Lines of ^{16}O 6.13 MeV), ^{14}N (.72, 1.63, and 2.31 Mev) are Indicated. Also Indicated are Weak Lines Associated with ^{14}N (2.12, 2.80, and 5.11 MeV). Note that the 5.11 MeV Line of N Contains also the Second Escape Peak of the Oxygen 6.13 MeV Line.

A REVIEW OF THE DEVELOPMENT OF A LUGGAGE EXPLOSIVE DETECTION SYSTEM

J. Bartko and F. H. Ruddy
Westinghouse Science & Technology Center
Pittsburgh, PA 15235-5098, U.S.A.

1. INITIAL CONSIDERATIONS

Nuclear activation technology has some powerful advantages over other technologies for determining the composition of concealed material. To a great extent this is due to the penetrating power of nuclear radiation, particularly, neutrons and gamma rays and the unique properties of their reactions with nuclei which enables a precise determination of constituent elements. The first step, then, in the evolution of a detection system was to identify an element or elements which would act as an indicator(s) of explosives. The element selected was nitrogen which is found in all common explosives in abundances ranging from ~15% to ~36%. Oxygen and carbon are also there in some abundance, but these are much more common and are more difficult to detect. Nitrogen, as we shall see, is an ingredient in some other materials, but it is considerably more rare in other materials.

There are three contending reactions that could be employed for detecting nitrogen which involve neutrons and gamma rays: $^{14}N(n,g)^{15}N$, $^{14}N(n,2n)^{13}N$, and $^{14}N(n,n'g)^{14}N$. The first was selected because it is initiated by thermal neutrons (easily produced from fast neutrons), its cross section is better (80 millibarns) than those of its competitors, and the resultant gamma radiation has some unique features. In ~15% of the reactions a 10.8 MeV gamma ray is produced. Gamma rays of this and higher energy are rare in other elemental neutron reactions and their production probability is considerable less than 15%.

Since the 10.8 MeV gamma rays are emitted promptly, a detection system based on this reaction must incorporate the means of producing the required thermal neutron flux, as well as the gamma ray detection apparatus. In routine neutron activation analysis studies, this is generally accomplished by constructing a cavity in neutron moderating material with a fast neutron source and detector(s) in close proximity to the cavity. A simple system is shown in Figure 1. The moderating material thermalizes the fast neutrons and deflects a fraction of them into the cavity creating a thermal neutron "field" therein. An item to be examined is inserted into the cavity and the resulting gamma ray activity is detected for elemental analysis. The sensitivity and practicality of this technique is dependent upon the achievable ratio of thermal neutron flux to fast neutron flux, the gamma ray detection efficiency and the capability of discriminating against potential false alarm materials. To optimize these aspects one must select the components, which are very interactive, with great care. These components are the neutron source, the moderator, the cavity, the gamma ray detection system and the shielding. Their selection or development will be discussed in the following section.

2. SELECTION OF SYSTEM COMPONENTS

2.1 Neutron Source

Fast neutron sources can be of the machine variety or isotope variety. Machine sources, electrically powered D-D or D-T generators, can be turned off but they are somewhat bulky and the periodic replacement of generator tubes makes them more expensive. The isotopic sources, e.g., ^{252}Cf, are smaller and lighter, but because they emit neutrons and gamma rays continuously, they must be shielded continuously. We selected ^{252}Cf as our source because of its convenient small size, ~1 cm diameter and ~3.8 cm length, and its low cost. The source intensity was ~1×10^9 n/sec.

2.2 Moderator Material

For moderation of the fast neutrons, hydrogenous materials are preferred. The thermal neutrons will be scattered back into the cavity where they will become part of the "thermal neutron gas cloud". In our early work paraffin was used but, because of its potential

of polyethylene was needed to produce the maximum thermal neutron flux in the cavity.

2.3 The Cavity

The dimensions of the cavity were prescribed by the FAA. The size was selected which would accommodate most of the baggage items stored in airplanes. The dimensions were ~40 cm wide, ~60 high and ~80 cm long.

2.4 The Gamma Ray Detector

There are three types of gamma ray detectors that are preferred for TNA: Ge detectors, NaI detectors and plastic scintillator detectors. Ge detectors have the best energy resolution, NaI detectors are the most efficient and the plastic scintillator detectors are the fastest. The selection of a particular one for a particular application is a complex process because of the many operational factors that must be considered. Additionally, one must also make decisions on the number and arrangement of the detectors.

We selected plastic scintillator detectors principally because of their speed, ease of obtaining different geometries and their low cost. Because the selection of these detectors was key to the detection system feasibility, i.e., it enabled us to succeed where others had failed, we will devote the next section to a more detailed discussion.

2.5 The Shielding

We mentioned earlier that only 5 cm of polyethylene was required for moderation. Thus, the size of the basic system is relatively compact. However, because the neutron and gamma ray radiation must be reduced to safe levels, a considerable amount of shielding was required, and in our studies the primary shielding material was polyethylene. Boron doped polyethylene was used to reduce the number of 2.2 MeV gamma rays resulting from neutron capture by hydrogen. The neutron capture cross section in boron is very high in a normal percentage of the captures and an easily shielded low energy gamma ray is produced. Sixty cm of borated polyethylene adjacent to the moderator produced safe levels. Finally, the ^{252}Cf source gamma rays were shielded by surrounding the source with 15 cm of Bi.

SYSTEM

The ^{252}Cf neutron source is also an intense source of gamma rays. The capture of neutrons by the hydrogenous moderator and shield material is an additional source of gamma ray background. Thus, the selection of ^{252}Cf for our neutron source and the selection of hydrogenous material for moderation and shielding presented us with a significant problem vis-a-vis the selection of a gamma ray detector. That problem was to find a detector which could handle the high counting rate without producing pileup pulses (overlap of two pulses) due to the intense background, which would interfere with the detection of the 10.8 MeV gamma rays from nitrogen capture. The solution was to select plastic scintillators which produce light pulses < 10 nsec in duration compared to the 250 nsec of the more efficient and widely used NaI detectors.

The poor energy resolution of a plastic scintillator detector was not a problem because of the exceptionally high energy (10.8 MeV) of the nitrogen capture gamma ray. There are no interfering gamma rays at that energy or higher.

The poor intrinsic efficiency of these detectors could be a problem if a high baggage throughput rate is desired. Because these detectors are inexpensive the solution was to simply increase the volume of the detector. The specific way in which the volume was increased was dictated by the solution of another problem - the problem of distinguishing between explosives and other nitrogenous materials normally found in suitcases, e.g., wool, nylon, orlon, silk and leather.

The key to the solution was the fact that although the nitrogen composition in these materials might be high, e.g., 26% for orlon, the nitrogen densities are significantly lower than that for explosives. Thus, an array of detectors, sensitive primarily to the nitrogen content immediately before it, could distinguish between explosives and other nitrogenous materials. To make a detector sensitive to the nitrogen content before it we took advantage of some aspects of the Compton interaction which is the governing interaction in plastic scintillators for 10.8 MeV gamma rays. The high energy electrons of the Compton tail are directed in a forward direction close to the axis of the incoming gamma ray. Thus, if one made a detector long and narrow, one would: 1) greatly increase the probability of interaction for a

gamma ray entering from the front compared to the side and 2) because of the forward direction of the high energy electron enhance its probability of depositing all of its energy within the scintillator. This would provide the detection directionality desired. Indeed, a Monte Carlo computer calculation of the counts and distribution of counts expected for an array of 5 cm diameter by 25 cm long plastic scintillator detectors monitoring a wool sweater and four sticks of dynamite, shown in Figure 2 verified this. Thus, by increasing the length we improved the efficiency and provided self-collimation.

4. TEST PROGRAM

4.1 The Laboratory System

With the development of a gamma ray detection system we were in a position to conduct a laboratory test program of the feasibility of this approach with the eventual goal of development of an airport system.

A test system consisting basically of a 25 cm polyethylene cavity shell surrounded by paraffin was designed and built (Figure 3). Along the right-hand wall can be seen the front surfaces of the six detectors (black circular areas) used in our study. The detectors used in the study were 5 cm diameter x 80 cm long NE102 plastic scintillator cylinders. The figure shows the cavity containing a Pullman-sized suitcase on a board used for positioning the suitcases to different areas within the cavity.

4.2 Data-Taking and Processing

After positioning the explosive and/or nitrogenous material within the suitcase, the suitcase was inserted into the cavity on the locating board shown in Figure 3. After taking 200 second counts (recorded on a computer), the suitcase was moved successively to different positions until one half of the suitcase had been scanned.

The FAA required extensive testing of differently sized suitcases filled with wool and orlon sweaters to various capacities, large pairs of shoes and/or simulated explosives. The key items to be determined by the tests were whether the system would be capable of detecting and discriminating the defined explosives against a background of other nitrogenous materials and the neutron source strength required to obtain detection in a throughput rate of bags per minute.

5. RESULTS AND DISCUSSION

The test results were grouped into three categories: (1) explosives alone in baggage, (2) false alarm tests, and (3) detection tests. It is obviously impossible to present all of the data from all of the tests. Instead, we will select the most revealing data for presentation in the paper.

5.1 Detection of Explosives Alone in Baggage

In the first run the package of eight sticks of simulated dynamite packed in a cylindrical array was placed on the floor of a large suitcase. Figure 4 is a computer printout of the results and shows the distribution of the counts in slightly more than half of the suitcase. Note that the counts increase toward the bottom-center of the suitcase. The dynamite package is sketched in at its location during the test.

Based on this run as well as the other explosive runs, we selected a threshold of 211 counts for obtaining an "image" of the explosives. The white numbers in Figure 4 represent this image. The dynamite is clearly delineated by a solid block of high counts covering its area.

5.2 False Alarm Tests

The results for 70% packing of wool (three medium and two large sweaters) in the large suitcase are shown in Figure 5. While there are many detector positions exhibiting counts above the threshold, there is no consistent pattern which would lead to a false alarm on the basis of the aforementioned criteria.

6. CONCLUSION

Based on the favorable results of the laboratory tests, the FAA initiated a follow-on program to examine real baggage. For this a detection system was designed and constructed in a trailer. The trailer was transported to four different airports and tests were conducted on a sizeable number of baggage or cargo items. The FAA would add simulated explosives to selected items to provide information on detection rates and false alarm rates. The results of the last two tests are shown in Table 1. The results pointed to the feasibility of moving to the prototype stage.

program, TNA explosive detectors are beginning to play an important role in airport security. Presently, there are four TNA systems established at airports and three others are planned. Improvements vis-a-vis detection of plastic explosives continue to be made.

Table I Results of Airport Tests

Airport	Number of Bags	Type	Detection Rate	False Alarm Rate
Chicago	1,403	Cargo	99.2%	1.6%
Philadelphia	815	Checked	96.3%	4.1%

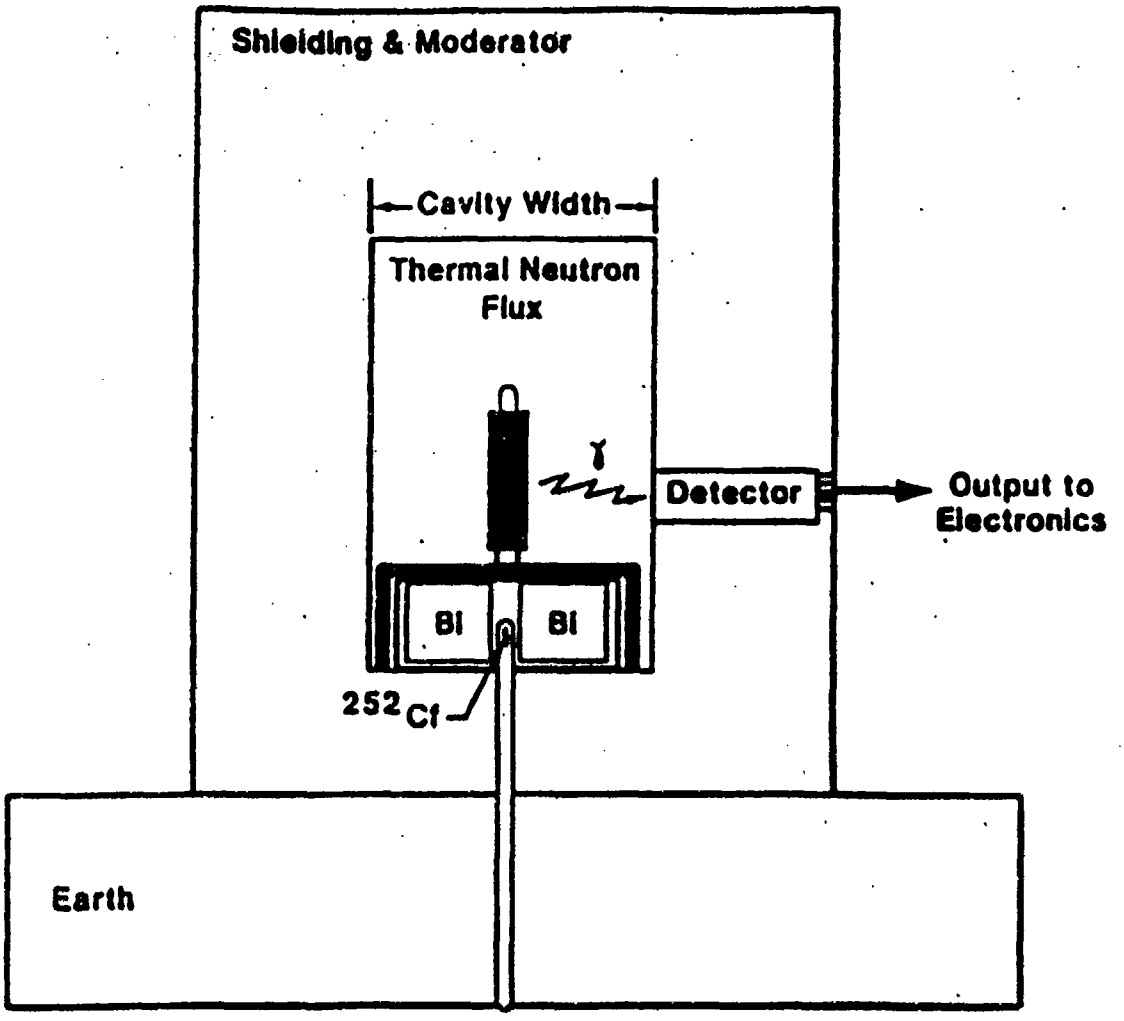


Figure 1 A Prompt Neutron Activation System

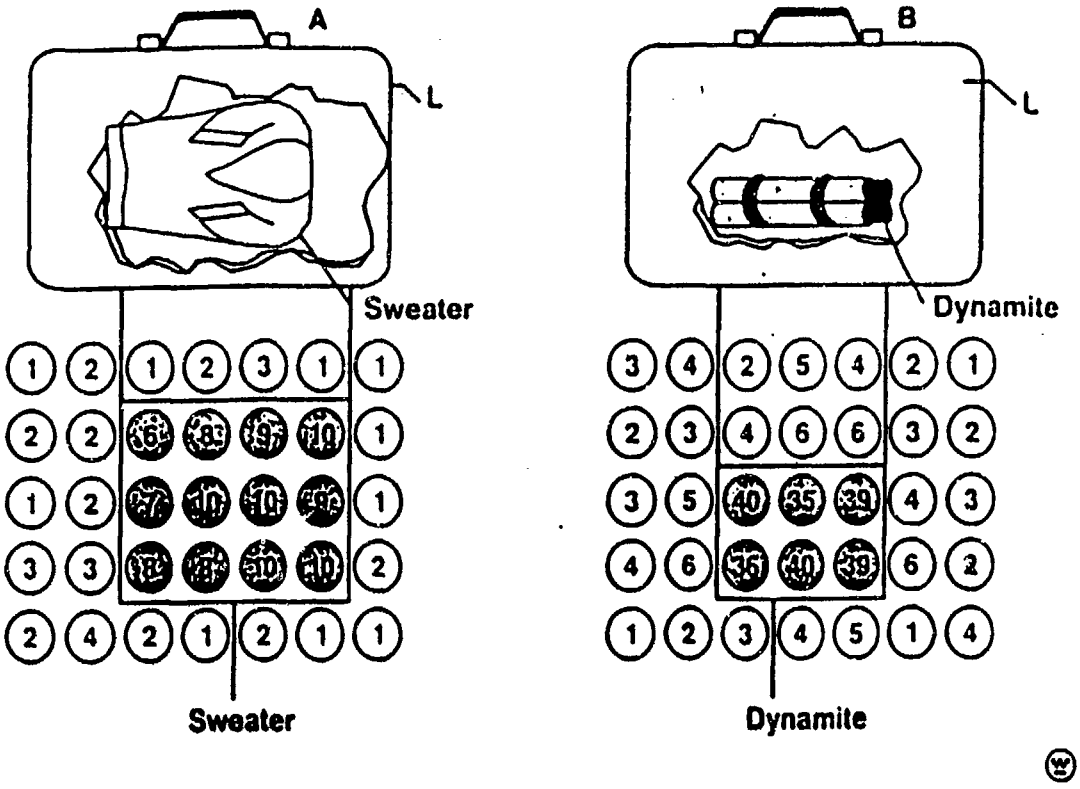


Figure 2 Comparison of the Gamma Ray Count Distribution Produced in An Array of Long Narrow Detectors by a Sweater and by Dynamite.

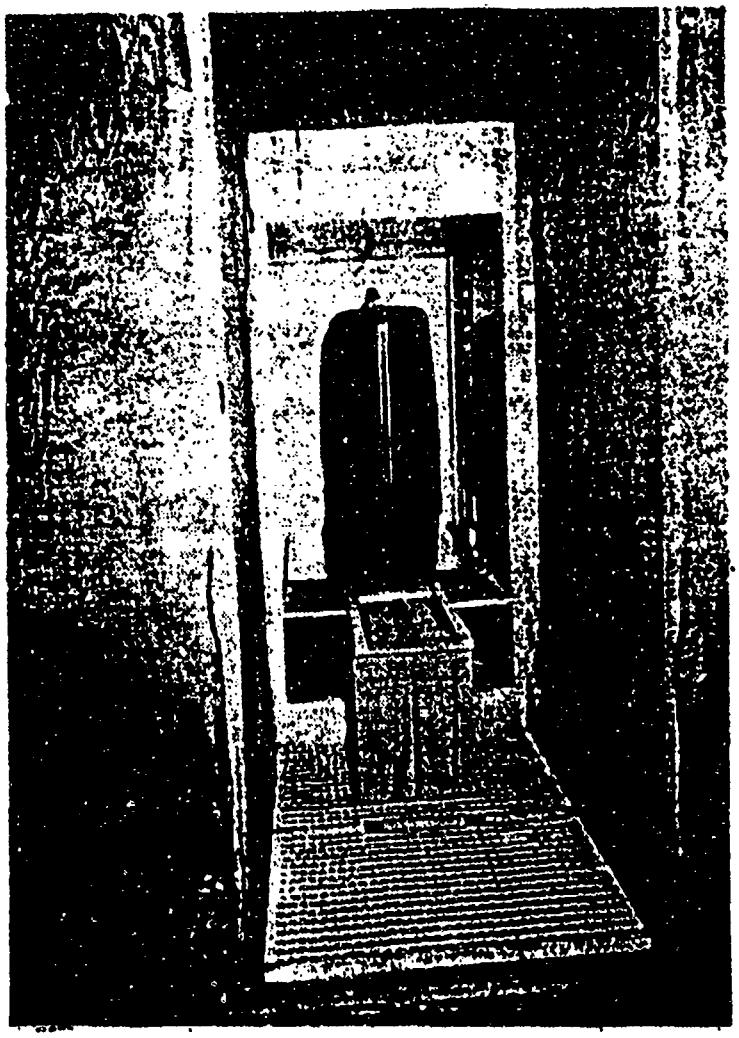


Figure 3 View of the Thermal Neutron Activation Cavity with a Large Suitcase Inside

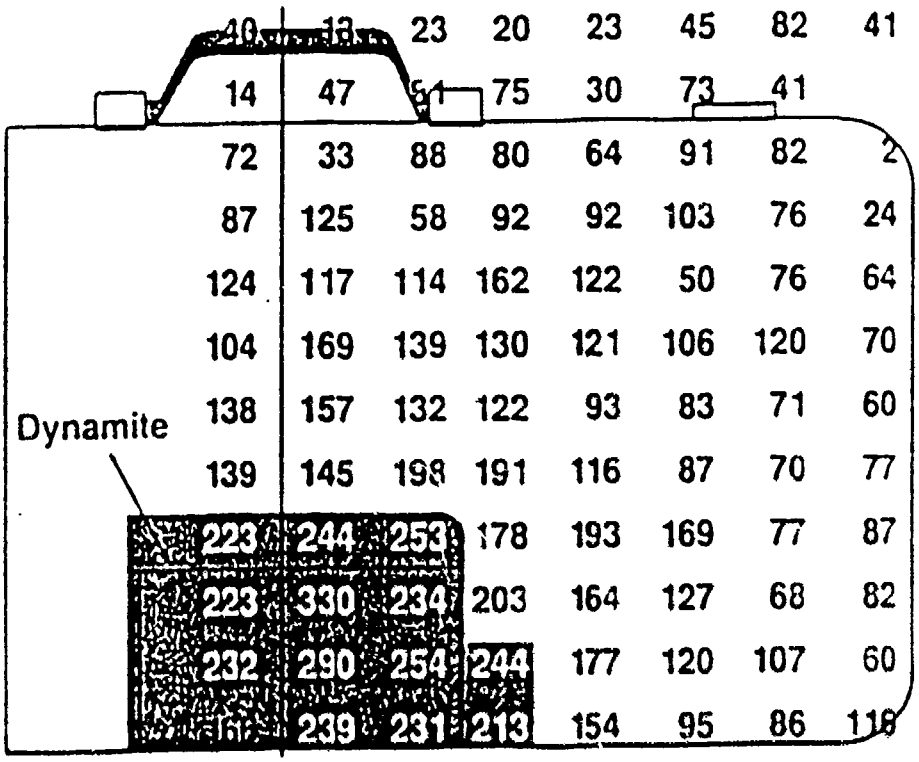


Figure 4 Count Distribution Produced by Dynamite in a Large Suitcase

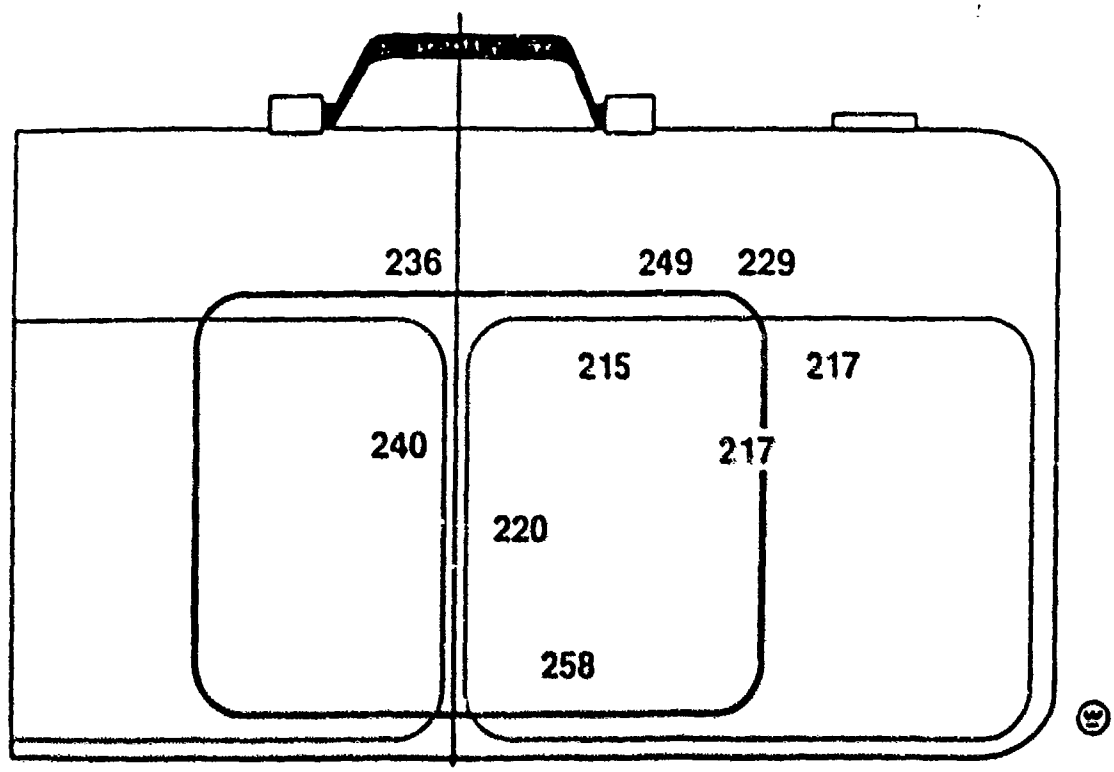


Figure 5 Woolen Sweaters Packed to 70% of Capacity in a Large Suitcase

A TRANSPORTABLE LUGGAGE EXAMINATION SYSTEM BASED ON NEUTRON INTERROGATION

D.B. Syme and G.D. James
Harwell Instruments, AEA Industrial Technology
United Kingdom

1. INTRODUCTION

A transportable TNA system suitable for the analysis of passenger luggage has been designed, built, and tested on airport luggage. The response of the system to passenger luggage and to luggage containing explosive simulant has enabled the detection performance of the system to be determined. The system uses a distribution of low strength 252Cf sources and an array of gamma-ray detectors bordering the luggage cavity. This arrangement gives positional information for bulk simulant but is otherwise equally sensitive to bulk and sheet simulant. The system weighs 1.7 tonnes and can be assembled in about one hour from components weighing less than 30 kg each. The radiological dose close to the analyzer is less than 1.5 μSv/h. Used in conjunction with an X-ray analyzer, the combined system would have low false alarm rate (FAR) and high detection performance.

2. THE TRANSPORTABLE TNA CONCEPT

In a TNA system, the gamma-rays produced by thermal neutron capture in nitrogen are detected and used as an indication of the presence of explosive material. The analyzer must exploit the difference between the distribution and level of signals obtained from the nitrogen content of ordinary luggage, and that obtained from luggage containing explosive material. A transportable TNA luggage analyzer has been designed, constructed, and extensively tested on luggage and simulated explosive material both in the laboratory at Harwell and at a military airport, and also by Home Office scientists at a civil airport. The system is suitable for use at conference or airport check-in desks, in a hotel foyer, on the apron of an airport, or on the platform of a suitable transport van given access to an electrical power supply. The system weighs 1.7 tonnes and can be moved to a new location in the form of sixty shielding blocks each weighing less than 30 kg. The system can be assembled in about an hour. The shielding is such that the radiological dose on contact, and the dose to the operator in loading luggage on to the analyzer, is acceptably low. The normal analysis time is 1 minute. In this time good detection rates are obtained when the false alarms from ordinary luggage are set to acceptable levels, e.g. 5%. These detection rates are almost independent of the form of the simulant in that both sheet and bulk simulant are detected with about the same probability. However, the arrangement of sources and detectors allows positional information to be obtained for bulk simulant. This information would be valuable in directing the attention of an operator at an X-ray analyzer. A system which combines the information from a transportable TNA system with an X-ray system would give a high detection performance with a false alarm level of about 0.3%.

3. THE TRANSPORTABLE TNA LUGGAGE ANALYZER

The upper part of Figure 1 shows a perspective sketch of the transportable TNA luggage analyzer. The lower part of the figure gives a cross sectional view which shows the cavity where luggage is placed for analysis, and the form of the surrounding neutron shielding. The shield measures 2.1 x 1.6 x 1.1 m and weighs 1.7 tonnes. Each of the sixty pieces into which the shield can be dismantled weighs less than 30 kg and can be taken through a standard 32.5 inch doorway. The cavity is lined with an arrangement of sources and detectors on each side of the suitcase position. The radiological dose rate on contact with the analyzer is about 1.5 μSv/h. The piece of luggage to be analyzed is loaded into the analyzing position on a trolley which is designed to provide good radiological protection for the operator both when it is fully withdrawn, and also when it is fully closed. It is estimated that the dose rate to the operator during an eight hour day is less than 2 μSv. The regulations governing the transport of radioactive material allow the sources to be transported in the shielding components which they occupy during operation. The doses received by operators involved

in the removal and reassembly of the analyzer were below measurements limits on a QFE.

In the present design the gamma-ray signals from the scintillation detectors are processed by Harwell Instruments proprietary series electronics, and then displayed, stored and accessed using a PC. The operating system must be given suspect count levels which must be determined from the count distribution of data from ordinary luggage. These levels can be set, at any chosen value of the false alarm rate, to indicate suspect luggage. For development purposes, and to maintain operational records, the data are stored for further analysis.

4. PERFORMANCE DEVELOPMENT

Extensive development work has been carried out on the shielding and disposition of detectors relative to the source arrangement to produce a system almost equally sensitive to bulk and shield simulants while retaining positional information on bulk simulants. Initially, reliable performance characteristics were determined by laboratory measurements on innocent luggage, on luggage loaded in a variety of ways with bulk, and sheet simulant, and with simulant material in isolation. These results were reinforced by independent measurements made at the Harwell Laboratory by Home Office scientists using eighty assorted suitcases, and extended by measurements on 300 suitcases at a military airport. These latter results are shown in Figure 2. They were found to be in very good agreement with the Laboratory data, giving much the same distribution of counts, the same weight dependence of counts, and thus the same counts at a chosen false alarm level.

The results obtained enable the detection probability to be determined as a function of simulant weight for any chosen false alarm level. At 5% false alarm, detection probabilities in excess of 90% are obtained for simulant weights below 2 kg. These are average values averaged over several bulk simulant positions. As a result of this averaging process, sheet and bulk simulants have roughly equal average detection probabilities.

Finally an extensive series of independent trials were carried out by Home Office scientists at a civil airport. Measurements using the transportable TNA system, and also using an X-ray system, were made on 722 pieces of passenger luggage. A large number of pieces were measured on the TNA system with and without simulant strapped on the outside of the luggage. Simulant weights of 700 g and 1 kg were used. Roughly equal number of measurements were performed with the simulant in bulk form and in sheet form. Experiments were also performed on isolated simulant, and on simulant placed in various positions inside experimental luggage. These extensive measurements allow the detection probability as a function of simulant weight to be determined in two ways, for a preset value of the false alarm rate. First, by combining the count distribution from passenger luggage with the response from isolated and specially packaged simulant. Second, by direct determination of the false alarm rate from innocent luggage, and of the detection rate from luggage to which a known weight of simulant has been attached. It is found that the results measured in these two ways are in good agreement. It was also possible to say that 46 of the 722 suitcases gave concern on first X-ray image examination, and required more detailed X-ray examination. Ten of these cases would have needed to be opened, to resolve suspicious or cluttered areas, on the basis of X-ray alone. This gives an upper X-ray false alarm level of 6.5% which could be combined with a 5% TNA false alarm level to give a combined operational false alarm level of 0.3%.

5. SUMMARY

The transportable TNA luggage analyzer considered in this report has been optimized so that it performs well on simulant explosive material in both bulk and sheet form. The performance characteristics determined in the laboratory have been confirmed by extensive measurements on passenger luggage at two airports. The system is radiologically safe and gives minimal exposure to operating staff. Within a reasonably short analysis time, the detection probability is high for an acceptably low false alarm rate. For bulk material the system gives useful positional information which can be used to assist subsequent X-ray analysis. For a combined TNA and X-ray system it has been shown that false alarm rates of 0.3% can be achieved.

ACKNOWLEDGEMENTS

The authors are grateful to the Ministry of Transport for supporting this work, and to Dr. R. Lacey and Miss Lynne Head of the Home Office for providing data on their measurements at Harwell Laboratory and at Luton Airport.

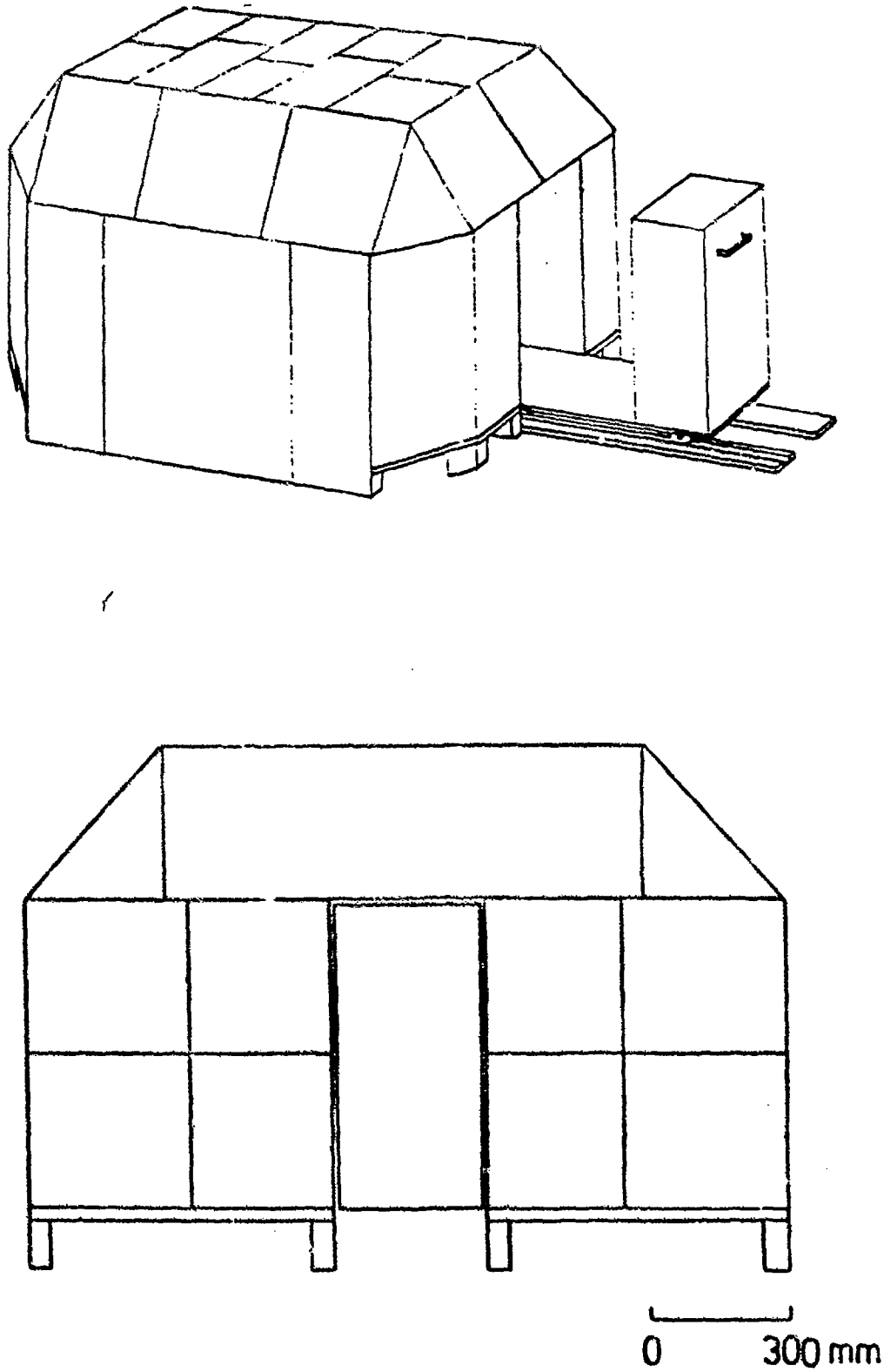


Figure 1. The Harwell Instruments TNA Luggage Analyser - a perspective sketch, and a cross-sectional view.

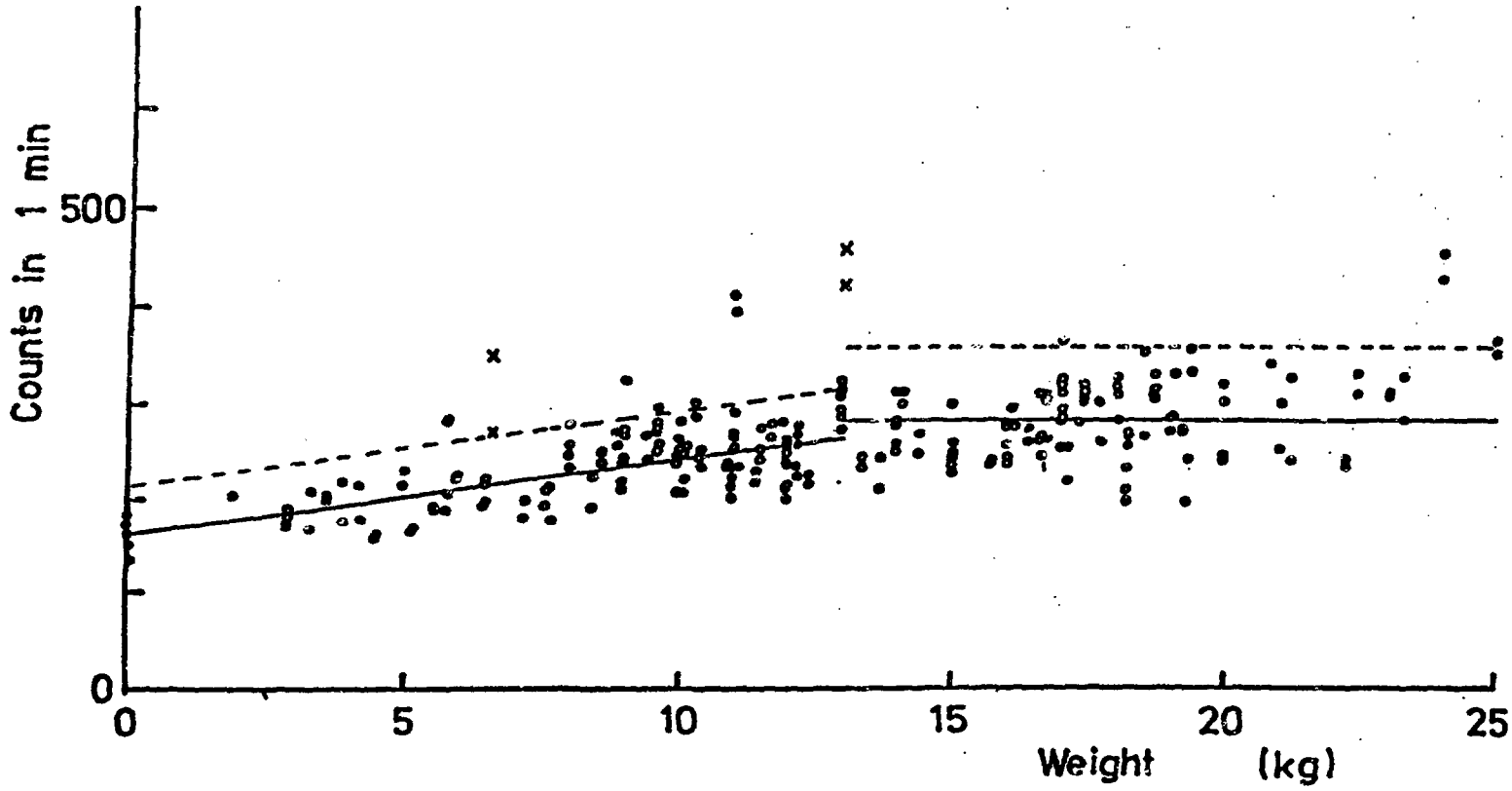


Figure 2. Data taken at an airport with the Harwell Instruments TNA Luggage Analyser. Open circles - data from passenger luggage as a function of suitcase weight. Crosses - data for suitcases containing simulant explosive.

AN APPROACH TO IMPROVING TNA EDS

Steven B. Buchsbaum and Duane Knize
Science Applications International Corporation
San Diego, CA 92121

Leon Feinstein
Science Applications International Corporation
Los Altos, CA 95054

Joseph Bendahan and Pat Shea
Science Applications International Corporation
Santa Clara, CA 94022

1. INTRODUCTION

Original FAA work in the use of TNA for explosive detection started in the mid 1970's with a contract to Westinghouse, which led to the development of a crude EDS using low resolution plastic scintillators and simple threshold level electronics. This early system development was aimed at the detection of bulk explosives. Nearly a decade later, in response to the bombing of the Air India flight out of Canada, the FAA issued requests for new innovations in non-vapor EDS systems. TNA technology was again chosen for funding. Science Applications International Corporation (SAIC) was awarded contracts to investigate the TNA system based on both an isotopic ^{252}Cf source and an electronic neutron generator (ENG). SAIC's experience in the application of TNA to non-destructive examination (NDE) of various bulk materials for over ten years and the proposed innovations for the application of the TNA technology to EDS were the keys to these efforts.

Although the SAIC proposal originally called for the detection of bulk explosives (C4 in bulk form, water gel, and dynamite), the specifications were later modified to include the detection of a reduced threat, and sheet explosives such as RDX/PETN or Semtex. These explosives had been found in various configurations in passenger luggage. When placed in thin sheets inside the lining of a suitcase, RDX/PETN and/or Semtex are practically undetectable, even in a hand search. During the TNA research and development, major breakthroughs were made in source moderation, system materials and construction, detector configurations, electronic signal processing, and decision analysis. In response to the accelerated schedule called for by the FAA, the two prototype EDS systems -- Cf-based and ENG-based -- were developed, designed, fabricated, and tested in the laboratory within 15 months. Subsequently, the two systems were taken to six airline locations (in SFO and LAX) and their performance were tested using over 40,000 pieces of mostly domestic luggage. Using a weighted distribution of simulated explosives, the systems were demonstrated to have a performance of approximately 95% probability of detection (P_d) and 5% probability of false alarm (P_{fa}). This was tested against the domestic bag distribution encountered, and for the FAA specified amount and varieties of explosives defined as a "threat level". For international bags, and for the FAA defined reduced threat, the P_d is somewhat reduced with a higher, but still usable P_{fa}.

Last fall, SAIC initiated a TNA EDS Performance Improvement Study to address the problem of detecting smaller quantities of explosives with TNA EDS, while maintaining or improving current levels of detection and false alarm performance. The purpose of this internally funded study was to develop a set of specific recommendations for signal processing changes, and system enhancements, to improve the TNA EDS performance, particularly to reduce false alarms, and to develop a full system simulation capable of predicting system performance against various threats, based upon threat specifications, clutter databases, and present and future design parameters.

2. PERFORMANCE EVALUATION AND REQUIREMENTS

In this section, we will develop, in engineering units, the performance of the present system, and the gains required to handle the reduced explosive threat.

TNA EDS Performance is specified by a pair of numbers: probability of detection, P_d, and probability of false alarm, P_{fa}, for a particular distribution of explosive types. This distribution was specified by the FAA as a distribution of explosive types at "full threat" amounts. The objective of the present program is to maintain current "full threat" detection performance for the FAA explosive distribution at a reduced threat level. The initial TNA EDS performance varies somewhat; for the most favorable case, summer-domestic luggage, $P_d \approx 95\%$, $P_{fa} \approx 5\%$ has been demonstrated. For winter-international baggage, performance falls to about $P_d \approx 90\%$, $P_{fa} \approx 12\%$. These two operating points are compared on Figure 1.

The chart plots operating characteristics, combinations of P_d and P_{fa}, on probability scales (sometimes referred to as ROC curves for receiver operating characteristics, using terminology developed by radar engineers). The result is that the P_d, P_{fa} pairs corresponding to a constant signal to noise ratio (for a constant signal, Gaussian noise model) fall on straight lines. Each line represents a level of performance. One can move along the iso-SNR lines simply by changing detection threshold. Real performance gains are achieved by moving across the iso-SNR lines toward the upper left. The FAA Goal for the present effort is a 5 dB performance gain.

3. PERFORMANCE OPTIMIZATION APPROACH

The required performance improvements can only be obtained through a systematic engineering and design approach using coordinated experimental measurements, data analysis, and modeling efforts. The current program evaluates in a unified quantitative framework, those elements of the TNA measurement technology and data processing stream that are most critical to the detection performance, and focuses our efforts on improvements in these areas. The present program has two goals: the first is to generate an optimal system design that can be implemented within the constraints of the present budget and schedule, and that will meet the FAA goals with regards to reduced threat performance, i.e. > 5 dB improvement. The second goal is to validate the TNASIM/TNASIR models, and this quantitative optimization approach to system design, for TNA EDS.

Within the scope of the present program we have available a baseline TNA EDS machine, and the opportunity to implement and test one new optimized machine design. We will collect data with both the baseline and optimized machines on a test set of luggage available in the laboratory. The luggage will be measured without explosives, and with full and reduced threats. These two machine designs operating against two threat levels will provide four performance points to compare with the TNASIM/TNASIR predictions. If it can be demonstrated that these tools can adequately predict performance as a function of system design and threat, then future designs to meet increased performance requirements, or to perform against more difficult threats, can confidently be projected.

The system engineering provides technical focus and coordination for the present program: estimating performance, performing design trade-off analysis using the TNASIM/TNASIR system response and performance model, defining areas where further measurements are needed, defining areas of particular focus for the analysts, and establishing a performance baseline. A performance baseline is being established by processing the luggage set collated in the laboratory with the unmodified TNA EDS. It is likely that the absolute P_d/P_{fa} results from this baseline may be biased relative to operational experience, due to the limited number of bags available in the lab. This same reference luggage set will be used for all tests as system hardware and processing algorithm modifications are implemented, and therefore the biases should be consistent for all the lab data collections. A second parallel baseline is established by using the present TNA EDS design parameters in the TNASIM and TNASIR models. It is through the relationship of the experimental and estimated baselines that predictions for paper designs are calibrated to real performance. When the optimized TNA EDS machine becomes available, this same luggage set will be processed, and an "improved" set of P_d/P_{fa}'s will be calculated. The absolute and relative performance of these two machine designs against the two threat levels will be compared to the absolute and relative performance predictions of the model suite. The initial comparisons of the model predictions with operational data show good agreement.

At the time of the writing of this paper we have evaluated twenty-eight candidate system designs. These designs are constrained to be relatively minor modifications to the baseline system hardware. We

anticipate evaluating more designs before a final candidate is selected, but already a couple of the candidates appear to meet the FAA requirements. The remainder of the discussion will be restricted to these twenty-eight designs for which the analysis is complete. It is important to note that the complete analysis of a candidate system design requires only a few hours on a workstation class computer (i.e. SUN SPARC 2), as opposed to the months of effort that would be required to perform the hardware modifications and testing required for laboratory evaluation of a design.

4. TNASIM - TNA SYSTEMS SIMULATOR

A complete, validated, end-to-end system model is required to efficiently probe the large parameter space of possible TNA system designs, and to quantify ultimate explosive discrimination performance for changes of detailed system parameters. The objective of such a model is to permit a large number of system design trades to be performed, and performance impact to be quantified, without the necessity of full experimental verification for each design configuration. In a system of this complexity most system modifications have numerous interrelated performance impacts, some beneficial, others detrimental. Detector modifications are one such example. The modification of a detector design to improve specificity, for example, could also lower overall counting rates, and therefore, signal counting rates. Further, optimal design settings for all such parameters must be determined if the best possible TNA EDS system performance is to be achieved; an engineering best estimate will not be sufficient.

This required performance model, TNASIM, is under continuing development, and has been validated by numerous experimental measures. All facets of the measurement and detection process are modeled, and the intent is to validate the model components against experimental measures wherever possible. It is anticipated that numerous system configurations; varying detector types, numbers of detectors, neutron source strengths, shielding configurations, auxiliary detector channels, and spatial configurations, will be tested within the context of the model, and only the most promising will need to be verified experimentally. The TNASIM model is capable of generating an estimate of machine response, as has been used for the present analysis. The model is also capable of generating a Monte Carlo realization of a luggage measurement set with any specified threat or luggage clutter distribution.

The TNASIM model uses extensive computational support from more sophisticated neutron transport models such as MORSE as well as experimental validation, for the modeling of neutron effects with regard to luggage and shielding interactions. TNASIM also relies upon MCNP and experimental measurements for detailed modeling of the detector spatial and spectral response, and noise performance estimates.

MCNP and MORSE are industry standard, general purpose Monte Carlo codes for neutron, electron and photon transport. MCNP was developed at the Los Alamos National Laboratory (LANL) over the past 35 years. MORSE represents a similar development effort from Oak Ridge National Laboratory. These codes use a Monte Carlo approach to theoretically duplicate a statistical process (such as the interaction of neutrons and photons with nuclei) and are extremely useful for complex problems involving many different kind of materials and geometries, that cannot be efficiently modeled by deterministic methods.

The detector model incorporated in TNASIM has also been calibrated against controlled experiments measuring the response of sodium iodide (NaI(Tl)) scintillators from a known source located at specified positions within the cavity. These experiments have been performed within a variety of detector configurations. We are also capable of modeling other types of scintillators for TNASIM such as bismuth germinate (BGO), and other more exotic materials. With multiple detector models, TNASIM can explore the consequence of utilizing a combination of different detectors in varying configurations and sizes.

The TNASIM has been used during the present effort to create a software realization of twenty-eight designs, and to evaluate the performance impact of these design for explosive discrimination.

5. TNASIR - TNA SIGNAL TO INTERFERENCE ESTIMATOR

TNASIR is a model to predict the performance of an idealized detection processor based upon a specified threat, noise and clutter statistics, and model inputs from TNASIM for the detailed system response. This allows for rapid analysis of the relative merits of various system designs. Within the accuracy of the assumed noise and system models, this processor provides an idealized best estimate of system

of achieving the performance of this idealized processor, this technique should provide good estimates of the relative performance of different configurations, and a modestly accurate estimate of absolute system performance. It is possible to include within the context of such an idealized processor performance losses to account for less than perfect processors. A simple approach to account for these losses will be presented.

Also under development is a detection processor that can analyze either simulated bag data sets produced by TNASIM, or real data, for any specified system configuration, TNASIR II. The detection processor will be constructed as a Maximum Likelihood processor, mimicking the idealized detection model. It is possible when working with real data, for a single system configuration, to produce a highly optimized discrimination processor, or ANS processor, that can outperform our approximation to a Maximum Likelihood processor, and this is indeed done for the operational system. The TNASIR II processor should be capable of providing near optimal performance, while still providing traceability to the model results, and thus will be very useful in highlighting deficiencies in critical areas of the modeling, as well as providing a second discriminator for the various system designs. The remainder of this section will provide a discussion of the structure of the TNASIR idealized detection processor, and results from that analysis.

The spirit of the analysis in the TNASIR processor is to model the most relevant system characteristics; signal, background, noise, clutter, and system response, for each candidate design, making approximations where necessary, and evaluate the performance of each design in a quantitative manner. If in this process, an assumption is needed for some system or environmental parameter, then the accuracy and sensitivity of the final results are tested as a function of the assumed parameter. If the results are found sensitive, then knowledge of this particular parameter is identified as an area in need of refinement. In general the figure of merit for the system design is P_d/P_{fa}, which is a logarithmic measure of the basic physics. Thus a complete quantitative treatment of the entire measurement/detection process usually provides good results, even if there are modest inaccuracies, and best guess assumptions in some of the basic environmental statistical factors.

chosen threat:

- SNR - Signal to Noise Ratio in the absence of clutter. In general this result is only of modest use, since for the bulk of the operation parameter space we find the performance to be limited by clutter.

- SIR - Signal to Interference Ratio. This is an estimate of the performance of the full system for a specified threat against both noise and environmental clutter. This is the primary figure of merit as it has direct traceability to P_d/P_{fa}.

- Estimation Accuracy. The inherent capability, and intrinsic errors of a particular system design to estimate important bomb parameters such as density, size, and position within the luggage are estimated by use of the Crammer Rao bound. These parameters provide an important second order measure of the system's performance, and of the overall measurement accuracy and specificity. These measures could become important to an on-line system algorithm if an attempt is made to estimate specific parameters of each detection in an effort to mitigate false alarms. These estimation accuracy bounds are also an important measure of the robustness of a particular system design.

We now present the structure of the calculations for the Signal to Interference Ratio - SIR, and estimation errors in the presence of clutter, the clutter free case can be recovered by setting the clutter covariance matrix equal to the identity. The signal is modeled as a 3-d rectangular volume of nitrogen in excess of the background. The dimensions of the volume can be chosen to match a bulk threat at either full or reduced strengths, and can also be chosen to match a sheet threat. The threat can be positioned anywhere within the bag; the SIR's are calculated for specific positions, and as average SIR's over an ensemble position within the luggage.

The background nitrogen distribution within a volume is denoted as $S(\vec{x})$, where $\vec{x}$ denotes position within the volume. We will model the nitrogen as a constant level μ, and a zero mean spatially varying

component (clutter) $S(\vec{x})$, i.e.:

$$S(\vec{x}) = \mu + \tilde{S}(\vec{x})$$

$$\langle S(\vec{x}) \rangle = \mu$$

For this analysis $\langle\ \rangle$ will imply an ensemble over a distribution of luggage. We will assume that the clutter is Gaussian distributed, and therefore it is completely characterized by its joint probability distribution. For the assumed zero mean process the joint covariance is:

$$C(\vec{x}_1, \vec{x}_2) = \langle \tilde{S}(\vec{x}_1)\tilde{S}(\vec{x}_2) \rangle = C(|\vec{x}_1 - \vec{x}_2|)$$

We nave also assumed that the covariance is spatially invariant, and therefore only depends on the sepsration distance, not the position within the bag. At this point we have made a number of significant assumptions about the statistical nature, and spatial structure of the clutter. We use our extensive database of luggage clutter collected by real operational field machines to calibrate the diagonal elements of our clutter covariance. The detailed spatial structure is assumed to fit an ad-hoc model. We have analyzed a number of different models for the detailed nature of the spatial structure, and we have found only a weak sensitivity of our final results on the choice of model. The relative performance of different designs that are presently under consideration are very insensitive to the detailed spatial structure of the clutter, and therefore, for the family of designs under present consideration we will assume our present model is sufficient. This is not to argue that clutter is unimportant in these calculations. Indeed the strength of the clutter, which we fit to real data is a critical parameter in our analysis. It is only the detailed spatial structure that is found to be relatively unimportant.

For the results that will be discussed later we will use a Gauss Markov model for the clutter:

$$C(|\vec{x}_1 - \vec{x}_2|) = \sigma^2 \mathrm{EXP}\left[-\sqrt{\left(\frac{\Delta x}{x_0}\right)^2 + \left(\frac{\Delta y}{y_0}\right)^2 + \left(\frac{\Delta z}{z_0}\right)^2}\right]$$

where σ^2 is fit to real data, and (x_0, y_0, z_0) are the correlation scale lengths in the different directions. The new designs have specifically been chosen to mitigate the effects of clutter in a manner that is sensitive to both signal and noise considerations. The absolute performance estimates are critically dependent on clutter strength; the relative performance for the designs presently under consideration are somewhat insensitive to clutter scale lengths. This seemingly counter-intuitive result does indeed make good physical sense. All of the new designs attempt to optimize signal while rejecting clutter on the scale lengths other than the spatial scales of the signal. The correlation scale lengths in the clutter model, (x_0, y_0, z_0), adjust the relative amount of clutter in the different spatial scales, target scale lengths *vs.* non-target scales, and thus the overall performance is affected. All of the designs chosen are reasonably effective at rejecting clutter on scales other than target scale lengths. The overall performance is found to be more sensitive to the signal and noise efficiency with which this primary clutter rejection is performed, rather than the detailed shape of the clutter rejection and its interaction with the shape of the clutter model. There are designs where the detailed clutter shape and clutter rejection patterns are critical to performance, but these designs tend to be very high performance designs where we are attempting to very precisely notch the response of the detectors to the signal, relative to the clutter, and are not realizable physically within the context of an airport and luggage environment.

The next important ingredient for the TNASIR analysis is the machine's response to a given distribution of nitrogen. The actual response is a very complicated function of detector geometry, source effects, cavity configuration, and unfortunately the luggage nitrogen content (and other elements). We assume that the machine response only depends on the detailed machine configuration, and an average bag elemental content. This is a linearization of the TNA system response for an average bag. The TNASIM model provides the complex response functions for each detector where a measurement in the ith detector is described by:

$$M_i = \int W_i(\vec{x}) S(\vec{x}) d\vec{x} + n_i$$

$$\langle M_i \rangle = \mu \int W_i(\vec{x}) d\vec{x}$$

where $W_i(\vec{x})$ is the detailed system response provided by TNASIM, and n is the noise estimated for the detector.

are fit to a parametric model of the form:

$$\langle n_i \rangle = 0$$

$$\langle n_i^2 \rangle = NF_i \langle M_i \rangle + \Gamma_i$$

where the ⟨Mi⟩ is the mean clean bag measurement, NF is noise figure for a given detector, and Γ is a noise floor, or dark current. The estimate for the parameters in the noise model are provided by a fit to existing data, and from estimates from TNASIM. The TNASIR calculations have identified these noise models as an area in need of further calibration, and a measurement program to improve our knowledge in this area is under way. The noise performance of the present system is well understood, although there is at present some uncertainty with regards to noise and interference effects for many of the paper designs.

Assuming an additive target we can now construct the expected value of a measurement in the absence of a bomb, the H0 hypothesis, and in the presence of a bomb described by the parameters $\vec{\alpha}$, the H1 hypothesis.

$$\langle \vec{M} | H0 \rangle = \mu \int \vec{W}(\vec{x}) d\vec{x} = \langle \vec{M} \rangle_0$$

$$\langle \vec{M} | H1(\vec{\alpha}) \rangle = \langle \vec{M} \rangle_0 + \int \vec{W}(\vec{x}) B(\vec{x}, \vec{\alpha}) d\vec{x}$$

where $B(\vec{x}, \vec{\alpha})$ is the spatial distribution of nitrogen for a threat with the parameters $\vec{\alpha}$. The parameters $\vec{\alpha}$ describe the width, position, and nitrogen content of a chosen threat. We will choose to work with mean removed measurements for the remainder of the analysis.

$$\langle \vec{M}' | H0 \rangle = \langle \vec{M} | H0 \rangle - \langle \vec{M} \rangle_0 = 0$$

$$\langle \vec{M}' | H1(\vec{\alpha}) \rangle = \langle \vec{M} | H1(\vec{\alpha}) \rangle - \langle \vec{M} \rangle = \hat{B}_{\vec{\alpha}}$$

where $\hat{B}_{\vec{\alpha}}$ is the bomb observable. Based upon the previous assumptions we now estimate the measurement covariance to be:

$$\langle M_i' M_j' \rangle = \iint W_i(\vec{x}_1) W_j(\vec{x}_2) C(|\vec{x}_1 - \vec{x}_2|) d\vec{x}_1 d\vec{x}_2 + \delta_{i,j} \langle n_i^2 \rangle$$

The last term is the noise term, which is uncorrelated from detector to detector.

that is normalized by both the noise and clutter correlations. This "half whitened" measurement is:

$$\vec{R} = A^{-T} \vec{M}' = A^{-T} \left(\vec{M} - \langle \vec{M} \rangle_0 \right)$$

where $A^T A$ is the Cholesky decomposition of the measurement covariance. In these coordinates the statistics of the observables are:

$$\langle \vec{R} | H0 \rangle = 0$$

$$\langle \vec{R} | H1_{\vec{\alpha}} \rangle = A^{-T} \hat{B}_{\vec{\alpha}} = \eta_i(\vec{\alpha})$$

$$\langle \vec{R}^T \vec{R} \rangle = I$$

This implies that these new "half whitened" measurements are uncorrelated and of unit variance. In these new coordinates the SIR is calculated as:

$$SIR = \sum_i \left(\eta_i(\vec{\alpha}) \right)^2$$

The calculation of the Fischer information matrix is greatly simplified in this new coordinate system:

$$J_{m,n} = \sum_i \frac{\partial \eta_i(\vec{\alpha})}{\partial \alpha_m} \cdot \frac{\partial \eta_i(\vec{\alpha})}{\partial \alpha_n}$$

The Crammer Rao bound implies that the error variance for an estimate $\hat{\alpha}_m$ of the parameter α_m is bounded below by:

$$\text{Variance}(\hat{\alpha}_m - \alpha_m) \geq J^{-1}_{m,m}.$$

An excellent reference for this material is provided by *"Detection, Estimation, and Modulation Theory"* (Van Trees, 1968).

We will now discuss some selected results from the above described analysis. Figure 2 shows the SIR for the twenty-eight candidate system designs. Design case number 1 is our model for the baseline machine. The estimated 10 dB performance can be compared to the 8 dB of performance displayed in

Figure 1 for winter international luggage with some caution. The clutter and the threat level for the TNASIR analysis has been calibrated to this winter international case. The performance displayed in Figure 1 is an average over threats and positions within the bag. Figure 2 displays the performance for a bulk threat, in the center of the luggage. Within the context of these limitations, the 2 dB spread in performance between actual and predicted is quite good. When this analysis is repeated for reduced threat levels the model predictions and experiments observations again provide good agreement.

The present analysis does not take into account performance loss due to a less than idealized processor. For example, one hundred measurements each of a signal to noise ratio of 1/10, are valued equal to a single measurement of signal to noise 10. This is unrealistic since engineering limitations conspire to make it difficult to accumulate many very small measurements for a detection. Figure 3 displays two estimates of SIR for each candidate design. The first "SIR - Threshold = 0.0" is the same plot as Figure 2. The second trace, "SIR - Threshold = 0.1", only accumulates individual measurements with a SIR greater than the threshold of 0.1 to the total system SIR. Though qualitative, this incorporates some measure of anticipated systematic errors from real world concerns. Notice that many of the candidate designs are significantly more robust to this measure than the baseline machine.

Figure 4 displays the rms estimation error for each of the candidate designs, for one of the intrinsic bomb parameters. In this case we display the average rms error for the estimation of the width of the explosive cube relative to an arbitrary baseline. This second order measure of performance is an important qualitative measure of the specificity and robustness a particular machine design has against a specific threat. These error measures may also become important for algorithms that estimate parameters for each detection, in an effort to mitigate false alarms.

Figure 5 provides an estimate of the TNA EDS performance in the absence of clutter. One of the authors has often suggested that passenger luggage should be ground to a uniform slurry before the addition of an explosive. We see that this practically difficult proposal would provide for a 9 dB performance improvement. Note that a 9 dB performance improvement roughly corresponds to the difference in the present performance of 90% P_d with a false alarm rate of one in ten (winter International), to a 98% P_d with a false alarm rate of one in ten thousand. A very important conclusion must be drawn from this result: If performance and analysis for the FAA explosive detection program are performed without specific, detailed inclusion of effects of luggage clutter, the results have little applicability to the real threat.

6. CONCLUSIONS

The conclusions that we look forward to making as this program matures, are that the optimized design chosen from the TNASIM/TNASIR modeling effort meets or exceeds the FAA performance requirement for reduced threat, and that our systematic design effort is capable of predicting TNA EDS performance for paper designs. The preliminary indications are encouraging, but much work is still to be done. The models predict an absolute performance for the reference system of 10 dB, which is to be cautiously compared to the observed 8 dB performance. The real test will be to demonstrate the 5 dB overall performance improvement for our soon to be made design selection.

One important conclusion can be drawn from the present analysis, and operational experience. All performance analysis for TNA EDS must include specific calculations for clutter effects to have any validity for airport performance.

REFERENCE

Van Trees, Henry L. *Detection, Estimation, and Modulation Theory*, John Wiley & Sons, New York, 1968, 697 pp.

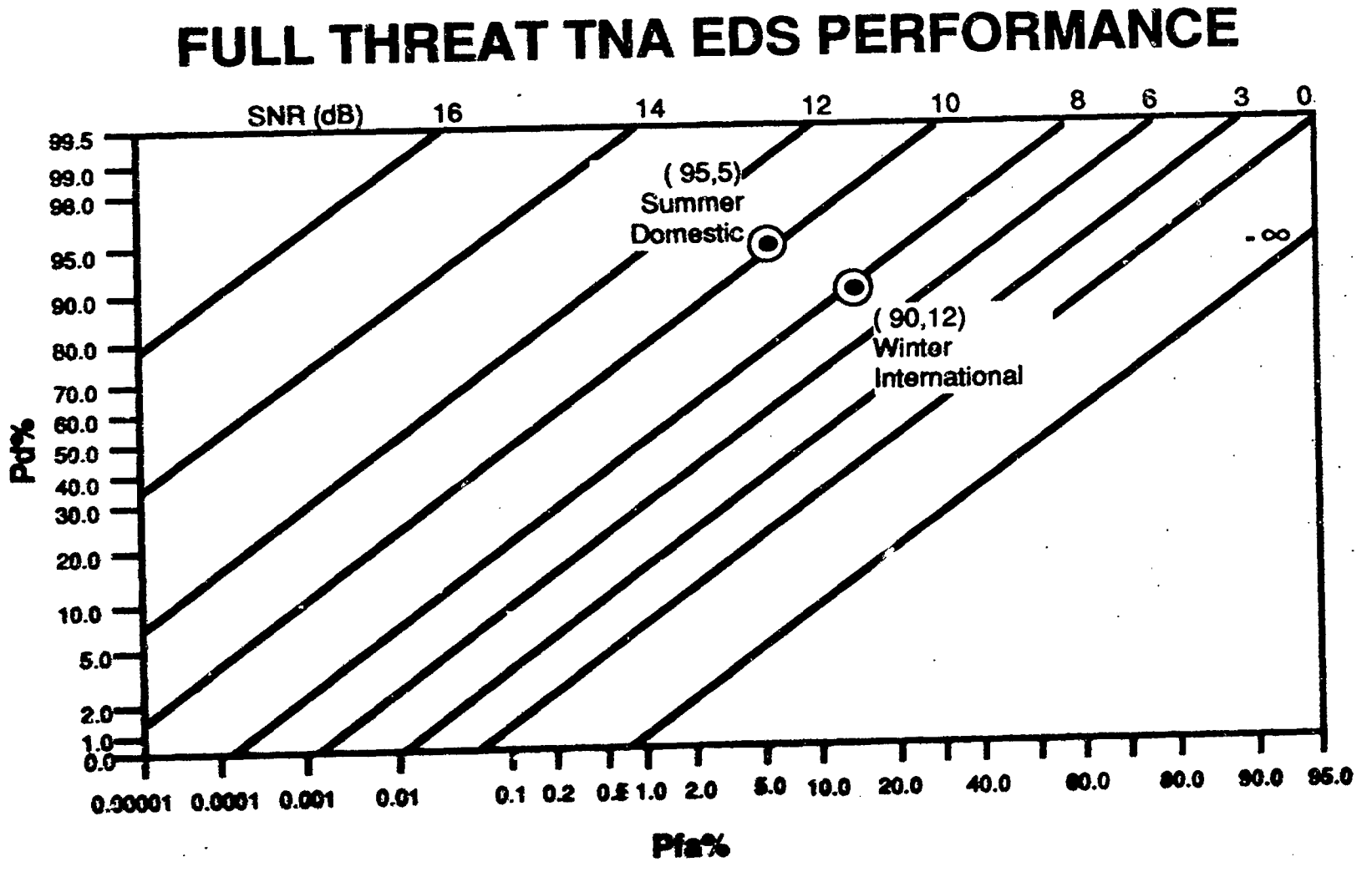


Figure 1 **Full Threat TNA EDS Performance**

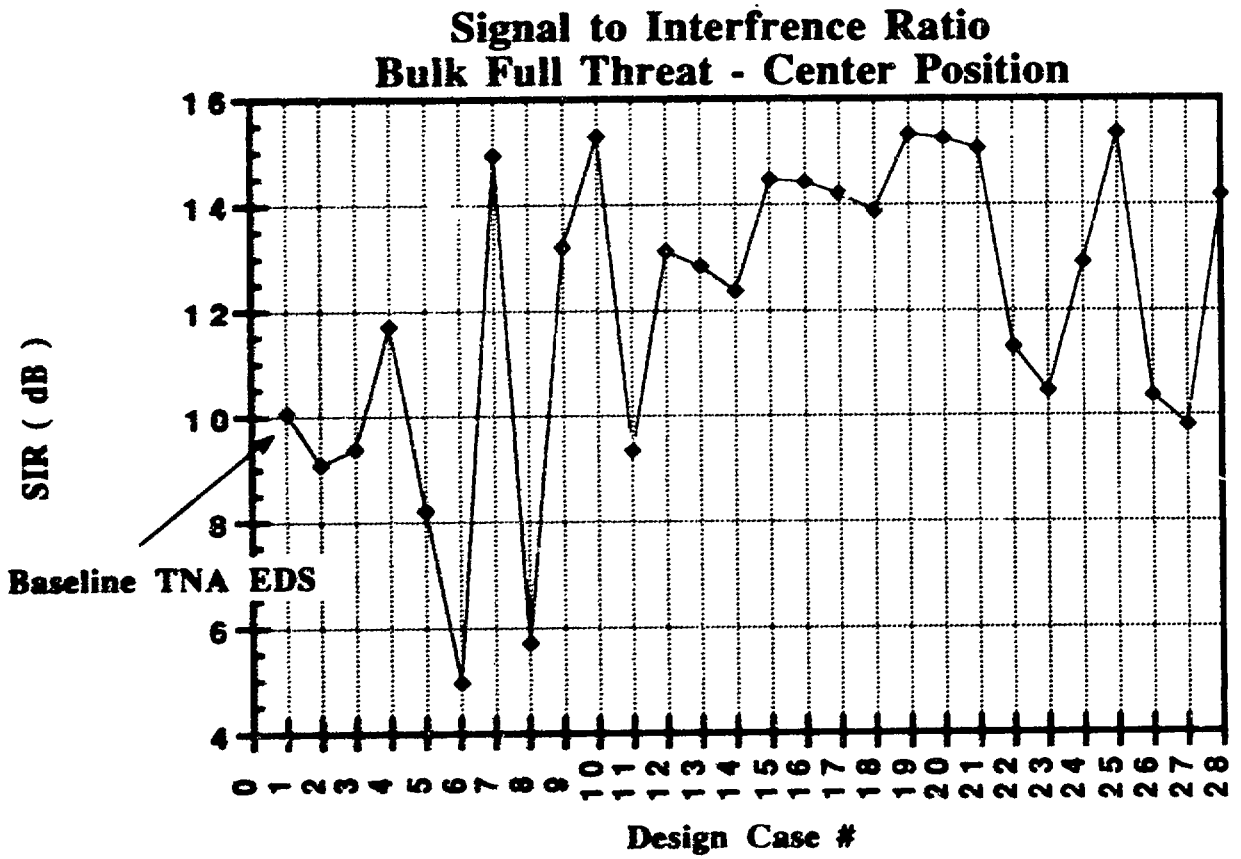


Figure 2 **Signal to Interference for Bulk Full Threat**

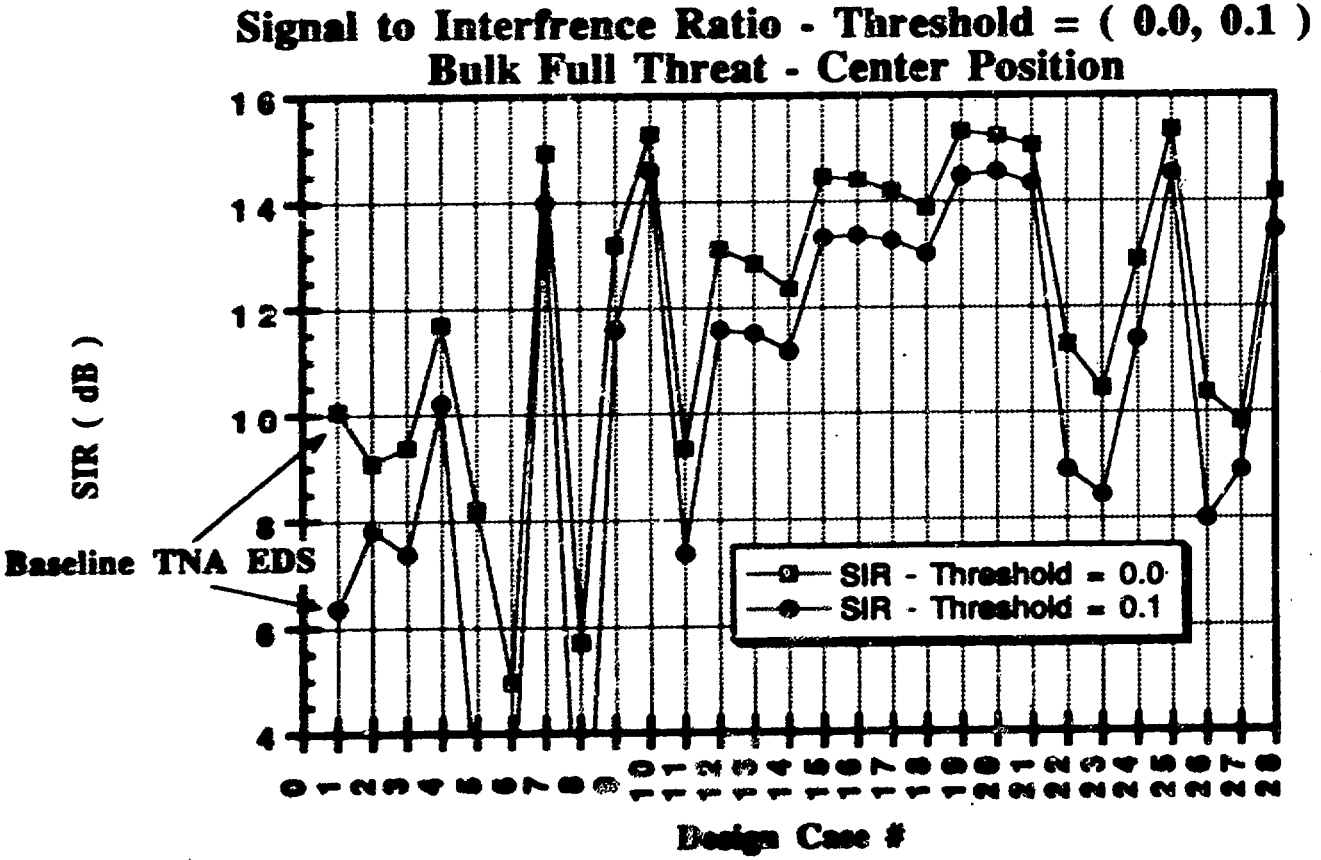


Figure 3 **Signal to Interference - Threshold (0.0, 0.1) for Bulk Full Threat**

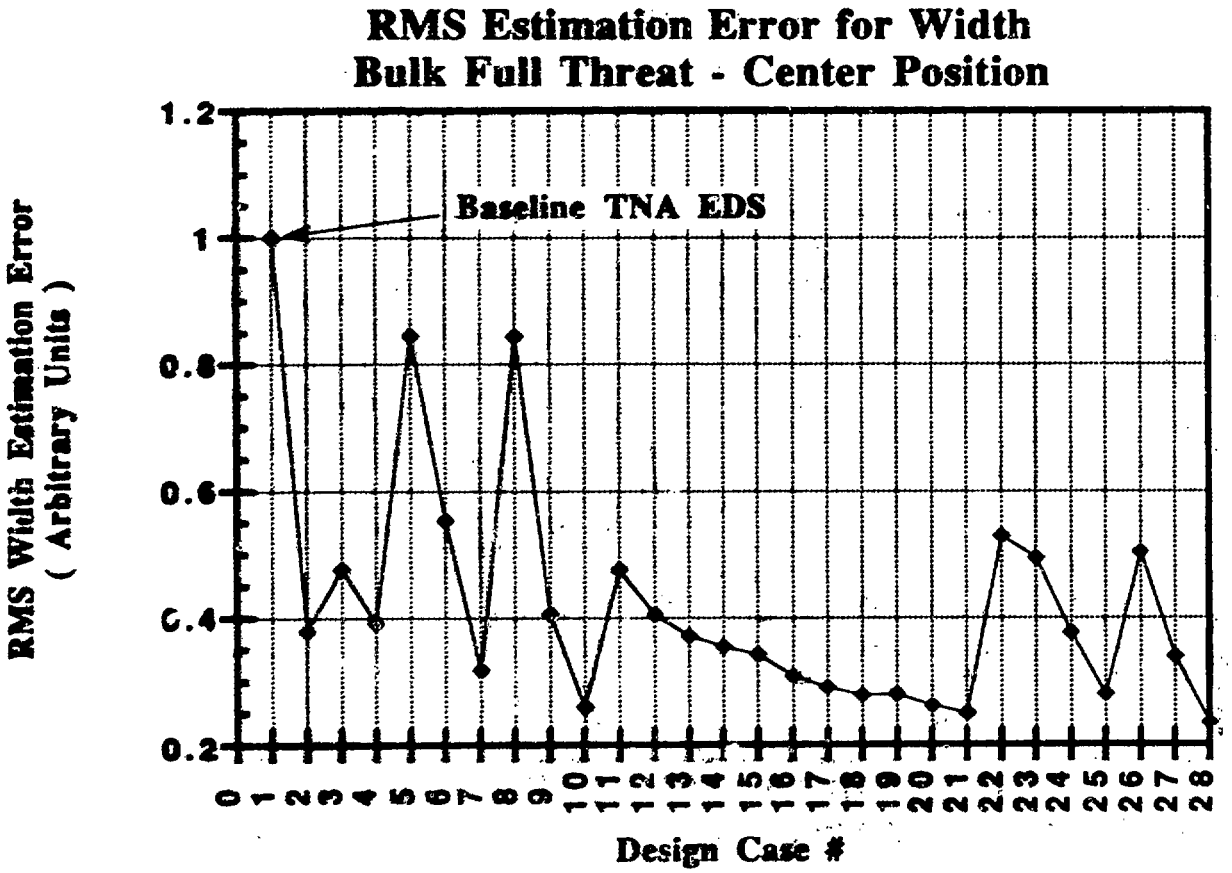


Figure 4 **RMS Estimation Error for Width**

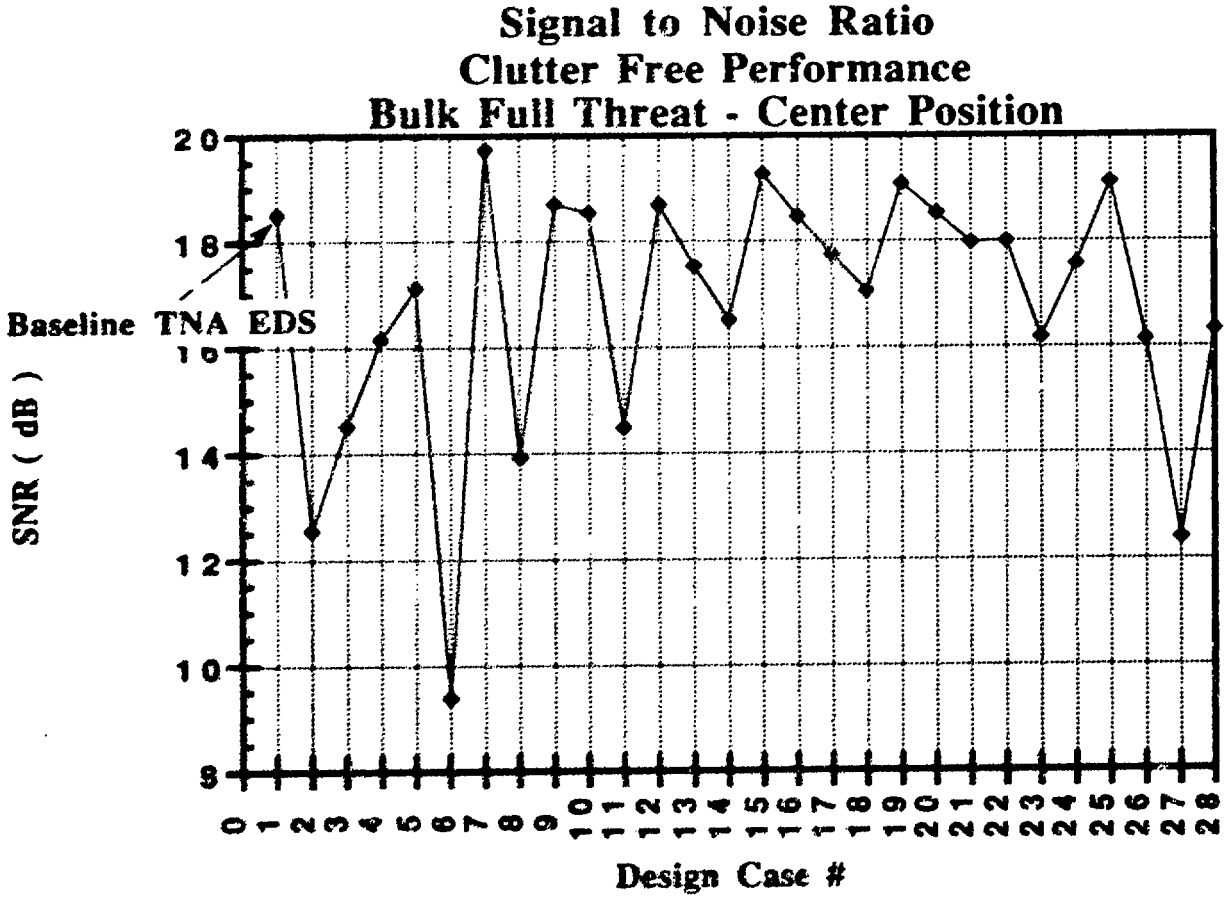


Figure 5 Signal to Noise Ratio, Clutter Free Performance

PFNA TECHNIQUE FOR THE DETECTION OF EXPLOSIVES

Zdzislaw P. Sawa and Tsahi Gozani
Science Applications International Corporation
2950 Patrick Henry Drive
Santa Clara, CA 95054

1. INTRODUCTION

Techniques for detecting chemical explosives in passenger luggage must be capable of unequivocally and rapidly identifying the threat in the luggage with a negligible rate of false alarms. This can be achieved by using nuclear radiations for a non-intrusive measurement of the chemical composition, including mapping of elements of the contents of luggage. Nuclear techniques have been used for a long time to measure chemical compositions. This paper describes a method of detecting explosives, based on the gamma-ray spectrometry in inelastic scattering of pulsed fast neutrons. This interaction leads to excitation of low-lying energy states of nuclei of all the elements of importance in explosives. The underlying nuclear technique is rather well understood and was developed in 1960-70 for studies of nuclear structures. The elemental compositions of explosives have a unique feature: a concomitant high content of nitrogen and oxygen in addition to hydrogen and carbon. This distinctiveness of explosives facilitates their detection in the presence of benign materials in the luggage by using time-of-flight gamma-ray spectrometry, which is at the core of the PFNA-technique conceived by SAIC in 1987[1]. The high contents of nitrogen and oxygen can be demonstrated most graphically (see Figure 1) by plotting a discriminant, which is the product of the masses (in g) of nitrogen and oxygen in 1 cm^3 of the explosives and in 1 cm^3 of the various common materials. It should be mentioned that other discriminants can also be useful in diagnosing explosives, for example, the ratio of the mass of oxygen to that of carbon in a given small volume. These and other discriminants can be used simultaneously to improve the detection probability and its specificity (i.e., one minus the false alarm probability) of explosives and/or narcotics.

A short description will be given in this paper of the concept underlying the PFNA technique. Also, some results will be presented of the ongoing extensive experimental program at SAIC in support of the PFNA technique development and engineering.

2. BASICS OF PFNA EDS

Science Applications International Corporation is presently developing an Explosives Detection System (EDS) which employs Pulsed Fast Neutron Activation (PFNA) for interrogation of passengers' airport check-in luggage. The irradiation of luggage with fast neutrons of sufficient energy and the measurement of the ensuing prompt gamma-ray spectra provide suitable means for an effective search of concealed explosives. It is based on the measurement of densities of carbon, nitrogen, oxygen, and chlorine in Voxels of Interest (VOI), i.e., small volume elements of the interrogated object (see Figure 2). The signatures of the oxygen (^{16}O), carbon (^{12}C), nitrogen (^{14}N), and chlorine ($^{35,37}Cl$) will occur in the gamma-ray spectra as lines, i.e., peaks, of intensities corresponding to the densities of O, N, C, Cl in the various VOIs. Pulsed neutrons of energy < 8.0 MeV, generated by the d+D reaction, are used in the current version of the PFNA. The pulsing of the neutron-producing deuteron beam provides short bursts of neutrons, facilitating the measurements of the gamma-ray spectra in well defined time intervals (time windows). The time distribution of events is obtained by measuring the total time elapsed between the creation of the neutron burst in the D target and the production of the gamma rays and their subsequent detection in the gamma-ray detector, e.g., NaI(Tl) crystal. By closing the window for spectral data acquisition when the neutron burst produces gamma-rays in the shielding and/or structural materials or in the NaI(Tl) crystal, itself, the background is either greatly reduced or completely eliminated. It is then a straightforward matter to obtain gamma-ray spectra in the time windows corresponding to the string of

VOI along the path of neutrons across the suitcase. The size of the VOIs is determined by the lateral shape of the neutron beam, i.e. the pixel, as defined by a collimator, and the depth, which is defined mainly by the duration of the deuteron burst and the time resolution associated with electronics. The digitized spectral data form a T_γ x E_γ matrix, where T_γ and E_γ are the pulse heights of the measured time of event (i.e. time-of-flight) and the gamma-ray energy deposited in the NaI(Tl) crystal, respectively.

The backbone of the PFNA technique is the gamma-ray spectrometry. The prompt gamma-ray transitions that are induced in carbon, nitrogen, oxygen, and chlorine nuclei by fast neutrons are measured with NaI(Tl) detectors. These detectors provide a good sample interrogation rate and satisfactory energy and time resolution for the detected photons. The measurement of the intensities of the fingerprint gamma-ray lines of explosives require that the measured gamma-ray spectra will consist of well resolved peaks. Though one can use higher energy neutrons, it was found analytically and corroborated experimentally that the energy of the bombarding neutrons should be well below 10 MeV in order to obtain high spatial resolution, strong and sufficiently resolved gamma-ray fingerprint peaks, while keeping the background and the radiological hazard low.

In the PFNA fingerprint lines of C, N, O, and Cl are produced predominantly in the $(n,n'\gamma)$ processes, however additional weak fingerprint lines stem from the $(n,\alpha\gamma)$, and the $(n,p\gamma)$ processes. It should be mentioned that the $(n,n'\gamma)$ processes involving light nuclei and low energy of bombarding neutrons are associated with strong resonances, which is reflected in the cross sections of the production of the gamma-ray lines and in the angular distributions of the gamma rays. All these aspects have been carefully studied experimentally by SAIC, since the current evaluated neutron data files are incomplete or insufficient for the PFNA objectives. The origin of the fingerprint lines of C, N, O, and Cl is indicated in Figure 3. It shows the low lying energy levels in ^{12}C, ^{14}N, ^{16}O, and $^{35,37}Cl$ and the prompt gamma-ray transitions which are utilized as the fingerprint lines of explosives in the PFNA.

3. MEASUREMENTS OF CONCEALED EXPLOSIVES USING PFNA

Some experimental data obtained in a recent PFNA investigations, will be shown in this section. This investigation was carried out at the Tandem Dynamitron of the Applied Physics Division in the Argonne National Laboratory, Argonne, Illinois. The pulsed deuteron beam had ~1.2 ns burst duration at 2 MHz repetition frequency with a time-average intensity of $\leq 3\ \mu A$. The neutron beam spot size was adjusted with the help of a W-Fe-CH_2 collimator, which also served as a shadow shield between the target and the gamma-ray detectors. For purposes of diagnostics and monitoring of the neutron beam, plastic scintillators, mounted on fast PMT, were used. They provide for both time-of-flight (TOF) measurements of the energy and intensity of the neutrons. The timing of the signals from the NaI(Tl) and the neutron detectors was measured relative to the signals from the time pick-off electrode in front of the target. The neutron TOF pulse height spectra were measured using PC-based multichannel analyzers, while the T_γ x E_γ data, provided by an array of four NaI(Tl) detectors, were stored in the appropriately divided memory of a commercial 2-D pulse height analyzer. An example of the quality of the gamma-ray energy spectrum obtained with the PFNA technique during irradiation of a simulant of C-4 explosive is shown in Figure 4. The measurements of the gamma-ray energy and time spectra were monitored on-line using the 2-D displays, (T_γ x E_γ), and the E_γ or T_γ spectra in the preselected time or energy windows, respectively. The data were transferred to magnetic tapes for a subsequent off-line analysis. Some typical results of the measurements are shown in the Figures 5a through 9b, which demonstrate the diagnostic power of the PFNA regarding the concealed explosives, i.e., simulants of C-4 or Semtex. In each case the amounts of C-4 or Semtex simulants were small compared to the mass of explosive needed to destroy aircraft in flight. The irradiation times of the strings of VOIs were kept sufficiently short to mimic the realistic conditions for a PFNA EDS for the passenger luggage, i.e., requiring high interrogation throughput.

Of some interest is the case of a portable radio receiver (mass ~2 kg). The energy pulse height spectra shown in Figures 8a and 8b were measured when the battery compartment of the receiver was partially filled with Semtex simulant and when the batteries were reinstalled, respectively. Note that not only the concealed Semtex simulant was detected (e.g., nitrogen fingerprints) but also the chemical composition of the batteries was established: MnO_2 + ZnO_2.

The PFNA technique allowed for the mapping of all the relevant elements in the interrogated objects, as demonstrated in Figures 5b through 5e. These figures show the distributions of C, O, and N concentrations along a string of voxels (pixel size 6 x 12 cm^2) across a Samsonite suitcase filled with fabric in which a small cube of the C-4 simulant was embedded. This capability of the direct 3-D imaging of the distribution of light nuclei inside the sample is highly advantageous over the 2-D imaging power of the x-ray technique for the following reason: two different chemical compositions may have the same electron densities and therefore be indistinguishable by the x-ray technique. In other words, two chemicals with the same mass density have the same electron density even though the nuclei are different. In the PFNA the neutrons interact with nuclei and prompt them to emit the characteristic gamma rays.

4. PRESENT STATUS OF PFNA EDS FOR LUGGAGE

SAIC has acquired from the National Electrostatic Corporation a 9SHD-2 Pelletron accelerator that is providing a pulsed deuteron beam burst of duration <1 ns at FWHM with beam repetition frequency of 12 MHz and time average intensity ≥ 20 μA. The planned PFNA EDS investigations aim at finding an optimum for the configuration of gamma-ray and neutron detectors and for the neutron beam delivery. In the next step we will build a small-scale demonstration EDS that will consist of a suitcase conveyor and a reduced-scale gamma-ray detection system. Furthermore, a careful experimental study of the radiological aspects of the PFNA EDS in the airport environment is planned.

SAIC is involved in the feasibility study and design of PFNA systems also for large objects such as trucks and shipping containers.

It is recognized that the data acquisition system will be quite complex, necessitating, e.g., distributed data processing and requiring a great computing power for the decision making. The design of the electronics front-end boards (analog and digital) is complete and their in-beam tests are in progress.

ACKNOWLEDGMENTS

The contribution of Dr. Peter Ryge and the enthusiastic assistance of Messrs. Tom Merics and Kurt Fankhauser from the very beginning of the experimental phase of the PFNA is gratefully acknowledged. We extend our thanks also to Dr. John Stevenson, who conducted the recent part of experiments in ANL with support of Drs. Joseph Krivicich, Robert Loveman, James Clayton, Ms. Diane Hsiung, Mr. Willis Lee, and Mr. David Mahood.

The cooperation of the staffs of the Tandem Accelerator in the Lawrence Livermore National Laboratory and of the Tandem Dynamitron Accelerator in the Argonne National Laboratory is deeply acknowledged.

NOTES

[1]P. Sawa, T. Gozani, and P. Ryge, "Contraband Detection System using Direct Imaging Pulsed Fast Neutrons", U.S. and overseas patent pending.

*Project partially funded by FAA, Contract DTFA03-87-C-00043.

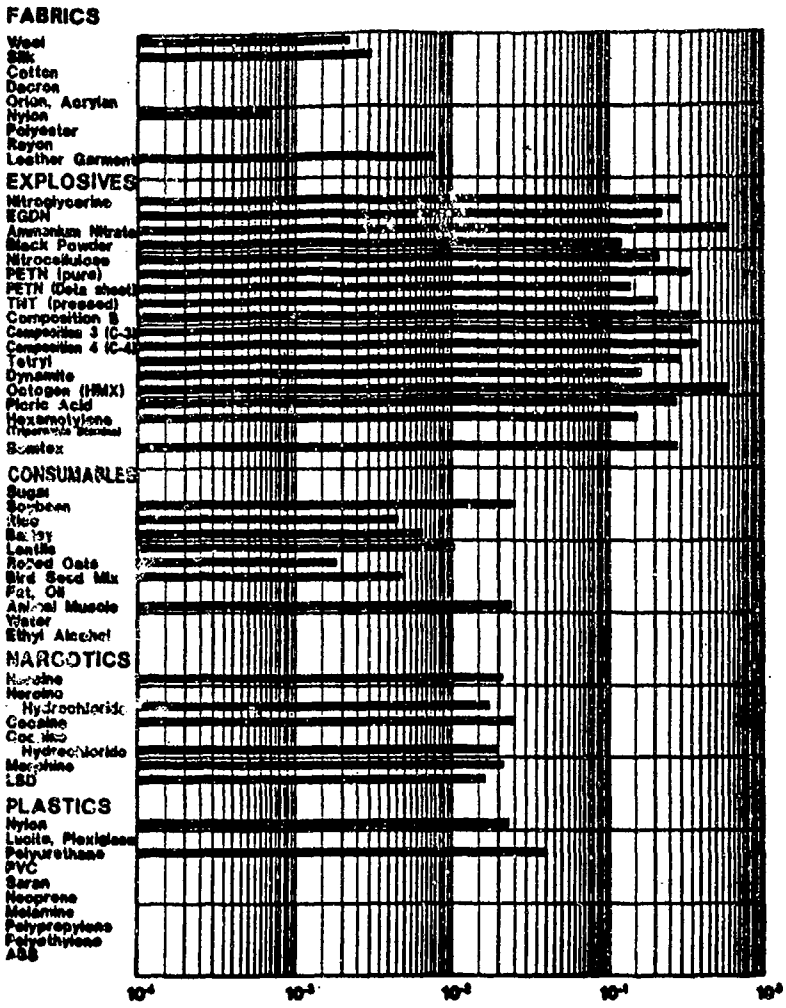


Figure 1 The product of nitrogen and oxygen densities in 1 cm^3 of explosives and of various common materials. The densities of the fabrics have been assumed to be .2 of the respective bulk materials. The density of the leather garment assumed .4 of the density of leather.

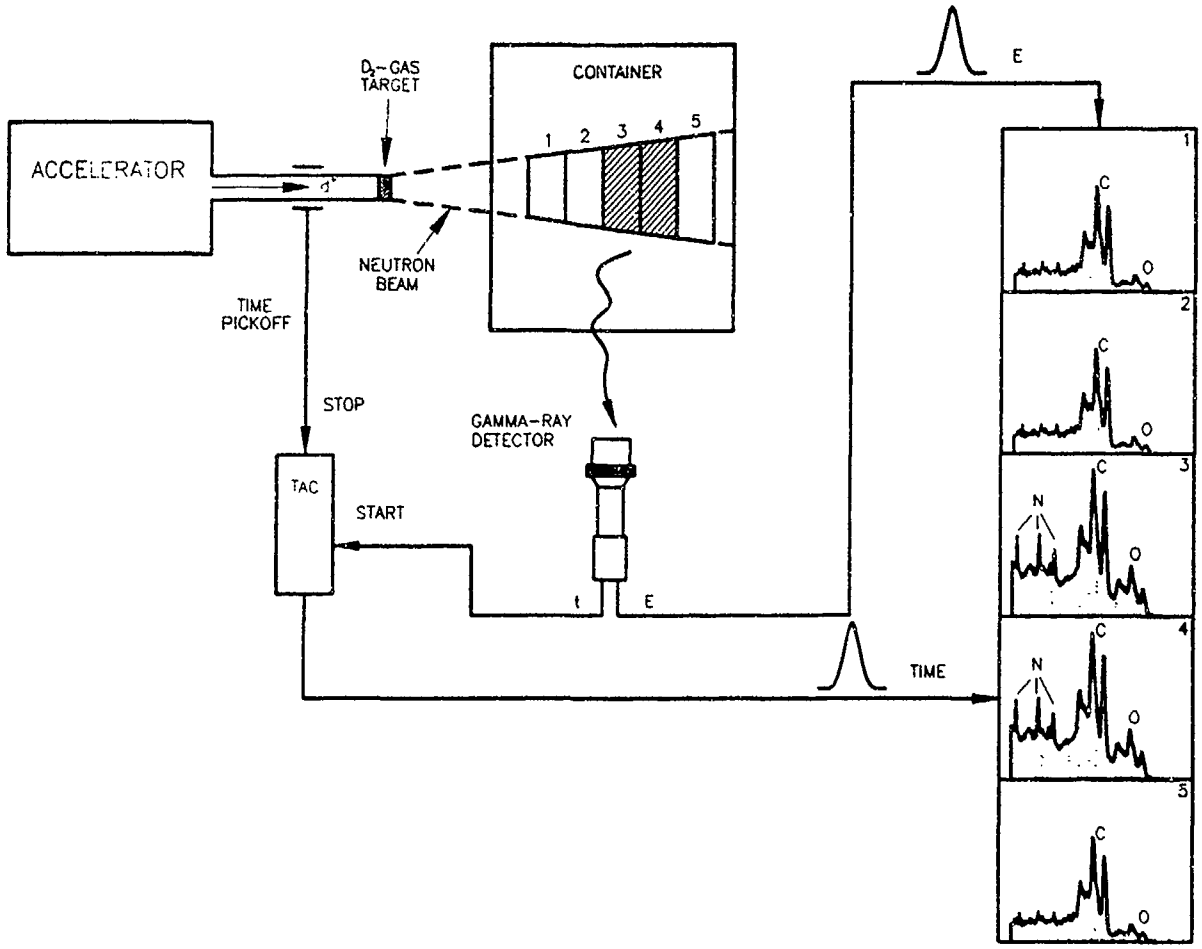


Figure 2 The principle of the detection of fingerprints of concealed explosives and of the direct imaging of densities of C, N, O, and Cl in the PFNA.

The five gamma-ray energy spectra shown on the right are viewed in the indicated five time windows which correspond to five Voxels of Interest (VOI) across the suitcase/container. VOIs 1, 2, and 5 are filled with fabrics, while VOIs 3 and 4 contain in addition C-4 simulant.

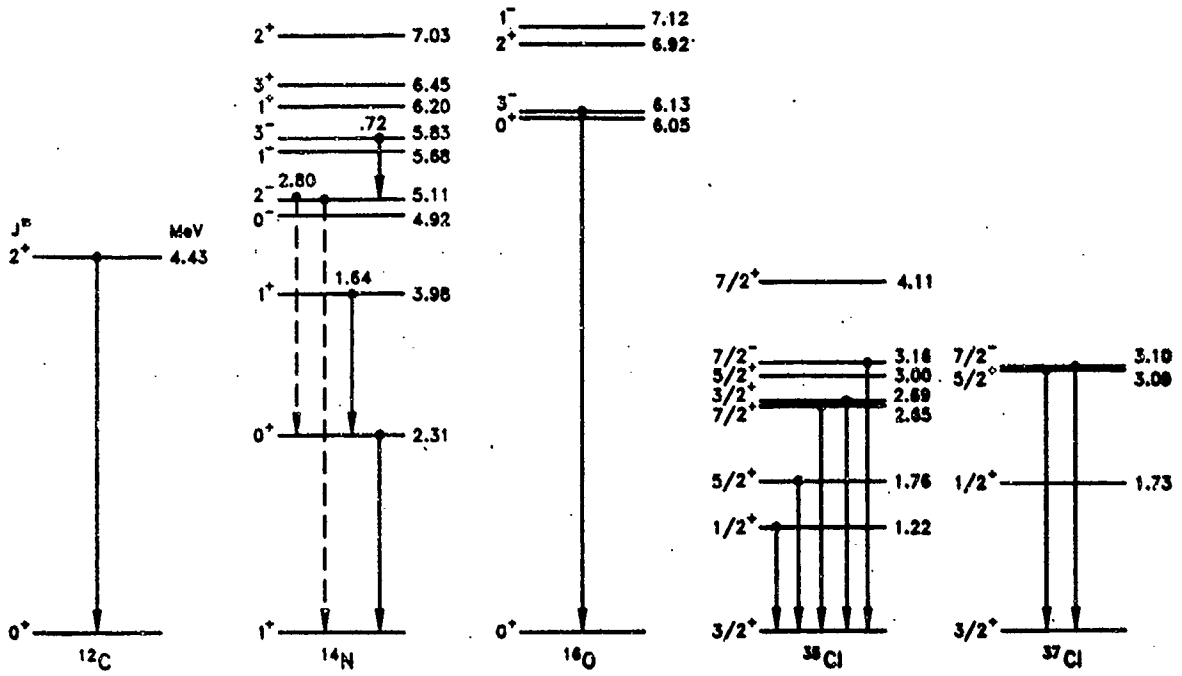


Figure 3 The nuclear energy levels in ^{12}C, ^{14}N, ^{16}O, and $^{35,37}Cl$ that decay by strong gamma-ray emission in the $(n,n'\gamma)$ processes induced by fast neutrons of $E_n \leq 8$ MEV. The main transitions employed in PFNA as the fingerprints of C, N, O, and Cl are indicated (bold lines).

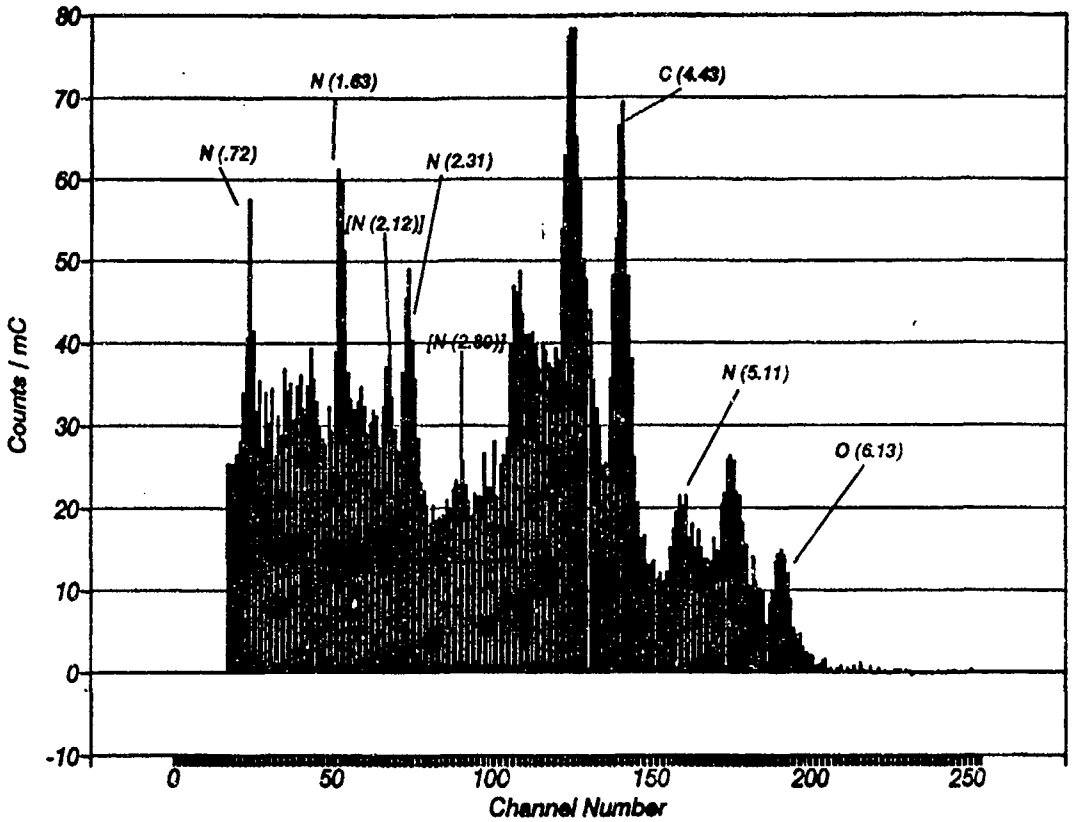


Figure 4 The gamma-ray energy spectrum measured with a NaI(Tl) detector for a small sample of C-4 explosive simulant. The fingerprint lines of ^{13}O (6.13 MeV), ^{12}C (4.43 MeV), and ^{14}N (.72, 1.63, and 2.31 MeV) are indicated. Also indicated are weak lines associated with ^{14}N (2.12, 2.80, and 5.11 MeV).

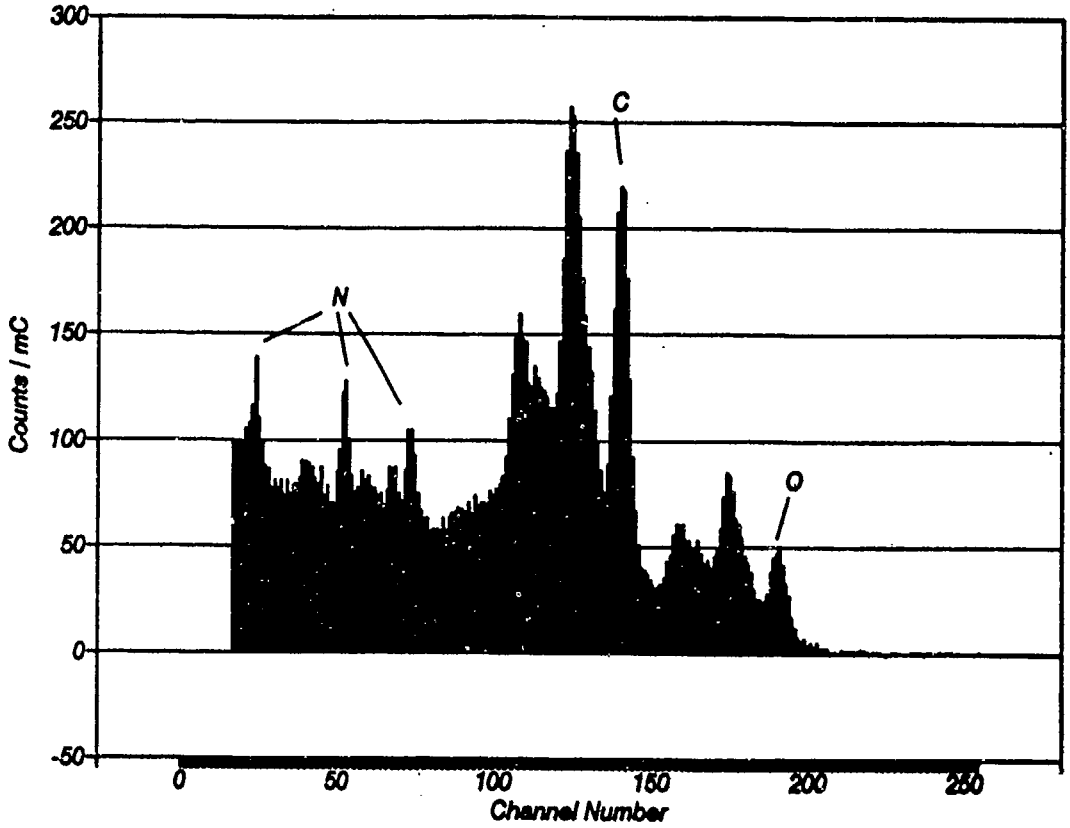


Figure 5a The gamma-ray energy spectrum measured for a VOI (V ~ 350 cm^3) in a Samsonite suitcase. The VOI contained a piece of suitcase lid, fabrics, and small amount of C-4 simulant.

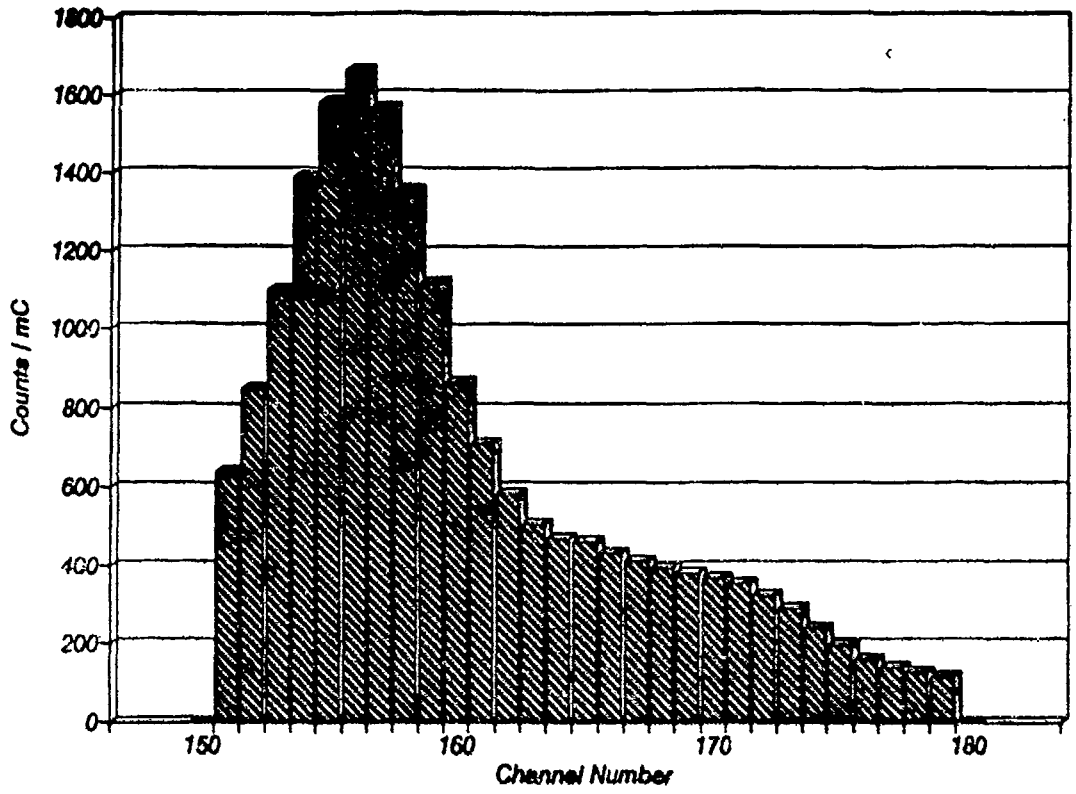


Figure 5b The time spectrum of gamma rays originating in a string of VOIs across the suitcase, refer to Figure 5a. The location of the C-4 simulant is clearly seen. (The location dispersion is ~ 1.0 cm/channel along the neutron beam.)

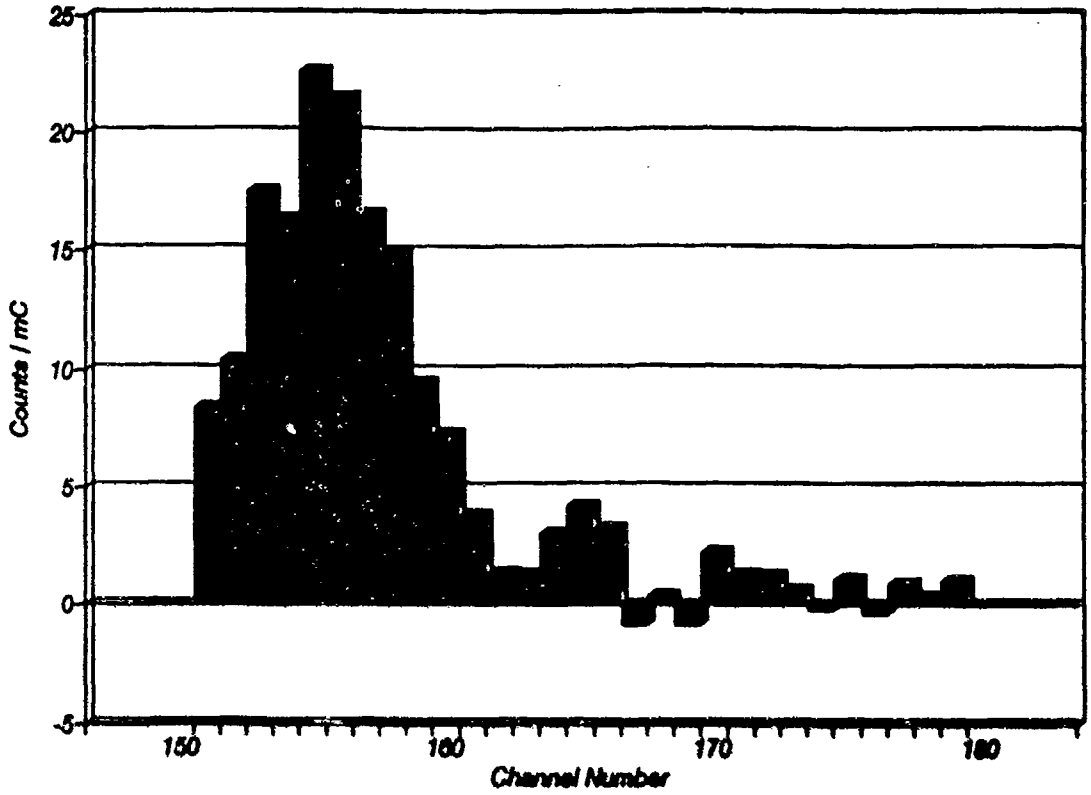


Figure 5c The nitrogen distribution (using the 2.31 MeV fingerprint) along the string of VOIs, refer to Figure 5b.

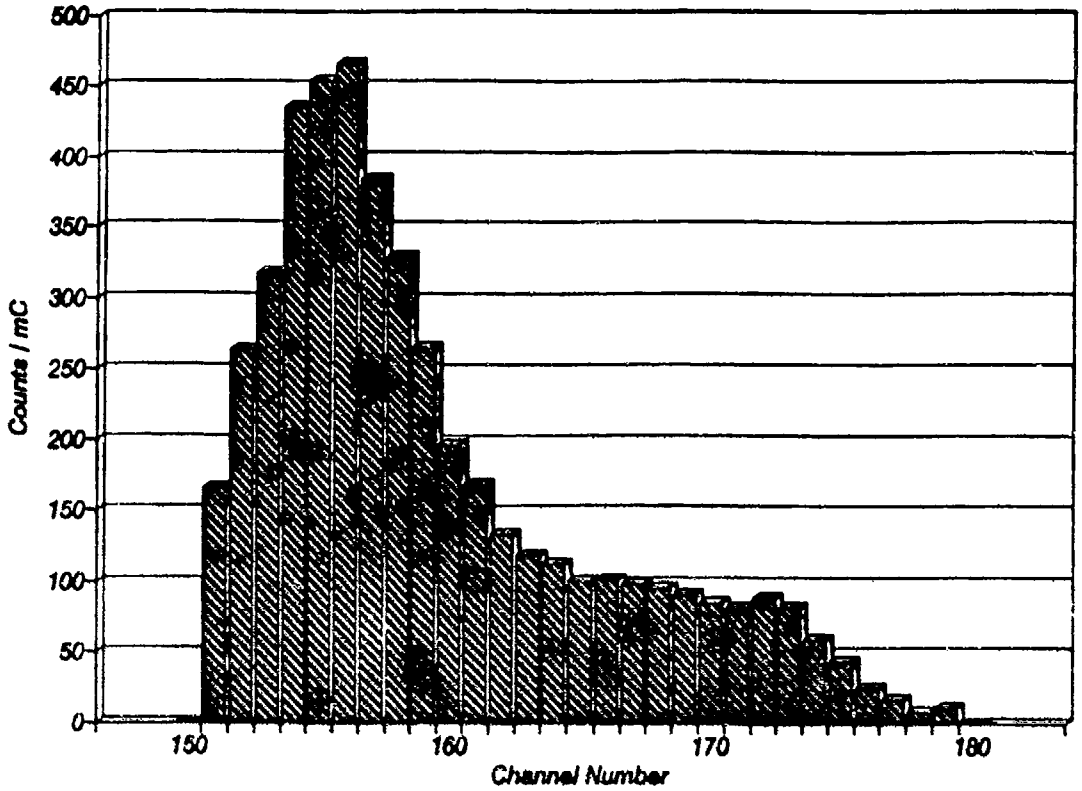


Figure 5d The carbon distribution, refer to Figure 5b.

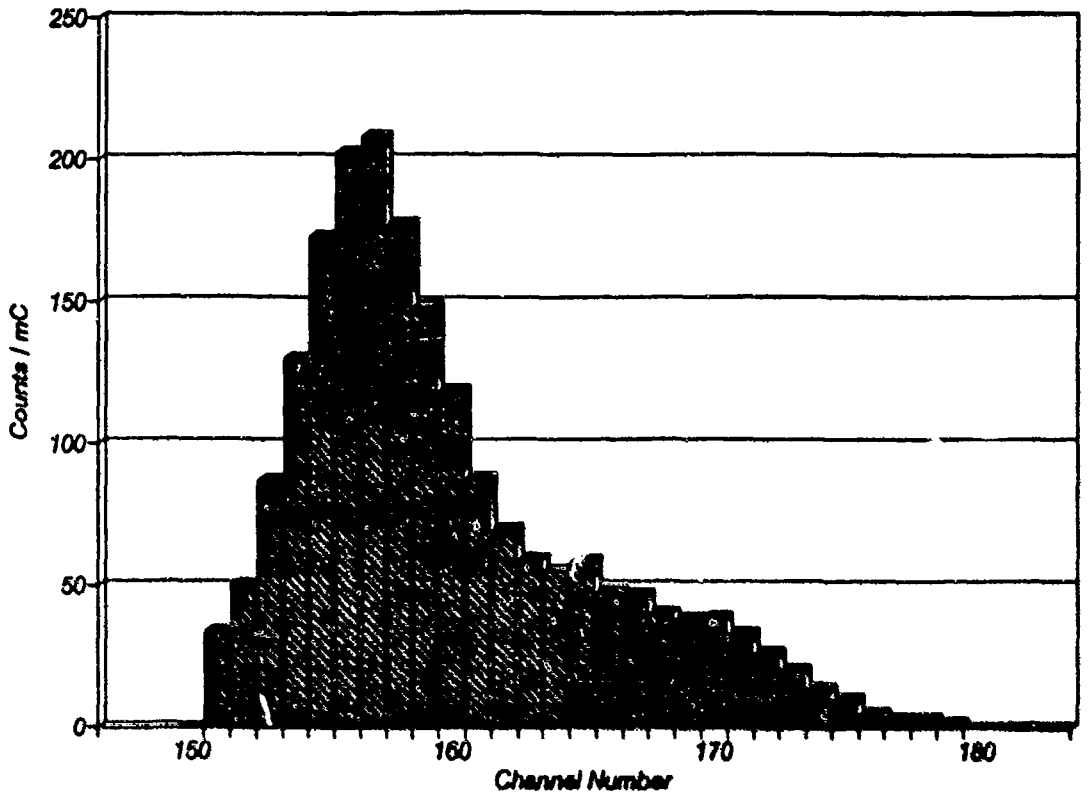


Figure 5e The oxygen distribution, refer to Figure 5b.

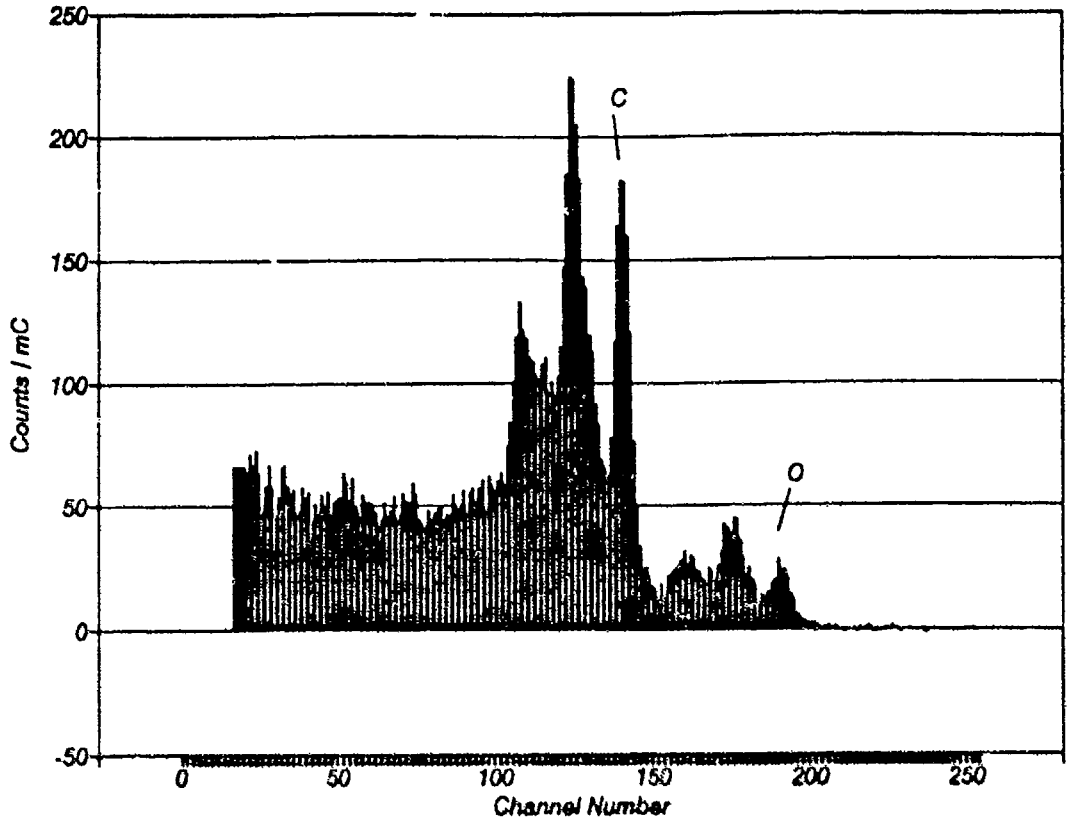


Figure 6a The gamma-ray energy spectrum measured for a Samsonite suitcase filled with fabrics only. The same VOI as in Figure 5a. Note the absence of the nitrogen fingerprints, and the lower intensity of the oxygen fingerprint, and low O/C ratio.

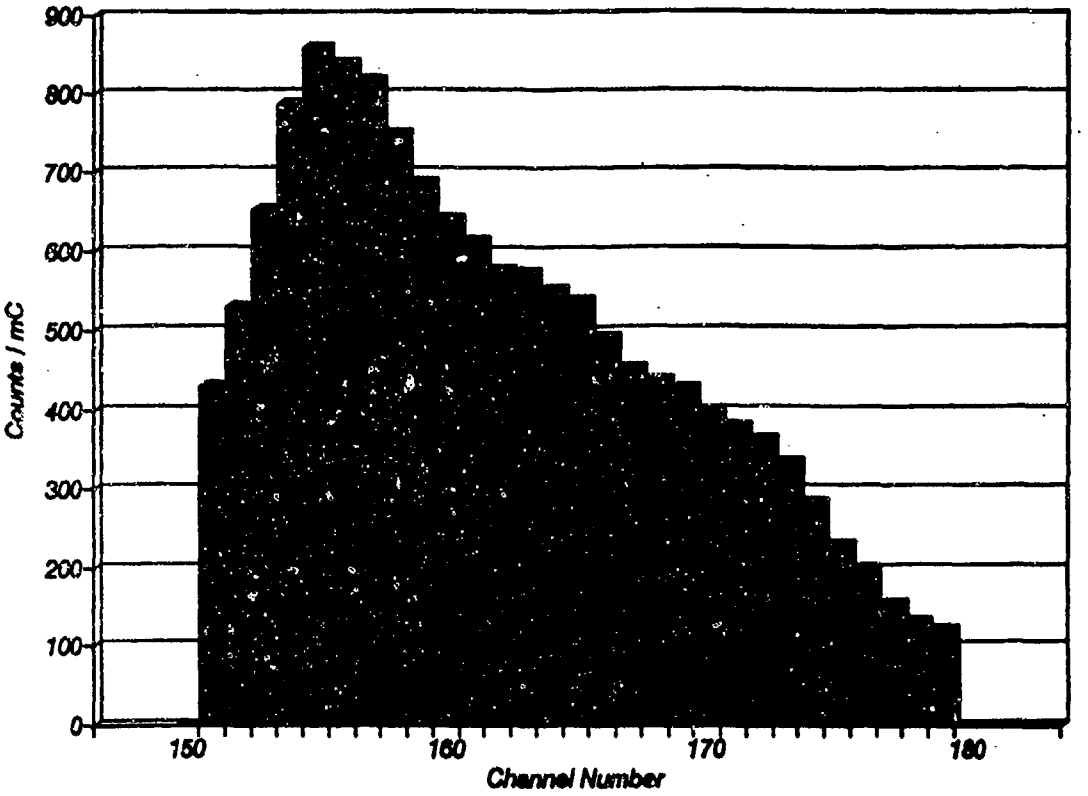


Figure 6b The time spectrum of gamma-rays originating in a string of VOIs across the suitcase, refer to Figure 6a.

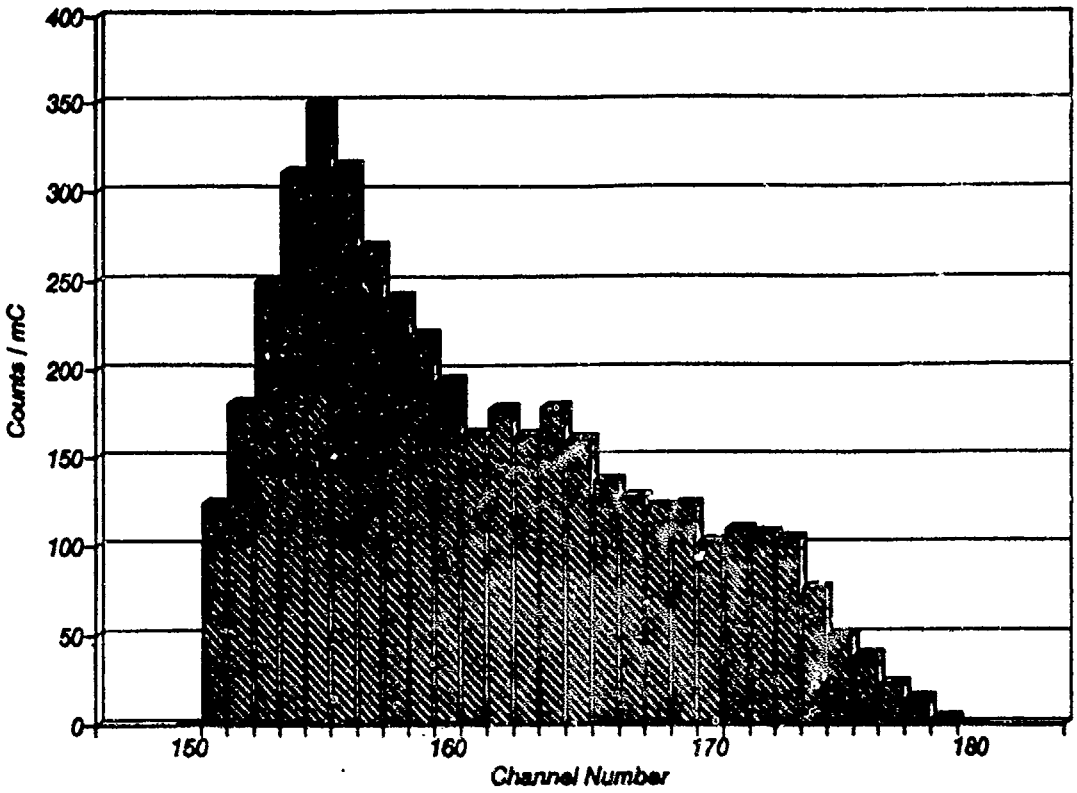


Figure 6c The carbon distribution, refer to Figure 6b.

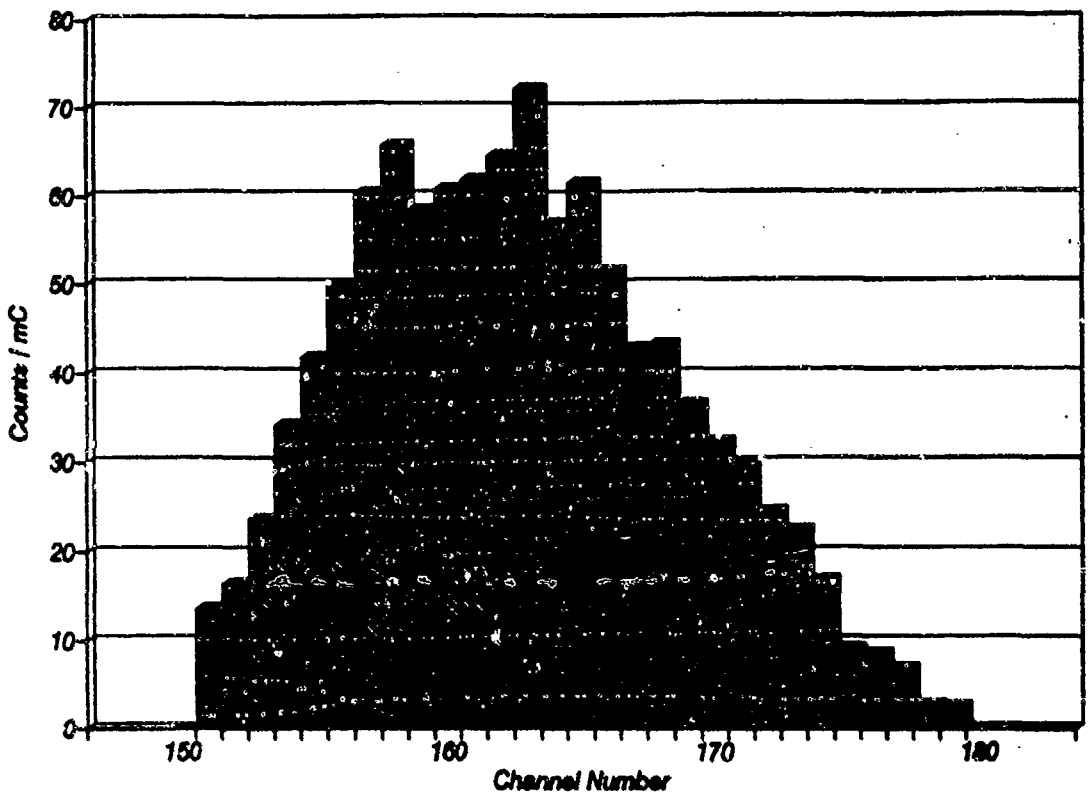


Figure 6d The oxygen distribution, refer to Figure 6b.

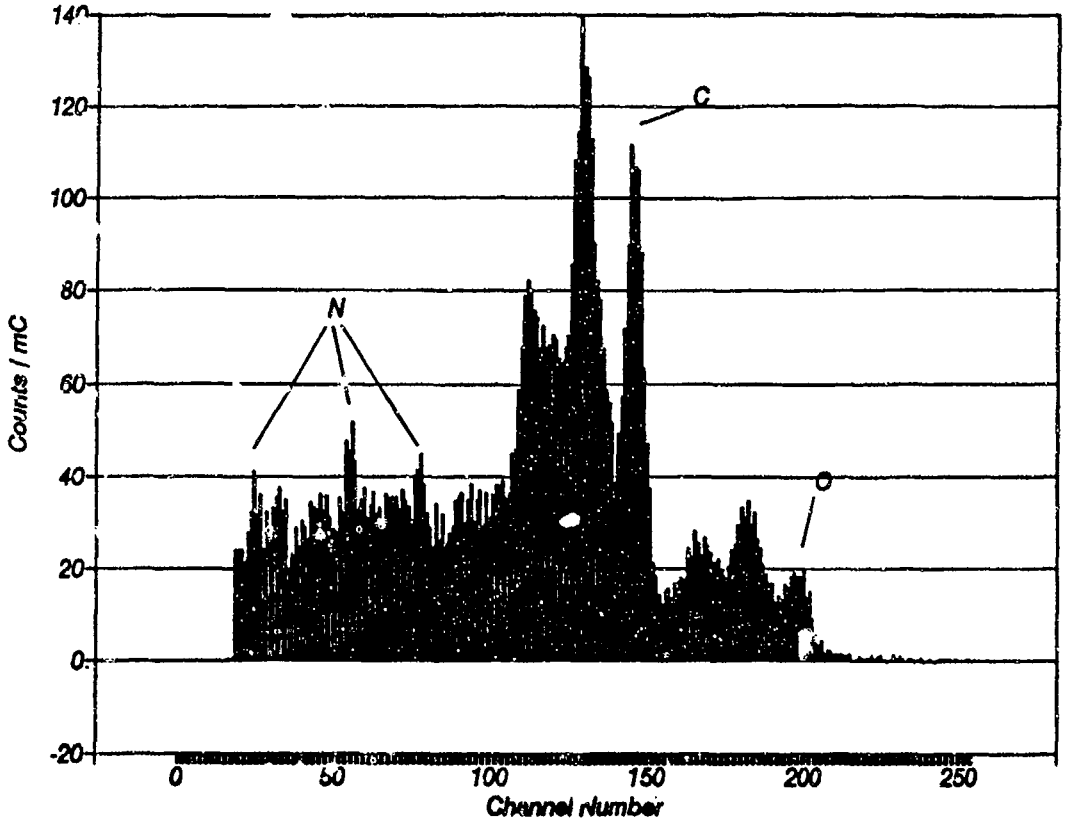


Figure 7a The gamma-ray energy spectrum for a deodorant-stick polymer wrapping filled with Semtex simulant.

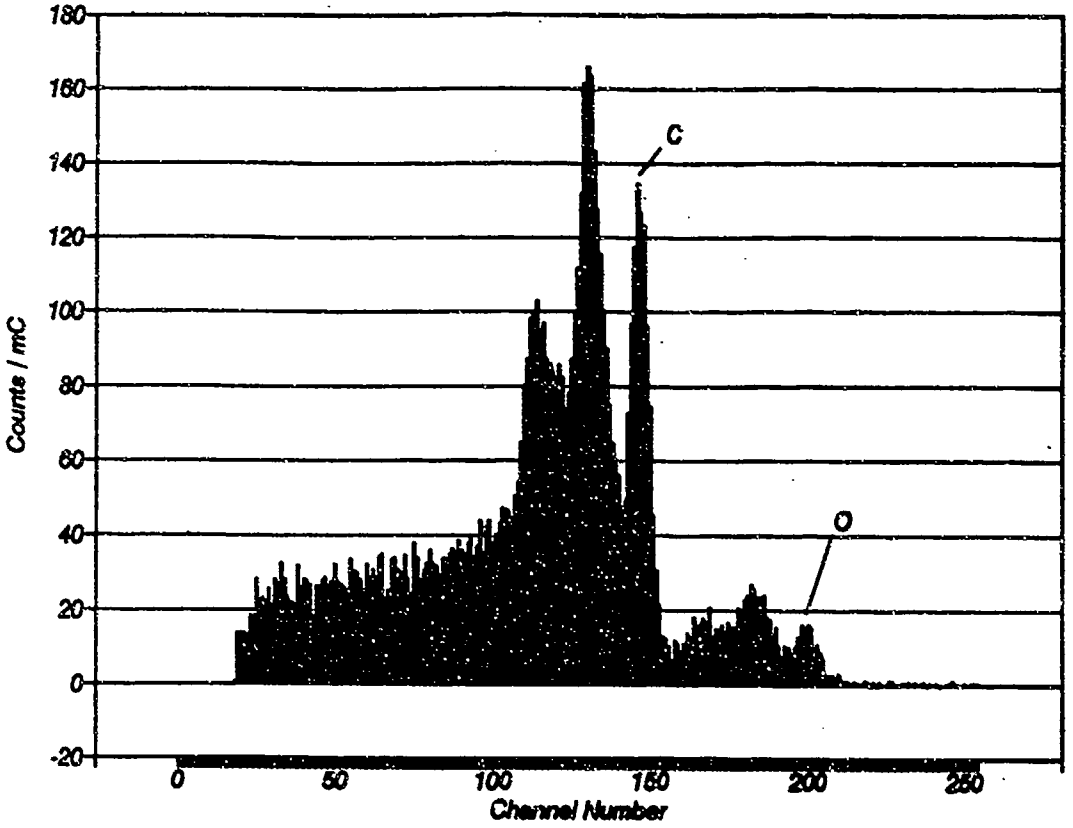


Figure 7b The gamma-ray energy spectrum for a genuine (w/o explosive) deodorant stick.

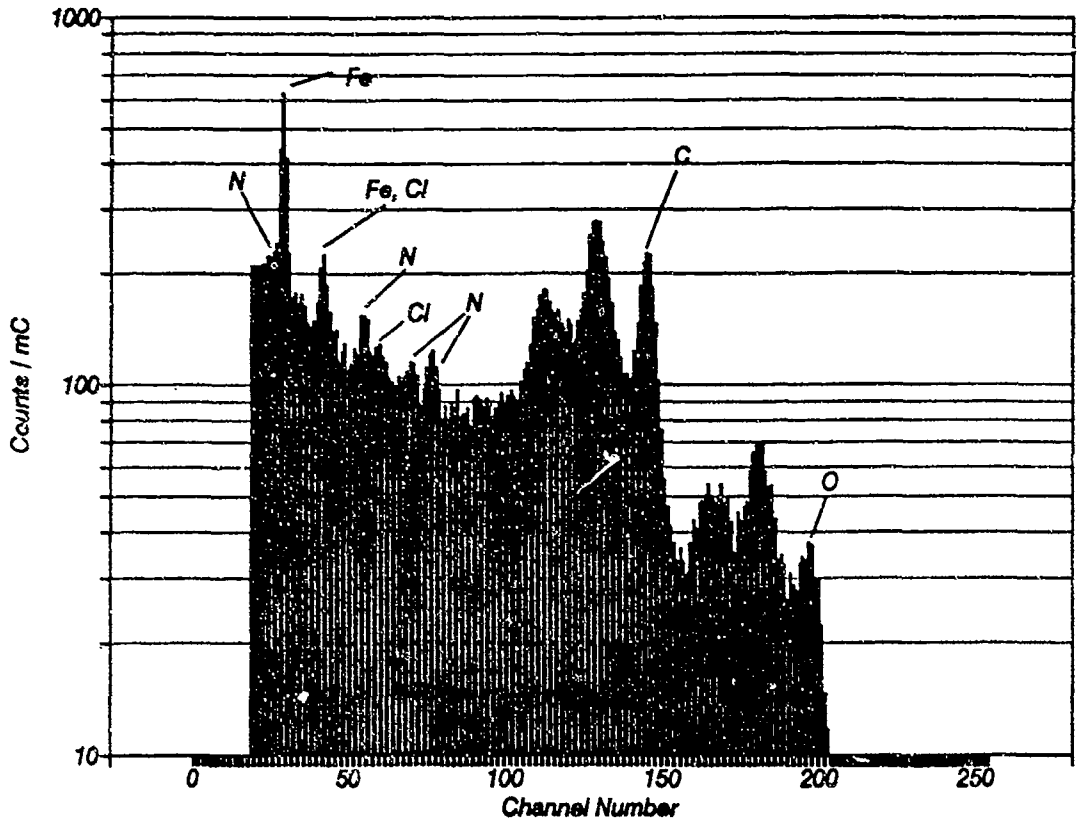


Figure 8a The gamma-ray energy spectrum for a portable radio receiver, battery compartment part of which was filled with the Semtex simulant. The VOI was centered on the battery compartment.

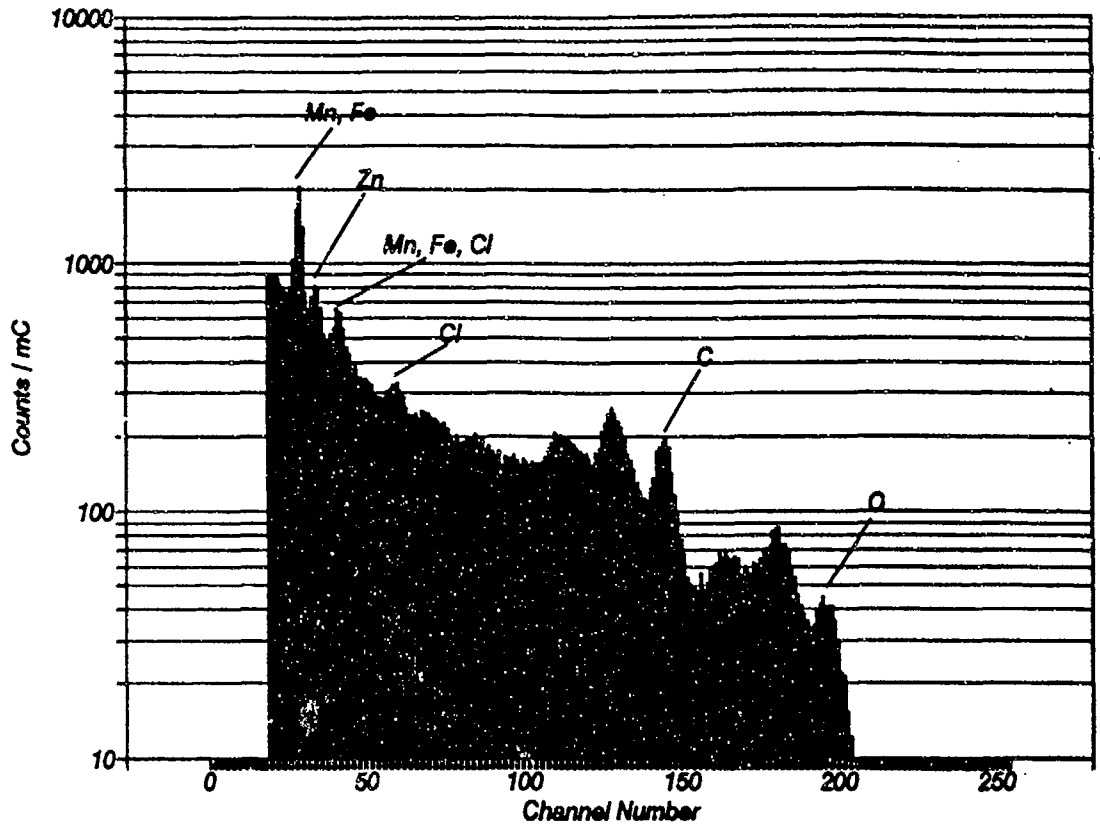


Figure 8b The gamma energy spectrum associated with the radio receiver with the batteries in place, refer to Figure 8a. Note the fingerprints of the batteries: the lines of Mn, Zn (and O).

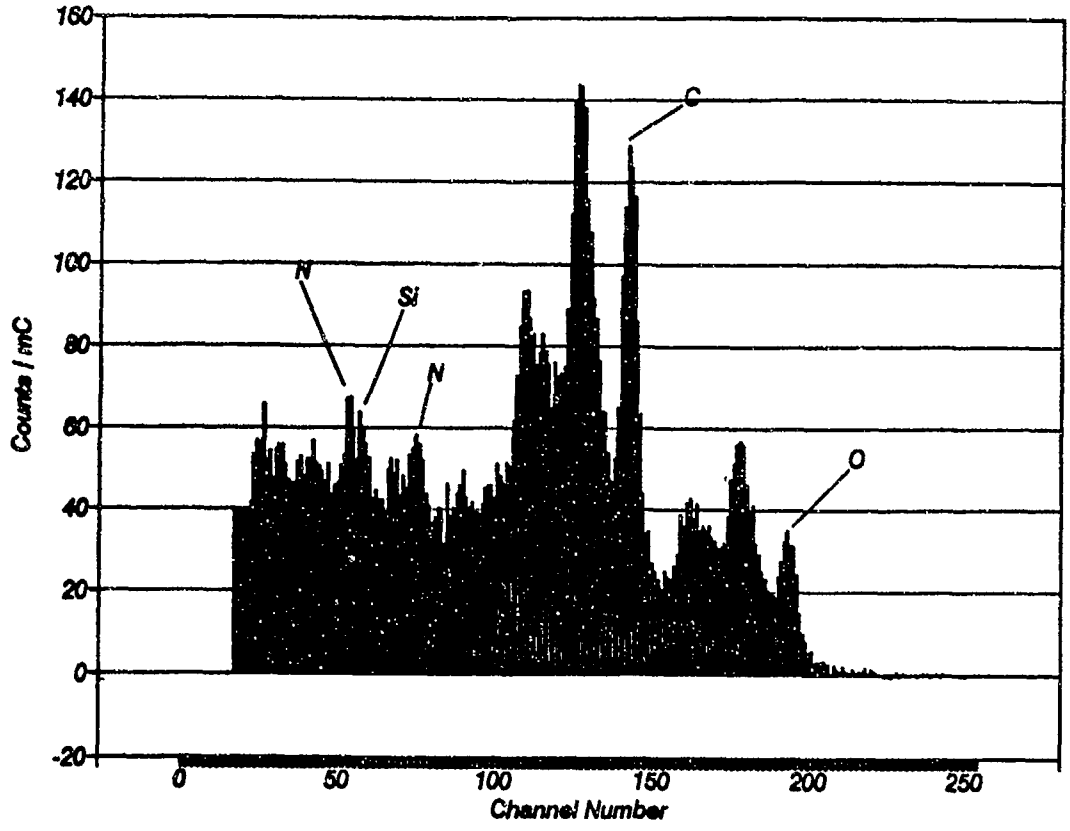


Figure 9a The gamma-ray energy spectrum for a heavy-duty leather boot (with silicon-rubber sole), toe compartment of which was filled with Semtex. The VOI was centered on the toe-compartment.

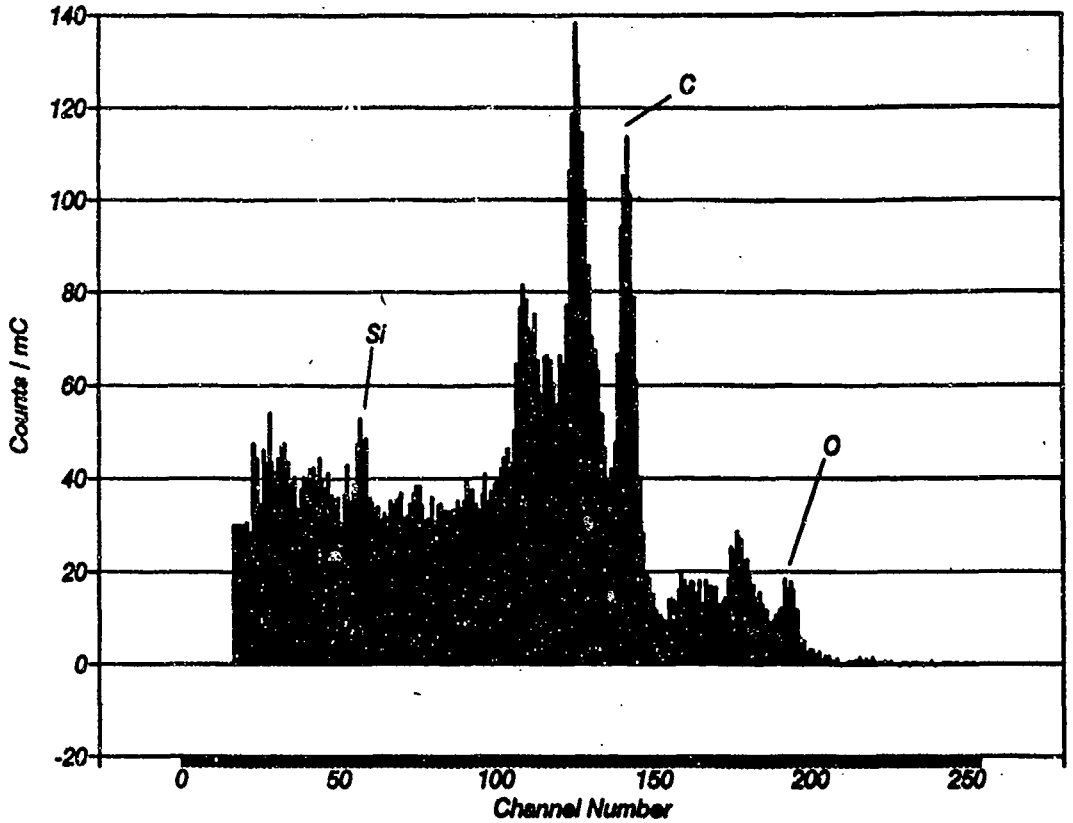


Figure 9b The gamma-ray energy spectrum for the same boot as shown in Figure 9a, but with the Semtex simulant removed.

A PULSED FAST-THERMAL NEUTRON INTERROGATION SYSTEM

G. Vourvopoulos
Department of Physics & Astronomy
Western Kentucky University
Bowling Green, KY 42101

F. J. Schultz
Office of Waste Management and Remedial Actions
Oak Ridge National Labortory
P.O. Box 2008
Oak Ridge, TN 37831

J. Kehayias
USDA/HNRC Tufts University
711 Washington Street
Boston, MA 02111

1. INTRODUCTION

Among the various analytical methods that could be used for the detection of explosives, a nuclear technique (thermal neutron activation analysis) was the first to show, in a practical way, the ability to detect small amounts of hidden explosives (Shea et al., 1990). The method uses a ^{252}Cf radioactive source that emits neutrons over a range of energies, with an average energy around 2.5 MeV. The neutrons are subsequently thermalized and interact with the N contained in the explosive through the $^{14}N(n, \gamma)$ reaction. The emitted γ-rays have an energy of 10.828MeV, which is the highest energy γ-ray to be produced by neutron capture. Although at this energy the detection efficiency of a NaI(Tl) γ-ray detection system has been reduced by 20% compared to a 1.5 MeV γ-ray, the advantage remains that the N γ-ray sits on practically zero background, making its identification easy and its area determination void of any corrections.

Given the fact that there are materials such as melamine equally rich or richer in N than the known explosives, the detection of N was shown to be inadequate in uniquely identifying an explosive (Grodzins, 1991; Grodzins, 1991). In particular, it was shown (Grodzins, 1991) that all explosives have a unique O-N profile. By determining the amount of these two elements contained in the interrogated material, the identification of hidden explosives would become more certain. C would be the third element that is common in all the explosives although it does not correlate uniquely with all known explosives. A system therefore that would be able to identify and quantify all three elements, C, N, and O would be able to provide more reliable information about the interrogated material.

Among the various options for the C, N, O identification, a pulsed fast-thermal neutron interrogation system is the technique that we utilize. In the following sections we present the advantages of the method, describe the characteristics of the various nuclear reactions, and present the data demonstrating the elemental identification.

2. PRINCIPLES OF THE METHOD

The three elements C, N, and O are identified via characteristic γ-rays emitted after the interaction of neutrons with the corresponding nuclei. To make the identification process most probable, there should not be a large number of γ-rays emitted, dividing the reaction strength in many channels. Table I shows the most important neutron reaction channels for C, N, and O along with the corresponding cross sections, minimum neutron energy and characteristic γ-rays.

Although other γ-rays are produced from the inelastic scattering of neutrons on N (Hall et al., 1959), the 2.31 MeV is the one that has the largest cross section (Perkin, 1964). The last reaction in Table I is actually the reaction $^{16}O(n,p)^{16}N$. ^{16}N beta decays

with a half-life of 7.13 s to the 6.13 MeV state of ^{16}O. The last reaction therefore, is a neutron activation.

From Table I we can see that all three elements could be observed with fast neutrons. The identification however of N through the n,n' reaction can be very difficult because it is located in the vicinity of some very strong γ-rays. This will be shown later in our data and will be discussed in the analysis of the results. A combination therefore of fast and thermal neutrons would obtain the desirable results. By pulsing the neutron source one can achieve two other important effects: a) the gating of the data acquisition system so that γ-rays produced from fast neutrons will not interfere with γ-rays produced from thermal neutrons and vice versa and b) possibility of timing the arrival of the neutrons at a particular position of the interrogated bulk, affording thus a depth analysis.

Fig. 1 describes the pulsing of the neutron generator and the measurements to be performed. Neutrons are produced in short pulses that last a few μs . During this time interval, a data acquisition system is gated and γ-rays produced from (n,n') and (n,p) reactions are accumulated. At the end of the neutron pulse, the fast neutrons pass through a neutron moderator and a percentage of them is thermalized (it would take several μs before a neutron is thermalized). The pulse remains off for approximately 100 μs. During that time a different data acquisition system is gated and γ-rays from (n, γ) reactions are collected. The process repeats itself for a number of cycles. Every few hundred cycles, the pulse remains off for a much longer period (a few ms). During this time a third data acquisition system is gated and γ-rays emanating from radioactive nuclei produced through neutron activation are collected. Three data acquisition regions can thus be separately triggered, eliminating appreciably the background.

3. EXPERIMENTAL RESULTS

The pulsed neutron generator used in the current experiments is based on a Zetatron tube. A full description of the system is given in Kehayias et al., 1987. Briefly, the generator was pulsed at an 8 kHz frequency and the pulse duration was 10 μs. The yield from the D-T reaction was 10^3-10^4 neutrons/pulse. For neutron thermalization, a nonoptimized moderator was utilized, composed primarily of water. Two detectors were employed for the characterization and collection of the emitted γ-rays: a 20 % efficiency high resolution High Purity Germanium detector (HPGe) and a 3 in x 5 in BGO detector. The HPGe detector was used for the correct identification of peaks, and the BGO detector which has a much higher efficiency but far worse resolution for the final data acquisition. Two Analog to Digital Converters (ADC) with conversion times less than 4 μs were separately gated in the acquisition system. The one ADC was gated with a 20 μs gate that opened at the beginning of the neutron pulse. The second ADC was gated by a 90 μs gate that started at the end of the neutron pulse. The current neutron generator set up did not allow us to stop the neutron generator for a predetermined quiescent period (e.g. every hundred pulses), in order to detect gamma rays from neutron activation only. Because of the low neutron yield and the experimental conditions, spectra were acquired over a 24 min interval. Three samples 12 kg each were utilized in this experiment: a coal sample that has a large number of elements in it but a very small amount of nitrogen, a sugar sample ($C_{12}H_{22}O_{11}$) and a urea ($(NH_2)_2CO$) sample. Urea has 25 % nitrogen atomic percentage which is in the range of the one in various explosives (Grodzins, 1991).

Fig. 2 shows a portion of the urea γ-ray spectrum taken with the HPGe detector. The ADC is gated on the neutron pulse, i.e. we observe primarily reactions due to fast neutrons. The 6.13 MeV O and 4.43 MeV C γ-rays along with their first and second escape peaks are clearly seen. The same energy region but without any sample in front of the neutron generator reveals a background that is void of any discernible peaks. Fig 3 shows a lower energy portion of the same spectrum, with two pronounced peaks from the neutron interaction with H (2.22 MeV) and with Pb (2.61 MeV). We are not able to detect in this high resolution spectrum any evidence for the 2.31 MeV peak from the N(n,n') reaction. The reason for this is the very high background under the 2.31 MeV peak due to the Compton tails of the large number of γ-rays with energies greater than 2.31 MeV. It is an example of the importance of the signal to noise ratio and not just of the signal.

To improve the signal to noise ratio, i.e. to lower the Compton background under the 2.31 MeV peak, one could use an anti-Compton shield for the HPGe detector. The use of such a shield has been demonstrated in the detection of S in coal through the S(n,γ) reaction (Vourvopoulos et al., 1989). The Compton background can indeed be suppressed

appreciably (by at least a factor of six) but with a large loss of available solid angle, making such measurements impractical. Fig. 4 shows a portion of the HPGe γ-ray spectrum around 10 MeV. The ADC now is gated after the neutron pulse, i.e. the detector is detecting mostly γ-rays from thermal neutron capture reactions . The 10.83 MeV N γ-ray is clearly seen in the urea spectrum, while the coal and the background spectra reveal the absence of other interfering peaks. It is worth noticing also in the urea spectrum, the N signal to noise ratio. Without any deconvolution of the data, we easily get a ratio of 5 while for the 2.31 MeV peak from fast neutrons, the ratio is barely over 1.

The data taken with the HPGe detector indicate that C,N, and O can indeed be identified through a combination of fast and thermal neutron reactions. Such a detector, however, because of its very low efficiency and susceptibility to neutron damage cannot be practically used in this application for the detection of γ-rays. To see if C, N, and O can be detected with a high efficiency but low resolution detector, a BGO detector was utilized. This detector was selected instead of a NaI(Tl) detector because of its higher material density, single light decay component and absence of elements that can be neutron activated. Fig. 5 shows the gamma ray spectrum with the ADC gated on the neutron pulse. The coal sample was substituted with a 12 kg sugar sample. The C γ-ray at 4.43 MeV is again clearly identified. The background in this energy region reveals no discernible structures. The shielding of the detectors from the water moderator was not adequate in this particular experiment. As a result, both HPGe and BGO detectors show an O 6.13 MeV γ-ray even when there is no sample. This situation did not occur in the previous run (Fig. 2) and it was remedied in the following runs. Turning to the ADC gated on the thermal neutrons, Fig. 6 shows a portion of the γ-ray spectrum above 8.7 MeV. A large peak at 10.3 MeV dominates the spectrum. This peak is also present in the fast neutron spectrum and cannot be attributed to a thermal neutron capture reaction. Around 10.8 MeV the N peak is clearly seen and this peak is absent from the sugar and the background spectra.

The data taken with the HPGe and BGO detectors clearly show that C, N, O, can be measured with a fast-thermal neutron combination. The BGO detector with its large efficiency can give a meaningful quantitative result without any interference from other γ-ray peaks.

For C and O, the γ-ray yield (Y_i for element i) can be written as:

$$Y_i = Y_i(C_i, \phi_{fn}, C_H, \rho, C_{HG})$$

where

C_i = concentration of the ith element in the material

ϕ_{fn} = fast neutron flux

C_H = Hydrogen concentration in the material

ρ = Mass of matrix material/unit volume

C_{HG} = concentrations of the elements producing higher γ-rays than the one analyzed (e.g. for C and for the sample in Fig. 5, these elements would be primarily O and Fe)

For N the γ-ray yield can be written as:

$$Y_N = Y_N(C_N, \phi_{th}, C_H, \rho)$$

where

ϕ_{th} = thermal neutron flux

As has been shown in previous cases of utilization of neutrons for elemental analysis (Baron et al. , 1991; Vourvopoulos et al., 1989), a linear equation connecting the γ-ray yield to the above parameters can be determined.

The yields that were obtained in this series of experiments, although far from maximized, indicate the feasibility of designing a system based on fast-thermal interrogation. The net yields that were obtained were $3x10^{-2}$ counts/kg/s for N and $3x10^{-1}$ counts/kg/s for C. Based on the HPGe results and the O reaction cross section, we estimate that the BGO yield will also be $3x10^{-1}$ counts/kg/s for O. These numbers, however, can be substantially increased. Systems already exist (SODERN) and others are in the design stage for sealed neutron generators producing 10^6-10^7 neutrons/pulse. Better source-interrogated material geometry and optimization of the neutron moderator could increase by a factor of three the fast neutrons and by a factor of 10 the thermal neutrons reaching the interrogated material. The electronics associated with the HPGe and BGO detectors as well as the ADC's have been designed to handle up to

500,000 counts/s (current rate is 5,000 counts/s). With the modifications stated above, an increase of the present counting rate by a factor of 10^3-10^4 can be realized. With these increased rates, a 10 s measurement would give precisions in the range 6% - 2% for N, 2% - 0.5% for C and O (per kg of explosive simulant material). The Minimum Detection Limit (MDL) can be calculated from the equation:

$$MDL = 3.29(B/t)^{1/2}/S$$

where S is the sensitivity in counts/kg/s, B the background rate in counts/s and t is the counting duration. In the worst case, the background will increase linearly with the net counts under the γ-ray peaks of interest. For a 10 s measurement with the precisions stated above, the explosive MDL is estimated to be between 0.3 and 0.5 kg.

Concerning the localization of the explosive within the interrogated volume, a pulsed neutron beam could be used for it. A 14 MeV neutron travels approximately 5 cm/ns. If the pulsed beam has a pulse duration of a few ns then from the time of flight of the neutron between the source and the interrogated material, we could obtain a volume localization of the explosive with a 5 cm resolution. The pulses that we are using however are a few μs wide and are not suitable for such localization.

4. CONCLUSIONS

The series of experiments performed indicate that a pulsed neutron interrogation system utilizing a combination of fast and thermal neutrons can be used for the detection of C, N, and O. The system utilizes a number of nuclear reactions and the emitted gamma rays can be efficiently detected with a BGO detector. In order for such a system to be of practical use, gamma ray yields must be increased by a factor of 10^3-10^4, a realistic goal indeed.

ACKNOWLEDGEMENTS

This presentation is based on work performed at the Oak Ridge National Laboratory, managed for the U.S. Department of Energy under contract DE-AC05-84OR21400 with the Martin Marietta Energy Systems, Inc.

REFERENCES

1. J. P. Baron and L. Debray, "Potential of nuclear techniques for on-line bulk analysis in the mineral industry", in Applications of Nuclear Techniques (Eds. G. Vourvopoulos and T. Paradellis), World Scientific (Singapore) 1991.

2. L. Grodzins, "Nuclear technologies for finding clandestine explosives", in Applications of Nuclear Techniques (Eds. G. Vourvopoulos, T. Paradellis), World Scientific (Singapore), 1991.

3. L. Grodzins, "Nuclear techniques for finding explosives in airport luggage", Nuclear Instruments and Methods B56/57, 829-833 (1991).

4. H.E. Hall and T.W. Bonner, "Gamma radiation from inelastic scattering of fast neutrons in ^{12}C, ^{14}N and ^{16}O", Nuclear Physics 14, 295-313 (1959).

5. J.J. Kehayias, KJ. Ellis, S.H. Cohn and J.H. Weinlein, "Use of a high repetition rate neutron generator for in vivo body composition measurements via neutron inelastic scattering", Nuclear Instruments and Methods, B24/25, 1006-1009 (1987).

6. J.L. Perkin, "Gamma ray spectra from fast neutron interactions", Nuclear Physics 60, 561-580 (1964).

7. P. Shea, T. Gozani, and H. Bozorgmanesh, "A TNA explosives-detection system in airline baggage", Nuclear Instruments and Methods A299, 444-448 (1990).

8. SODERN, Neutron Generator Bulletin.

9. G. Vourvopoulos, D.L. Humphrey, P.L Setters and K. Lamkin, "On-line elemental analysis of coal via high resolution PGNA", Nuclear Instruments and Methods, B40/41, 853-856(1989).

10. G. Vourvopoulos and P.C. Womble, "On-line sulfur determination in coal with prompt gamma neutron activation", Nuclear Instruments and Methods B36, 200-205 (1989).

Table I Neutron (fast and thermal) induced nuclear reactions on C, N, O.

Element	Reaction	E_n^{min} (MeV)	Cross Section (mb)	Eγ (MeV)
C	n,n'	4.8	200°	4.44
N	n,n'	4.7	70°	2.31
N	n,γ		75	10.83
O	n,n'	6.4	96°	6.13
O	n,p	10.3	38°	6.13

° Measured at E_n = 14 MeV

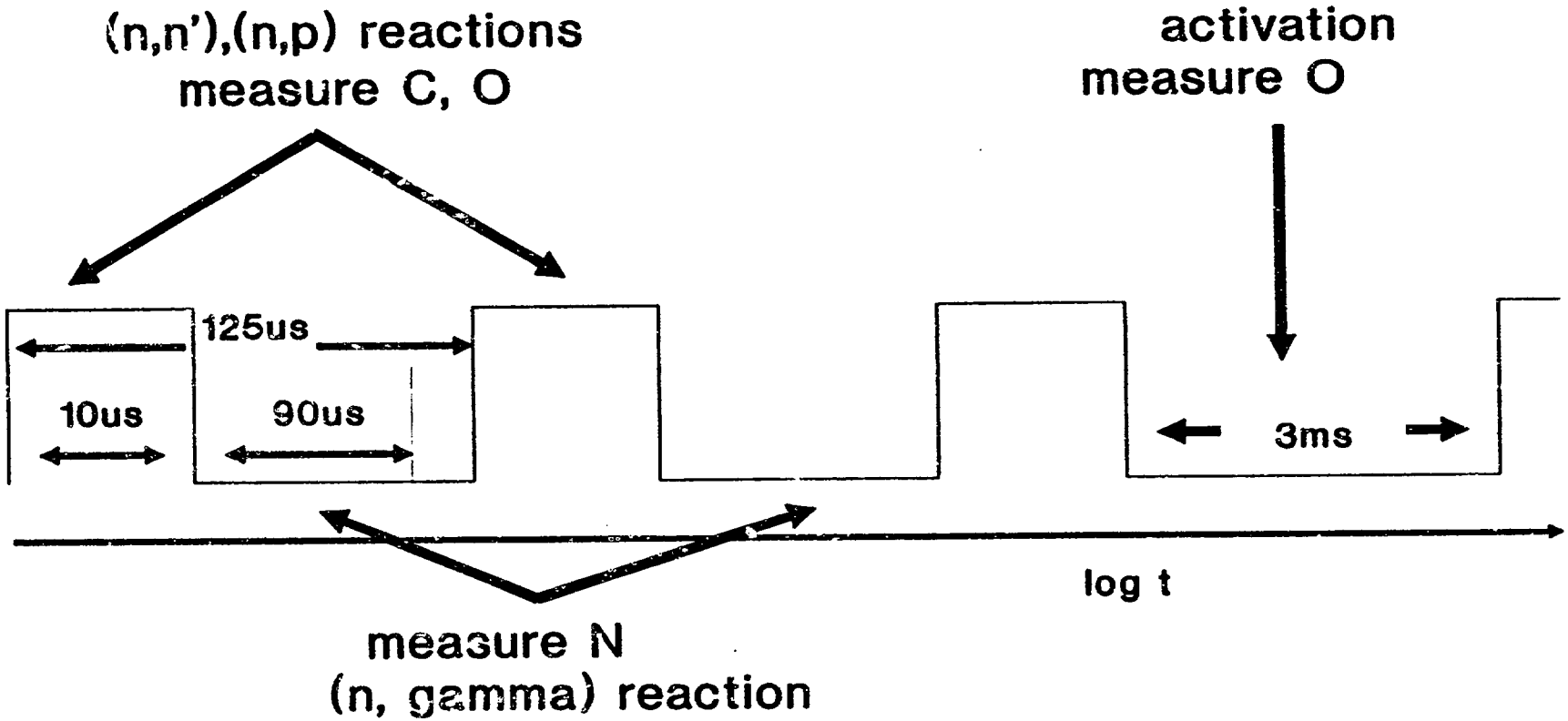


Figure 1. Schematic diagram of the neutron generator pulsed output.

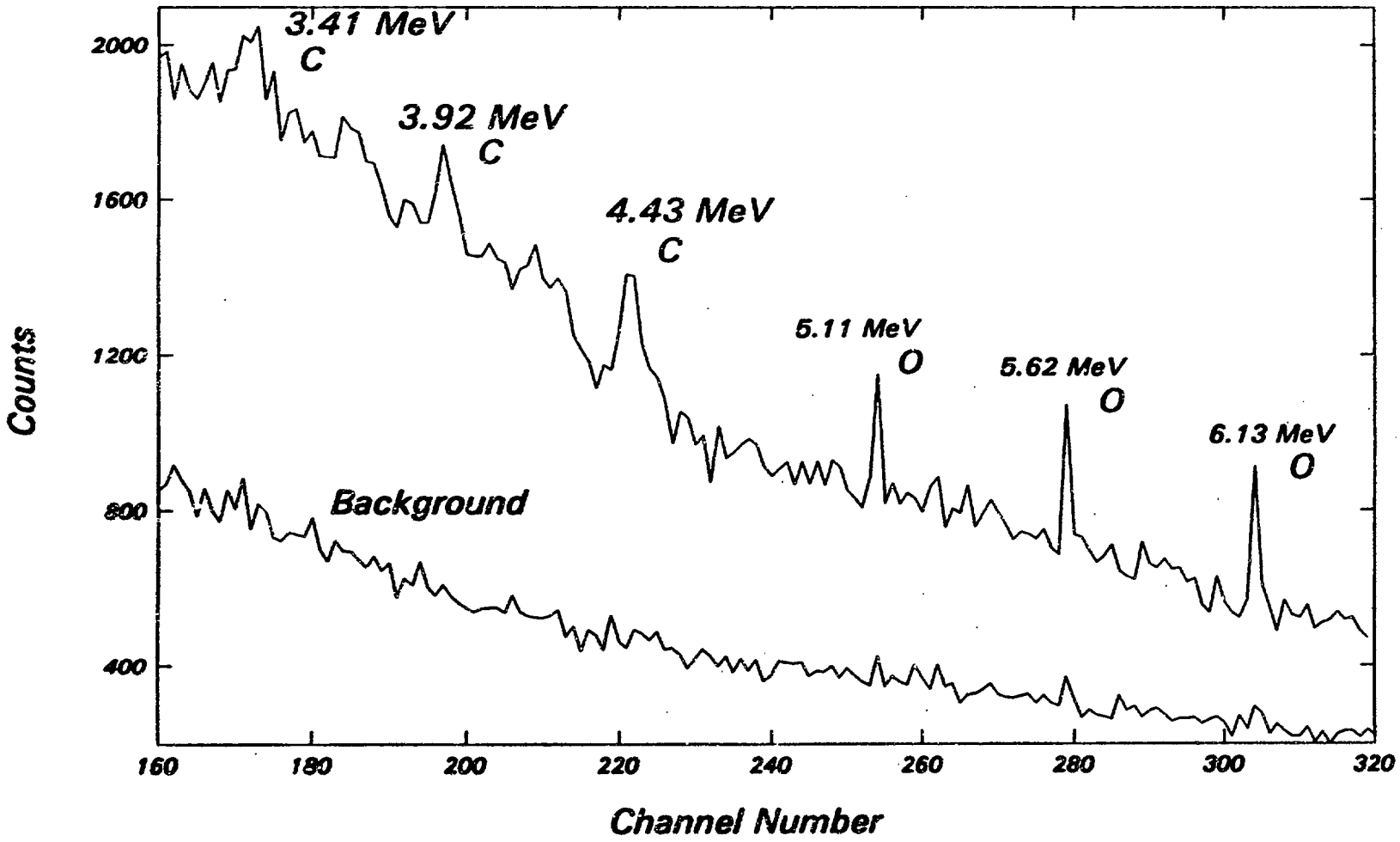


Figure 2. Portion of the HPGe gamma ray spectra of the urea sample and of the background, gated on the neutron pulse (fast neutron reactions). The relevant O and C peaks are marked.

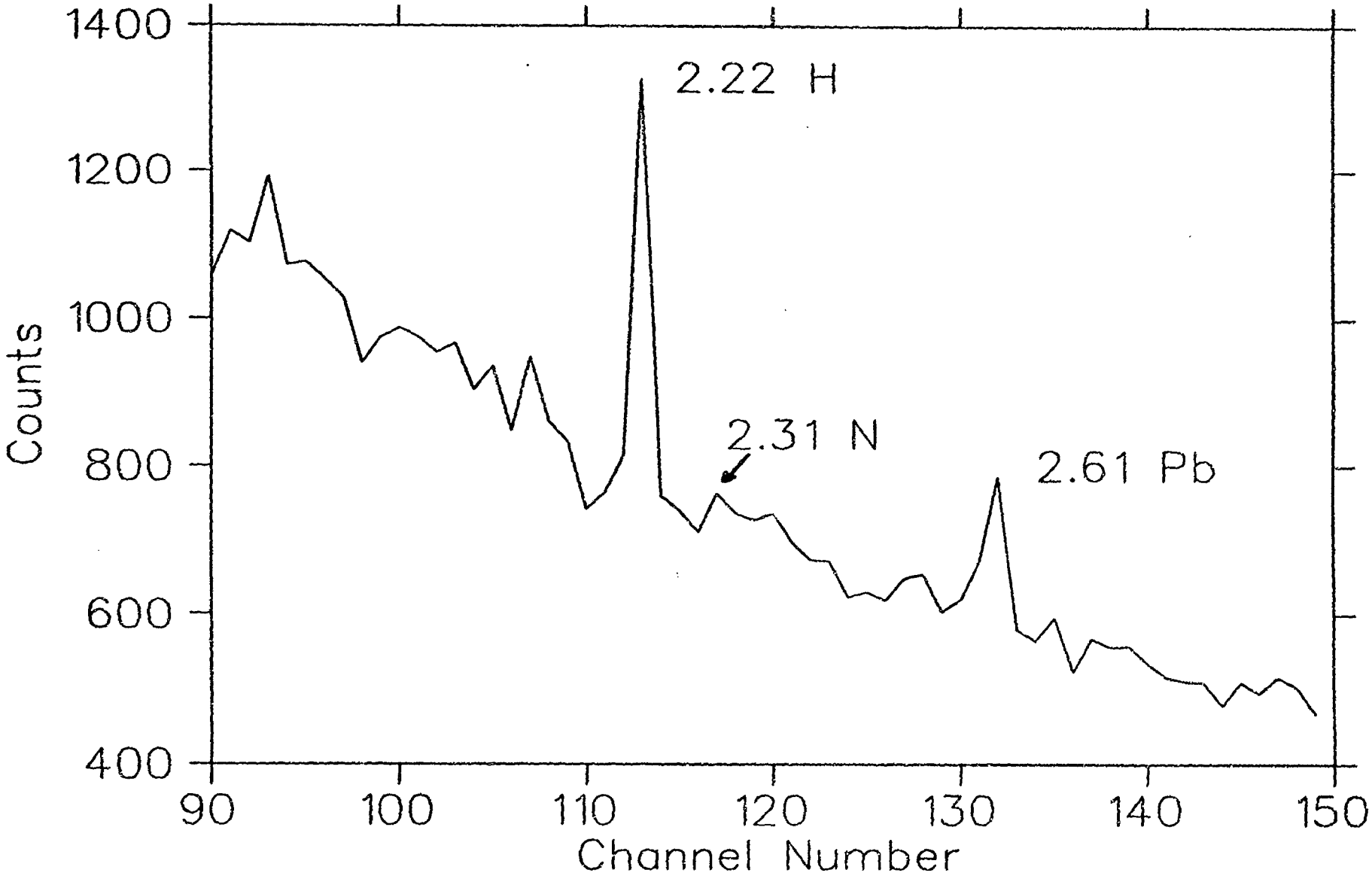


Figure 3. Portion of the HPGe gamma ray spectrum of urea, gated on the neutron pulse (fast neutron reactions). Peaks corresponding to H, N, and Pb are marked.

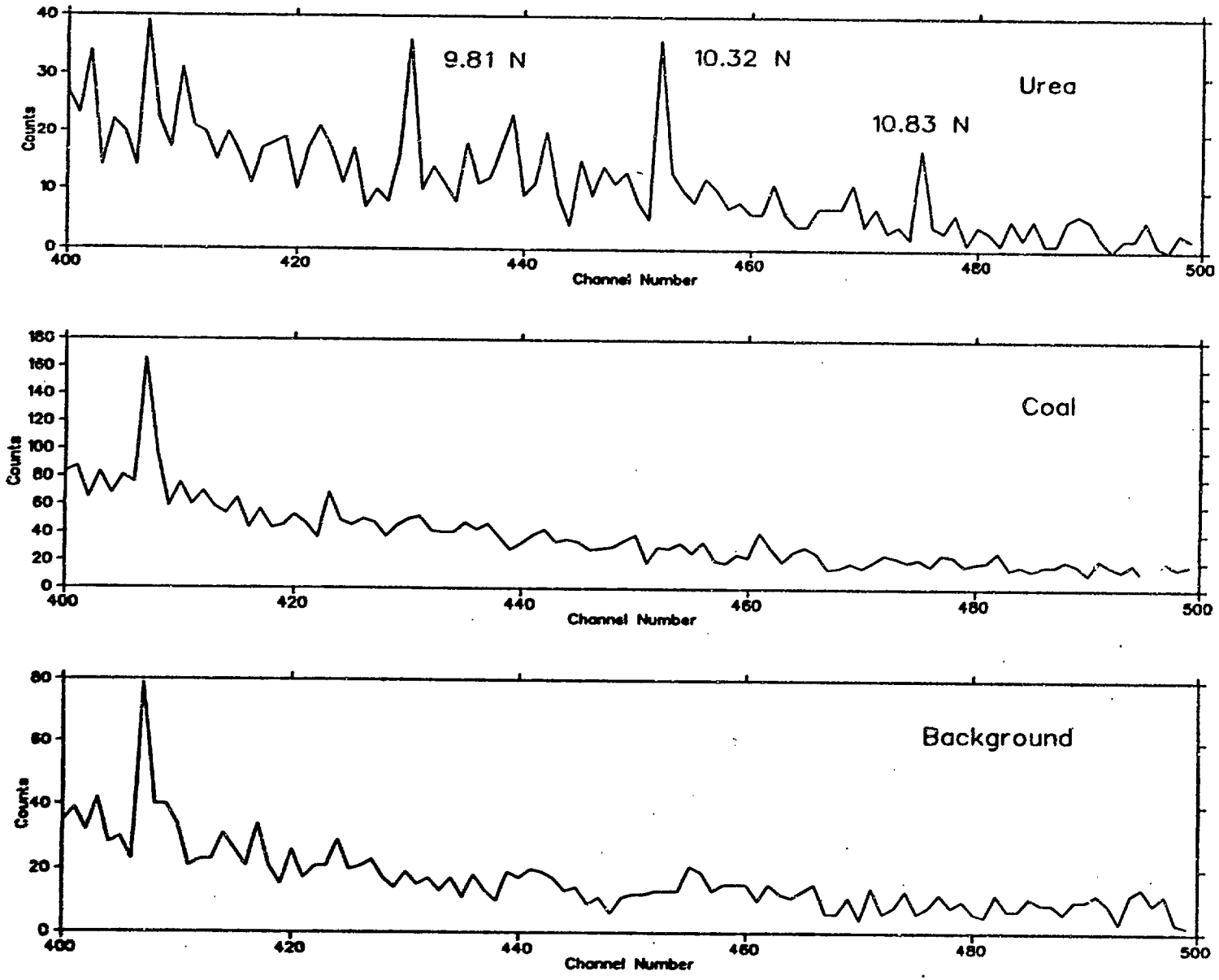


Figure 4. Portion of the HPGe gamma ray spectra of urea, coal and background, gated after the neutron pulse (thermal neutron reaction). Relevant N peaks are marked.

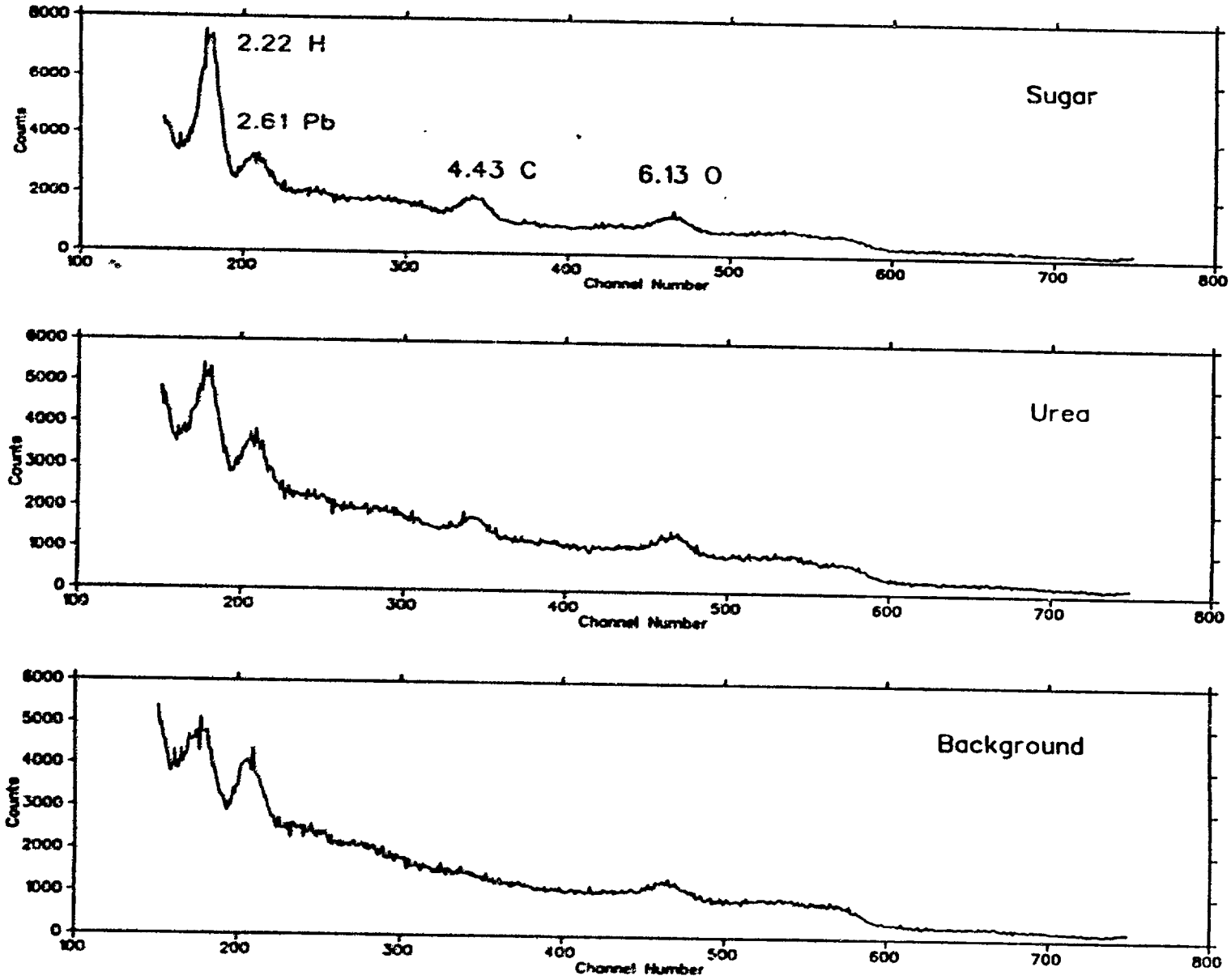


Figure 5. BGO gamma ray spectra of urea, sugar, and background, gated on the neutron pulse (fast neutron reactions). Peaks corresponding to H, Pb, C, and O are marked.

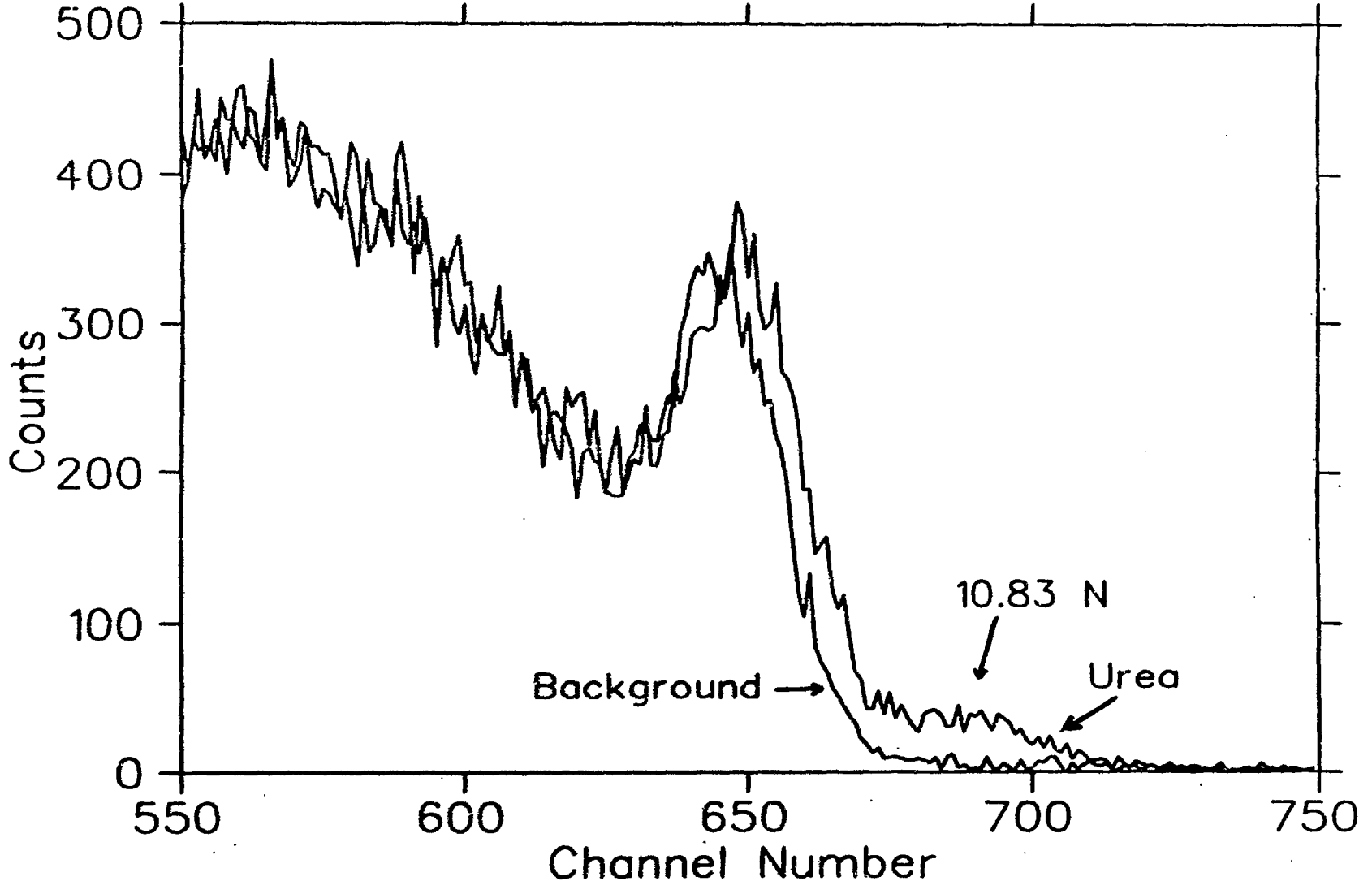


Figure 6. Portion of the BGO gamma ray spectra of urea, and background, gated after the neutron pulse (thermal neutron reaction). The N peak at 10.83 MeV is marked

THE NITROGEN CAMERA: A NEW EXPLOSIVE DETECTOR

W. P. Trower
Physics Department
Virginia Polytechnic Institute and State University
Blacksburg, VA 24061

1. INTRODUCTION

The Nitrogen Camera has much in common with conventional cameras -- photographic, x-ray, and positron -- but rests on different physics. In the photographic camera visible light with energy of a few eV is scattered by an object, is manipulated by a variety of optical devices, falls onto an aperture, and is recorded on an electronic or chemical media. The x-ray camera uses photons of a few keV, which are scattered as they pass through an object, fall unmanipulated onto an aperture, and are recorded. In the PET camera, a radioisotope, with a half-life of hour to days, is injected into an object. Decay positrons of a few MeV lose energy by a succession of bremsstrahlung collisions, finally annihilating into two oppositely-directed gamma rays, the signals from which are manipulated to produce three-dimensional images.

2. THE PHYSICS

In the Nitrogen Camera high-energy photons are flashed into an object in which they create a wide variety of radioisotopes. Many of these isotopes emit gamma rays directly. Some decay with electrons or positrons which produce a plethora of bremsstrahlung gamma rays, logarithmically increasing in number with decreasing energy. If positrons are present, two annihilation gamma rays are also produced. It is the totality of these gamma rays detected in time after irradiation which constitute the Nitrogen Camera signal.

For photon energies of 50 MeV only two radioisotopes are produced in appreciable quantity and decay rapidly, in tens of milliseconds: nitrogen-12 and boron-12 whose half-lives (end point energies) are 11.0 (17.3) and 20.2 ms (13.3 MeV), respectively. Their production probability for photons on nitrogen-14 increase with photon intensity and energy above their respective production thresholds, $\sim$ 30.6 and 25.1 MeV.

All the gamma rays which result from these two reactions are our nitrogen marker. With photons from 50 MeV electron collisions in a thin tantalum radiator, the production reactions of interest are,

$$\gamma + {}^{14}N \rightarrow {}^{12}B + 2p;$$

$${}^{12}B \rightarrow {}^{12}C\ \upsilon_e\ e^-,$$

$$\gamma + {}^{14}N \rightarrow {}^{12}N + 2n;$$

$${}^{12}N \rightarrow {}^{12}C\ \upsilon_e\ e^+;$$

$$e^+ + e^- \rightarrow 2\gamma\ (511\ \text{keV}),$$

while a third reaction,

$$\gamma + {}^{13}C \rightarrow {}^{12}B + p;\ {}^{12}B \rightarrow {}^{12}C\upsilon_e\ e^-,$$

provides the sole interference signal. Unfortunately, these two-nucleon reactions have cross sections for 50 MeV electrons about a hundred times smaller than for single-nucleon reactions whose production thresholds are $\sim$ 20 MeV. With the solitary exception of our interference signal, all single knock-out nucleon produced isotopes are relatively stable, with lifetimes from seconds to days, and so form a constant and well defined background to our signal. Three-nucleon reactions, some hundred times less probable than two-nucleon reactions and with thresholds $\sim$ 50 MeV, produce several unstable radioisotopes which would mimic our signal if we went to substantially higher excitation energy.

A concrete, albeit unrealistic, example serves to illustrate the Nitrogen Camera physics. Consider the consequences of irradiating a pure nitrogen object with a short burst of sufficiently energetic photons to produce only two reactions, ${}^{14}N(\gamma,2n){}^{12}N$ -- the "signal" -- and ${}^{14}N(\gamma,n){}^{13}N$ whose half life is $\sim$ 600 seconds -- the "noise". During the first 10 ms after irradiation half of the produced nitrogen-12, while only $\sim$0.0001 of the produced nitrogen-13, would decay. So even if the single-nucleon cross section is

a 100 times than that for two-nucleons, the signal-to-noise in the first 10 ms would be $\sim$ 500/1.

The real situation, however, is more complicated in several ways. First, the thresholds for producing these reactions are different as are the energies of their production maxima and their cross sections are only vaguely known. Second, the incident photons produced by an electron beam in the radiator will have yields that depend not only on the beam energy and intensity, but also on the geometry and material of the radiator. Third, substantial extraneous radiation produced during and immediately after the acceleration process cause counts in the detectors. Finally, we have not considered all the other long-lived "noise" reactions which will elevate the background on which our nitrogen signal sits.

3. THE DATA

We have constructed extensive calculations to "prove" the Nitrogen Camera's ability to detect explosives in a variety of applications and in myriad of environments. However, physics is ultimately an experimental science and no calculation should suffice to convince: For that only data will do. Having said so, I now explicitly omit a discussion of radiation hazards to operators and the environment for brevity since we have found both by calculation and experiments to date that the radiation levels generated lie within the prescribed international limits.

Figure 1 displays a typical time spectra taken at the 50 MeV electron racetrack microtron of the Royal Institute of Technology's (KTH) in Stockholm, Sweden where the experimental work is being performed. The target was 1 kg of melamine ($\sim$ 66% nitrogen by weight) explosive simulant located $\sim$ 25 cm from a 2 mm thick tantalum radiator and $\sim$ 25 cm from a detector -- a 5" fast photomultiplier tube coupled to a 5" diameter, 2" thick scintillator. The beam was $\sim$1 mA delivered in $\sim$ 5 ms-long pulses.

The first panel is the raw spectrum containing 593,294 counts (the first bin has 74,843 counts, the last 434) and was taken in 1,681 bursts. The three distinctive features are:

- A long-time background which appears equally in each bin, its magnitude proportional to the number of bursts, N, and the counting time, n $\sim$ 102 ms, as $\sim n\Sigma N_i = n(N/2)(N+1)$. If the irradiation had been delivered in a one burst, as in our eventual operational single-shot mode, this background per bin would be negligible. Thus, the next panel shows the spectra with this large-time background subtracted.

- A short-time background appears immediately after irradiation, has a half life of $\sim$1.3 ms, produces $\sim$ 65% of the counts, and is seen isolated in the last panel and shaded in the others. I attribute this to radiative neutron capture on all the material in the counting room, the neutrons being copiously produced in the accelerator, radiator, target, and counting room walls. In the operational mode far fewer of these counts will be present because the beam will only travel $\sim$ 1 m in air before spending itself in the object. How much this background will be reduced awaits a Monte Carlo calculation, however, crude estimates indicate that it will be at least three times less.

- The signal, seen in the third panel, contains 103,746 counts, $\sim$ 17% of the total counts and has a half life of $\sim$18.6 ms which when apportioned between nitrogen-12 and boron-12, gives $\sim$ 83% of the signal to the latter.

The resultant nitrogen-signal/burst is $\sim$ 50 counts above a negligible background. An operational system will benefit from multiple detector cells (x4) and greater beam intensity (x20), but will suffer from lower target nitrogen concentrations (x1/2) and amounts (x1/5) as well as a larger standoff distance (x1/3). Thus, a prototype system should comfortably operate within the constraints of this parameter envelope.

4. INTERFERING SIGNALS

I search for interfering signals with a computer code using the National Nuclear Data Center compilation. I looked for the reactions (γ,p), (γ,n), (n,p), (n,γ); $(\gamma,2p)$, (γ,pn), $(\gamma,2n)$; and $(\gamma,3p)$, $(\gamma,2pn)$, $(\gamma,p2n)$, $(\gamma,3n)$ on all stable isotopes with isotopic abundance >0.1% for incident photon energy of 100 MeV. Reaction products which could produce interference signals were those with a half live <100 ms, ten times that of the nitrogen-12 signal. I list these

candidates in Table I. The isotopic and chemical (earth's crust) abundance percentages, threshold energy, and a crude indication of the relative yields at this specific excitation energy are also given. In the first column is the number of knock-out nucleons with the sign of the decay beta particle.

Of the nine possible fast reactions at Eγ = 100 MeV, six are on nitrogen isotopes, three on oxygen, and one each on carbon-13 and boron-11, the latter being produced by neutron capture. From abundance considerations only those reactions in bold type need be taken seriously. At ~ 20 MeV excitation energy only the carbon reaction contributes, at ~ 40 MeV nitrogen also produce an appreciable signal, and at 100 MeV oxygen may dominate the signal.

I obtained experimental spectra for medium and small (plastic) and small (metal) land mine simulants; air, brass, dirt, glass, granite paving block, particle board, sand, steel, wood; Al, C, Cu, Fe, Mg, Pb; and $CaSO_4$, FCl, H_20, KBr, MnO_2, $N_2H_4O_3$, $N_6C_3H_6$, $NaBiO_8$, NaCl. The targets included all but one (titanium) of the 10 most abundant elements in the earth's crust (99.48% by weight) as well as 17 other elements. I saw signals only from nitrogen and carbon-13.

Figure 2 shows these spectra typical of these other materials: One kilogram of table salt taken under irradiation conditions similar to that of the melamine already mentioned. This spectra shows no indications of a nitrogen signal, however, detailed analysis reveals a nitrogen signal which can be fully accounted for by the room air.

Thus only carbon-13, which constitutes 1.1% of naturally occurring carbon, provides an interfering signal. The carbon-13 created signals can be verified (and therefore its interpretation as a nitrogen signal falsified) using the unique ability of the racetrack microtron to change energies in milliseconds: When scanning with the 50 MeV beam, a nitrogen signal is confirmed by halving the electron beam energy on the next burst to 25 MeV and re-irradiating the pixel - if no signal is seen then the original signal was from nitrogen.

5. IMAGING

A variety of natural and man made objects, from wool sweaters to polish sausage, have a large nitrogen content similar to explosives. It is therefore essential for any operational explosive detection system to not only detect but also to image, nitrogenous objects since often function can be implied from form.

To see how imaging may be accomplished with the Nitrogen Camera we construct again a simplistic example. Imagine a nylon cube whose dimensions are that of our pixel, ~ 6.3 cm on a side, and contrive a scanning procedure so that the cube lies completely within a single scan pixel. Make the detection interval ~ 10 ms, to correspond to the half life of nitrogen-12 which we assume falsely to be the only nitrogen marker produced. Further, assume that short- and long-time backgrounds can be adequately subtracted. Then the number of counts from each scan pixel before encountering the cube will be consistent with that of the intervening air and so can be subtracted as a pedestal constant. Once the cube is irradiated N counts will appear in the first counting interval. When the next, and cubeless pixel is irradiated, N/2 counts will be recorded even though no nitrogen is present in the most recently irradiated pixel. Similarly, subsequent counting intervals will give N/4, N/8, N/16, and so on, counts. Desmearing this image can then be accomplished by taking the cube pixel as containing 2N counts and then subtracting the calculated tail from the subsequent pixels. Such a procedure can be generalized for real world non-ideal conditions at only a cost of complexity.

A prototype detector section -- 4 5" cylindrical scintillation detectors read out by photomultilplier tubes whose power supplies are operated under computer control -- is being built to explore the imaging capabilities of the Nitrogen Camera. Each tube output is to be fed into a four-channel customs electronics module that will initially reside in the back plane of an IBM compatible 486 computer. These individual electronic channels will contain a computer controlled discriminator and a 256 element, 2^{14} range, memory which will multiscale at 1 ms, or factors of 2 thereof, under computer control. The start/stop signals will originate in the external logic and be initiated by signals from the accelerator electron gun.

6. PROSPECTS

For the Nitrogen Camera technique to have a chance of succeeding as an explosive detector, four now experimentally verified facts had to be established:

- That the abundant long half-life noise is at worst well behaved (and so can be reliably

Table I. Reactions produced at 100 MeV with decay products faster than 100 ms.

eN	Reaction	E_{thres} (MeV)	$t_{1/2}$ (ms)	Abundance (%) Isotopic	Chemical	Relative Yield
0	boron-11 → boron-12	-3.4	20.	80.1	0.001	-
−1	carbon-13 → boron-12	17.5	20.	1.1	0.020	.01
−2	nitrogen-14 → boron-12	25.1	20.	99.6	0.002	.15
+2	nitrogen-14 → nitrogen-12	30.6	11.	99.6	0.002	.19
−2	nitrogen-15 → boron-13	31.0	17.	0.4	0.002	.20
−3	nitrogen-15 → boron-12	35.9	20.	0.4	0.002	.21
+3	nitrogen-15 → nitrogen-12	41.5	11.	0.4	0.002	.24
−3	oxygen-16 → boron-13	43.2	17.	99.8	46.400	.25
−3	nitrogen-15 → beryllium-12	46.8	24.	0.4	0.002	.27
−3	oxygen-18 → boron-15	51.6	9.	0.2	46.400	.30
+3	oxygen-16 → oxygen-13	52.1	9.	99.8	46.400	.31

subtracted) and at best can be ignored in a single-shot operational mode;

- That the overwhelming small half-life noise attending acceleration and targeting is both sufficiently well behaved and of brief duration that it can be either subtracted or its time domain ignored;

- That the signal strength is sufficient so as to be measurable above these backgrounds when produced by a single burst from the accelerator; and

- That the known nitrogen-faking signal from carbon-13 can be falsified in real time.

The above accomplished, what now needs to be demonstrated is:

- That imaging capabilities -- resolution, pixel size, etc. -- are sufficient;

- That methods of sweeping the beam can be found;

- That automatic analysis algorithms can be developed;

- That data taking, beam sweeping and data analysis can be synchronized; and

- That the Scanditronix medical microtron can be reduced in size and weight.

The above list is necessary, not sufficient. The failure to accomplish any of these tasks will result in the Nitrogen Camera being a sterile technology. The achieving all of them, however, will not assure that it will become an economically and societally acceptable device. Whatever is the eventual result it is great good fun trying, for a change, to solve, rather than create, a social problem with nuclear physics.

ACKNOWLEDGEMENTS

Staffan Rosander at KTH helped create the racetrack microtron on which my experimental work is being done, and skillfully operates it during data runs. This work was motivated by the late Luis W. Alvarez.

Support has been provided by the Swedish Technical Development Board (89-01526P), the U.S Army (DAAK70-91-C-0034), and Defense Advanced Research Projects Administration (DAAK70-92-C-0001).

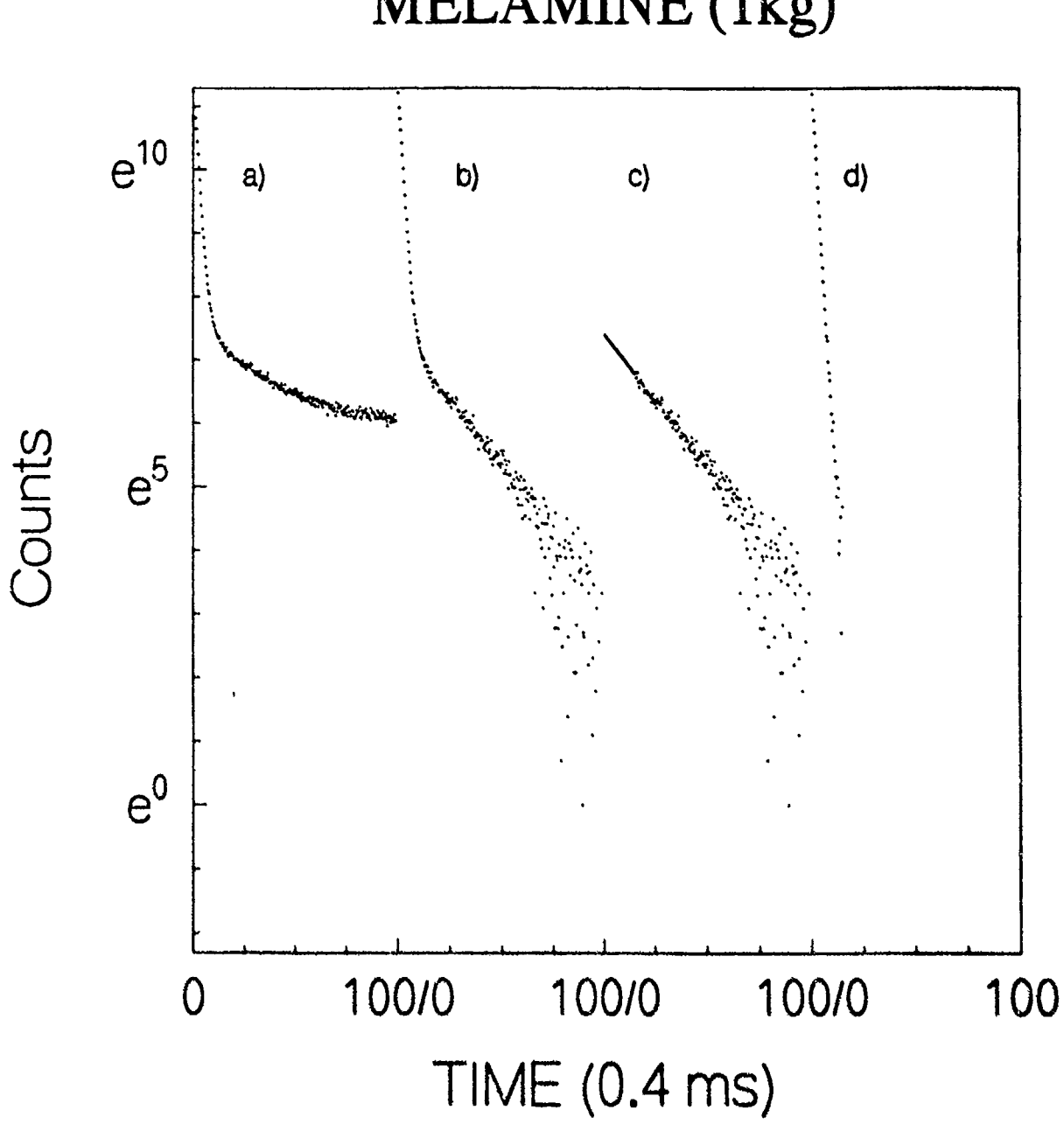


Figure 1. Typical time spectra using 1kg of melamine.

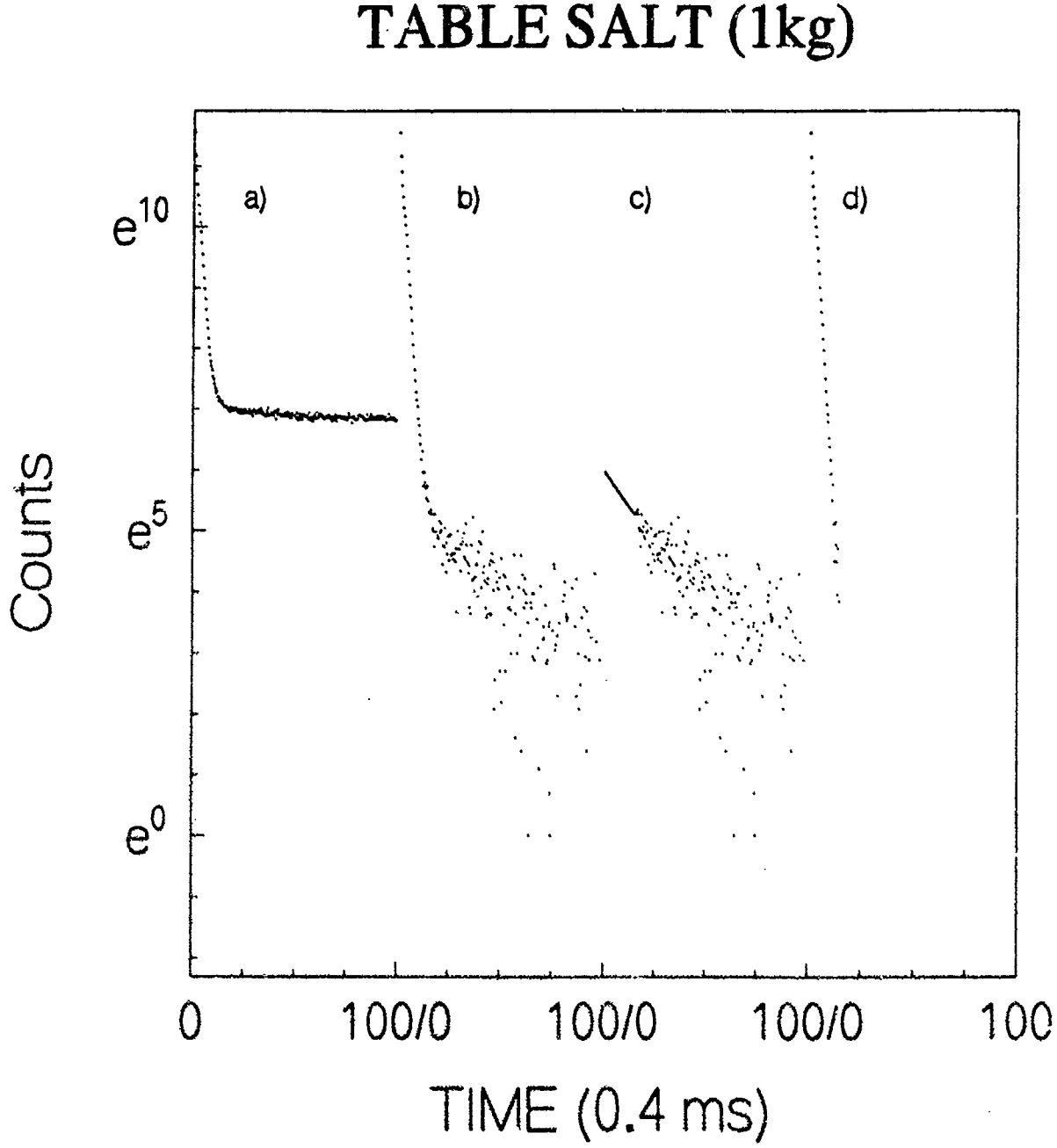


Figure 2. Typical time spectra using 1kg of table salt.

NEUTRON ELASTIC SCATTER (NES) FOR EXPLOSIVES DETECTION SYSTEMS (EDS)

Dr. Henry J. Gomberg
PENETRON, Inc.

Dr. Brian G. Kushner
BDM International

1. BACKGROUND

PENETRON, Inc. was created in 1987 as a joint venture between the Environmental Research Institute of Michigan (ERIM) and Ann Arbor Nuclear, Inc. (A^2N) for development of new, innovative search systems for detection and location of contraband such as hidden explosives, and subsequently, concealed narcotics. The NES system concept described below resulted from the initial joint venture for explosives detection.

BDM and PENETRON formed a team in April 1991 to pursue development further and to implement the NES technology.

The systems are based on Neutron Elastic Scatter (NES) which incorporates two patented techniques, Neutron Resonant Elastic Scatter (NRES) and Neutron Elastic Back Scatter (NEBS), in a proprietary technology. The first patent (4,864,142) on the NRES technology issued on September 5, 1989 and a second patent, on the NEBS technology (4,918,315), issued on April 17, 1990.

The development started in 1986, in response to a perceived need for new methods of contraband detection that would be sensitive, difficult to counter, and have a low false alarm rate.

The chemical and physical properties of the common explosives were analyzed (from the literature) and the methods for their detection which were known to be in use or under development were reviewed. There were many! In addition, chemical and physical processes which were not under development were explored. This study produced the realization that the large elastic scatter cross sections of the nuclei of the light elements for fast neutrons which are well known in nuclear physics were not being used as a basis for an explosives identification system. The initial analytical work, which ran for about a year within Ann Arbor Nuclear but in close collaboration with ERIM, was followed by formation of PENETRON as a joint venture and the initiation of an experimental testing and verification program. The experiments were carried out at the Nuclear Physics Research Laboratory of the University of Kentucky at Lexington under the supervision of Professor Marcus McEllistrem.

These studies form the base from which the BDM-PENETRON team is moving towards prototype systems for demonstration and toward production of fieldable systems.

2. INTRODUCTION TO TECHNICAL DISCUSSION

The detection and location of concealed explosives by Neutron Elastic Scatter (NES) is based on detection of the atomic constituents and measurement of their respective concentrations. Using Carbon, Nitrogen, and Oxygen as the primary targets, the presence and amount of each is measured and the Carbon-Nitrogen and Oxygen-Nitrogen ratios established. As shown in Table 1, the principal explosives have C/N and O/N ratios which fall into a fairly narrow range. The densities range between 1.5 and 2, and the concentration of Nitrogen is high, 15 to 35%.

There are many innocent articles of commerce, however, which contain Nitrogen. Here, the concentration of Nitrogen is lower or the ratios are different.

It is important that a probe technique be sensitive enough to detect the concentrations of Nitrogen, but also be able to evaluate the setting in which it is found; to determine the ratios or "signature."

3. PRINCIPLES OF NES

The common explosives contain predominantly light

atoms; Hydrogen, Carbon, Nitrogen, and Oxygen. Fast neutrons will interact strongly, primarily by elastic collision, with the light nuclei in contrast with X-rays which show relatively weak interactions. In elastic collisions there is no change in the structure of the nucleus hit by the neutron.

From a beam of neutrons with same energy impinging on target nuclei, the neutrons scattered in a particular direction have a new, unique reduced energy determined by the mass of the nucleus hit.

By measuring the change between neutron velocity in and the velocity out, the nucleus struck can be identified. Carbon, Nitrogen, and Oxygen all produce different back scatter velocities (see Figure 1).

From the intensity of the back scattered signals, the amounts of the chemical elements doing the scattering can be automatically calculated, and from the ratios of their signals, the composition can be estimated. Not only is Nitrogen detected and measured, but also the ratios of Nitrogen to Carbon, Nitrogen to Oxygen, etc. can be established automatically. Neutron Elastic Scatter provides a quick and sensitive way of doing a remote chemical identification.

Up to this point, we have assumed that the nuclei of the different light elements (C, N, O) display the same cross section; the same size and shape targets to the incoming neutrons. The targets differ only in mass or weight.

For some neutron energy regions this can be reasonably accurate, but for particular energies, individual elements can show unique changes in cross section because they no longer are essentially spherical. Instead, they scatter the neutrons more effectively in one direction (back scatter) than another (side scatter) and the effective size, the cross section, may increase several fold, or it may even almost disappear making the element "transparent."

We refer to the peaks in the scatter cross section at particular energies as "resonances." This may be seen in Figure 2 for the elements H, C, N, and O. The differential cross section for Nitrogen as a function of angle, with neutron energy as a parameter is shown in Figure 3. Note that for back scatter ($\cos \sigma = -1.0$) the cross section for 1.78 MeV is higher than for 1.59 MeV. The total cross sections (see Figure 2) are in reverse order. When the back scatter spectrum for Nitrogen is compared with the averaged cross section as a function of neutron energy, important differences emerge. The back scatter resonances are usually higher, enhancing sensitivity, but in some cases (1.59 MeV) there is no back scatter peak (Figure 4).

These back scatter resonances can be found at energies up to about 10 MeV, as seen in Figure 5 for Nitrogen. This sets an effective energy limit on the NRES technique. The NEBS technique which is used to generate the "signatures" remains effective to 20 MeV and higher; as long as elastic scatter is dominant.

Similar properties are displayed by Carbon and Oxygen. Backscatter spectra for C, N, and O are shown in Figure 6.

The nuclear data presented has been developed from sources in the open literature and in particular, data from the National Nuclear Data Center at Brookhaven National Laboratory.

4. LABORATORY TEST RESULTS

Up to this point we have dealt with concepts. The NES technology has been successfully demonstrated in the laboratory. Spectra have been experimentally observed for "innocent materials" (plastics) versus simulated explosives. The results at one neutron energy (application of the NEBS principle) are shown in Figure 7. The difference, particularly in the detection of Nitrogen, along with Carbon and Oxygen, are clear. It should be noted that the complete spectrum of elements is generated using one input energy.

Three spectra for the simulated explosive taken at different neutron energies (application of the NRES principle) illustrate in Figure 8 the change in contrast and how the Nitrogen signal is enhanced. The spectra were normalized to the Carbon signal. A shift of 30 KeV (1.78 to 1.75 MeV) would change only the Nitrogen peak, thus providing a test for false alarms.

The preceding figures were "smoothed" for clarity of presentation. A computer printout of the actual data points showing standard deviations for each channel count and the derived spectrum using the SAN-12 code is presented in Figure 9. The experiments were carried out in the accelerator laboratory at the

University of Kentucky under the supervision of Professor Marcus McEllistrem.

One other example is given. Thin sheet explosives are a known problem. Figures 10 and 11 show the experimentally generated spectra for a thin sheet alone and for the same sheet behind aluminum as in an attache case. It is easily detected, and a typical cover makes no difference.

5. POSTULATED PROBLEMS

5.1.False Alarms
We have examined several sources of postulated false alarms and find that either the NES system can reveal spurious signals in its normal configuration or is readily modified to meet the problem. The basic protection comes from the fact that:

5.1.1. "Signatures" are generated and these are characteristic of the material being examined.

5.1.2. The resonance technique allows quick routine and automatic check on the authenticity of signature, that is, is a given peak really due to Nitrogen?

Our thinking on these and other postulated false alarms is summarized in Table 2. We believe the problems can be met.

5.2. Radiation Protection Calculations indicate that for the proposed neutron energy range (to 3.5 MeV), an operator and the general public can be readily protected by light (water tank or equivalent) shielding less than 1 meter thick; about one third of that required for 14 MeV neutrons.

On the matter of induced radioactivity, the basic process depends on elastic scatter which is the dominant reaction by orders of magnitude. In Table 3, we have summarized our findings for examination of an aluminum case. The initial dose rate from the surface of a freshly examined case is calculated to be less than 1×10^{-4} of the ambient sea level dose.

For an experiment similar to that shown in Figure 7, no radioactivity could be measured with a safety survey (G.M.) type meter after the source was turned off and the case brought out from behind the shield.

6. COMMENTS IN CONCLUSION

- NES is based upon a primary effect, and is thus more precise, reliable, and quicker for detection of concealed explosives.
- NES is based on current and available technology.
- NES has measured data from laboratory demonstrations
- NES produces negligible residual radioactivity.
- NES can be in production, pending funding and resolution of system engineering issues, in 3-5 years.

Table 1. Elemental Ratios, Concentrations, and Densities for Explosives

	Hydrogen/ Nitrogen Ratio	Carbon/ Nitrogen Ratio	Oxygen/ Nitrogen Ratio	Nitrogen (Weight %)	Density
EXPLOSIVES (FUEL & OXIDIZER)					
Nitroglycerine	1.67	1	3	18.5	1.70
TNT	1.67	2.33	2	18.5	1.75
RDX	1	0.5	1	38.0	1.6
PETN	2	1.25	3	17.7	1.5
AN	2	0	1.5	35.0	1.7
COMMERCIAL ARTICLES					
Wool	4.8	3.3	1.1	12	0.2
Silk	4.5	3.0	1.2	15	0.2
Collagen (Leather)	4.8	3.1	1.3	15	1.0
Orlon	3+	3+	0	26.4	0.2-0.4
Nylon	11	6	1	12.4	0.2-0.4
Peanuts	14	10	3	4.4	(1)
Navy Beans	13	10	8	4.1	(1)
Melamine	1	0.5	0	66.0	1.5

Table 2. False Alarms

PROBLEMS

A. A false alarm has been postulated for a bag in which light, innocent (C, O, H) materials are in front of heavier materials. Faster neutrons from the distant layer may arrive in the "N" time slot for the lighter material. This can be detected as follows:

1. The use of resonance peaks for a critical element like N, followed by off-resonance excitation will cause modulation of the C, N, O signature. If the "N" slot signal is due to neutrons scattered from other elements, the modulation will not be observed.
2. The normal detector distance for resolution of C, N, O within the signature is 2 meters. A second detector at 1 meter will display the signature envelope but without resolving the elements. If, however, one constituent of the signature is from distant scatter, the envelope will change, indicating a false alarm.

Both of the above can be operated routinely. Another simple test is:

3. If an alarm signature is seen, the bag can be rotated 180°. A false signature will break up; a genuine signature remains intact.

B. Generalized Scatter of Radiation

1. These will lead to background noise at lower energy levels and will not generate "signatures."
2. Where double scatter is postulated leading to neutrons entering the "Nitrogen" slot, we find:
   a. the signal will not respond to resonant modulation.
   b. the probability for back scatter with the correct energy is very low.

Table 3. Induced Radioactivity

For exposure to 1 x 10^6 fast neutrons per square centimeter in a period much shorter than the product half life, the following activity-inducing reactions and levels may be anticipated:

Reaction	Dis/sec-gram	Energy (MeV)
Na 23 → F 20	0.13	1.63
Na 23 → Ne 23	0.72	~1.00
Al 27 → Mg 27	0.11	~1.00
Si 28 → Al 28	0.65 (0.6 per gm Si)	1.78
Si 29 → Al 29	1.0 (0.05 per gm Si)	1.28

Taking an aluminum attache case as an example, the gamma ray intensity will be 0.03 gamma rays/sec-cm^2 for an initial dose rate at the surface of 1 x 10^{-9} R/minute.

The total dose delivered, essentially over the first hour, is 1.4 x 10^{-8} R.

The permitted dose to the general public is 2 x 10^{-3} R in a one hour period or 0.05 R in one year; 10CFR20 (1991).

The permitted dose for one hour is 140,000 times that from the case.

Background at sea level is 0.145 R/year; about 1,000 times the initial rate from the case.

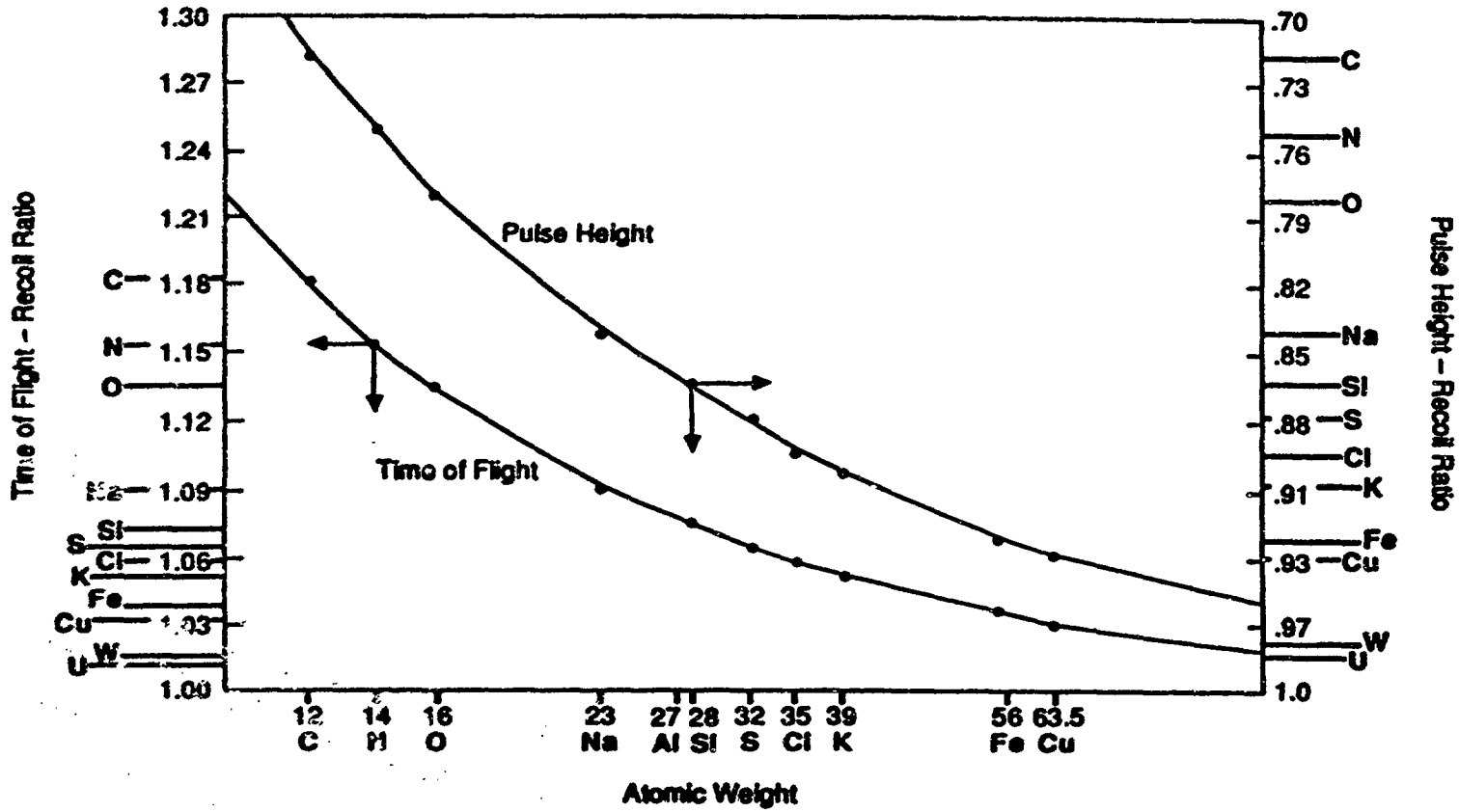


FIGURE 1. NEUTRON BACK SCATTER FROM TARGET NUCLEI

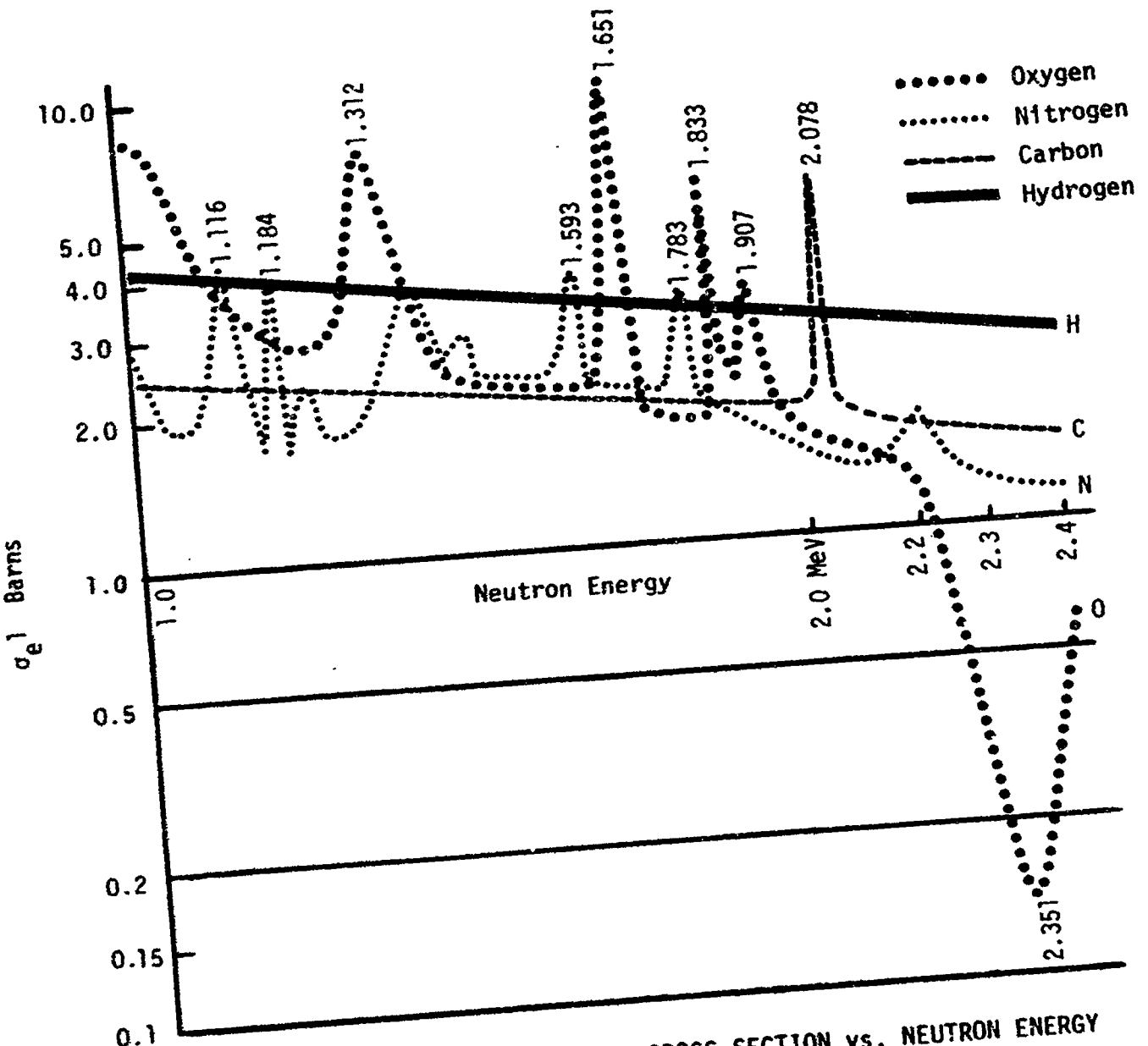


FIGURE 2. NEUTRON ELASTIC SCATTER CROSS SECTION vs. NEUTRON ENERGY

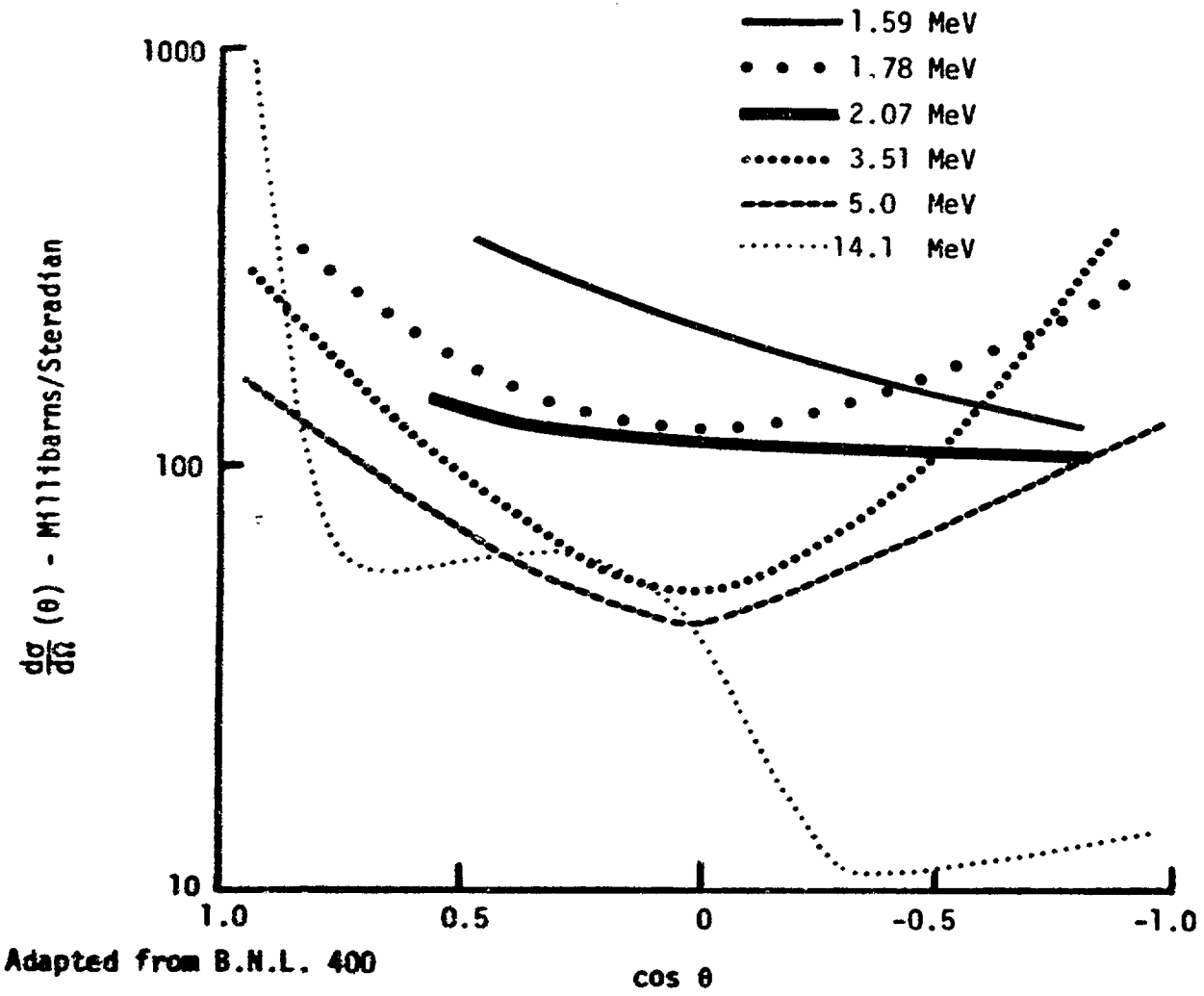


FIGURE 3. DIFFERENTIAL CROSS SECTION VS. SCATTER ANGLE
Neutron Elastic Scatter from Nitrogen

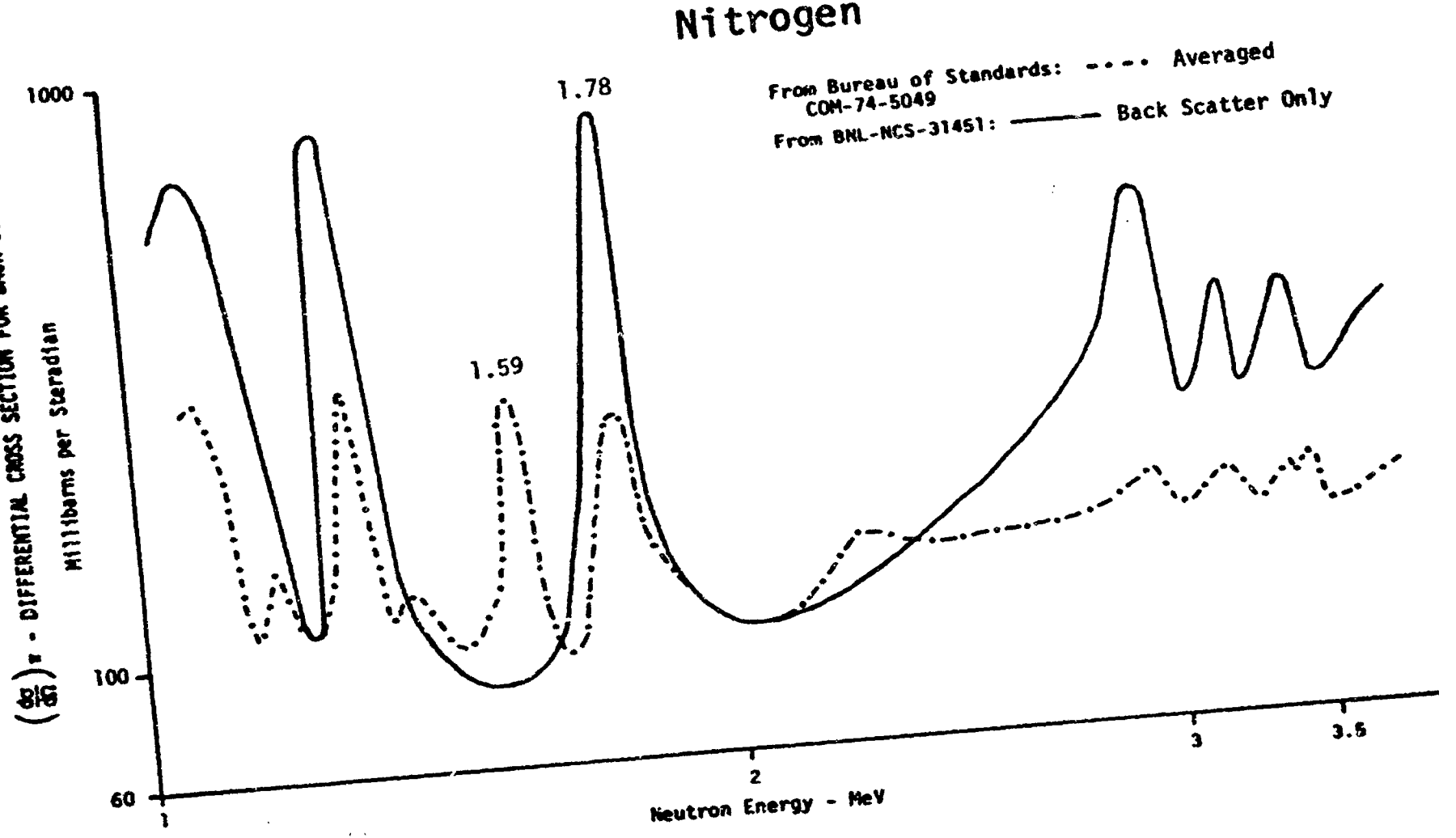


FIGURE 4. DIFFERENTIAL CROSS SECTION FOR BACK SCATTER VS. NEUTRON ENERGY

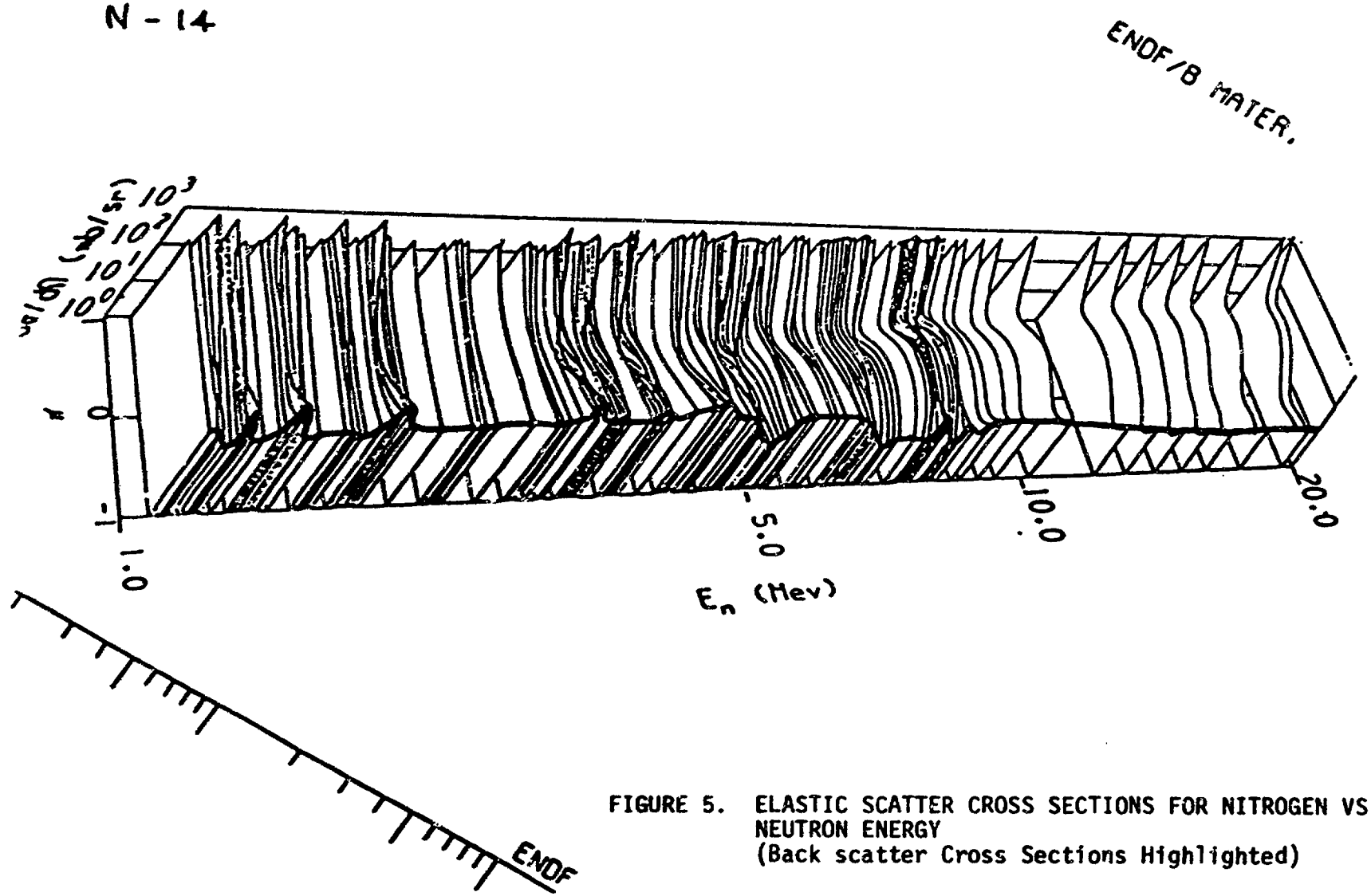


FIGURE 5. ELASTIC SCATTER CROSS SECTIONS FOR NITROGEN VS. NEUTRON ENERGY
(Back scatter Cross Sections Highlighted)

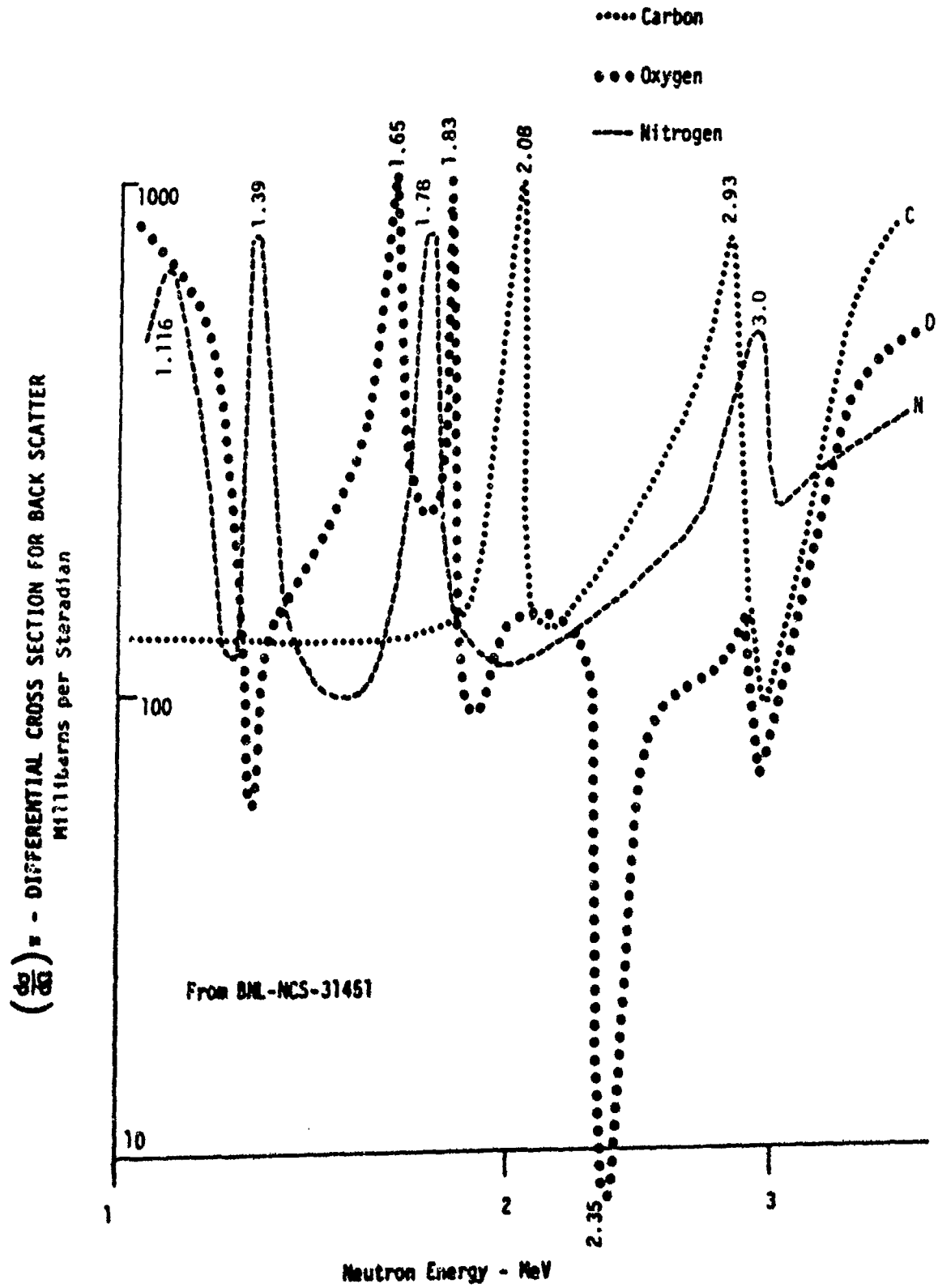


FIGURE 6. DIFFERENTIAL CROSS SECTION FOR BACK SCATTER VS. NEUTRON ENERGY

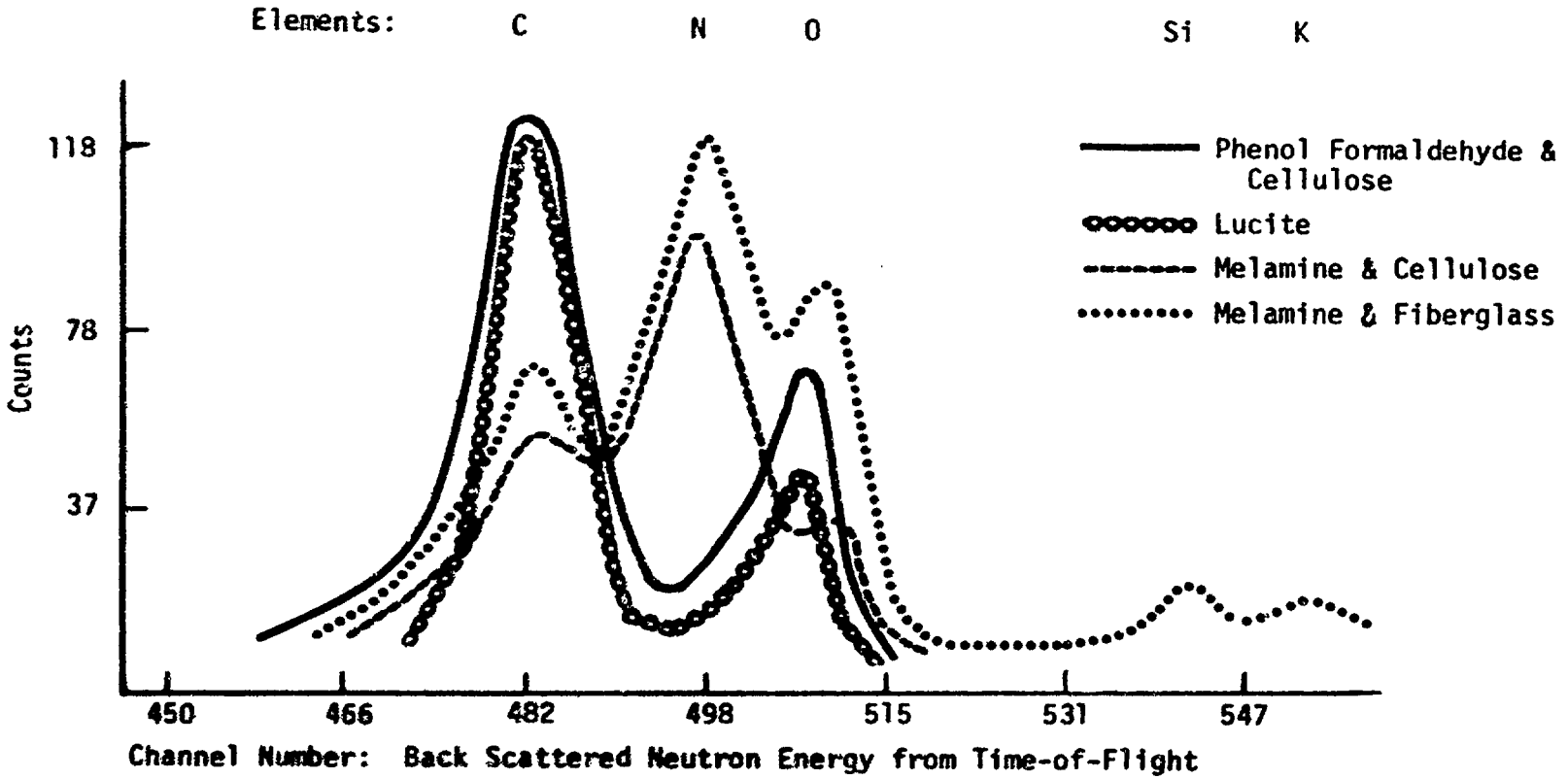


FIGURE 7. SPECTRUM OF BACK SCATTERED NEUTRONS FROM PLASTIC TARGETS WITH AND WITHOUT NITROGEN
Input Beam Energy — 1.78 MeV (Nitrogen Resonance)

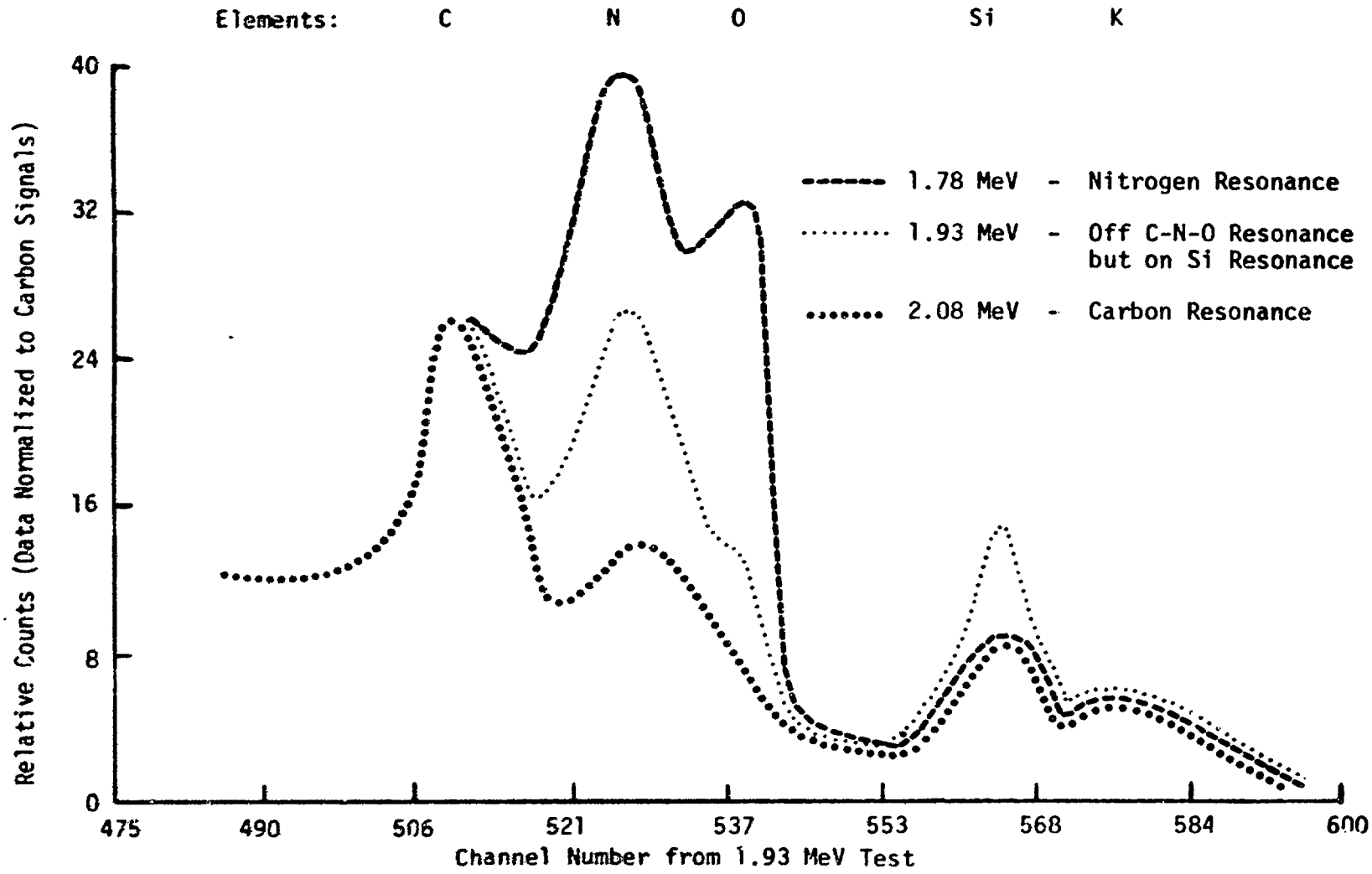


FIGURE 8. SPECTRUM OF BACK SCATTERED NEUTRONS FROM MELAMINE + FIBERGLASS FOR DIFFERENT INCIDENT NEUTRON BEAM ENERGIES

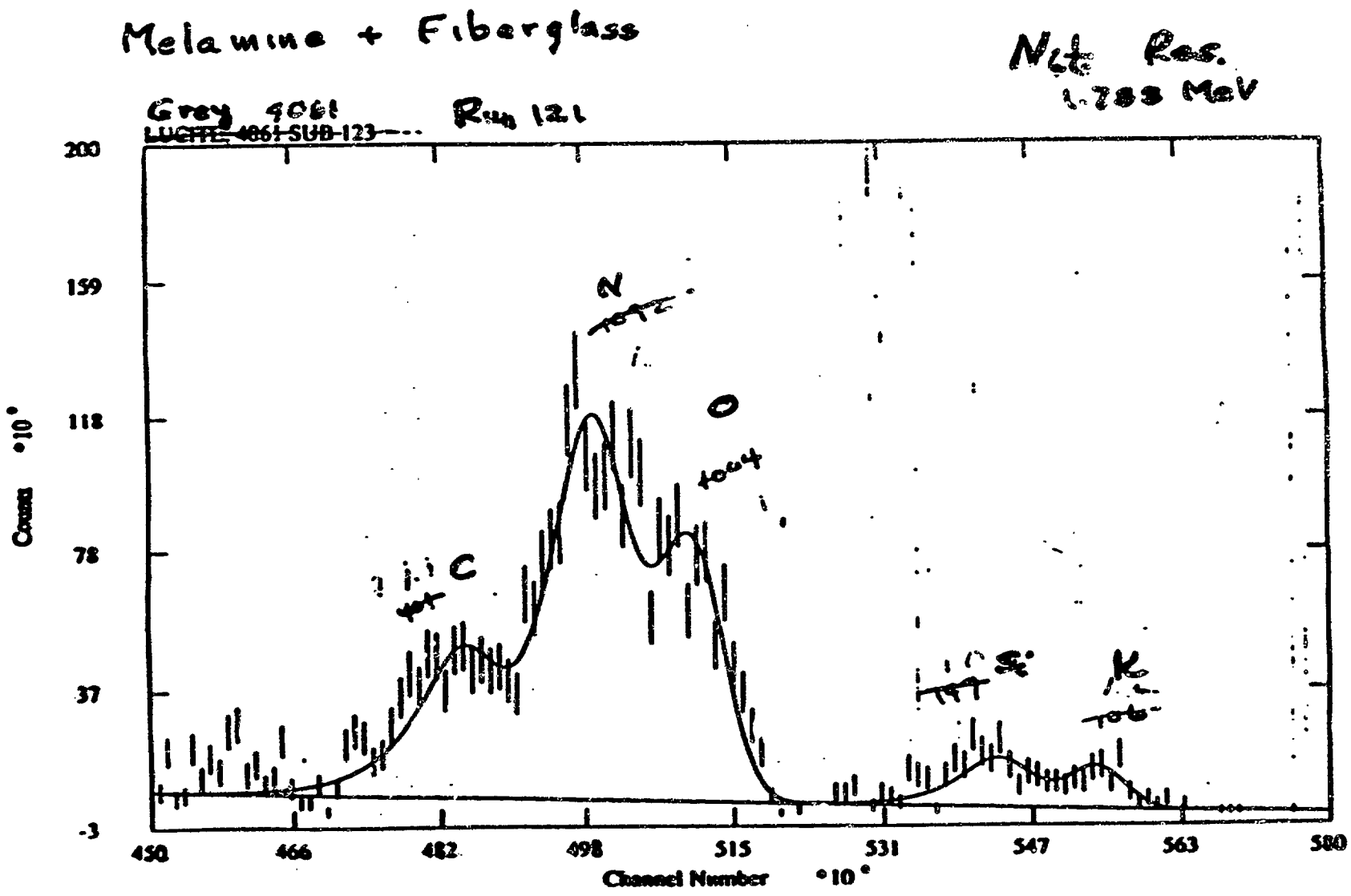


FIGURE 9. COMPUTER PRINTOUT OF MELAMINE AND FIBERGLASS SIGNATURE

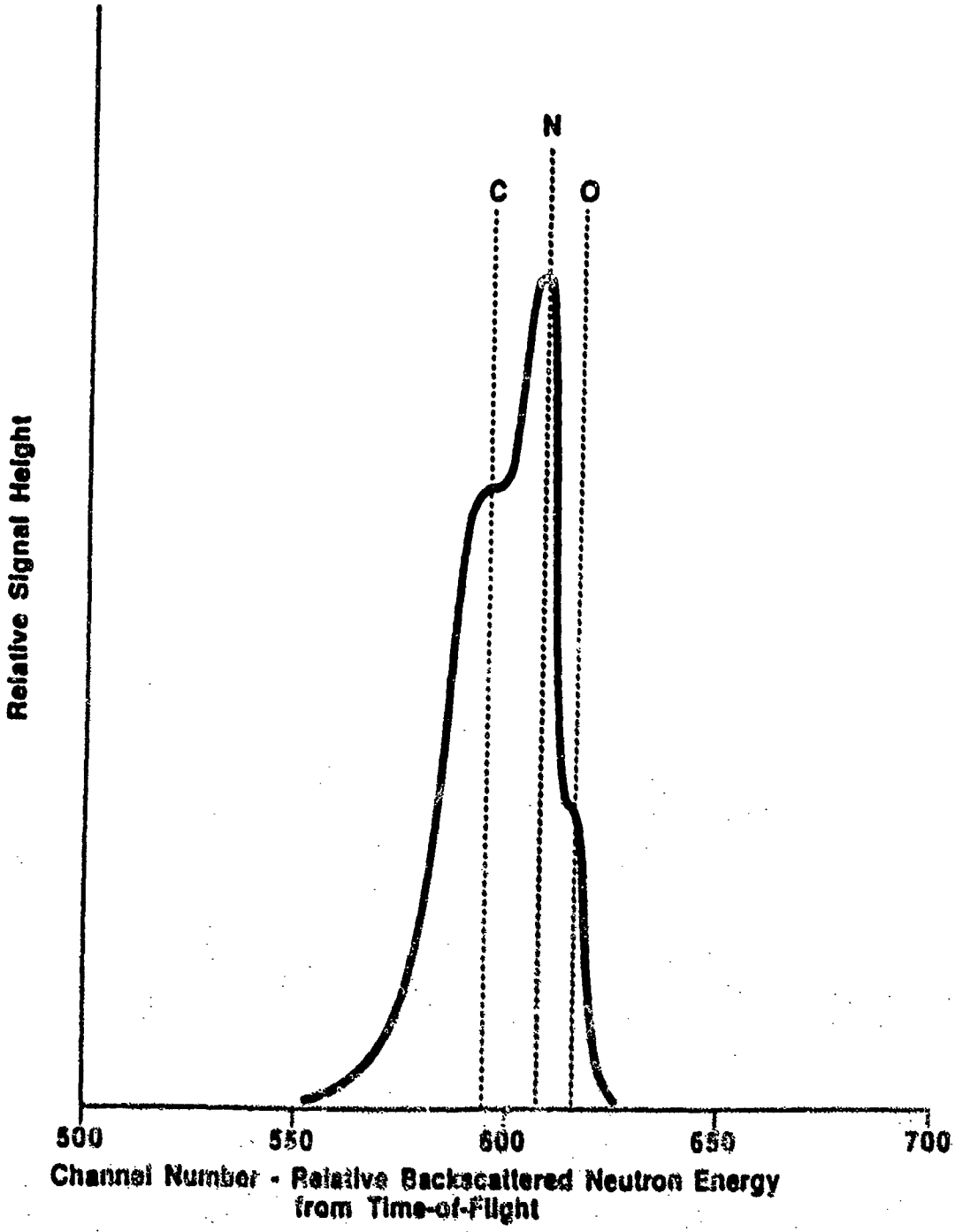


FIGURE 10. SPECTRUM OF BACK SCATTERED NEUTRONS FROM SIMULATED SHEET EXPLOSIVE
(1/4 inch of Melamine + Cellulose)
Beam Energy: 1.78 MeV (Strong Nitrogen Resonance)

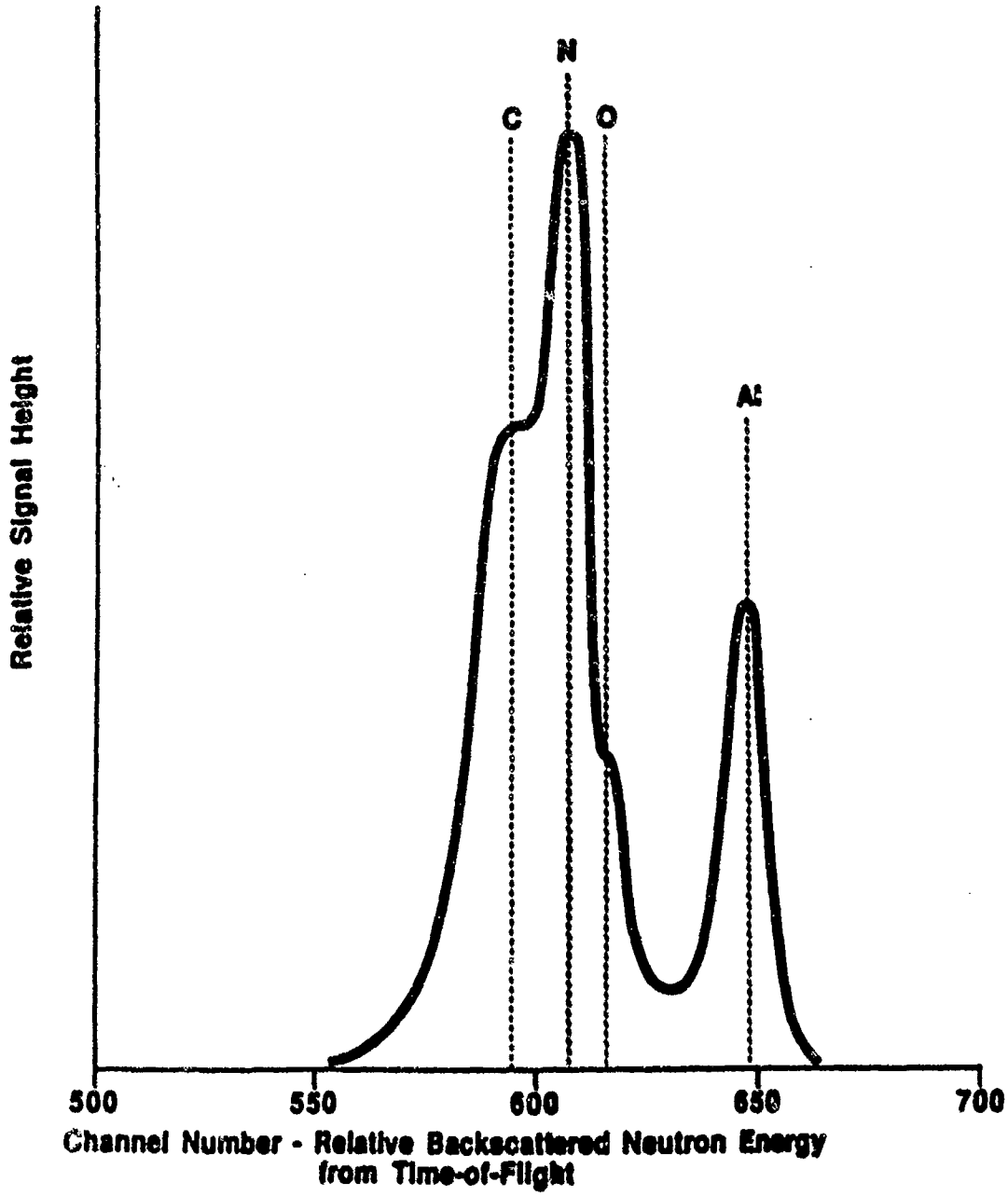


FIGURE 11. SPECTRUM OF BACK SCATTERED NEUTRONS FROM SIMULATED SHEET EXPLOSIVE
(1/4 inch of Melamine + Cellulose)
COVERED BY 1/8 inch SHEET OF ALUMINUM
Beam Energy: 1.78 MeV (Strong Nitrogen Resonance)

EXPLOSIVE DETECTION SYSTEM

Willis Lee, Joseph Bendahan, Peter Ryge, and Tsahi Gozani
Science Applications International Corporation
Santa Clara, CA

1. INTRODUCTION

The gamma ray scintillators form the basic detection system for three nuclear-based explosive detection systems, namely the thermal neutron analysis (TNA), fast neutron analysis (FNA), and pulsed fast neutron analysis (PFNA). These scintillators are required to distinguish gamma ray lines of interest from a variety of background that comes from non-explosive materials as well as the detector material itself. The gamma ray of interest in the case of TNA is the 10.83 MeV thermal neutron capture line from nitrogen. The lines of interest in FNA and PFNA are the 6.13 and 4.43 MeV lines from inelastic scattering of fast neutrons in oxygen and carbon, respectively, among others.

Various types of scintillators were evaluated. The list included thallium activated sodium iodide (NaI(Tl)), bismuth germanate ($Bi_4Ge_3O_{12}$, also known as BGO), and barium fluoride (BaF_2).

2. ENERGY AND TIME RESOLUTION

Good energy and time resolution are key factors in the detector selection process. They enable the separation of the gamma ray of interest from other interfering lines and background. In the case of the TNA, there are several gamma ray lines that lie just below the nitrogen region (10 - 11 MeV), causing interference. Some of these interfering lines are the 9.7 MeV chromium capture line, the 9.3 MeV iron capture line, the 9 MeV nickel capture line, and the 8.6 MeV chlorine capture line. The poor energy resolution makes the separation between nitrogen signals and deleterious signals from the interfering materials very difficult. The main background comes from pileup where two or more gamma rays, whose combined energies fall in the nitrogen region, are incident on the detector within the resolving time of the electronics.

When the energy resolution is compared at 662 KeV, the NaI(Tl) detector has the best resolution of about 7%, followed by the BaF_2 at 10%, and the BGO at 13%[1,2,3]. The BGO detector is inferior to the NaI(Tl) in energy resolution by about a factor of two and tends to trap the scintillation light because of its high index of refraction.

The time resolution for the 3"x3" NaI(Tl) detector is around 0.6 ns and for the 4" cube is 1.1 ns at 6.13 MeV. The time resolution for the BGO is little worse (around 1.4 ns) at 6.13 MeV and deteriorates rapidly towards lower energies. The BaF_2 detector is the fastest of the group; resolution time of 230 ps can be obtained with the 1"x1" scintillator. The timing resolution also improves with size.[4] This means better timing resolution can be obtained by using smaller crystals.

3. DETECTION EFFICIENCY

The detection efficiency increases with the density and atomic number of the scintillator material. The BGO has one of the best photopeak efficiencies (see Figure 1). It has an extremely high stopping power because of the high atomic number of bismuth (Z=83) and its high density (7.13 g/cm^3). A high stopping power is required to detect the very high energy gamma ray of 10.83 MeV in the TNA. Despite the inferior energy resolution, the BGO has a high peak to compton ratio and produces a lower contribution in the forms of single and double escape peaks. The former is 3 times and the latter 50 times smaller than the full energy peak, enhancing the separation of a nitrogen signal from that of chromium and iron.

In order to quantify the gamma ray detection efficiencies for various sizes and types of detectors, the detector responses were simulated using EGS4 (Electron Gamma Shower version 4) code. The input geometry included only the bare crystal. The gamma

ray sources were located 25 cm from the face of the detectors at an angle of 0 degree. The simulation results showed good agreement with the experimental data for a few benchmark cases (see Figure 2). From the simulation results, one can conclude that the BGO detector is over 2 times more efficient than the NaI and 1.5 times more efficient the BaF_2, for the same crystal size.

4. COMPARISON OF THE NaI(Tl) AND BGO SCINTILLATORS

A measurement was done to characterize and compare the NaI(Tl) and BGO scintillators of various sizes. The following types and sizes of the scintillators were studied: a 4"x4"x4" (cubic) NaI(Tl), and cylindrical shape: 3"x3" NaI(Tl), 2"x4" NaI(Tl), 3"x3" BGO, and a 2"X2" BGO detector. These detectors were tested in a prototype carry-on explosive detection system (COEDS). Two different widths of nitrogen regions were evaluated, namely a wide region (9.4 MeV - 11.3 MeV) and a narrow region (10.05 MeV - 11.3 MeV). The wide region included a 10.83 MeV full energy peak all the way down to the double escape peak, and the narrow region excluded the double escape peak. The wide region favors the smaller detectors while the narrow region favors the large 4"x 4"x 4" NaI(Tl). For instance, since smaller detectors lack a detection efficiency and have a higher probability of producing single and double escape peaks, a wider region would be more beneficial.

Table 1 summarizes the comparison of net signal, signal to background ratio, and figure of merit. The figure of merit (FOM) is defined as:

$$FOM = \frac{S}{\sqrt{S+2B}} = \frac{S\sqrt{B}}{\sqrt{2+S/B}}$$

where S represents count rate due to the source alone without background and B represents count rate due to background. The FOM measures the ratio of signal to statistical background in terms of the number of (counting statistics) standard deviation. This measure is especially important in TNA because of its short acquisition time.

The results seem to indicate that there will probably be more losses than gains by going with a 2"x4" NaI(Tl) detector. For example, the figure of merit dropped by more than a factor of two between a 4"x4"x4" and 2"x4" NaI(Tl) detector while signal to background ratio improved a little for the wide region and remained same for the narrow region. A 3"x3" NaI(Tl) detector faired slightly better, but the improvement in signal to background ratio was not enough to offset the deficiency in the net signal and figure of merit. However, these smaller detectors could fare better if the source intensity could be increased.

The 3"x3" and 2"x2" BGO detectors were then compared against the 4" cube NaI(Tl). In order to reduce the interference from neutron capture gamma rays in ^{73}Ge, the BGO detectors were encased in appropriate shielding. The detector signals were passed through a preamplifier and a conventional spectroscopy amplifier (Canberra 2020). Its output was then fed to an ADC which was part of the Nuclear Data Accuspec PC-based MCA board. Table 2 shows some basic comparisons between the detectors, namely the front surface area, the volume of the crystal and their total input count rates.
As might be expected, the count rate is roughly proportional to the surface area ratio. Figure 3 shows the spectral comparison between these three detectors. The resolution measurements were done at three different gamma ray energies, namely 2.22 MeV (hydrogen capture), 4.95 MeV (carbon capture), and 10.83 MeV (nitrogen capture).

The resolution comparison (see Table 3) confirms that the NaI(Tl) detector has a superior resolution than the BGO detectors. For example, at 10.83 MeV the 3"x3" BGO detector has about a 28% poorer resolution than the 4" cube NaI detector, and the 2"x2" BGO has a 41% inferior resolution than the 4"x4"x4".

The efficiencies of these detectors are also compared. To compare efficiencies of the detectors, a following method of calculating the detector efficiency was used:

Efficiency = Total output count rate above 2 MeV / Total input count rate above noise.

This counting efficiency measures the intrinsic detection efficiency for high energy gamma rays (above 2 MeV) with respect to all gamma rays recorded by the detector.

For the 4" cube NaI(Tl) and the 3"x3" BGO, the

calculated efficiency was identical at about 17% while the 2"x2" BGO efficiency was somewhat lower at about 14%.

5. CONCLUSION

Other factors to consider in the detector selection process are cost, availability, handling, and sensitivity to neutron backgrounds. Table 4[1,5] summarizes the basic properties of various scintillators. The NaI(Tl) is the most available and relatively inexpensive detector. Its energy resolution is one of the best among inorganic scintillators, but its time resolution and detection efficiency are only average. It needs to be handled with care since it is hygroscopic and fragile[1]. The BGO detector is the most efficient of the group, with its high stopping power and high peak to compton ratio. It is also non-hygroscopic and much more rugged compared to the NaI(Tl). Its disadvantages include poor energy and timing resolution, high cost, and low availability. The BaF_2 detector has the fastest timing resolution of the group. Its efficiency is between that of the BGO and NaI(Tl) detectors. Figure 4 shows the comparisons of spectra taken in a laboratory FNA system. However, its disadvantages are poor resolution, high cost, and low to medium availability.

In nuclear based systems, detectors are exposed to neutron fluxes of different energies. These neutrons may create backgrounds in the various gamma energy region and may also add to the overall count rate in the detector. The calculated cross section for thermal neutron capture in a NaI detector is 2.7×10^{22} barns per gram while the cross section in a BGO is only 3.4×10^{21} barns per gram[6]. The factor of eight reduction in the cross section for the BGO means significant reduction in the background. In the case of the NaI(Tl), neutrons impinging on the crystal creates cascade of gamma ray lines around 6.8 MeV due to resonance capture of neutrons in iodine. On the other hand, a BGO manifests a 10.2 MeV gamma ray line which comes from cascade gamma rays emitted as a result of neutron capture on ^{73}Ge (7.8% abundant isotope of Ge) within the crystal (see Figure 5). This high energy gamma ray falls within the nitrogen region in the TNA and thus poses a problem. Fortunately, it has been proven that this line can be sufficiently reduced by surrounding a BGO detector with adequate shielding. The same is true with a NaI(Tl) detector. A BaF_2 detector is the least problematic in this area because of its low cross section to neutrons, and its background gamma rays do not interfere with the gamma rays of interest.

NOTES

[1]Harshaw Chemical Company, Solon, Ohio.

[2]Rexon Corporation, Macedonia, Ohio.

[3]Bicron Corporation, Newbury, Ohio.

[4]E. Dafni, Nuclear Instruments and Methods in Physics Research A254 (1987) 54-60, North-Holland, Amsterdam.

[5]W.C. Kaiser, Anal. Chem. 38 (11), 27A (1966).

[6]S.A. Wender, IEEE Transactions on Nuclear Science, Vol. NS-30, No. 2 (April 1983).

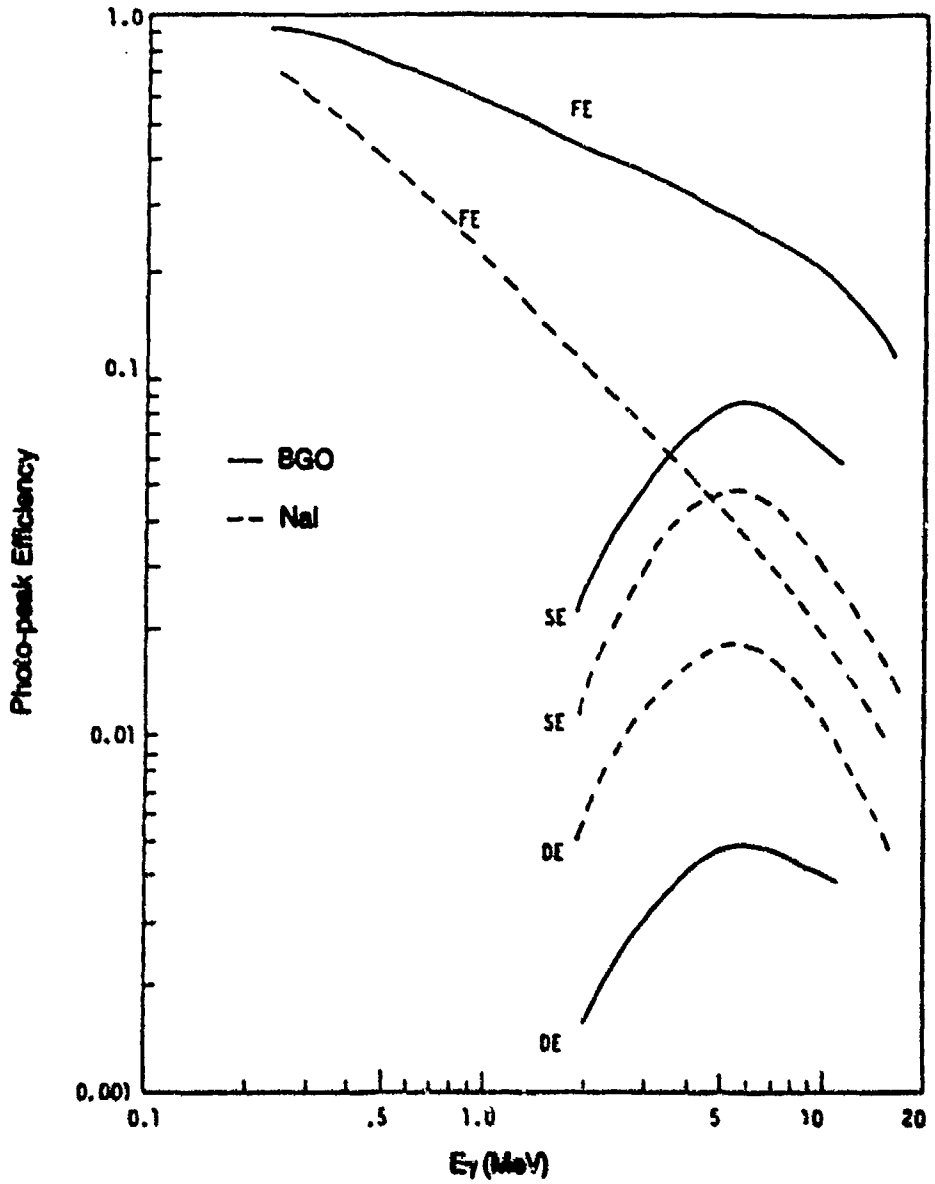


Figure 1 Comparison of Photo Peak Efficiency Between NaI(Tl) and BGO Detectors.

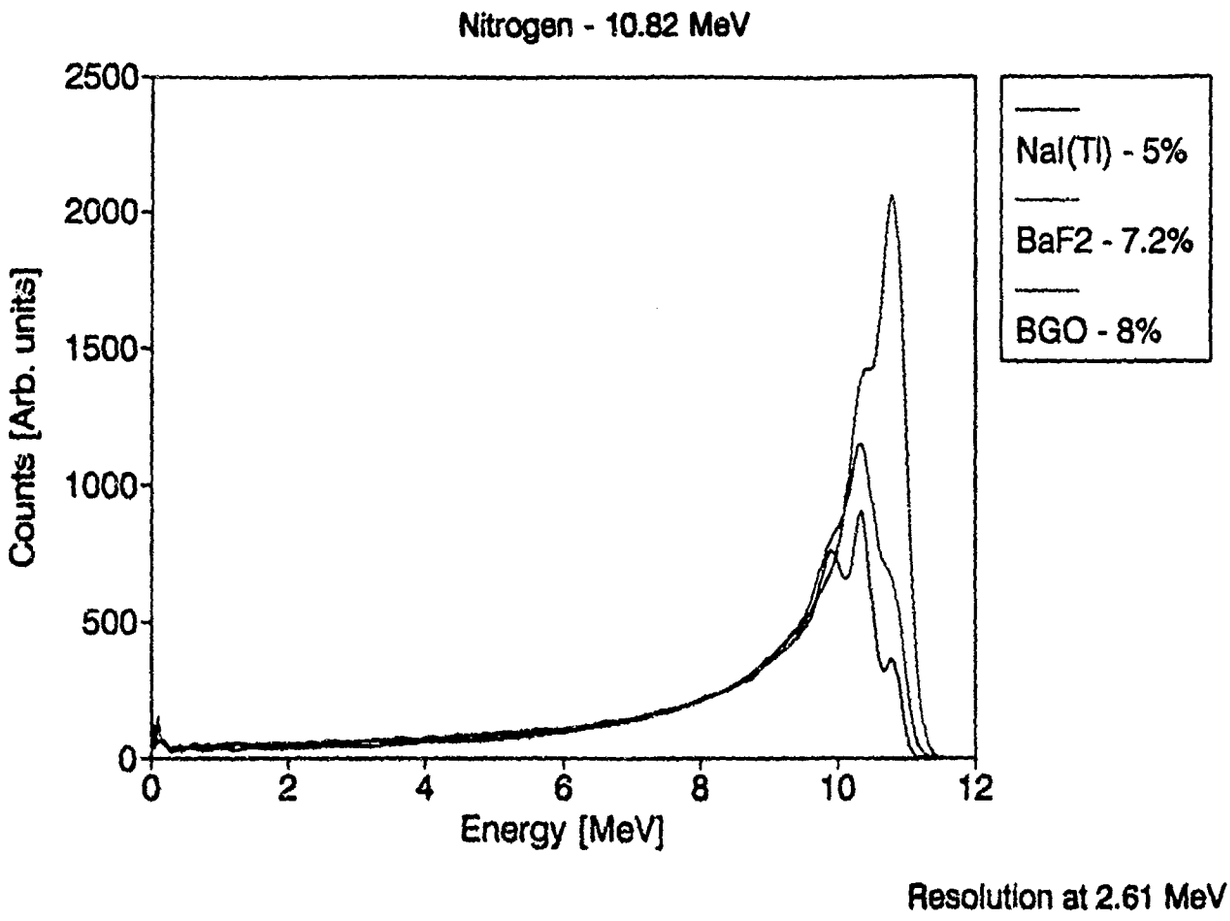


Figure 2 Detector Response (3"x3")

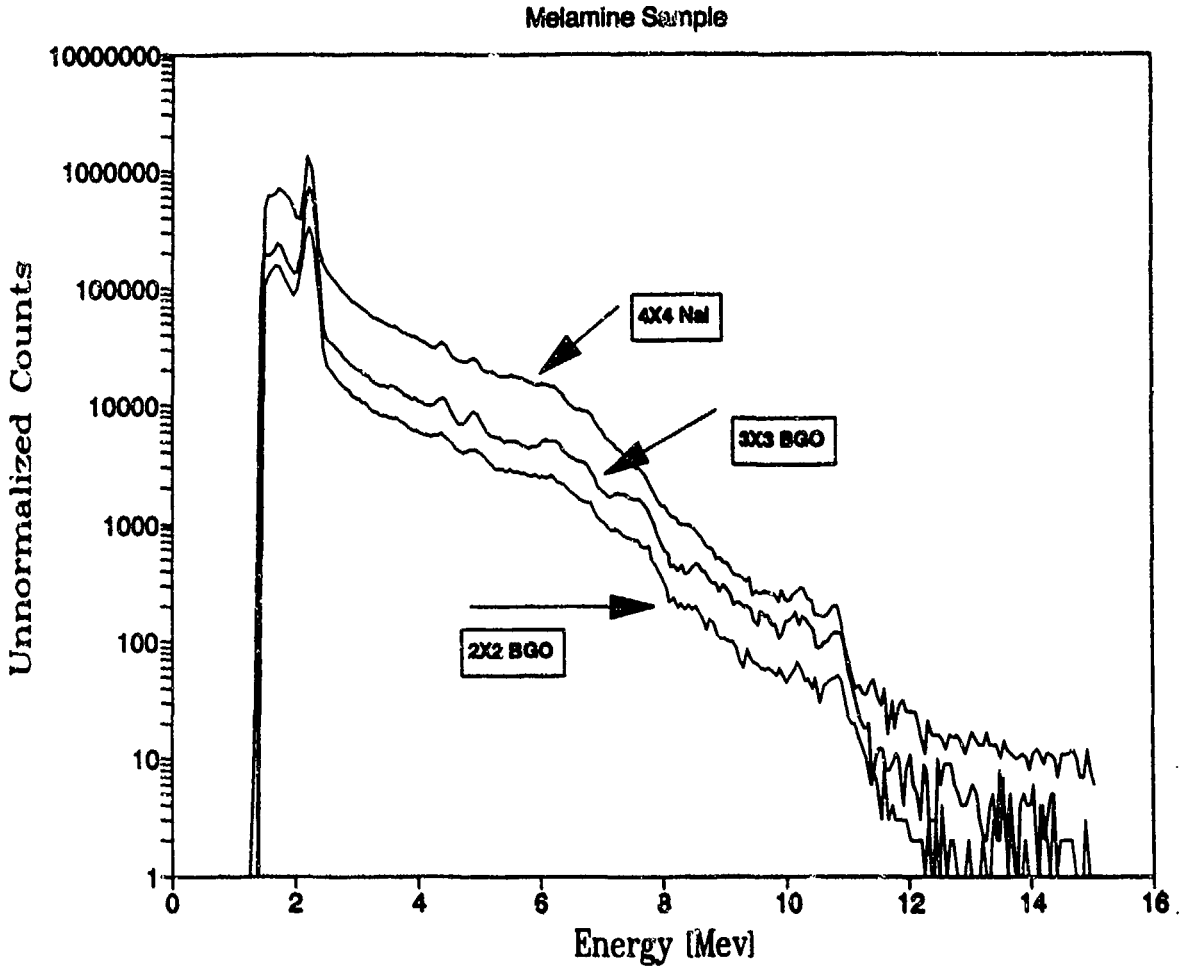


Figure 3 Detector Comparison Using COEDS

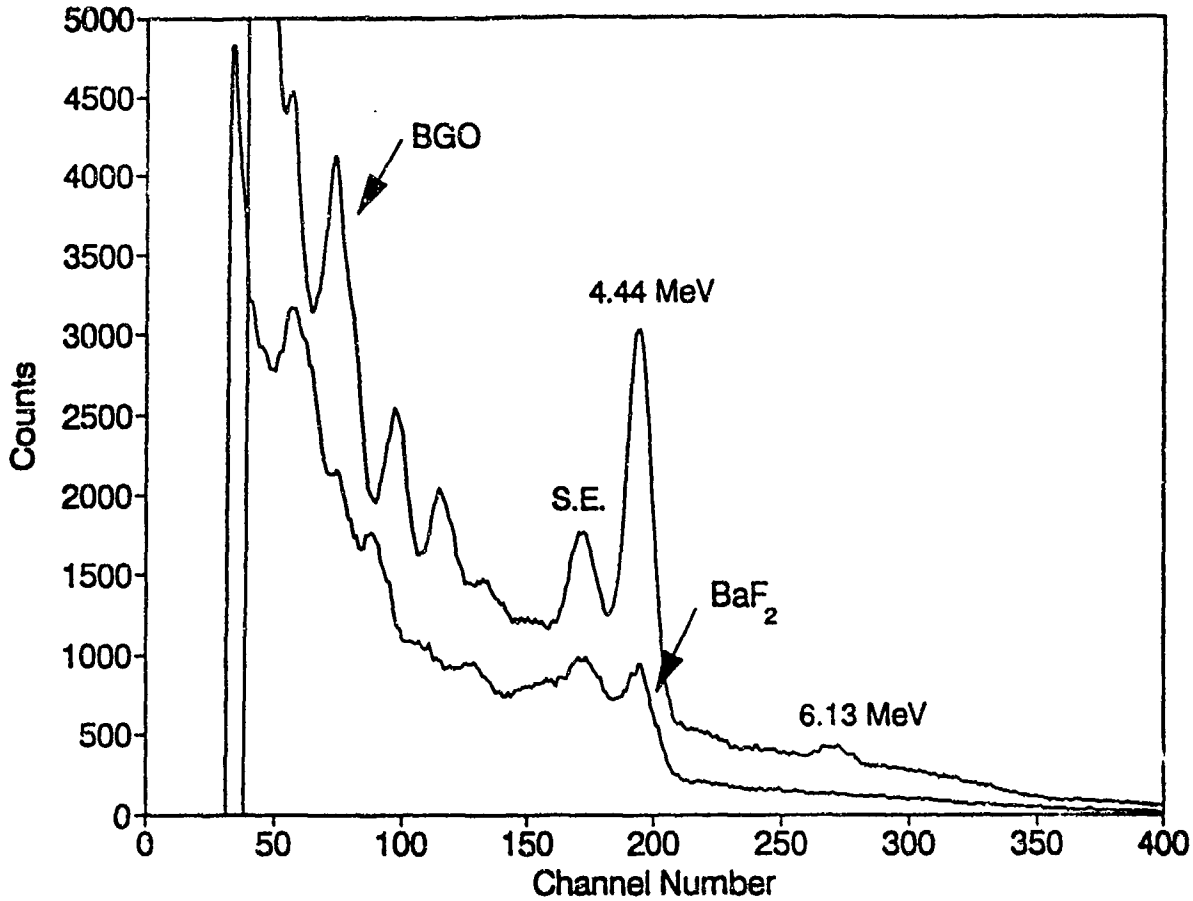


Figure 4 Comparison between a 3"x3" BaF_2 detector (bottom) and a 3"x3" BGO detector for a 2"x2"x4" graphite sample in a laboratory FNA system. Observe the lower efficiency and background of the BaF_2 detector.

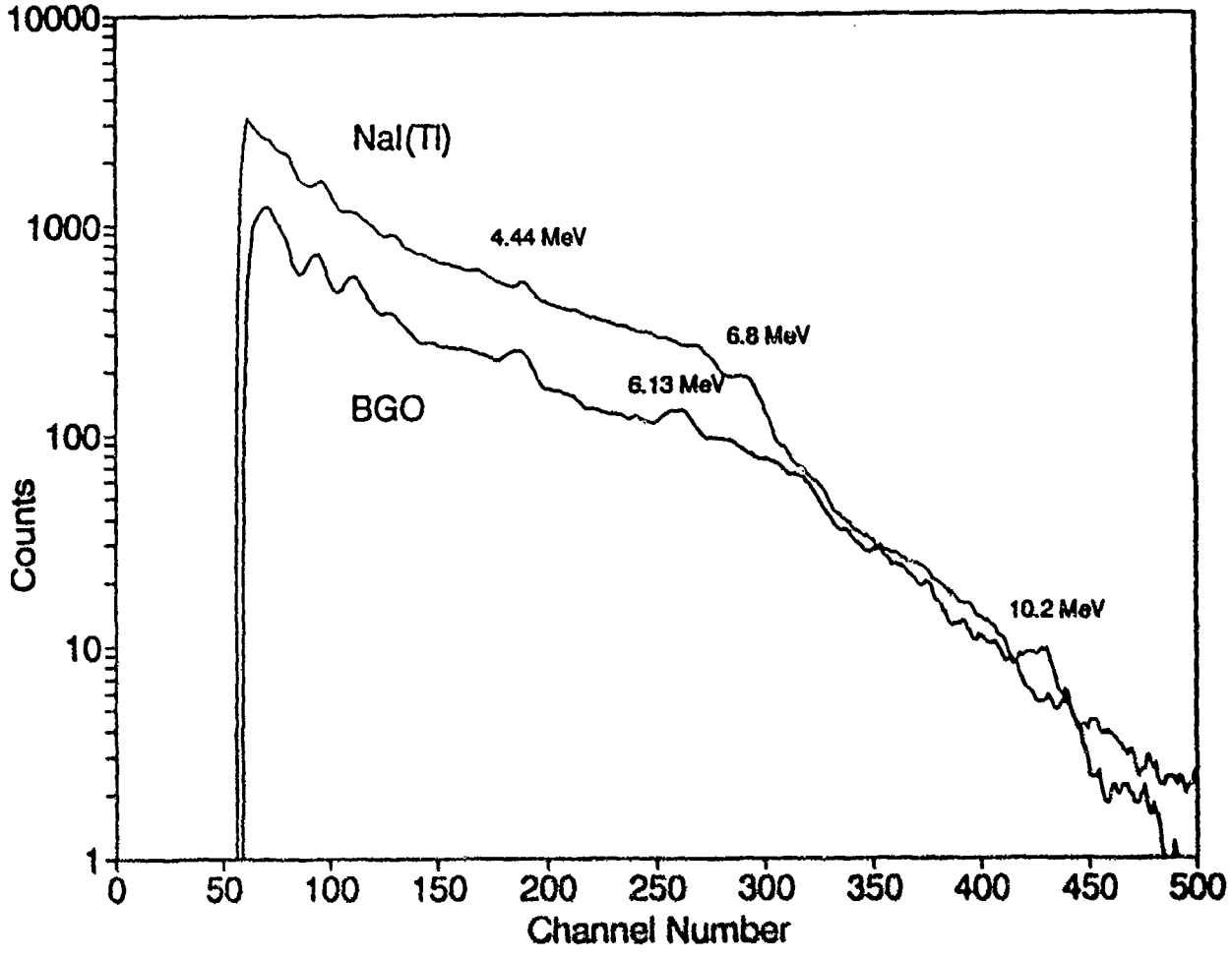


Figure 5 Comparison between a 4"x4"x4" NaI(Tl) (top) and a 3"x3" BGO (bottom) detectors under the same conditions. Observe the 6.8 MeV gamma ray and lower energy continuum emitted by neutron capture in Iodine. The counterpart in the BGO detector is the 10.2 MeV emitted by neutron capture in ^{73}Ge isotope.

Table 1

FOM Comparison Between Various NaI Detector Sizes

Wide Region: (9.4 MeV - 11.3 MeV)			
Detector Size	Net	S/B	FOM
4x4 (det 33)	10.89	2.23	2.40
4x4 (det 48)	11.18	2.64	2.52
3x3 (det 47)	3.61	3.44	1.51
2x4 (det 34)	1.69	3.31	1.03
Narrow Region: (10.05 MeV - 11.3 MeV)			
Detector Size	Net	S/B	FOM
4x4 (det 33)	7.17	3.22	2.10
4x4 (det 48)	6.92	3.41	2.09
3x3 (det 47)	1.79	3.65	1.08
2x4 (det 34)	0.80	3.20	0.70

Table 2

Description of the Scintillators

	4"x4"x4" NaI	3"x3" BGO	2"x2" BGO
Area	16 in^2	7.1 in^2	3.1 in^2
Volume	64 in^3	21.3 in^3	6.2 in^3
Count Rate	23.6 kcps	11.5 kcps	7.1 kcps

Table 3

Energy Resolution Comparison

Detector	Element	Energy	FWHM % Resolution
4"x4"x4"	H	2.22 MeV	5.8
3"x3"	H	2.22	7.4
2"x2"	H	2.22	8.7
4"x4"x4"	C	4.95	3.3
3"x3"	C	4.95	4.0
2"x2"	C	4.95	5.8
4"x4"x4"	N	10.83	1.8
3"x3"	N	10.83	2.3
2"x2"	N	10.8e	2.5

Table 4

Basic Properties of Various Scintillators

	Density (gr/cm^3)	Energy Resolution at E=0.662 MeV	Time Decay τ	Radiation Length (cm)	Price* $/cm^3	Availability	Observations
NaI (Tl)	3.67	7%	230 ns	2.6	1.70-2.50	Good	
BGO	7.13	13%	300 ns	1.1	14-18	Fair	
BaF_2	4.80	30% (fast) 10% (total)	0.6 ns 600 ns	2.1	8-10	Fair	Requires quartz window
CsI	4.5	18% (fast) 16% (total)	10 ns, 30 ns 1 μs	2.0	5	Good	Requires quartz window
CsI(Tl)	4.5	8%	1 μs	2.0	5	Good	
CsI(Na)	4.5	7.2%	630 ns	2.0	5	Good	
NaI	3.67	>5.5% (?)	60 ns	2.6	2.50	Good	Requires quartz window. Characteristics at 77° K.
GSO	6.71	7.8%	60 ns 600 ns	NA	NA	Poor	τ depends on Ce concentration

* Price for single detector. For bulk order the price is significantly lower.

EXPLOSIVE DETECTION SYSTEM BASED ON ELECTRONIC NEUTRON GENERATOR (ENG)

Willis Lee, David B. Mahood, Peter Ryge, Joseph Bendahan, and Tsahi Gozani
Science Applications International Corporation
2950 Patrick Henry Dr.
Santa Clara, CA 95054

1. INTRODUCTION

Under FAA sponsorship, thermal neutron analysis (TNA) explosive detection systems (EDS) for inspection of checked airline baggage have been developed and demonstrated. Two parallel development paths were initiated, one using a californium-252 radioisotope source and one using an electronic neutron generator (ENG) consisting of a small particle accelerator with a neutron production target. A second generation development produced the californium-based TNA presently deployed in various airports.

Each of these neutron sources has its advantages over the other. The californium source is more compact, economical and absolutely reliable since neutrons are emitted constantly (whether desired or not). A neutron generator is more bulky, expensive, and, like any equipment, not totally reliable. However, since it can be turned off and thereby cease emitting radiation, it was considered inherently safer and expected to be less difficult in terms of regulation and licensing. It was also expected that the ENG-based EDS would be less subject to the extreme sensitivities of some individuals to the presence of radioactive materials in a public application.

The Kaman A711 was the least costly neutron generator capable of providing the necessary neutron flux and was therefore selected for the ENG-EDS development. A prototype EDS using it was designed, constructed and evaluated.

2. THICK TARGET YIELDS

Various deuteron beam reactions can be employed for producing neutrons. Neutron production yields are shown in Figure 1 for various reactions.[1] The prolific $T(d,n)^4He$ reaction is not suitable for TNA application because the 14 MeV neutrons emitted are too difficult to shield and produce excessive background.

The $D(d,n)^3He$ reaction has a high yield with low particle energies and was used in the compact Kaman generator. The energy distribution of the neutrons emitted from the $D(d,n)^3He$ reaction at low deuteron beam energy is almost monoenergetic, resulting in a good neutron thermalization efficiency. The Kaman accelerator produced a 180 keV deuteron beam with currents of up to 4.0 mA which resulted in a total neutron output of $5x10^8$ n/sec at an energy of about 2.6 MeV.

The $^9Be(d,n)^{10}B$ reaction was also employed for the production of neutrons. The neutron yield from the reaction is isotropic about the target and the energy distribution is shown in Figure 2. The neutron spectrum of interest is from the 1.0 MeV deuteron beam produced by the National Electrostatic Corporation (NEC) accelerator.

Figure 3 shows the expected neutron production from the $^9Be(d,n)^{10}B$ reaction at various bombarding energies. A 1 MeV deuteron beam should produce a neutron output of about $1x10^8$ n/sec-μA. The NEC accelerator was rated at a maximum beam current of 20 μA at 1 MeV energy with stable, reliable operation, giving neutron outputs as high as $1x10^9$ n/sec.

3. ADVANTAGES AND DISADVANTAGES OF THE $D(d,n)He^3$ AND $Be^9(d,n)B^{10}$ REACTIONS

The major advantage of the $D(d,n)^3He$ reaction is that high neutron yields can be achieved at low voltage or beam energy but requires high beam current. The monoenergetic output results in more efficient thermal neutron production.

The principal disadvantage is that the target is short lived due to deuterium sputtering erosion which occurs at the high beam currents needed to supply adequate neutron yield.

The $^9Be(d,n)^{10}B$ reaction has the advantage of producing high neutron output but requires higher

beam energy. The major advantage of the reaction is that solid beryllium neutron production targets can be employed and will last indefinitely. A disadvantage is the production of gamma rays along with the broad neutron spectrum resulting in a higher background which must be taken into account.

4. NEUTRON GENERATOR SYSTEMS

4.1 Kaman Model A711 Neutron Generator

The Kaman A711 Neutron Generator is shown schematically in Figure 4 integrated with the prototype EDS. The compact accelerator head is located within the shielding above the baggage-carrying conveyor belt. The head consists of an SF_6 insulated pressure vessel containing the glass and metal sealed accelerator tube, comprised of a deuterium ion source, acceleration electrodes and neutron production target. This sealed tube was an expended component, replaced at a cost of $17,000, requiring about eight hours. The high voltage power supplies and cooling systems are placed on top of the conveyor shielding at the ends of the EDS.

The Kaman accelerator was operated by a laboratory technician. The control system for the accelerator was found to be unstable, so a microprocessor based controller was developed to automatically maintain a fairly constant neutron output. The A711 was used for development and testing in the laboratory and was later installed at airport locations in the prototype EDS.

Reliability of the accelerator was found to be unsatisfactory due to failure of the sealed accelerator tubes. The accelerator was operated near maximum voltage and beam current in order to obtain the required neutron output. The neutron yield dropped considerably in some tubes in relatively short periods of time.

Explosive detection performance of the EDS with the Kaman generator was tested at San Francisco and Los Angeles airports on passenger baggage and at San Francisco on air cargo. Probability of detection, probability of false alarm and throughput goals were met.

The useful life of the tubes varied considerably but was generally about 250 hours of continuous full output operation.

4.2 National Electrostatic Corporation Model 3SH Accelerator

The National Electrostatic Corporation (NEC) Model 3SH accelerator was installed and tested in the EDS prototype previously used with the Kaman. A thick, solid beryllium target was brazed to the end of the beam tube. Figure 5 shows the schematic diagram of the NEC accelerator mounted on the EDS. The Model 3SH is contained in a sealed tank filled with SF_6 to insulate the ion source, accelerator column, and pellet-chain high voltage charging system.

During initial installation and testing of the accelerator some minor modification and repairs were necessary but all of the problems were resolved within the first 2000 hours of operation and the total time required for the modifications and repairs was about 4 days.

Operation of the accelerator was fairly simple and required an operator at a laboratory technician level with an understanding of accelerator maintenance. The stability of the neutron output was excellent and did not require modifications to the control system as did the Kaman unit. Other than minor adjustments of the corona probe used for voltage regulation, the NEC accelerator has been operated continuously with no major faults or maintenance required for a period of 10,000 hours. At the time that this report was written the neutron generator had been run for 12,649 hours. The NEC Model 3SH pelletron has proven to be a reliable, safe, and economical neutron generator.

5. EXPLOSIVE DETECTION PERFORMANCE OF NEC ACCELERATOR BASED EDS

A large number of bags must be run through the system in order to establish its performance with statistical validity. This process is very time consuming. Therefore, a simpler technique for estimating the performance from a smaller number of measurements was desired. This simpler technique involves measuring ten standard bags with and without explosives. For convenience reasons, explosive simulants were used in place of actual explosives. The bags were chosen to cover the full range, as measured by the nitrogen content and flux absorption, of actual suitcases encountered in airports. The EDS computer makes explosive detection decisions by discriminant analysis [2] of features which are a mathematical combination of the detector counts measured by the system. The distance between the centers of the two clusters (with

and without explosives) in feature space can be used to predict the performance and compare different EDS systems.

To compare between systems on a common ground, the same set of ten bags are used repeatedly, and the five best features are deduced by the stepwise discriminant procedure. Since the ten bags are chosen to represent the extremes of the distribution of passenger bags, there is a high correlation of the distance between the two clusters as measured by the ten bags with the detection and the false alarm rates measured on the more numerous passenger bags. The separation is calculated from the means for the two clusters in units of the standard deviation of the points about the mean. This measure of separation, also known as the Mahalanobis distance D, is computed by SAS [3] procedure DISCRIM. Its formula is as follows:

$$D^2 = (X_i - X_j)^T \, COV^{-1} (X_i - X_j)$$

where the i and j refer to two clusters, X is the mean vector for the cluster, and COV^{-1} is the inverse of the covariance matrix between the clusters. The calculated Mahalanobis distance showed that the performance of the NEC accelerator based EDS was comparable to that of the californium-based TNA units.

One of the advantages of an electronic neutron generator is its ability to produce variable neutron output by the adjustment of its beam current. This unique feature was exploited, and the detector performances were compared at three different beam currents, namely 2 μA, 5 μA, and 10 μA. The detector performance is measured in terms of its figure of merit (FOM), which is defined as

$$FOM = S/\sqrt{S+2B} = S\sqrt{B}/\sqrt{2+S/B}$$

where S represents count rate due to the source alone without background and B represents the count rate due to background. The FOM measures the ratio of signal to statistical background in terms of the number of (counting statistics) standard deviations. This measure is especially important in EDS because of its short measurement time. The signal of interest, is the 10.8 MeV γ-ray from the thermal neutron capture in nitrogen. For the FOM calculations, a wide region including the full-energy, single and double escape peaks was used. Figure 6 shows the pulse height spectrum acquired at the three beam currents and their respective FOMs. It is evident that the FOM increases with neutron output in this range. As count rate increases further, the background increases and FOM deteriorates above an optimal point.

6. CONCLUSION

Experience with the prototype ENG-EDS has shown that an operational airport baggage inspection system based on an electronic neutron generator can be built and would be a practical and effective alternative to a system employing radioactive materials.

REFERENCES

1. Burrill, A. E., "Neutron Production and Protection", High Voltage Engineering Corporation, Burlington, MA.

2. Anderson, T.W., Introduction to Multivariate Statistical Analysis, 1958.

3. SAS User's Guide: Statistics Version 5, 1985.

NOTES

1. Work was conducted under FAA Contract No. DTFA03-85-C-0049.

2 KAMAN Instrumentation Corporation, Colorado Springs, Colorado.

3. National Electrostatics Corporation, Middleton, Wisconsin.

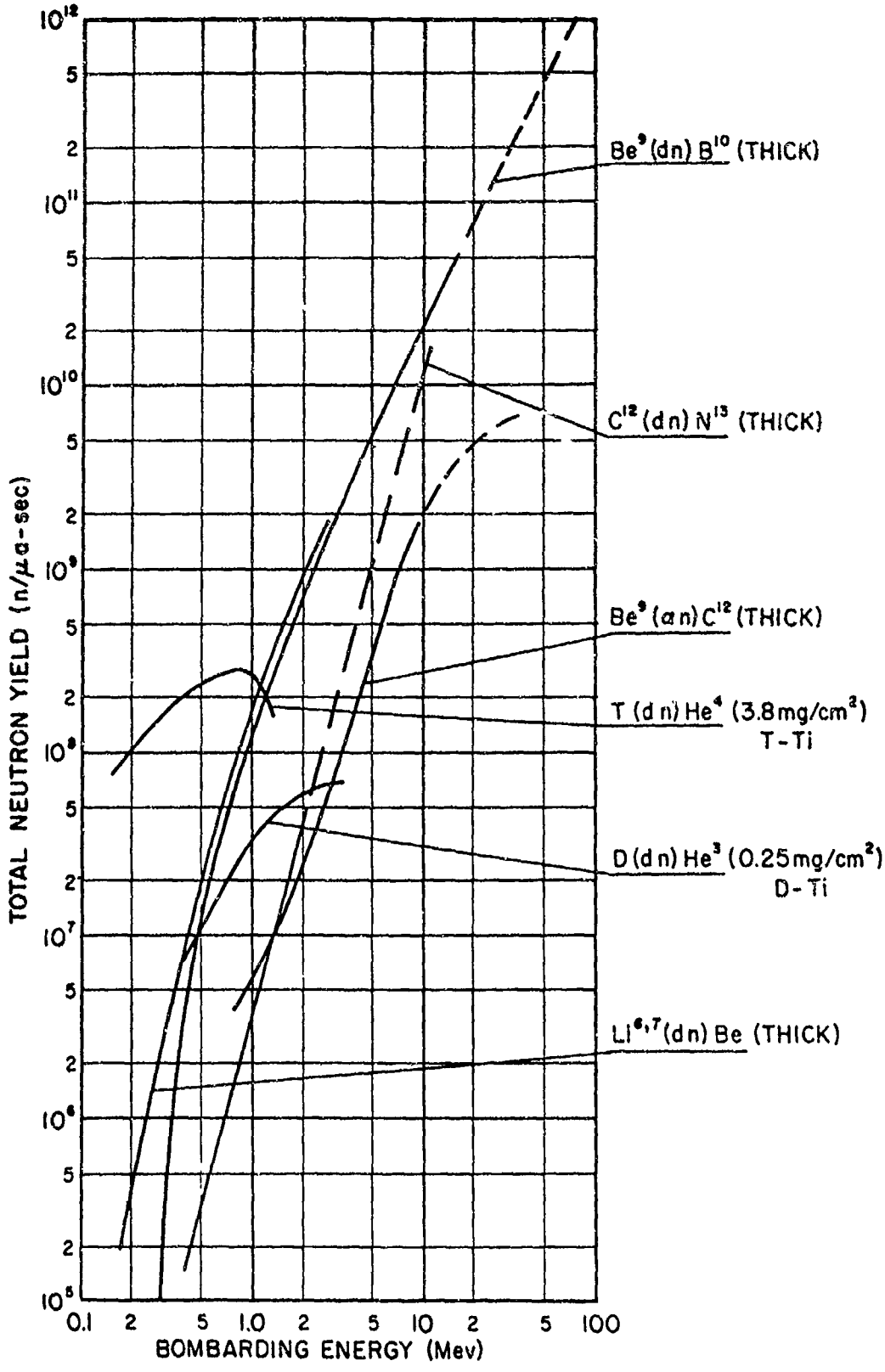


Figure 1 Neutron Yields - (d,n) and (α,N) Reactions

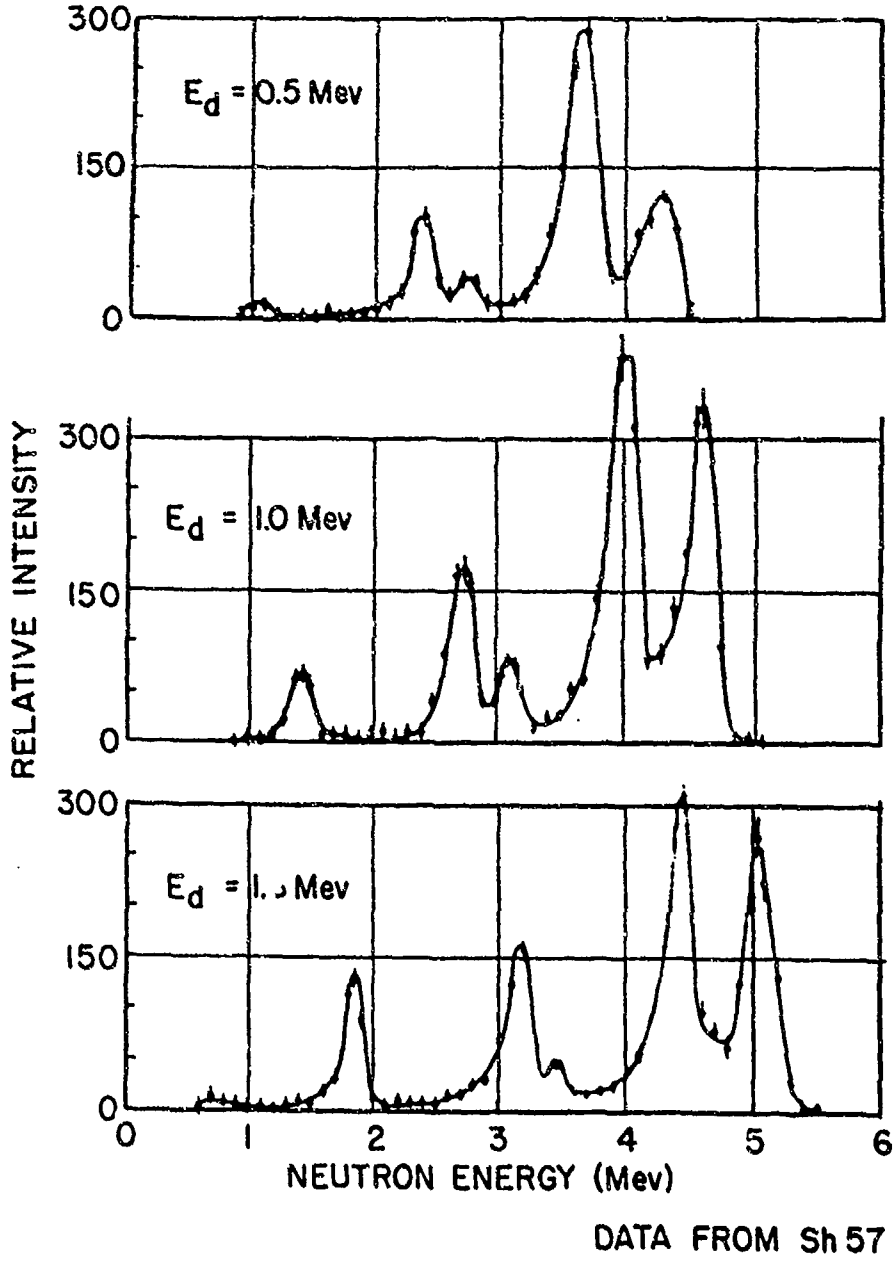


Figure 2 **Neutron Spectra from $^{9}Be(d,n)^{10}B$ Reaction - Low Energy**

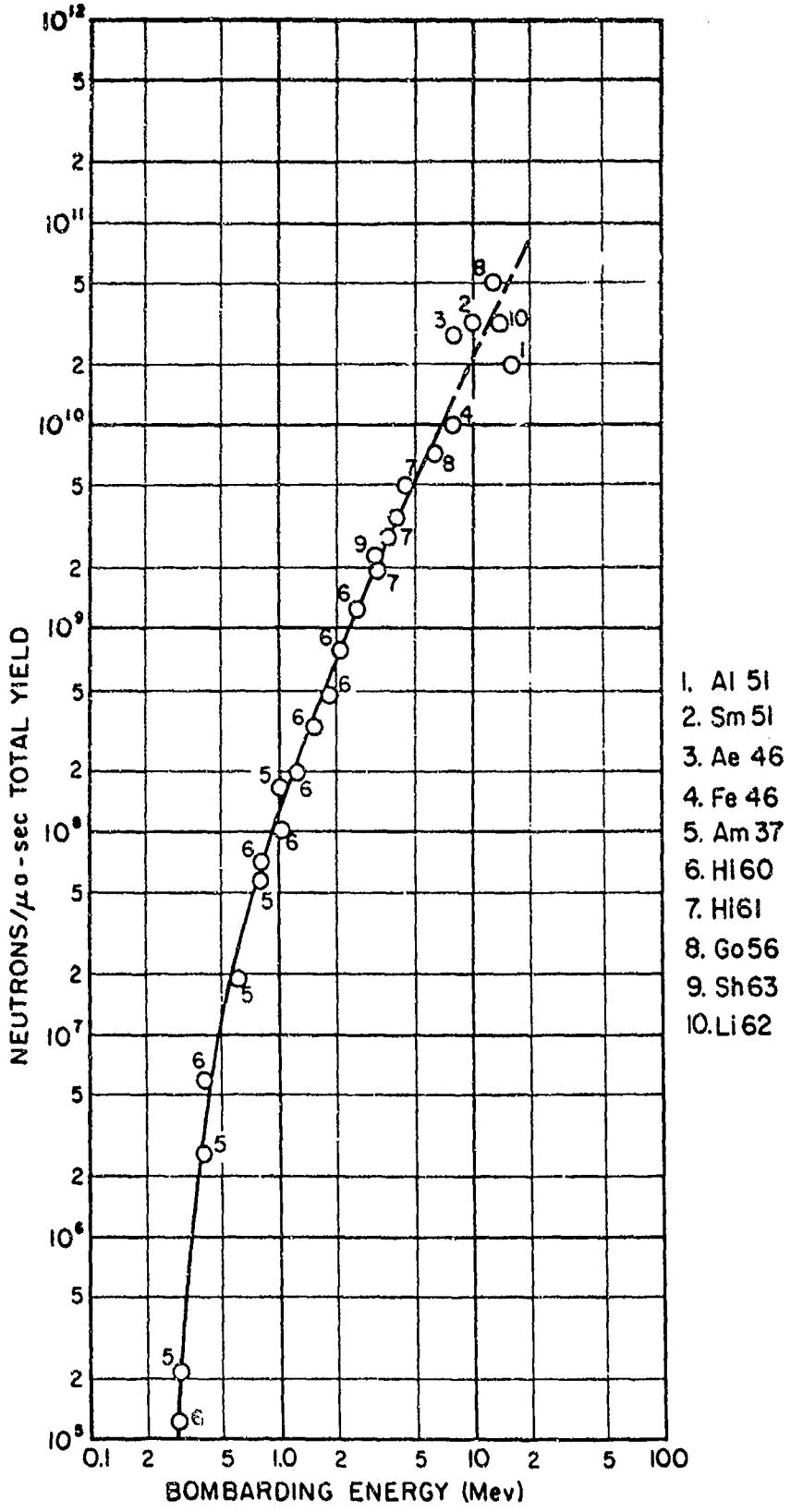


Figure 3 Neutron Yield from $^{9}Be(d,n)^{10}B$ Thick Target

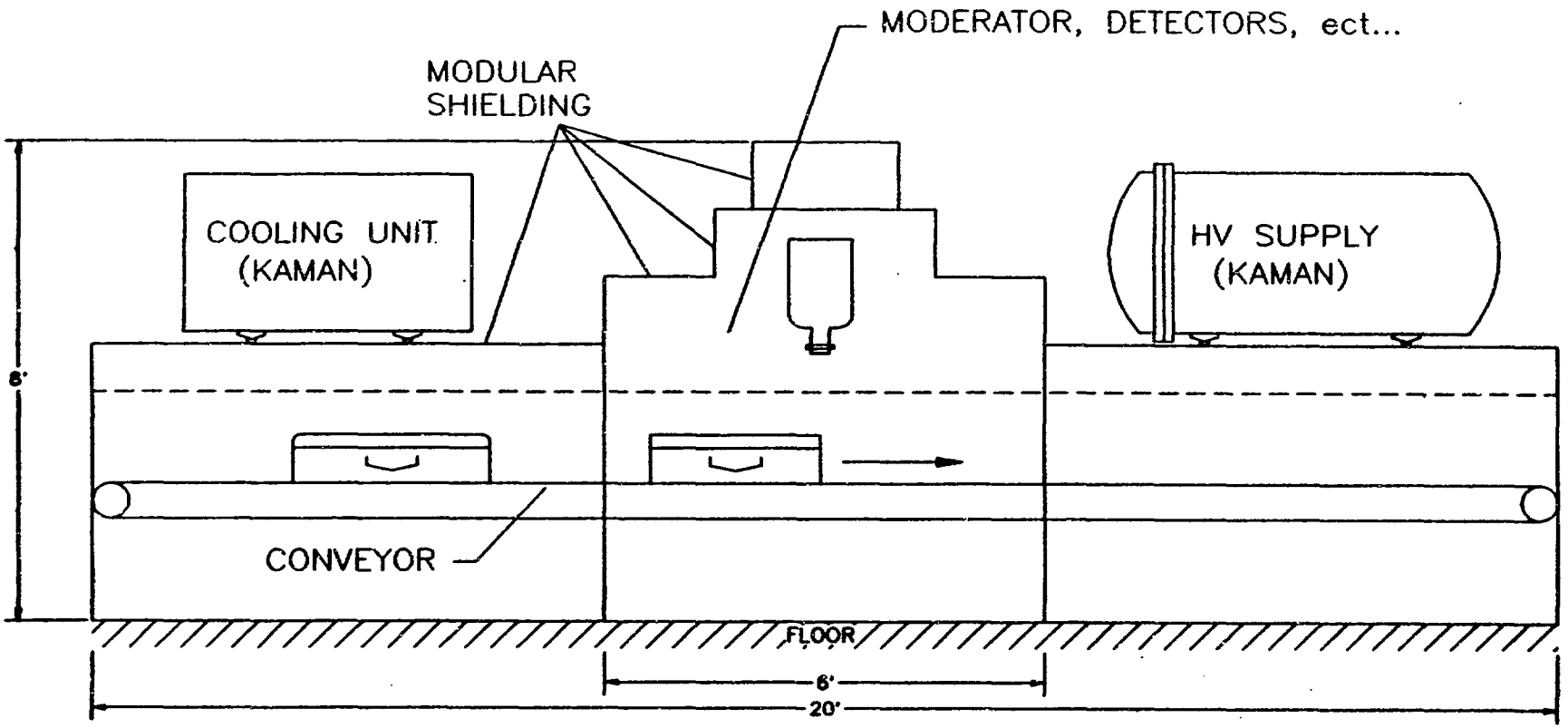


Figure 4 Kaman A-711 neutron generator integrated with prototype EDS.

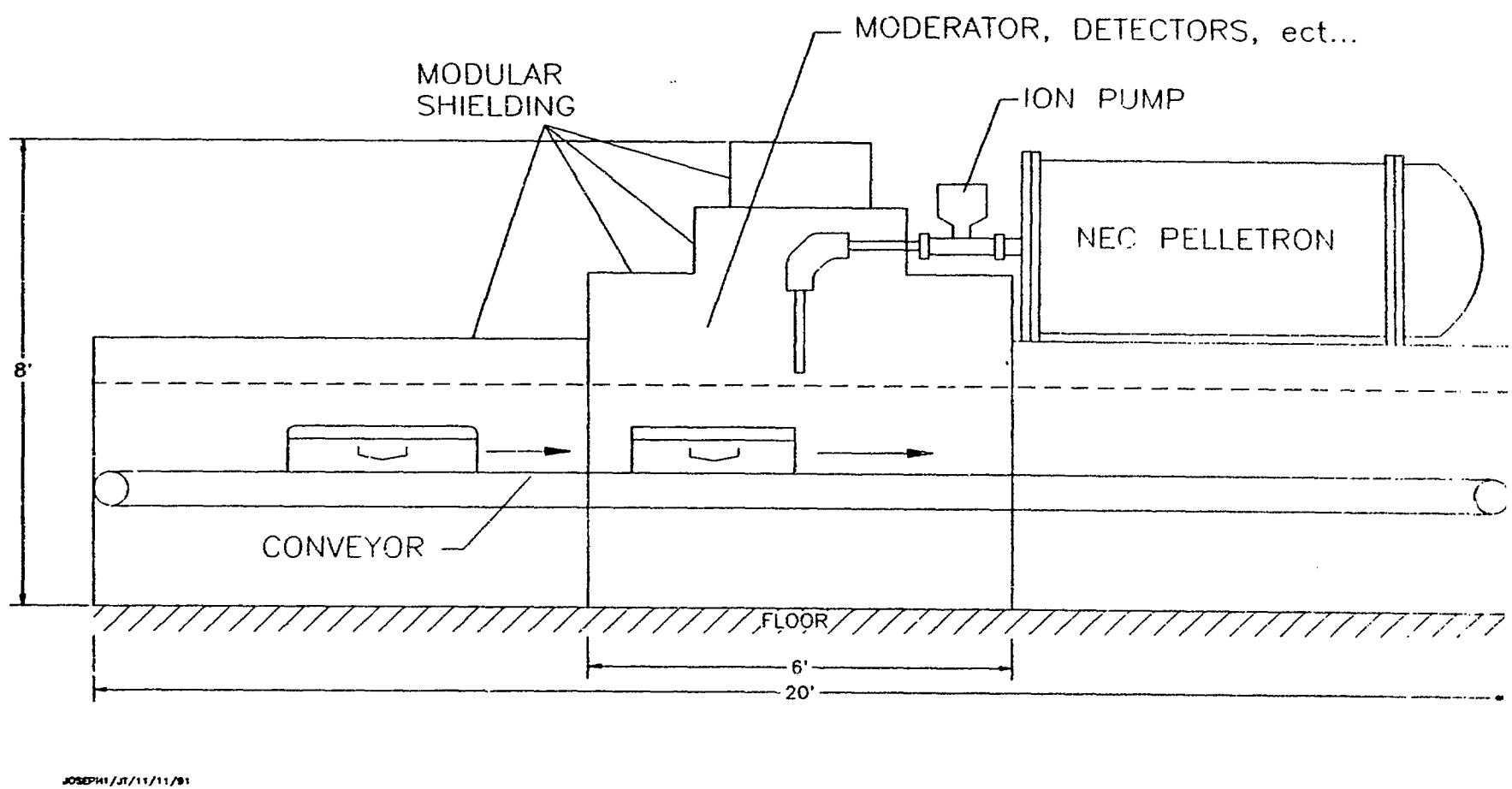


Figure 5 NEC Accelerator integrated with prototype EDS.

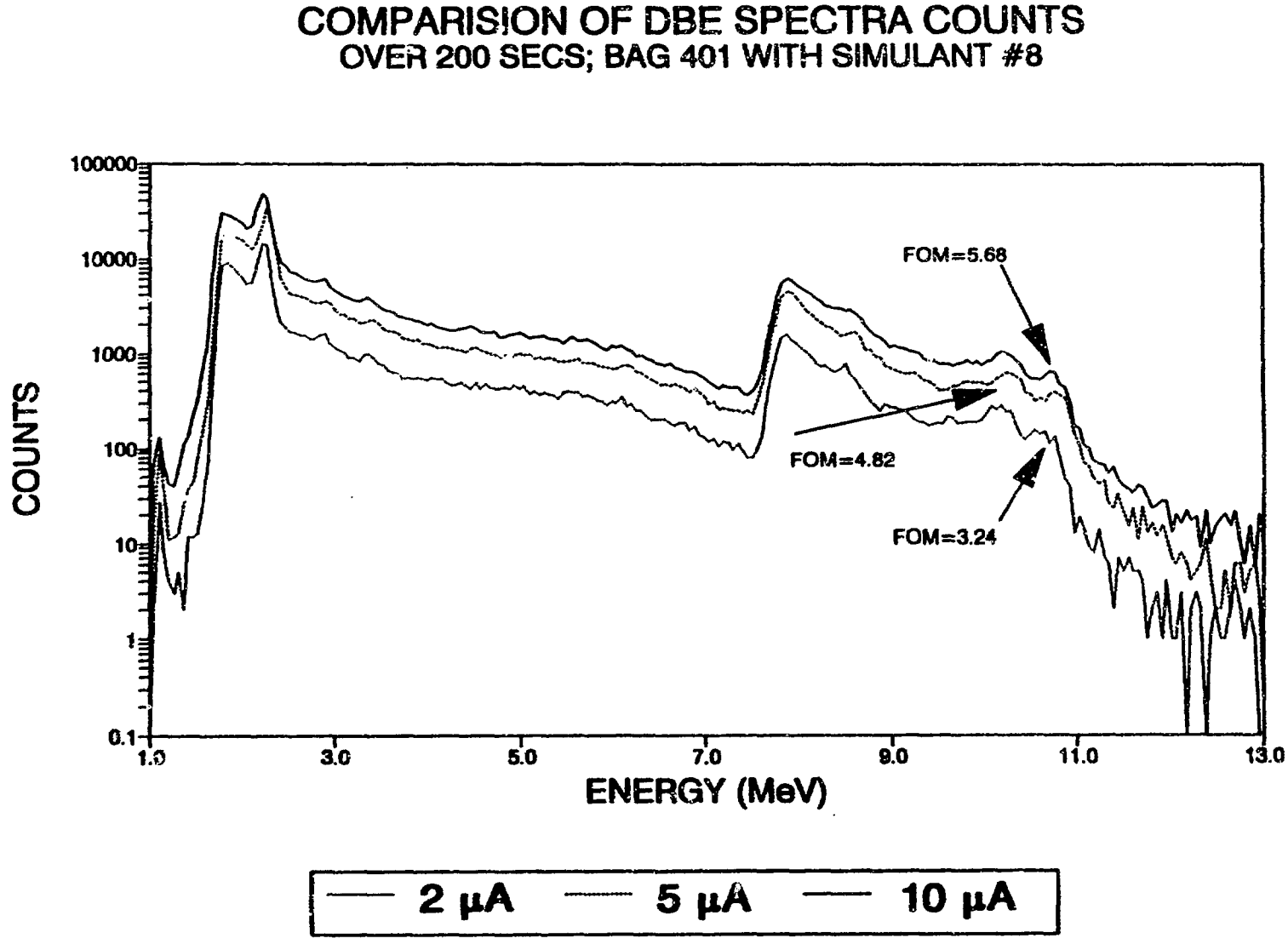


Figure 6 Gamma ray spectra from NEC-EDS at three beam current values.

ASSOCIATED PARTICLE IMAGING

Albert Beyerle, Robin Durkee, Garrett Headley,
J. Paul Hurley, and Laura Tunnell
Special Technologies Laboratory
Santa Barbara, CA

1. INTRODUCTION

An associated particle imaging (API) system has been built and some first images recorded. These images are presented in this paper. Design of the system has been reported previously[1].

Associated particle imaging uses the direction and time correlations between fast (14 MeV) neutrons and alpha particles produced in a small accelerator via the deuterium-tritium reaction. Detection of the alpha particle with a position-sensitive detector provides the direction of flight and time of emission of the associated neutron. The neutron may then interact (most probably scatter inelastically) with the target nucleus to produce a gamma ray whose energy is characteristic of the target material. The time-of-detection of the gamma ray gives the neutron interaction time and is used to locate the neutron-nucleus interaction and, hence, the target material, while measurement of the gamma-ray energy identifies the elemental composition of the target. The system is information rich, since it can use the geometric and elemental data recorded with each event to generate real-time, fully manipulable, three-dimensional images of identified materials. API permits single-sided, non-intrusive inspection of the internal contents of sealed packages and containers, and will image all elements except hydrogen and helium. The technique images 14 MeV neutron interactions in the material of interest.

The associated particle T(d,n)^{4}He technique as a means of "electronic collimation"[2] has been used for 40 years[3] with many examples of its use[4]. C. W. Peters, et al[5] constructed a proof-of-concept imaging system. Groups at LANL[6,7] and ANL[8] have also been working with the technique.

2. COMPONENTS OF THE SYSTEM

The associated particle imaging system consists of several components. Neutrons are produced in the sealed-tube neutron generator (STNG). The STNG tube also records the alpha particle associated with each neutron which defines the time of creation and direction of flight for each neutron. A sample to be imaged is placed in front of the STNG tube (opposite the alpha detector) and neutrons are allowed to interact with it. Gamma rays characteristic of each interaction are counted by gamma-ray detectors viewing the sample. A computer is then used to process these complex position, energy, and timing data for presentation to a user in an intelligible form.

The design and manufacture of the prototype sealed-tube neutron generator (STNG) encompasses five separate tasks: ion source studies; electrode geometry design, including beam optics computer studies; alpha particle detector studies; high voltage power supply (HVPS) design; and selection of an appropriate fabrication site. All of these are now complete. The design lifetime goal for the STNG tube when used in API applications has been set at 1000 hours, with every expectation that this figure will be exceeded.

Five STNGs have been manufactured. The first four have been used for beam optics studies, while the fifth tube is now generating neutrons. As of the time of this writing, that tube will have been operating for more than 700 hours (as of 10/15/91; see above), at a continuous neutron flux of $\sim 2 \times 10^9$ n/s, a rate that is limited by the performance of the existing alpha particle electronics. The tube is operated at an $\sim$75 kV acceleration and $\sim$1.4 uA current on target. Designed for direct beam observations and for ease in making modifications, the beam optics tubes were manufactured with a glass envelope, a clear glass view port, a fluorescing glass target, and a removable conflate flange assembly. The fifth tube is similar to the first four, using the same glass envelope and flange assembly. However, in order to generate neutrons and detect the associated alpha particles, the glass target was replaced with a target containing tritium and the clear glass view port was replaced with an alpha detector.

The ion source, a Penning cell which operates on ambient gas in the tube, is one whose design has long been used in commercial tubes[9]. The first tube was used primarily to characterize the performance of the ion source. The relationship between ion source current, ion source (tube) gas pressure, and ion source voltage was studied. This was important to understand the mode switch point in the ion source between modes I and III. For a discussion of mode switching in ion sources, reference is again made to the discussions by Hooper[10]. For the low target currents appropriate to API, these tubes will be operated well below the switching point, where the ion source current is low, and the pressure versus current slope is positive for good feedback control.

A unique aspect of the API STNG tube is the requirement for a tightly focused beam. Most STNG's intentionally defocus the beam to avoid target heating problems. STNGs 2-4 were used primarily to measure beam spot parameters including those controlling beam current and beam focus. The results confirmed the computer studies[1], showing that the focal plane is adjustable through a distance ranging from before the target to well beyond it, that the beam is cylindrical in cross section and, when focused on the target, has a diameter of approximately 0.8 mm, a measure that exceeds expectations ($\sim$ 1 mm) for the first tube, and is acceptable for API applications. The measurements also define the focus voltage as a function of acceleration voltage for smallest beam spot.

For this work a 3" x 3" BaF_2 detector has been used. It provides good detection efficiency, good timing, and moderate energy resolution at reasonable cost. It would be desirable to have a huge array of high-resolution Ge detectors in addition to scintillators, but they are expensive and timing is poor. Any final API system will probably comprise several detector types, all working in concert.

Two main factors influence the lateral position resolution of the system, and both relate to the precision of the measurement of the alpha-particle direction. The first of these is the size of the ion beam spot on the target and the second is the position resolution of the alpha detector. The extent to which the precise locations of the origin of the alpha particle and its impact on the detector are undetermined contributes to an uncertainty in the direction of the neutron. This uncertainty defines the minimum resolvable angle between sample features.

One of the count-rate limitations of any timing technique is the need to limit random coincidences. API is no different in this respect. The technique tracks an individual neutron to an interaction site and then a gamma-ray from the interaction site to a gamma-ray detector. If two neutrons are produced in a coincidence window, the system has no way to know which neutron produced the gamma ray. Therefore, the neutron production rate must be kept low enough so that the interactions do not interfere. In the case of the API system, to image objects out to 2 meters, the longest flight times are about 50 nsec. This corresponds to a frequency of 20 MHz. Since the neutrons are produced by a random process, rather than at fixed intervals, the rate must be kept low enough to avoid these random coincidences. A factor of about 10 lower in average rate will yield about a 10% random coincidence rate. Thus the API system is limited theoretically to about 2×10^6 neutrons produced traveling in the direction of the target. If the neutron production rate is pushed much higher than this little is gained, because data are confused due to random coincidence events. This is a fundamental limitation on API count rate and it is the price that is paid for the 4-dimensional information the technique provides.

3. IMAGES

The images we have taken with the API system thus far have all been obtained with roughly the same operating parameters. The beam current in the system has been limited to about 1.1-1.5 μA beam current on target. This produces 3000-6000 α-particles/sec in the alpha detector. We are currently using a 1 μsec pulse shaping time in the α detector, so the rate must be kept low to avoid pile up. Above about 7000 cps a pile-up "phantom" begins to appear in the middle of the image. This rate limitation is imposed by the existing alpha-detector electronics. Our calculation indicates that this corresponds to a neutron production rate of $\sim 10^5$ n/sec. There is a total gamma-count rate of about 3,000 γ/sec. This results in about 1 coincidence-event/sec (depending of course on the mass of the target). The coincidence window is <70 nsec for the coincidence between alpha and gamma. The gamma-detector is a 3" x 3" BaF_2 scintillator. It is located about 90° from the beam axis, just out of the direct flux of the neutron beam, about ½ meter from the center of the target.

We have taken an image of two one quart containers; one partially filled with salt, the other filled with water. The intent of this measurement was to test the

ability of the system to resolve objects spatially as well as chemically.

The experimental configuration is shown in Figures 1 and 2. The figures show the arrangement of the two containers relative to the origin. The containers are 8 cm (X) x 8 cm (Y) x 8 cm (Z). Also indicated is the viewing angle of the STNG ($\sim$13°), and the slightly larger viewing angle of the shield surrounding the STNG ($\sim$17°). The position of the BaF_2 gamma-ray detector is indicated in the top view.

Figures 3 and 4 are shadowgram images of the objects obtained by integrating out the energy dependence and one of the spatial dimensions. Figure 3 is a front view. This is the view of the objects from the location of the STNG. Figure 4 is a top view. This is the view, from above, down on the object. The side view is available in the same data but is not presented.

One of the great virtues of the API system is the 3-dimensional imaging capability. Conventional radiographs are shadowgraphs of data, with one of the spatial dimensions integrated out by the nature of the technique. The presentations in this paper are necessarily two-dimensional, but this is a limitation of the medium rather than a limitation of API. In this section we will go through a slicing up process of the data to demonstrate the power of this spatial isolation. All of the data in this paper are different views of the same 4-D image.

Figure 5 shows the Z distribution of all events, regardless of their X-Y-E value. The salt can be seen near Z = 70, and the water, near Z = 90. The largest peak near Z = O is from the shielding and warrants some discussion later.

The depth (Z) data can be used to isolate objects of interest. In order to spatially isolate either the water or the salt, the data can be sliced or windowed in two coordinates and then viewed in the third. The horizontal (X) distribution of all events (no slicing) is shown in Figure 6. The peak at X = 10 cm is the water and the peak at X = -7 cm is the salt. Figure 7 shows the X distribution of the water after being windowed in Y and Z. Now the water is the dominant peak at x $\sim$ + 10 cm. The salt data are still present, although much reduced, because the objects overlap in Y and the timing does not completely separate the Z. The large overall background, which is due to the large peak near Z = O in Figure 5 is much reduced.

API imaging provides isotopic information via the spectra produced by neutron induced gamma rays. A 3" X 3" BaF_2 scintillator detects gamma-rays to provide timing and energy resolution. The energy resolution of this detector is about 3.5% at 6.13 Mev.

Energy spectral peaks from Na and Cl are expected in the salt. Spectral lines from O are expected in the water since hydrogen has no fast-neutron gamma-ray lines. Figure 8 shows the entire energy spectrum for the arrangement of Figures 1 and 2. The most prominent lines are those due to hydrogen thermal neutron capture, ($H(n_{thermal},\gamma)D$) at 2.22 Mev, and carbon ($^{12}C(n_{fast}, n')^{12}C$) at 4.43 Mev (escape triplet peaks). Oxygen lines are barely visible as 6.13 Mev (escape triplet peaks). Major lines are identified in Figure 8.

The major lines in this spectrum are due to hydrogen and carbon which are constituents of the shield, not the targets. Hydrogen capture is not prompt, since the neutrons must undergo many collisions before they slow down enough for this reaction to take place. Upon examination of the following energy spectra, note that the hydrogen-capture line is gone. It does not appear in any of the spatially correlated slices because it is a general random-coincidence "fog" throughout the picture.

Figure 9 is the spectrum due to the Z = O peak of Figure 5. The prominent peaks correspond to carbon (4.43 Mev and escapes). These gamma-rays are time-correlated fast-neutron capture peaks from the shield. The shield is out of the direct path of coincident neutrons. This interaction must be a multiple-scattering effect, where the STNG itself scatters neutrons out of the exit cone of the shield. The shield is very massive. It is about 1000 times more massive than the target so that a small diverted neutron flux will cause a huge effect.

Figure 10 is the energy spectrum resulting from spatially isolating the water. Although the count rate is low, the gamma ray lines due to oxygen predominate. The low count rate may be attributed to the degraded efficiency of the BaF_2 at higher energies. Despite this, the gamma-rays from other objects are greatly suppressed (compare to Figure 8). The hydrogen capture at 2.22 MeV is gone. The carbon 4.43 MeV gamma-ray peak which would fill in the valley between the two oxygen groups is not present.

Figure 11 is the energy spectrum of the salt region. Both Cl and Na have many low energy lines. These lines show a correspondence to the peaks in the spectra. Note that the line at 2.2 MeV is present in this spectrum but not in the water. This is the Cl 2.19 MeV gamma-ray which is swamped by the 2000 pound shield until the salt is spatially isolated.

4. DISCUSSION

An associated particle imaging system has been built. Preliminary images which have been recorded show clearly the objects being imaged. Analysis of the data reveals elemental information for two real objects and one phantom caused by shielding required for radiological safety reasons. A duplicate image has been taken through 1/4" of steel which shows similar character to the image presented but is not presented in this paper due to space limitations, as the analysis requires more steps.

Although quantitative system parameters have not yet been measured, the system resolving power is on the order of a few centimeters in any direction. The imaging seems to offer great promise as a background interference technique, as well as in its own right, in that interference from a massive shield can be eliminated. Weak gamma-ray signals can be enhanced by spatial isolation. The count rate is low but we expect almost a factor of 100 in neutron flux increase once certain electronics problems are dealt with, and more detectors can be added to increase count rate. We expect a factor of 1000-10,000 faster count rate in a production system.

ACKNOWLEDGEMENTS

This work has relied upon the expertise of many people. Special thanks to many people at EG&G Amador Valley Operations who have constructed the tube; Fred Frey and others at M. F. Physics who filled tubes with deuterium gas and installed tritium targets; and Neal Norris with whom we had many useful discussions concerning beam optics evaluation.

Work supported by the U.S. Department of Energy, Field Office, Nevada under contract number DE-AC-08-88NV10617.

REFERENCES

1. Design of an Associated Particle Imaging System, Alben Beyerle, J. Paul Hurley, and Laura Tunnell, Nucl. Instr. and Meth. A299 (1990) 458.

2. S. Tagesen and R. Nowotny, Osterr. Akad. Wiss. 4 (1971) 67.

3. H. H. Barschall, L. Rosen, and R. F. Taschek, Rev. Mod. Phys. 24 (1952) 1.

4. CRC Handbook of Fast Neutron Generators, Julius Csikai, CRC Press, Boca Raton, Florida, 1987.

5. C.W. Peters, Nuclear Diagnostics Systems, Springfield, Va., Private communication.

6. The Associated-Particle Technique for One-Sided Imaging, L. E. Ussery, C. L. Hollas, and G. J. Arnone, Report # LA-CP-89-331.

7. R. Morgado, Los Alamos National Laboratory, Private communication.

8. E. Rhodes, Private Communication 8/91.

9. Manfred Frey, M.F. Physics, Colorado Springs, Co., Private communication.

10. A Review of Reflex and Penning Discharges, E.B. Hooper, Advances in Electronics and Electron Physics 27 (1967) 295.

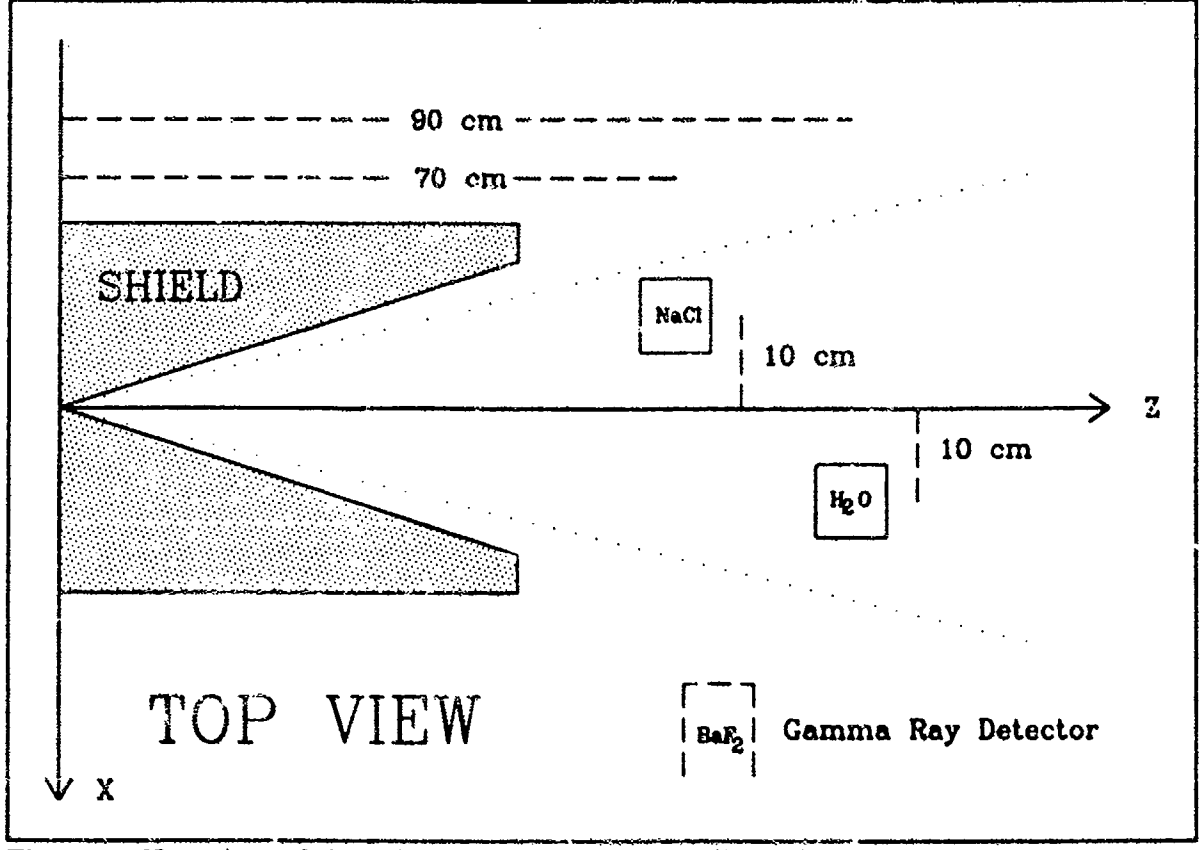


Figure 1 Top view of the salt and water image configuration.

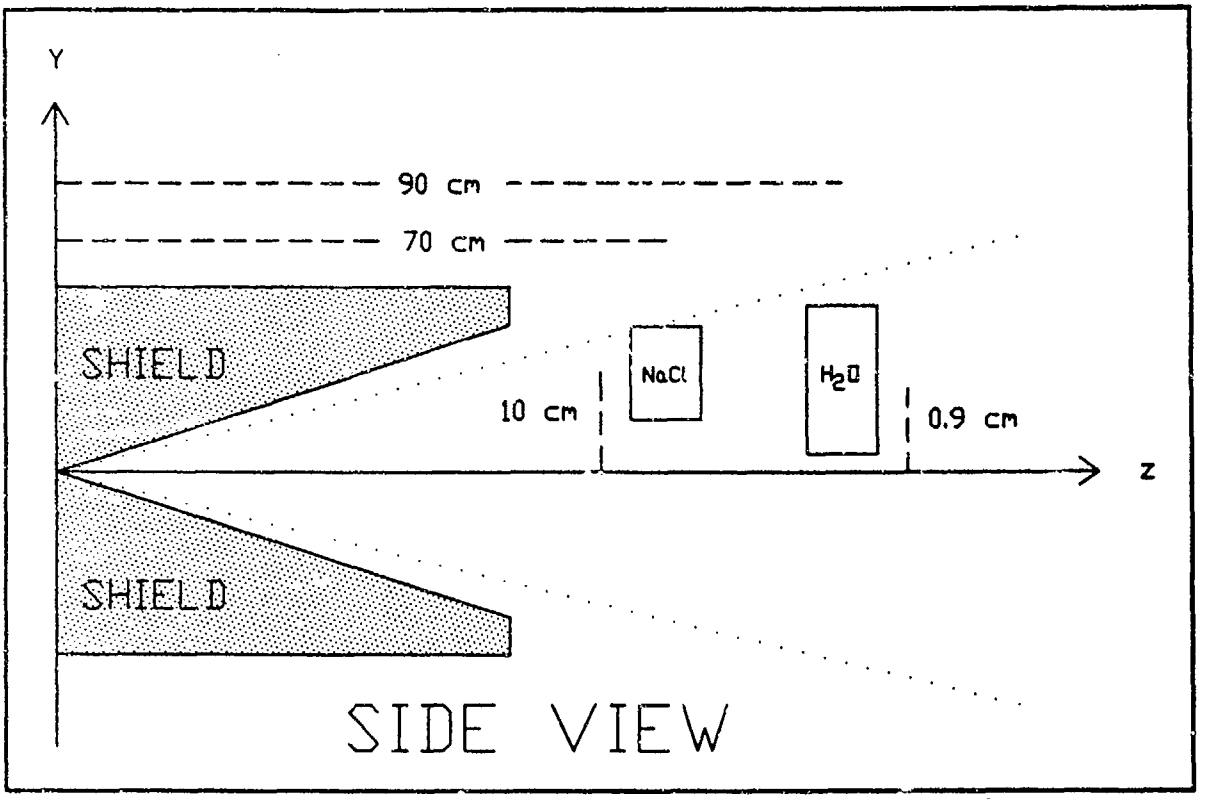


Figure 2 Side view schematic of target arrangement for salt and water image.

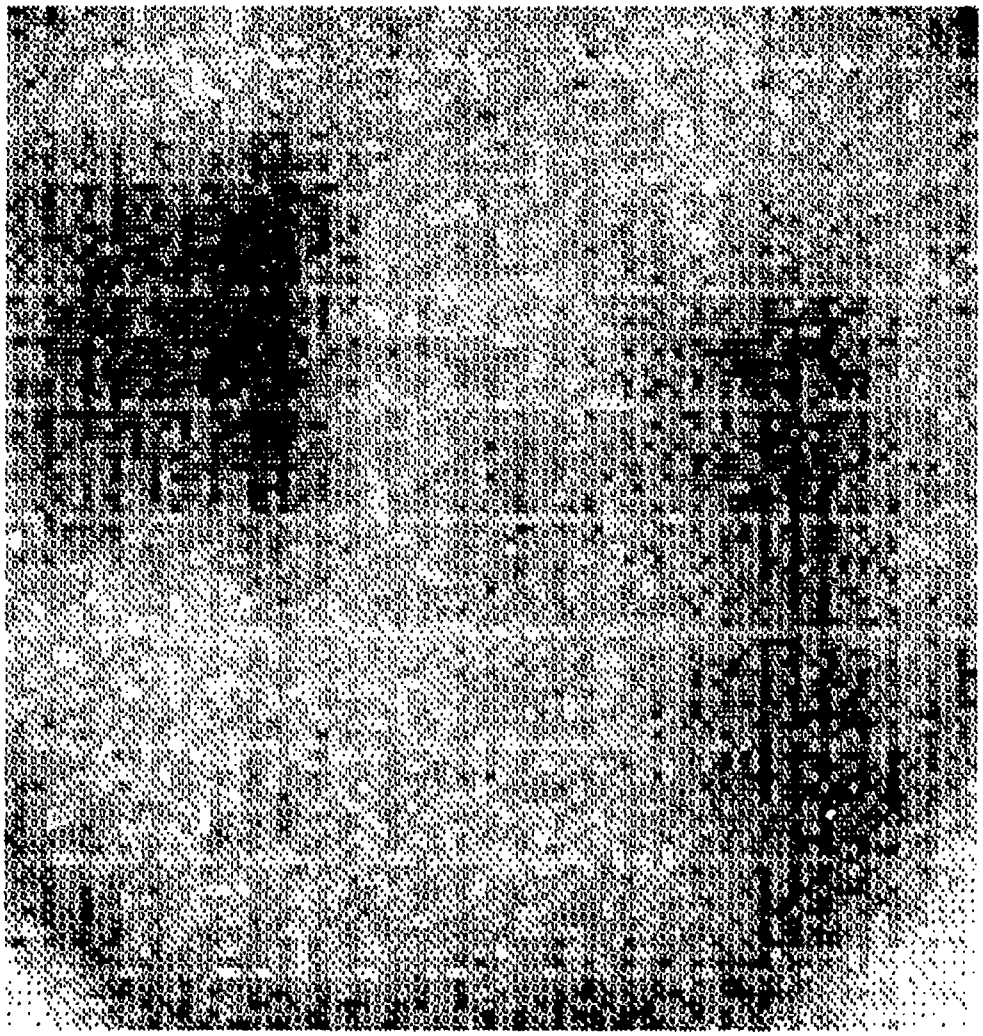


Figure 3 Front view ($X^{\rightarrow}$-$Y^{\uparrow}$) shadowgram image of the salt and water.

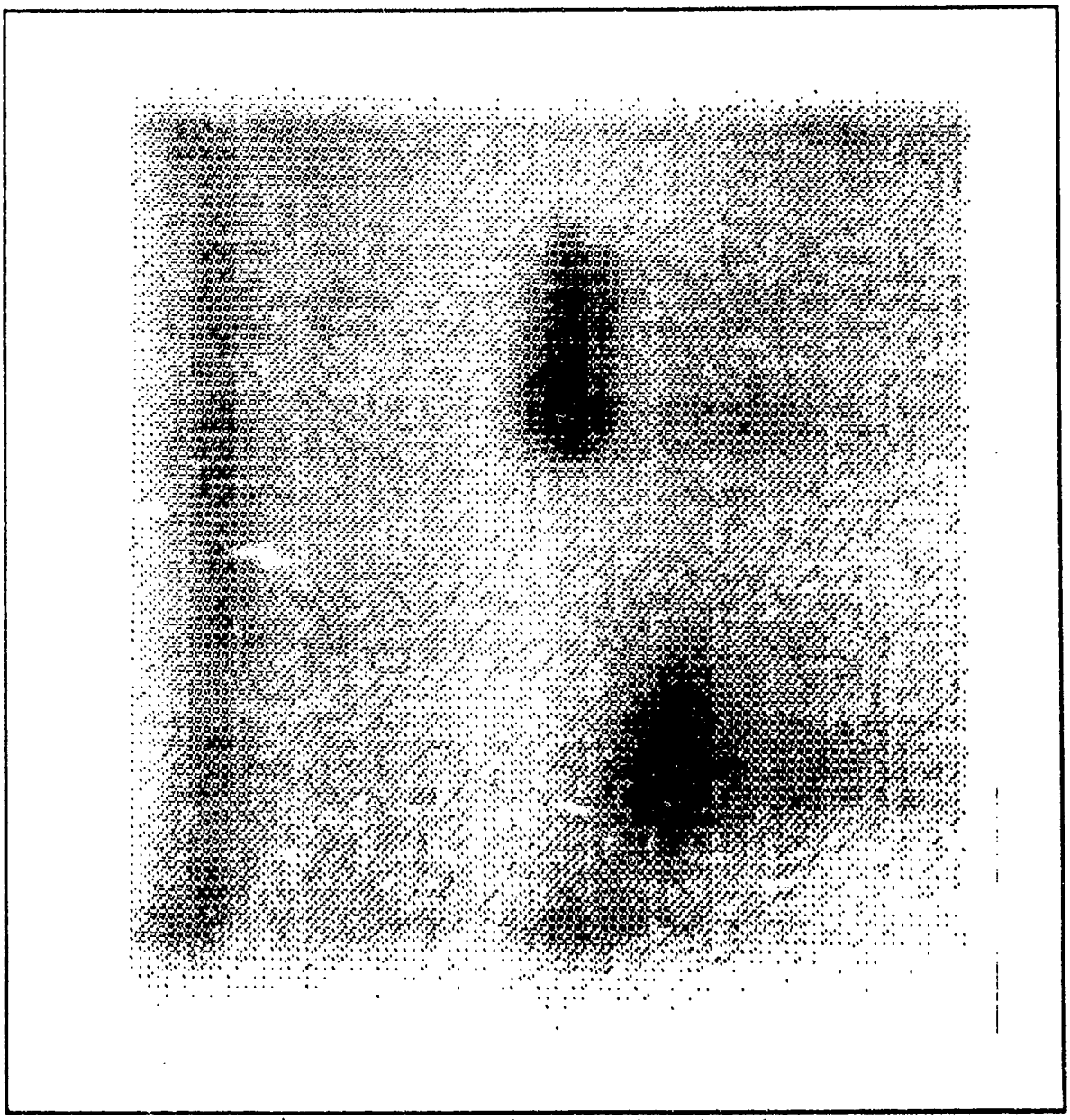


Figure 4 Top view ($X^{\downarrow}$-$Z^{\rightarrow}$) shadowgram image of the salt and water.

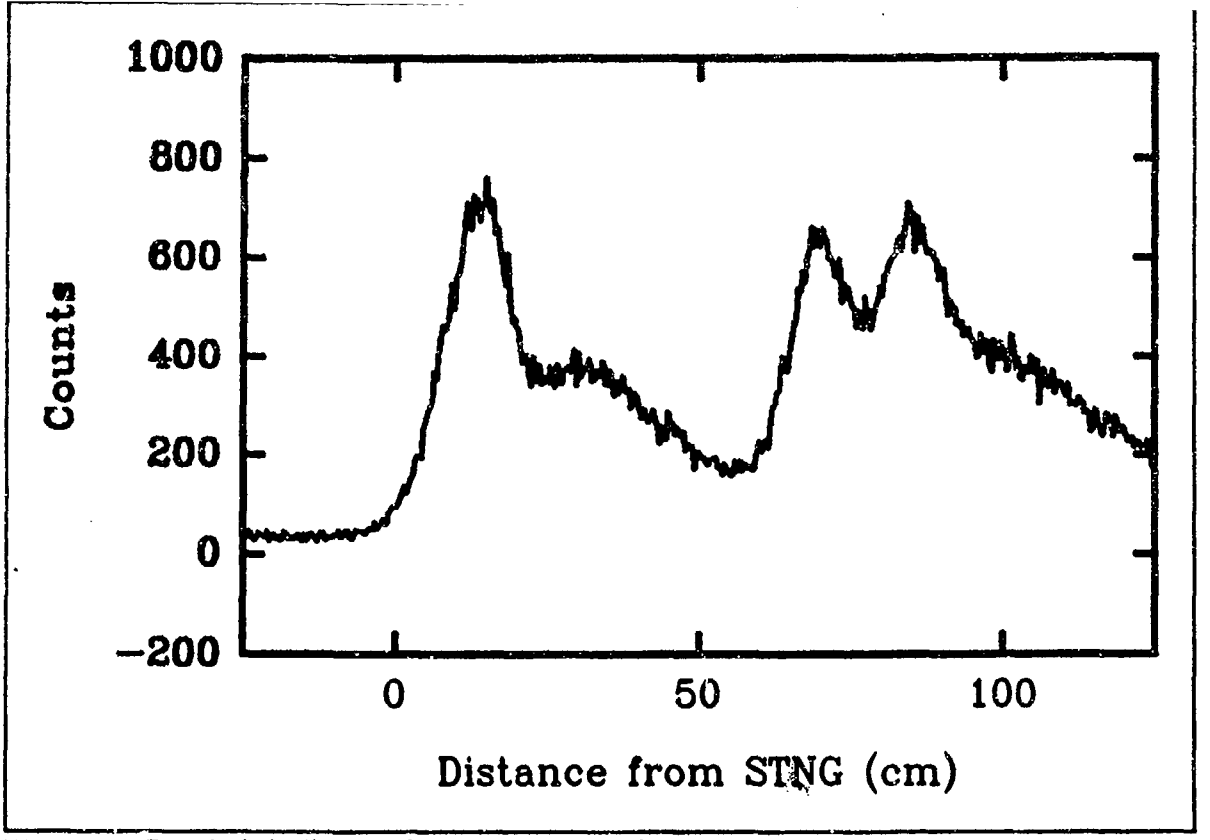


Figure 5 Depth (Z) distribution of all counts in the salt and water image.

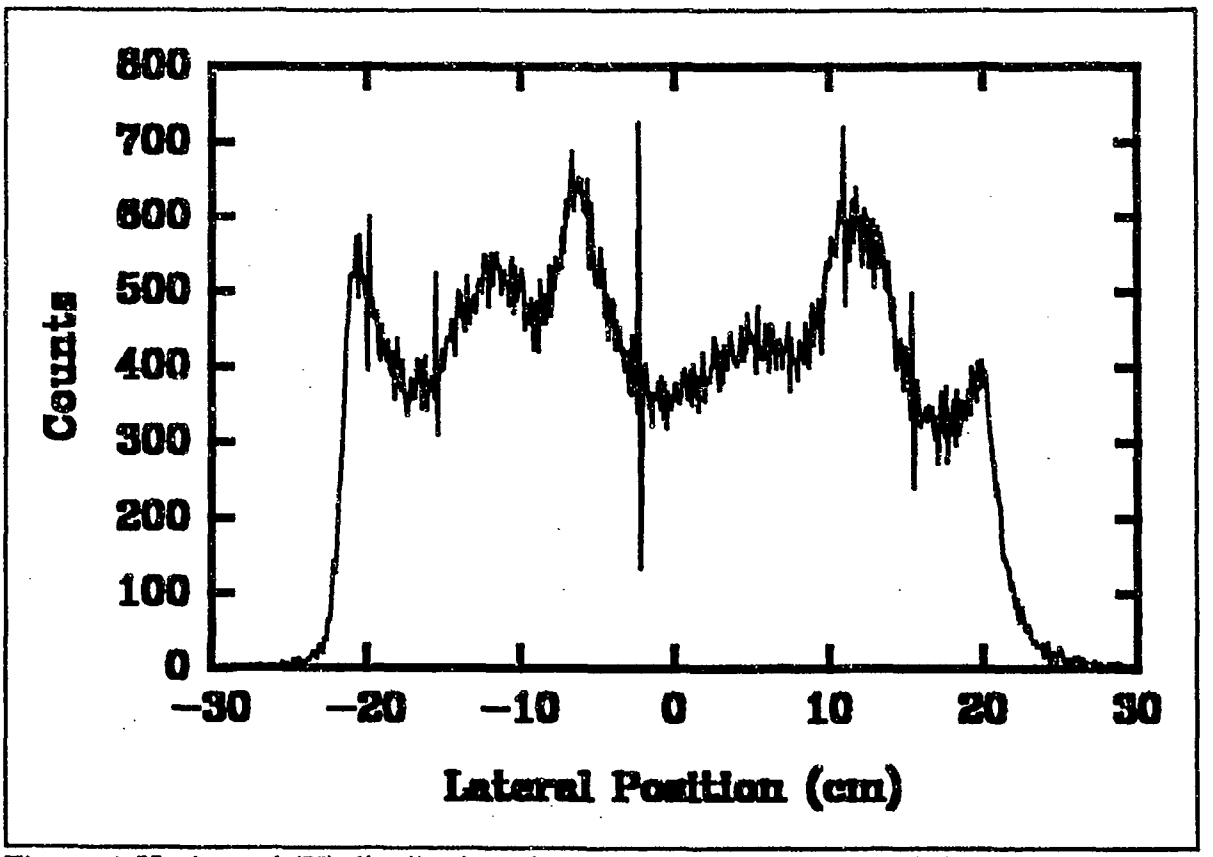


Figure 6 Horizontal (X) distribution of events for the entire field of view for the salt and water data.

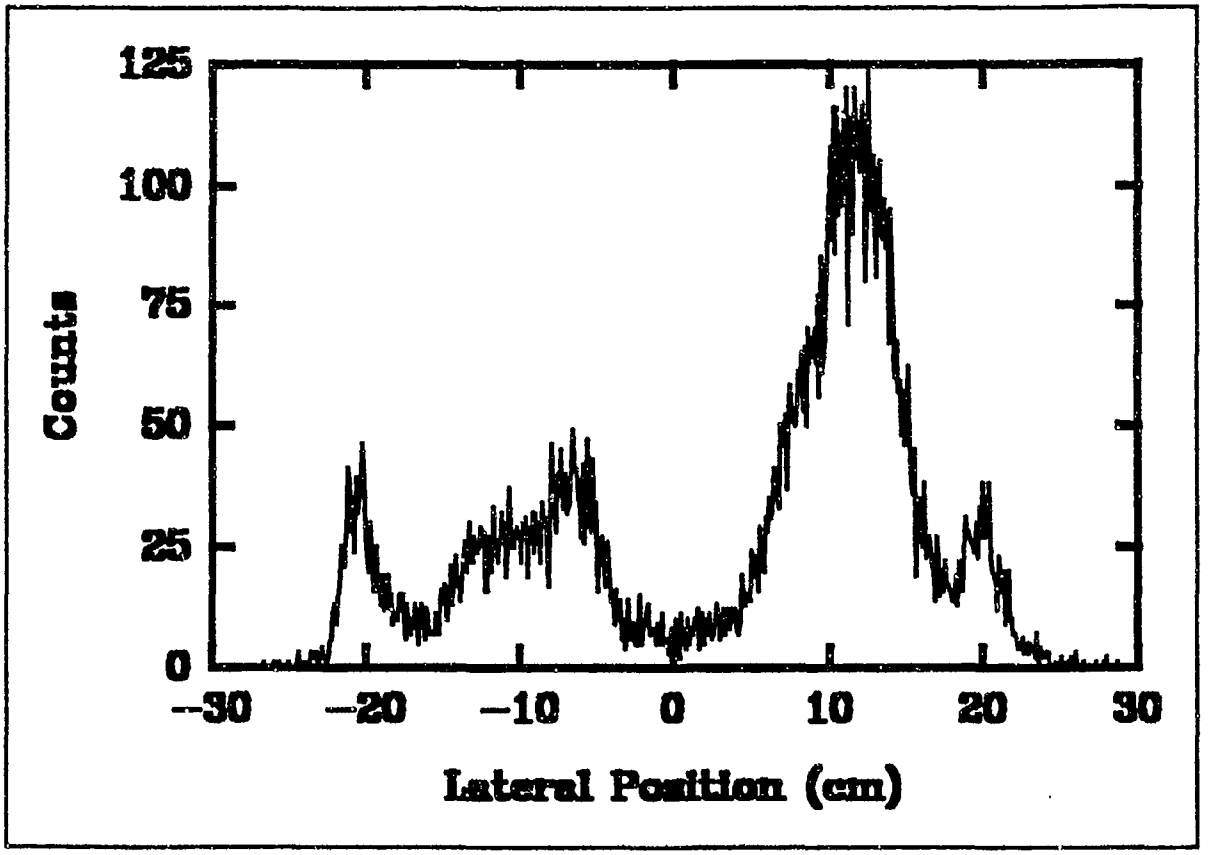


Figure 7 Horizontal (X) distribution of events (for Z and Y corresponding to the water) only for the salt and water image data.

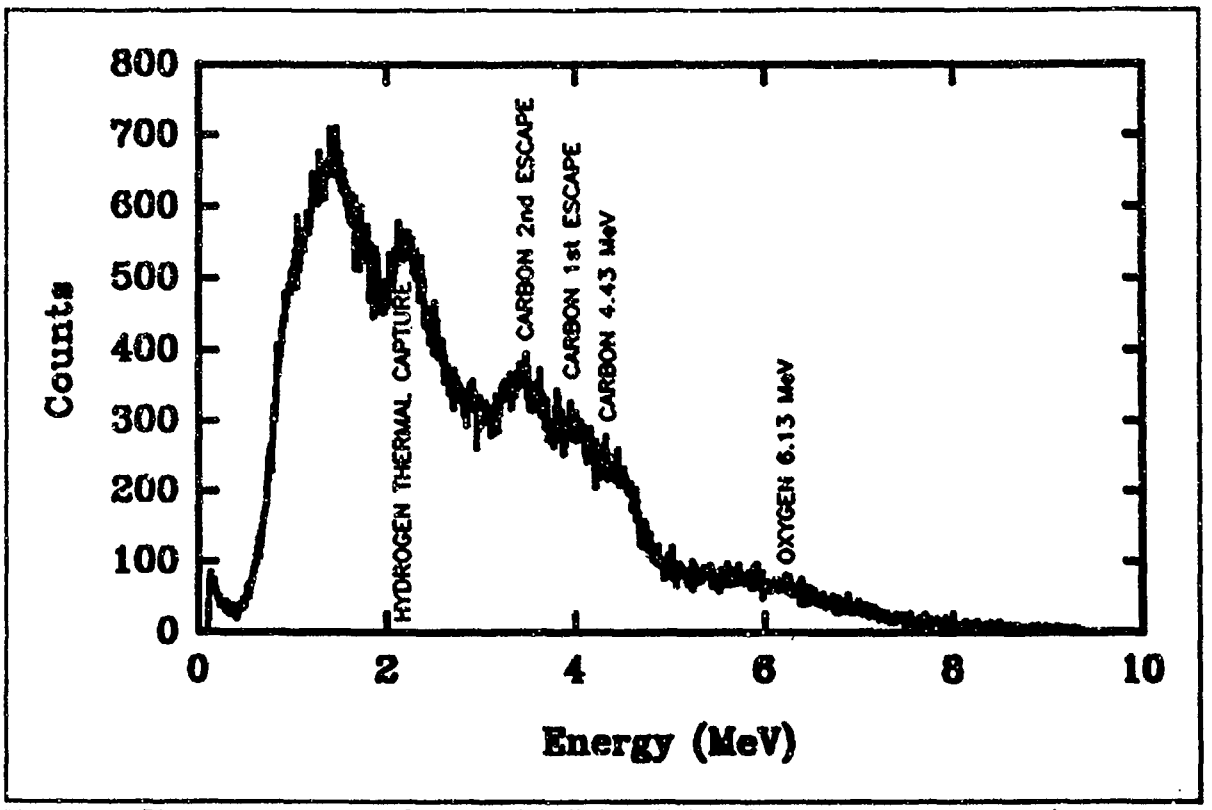


Figure 8 Energy spectrum of the entire field of view for the salt and water image.

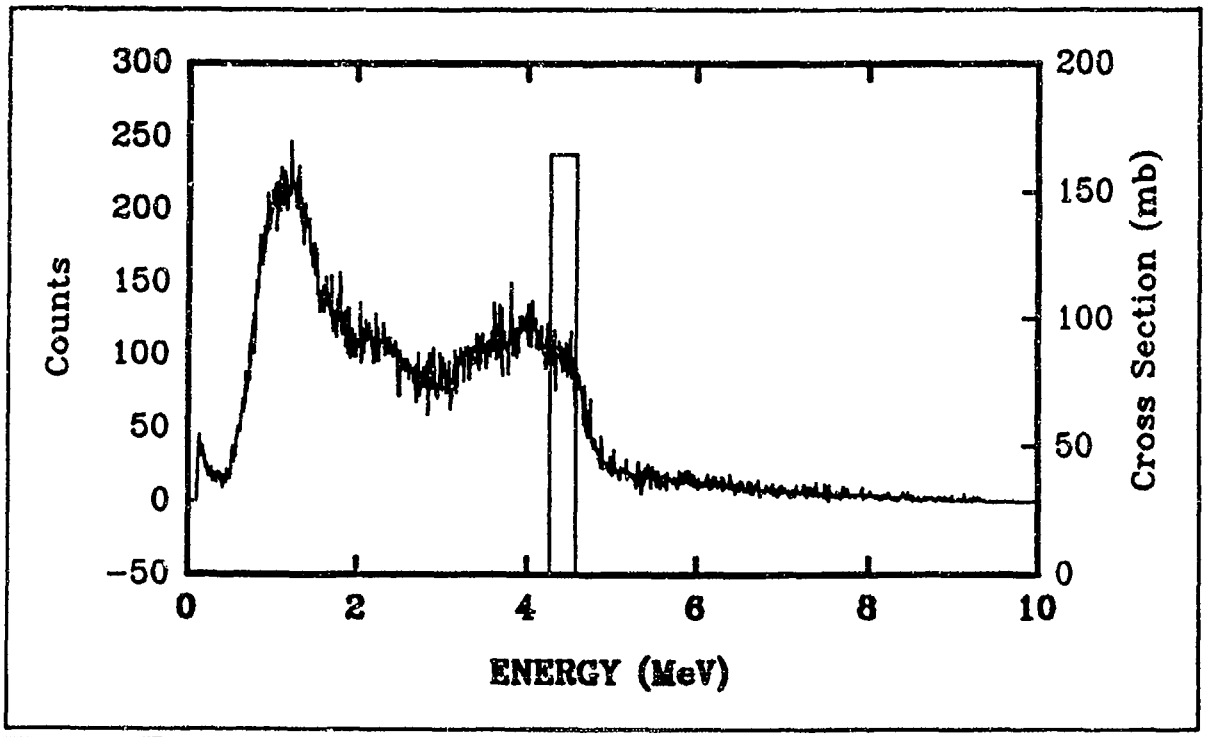


Figure 9 Energy spectrum of the "object" near the STNG.

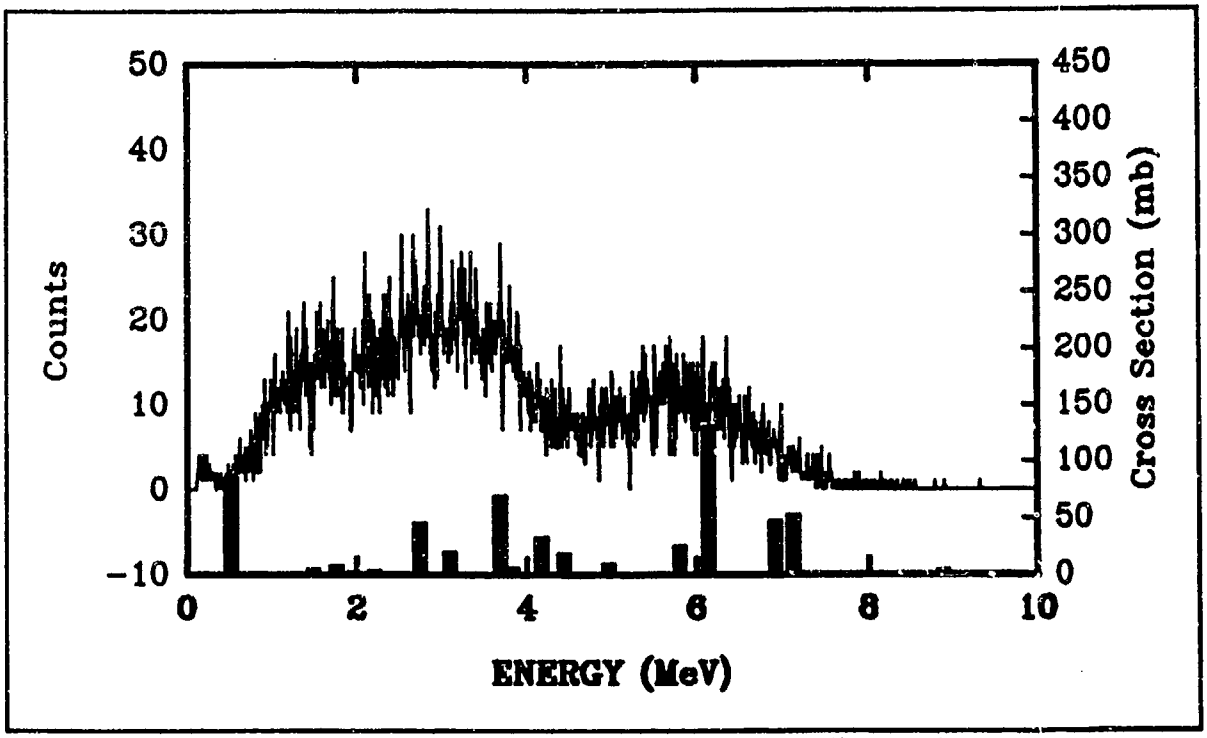


Figure 10 Energy spectrum of the spatial region corresponding to the water.

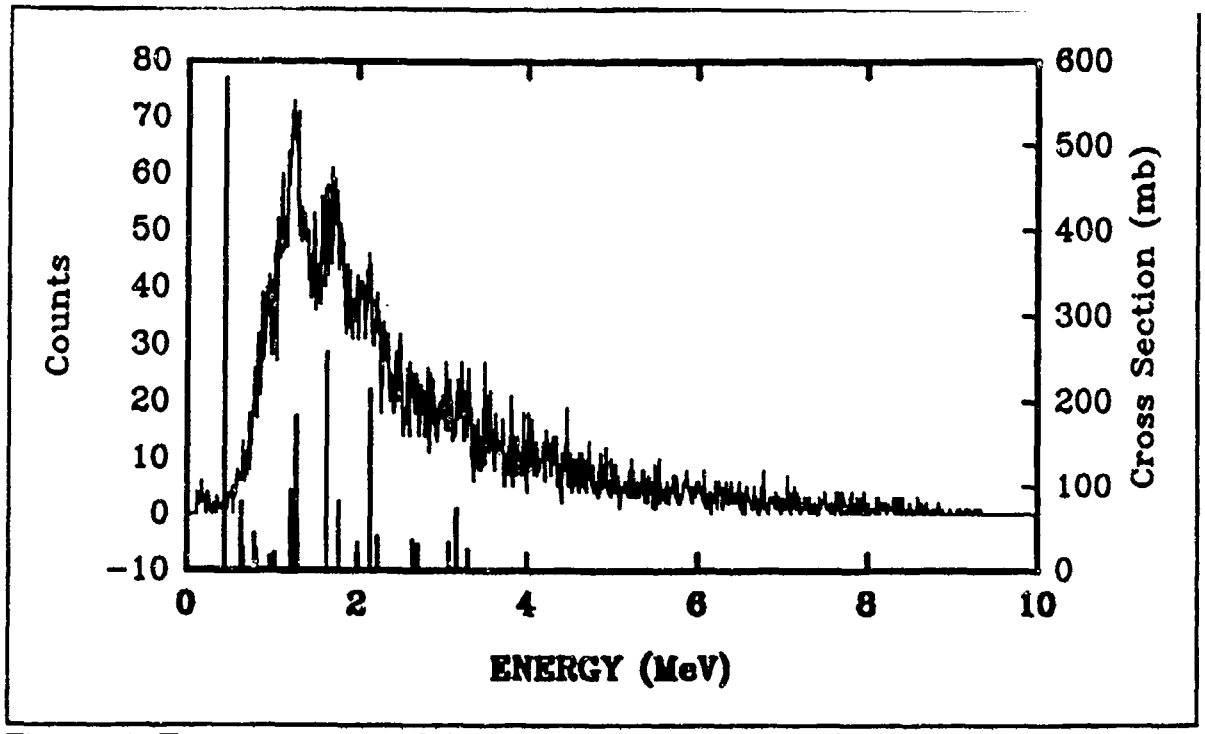


Figure 11 Energy spectrum of the spatial region corresponding to the salt.

ACCELERATORS

THE RFQ LINAC: A HIGH-CURRENT COMPACT ION ACCELERATOR FOR EXPLOSIVE DETECTION

Robert W. Hamm
AccSys Technology, Inc.
1177-A Quarry Lane
Pleasanton, California 94566

1. BACKGROUND

The linear accelerator (linac) has been the accelerator of choice for generating high-current, high-energy ion beams since its invention by Alvarez in 1934. However, prior to the demonstration of the RFQ linac in 1980 by Los Alamos National Laboratory [Stovall], ion linacs were very large accelerators used primarily at high-energy physics research facilities. The successful operation at Los Alamos of a compact version of this unique new device, first proposed in 1970 by Kapchinskii and Teplyakov [Kapchinskii] and demonstrated in the Soviet Union in 1974 [Golosai], immediately made it obvious that the RFQ would be a useful tool for the generation of high-current ion beams for many practical applications. An intense development program was begun at a number of accelerator laboratories worldwide after the U.S. activities were published, resulting in widespread acceptance and use of the RFQ linac for research applications. By 1986, it was reported [Staples] that more than 50 RFQ accelerators were in various stages of development and that commercial development of these structures had been initiated by AccSys Technology, Inc. At the present time, at least five companies worldwide now offer RFQ linacs, and laboratories in at least ten countries are developing new versions. In addition to its continued use in physics research, mostly as an injector for high-energy physics accelerators, the RFQ is now being developed for several industrial and medical applications other than explosive detection. These include particle-beam cancer therapy, isotope production, ion implantation, and neutron activation and radiography. Many other practical applications requiring intense, energetic ion beams are expected to benefit from the use of this powerful but simple-to-operate accelerator.

2. RFQ DESCRIPTION

The RFQ, which has been thoroughly described and reviewed during the past decade by several authors [Klein; Schriber; Stokes], is essentially an rf-driven quadrupole-focusing channel consisting of four electrodes that have been modulated, as seen in Fig. 1, to provide not only a radial focusing field but also an axial accelerating potential. The axial field component is adiabatically turned on by a careful tailoring of the electrode pole tips [Crandall] to enable the RFQ to capture almost entirely a low-energy dc ion beam that is injected into it. Several successful techniques have been developed for the tailoring of the modulations to capture the ion beam in the rf acceleration "buckets" of the structure, depending on the ion beam current and ion specie being accelerated [Yamada; Gough]. Once the injected ions have been captured, the vane modulations are used to simultaneously focus and accelerate the beam to its final energy of a few MeV. The RFQ linac becomes inefficient beyond these energies, so if higher energies are required, the beam from the RFQ is usually injected into the conventional linac structures used for many decades.

The uniqueness of the RFQ linac is its simplicity. Following a very sophisticated design and fabrication procedure, this accelerator can provide simultaneous bunching, focusing, and acceleration of a high-current, low-energy ion beam injected into it through the use of only the electric fields created by rf power coupled into the structure. Hence, no large high voltages are required in the system; no large magnets are needed to focus or contain the ion beam; and only one parameter (rf input power) is adjusted to operate the device.

Within the constraint imposed by sparking of the high voltage applied between the neighboring vane tips (usually 30-100 kV), the RFQ can be designed with great flexibility in its input energy, vane modulation, and vane-tip bore diameter to accommodate a wide range of beam currents, from a few microamperes to as much as several hundred milliamperes. The output beam properties (output phase space and beam transmission) can also be traded against the required RFQ vane length and input rf power. A wide range of

operating frequencies (10 MHz to 1 GHz) can be used for the RFQ, depending on the mass of the ions to be accelerated, the desired size of the RFQ, and other physical constraints. Higher frequency RFQs (>200 MHz) are usually implemented as vane-loaded resonant cavities (Fig. 1b), while lower operating frequencies are employed with resonant circuit geometries, the "four rod" approach (Fig. 1a).

It is this flexibility in the design and implementation of the RFQ linac that makes it an ideal accelerator for several proposed nuclear techniques in explosive detection. Coupled with its proven reliability and simple, reproducible operation, the high-current capability and compact size of the RFQ also make it the most practical accelerator for deployment of these systems in airports. It can be designed for the production of neutrons or gamma radiation, both of which can be used for explosive detection.

3. APPLICATIONS IN EXPLOSIVE DETECTION

The applicability of the RFQ linac in explosive detection covers several of the nuclear detection techniques described by Grodzins [Grodzins], including thermal neutron activation (TNA), nuclear resonance absorption (NRA), neutron elastic scattering (NES), neutron attenuation transmission analysis, and pulsed fast-neutron activation (PFNA). The flexibility of the RFQ as a neutron generator allows it to be used to generate either fast or thermal neutrons. A wide selection of targets and bombarding particles, energies, and currents allows the explosive-detection system designer a wide range of neutron flux and neutron spectra. Fig. 2 shows the most common neutron-producing reactions that are available using the RFQ linac, along with the yields and threshold for each. For comparison, the reported yields for commercial sealed-tube neutron generators is included in this figure. The output neutron spectra from these reactions vary greatly in both energy and spatial distribution, allowing one to choose the appropriate reaction for a given application. Monoenergetic neutrons can even be produced by using the RFQ to bombard a tritiated target with deuterons at several hundred keV energy or by bombarding other targets such as vanadium or scandium with high-energy protons.

Very compact neutron sources producing a continuum of neutron energies are available using the Be(d,n) reaction, since the negative Q value of this reaction also allows low bombarding energies. These compact systems can be used with a modest-size moderator to produce thermal neutrons because the high-quality beam from the RFQ can be transported through a small beam tube to a target located inside the moderator. Primary neutrons with much lower energies than those in the Be(d,n) reaction can be produced using the Li(p,n) or Be(p,n) reactions, but the input ion energy must be higher, making the accelerators somewhat larger. A 4.0 MeV proton RFQ linac capable of delivering 1 mA average current is currently being assembled by AccSys for use as a neutron source for thermal neutron radiography.[1] This transportable system is expected to produce more than 10^{12} neutrons/second with energies of up to only 2 MeV.

As proposed by Schempp [Schempp], the RFQ can be configured with multiple acceleration stages, each operating at a different frequency, in order to produce intense, short beam pulses of ions separated by long periods. These ion beam pulses can then be used to produce pulsed fast-neutron bursts for PFNA analysis, NES, or pulsed neutron absorption analysis. For example, an RFQ with three sections operating at frequencies of 240/320/340 MHz would produce a beam structure with pulses of less than 0.5 nsec width at intervals of 50 nsec, with an intensity reduction of only 15 from the injected dc beam current.

In contrast, the RFQ linac can also be used to produce gamma rays to detect explosives using the gamma-ray resonance absorption technique. The RFQ can easily accelerate the 1.7476 MeV protons required for this technique at average currents of several milliamperes, and it has a minimal phase space growth in the injected ion beam if designed properly. Since the RFQ can utilize an H^+ beam, very low phase space ion sources such as the duoplasmatron are available for this application. Although the RFQ linac does not have an intrinsically low output beam energy spread, due to the fact that it is an rf accelerator with a pulsed beam structure, the output beam can be de-bunched in a separate rf cavity to reduce the beam spread significantly, with little loss in intensity.

4. RFQ TECHNOLOGY STATUS FOR EDS

Several RFQ linac systems pertinent to the detection of explosives are currently being fabricated or tested by AccSys Technology, Inc., the leading commercial supplier of RFQ linacs. These systems include the prototype Model DL-1 RFQ linac system shown in Fig. 3, which was developed for the FAA under an SBIR contract[2] as an electrically-driven neutron source

for TNA. This compact RFQ linac is only 70 cm in length and produces a 900 keV deuterium beam at a maximum current of more than 100 μA. The deuterium beam bombards a beryllium target attached at the end of a 22 cm beam pipe to produce up to 10^{10} neutrons/second. These neutrons have a continuum of energies of up to 5 MeV, with an average energy slightly higher than that of the neutrons produced by Cf-252.

A cross-sectional view of this accelerator is shown in Fig. 4, revealing the duoplasmatron ion source and electrostatic einzel lens used in the 25 kV injector, and the RFQ resonator located within the vacuum chamber. By using cryopumps on this system (one for the gas load from the ion source and one for the RFQ section), the accelerator is lightweight and free from hydrocarbon contamination. It also has no restriction on orientation, allowing the unit to be used either vertically or horizontally. The entire system is computer-controlled and can be operated at a repetition rate of 1500 Hz with a duty factor of 0.0225 to produce a quasi-continuous thermal neutron flux. Preliminary measurements made at Gamma-Metrics[3] in a prototype TNA system with a fission chamber gated 50-1000 μsec after the beam pulse indicated that the Model DL-1 prototype was producing thermal neutrons in this particular moderator geometry equivalent to a 454 μg Cf-252 source [Hurwitz], even though the beam current on target was only about 60 μA. No measurements have been completed on the total fast-neutron output from the beryllium target.

An even smaller version of this compact linac neutron generator has been designed. The Model DL-½ RFQ linac has a deuteron output energy of 500 keV and produces a maximum neutron flux of $5x10^8$ neutrons/second. This smaller system uses a 600 MHz RFQ (as opposed to 425 MHz in the Model DL-1), reducing its diameter from 30.5 cm to about 22 cm. A 1.5-meter high, double-bay electronics cabinet houses all of the electronic equipment required to power and operate this system.

Both of these compact linac neutron generators were designed to replace radioactive Cf-252 sources, which have inherent safety hazards and increasing regulatory restrictions, as well as sealed D(d,n) neutron generator tubes, which have shorter lifetimes and lower neutron outputs.

Another existing RFQ linac that has potential uses in the area of explosive detection is the Model PL-2 proton accelerator system shown in Fig. 5. This standard commercial system, of which seven have been sold, has a maximum proton energy of 2.0 MeV. Along with medical and beam research applications, it is also being used as a neutron generator for nuclear waste assay [Karvinen] and as a gamma ray source for high-energy physics detector calibration [Ma]. One system is currently being assembled at AccSys to accelerate protons to 1.75 MeV, with the standard Model PL-2 resonator length of 1.6 m used to obtain higher beam transmission, lower beam emittance growth, and a lower energy spread. This system uses a single-gap cavity placed at the output of the RFQ to further reduce the beam energy spread to a final value of $\pm$6 keV. All of the existing Model PL-2 RFQ linacs produce a pulsed output current of up to 25 mA, and the recent systems, made with copper-plated aluminum RFQ resonators, can operate at duty factors of 0.25 using appropriate rf power sources.

Finally, recent experimental data [Delayen] have revealed that a superconducting RFQ geometry has the potential for yielding a high-current continuous-wave (CW) accelerator that is very compact. AccSys, in collaboration with Argonne National Laboratory under an SBIR grant sponsored by the Department of Energy,[4] is currently designing a prototype superconducting RFQ for accelerating high-current proton beams. Preliminary design results reveal that a 1.75 MeV RFQ operating with a current of 10 mA would be less than 1 meter in length and would require only 18 kW of rf power. Further beam dynamics calculations will be completed during the next few months, along with the mechanical design of a prototype resonator to be tested with beam.

5. CONCLUSION

The RFQ linac is well-suited for use in the detection of explosives. As a proven, commercially available ion accelerator, the RFQ linac has no equal in the generation of high-current, high-quality beams. The flexibility of the RFQ and the implementation options available enhance its ability to be the most appropriate accelerator available for several of the proposed nuclear detection techniques. Its compact size, high current capability, and ease of operation and maintenance have already made the RFQ the accelerator selected for several new systems under development.

Although the technology is now well-established, development of the RFQ is continuing vigorously at many companies and research laboratories worldwide. These new technical improvements, coupled with the

commercial availability of RFQ systems, should ensure that the RFQ will remain the principal tool in these applications.

REFERENCES

1. Crandall, K.R., R.H. Stokes, and T.P. Wangler, Proc. 1979 Linac Conf., Brookhaven Natl. Rep. BNL-51134 (1979) 129.

2. Delayen, J.R. and K.W. Shepard, Appl. Phys. Lett. (57) (1990) 5.

3. Golosai, N.I. et al., Atom. Energy 2 (1975) 123.

4. Gough, R. et al., Proc. 1986 Linac Conf., Stanford Linear Accel. Rep. SLAC-303 (1986) 260.

5. Grodzins, L., Nucl. Instr. and Meth. Phys. Res. B56/57 (1991) 829.

6. Hawkesworth, M.R., Atomic Energy Rev., Vol. 15 (2) (1977) 169.

7. Hurwitz, M., Gamma-Metrics, San Diego, Calif., private communication.

8. Kapchinski, I.M. and V.A. Teplyakov, Prib. Tekh. Eksp. 2 (1970) 19.

9. Karvinen, R., Transuranic and Hazardous Waste Characterization Information Exchange Meeting, Pocatello, Idaho (July 1991).

10. Klein, H., IEEE Trans. Nucl. Sci. NS-30 (4) (1983) 3313.

11. Ma, H. et al., Nucl. Instr. Meth. Phys. Res. (A274) (1989) 113.

12. Schempp, A., New Techniques for Future Accelerators, Plenum Publishing Corp. (1987) 201.

13. Schriber, S.O., IEEE Trans. Nucl. Sci. NS-32 (5) (1985) 3134.

14. Staples, J.E., Proc. 1986 Linac Conf., Stanford Linear Accel. Rep. SLAC-303 (1986) 227.

15. Stokes, R.H. and T.P. Wangler, Ann. Rev. Nucl. Part. Sci. (38) (1988) 97.

16. Stovall, J.E., K.R. Crandall, and R.W. Hamm, IEEE Trans. Nucl. Sci. NS-28 (2) (1980) 1508.

17. Yamada, S., Proc. 1981 Linac Conf., Los Alamos National Laboratory Rep. LA-9234-C (1982) 313.

NOTES

1. Funded by Naval Weapons Center, China Lake, Calif., under Contract No. N60530-90-C-0226.

2. Funded by Federal Aviation Administration, Department of Transportation, under Contract No. DTRS-57-89-C-00013.

3. Funded by Federal Aviation Administration, Department of Transportation, under Contract No. DTFA 03-90-C-00040.

4. Funded by U.S. Department of Energy under Contract No. DE-FG03-91ER81098.

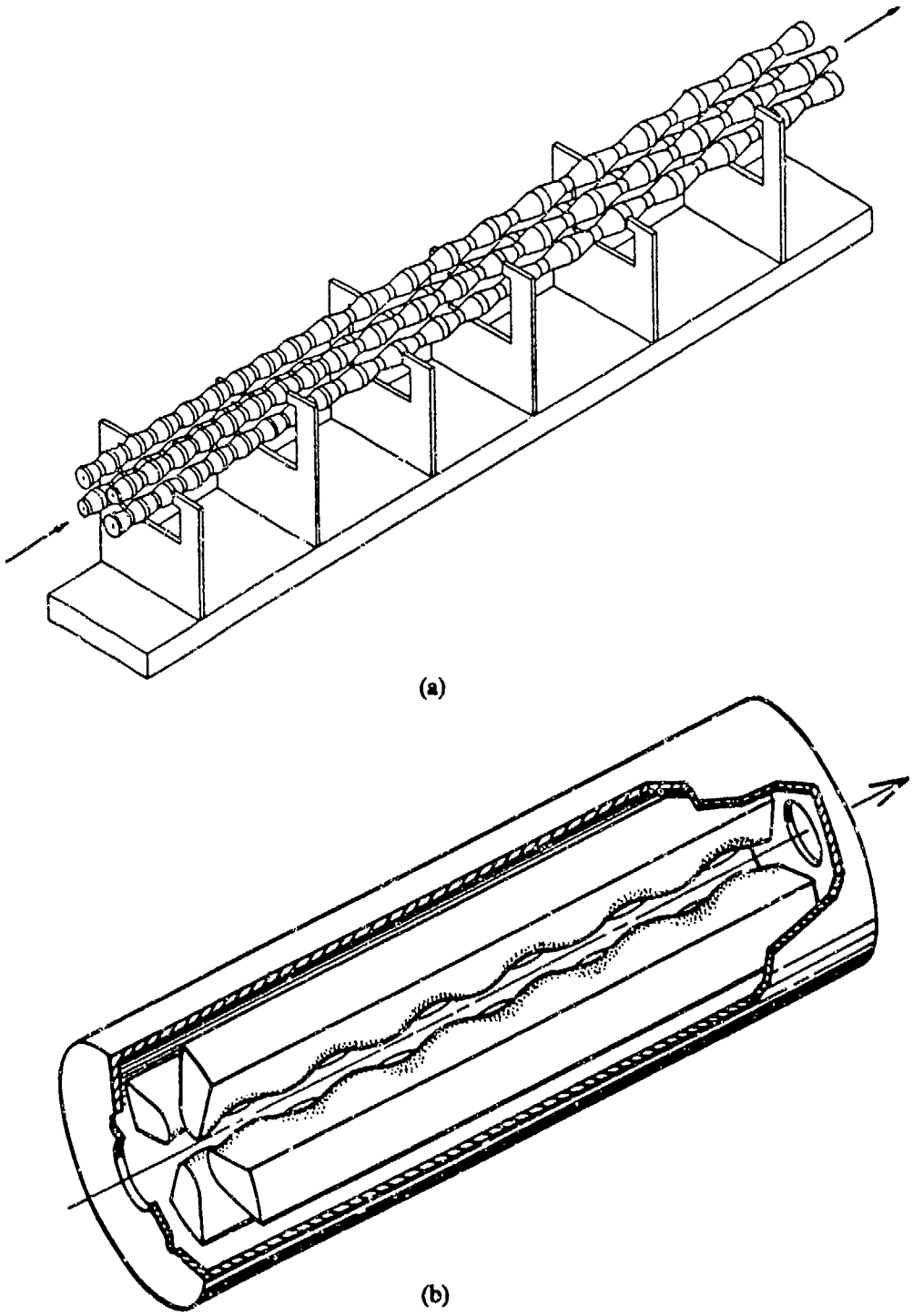


Fig. 1 RFQ accelerator configurations: (a) resonant circuit and (b) resonant cavity

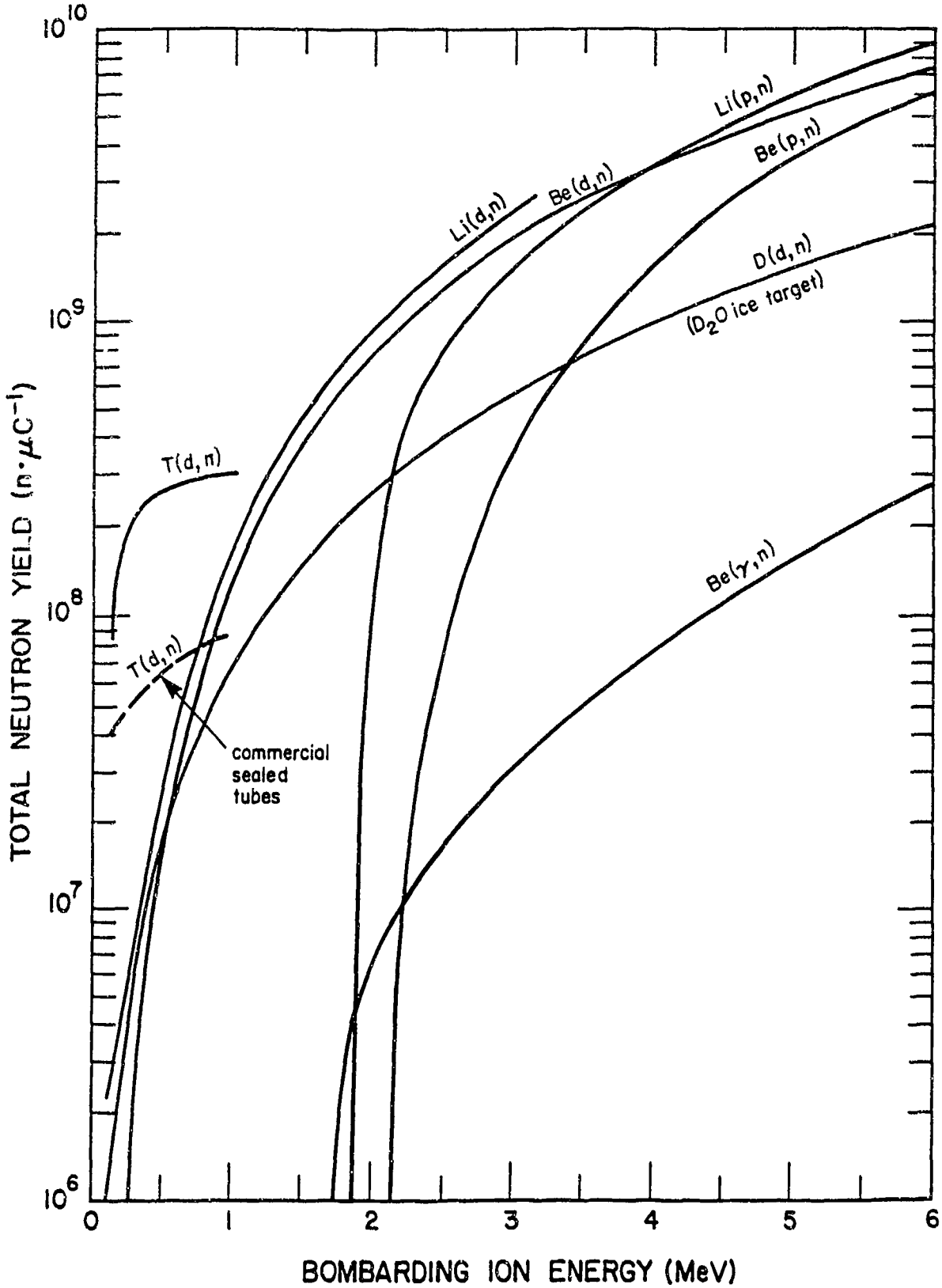


Fig. 2 Accelerator-based neutron production reactions [Hawkesworth]

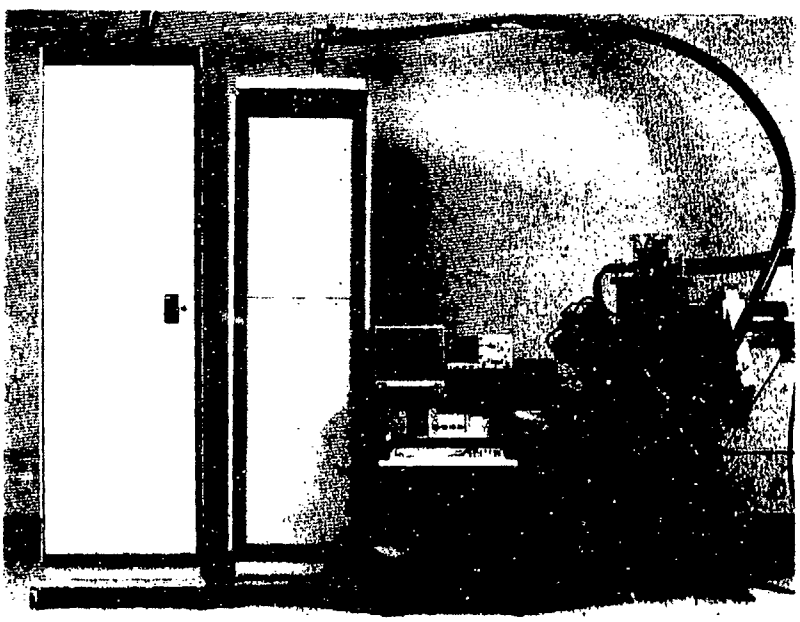


Fig. 3 Prototype Model DL-1 RFQ linac neutron generator

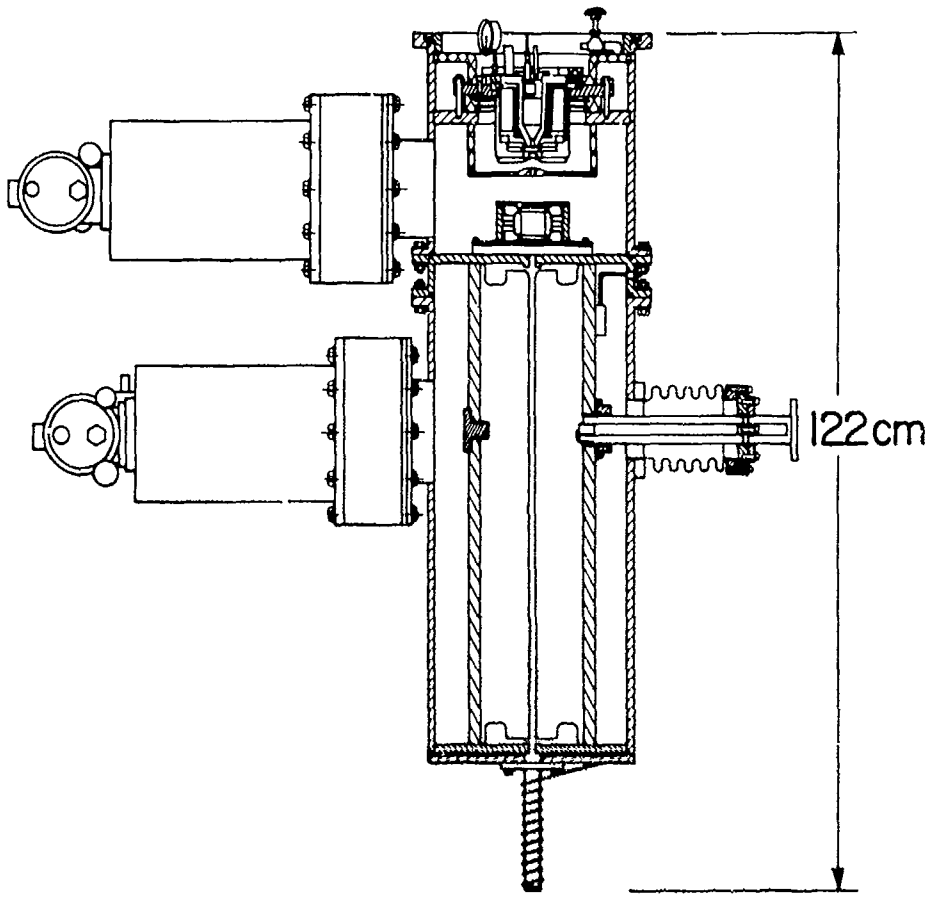


Fig. 4 Model DL-1 accelerator cross-sectional view

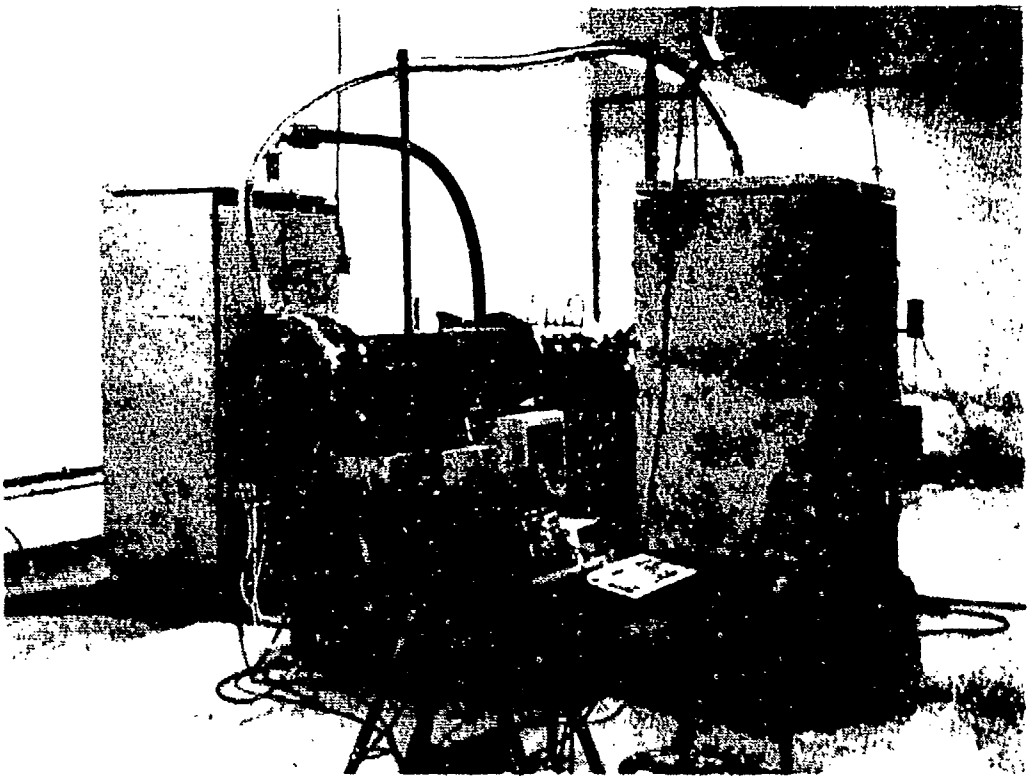


Fig. 5 Standard Model PL-2 RFQ linac system

DESIGN OF A HIGH CURRENT PROTON ACCELERATOR

A. M. M. Todd, C. C. Paulson, J. W. Rathke, and M. F. Reusch
Grumman Space Systems Division
4 Independence Way, Princeton, NJ

O. A. Anderson and K.-N. Leung
MFE Group, Lawrence Berkeley Laboratory
Berkeley, CA

1. INTRODUCTION

Gamma(γ)-ray resonance absorption analysis is based on the preferential absorption of 9.172 MeV γ-rays by Nitrogen 14 (^{14}N), which occurs at higher density in explosives than in almost all other common luggage materials. The γ-rays are generated in carbon foil targets by the proton resonance absorption ^{13}C (p,γ) ^{14}N, as shown schematically in Figure 1.

The reaction occurs when protons irradiate a ^{13}C foil at an energy of 1746.6 ± 0.9 KeV[1]. The width of the resonance has been measured to be 135 ± 9 eV[2]. Due to the center of mass energy, γ-rays at an angle of $80.8 \pm 1°$ to the reaction plane have the precise energy required for reabsorption by ^{14}N in the luggage. Imaging of the nitrogen density distribution in the luggage results from normalization with other off-angle high energy γ-rays to determine the resonant absorption due to ^{14}N.

This paper principally addresses the physics design, to nominal performance criteria, of the accelerator system which produces the 1.76 MeV proton beam incident on the ^{13}C target system. Electrical, radio-frequency (RF), thermal, vacuum and mechanical design of the various components shown schematically in Figure 2, have also been performed. Target and resonance or non-resonant scintillator detector issues are not discussed here.

The resonance absorption EDS requires that the accelerator meet the qualitative performance goals identified in Table 1. An approach to solving these issues is identified and discussed in greater detail below. Some specific Table 1 requirements depend on details of the target system, such as foil thickness.

2. ION SOURCE

An LBL H^+ multi-cusp ion source has been chosen because of the excellent characteristics of this source with respect to beam performance, gas efficiency, reliability and maintainability. Such a source, schematically illustrated in Figure 3 with filaments, permanent magnets and filter, has been consistently measured to deliver quiescent CW proton beams ($\leq \pm 1\%$ current fluctuation and $\leq 1\%$ dropout rate) with very high species purity and very low beam emittance at the current levels required.

In particular, proton fractions approaching 90% are achieved as shown in Figure 4. This is important, not only because it reduces the total extracted ion current which in turn leads to lower values for the emittance, but also because the H_2^+ and H_3^+ species are not accelerated through the RFQ and thus represent a CW thermal load on that component. At the present time, the CW hot cathode mode of operation is baselined. However, the ongoing RF drive development program at LBL in support of the SSC (Superconducting Super Collider) source will lead to the adoption of this lower power, higher reliability and higher performance operating mode in the near future.

3. LOW ENERGY BEAM TRANSPORT (LEBT)

In addition to RF drive, the SSC injector requires an electrostatic LEBT because of the short timescale of its macropulses. The electrostatic approach leads to a lower power, shorter length component with no gas neutralization for the present application. The absence of gas neutralization greatly reduces the LEBT gas load and enhances beam stability and quiescence.

The SSC acceleration-deceleration scheme has been selected because it gives low extracted source emittance, little LEBT emittance growth and the ability to generate a good match to the RFQ

acceptance ellipse. The specific design utilizes the proven ring lens approach shown in the simulation of Figure 5. Here, the various LEBT electrodes, their voltages and associated electric potential contours are plotted. The space charge forces within the overlaid extracted beamlets is self-consistently modelled. The source is biased to 30 KV and the first gap extraction voltage is -43 KV. The extraction optics decelerate and expand the beam with 30 KV at the ring lens and then deliver a highly convergent beam at zero potential in the RFQ match plane. The RFQ design has used an input normalized transverse rms emittance value of 0.08 π mm-mrad, but such sources and LEBTs have been consistently measured to deliver significantly better 10 mA H^+ performance.

4. RADIO FREQUENCY QUADRUPOLE (RFQ)

The proton accelerator is a conventional four vane Radio Frequency Quadrupole (RFQ) device whose symmetric point cross-section is illustrated in Figure 6. In order to provide long term performance stability and eliminate the requirement for periodic structure retuning, we propose to electroform the accelerator. It is believed that operating cost savings and the increased reliability will easily defray the higher manufacturing cost of electroforming as opposed to more conventional design approaches. The electroformed BEAR (BEam Aboard Rocket) RFQ demonstrated the same performance characteristics throughout a space flight and after a subsequent 70-g landing, without any hardware changes or retuning. A higher-current, higher-power CW cryogenic RFQ has already been designed and fabricated for the Continuous Wave Deuterium Demonstrator (CWDD) project, and hence CW operation with the present 10 mA proton current causes no particular thermal or mechanical problems for the engineering design. Details such as the thermal load of the CW proton, H_2^+ and H_3^+ currents collected inside the RFQ have been factored into the thermal design of the accelerator.

With cost and practicality in mind, the RFQ design drivers were adequate output brightness at minimum length and power consumption. The selected design has a 1.6 mm constant average aperture (r_o), 3/4 r_o vane tip radius, and the relatively low operating potential of 46 KV. This minimizes the power consumption and the peak surface electric field (PSEF) while maintaining satisfactory current transmission (79%) and an adequate current limit (28 ma) for off-nominal performance. The length was minimized principally by the choice of the axial vane modulation variation. It has been verified that the design will accommodate the projected levels of input beam misalignment, mismatch and performance fluctuation within the desired output performance envelope. As an example, Figure 7 shows the variation of output centroid energy as a function of vane voltage. Given a 1° phase and 1% amplitude RF control system, the output energy stability will be on the order of $\pm$ 1.0 KeV and will thus require no feedback control.

A summary of the principal RFQ design parameters and the performance values projected by beam dynamics analysis such as is illustrated in Figure 8, is given in Table 2. Emittance values are in rms normalized units. Figure 8 shows the achievement of about $\pm$ 35 KeV total beam energy spread at the end of the RFQ, and the dominant transmission loss as ions fall off-energy and out of the RF bucket in the gentle buncher region of the accelerator.

5. HEBT

The HEBT is required to transport the RFQ output beam to the foil target. Typical target requirements are an approximate 10 mm spot with a divergence of $\leq$ 5 mrad and a spot uniformity of better than $\pm$ 20%. Additionally, the long term variation of the centroid beam energy and the bunch energy spread should be less than $\pm$ a few KeV and approximately $\pm$ 10 KeV respectively, in order to maximize the γ-flux in the sharp resonance cone angle. The output emittance values and energy stability of the RFQ are sufficient to accommodate these requirements, but it is necessary both to expand the beam thus increasing the spot size while decreasing the divergence angle, and to energy compact the bunches after a drift in order to achieve the low energy spread.

A summary of proposed HEBT transport elements is provided in Table 3. The principal function of elements 1 through 9 is to provide a parallel expanded beam of the appropriate spot size in the vicinity of the target beyond element 15. This can be seen in the beam envelope behavior shown in Figure 9, where each element is numbered as per Table 3. The nominally zero strength electromagnetic quadrupole (EMQ) spot trim coils and drift of elements 13 through 15 will be site geometry dependent and hence while the qualitative function is relevant, the detailed sizing of this HEBT design is only illustrative. Additionally, if it is desired to locate the beamline above or below the target area, oriented vertically, then a 90° bend will be needed in

the HEBT before the target. HEBT steering will either be provided by misalignment of PMQs 2 and 5 or by separate small electromagnetic dipoles placed in the beamline.

The synchronous energy and energy spread control is performed with the element 11 single 425 MHz fundamental RF cavity, which should be placed as near to the target as possible to minimize the beam energy spread after bunching. The drift length from the end of the RFQ is set by the desired phase spread at the buncher, which in turn derives from the RFQ output longitudinal emittance and desired target energy spread. Using phase and amplitude control, the buncher, nominally at -90° and 34 KV respectively, provides the fine tuning on the output energy by varying the synchronous phase from about -80° to -132° while the amplitude changes from about 34.6 KV to 45.9 KV respectively. The HEBT longitudinal emittance at the beam edge, defined here as five times the rms emittance (> 90% of the beam), has a value of 375 KeV-°. This can be manipulated by the HEBT to yield ± 8.3 KeV by ± 45 ° thus satisfying nominal target requirements. In the Figure 9 example, some growth in beam size and energy spread following the element 13 delivery point can be seen. Specific site design would greatly reduce this growth.

The last function of the HEBT is to deliver a beam of high uniformity. Octupoles [3,4] are used to fold the wings of the "X" and "Y" plane transverse beam distributions back upon themselves. Figure 10 demonstrates this effect in the "X"-plane with the addition of element 3. Each octupole is optimally placed at a waist in each plane and again, since the final drift to the target is critical for the placement and strength of these magnets, the final design will be site dependent.

6. CONCLUSIONS

A high-current proton beamline design applicable to the gamma ray resonance absorption EDS technique has been completed. Projected beamline performance parameters and anticipated reliability levels will lead to a viable detection system. Cost and complexity, the principal drawbacks of the proposed system, are being addressed.

ACKNOWLEDGEMENT

This work was performed with Grumman internal research funds.

REFERENCES

1. F. Ajzenberg-Selove, *Nucl. Phys.*, A 268(1976) 1.

2. W. Biesiot and P. B. Smith, *Phys. Rev.*, C24 (1981) 2443.

3. P. F. Meads Jr., *IEEE Trans. Nucl. Sci.* 30 (4) (1983) 2838.

4. A. J. Jason, B. Blind, and E. M. Svaton, *Proc. 1989 Particle Accelerator Conference*, Chicago, Ill., 192.

Table 1: Qualitative Beamline Requirements and Design Approaches Adopted

REQUIRMENT	APPROACH
Quiescent Proton Beam	H^+ Multi-Cusp Ion Source
Short, Un-Neutralized LEBT	Eletrostatic & Ring Lens
10 mA CW H^+Current	425 MHz CW RFQ
Tunable Energy	1,76 Me V RFQ + 425 MHz RF Cavity
Good Energy Stability	1° Phase and 1% Amplitude RF Control
Low Energy Spread	Low Longitudinal Emittance & Energy Compaction System
$\sim$ 10 mm spot diameter, $\leq$ 5 mrad divergence & good spot uniformity	Beam Expanding HEBT + Low Transverse Emittance + Multipole Correctors

Table ?: RFQ Design & Performance Parameters

Frequency/Pulse Length	425	MHz / CW
Energy In	0.03	Mev
Energy Out	1.76	MeV
Current In	12.8	mA
Current Out	10.0	mA
Transverse Emittance In	0.08	π mm-mmrad
Transverse Emittance Out	0.13	π mm-mrad
Longitudinal Emittance Out	75.0	π KeV-°
Synchronous Phase Out	-22	°
Number of Cells	154	
Average Aperture	1.6	mm
Peak Modulation	3.0	
Current Limit	28	mA
Peak Surface Electric Field	1.8	Kilpatrick
Intervane Voltage	46	KV
Length	1282	mm
Cavity Power	76	KW
Total Power	110	KW

Table 3: Summary of HEBT Elements

No	Element	Length (mm)	Strength	Comment
1	Drift	10.66	-.-	
2	PMQ	20.00	-165.6 T/m	Steering Trim
3	Octupole	20.00	-.- T/m3	
4	Drift	4.14	-.-	
5	PMQ	20.00	85.5 T/m	Steering Trim
6	Drift	405.30	-.-	
7	Octupole	20.00	-.- T/m3	
8	Drift	4.14	-.-	
9	PMQ	20.00	-78.6 T/m3	
10	Drift	333.24		
11	RF Cavity	10.00	34.1 KV	425 Mhz @ -90
12	Drift	100.00		
13	EMQ	20.00	0.0 T/m	Focus/Spot Trim
14	Drift	1250.00	-.-	
15	EMQ	20.00	0.0 T/m	Focus/Spot Trim

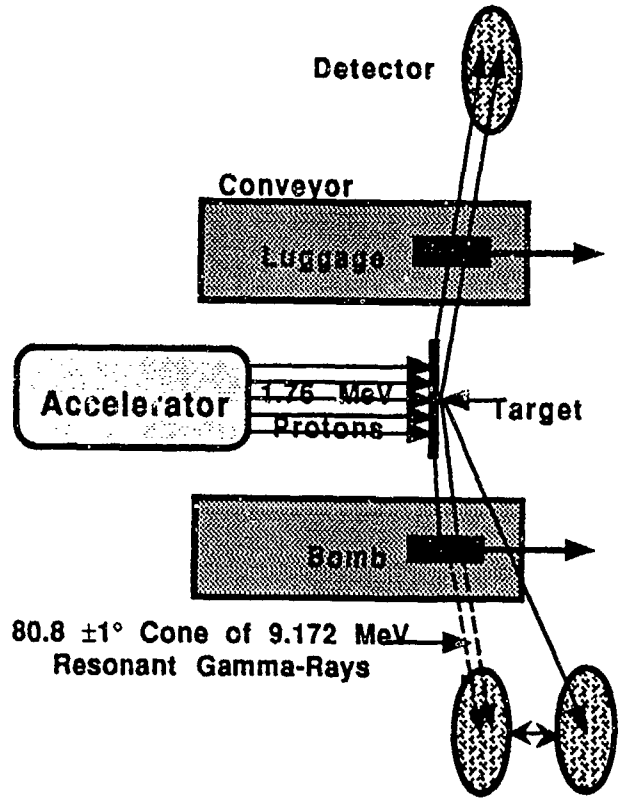


Figure 1: Schematic of the γ-ray resonance absorption technique used for explosive detection

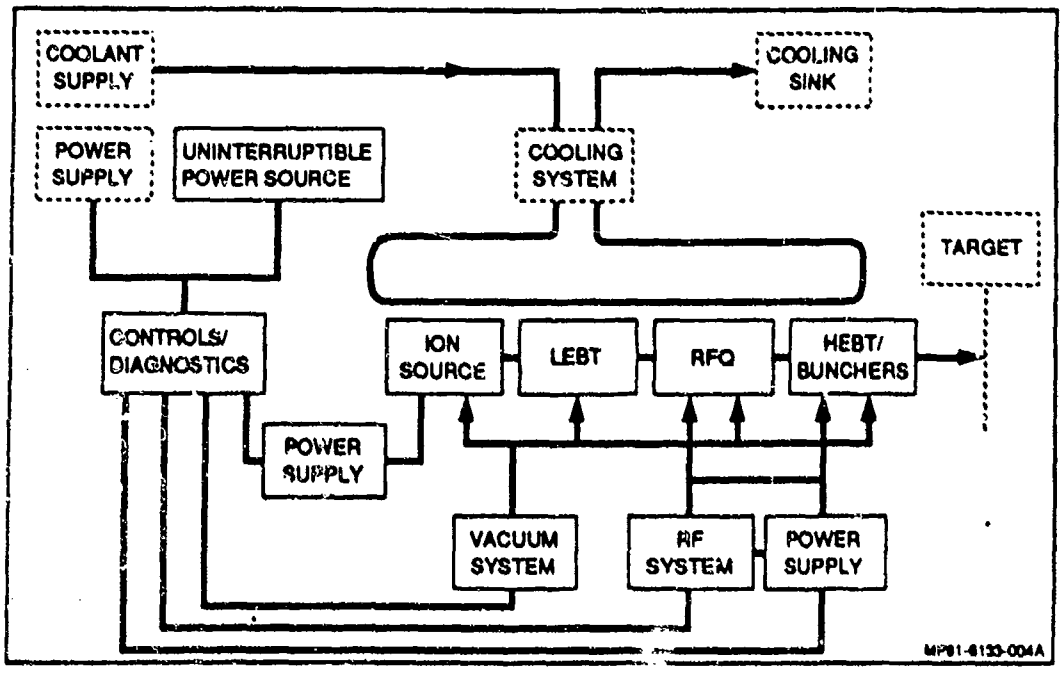


Figure 2: Block diagram of accelerator components

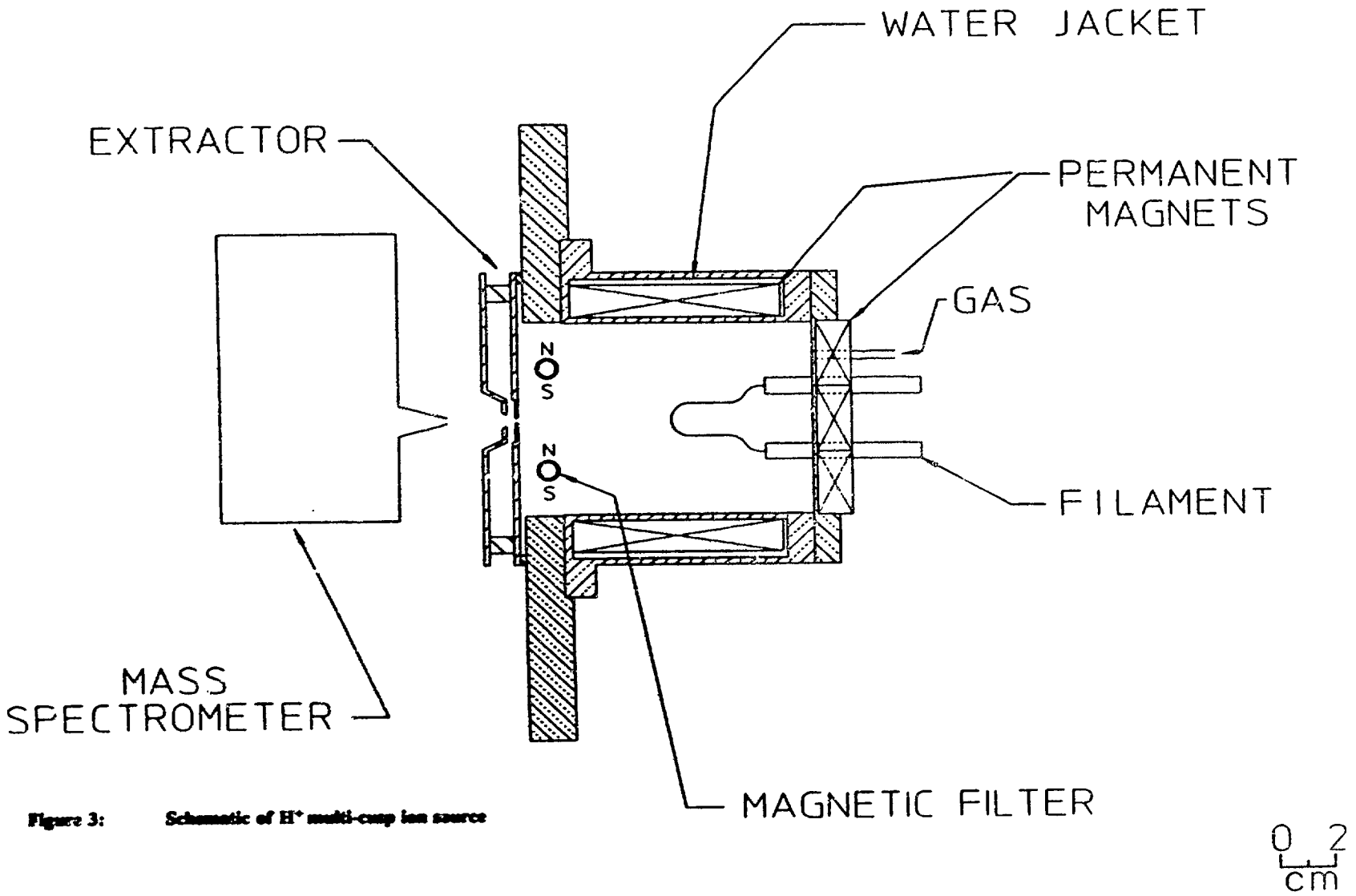


Figure 3: **Schematic of H^+ multi-cusp ion source**

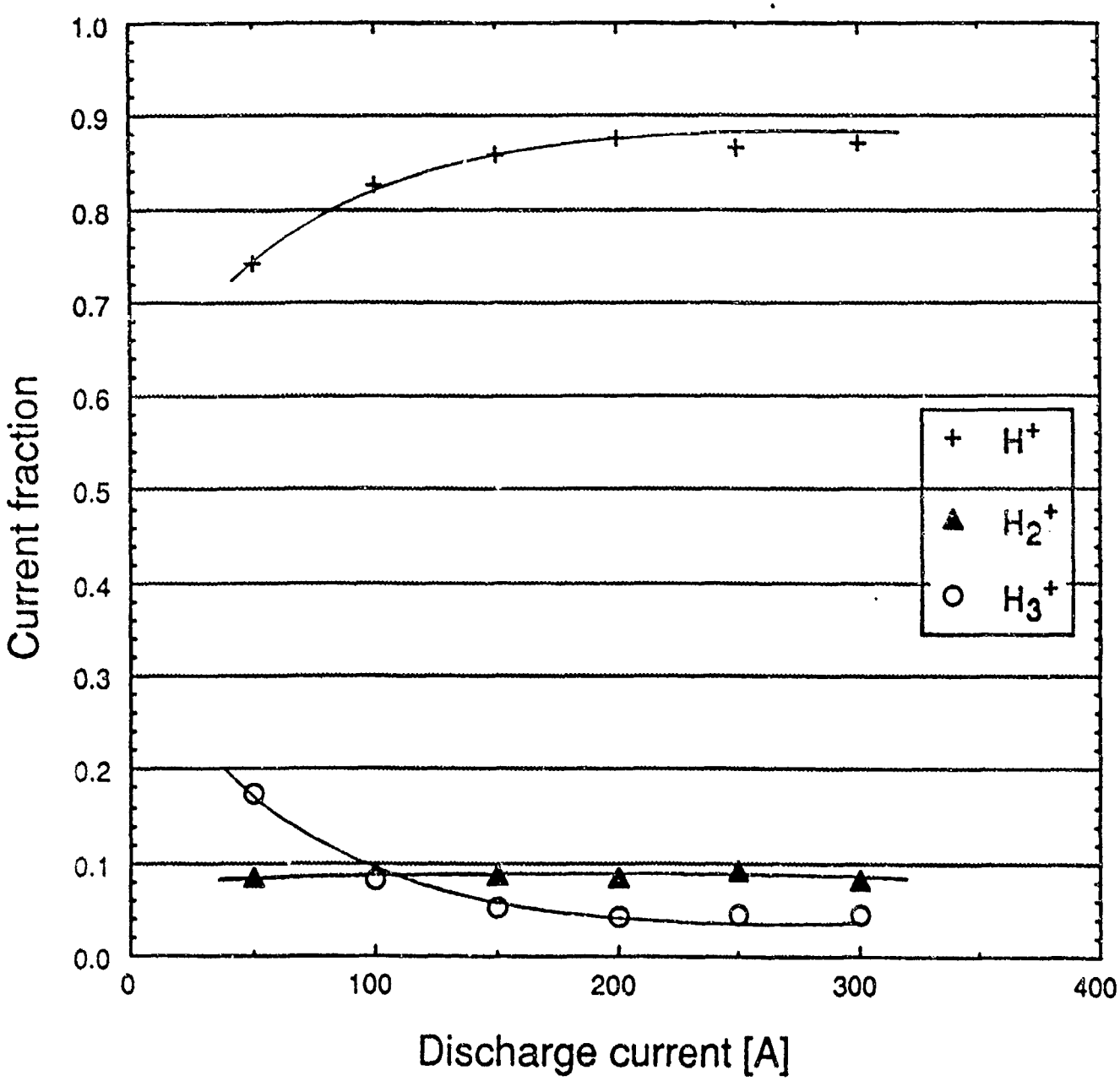


Figure 4: **Hydrogen species fractions with arc current**

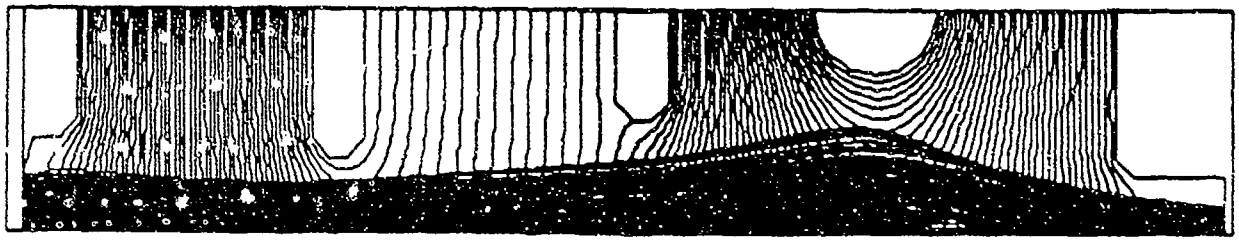


Figure 5: Ion trajectories and potential contours in the extraction grids and LEBT

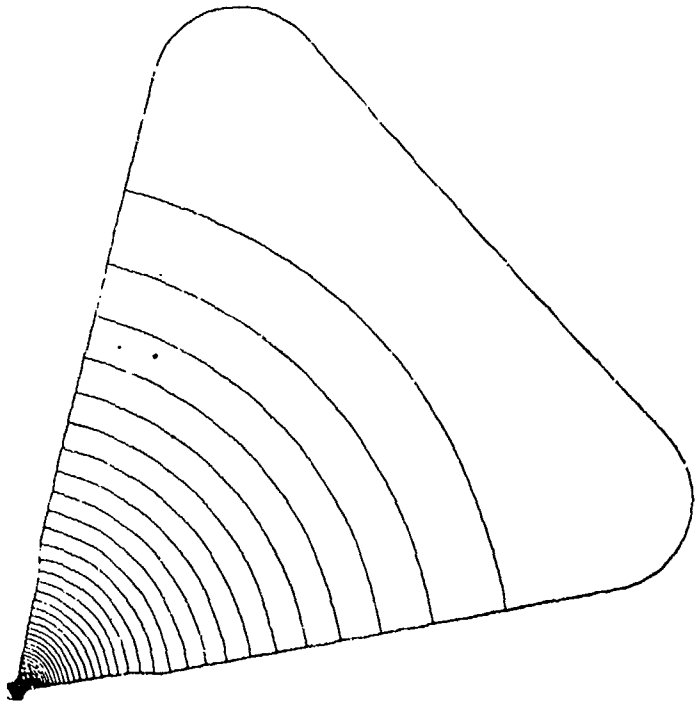


Figure 6: Potential contours in a single RFQ quadrant

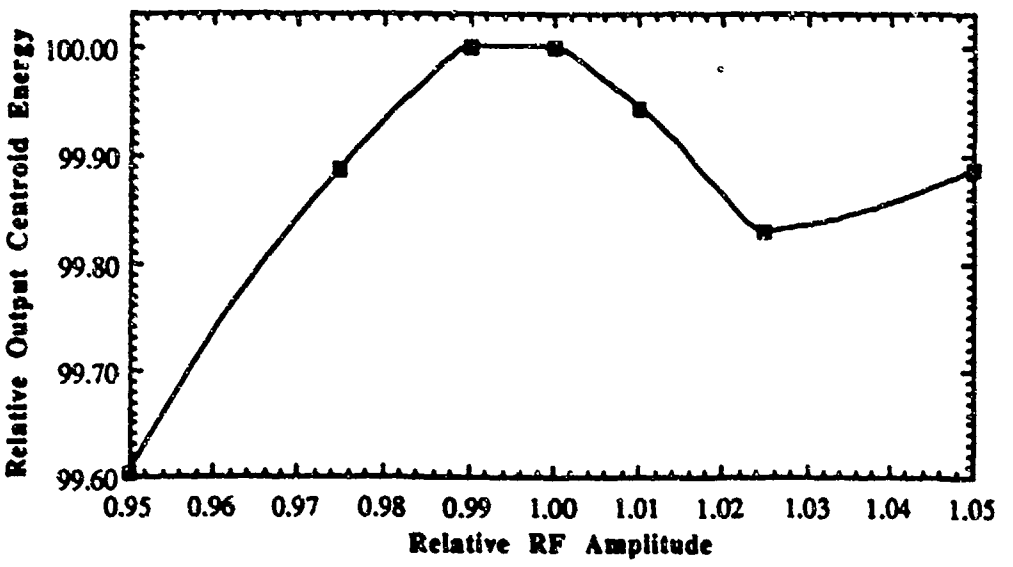


Figure 7: **Energy centroid variation (% of nominal) with RF amplitude fluctuation**

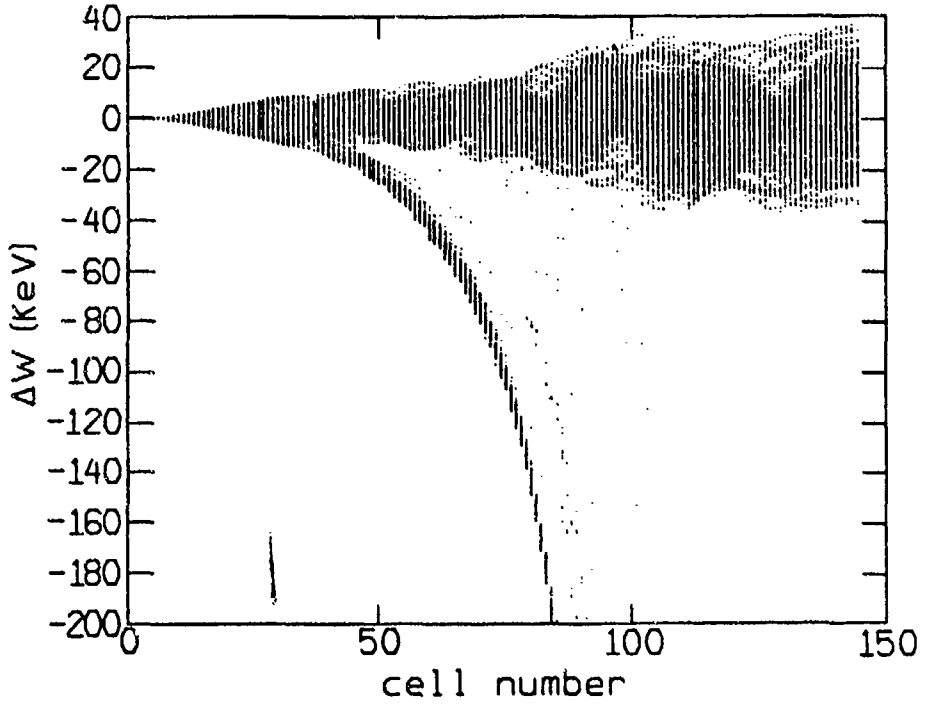


Figure 8: **Energy spread along the RFQ length showing the transmission loss in the gentle buncher**

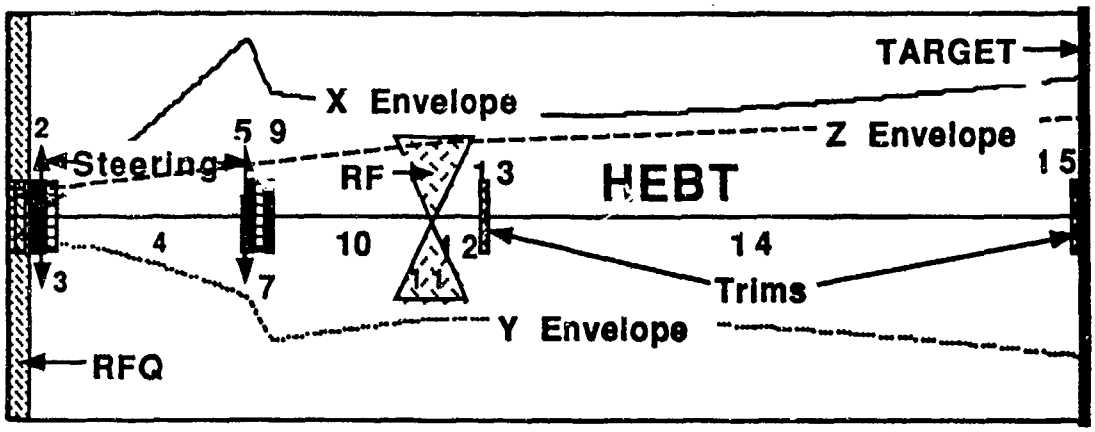


Figure 9: 5ϵ beam envelopes along the HEBT - "X" and "Z" (dashed) are above while "Y" is below. The transverse and longitudinal box scales are 10 mm and 180° respectively.

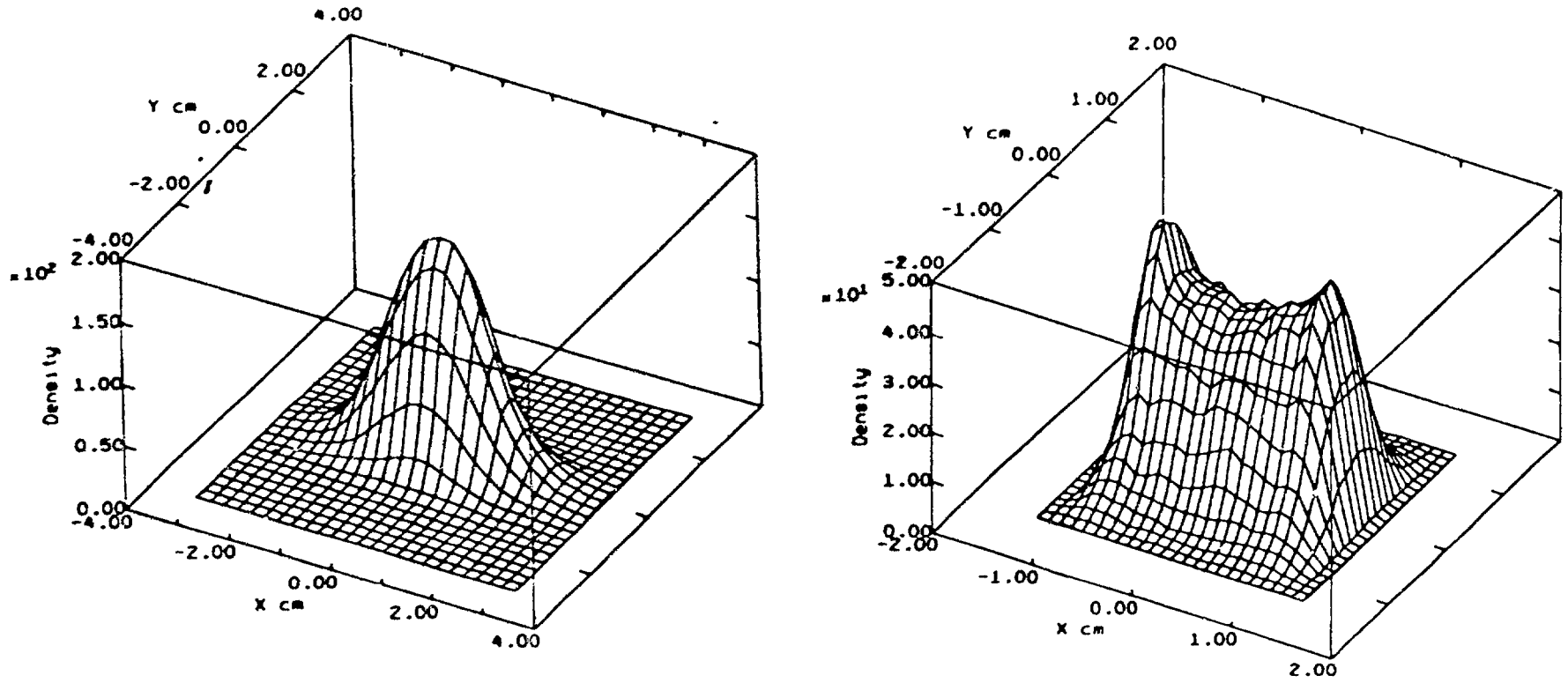


Figure 10: **Beam dynamics simulation of target transverse plane beam intensity profiles for an uncorrected (upper) and octupole corrected "X"-plane (lower) beam**

AN H^- ION SOURCE FOR RESONANT GAMMA PRODUCTION

P. W. Schmor and L. Buchmann
TRIUMF, 4004 Wesbrook Mall, Vancouver, B.C., Canada V6T 2A3

1. INTRODUCTION

1.1 Gamma Ray Absorption

Resonant gamma (γ) rays are produced by 1.75 MeV protons striking a ^{13}C target[1],[2]. Those γ-rays which are suitable for resonant absorption in ^{14}N are confined to a cone of small angular width. This angular width depends on the spot size and the angular divergence (i.e., emittance) of the proton beam at the target. Good image resolution requires that this width be made as narrow as possible.

1.2 Accelerator

Although there are a number of different accelerator techniques which should work, the electrostatic tandem accelerator, in particular, has several advantages. The unmodulated dc beam, from any electrostatic accelerator, simplifies the detection electronics. As the beam is unbunched the momentum spread is inherently small and the longitudinal emittance requirements for gamma ray resonance can be met with conventional techniques. The complexity of the high voltage system is minimized by the tandem system which reduces the total required voltage by a factor of two. Reliable, high-current (100 mA), 1 MeV power supplies already are routinely being used in industry. Ion source operation, maintenance and complexity are all simplified if the ion source is made to operate near ground potential. The ion source power supplies require considerable line power which can be provided much easier and more economically when the ion source is near ground potential.

1.3 Emittance

The emittance of an ion beam is the six dimensional (x, x', y, y', p, δp) volume containing the beam, where (x,y) are the transverse coordinates of ions within the beam, (x',y') are the divergence of the ions at this point, and (p,δp) are the longitudinal momentum and momentum spread of these ions. The emittance, normalized by $(\beta\gamma)^3$ where $\beta\gamma$ are the normal relativistic parameters, is an invariant of motion under the influence of linear forces. For most systems the emittance volume can be characterized by the three independent projections (x,x'), (y,y') and (p,δp). Initial estimates have been made for the transverse beam emittance requirements. Although the vertical and horizontal requirements are slightly different, a reasonable and achievable design goal is 0.13 π mm-mrad for a normalized rms emittance. The energy spread is dominated by the power supply stability.

1.4 Emittance Growth

Emittance growth, invariably, occurs during the acceleration process in all accelerators. The beam optics of an electrostatic accelerator can be optimized for minimum emittance growth by using large apertures in all optics elements, including the accelerator columns. However the main contribution to the increase in emittance is from the H^- to H^+ gas stripper. This stripper is a compromise between the conflicting constraints of maximum fraction stripped and minimum Coulomb scattering of the beam by the stripper gas nuclei. Because of this compromise, there is an optimum gas pressure for any given geometry and gas type. Requiring a maximum transverse emittance of 0.13 π mm-mrad at the stripper exit, the fraction of beam lost due to scattering and non-stripping is a fraction of the input emittance. This fraction depends on the geometry of the stripper. In order to maintain at least 90% of the initial ion source beam within the 0.13 π mm-mrad it is necessary to have an ion source emittance less than 0.09 π mm-mrad for a stripper canal 1 meter long and 2 cm in diameter.

1.5 Beam Current

The precision of the nitrogen density measurements and the length of time to obtain the required statistics

depend on the γ-ray flux. The γ-ray flux is proportional to the proton current. The precise proton current required depends on a number of factors. It is estimated, based on the results of a feasibility experiment performed by TRIUMF scientists, that a current of about 5 mA is required to meet existing specifications.

1.6 Ion Source

Given the above, a nitrogen detection system for explosives requires an H^- ion source with a current of at least 5 mA dc within a normalized rms emittance of 0.09 π mm-mrad. These specifications are met by a multi-cusp ion source and ion extraction system which was developed at TRIUMF[3]. This ion source is being used on a cyclotron for the commercial production of radio isotopes. The cyclotron has been in operation for slightly more than one year. During this period the ion source has operated without problem, requiring only regularly scheduled filament changes. Some of the important criteria for the ion source in this application include: a) current stability, b) reliability, c) ease of operation, d) reproducibility, and e) minimal maintenance requirements. All of these features are needed for a practical explosives detector.

2. ION SOURCE

2.1 H^- Production

During the last three decades, the application of H^- ions in accelerators has been growing. Two basic techniques are used for H^- production; namely, either volume production or surface conversion. These processes have been studied in a number of laboratories[4],[5]. Surface conversion ion sources produce H^- very efficiently but they generally require cesium; a distinct disadvantage for accelerators! The TRIUMF source uses volume production, where H^- ions are extracted from a hydrogen plasma which contains positive ions as well as electrons and a small number of negative H^- ions. These negative ions are created at energies less than 1 eV through dissociative attachment. (Cesium is not used to enhance the negative ion production, as the problems this creates for the accelerating structures are considerably worse than the benefit.) The H^- beams are characterized by low emittance, high brightness, stable output and low noise. These properties, along with the inherent simplicity of the volume source and the relatively long filament lifetime make it a practical choice for accelerators with external dc H^- injectors.

2.2 Source Description

The TRIUMF source consists of a cylindrical, all-copper, water-cooled plasma chamber (anode) which is surrounded by 10 axial rows of $SmCo_5$ permanent magnets for plasma confinement. The chamber is 10 cm diameter by 15 cm deep and is divided into two regions by a transverse magnetic field. A filament which extends into the chamber is mounted on the back flange. The front face forms the first electrode of the ion extraction system, is electrically insulated, is biased at a few volts positive with respect to the anode, and contains an 11 mm diameter aperture through which the H^- ions are extracted. The extraction system is an axially symmetric, four-electrode structure designed to produce a 25 keV ion beam. A collimator on the final electrode makes possible differential pumping and minimizes gas stripping of the extracted ion beam. A turbo-molecular pump is used to achieve a pressure of the order of 10^{-5} torr in the region between the collimator and plasma generator, while a cryo-pump downstream of the collimator yields an adequate vacuum in the beam line (approximately 10^{-6} torr). The gaps between the electrodes have been experimentally obtained by optimizing the beam brightness (proportional to the current divided by the emittance squared) for a 25 keV ion beam with current in the range of 1 to 6 mA.

2.3 Emittance Measurement

The beam emittance is determined by a method developed at LAMPF which uses a pair of electrostatic deflecting plates located between two slits and a linear feed screw to precisely position the system in the ion beam[6]. A portion of the beam passes through the first slit and is deflected by the electrostatic plates. Any current going through the second slit is measured on a Faraday cup. The plate voltage (angular beam deflection) can be stepped up uniformly by computer control and the Faraday cup current is digitized at each voltage step. The detector is moved and a set of curves is generated whose width is proportional to the angular spread at each position. The computer is used to calculate the emittance and plot the contours.

2.4 H^- Current

The H^- current is measured on a Faraday cup approximately 2 meters downstream of the ion source. The total current from the source depends on

the area of the extraction aperture. For an 11 mm diameter hole, a 7 mA H^- beam has been obtained within a normalized rms emittance of 0.085 π mm-mrad at an arc current and arc voltage of 27 A and 127 V, respectively. The output current is stabilized to the few percent level for periods of 24 hours with an electronic feedback loop which regulates the arc power. Long term current stabilization of weeks is maintained by computer control. The filament lifetime at 5 mA is approximately 4 weeks.

2.5 Controls

The ion source is controlled by a commercial programmable logic controller (PLC) which is monitored by an IBM personal computer. The ion source control system uses high level macros to operate the electronics, vacuum pumps and valves and thus reduce the need for highly trained operators. For instance a single set command at the console can turn the ion source on, through a predefined process, to preset values. The console screen contains colour-coded icons of the system which rapidly allow problems to be diagnosed. Various pages allow the operator to call up Help screens, interlock status of devices as well as the interlock logic step ladder. The diagnostic system is very user friendly and can be quickly mastered by individuals familiar with personal computers.

2.6 Reliability

The ion source has operated for over one year on a cyclotron which is being used for the commercial production of radio active isotopes. The source is required to run at 5 mA continuously. Regular maintenance periods are scheduled in advance. The ion source filament is changed during a scheduled maintenance approximately every four weeks. The computer is used to monitor the filament current and voltage to predict the anticipated lifetime of a given filament. The time dependent filament characteristics allow the operators to extrapolate and estimate the lifetime more than one week in advance.

ACKNOWLEDGEMENTS

A number of other TRIUMF scientists have contributed to this paper. G.Stinson, R. Ruegg and F. Bach assisted in carrying out the feasibility experiment. A. Altman has contributed to the caculations of resonant γ-ray fluxes and ion beam requirements. H. Schneider examined accelerator requirements. R. Baartman examined ion source matching conditions and emittance growth effects. K. Jayamanna, M. McDonald and D. Yuan obtained the ion source data.

REFERENCES

1. W. Biesot and P. B. Smith, Phys. Rev. C24 (1981) 2443

2. D. Varsky *et al*, Nucl. Phys. A505 (1989) 328

3. D. H. Yuan *et al*, Fifth Int. Symposium on Production and Neutralization of Negative Ions and Beams, AIP Conf. Proc. No. 210, Particles and Fields Series 40, (1990) pp 323-328

4. K. N. Leung, Proc. of the 10th Symposium of Fusion Engineering, Philadelphia, Pa (1983)

5. K. N. Leung *et al*, Ref. Sci. Instrum. 54 (1983) 56

6. P. W. Allison *et al*, IEEE Tran. Nucl. Sci. NS-30 (1983) 2204

X-RAY AND GAMMA RAY TECHNIQUES

PHOTONS IN - PHOTONS OUT: NON-DESTRUCTIVE INSPECTION OF CONTAINERS USING X-RAY AND GAMMA RAY TECHNIQUES

L. Grodzins
Massachusetts Institute of Technology
Cambridge, MA

1. INTRODUCTION

The non-invasive examination of containers for light-element contraband presents different challenges depending on whether we seek explosives or narcotics or foodstuffs; whether we are examining hand bags, or hold luggage or cargo containers; whether we have 5 seconds or 50 seconds; whether we have constraints or foreknowledge. There is no universal solution. Indeed, at this time there is no single detector that promises to solve more than a sub-set of our problems. We therefore seek a systems approach that presents a gauntlet of barriers whose sum will deter the most determined.

It is also clear that the search for explosives, the subject of this paper, is inherently different from the search for narcotics or foodstuffs. Explosives are expected in but one in a billion pieces of luggage; narcotics may be in more than one in a hundred. If but one explosive in ten passes our surveillance we have a tragedy; the system has failed. If we find one out of ten stashes of narcotics that wouldn't have been found otherwise, the system has been a success.

The evaluation of different explosive detection devices (EDDs), which integrate into a system called EDS, implies criteria of performance. If such exist, I don't know them. In the absence of such knowledge, I have adopted my own guidelines in order to evaluate different EDS approaches. The following qualitative criteria are a sub-set needed for the paper.

1. Testing must be automated and not rely on human judgement.

2. The probability of detecting a potential threat should be close to 100% for bulk explosives that terrorists use.

3. The probability of false positive alarms can be substantial if passengers are with their luggage, but must be negligible with passengers absent.

4. The system must be difficult to thwart or circumvent. Camouflaging the explosive must alarm the system.

The minimum weight and thickness guidelines are classified. In order to make calculations I have assumed minimum weights and thickness that, according to well-published reports[1], have been used successfully by terrorists. These are but a fraction of the weight and size of typical bags. They pose daunting challenges to technology. Nevertheless, I believe that we are not far from demonstrating a credible system that will meet the full set of guidelines, with a low enough alarm rate as to make the frequency of hand searches acceptable.

The paper begins with a discussion of the physical properties that distinguish an explosive. We then consider x-ray techniques, including simple transmission, Compton backscatter, multiple energy, and multiple view. We omit coherent scattering and detonator detection. We then make up Mev x-ray imaging for investigating large containers, which leads into the use of Mev x-rays for nuclear resonance absorption, a new technique not previously discussed. Recent progress in the Soreq technique of nuclear resonance absorption is then summarized. The final section suggests a gauntlet of different EDD x-ray machines, that either are or will be available soon, which together with profiling and hand searches could, I believe, be a formidible deterrent against terrorists.

2. THE UNIQUENESS OF BEING AN EXPLOSIVE

2.1 Chemical

Every type of explosive has a unique chemical formula and its vapors contain singular molecules.

2.2 Elemental

Explosives of concern in EDS are composed of hydrogen, carbon, nitrogen and oxygen. So, too, are many common organic and inorganic materials. As a class, explosives are rich in nitrogen and oxygen, poor in carbon and hydrogen. Atomic concentrations are not a particularly good discriminant since many common non-explosives have high atomic concentrations of oxygen (dacron, silk, cotton) and nitrogen (wool, silk, orlon). A more significant discriminant is the atomic densities of oxygen and nitrogen, measured in moles per cc. Still, many common materials (water, sand) have high densities of oxygen. Very few, however, have high densities of nitrogen; the most cited exceptions being certain plastics (melamine, polyurethene, and solid nylon). Nitrogen density is the most effective single elemental discriminant.

2.3 Crystalline

Most explosives have a crystalline structure that can be measured by modern x-ray Bragg scattering techniques. The detection probabilities and the false alarm rates remain to be determined. So too is the ability of Bragg system to scan luggage in desired airport conditions. But we know, a priori, that many light materials are not crystalline and that metals have very special Bragg signatures that will not confound the method. In my view, this technique, which is not discussed in this paper, has a definite role to play in a security system and should be exploited as fully as possible.

2.4 Mass and Linear Attenuation Coefficients

The ubiquitous airport x-ray machines measure the attenuation of x-rays of energies between about 60 kev and 120 kev. The subject is gone into in greater detail below. Suffice it to emphasize that the mass attenuation factors that are the quantitative results of such measurements cannot give unique signals for explosives since most light materials (plastics, paper, clothing) have essentially the same absorption effects as explosives. The example in Table 1 makes the point by comparing sugar with the military explosive C-4.

The mass attenuation coefficients, μ measured in cm^2/g, and the densities are the same within a few percent; they cannot be distinguished by x-rays. Nevertheless, as we will emphasize, x-ray interactions may well be the most important single security tool for detecting explosives.

Linear attenuation coefficients of materials, which are measured by three-dimensional x-ray imaging techniques such as computerized axial tomography, are a much more discriminating characteristic. The data are presented in Figure 5.

2.5 Density

The densities of explosives, shown in Figures 4 and 5, can vary over a wide range but the densities of high performance, robust explosives that terrorists use are tightly clustered between about 1.5 and 1.9 g/cm^3. If the density of objects in luggage could be measured, we would be able to eliminate from consideration a large number of confounding materials.

2.6 Correlations

Not a single attribute of explosives, apart from the molecular structures, is a unique signature of an explosive, but several have but a limited number of confounders. The measurement of two or more attributes in a single volume has the potential for eliminating or at least severely restricting the false alarm rates. In this subsection we examine a few two-parameter correlations.

- Nitrogen versus Oxygen: In previous publications we have called attention to the fact that the correlation of high atomic densities of nitrogen and oxygen is a unique signature of explosives. Figure 1 shows, in a plot of moles/cc of nitrogen versus the corresponding moles/cc of oxygen, that all explosives fall within a rectangle that contains no non-explosive, and innocuous materials are far from the rectangle and generally clustered in the lower left corner of the graph; i.e. the concentrations are low. A measurement of the oxygen and nitrogen densities to uncertainties of 20% gives a unique separation of explosives from other materials.

- Carbon versus Hydrogen: Figure 2 shows the correlation between carbon and hydrogen. Explosives (black squares) are for the most part will separated from innocent materials which contain either much more or much less of both carbon and hydrogen. Unfortunately, the exploitation of the distinction demands highly

accurate measurements, and methods for making such measurements, especially of hydrogen, are unknown to this author.

- Carbon versus Oxygen: An important discriminating signature is the correlation between the oxygen and carbon densities, shown in Figure 3. Measuring this correlation, which, in principle, can be done with some accuracy by several techniques, could greatly reduce false alarm rates.

- Mass attenuation coefficients versus density: The degeneracy of mass attenuation coefficients, μ, is lifted to some extent if the densities of the object can be measured as well. Figure 4 shows the correlation of μ vs ρ for 80 kev x-rays for a number of substances. The explosive group (black circles) is rather tightly constrained on this plot, though ambiguities with innocuous materials are inevitable, as already noted in Table 1. Nevertheless, if a correlation measurement can be made it would greatly reduce false alarms from clothing, liquids and foodstuffs. After all, what percentage of passengers carry a pound of sugar in their luggage?

- Linear attenuation coefficients versus density: The linear attenuation coefficient λ is the product of μ and ρ. A single measurement of λ, obtained, for example, by computerized axial tomography, gives the separation implied by the correlation in Figure 4. If ρ can be measured as well as λ then a further separation is obtained as shown by the correlation graph of Figure 5.

- Mass attenuation versus elemental concentrations: A number of systems propose to reduce false alarm rates by combining images of atomic concentrations with those of x-ray attenuation. Such correlations are, a priori, a "good thing" since any new information is valuable, but the correlation will be especially useful if the parameters are uncorrelated. For example, the nitrogen density of light materials is, to first approximation, uncorrelated with the x-ray attenuation coefficients and independent measurements of these quantities would help considerably in distinguishing explosives. Carbon densities, on the other hand, are not uncorrelated with μ values, so that the measurement of both gives little more information than the measurement of either.

3. THE INTERACTION OF PHOTONS WITH MATTER

The absorption of a beam of X-rays of energy E and intensity I_o (photons/sec) passing through material (atomic number Z, atomic weight A and density ρ) is described by an exponential attenuation,

$$I = I_o \exp(-\sigma_{tot} n t) \qquad (1)$$

where I is the measured intensity after the beam has traversed material of thickness t having n atoms per cc. Taking the log of both sides and writing n explicitly, we obtain,

$$\ln(I_o/I) = \sigma_{tot} n t = \sigma_{tot} N_o/A \; \rho t. \qquad (2)$$

N_o is the number of atoms per mole (Avogadro's number), A is the number of grams per mole (atomic weight), and ρ is the density. Equation 2 is usually written in a condensed form,

$$\ln(I_o/I) = (\sigma_{tot} N_o/A)(\rho\, t) = \mu(\rho t) = \mu x, \qquad (3)$$

where $\mu(cm^2/g)$ is the mass attenuation coefficient, and $x = \rho t$ is the areal density in g/cm^2. For some purposes it is more appropriate to use the linear attenuation coefficient $\lambda(cm^{-1}) = \mu\rho$:

$$\ln(I_o/I) = (\sigma_{tot} N_o/A\rho)t = \lambda t. \qquad (4)$$

The total cross section per atom σ_{tot} is the sum of four independent cross sections:

$$\sigma_{tot}(Z,E) = \sigma_{p.e.}(Z^5, E^{-7/2}) + Z\sigma_{es}(E) + \sigma_{p,p}(E,Z^2) + \sigma nu. \qquad (5)$$

$\sigma_{p.e.}(Z,E)$, is the photoelectric cross section that measures the probability that a photon will be absorbed by an atom, ejecting an electron whose kinetic energy is equal to the photon energy less the binding energy of the electron to the atom. The photoelectric effect, which increases as the fifth power of the atomic number and decreases as the 7/2 power of the photon energy is most important for x-ray energies below about 100 kev and for heavier materials.

$\sigma_{es}(E)$ is the cross section for photon scattering by electrons. At low photon energies, of the order of the binding energies of the atomic electrons, the scattering has a strong coherent component. As the energy of the photon increases, that component becomes small and the scattering is dominated by the

Compton effect in which the photon, acting like a particle, scatters from free electrons. We emphasize here, and again below, that the probability for Compton scattering is almost independent of Z since, as seen by Equations 4 and 5, it is proportional to $(Z/A)\sigma_{sc}$; Z/A apart from hydrogen, deviates little from 0.5, and σ_{sc}, the cross section per electron, is independent of Z.

$\sigma_{p,p}(E,Z^2)$ measures the probability that the photon transforms into a positron and electron. Since this can only occur at energies greater than 1.022 Mev, it is important only for Mev photons.

σ_{Nu} is the cross section for the photon to excite a nuclear state. This is an idiosyncratic phenomenon of importance only for very special photon energies matched to specific nuclear isotopes. In general σ_{Nu} is negligible, but there are a few exceptions in which the cross section is comparable to and may even dominate the electronic cross sections of Equation 2.

4. EXPLOSIVE DETECTION SYSTEMS (EDS)

There are a number of ways in which the fundamental interactions outlined in Section 3 can be used to identify materials in containers. We begin by discussing methods using x-ray generators with terminal voltages well below the pair production or nuclear excitation thresholds. A later section will consider EDS based on x-ray generators in the Mev range where both pair production and nuclear effects are significant. Finally, we will consider gamma ray schemes which make specific use of the nuclear interactions for measuring the distribution of specific elements.

4.1 Airport X-Ray Scanners

The ubiquitous airport scanner is shown schematically in Figure 6. These typically operate with electron energies of 120 kev impinging on a tungsten target. The resulting x-ray spectrum, sketched in the lower part of Figure 6, consists of the characteristic x-ray energies of tungsten (~60 kev) superimposed on a broad bremsstrahlung spectrum whose maximum energy is the electron energy (120 kev) and whose intensity per energy interval is inversely proportional to the x-ray energy. The luggage absorbs the lower energy x-rays preferentially and the exiting spectra, also sketched in the figure, is "hardened" to a degree that depends on absorbing material. The mean energy of the beam exiting from the luggage is typically around 80 kev.

Airport x-ray imaging systems were introduced to combat hijacking. The devices were designed to give high resolution pictures with excellent gray scale dynamic range so that the security operator could identify weapons made of metals in characteristic shapes. We now ask that these devices make evident explosives made from light materials with no characteristic shape. X-ray machines now being offered as EDS systems are, for the most part, adaptations of existing technologies to the EDS problem.

Attenuation: The most elementary approach to an EDS is to use the attenuated signal as a measure of potential threat. Consider the x-ray signal obtained in a simple two-dimensional projected image of an explosive shown idealized in Figure 7. The integrated signal, S, is simply:

$$S_{bomb} = N \log(I_o/I) = N\sigma_{tot}(N_o/A)\rho t\, a = \sigma_{tot}(N_o/A)M \quad (6)$$

where N is the number of pixels covering the bomb's projected area, a_i is the area of each pixel and M is the mass of the bomb. The sum of the logs of the attenuation ratios, due only to the bomb, is proportional to the mass of the bomb and is essentially independent of the type of explosive. We have assumed, for simplicity, a constant thickness of penetration but the answer is a general one, independent of shape.

The total signal from a bag is the sum of the signals S from every component in the bag. That is, the log of the attenuations add linearly and the total signal depends on the bag's mass. Thus, a small explosive in a large, heavy suitcase filled with light material will yield a bomb signal S_{bomb} that is only a few percent of S_{bag}. If heavier materials, such as iron, are present then the ratio will be greater. If we set our threshold equal to S_{bomb}, we will false alarm on almost every heavy bag. The total attenuation is therefore not by itself a useful measure for finding small bombs, though it will be an important input in more general EDS schemes.

Dual Energy: Commercial x-ray systems at airports now feature dual energy analysis to measure the atomic number of the material in the bag, a vital piece of information for the security operator. Figure 8 shows a schematic of the method. The method

makes use of the fact that the photoelectric effect is strongly Z dependent. To see the power and limitations of the method consider again the simple object of Figure 7. The log of the attenuation signal obtained at a mean x-ray energy, E_1 is given in Equation 7.

$$\ln(I_o/I_1) = [\sigma_{p.e.}(Z,E_1) + Z\sigma_{sc}(E_1)](N_o/A)\rho t \quad (7)$$

There are too many unknowns in Equation 7 to get much information from a single measurement. In particular, a thin, high Z material will have the same attenuation signal as a thick, low Z material. But two measurements obtained with two different energies, as indicated in Figure 8, can unravel some of the mystery about a single object.

The division of the two signals cancels the common factor of $\mu\rho t$. The result is,

$$\ln(I_2/I_1) = [\sigma_{p.e.}(Z,E_1) + Z\sigma_{sc}(E_1)][\sigma_{p.e.}(Z,E_2) + Z\sigma_{sc}(E_2)]^{-1} \quad (8)$$

This ratio shows strong discriminating power at lower energies and heavier Z. But there is little discriminating power among the lighter materials. Figure 9 presents the ratio of mass attenuation coefficients for a number of materials and for two energy ratios: the black squares are for 80 kev to 40 kev mean energies: the open circles are for 100 kev to 60 kev. Not surprisingly, the lower the lowest mean x-ray energy, the better the discrimination power. But the lower energy x-rays are strongly absorbed and it is very doubtful that present x-ray systems can produce useful signal strengths with 40 kev radiation passing through heavy luggage. The 100/60 results show reasonable discriminating power (if the measurements can be made to an uncertainty of 10%): materials with a modest component of heavier elements, such as black powder with its potassium, sand with its silicon, saran and PVC with chlorine can be distinguished, as can all of the metals heavier than sodium.

The dual energy method applied to a simple object also yields the areal density ρt and that in turn gives a measure of the density and the thickness, since the atomic number has been determined. (That measure could be reasonably precise for heavier materials but is expected to have large uncertainties for light objects since the densities of objects with the same effective Z and μ can have densities that range from 0.2 to values close to 2.)

But simple objects for which Equation 8 applies are rarely seen at airport gateways. The contents of actual luggage is infinitely varied and only occasionally neatly packed. And, terrorists camouflage their bombs. The dual energy method when applied to real luggage no longer gives the atomic number of the object, but only an effective atomic number, and the areal densities are poorly known. In the real world, simple dual energy analysis, while an improvement over single energy analysis, is easily confounded and cannot be used for automated screening. To improve the method one must separate the objects in a complex image. Several approaches are being vigorously pursued.

- Multiple views: Two views are better than one; three better than two. Figure 10 shows a system in which two orthogonal views are obtained so as to uncover some objects hidden from one view. In this idealized drawing, the five objects that are observed to be one continuous object in the horizontal view, are revealed in the vertical view to be at least 4 separate objects. A modest amount of computerology should be allow all 5 objects to be identified.

A dual view system when combined with dual energy, represents a significant advance. In some cases , the two views can, in principle, give sufficient information to derive the volume of the objects, and hence their densities; in principle, because the computerology of the image reconstruction has not been demonstrated to my knowledge. Obviously, two views still contain ambiguities and degeneracies, so the more views the better; the limit is a full computerized tomographic scan taking as many independent views as there are independent voxels.

- Compton scattering plus absorption: A competing technique to dual energy analysis makes use of images formed by absorption together with back-scattering. Figure 11 is my cartoon of the AS&E method in which a beam of x-rays scans the luggage; the Compton scattered x-rays together with the transmitted x-rays are counted in registration with the beam position.

It is sometimes said that the AS&E method and the dual energy method of x-ray analysis give equivalent information since they both, in principle, separate and identify the photoelectric and Compton components. That argument ignores the competition between the two effects, which allows Compton backscattering to provide information that cannot be obtained in

practice by dual energy. The proper comparison of dual energy analysis is to the combination of transmission attenuation plus forward Compton scattering. Backward Compton scattering has special advantages as the following simple calculation makes clear.

Compton backscattering gives information about light material in the near surfaces of luggage that is difficult to obtain otherwise. The principal reason is that the Compton signals from heavier material are suppressed by the photoelectric attenuations. The backscattered intensity, I_b, from a sheet material of areal density $d(g/cm^2)$, into a detector that subtends Ω of a sphere is given by,

$$I_b = I_o(\sigma_{sc}/2\sigma_{tot})\Omega[1-\exp(-2\mu_{tot}d)]. \quad (9)$$

Assume for simplicity that the incident x-ray flux is uniform from 30 kev to 60 kev and that the thickness is such that $2\mu_{tot}d=1$ for plastics. The intensities I_b/I for plastic, aluminum and iron are they in the ratios of 1:0.8:0.2. The signals from the heavier materials are suppressed, allowing the light materials to stand out clearly. By the proper choice of beam conditions, the light materials in the near surfaces (and to a lesser degree in the interior) can be strongly enhanced for either visual or automated discrimination.

Compton backscatter imaging is, at this time, unique in finding thin explosives, especially near surfaces. That uniqueness, which I have described for examining luggage, is being applied by AS&E and by IRT to the search for explosives and other contraband on the surfaces and clothing of people.

- Pattern recognition with object subtraction: An operator examining a high-resolution, wide dynamic-range x-ray image can highlight individual objects by examining the images at each level of grey scale. Companies claim to have written programs that do this automatically. That is, objects are identified by pattern recognition schemes and are isolated by subtracting the signals representing the background materials. If dual energy analysis is carried out on the separated objects, then the analysis of Equation 8 applies and the device has the potential for being an automated detector of potential explosives.

- A comment on the need for two dimensional as opposed to linear x-ray detector arrays: I have no doubt but that pattern recognition, especially obtained from multiple views, will eventually, if not now, be able to identify a considerable number of objects in luggage, provided that the data is robust enough. But my own estimates of counting rates raise doubts as to whether the counts per pixel are sufficient for many levels of image manipulation. State of the art x-ray tubes used at airports have beam power levels of about a kilowatt. The total detected x-ray fluence, in rapid, dual-energy scan of a large suitcase, must be divided into thousands of pixels. The number of counts per pixel is limited, especially through denser sections of a bag. Each successive subtraction introduces statistical fluctuations so that the final, isolated object may be very poorly characterized. A thin sheet of explosive that weighs but a fraction of the bag poses a severe challenge since its identification requires the subtraction of two signals that may not differ by more than 1%. There are a number of ways to enhance the signal strength per pixel. Perhaps the most obvious is to use areal rather than linear arrays of detectors so that image information can be taken in parallel in two dimensions.

- A comment on the advantages of digitized pulse counting, as opposed to digitized current measurements: The x-ray systems in place at airports digitize the charge currents obtained when the x-ray beam strikes the detector; the effective x-ray energy is a convolution of the x-ray energy spectrum and the detector efficiency function. Dual energy images can be obtained by several methods, the most straightforward being the taking of sequential views, each at a different x-ray tube potential, Figure 8. The analyses obtained in this way suffer from the problem of "beam hardening;" i.e., the lower energy x-rays are preferentially absorbed. It is difficult, with current digitization, to obtain an x-ray image at low x-ray energies where the sensitivity to atomic numbers is greatest. Pulse counting, in which the energy of each detected x-ray is measured and stored, cures the problem. Dual energy analysis is carried out with specific knowledge of the detected energies and is independent of beam hardening. The low-energy x-ray image is obtained at the lowest that is practical for each area of the luggage. Digitizing individual pulses at very high rates in arrays of detectors was once prohibitively expensive but the cost has come down dramatically in recent years and systems

with hundreds of detectors, digitizing at rates of 10^8/sec, are practical.

- Computerized axial tomography: CAT scanning, so well developed for obtaining 3-dimensional images of the insides of people and commercial objects, is now being applied by Imatron to the surveillance of luggage. It is an exciting development since the voxel size is fixed by the system parameters so that the x-ray absorption yields the linear absorption coefficients rather than the mass absorption coefficients. The linear coefficient, as Figure 5 shows, is the more informative parameter. Only a few common materials such as sugar and polyurethane will likely be confused with high-performance bombs.

The present Imatron system, while considerably faster than most CAT systems used for people, is still too slow for use as a screener at airports. Part of the slowness is due to deficiencies in computer power, but that will disappear in a few years with the inexorable advances in computer capabilities. More fundamental is the deficiency in x-ray fluence which is limited by available x-ray tubes and the scan time. That limitation prompts a general remark about the development of x-ray systems for airport security.

- Automated x-ray security systems: All of the present x-ray security systems are patched up and augmented versions of the original designs aimed at thwarting hijacking by showing security personnel the clearest possible image of the interior of a suitcase. The Imatron CAT-EDS had its origin in a portable medical scanner, where again, the principal goal was clearest visual images. A device or system designed for automated decision making rather than viewing will likely have very different specifications than present systems. The subject is an involved one and I will illustrate my point with but one example.

In CAT imaging, and no doubt in other x-ray imaging systems as well, there is a fundamental relationship between the total fluence that passes through the test object, the limits in spatial resolution Δx_i, and the precision of measuring the linear attenuation coefficient $\Delta\lambda/\lambda$. That relationship is simply

$$FT = K(\Delta x)(\Delta y)(\Delta z)(\Delta\lambda\lambda)^{-2} \qquad (10)$$

where F is the transmitted flux of x-rays in number/cm^2/sec, T is the total interrogation time on the sample and K is a constant that depends on the size of the object and its average λ. The linear attenuation coefficients for explosives have a spread of about 10% and there is little to be gained by having the ability to measure λ to better than say half that value. Similarly, there is little merit in having a spatial resolution that is more precise than is needed. If our aim is to find explosives, we should be designing the computer algorithms to recognize a volume of material with x-ray attenuation coefficients implicative of an explosive. The CAT specifications will then be much less severe than for image visualization or object identification and the fluence needed per slice, as well as the needed computation power, may well be reduced by one or two orders of magnitude. It might be possible to now design an Imatron-type system that can fully scan every piece of luggage in a few seconds. The technology will doubtless require a totally new x-ray detector system, though one that is well within the state-of-the-art.

4.2 High Energy X-Ray Imaging

X-rays of 80 to 100 kev are marginally capable of examining the heavier and bulkier pieces of checked luggage. As the x-ray energies are raised so as to increase the penetrating power, the interactions become dominated by the forward Compton cross section, which does not give measure of atomic numbers or masses. In order to affect such discrimination we must increase the energy into the Mev range where the pair production cross section is important.

Several manufacturers have commercial, Mev-class, x-ray systems for investigating the interior of large containers; some include dual energy to obtain atomic number information, and there are even computerized tomographic systems available. These systems will play no role in checked or hand luggage, though they may have uses in scanning cargo containers. If so, they will be housed in special buildings since the commercial systems require large amounts of shielding. The systems that use 10 Mev beams from linear accelerators are enormous.

As we have shown above, attenuation measurements made at one energy can only give morphological information. To obtain measure of the atomic number of the absorbing material one needs two measurements taken at different effective energies. The ratios of attenuation coefficients calculated at 10

Mev and 5 Mev for various materials are shown in Figure 12. Just as with dual-energy x-rays, there is little difference in the ratios for materials consisting of hydrogen, oxygen, carbon and nitrogen. But concrete, sand and metals show up clearly. The discriminating power at energies in the Mev range is at least as great as that in the 50 to 100 kev range.

4.3 Nuclear Excitations by High-Energy X-Ray Beams

A high energy x-ray beam contains a white spectrum of photons. At certain special energies characteristic of the individual nuclear species, the nuclear part of the interactions, Equation 5, becomes comparable with the electronic absorption. An excellent general reference is F. Metzger, Resonance Fluorescence in Nuclei.[2]

The probability for nuclear excitation by photons is given by the Breit-Wigner formula:

$$\sigma_o(E_\gamma) = (\lambda^2/4\pi)\Gamma\Gamma_\gamma[(E_\gamma - E_o)^2 + \Gamma^2/4]^{-1} \qquad (11)$$

where σ_o is the cross section in cm^2, λ is the wave length of the photon in cm., Γ is the total width of the state being excited and $\Gamma\gamma$ is the partial width for deexcitation to the ground state, E_o is the energy of the eigenstate and $E\gamma$ is the energy of the photon; spin terms have been omitted.

The maximum cross section, σ_o, occurs when the photon energy is exactly on resonance ($E\gamma - E_o = 0$).

$$\sigma_o(E\gamma = E_o) = \lambda^2/\pi\frac{\Gamma\gamma}{\Gamma} = \frac{5 \times 10^6}{E_o^2}\frac{\Gamma\gamma}{\Gamma} \qquad (12)$$

where σ_o is in barns (10^{-24} cm^2) and E_o is in MeV; spin dependent terms have again been omitted. If the excited state only decays to the ground state then $\Gamma\gamma/\Gamma = 1$ and a 10 Mev state can have an absorption cross section of order 50 barns, which is 100 times the electronic stopping cross section for 10 Mev photons in light materials.

Table 2 lists some of the states in carbon, nitrogen and oxygen that are candidates for resonance fluorescence. The data have been taken from the Nuclear Physics articles of Ajzenberg-Selove.[3] Note that the widths of the states vary over factors of 10^6, from milli-electron volts (mev) to kilo-electron volts (kev).

The first column gives the energy of the states; e.g., the first excited state of carbon is at 4.4 Mev. The spin and parity of the states are given in the 2nd column. Column 3 displays the total width of the states, while the partial width for the transition to take place directly to the ground state is given in column 4. Column 5 gives the maximum gamma ray absorption cross section, in barns, including the effects of spin. The last column gives a figure of merit for excitation, defined as the total width in electron volts multiplied by the peak cross section in barns.

Consider the example of the 15.11 Mev state of ^{12}C. Its width is 43.6 electron volts and, once formed it decays mainly to the ground state emitting a 15.11 Mev photon. The peak cross section is 29 barns, almost 100 times the electronic cross section. That is, at the precise energy of resonance, the mass absorption coefficient due to nuclear excitation is 1.45 cm^2/g, while the mass absorption coefficient due to the Compton plus pair production effects is only 0.018 cm^2/g. At this energy, the mean free path in carbon is only 7 mm, rather than 55 cm, which it is at energies only a 100 electron volts away.

There are a number of ways of exploiting nuclear resonance absorption to measure the concentration of particular nuclei. One way, that utilizes the high energy x-ray beam discussed above, is outlined here; a fuller discussion will be the subject of a forthcoming paper.

Figure 13 shows, in schematic form, an EDS method that utilizes a high energy x-ray beam to measure simultaneously the distribution of the bulk material and projected concentrations of a number of elements in a cargo container.

A highly collimated x-ray beam, produced by electrons of say 10 Mev, is attenuated on passing through a cargo container that contains carbon, oxygen and nitrogen. (The method also applies to other elements, in particular chlorine.) The idealized incident spectrum, shown in the top right of the figure is attenuated by electronic interactions to produce the fictional transmitted spectrum shown. At certain specific narrow energy bins, corresponding to the nuclear excitations in carbon, oxygen and nitrogen, there are sharp dips in the spectrum. For example, oxygen should show a dip at an energy of 6.917 Mev; nitrogen should have a dip at 9.17 Mev, and carbon dip at 4.4 Mev. To measure the strength of the absorption we propose to use resonant

detectors that are sensitive only to the resonant energies and insensitive to the non-resonant photons.

An example of a resonant detector for oxygen is shown in Figure 14. An oxygen target, such as water, is placed in the path of the beam exciting the cargo container. Emerging from the sides of the water target are the Compton scattered photons, annihilation radiation, and the 6.917 Mev gamma rays that deexcite the ^{16}O nuclei that have been excited by the x-ray beam. The energy of the annihilation radiation, produced by the positrons created in pair production, is concentrated at 0.511 Mev, a factor of 14 below the gamma ray energy. The energies of the Compton scattered photons depend on the angle of scattering; at scattering angles of 90° and 180°, the maximum energies are 0.511 Mev and 0.255 Mev respectively. Thus, if we view the water target from the back direction with a well shielded detector, as shown in the figure, we should be able to measure the strength of the nuclear interactions in the cargo container as signaled by the yield of 6.917 Mev fluorescent gamma rays from the water target. The signal to background strengths, calculated with Monte Carlo codes, indicate that it should be possible to scan cargo size containers in less than 5 minutes to produce quantitative images of the projected densities of the elements of most interest.

4.4 Soreq Method of Nuclear Resonant Absorption

The final topic in this survey of photon-photon methods of EDS is the Soreq method of finding nitrogen through the use of the 9.17 Mev nuclear gamma ray resonance. Figure 15 is a schematic depiction of the method. The basic idea has been described earlier.[4] We address here two recent advances that have not previously been reported.

Gamma rays of precisely the right energy to excite the 9.172 Mev state in ^{14}N nuclei are passed through the examined luggage. If nitrogen is present, those gamma rays will be absorbed; the amount of absorption is a measure of the projected nitrogen concentration in the luggage.

The requisite gamma rays are obtained by the resonant capture of 1.7476 Mev protons by ^{13}C. That is,

1.7476 Mev $p + {}^{13}C \rightarrow {}^{14}N^{*}(9.172\ \text{Mev}) \rightarrow {}^{14}N + 9.172\ \text{Mev}\ \gamma$.

The lifetime of the 9.172 Mev state is so short that the deexcitation gamma ray is emitted before the recoiling nucleus can slow down and the fluorescent gamma ray suffers a Doppler shift proportional to the cosine of the emission angle with respect to the beam direction. Every gamma ray emitted at a cone angle of 80.5° has precisely the right energy to excite nitrogen nuclei in luggage.

The Soreq method is powerful with many striking merits. The radiation levels are extremely low; neither neutrons nor radioactivity are produced; the method cannot be thwarted; a normal radiographic image is produced together with the image of the projected nitrogen concentration; the spatial resolution in the projected direction is excellent. The method has two obvious disadvantages. First, the yield from the production reaction is low so that exceptionally high currents of protons are needed if luggage must be scanned in a few seconds. Second, the method is keyed to nitrogen, which is not a unique marker for explosives. We have begun to address both those concerns. The following is the briefest of progress reports.

- The accelerator target: The primary reason for the low yield of 9.172 Mev gamma rays (about 1 in 10^8 protons) is that the effective thickness of the target is equal to the resonant width of 140 e.v.; i.e. about 1 $\mu g/cm^2$. We have been exploring the possibility of amplifying the output by using multiple foils (or gas cells) and reaccelerating the protons in the path between the foils (or gas cells). Figure 16 shows a schematic drawing of the basic idea for a 5 element target with a magnetic field to suppress the electrons.

Celeste Chang and I have carried out a detailed theoretical analysis of the limits of the amplification factors imposed by energy straggling and multiple scatterings in the foils. The conclusion, detailed in Chang's Senior Thesis[5], is that amplification factors greater than 50 will be difficult to attain, primarily because of energy straggling in the foils; the 5 element target of Figure 16 is expected to have a gain of about 4. The major unknowns are the practical ones: How long will thin carbon foils last under the intense beams? How thin can one make a stack of thin foils? How easy is it to replace ruptured foils? Can we deal effectively with the secondary electrons emitted from the foils?

Oxygen Concentrations. The 6.9 and 7.1 Mev states in ^{16}O have excellent resonant absorption properties

and the states have been studied in some detail by resonance techniques. We have been examining the practicality of using the same 1.7 Mev proton beam, used for measuring nitrogen distributions, for measuring the ^{16}O.

The central idea is to make use of the fact that the 6.9 and 7.1 Mev states in ^{16}O can be produced by the reaction of 0.5 to 1.7 Mev protons on ^{19}F. The reaction, which has many resonances, proceeds as follows:

$$^{19}F + p \rightarrow {}^{20}Ne^* \rightarrow {}^{16}O^* + \alpha.$$
$$^{16}O^* \rightarrow {}^{16}O + 6.9 \text{ Mev } \gamma$$

The 6.9 Mev (and 7.1 Mev) gamma rays are Doppler broadened by about 100 kev on emission from the fast moving ^{16}O nuclei and only about 1 gamma ray in 10,000 is in resonance. To detect the resonant signal we again need a resonant detector but this time it can have close to 4π efficiency since the count rates are moderate and the incident gamma rays are nearly monochromatic. A schematic drawing of the method is shown in Figure 17.

Whitney Edmister and I have modeled this method on a computer to determine its merits and limitations. Our conclusion, detailed in Edmister's Senior Thesis[6], is that it is practical to use a composite target of ^{13}C plus ^{19}F and a single beam of 1.7 Mev protons to detect both the projected nitrogen density and the projected oxygen density. The efficiency of the latter is significantly smaller than that of the former, however, so that the measurement of oxygen can neither be carried out quickly nor with high resolution. What does appear practical with the same accelerator system is to investigate the nitrogen quickly, with high resolution. If an area of a bag is suspect, it would be investigated over longer periods of time with the special oxygen detector.

5. A POSSIBLE SECURITY SYSTEM

During the past decade, a wide variety of methods have been proposed for finding explosives in airport luggage. Some of these methods have gone beyond the proof-of-principle phase to the prototype phase, and a few are in commercial production. And as this conference makes abundantly clear, there is no lack of new ideas for explosive detection schemes. In the fullness of time and funding, the nation will have an automated explosive detection system that will meet the most stringent requirements of security. In the meanwhile, I suggest that we are within reach of having a practical, semi-automated airport security system that will be a strong deterrent to terrorists, even though it is not the ultimate that we desire. My scenario does not include future technologies. Nuclear techniques, despite their promise, are not yet at the stage to be considered for today's EDS.

The flow diagram for the suggested system is shown in Figure 18. Every piece of luggage must be examined in the presence of the passenger. The most obvious place for the system is close to the check-in counter. The system consists primarily of a series of x-ray detectors that would look quite similar to the x-ray systems passengers go through now. Every passenger must be profiled. Every bag must be passed through a series of detectors each of which has a special as well as a general purpose.

- The first line of defense is the profiling and the questioning of the passengers. I doubt if we will ever give up this primary hurdle.

- The second line of defense is an x-ray system designed specifically for detecting detonators. Detonator detectors may never be perfect but even those presently available are better than no detonator detector system at all.

- The third line of defense is a Compton backscatter-transmission system whose primary function is to examine the near surfaces for potential thin explosive-like material. I expect that that would not be difficult to do with computer software but until that is proven, the examination should be visual. One can expect that this system will be implemented with dual-energy capabilities in the not distant future. The AS&E system purports to do much more than find contraband in surfaces, and that is all to the good. But the primary purpose of the detector in the present EDS is to find what other detectors cannot.

- The fourth line of defense is a multi-view, multi-energy x-ray examination whose primary function is to ascertain whether there are potential blocks of low-z material that have the critical mass.

- Any or all of the three x-ray systems should be able to automatically detect the possible presence of batteries and wires.

- All systems must alarm if there is a potential for camouflaging, and must alert the operators as to the suspect areas.

- The first generation systems will have substantial problems. There will surely be high false alarm rates that will necessitate hand searches. But these rates will fall with each improvement in hardware and software, and with the integration of each device with the rest. The critical questions are whether the false alarm rates of a mature system will be tolerable and whether the detection probabilities will be high; I predict that the answer to both questions will be yes. I emphasize that the tests for explosives must not only be the conventional ones to determine that the system will alarm when explosives are introduced into "standard" bags, but that the tests include those by a "red" team that is trying its best to defeat the system.

- Alarming luggage should be channeled to one of several possible detectors, including, finally, a hands-on, vapor-detector search of the opened suitcase. CAT scanning to carefully examine a few individual areas of a bag should be available soon. Coherent x-ray scattering to examine suspect parts of a bag, especially "black boxes" that can't be conveniently opened, should also be available in the not distant future.

In sum I believe that we already have sufficient technology to implement a credible security system at or close to the check-in counters. What is required is the early installation and testing, under airport conditions, of each new x-ray system that advances the state of the art of EDS. The testing, improvement and retesting should be a cooperative venture of the FAA, the manufacturer, the airport security people, and an independent testing team who will make the final judgements.

REFERENCES

1. Statement of Billie Vincent: Hearings before the Government Activities and Transportation Subcommittee of the Committee on Government Operations, House of Representatives. September 25, 1989.

2. F. Metzger, Resonance Fluorescence in Nuclei. Progress in Nuclear Physics, Vol. 7, 54 (1959).

3. F. Azjenberg-Selove, Energy Levels of Light Nuclei. Nucl. Phys. A336 (1980) 1; Nucl. Phys. A360 (1981) 1; Nucl. Phys. A375 (1982) 1.

4. L. Grodzins. Nuclear Technologies for Finding Clandestine Explosives. International Conference on the Applications of Nuclear Techniques, Crete, Greece, June 1990, Editors, G. Vouvopoulos and T. Paradellis. World Scientific Press, 1991, pp. 338-360. Nuclear Techniques for Finding Chemical Explosives in Airport Luggage, Nucl. Inst. and Meths. B56/57 (1991) 829-833. Nuclear and x-ray Technologies for Airport Security, MIT Symposium on Technological Measures for Airport Security. April, 1990.

5. Celeste Chang, An Analysis of Factors Limiting the Amplification of Resonance Fluorescence in a Carbon 13 Accelerator Target. Bachelor of Science Thesis in Physics, June 1991.

6. Whitney Edmister, Oxygen Density Measurements Using Nuclear Resonance Fluorescence. Bachelor of Science Thesis in Physics, June 1991.

Table 1

Material	density g/cm^3	μ 40 kev	μ 60 kev	μ 80 kev	μ 100 kev	μ 150 kev	μ 200 kev
sugar	1.6	0.236	0.190	0.174	0.162	0.144	0.133
C-4	1.64	0.235	0.187	0.170	0.159	0.141	0.139

Table 2

E (Mev)	J^{π}	Total Width Γ	Partial width to ground state. Γ_{γ}	σ_o barns	Figure of Merit $\Gamma\sigma_o$ (ev-barns)
Carbon 12					
4.44	2^+	10.8 mev	10.8 mev	634	7
12.71	1^+	18.1 ev	0.35 ev	0.9	16
15.11	1^+	43.6 ev	38.5 ev	29	1300
17.23	1^-	1,150 kev	44 ev	0.001	1150
Nitrogen 14					
2.31	0+	7.2 mev	7.2 mev	156	1
3.94	1+	140 mev	5.5 mev	6.3	0.9
4.91	0-	8.2 mev	8.0 mev	35	0.3
6.44	3+	1 mev	0.7 mev	98	0.7
7.03	2+	0.12 ev	0.12 ev	84	0.8
7.97	2-	2.5 ev	18 mev	0.47	1.1
8.06	1-	30 kev	10.3 ev	0.01	300
8.49	4-	27 mev	5.6 mev	22	0.7
8.62	0+	7 kev	1.2 ev	0.002	15
8.79	0-	460 kev	43 ev	0.001	460
9.17	2+	140 ev	7.3 ev	2.6	360
10.43	2+	33 kev	12.1 ev	0.014	460
Oxygen 16					
6.13	3-	0 .024mev	.024 mev	466	0.01
6.917	2+	95 mev	94 mev	261	25
7.117	1-	54 mev	54 mev	148	8
8.872	2-	3 mev	0.24 mev	13	0.04
9.847	2+	625 ev	6 mev	0.001	0.6
11.52	2+	74 kev	0.61 ev	0.0008	60
12.96	2-	2 kev	0.08 ev	0.003	5.9
13.09	1-	130 kev	32 ev	0.01	1300
13.66	1+	68 kev	8 ev	0.005	340

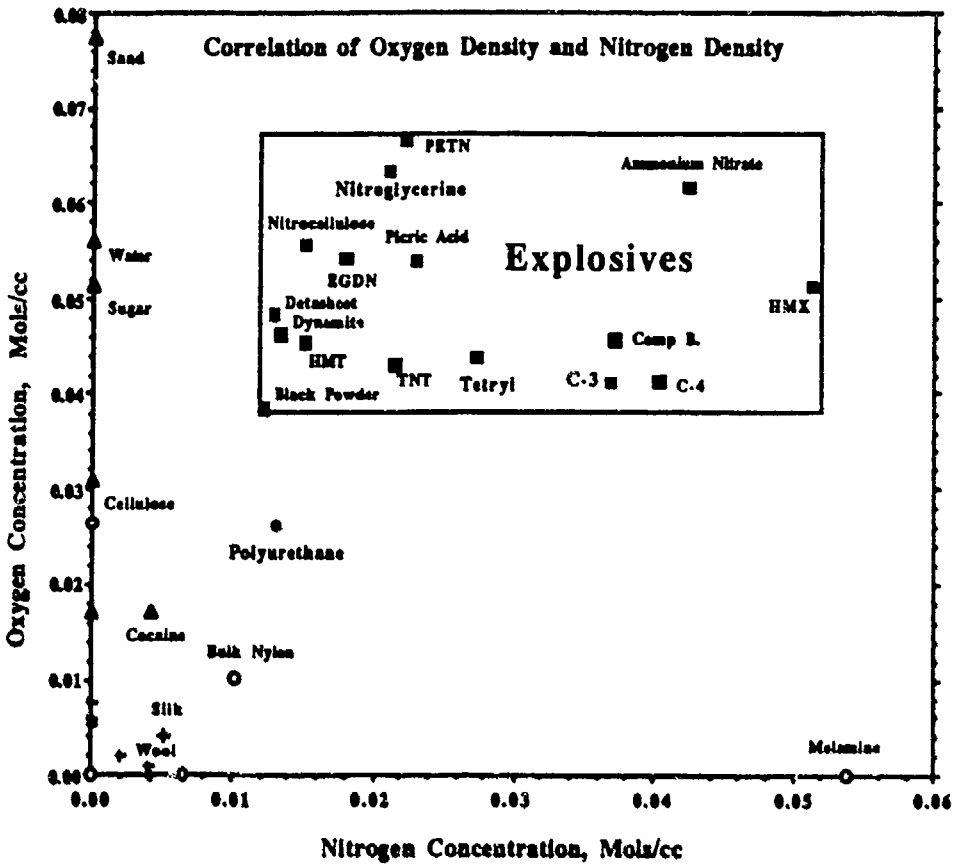


Figure 1. The atomic densities of nitrogen and oxygen are plotted for a number of types of explosives (black squares), clothing (crosses), plastics (open circles), and miscellaneous (open triangles).

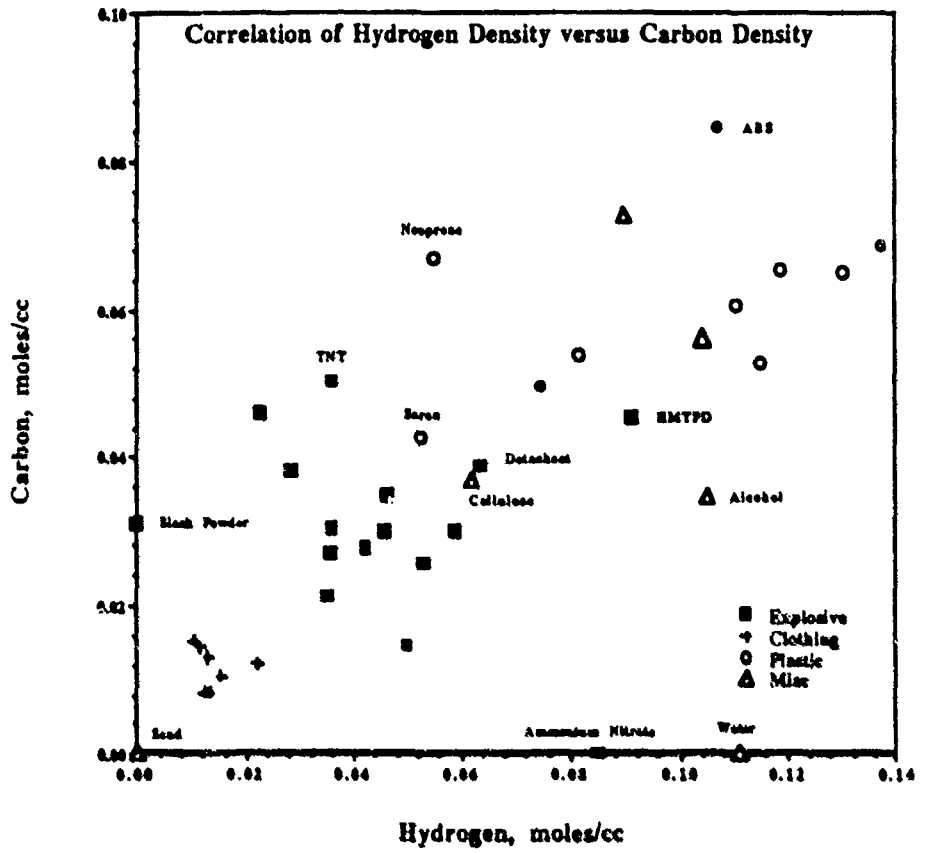


Figure 2. The atomic densities of carbon and hydrogen are plotted for a number of types of explosives (black squares), clothing (crosses), plastics (open circles), and miscellaneous (open triangles).

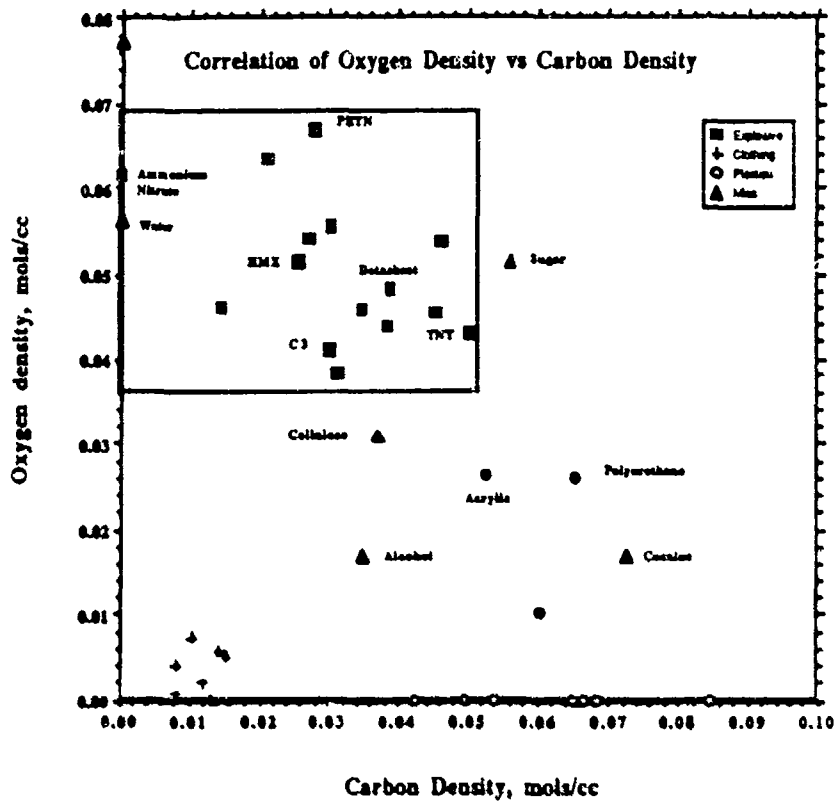


Figure 3. The atomic densities of carbon and oxygen are plotted for a number of types of explosives (black squares), clothing (crosses), plastics (open circles), and miscellaneous (open triangles).

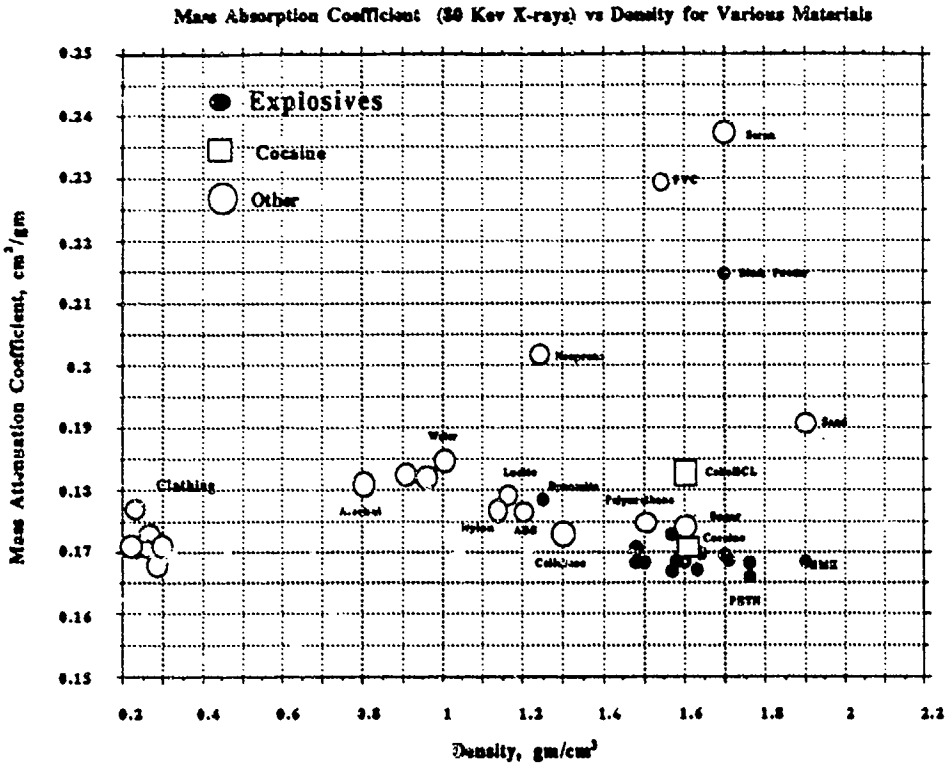


Figure 4. The mass attenuation coefficients are plotted against the density of explosives (black circles) and innocent materials (open circles). Illicit substances (cokeHCl and cocaine, open circles) have μ and ρ similar to explosives.

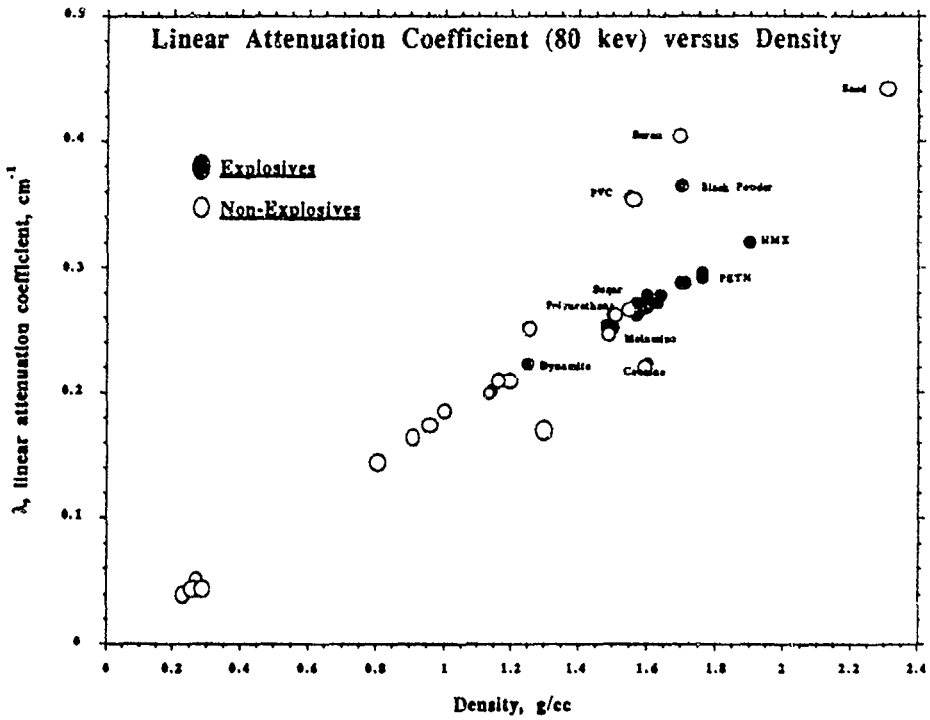
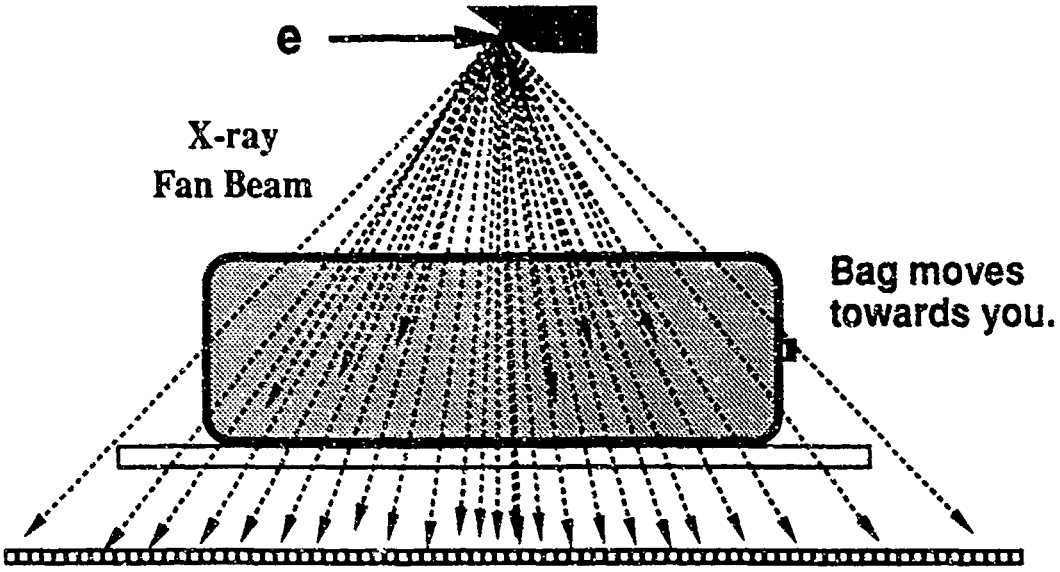


Figure 5. The linear attenuation coefficients are plotted against the density of explosives (black circles) and non-explosives (open circles).



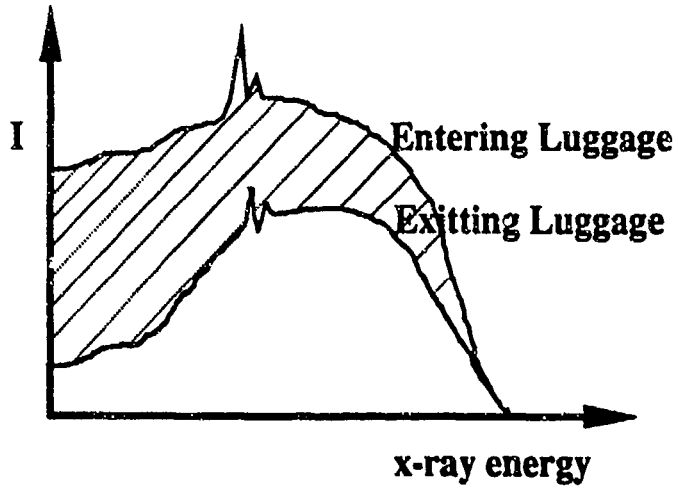


Figure 6. Schematic of a single view, single mean x-ray energy system used for the surveillance of luggage at airports. The lower figure depicts the change in the x-ray spectrum resulting from the absorption in the luggage being investigated.

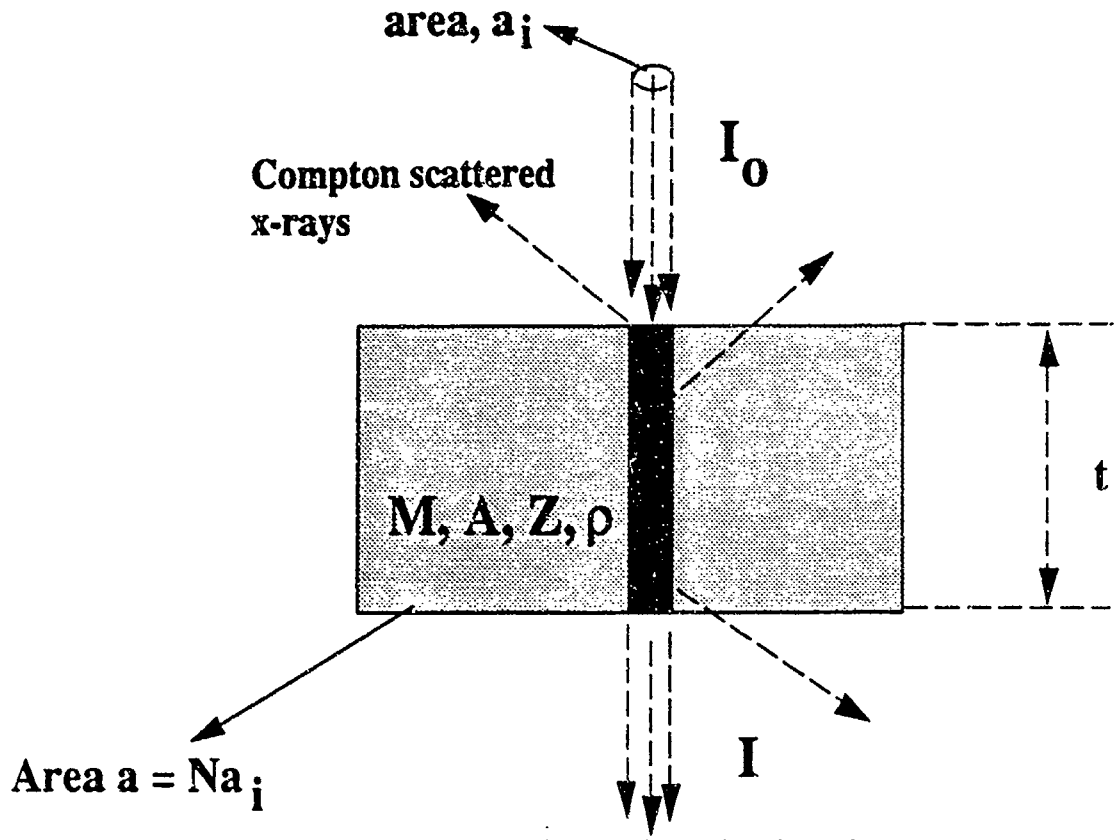


Figure 7. Sketch showing the parameters of x-ray absorption through a rectangular block of uniform material of mass M, density r, thickness t area a, atomic number Z, and atomic weight A. The incident beam flux I_o (photons/cm2/sec) has an area a_i so that there are N = a/a_i pixels covering the block.

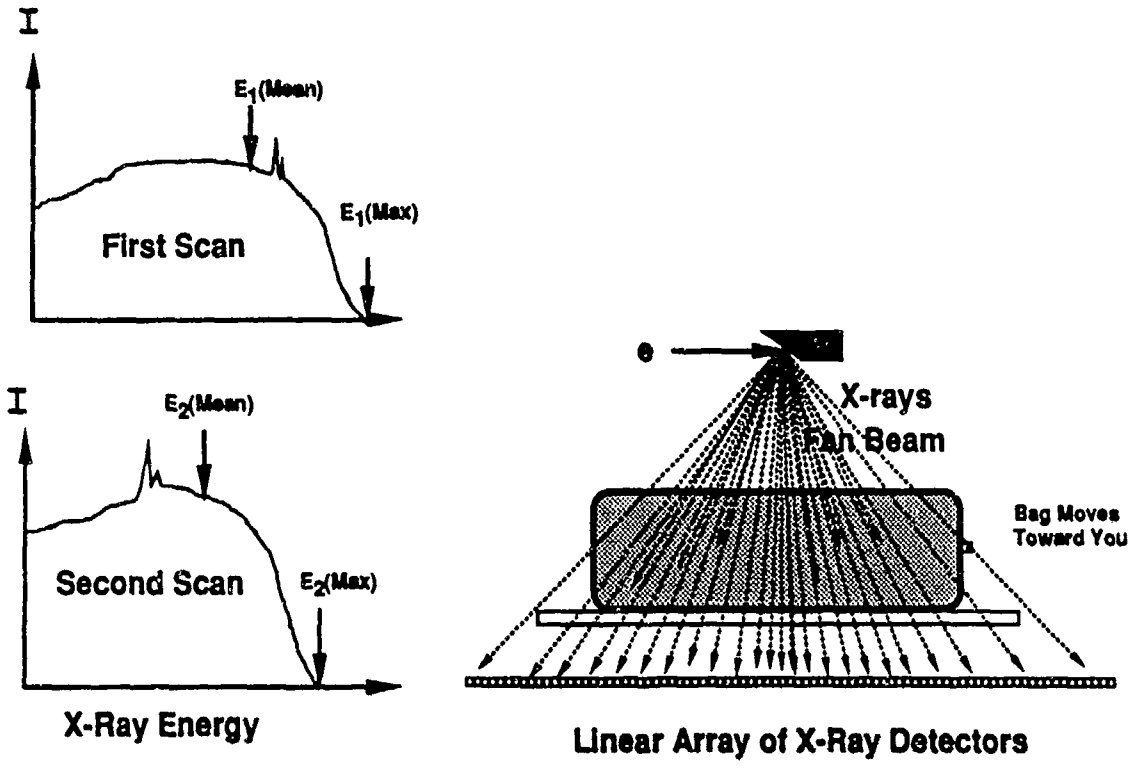


Figure 8. A schematic of a dual-energy system in which the anode voltage and the anode material are both changed to obtain different mean energy spectra.

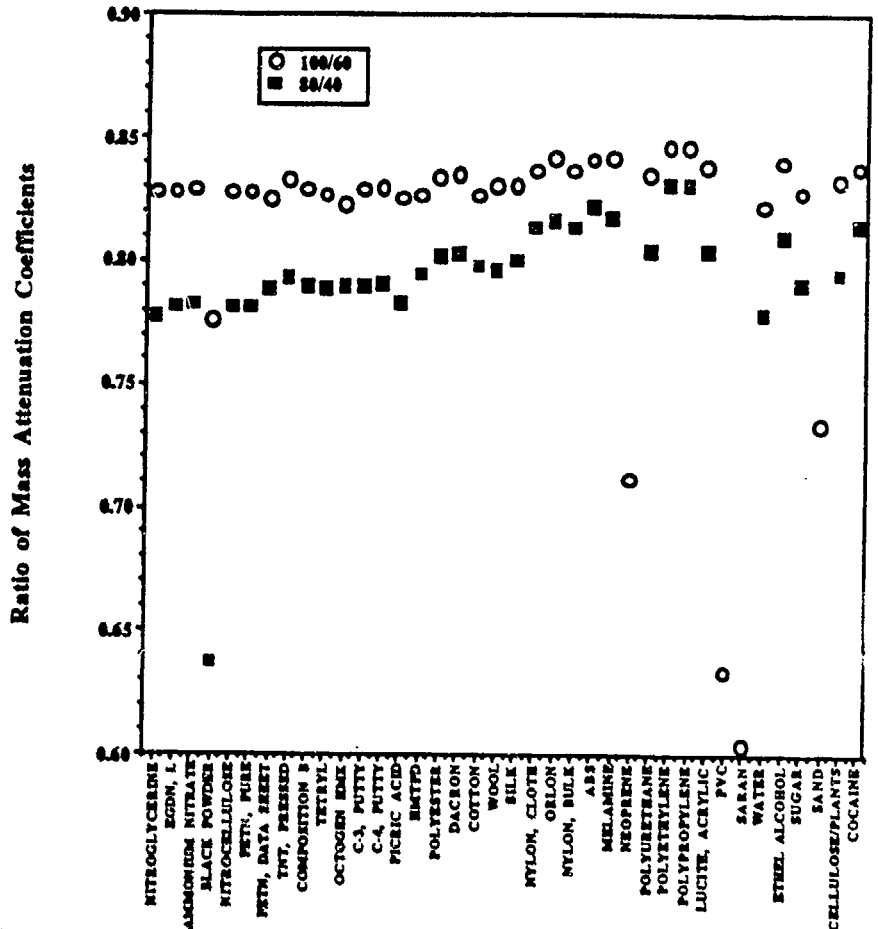


Figure 9. The ratio of mass attenuation coefficients for various materials and for two x-ray energy ratios: 100 kev to 60 kev (open circles) and 80 kev to 40 kev (black squares).

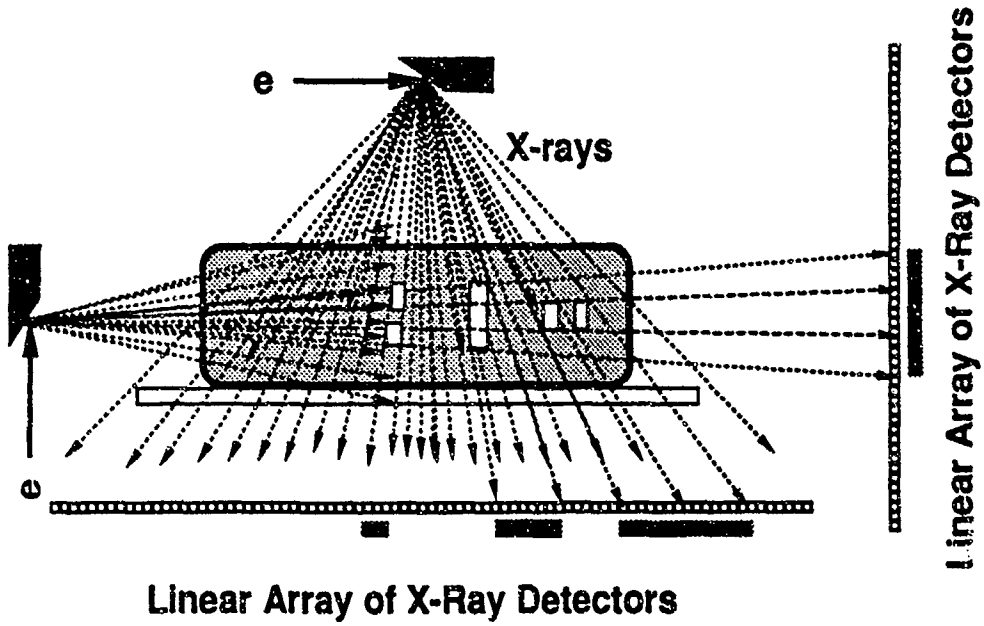


Figure 10 A schematic of a two-view system using two separate x-ray sources and detector arrays arranged orthogonally.

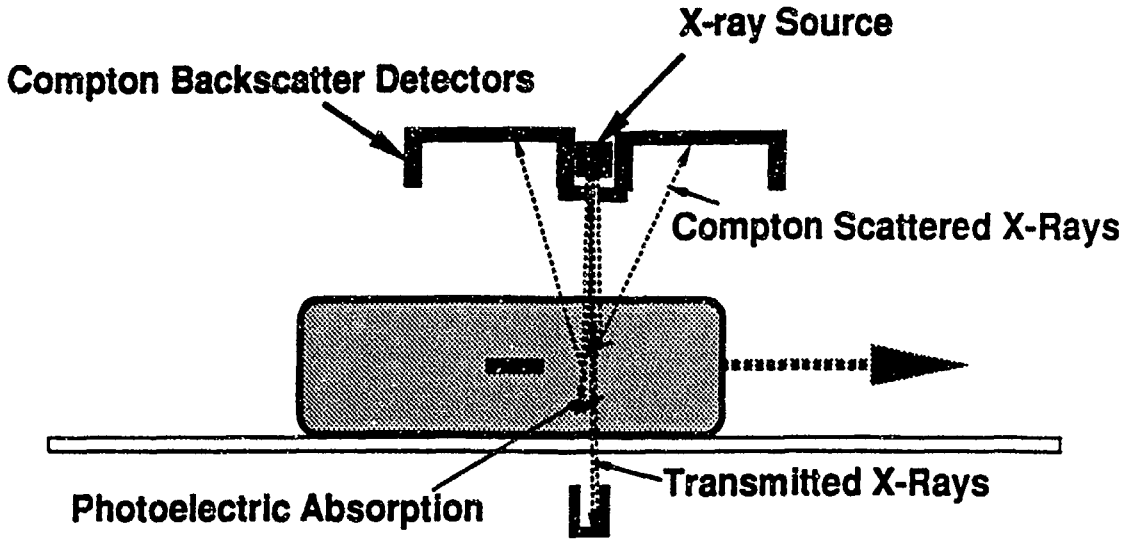


Figure 11. A schematic of the x-ray transmission plus back-scatter Compton method. The x-ray beam is raster scanned perpendicular to the direction of the bag's travel. The x-ray counts in the detectors are registered in time with the beam position to give images of the transmitted and backscattered intensities.

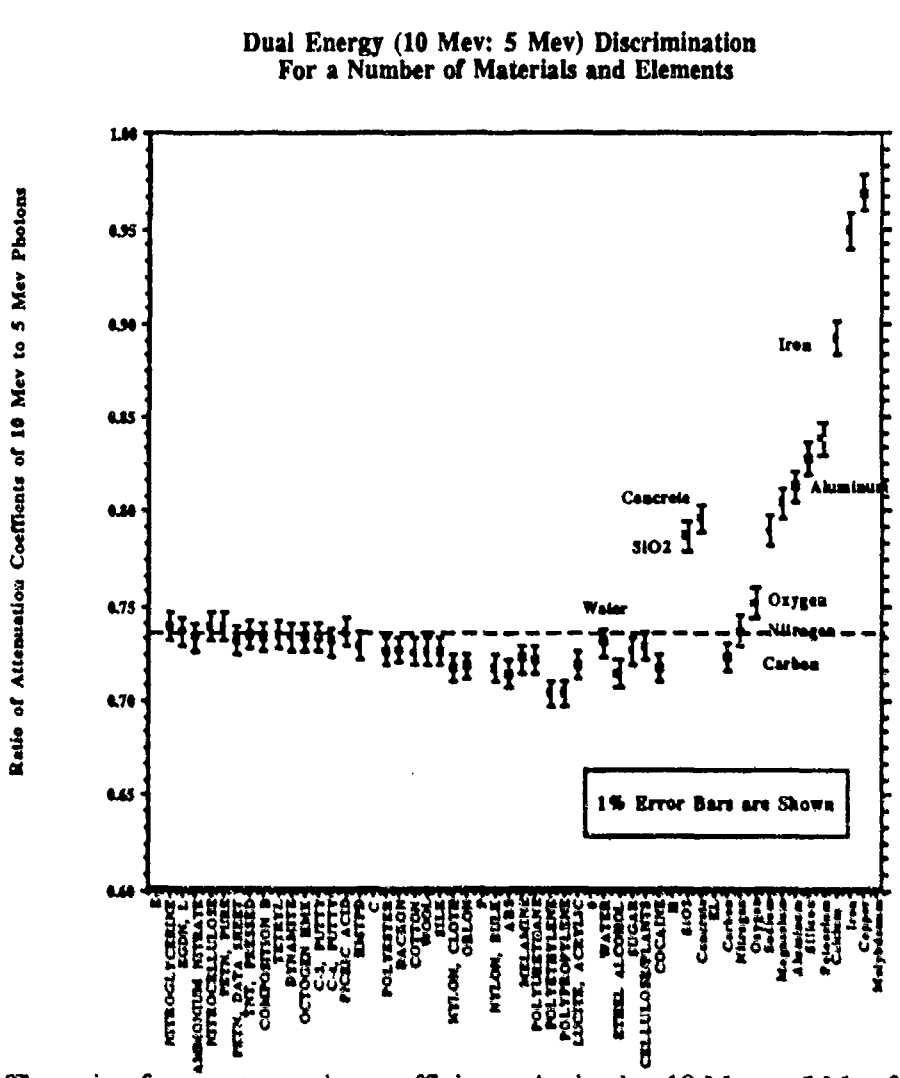


Figure 12. The ratio of mass attenuation coefficients obtained at 10 Mev to 5 Mev for various materials

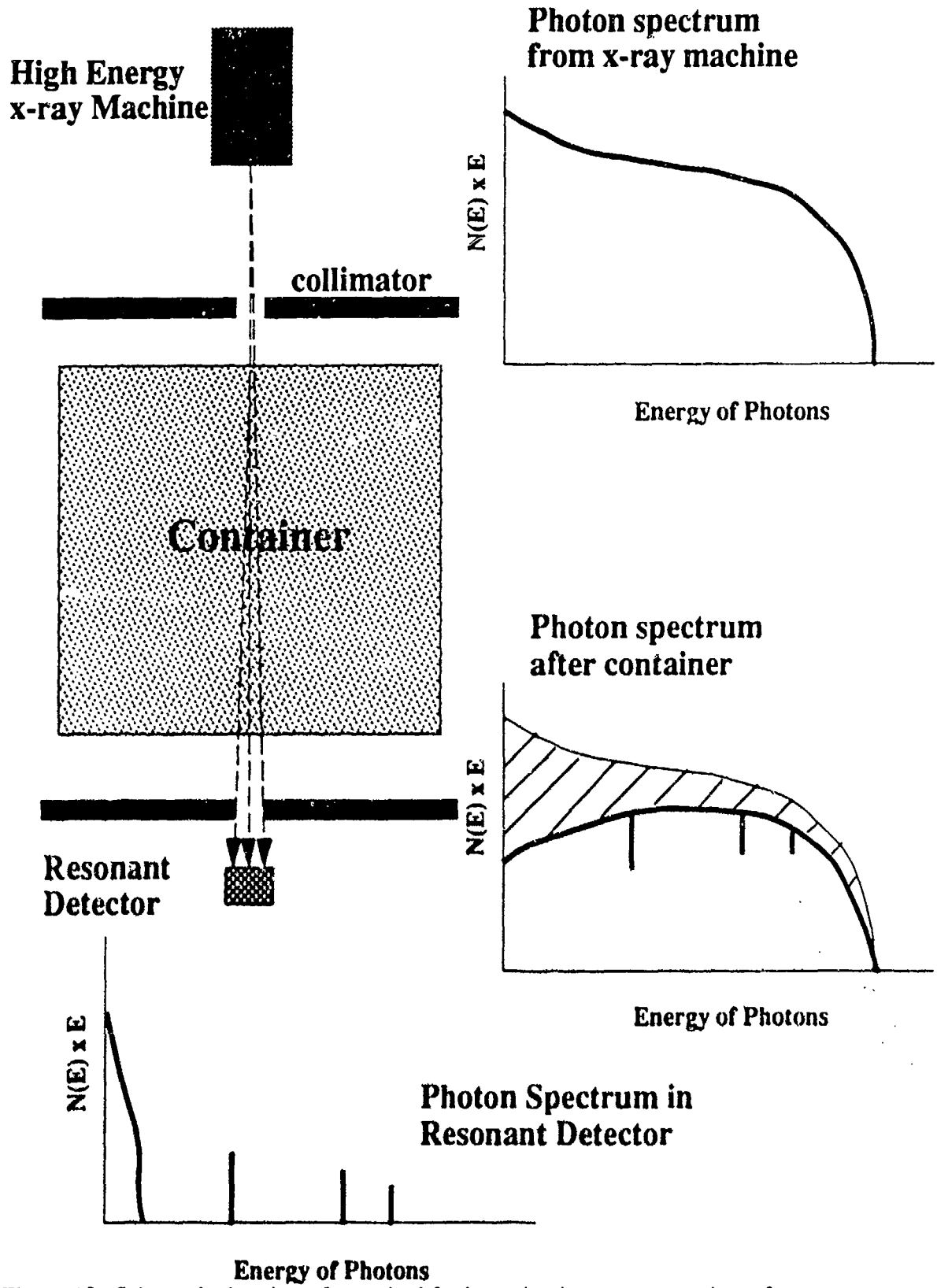


Figure 13. Schematic drawing of a method for investigating cargo containers for explosives and other contraband, using nuclear resonant absorption.

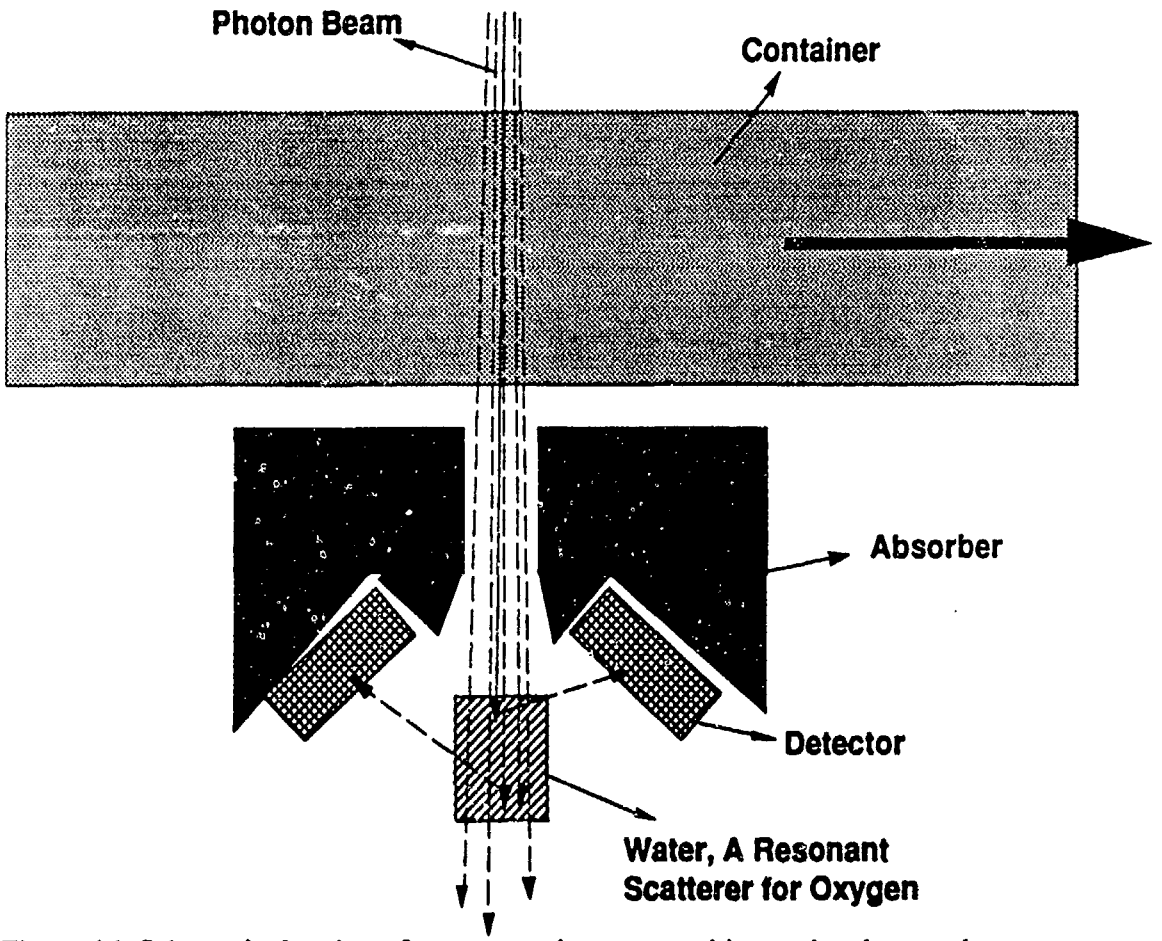
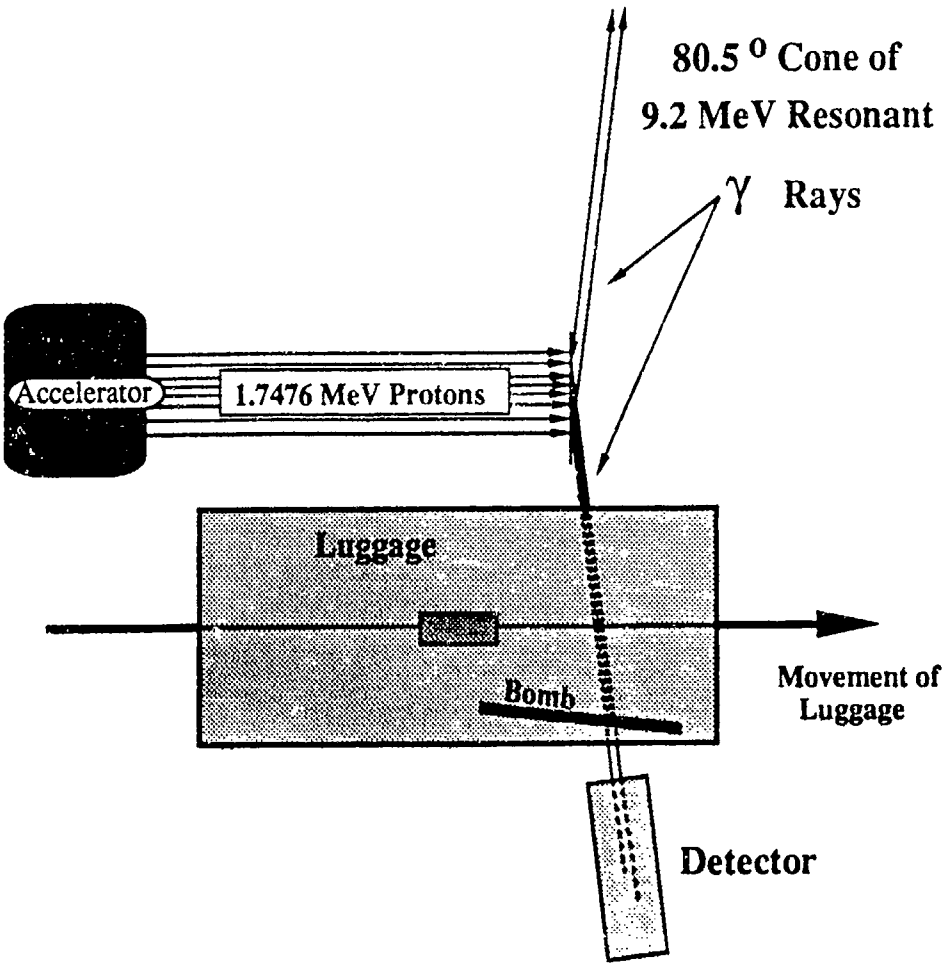


Figure 14 Schematic drawing of a resonant detector sensitive to the photons that can resonantly fluoresce in the scatterer.

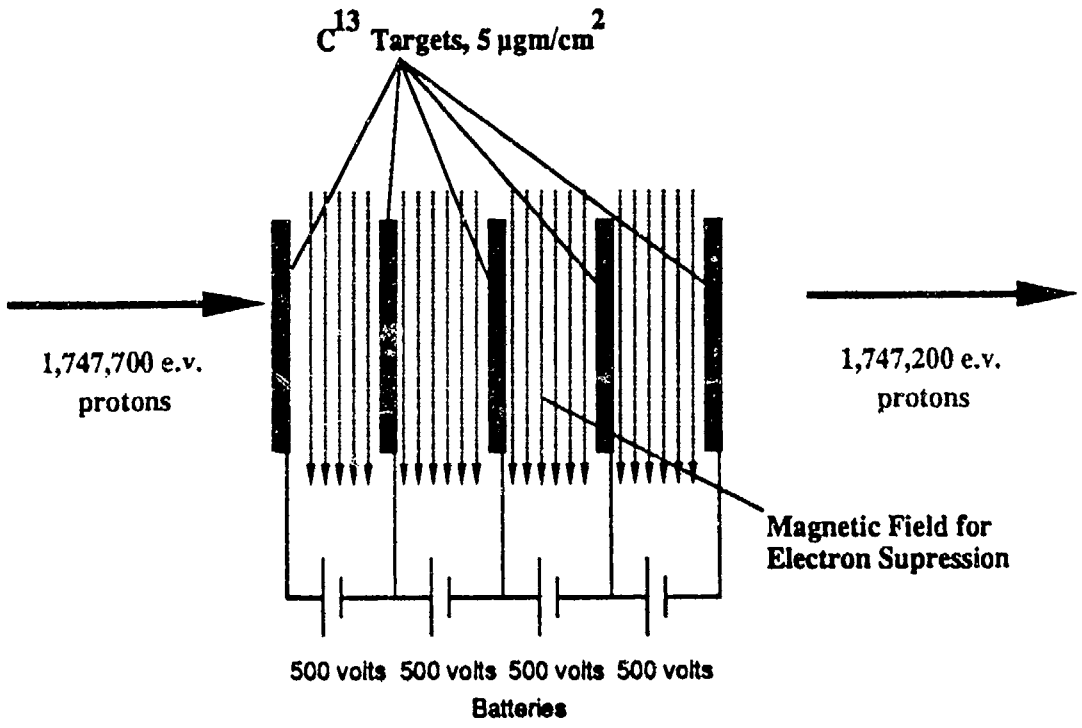


Production: $C^{13} + p \longrightarrow N^{14*} + 9.172\ \text{MeV}\ \gamma$

Resonance: $9.172\ \text{MeV}\ \gamma + N^{14} \longrightarrow C^{13} + p$

$N^{14} + \gamma\ (5\%)$

Figure 15. A schematic drawing of the gamma-ray resonance absorption method using the 9.17 Mev γ-ray of ^{14}N produced by proton absorption on ^{13}C.



Five Component Resonance Target

The Energy Lost in Each Target is 500 electron volts.

Figure 16. An accelerator target for amplifying the yield of 9.17 Mev gamma rays from 14N excited by 1.7 Mev protons.

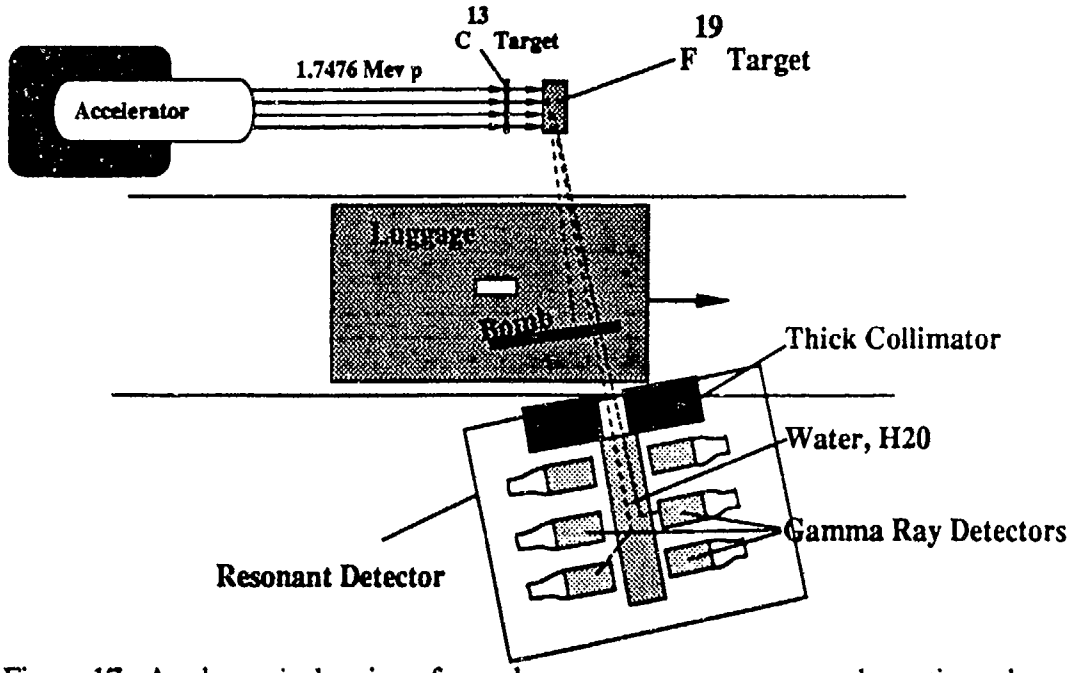


Figure 17. A schematic drawing of a nuclear gamma ray resonance absorption scheme for measuring the oxygen in luggage, using the same accelerator and baggage handling system as used for the Soreq scheme of resonance absorption in nitrogen.

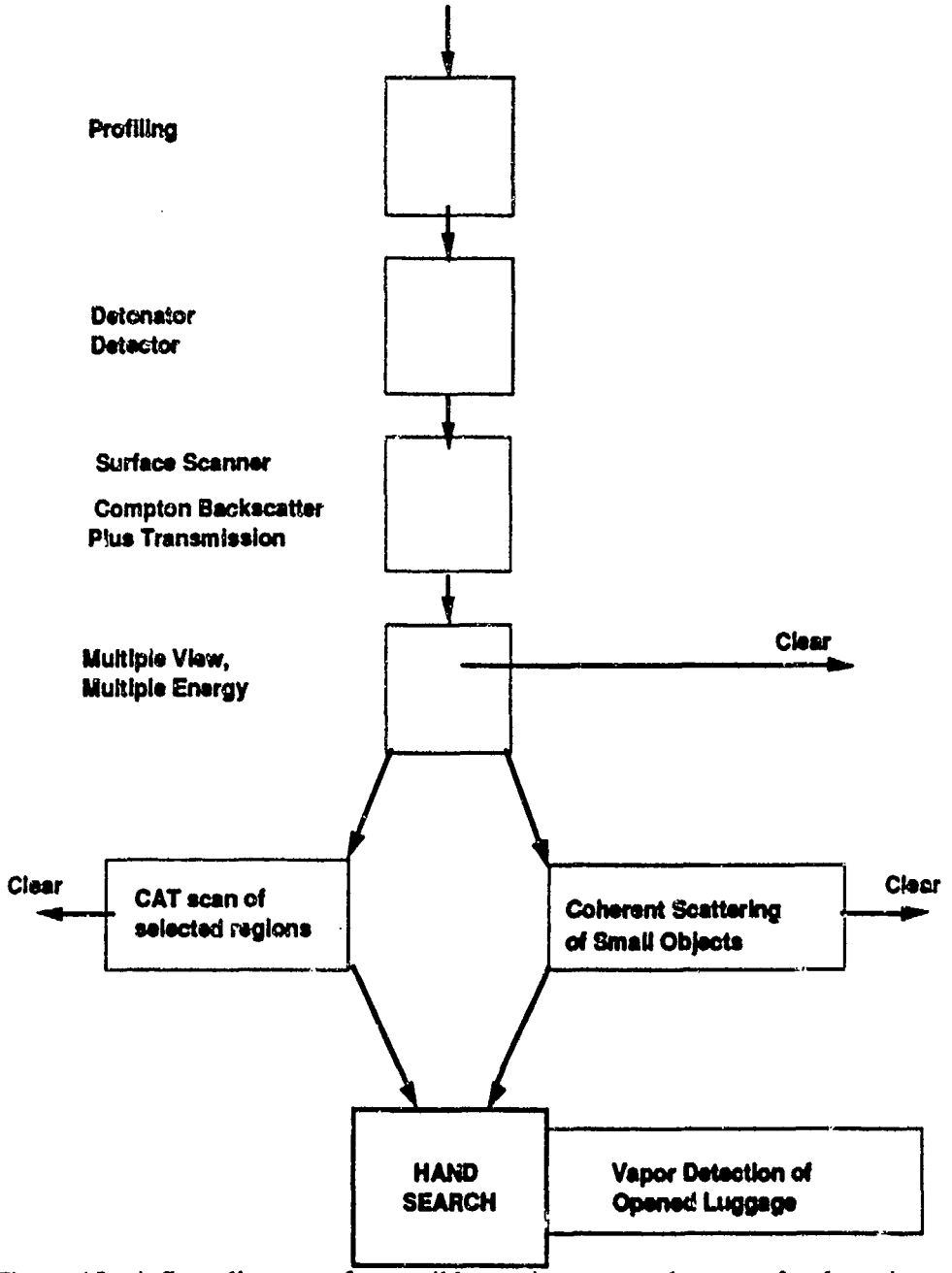


Figure 18. A flow diagram of a possible semi-automated system for detecting explosives in luggage at airports.

THREE DIMENSIONAL X-RAY SYSTEMS AND IMAGE ENHANCEMENT TECHNIQUES

Dr. Max Robinson and Mr. Paul Evans
Nottingham Polytechnic
i2i Vision Limited
Nottingham, England

1. INTRODUCTION

X-ray images are by their very nature difficult to understand. Interpretation of these images is based solely on shape and grey shade information. For most security applications these images are presented on standard video monitors.

Not only do the images usually contain no information concerning 3-D space they are often presented in ways that have paid little heed to the psychology of the human visual system.

Two distinctly different developments are considered in this paper both of which provide x-ray information in ways which make human interpretation an easier task.

2. X-RAY IMAGE ENHANCEMENT

Most security x-ray systems currently in use are capable of providing at least 256 grey levels of information. This is a convenient 8 bits of digital sampling which has become a common standard with which to work. However, a human observer is incapable of discriminating grey level differences with such contrast sensitivity. For example, some security x-ray systems will display 16 grey level bars at start up, ranging from what the display determines as complete black to complete white. Each of these grey level bars consists again of 16 more grey levels giving 256 in all (ie 16 x 16). This extra detail is not readily discernable by a human.

It is not possible to put an absolute figure on the contrast sensitivity of the human eye since so much depends upon the viewing conditions. Even assuming a very liberal figure for this of 1% contrast difference[1] this still only represents a 40% discrimination in 256 levels of grey. Viewing a video monitor in typical artificial ambient lighting may well reduce this contrast sensitivity quite considerably.

In order to present all the grey level information that the machine has detected in a manner that can be discriminated by a human observer a number of image processing routines have been developed. It has been found that no one particular routine is ideal for every image situation, nor in any given situation do all observers favour one specific display. It has also been important to ensure that the operational environment and practices are not unduly altered by using such techniques. In addition, although powerful, digital image processing is employed an operator does not have to be computer literate to operate it. No keyboard exists, but rather a simple operator input device which allows interactive control of the image.

This work has reached the stage where fully operational equipment is available and currently in use at certain security installations in the UK.

3. THREE DIMENSIONAL X-RAY SYSTEMS

Work has been carried out for a number of years on the development of three-dimensional (ie binocular stereoscopic) imaging systems based on closed circuit television cameras. The main application areas of this technology has been in remote control vehicle guidance [2] and manipulator arm control in hazardous environments [3]. Much of the attention in this work has been directed to the development of suitable image sensor packages. Over a period of time, considerable expertise has been built up on the production of novel stereoscopic sensors [4].

As a natural extension of this work and as the result of a requirement by HM Customs & Excise, a prototype stereoscopic x-ray system was produced [5]. This was based on linear array

detectors and is effectively a three-dimensional imaging system using one-dimensional sensors.

In recent years the security industry has become used to using new types of linear array in x-ray screening equipment. Two particular developments are the use of folded arrays for complete tunnel coverage and dual energy sensors for materials identification.

A project is currently under way with the Department of Transport and the Home Office to develop a 3-D x-ray machine incorporating both of these features. A theoretical design has already been produced and work has now commenced on the construction of the machine. Further mention of this will be made in Section 3.6.

In order to put into context the new three-dimensional x-ray system, a brief description of the way in which humans perceive the 3-D world will be presented.

3.1 Three-Dimensional Human Vision

Human beings determine the positions of objects in the real, three-dimensional world via a variety of distinctly different depth cues. Some of these are purely psychological such as interposition, linear perspective and the effects of shades and shadows. In general, it is relatively easy to disguise the reality of a situation when only psychological cues are used. However, a number of powerful physiological depth cues are also available to enable us to determine the relative positions of objects in space.

Prominent amongst these are the linked binocular mechanisms of convergence and accommodation and also monocular movement parallax. The most powerful cue employed by humans over a short range, however, is that of binocular parallax. Simply put, this means that objects at different distances from an observer will have images on each retina having different relative lateral separations. The eyes are capable of discriminating very small variations in this parallax information and translating them into depth information.

3.2 Three-Dimensional Computer Graphics

The computer graphics fraternity have in recent years advertised their products as having a three-dimensional capability. In most instances this has not meant a binocular stereoscopic display. There is now effectively a crisis of terminology because of this. A computer-aided design (CAD) system having a so called three-dimensional display usually means that certain psychological depth cues such as linear perspective and interposition have been introduced. Even with the addition of the effects of shading and shadows, the displays contain fewer three-dimensional depth cues than a broadcast television signal. It is inconceivable that any television station would claim that their current transmissions are three-dimensional.

A few notable exceptions exist, however, where CAD systems do produce full stereoscopic images, but the step-up in computing power necessary to manipulate such an image from that required for a pseudo three-dimensional image is quite considerable.

Caution must be exercised, therefore, when claims of three-dimensional capability are made to establish exactly what combination of depth cues are being presented.

3.3 Three-Dimensional X-Ray Images

X-ray imaging in a variety of forms has become a standard analytical technique in many diverse fields. Prominent amongst these are the multiplicity of uses employed by the medical profession and also the many applications of quality control and assessment used in industrial non-destructive testing (NDT).

In all of these situations, except for a few specific laboratory set-ups, the images produced are two-dimensional in nature. Interpretation of these images, whether from photographic film or more recently from a variety of display monitors, is based solely on flat image shape and grey level information related to the penetration of the particular range of x-ray energies being employed.

X-ray imagery is unique in that many of the usual powerful three-dimensional depth cues that humans are able to extract from two-dimensional images are missing. Examples of these cues are interposition, the effects of shading and shadows, texture gradient and to some extent, linear perspective. Almost all of these cues and others are available, for example, in an ordinary photograph. The difference is that a photograph is produced by reflected light whereas an x-ray

picture is derived from transmitted radiation. This consequent loss of depth cues can, and does, cause serious ambiguities to arise in the interpretation of complex images.

Attempts to overcome this inherent problem with x-ray imagery have in the past involved using bulky equipment, employing tedious operating procedures, and have usually been time-consuming and expensive.

For example, stereoscopic pairs of x-ray plates have been produced by the medical world in the past. They usually require the patient to be motionless for some considerable time whilst each perspective view (left and right) is taken sequentially. Further delays occur before the images may be viewed, usually via a stereoscope, and should any three-dimensional measurements be required, then the use of some kind of stereo-comparator would be necessary.

Pseudo three-dimensional x-ray images are currently derived from standard computer tomography (CT) scanners. These enhanced images are not readily available since they are very computer intensive and consequently costly in their production. They involve the introduction of a number of depth cues into the images by "computer-aided joining together " of a number of CT scan slices. This is obviously an approximation since any irregularity between adjacent slices cannot be seen.

A major departure from all these techniques has been the development of a three-dimensional (ie. binocular stereoscopic) x-ray system based on linear arrays.[5]

In the normal two-dimensional mode of operation a linear array x-ray system operates as follows. A thin collimated curtain of x-rays is derived from an x-ray source and targeted onto the linear detector. Relative movement now between the object to be imaged and the x-ray beam causes an image to be built up when the linear detector electronically scans in synchronism with the speed of object movement. The digitised image information which is captured is then loaded directly into a frame store. The three-dimensional version of this technique can take two forms, either of which are able to acquire a left and right perspective view of the object under inspection during one single pass.

In one configuration two linear detectors and two x-ray sources are used. A more elegant technique, however, is to use only one x-ray source and to derive two collimated beams from it; again two linear detectors are required. The amount of depth perceived in the stereoscopic image by an observer will be controlled to some extent, but not entirely, by this x-ray beam/linear detector array geometry.

Solutions to the problems of manipulating the x-ray intensity information received from two sensors, which are usually scanning different parts of the same object at the same time, and of designing the x-ray beam geometry such that successful reconstruction of real three-dimensional image of an object is possible, have been derived.

3.4 Viewing The Image

The method selected for observing the three-dimensional x-ray image is known variously as the time division or field sequential type of display. The technique takes advantage of the interlace facility used in normal video displays and the short retention memory capability to visual stimuli of the human eye/brain combination. Left and right perspective views are displayed sequentially on the monitor screen whilst the observer views that image through liquid crystal glasses which are switching, transparent and opaque in synchronism with the display. The speed of switching is at twice the standard video rate and so a solid 3-D image without any perceived flicker is observed. An alternative method used has been to place an active liquid crystal plate in front of the monitor screen and then to view the image using polaroid (circularly polarized) glasses. The left or right two-dimensional image can also be viewed in this way.

Two interesting and useful phenomena have been observed. Firstly, since normal x-ray images contain very few, if any, depth cues, it has been shown that by altering the phase of the viewing glasses (ie. presenting left eye information to the right eye and vice versa) a three-dimensional view of the object from the opposite side may also be obtained. Quite simply one may observe the three-dimensional image of the object from the position of the x-ray source, or alternatively the position of the linear detectors. This is possible since the only depth cue being presented is binocular parallax. This technique would not work with a stereoscopic

image derived from television cameras since other conflicting depth cues would also be presented.

A second useful artefact of the images is an apparent pseudo-movement parallax. Normally, movement parallax manifests itself as an increased movement of foreground object relative to background when an observer moves laterally with respect to a scene. In stereoscopic images an "apparent" greater movement of the background occurs. This can be used as a powerful depth cue especially for complex images. Other effects are also possible such as electronically "shifting" the image in and out of the monitor screen. This technique ensures that the complete stereoscopic depth of field is utilised.

3.5 Measurement in Stereoscopic Displays

A technique has been developed for measuring x, y and z coordinates in stereoscopic video images [6]. The method uses measuring markers inserted into the left and right perspective views. The disparity information obtained in this way of conjugate points in each image is a measure of the z-coordinate. It is necessary to calibrate the system initially in order to eliminate distortions in the display due to geometrical misalignment, the electron optics of the display and the inherent distortion due to point source illumination in an x-ray image.

The calibration technique [7] is a derivation of tried and tested methods used in standard close-range photogrammetry.

Each individual pixel separation in a display between left and right conjugate points gives rise to an individually resolvable depth plane. In a correctly constructed image this number could be quite large. Consequently, images are produced with a considerably higher density of depth planes than would be obtained from the normal use of a CT scanner. This occurs in a matter of a few seconds without the need for expensive computing equipment.

3.6 Latest Developments

As stated previously, a new generation of 3-D x-ray machine is under construction which is aimed primarily at security applications.

Particular problems associated with the use of folded-array, dual-energy linear sensors have been identified and specific solutions have been proposed. A continuing theme throughout the development presented in this paper has been the importance of displaying x-ray information in ways which are conducive to accurate human interpretation.

To this end, new techniques of depth plane isolation based on perspective subtraction are to be investigated. It has already been shown by the authors that images can be produced having a high visual impact which are not unlike edge illuminated microscopy displays. This is a well known technique for enhancing 3-D surface features. A dynamic sequence of such images which effectively peels away depth planes in the stereoscopic image has also been shown to be possible. Using the organic/inorganic discrimination of this new machine it is proposed that volume estimations of objects will also be possible.

The results of the work which is supported by the UK Department of Transport and the Home Office will be reported in due course along with information relating to trials of the equipment in a real operational environment, possibly an airport.

REFERENCES

(1) Freeman M H Optics (10th Edition) Ch 10, Butterworth Press (1990) ISBN 0-407-00530-7

(2) Robinson M, "Remote Control Vehicle Guidance using Stereoscopic Displays", Proc US Human Factors, Vol 28 1984 p 809.

(3) Robinson M, "Three-dimensional Vision for Bomb Disposal", 8th Int Conf Special Equipment for the Police, INTERPOL HQ Paris, 1983.

(4) Robinson M, Shuttleworth P, "The Development of Stereoscopic Vision Systems for Use in Hazardous Environments" Proc Int Symp Teleoperation and Control, The Ergonomics Society 1988, pp 191-195.

(5) Robinson M "Three-dimensional Visual Screening System", British Patent Application No 8623196, Sept 1986.

(6) Robinson M, Sood S C, "Calibration and Depth Resolution of a Stereoscopic Video Display", SPIE Vol 402, 1983, pp 162-165.

(7) Robinson M, Ariyaeeinia A M, "An Active Coordinate Imaging System for Robot Vision", SPIE Vol 657, Applications of Artificial Intelligence, 1986, pp 144-151.

AN EXPLOSIVE DETECTION SYSTEM FOR SCREENING LUGGAGE WITH HIGH ENERGY X-RAYS

Jerome R. Clifford, R. Bruce Miller,
William F. McCullough, and Kerry W. Habiger
TITAN Spectron
Albuquerque, NM 87106

1. INTRODUCTION

Since the downing of Pan Am Flight 103 over Lockerbie, Scotland, on December 21, 1988, the airline community has been searching for a technology that can detect a terrorist device with less than one pound of high explosives. The search has focused on an explosives detection system for checked baggage which has more sensitivity and less false alarms than the thermal neutron activation technique, which was designed for a 2.5 pound TNT threat. The techniques explored, including vapor detection, x-ray systems, electromagnetic and nuclear techniques, have attempted to identify explosive materials by their unique combination of elements, their densities or their chemical structures.

TITAN has developed an explosives detection technology that relies on the unique combination of nitrogen density and physical density within most commercial or military high explosives. Explosives which have been used by terrorists have nitrogen densities between 0.15 and 0.60 g/cm^3 and physical densities between 1.2 and 1.8 g/cm^3. Figure 1 compares the characteristics of bulk explosives with common plastics and other high-nitrogen concentration materials. Of the most common materials, including foodstuffs, fabrics, plastics, organic compounds, and drugs, only solid polyurethane and melmac have physical densities and nitrogen concentrations similar to explosives.

Our EXDEP technique measures the nitrogen concentration of materials on a per unit-volume basis. Together with a conventional x-ray scanner to measure the physical density, an EXDEP-based system will detect bulk explosives with a high probability and very few false alarms.

This paper focuses on the EXDEP technique and the experimental results which show the capability to detect explosives, to image the explosives, and to discriminate explosives from other materials. The accompanying paper, "Explosive Detection for Checked Luggage by DETEX, a Combined X-ray and Positron-Tomography System" by Hans Pongratz of MBB (Germany), presents details on an EXDEP-based explosives detection system and shows simulation results for detection of sheet explosives using a combination of EXDEP and standard x-ray.

2. THE EXDEP CONCEPT

The EXDEP concept is shown schematically in Figure 2. A radio frequency linear accelerator (RF LINAC) is used to produce an electron beam with an energy of 13.5 MeV. The electrons strike a tantalum or tungsten target and produce bremsstrahlung radiation with a maximum energy equal to the electron beam energy. The x-rays interact with the explosive and activate the nitrogen via the photoneutron (γ,n) reaction. The stable nitrogen isotope ^{14}N thus becomes the radioactive isotope ^{13}N, which then decays with a 10-minute half-life via positron emission to ^{13}C. The positron immediately slows down and annihilates, producing two coincident 511-keV photons that are oppositely directed. These photons are easily detected and counted in coincidence using standard scintillation detectors.

The high-energy bremsstrahlung photons from the accelerator penetrate easily through most materials and, therefore, are excellent probes for inspecting luggage and cargo. The bremsstrahlung photons are attenuated significantly only by Compton scattering and pair production. The 10-15-MeV photon attenuation coefficients range from 0.018 cm^2/g for low-Z elements (C, N, O, Al) to 0.030 cm^2/g for Cu. Assuming that luggage contains mostly low-Z elements and that the bulk density is 0.2 g/cm^3, the 1/e attenuation length for the illumination photons is 2.8 m. The attenuation through 75 cm of luggage is less than 27%.

The positron range is typically only a minor factor in determining the resolution that is possible with

EXDEP. The positrons produced in the decay of the activated elements lose energy primarily through inelastic collisions. Their range in g/cm^2 is approximately half their energy in MeV; and typical positron energies are only about 20-58% of these values. Thus, a positron from the decay of ^{13}N travels at most 3.75 mm in the explosive before annihilation with an atomic electron. The same positron travels at most 3 cm in clothing and 4 m in air. For a 3-mm thick piece of detasheet explosive with a large surface-to-volume ratio, a small fraction of the positrons will escape the explosive. For those positrons that escape the explosive, however, the positions where the annihilations occur are dispersed throughout the luggage and no one source produces sufficient activity concentration to be detected as a false alarm.

The 511-keV photons which result from the annihilation of the positrons are attenuated by photoelectric and Compton scattering interactions, but most of them will escape from the baggage and be detected. Most luggage items contain low-Z elements with an attenuation coefficient of 0.087 cm^2/g and average bulk densities of 0.2 g/cm^3, which gives a 1/e attenuation length for the 0.511 MeV photons of 58 cm. A book or large report has significantly greater attenuation due to the larger bulk density. For example, a 5-cm thick report attenuates the annihilation photon flux by almost half. It would take a 0.8-cm thick steel sheet to obtain the same reduction. The attenuation of the annihilation photons is the most important limitation in the EXDEP performance. Calculations including these attenuation factors and experiments with buried mock explosives, which will be described in subsequent sections, show that EXDEP should effectively detect explosives in luggage in spite of this limitation.

3. EXPLOSIVES DETECTION RESULTS

We conducted three sets of experiments to show that the EXDEP technique is effective at detecting concealed explosives. The first was a proof-of-concept experiment performed by TITAN using the RF LINAC at Lawrence Livermore National Laboratory (LLNL). A second set of experiments was done at the 90° port of the DOE LINAC operated by EG&G at Santa Barbara, California, to benchmark the model and calculations. Finally, a third experimental series was done at the Naval Research Laboratory LINAC in Washington, DC, to obtain improved experimental results necessary for the design of a portable system. These efforts were sponsored jointly by Sandia National Laboratories (SNL) and the Defense Advanced Research Projects Agency (DARPA).

Under the SNL and DARPA programs, TITAN designed and built a portable LINAC for testing against mock land mines. The LINAC uses a Varian Linatron 6000 centerline and electron gun and a Thompson 6.5 MW klystron. Figure 3 shows the accelerator mounted in TITAN's laboratory, with a cart containing sand and a mock mine in the illumination position. The LINAC produces a 13.5 MeV beam with peak current of >200 mA and a pulse width of 5.8 μs at a pulse rate of 200 Hz.

For safety reasons, a mixture of melamine and glucose was used to simulate TNT explosive; the elemental composition was essentially the same. The mock explosives were buried a few inches deep in silica sand and peat. The sand is reasonably free of trace elements, consisting primarily of silicon and oxygen. Since both of these elements have very high (γ,n) thresholds, essentially no activation was anticipated when the electron beam kinetic energy was kept below the oxygen activation threshold of 15.8 MeV. The peat, on the other hand, is rich in organic matter and trace minerals which give measurable background signals. The primary experimental objective was to demonstrate that the EXDEP photon activation technique can detect the explosive within a background resulting from (γ,n) reactions in common elements. The soil also provided for attenuation of the 13.5 and 0.511 MeV photons.

The mock explosive targets were mounted on a carriage assembly whose position was remotely controlled using a constant-velocity motor. A sketch of this experimental geometry is shown in Figure 4. The cart/explosive was stationary in the beam during irradiation, after which it was moved down the track and in front of the detectors. The cart was moved to the detector location at ~1 mph, such that the delay between irradiation and detection was typically a few seconds.

A single 258 cm^2, 1.27-cm thick bismuth germanate scintillation detector was used for the following tests. BGO was selected because it is not sensitive to neutron activation, whereas NaI(Tl) crystals are. The detector had an energy resolution of 19% at 511 keV. The scintillation detector was located ~3 m from the beam line and 0.3 m from the sand surface. A ^{22}Na

radioactive source was used to calibrate the detector and electronics.

Following illumination of the sand and mock explosive, both multi-channel and single-channel data were taken. Figure 5 shows a typical multichannel-analyzer spectrum of the mock explosive; the 511-keV photopeak stands clearly above the background photons from other decay processes. There are no extraneous gamma peaks from the target which could give spurious background contributions. The single-channel-analyzer data, with the window set for the 511-keV photopeak, were taken to count the annihilation photons.

With the detector's low background, the measured signals from the explosives were clearly and consistently observed above the soil background. Figure 6 shows the number of counts verses time after illumination for a 1.5-kg and 9.2-kg TNT mock explosive surface-buried in sand. The explosives were illuminated with x-rays from 30 μC of charge deposited on the converter. The count times were 10 seconds per data point. Figure 7 shows a similar plot for data from the NRL experiment with the 1.5-kg mine buried at up to 2 inches in sand.

These data verify that EXDEP can detect concealed explosives using only crude collimation. The two questions which remain for luggage inspection are: Can a small quantity of explosives be detected in the background of a suitcase? Can the explosive be distinguished from the myriad of objects found in a suitcase? We will examine these questions next.

4. IMAGING OF EXPLOSIVES

EXDEP has excellent resolution because the two oppositely-directed, coincident, 511-keV photons are counted simultaneously. The explosive lies on the line between the two detectors measuring the event. As many nuclei decay, there are multiple lines that intersect at the explosive's location, as shown in Figure 8. The positron range (the distance that a positron travels before annihilation), Compton scattering of the annihilation photons before exiting the baggage, and uncertainty in the location of the photon interaction within the detector crystal blur the image somewhat, but the resolution still remains about one centimeter. This type of imaging, called positron emission tomography (PET), is used routinely in modern medical diagnostics.

To demonstrate the imaging capability of EXDEP, we did a series of four tests using the UGM PET camera at the University of Pennsylvania Medical Center. While this PET camera is not designed for our application, it did provide good evidence that PET imaging would be effective. Based on previous experiments, a half-kilogram of TNT illuminated with x-rays from a 1-mA beam at a luggage throughput rate of 30 bags per minute should produce an activity of 0.9 μCi over 300 cm^3 or 3.0 x 10^{-3} μCi/cm^3. Therefore, we used 0.1-μCi point sources of ^{22}Na and a solution of ^{68}Ga in water diluted to 6.8 x 10^{-4} μCi/cm^3 to simulate the distributed activity from the illuminated explosive.

In one test, three 0.1-μCi point sources were placed 5 cm apart near the center region of the camera. Figure 9 shows the raw data (in sinograph format) for four slices through the volume containing the ^{22}Na sources. The data was collected for a 20-sec count time. The resolution for the data appears to be approximately 1 cm.

In another test, a 0.1-μCi point source was immersed within the water solution containing 1.7 μCi of ^{68}Ga. The beaker had a 9-cm radius and a 10-cm depth and contained 2500 cm^3 of water. The count time was 20 seconds. This is equivalent to counting a 2.3 x 10^{-3} μCi/cm^3 source for a 6-sec count time, which is very close to the activity we expect in the explosive. Figure 10 shows the raw data (in sinograph format) for six slices across the beaker. The activity shown in the last slice is decreased because the slice includes a smaller cross section of the beaker. The 0.1-μCi point source is also visible in the distributed activity in the fourth slice.

These experimental results clearly demonstrate that the activity levels which we expect to produce using the EXDEP accelerator are observable using a PET camera. Moreover, the linear resolution that is achievable is approximately 1 cm, which should be sufficient to detect sheet explosives.

The excellent resolution achievable with EXDEP directly reduces the false-alarm rate of a system. With low resolution, e.g., the 1000 cm^3 that is achievable by collimation in TNA, only an average nitrogen concentration in a given volume is measured. A volume containing a large cheese may give the same count rate as a volume containing a small explosive and some cotton clothing. With high resolution, e.g., the 1 cm^3 with EXDEP, the nitrogen concentration of individual items are measured over

a small enough volume to distinguish explosives from most other nitrogenous materials.

From our experimental data and our EXDEP model, we have estimated the count rate that a high-efficiency PET detector system might encounter. Assume that 1 kg of TNT (nitrogen concentration equals 0.18) is located in the center of a typical suitcase with dimensions 30 cm x 60 cm x 75 cm and a mass of 30 kg. Using an average absorption coefficient for 10-15 MeV photons of 0.02 cm^2/g gives a 14% attenuation. If the bags pass on a conveyor through a 1-m^2 tunnel at 30 cm/sec, the throughput past the illuminator is 60 bags/min. If the LINAC operates at 14 MeV with an average current of one milliampere and the irradiation coverage is over A = 100 cm x 30 cm = 0.30 m^2, then the total number of activated ^{13}N atoms created in the explosive is

$$N_{13} = 2.4 \times 10^7 \text{ atoms} \quad (7)$$

For an array of NaI(Tl) scintillation sheet detectors located around the conveyor belt, the average detector solid angle coverage is 4.2 sr, and the crystal efficiency is 0.7. Ten seconds following the irradiation of the 1-kg explosive, the coincidence count rate from the activated ^{13}N atoms in the explosive is

$$C_c = 1345 \text{ cts/sec} \quad (8)$$

Assuming that the explosive is a simple cube approximately 8.5 cm on a side, then the count rate per unit volume is C_c = 2.0 $ct/cm^3/sec$. For the 10 seconds that the bag is in the detector array, each cubic centimeter of the explosive will produce 20 cts. The count rate is low enough that the detection electronics will not be saturated, yet high enough to be detectable.

5. DISCRIMINATION OF EXPLOSIVES

The relatively low nitrogen photonuclear activation threshold energy at 10.6 MeV and the subsequent ten minute half-life positron decay is a unique combination which makes it possible to discriminate explosives from other items. Most other elements common in luggage have photonuclear reaction thresholds above 13 MeV, produce no positron, or have very short or very long half-lives. Those few elements which do react similarly to nitrogen, and thus could contaminate the nitrogen signal, have different activity concentrations or densities which distinguish them.

Since the nitrogen in the explosive has a photoneutron threshold which is substantially lower than that of the most common elements, proper adjustment of the electron beam energy allows activation of the nitrogen in the explosive without activating the nuclei of most of the surrounding materials. This is shown schematically in Figure 11, where the bremsstrahlung spectrum is overlaid on the cross sections for nitrogen, oxygen, and aluminum. Tuning the accelerator can maximize the overlap of the bremsstrahlung spectrum with the nitrogen cross section while minimizing the overlap with other elements. Calculations and experiments have shown that the best nitrogen-signal-to-background ratio is achieved when the electron beam energy is around 13-14 MeV.

The limited number of isotopes which are detectable for the EXDEP technique are shown in Table 1. Fourteen elements are identified in the "Atlas of Photonuclear Cross Section Obtained with Monoenergetic Photons" (Ref: Atomic Data and Nuclear Data Tables, Vol 38, No 2, March 1988) as having photonuclear thresholds below 13 MeV and producing a positron decay. The rare earths (praseodymium, samarium, and erbium) are not present in any significant amount in luggage. The metals (nickel, copper, zinc, gallium, zirconium, molybdenum, and silver) have mass densities which distinguish them from nitrogen. Moreover, the reaction cross section, density, and half-lives of these metals make the activity concentration significantly higher than that for nitrogen. Fluorine is found in trace amounts except for the compound teflon, which has a density of 2.2 g/cm^3. Phosphorus, chlorine, and bromine are elements which would not be expected in luggage and, if found, should indeed be identified as potentially hazardous.

Figure 12 shows on a log plot the activity concentrations vs physical density expected for various benign items containing those isotopes identified as EXDEP detectable, i.e., items containing copper, zinc, silver, nickel, and fluorine. None of the items overlap the explosives. Therefore, these potential false alarms are in fact easily discernible. There may be items in luggage that contain combinations of these isotopes which would make them look like explosives, but we have not been able to identify any. Empirical examinations of

checked luggage using EXDEP will determine if there are many such false-alarm targets.

Consider a [illegible] cm x 60 cm x 75 cm piece of luggage. It would be imaged using the EXDEP detector system into 135000 individual cubic centimeter cells. From the previous model calculations, a TNT explosive would produce 20 counts in a 10 sec count interval if there were 50% attenuation for each annihilation photon. If there were 10% attenuation, then the TNT would produce 65 counts in the same time. A 1-lb piece of TNT would occupy 275 cells. Ten pennies in a cell would produce almost 800 counts in the same time interval with 50% attenuation and 2600 counts with 10% attenuation. The background count rate per cell is less than 1 count per 10 sec.

For a suitcase with pennies, a brass ring, a piece of sterling silver jewelry, and 1-lb TNT explosive, a histogram of the counts might look like Figure 13a. A two-dimensional slice through the bag may look like Figure 13b, where the gray scales correspond to the counts. Either representation clearly shows the presence of the explosive.

6. RADIATION ISSUES

The bremsstrahlung radiation dose rate at 1 meter from the accelerator converter is given by

$$D(\text{rads/sec}) = 1.1 \times 10^{3} [V(\text{MeV})]^{3} I(A) \qquad (1)$$

where V is the electron energy and I is the beam current. For a 1-mA, 13.5-MeV beam, the radiation dose is 1.6 kR/s at 1 meter. If the accelerator pulses 200 times per second and the beam is directed such that each portion of the bag receives illumination from four pulses, then the radiation exposure to any part of the bag would be 30 R from the primary x-ray beam. The scattered radiation dose to the bag is down by a factor of 0.4×10^{-3} and does not contribute appreciably to the dose to the bag. At this dose, no material other than film should be affected.

The neutron dose comes mainly from the converter and is proportional to the x-ray flux and the converter thickness. We used the TIGER spectra (see the next section) to calculate the x-ray flux and Berman's Atlas of Photoneutron Cross Sections for the tungsten cross section as a function of energy. We also assumed that half the converter thickness was used to produce neutrons. For a 1-mA beam striking a 0.25-mm thick tungsten converter, a neutron flux of 10^{11} nt/sec is produced, and is emitted isotropically. Most of these neutrons will be absorbed by the shielding immediately surrounding the converter.

We have calculated the activity generated in the luggage from the direct bremsstrahlung radiation. It is quite low because the threshold for activation of most common materials is above the maximum energy of the illumination photons. Also, the secondary radiation from Compton scattering is well below the photonuclear thresholds for the bag contents and thus causes no additional activation. The result is that most contents of checked luggage, including food, clothing, plastics, and drugs, whose primary elements are carbon, hydrogen, and oxygen, will acquire no activity.

For an example of residual activity, consider luggage with a 1-kg TNT explosive, 25 g of copper, 10 pennies, or 16 g of sterling silver. It is irradiated with photons from a 1-mA electron beam per 0.3 m^2 of x-ray coverage. Less than 10^{-15}% of the nuclei become activated and produce less than 1 μCi of activity. This is equivalent to a dose of 0.0004 mR/hr. For comparison, the average annual individual doses for some common activities are: medical and dental x-rays - 400 mR, living in a brick building - 7 mR, air travel - 3 mR, and watching television - 1 mR. (Ref. "The Effects on Population of Exposure to Low Levels of Ionizing Radiation," National Academy of Science, 1980.) It would take 500 such suitcases within one meter of a person to exceed the recommended environmental exposure limit. Even that slight amount of activity decreases during an hour to less than 1/64 of the original amount. The exceedingly slight amount of radiation present is detectable only with an extremely sensitive detector system.

The EXDEP accelerator for luggage screening would require shielding equivalent to that for a medical cancer treatment facility, but only for the suitcase volume. The accelerator would preferably be oriented downward on the ground floor so that the soil would be the primary shielding. The detectors would be outside the shielded area. The radiation exposure to the suitcase, the passengers, and the baggage handlers would be well below government regulations for environmental standards.

7. CONCLUSION

The final evaluation criteria for an explosives detection system will be the cost per bag to perform adequately. This includes the costs of the hardware,

operations, and facilities. The hardware costs and size for any nuclear technique will be approximately the same. The processing speed and the performance capabilities of the EXDEP/CTX system, however, should be significantly better, so that the cost per bag should be significantly less. The EXDEP/CTX system should truly be a second generation explosives detection system.

Table 1. Isotopes Detectable by EXDEP.

Isotope	%	Threshold (MeV)	Cross Section (mb) at 13 MeV	Half-Life	% $\beta+$	$E_{max}\beta^+$ (MeV)
Nitrogen (^{14}N)	99.6	10.6	1	10 m	100	1.198
Fluorine (^{19}F)	100	10.4	2	110 m	97	0.635
Phosphorus (^{31}P)	100	12.3	<1	2.6 m	99	3.24
Chlorine (^{35}Cl)	75.8	12.8	2	32.3 m	50	2.5
Nickel (^{58}Ni)	68.3	12.2	5	36 hr	50	0.85
Copper (^{63}Cu)	69.2	10.9	20	9.8 m	97	2.93
Zinc (^{64}Zn)	48.6	11.9	10	38 m	92	2.34
Gallium (^{69}Ga)	60.1	10.3	30	68 m	87	1.9
Bromine (^{79}Br)	50.7	10.7	?	6.5 m	92	2.5
Zirconium (^{90}Zr)	51.4	12.0	25	78 hr	22	0.9
Molybdenum (^{92}Mo)	14.8	12.7	20	15.5 m	94	3.4
Silver (^{107}Ag)	51.8	9.5	75	24 m	60	1.96
Praseodymium (^{141}Pr)	100	9.4	150	3.4 m	50	2.37
Samarium (^{144}Sm)	3.1	10.5	250	8.9 m	50	2.47

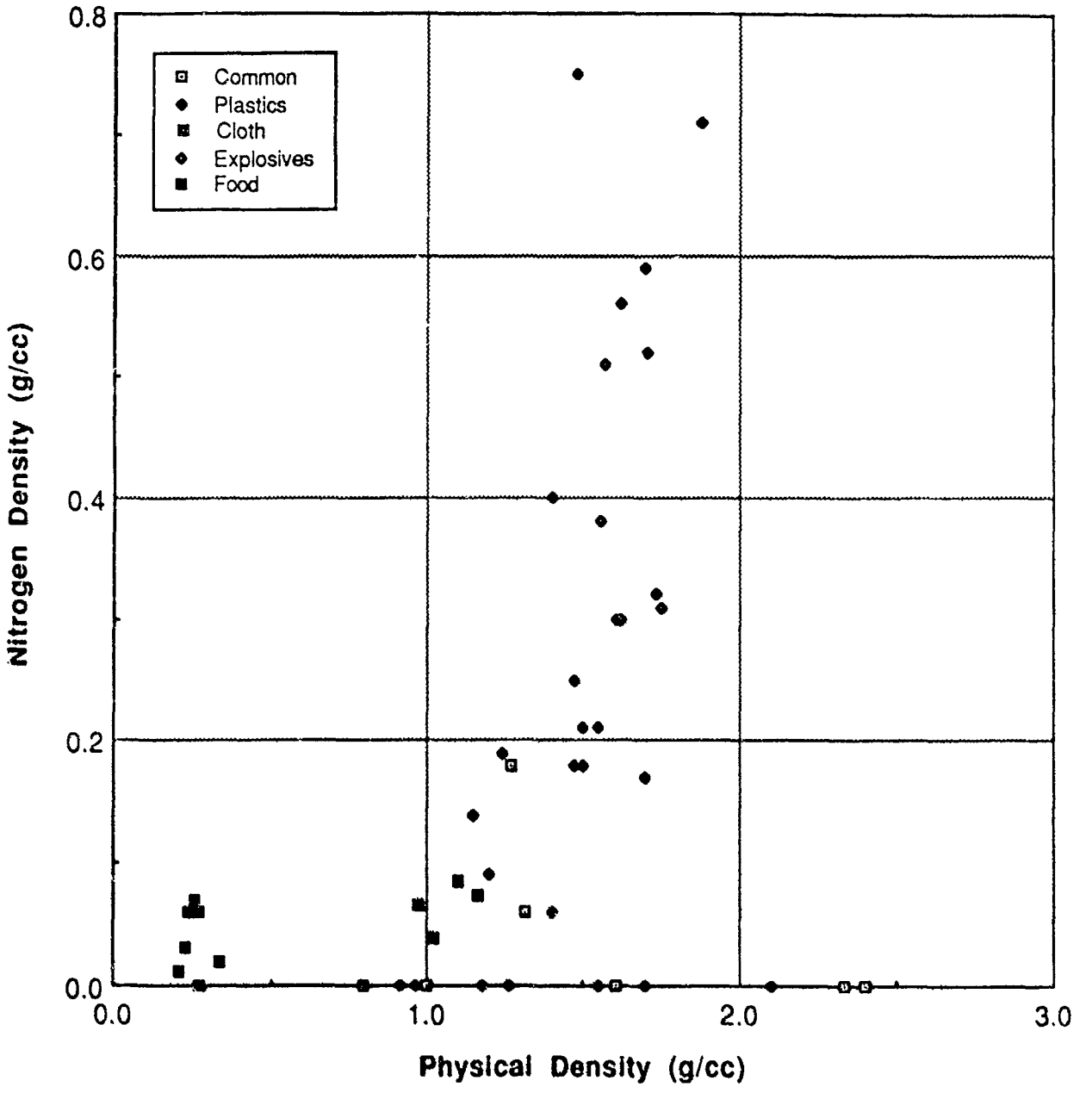


Figure 1. Plot of physical density vs nitrogen density for common materials and explosives.

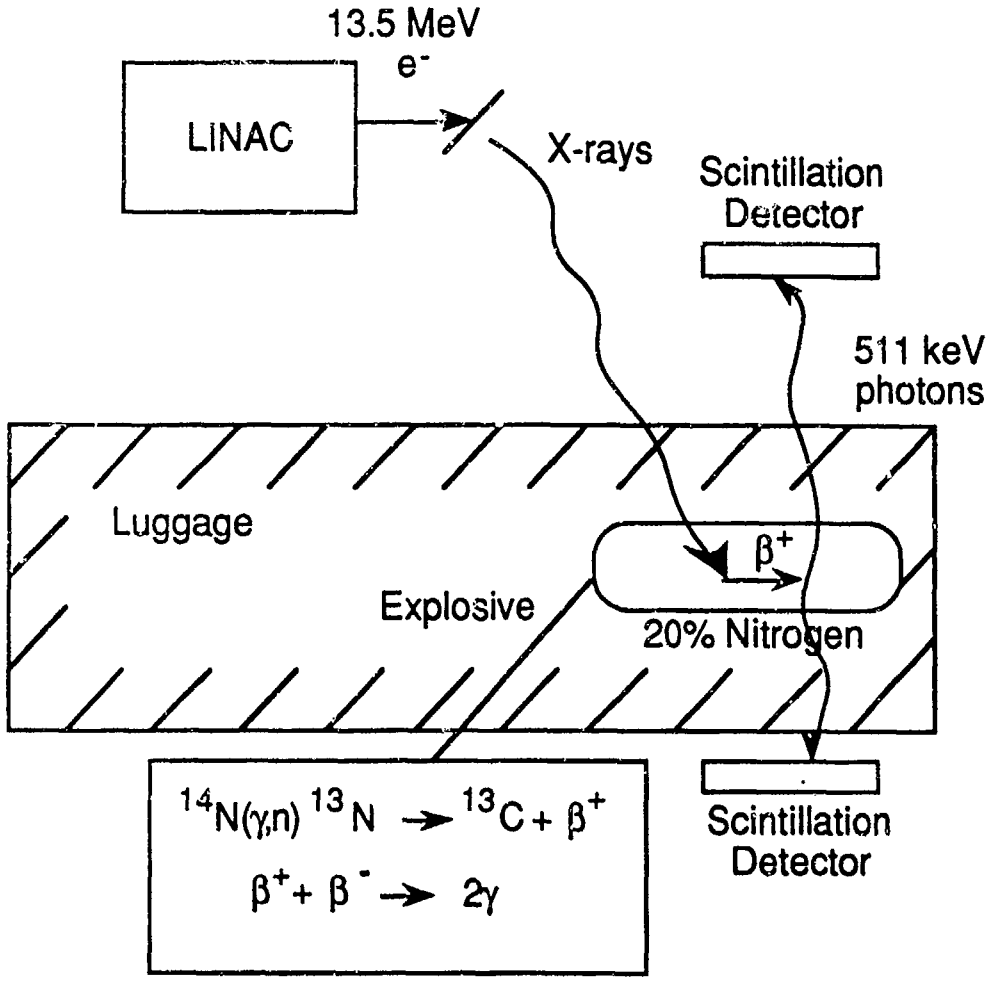


Figure 2. EXDEP concept.

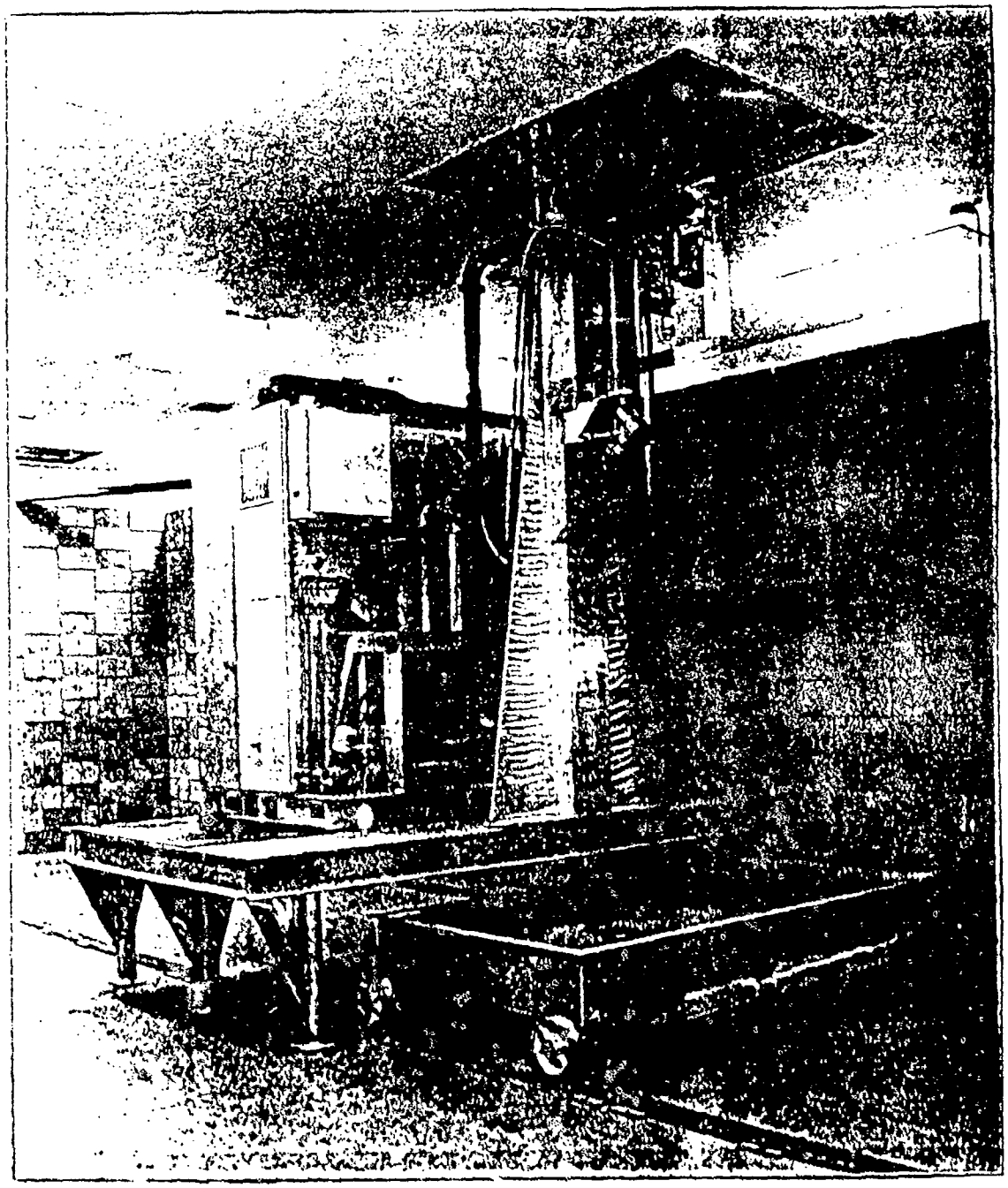


Figure 3. The EXDEP accelerator is shown in the TITAN laboratory with the cart in the illumination position.

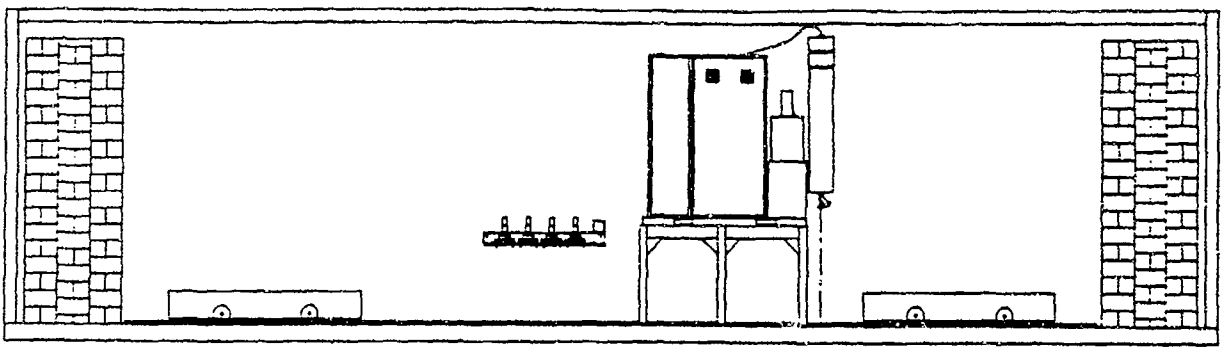


Figure 4. Experimental configuration for detecting explosives with electron beams.

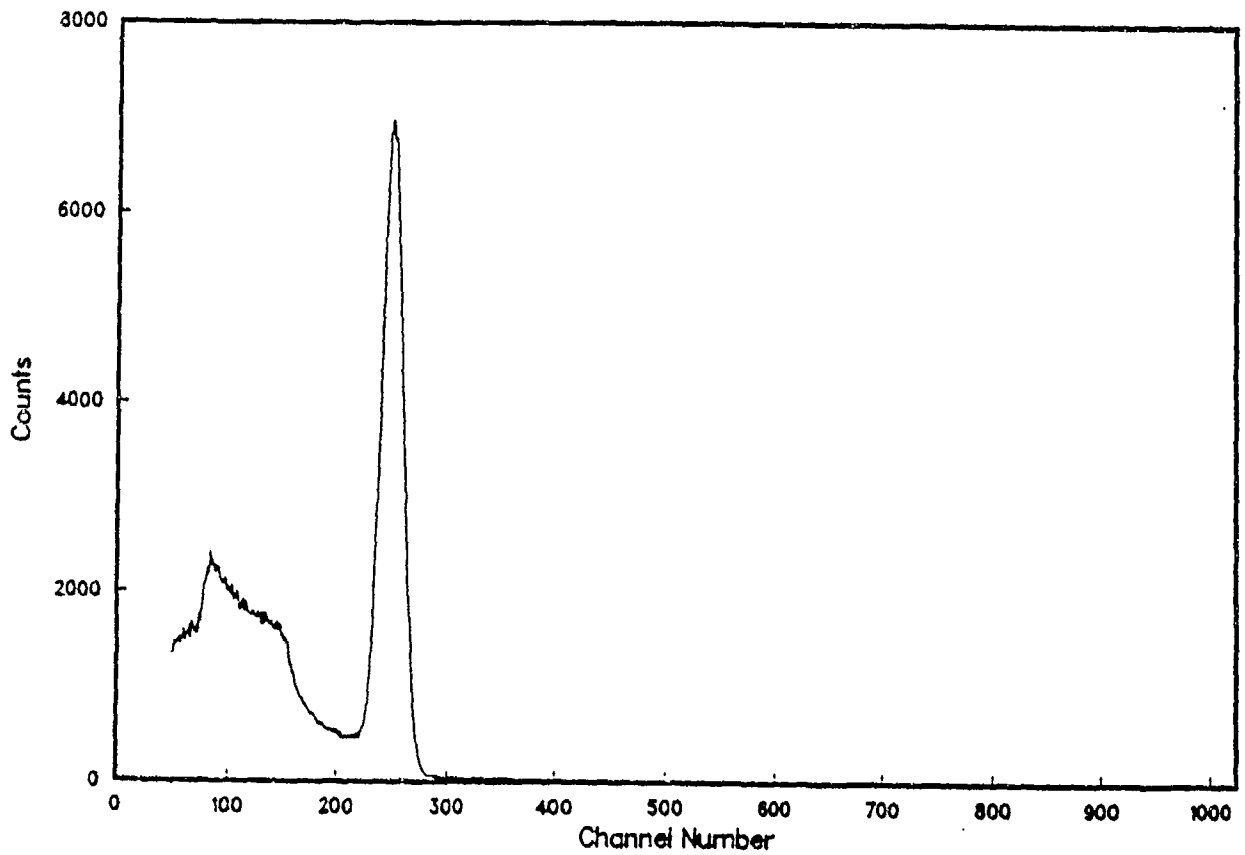


Figure 5. Multichannel analyzer spectrum showing 511-keV photopeak with little background from surroundings.

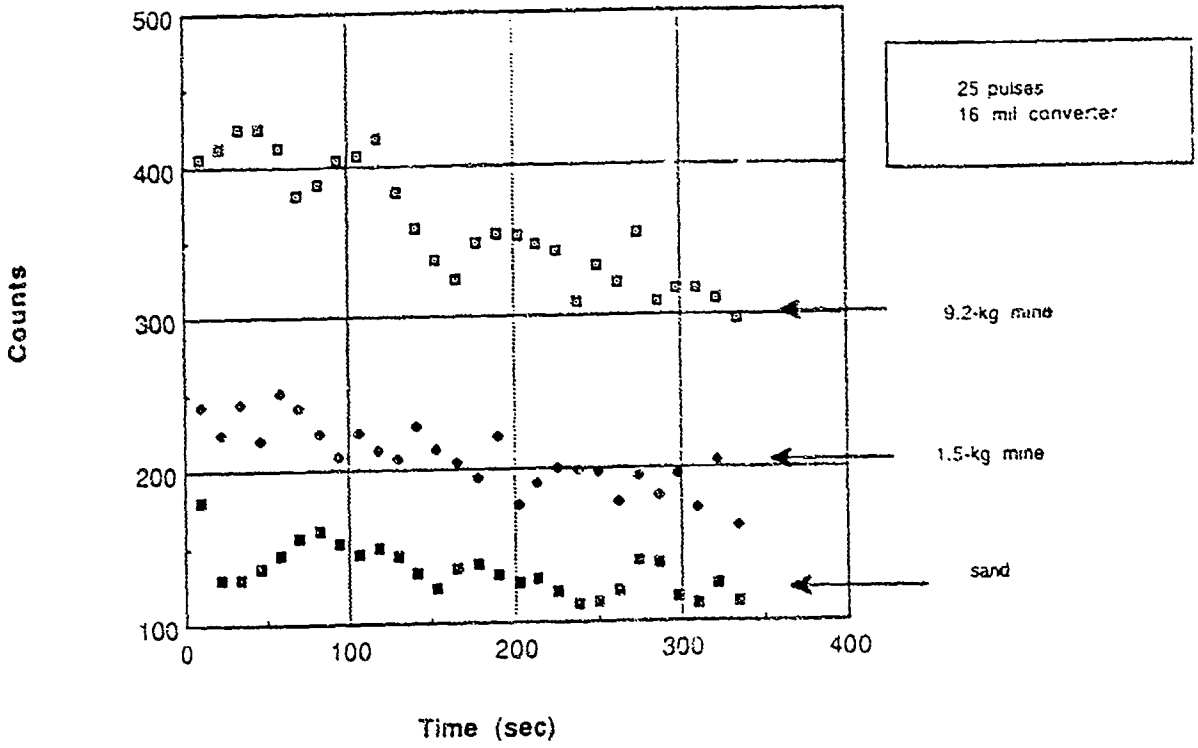


Figure 6. Plot of counts verses time after illumination for sand, and surface-buried 1.5-kg and 9.2-kg explosives.

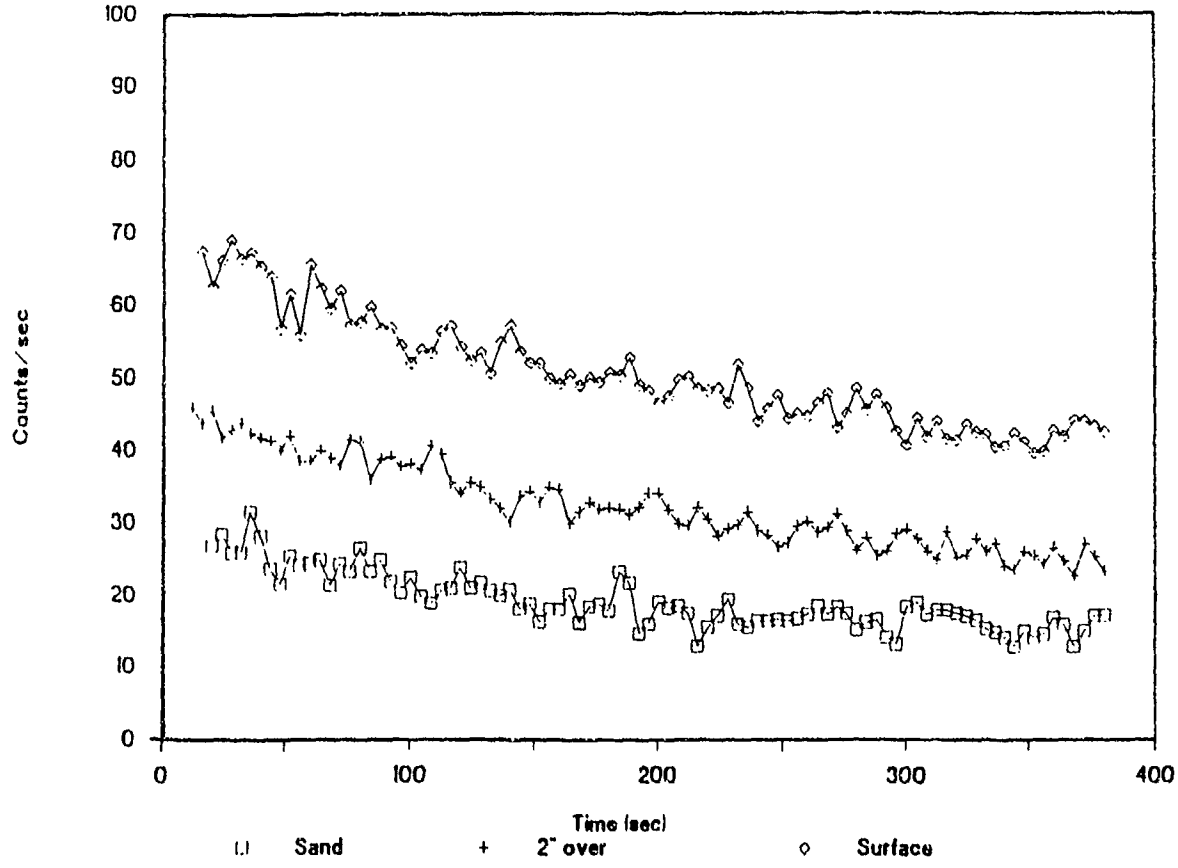


Figure 7. Plot of counts vs time for a 1.5 kg TNT mock explosive at different soil depths.

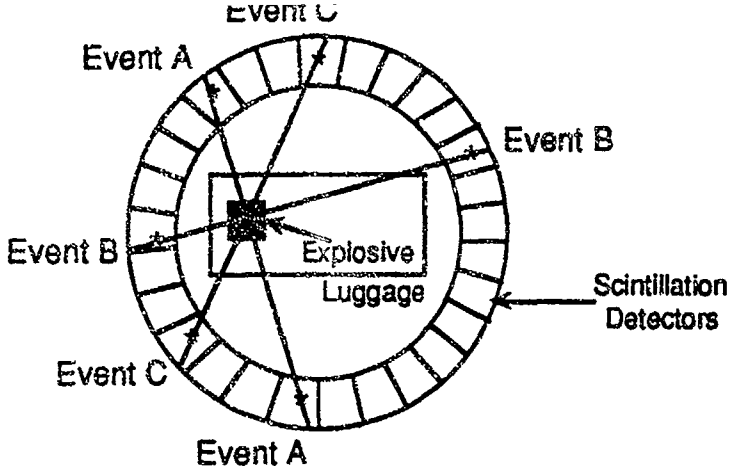


Figure 8. The EXDEP resolution will be 1 cm using coincidence counting of oppositely-directed photons from positron annihilation.

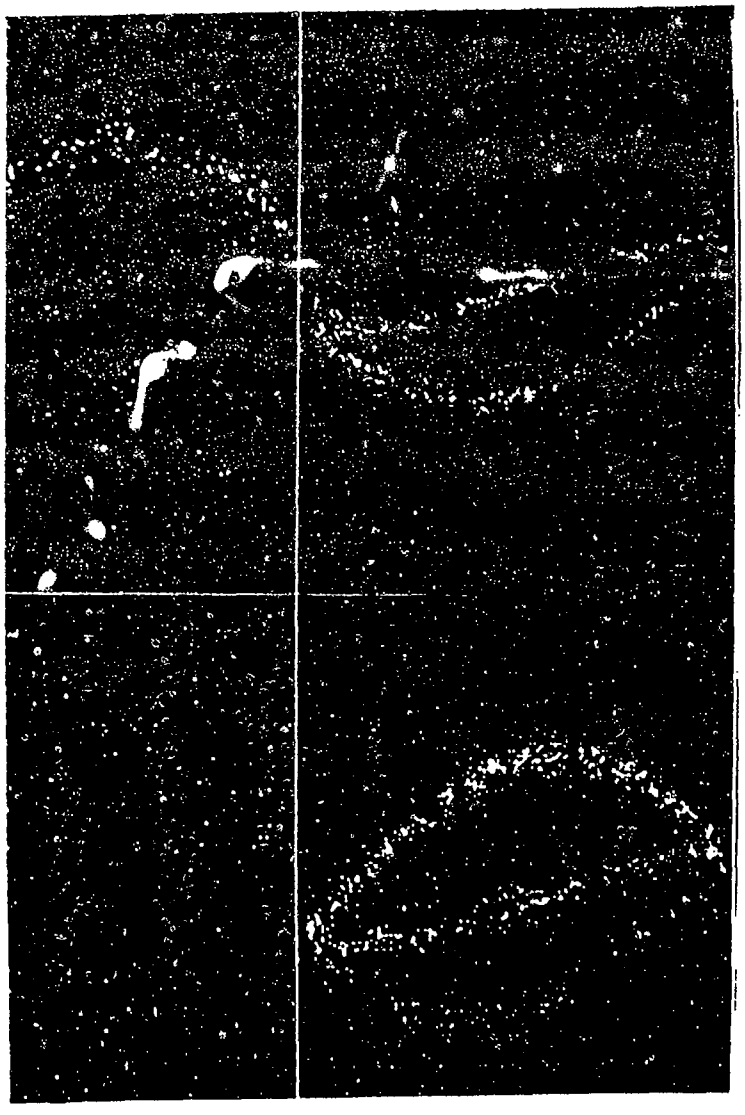


Figure 9. Data (in sinograph format) showing excellent resolution for three 0.1μCi ^{22}Na point sources 5 cm apart.

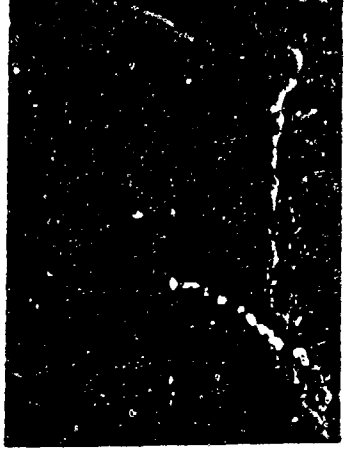


Figure 10. Raw data for six slices across the beaker.

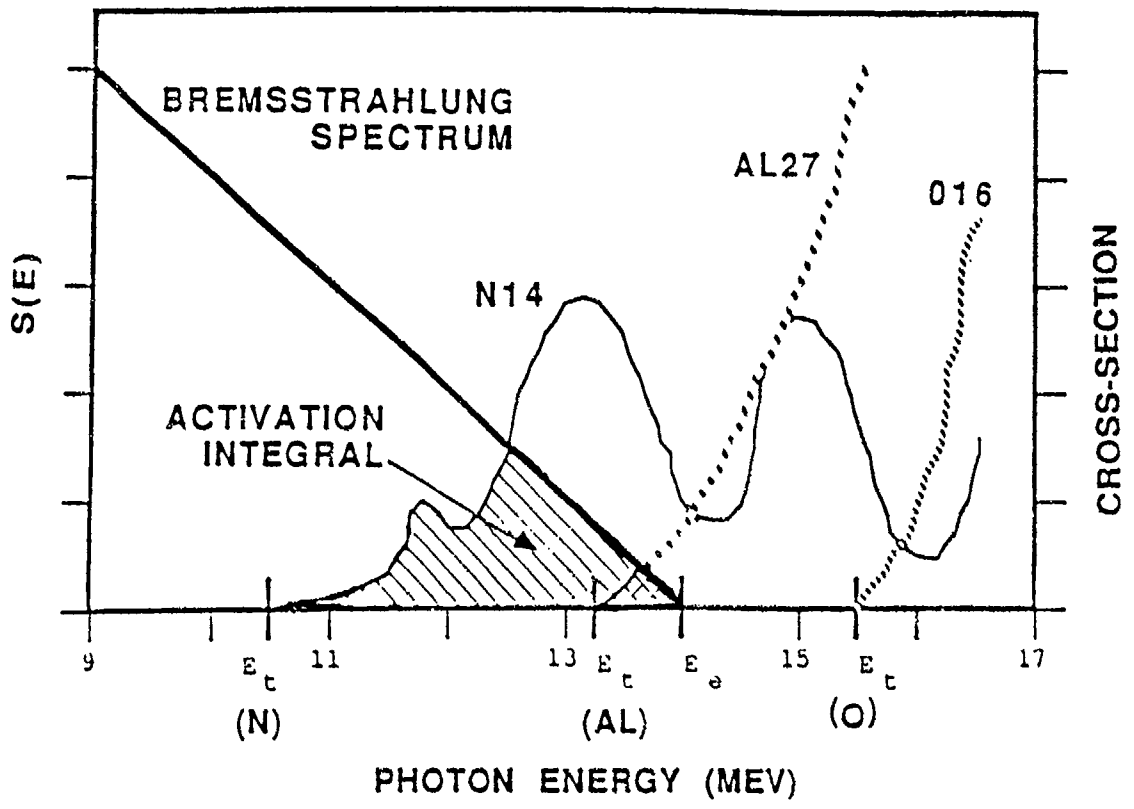


Figure 11. The endpoint energy of the bremsstrahlung beam lies above the activation threshold of ^{14}N but below those of ^{28}Al and ^{16}O (and ^{12}C as well).

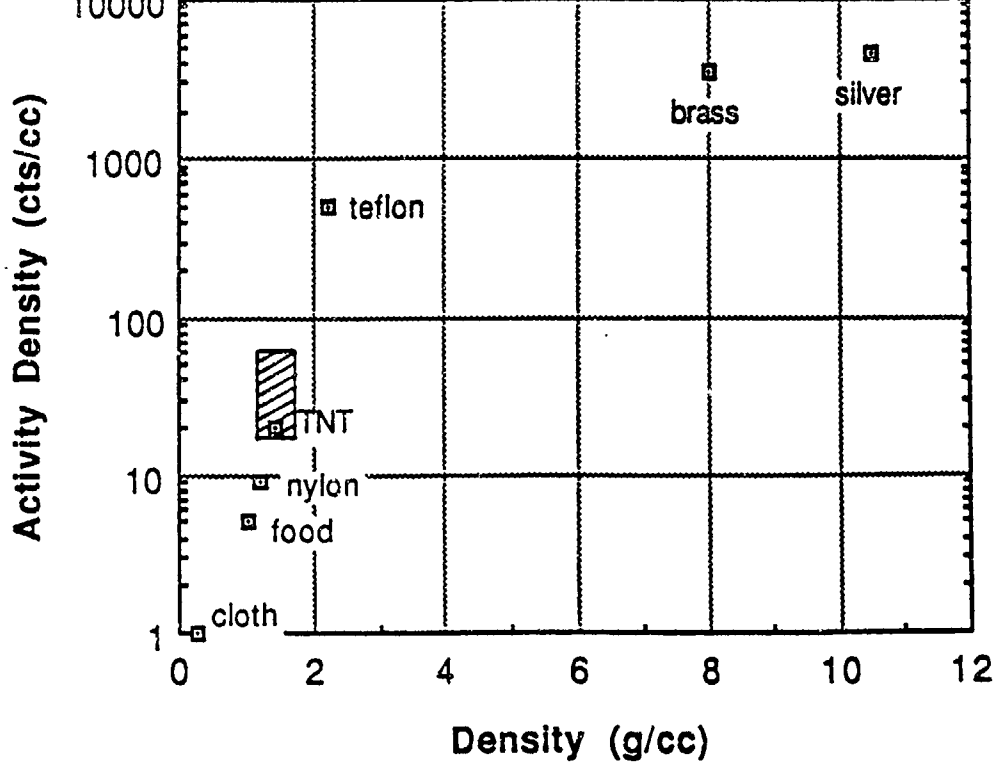


Figure 12. Log plot of activity concentration vs physical density for explosive and other items in luggage.

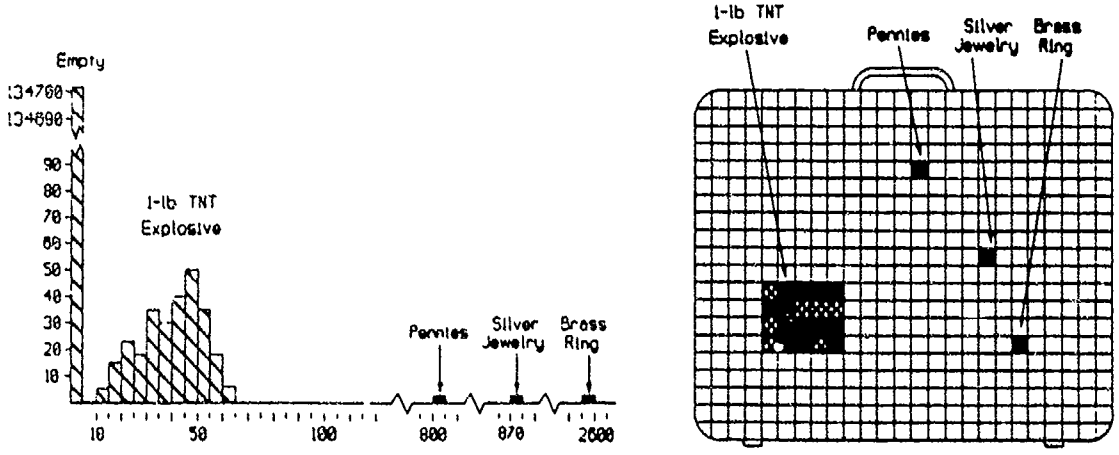


Figure 13. (a) Histogram and (b) Image from EXDEP screening of luggage with pennies, a brass ring, silver jewelry, and 1-lb of TNT.

EXPLOSIVES DETECTION LIMITATIONS USING DUAL-ENERGY RADIOGRAPHY AND COMPUTED TOMOGRAPHY

K.W. Dolan, R.W. Ryon, D.J. Schneberk, H.E. Martz, and R.D. Rikard
Lawrence Livermore National Laboratory
Nondestructive Evaluation Section, L-333
P. O. Box 808, Livermore, CA 94551

1. INTRODUCTION

Computed tomography (CT) provides volumetric mapping of x-ray attenuation in objects. X-ray attenuation is a function of composition and density. By making measurements at two or more energies, density and "average composition" (or effective atomic number) can be separated. Dual energy CT has therefore been suggested as a means for positive identification of small explosive quantities in baggage, boxes, containers, etc. That is, tomographic volumetric mapping and cross correlation of density and effective atomic number may provide the key for explosive materials detection with reduced false alarm rates. For example, we have used the dual energy CT method successfully to determine density and effective atomic number of explosives and mock material with accuracies of a few percent on density and better than $\pm$ 1 atomic number [Ref. 1]. Our dual energy CT work has been done in a materials analysis context. Two methods have been used:

- Isotope sources,which emit discrete energy (monochromatic) x-rays, coupled with energy discriminating x-ray detectors;
- X-ray tube sources, which emit a continuum (bremsstrahlung) energy distribution of x-rays, coupled with nondiscriminating detectors [Ref. 1,2,3].

We have developed beam hardening correction procedures for CT with polychromatic x-ray tube spectra [Ref. 3]. Dual energy CT with polychromatic sources is implemented by any technique that modifies the x-ray spectrum at either the source or the detector. This is accomplished by using two accelerating potentials, beam filtration before or after the sample, or energy selective detectors. The polychromatic option provides high flux source intensities which would be needed for routine high throughput explosives detection. We have also used transmission anode x-ray tubes, which produce nearly monochromatic radiation, for x-ray gauging. Such tubes may be useful for baggage inspection CT.

2. BACKGROUND

X-ray transmission through an object is a function of material composition, density, and thickness. Film and real time radiography produce two-dimensional "shadowgraph" images of an object with internal features superimposed in the image. Each point in the shadow image is a function of the attenuation of the x-ray beam along the path from source to image point. For each ray-path, the total linear attenuation coefficient is the sum of the attenuation coefficients of each volume element in the path. Computed tomography (CT) produces cross section (i.e. planar slice) images of an object by reconstructing a matrix of x-ray attenuation coefficients. These images can be volume rendered to provide three-dimensional information. In the slice or volume rendered images, the reconstruction algorithm determines the linear attenuation coefficient for each volume element of the image. The linear attenuation coefficient is a function of the composition (effective atomic number), density, and volume element dimension. The term "effective atomic number" is the atomic number of that hypothetical single element which gives the same x-ray attenuation as a compound or mixture being measured. Since the volume element dimension is known from the geometry of the CT scanning system, the attenuation coefficient becomes a function of only two variables, effective atomic number and density. Separation of these variables is done by taking CT data at two separate source energies, and essentially solving two equations in two unknowns. Thus, the volume elements can be mapped according to effective atomic number and density, and correlation of these variables can provide both feature and material identification

3. EXISTING TECHNOLOGY AND CAPABILITIES

Dual energy radiography for explosives detection is a research activity funded by the FAA [Ref.4]. It has been suggested that dual energy computed tomography might provide enhanced detectability for explosives. The high throughputs required for baggage inspection necessitate the use of very fast scanning and analysis. For example, x-ray scanning, reconstruction processing, and decision analysis needs to be accomplished in less than about 10 seconds. The technology associated with fast medical imaging systems already provides the capability of fast scanning, and these scanners could be extended to incorporate dual energy features. We have used parallel processors to reduce CT reconstruction times to the order of seconds. Decision making by artificial intelligence (AI) methods could be used to provide near real-time decisions. Image display and image analysis of CT image slices have been developed extensively here for visual interpretation. The technology elements are all available for high throughput inspection for explosives detection by dual energy CT. A prototype scanner combining these capabilities could be used to demonstrate speed, false alarm probabilities, detection limits, and "spoofability". But before launching such an effort, we performed a preliminary analysis to test the potential success of the concept.

4. DUAL ENERGY COMPUTED TOMOGRAPHY METHODS

Dual energy CT provides an additional parameter (i.e. effective atomic number) to the usually measured density that may provide another means of distinguishing explosives from common materials. We have used dual energy CT to advantage in several applications [Ref. 1,2]. Based on this experience, we consider dual energy CT a possible candidate technique for explosives detection, or perhaps as a secondary technique used to resolve false positive identifications made by other methods

A thorough treatment of multiple energy CT analysis is given in a previous publication [Ref 3], and only the concept of effective atomic number will be covered here. Effective atomic number (Z_{eff}) as used in x-ray CT is defined as the atomic number of the single element that attenuates the x-ray beam most like the multicomponent object. This concept is conveyed by the relationship

$$(\mu/\rho)(Z_{eff},E) = \Sigma\, (\mu/\rho)_n(Z_n,E)\,w_n$$

where the mass attenuation coefficient (μ/ρ) is a function of atomic number (Z) and x-ray energy (E), ρ is the material density, w_n is the weight fraction of component n, and Σ represents a summation over all components. Effective-Z values are not solved explicitly, but are obtained from interpolations of tabulated x-ray mass attenuation coefficients, or from interpolations on a basis set of materials. Effective-Z is a function of both material composition and x-ray energy, and every volume element in a sample can be characterized by both an effective-Z and a material density.

Since x-ray absorption at a particular energy is a function of both material (i.e., effective Z) and density, the two parameters may be separated by making measurements at two (or more) energies.

At energy 1, the x-rays are attenuated by the familiar exponential equation

$$(I/I_o)_1 = \exp(-(\overline{\mu/\rho})_1\, \rho\, t)$$

where $(\mu/\rho)_1$ is the summation Σ

$(\mu/\rho)_n(Z_n,E_1)w_n$ at energy E_1, and t is the thickness. At a second energy, we likewise have

$$(I/I_o)_2 = \exp(-(\overline{\mu/\rho})_2\, \rho\, t).$$

By using the ratio of the logarithms of the measured quantities (I/I_o) at the two energies, the density and thickness are eliminated:

$$\ln\{(I/I_o)_1\} / \ln\{(I/I_o)_2\} = (\overline{\mu/\rho})_1 / (\overline{\mu/\rho})_2 .$$

Examples of the ratios as functions of atomic number are shown in Figures 1 and 2. Effective Z's can be determined by interpolation using such curves.

5. EXPLOSIVES DETECTION CRITERIA AND PRELIMINARY FEASIBILITY ANALYSIS

In order to positively identify explosives, there must be one or more nearly unique signatures from the measurements. Since dual energy x-ray measurements yield the two parameters density and effective Z, the correlation of the two values could greatly diminish the possibility for false positive results. However, a further consideration is that the precision of the

measurements must be sufficient to eliminate ambiguity. X-ray measurements are subject to statistical fluctuation proportional to the square root of the number of photons detected (and therefore of the measurement time). We will not carry out an explicit error analysis here, but we will show by example the range of results which accrue from measurement errors.

A complete analysis of the feasibility of dual energy CT would require, first, an extensive compilation of the compositions of explosive and common materials, and second, radiation transport modeling of these materials using a variety of x-ray source spectra. Tables 1-3 give a first cut, short version of such an analysis. While not complete, it is possible to make some significant inferences.

In Table 1, we see that explosives tend to have higher densities than common hydrocarbon fibers and plastics. X-ray attenuation is therefore greater for explosives. There are marked differences in attenuation at optimum energies around 10 keV for thin materials. However, baggage inspection requires considerably higher energies, 50-150 keV, in order to penetrate the thickness of baggage. At these higher energies, a thin sheet explosive is almost transparent to x-rays, and there is very little difference from one material to the next. The latter point is emphasized in Table 2, where relative transmittances are given. There is only a percent or two difference between any of the materials at higher energies. It would be difficult to achieve precision better than several percent for any volume element in a fast CT scanner.

Regardless of the inherent limitation in the x-ray measurements, we may proceed further and look at the effective atomic numbers, given in Table 3. The values in Table 3 were derived from Figures 1 and 2. If the measurements could be very precise, there are clear distinctions between the effective Z's of explosives and many hydrocarbon materials. An exception is wool. This is an unfortunate exception, since the nitrogen in wool also gives a false positive result in thermal neutron activation (TNA) scanners. The other unfortunate result is the error bars. Even at low energies, 2% measurement errors lead to effective Z ranges which obscure distinctions between materials. It would be difficult to obtain 2% precision even in ideal laboratory environments where x-ray energies can be optimized and long counting times are possible. At the higher energies needed for baggage scanners, small measurement errors completely obliterate all distinctions. This results both from the very small attenuation (Table 1) and from the great sensitivity in effective Z to small changes in the measurements (Figure 2). At high energies all materials "look alike" to x-rays, since the primary interaction is Compton (inelastic) scatter which is primarily a function of the number of electrons present (i.e., electron density).

In the short list of materials reviewed here, explosives stand out from other organic materials and polymers principally in density. Dual energy radiation techniques, which yield effective Z's, seems to offer little help. The only way to obtain the required precision through signal averaging is to use many volume elements in a model-based analysis scheme.

6. CONCLUSIONS

We have shown that dual energy CT can be used to provide separate images of density and effective atomic number in laboratory situations. However, preliminary analysis suggests that unique correlations between density and atomic number would be very difficult to obtain in a practical baggage scanner due to inherent limitations in sensitivity and measurement precision. More thorough modeling and computational testing are required to evaluate this technique. It is likely that very sophisticated data processing, using correlation schemes and model-based analysis, will be needed for this technique to succeed. While composition (effective atomic number) adds some discrimination, it is primarily density which distinguishes explosives from other hydrocarbon materials.

If the inherent limitations *can* be conceptually overcome, a high throughput prototype scanner could be assembled, and parallel processing techniques could be developed for fast reconstruction and decision analysis. Testing would be needed to demonstrate speed, detection limits, false alarm rates, and "spoofability".

REFERENCES:

1. H. E. Martz, D. J. Schneberk, G. P. Roberson, S. G. Azevedo, and S. K. Lynch, "Computerized Tomography of High Explosives", Lawrence Livermore, CA, UCRL-102345 (1990).

2. H. E. Martz, G. P. Roberson, D. J. Schneberk and S. G. Azevedo, "Nuclear Spectroscopy-Based, First Generation, Computerized Tomography Scanners", Lawrence Livermore National Laboratory, Livermore, CA, UCRL-JC-104187 (1990).

3. D. J. Schneberk, H. E. Martz and S. G. Azevedo, "Multiple-Energy Techniques in Industrial Computerized Tomography", Lawrence Livermore National Laboratory, Livermore, CA, UCRL-JC-103762 (1990).

4. Aviation Week and Space Technology, March 25, 1991, pp. 60-62.

Table 1. Compositions, densities and transmittances (I/I_o) at various x-ray energies for some explosives and common materials

Material	Composition	Density (grams/cc)	fraction transmitted (I/I_o) by 1.0 mm 10 keV	25 keV	50 keV	100keV
explosive 1	PBX9502	1.9	0.4030	0.91360	0.9614	0.9710
explosive 2	Comp B	1.71	0.4925	0.9290	0.9660	0.9739
explosive 3	Comp C-4	1.65	0.5087	0.9315	0.9670	0.9746
explosive 4	PETN	1.76	0.4451	0.9226	0.9644	0.9730
polystyrene	$(C_6H_5CHCH_2)_n$	<1.0-1.0+	0.8112	0.9689	0.9810	0.9843
paraffin	$(CH_{2.06})_n$	0.88-0.92	0.83381	0.9717	0.9819	0.9850
polyethylene	$(-CH_2-)_n$	0.92-0.95	0.8318	0.9706	0.9813	0.9844
Nylon	$(C_6H_{11}NO)_n$	<1.0-1.14	0.7462	0.9600	0.9773	0.9816
wool (keratin)	17 amino acids	<1.0-1.0+	0.6201	0.9521	0.9787	0.9840
wool	@65% humidity	<1.0-1.0+	0.6062	0.9514	0.9788	0.9842
water	H_2O	1.00	0.5961	0.9507	0.9777	0.9832
aluminum	Al	2.7	0.00088	0.6080	0.9049	0.9550
steel	Fe	7.86	10^{-58}	2.1×10^{-5}	0.2140	0.7457

Explosive components and atomic composition:

PBX9502: TATB(95%), Kel-F(5%); $[C_{2.30}H_{2.23}N_{2.21}O_{2.21}Cl_{0.038}F_{0.13}]$

Comp-B: RDX(63%), TNT(36%), wax(1%); $[C_{2.03}H_{2.64}N_{2.18}O_{2.67}]$

Comp C-4: RDX(91%), Di(2-ethylhexyl) sebacate(5.3%), Polyisobutylene(2.1%), Motor oil 1.6%); $[C_{1.82}H_{3.54}N_{2.46}O_{2.51}]$

PETN: $[C_5H_8N_4O_{12}]$ Detasheet: PETN(85%), binder(15%)

wool $C_{4.00}H_{6.69}N_{1.11}O_{1.65}S_{0.104}$
at 21.2°C and 65% humidity, add 16% water

Table 2. Relative transmittance (I/I_o) for the explosives and common materials listed in Table 1.

Material	Composition	Density (grams/cc)	transmittance of 1.0 mm relative to water 10 keV	25 keV	50 keV	100keV
explosive 1	PBX9502	1.9	0.676	0.961	0.983	0.988
explosive 2	Comp B	1.71	0.826	0.977	0.988	0.991
explosive 3	Comp C-4	1.65	0.853	0.980	0.989	0.992
explosive 4	PETN	1.76	0.747	0.970	0.986	0.990
polystyrene	$(C_6H_5CHCH_2)_n$	<1.0-1.0+	1.361	1.019	1.003	1.001
paraffin	$(CH_{2.06})_n$	0.88-0.92	1.406	1.022	1.004	1.002
polyethylene	$(-CH_2-)_n$	0.92-0.95	1.395	1.021	1.004	1.001
Nylon	$(C_6H_{11}NO)_n$	<1.0-1.14	1.252	1.010	1.000	0.998
wool (keratin)	17 amino acids	<1.0-1.0+	1.040	1.001	1.001	1.001
wool	@65% humidity	<1.0-1.0+	1.017	1.001	1.001	1.001
water	H_2O	1.00	1.0000	1.0000	1.0000	1.0000
aluminum	Al	2.7	0.0015	0.640	0.925	0.958
steel	Fe	7.86	10^{-58}	2.2×10^{-5}	0.219	0.758

Table 3. Effective atomic numbers (Z_{eff}) at selected x-ray energies for the explosive and common materials listed Table 1 using ratio method

Material	Composition	Density (grams/cc)	Z_{eff} from ratio $\ln(I/I_o)$ with 2% meas. error Zeff(μ10/μ25)	Zeff(μ50/μ100
explosive 1	PBX9502	1.9	7.45±0.68	7.51±7.0
explosive 2	Comp B	1.71	7.22±0.79	7.17±8.0
explosive 3	Comp C-4	1.65	7.17±0.81	7.12±8.3
explosive 4	PETN	1.76	7.45±0.77	7.36±7.7
polystyrene	$(C_6H_5CHCH_2)_n$	<1.0-1.0+	5.73±1.36	5.58±>10
paraffin	$(CH_{2.06})_n$	0.88-0.92	5.59±1.48	5.50±>10
polyethylene	$(-CH_2-)_n$	0.92-0.95	5.51±1.38	5.30±>10
Nylon	$(C_6H_{11}NO)_n$	<1.0-1.14	6.00±1.06	6.09±>10
wool (keratin)	17 amino acids	<1.0-1.0+	7.28±1.28	7.48±>10
wool @65% humidity		<1.0-1.0+	7.45±1.34	7.60±>10
water	H_2O	1.00	7.55±1.36	7.44±>10
aluminum	Al	2.7	13±0.2	13±2.2
steel	Fe	7.86	26±0.02	26±0.4

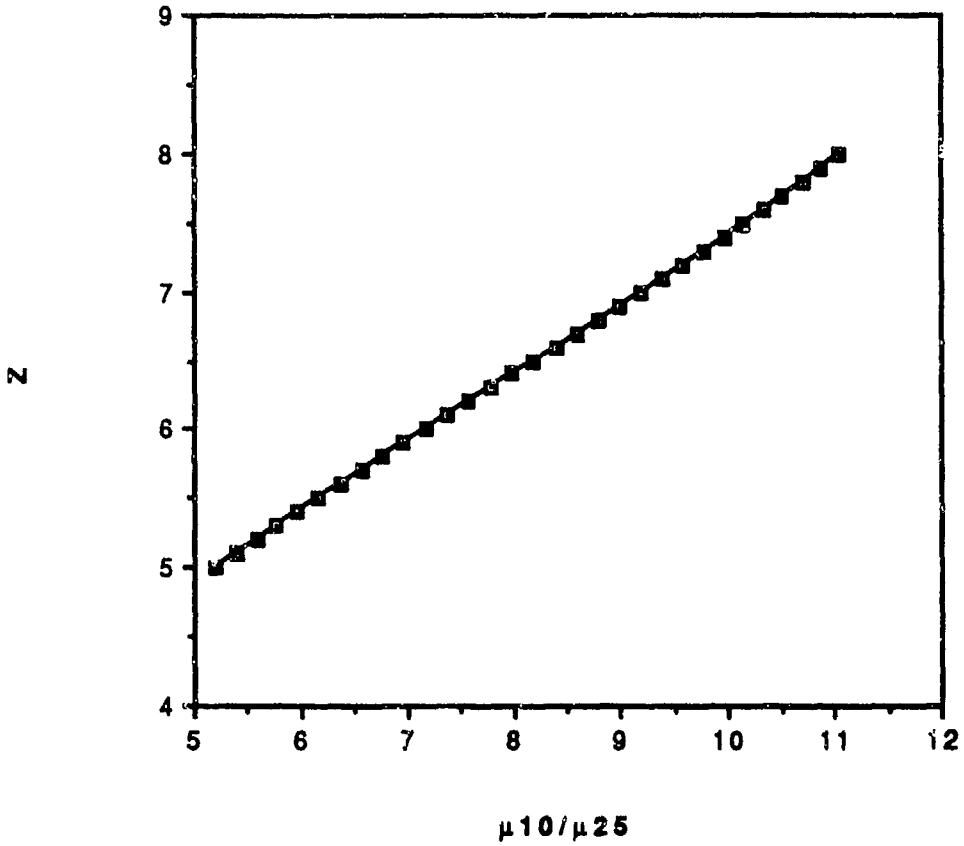


Figure 1. Effective atomic number (Z_{eff}) as a function of ln{(I/Io)@10 keV}/ln{(I/Io)@25 keV) which is equivalent to (μ @ 10 keV)/(μ @ 25 keV). Note that the approximate slope (sensitivity) $\Delta Z/\Delta ratio = 0.51$

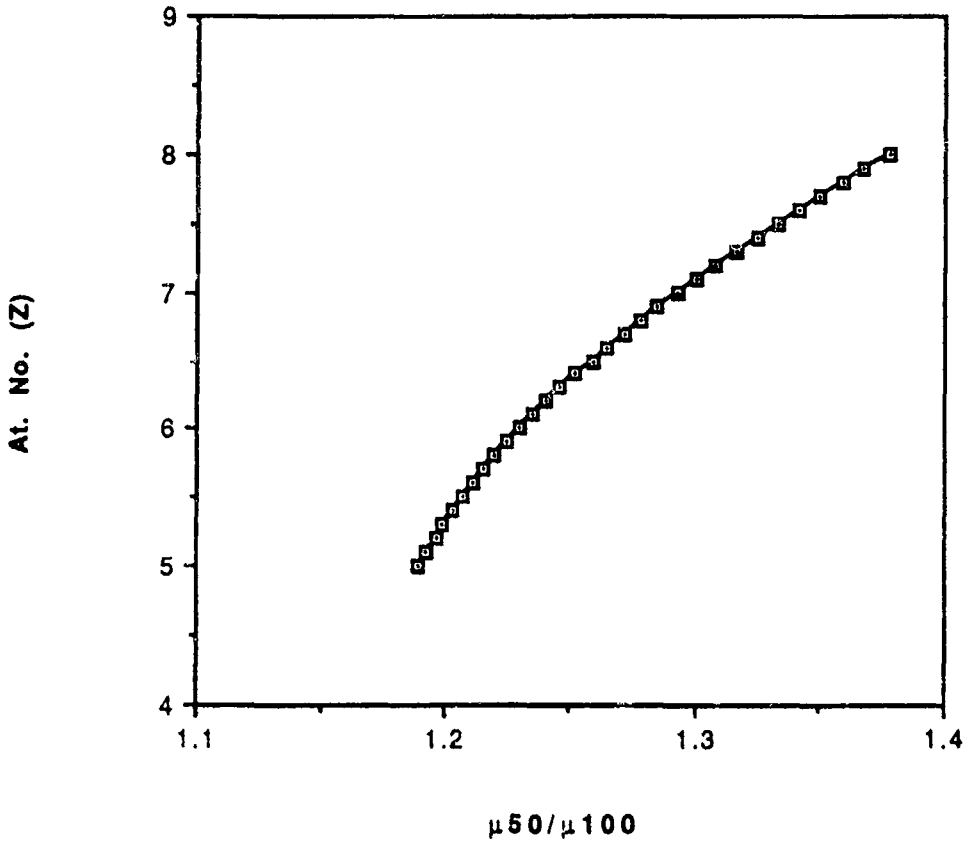


Figure 2. Effective atomic number (Z_{eff}) as a function of ln{(I/Io)@50 keV}/ln{(I/Io)@100 keV) which is equivalent to (μ @ 50 keV)/(μ @ 100 keV). Note that the approximate slope (sensitivity) ΔZ/Δratio = 15.

DETECTION OF OBJECTS CONCEALED UNDER PERSONS' CLOTHING USING THE "SECURE" SYSTEM

Steven W. Smith, Ph.D.
IRT Corporation

1. INTRODUCTION

The problem of detecting weapons and contraband concealed under the clothing is very old. Airline hijackings in the 1970's focused the problem on detection of metal firearms and knives. The technological challenge of the 1990's, and beyond, will be detection of non-metallic weapons, explosives and illegal drugs. While metal detectors and chemical sniffers may be used for the detection of larger metal objects and certain chemical substances, no system is currently available that can detect a wide variety of concealed objects and materials. Security personnel have little option but to hand search persons suspected of concealing many kinds of threats. This paper describes the operating principles and test results (1) of a new technique developed to address this need.

The method used to detect concealed objects is referred to as: Subambient Exposure, Computer Utilized Reflected Energy, or more simply, SECURE. As the acronym implies, SECURE is a back-scatter x-ray technique that produces images of subjects and any objects concealed under their clothing. Two operational models of the SECURE system have been constructed and tested. These systems are referred to as the SECURE 1000. In physical appearance, the SECURE 1000 is self contained in an enclosure 82 inches high by 48 inches wide by 32 inches deep. Persons being inspected stand about 6 inches in front of the system and must remain relatively motionless for 3 seconds. Almost immediately, a computer enhanced image appears on a display monitor showing the outline of the person and any concealed objects. A typical image acquired on the test system is shown in Figure 1. Each 3 second scan produces an image of one side of the person. Multiple views, such as front, rear, and sides, require the subjects to turn their bodies for additional scans.

Techniques for producing images using x-rays have been in common use for nearly one-hundred years. In the same context, adverse health effects from significant exposure to x-rays have also been known for nearly this long. Until the development of the SECURE technique, the overwhelming view of both the security and radiation protection communities was that x-ray imaging could not be used to detect concealed objects on persons because of the health implications.

Using this as a background, the important technological features of the SECURE technique can be appreciated. Through the use of back- scatter x-ray detection, an optimized imaging geometry, and computer image enhancement, the SECURE technique requires only a small fraction of the radiation level previously thought possible. Radiation exposure to examined persons is so low as to be trivial compared to naturally occurring environmental radioactivity. In accordance with accepted radiation safety standards, these levels are completely negligible, and do not need to be considered for purposes of radiation protection.

2. PRINCIPLE OF OPERATION

The block diagram shown in Figure 2. illustrates the operation of the SECURE system. A small x-ray source provides a very narrow "pencil" beam of x-ray directed at the body of the person being examined. One of three things will happen to each individual x-ray striking the body. First, the x-ray may pass completely through the body without interacting. At the relatively low x-ray energy used in the SECURE method, virtually none of the x-rays will be able to achieve complete penetration. The second event that may happen is the x-ray interacting in the body by the photoelectric effect. The final result of this interaction is that the x-ray is absorbed, releasing its energy into the body. The third event that may occur is an interaction of the x-ray by Compton scattering. This can be most simply viewed as an x-ray colliding and bouncing off of an electron in the body. The important point here is that Compton scattering does not destroy the x-ray, it only

changes its direction and energy. Many of the x-rays striking the body will penetrate a few centimeters, interact by Compton scattering, and exit the body through the same surface that they entered the body. These "back-scattered" x-rays can then be detected by large area x- ray detectors placed near the x-ray source.

The main detection principle used in the SECURE method is based on the relative magnitude of Compton scattering as compared to the photoelectric effect. X-rays passing through materials composed of low atomic number elements are most likely to interact by Compton scattering. X-rays passing through materials composed of high atomic number elements are more likely to interact by the photoelectric effect. As shown in Figure 3, this results in the number of back-scattered x-rays being a strongly varying function of the atomic number of the material the x-rays were scattered from. Low atomic number elements produce much more back-scatter than high atomic number elements. The actual number of x-rays detected as back-scatter will depend on many fixed parameters including x-ray energy and imaging geometry. When the x-ray beam used in the SECURE 1000 is directed against soft tissue, approximately 7 percent of the incident x-ray beam can be detected as back-scatter. This can be compared to medical radiography, where typically only 0.1 percent of the incident x-rays are detected passing through the body.

Using the above method, the relative amount of back-scatter, and therefore the relative atomic number, can be measured at the point the x-ray beam strikes the body. Additional points on the subjects' body are examined by rapidly scanning the x-ray beam in a raster scan pattern. These measurements are assembled to form an image of the person and any objects concealed under the clothing. Body tissue, organic matter and plastic appear light in the image indicating a low atomic number material. Metals and bones near the surface of the skin appear dark indicating a high atomic number composition. Before displaying on the image monitor, each image is digitally processed using various non-linear spatial filters to provide easier image interpretation.

Because the x-rays penetrate only a few centimeters below the skin, the images displayed by the system show only those features within about 1-2 centimeters of the body surface. This allows detection of objects concealed under the clothing without imaging the body's internal anatomy. An exception to this is bones in the lower legs which are near enough to the skin to be seen in the acquired image.

3. RADIATION SAFETY

Each scan using the SECURE technique exposes the subject being examined to a 3 microRem dose of x-ray radiation. For comparison, medical x-rays typically expose patients to 30,000 to 300,000 microRem per examination.

Every person is continually exposed to radiation from naturally occurring radioactive materials in the air and soil. The level of this "background" radiation ranges between 10 and 20 microRem per hour (2), depending on local conditions. Cosmic radiation from space also provides a significant radiation level that increases with elevation. For example, commercial airline passengers are typically exposed to 500 microRem per hour (3) during a flight at 35,000 feet above sea level.

The radiation dose values listed above are measured at the skin of the subject. The average energy of background radiation is significantly higher than used in the SECURE technique. As shown in Figure 4, this results in background radiation penetrating more deeply into the body than radiation used in the SECURE system. Each SECURE 1000 scan produces a radiation dose of 3 microRem at the subject's skin. This same 3 microRem is produced at the subject's skin each 10 minutes from exposure to normal background radiation. Tissue below the skin receives less dose because it is partially shielded by the outer layers of tissue. Near the center of the body, 10 to 15 centimeters below the skin, a single scan from the SECURE technique produces less radiation dose than a I minute exposure to background radiation. As an average between these values, the radiation dose resulting from a SECURE 1000 examination is equivalent to the radiation dose all persons receive each 5 minutes from normal background radiation. Passengers flying aboard commercial airlines are exposed to this same level of radiation about every 20 seconds.

Front and rear scans are normally required to determine if a subject is concealing an object. In some cases, side views are also required. These additional views do not raise the radiation exposure beyond the stated comparisons to background radiation. Each additional view exposes a different side of the body to the x- ray beam. For example, after a front scan, the front of the subject has been

exposed to 3 microRem of radiation, however, the rear of the subject has received virtually no dose. Only after all four views are completed has the subject received 3 microRem over the majority of his body. Since background radiation produces a dose over the entire body, 5 minutes of exposure to background radiation is equivalent to a SECURE examination composed of 4 views.

As the above analysis shows, the radiation exposure from the SECURE system is small compared to the radiation exposure from naturally occurring background radiation. Even more importantly, the SECURE dose is small compared to behavior induced variations in the background dose. Every person receives 250 to 500 microRem of radiation dose each day from background radiation. Variations in this level result from local conditions, elevation, housing material and even clothing. For example, deciding to wear a sports coat instead of a sweater produces a few percent change in the background radiation reaching the body. Over the period of a few hours, this results in a few microRem change in dose. In this manner, a scan from the SECURE technique is literally equivalent in risk to wearing a sports coat instead of a sweater, or eating lunch on an outside patio instead of an inside dining room. These comparisons provide the strongest claim for the safety of the SECURE technique. The SECURE technique is safe, because its risks are no larger than the risks from daily activities and behaviors that are considered unconditionally safe.

The commercial version of the SECURE system will be capable of performing approximately 600 scans per hour. Based on a single scan emission of 3 microRem, this results in a total maximum radiation emission of 1800 microRem per hour. This can be compared with Federal regulations classifying locations with respect to their radiation levels. Under Part 20.105.b.1, Title 10, Chapter I of the Code of Federal Regulations, locations with radiation levels less than 2000 microRem per hour are classified as "unrestricted," the lowest category. Access to unrestricted areas is not controlled for purposes of radiation protection, and radiation warning signs are not required. Even with intentional operator misuse, the SECURE system cannot emit significantly higher levels of radiation at any point on the exterior of the enclosure.

The National Council on Radiation Protection and Measurements (NCRP) has recommended an annual effective dose limit for members of the general public of 100,000 microRem per year (4). Accepted radiation safety procedures require that efforts be taken to keep this exposure as low as reasonably achievable (ALARA), with economic and social factors being taken into account. In 1987, the NCRP specifically addressed the issue of very low level exposure to radiation. In report No. 91, Recommendations on Limits for Exposure to Ionizing Radiation (4), the NCRP recognizes a lower limit below which further effort to reduce radiation exposure to the individual is unwarranted. They refer to this as the Negligible Individual Risk Level (NIRL) and assign a value of 1000 microRem per year from any one individual source or practice. Radiation exposures at or below the NIRL are regarded as trivial, completely insignificant, and are not required to be considered for purposes of radiation protection.

In another publication (5), the NCRP addresses the use of radiation in consumer products:

"In certain cases the use of radiation, although not mandatory, enables a task to be performed more rapidly and/or economically. In a few cases, there may be no technologically better way of conducting the given operation. As long as the associated individual and collective radiation doses are small, such applications appear to be acceptable. Examples include airport luggage inspection systems and gas and aerosol (smoke) detectors."

The SECURE technology clearly falls within both the letter and spirit of these radiation exposure recommendations. Even when individuals are examined up to 300 times per year, the accumulative radiation dose falls within the NIRL. This should not be interpreted to mean that all persons must be restricted to less than 300 scans per year. The NCRP emphasizes that the NIRL is not a radiation exposure limit and that exposure to small dose increments above the NIRL are of little significance.

4. TESTING RESULTS

A fully operational SECURE 1000 prototype was tested by Sandia National Laboratories during the period July 23-25, 1991. Detection capabilities of the system were evaluated by concealing objects on volunteers and then scanning them with the SECURE 1000. The acquired images were then inspected to determine if the concealed items could be detected. The testing included actual samples of explosives, weapons, and illegal chemical substances. More than

200 scans of concealed objects were acquired during the testing period. Additional tests were made to confirm radiation exposure levels and investigate system safety. The following comments and conclusions are taken from Sandia's report of the testing (1).

Explosive testing included the use of actual explosives, including: C4, Detasheet, Kinemax and WaterGel. The primary test samples were 100 gram blocks of Detasheet and C4. Both of these samples could be detected without question on any subjects' chest area. Explosives located in overt positions on a subject's body could be detected in a single scan. Explosives placed in covert positions (e.g., small of back, top of head, ankle area, inside thigh), were always detected by a combination of two scan views, e.g., front and side.

Weapon testing included: North American Arms MR (mini-revolver), FIE "The Best" .25 cal, American Derringer, Excam (,T-27, Ramline .22 (plastic and metal), 5" hunting knife and a Special Nuclear Materials (SNM) container. These weapons were detected in both overt and covert locations. Metallic objects on the side of the person blend in with the background and may be unobserved; however, a side scan would provide an image of the object.

Illegal chemical substance testing used evidentiary materials from past court cases including : cocaine, Mexican heroin, marijuana, and anabolic steroids in various forms, i.e., pills, capsules, filled hypodermics, and vials. Various scenarios were used, attempting to mimic some of the methods used to attempt transport of illegal chemical substances across borders. The items could usually be detected by a combination of scans, i.e., side and front.

Measurements taken on the system showed the radiation exposure during normal scanning to be 2 +/-1 microRem. Interlocks and safety systems on the scanner were tested and there appears to be no danger for excessive radiation exposure due to a mechanical malfunction.

5. CONCLUSION

The feasibility and usefulness of the SECURE technique depends on two factors: first, radiation safety, and second, detection capabilities. Safety of the system is certain. Any health risk associated with the techniques is no greater than the risks associated with everyday activities that are considered unquestionably safe. The full detection capabilities of the system will be determined through future field tests, however, summarized in the report from Sandia Laboratories, "The primary conclusion which can be made is that the SECURE 1000 does have applicability to the detection of contraband material(s) on personnel. This includes explosives, illegal chemicals, weapons and SNM.

REFERENCES

1. Kenna, B.T. and Murray, D.W. "Test Report of IRT SECURE 1000 System," July 1991, Sandia National Laboratories, Albuquerque.

2. Knoll, G.F., "Radiation Detection and Measurement," 1979, John Wiley & Sons, New York, pg 799.

3. NCRP Report No. 45, "Natural Background Radiation in the United States," Nov 1975, Figure 10, pg 20, National Council on Radiation Protection and Measurements, Bethesda, MD.

4. NCRP Report No. 91, "Recommendations on Limits for Exposure to Ionizing Radiation," June 1987,pg 43, National Council on Radiation Protection and Measurements, Bethesda,MD.

5. NCRP Report No. 95,"Radiation Exposure of the U.S. Population from Consumer Products and Miscellaneous Sources," June 1987, pg 67, National Council on Radiation Protection and Measurements,Bethesda,MD.

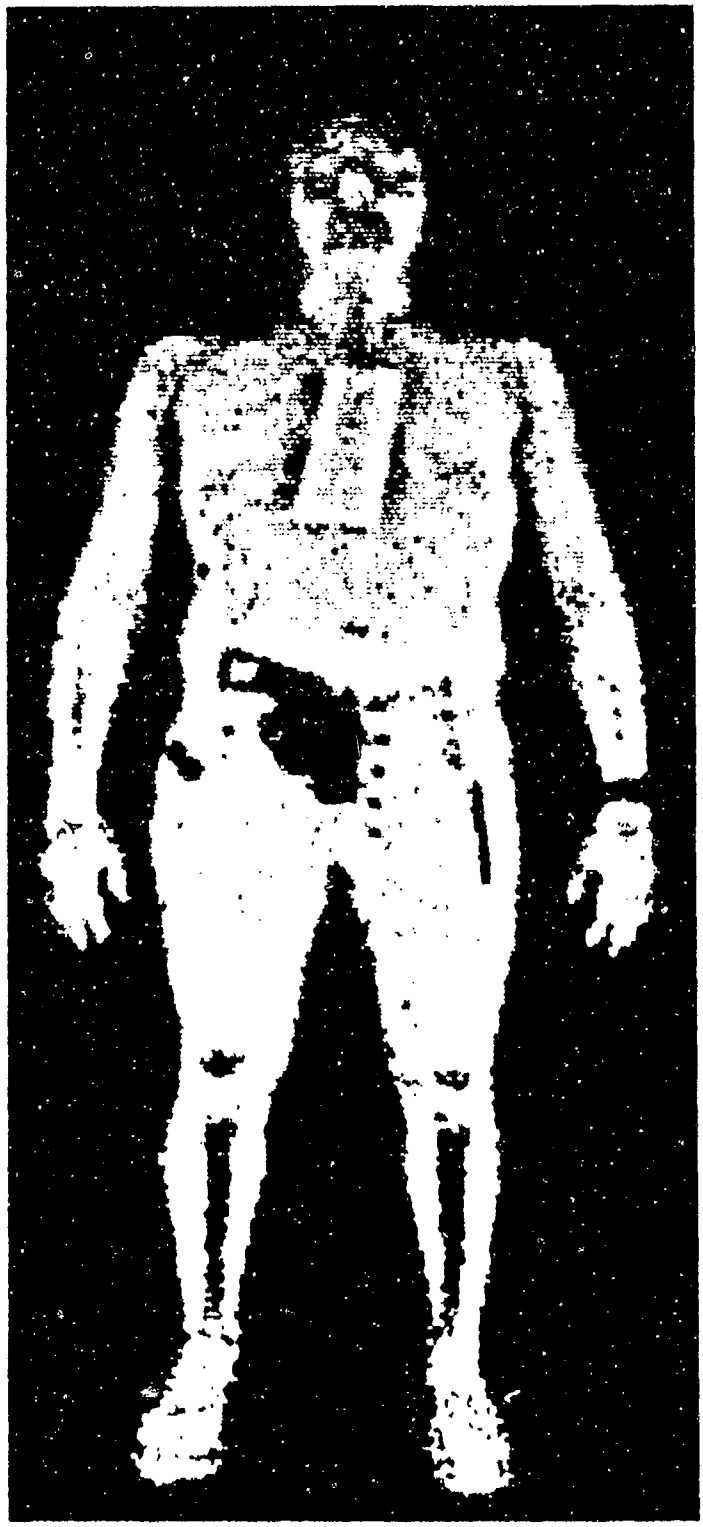


Figure 1. **The following concealed objects can be identified in this actual SECURE 1000 image: simulated one-half pound plastique explosive charge; .38 caliber handgun; two quarters; screwdriver with a plastic handle; metal watchband.**

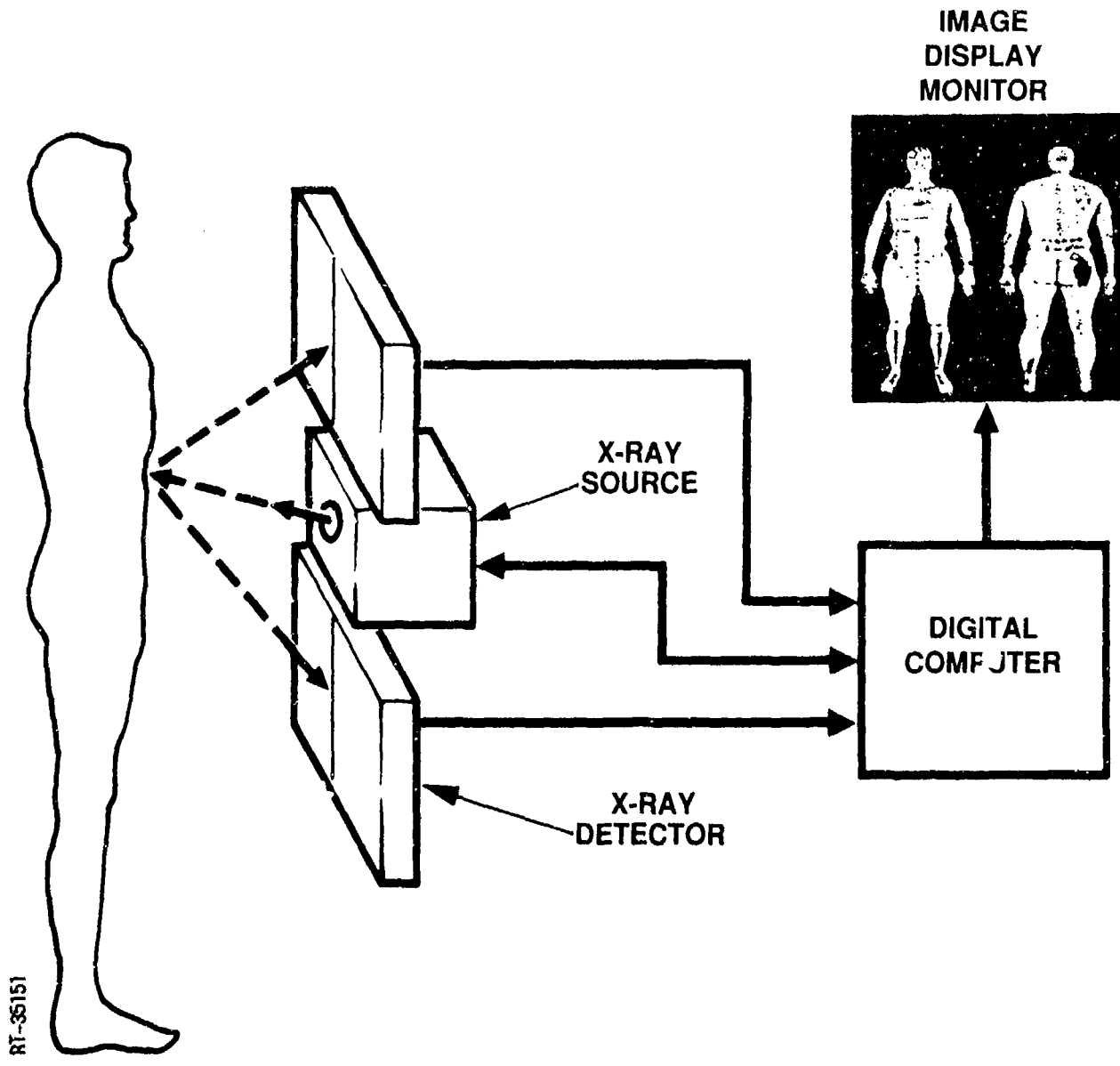


Figure 2. **The SECURE technique uses a scanning "pencil" beam of x-rays, back-scatter x-ray detectors, and computer processing to generate an image of the subject.**

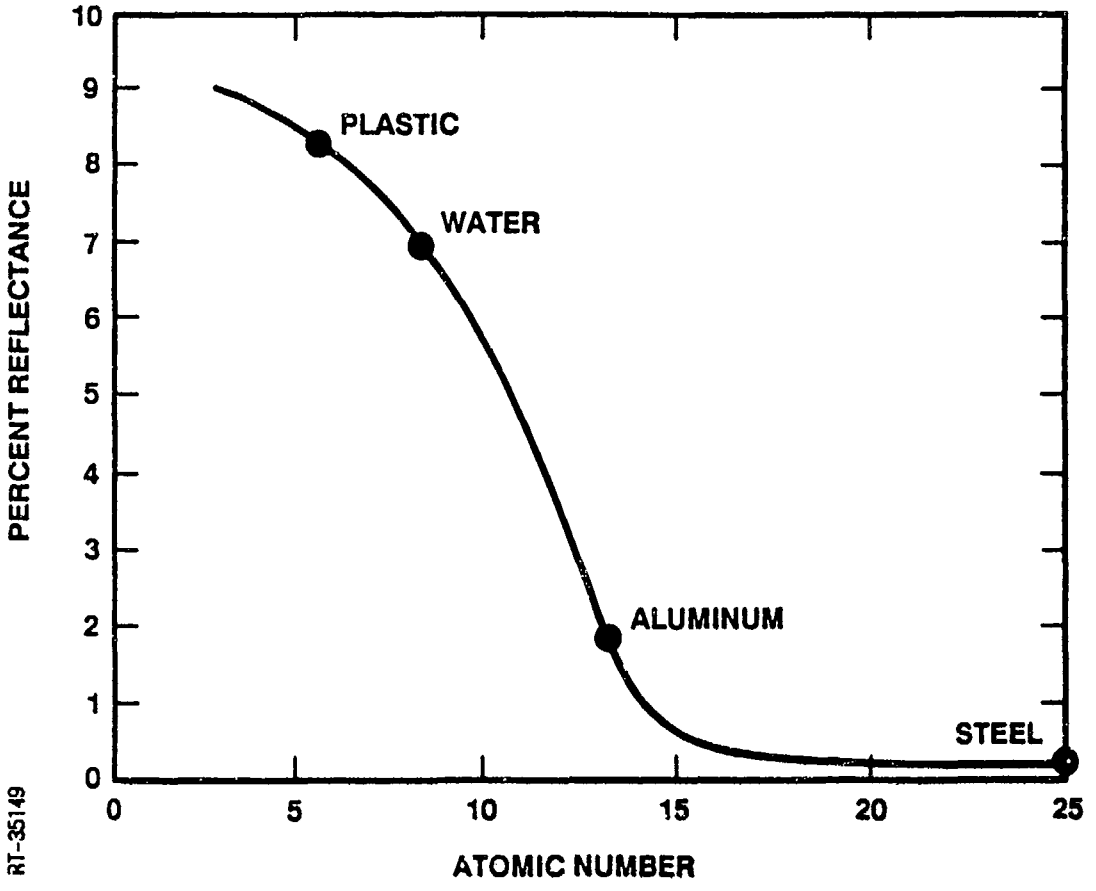


Figure 3. Low atomic number materials produce a much higher level of back-scattered x-rays than high atomic number materials.

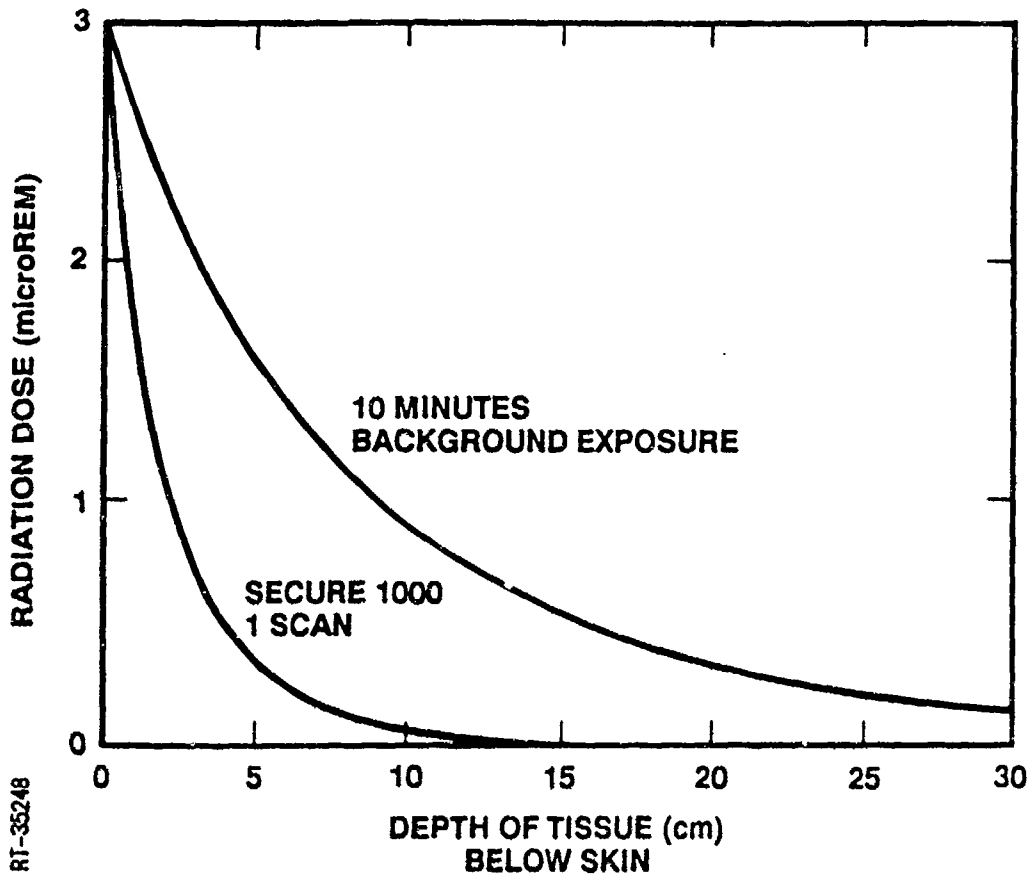


Figure 4. Naturally occurring background radiation is of significantly higher energy than used in the SECURE technique, resulting in deeper penetration into the body.

NEW X-RAY TECHNOLOGY FOR THE DETECTION OF EXPLOSIVES

D. Schafer, M. Annis, and M. Hacker
American Science and Engineering
Fort Washington
40 Erie St.
Cambridge, MA 02139

1. INTRODUCTION

Traditional X-ray transmission systems are not well suited to detection of low Z threats such as plastic explosives. Several different approaches have been implemented, such as backscatter and dual energy, to use X-ray imaging to detect these threats. The physical principles of X-ray interactions are used to interpret the results and to deduce the types of materials present in the luggage. These X-ray technologies are sensitive to the overall density and atomic number of the constituents and since plastic explosives are typically characterized by low atomic number (low Z) and high density (relative to other low Z materials), these techniques can be effective in locating explosive threats in many situations.

In an attempt to improve on the detection capabilities of the AS&E Model 101Z™, a new approach, based on forward scattering, has been investigated at AS&E. The physical background for this technology as well as some preliminary results of this investigation are presented.

2. BACKGROUND

AS&E manufactures and sells X-ray inspection equipment based on a flying spot technique. The technique is shown schematically in Figure 1. A rotating chopper wheel and a stationary slit form a thin pencil beam of X-radiation which is used to raster scan a bag. A single detector collects the transmitted radiation and converts it to an electrical signal. This signal is digitized, stored and used to create a visual image of the transmission of X-rays through the bag.

X-rays are removed from the pencil beam in one of two ways. They are either absorbed (photoelectric absorption), or they are scattered (Compton Scattering) by material in the bag (note: this approximation is only true in the energy range typically used to screen airport luggage; at higher energies, pair production must be considered). For transmission imaging, both processes contribute to the signal. The resultant signal is given by the formula in Figure 2. The integral is over the energy spectrum of the incident radiation. The exponential term is the attenuation along the line of sight associated with a given pixel for a given energy photon. Completing the equation is the probability of detection in the transmission detector times the energy of the photon (only true in energy sensitive detectors; in photon counting detectors this energy factor is not present). The transmission at any energy depends on the density of the material and on the total mass attenuation coefficient (μ_t) which describes both the scattering and absorption.

The total attenuation coefficient consists mainly of contributions from Compton scattering and from photoelectric absorption. Since the photoelectric absorption cross section is strongly energy dependent, the total attenuation coefficient is also strongly energy dependent in the region where the photoelectric effect is dominant. For metals such as iron, this is generally true up to energies in the range 100-150keV whereas for organic material (e.g. the element nitrogen, and plastic explosives), the Compton effect dominates at energies above approximately 20keV. Since the total absorption cross sections for low Z and high Z materials are different , it is possible to make two separate measurements at different energies to determine the amount of metal and the amount of low Z material present in an object. Traditional dual energy systems will employ the equations of Figure 2 using either two input energy spectrums, or two detectors with different $P_d(E)$, and some mathematical analysis to separate the amount of high and low Z materials.

When an incident x-ray photon undergoes a Compton scattering interaction there is a scattered X-ray photon whose energy is not far different from the incident X-

ray photon (the actual scattered photon energy is a function of the scattering angle). This scattered X-ray photon can also be detected. The Z technology manufactured by AS&E uses a flying spot technique coupled with detection of Compton backscattered radiation to produce images that directly highlight high-density, low-Z materials. Figure 3 shows a schematic of a Model 101Z backscatter system. Figure 4 shows the equation describing the expected measured signal from such a backscatter system using the same notation as in Figure 2. Again the first integral is taken over the incident X-ray spectrum as a function of energy. The next integral is taken along the line of sight in the bag. The scatter signal detected from each depth into the bag is treated differentially. The first term in the square brackets describes the attenuation of the beam from the front surface of the bag to the depth Z'. The second term in square brackets describes the probability of scatter per photon in the region of the pencil beam from Z' to Z'+ dZ'. The third term in square brackets describes the attenuation of the scattered radiation as it travels from the region of scatter to the scatter detectors over the total solid angle of those detectors, and therefore must be integrated over the solid angle subtended by the detectors. The factor $(P_d(E')E')$ again represents the detection efficiency for an energy sensitive detector. X-ray backscatter imaging is effective for detecting high-density, low-Z materials such as plastic explosives and narcotics in cluttered environments.

X-rays scatter from the object in all directions according to the Klien-Nishina formula for the differential scattering cross section. Since the X-rays that scatter in the forward direction must also traverse the remainder of the object, the raw forward scatter image contains a measure of the scatter probability as modulated by the total attenuation properties of the surrounding material. If the transmission image is also measured, an algorithm can be developed to produce separate images of low and high Z materials.

3. FORWARD SCATTER IMAGING

A new technique for detecting low Z materials with X-rays utilizes detection of forward scattered X-radiation. Figure 5 shows a forward scattering system in schematic terms. Figure 6 shows the equations for forward scattering for a monoenergetic beam of X-rays using the same notation as the previous equations. Note that as with backscatter, there is an integral over the thickness of the object; however, the second attenuation term is now integrated over the range from Z' to L. If the scattering angle is small the equation reduces as shown in equation 6a.

The more interesting case occurs when there are both high and low z materials in the beam. This situation is illustrated in Figure 7. The two equations in two unknowns can be solved to obtain the thicknesses of the two materials, as shown in the two equations. The above analysis is appropriate for a monoenergetic X-ray spectrum. Since it is not obvious that the technique will also work with the polychromatic spectrum produced by an X-ray tube, a Monte Carlo computer analysis was performed to simulate this situation.

4. MONTE CARLO CALCULATION

To test the Monte Carlo program, a monochromatic X-ray beam was used initially. Assumptions were made for energy efficiency for the transmission and scatter detectors based on the design of these detectors. Cross section information was included from the Compilation of X-ray Cross Sections[1]. Input parameters to the program included the amount of material of iron (X gm/cm^2) and the amount of plastic (Y gm/cm^2), and the X-ray energy. Each combination of material thicknesses is represented by a point on a graph of transmission signal vs. scatter signal. The results for 140kV X-rays are shown in Figure 8. From this Figure we can see that over the useful range of material thickness, there is a one to one mapping relating the pair of values (X,Y) to the pair of measured values (T,S), and therefore such a system could use the two measured values to deduce the material thicknesses.

Next the model was expanded to include a polychromatic spectrum typical of a filtered X-ray tube. It was not known whether the technique would extrapolate to this situation because of the way the cross sections, and therefore the total attenuation and scatter signals, change with energy. Figure 9 shows the results of this calculation. Again different amounts of plastic and metal are represented by different combinations of transmission and forward scattering signals. The separation between these points indicates that forward scattering technology can be used to separate high and low Z material in a practical system.

5. LABORATORY TESTING

A laboratory test was conducted to evaluate the

forward scattering technology. A two dimensional step wedge was constructed by placing a horizontally varying plastic step wedge behind a vertically varying steel step wedge to produce a pattern of rectangular regions each of which has different thicknesses of metal and plastic. A model 101Z source and transmission detector were used in addition to forward scatter detectors with electronics taken from a model 101Z backscatter detector. Each detector produced a separate image of the phantom, one in transmission and the other in forward scattering. Each of the rectangles was analyzed to obtain the average and standard deviation of the signal level for both detectors, and the results are plotted in Figure 10. The separation of the data points shows that forward scattering can be used to separate the high and low Z materials in this thickness range.

6. CONCLUSIONS

A Monte Carlo computer simulation and a simple experimental system was used to test the idea of using forward scatter and transmission data to measure the amount of high and low Z material in the path of an X-ray beam. These data indicate that a forward scattering system will have the capability to separate high and low Z material using a simple look up table of values of thickness for given signals. A system that uses this technology could then show separate images of metal and plastic only over a wide range of material thickness. This system will have certain advantages over both backscatter imaging and dual energy imaging. AS&E plans to implement forward scattering into the model 101Z systems under a later phase of a currently awarded contract (contract # DTFA03-90-C00047) with the FAA Technical Center to develop and test a automatic explosives detection system (EDS).

NOTES

1) Compilation of X-ray Cross Sections, W.H. McMaster, N. Kerr Del Grande, J.H. Mallett,and J.H. Hubbell, National Bureau of Standards, TID-4500,UC-34 Physics,UCRL-50174 Sec II, Rev 1

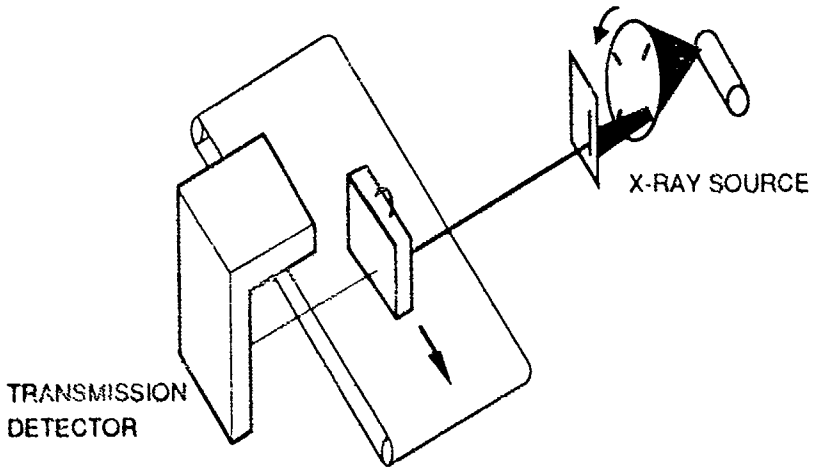


Figure 1.- Schematic diagram of Flying Spot System for Transmission only

$$T(x,y)=\int dE\, N(E)\, e^{-\left\{\int dz\, \mu_t(x',y',z',E)\, \rho(x',y',z')\right\}} P_d(E)\, E$$

where

$T(x,y)$ = the transmission at the x and y coordinates of the projected image.

$N(E)$ = number of incident X-ray photons between E & E+ δE

$\mu_t(x',y',z',E)$ = the total mass attenuation (cm^2/gm) coefficient as measured along the X-ray line of sight

$\rho(x',y',z')$ = the density (g/cm^3) of the materials in the bag along the X-ray line of sight.

$P_d(E)$ = the probability of detection of a photon of energy E incident in the detector

E = photon energy

This may be written in a simplified form:

$$T(x,y) = \int dE\, N(E)\, T(x',y',E)\, P_d(E)E \qquad (2a)$$

where

$T(x',y',E)$ = the transmission of the bag at energy E along the X-ray line of sight.

Figure 2

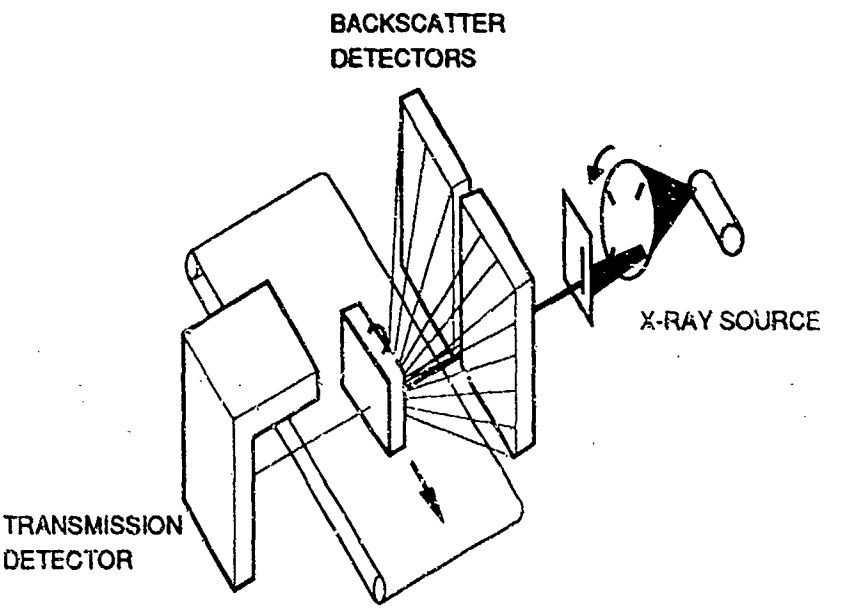


Figure 3.- Schematic diagram of Flying Spot System forTransmission and Backscatter

$$S(x,y)=\int dE\, N(E) \int dz' [e^{-\{\int_0^{z'} dt\, \mu_t(x',y',t,E)\, \rho(x',y',t)\}}][\, \mu_c(E)\, \rho(x',y',z')]$$
$$[\int d\Omega\, e^{-\{\int_{z'}^{0} dt\, \mu_t(x'',y'',t'',E')\, \rho(x'',y'',t'')\}}\,]\, P_d(E')\, E'$$

where the notation is the same as for the transmitted radiation, except

$S(x,y)$ = the scattered photon signal from the position (x,y) of the projected image.

Z = depth into the object along the pencil beam.

$\mu_C(E)$ = The Compton scattering cross-section as a function of energy. The cross section is also a function of angle. However the backscatter detectors used here sample a range of angles over which the cross section is nearly flat. This angular dependence is dropped for simplicity.

E' = The photon energy after scattering.

This may be simplified as :

$$S(x,y)=\int dE\, N(E) \left\{ \int_0^D dz'\, T(x',y',z',E)\ \mu_c(E)\rho(x',y',z')\ T'(x'',y'',z',E') \right\} P_d(E')\, E' \qquad (4a)$$

where:

$T(x',y',z',E)$ is the transmission of the bag at energy E along the X-ray line of sight to a depth Z', and

$T(x'',y'',z',E')$ is the transmission of the bag at E' from the depth z' averaged over the total solid angle of the scatter detectors.

Figure 4

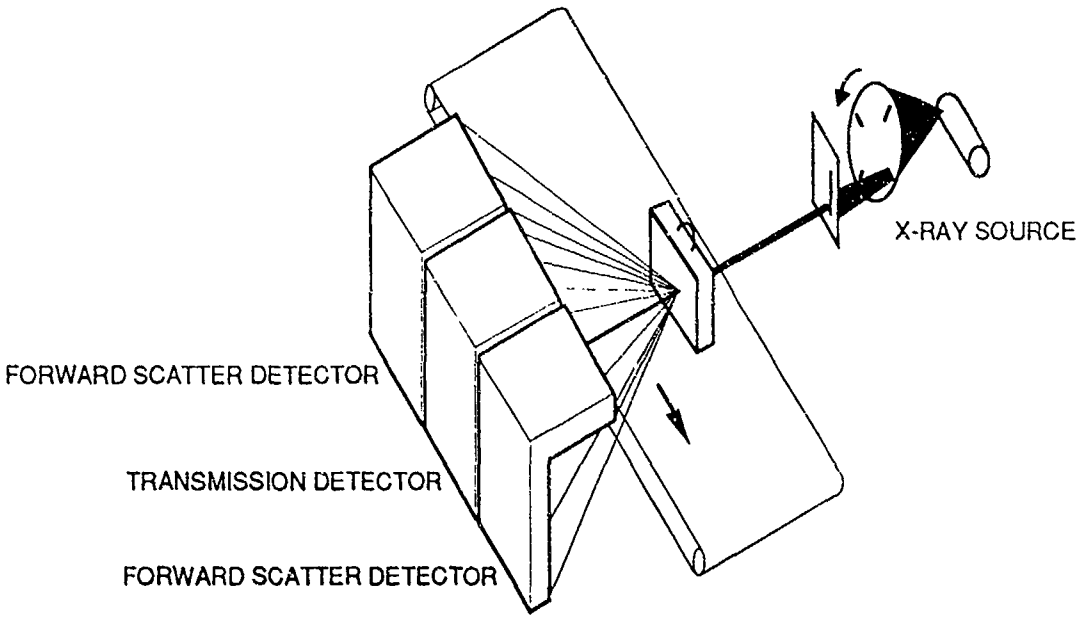


Figure 5.- Schematic diagram of Flying Spot System forTransmission and Forward Scatter

$$F(x,y)=\int dE\, N(E) \int dz' [e^{-(\int_0^{z'} dt\, \mu_t(x',y',t,E)\, \rho(x',y',t))}][\, \mu_c(E)\, \rho(x',y',z')]$$
$$[\int d\Omega\, e^{-(\int_{z'}^{L} dt\, \mu_t(x'',y'',t'',E')\, \rho(x'',y'',t''))}]\, P_d(E')\, E'$$

where the notation is the same as for the transmitted radiation, except

F(x,y) = the scattered photon signal from the position (x,y) of the projected image.

Z = depth into the object along the pencil beam.

$\mu_C(E)$ = The Compton scattering cross-section as a function of energy. The cross section is also a function of angle. However the Forward scatter detectors used here sample a range of angles over which the cross section is nearly flat. This angular dependence is dropped for simplicity.

E' = The photon energy after scattering.

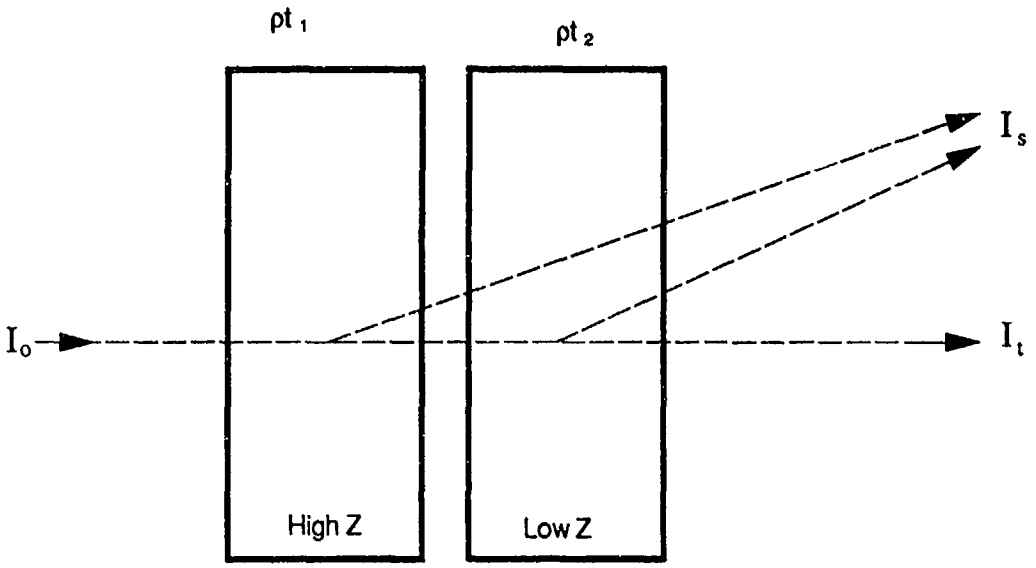
Since for small angle forward scattering, the photon energy is nearly unchanged and the scattered photon passes through nearly the same material as the primary beam, this may be simplified as :

$$F(x,y)=\int dE\, N(E) \left\{ \int_0^L dz'\, T(x',y',L,E)\, \mu_c(E) \rho(x',y',z') \right\} P_d(E')\, E' \qquad (6a)$$

where:

T(x',y',L,E) is the transmission of the entire bag at energy E along the X-ray line of sight.

Figure 6



$$I_s = I_o (\mu_{c1} \rho_1 t_1 + \mu_{c2} \rho_2 t_2) e^{-(\mu_{t1} \rho_1 t_1 + \mu_{t2} \rho_2 t_2)}$$

$$I_t = I_o e^{-(\mu_{t1} \rho_1 t_1 + \mu_{t2} \rho_2 t_2)}$$

Figure 7.- Geometry for separation of materials using forward scattering

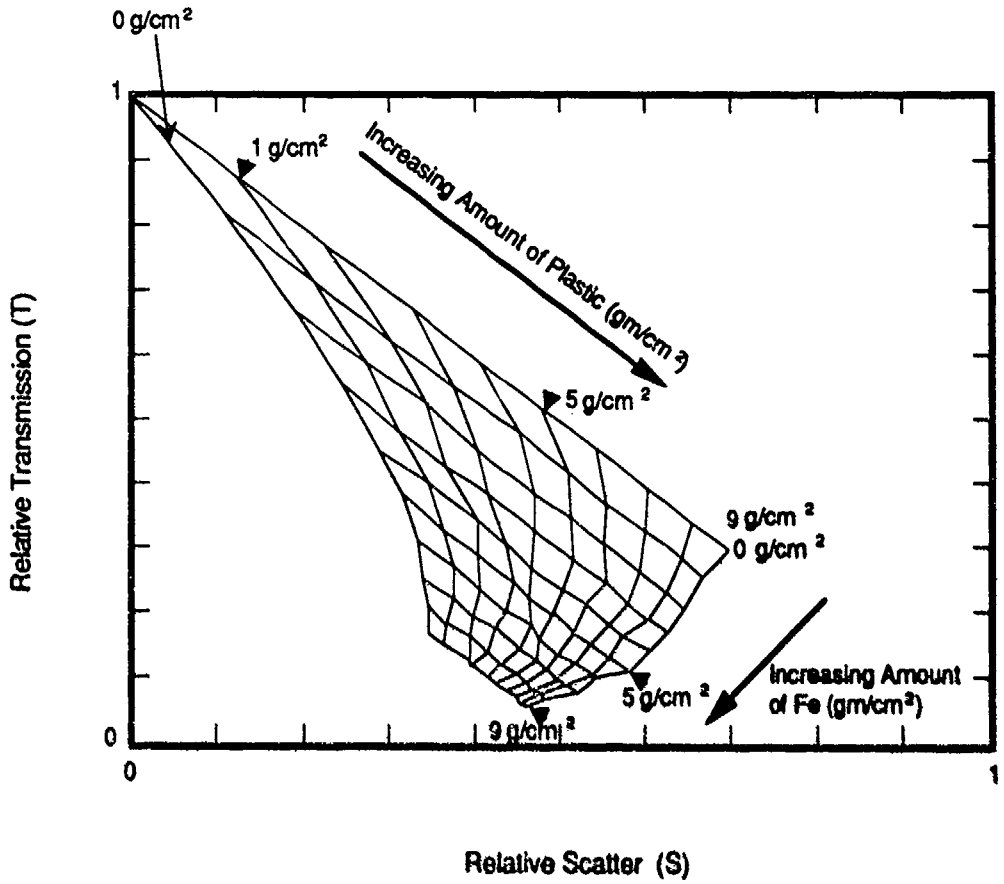


Figure 8.- Forward Scatter Monte Carlo calculation for 140 keV X-rays.

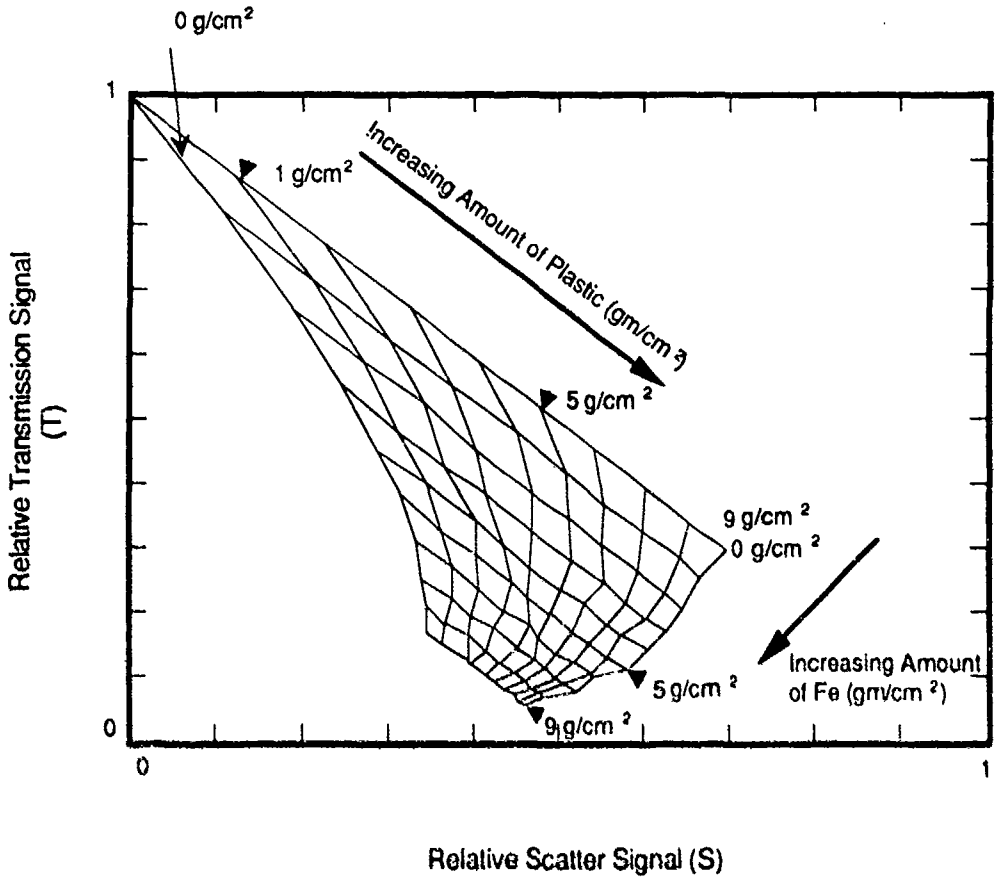


Figure 9.- Forward Scatter Monte Carlo calculation using X-ray tube energy spectrum.

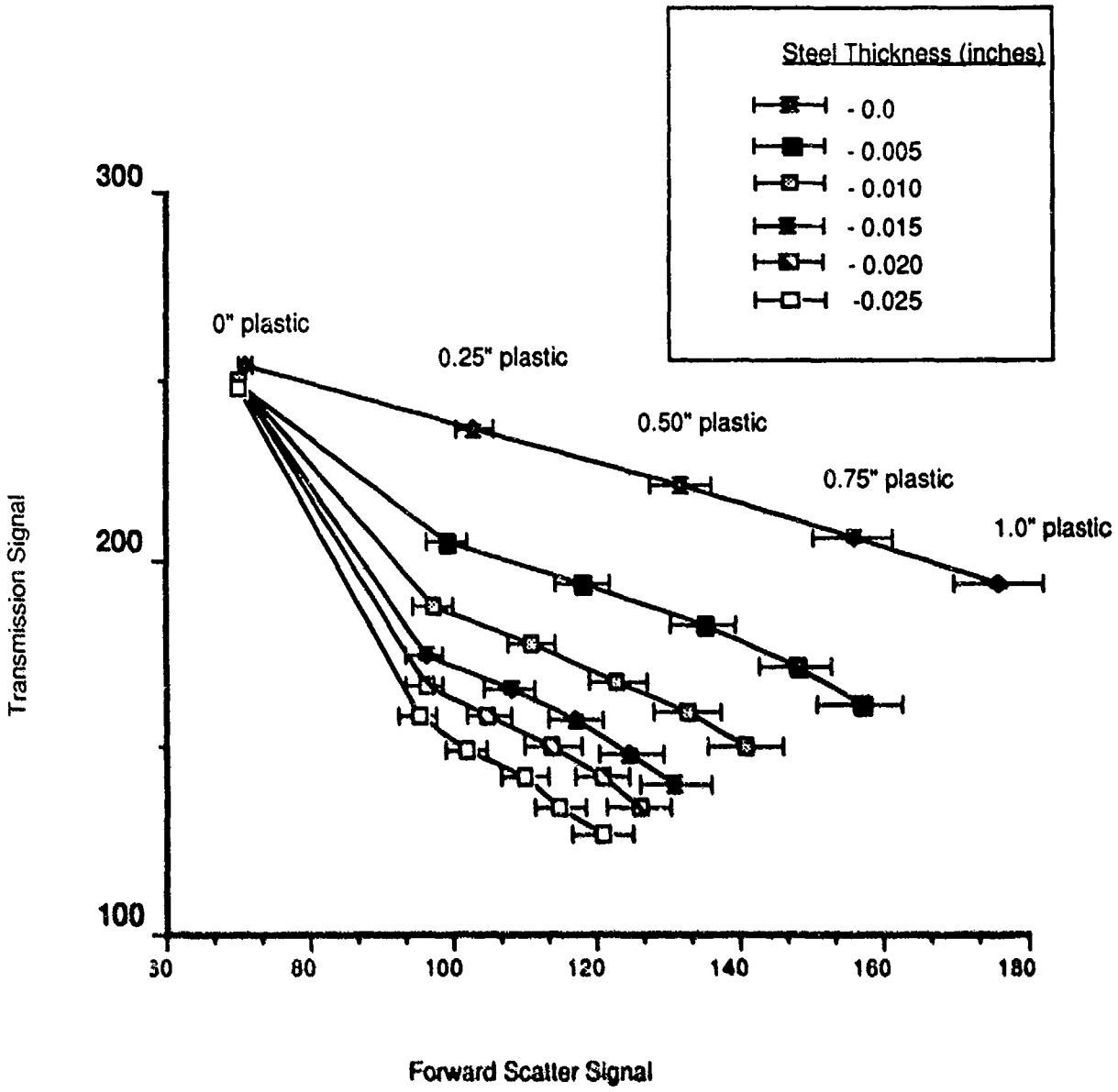


Figure 10. · Forward Scatter vs. Transmission · Data collected using a model 101Z X-ray source operated at 140kV, and Model 101Z transmission detector and backscatter detector located to collect forward scattered radiation.

ADVANCED DUAL ENERGY X-RAY FOR EXPLOSIVES DETECTION

Kristoph D. Krug and Jay A. Stein
Vivid Technologies
Waltham, MA

1. INTRODUCTION

The Vivid Rapid Explosives Detection System is a precision materials analysis instrument designed to automatically inspect airport baggage for the presence of explosive materials. The unit also features a high quality image and many imaging enhancements to aid human operators in baggage inspection and in visually clearing false alarms. The system is designed to physically resemble imaging-only x-ray machines now in place in airports around the world and is able to be used in any location where a conventional x-ray machine is currently installed.

2. SYSTEM COMPONENTS

The Vivid system combines an ultra-stable dual energy x-ray scanner, a high performance computer, and an advanced imaging system together with a unique software algorithm to achieve true materials analysis on objects in airport baggage.

The dual energy scanner provides precision high voltage pulses to an industrial quality x-ray tube to produce alternating x-ray pulses with 2 different energy spectra. This technique, in conjunction with an array of 960 detectors utilizing proprietary detector circuitry, provides high resolution and quality x-ray data with an accuracy, stability and reproducibility unmatched in the industry.

This data stream is sent to a high performance array of "super-micro" computers, based on transputers, manufactured by Inmos Ltd., and i860's, manufactured by Intel Corp. This computer power, which achieves peak rates of 200 million floating point operations per second (Mflops), is configured as a parallel processor with a very high Input/Output data rate and is expandable to over 400Mflops for future algorithm features and enhancements. Additionally, the machine is "network ready" incorporating an industry standard Ethernet(tm) connection utilizing standard protocols.

The operator's screen is a high resolution million pixel display commonly used in engineering CAD applications which provides bright and sharp black and white and color images.The software provides many advanced image enhancements with several unique image and threat analysis modes. The operator interface is designed to be familiar to current x-ray machine operators and compatible with airport operations and facilities.

The machine incorporates high reliability components and features extensive self-test and diagnostic capabilities to insure the high level of accuracy in an airport environment. It continuously monitors internal voltages, temperatures, and interlocks. An integral modem allows remote diagnosis for more accurate field service calls to minimize mean-time-to-repair. VDE/TUV certification is standard.

Current x-ray machines create images that roughly depict the composite atomic number, coded as a color change in the case of 'E-Scan'[1] or 'HiMat'[2] or as a white on black image for organic objects near the surface of a bag in the case of backscatter-based x-ray machines.

The composite atomic number methods are only able to broadly classify objects in bags as organic, inorganic, or metallic. Typical baggage contains mostly organic objects and so these images provide little discrimination between normal objects and the high explosives. Additionally, overlying objects and materials can shift the composite atomic number which confuses the ability to discern the composition of the object of interest.

The backscatter method images organic materials near the surfaces of bags but the backscatter photons generated have little penetrating power and are easily masked by overlying objects and materials.

The Vivid materials analysis system compares each object in a bag to its local background to determine the effective atomic number of the material in that

object. The effect of overlying objects and materials is effectively subtracted out thus yielding a measurement that is independent of other objects in the bag as well as the bag itself. This can only be done with data taken on an absolutely characterized and stable x-ray system and requires an extremely high level of computation, on the order of 500 million floating point operations per bag.

Typical detection images shown represent 2 organic objects with equivalent mass and densities and differing slightly in effective atomic number. One of the objects is, in fact, C4 high explosive. Detection is unchanged with the addition of a 1 inch thick aluminum plate. The C4 explosive in both cases is highlighted in red over the grey-scale image, the other object is rejected and is shown in normal grey scale.

The next image shows the same 2 objects in a different bag, and in a bag with a 1/16 inch steel plate overlaying the objects. The composite 'TriMaterial' image shows that the plate changes the color of the organic objects into the inorganic range. The Vivid detection image again shows detection of the explosive and rejection of the other organic material despite the intervening steel plate.

The effective atomic number of a material is shown to be an effective way to discriminate the 'plastic' explosives consisting of RDX and PETN-based materials. The window in effective atomic number is a relatively narrow slice of an admittedly large population of materials that can be found in airport baggage. Other explosives, due to their high nitrogen and oxygen contents such as TNT, also fall within this narrow window. The Vivid system is architected to allow for multiple 'windows' placed anywhere in the entire organic spectrum to simultaneously detect multiple types of materials, e.g. other types of explosives or drugs.

3. VIVID DETECTION ALGORITHM

The Vivid detection algorithm is an effective expert system for the detection of threats and contraband in baggage. The algorithm architecture is a multilevel analysis responsive to the full spectrum of explosive devices and baggage contents. Information utilized by the algorithm includes, but is not limited to, composition analysis, identification of bomb components, shape and other heuristics, as well as object definition, isolation and mass. Currently, over 150 separate parameters govern the performance of the algorithm. This parameter set can be tuned to a wide range of Probability of Detection/Probability of False Alarm rate settings, offering the user the capability of adjusting the machine in response to the local or changing levels of threat.

Testing and tuning of the algorithm is done on an extensive database of recorded baggage data. The bomb-free set was recorded at Logan International Airport in Boston, Ma. Over 1500 checked bags from 9 international carriers was recorded during a 2 week period in October 1990. The bomb set currently numbers over 700 and consists of various explosives concealed in heavily packed baggage.

The Vivid Rapid Explosives Detection System is designed to be an integral part of a multi-sensor Explosive Detection System (EDS) as well as a standalone security system. The Vivid Information Protocol is designed to allow information to be passed from the Vivid machine to other devices downstream to speed inspection and provide a high clearing rate. Industry standard networks (Ethernet) and protocols provide an easy and reliable interconnection.

Capabilities include machine control and status to enable integration with a high level host program, bag information, which can include ID, total mass of the bags, suitcase composition (cloth, metal, plastic), image data (for recording and display), and threat object information such as object ID, object location and size, object mass and estimated density.

This protocol could be utilized to implement a 'one-up review' system, which allows an explosives expert equipped with a Sun-based workstation which is networked to many Vivid machines to review images which cannot be cleared by the machine operators. This would allow a human expert to consult with each operator as required without moving from his remotely located workstation. Information could also be passed to a display system which would guide security personnel in hand inspections.

4. SUMMARY

In summary, the Vivid Rapid Explosives Detection System is an effective tool for airport security, available now and for the future. It can be utilized as part of an automated system of detection devices or as a standalone device combining machine decision threat detection with the best image, penetration, and resolution in the industry.

NOTES

1. Trademark EG&G Astrophysics, Long Beach CA.

2. Trademark Heimann GmbH, Weisbaden, West Germany.

3-DIMENSIONAL X-RAY IMAGING FOR THE DETECTION OF CONTRABAND

D.C. Shreve, R. Schirato, R. Polichar, and V. Orphan
Science Applications International Corporation
4161 Campus Point Court
San Diego, CA 92121

1. INTRODUCTION

Standard transmission radiography is used in many types of inspections. We are all familiar with the technique. Radiography allows the examination of the interiors of objects. X-ray images yield information about the shape and density of the items inside of an object.

One potential problem with transmission radiography for the detection of explosives is the difficulty in image interpretation when dense items obscure or confuse the observation of lower density objects. Our experience has shown that this can certainly be the case when one desires to detect explosives on the interior of containers which also contain metallic objects. The clutter caused by overlapping objects can be a serious problem in image interpretation.

This paper will describe X-ray laminography, a 3-dimensional inspection technique that can reduce the problems caused by overlapping objects in normal transmission X-radiography. An example of the technique will be presented.

2. TECHNICAL DISCUSSION

Laminography, or Tomosynthesis[1] as it is sometimes called, is a technique which produces images of "slices" through the object. These slices are generated from normal transmission radiographs taken at multiple angles.

The resulting individual slice images are similar to those obtained using computed tomography, but can be obtained in a fraction of the time necessary for a complete CT inspection. These slices can be combined to produce a fully three dimensional representation of the contents of the inspected object.

Laminography is based on a very simple geometric property. This basic principle is shown in Figure 1. The length of the projection of a line of length L is given by the equation

$$P = \frac{LH}{H-O}$$

where P is the length of the projection.
L is the length of the object line.
H is the distance between the source and image planes.
O is the distance between the image plane and the object line.

The length of the projection P on the image plane is seen to be independent of the lateral position of the source.

The two dimensional geometrical principle shown in Figure 1 can be extended to three dimensions as shown in Figure 2. In this figure we show three sketches of the projections of a two layer object with the X-ray source at different positions. The source is constrained to move in a plane which we call the source plane. The projections are measured on a second plane, parallel to the source plane, labeled the image plane. The object is assumed to have a Cross (X) on one of the layers and a Plus (+) on the other layer.

The positions of the projections move on the image plane as the source moves; but, by the geometrical argument given above, both the shape and size of the X-ray image are unaffected by the source position.

If one moves the imager as the source is moved (as shown by the box around the Plus) then the image of the Plus will be fixed at the same location on the imager as the movement progresses. Integration of the image during the motion will produce a sharp image of the Plus. The position of the X is seen to move across the image as the integration takes place. This will produce a blurred image of this feature.

The above example showed a linear motion of the source and imager. The motion of the source could

have been circular or, indeed, could have been along any arbitrary path.

Also, since only the relative motion is important, any two of the three components (source, object, and imager) could have been moved.

There are two data collection options when considering laminography. The first option of integrating during the motion was discussed above. In this method, the image of a single slice through the object is obtained.

In the second option, one takes "snapshots" of the X-ray image as the source is moving. The reconstruction of any slice through the object can then be obtained by properly shifting and adding the individual snapshots. This shift and add process is easily performed on digital images using an image processor.

This "multi-planar" approach is shown in Figure 3. In this figure we show a series of simulated X-ray snapshots of an object with three planes. The planes are assumed to have an O on top, a Plus in the center and an X on the bottom.

The snapshots are assumed to be obtained as the source and imager move in straight lines, with the center of the imager moving so that the Plus remains at the center of the image. The center column of images is shown unshifted. It is seen that the X and O move as the angle is changed. The other columns show the same snapshots after they have been scrolled.

The results of adding and normalizing the snapshots are shown at the bottom of the figure. If the images are simply added as shown in the center column, the image of the Plus adds coherently, producing a sharp image. The other two layers in the object produce multiple, lower intensity features in the summed image.

The right-hand column shows the addition after scrolling all of the images so the X adds coherently. The Plus and the O now produce blurred images.

The left-hand column shows the shift and add procedure so that the O is added coherently. In this case the Plus and X are blurred.

For the linear geometry shown in this case, the shift applied is simply a linear function of the source position. For other data collection geometries (eg. circular or elliptical), the shift necessary to produce the reconstructions will also be a simple function of the data collection geometry.

By properly shifting and adding the individual snapshots, one can obtain the reconstruction of any plane in the object.

3. RESULTS

In the present experiment, we examined a suitcase that was packed with a number of dense objects that could be found in typical suitcases. The objects included coat hangers, shoes with shoe trees, an aerosol can, coins, and other metallic objects. Also included was a sawed-up broom handle that was intended to simulate sticks of a low density explosive, and a hand calculator and battery pack intended to simulate a timing device. Wires connected the simulated timing device to a piece of solder used to simulate a detonator.

(This experiment was designed to demonstrate the principle of laminography. Neither the objects in the suitcase nor the simulations were designed to be representative of actual threats.)

A sketch of the experimental geometry is shown in Figure 4. The suitcase was placed on a large area, real-time X-ray imager and exposed by a 220 KVCP X-ray beam at about 30 degrees to the normal. The X-ray imager and the supported suitcase were rotated under computer control through 360 degrees with images being obtained every 4 degrees. These transmission radiographs were stored digitally and used to reconstruct the laminographic slices. (This is not the most appropriate geometry for laminography. Better results would have been obtained if the suitcase had been rotated on a separate table so that the plane which requires no shift in the addition process would have been located at the center of the suitcase instead of being below it. This would have allowed a much better use of the imager's available field-of-view.)

Figure 5 shows a transmission radiograph of the suitcase. The high density objects are easily identifiable. We can see the coat hangers, the aerosol can, and the shoes with the shoe trees. The simulated explosive and timing device are visible in this radiograph, but difficult to interpret. Laminographic reconstructions were obtained by shifting and adding these individual images. For the geometry used, these

shifts were

$$X_{shift}=V\cos(\theta-\theta_0)$$

$$Y_{shift}=V\sin(\theta-\theta_0)$$

where V is the height of the reconstruction,
θ is the angle of the individual measurement,

and θ_0 is the angle at which the measurements started.

It should be noted that there is only one parameter, θ_0, that must be determined experimentally.

Various heights were reconstructed by varying the parameter V.

Figures 6 to 9 show laminographic reconstructions through several sections of the suitcase. The objects at each layer are easily interpreted.

Figure 6 shows a slice approximately 3 inches above the bottom of the bag. The shoe trees and the top of the aerosol can are visible.

Figure 7 shows a slice about 2.3 inches above the bottom of the bag. The heels of the shoes, coat hangers and the bottom of the aerosol can are visible.

Figure 8 show a slice at an elevation of about 2 inches. The bottom of the heels of the shoes are visible along with coat hangers, coins and a cigarette lighter.

Figure 9 shows the reconstruction through the simulated explosive. The individual wooden sticks are visible as are the wires, batteries and simulated timing device. The presence of the other objects is almost completely eliminated in this image.

4. CONCLUSIONS

The conclusions of this demonstration are:

- Laminography can reduce the effects of clutter in radiographic images and aid in the detection of threats.

- Laminography presents 3-dimensional information of the inspected object.

The data collection and processing shown here could be performed in from 0.2 to 0.3 seconds per reconstructed slice using a modern imager processor[2]. (The time for reconstruction will depend on the number of individual images collected during a scan.)

In addition to the conclusions that can be drawn from this demonstration, we would also like to point out that laminographic techniques might be very useful for correlation with other 3-dimensional inspection techniques that are more specific for the detection of explosives.

The X-Ray Enhanced, Neutron Inspection System (XENIS) produced by Science Applications International Corp. several years ago attempted to correlate low resolution, 3-dimensional thermal-neutron-activation (TNA) data that detected the presence of nitrogen in an inspected object with high resolution, 2-dimensional transmission X-ray images. The correlation of high nitrogen concentration with relatively high X-ray attenuation indicated the presence of a potential explosive.

This correlation was hampered since the X-ray inspection system produced transmission radiographs. The images of metallic objects superimposed on low density objects with high nitrogen concentrations could cause large correlations with the TNA data, yielding false alarms, even though the metallic objects and the high nitrogen concentration objects were physically separated. The use of a laminographic X-ray inspection technique could increase the usefulness of the correlation technique.

REFERENCES

1. H. H. Barrett, W. Swindell, *Radiological Imaging, The Theory of Image Formation, Detection, and Processing, Vol II*, Academic Press, New York (1981), p 368.

2. For example, Recognition Concepts, Trapix Plus Image Processor. Recognition Concepts, Inc. 5200 Convair Drive Carson City, Nevada 89706.

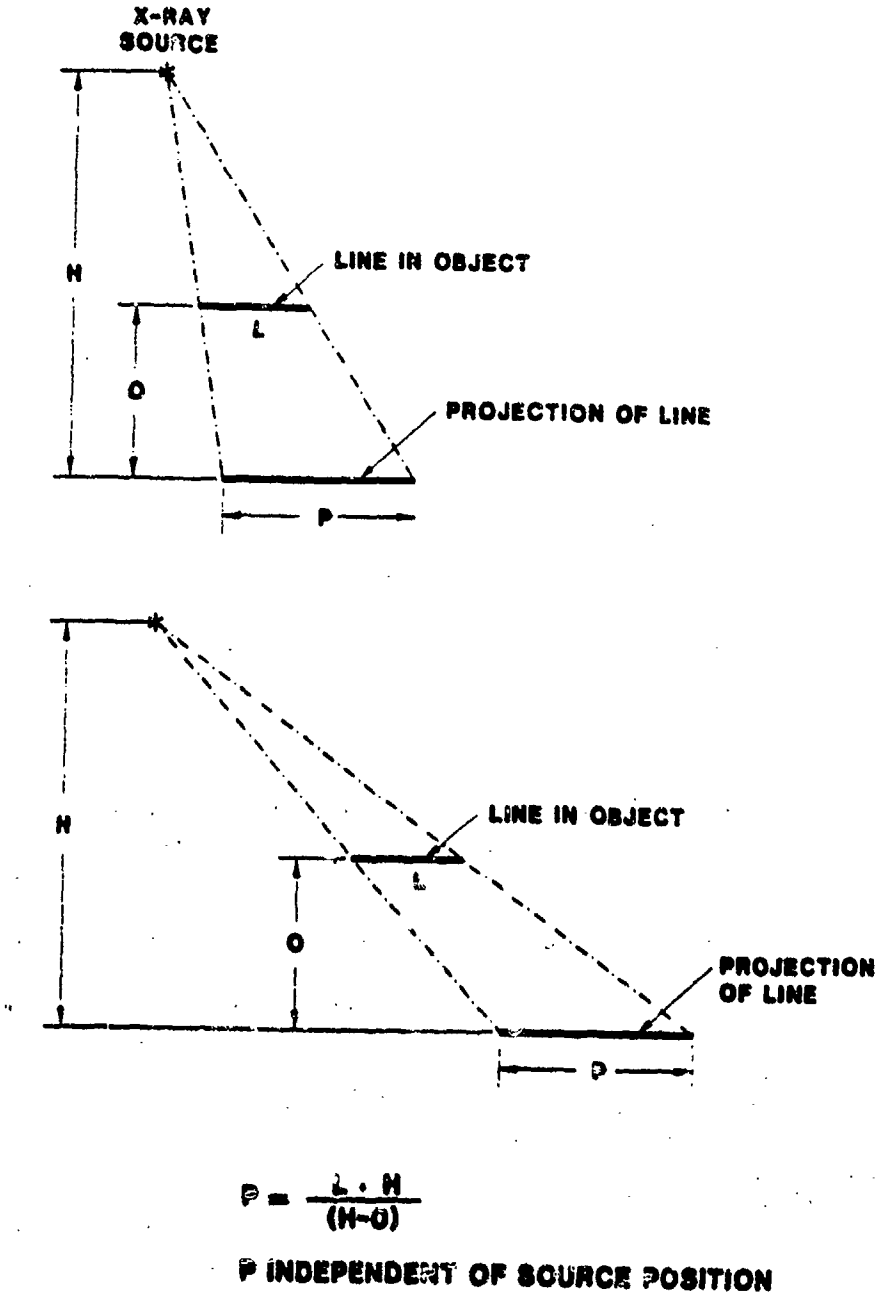


Figure 1. Geometrical Basis of Laminography. The length P of the projection of a line of length L is independent of the lateral position of the source.

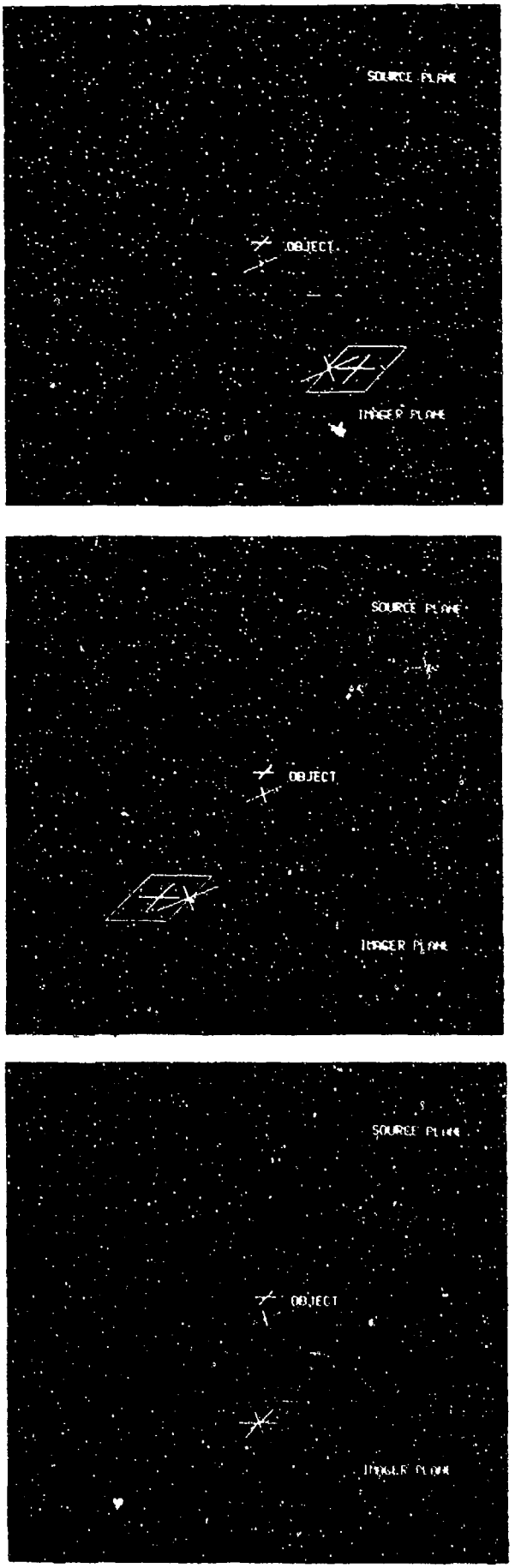


Figure 2. Three-Dimensional Sketches of Laminographic Geometry. The X-ray source is constrained to move in a plane. The three sketches show the source at three different positions and the resulting projections.

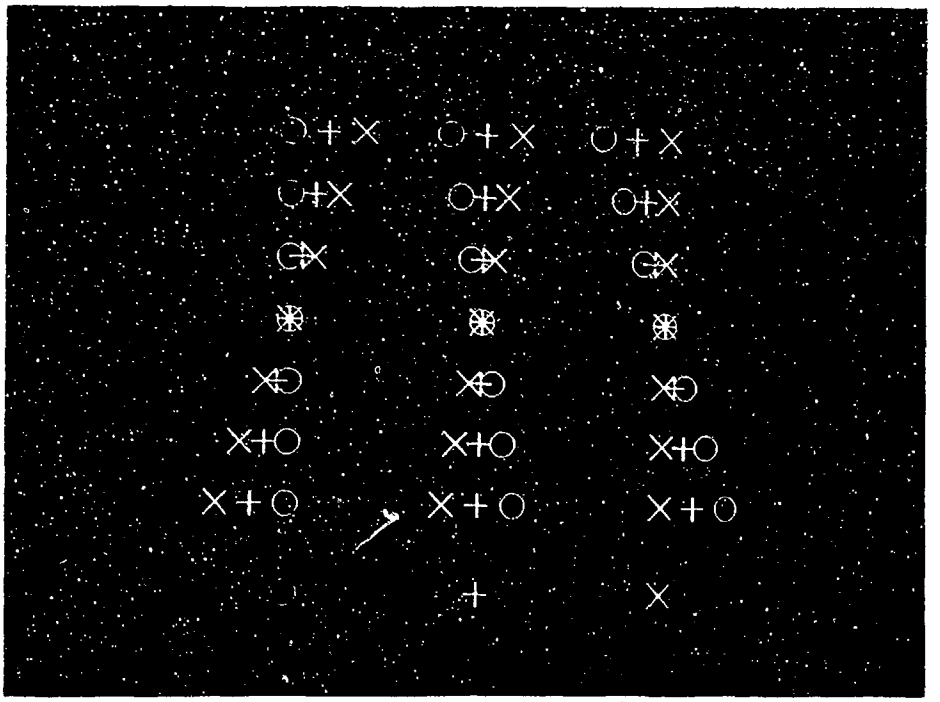


Figure 3. Illustration of the Process of Shifting and Adding Individual X-ray Images taken at Different Source Positions. The three columns show the same set of 7 simulated X-ray images with the horizontal positions of the images in each column being displaced before addition. The bottom row of images are the normalized sums of the images above them, showing the reconstruction of different layers in the object.

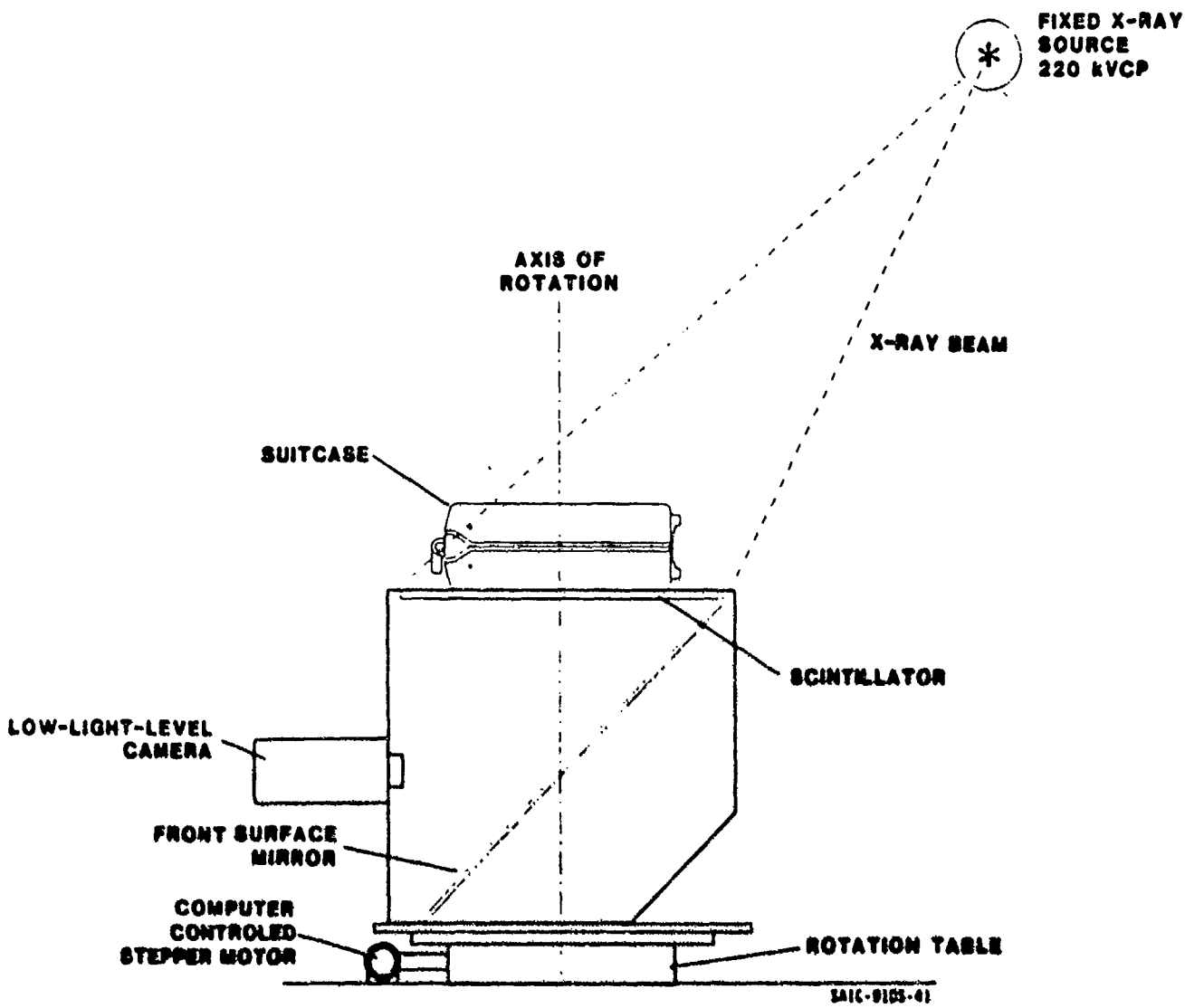


Figure 4. Sketch of the Experimental Geometry. The suitcase was placed on a rotating X-ray imager and illuminated by an X-ray source at about 30 degree orientation to the axis of rotation. Images were taken at 4 degree increments during a complete revolution of the imager and suitcase.

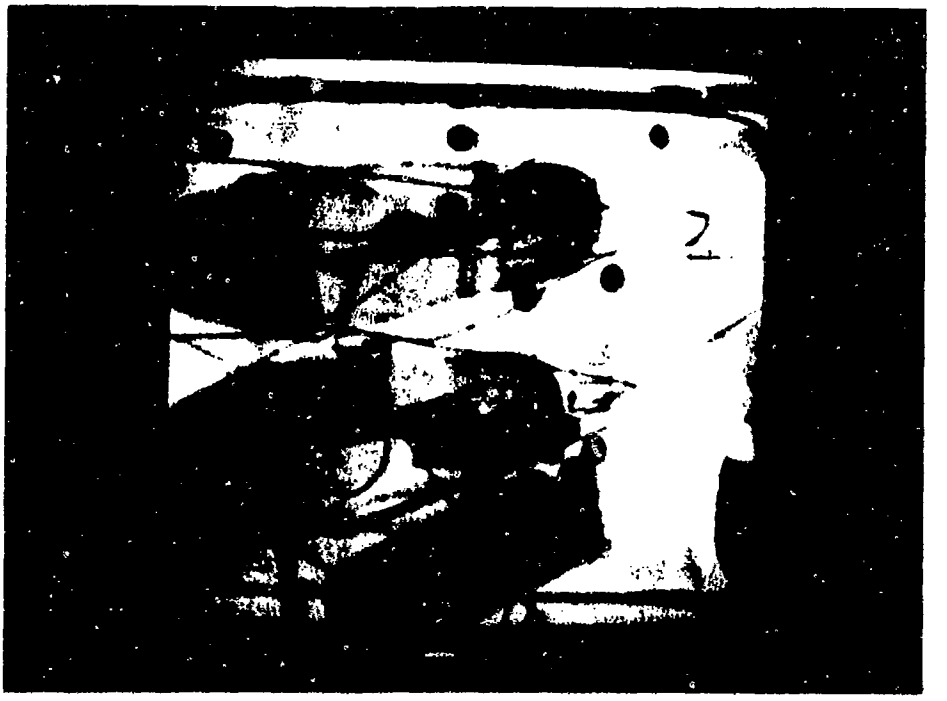


Figure 5. Transmission Radiograph of the Suitcase. The dense objects such as coat hangers, shoes with shoe trees, belt buckles, etc. are readily visible. The simulated explosive is visible, but difficult to interpret as a potential threat.



Figure 6. Laminographic Reconstruction of a Layer in the Suitcase 3 Inches above the Bottom. The shoe trees and the top of the aerosol can are visible.



Figure 7. Laminographic Reconstruction of a Layer about 2.3 Inches above the Bottom. The heels of the shoes, coat hangers, and aerosol can are visible.

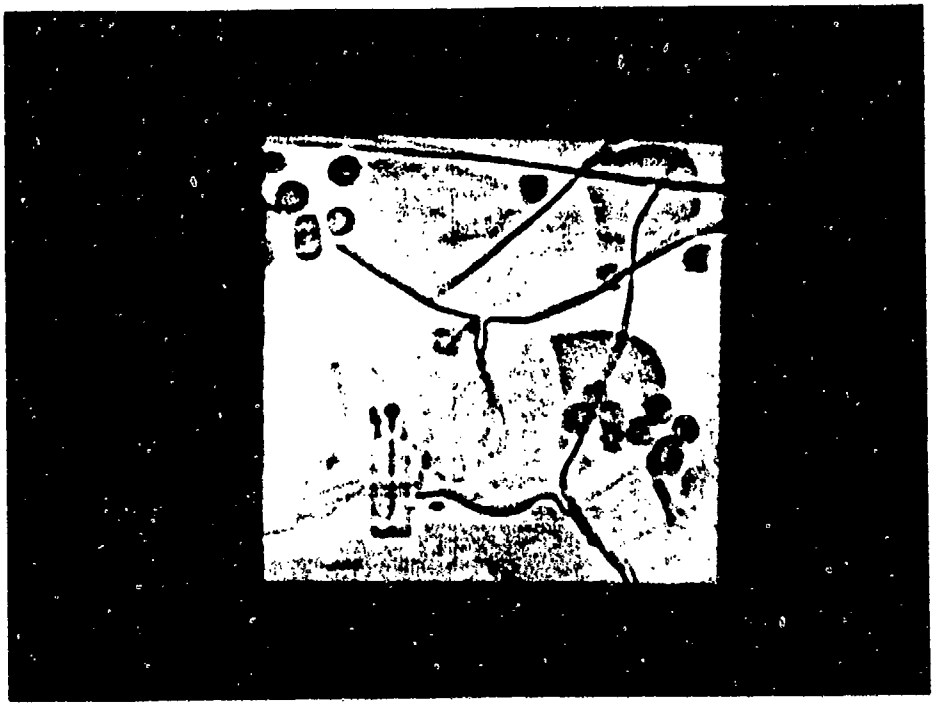


Figure 8. Laminographic Reconstruction of a Layer about 2 Inches above the Bottom of the Suitcase. The coat hangers, coins and a cigarette lighter are visible.

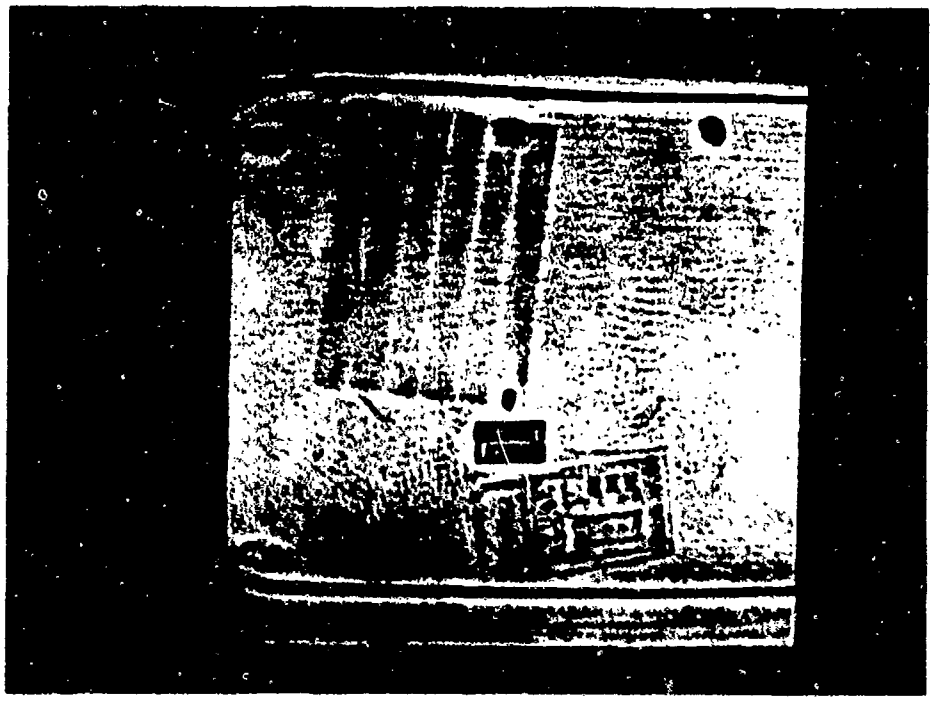


Figure 9. Laminographic Reconstruction of a Layer 0.3 Inches above the Bottom of the Suitcase. The simulated explosive, a battery pack, a pocket calculator, and wires are clearly visible. There is very little evidence of the overlapping structure that is apparent in the transmission radiograph.

THE EVOLUTION OF COMPUTED TOMOGRAPHY (CT) AS AN EXPLOSIVES DETECTION MODALITY

Fredrick L. Roder, Ph.D.
Imatron Federal Systems, Inc.

1. INTRODUCTION

There was a revolution in diagnostic radiology in 1972 - Godfrey Hounsfield announced the development of the world's first computed tomographic (CT) scanner. For the first time, radiologists did not have to decipher the vague x-ray shadows which spelled the difference between normal anatomy and ominous tumors. The scanner allowed organs to be seen directly and individually, just as they would have appeared to a surgeon, had a biopsy been necessary. Today, to physicians throughout the world, diagnosis without the added dimensions provided by CT scanning would be unthinkable.

The parallel between detecting a tumor in the body and an explosive device in a packed suitcase extends beyond the dire consequences of a misdiagnosis. Suitcases contain a varied array of innocuous materials - organic and inorganic; high density and low - which, when superimposed in conventional x-ray images, produce complex and cluttered shadow images not too dissimilar from the complex images produced by the interplay of internal organs and bones. Just like a tumor, an explosive device can easily be missed. Even in its infancy, when eight minutes were required to perform a CT scan, the applicability of this technology to the explosive detection problem was obvious.

The first CT explosives detection experiments were performed on the first CT scanner built in the United States - the ACTA I scanner at Georgetown University. The results of that study were presented at the March 1978 joint meeting of the Biophysical and American Physical Societies[1] and more fully in a technical report published by The Aerospace Corporation.[2] Despite the promising results of this and subsequent studies of CT explosives detection, however, this technique remained in the province of research because the small aperture and relatively long image acquisition and reconstruction times of existing medical scanners made them ill-suited to the explosives detection application. For CT explosives detection to be practical, a scanner would have to:

1. Have a physical and image aperture of sufficient size to accommodate large luggage.
2. Rapidly acquire image data.
3. Rapidly reconstruct these data into cross-sectional images.
4. Produce images with sufficient resolution to allow the automated detection of sheet explosive.
5. Perform these functions continuously, over extended time periods.

In this paper, we will trace the progress made toward each of these goals, culminating in the current development of the CTX Explosives Detection System. We will also briefly discuss the tests to date which have demonstrated the efficacy of this technique, and extrapolate to the manner in which a CTX system will be used in an airport.

2. THE EVOLUTION OF CT EXPLOSIVES DETECTION

2.1 Scan Speed

The first CT scanner, the EMI Mark I, used a single detector in a translate-rotate geometry and required four minutes to acquire the data for one image. Increasing the number of detectors to approximately 20 (a "second-generation" geometry) reduced the scan speed to about 20 seconds. "Third-" and "fourth-generation" geometries, which utilized hundreds or even thousands of detectors in a rotate-only mode, allowed scan times to be reduced to about one second. Further reductions proved infeasible for any system which required physical motion. The next advance was achieved by Imatron, which, in 1984, shipped its first Ultrafast CT scanner (Figure 1).

This scanner, developed to provide three-dimensional motion pictures of the beating heart, used electron beam technology to acquire up to 34 images/second. The decrease in scan time from 1972 to the present is shown in Figure 2.

Scan speed in a medical CT scanner is of paramount importance to image quality: motion during a scan degraded the resulting image, and the human body is in constant motion. However, a subsecond scan speed does not necessarily mean a large number of scans/hour. The x-ray tubes in conventional medical scanners overheat if too many scans are taken in succession, and even the Imatron Ultrafast scanner (which is not subject to overheating) is subject to data handling and image reconstruction limitations. As a result, less than 100 scans/hour are obtained by conventional hospital-based CT scanners. Increasing scanner throughput (scans/hour) required a fresh look at the problem.

2.2 Throughput

The throughput problem was addressed by Imatron in 1987, under the auspices of the U.S. Army Medical R&D Command. The Army needed a CT scanner for use in military field hospitals for mass casualty care, where time is of the essence, and surgeons cannot wait for a CT scan to be scheduled, executed, and interpreted. In response Imatron produced the FMS 5000, the first CT scanner designed for continuous operation and pipelined reconstruction. See Figure 3. In addition to its continuous duty cycle and high-speed reconstruction, the small size, light weight, and low power requirements of this scanner represented major design breakthroughs. The designed principles developed and implemented in the FMS 5000 have been employed and extended in the CTX 5000 Explosives Detection System. Figure 4 illustrates the increase in throughput (scans/hour) of CT systems from 1972 to the CTX 5000.

2.3 Image Reconstruction Time

With the development of the electron beam Ultrafast CT, scanning speed ceased to be an issue. Only image reconstruction speed limited CT explosives detection performance, and this was a limitation entirely within the domain of the rapidly advancing computer industry. The FMS 5000 demonstrated that a high-resolution (512 X 512) cross sectional image with extremely high density resolution (4,000 grey levels) could be reconstructed in 13 seconds. Thanks to continuing advances in computer technology, the CTX Explosives Detection System (Figure 5) will have an image reconstruction time of less than 3 seconds, and shorter reconstruction times can be expected in future generations. The decrease in image reconstruction time since 1972 is illustrated in Figure 6.

2.4 Aperture and Image Matrix Size

The first CT scanner, the EMI Mark I, had an image diameter of 25 cm and a reconstruction matrix of 160 X 160 pixels. The CTX Explosives Detection System has an image diameter of 80 cm (more than enough to accommodate a 16 X 26 X 32 in. suitcase) and a reconstruction matrix of 512 X 512 pixels. The increase in CT image diameter and reconstruction matrix size since 1972 is shown in Figures 7 and 8, respectively.

3. EFFICACY OF CT EXPLOSIVES DETECTION

Initial studies of CT explosives detection involved a few explosive samples, a few simulants, and as wide a variety of innocuous materials as could be conceived of by the researchers involved. In addition to the Georgetown University and Aerospace studies, experiments were conducted by Varian Associates[3] and by UCLA.[4] From these studies, it became apparent that explosives could be characterized as dense organic materials, and, as such, could be differentiated from the vast majority of objects which could be expected to be commonly encountered in suitcases. However, without a substantial data base for explosives and for the population of objects actually encountered in suitcases, the efficacy of CT for explosives detection remained, at best, problematical. Certainly, materials existed which mimicked the CT characteristics of explosives. The real question, however, was the frequency with which these materials would be encountered in checked luggage in the real world. The first serious attempt to address this question was a study performed by Imatron during the summer of 1987. This study was funded by the FAA and performed under a subcontract from UCLA.[5]

The explosives characterization study was performed at the Bureau of Mines (BoM) in Pittsburgh. In this study, ninety three distinct explosive products were

examined using a medical CT scanner, as well as a set of sheet explosive samples differing only in thickness. These explosives constituted all the cap-sensitive products resident in the BoM magazines at that time. Included were 31 water gels, 15 emulsions, 28 dynamites, and 18 products which contained military explosives. While it is believed that this represents the most extensive explosives characterization study ever performed for purposes of explosive detection research, this number of explosives products is still negligible compared to the total number of products produced in the United States and throughout the world.

The suitcase characterization study was performed using the same medical scanner at Los Angeles International Airport (LAX). Data from a total of 700 suitcases were compiled, measuring the CT values for the six most explosive-like materials in each suitcase.

The BoM-LAX study (and all previous CT explosives detection studies) included the acquisition and analysis of dual-energy as well as single-energy data. Dual-energy x-ray techniques were originally developed as an adjunct to computed tomography. Initial studies included the explosives detection cited above, as well as medical research conducted by Rutherford et al.[6] in the United Kingdom and by Brooks and DiChiro[7] in the United States at the National Institutes of Health. However, it was the technique developed by Alvarez and Macovski[8] at Stanford University which established dual-energy CT as a valid quantitative measure of the average atomic number and electron density of each region within a cross sectional image. A variant of this technique will be employed on an "as-needed" basis by the CTX Explosives Detection System.

The results of the BoM-LAX study were promising, both in terms of the automated detection of explosives in general and plastic and sheet explosives in particular, and in terms of the information which CT images were demonstrated to provide to an operator, permitting the fast and unambiguous resolution of potential alarms. On the basis of these results, Imatron initiated the in-house development of a CT explosives detection system, the progenitor of the CTX.

4. OPERATIONAL DEPLOYMENT OF THE CTX EXPLOSIVES DETECTION SYSTEM

The CTX will operate continuously and automatically, simultaneously acquiring image data, reconstructing images from these data, and analyzing the resulting images to automatically detect and identify threats. Each image cycle will require less than 3 seconds. Images identified by the CTX as containing possible threats will be provided to a system operator. The possible threat object will be identified to the operator both in the image and by other measured characteristics. If the operator cannot identify and exclude the possible threat object as innocuous, the system continues its analysis, obtaining a full three-dimensional data set for the now-suspect object. The three-dimensional data may be analyzed by the same operator, or transferred to a better-trained "expert" operator. If the suspect object cannot be identified as innocuous by the expert operator, given all the information provided by the CTX system, we believe that it is time to call the bomb squad.

The CTX Explosives Detection System may be employed as either a stand-alone system, embodying primary, secondary, and tertiary detection and decision functions; or in conjunction with an inclusive primary screening device, in which case it will serve secondary and tertiary detection and decision functions.

In a stand-alone configuration, the scan planes are selected automatically, on the basis of x-ray projection data obtained by the CTX. The number of scan planes selected will be determined by the defined threat and by the nature of the suitcase population. A minimum number of scans will be required in any case to identify sheet explosive, which is essentially invisible in projection data.

Alternatively, the CTX may be used in conjunction with another explosives detection device, even if that device identifies a large fraction of suitcases as containing threats, provided that that device is inclusive (i.e., that it does not miss any explosives). Primary screening devices that generally localize possible threat objects aid in the scan plane selection process, and will increase overall system throughput.

5. CONCLUSIONS

Since its development in 1972, computed tomography has evolved rapidly in terms of scan speed, throughput, reconstruction time, aperture, and image matrix size. As a result, it is now possible to consider the deployment of a CT explosives detection system as practical and operationally viable. The

efficacy of CT as an explosives detection modality has long been proposed, and field data obtained to date support this proposition. The current development of a field prototype CT Explosives Detection System under the auspices of the FAA Technical Center will provide the tool to fully explore the capabilities of this modality in real-world environments, both as a stand-alone system and in conjunction with other explosive detection devices.

REFERENCES

1. F.L. Roder, H.K. Huang, and M. Cerroni, "Determination of the Atomic Number and Electron Density of Biomaterials by Dual-Energy Tomography," Abstracts of the Joint Meeting of the Biophysical Society and the 22nd Annual Meeting of the American Physical Society (American Institute of Physics, New York, 1978).

2. F.L. Roder, "Preliminary Feasibility Investigation -Explosives Detedtion by Dual-Energy Computerized Tomography" (The Aerospace Corporation, El Segundo, California, 1978), ATR-78(3860-06)-1ND.

3. R.E. Alvarez, J.T. Arnold, and J.P. Stonestrom, "The Characterization of the Ablilty of a Conventional Dual Energy Medical CT X-Ray Scanner to Distinguish Explosive," Varian Associates, Inc. Final Report on FAA Contract No. DOT-FA78-W-4247 (1979).

4. H.K. Huang, "New Detection Concepts," Phase I Final Report on FAA Contract No. DTFA03-85-C-00037 (1986).

5. "Dual-Energy Computed Tomographic Explosive and Suitcase Characterization Study, "Imatron Final Report to the Department of Radiological Sciences, University of California, Los Angeles under FAA Contract No. DTFA03-85-C-00037.

6. R.A. Rutherford, B.R. Pullan, and I. Isherwood, Neuroradiology **11**, 15 (1976); **11**, 23, (1976).
7. R.A. Brooks and G. DiChiro, Radiology **126**, 255 (1978).

8. R.E. Alvarez and A. Macovski, Phys. Med. Biol. **21**, 733 (1976).

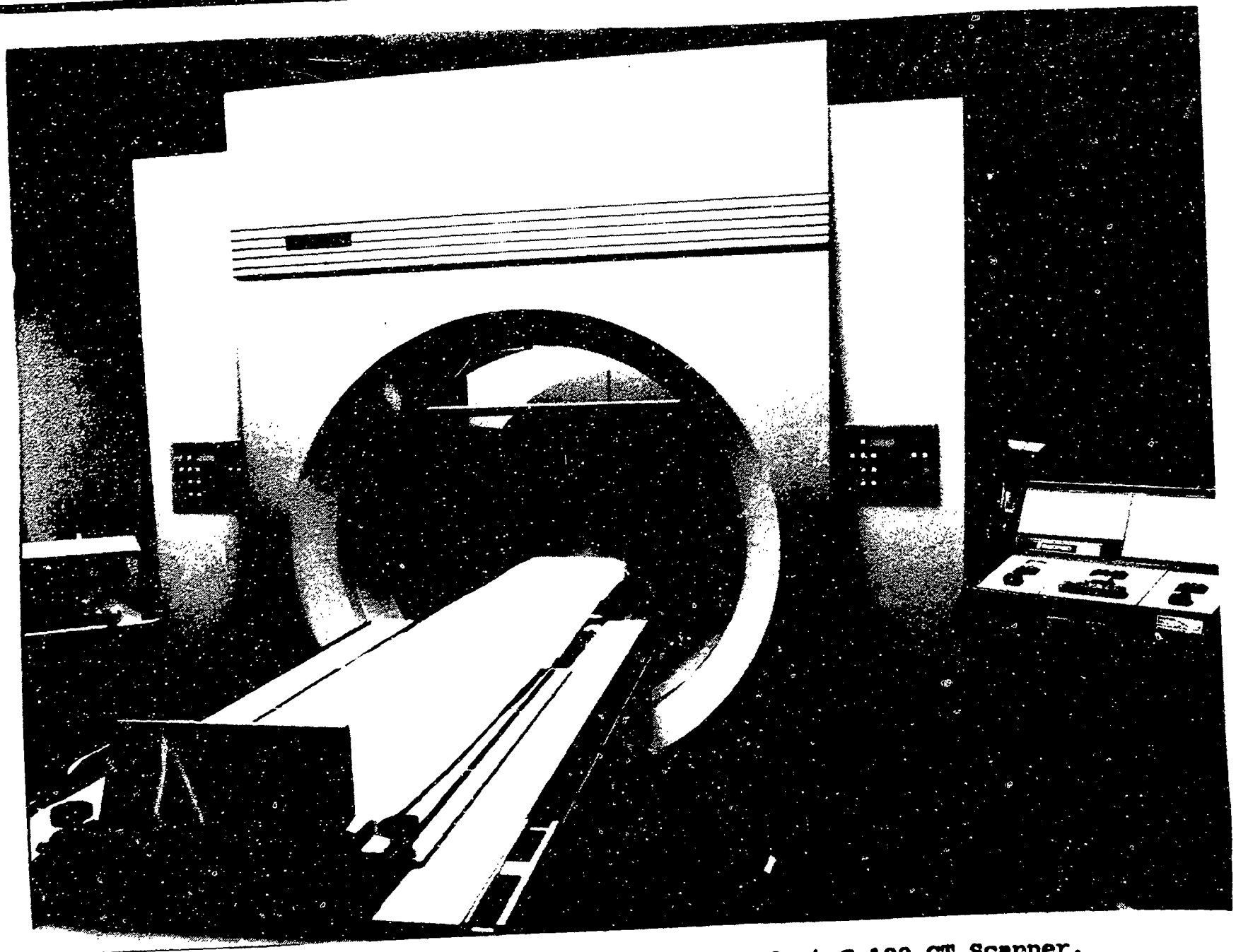


FIGURE 1. The electron beam Imatron Ultrafast C-100 CT Scanner.

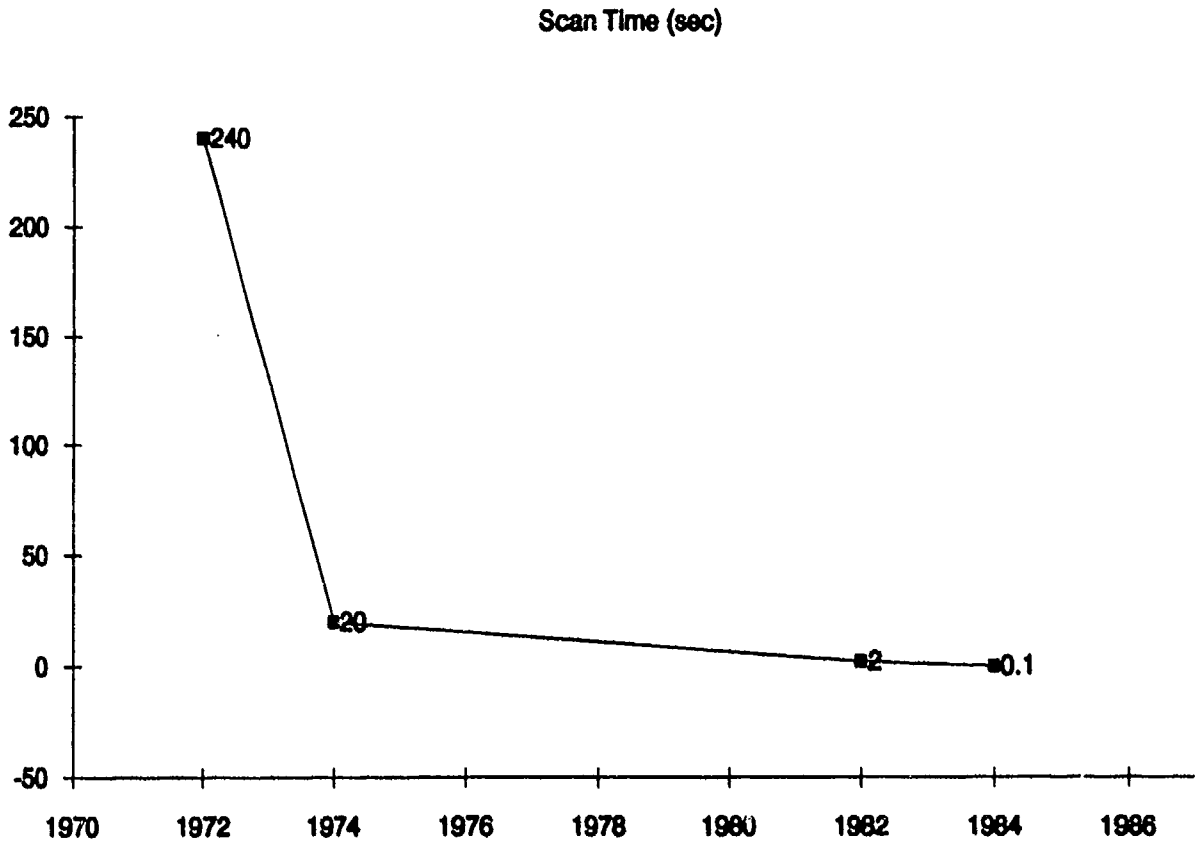


FIGURE 2. Decrease in scan time per image (1972 - present).

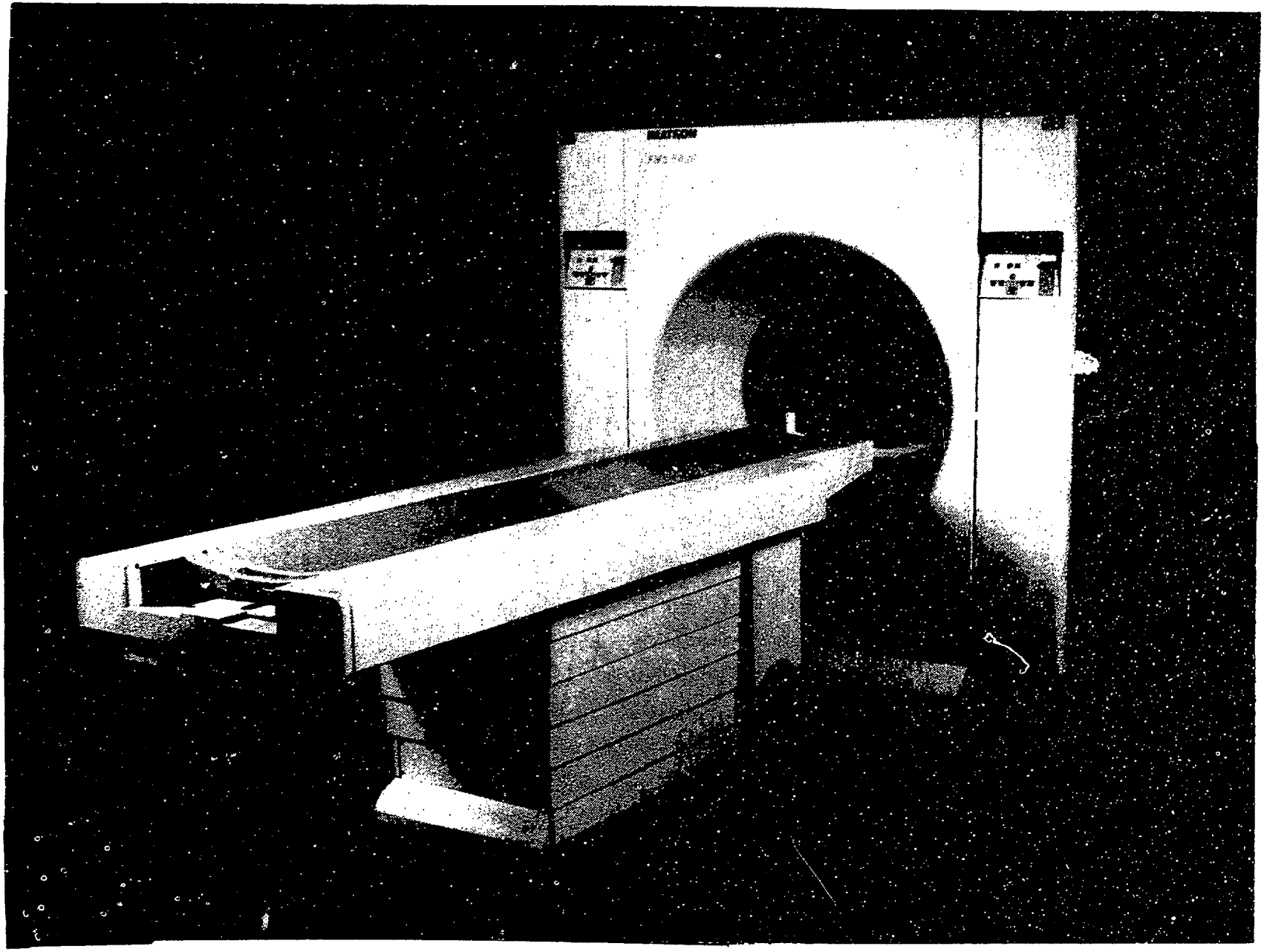


FIGURE 3. The high-throughput Imatron FMS-5000 CT Scanner.

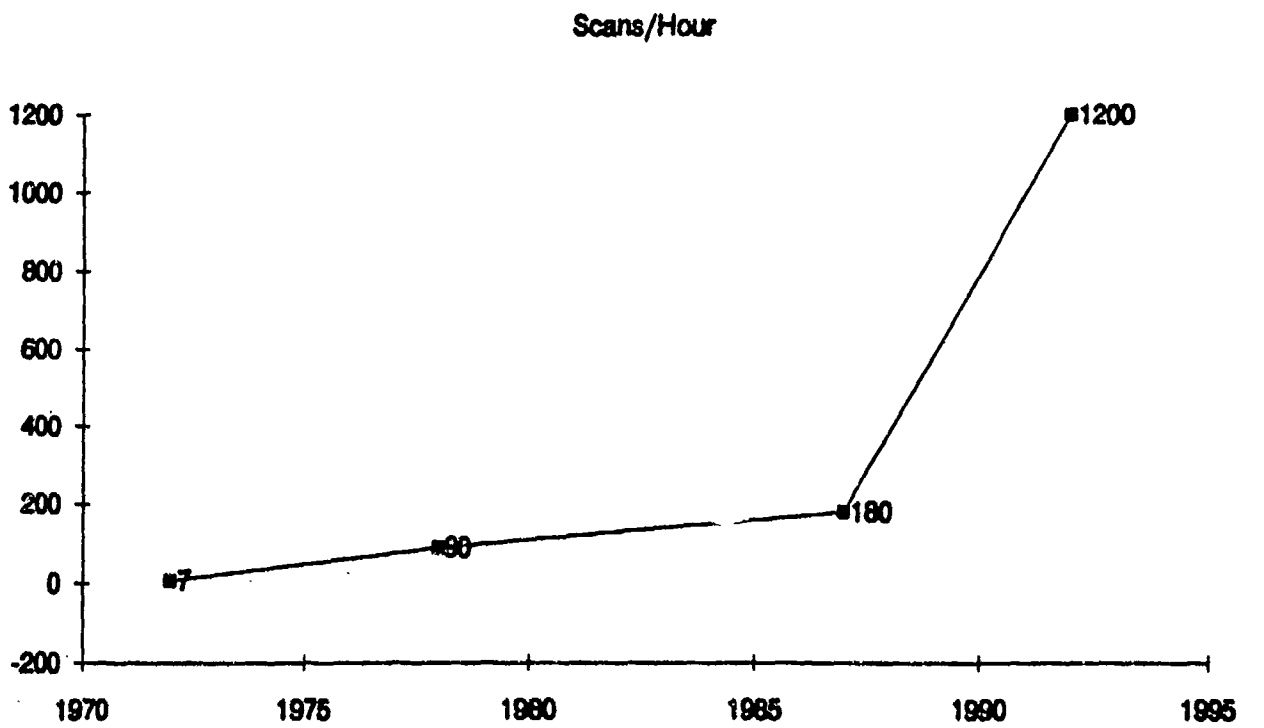


FIGURE 4. Increase in CT scanner throughput (1972 - present).

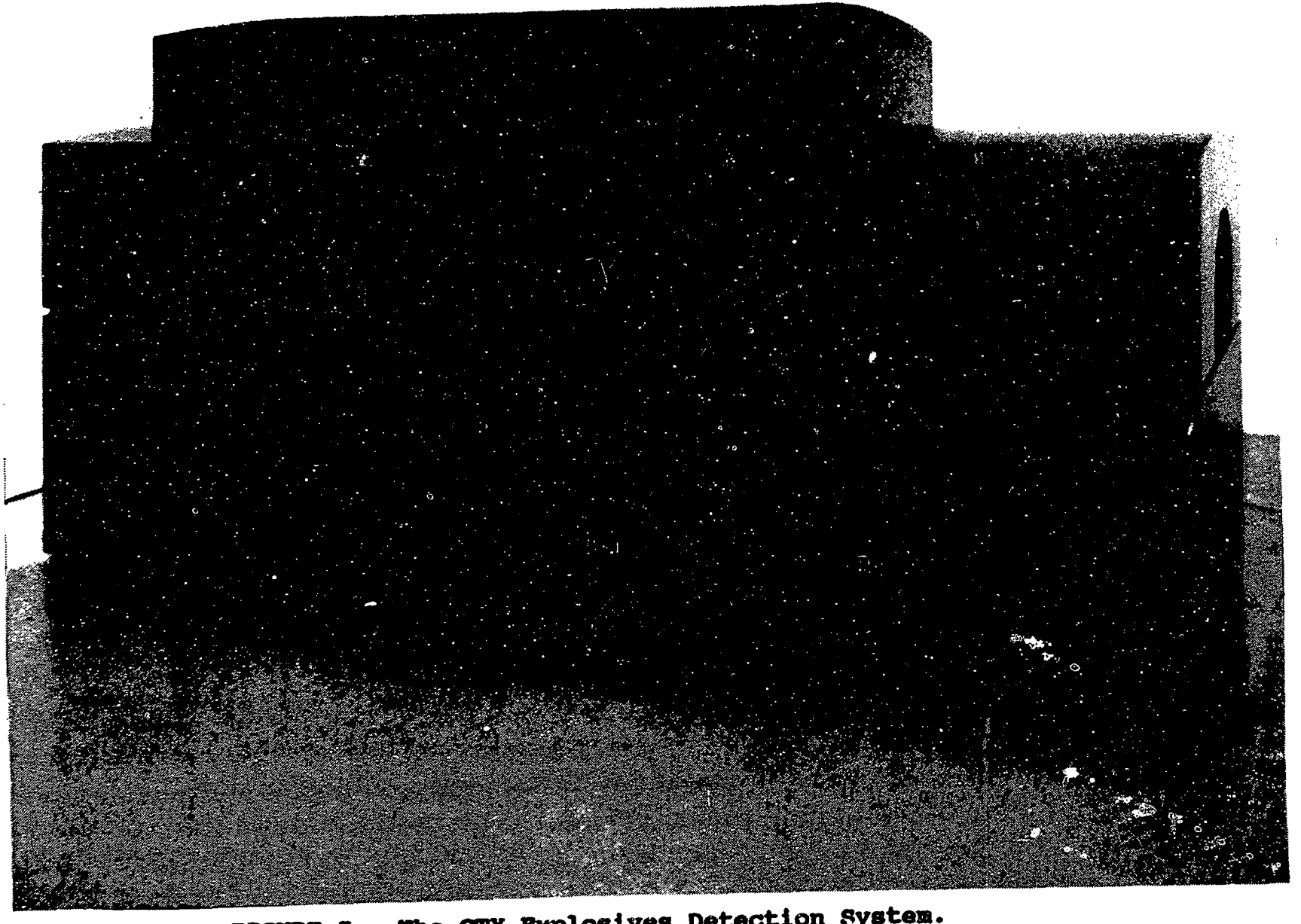


FIGURE 5. The CTX Explosives Detection System.

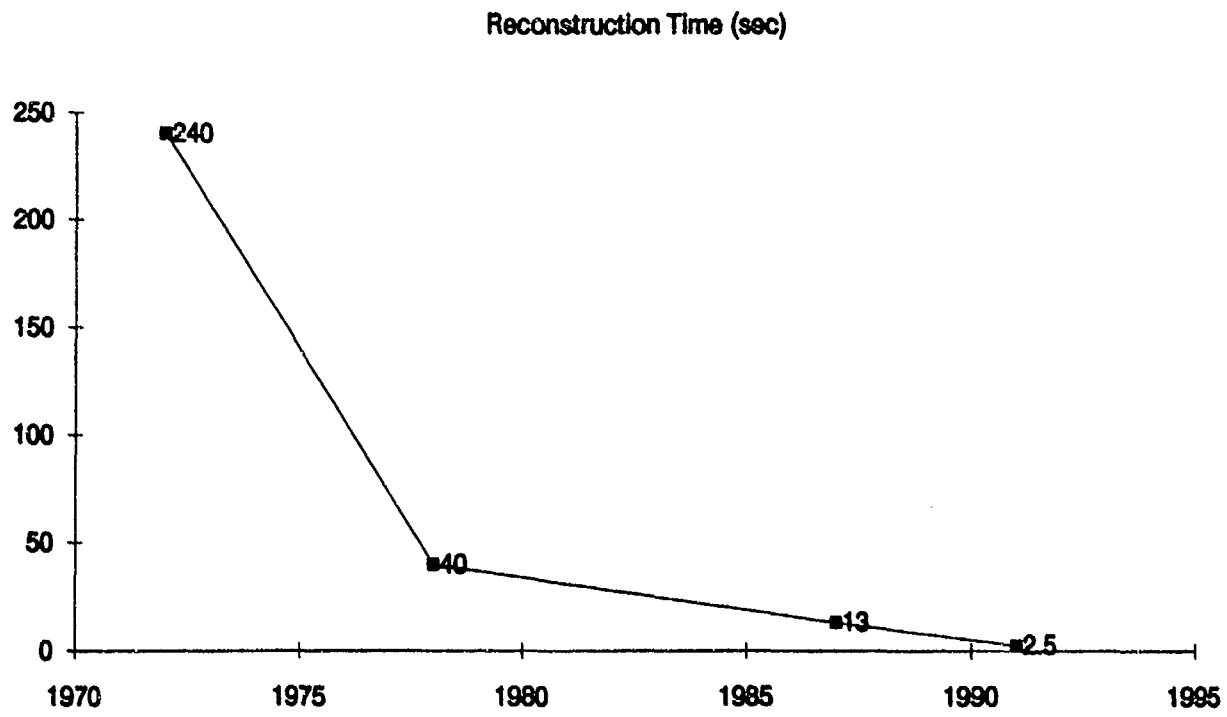


FIGURE 6. Decrease in image reconstruction time (1972 - present).

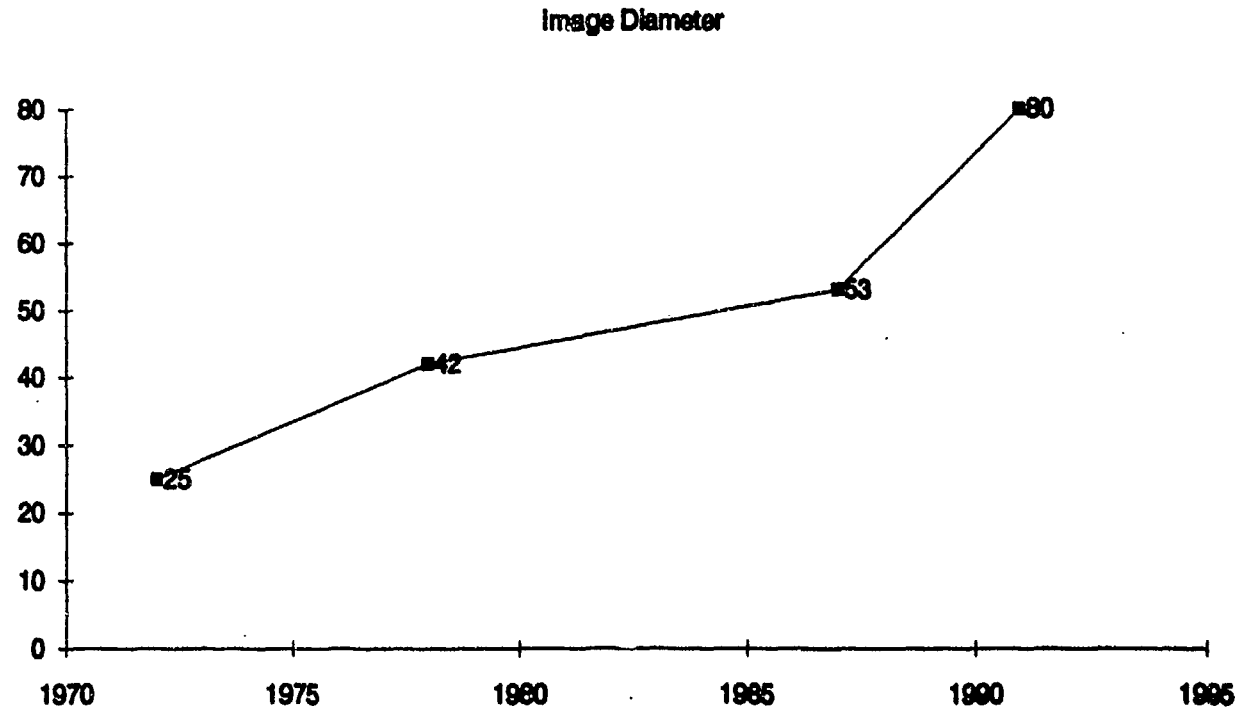


FIGURE 7. Increase in CT image diameter (1972 - present).

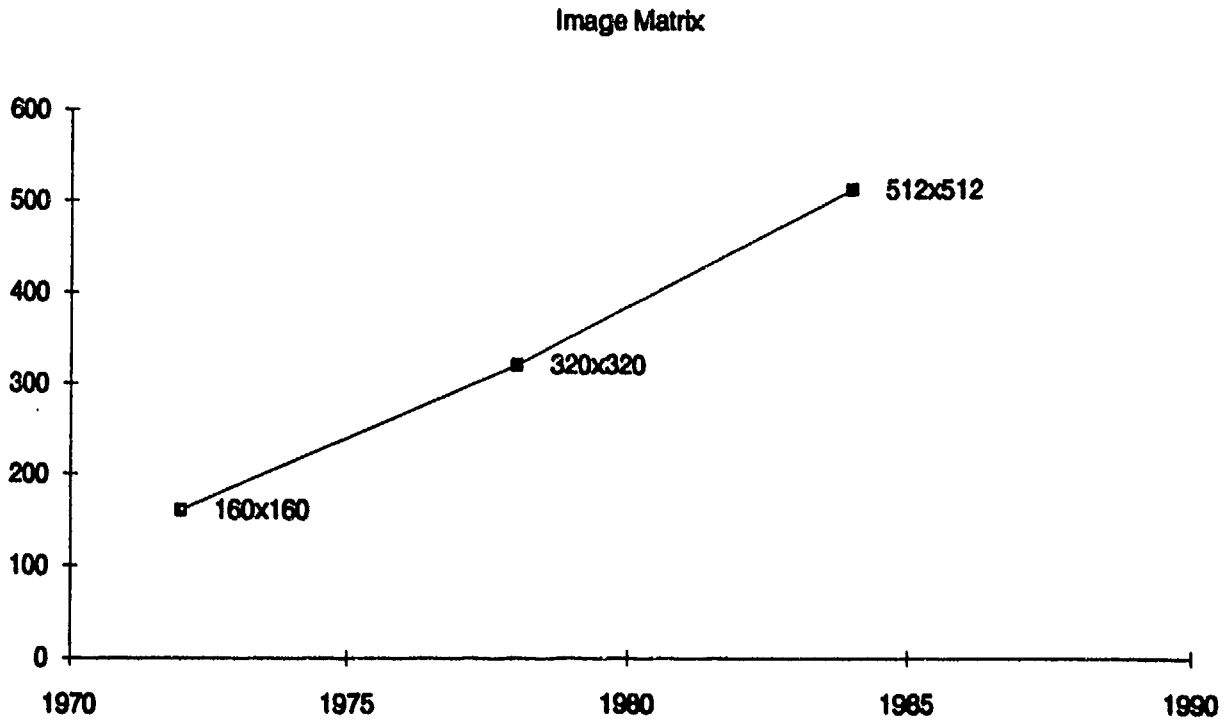


FIGURE 8. Increase in reconstruction matrix size (1972 - present).

COMBINATIONS OF X-RAY, NUCLEAR, AND OTHER TECHNIQUES

EXPLOSIVE DETECTION USING X-RAYS AND THERMAL NEUTRON ACTIVATION

T. R. Wang and P. J. Bjorkholm
EG&G Astrophysics, Long Beach, CA

R. Scarlet
EG&G, Wellesley, MA

S. Goldberg
EG&G Electro Optics, Salem, MA

1. INTRODUCTION

For the last fifteen years, EG&G Astrophysics has been actively involved in research, development, and implementation of various weapon and explosive detection systems which can be used in airports, government facilities and other institutions for overall security. Since the Pam-Am 103 accident in 1989, there has been heightened concern from the public, congress, and the FAA regarding aviation security. One of the biggest concerns has been the potential threat from plastic explosives.

The detection of an explosive is often accomplished by scanning a bag with various forms of radiation, such as x-rays, gamma-rays, and neutrons, to map the physical and chemical properties of the materials in it. While each technology has its strengths and limitations, none is an ideal solution to the threat detection problem. Since different technologies can complement each other, it is desirable to consider the best way to design a system that can exploit several methods at once.

EG&G Astrophysics has developed an explosive detection system that uses a dual view dual energy (DVDE) x-ray system. In conjunction with the FAA, EG&G is continuing its own development of DVDE in combination with thermal neutron analysis (TNA) to identify both metallic weapons and plastic explosives in baggage. This approach allows the analysis to fully utilize data sets from DVDE and TNA to their best potential, and to objectively define tradeoffs among the costs and performances of the differing sensors.

2. DVDE

The interaction of x-rays with material can be described as a combination of photoelectric, Compton and pair production processes. For medium energy x-rays ($E\gamma < 140$ keV), the interaction of x-ray with material is dominated by photoelectric and Compton scattering. While the cross section of Compton scattering with an atom is roughly proportional to atomic number Z, the cross section of photoelectric effect has strong Z dependence ($\sim Z^{4.5}$)[1]. In a dual energy x-ray system, the drastically different Z dependence of the Compton scattering and the photoelectric effect is used to extract the atomic number, and density of the contents of a bag.

In a DVDE system, the x-ray module consists of two separate, well calibrated EG&G dual energy x-ray imaging devices. One system provides a normal lateral projection and the other provides an oblique projection from the bottom. The data from both views are analyzed to extract the line of sight organic density information. These two organic images are then used to reconstruct a three dimensional model of the scanned object using Algebraic Reconstruction Techniques (ART)[2] with specially developed mathematical representations of physical constraints. The three dimensional model is examined for contiguous volumes that have a physical density within preset limits. The identified regions are then examined to determine if any exceed a previously defined mass level.

It is well known that two views are inadequate to reconstruct a tomographic image. In general one needs the product of the views and the number of rays per view to be equal to the number of pixels in the cross sectional image. In the case of DVDE this means we have only 2N values to determine N^2 pixel densities. In order to obtain a reasonably accurate reconstruction, additional physical constraints are invoked which restrict the potential solutions to this underdetermined problem. These constraints range from the very obvious (nonphysical density is not

allowed) to more obscure observationally based constraints (limits on the frequency content of object reconstructions).

Experimental results have shown that although any single slice has serious ray artifacts, objects with a density typical of the explosives of interest can be identified, followed in contiguous slices, and have their mass determined with a reasonable degree of accuracy.

3. TNA

For two dozen different types of plastic explosives which are available, most of them have high concentrations of nitrogen and oxygen[3]. One concept to detect the ^{14}N content in an explosive is through thermal neutron capture which results in high-energy γ-rays (10.8 MeV) which can be observed by various types of γ-ray detectors. Indeed, SAIC[4], building on earlier Westinghouse efforts, made use of this fact to develop the first prototype thermal neutron analysis (TNA) system for airport security .

In Astrophysics' TNA system, bags move through a sea of thermal neutrons produced by a $^{252}C_f$ source and neutron moderator. The 10.8 MeV γ-rays from $^{14}N(n,\gamma)\ ^{15}N$ reaction are analyzed to give the spatial distribution of nitrogen, and in turn, plastic explosives. The cross section of thermal neutron capture on ^{14}N is 75 mb, where the branching to ground state of ^{15}N is 13.8%[3]. In order to provide a reasonable yield of γ-rays from thermal neutron capture on ^{14}N, an intense neutron source is required. This raises a series of problems: neutron moderation, neutron shielding, pile-up in detectors, elastic and inelastic neutron scattering etc. A great effort is needed to optimize the performance of TNA while cutting the overall volume, weight, and cost.

Although implementation of a TNA at airports is not a trivial task, TNA does provide very unique information, i.e. ^{14}N content of an explosive. By jointly interpreting the information from the DVDE and TNA subsystems, one is able to make a better determination of the properties of objects which appear in the baggage than can be made from the separate data sets.

4. PRESENT STATUS

The x-ray and neutron modules have been tested independently for sensitivity to various types of explosives, masses, configuration and location within normal check-in baggage. Algorithms for processing the DVDE and TNA data sets separately and in combination have been tested and verified. The system is automatic and is designed to process 720 bags per hour. The output will be the standard x-ray screening images for a cleared bag. For a bag with an identified threat there will be an alarm, and the images will have a graphic overlay indicating the location of the threat within the bag and the size of the threat. We have also started a viability study of a multi-view (number of view > 2) dual energy system.

ACKNOWLEDGEMENT

We thank the FAA for their support, advice and assistance. This work is supported in part by FAA contract DFTA03-91-C-00041.

REFERENCES

1. C. M. Davisson, Alpha-, Beta-, and Gamma-Ray Spectroscopy, Edited by Kai Siegbahn, p. 37, 1966, North-Holland Publishing Company.

2. R. Gordon, R. Bender, and G. Herman, Algebraic Reconstruction Techniques for Three Dimensional Electron Microscopy and X-ray Photography, J.Theor. Biol. 29, 471-481 (1970).

3. Lee Grodzins, Nucl. Inst. and Methods, B56/57, 829-833 (1991).

4. P. Shea, T. Gozani, and H. Bozorgmanesh, Nucl. Inst. and Methods, A299, 444-448 (1990).

5. F. Ajzenberg-Selove, Nucl. Phys. A360, 129 (1981).

FUSION OF THE NUCLEAR AND DIFFERENT X-RAY TECHNOLOGIES FOR EXPLOSIVES DETECTION

V. Leung, P. Shea, F. Liu, and M. Sivakumar
Science Applications International Corporation
Santa Clara, California

1. INTRODUCTION

Explosive Detection Systems (EDS) are to be used in airports to detect explosives concealed in baggage. They have an important role in the security system protecting human life and property from being destroyed by acts of terrorism. The basic criterion of an effective EDS is to be able to distinguish explosives from any other materials and automatically identify explosives hidden in baggage without human intervention. The most significant signature of explosives compared to benign materials is the high content of nitrogen in explosives. Among the existing explosive detection techniques, the one which can achieve the highest total sensitivity to nitrogen is the Thermal Neutron Activation (TNA) technology. The TNA-EDS, designed and developed by Science Application International Corporation (SAIC), is able to detect explosives with high probability of detection (PD) and an operationally acceptable probability of false alarm (PFA).

False alarms impede the baggage circulation processes because of the need to further screen them. In order to decrease the PFA, a secondary inspection system has been added to the TNA-EDS. X-Ray radiography, which measures the densities of objects in suitcases with high spatial resolution, has proven to be a good secondary inspection unit to the TNA-EDS in reducing the PFA. The fusion of the most prominent pieces of information from both the TNA and the X-Ray reinforces the EDS ability to identify the presence of explosives in suitcases more accurately. This combined system, the X-Ray Enhanced Neutron Interrogation System (XENIS), was designed and developed by SAIC using the Astrophysics X-Ray Transmission Linescan System, and is currently used by the U.S. Federal Aviation Administration (FAA) in several airports in the U.S. and Europe.

This paper describes the basic principles of the XENIS, and the complex data analysis and automated decision algorithms developed by SAIC for the realization of this technology. It also discusses the issues involved in the practical application of the XENIS in airports. Two new X-Ray techniques were investigated for the future upgrade of the XENIS. They are the X-Ray Transmission Computed Tomographic (CT) Scanning technique built by Imatron, Inc. and the X-Ray Transmission and Backscatter Tomographic (ZT) Scanning technique built by American Science and Engineering (AS&E). Both techniques were investigated by SAIC and tested by the FAA, and are described in this paper.

2. XENIS PRINCIPLES

The underlying principle of the XENIS is the mathematical fusion of the characteristic physical parameters of explosives detected by the TNA-EDS and the X-Ray system. As mentioned earlier, the first and the foremost signature of bulk explosives is the high content of nitrogen. As of today, TNA is the technique which gives the highest sensitivity to nitrogen, making TNA the best existing technology in bulk explosives detection.

The neutron interrogation technique of the TNA-EDS is based on the neutron-gamma modality. The essential components of the TNA-EDS are the neutron source and the gamma ray detectors. When thermal neutrons emitted by the neutron source hit the materials in the suitcase being scanned, a few specific nuclear reactions are induced resulting in gamma ray emission. The energy distribution of the detected gamma ray signifies the presence (or absence) of nitrogen in the suitcase. The number of detected gamma rays at the nitrogen energy level indicates the amount of nitrogen being detected.

Owing to the high nitrogen count rate of the detectors in the TNA-EDS, a direct fundamental output from

the neutron interrogation is the amount of nitrogen present in the suitcase. This is one physical parameter that the TNA-EDS uses to detect explosives. Another key output from the neutron interrogation is the reconstructed nitrogen image. The orientation of the neutron source and the detectors of the TNA-EDS are designed in such a way that a 3-D nitrogen image can be reconstructed by using the nitrogen signals detected in the array of detectors. This TNA nitrogen image is a good indication of the threat level within the suitcase. However, due to the limitation on the practical sizes of the gamma detectors, the spatial resolution of the image is coarse even though the TNA image is very nitrogen specific.

The best way to improve the spatial resolution of the nitrogen image is to correlate it with a high-resolution density image. X-Ray radiography is currently the most efficient technique for obtaining a high resolution, 2-D density image of an object. Although the X-Ray does not deliver any information about the elemental composition of the materials in suitcases, the spatial resolution in two dimension that it can deliver is far beyond what neutron based systems can provide. The idea of the XENIS is to make use of the most prominent attributes of the TNA and the X-Ray modalities. The TNA image is very specific to nitrogen but has coarse spatial resolution. The X-Ray image has no specificity of nitrogen but has high spatial resolution. By mathematically correlating the two images, a much more accurate and precise image of nitrogen bearing materials is obtained. The fusion of these two pieces of orthogonal information is the scientific basis for the effectiveness of the XENIS as an EDS.

The basic concept of the XENIS, which is the merging of the strengths of the TNA-EDS and the X-Ray system into a single system, is called the multi-mode approach. The advantage of this approach is its great flexibility and versatility. The XENIS can be upgraded (by replacing the current X-Ray by a new generation X-Ray) or expanded (by incorporating a third subsystem) with minimal modifications on the existing design. The overall system performance of the combined TNA-EDS and X-Ray system is far better than any of the individual system can deliver as shown on the PD/PFA curve in Figure 1. This curve indicates how much the XENIS has reduced the TNA-EDS PFA. It is generated from the set of bags (used for the FAA test in San Francisco International Airport) that is considered a threat by the TNA-EDS alone. PD represents the percentage of bomb cases in that set that was confirmed by the XENIS. PFA represents the percentage of clean cases in that set that was alarmed by the XENIS. The percentage of the false alarm reduction (100% - PFA) can be extracted from the plot at the point where the curve leaves the 100% PD line. The ultimate goal of the XENIS is to maintain the high PD from the TNA-EDS and minimize the PFA by using the X-Ray system.

3. XENIS TECHNIQUE

The XENIS is a highly efficient and intelligent EDS. It is able to scan a suitcase with TNA followed by X-Ray, perform real time data analysis, and come up with an automated decision of bomb or no bomb, all within six seconds. The XENIS final decision is based solely on mathematical analysis without any human intervention. The intelligence of the XENIS lies in the software which is the most complex and unique part of the system. The software is responsible for three main functions:

3.1. Data Acquisition
3.2. Data Reduction, and
3.3. Decision Analysis

These three sections are briefly described below.

3.1 Data Acquisition

The main purpose of the data acquisition module is to acquire raw data from the TNA and the X-Ray scanners to generate images. The data acquisition module performs two tasks:

(i) TNA Image Acquisition
(ii) X-Ray Image Acquisition

The TNA image acquisition is done by a data acquisition package custom designed and developed by SAIC. When a suitcase passes through the TNA-EDS, the nitrogen signals acquired by the gamma detectors are passed to the image reconstruction algorithm to generate a 3-D nitrogen image of the suitcase. This image is analyzed by the TNA-EDS data analysis module. When a TNA-EDS automated decision is reached, the image is then transferred to the XENIS data analysis module for image correlation.

The X-Ray image acquisition system uses a modified Astrophysics Linecan System Five which provides a 2-D transmission top view and a 2-D transmission side view of the scanned suitcase. Once acquired onto a specialized image processor, the XENIS data reduction module performs image correlation.

3.2 Data Reduction

The data reduction module performs the fusion of the TNA and the X-Ray images. Before the actual image correlation takes place, both the TNA and the X-Ray images require preprocessing.

The first step in the image preprocessing is the conversion of the dimensionality of the TNA image to that of the X-Ray image. This is done by projecting the 3-D TNA image onto the 2-D X-Ray image plane. There are two image projection methods. One, known as the straight-projection method, collapses the 3-D image along parallel rays perpendicular to the plane of projection as shown in Figure 2. This method does not account for the X-Ray magnification due to the fan shape of the X-Ray beam. The other, known as the warped-projection method, compensates for fan-beam magnification by progressively magnifying slices of the 3-D image which are closer to the projection plane before collapsing as in the straight-projection method as shown in Figure 3. Warped-projection is more computationally intensive than straight-projection but certainly produces an image that corresponds more closely to the fan-beam configuration of the X-Ray system.

The next steps in the image preprocessing are image rescaling and image convolution. The size of the reconstructed TNA image is different from that of the acquired X-Ray image due to the difference in the data acquisition systems. It is important to match up the sizes of both images before correlation is performed. On the other hand, the vast contrast in the spatial resolution between the TNA and the X-Ray images requires the X-Ray image to go through image convolution. Image convolution helps to adjust for the resolution mismatch between the TNA and the X-Ray images by filtering the X-Ray image. This will lower the image noise level and smooth the X-Ray image.

Upon the completion of image preprocessing, the TNA and the X-Ray images are correlated. Image correlation is carried out mathematically by a SAIC specially designed algorithm. The challenge in image correlation is to merge the TNA and the X-Ray images with about the same average sharpness but not to lose the important spatial information that the original X-Ray high resolution image contains. This is the most crucial part in image correlation. Another important part is that the intensity of the TNA and the X-Ray images have to be well balanced according to their significance level. If the correlated image is dominated by either the TNA or the X-Ray image, the information extracted from this resulted image would be biased, which would directly affect the accuracy of the automated decision.

The last steps in image correlation are image regularization and edge enhancement. The purpose of these procedures is to regularize the rough spots in the image and to make the different objects in the suitcase stand out from the background and from each other. The final image, hence, becomes a smooth and fine tuned correlated image which contains the most important information from both the TNA-EDS and the X-Ray system.

Once a final correlated image is created, the useful information contained in the image are extracted. This information is expressed as quantitative variables, or features. There are two types of features available from each image. One type is the global features. Global features show the average information of a bag with no regional specific detail. One value is obtained for each global feature for each image. The other type is the local features. Local features show the localized information within a suitcase by using the agglomerization technique. The function of this technique is to identify one or more high threat level regions within the suitcase.

It is important for the decision algorithm to distinguish explosives not only based on the average bag information, but also specifically on the different objects within the suitcase. The way to perform agglomerization is to threshold the intensity of the correlated image with preset values. If there is any localized region that exceeds the threshold, this region is identified as a blob. A blob means the identified region in the suitcase has high density and high content of nitrogen, or in other words high threat level. Each image may contain more than one blob, depending on the nitrogen content of the objects, the density of the objects, and the number of objects contained in the suitcase. In contrast to the global features, each image may have many local

feature values. For example, if three blobs are identified in an image, three values of a local feature would be produced.

The agglomerization technique is important in providing the decision algorithm a much clearer and more regional specific picture of the scanned suitcases, especially for dense suitcases. The local features of explosives in a dense suitcase have much stronger indications of its presence than the global features.

3.3 Decision Analysis

The multi-mode approach of the XENIS makes the system inherently complex. The abundant raw and processed data from both the TNA-EDS and the X-Ray system result in the generation of more than a hundred features. By utilizing these features, a fully automated threat or no threat decision is made.

The classification theory, discriminant analysis[1], is used to make the XENIS decision. Discriminant analysis is a statistical technique for classifying individual objects into mutually two or more exclusive and exhaustive groups on the basis of a set of independent variables, or discriminant features. Its objective is to derive a linear combination of the independent discriminant features that will discriminate between *a priori* defined groups (bags with or without threat) with minimum misclassification error rates.

Discriminant analysis for the XENIS can be thought of in terms of a simple "scoring system". Given a calibration bag data set with known status (with or without threat) of each bag, a score, which is essentially a weighted average of the independent discriminant features, is assigned to each bag. Once a score is determined, it can be transformed into an *a posteriori* probability that gives the likelihood of the bag belonging to each of the (with or without threat) groups. Fisher's approach is used in generating this probability. It is accomplished by maximizing the between-group variance relative to the within-group variance.

The accuracy of the XENIS decision depends on the robustness of the XENIS calibration which is dependent on many factors. The most significant one is the distribution of the calibration data set. The way the XENIS discriminates bags into different (with or without threat) groups is by following the rules established by the discriminant analysis of the calibration sample. If the distribution of the data in the calibration sample are not representative, no matter how fine tuned the system calibration is, the discrimination rules established based on the invalid data set would not be optimal, resulting in a non-robust automated decision.

4. PRACTICAL EXPERIENCE OF THE XENIS

System integration plays an important role in building the XENIS. Many technical problems were encountered and solved before the XENIS was fully operational. They include the assembly of the TNA-EDS neutron source, gamma detectors, neutron flux moderator, scanning cavity, shielding walls, shielding doors, the physical integration of the TNA-EDS with the X-Ray system, the conveyor belt common to both subsystems, the electronics for data acquisition, the data transfer from the TNA-EDS to the XENIS, the interface for the hardware, software, and image processor, and the system throughput.

The XENIS performance depends on the optimization of the above components beside software implementation and the XENIS calibration. In addition to the optimal operation of each individual component, the integration of all components at final installation affects the features values used in the decision making. The key requirement in making sure every part of the XENIS is working optimally is ample experience with on-site operation. The application of the XENIS in airports in the U.S., the Middle East, and Europe has shown that different airports in different seasons have different needs from the system. Each XENIS has to be adjusted differently in order to suit different airports' specific requirements. The system adjustment procedure has been made convenient through telecommunications. The SAIC main computer system can make adjustments to the on-site XENIS anytime without interruptions to the normal daily operation of the system. Off-line analysis of the on-site data can also be performed on the same day through telecommunications.

The collected data that the XENIS obtained from passengers' bags provide a valuable statistical database for decision analysis. The robustness of the XENIS calibration depends on the distribution of these data. Without this important piece of information, it is impossible for any kind of EDS which makes automated decisions to be able to

perform optimally because of the lack of valid information to train the decision algorithm.

The robustness of the XENIS calibration also depends on the simulants, which are materials containing the same characteristic features as in the explosives but has no risk for explosion. The experience in making different types of simulants and developing the methods to qualify the simulants are very important. If the errors between the qualities of the simulants and the explosives exceed certain limits, the collected data using these simulants will carry false information, which certainly reduces the robustness of the XENIS calibration. For instance, if the XENIS is trained with one set of simulants, when it is tested with real life explosives, or, even worse, simulants which are not thoroughly qualified, the system performance would most probably be lower than its normal performance because there are discrepancies between the information carried in the calibration data set and the information observed in the test. The only way to avoid this problem is to utilize the experience of dealing with simulants, figure out which features are important in qualifying simulants, and design a detailed and complete simulant qualifying test to minimize the errors of those features.

All the above observations are solely based on the practical experience of the XENIS in airports. It is observed that detailed decision analysis on airport bag information is essential to obtain a robust calibration, even though all the software implementation have been finished and the system is up and running. How well the XENIS performs directly depends on how valid the calibration data set is, how detailed the decision analysis has been done, and how much has been learned from on-site operational experience.

5. INVESTIGATION FOR THE XENIS UPGRADE

The multi-mode design of the XENIS makes the system very flexible for future upgrades without requiring any major modifications on the existing design. Two new X-Ray technologies were investigated to assess the possibility of replacing the current Astrophysics X-Ray Transmission Linescan System. They are the X-Ray Transmission Computed Tomographic (CT) Scanning technique built by Imatron, Inc, and the X-Ray Transmission and Backscatter Tomographic (ZT) Scanning technique built by American Science and Engineering (AS&E).

The advantage of the CT Scanner is that it provides a 3-D X-Ray image. If this 3-D X-Ray image is used to correlate with the TNA image, the projection of the 3-D TNA image onto a 2-D plane would no longer be required. The correlated image would be more spatially specific and the resultant blobs from agglomerization would be more precise. The preparation for the FAA test of the combined TNA-EDS and CT Scanner required very minor TNA-EDS modifications.

The advantage of the ZT Scanner is that it provides backscattering as well as transmission information on the 2-D X-Ray images. The backscattering X-Ray image indicates the presence of materials with low atomic numbers, which may be useful in distinguishing plastic explosives. The preparation for the FAA test of the combined TNA-EDS and ZT Scanner requires minor modifications, which is consistent with the idea of the multi-mode approach.

6. CONCLUSION

The high nitrogen sensitivity of TNA makes it the best existing technology for the detection of bulk explosives concealed in baggage. The XENIS, the fusion of the TNA and the X-Ray technologies, successfully developed by SAIC, significantly enhanced the effectiveness of explosives detection. The rigorous correlation of the TNA 3-D nitrogen image with the X-Ray 2-D high density image, the novel agglomerization technique, the detailed discriminant analysis of an extensive database acquired on site, and the thorough qualification process of simulants used for calibration, all contribute to the robustness of the XENIS automated decision. The extensive airport operational experience of the XENIS has proven valuable in identifying the factors critical to the success of the XENIS. The multi-mode design of the XENIS has made the system very flexible for future upgrades, as demonstrated in the investigation of the CT Scanner and the ZT Scanner.

NOTE

1. Linear Statistical Inference and Its Applications by C. Rao, 2nd ed., Wiley and Sons, 1973.

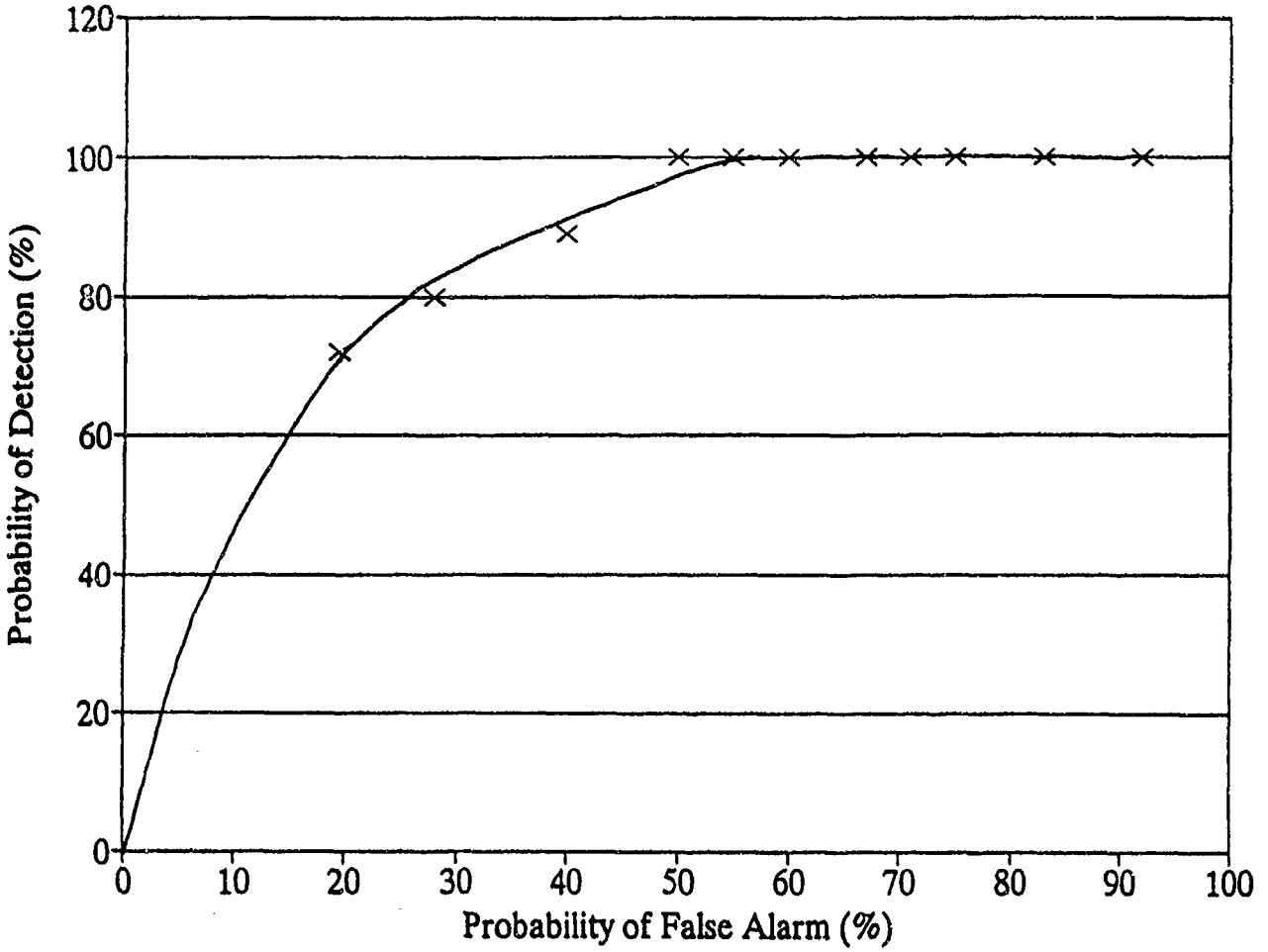


Figure 1 PD vs. PFA Plot

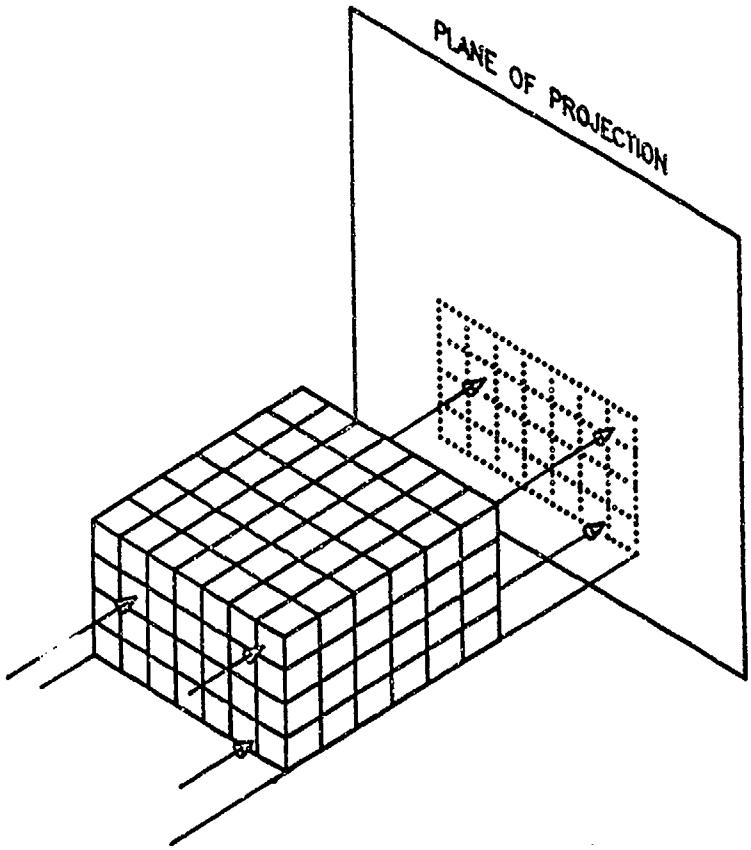


Figure 2 Straight Projection Method

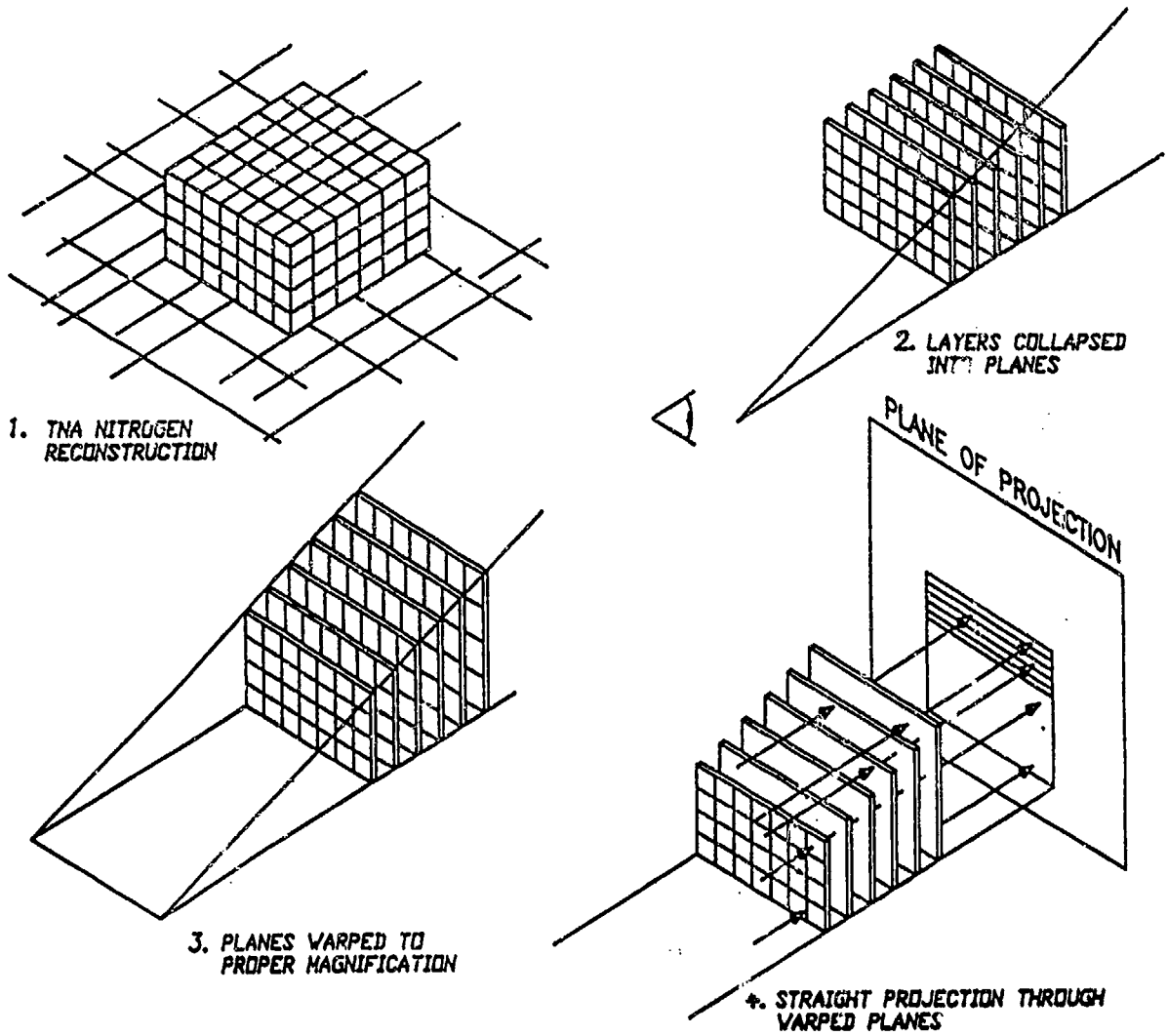


Figure 3 Warped-Projection Method

EXPLOSIVE DETECTION FOR CHECKED LUGGAGE BY DETEX, A COMBINED X-RAY AND POSITRON-TOMOGRAPH SYSTEM

Hans W. Pongratz
DASA-MBB
Munich, Germany

1. SCOPE

The DETEX—System (DETection of EXplosives) is a multistage, automatic detection system for explosives in checked luggage on airports. The operating principle of DETEX combines a two energy x-ray machine performing three-dimensional reconstruction and a bremsstrahlungs source with a positron tomograph system and automatic threat assessment algorithms. Special reconstruction algorithms for the positron tomograph have been developed for three-dimensional reconstruction of activity distribution at low count rates. Results of simulations and measurements are presented and discussed.

2. SYSTEM REQUIREMENTS

Investigations in recent terrorist attacks showed that explosive charges smaller than one pound can destroy an aircraft. At the moment a detection threshold of sub-kilogram quantity of explosives in a camouflaged format, found with a false alarm rate of less than 0.1% at a detection probability of greater than 99% seems adequate. Smaller charges should be found with higher false alarm rates (Fig. 1).

The system shall have low susceptibility to camouflage (shielding, sheet explosives, gastight enclosement) and deception.

The system shall have a high throughput of at least 600 bags per hour and shall be expandable to 3000 bags per hour.

The system shall operate fully automatic until alarm generation and must be integrated into standard luggage handling systems on airports. Low false alarm rate is important to allow uninterrupted luggage handling operations.

The system shall be able to find nitrogen based high performance explosives like TNT and SEMTEX and other mixtures based on chlorates, perchlorates and other oxidation agents in larger quantities (Fig. 2).

3. DETEX CONCEPT

The DETEX-concept is a multistage and multisensor approach to the explosive detection problem. It combines two energy x-ray systems which can take at least three projections of a luggage sample and create a three-dimensional approximation of the absorption density and the atomic number distribution of materials with an activation unit and a positron tomograph system with good spatial resolution which can create a nitrogen and oxidation agent density distribution of the checked luggage piece.

A survey into possible materials in a piece of luggage shows that nitrogen- or oxidant-agent carrier density alone is not selective enough as a decision criteria. Taking physical density and atomic number as well into account gives a reasonable selective criteria, if the spatial resolution is high enough to avoid excessive false alarms (Fig. 3).

The nuclear measurement component works by activating nitrogen and other low threshold materials by bremsstrahlung, which is a spectrum of hard x-rays. The bremsstrahlung is produced by a 14 MeV electron beam striking a heavy metal target.

The x-ray components above the threshold of 10.8 MeV generate a (γ, n)-reaction which transforms ^{14}N into ^{13}N. ^{13}N reacts further to ^{13}C and a positron. The positron gets slowed down in the material and eventually annihilates with an electron producing two γ-quanta in opposite directions. These coincident (in time)γ -quanta can be measured on opposing position sensitive detectors. Thus a line can be defined where the event must have been with a resolution of about 1 cm (Fig. 4).

From the sum of the events a reconstruction algorithm can reproduce the activity density in the measured sample. Activity densities of cloth material, drugs, explosives and metals are sufficiently apart to discern regions of possible explosives with a resolution of about 2 cm.

The resulting 511 keV annihilation radiation is hard enough to penetrate usual luggage materials and to allow nondestructive measurement of the activation.

Measurement can be in a small energy band (energy resolution about 10%) which results in high signal to noise ratios. With this kind of energy resolution some γ-quanta which are compton-scattered still can enter the measurement device and result in some softening of the resulting image. However, this effect remains in tolerable limits due to the operation of the reconstruction algorithm which tends to suppress stray signals.

The complete DETEX-System operates in three stages (Fig. 5). In the first stage the bags are activated in the illumination chamber. Then the x-ray machine takes three projections from the bag in two energy bands. From these an absorption density and an atomic number distribution of the bag is produced. The (Fig. 6) activation is measured in the Anger camera as a list of coincidence events. From these an activity density map is produced. Mass and activity density are correlated and coherent objects identified and classified. These objects are used for a first threat analysis. Unsuspect bags are cleared from the process at this stage. Suspect bags are transferred into a high precision computer tomograph which produces a high resolution outline and density map of suspect areas which takes some time and cannot be performed on every bag in reasonable time. This is the second stage of the process. Bags that can be cleared are taken from the system now. Bags which are still suspect enter the third stage of the process. Here the bags are recycled and reactivated at 17 MeV - at the suspect areas only to avoid excessive activation. At 17 MeV ^{16}O gets activated at a notable scale and allows assessment of ^{16}O contents in the suspect area (Fig. 7).

Areas which contain enough nitrogen or oxidant agent carriers like chlorine, phosphorus and fluorine and enough oxygen to comprise an explosive charge of sufficient size are considered as bombs and trigger an alarm to initiate separate treatment by the operator of the possible bomb.

4. MEASUREMENTS AND SIMULATIONS

Activation measurements with 14 MeV bremsstrahlung to confirm the cross-sections for the (γ-n) activation reaction have been performed by the TITAN Company of Albuquerque, USA.

Measurements with an Anger camera to prove the spatial resolution at the anticipated low count rates have been performed at UGM Medical Systems of Philadelphia, USA and showed that a resolution of 1 cm can be reached (Fig. 8).

A detailed measurement simulation of both the x-ray and the (Fig. 9) Anger camera and a first version of the reconstruction algorithms showed that TNT sheet explosives as thin as 3 mm and down to about 50 g of mass can be reliably found in a standard luggage environment. As well a shielding of 5 mm copper, which is activated by itself much stronger than the explosive, can be penetrated and allows, for example, to see whether a hollow cube of 5 cm edge length and 5 mm copper walls contains explosives or not (Fig. 10).

Materials like copper, silver or gold get activated much stronger than nitrogen. This results in some problems around the edges of thick materials, where a halo is created, which could be mistaken as a sheet of explosive on the metal and cause a false alarm. These cases can be resolved in part by taking the x-ray images and inspecting the edges whether a sufficient dense plastic material is actually there to constitute an explosive lining or not. This is where the high resolution of the computer tomograph is needed and where the false alarm rate can be reduced over that attainable in the first stage alone.

5. CONCLUSION

Taking these results together there is a good chance for the DIX-Concept to answer the needs for an effective explosive detection device which is operable in an average airport (Fig. 11) environment. A vital advantage is by separating illumination and measurement resulting in a long life expectancy for the Anger camera (20 000 h). There is permanent access without radiation hazard except to the illumination chamber.

The illumination unit as well has long life expectancy (30 000 h).

The system is highly modular and adaptable. High spatial resolution translates into good resistance to countermeasures.

The residual activity of the luggage is far below allowable limits for free handling and has short half life (order of 10 minutes), which improves the chance for public acceptance (Fig. 12).

System Requirements

- Detection Threshold: Sub-kilogram quantity of explosives
- Throughput: minimum 600 bags/hour
- Detection Probability: 99 %
- False alarm rate: smaller than 0,1 %
- Reliability: Small susceptibility to camouflage (shielding, gastight enclosement, sheet explosives)

Fig. 1

System Requirements

Explosives Examples:

Nitrogen based explosives:

- TNT
- HEXOGEN (SEMTEX)
- OKTOGEN
- PETN

Others:

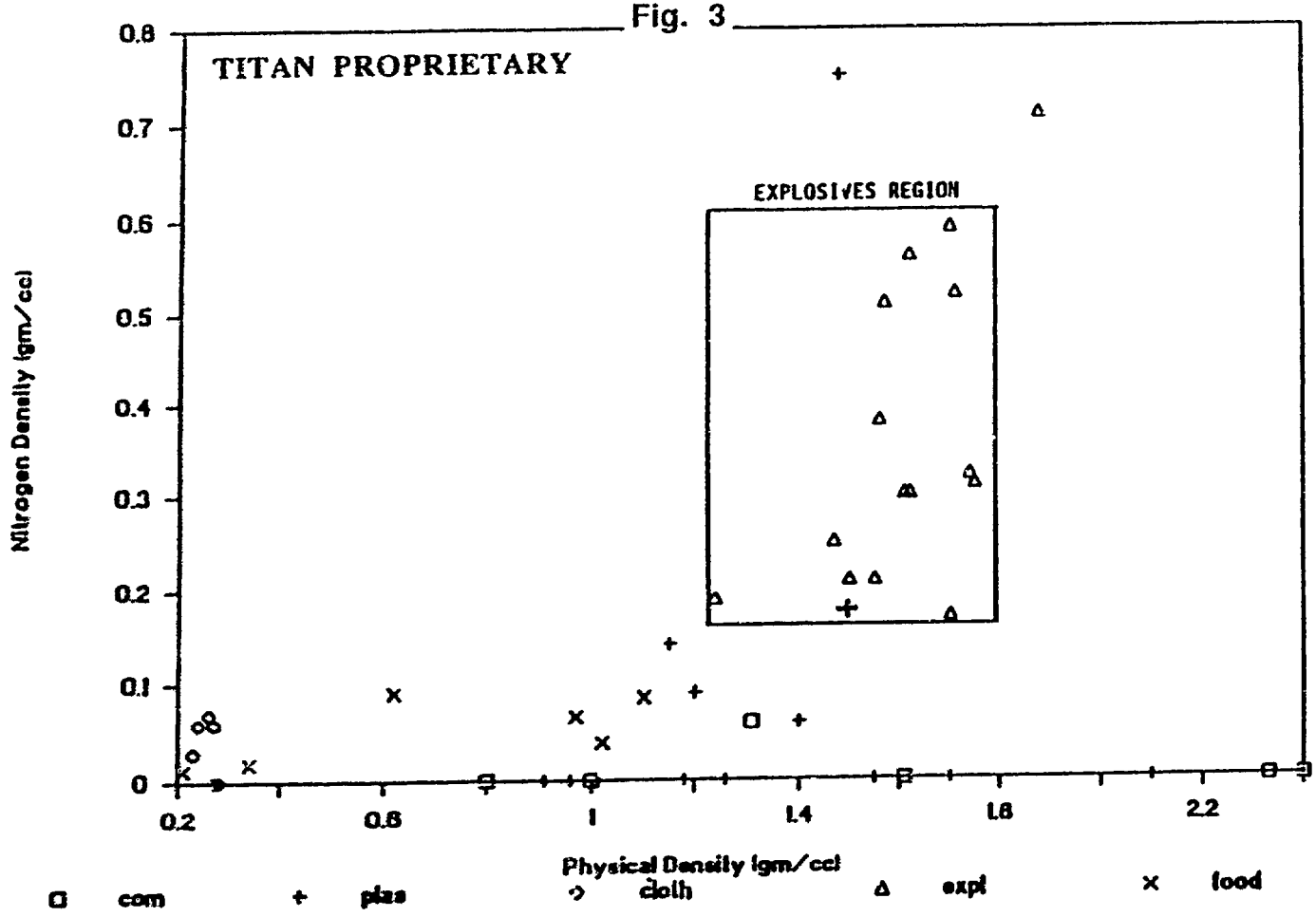
- CHLORATE
- PERCHLORATE
- NITRATE

FIG. 2

MBB
Deutsche Aerospace

DETEX Concept

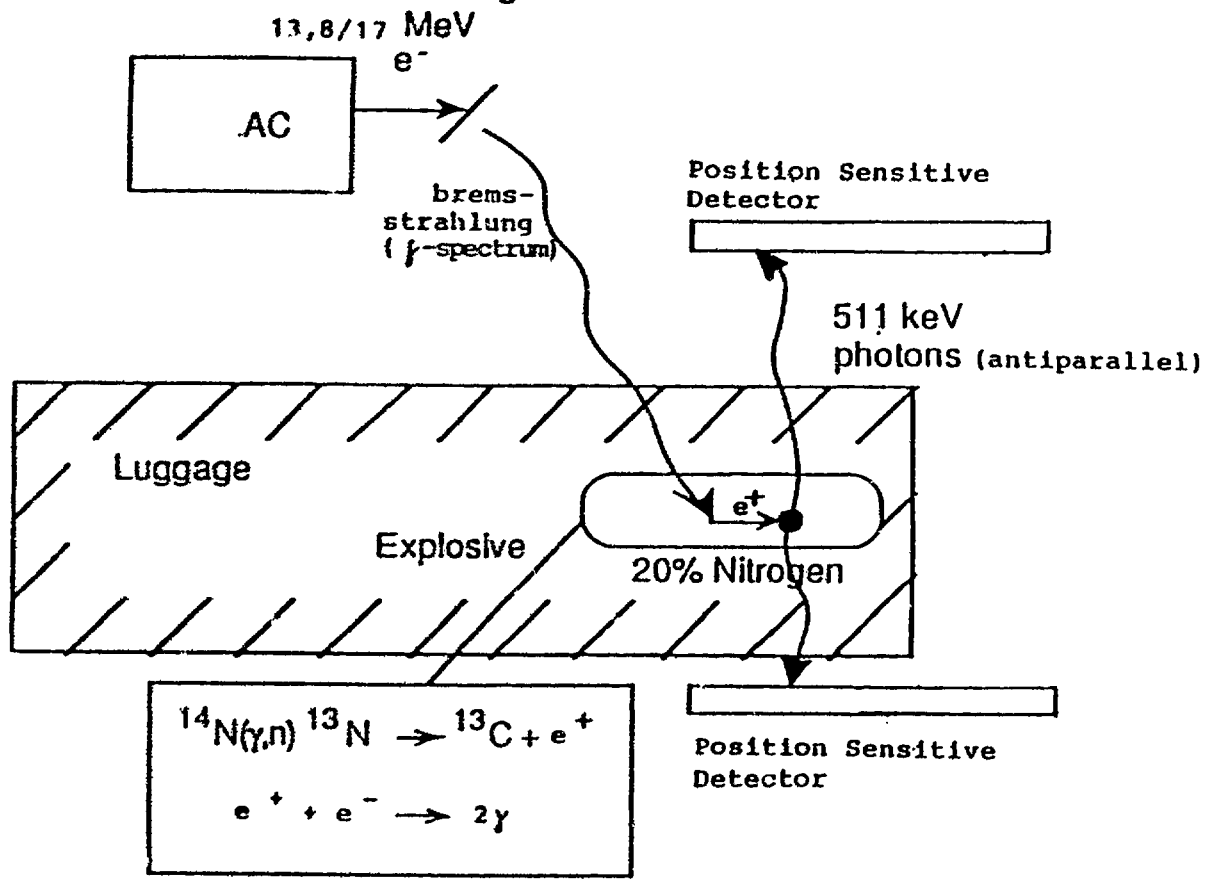
Fig. 3



MBB
Deutsche Aerospace

DETEX Concept

Fig. 4



TITAN PROPRIETARY

DETEX Concept

Components:

- Illumination chamber and AC, bremsstrahlung source
- 2D-X-ray, 3 images
- Anger camera as position sensitive detector
- 3D-X-ray computertomograph
- Signal processing computer

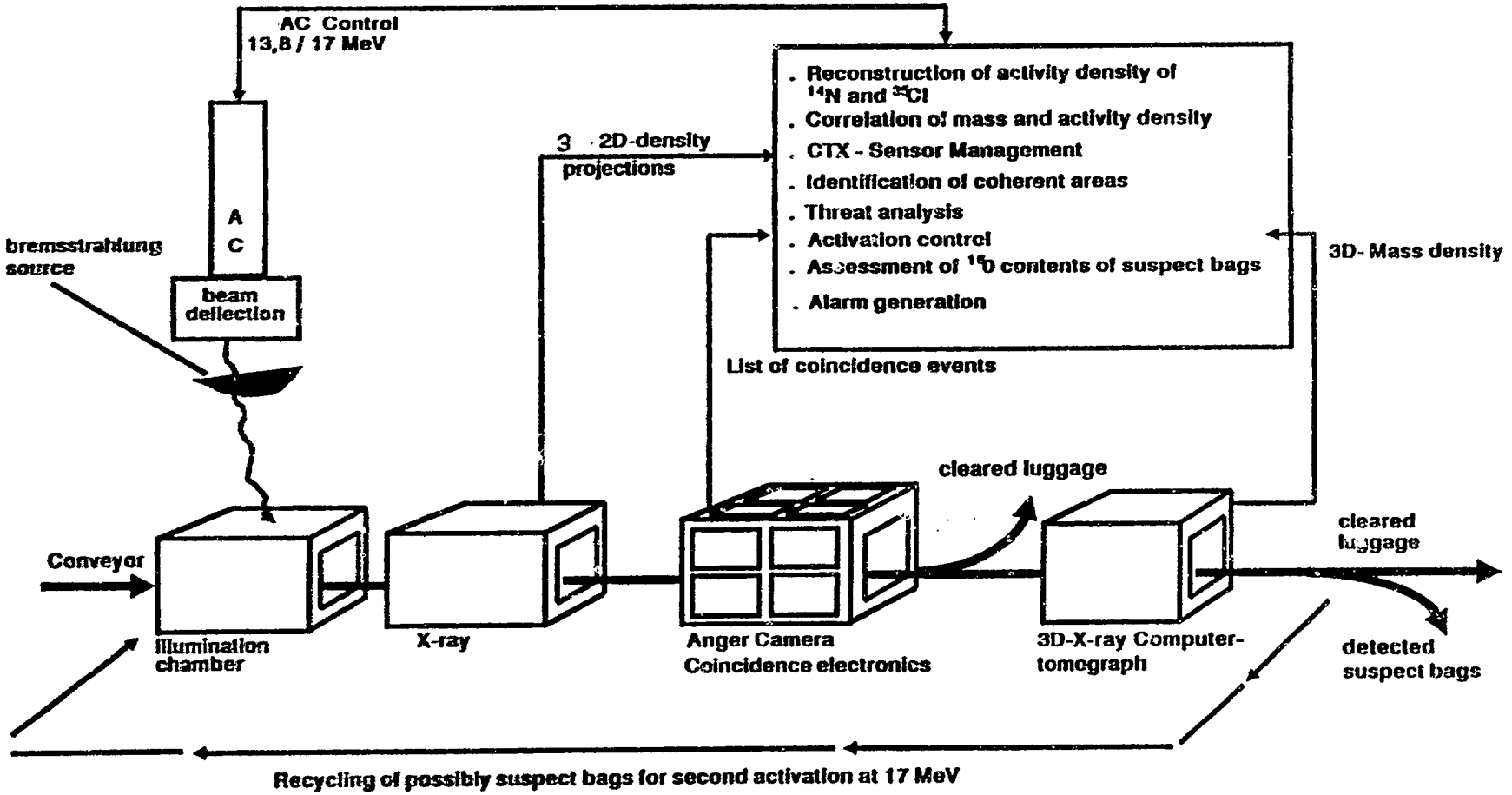
Fig. 5

Detection of Explosives
DETEX

MBB
Deutsche Aerospace

DETEX Concept

Fig. 6

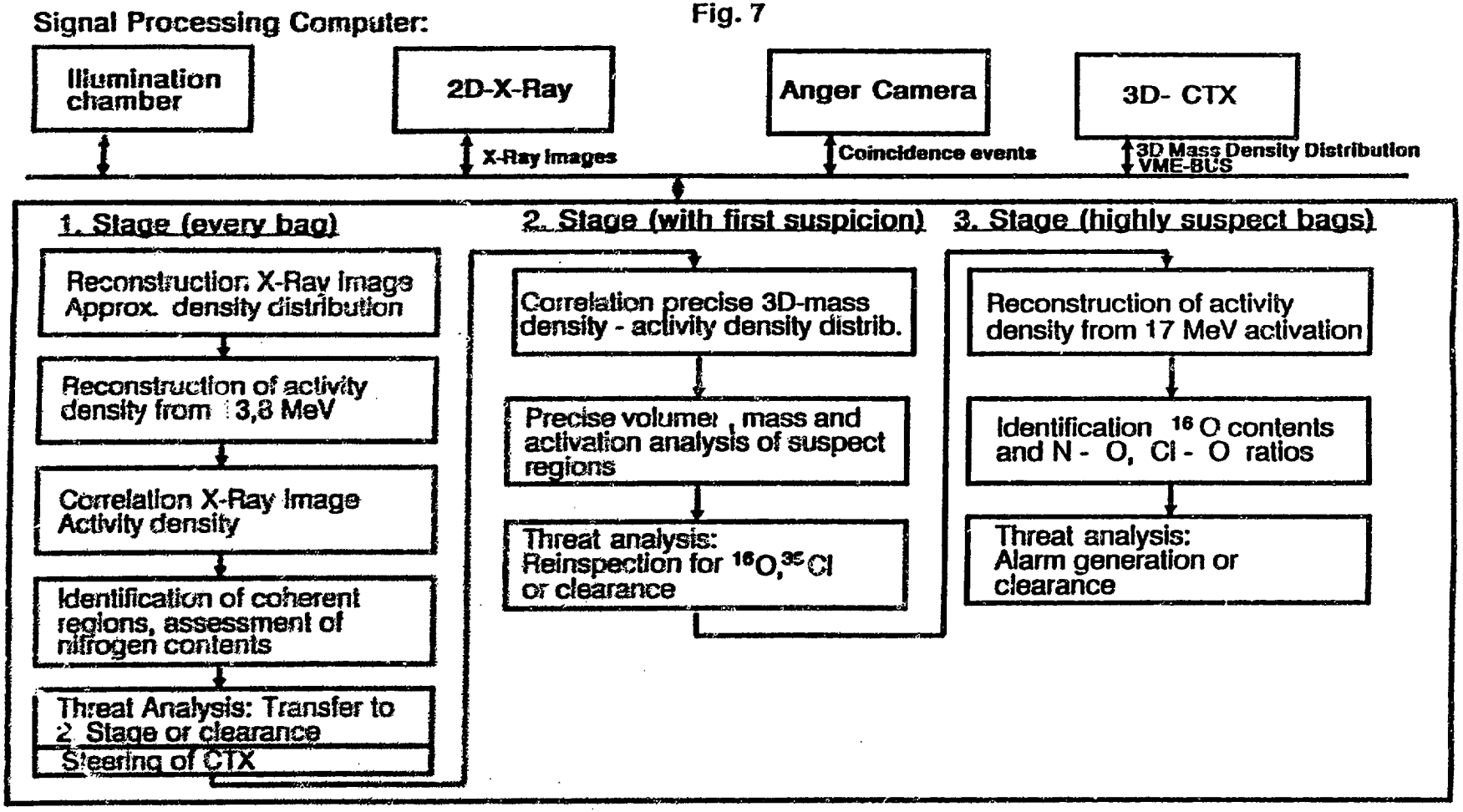


Detection of Explosives
DETEX

Deutsche Aerospace

Layout of System Components

Fig. 7

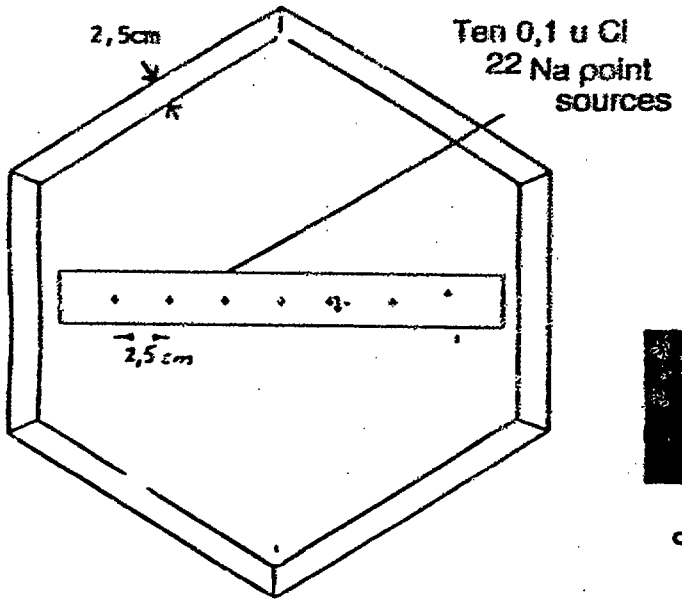


Detection of Explosives
DETEX

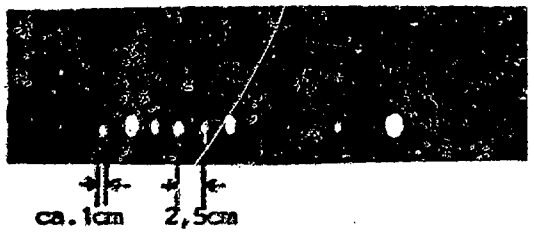
MBB
Deutsche Aerospace

Layout of System Components

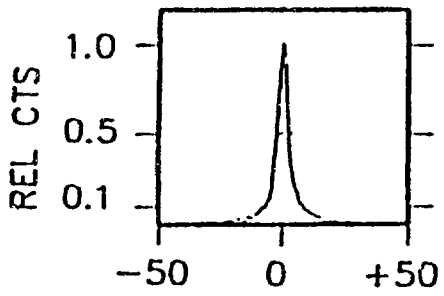
Fig. 8



Free passage = 88 cm
Detector length = 50 cm



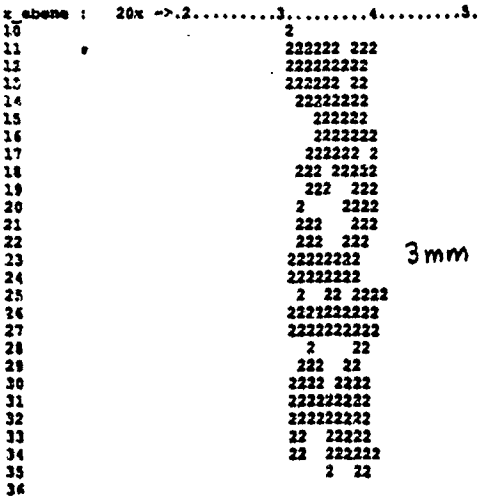
Reconstructed image
(Photo from tomograph
screen)



2D Point-Spredel Function
at low count rate (point
source)

Experimental results for the projected detector concept
UGM Medical Systems Inc.

ANGER CAMERA RECONSTRUCTION



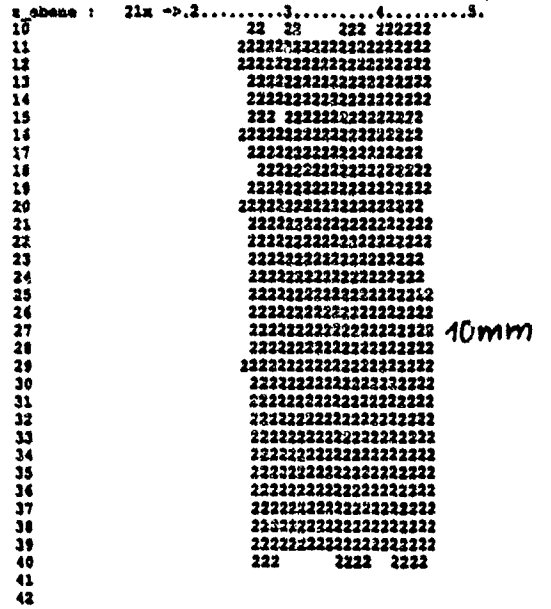


Fig. 9

ANGER CAMERA RECONSTRUCTION

Fig. 10

Detection of Explosives
DETEX

Conclusions:

- DETEX meets all requirements
- Vital advantages by separating illumination and measurement:
  - Long life expectancy of Anger Camera (20.000 h)
  - Permant access without radiation hazard for operating and maintenance except illumination chamber
- Long life expectancy of illumination unit (30.000 h)
- All important system components verified by experiments
- High modularity
- Best spatial resolution of all discussed methods results in highest sensitivity and high resistance against counter measures
- Residual activity of luggage far below allowable limits
- MBB has processing license for handling of explosives for test measurements

FIG. 11

Layout of System Components

Fig. 12

Residual Activation of Bags:

Example of a typical bag contents:

Contents	Amount	Half life time	Activity Bequerel (Bq)		
			after illumination	after 30 min.	after 3 h
Coins	10 g	24 min.	10 730	4 511	60
Brass Belt Buckle	7 g	9,8 min.	7 400	886	0
Silver Jewelry	3,5 g	24 min.	4 440	1 867	25
Copper Wire	5 g	9,8 min.	5 550	665	0
Nylon Cloth	500 g	10 min.	2 220	280	0
Leather Jacket	2000 g	10 min.	8 880	1 110	0
Drug containing Iodide (Iodide)	50 mg	13 Tage	0.5	0.5	0.5
Cheese	500 g	10 min.	1 480	185	0.4
Sum of residual activities			40 700.5 Bq	9 504.5 Bq	85.9 Bq

Activity of natural ^{40}K contents of human body: ca. 4 000 Bq
Limit for free handling of comparable radiation source 500 000 Bq

- Radiation dose is far below accepted limits and comparable to natural fluctuation levels from other sources.
- Luggage handling requires no special radiation precautions to personnel.

SELECTIVE GAMMA RAY RESONANT ABSORPTION FOR EXPLOSIVES DETECTION

Colin Nicholls & J. Derwin King
Instrumentation and Space Research Division
Southwest Research Institute
San Antonio, TX

Floyd McDaniel
Ion Beam Modification & Analysis Lab
University of North Texas
Denton, TX

1. INTRODUCTION

The provision of improved security for passengers in domestic and international travel is a high priority need of the Federal Aviation Administration (FAA) and other government agencies. One technique currently under investigation is based on the resonant absorption in nitrogen of 9.17 MeV gamma rays. Since explosives contain a higher proportion of nitrogen than most common materials, a high nitrogen absorption can be used to infer the presence of explosives. This technique is attractive in that the gamma rays used are of sufficiently high energy that they can penetrate most shielding that could reasonably be incorporated into a suitcase. However the method is more accurately a nitrogen concentration detector rather than a specific explosive detector and so false alarm rates from this approach could be high. If a degree of chemical selectivity (i.e. detection of explosives, rather than nitrogenous compounds) could be incorporated into the method, then false alarm rates might be reduced to a low enough level to make this a particularly attractive technique. SwRI has identified a promising method to achieve this and has filed for a patent. In this modified method, high energy gamma rays are used to penetrate metal shields while a magnetic field is applied to modulate the nuclear energy levels of selected nuclei (^{14}N) in the material being tested. This modified resonant gamma ray absorption approach will potentially provide chemical sensitivity and specificity to selected nitrogenous compounds, including some explosives.

2. TECHNICAL BACKGROUND

Despite the increasing threat from terrorist attacks and substantial R&D expenditures by the FAA, no entirely satisfactory technique for detecting explosives concealed in airline baggage or mail has yet been developed. The previously developed methods are not specific to explosives, have too high a false alarm rate or they are not able to inspect all bags.

However, some time ago, one of us (J.D.K.) filed an invention disclosure which described a technique which relies on combining the resonant absorption of 9.17 MeV gamma ray photons by ^{14}N with additional features that provide specificity to selected compounds. Any nitrogenous materials placed in a beam of 9.17 MeV gamma rays will absorb these photons with a relatively high cross-section. However, nitrogen in some explosives (notably TNT and C4--the high-threat plastic explosive) has nuclear quadrupole resonances (NQR) at various frequencies in the 1-5 MHz range. Application of a magnetic field of the appropriate intensity (generally in the 200 - 1500 Gauss range) causes the nuclei of hydrogen atoms, which are also present in the explosive materials, to have an NMR frequency co-incident with the nitrogen NQR frequency. From our previous NMR work (Ref. 1,2), it is known that this frequency co-incidence allows greatly enhanced energy transfer between the hydrogen and nitrogen nuclei and this effect strongly influences the proton NMR characteristics (for example, the NMR spin lattice relaxation time, T_1, of protons in C4 is reduced by a factor of several thousand - Ref 3). Our present NMR system for explosives detection utilizes this cross coupling effect. It was postulated that this coincidence would also affect the nitrogen resonant absorption of gamma rays, possibly by changing the width of the resonance line or by shifting the resonant energy level by a small amount. Hence, by varying the intensity of the applied magnetic field about the level that causes coincidence of the ^{1}H-NMR and ^{14}N-NQR in the

material under test, it was anticipated that any effects due to this coincidence will be shown as variations in the absorption characteristics of the resonant gamma rays. For example, if the resonance is broadened then gamma ray energies which were previously outside the resonance absorption line would be attenuated as they move under the resonance curve. Similarly, if the resonant energy shifted, then the attenuation of "on-resonance" gamma rays will be affected. Recently the basic measurements needed to verify the existence of such effects were carried out. It was believed that the success of the measurements would demonstrate the feasibility of a detection scheme which combines the chemical selectivity of NMR with the capability to penetrate dense metallic shielding. These are fundamental requirements for an entirely successful explosives detector to meet the needs of airport security as well as other portal inspection applications.

3. APPROACH

The experimental investigations were conducted at the University of North Texas. The tandem accelerator at the University of North Texas was used to generate protons of approximately 1.7 MeV required for the studies. Collision of these protons with a carbon-13 target generates high energy gamma rays (Figure 1). At an angle of approximately 80.7° to the proton beam, the doppler shift is of exactly the correct value to produce a beam of gamma rays at an energy of 9.17 MeV -- the value required for resonant (maximum) absorption by nitrogen-14 (Figure 2). These gamma rays were directed through an explosive simulant (powdered hexamethylenetetramine - HMT) which contains ^{14}N in a molecular (crystalline) environment that causes a nuclear quadrupole resonance to be present. It was necessary to use explosive simulants such as HMT to avoid difficulties in handling and shipping explosive materials. Future studies will use real explosives. Nitrogenous materials with no known NQR resonances (e.g., liquid nitrogen) were to be used as controls but difficulties with the accelerator severely limited the useful beam time available to the study. Controls were therefore achieved by other means, which are described below. The test materials were located in a magnetic field and irradiated with the resonant gamma rays. The intensity of the gamma ray transmission was monitored as the scattering angle between the incident proton beam and the emitted gamma ray beam was varied. Since the doppler shift varies with scattering angle, by sweeping the detector through various angles the incident gamma ray energy is effectively varied.

To compensate for the effects of beam current fluctuations and the presence of magnetic fields, a second gamma ray detector was used on the side of the beam line opposite to the sample system. This detector was used to detect the emission of 9.17 MeV gamma rays (which are emitted in a cone of constant scattering angle - $\theta = 80.7°$). A gamma ray spectrum obtained from this detector during one experiment is shown in Figure 3. The peak centered at channel number 2550 is the 9.17 Mev Gamma ray photopeak, and the smaller, broader peak centered at channel number 2400 is the first escape peak. Both peaks were included in the data window, since both peaks represent the arrival at the detector of a 9.17 MeV gamma ray. When the magnet was switched on, the fringe field altered the photomultiplier response, effectively reducing the photomultiplier gain by about 30%. The 9.17 MeV peak thus accumulated in channels centered around 1700. The counts detected in the sample detector were normalized by dividing by the counts detected in the reference detector. In order to properly define the scattering angle (and hence the gamma ray energy) the sample detector was collimated with four inches of lead, except for the entrance aperture which was 2 mm wide. This represents an angular width of approximately 0.25°.

After the proton beam had been calibrated to ensure that the requisite 1.7 MeV protons were incident on the ^{13}C foil, the first experiment was performed using a melamine sample. This material was chosen because it has one of the highest nitrogen concentrations available in a conveniently handled material (~80% that of liquid nitrogen). With a 10" long powdered sample in no magnetic field, the scattering angle was varied to map out the resonance which is shown in Figure 4. The absorption dip is clearly seen. The depth of the dip agrees with calculations based on published data [Ref 4.]. If the sample goniometer were exactly aligned with the proton beam axis, then the center of the resonance should occur at 80.7°. The data shows a goniometer offset of approximately 1.1°, but since this is just a constant offset which is defined by the goniometer position, no adjustments were made.

After this result had been obtained, several experimental difficulties severely reduced the available beam time, during which useful experiments could be performed. All of these problems were identified and corrected, but they so severely reduced the time available on the apparatus that only one sample with an NQR signature could be studied. Fortunately this one sample was enough to indicate the possibility of the approach being feasible.

In this experiment a 10" long cylindrical sample of HMT powder was placed inside the magnet with its axis aligned along the gamma ray beam. The scan was begun at a scattering angle of 80° and the angle was incremented in 0.2° steps except around the center of the resonance where 0.1° steps were used. At each position data was collected with no magnetic field applied and then repeated, without moving the sample, with an applied field of 800 gauss at the center of the magnet. The homogeneity of the field was such that the field at the sample was everywhere within the range 780-800 gauss. Since the proton NMR/ nitrogen NQR cross-over region in HMT occurs at fields from 750 gauss to 820 gauss, all parts of the sample were subjected to magnetic fields which satisfied the crossover condition. The results are shown in Figure 5.

4. RESULTS & DISCUSSION

Examination of Figure 5 shows there is appreciable scatter present in the data. However there are certain differences between the data sets, the most obvious of which is that the 'Magnet on' data has a higher baseline than the 'Magnet Off Data'. Unfortunately this may not be significant, since the baseline, defined by the ratio of the counts at the reference detector to the counts at the sample detector far from resonance may be influenced by the experimental configuration. It is possible that the differences seen in the two baselines might be due to a shift in the sample detector calibration in the fringe field of the magnet. The two calibrations (with and without magnetic field) required two sets of energy windows to be set to observe the 9.17 MeV peak. Small differences between the true widths of these two windows could account for the small baseline shift (1% of reference detector count rates) observed here.

To more quantitatively assess the differences between the data sets, a computer program was written to fit the data to a Lorentzian line shape of the form :

$$Y = A + B\,(1 + ((\theta-\theta_o)/\Delta)^2)^{-1}$$

where

Y	is the ratio of the counts in the two detectors
A	is the basline ratio (far from resonance)
B	is the depth of the resonance dip
θ	is the scattering angle
θ_o	is the center of the resonance
Δ	is the width of the resonance.

The fits to the entire data set, shown in Figure 5 gave the following values

	Baseln	Depth	Width	Center
Magnet Off	0.1201	0.0296	0.569°	81.89°
Magnet On	0.1301	0.0241	0.343°	81.78°

As part of the fitting process, a technique called a jack-knife fit (Ref. 5) was used to estimate the error in the fitted parameters. This procedure works by taking the entire data set, dropping the first point and then calculating the fitted parameters. The first point is put back in the data set, the second point is dropped and a new set of fitted parameters is obtained. This procedure is repeated dropping each of the n points in turn and generating n sets of fit parameters. The uncertainty in the fit parameters is then estimated by taking the standard deviation of the n sets of fits. However a standard Chi Squared value is also generated as part of the fit and it was noted that when either of two points (point numbers 2 & 5, corresponding to scattering angles of 81.2° and 81.5°) were dropped, the Chi Squared parameter dropped by almost a factor of two suggesting that these points were outliers. Examination of Figure 5 supports this hypothesis. The fits were repeated excluding these points and the data of Table 1 were obtained.

The first line in Table 1 shows the parameters obtained from fitting all points except the two that had already been identified as outliers. The lower portion of the table shows the parameters obtained when the point number identified in column 1 was dropped. The second line in Table 1 (labelled 'Mean') represents the means for the parameters shown in the lower table and the third line shows the standard deviation of these parameters. For visual comparison, the data is presented in graphical form in Figures 6-8. Note that no graph is shown for the baseline parameter, because the differences observed in this parameter could be an experimental artefact, as previously described.

Examination of Figures 4-6 appears to show significant differences between the 'Magnet Off' and 'Magnet On' states. In particular the 'Magnet on' data appears to

have a narrower and deeper resonance than the 'Magnet Off' data and to be shifted by approximately 0.1°. It is not known what causes these changes.

The total absorption of the sample under the resonance can be calculated by integrating the equation for the resonance line shape. This yields an expression of the form

$$\Gamma(x) = B\Delta \, \mathrm{Tan}^{-1}(x)$$

Where the baseline parameter A has been arbitrarily set to 0.

Calculation of the integral over a range of 1.2° using the values .215, .3, and .172 and .4 for B and Δ for 'Magnet On' and 'Magnet Off' respectively, gives areas Γ_{on}= 9.80 and Γ_{off}=9.85, which are identical to within the experimental uncertainties.

5. CONCLUSIONS

The data from these experiments appear to show that there are significant differences in the resonant absorption characteristics in a magnetic field intensity selected to maximize the ^{1}H-^{14}N cross-coupling effects compared to that in no applied magnetic field. It is still uncertain whether these effects are of a magnitude large enough to be practically useful in the detection of explosives in suitcases. It is also unknown what the effects will be on real explosives, on materials with no NQR resonance, on materials with NQR resonance but at other fields or on materials with NQR resonances irradiated with RF at their resonant frequency. The various problems with the apparatus precluded these determinations and further work is required to fully address these issues.

REFERENCES

1. "Nuclear magnetic Resonance Techniques for Explosives Detection Parts I - IV", J.D.King, W.L. Rollwitz et al., U.S. Army MERADCOM Final Report, AD-BO26059, Feb. 1978

2. "Development & Evaluation of a Prototype Checked Baggage System " A.De Los Santos, J.D.King, W.L.Rollwitz, U.S.Dept Transportation, Federal Aviation Administration Final report contract DOT-FA77WA-3966,FAA-RD-8-46, Feb 1981

3. "Hydrogen-nitrogen Cross Relaxation in Hexamethylenetetramine" R.Gonano et al. 3rd Int. NQR Conf., Tampa Florida April 1975

4. "Feasibility of Detecting FAA-Threat Quantities of Explosives in Luggage & Cargo using Nuclear Resonance Absorption in Nitrogen",Los Alamos nuclear Laboratory, Advanced Nuclear Technology N-2, October 1989

5. "Estimating Error Limits in Parametric Curve Fitting" M.S. Caceci, Anal. Chem. 61 (20) 1989 p 2324-2327

TABLE 1

	Magnet Off				Magnet On			
	Base	Depth	Width	Center	Base	Depth	Width	Center
Fit	1118.4	171.79	0.398	81.89	1277.2	215.43	0.299	81.78
Mean	1120.0	173.47	0.404	81.89	1277.5	216.09	0.300	81.78
Std Dev	13.3	11.30	0.054	0.0126	6.7	7.14	0.017	0.0048
Drop Pt. #								
1	1093.3	150.43	0.329	81.88	1274.6	213.15	0.296	81.78
2	1117.1	169.89	0.411	81.88	1277.1	215.46	0.299	81.78
3	1118.2	171.67	0.397	81.89	1281.2	218.44	0.322	81.77
4	1118.2	171.54	0.397	81.89	1275.5	212.25	0.293	81.79
5	1117.9	169.65	0.397	81.89	1279.3	207.77	0.316	81.79
6	1123.7	171.22	0.429	81.90	1271.2	227.80	0.262	81.78
7	1114.3	171.86	0.375	81.89	1277.2	215.41	0.300	81.78
8	1118.2	179.13	0.382	81.90	1274.5	212.87	0.291	81.78
9	1118.4	173.02	0.395	81.89	1278.2	216.52	0.303	81.79
10	1117.4	166.31	0.405	81.88	1280.0	216.57	0.313	81.79
11	1107.7	162.90	0.353	81.87	1278.2	220.18	0.282	81.78
12	1120.6	173.45	0.408	81.89	1276.9	215.02	0.300	81.78
13	1159.8	205.07	0.582	81.93	1263.7	201.32	0.287	81.79
14	1119.1	175.51	0.375	81.88	1279.2	217.35	0.302	81.78
15	1126.7	181.43	0.401	81.88	1296.0	231.25	0.334	81.78
16	1129.9	182.42	0.426	81.89				

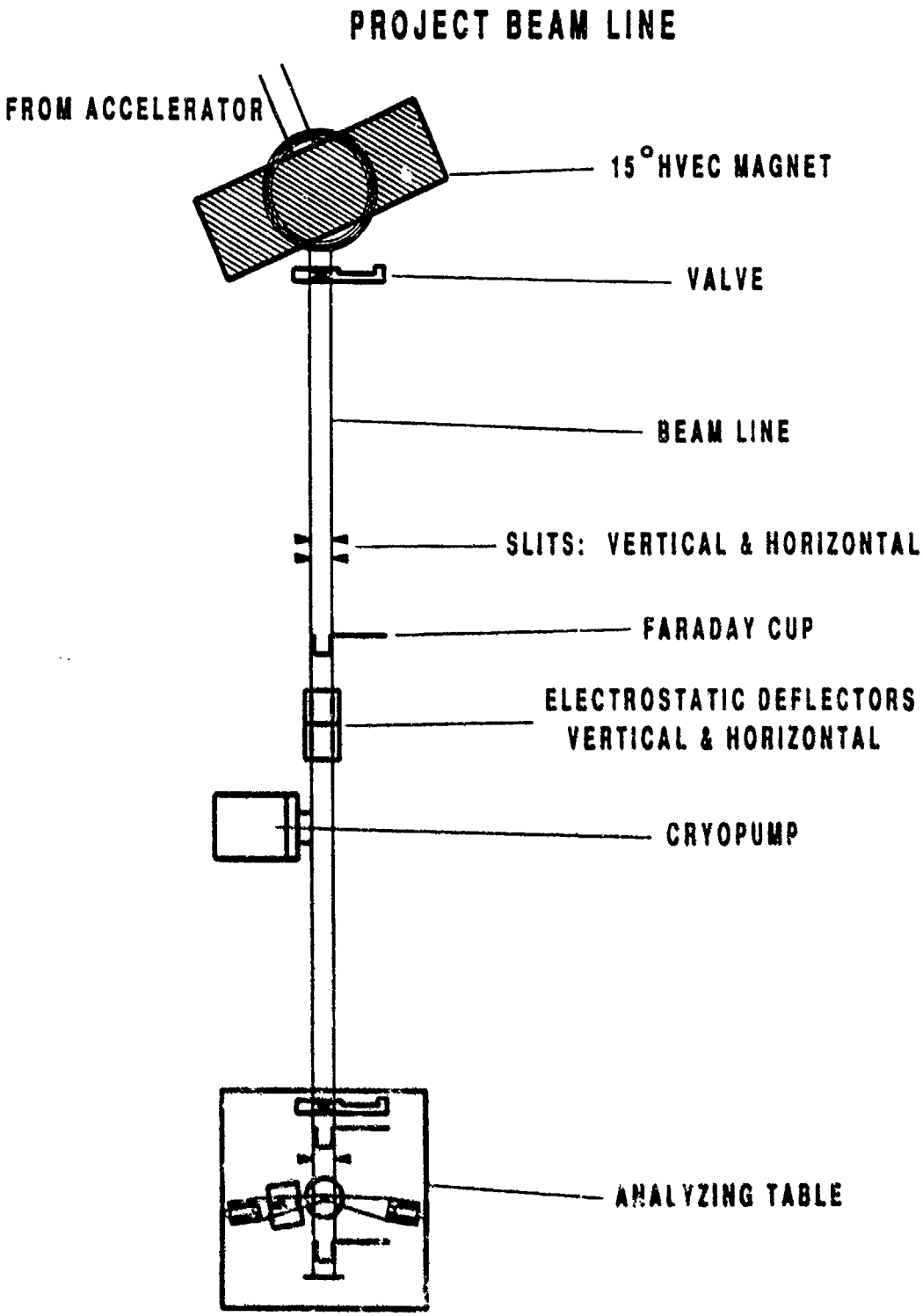

PROJECT BEAM LINE
FROM ACCELERATOR
15°HVEC MAGNET
VALVE
BEAM LINE
SLITS: VERTICAL & HORIZONTAL
FARADAY CUP
ELECTROSTATIC DEFLECTORS
VERTICAL & HORIZONTAL
CRYOPUMP
ANALYZING TABLE

FIGURE 1.

ANALYZING TABLE

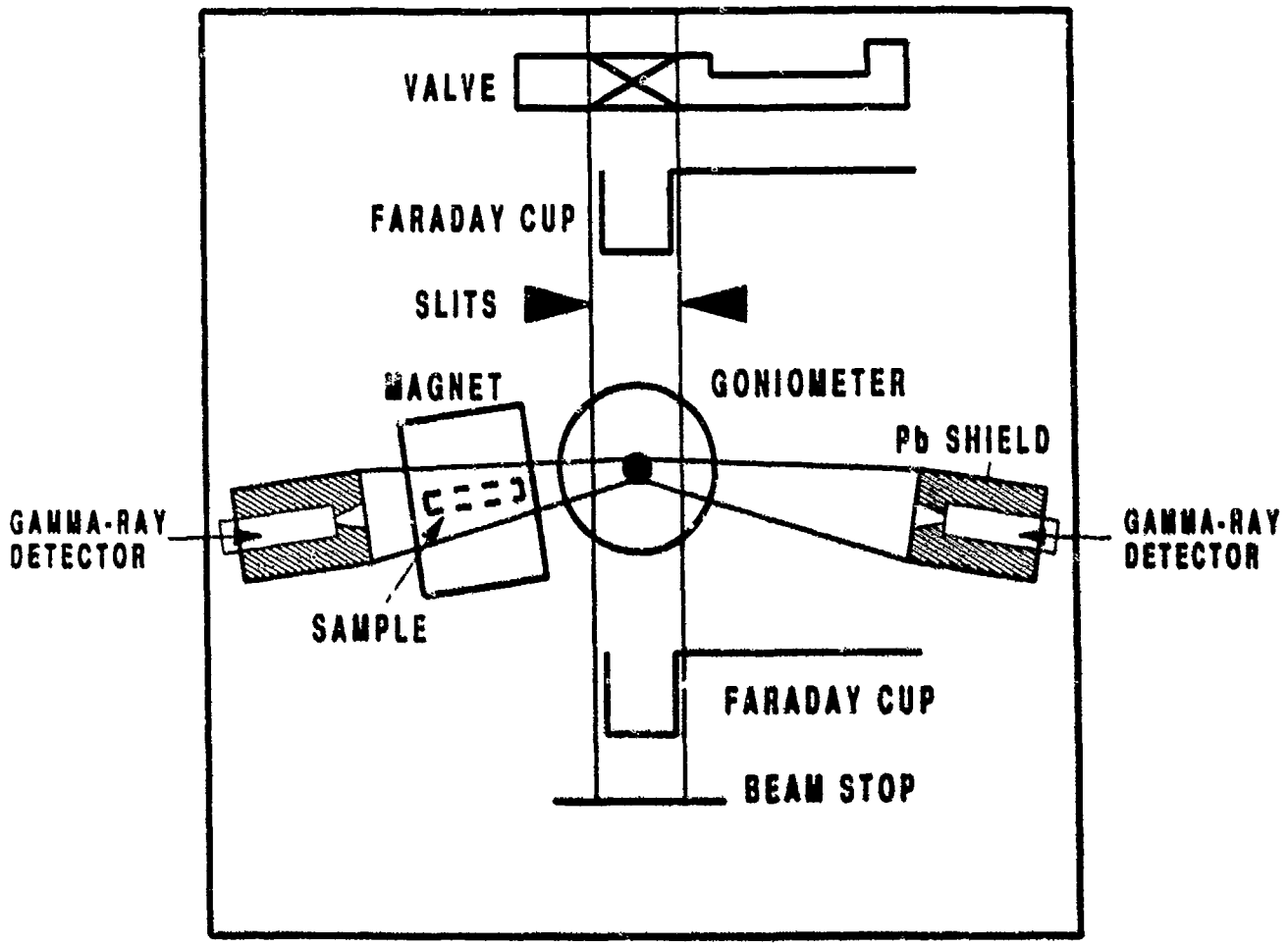
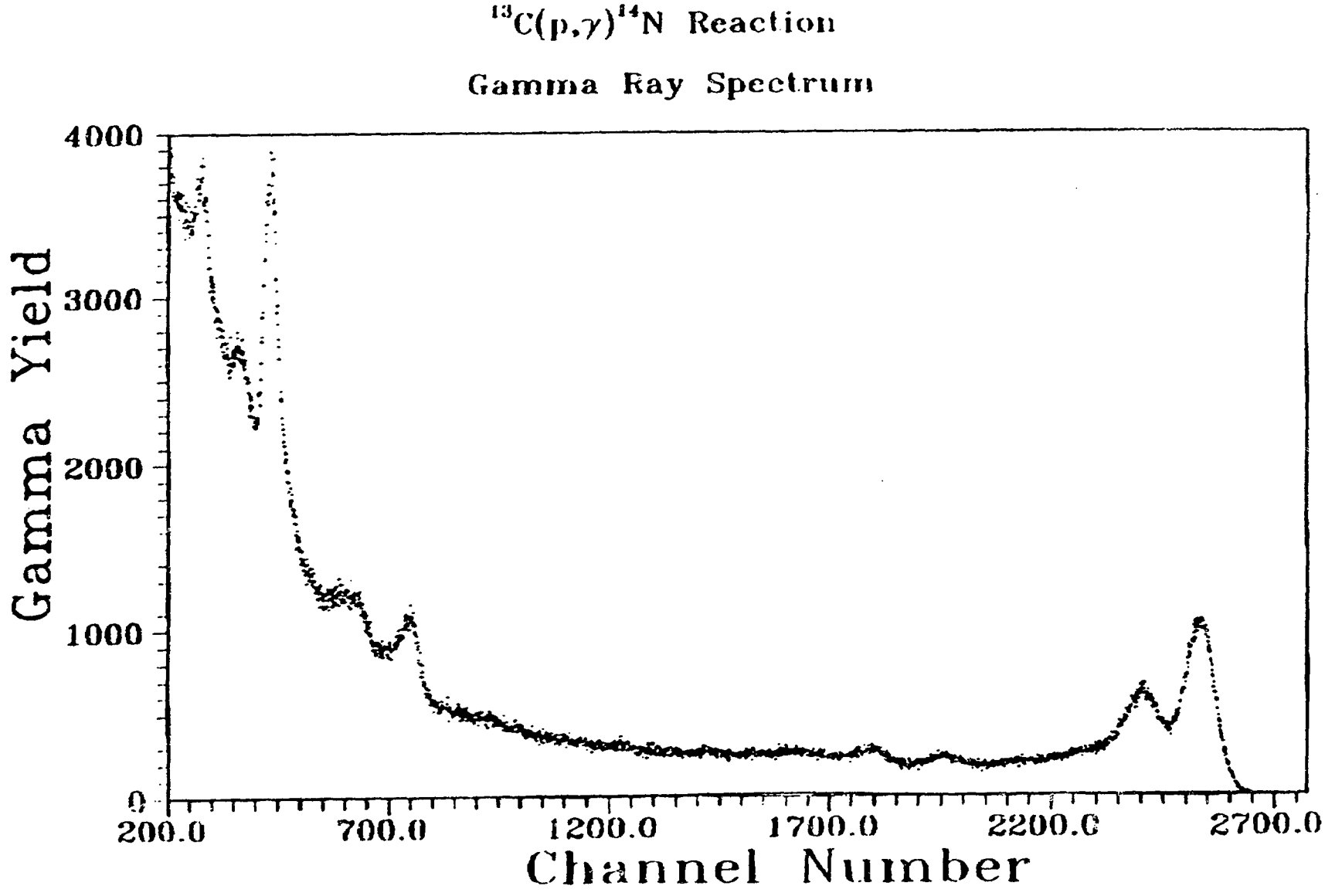


FIGURE 2.


$^{13}C(p,\gamma)^{14}N$ Reaction
Gamma Ray Spectrum
Gamma Yield
4000
3000
2000
1000
0
200.0
700.0
1200.0
1700.0
2200.0
2700.0
Channel Number

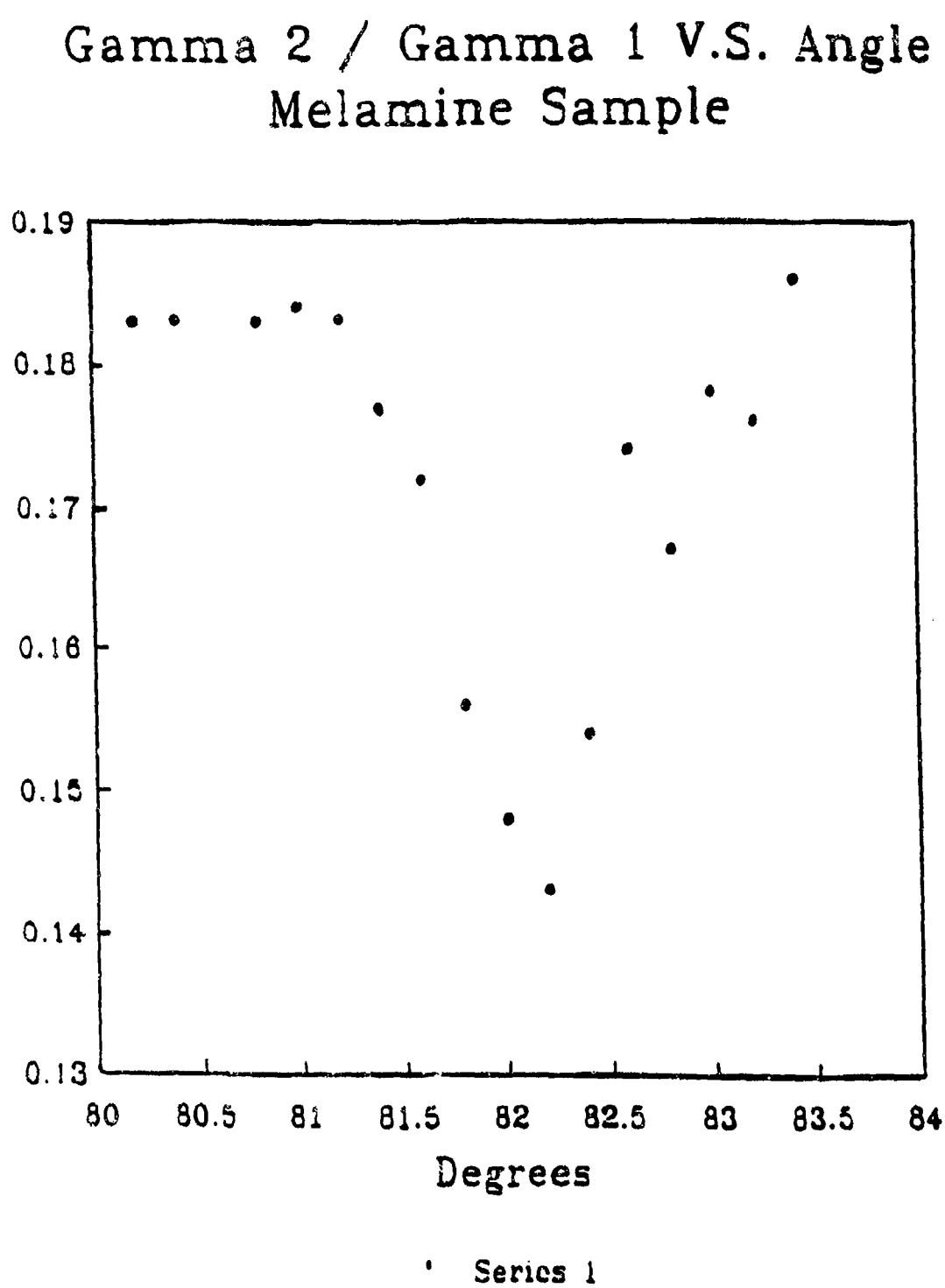

Gamma 2 / Gamma 1 V.S. Angle
Melamine Sample
0.19
0.18
0.17
0.16
0.15
0.14
0.13
80
80.5
81
81.5
82
82.5
83
83.5
84
Degrees
Series 1

FIGURE 4.

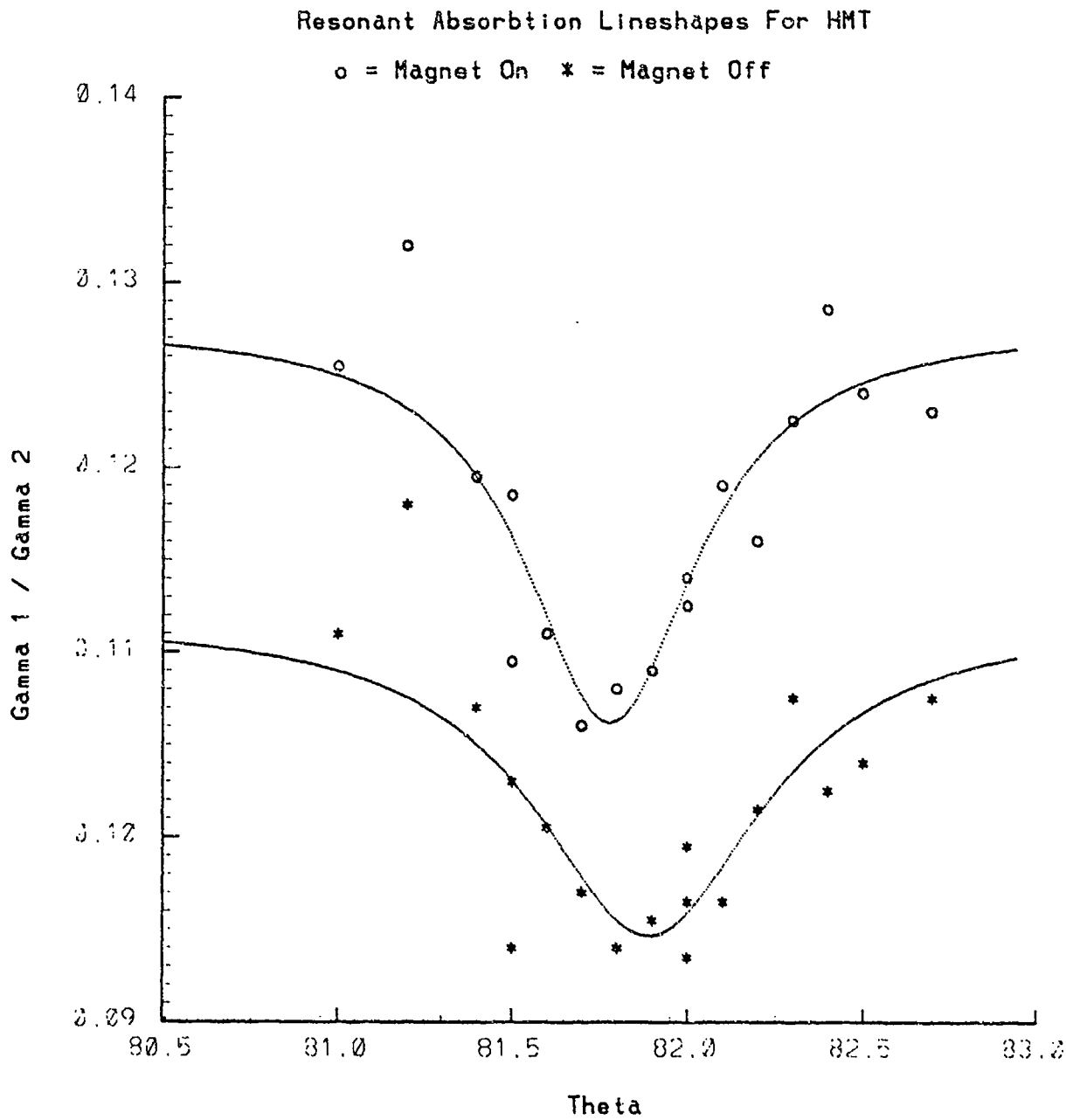

Resonant Absorbtion Lineshapes For HMT
o = Magnet On * = Magnet Off
Gamma 1 / Gamma 2
0.14
0.13
0.12
0.11
0.10
0.09
80.5
81.0
81.5
82.0
82.5
83.0
Theta

FIGURE 5.

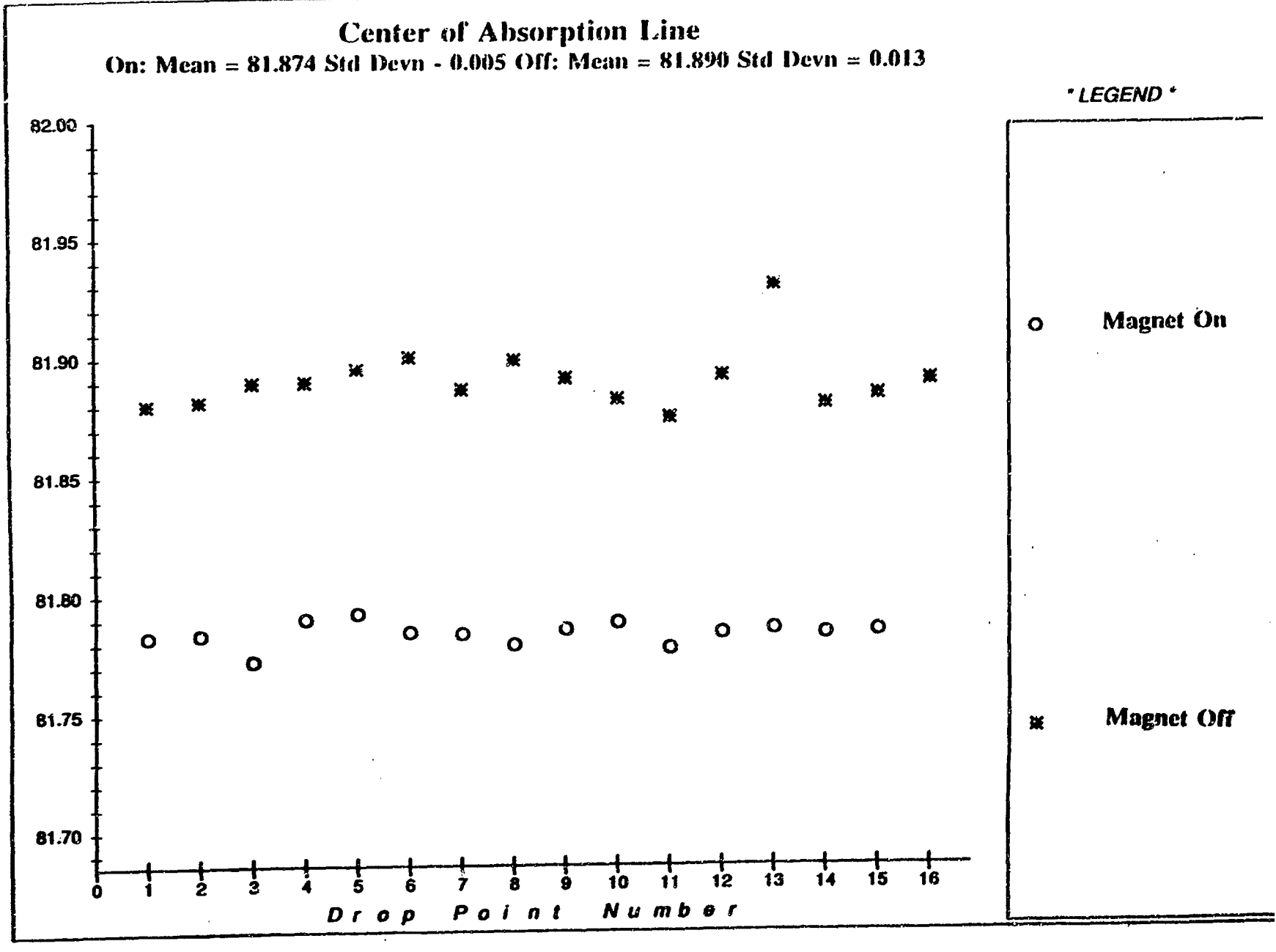
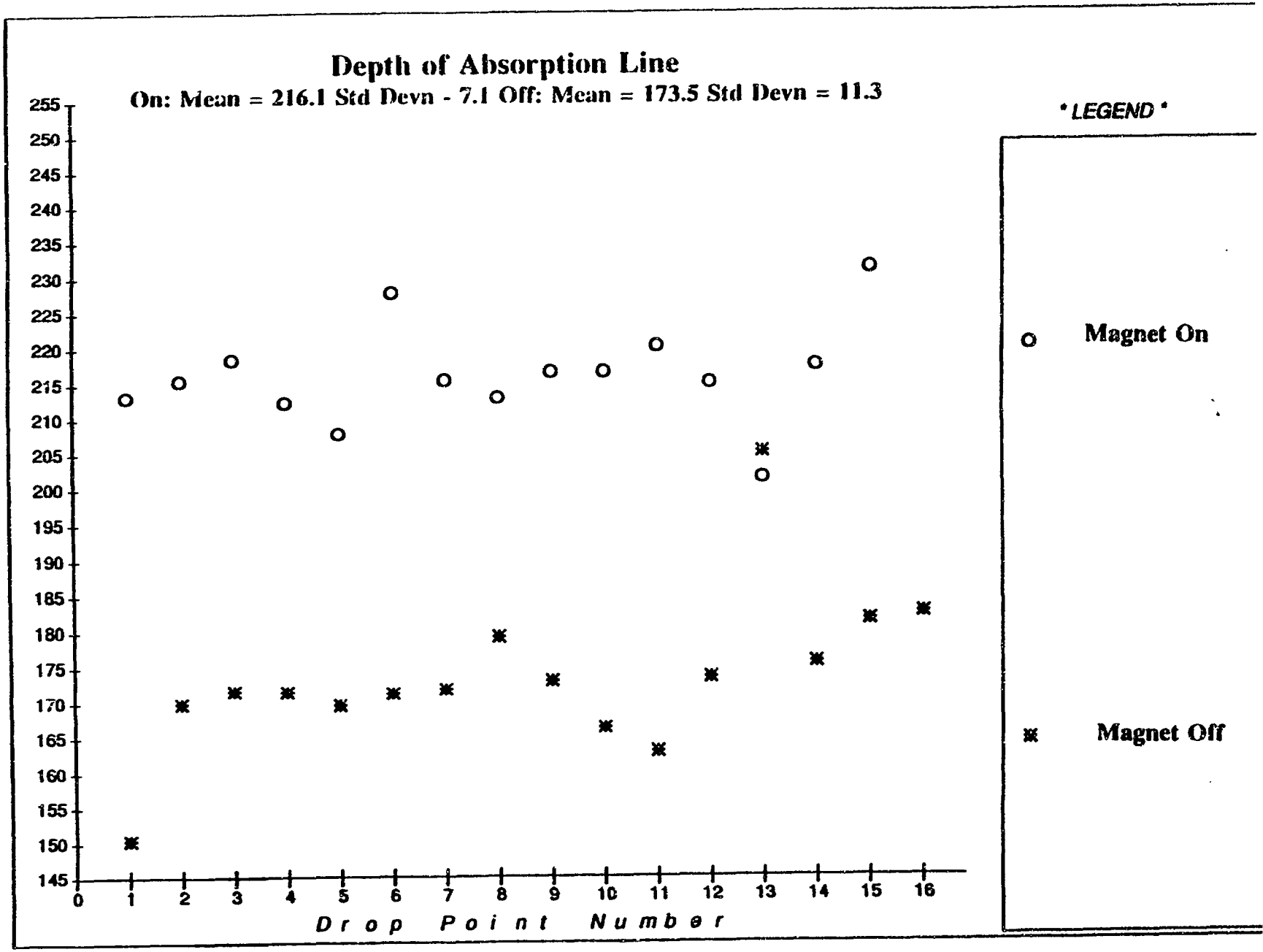

Center of Absorption Line
On: Mean = 81.874 Std Devn - 0.005 Off: Mean = 81.890 Std Devn = 0.013
82.00
81.95
81.90
81.85
81.80
81.75
81.70
0 1 2 3 4 5 6 7 8 9 10 11 12 13 14 15 16
Drop Point Number
* LEGEND *
Magnet On
Magnet Off

FIGURE 6.


Depth of Absorption Line
On: Mean = 216.1 Std Devn - 7.1 Off: Mean = 173.5 Std Devn = 11.3
255
250
245
240
235
230
225
220
215
210
205
200
195
190
185
180
175
170
165
160
155
150
145
0 1 2 3 4 5 6 7 8 9 10 11 12 13 14 15 16
Drop Point Number
* LEGEND *
Magnet On
Magnet Off

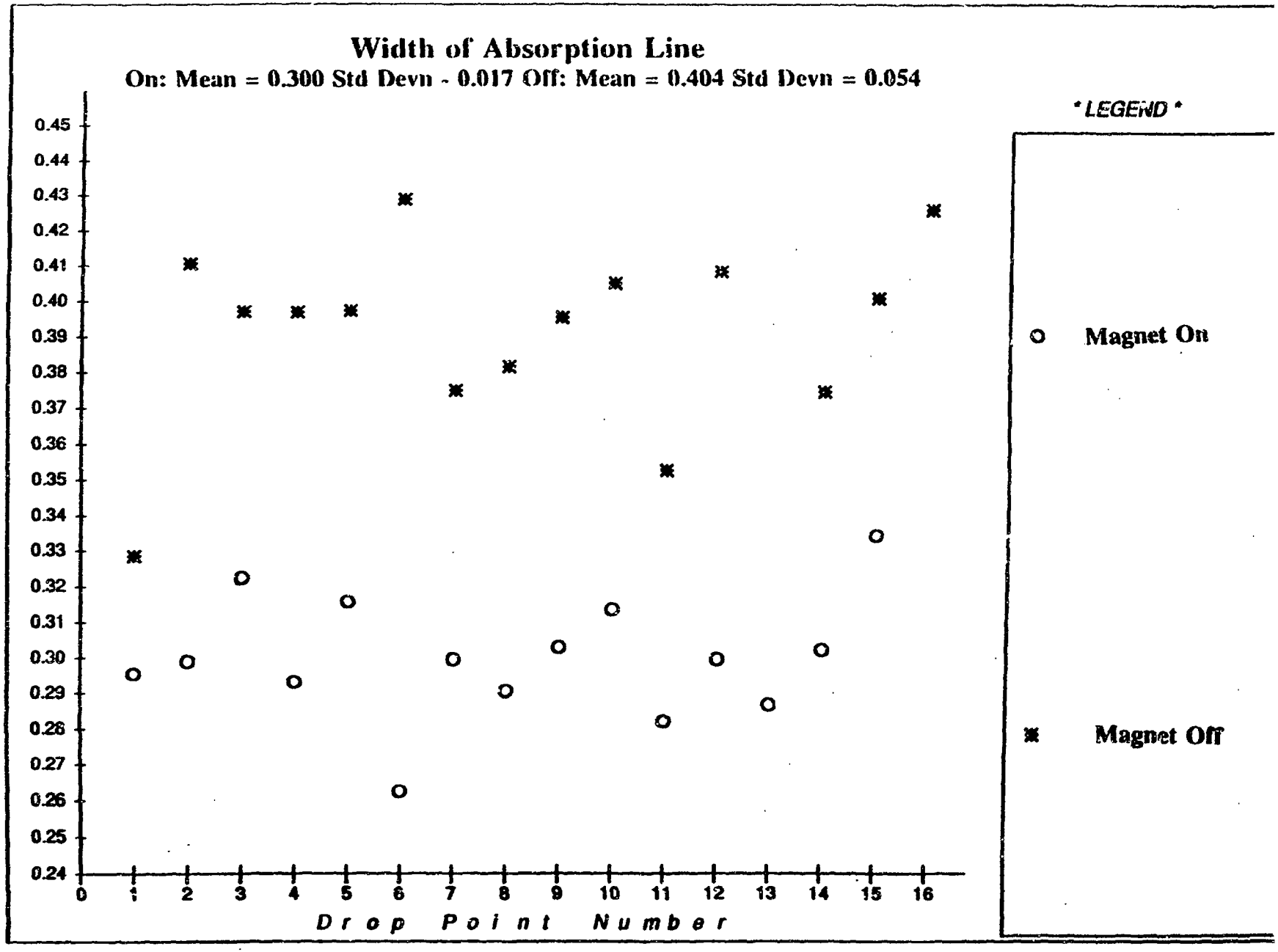

Width of Absorption Line
On: Mean = 0.300 Std Devn - 0.017 Off: Mean = 0.404 Std Devn = 0.054
0.45
0.44
0.43
0.42
0.41
0.40
0.39
0.38
0.37
0.36
0.35
0.34
0.33
0.32
0.31
0.30
0.29
0.28
0.27
0.26
0.25
0.24
0 1 2 3 4 5 6 7 8 9 10 11 12 13 14 15 16
Drop Point Number
* LEGEND *
Magnet On
Magnet Off

FIGURE 8.

TESTING AND FIELD EXPERIENCE

A GENERAL PROTOCOL FOR OPERATIONAL TESTING AND EVALUATION OF BULK EXPLOSIVE DETECTION SYSTEMS

Dr. Joseph A. Navarro
JAN Associates, Inc.

Mr. Donald A. Becker
NIST

Dr. Bernard T. Kenna
Sandia National Laboratory

Dr. Carl F. Kossack
Consultant

1. INTRODUCTION

In March 1990, the FAA Technical Center established a Task Force of independent consultants to undertake testing and evaluation of the TNA technology as implemented by SAIC at the JFK airport. As a result of its work, the Task Force was asked to prepare a protocol for the conduct of operational testing of explosive detection systems (EDS) for checked or carry-on airline baggage (bags, containers, etc). These results, in part, would also be used to decide on FAA certification of bulk explosive detection systems. This protocol is specific to testing of production hardware, as opposed to R&D brass/bread board models or prototype versions of the system. This protocol is applicable to systems which are automated (i.e., no human intervention used for the detection process) and for those systems which do not change the characteristics of the tested item as a result of the item being tested. This protocol is only applicable to systems based on detection of explosives in bags via bulk properties (i.e., vapor detection systems are excluded). Finally, although this protocol was written to be applicable for the detection of explosives in bags, much of it is applicable for the detection of explosive devices.

Since different technologies may be considered in this application, the protocol does not provide sufficiently detailed plans and procedures to allow one to test and evaluate any specific hardware system. However, it provides the guidance and framework to ensure that all explosive detection systems, meeting the above conditions, will be tested with the same rigid standards.

For each application, the FAA will establish the specific threat package (including size, shape, amount and type of explosive) to be detected by the system. Although there will be only one overall threat package, one could envision (in a long range plan) where technologies could be appropriate for, or apply to, a subset of the threat package but not the total package.

In order for the FAA to make a decision on the operational effectiveness of the system, the FAA will need to consider the:

- Potential locations of the EDS;
- Fraction of detections, f(d), of explosives observed in the operational testing and evaluation (OT&E) of the EDS;
- Fraction of false alarms, f(fa), observed;
- Rate of processing of the containers, R.

The FAA may also be interested in the trade-off between the two fractions, especially for those technologies/systems which could readily adjust detection thresholds (thus affecting these fractions). Other factors which may be considered by the FAA in determining the effectiveness of the system include:

- Reliability, maintainability, availability;
- Cost, initial and annual;
- Significant operational constraints (environment, manpower, etc.);
- Processing time distribution.

The FAA will determine when the test will take place, and will provide the test team, which will be responsible for generating the detailed test plan, preparation and execution of the test, analyses and evaluation of the test data, and finally prepare a report on the findings of all aspects of the operational testing. The test team should have a test director, and be composed of experts in the technology being tested, test and evaluation planners, and analysts who can design the statistical plan and conduct the evaluation of the test results. An independent observer should also be a member of the test team. The individual should comment on all activities associated with the testing and evaluation of the EDS.

All test baggage and test articles, threat explosives (explosives or simulants) and personnel will also be provided by the FAA.

Section 2 provides some general requirements associated with the operational testing process. Section 3 addresses a set of issues that must be considered and specific requirements that must be fulfilled prior to the development of a detailed operational test and evaluation (OT&E) plan. In Section 4, specific aspects of the detailed OT&E plan are discussed. Section 5 deals with issues related to the conduct of the test, while Section 6 discusses the data analyses and evaluations of the test data. Finally, the appendices contain the statistical approaches suggested for the analyses of the test data.

2. GENERAL REQUIREMENTS

In order to develop a specific test plan, the test team must consider all of the factors that may: (1) influence the conduct of the test; (2) bias the measurements related to the detection system under test; (3) affect the results obtained from the test and/or the reliable interpretation of those results. The test team must establish the conditions under which the test is to be conducted and the characteristics (i.e., attributes, variables) of any bag as it is processed by the system. There are a number of steps or topics which must be considered before development of a final specific test plan for the system under test. These may be separated into two groups, general topics and specific topics. The general topics are discussed in this section, while the specific topics will be covered in the next section. However, since this is a generic protocol for a variety of explosive detection systems (using different technologies), there may be some additional factors which may need to be considered, and the discussions that follow should not prevent any additional factors from being included in the final test plan if those factors are considered to be relevant.

2.1 Identification of the Measured Characteristics

Once the system to be tested has been identified, the set of characteristics of the explosives that will be measured in order to determine if a detection has occurred has to be identified and specified. For example, for the TNA system, one of the primary characteristics of the explosive being measured is the nitrogen content. Having done this, the test team must determine if simulants can be identified which will exactly mimic the explosive characteristics under test. This determination must be made especially when the use of explosives will be prohibited in the operational test and evaluation (OT&E) of the system at airport facilities.

In addition, any countermeasure techniques to be included in the testing should be identified prior to the test initiation by the FAA, or by the test team in consultation with the FAA. Some systems have relatively simple and effective countermeasures which are obvious, while others may not have any known countermeasures or only difficultly applied countermeasures.

2.2 Identification of the Set of Threat Explosives

The set of threat explosives (type, shape and weight) to be used in the OT&E testing must be specified by the FAA. For example, the FAA may include as part of the threat, that testing must be done using 2.0 pounds of sheet explosive of RDX/PETN base (Semtex). The FAA must also specify the relative frequency of expected occurrence for each item in the set of threat explosives. The FAA should identify where in the containers the explosives should be placed. For example, some explosives may be more difficult to detect when placed on edge, or along a wall of the container. Some systems will be more sensitive than others and thus this requirement assumes knowledge of the system characteristics.

2.3 Identification of Potential Bag Populations

Since the FAA will designate where the EDS will be located, the test team must determine the characteristics of bags typical of those that will be processed by the system when placed at those designated airports. Thus, data must be collected on actual passenger bags that will be processed at those facilities. Further, data may need to be collected over a sufficiently long period of time in order to be able to reflect seasonal and bag destination differences, unless that data is already available from other sources. The data base should cntain observations of all the major characteristics that will be measured by the detection system being tested. This database will be used by the test team to select representative groups of test bags, when required to do so. The actual set of bags used for testing could be: (l) actual passenger bags; (2) fabricated by the FAA appointed team; or, (3) selected from the set of FAA "lost" bags. Bag selection is a crucial topic in designing a test plan which is fair and effective. For additional information on bag selection techniques, see subsection 3.1.

2.4 System Calibration and Threshold Settings

This protocol was developed for systems which are totally automatic in their response. That is, they are to be operator independent. The manufacturer will not be allowed to change or modify the settings of the system once the test for a given bag population has been initiated. Thus the manufacturer should be allowed to have access to the set of bag populations that will be used for the OT&E testing so that they can determine the associated response of the system to the characteristics, and thus calibrate the system and establish the threshold settings prior to any testing by the FAA. However, the manufacturer should not be given any details as to the relative frequency of threat occurrence and location of the threats in the bags, since it is the intent to make the tests as blind as possible. The manufacturer should provide the FAA with the complete calibration protocol.

While the manufacturer is establishing the threshold settings, they should also be required to provide the FAA test team with the relationship between f(fa) and f(d), as a function of the threshold setting. This data should be made available prior to the OT&E testing to help answer the "What If" questions. If the system being tested can store the basic data so that, after the fact, the- what would happen to the f(d) if the threshold was raised (or lowered)- question can be answered, then the above requirement on the manufacturer would not be necessary.

2.5 Manufacturer/Contractor Participation

Although the test team may be required to rely heavily on the manufacturer/contractor personnel for support in conducting the testing, procedures should be established to minimize the possibility the manufacturer could affect the results of the tests. Toward this end, the manufacturer may be required to train FAA chosen personnel to operate the system during the test. The personnel chosen should be representative of the types that will be expected to operate the system if it is indeed placed in the hands of the airport/airline companies.

2.6 Test Sites

All EDS hardware should be tested at either the airport facilities where they might be located, or at an FAA dedicated test site designed to accommodate the OT&E process. If the testing is at an FAA dedicated site, the distinct bag population samples need to be generated; however, there should not be a need to use simulants since the use of explosives should be allowed. If the testing is conducted at airports, then the bag populations are available (passenger bags), assuming the tests are conducted over the various seasons which might influence the characteristics of the bags. In most cases, the use of explosives will not be acceptable and simulants will be required. (In either case, simulants may be needed if one wants to check the systems while they are operational at the various airports.) A major disadvantage of airport testing is that the testing could interrupt operations at the airport. On the other hand, if the EDS is to be used in conjunction with other systems, already in place at the airport, there would be no need to have to provide the other hardware at the dedicated site.

All things taken into account, the preferred test site would be an FAA dedicated site. However, at this time, the protocol must be written for airport facilities, since realistically, it would take several years to obtain such a site, and in the interim the only practical test sites would be the airports.

3. SPECIFIC REQUIREMENTS

Before a test plan can be developed, it is essential to know where the tests will take place and the constraints that will be placed on the use of threats

during the tests. The preferred location of the tests should be at the airports where the hardware systems will be used. Further, it is preferred that actual explosives samples be used when testing for the detection capability of the system. Finally, it is preferred that actual passenger bags be used when testing for both the detection and false alarm capability of the system. Unfortunately, it may not be possible to conduct the operational tests in the above preferred manner. The test team must first determine what deviations will take place and use alternative methods for achieving as realistic and meaningful tests as possible, given these deviations.

If the tests can not be conducted at airport facilities, it most likely will not be possible to use passenger bags to test for the fraction of false alarms, f(fa). It may also be difficult to address operational processing rates of bags through the system. If on the other hand the tests can be conducted at airport facilities, then it may not be possible to use actual explosive samples, but may require the use of simulants. Under either situation, the test team must determine the set of bags that should be used in testing for both f(d) and f(fa). The selection process will be depended on where the testing will take place.

In summary, the three specific areas that may have to be addressed before the test team can develop the detailed test plan for the conduct of the OT&E of any system are: i) identification of the set of distinct bag populations that must be used in the OT&E of the system, ii) identification and selection of the threat package to be used in the testing of the system, and iii) specification of the procedures used to measure baggage processing rates.

3.1 Identification of Distinct Bag Populations

One of the most important aspects of the test plan and subsequent analyses is the selection of the bags to be used for the tests. These bags must reflect the type of bags that will be operationally encountered and processed by the system, over time and at various locations. Bags which are destined for one location, at a given time of year can be expected to be packed with different items than bags going to a different location, or even going to the same location, but at a different time of year. The contents of the processed bags, and the effect it will have on the measurements that will be taken of the characteristics of the explosive, must be considered in any test plan. Toward this end, the FAA will specify the constraints/conditions placed on measurements associated with f(d) and f(fa) determinations. For example, the size and weight of a test bag may be restricted, their destination and/or time of year may be specified, etc. One must first address the issue of the number of different populations of bags which the system will be expected to process. Different applications or situations may be such that the distribution of the observed values of the characteristics being measured by the system will change significantly from one application to another. If it is determined that these differences are important to the determination of f(d) and f(fa), then the different bag populations should be used for the OT&E testing.

At this stage of the planning phase, it is assumed that the test team has identified the potential set of different bag populations. Further, the test team has established the various factors which are significant in determining if an explosive has been detected. The test team now needs to collect data to determine the final set of populations that will be tested. In order to evaluate these bags, the data collected should be the numerical values of the measured characteristics, as opposed to detect/no-detect.

In order to collect this data, it is recommended that the system under consideration be physically located at those airport facilities for which the potential baggage populations can be observed. For each of these locations, the system manufacturer should be informed by the FAA what maximum fraction of false alarms will be acceptable, so that the system can be properly calibrated and the threshold (for alarming) established.

For each of the potential bag populations, the manufacturer will process passenger bags from these populations and provide the test team with the observed measurements of the explosive characteristics for each processed passenger bag. A sufficiently large sample of processed bags is required, so as to obtain a reasonable estimate of the multi-variate frequency distribution of the set of characteristics being measured (for each of the populations). At the same time, data will be collected on the f(fa), which could be of use to the manufacturer in establishing and/or reconfirming the calibration and threshold setting. If the distributions for one or more of the potential populations are not statistically different, then the data from those populations should be pooled to represent one population. In this manner, a new set of populations

will be established which will represent the final set of populations that will be tested during the OT&E. It should be mentioned that the pooling process is not rigorously defined and will require a considerable amount of judgement.

Some statistical approaches for making this determination are given in Appendix A.

If it is not physically possible to conduct the testing at the airport facilities, then the test team must prepare a set of bags from each of the potential bag populations, and conduct the tests at alternative sites. This will require the test team to know the bag characteristics, as measured by the system, for each of the populations. To this extent, some uncertainty will be introduced into the OT&E process, since the true bag populations are defined by the actual passenger bag populations and the test team is generating artificial populations. In this situation, the test team must attempt to prepare these sets of bags to be as close to the populations of interest as possible.

3.2 Identification and Selection of the Threats

The threat as specified by the FAA for the EDS should include:

- type of explosive (C-4, PETN, etc.);
- minimum quantity (mass);
- shape (bulk, sheet,thickness, etc.);
- relative frequency of use of each threat;
- the location of the threat in the container;
- the set of containers to be used (bags, electronic devices, etc.) and any pertinent features;
- potential countermeasures.

As has been stated before, any detection system must measure a set of characteristics associated with the explosive/bag as it passes through the system, and based on these measurements, decide if a threat is present. In order to develop a meaningful test plan, the test planners need to know the characteristics of the explosive that are being measured by the system and how these measurements might be affected by the container in which the threat is placed. In order to select the appropriate groups of test bags (when this is required) and/or produce simulants of explosives (when this is required) the following needs to be established:

- The characteristics of the explosive that are being measured.
- The bag related items which affect the characteristics, and if the system readings of that characteristic, with an explosive in the bag are additive (that is, will the observed value of the characteristic of an explosive in a bag, be statistically equal to the observed value of the bag plus the observed value of the explosive without the bag?).
- The relationship between the measured values of the characteristics and the shape, weight and type of explosive being considered.
- The distribution of the observed measurements on the characteristics of the explosive. Are the different characteristics related or independent of each other?
- The discriminate function being used to assimilate the observed values of the characteristics into a detect/no-detect decision. This will be important to know if simulants will be required in conducting the OT&E.

If at all possible, the OT&E testing should be done using samples of the explosive threats defined by the FAA. All explosive samples must be verified relative to type, purity, weight, and chemical composition, if that characteristic is significant for the system being tested. This testing should be done by an independent laboratory. The number of samples of each threat type is determined by the test design, that is the number of different bags being processed and the variability of the measurements of the characteristics of different samples of each threat type.

If, however, simulants must be used instead of explosives because the explosives to be tested will not be allowed at the airports, then it is important to ensure that the simulants faithfully represent the explosives relative to the characteristics of the explosives that are measured by the system and used for the detection process. In order to do this, each simulant, representing a specific mass of a particular

explosive, must be compared to the actual mass of real explosive material with the system being tested. The simulant and explosive should both be in the same geometrical shape, i.e., sheet or block.

To ensure that the explosives are what they were purported to be and to inspect their purity, duplicate analyses of each explosive should be performed by an independent laboratory. Samples for the analyses should be taken from the explosives under the supervision of the test team.

Once the explosives have been checked and the simulants produced (the number of each simulant type should be determined by the test team and should be adequate to ensure that a sufficient quantity will be available for the OT&E testing), a validation test is required to verify that the simulants are faithfully representing the explosive. Obviously, the validation testing cannot be done at an airport facility. The following outlines the recommended procedure for the validation testing of the simulants.

1) Test Procedures. The simulant validation test design should be based on placement of the explosive in bags representative of the total set of population of bags being tested, and recording the value of each of the characteristics the system uses in the detection process. Using the same set of bags and replacing the explosive with its simulated explosive in the same location, the test is repeated. Each time, the explosive (or simulant) is placed in the same location of the bag. Note: if possible, the selection of the location should be such as to provide high signal-to-noise ratio in order to facilitate the explosive-simulant comparison. All bags should be sampled at least ten times with the explosive, with the corresponding simulant and with neither. By comparing the average and the variances of the readings of the characteristics with explosives in the bag, with the average and the variances of the readings of the characteristics with the simulated explosive in the same bag, one can determine the validity of each simulant.

For example, in order to test, say, simulants of ten explosive types identified by FAA, fifteen bags, covering the population range of the characteristics being measured, are recommended for use. Five empty bags (containing neither explosive nor simulant, but only the contents of the bag) would be randomly placed among the ten bags containing either explosives or simulants on every one of the major runs that are used to obtain data on the explosives and the simulants. One purpose of using the same empty bags on each run is to collect data to evaluate if the system has "memory", in that if higher values of characteristics are being measured on a given run (as a result of ten bags containing explosives or simulants) then the system might be reading higher on all bags, including the empties. A second purpose is to collect large quantities of data of a selected number of bags to estimate the variability of the measurements from the selected bag set. This should be used to reconfirm the bag selection process for validation testing and to help guide the test team in the bag selection process for testing at an airport terminal. The test team must monitor all aspects of the validation testing, record data for each bag processed, verify the sequencing of bags through the system, place all explosives and simulants in the appropriate bags, and observe the verification tests of each of the samples of explosives used for comparison against the simulants.

2) Test Results. The detailed data collected on each bag will be maintained by the FAA. The mean value and standard deviation of the measurements of the characteristics for empty bags, the bags with explosive and the same bags with the simulated explosive should be recorded and compared. For each characteristic, its mean value for the bags with an explosive is compared to its mean value for the bags with the simulated explosive and F-tests and t-tests are conducted. A priori, the test team should select the critical region for both the F and t-test (reject the hypothesis that the simulant is representative of the explosive with respect to the characteristics being considered), usually selected to be at the $\alpha=5\%$ level.

Based on this data, one accepts or rejects those simulants using the t test. The rejected simulants may be reworked (if possible) and rerun through the system. This process may be continued in an attempt to validate as many simulants as possible. For overall confirmation, one can run an Analysis of Variance, testing that the differences of the mean value of the characteristic of the bags with explosives from the mean value of the characteristic of the bags with simulated explosives were zero (the F-test, with the associated test of homogeneity). The detailed statistical approach that can be used for the validation process is contained in Appendix B.

The validated simulants should immediately be put in the custody of the test team who will then deliver them to the test site at the appropriate time. If the

simulant characteristics can change over time, the simulants should be revalidated after appropriate time periods.

3.3 Bag Processing Rates

A very significant aspect of the operational suitability of the system is the average time required to process each bag, R. If this time is excessive, the airlines will have difficulty in incorporating the system so as to not affect its schedule of activities. It will be necessary to collect data on this operationally important issue, while conducting the various tests associated with the estimation of the detection and false alarm rates.

The first time that operational data can be collected is when the test team is testing to determine the final set of bag populations. During these tests, procedures should be established to ensure that meaningful data is collected on the time required to process the bags being tested. It will be important to collect individual processing times for each bag, as opposed to the total time required to process a number of bags, so that the mean and the variance of the processing time can be determined. The second time that operational data can be collected is during the OT&E tests. It may be more difficult to collect data at this time since more test activity is being conducted (such as placement of explosives in bags, marking bags, etc.) which might have an effect on the process times. However, with care, additional processing time data should be available from these tests.

If the above testing is conducted at airport facilities, the collected processing time data should be fairly descriptive of the operational processing time of the system. If however, the testing cannot take place at an airport facility, then the test team must set up the testing facility to mimic the airport facilities of interest. Here again, some artificiality will be built into the collection of this data.

Since almost all of the operational processing will take place with passenger bags (not containing explosives), the processing rate data should be generated with that testing associated with the false alarm rate estimation. Toward this end, processing time should be associated with each bag, including the re-processing of a bag when an initial false alarm has occurred.

The test team should record any malfunctioning of the system, unusual processing activity, manual interference with the automated processing function, etc., which should be reported in the final report on the OT&E activities.

Appendix C provides the statistical approach for analyzing and reporting the bag processing rate.

3.4 Pre-Testing

Prior to the full scale operational testing, the test team should conduct a pre-test to determine if the system can meet the FAA requirements against a standard but limited number of target bags randomly intermingled with a standard but limited number of normal bags. In this manner, the test team can pre-screen systems without having to undergo the complex ritual of the OT&E, since most systems' test results do not tend to be "near misses" and could easily be sorted out in such a pre-test. The above standards could also serve as system cross comparison set.

4. DEVELOPMENT OF THE OT&E PLAN

4.1 General Factors

At this point in time, the test team should be aware of all factors that may influence the conduct of the test as well as the measurements related to the detection process as implemented by the technology being used in the EDS and be ready to develop the OT&E. The following items address various factors that should be considered in developing the detailed test plan.

- The test design should be as robust as possible so as to lend itself to studies of as many operational factors as possible. All planned pre- and post-test activities should be clearly identified, as well as the test activities, to all concerned parties--who, when, how, where, why, etc.

- Data collection should be automated (if possible) and also manually recorded by independent data collectors. At a minimum, the collectors should identify and record the order and bag number of each bag entering the system and record each alarm response and appropriate data. All runs should be numbered, and the time of each run recorded. Basically, one should collect sufficient data to be able to recreate the complete time history associated with each

bag and with each threat. Toward this end, the test team should consider the use of blind bar graph labeling techniques, with all reading done by hand-held bar graph readers, with the data automatically fed to a central processing unit. All bags, threats and countermeasure items should be bar graph labeled.

- Test conditions should be clearly understood and agreed to by the system operators. Specific evaluation plans, including all test conditions, should be reviewed by the system manufacturer and the system operators. The FAA test director will determine if the plan is complete and suitable for the system under test.

- If appropriate, the acceptable minimum f(d) and maximum f(fa) required to certify the EDS should be clearly identified to the test team. All confidence statements will be made at the 95% level.

- The primary response variable is binary, i.e., detection/no detection.

- How the bags will be screened through the system should be determined including where operators will be required in this process and the typical time required to process a bag, or a group of bags.

- Will the system be able to automatically adjust the detection threshold and how? What is the relationship between the fraction of detection, f(d), and the fraction of false alarms, f(fa), as a function of the detection threshold level? This relationship will require the contractor to conduct testing of various bag populations while the threshold is varied.

4.2 Data Analysis Plan

The specific analysis plan should be developed prior to any testing. The analysis plan must describe the data that will be required to be collected during the test, show how the data will be analyzed, and the statistical tests that will be used in analyzing the collected data. It is advisable to exercise the data analysis plan by generating artificial data and performing the analysis on that data. The resulting proposed data collection and analyses should be the prime part of the test plan. It should be emphasized that the test team should be allowed flexibility in case of unanticipated data outcomes, and they should not be rigorously held to the initial plan. However, the initial hypotheses of interest and the associated criteria should not be changed.

4.3 Selection of Test Bags

In order to determine the number and the characteristics of the bags from a distinct population of bags (generated by the process described in Section 3), to be used in the testing, it is assumed that data collected on bag characteristics from that population have been collated so as to statistically describe the multi-variate frequency distribution of the characteristics. The data base for a specific population should be used by the test team to assist in the selection of the actual set of test bags that will be used in the OT&E test. The set of bags to be used could be (i), selected from FAA-held "lost" bags; (ii), fabricated by an FAA appointed team; or (iii), actual passenger bags. When non-passenger bags must be used, it would be beneficial if the test team could use several groups of bags, for each given population, each group representing a typical set of bags for that population.

For each of these different populations, there are three different methods for selecting bags.

1) Selecting Representative Bags When Non-Passenger Bags Are Required. For each of the different populations, designated in Section 3, a set of test bags needs to be available, which reflect the multi-variate frequency distribution of the characteristic measurements of bags from that population. In this method, one should try to use a stratified sample of bags from that population. For each characteristic, its range is partitioned so that an equal frequency of observations are observed in each of the partitions. This generates a number of multi-dimensional cells such that the marginal frequencies of occurrence of each characteristic are equal. Then the multi-variate frequency in each cell is observed and a proportional number of bags are selected to represent each of the cells.

For example, if 20 cells are established (each cell representing 5% of the population which has the multi-variate frequency of the characteristics as represented by that cell), one bag should be selected from each of the cells, each bag having the characteristics associated with that cell. This would

generate a sample of 20 test bags representative of the population. If a sample size of 40 is required, then 2 bags should be selected from each cell, etc.

If it is not possible to do the above because, for example, the number of characteristics is too large to allow for this approach, delete the least critical characteristic and continue, reducing the set of characteristics until the process can be accomplished. The unaccounted-for characteristics can then be handled by statistical techniques. Alternatively, ensure that at least one bag is selected for each of the non-zero cells, and then use the same statistical techniques to account for the non-representative sample of bags.

Another possibility is to estimate the correlation between the variables being measured and attempt to use a transformation function which might assist in the above process.

2) Selecting Bags at Random. If the above process is not possible, because of the large number of characteristics or not having an understanding of the correlation between the characteristics, etc., one can take statistically random samples from the population of bags.

3) Using Passenger Bags. If the system is set up at an airport terminal, which is the preferred location for conducting the OT&E (that terminal handling bags from one of the chosen populations), one can use passenger checked bags to test for the false alarm rate of the system (as was discussed in Section 3). To test for the detection rate, one can, with the cooperation of the passengers, use their bags for incorporating explosives (or simulants), or by using a "Red Team" to package bags, with explosives or simulants, going to the same destinations as the other passenger bags. These bags should be clearly identifiable to the test team (but not the system operators) so that they can be retrieved once they have been processed. Under this approach, the "Red Team" determines what will be placed in the bag and where it will be located. This approach will provide f(fa), for the time period being observed, using actual passenger bags, and f(d) either using the modified passenger bags or fabricated bags.

The recommended approach is to use passenger bags ("Red Team" approach), if that is possible; if not the second choice would be using selected representative bags.

4.4 Number of Test Bags Required

The number of observations required for the test will depend on the values of the FAA-provided minimum f(d) and the maximum f(fa). The required number of tests against bags with explosives will vary between 4500*f(d)*(1f(d)) and 15000*f(d)*(1-f(d)), depending on the assumptions underlying the analyses and the methodology used for acceptance. For bags without explosives, one replaces f(d) with f(a) and uses the same formula. (See Appendix C for detailed formulation of the required sample size as a function of the assumptions on confidence statements and/or hypothesis testing.) When passenger bags are not being used, it is recommended that the number of observations be obtained by sampling a given bag without the explosive and the same bag with the explosive threat a minimum of six times each, thus requiring approximately 1/6 of the above numbers. It is further recommended, that these bags be chosen such that there are multiple groups (i.e., 6 groups of bags) which are each representative samples of the population being considered.

If the "Red Team" approach is being used, it may not be possible to test each bag with and without explosives.

4.5 Selection of the Number of Threat Articles

The number of threat articles (explosives or simulants) to be used for the fraction of detection determination will depend, in part, on the number of bags available to conduct the testing. For each defined threat, multiple samples may be required to facilitate the testing. For example, if there are 5 distinct threats (one threat could be 2.5 pounds of TNT), then, one might want 4 samples of each threat so as to provide 20 test articles. The determination of the number of detection test articles must be made early in the planning process if simulants are required, so that the simulant validation testing can be conducted prior to the OT&E testing.

5. TEST EXECUTION

For the purposes of this section, it is assumed that all parts of the previous sections of this protocol have been carried out. Thus the test team has examined and learned about the explosive detection system to be tested, and has a complete understanding of all the relevant technical issues and characteristics of the system. (If the test team does not fully understand the system to be tested, they may not be able to assure

the FAA that the system has been adequately tested.) It is also assumed that the test team has access to the raw data as well as any processed data of the critical characteristics of the explosives and the baggage as being measured by the system. They have selected the set of bags to be used in the testing and understand how these bags represent the population of bags being considered. Finally, it is assumed that the test team has determined the threat samples to be used for the OT&E testing.

The following areas should be considered by the test team in the execution of the OT&E testing.

5.1 Contractor Independence

Although the test team may be required to rely heavily on the contractor personnel for support in conducting the tests, procedures need to be established to minimize the possibility that the contractor could affect the results of the tests. Toward this end, at least one member of the test team should:

- Participate in supervising and overseeing all operations of each test including placement of threats in bags, numbering and sequencing bags through the tested system, and identifying and manually recording data on each bag as it was being processed;
- Verify that any internal computer identification system does not affect the measurement system;
- Disconnect computer modems and any other outside manipulative devices to isolate the system from the outside world. If at all possible, the system manufacturer should train FAA chosen personnel, who will operate the system during the test. The personnel chosen to operate the system should be representative of types that are expected to operate the system when it is in the field, in terms of education, experience, IQ, etc.

5.2 System Reproducibility

During all test periods, the test team should collect data on measurement reproducibility by taking repeated measurements of a controlled set of bags. For example, over the test period, a set of control bags should be repeatedly processed before, during and at the conclusion of each day's test, in order to provide assurance and documentation that the system response has not changed significantly during the test sequence. If the test team determines that the system response has changed over the testing period, the test may have to be repeated, unless an acceptable answer to why it occurred can be provided to the test team.

5.3 Other Areas

- The test team shall directly supervise the placing, moving or removing the threats in the bags being tested.
- The test team should control the threats with an established chain-of-custody procedure.
- At the end of each day of the testing, print outs of all test data should be collected by the test team; a backup package should be available for the FAA, and this data retained for possible future use/confirmation.
- All available data should be collected, even if some will not be used immediately. At a minimum, threshold values and alarm/no-alarm readings on each item tested should be recorded. All parties should sign off on the data packages each day.
- The system manufacturer should be informed of all data requirements (by the test team) as early as possible.
- Prior to any testing, dry run each significant set of test conditions, to insure that the system is functioning in an operational mode.
- If possible and appropriate, all tests and test activities should be video/audio recorded.
- The system being tested will be used as set up by the manufacturer, i.e., there will be no non-routine changes or adjustments made during the evaluation testing.

5.4 An Example

In order to provide a model that could be used for the actual testing, the following is provided. For explanatory purpose only, it will be assumed that 20 threats are available to conduct the test. If passenger

bags cannot be used, then it is suggested that for each of the bag populations, six groups of twenty bags should be selected to be representative of that population. If it is not possible to "reproduce" the distribution because an adequate number of bags to select from is not available, one could correct for this discrepancy by using a statistical weighing process on the data to better match the distribution.

After having selected the six groups of twenty bags, randomly order the bags in each group with the first group, called A1, A2, ..., A20, the second group called B1, B2, ..., B20, etc. To accomplish this, one can use a random number generator, such as a table, and select a number. Next, the first 10 B bags are randomly intermingled with the first 10 A bags and the second 10 B bags with the second 10 A bags. Twenty threats are then randomly assigned to the 20 A bags. Each newly defined group of ten A and ten B bags are then processed through the system. Each time the group of twenty bags is processed, the threat location in the bag is changed by flipping and/or twisting the bag; see Figure 1 for the 15 locations in the bag and the 9 starred locations that should be used. The threats are then transferred to the B bags in the group and again processed through the system. In this manner, one is able to obtain measurements on A bags with threats and B bags without and on B bags with threats and A bags without, obtaining 9 observations on each bag. One then moves on to test with C & D bags (using the same process - replace A with C and B with D) obtaining 9 observations on each combination. Finally one tests with E & F bags (using the same process--replacing C with E and D with F) obtaining 9 observations on each combination. The total number of observations on empty bags is 1080 while the number of observations on bags with threats is 1080, with each threat being tested in 6 different bags, and in 9 locations in each bag.

Before running the six groups of twenty bags through, two control bags should be processed through the system 10 times (one bag without a threat and the second bag containing one of the threats). This set of two bags should be processed in a similar manner at various times during the tests and also at the end of each day. Comparing these measurements assures the test team that the system readings are not varying over the duration of the tests.

6. ANALYSIS AND EVALUATION OF OT&E TEST

Once the OT&E tests have been completed, the test team will be required to prepare a report of the test findings. The testing program should have produced most of the following data and information:

- Detection characteristics measured;
- Set of explosives/simulants used;
- Bag populations used, including justifications;
- System calibration results;
- Threshold settings used;
- Number of bags used and the selection process;
- Simulant validation data, as appropriate;
- Detections observed data;
- False alarms observed data;
- Bag processing rates data.

Using procedures such as those presented in the appendices, the above information will provide the following:

- The fraction of detections observed, for different bag populations and different threats;
- The fraction of false alarms observed for different bag populations;
- The processing rate of baggage through the EDS.

Although the appendices provide procedures for calculating the above three items, it should be understood that there may be modifications to the procedures to accommodate different systems undergoing the testing and testing conditions. Thus the appendices are suggested procedures but the test team has the responsibility to correctly apply those procedures or to modify or revise them to provide scientifically correct and defensible data analysis methods.

tested bag populations are equally likely, stratified sampling of the bag populations is used, and all threats and locations tested are equally likely, then

- f(d)=(# of detections)/(total # of possible detections);
- f(fa)=(# of false alarms)/(total # of possible false alarms);
- R=(time required to process all bags)/(# of bags processed).

If any one of the above assumptions is not true, then these fractions must be computed for appropriate subsets of the test data and these fractions weighted to account for any differences (for example, if the bag populations or threats are not equally likely). How this can be done is described in Appendix C. At some point the test team should provide a composite fraction for the OT&E test for use by the FAA.

Finally, the test team report should contain all of the raw data generated in the testing, as well as the reduced data, and include all of the detailed calculations showing the complete test design and how the results were obtained from the data collected. This report should be sufficiently detailed and transparent so that any competent technically trained individual should be able to completely follow the testing system and results to its logical conclusion.

APPENDIX A: SELECTION OF BAG POPULATIONS

Given that a set of potential bag populations has been identified and data collected on each of these populations (data in terms of the measurements of the characteristics being obtained by the system being tested), the test team must determine the final set of populations to be used. There are a variety of approaches that can be used. One approach would be to use all of these populations of bags and ignore the fact that several of these populations might be statistically the same. This approach might be required if data cannot be collected to compare these populations. A preferred approach is to reduce the number of different populations that need to be tested to a minimum by comparing each of the populations with each other and combining those that are statistically the same.

In order to do this, one must be able to compare the bag populations as defined by the measures of the critical characteristics used by the EDS in its attempt to detect the existence of an explosive threat. Thus an operational system must be placed at each airport being considered, so that each of the associated bag populations can be processed through the EDS. This does not have to be done simultaneously so a single system could, if necessary, be moved from airport to airport or be operated over different seasons. The system should be recalibrated for each airport/season so as to produce the FAA specified f(fa) for the population being considered.

Once the EDS is installed and properly calibrated, the data base for the population should be developed by recording the observed values of the characteristics, a{}, and whether or not a false alarm has occurred. This should be done for a large number of bags that are routinely checked at the airport. The number of bags so processed should exceed 5000 for each season of interest. Once the data base has been developed for all airports/seasons of interest, one can compare the associated a{} for each airport/season to determine if any of the populations are statistically the same and hence can be pooled. A multi-variate Analysis of Variance can be used to test the null hypothesis that there is no difference between any of the populations as far as their multi-variate means are concerned. Of course, one must test for homogeneity first. If this hypothesis is accepted, then there would only be one distinct bag population to use in the test. If, however, the hypothesis is rejected, then some type of outlier, or cluster analysis technique should be used to determine which of the populations should be pooled into a single population. Such a pooling procedure should then be followed by a repeat of the Analysis of Variance test. The combined approach should be repeated until the null hypothesis is accepted separately for each of the pooled populations.

To further elaborate on this procedure, for each of the potential bag populations, one would generate an n-dimensional set of cells (where n represents the number of characteristics that are being measured), and in each cell, observe the frequency of occurrence of the bags. Thus, let a{i,k} be the measurement of the i-th characteristic in the k-th bag. The range for each of the characteristics should be divided into a fixed (small) number of intervals, say n. Let these divisions be designated by $a_i(r)$, with r=1,...,n. Then the number of bags with a{i,k} between $a_i(r)$ and $a_i(r+1)$ for all of the i divided by the number of bags in the set, would represent the frequency of occurrence of those bags in the cell identified by the $a_i(r)$ and $a_i(r+1)$. If there were only two populations to be compared, and only one characteristic being measured, a paired comparison test of the two populations can be conducted to determine if the samples are statistically the same. (Alternatively, a Chi-Squared test can be used to test for significant differences.) However, the number of populations will most likely exceed two, and the number of characteristics being measured could very well be larger than one. In these cases, the comparing of the bag populations can be very difficult and more exotic techniques might be required.

APPENDIX B: VALIDATION OF SIMULANTS

The decision to be made is whether or not a given simulant gives a similar enough response to that given by the real explosive as far as system operation is concerned, namely detect or no detect. The following testing is recommended for the validation process.

We start with a representative group of J + Q bags where J equals the number of different explosive types being simulated and Q represents a small number of additional bags. For the j-th explosive type, there are m(j) simulants which need to be validated. Here the m(j) depends on the OT&E test design. These J+Q bags are run through the system N times for each of the three conditions, (1) with the explosive, (2) with the matching simulants, and (3) with neither (to check on additivity of the measurements and to ensure that the bag characteristics have not changed over the testing period). The explosive and its matching simulant are also placed in the same bag in the same position, that position being where the measurements of the characteristics are considered to be optimal for measurement purposes.

The set of characteristic measurements of the bag as determined by the system are the determining operational variables used in the test. Thus the primary data can be considered as three matrices:

(1) a{i,k}
(2) a{i,E(j),k}, and
(3) a{i,S(j,m),k},

where (1) is the observed value of the i-th characteristic in the k-th bag, (2) is the observed value of the i-th characteristic with explosive type E(j) in the k-th bag, and (3) is the observed value of the i-th characteristic with the explosive replaced by the m-th simulant of the j-th type explosive, S(j,m), in the k-th bag. Here,

$i=1,\ldots,I$
$j=1,\ldots,J$
$k=1,\ldots,K=J$
$m=1,\ldots,m(j)$

The following process is recommended:

(i) Run K+Q bags through N=10 times without explosives or simulants. This data is needed to ensure that the bags being used are representative of the bag population they are thought to be representing and to check for additivity of the measurements;

(ii) Place the J explosives in the K bags, selecting the assignment at random, all in the same location, that being where the a{} readings are expected to be least variable. If appropriate, use the flip\twist\move procedure, described above, to sample the a{} at different relative locations in the system. Run the K+Q bags through N=10 times;

(iii) Replace each of the J explosives with a simulant of that explosive, S(j,m), and repeat (ii), continuing this until all simulants have been tested in bags which contained the appropriate explosive;

(iv) At the beginning of each new day of testing and at the end of the testing, repeat (i).

The above procedure would require a total of 10x(J+J+M) passes through the system, of bags containing either an explosive or a simulant, with each pass providing observations on the I characteristics. Here M=m(1)+m(2)+...+m(J). In addition to the above, for each set of K bags processed through the system, the Q control bags should be randomly located within the K bags. These bags and the associated measurements will be used to measure consistency of the operation of the system, over time.

B.1 Analyses for the Validation of Simulants

Let

$$A\{\}=\Sigma a\{\}/10$$

be the mean value of the respective reading, taken over the 10 observations on the k-th bag and

$$v(\ )=\Sigma[a\{\}-A\{\}]^2/9$$

be the sample variances. In order to validate a simulant, we are testing the hypothesis that the population mean as estimated by A{i,E(j),k} is equal to the population mean as estimated by A{i,S(j,m),k}, given the populations are normally distributed with equal variances. Three statistical tests can be used to determine if these samples came from the same distribution, so as to justify the validation of the m-th simulant of the j-th type explosive.

1. The Significance of the Difference Between Two Sample Means. In this approach only one bag is used for the testing of the explosive and the simulant of that explosive. That bag (say the k-th bag) should be randomly assigned for a given simulant and explosive pairing.

For a simulant of the j-th type explosive, one now tests that $A\{i,S(j,m),k\}=A\{i,E(j),k\}$, for all $m=1,\ldots,m(j)$ and for all characteristics $i=1,\ldots,I$. If, for each of the I characteristics, the two sample means are not significantly different at the $1-\alpha$ level of significance using the two-sided alternative, we will declare the m-th simulant to be validated, at the $1-(1-\alpha)^I$ level of significance.

To make such a statistical test, one must first determine if the two observable random variables, for each of the I characteristics, have equal variances or not. To test this one uses the Snedecor F statistic computing

$$F(9,9)=V(i,j,m)/v(i,j,m),$$

where by convention V( ) represents the larger of the two variances and v( ) the smaller and (9,9) are the respective degrees of freedom.

If the F value proves to be not significantly different than 1, using once again the $1-\alpha$ level of significance, one can pool the two variances into a single variance

$$v(i,j,m)=[9v(i,E(j))+ 9v(i,S(j,m))]/18$$

Then the Student-test statistic is

$$t(18)=[A\{i,E(j),k\}- A\{i,S(j,m),k\}]/ [v(i,j,m)*2/10]^{.5}$$

If $|t(18)|<t(18\,|\,1-\alpha/2)$, for each of the I characteristics, the simulant will be declared to be validated at the $1-(1-\alpha)^I$.

If, however, the F test of the two variances shows them to be significantly different, then the simulant does not exhibit the same properties as the explosive and should be rejected. In this validating approach each of the M simulants is considered independently even though some of them are simulating the same type of explosive.

2. The Paired Difference Approach. Since the values of a{} come from the same bag with the explosive and its matching simulant in the same position in the bag, it is natural to consider the paired difference approach to test the correspondence between a simulant and the explosive. In this approach, one uses the differences

$$d\{i,j,m\}=a\{i,E(j),k\}- a\{i,S(j,m),k\},$$

where the pairing over the 10 observations are randomly assigned. The population of such differences has an expected value, $E(d\{i,j,m\})=0$ if indeed the m-th simulant faithfully represented the j-th explosive for the i-th characteristic. An appropriate null hypothesis to test would be

$$H(0):\ E(d\{i,j,m\})=0,$$

against the two-sided alternative,

$$H(1):\ E(d\{i,j,m\}) \neq 0.$$

Once again we could accept the m-th simulant as being validated if the null hypothesis is not discarded at the α level of significance for all of the I characteristics. The test statistic to use in making this test is:

$$t(9)=D(i,j,m)/[v(d(i,j,m]^{.5}$$

where $D(i,j,m)=\Sigma d(i,j,m)/10$, taken over the 10 samples, and

$$v(i,j)=\Sigma[d(i,j,m)-D(i,j,m)]^2/9.$$

Note that in using this test we have lost 9 degrees of freedom and as a result this test would be preferred only when there is a relatively high correlation between a{i,E(j),k} and a{i,S(j,m),k}. Here again, each simulant would be subject to its own validating decision.

3. The Analysis of Variance Approach. It should be noted that d(i,j,m) as defined above, can be considered in an Analysis of Variance for each explosive type j. The Analysis of Variance approach provides a statistical test of the composite null hypothesis:

$$H(0):\ E[D(i,j,m)]=C, \text{ for all i and m}$$

against the alternative,

$$H(1): E[D(i,j,m)] \neq C, \text{ for some } i \text{ or } m.$$

We test the above hypothesis by selecting the level of significance α and assuming homogeneous variance, establish the critical region (reject H(0)) as

$$F > F_{1-\alpha}(m(j)-1,\ m(j)*(I-1))$$

where

F is the ratio of the mean of the sum of squares amoung simulants to the mean of the sum of squares within simulants.

This test can then be applied for every one of the J explosives. Tests such as this are available on most computers' statistical packages.

If the null hypothesis is accepted, then one needs to test the hypothesis that the constant $C=0$. One approach to this test is the use of the t-test.

In using this test if the composite null hypothesis is not discarded all simulants of the j-th type explosive would be declared to be validated. However, if the null hypothesis is discarded, none of the simulants would be validated. There is an approach that allows one to also examine a wide variety of possible differences, including those suggested by the data itself. This test is based on the range of the m(j) observed means (we are looking at the difference between the smallest and the largest observed values). The reader is referred to Introduction to Statistical Analysis, Dixon & Massey, Second Edition, pages 152 to 155.

4. Measurement Additivity. As was mentioned above only one bag is used to validate the simulants of a given explosive. This is acceptable if the measurement system is additive, that is, if the measurement of the characteristic of the explosive plus the measurement of the characteristic of the bag, statistically equals the measurement of the explosive in the bag. If this is not the case, then the validation of the simulants will require testing over a representative set of bags, for each explosive threat. Hence one must test for additivity of the measurements. This is done by taking measurements of the explosive in the absence of any background which would interfere with the measurement of the characteristics of the explosive. These measurements are repeated 10 times (as in the above). One then compares the sum of average reading of the explosive and the average reading of the bag (which is associated with the testing of that explosive, but not containing the explosive) with the average reading of the bag with the explosive. The above Analysis of Variance approach is suggested for testing for additivity of the measurements.

B.2 A Recommended Approach for Validating Simulants

Repeated use of the Analysis of Variance approach appears to be appropriate. If in its initial use, the set of simulants are not validated, an individual t-test should be run and the simulant which differed most significantly from its null hypothesis would be declared to be invalidated and dropped from the group of simulants being tested. The Analysis of Variance approach would then be repeated using the reduced group. This process would be repeated until a final reduced group of simulants would be declared to be validated. This is then repeated for all of the J explosives.

APPENDIX C: STATISTICAL PERFORMANCE TESTS

C.1 Statistical Analysis Plan

To determine how best to measure the operational effectiveness of the system one must consider the form of the data that will be evolved by the testing program.

The test data will come as a 0, 1 vector of observations for each of the bags as they are processed through the system.

In this analysis the operational parameters of the system are P_D, the probability of the system detecting an explosive and P_{FA}, the probability of the system giving an alarm when no explosive is present.

Let the n-th population being tested be subdivided into K categories, each designated by $c_n(k)$, and let $c_n(k,m)$ be the condition that the bag in the k-th category from the n-th population is being sampled for the m-th time. Here, $N(c_n(k))$ is the total number of times the bag is sampled.

Let r( ) represent the alarm response variable, r( )=0, when there is no detection and r( )=1, when there is a detection. Let $r(c_n(k,m),0)$, $m=1,\ldots,N(c_n(k))$, be the vector of responses obtained for the $N(c_n(k))$ times an empty bag from category $c_n(k)$ is passed through the system, with $k=1,\ldots,K$. Let $r(c_n(k,m),j)$, $m=1,\ldots,N(c_n(k))$, be the vector of system responses for the $N(c_n(k))$ times a bag containing a j-th type threat is passed through the system, with $j=1,..,J$ and $k=1,\ldots,K$. Further, let the estimates of the detection probabilities of the j-th type threat in bags from population category $c_n(k)$ and the false alarm probabilities of the bags in category c(k) be given by

$$P(c_n(k),j)=\Sigma r(c_n(k),m),j)/N(c_n(k)), \quad (1)$$

$$P(c_n(k),0)=\Sigma r(c_i(k),m),0)/N(c(k)),$$

$$m=1,\ldots,N(c(k))$$

The error variances of the P( ) are given by

$$V(P(c_n(k),j))=P(c_n(k),j)*(1-P(c_n(k),j))/N(c_n(k)), \quad (2)$$

$$V(P(c_n(k),0))=P(c_n(k),0)*(1-P(c_n(k),0))/N(c_n(k)).$$

We can use the weighted fraction of P(c,)'s to estimate the probabilities of detecting the j-th type threat and the probabilities of false alarms by,

$$P_D(c_n,j)=\Sigma P(c_n(k),j)*g(c_n(k)), \text{ and} \quad (3)$$

$$P_{FA}(c_n)=\Sigma P(c_n(k),0)*g(c_n(k)),$$

$$\text{for } j=1,\ldots,J$$

where $g(c_n(k))$ are the frequencies of that $c_n(k)$ category as given by the bag distribution for the n-th population. The error variance of the estimates in (3) are given by

$$V(P_D(c_n,j))=\Sigma g^2(c_n(k))*V(c_n(k),j), \text{ and} \quad (4)$$

$$V(P_{FA}(c_n))=\Sigma g^2(c_n(k))*V(c_n(k),0),$$

$$j=1,\ldots,J.$$

In order to provide an overall measure of effectiveness of the system, one can weight the fractions as defined by (3) by the weight assigned by FAA relative to the expected frequency of occurrence of the j types of explosives. Hence, the overall fraction of detection is given by

$$P_D(c_n)=\Sigma P_D(c_n,j)w(j), \quad (5)$$

$$\text{with } j=1,\ldots,J,\ \Sigma w(j)=1,$$

and the fraction of false alarms, $P_{FA}(c_n)$ is given by (3). Here the w(j) are the expected frequency of occurrence of the j-th type explosive. The estimate of the error variance for $P_D(c_n)$ is given by

$$V(P_D(c_n))=\Sigma w^2(j)V(P_D(c_n,j)) \quad (6)$$

With the above statistics, techniques are available which will allow the test team to determine the sample size needed to provide confidence bands about the estimates of $P_D(c_n)$ and $P_{FA}(c_n)$ or to test hypotheses about the corresponding population

probabilities. The next section describes several approaches to the determination of the sample size N.

1) False Alarm Rate. One method for the determination of the sample size is to use a confidence band approach. The true population value of the false alarm rate, P_{FA}, can be estimated by $P_{FA}(c_n)$, as given by equation (3) and the population variance estimated by $V(P_{FA}(c_n))$ as given by equation (4) in the above. Then for large N, the following confidence statement can be made:

$$P\{P_{FA}(c_n)-z(1-\alpha/2)*V(P_{FA}(c_n))^{.5} < P_{FA} < P_{FA}(c_n)+z(1-\alpha/2)*V(P_{FA}(c_n))^{.5}\} = 1-\alpha.$$

An upper bound on P_{FA} is given by

$$(7) \qquad P\{P_{FA} < P_{FA}(c_n)+z(1-\alpha)*V(P_{FA}(c_n))^{.5}\} = 1-\alpha$$

From (7), if we replace $P_{FA}(c_n)$ with the maximum acceptable value of f(fa), say F(fa), then, for $P_{FA}(c_n) < F(fa)$,

$$(8) \qquad P_{FA} < F(fa)+z(1-\alpha)*[(F(fa)*(1-F(fa))/N]^{.5}$$

or

$$(9) \qquad N < z^2(1-\alpha)*[F(fa)*(1-F(fa))/(P_{FA}-F(fa))^2$$

Table 1 displays N as a function of F(fa), $\alpha = .05$ and using $|P_{FA}-F(fa)| = .3*F(fa)*(1-F(fa))$ for the confidence interval half width.

Alternatively, (7) yields,

$$P_{FA}-P_{FA}(c_n) < z(1-\alpha)*[P_{FA}(c_n)*(1-P_{FA}(c_n))/N]^{.5}$$

and solving for N yields

$$N \leq z^2(1-\alpha)*F(fa)*(1-F(fa))/(P_{FA}-P_{FA}(c_n))^2.$$

and Table 1 can be used again to determine the necessary sample size for a given F(fa), α and the confidence interval half width.

In the above approach, there is no attempt to protect the decision maker from making an error of the second kind, ß. Only the error of the first kind, α, is specified. An approach which considers ß in determining the sample size is to use hypothesis testing. In this approach one tests

$$H(0): P_{FA} \geq F(fa) \text{ versus}$$

$$H(1): P_{FA} < F(fa)-D, \quad D>0$$

One specifies the error of the first kind, α, and the error of the second kind, ß. Then, under H(0), and for a large sample size, N, H(0) is rejected when

$$N^{.5}*[P_{FA}(c_n)-F(fa)]/[F(fa)*(1-F(fa)]^{.5} < z(\alpha),$$

where $z(\alpha)$ is the value of the normal variate (with zero mean and unit variance) for which α percent of the population fall below. If one also requires that given H(1) is true, N is determined so that we would select H(1) when H(1) is true, 1-ß of the time. Then

$$z(1-ß) = [z(\alpha)(F(fa)*(1-F(fa))/N)^{.5}+D]/[(F(fa)-D)*(1-F(fa)+D)/N]^{.5}$$

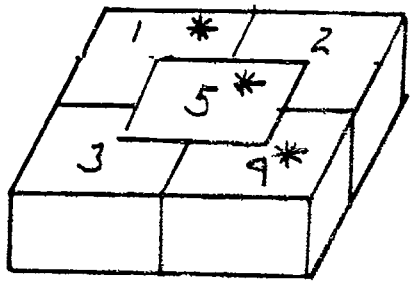
and solving this for N yields

$$N = \{z(\alpha)*[F(fa)*(1-F(fa))]^{.5} - z(1-ß)*\{(F(fa)-D)*(1-F(fa)+D)]^{.5}\}^2/D^2$$

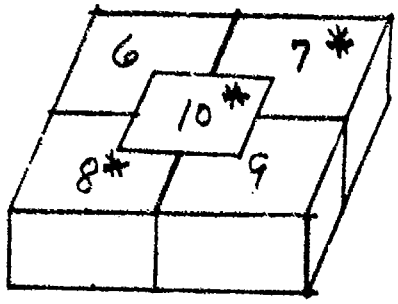
Table 2 displays N versus $\alpha = ß = .05$, F(fa) and D. Here D was chosen to be equal to $.3*F(fa)*(1-F(fa))$. For different values of the parameters, one can use the above equation to calculate N.

This approach to determining N is preferred over the confidence band approach, since it allows the tester to statistically control both errors α and ß. It does, however, require a sample size on the order of 3.5

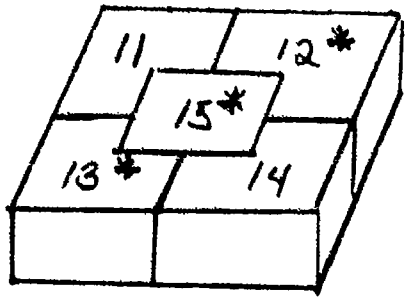
FIGURE 1. THREAT LOCATIONS IN BAGS



TOP



MIDDLE



BOTTOM

times more than the former approach.

2) Detection Rate. The unbiased estimate of P_D is given by equation (5) above. With probability $1-\alpha$, the true value of P_D will fall between

$$P_D \pm z(1-\alpha/2)*V(P_D)^{.5}$$

where $V(P_D)$ is given by equation (6). In like manner as above, the test team can again determine the sample size needed when testing for the fraction of detections, by using either the confidence band approach or the hypothesis testing approach.

An excellent source for determining sample sizes is How to Choose the Proper Sample Size, American Society for Quality Control Statistics Division, Milwaukee, WI, 1988. There are many other text-books that can be used as well.

3) Through-Put. The unbiased estimate of the through-put, R, is given by $R(I)=\Sigma R(i)/I$, where R(i) is the time required to process the i-th bag and $i=1,\ldots,I$. Assuming that I will be large, then with probability $1-\alpha$, the true value of R will fall between

$$R(I) \pm z(1-\alpha/2)*s(I)$$

where s(I) is the sample standard error of the R(i). If one imposes a confidence interval half width of size r, then the sample size needed is given by

$$I = z^2(1-\alpha/2)*R(I)*(1-R(I))/r^2.$$

C.2 Testing for Consistency of the Operation of the System

Data must be made available for checking the consistency of the operation of the system. It is recommended that this data be generated through the use of a set of bags, (say T in number) randomly selected, half containing a representative type threat and the other half "empty". These bags are run through the system in between operational test runs, n times at the initiation of the test runs and n times during several selected times during the course of the test program. For all of these runs both the main characteristic measurements and whether a detection has occurred should be recorded.

There are several approaches that can be used to check on consistency. One approach would be to determine the P_D and P_{FA} for the first run of n and considering these values as representing the population probabilities ask, using the exact approach for Binomial random variables, if the number of "successes" realized in a subsequent run could have come from a Binomial with these values for probability of success.

Let N(t,1) be the number of alarms realized on the t-th run of n for the bags with the threats. Assuming $N(t,1) > n_D$, the expected number of successes, one computes

$$P(N(t,1)) = \Sigma C_j^n P_D^j (1-P_D)^{n-j},$$

with the sum taken over all values of j larger than N(t,1). If $P(N(t,1)) < 1-\alpha$, one can assume that the system is operating in an inconsistent fashion. A similar computation could be run for the experience with the empty bags.

This test requires a large sample size in order to have any reasonable power.

An additional method would involve using some type of quality control chart, using the central line as $p=P_D$ and the Upper and Lower Control Limits by $P_D \pm 3[P_D(1-P_D)]^{.5}$. The successive values of P_D could then be plotted on the chart and from them a consistency of operation decision made.

Characteristic measurements are also available for these consistency check runs. In an a posteriori fashion, one can look at the complete set of data using an Analysis of Variance type analysis, separately for each type bag. For each bag, Q (the number of different runs) runs of n observations of s() will be available. A multi-variate Analysis of Variance can be used to test that the expected value of the average (over n and T) reading of the i-th characteristic is constant over the Q runs and for all measured characteristics. If this hypothesis is discarded, then the OT&E results need to be more carefully analyzed to insure that the lack of consistency is not significant in the outcome of the test results. If it is, then the test director must determine if the test needs to be redone after the correction for the lack of consistency has to be made.

TABLE 1. SAMPLE SIZE USING CONFIDENCE BAND APPROACH

F(fa)	$\lvert P_{FA}-F(fa) \rvert$	N
.05	.014	633
.10	.027	335
.15	.038	236
.20	.048	188
.25	.056	161
.30	.063	143
.35	.068	133
.40	.072	126
.45	.074	121

TABLE 2. SAMPLE SIZE USING HYPOTHESIS TESTING

F(fa)	D	N
.05	.014	2171
.10	.027	1165
.15	.038	836
.20	.048	677
.25	.056	587
.30	.063	533
.35	.068	500
.40	.072	481
.45	.074	474

PERFORMANCE TESTING OF EXPLOSIVES AND WEAPONS DETECTION SYSTEMS

T. G. Sheldon, Dr. R. J. Lacey, N. C. Murray, and G. M. Smith
U.K. Home Office
Police Scientific Development Branch

1. INTRODUCTION

Many agencies, all over the world, have an interest in explosives and weapons detection and carry out tests on detection equipment. There is probably no single organisation which can afford the time or resources needed to evaluate every piece of equipment with all its possible uses, but all can contribute something to the body of knowledge of this subject. It is probably fair to say that every group working in this field knows something that the others do not.

Unfortunately, the exchange of this information is hampered by the differing approaches these organisations take towards planning and carrying out tests, and sometimes, sadly, by the poor standard of some evaluations. The picture is further obscured by the odd snippets of imformation which leak into the public domain, unqualified by any supporting information as to methods, materials used, purpose of trials and so on.

This paper describes the philosophy and methodology underlying equipment tests carried out by the Home Office Police Scientific Development Branch. This organization carries out, amongst other things, development and testing work on explosives and weapons detection systems on behalf of three main customers: Police Forces, the Prison Service and the Department of Transport.

It describes the steps in planning and carrying out trials and some of the pitfalls to avoid. It refers to past and current evaluations and tests for different types of equipment are outlined. The possibility of standardising certain tests is also discussed.

It is not intended to suggest that PSDB's trials philosophy is better than anyone else's, but to provoke comment and discussion and thus, one hopes, to improve the exchange of usable imformation.

2. WHY DO TRIALS?

In general terms, when we test a piece of explosives or weapons detection equipment, it is because we want to know whether it will reliably detect the explosive or weapon we are looking for in the operational situation in which we envisage the equipment being deployed. There are other aims, however, and, depending on available resources and on what we already know, we may do a trial for the following reasons:

- To determine whether an entirely new detection technique is useful;
- To compare similar instruments, or an old instrument with a new version;
- To determine whether a piece of equipment meets predetermined performance standards.

In addition to the above, it is to be hoped that doing trials will increase our understanding of why a piece of equipment behaves like it does, and when it can and cannot be used. This understanding is something you can take away from a trial and use over and over again to predict roughly the behaviour of the equipment in circumstances other than those of the trial.

The reasons for testing a piece of equipment make a difference to how the trial is done. If we are looking at a new technique, we will do a fairly informal set of trials, bearing in mind that we won't know exactly how to use the equipment, and may need to adapt our test methods to suit the technique. A more rigid set of tests may come later.

To compare similar instruments we must be sure that all our tests are equally applicable to each system, and we may need a large number of tests to show up small differences in performance. Consistency is very important in this type of trial, as is experience of using each system.

Testing against a predetermined set of performance standards is not too difficult in itself. The hard part is determining the standards and deciding which are more or less important. The thing to avoid is rejecting equipment which offers real benefits because it fails to meet some arbitrary or outdated standard. For this reason the standards need to be reviewed regularly.

None of these things should be done without considering the requirement, for this will largely determine what kind of trials you will do.

3. MATCHING THE TESTS TO THE REQUIREMENT

When we start testing a piece of equipment, we obviously have some possible applications in mind. We will also have some ideas about the constraints each application will put on the use of the system. General aspects of the requirement include:

- The threat: what explosives and weapons do we expect and in what quantities, and how might they be concealed?
- Operational constraints: portability, environment, ease of ease so on;
- Throughput and speed of response;
- Acceptable false alarm rate: This depends on what the user will do when an alarm occurs and how much disruption will be caused;
- Safety: many systems have radiological or other hazards which may restrict their use.

To give an example: for screening aircraft hold baggage the detection system must be capable of screening the bags in a limited time. It may have to be capable of doing this without opening the bags, and to both detect a small amount of explosives and to have a low false alarm rate. The user may also feel that only, say, plastic explosives are a threat.

Some of these constraints could be got around by changing operational procedures - throughput could be increased by using more systems; screening could be done at check-in and bags could be opened - but some, like detection capability and false alarm rate, depend mostly on the detection system itself so these are the main things we would want to test. Throughput we could measure easily but we must also determine whether changing throughput affects detection. We may also have to determine whether opening bags affects our detection capability.

Essentially, we must measure the detection and false alarm performance of the system in the situation in which it is likely to be used, and relate the test to a realistic threat, but keep in mind the variations which may be made in operating procedures, and how these may alter performance.

It is very important to consult the prospective users about this, and maybe become involved in some of their operations. This will lead rapidly to an appreciation of what can and can't be done operationally.

4. DEVISING A TEST PROTOCOL

By a protocol, I mean a written-down plan of what tests we are going to do and why. The protocol is not a completely inflexible document. It can be discussed with interested parties and may be altered as a result, or it may be altered after the first few tests. Any changes, however, should be made for a good reason and properly recorded.

At PSDB we have devised a generalised protocol on which to base all others. This divides the trials into three stages:

1. Laboratory tests. These measure fundamental parameters like sensitivity and crude selectivity.

2. Semi-realistic tests. Attempting to detect the weapon or explosives in a realistic situation, but with no attempt to simulate operational conditions, or to do blind tests.

3. A large scale blind test in which an operation is simulated, and false alarm rates and/or detection rates are measured.

After any stage the tests may be curtailed for a variety of reasons. The system may not perform well enough in the laboratory, or we may decide we know enough to sensibly relate its performance to an existing system. The last stage is much more complicated and difficult to set up than the others, so it may be left until several similar systems can be tested together or until faults found in the first two stages have been corrected.

We would normally pass the protocol to the potential user of the equipment and to the manufacturers for comment. We may then revise the protocol in the light of these comments. This part of the process is very important. The users will have their own questions about a system, and we want to make sure that these are addressed in our trial. The manufacturer knows how his instrument should be used, and can often tell us how to get the best out of it.

Full consultation at this stage largely allays the mutual suspicion which sometimes develops between manufacturers who think that their equipment is being unfairly tested and testing agencies who think something is being hidden from them. Not that the manufacturers should dictate the tests, of course, but if there is to be any argument, it is better to have it before going to all the trouble of doing the trials.

So, having agreed our protocol (remembering that we can still vary it, with consultation, after we start the trials) we now have to carry out the tests. The first two stages whilst important and often complicated, consist of fairly obvious tests, and it is not proposed that they be discussed in detail here. Blind tests and simulated operations are, perhaps, more difficult to do and so some comments on their more general aspects may be worthwhile.

5. BLIND TRIALS AND OPERATIONAL SIMULATIONS

Blind operational simulations can provide an excellent overview of a detection system's capabilities in a realistic scenario, but they are complicated and difficult to do. The difficulty is in organising a fairly big event, with lots of people and equipment involved, often at a venue remote from the laboratory, sometimes with large quantities of explosives (or even viable explosive devices) around and with considerations of safety, security and commercial confidentiality and so on and yet still preserve the scientific integrity of the trial.

The scientific requirements of the trial include the following:

- The trial should simulate as closely as possible an operational scenario;
- A large number of individual searches will need to be done for statistical reasons;
- The trial should be blind -equipment operators should not know, or be given any chance of finding out, where the target items are;
- The number of variables should be limited, since more variables mean even more searches;
- The targets must be made and concealed in a realistic way;
- The detection systems under test must be used properly.

The organisation of the trial must be carried out with these considerations to the fore. A good idea is to appoint a trials director. The trails director should be a person who is thoroughly conversant with the equipment under test and familiar with explosives and weapons detection generally. They should preferably have been involved with stages 1 and 2 of the testing programme. The director needs to devise the protocol, discuss it with interested parties and organise and supervise the trial itself. They should therefore be given the freedom to negotiate with the users, manufacturers and the providers of the venue and helpers. The director has to be sure, before the trial begins, that all the scientific criteria above are met and that everyone involved knows what they are doing. Often, non-scientific staff will not understand all the requirements, so they must be thoroughly briefed and allowed to discuss their rôle before the trial begins.

The first thing to be sorted out is usually the venue. There needs to be room to accommodate all the equipment involved, and operators, experimental subjects, baggage or whatever. If vapour or trace detection equipment is being tested the venue must be free from explosives vapours or traces, so civilian premises may be preferred.

Helpers and possibly experimental subjects may need to be found, and all must be briefed. In cases where cross contamination is a problem, they must not be allowed to contaminate one another. If some subjects are carrying target materials they should not know this in case they communicate this knowledge to the equipment operators. Substitute materials could be given to some subjects so that everyone is carrying something.

A system of keeping records must be devised. Two separate records are needed, with some way of tying them up. We need to record, firstly, where the targets were placed and, secondly, where instrument responses occurred. Incidental details and comments may also be needed. At PSDB we favour using forms which have spaces for each piece of information. For example, fig. 1 shows a form used for recording EGIS responses on a train. Each carriage was divided up into search areas with one sample per area and these areas are shown on the diagram at the top right. The vehicle number (all railway rolling stock is numbered) is recorded by the searcher along with the search area and a description of the area is included in case of error. The searcher also records start and finish time and any comments. The form then accompanies the sample back to EGIS where the analysis results are recorded at the bottom.

Other aids to record keeping include video (essential with baggage X-Ray machines) and computers. Checks should always be included so that one type of record does not get out of step with another. Where live explosives or weapons are used record keeping should be designed to ensure that all of them are returned at the end!

The movement of people, bags equipment and so on through the trial area may need to be controlled to prevent cross-contamination or to prevent the 'blindness' of the trial from being compromised. If several detectors are being tested together they should be arranged so that operators of one system cannot see the others. In some cases it should be remembered that use of two systems one after another may not be practical, since one search may affect subsequent tests (for example, using a particulate sampling system on a bag will reduce the number of particles available for subsequent tests, or may introduce contamination).

Samples of target materials used in the trial should be in good condition. Explosives especially tend to cross-contaminate (EGDN is the usual contaminant) so the purity of samples should be checked before the trial. Equipment used for checking purity should be at least as sensitive to the contaminant as the equipment under test. For vapour detectors, it is the purity of the vapour from the explosive that counts, rather than the explosive itself. An alternative approach is to get the explosives straight from the factory and isolate them from possible contaminants. Non-volatile explosives tend to contaminate other items through physical contact. As a precaution, we tend to assume that all our equipment, staff and laboratories are contaminated in this way. The best way to limit further contamination is for all persons not meant to be placing explosives to wear disposable coveralls, gloves and overshoes and to change them regularly.

The director should be convinced that all these details have been fully worked out before the trial. If mistakes are discovered on the day it may be too late to do anything about them.

The usual approach to a simulated operational trial is to measure the detection capability and false alarm rate at the same time, in the same conditions. For some types of instrument, like particulate explosives detectors where cross contamination is a problem, this may be very difficult. A possible alternative approach is to determine the detection capability in the laboratory and then to measure the false alarm rate in operational conditions. It is very important that search techniques used in the laboratory are reproduced in the field and that the calibration of the instrument is not changed.

To summarise, then, operational simulations are complicated and expensive. To get the most out of our investment in time and resources, a thorough understanding of the instruments we are testing, coupled with meticulous planning, are essential.

6. USE AND ABUSE OF RESULTS

The result of each stage of our trials should tell us the things we set out to discover. We can use them to decide whether a detection system is useful, whether it needs improvement or whatever, depending on how we designed the tests. The same results can also be taken out of context and obscure the truth about a system. This is especially likely to happen with the results of large scale field trials and blind tests, perhaps because they are difficult to set up and to repeat, so the results are quoted more widely and with less qualification than they should be.

An important point about these large blind trials is that, whilst they are a very good way of measuring false alarm rates, they do not always provide as much information about detection capability as we would like. This is because often, in setting up a trial of this sort we make implicit assumptions about the terrorists and their methods. A good example is the testing of baggage X-Ray systems. Suppose we

make 20 dummy bombs, put them into packed bags, mix them with 100 other bags and then put them through an X-Ray machine. The operator spots 15 of them. Does this mean that the probability of detecting a terrorist bomb is about 75%?

No!

Ignoring for a moment the human factors (if you tell an operator you are putting bombs through he may pay more attention or be more cautious than usual) there is an assumption built into this test that our bombs are typical of the terrorists'. Some bombs are more easily spotted than others and we will probably have used a variety of types. We do not know that the distribution of 'ease of identification' of our bombs is typical of what terrorists will produce. The database of real bombs (in aircraft baggage) is too small to tell us much. A terrorist knowing that his work is to be X-Rayed may well produce only well-disguised bombs, which may all resemble the 25% that we missed.

The point of this is that the figure of 75% is perfectly good for comparing the system with similar X-Ray systems, tested under similar conditions with the same set of dummy bombs. It cannot, though, be used to compare an X-Ray system with, say, a vapour detector, because the performance of a vapour detector is affected by a completely different set of constraints.

This leads to the unfortunate conclusion that the often-used term 'probability of detection' is meaningless when unsupported by details of trials methods, or for comparing different kinds of detection system. The performance of complicated systems cannot be reduced to a few percentages. A far deeper understanding is required.

At PSDB we usually give the manufacturers full details of trials methods and results, excluding, of course, information on competitors' systems. There is seldom any good reason why this cannot be done, provided it is made clear that the information is not given to third parties without permission and also that parts of the report (the good parts) are not taken out of context.

In general, testers should be aware of the uses which may be made of their results and guard against both possible unauthorised disclosure and simply reading things into the results which are not there.

7. SOME EXAMPLES

Below are some examples of different detection systems, with some ideas as to what can be measured in each case.

7.1 Vapour and Trace Detectors

Stage 1. Sensitivity of analytical system, efficiency of sampling, effect of impurities and dirt in sample, effect of commonplace chemicals

Stage 2. Can explosives of various types be detected in baggage, in electrical devices, in cupboards, cars? Are they detected by sampling vapours or particles? How is this best done? Effect of handling explosives, wrapping etc.

Stage 3. False alarm rates in specified situations. Detection capability for specified explosives and concealment methods, but this may be difficult to do and of limited value.

The main difficulty in testing vapour and trace detectors is cross-contamination. Explosives samples may be contaminated with other explosives (notably EGDN) and supposedly 'clean' objects and places may be contaminated with particles of explosives. Extreme precautions may need to be taken to avoid contamination, and false alarms should be checked to ensure that they are really false.

7.2 Bulk Detectors

Stage 1. Response to various masses of different explosives, response to other materials, screening effects of various materials, variation in response with target distance or position, radiological safety.

Stage 2. Detection in realistic situations (e.g. in packed baggage, behind walls etc.)

Stage 3. Blind trial to distinguish, say, bags with explosives or simulants in from 'normal' bags. Measure detection rate and false alarm rate. Also need to test effect of position and size and shape of explosives.

Difficulties in testing bulk detectors for baggage include:

i. Formulating realistic explosives simulants, as large quantities of explosives would otherwise need to be used.

ii. Getting enough bags to do the blind trial. Bags belonging to the general public can often only be used as blanks, so the 'live' bags must be acquired and packed specially. The packing has to resemble real bags as closely as possible, and for a large scale trial this can be difficult. (Think of what you normally pack on a foreign trip, multiply it by 100 or so and imagine the amount of trouble involved in acquiring it all).

7.3 X-Ray Machines

Stage 1. Resolution, imaging of fine wires, penetration (amount of material which can be interposed between the source and the object of interest without obscuring the object), discrimination between materials, radiological safety, effect on photographic materials and magnetic media.

Stage 2. Visibility of various items in baggage, effect of overlap

Stage 3. Blind trial with bags having weapons or bombs mixed with 'normal' bags to determine number of detections and number of false alarms. Operator comments.

It is important in X-Ray trials to remember that their performance depends on the operators. Operators should not only be experienced in X-Ray interpretation generally but should have training and experience on the actual system under test (for instance, operators used to monochrome may take some time to adapt to colour and use it effectively. In our tests, operators were actively hostile to dual energy systems but still produced better results than with monochrome). It can be difficult to decide what objects to put in the bags and how many of each type to use, bearing in mind that more variables inevitably mean a bigger trial.

We may wish to distinguish genuine detections - where the operator spots the weapon or bomb - from those where the operator rejects a bag for some other reason and does not spot the weapon in it. This cannot usually be done with non-X ray systems, but it provides useful information.

7.4 Metal Detecting Doorway

Stage 1. Response to standard test objects (metal rings, blocks of various metals, weapons) in different positions and orientations and at different speeds. Electromagnetic interference. Other environmental factors.

Stage 2. Response to objects carried on the person, with and without 'legitimate' metal items (keys, pens, watches).

Stage 3. Trial to determine false alarm rate. The doorway is set at a sensitivity setting determined after stages 1 and 2.

Testing metal detecting doorways may be complicated by the large number of adjustments available on some instruments. One way around this is to specify some simple detection criteria and ask the manufacturers to set the instrument up to meet these. We now have a detailed general test protocol for metal detecting doorways.

8. STANDARD TESTS AND SHARING OF RESULTS

So, what about standardising all our test methods so that we can all test different instruments and then swap the data? I do not think this is possible for all the types of detection systems around. To fully test a detection system as described above is complicated, and the test methods depend on both the system itself and on the requirement. However, some tests will always be the same for certain types of equipment, and these tests can form the basis of information exchange. For instance, the sensitivity of vapour detection systems is a useful indicator of performance, as is the resolution of an X-Ray machine. There is probably scope for standardisation of tests of things like archway metal detectors, since they have been around for a long time and all do roughly the same thing. The ICAO tagging programme produced some standard test procedures for vapour detectors, which deserve consideration. It is important, however, that it is the test method and the presentation of results that is standardised and not the interpretation of the results. Only the user can decide whether an instrument fits their requirement.

For those detection systems which do not lend themselves so readily to standardised tests the answer is probably to be more specific when sharing information. If a figure needs qualification, we should qualify it. If our test procedures are unconventional, we should explain them. This is not always easy. No-one wants to wait months for full, departmentally sanctioned, glossy covered, fully

illustrated reports, but there must be a middle ground between this and the cursory "we tested it and it was very good/bad". A clear statement of what was tested, how it was done and what the results were is what we need.

9. CONCLUSION

The useful exchange of performance data depends on the understanding of the differing aims and approaches of the testing agencies involved. It also depends on those agencies building their own credibility by carrying out well planned tests, presenting results in a useful way, with the limitations of the tests made clear, and by openness with others working in the same field. I have endeavoured to explain our aims and our approach and, I hope, enhance our credibility a little.

Fig. 1 Example of Trial Record Form

EGIS: Train Search Sample Record Form

Sample No.

Part 1. Searcher's Record

Searcher:

Vehicle No:

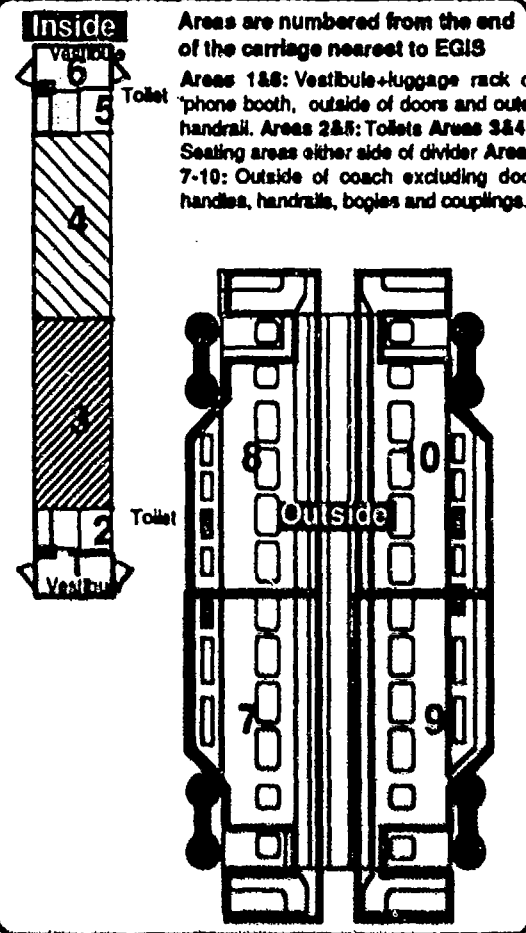
Search Area:

Description:

Start Time:

Finish Time:

Comments:



Areas are numbered from the end of the carriage nearest to EGIS

Areas 1&8: Vestibule+luggage rack + 'phone booth, outside of doors and outer handrail. Areas 2&5: Toilets Areas 3&4: Seating areas either side of divider Areas 7-10: Outside of coach excluding door handles, handrails, bogies and couplings.

Part 2. EGIS Operator's Record

Time: Sampler No: Printout No:

EGIS Response	Bars			Peak indications		
	NG	TNT	PLA			
First run						
Second Run						

Comments

A FRAMEWORK FOR THE OBJECTIVE TEST AND EVALUATION OF EXPLOSIVE DETECTION TECHNOLOGY

Donald R. Greenlee
Science Applications International Corporation
Falls Church, VA

1. INTRODUCTION

The critical need for effective explosive detection capabilities in support of aviation security has stimulated the research and development of a variety of potentially applicable technologies. Prior to any major investment in the acquisition of equipment for actual deployment, however, each candidate technology (or combination thereof) should be subjected to test and evaluation (T&E) in an operationally realistic setting adequate to verify its effectiveness and suitability. A framework for the objective approach to this testing and evaluation should promote test requirements definition, test concept development, test design, technical and operational test planning, test instrumentation and facilities, the role of modelling and simulation in support of test and evaluation, test conduct and monitoring, data collection, reduction, processing and analysis, and assessment of results adequate to determine "How much testing is enough?", the most difficult question in the relationship between T&E and acquisition or deployment. The costs of test and evaluation, particularly where advanced technology, sophisticated threats, environmental constraints and hazards to safety exist, coupled with inevitable programmatic, political and schedule pressures on the system under test, create forces tending to minimize the type, amount and duration of testing. Conversely, the need for technical and operational information about the system and its behavior, and for proof by demonstration that the system satisfies the requirements it was developed to meet, gives rise to the desire for maximizing testing and its support functions to accommodate the system's developers, users and overseers. Since testing per se does not improve the performance of a system, T&E is technically a "zero value added" process, except for the information it provides. The projected information value of a test in reducing risks in the acquisition/deployment decision process, then, provides a basis for solving the indicated "minimax" problem.

2. WHY WE TEST

As a working hypothesis, we assume that, at least in theory, testing is an information generation activity with the objective of reducing the risk of doing something. Or in very general terms, we test to generate information to reduce the risk in applying new technology or in using old technology in new ways. Then we stop testing when that risk has been reduced to a level generally acceptable to those responsible for the application. (Many other factors tend to intrude, however, as noted below.) Since the uncertainties introduced by new technology or its novel applications drive T&E, testers tend to be challenged most by the very features and characteristics which make new systems effective. It has been noted that, despite its utility, "Testing is a zero value-added activity", since no system is ever improved by the act of testing alone. Testing is usually performed either to find out something (experiment) or to prove something (demonstration), of either an operational or technical nature, with the ultimate goal of reducing the risk of an unwanted result of taking some action. Although ideally testing proceeds until adequate risk reduction has been achieved, numerous other constraints tend to affect the type, amount, and duration of T&E:

- Resource Constraints
- Schedule Constraints
- Environmental and Safety Constraints
- Pressing Need to Use, Deploy, or Market
- Desire to Exploit A Technique, Technology or Opportunity
- Security Limits on Capability Exposure
- Programmatic Perturbations
- Political, Social, and Cultural Considerations.

3. THE TEST AND EVALUATION PROCESS

The T&E process, like the system design process, begins with the statement of a general need. This statement should not define a specific system to meet

the need, much less the quantitative parameters of such a system. For example, the need for "a combination of sensor equipment and operational procedures to prevent the transportation of explosives aboard aircraft and their subsequent detonation" could serve as such a statement. The "user", or authority ultimately responsible for acquiring and deploying the system, should issue this statement.

This general statement of need should then be translated into a set of operational requirements; these should be as specific and quantitative as possible, but couched in operational, rather than engineering terms. Again, the articulation of operational requirements should not explicitly define the design of a system to satisfy these requirements. For explosive detection systems, the traditional parameters of detection probability and false alarm rate, when specified in relation to a particular type and amount of threat explosive, serve as examples. Other characteristics, such as throughput rate and physical attributes (size, weight, etc.) can either be specified as requirements or held out as variables to be used as discriminants in the selection process for alternative system candidates. Again, the user is responsible for articulating operational requirements, based, presumably, on some analysis of the operating environment and real-life constraints. These operational requirements are also used to generate a set of critical operational issues or questions to be addressed later by operational testing.

Based on the operational requirements, then, the "developer" can create technical or engineering specifications for one or more systems which are feasible candidates to meet the operational requirements. The technical specifications in turn lead to critical technical issues, or engineering questions to be addressed by technical testing. Since the technical specifications, unlike the operational requirements, are peculiar to each system design, they can vary widely in number and type. Technical specifications appropriate to an X-ray device, for example, would probably not be suitable for a device attempting to exploit vapor detection phenomenology. The developer, usually in cooperation with the contractor actually responsible for the design and fabrication of the system, will perform developmental or technical testing against the technical specifications to determine whether, and to what degree, they are met. Technical testing is in the nature of an "experiment", in that the results may be used, often with numerous test-analyze-fix iterations, to improve the system performance.

After a system is viewed as having satisfactorily passed its technical tests, it becomes a candidate for operational testing against the operational requirements. (An important point to note, however, is that a system can fail to meet one or more of its technical specifications, and still satisfy the operational requirements, just as a system can pass all of its technical tests, yet be found unacceptable in operational testing. Thus technical specifications must be treated very carefully when they are being used to assess systems as candidates for operational testing.) Ideally, to maximize the objectivity of results, operational testing should be conducted and evaluated by an agent who is independent of the user and the developer/contractor, but who is nevertheless as informed about the system as the latter and yet a worthy surrogate for the former. (This is sometimes difficult to arrange institutionally, but adds greatly to the credibility of the process.) Operational testing obviously should take place in an environment and under conditions as nearly operationally realistic as practicable, e.g., using actual items (baggage), personnel (handlers) and threat replicas (explosives).

Finally, the results of operational testing are compared with the operational requirements and critical operational issues and an assessment made of the system's operational effectiveness and suitability to the user's original need. ("Effectiveness" here relates to performance factors, whereas "suitability" refers to factors affecting the satisfactory installation and employment of the system, e.g., reliability, availability, maintainability, etc.) Upon this assessment, a decision whether to acquire and deploy the system can be made. Normally, other factors enter the decision process at this time, both quantifiable (e.g., cost of the system in relation to its effectiveness) and non-quantifiable (e.g., the presumed deterrent effect of having the system in place). In addition to forming the basis for an informed "buy" decision, the results of operational testing can, if appropriate, be used to modify the user's expectations as to operational requirements or even the basic need, just as the results of technical testing are employed in an iterative fashion to adjust system design, construction and even specifications.

4. TEST AND EVALUATION OF EXPLOSIVE DETECTION TECHNOLOGY

Within the general framework outlined above fall a number of crucial considerations specific to the test and evaluation of explosive detection technology. First, both in time and importance, is the

establishment of the need for the technology and the equipment by which it is implemented. This need is presumably based on some real explosive threat, and so, unless the threat disappears, the need, once articulated, remains to be met. Thus the user may choose to accept the technology which comes closest to meeting this need, even though the operational requirements are not all fully met, in order to avoid the situation wherein no constructive action is taken. System acquisition theory offers a formal solution to this predicament in which no currently existing technology is completely satisfactory, namely the "evolutionary strategy". In this approach, formal acknowledgement is made of the circumstance that the operational requirements are not completely stated (e.g., because of an insufficiently precise threat definition) and/or the technology is not completely in hand to satisfy the requirements (although the expectation exists that such technology will eventually be available). An attainable increment of "core" capability is then defined, implemented, tested and deployed. Subsequently, when the requirement is better understood and/or the technology improved, a second increment of capability is fielded. This cycle is repeated as necessary until the final system evolves, with technical and operational testing conducted against the provisional requirements at each stage. Thus the user is able to promptly enjoy the benefits of the best existing technology while, in a disciplined and justifiable way, addressing the (possibly changing) requirements with gradually improving technology. In the case of explosive detection technology, the user also gains from the deterrent power of having an actual system whose limitations may not be understood (and hence must be respected) by a threat agent.

Having decided that his explosive detection need must be met to the maximum (if not total) extent, the user must articulate quantitative operational requirements, beginning with a characterization of the threat. Although the simplest formulation of the threat standard would be a minimum detectable amount (e.g., the selected technology must be able to detect at least X pounds of different types of explosives), care must be taken not to set an impossible problem. As noted above, adequate freedom should be built into the threat specification to allow proceeding with otherwise acceptable technologies which do not completely meet the criterion; otherwise, all progress is blocked. Other characteristics of the threat which are necessary to make the explosive a problem for the detection system user (e.g., timers, pressure sensors, detonators, wiring, etc.) should also be considered in the threat definition. Other candidate parameters traditionally offered as operational requirements include probability of detection Pd, probability of false alarm Pf, throughput rate V and system cost (fixed initial plus recurring operation and maintenance) C. This set defines a four-variable simultaneous stochastic optimization problem. Because of the very different nature of C from the other parameters, it is probably best considered separately, either in the manner of a cost-benefit analysis, or as simply a factor in the eventual procurement process, to be driven out by market forces. Furthermore, in many candidate technologies, Pd and Pf are directly correlated (and inversely joy-producing), so that a joint specification which allows the system designer to accomplish tradeoffs may be appropriate. In any event, the operational requirements and critical operational issues are to be derived from the need statement and not tailored to the prospective technologies; all systems should undergo operational testing against the same objectives.

With the universal operational requirements and critical operational issues, together with the technical specifications and critical technical issues specific to each technology derived from them in hand, the test planning process can begin. The overall test concept, leading to detailed test designs, leading in turn to detailed technical and operational test plans, should, in addition to prescribing exactly how the tests should be conducted, monitored and reported, relate the results of testing to the ultimate decision about acquiring and deploying the candidate technologies. That is, in addition to providing data about the technologies ("experiment" function) or showing that some forecast detection capability actually exists ("demonstration" function), the ultimate output of the test program should be sufficient information and answers to permit an acquisition decision to be made with minimum risk (variously characterized as the "final exam", "live-or-die" or "Sunday game" function). The test plans should also specify the test resources (facilities, instrumentation, test units, etc.) which will be required, together with any limitations on testing scope or realism which the evaluator must cope with later. For explosive detection systems undergoing operational testing in an actual working airport environment, these constraints can be significant.

One obvious tool which can greatly assist the system tester, as well as the system designer, is a computer simulation of the system. Such a model, which need

not necessarily incorporate the detailed physics and mechanics of the system, can be used in the test planning phase to suggest the most useful configurations for actual testing (thereby minimizing low information content events), as well as in the post-test analysis and evaluation phase to extend the results of testing to additional configurations; both modes potentially save time and money. If the simulation is available early enough in the design phase, it can of course be used to experiment with various combinations of technologies and their interconnections, along with methods and procedures for their use.

5. HOW MUCH TESTING IS ENOUGH?

What constitutes "enough" testing lies, like beauty, in the eye of the beholder. A system of any appreciable significance will normally have a diverse set of constituents, each with a view on the sufficiency of testing:

- The Program Manager
- The Contractor
- The User
- The Tester
- The Review and Audit Community
- The Analytical Community
- The Taxpaying Public
- The Media
- "The" Congress.

The rightful entitlement of each party to his special perspective is not disputed; however, the tester is expected to supply special contributions, including independence and technical expertise in his craft. Discussions of how much testing is enough have traditionally focussed on analytical approaches to the determination of test sample size. Statistical considerations are essential (and certainly comforting), but may not embody all of the real-world factors, as the examination of some prominent programs and their associated amounts of testing tends to suggest:

- One Is Optimal (Anti-Satellite System)
- None Is Plenty (Continuity of Government Programs)
- Any Is Appreciated (Electronic Warfare Systems)
- A Little "Bit" Would Have Sufficed (Mariner)
- This Is OK, We Can Always Tweak It Later (Hubble)
- Every Day's Worth Makes Us Happier (Lotus 1-2-3/G)
- If It Works In Practice, "Whatever" Was OK (Numerous)
- None Is The Least We Can Get Away With (Various)
- Some Is Exactly Right (?).

The last reference acknowledges the difficulty of identifying systems or programs in which the amount of testing was precisely enough; instances of insufficient testing are much easier to cite, and "overtesting" is a difficult notion, if not an oxymoron. Nevertheless, part of the tester's job is to determine (expertly) how much testing is enough, assess and articulate the adequacy of testing, and defend his vision of testing sufficiency against those of other constituencies. This is to be done, furthermore, under very general T&E policy guidance, directives, and regulations which are virtually free of glaring strengths regarding how much is enough. A variety of approaches has been used to attempt to answer the question "When can we stop testing?". These include classical statistics, Bayesian statistics, game theory, decision theory, and modelling and simulation. Most approaches view a test as an event characterized by a binary choice of outcomes, viz., success or failure. But most systems of any non-trivial degree of complexity don't simply "pass" or "fail". Furthermore, if, as assumed in the discussion above, the fundamental objective of testing is to obtain information, it seems reasonable to measure the information generated by testing and stop when we have enough of it to reduce the risk to some acceptable level. In this approach, a test of a system can be viewed as a multi-state stochastic process, the system proceeding from state to state in accordance with assumed probability distributions (or else the outcome of the test would be fixed) and residing in different states for periods of time determined in accordance with other assumed probability distributions. The passage of the system through each test state generates a specific, quantifiable amount of information. The total amount of information generated by the test is then the sum of the information generated by the sequence of realized states. Since the risk is inversely proportional to the total information, it decreases monotonically with increasing testing. Testing (i.e., information generation) continues until risk is reduced to the

desired level, or conversely, we stop testing when the information generated exceeds the reciprocal of the acceptable risk level.

The mathematical description of the stochastic evolution of a process such as the above characterization of a test has been worked out and described by the author. Although the approach is valid in principle for arbitrarily complex processes (i.e., arbitrarily large number of possible states), the actual calculations can become laborious for complicated systems. Fortunately, numerical methods can be applied to generate the numbers by computer, so that closed-form analytical expressions need not be derived. The handling of information by quantitative methods is discussed in any competent text on information theory.

VALIDATION OF SIMULATED EXPLOSIVES FOR TESTING TNA EXPLOSIVES DETECTION SYSTEMS

Michael J. Hurwitz
and
Wilbert P. Noronha
GAMMA-METRICS
5788 Pacific Center Blvd
San Diego, CA 92121

1. INTRODUCTION

GAMMA-METRICS has developed an explosives detection system (EDS) for airline checked baggage. This system is based upon prompt gamma neutron activation analysis,(PGNAA), often referred to as thermal neutron analysis. In this technique the checked baggage is placed in a chamber filled with thermal neutrons. The thermal neutrons readily penetrate the contents of the checked baggage and are absorbed by the various chemical elements. Each element then emits characteristic gamma-rays which are then detected and analyzed by a large bank of scintillation detectors. Primarily this technique is based upon the detection of the 10.8 MeV gamma-ray from the absorption of neutrons by nitrogens atoms.

In the development and testing of such systems it would be normal to place the target materials in the system in order to obtain realistic signals and to measure the performance. However, explosives are highly regulated materials and special licenses and permits are required for their handling and storage. In fact we have been unable to obtain a permit to store explosives in our facility.

We are now also engaged in airport testing of our EDS. This also requires a suitable target but it is difficult, if not impossible, to bring real explosives onto the airport where we are performing the tests.

The alternative is to create a suitable inert simulated explosive which will produce the same gamma-ray signatures that are produced by real explosives. The simulants ideally should comprise precisely the same elements in the same proportions and mass as are found in the real explosives which we wish to detect. The explosives are primarily composed of carbon, hydrogen, oxygen, and nitrogen. It is possible for the simulant to have some differences from the real explosives and still be a suitable substitute. The simulant should have the following characteristics:

- The nitrogen content should be accurately matched to that found in explosives, since the nitrogen gamma-ray is the primary signal which is used for the detection of the explosives.
- The hydrogen content should be approximately matched since hydrogen absorbs and moderates the neutrons which probe the contents of the checked baggage and cause the emission of the characteristic gamma-rays.
- The density and average atomic number should be matched approximately so that the simulant will absorb the emitted gamma-rays to a similar extent. However, for the size of explosives generally sought there is relatively little absorption of the gamma-rays in the simulant so the match can be fairly crude.
- The form and weight of the simulants should also be similar to that of real explosives for the above reasons and also so that they displace material within a suitcase in a similar way. Simulants which are used for both TNA and X-ray systems must be much more carefully matched in density, average atomic number, and form.

We have chosen some fairly common and convenient materials to create simulants for the TNA EDS. Melamine is a relatively inexpensive and inert powdered plastic material which contains 66% nitrogen by weight. Polyester resin with an organic

catalyst is the binder and provides some hydrogen. Sand and graphite are used as fillers and they control the density and pourability of the mixture as it is cast into molds. The oxygen, carbon, and silicon in these filler materials have relatively minor effects upon the neutrons.

Table 1 provides a comparison of the percentage of nitrogen and hydrogen by weight of the real explosives and simulants. The nitrogen matches exactly for all for the simulants. The hydrogen content and density are similar. Table 2 provides the proportions used in our simulants. We have found these mixtures can be fairly readily mixed and poured. They result in fairly durable simulants and they do not segregate significantly in the time it takes for the resin to solidify. We have found that the mesh size of the powders which we use is important in controlling the mixability and pourability of the mixtures.

Three types of tests were performed in validating that the simulants do indeed give the same results as real explosives. Total net nitrogen counts were measured to demonstrate that the nitrogen signal is the same. Gamma-ray spectra were obtained to demonstrate that other significant gamma-rays were comparable. Finally, the C4 simulant and real C4 explosives were placed in the same position in 10 suitcases of differing weight to demonstrate that the contents of suitcases did not produce any significant differences between the simulants and the real C4.

In these tests 6 types of explosives were used: C4, Detasheet, water gel, Tovex, semtex, and TNT. The quantities were not the same as the FAA defined explosives, but they were close enough that if these simulants are suitable, the properly sized simulants should also be suitable.

Each simulant and explosive was run through the EDS 10 times in the same location at the same belt speed used for inspecting luggage. They were tested alone and also in the center of an average size suitcase (29 lbs). The mean values and standard deviation of the total net nitrogen counts for the 10 runs were computed and compared. Table 3 provides the results. Generally the 95% confidence band was $\pm$ 9%. This degree of precision is sufficient since explosives which must be sensed by the system vary quite widely. Most of the comparisons lie within the 95% confidence band but several do not. We performed tests with the t statistic on the results. Some of the differences were statistically significant but the simulants are still close enough to be useful for purposes of testing the EDS. The low value for the bare semtex is probably because of the low hydrogen content of the simulant. The Tovex simulant was low in nitrogen by about 20% because we did not know the nitrogen content of the Tovex before the tests and therefore we did not make an exact simulant.

Figure 1 shows a comparison of the upper third of gamma-ray spectra obtained for real and simulated C4 and for the empty test chamber. The spectra of the C4 and the simulant were virtually identical. The broad peak at channel 10 seen in the difference between the C4 (real and simulated) and the empty tunnel is due to the 10.8 MeV nitrogen gamma-ray and the escape peaks. The spectra of the other simulants also agreed well.

Table 4 provides the results of the tests of comparing the simulated and real C4 explosive in 10 suitcases of differing weights. Each case was run through the system 5 times and mean values and deviations of the total net nitrogen counts were computed. The percentage error in the difference between the simulant and the real explosive is provided. There is no particular trend in variation with weight. Tests with the t statistic showed that 3 of the cases had statistically significant differences. We believe that these variations are probably due to not placing the simulants and explosives in exactly the same location in the suitcase.

2. CONCLUSION

Practical simulated explosives for several common explosives were described. All of these simulants (with the possible exception of the TOVEX simulant) are similar enough to real explosives that they may be used for testing of TNA systems, but some are measurably different from the real explosives. The differences show that great care should be taken in creating simulated explosives and that it is not trivial to get exact matches to real explosives.

	Real Explosive			Simulant		
	N%	H%	Density	N%	H%	Density
C4	34.5	2.0	1.68	34.5	3.7	1.47
SEMTEX	25	2.0	1.40	25	4.0	1.45
WATERGEL	23	3.0	1.28	23	3.7	1.34
TNT	19	2.0	1.47	19	3.0	1.47
DETASHEET	15	4.3	1.48	15	2.8	1.48

Table 1 Comparison of explosives and simulants

	Melamine	Polyester Resin	Sand	Graphite
C4	51.7	33.0	15.3	0
SEMTEX	37.5	37.5	12.5	12.5
WATERGEL	34.5	55.5	0	10.0
TNT	28.5	44.5	17.0	10.0
DETASHEET	22.5	45.4	17.1	15

Table 2 TNA Simulant Mixtures (percentage by weight)

	Bare	29lb Suitcase
C4	- 4%	8%
Data Sheet	8%	15%
Watergel	- 5%	14%
Semtex	- 22%	-1%
TNT	- 5%	-2%
Tovex	20%	19%

Table 3 Comparison of total nitrogen counts from simulants and real explosives, with/without suitcase. The numbers shown are 100* $(N_{sim} - N_{exp})/N_{exp.}$ The suitcase was 29lbs

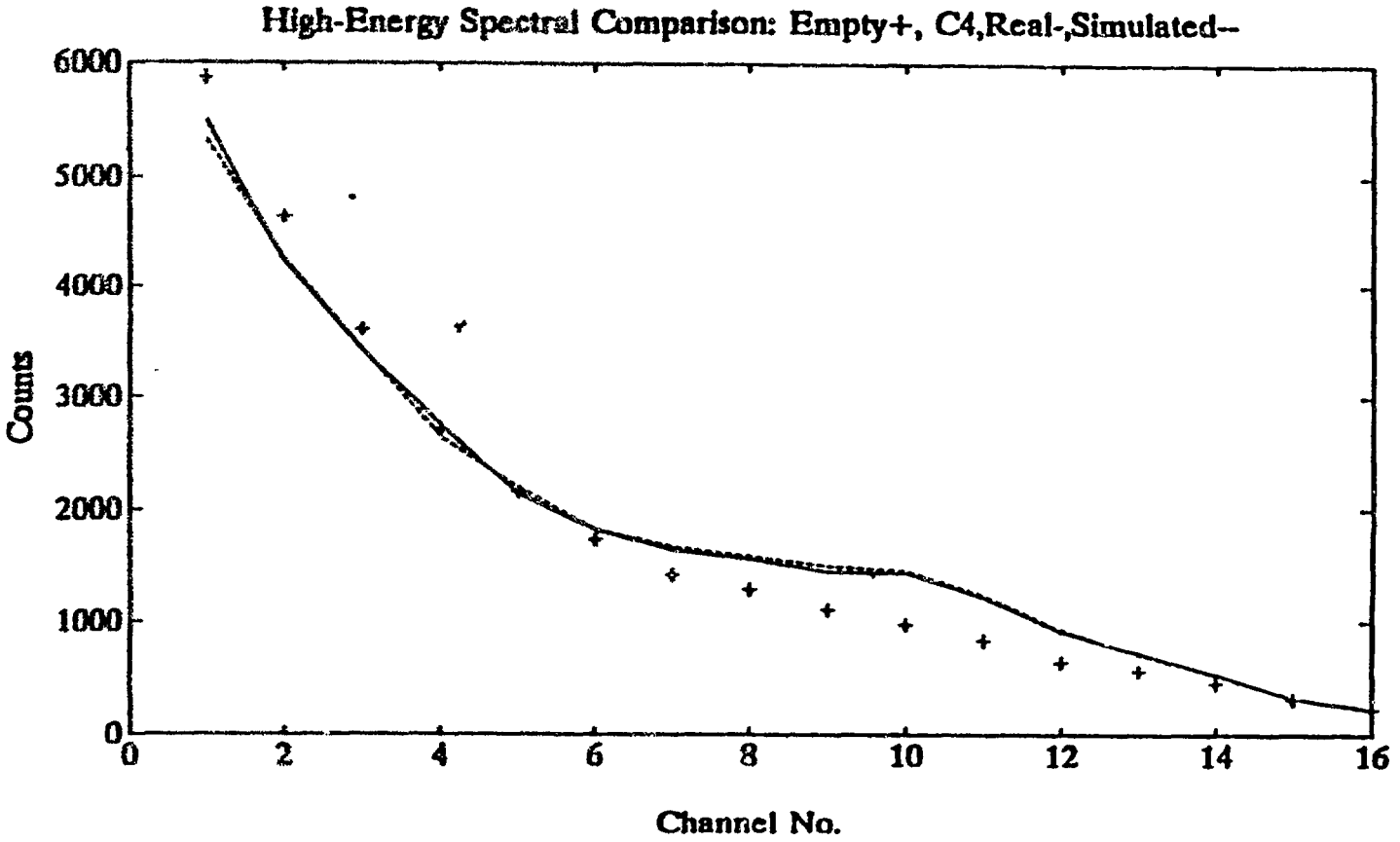


Figure 1 Comparison of Real and Simulated C4 Spectra

SUITCASE WEIGHT (LBS)	PERCENTAGE ERROR OF SIMULANT (%)
40	- 4
34	-19
33	0
32	11
29	5
22	- 6
22	- 7
16	- 4
15	-12

Table 4 Percentage Deviation in Total Nitrogen Counts between Simulated and Real C4 in Suitcases of differing weight.

AIRPORT TESTING OF A NEW THERMAL NEUTRON ANALYSIS EXPLOSIVES DETECTION SYSTEM

M.J. Hurwitz, W.P. Noronha, and T. A. Atwell
GAMMA-METRICS
5788 Pacific Center Blvd
San Diego, CA 92121

1. INTRODUCTION

GAMMA-METRICS has developed an explosives detection system (EDS) for airline checked baggage. This system is based upon prompt gamma neutron activation analysis (PGNAA), often referred to as thermal neutron analysis. In this technique the checked baggage is placed in a chamber filled with thermal neutrons. The thermal neutrons readily penetrate the contents of the checked baggage and are absorbed by the various chemical elements. Each element then emits characteristic gamma-rays which are detected and analyzed by a large bank of scintillation detectors. Primarily this techniques is based upon the detection of the 10.8 MeV gamma-ray which results from the absorption of neutrons by nitrogen atoms.

This system is designed to use a long-lived SODERN electronic neutron generator, but it can also use a californium-252 neutron source. Among the other features of this system are the use of a larger number of detectors and provision for the use of an integrated X-ray system in order to improve the detection versus false alarm performance for smaller explosives. As shown in the line drawing, in Figure 1, the EDS is made up of 5 modules so that it may be readily assembled in the field. Figure 2 shows a photograph of the system which is currently deployed in an extensive data collection and testing program in the baggage make-up room of Delta Air Lines at Los Angeles International Airport (LAX). This testing program is being supported under an FAA contract.

2. AIRPORT TESTING

The preparation and performance of airport data collection and testing requires a great deal of planning and negotiation. This process can normally be expected to require about 4 to 6 months.

Among the issues and operations required for the preliminary arrangements for the airport test are the following:

- Airline selection
- Airport site selection (baggage room, concourse, etc.)
- Detailed site inspection
- Airline approval:
  - Local
  - Corporate
- FAA approval of site
- Adequate baggage flow
- Radiation safety approval from federal, state and local authorites
- Coordination with local FAA liaison office
- Insurance
- Personnel access and badging for airport security
- Baggage handlers
- Site preparation (power, walls, base for the system, etc.)
- Preparing and validating simulated explosives
- Test Plan
- Plans for transport and assembly of the system

Figure 3 is a top view line drawing of the installation at LAX. A significant amount of site preparation was necessary. A level base for the system was prepared. Walls were erected for protection of the system from rain. Feed and exit conveyors were installed. Power and lighting was installed. Barriers were installed to protect the system from collisions by airline vehicles such as baggage carts.

The airport mission itself also requires many steps including:

- Assembly of the system without impacting normal operations
- System checkout
- System calibration

Collection of data on real airline checked baggage
Maintenance
Training of neural network explosive discrimination algorithm
Performance verification testing
Disassembly and removal of the system

3. TEST PLAN

For developing the explosives discrimination algorithm we must obtain data with real explosives or properly validated simulated explosives and we must also collect a large body of data for baggage without explosive or simulant. Ideally one would use real airline baggage without simulated explosive and then place simulated explosives in these same suitcases. This is not possible since one can not open checked luggage or readily place simulants in it.

One unsatisfactory alternative which was used in early work was to place the simulants on the side of the luggage. As shown in figure 4 the situation is quite different if a simulant is placed outside rather than inside a suitcase. First, the system develops a three dimensional nitrogen density distribution which would clearly show a concentration of nitrogen outside the suitcase and this would clearly indicate the presence of the simulant. This is not typical of the situation in which the EDS must work. Second, the simulant would be too close to the neutron source and too close or too far from certain of the detectors. Third, the simulant should displace normal materials within the suitcase.

We have elected a different procedure. False alarm data is gathered using real airline checked baggage. Data with simulants is collected using unclaimed (lost) airline luggage purchased from the airlines. Simulants are placed in random positions within the unclaimed luggage.

Of course, it is essential to insure that the real airline luggage and the unclaimed airline luggage are indeed equivalent as seen by the EDS system. This is confirmed in three ways. First, the weight and size of the bags in these 2 sets are compared. Second, the distribution of total nitrogen counts of the two sets of baggage is compared and the unclaimed baggage set is adjusted to match the real airline checked baggage. Third, data is acquired without simulants in the unclaimed luggage and ultimately, the false alarm performance of the two sets of bags is compared.

Figure 5 shows the distribution for total nitrogen counts in domestic luggage, international luggage, and for the GAMMA-METRICS' set of unclaimed luggage. The GAMMA-METRICS' set was found to have too many bags in the region around 4000 total counts and too few suitcases in the region around 11000 counts. Subsequently, we revised the distribution of the GAMMA-METRICS unclaimed baggage by emptying some of the baggage with counts around 4000 and stuffing more items heavily laden with nitrogen with counts around 11000 into the bags. Most of the real luggage with very high counts at LAX appeared to be more like air cargo rather than normal luggage.

4. AIRPORT TEST STATUS

The airport data collection is still underway. We have collected data on about 9500 suitcases as shown in table 1. Despite the best efforts of our host, Delta Air Lines, we have found that we have not been able to gather data on as many real airline bags as hoped. The primary problem has been that there is very little time for the airline to bring us carts of suitcases before they must be taken to the airplane and, obviously, we can not delay any of the luggage.

At this time we are beginning to analyze the airport data and train our bomb discrimination algorithms. Once we have trained the bomb discrimination algorithm which employs an artificial neural network we install this algorithm in the real-time system and perform verification testing.

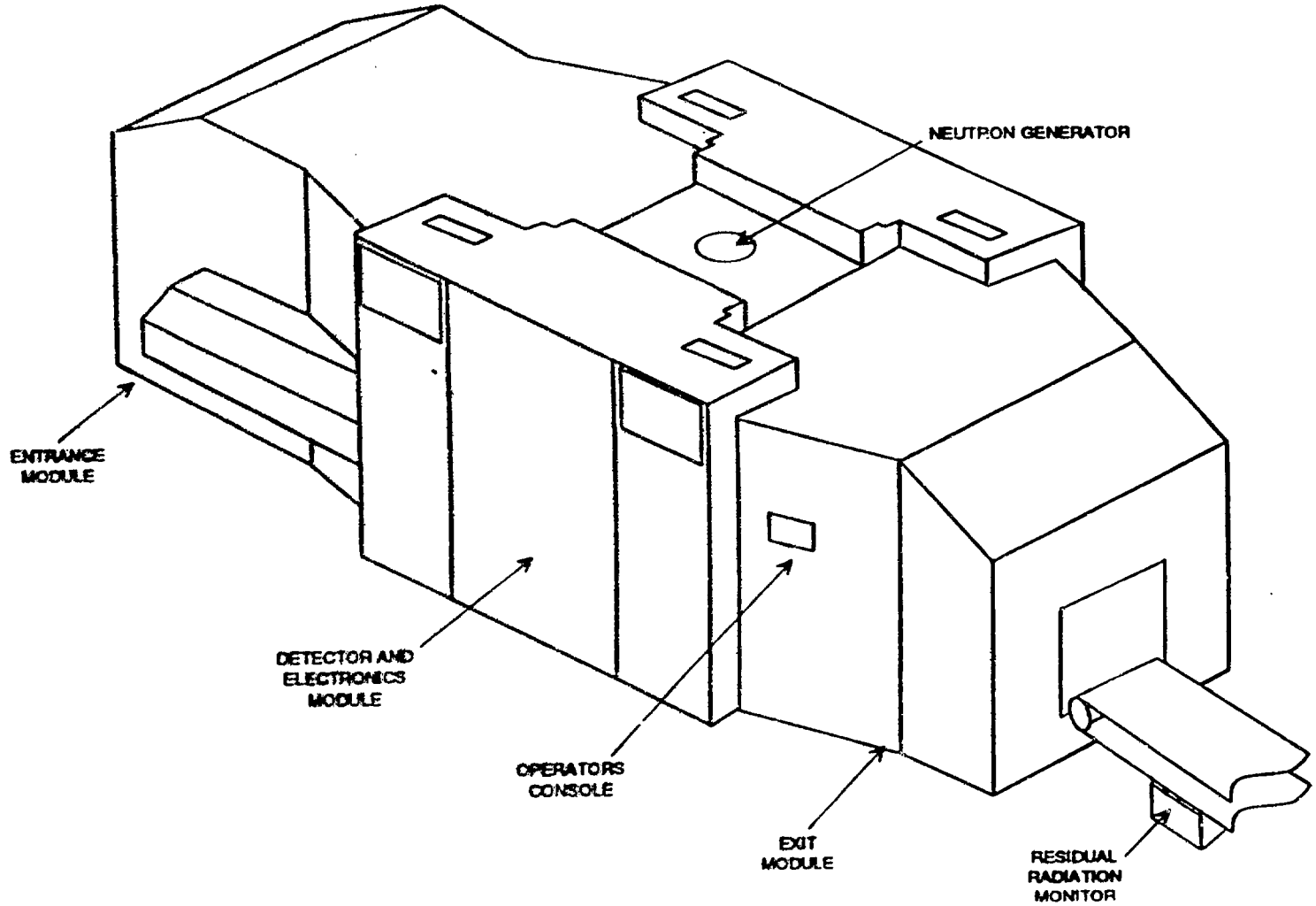


Figure 1 Line Drawing of the GAMMA-METRICS Explosive Detection System

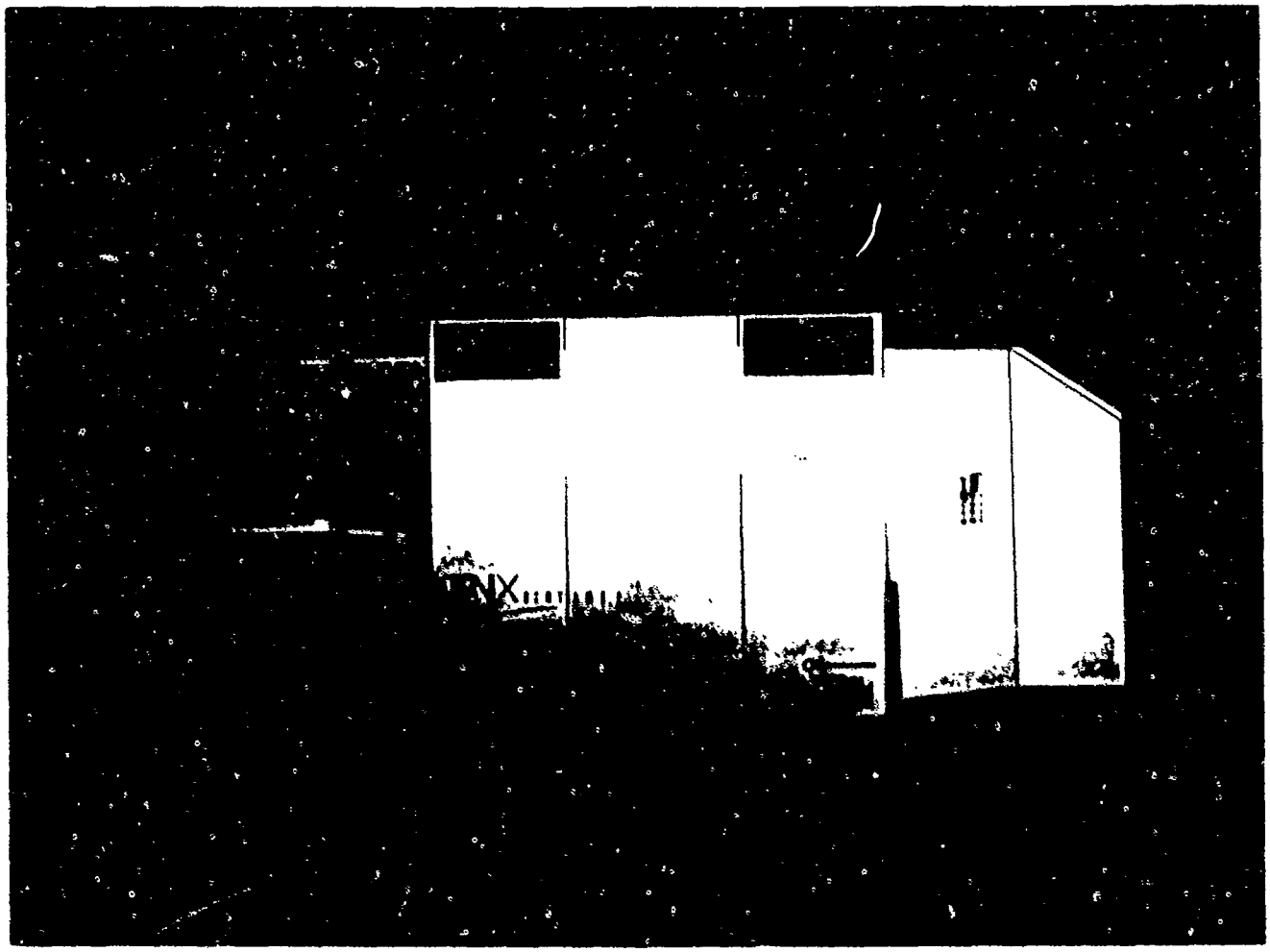


Figure 2 Photograph of the GAMMA-METRICS Explosive Detection System

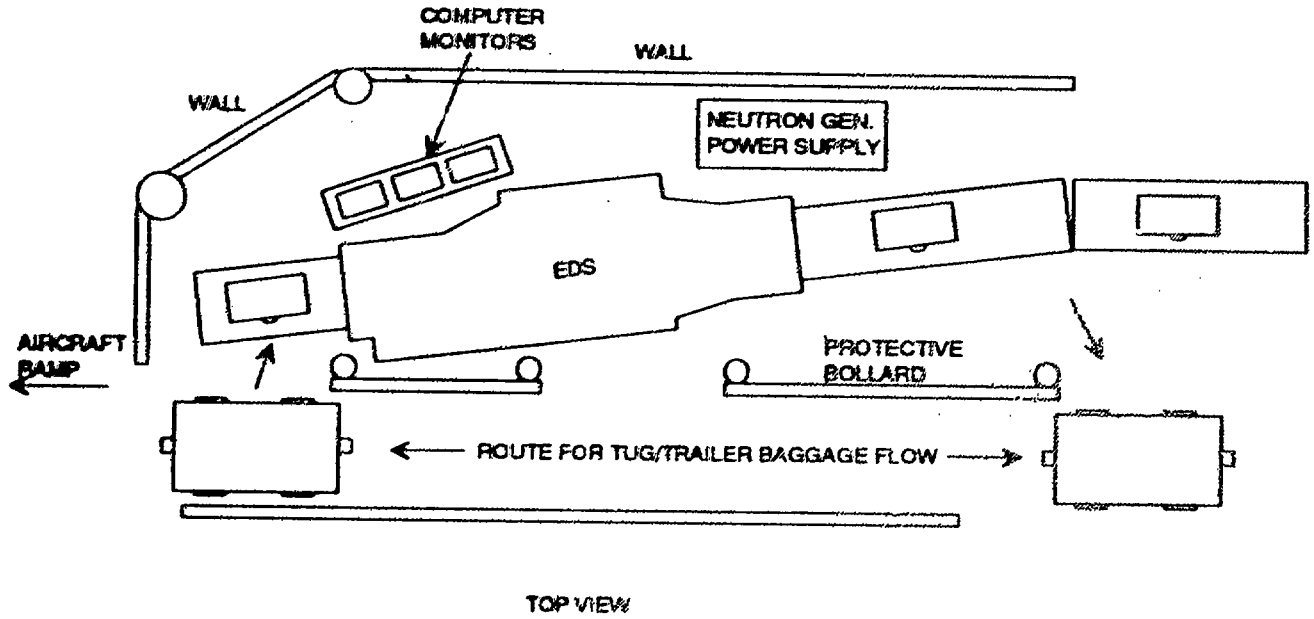


Figure 3 Line Drawing of the Explosives Detection System Installation at Los Angeles International Airport

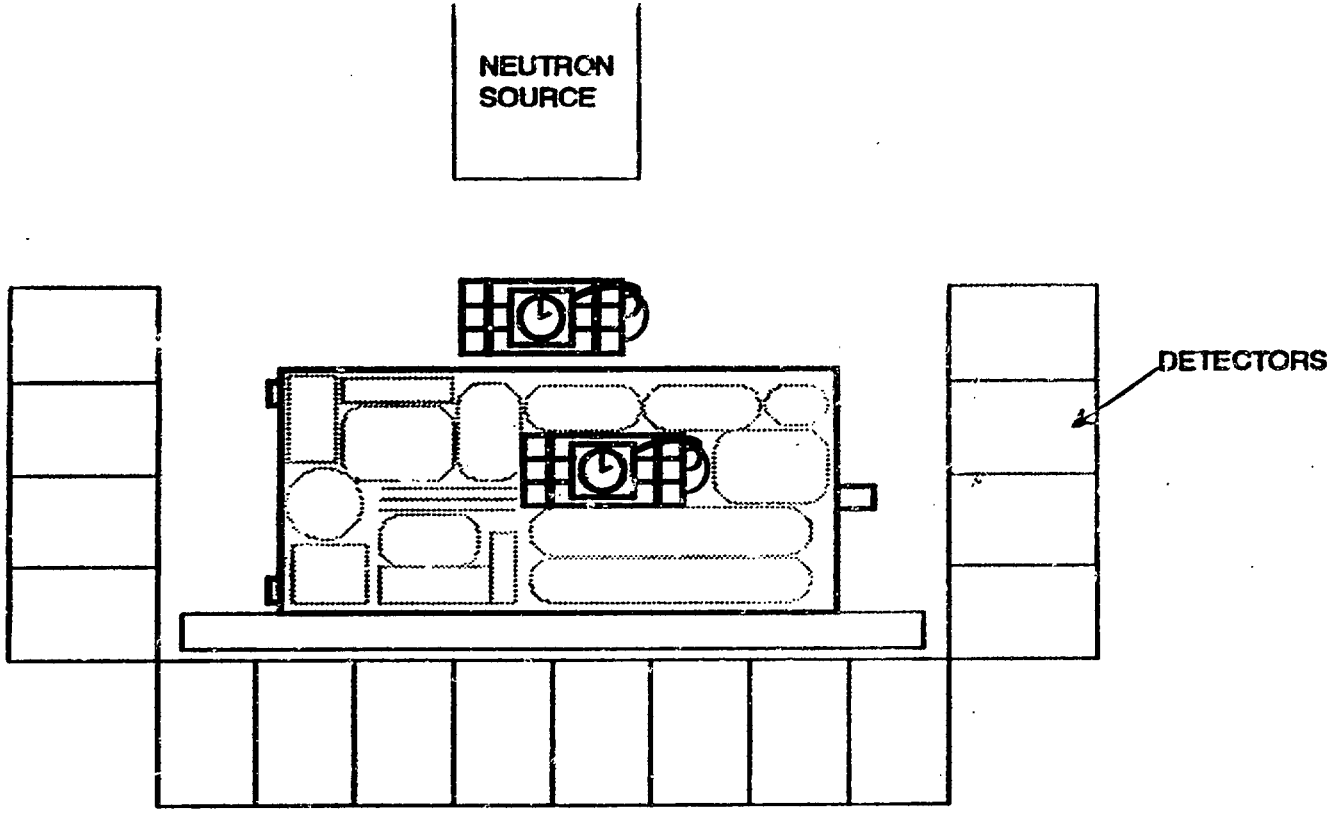


Figure 4 Possible Locations for the placement of Explosives Simulants for Airport Performance Tests

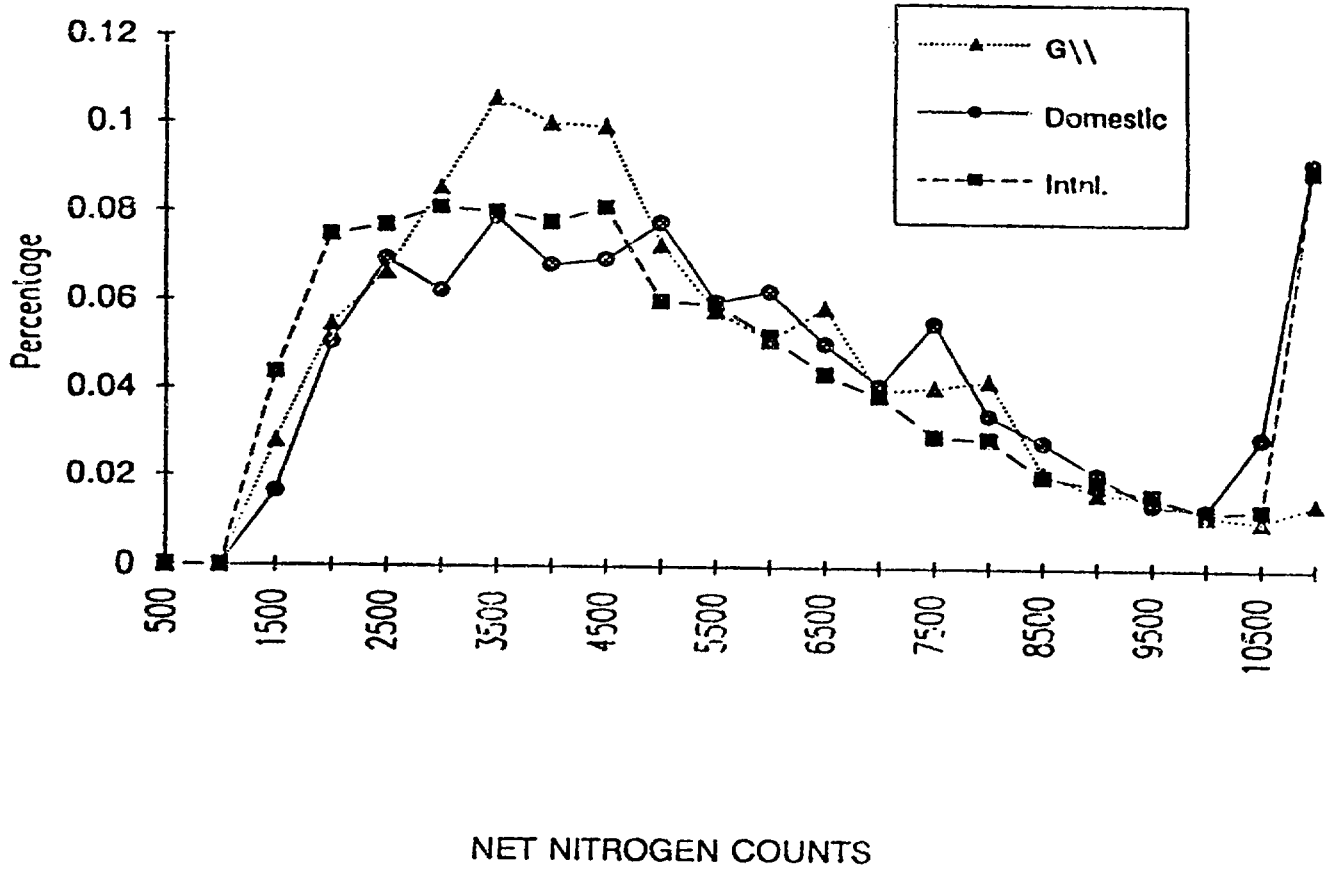


Figure 5 Distribution of Total Nitrogen Counts in Unclaimed Luggage and International and Domestic Checked Baggage at Los Angeles International Airport

DATA COLLECTED

2000	Delta Airlines International - Clean
1000	Delta Airlines Domestic - Clean
2000	Lost Baggage - Clean
4500	Lost Baggage - Simulant

Table 1 Data collected at Los Angeles International Airport
October 24 - November 15, 1991

RADIOLOGICAL SAFETY ASPECTS OF TNA DEPLOYMENT

I. M. Bar-Nir, Ph.D., and P. Ryge, Ph.D.
Science Applications International Corporation (SAIC)
Santa Clara, California

1. INTRODUCTION

Active nuclear interrogation techniques enable non-invasive explosives detection. These techniques use neutrons or high energy γ rays as probes. They study the products of the interactions of these probes with individual atoms in the inspected object to determine the presence of specific elements characteristic of explosive materials. These active techniques provide highly penetrating probes that generate distinguishable and detectable reaction products from the different elements constituting the various substances present inside the inspected object. Thermal neutron analysis (TNA) is currently the only nuclear technique incorporated in a practical and tested explosive detection system (EDS). The deployment and use of nuclear based devices in areas accessible to the general public (e.g., the concourse of an airport) raise concerns about potential radiation related hazards. A major part of the effort put into the TNA program was to ascertain that its installation and operation are harmless both to personnel and to members of the general public. Section 2 provides a brief description of the technology and how it is implemented. Section 3 describes the safety issues and how they were addressed in the TNA devices.

2. TNA AND ITS MODE OF OPERATION

2.1 TNA Techniques

The basic physics behind Thermal Neutron Analysis (TNA) is well-understood and has been applied to a wide variety of assay problems. The technique is used, for example, in laboratory sample analysis, on-line monitoring of coal and cement quality, and borehole logging[1,2]. In TNA the object to be inspected is exposed to a thermal neutron flux; each of the elements composing the materials in the object has a known reaction rate with these neutrons. The neutrons are captured and the resulting nucleus has excess energy. If this energy is released in a short time (on the order of 10^{-12} seconds) then the emission is called prompt. For most materials encountered in passenger bags, the emission of prompt γ rays is the most common reaction that forms the basis of the detection process. A nucleus which has absorbed a neutron will emit γ rays of characteristic energy at a known rate. In particular, a nitrogen nucleus will emit a 10.8 MeV γ ray about 14% of the few times that it absorbs a neutron in a radioactive capture process. By knowing the number of γ rays received in a detector, the number of neutrons bombarding the sample, and the known reaction rates for the elements in the sample, the amount of a particular element in the sample can be determined.

Delayed emissions (which occur on the order of seconds after irradiation) are of concern only as regards the safety of the system. These are the subject of the present paper.

Neutrons can be obtained from either radioisotopes (e.g. californium-252) or from electronic neutron generators. All the operational TNA units at present are californium based. A neutron generator based unit was built and successfully tested as well. It is envisaged that in situations where the use of radioactive materials is precluded, the generator will be used instead. In either technique the neutrons are produced at a broad spectrum of energies. Thus, the design of the system must incorporate materials to slow the neutrons down to thermal equilibrium. The resulting energy spectrum of the neutrons hitting a suitcase to be inspected is thus rather complex. It would be therefore probably incorrect to describe the system as a purely Thermal Neutron Analysis system. However it was designed so that those interactions dominate. The requirements for the design of moderating assemblies can be found in the literature[3]. A more detailed description of the technical aspects of the TNA system and its implementation can be found elsewhere[4].

2.2 The TNA Device

Figure 1 shows the TNA with its major components. Bags move through the system, traveling on a conveyor belt, passing through a cavity bathed with thermal neutrons and encircled by detector arrays.

Signals from the detectors are processed by the TNA computer which automatically makes a determination to clear the bag or not. The presence of suspect materials inside the luggage triggers an alarm that generates an audio signal and sends a visual message on the operator's monitor screen. Bags containing suspect objects are automatically removed from the luggage flow by the diverter.

Figure 2 is a "see through" view of the system showing in greater detail the process of bag inspection. Also indicated is the shielding incorporated into the system design. The massive shielding provided, was reflected in the system's size. TNA by itself is 13' x 8' and its weight is 28,000 Lbs. As a consequence, the installation of the TNA into airports entailed careful planning and rather involved logistics.

2.3 The TNA Use in Airports

Passengers with overseas destinations have their luggage examined prior to their departure from major international airports in the United States and overseas. At present only luggage from outbound international flights is screened, but this may change in the future and baggage going to domestic destinations may be examined as well. The number of airline passengers whose luggage would be examined was estimated to be 1.1 million per year per system. Based on an average of 2 bags/passenger, the number of pieces of luggage exposed to neutrons can therefore be as high as 2.2 million per year (at the time these lines are written, the total count of baggage items that underwent TNA inspection is about 650,000). The bags would pass through the TNA on the conveyer belt and would normally be inside the system for approximately 20 seconds during which they would be exposed to the neutron flux from the ^{252}Cf source. However, the flux is sharply peaked near the source. Thus, most of the neutron irradiation occurs within a shorter time frame (approximately 6 seconds). The effects of the neutron irradiation on the bags' contents are discussed in detail in Section 3.2, while the effects of a possible longer exposure due for example to a baggage jam in the system are addressed in Section 3.3.

Checked luggage has been the focus of the first application of the TNA technology, but threats from attacks in carry-on luggage may be equally great. In fact, approximately half of the explosive attacks against aircraft have been made through carry-on luggage. Standard X-ray screening that carry-on bags are subjected to is designed only to detect weapons, and has proved to be ineffective against explosives. SAIC has designed and tested (under contract to the FAA) a system for screening carry-on luggage.

3. SAFETY ISSUES

The use of radioactive materials in airports raises the issue of possible radiation exposure to TNA operators, other airport personnel and members of the public. Potential exposure pathways include the following:

- Radiation leakage through the system's shielding in the course of its normal operation and its impact on the immediate environment of the system.
- Induced radioactivity of the contents of the inspected luggage caused by the neutron interactions. Both potential external exposure from activated objects and potential internal exposure through ingestion of food stuffs carried in the examined baggage have to be considered.
- Potential radiation hazards in the event of a system malfunction (e.g., jams or power failures) or accidents. In particular, the potential for radiation hazard in the event of a bomb exploding inside the system or as a result of fire .
- Shipping and handling of the radioactive source of the system. In particular, source loading and retrieval.

As regards the handling of radioactive materials or the use of any ionizing radiation generating device for that matter, a universally accepted guideline is the following: "...the magnitude of individual doses, the number of people exposed, and the likelihood of incurring exposures where these are not certain to be received should all be kept as low as reasonably achievable (ALARA), economic and social factors being taken into account[5]."

3.1 Potential Radiation Exposure in the Immediate Vicinity of the TNA

Individuals who might be exposed to radiation due to normal operation of TNA are divided into two categories. The first group consists of workers who

handle the baggage and operate the system. These people spend significant amounts of time in the immediate vicinity of the system. Baggage handlers may also be specifically assigned to the TNA. The second group consists of members of the public, primarily airline passengers. Figure 3 shows the layout in one of the TNA installations, indicating the flow of bags and passengers through the system.

Two factors determine the effects of radiation: the radiation level and the exposure time. The biological effects of radiation depend on the total dosage absorbed and are cumulative. A certain level of radioactivity is always present in the background. This background radiation has its origins in a variety of sources. Primarily it is caused by natural sources (e.g., cosmic rays and naturally occurring radionuclides such as potassium-40). A small part of it, however, is man made (e.g., home appliances such as TV sets and computer monitors, or medical devices such as X-ray machines). This background radiation results in an effective annual dose of approximately 1 mSv (100 mrem/yr) at sea level. At high altitudes (e.g., Denver CO or Mexico City), due to the increasing contribution from cosmic rays, it can be as much as twice as high (the same is true for the altitudes of commercial flights)[6]. The International Commission on Radiological Protection (ICRP) guidelines call for maintaining the dose rates in areas accessible to the public ("public areas") near any nuclear installation at such levels that ensure that the resulting annual effective dose does not exceed this background of 1 mSv. The upper limit recommended for instantaneous dose rate for members of the public is 0.5 μSv/hr (0.05 mrem/hr).

The TNA design incorporates massive shielding to reduce the internal neutron and γ ray radiation to very low levels. Figure 4 shows the shielding and the doors arrangement in the TNA. The mechanical structure of the TNA is made of aluminum, with a welded-on outer shell of 3/16 in. aluminum (aluminum is preferable to other choices, such as steel for instance, due to its low interaction rate with neutrons). The structure is filled with moderators of low atomic number which is then cast into place. Additional shielding, consisting of 1/4 in. thick lead and 1 in. thick polyethylene plates, further reduces the exterior dose rate. The measured dose rates at any distance of one foot from the systems surface were found to be less than 3 μSv/hr (0.3 mrem/hr)[7]. For comparison, during a typical chest X-ray, one is exposed to 1,000 times the dosage absorbed next to a TNA in a whole year.

The door arrangements at both ends of the system are made of 4 in. thick plates. The end panels swing about vertical axes with return springs. The four inner panels hang from a horizontal pivot point with a cam-spring arrangement. In the event of a spring mechanism failure, the weight of the panels will keep them in the closed position. Individual position sensors for each panel are coupled to an indicator light on the main panel to show that the doors are closed when there is no luggage. The arrangements for loading and unloading of the bags are such that no one has to spend any length of time directly in front of the openings. Additional safety features include the following:

- The outer shield doors are key locked when the system is unattended.
- The outer shield doors are interlocked so that if the system operator removes the computer system key before locking the shielded doors, an alarm sounds.
- The source can be drawn manually to a retracted position, so that in the event of a baggage jam, retrieval can be affected with lower radiation fields.
- The source is always confined within several layers of shielding, and a locked panel covers the Teleflex cable to which it is mounted.
- A tamper indicating seal is used to show if tampering with the system has been attempted.
- Environmental monitors are used to monitor possible radiation doses in the area.

All this was achieved at a price: the system's dimensions and overall weight are rather large and its installation into an airport calls for some careful planning.

All the workers directly associated with the TNA operation are extensively trained. They are taught basic information about radiation and exposure to it, how to minimize their own exposure, and how to use survey instruments. The operation is supervised by a highly trained responsible operator. In addition, informative briefings are held for all personnel who might occasionally have to access the system area

(e.g., baggage handlers, supervisors, ramp managers etc.).

Survey instruments are provided at each airport location and doses to the operators are monitored using personal dosimeters. Explanatory and warning signs are posted at visible locations around the system for the general public.

TNA devices have undergone extensive radiation safety evaluation both by the health authorities of the State of California, where the systems are manufactured, and by the NRC. The environmental assessment determined that: "...for normal operation of the EDS and anticipated abnormal events, the radiological impact to both the worker and the public is well below NRC and the environmental protection agency (EPA) dose guidelines and is acceptable[8]." An additional environmental assessment performed in order to demonstrate TNA's suitability for operation in areas accessible to the public (e.g., airport concourse) resulted in a "Finding of No Significant Impact[9]."

At no time during the two years of operation was there any incident of the radiation levels in the areas around any of the TNA systems approaching that of the natural background.

3.2 Assessment of the Induced Radioactivity In Luggage Contents

Since the interactions of neutrons with the elements in the interrogated bags results in their becoming slightly radioactive it was necessary to demonstrate the safety (both to personnel and passengers) of handling the luggage after it had undergone TNA inspection. The TNA inspection time was determined so as to keep this induced radioactivity at a minimum. Most of it decays within a few seconds to a few minutes. By the time a bag exits the system, its radioactivity is below the natural background and no longer measurable. Detailed descriptions of the calculations and measurements performed to establish the levels of induced radioactivity in the inspected bags are provided elsewhere[10,11]. In all the examples, worst case scenarios were assumed. As an added precaution, every bag's radioactivity level is monitored at the exit from the system and whenever it exceeds the background that bag is shunted aside by the system's diverter and the operator is warned. The bag's radioactivity level is then manually checked and only after it has been verified to be below the regulation limit for non-radiative shipment (at present 5 μSv/hr) the bag is released for loading on the plane.

A few of the neutron interactions result in radionuclides with somewhat slower decay rates (longer half life) (e.g., gold or sodium with half life values of 2.7 days and 15 hours respectively). Even in these cases the risk is low as can be seen from the following two examples.

Case 1: External irradiation by elements that had undergone TNA inspection. The largest potential radiation source is gold. Because of its relatively long half life nearly all the induced radioactivity in gold will be present when the passenger claims his luggage (assuming that he carries his gold jewelry in his checked luggage). To make things worse, we omit the delay time, and have the passenger access his bag immediately after the TNA scan. If that passenger were to wear a 40 gram (approximately 1.4 ounces) gold medallion continuously for 10 days (24 hours a day), the total effective dose equivalent would be 4×10^{-5} mSv. This is only one eighth of that resulting from the natural potassium content of his average daily food intake.

Case 2: Ingestion of foods carried in bags that had undergone TNA inspection. Table 1 shows the daily intakes of the elements that are the principal contributors to the dose that would be received and the dose estimates for each element under the assumed conditions. The results of Table 1 show that salt is the principal source of radiation exposure from consumption of food that has passed through the TNA. About 90% of the effective dose equivalent of 1.7×10^{-7} mSv would be due to ingestion of sodium and chlorine. This means that although the assumed scenario is unlikely, its equivalent could occur. As a specific example, if a passenger were to consume in one day 2 ounces of salt, approximately 27 grams of sodium, (this excessive amount is the highest daily reported salt consumption encountered in some exotic Japanese diets) right after being inspected by TNA, the radiation dose absorbed would be less then 0.4% of that resulting from naturally occurring potassium in food. In general, however, passengers gain access to their luggage only after the flight has reached its destination, which for most international flights means a delay of many hours before the passenger recovers his luggage.

Another issue concerns the integrity of the contents of bags undergoing TNA scans; in particular foods, electronic and photographic media and

pharmaceuticals. Existing federal guidance and laboratory data both provide assurance that neutron irradiation of luggage as proposed will not cause deleterious effects. The Food and Drug Administration (FDA) has approved neutron irradiation of food using ^{252}Cf sources to determine its moisture content. Such irradiation is permitted for absorbed doses of up to 2 mGy[12]. Examination of luggage is estimated to produce an absorbed dose from neutrons of about 0.01 mGy under normal TNA operating conditions. It is estimated that one bag in 6000 could be exposed for about 45 seconds due to a baggage jam. In that case, the absorbed neutron dose is estimated to be about 0.1 mGy, still well below the FDA dose guideline.

Gamma irradiation of food has been approved for much higher dose levels, $\sim 10^4$ Gy[12]. The gamma ray doses from passage through the TNA are far lower, about 0.02 mGy. This has been determined by integrating dose rates (measured with a survey meter), and by passing a dosimeter through the system in various pieces of baggage.

Passage through the TNA would expose a medicine, lotion, or other item in the suitcase to a flux of 8 x 10^5 neutrons/cm^2 if the item were located at the peak flux. This neutron exposure is comparable to that experienced from cosmic rays in Denver each year (about 1 x 10^6 neutrons/cm^2).

The effect of the system on photographic film is undetectable under normal conditions. This was determined by testing several types of film with single and multiple passes through the system.

3.3 System Malfunction and/or Accidents

The system's built-in radiation shielding is sufficient to ensure that even during a potential system malfunction, the emitted radiation level will not increase. However, system failures (caused by power interruptions or by jamming of the conveyor belt mechanism) can result in the baggage being exposed to neutrons for longer periods of time than under normal operation. The potential effective dose equivalent from wearing gold jewelry for 10 days following its irradiation in a suitcase that was caught in a baggage jam would be about 0.003 mSv but could perhaps be as high as 0.01 mSv. If this occurs for one gold medallion per year, the resulting effective dose equivalent would be 1 x 10^{-5} person-Sv, about 2.5 % of the effective dose. In the event of bags caught in a baggage jam, the relevant luggage items are manually taken out of the system and kept aside until the measured radioactivity level is found to be below the regulation limit for non-radiative shipment before being allowed to be loaded on the plane.

The radiation safety of the TNA in the event of an accident was assessed independently. The U.S. Bureau of Mines built a mock-up of the system and an empty capsule used to contain the radioactive source was exposed inside it to the blast from an explosion of a large amount of high explosives. It remained intact[13]. The potential radiation resulting from an accident followed by a fire was addressed as well[14].

3.4 Source Shipment and Handling

The components of the TNA are shipped individually and are assembled in situ within the airport where the device is to be used. No radiation exposure of workers or members of the public results from either shipment or assembly of the TNA because the radiation source is not in the system during this stage of the operation.

The ^{252}Cf source is shipped separately in a single shielded cask. The source contains 150 micrograms of ^{252}Cf (approximately 80 mCi or 3 x 10^6 Bq). Following the assembly of the TNA, the source is transferred from the cask to the TNA. Radiation exposure of individuals can occur due to transport of the ^{252}Cf source and during the source installation at the airport location. In assessing the effects of source transport, it is assumed that the ^{252}Cf source is shipped by a truck from a manufacturer in Ohio to the various airports. An average travel distance of approximately 1200 highway miles is estimated for assumed airport locations. Because the ^{252}Cf source decays (with a half-life of $\sim$2.64 years), periodic replacement of the source would be necessary. It is estimated that a new source would have to be installed as frequently as once every 18 months. The operational lifetime of the TNA systems is estimated to be 15 years, so a total of 10 source shipments is anticipated per system.

The expected radiation dose rates outside a shipping cask loaded with a 150-microgram source of ^{252}Cf are shown in Figure 5. The dose rates along the cylinder's axis are somewhat higher than those perpendicular to that axis. The cask would be transported in a truck. The nearest point of public

access is likely to be ~3 m and the dose rate would be expected to be less than 0.01 mSv/h at that point.

Radiation doses to the truck drivers, who might spend 24 hours at a distance of 2 m from the cask while transporting a new source from the manufacturer to an airport, are estimated to average about 0.16 mSv per delivery. Assuming two drivers per truck and that the used source is returned to the manufacturer, periodical replacement of the source is expected to result in a collective dose to drivers of 0.0004 person-Sv per TNA system. If the average cask-driver separation is 3 m, then the expected collective dose would be 0.004 person-Sv. The dose to an individual member of the public seems unlikely to exceed 1 mSv, although following the truck at a distance of 5 m from the cask for 5 hours could produce a dose of that magnitude.

The source carrying cask has an interfacing mechanism with the TNA enabling the source to be loaded and retrieved from the system without being exposed to the environment and without having to be touched by human hands. Padlocks prevent any unauthorized access to the source (either in the cask during shipping or in the system during operation). Only appropriately trained system operators, who are specially trained in radiation safety and handling of radioactive materials, have keys to these padlocks.

The radiation dose to operators from relieving a baggage jam is expected to be no more than 0.05 mSv. Experience with TNA indicates that baggage jams are infrequent, and the vast majority of those can be cleared without resorting to entering the cavity; in fact this has not yet occurred in even one case.

Major maintenance of the system, such as to repair a broken conveyer or to replace of the detectors, requires partial disassembly of the TNA. In that event the ^{252}Cf source is retrieved from the system and placed in the shipping and storage cask. Thus, radiation exposure during major maintenance is minimal.

4. CONCLUSIONS

The deployment of TNA systems in airports shows that nuclear based explosives detection systems can be readily integrated into public areas. Potential radiological related effects are minimal, and the measures undertaken to ensure the safe operation of the systems are appropriate.

NOTES & REFERENCES

1. T. Gozani, "Physics of Recent Applications of PGNAA for On-Line Analysis of Bulk Minerals", 5th International Symposium on Capture γ-Ray Spectroscopy and Related Topics, American Inst. of Physics, September 1984.

2. T. Gozani, "Advances in Bulk Elemental Analysis Using Neutron Interactions", Nucl. Geophys., Vol. 2, No. 3, pp. 163-170, 1988.

3. T. Gozani, "Active Nondestructive Assay of Nuclear Materials -- Principles and Applications", U.S. Nuclear Regulatory Commission, NUREG/CR-0602, NTIS, Springfield, VA, 1981.

4. P. Shea, T. Gozani and H. Bozorgmanesh, "A TNA explosives-detection system in airline baggage", Nucl. Instr. & Meth. in Physics Research, A229, pp. 444-448, 1990.

5. "Annals of the ICRP", Vol. 21, No. 1-3, p. 71, ICRP Publication 60, Pergamon Press 1991.

6. Loc. cit., par. 191, p. 45.

7. C. G. Jones, "Environmental Assessment of the Thermal Neutron Activation Explosive Detection System for Concourse Use at U.S. Airports", U.S. Nuclear Regulatory Commission, NUREG-1396, section 5.4.2, Office of Nuclear Materials Safety and Safeguards, August 1990.

8. Federal Register, Vol. 54, No. 156, pp. 33636 - 33639/ Aug. 15, 1989.

9. Federal Register, Vol. 55, No. 41, pp. 7390 - 7393/ Mar. 1, 1990.

10. See sections 5.4.3 and 5.4.4 of ref. 7.

11. D.A.Becker, "Quantitative Assessment of Induced Radioactivity in Baggage", Nuclear Methods Group, Center for Analytical Chemistry, National Institute of Standards and Technology, March 1989.

12. Code of Federal Regulations (CFR), Title 21, "Food and Drugs", Part 179.

13. U.S. Bureau of Mines, "Report of Tests on the Survivability of the Neutron Source Capsule of the SAIC Nitrogen Explosive Detection System", Pittsburgh, Pennsylvania Sep. 1988.

14. See section 6.3 of ref. 7.

Table 1 EFFECTIVE DOSE EQUIVALENT FROM DAILY INTAKES OF ELEMENTS ONE HOUR AFTER IRRADIATION DURING PASSAGE THROUGH THE TNA

Element	Mean Daily Intake (g)	Induced Radionuclide	Effective Dose Equivalent (mSv) from 1-day Intake One Hour Delay	No Delay
Sodium	4.4	^{24}Na	1.3×10^{-7}	1.4×10^{-7}
Chlorine	5.2	^{38}Cl	2.3×10^{-8}	7.3×10^{-8}
Potassium	3.3	^{42}K	1.0×10^{-8}	1.1×10^{-8}
Manganese	0.0037	^{56}Mn	3.5×10^{-9}	4.6×10^{-9}
Phosphorus	1.4	^{32}P	2.6×10^{-9}	2.6×10^{-9}
Arsenic	0.001	^{76}As	1.9×10^{-10}	1.9×10^{-11}
Bromine	0.0075	^{80}Br	1.4×10^{-10}	1.5×10^{-9}
		^{80m}Br	1.0×10^{-10}	1.2×10^{-10}
Copper	0.0035	^{64}Cu	7.9×10^{-11}	8.4×10^{-11}
Iodine	0.0002	^{128}I	7.9×10^{-12}	4.2×10^{-11}
Rubidium	0.0022	^{86}Rb	9.0×10^{-13}	1.0×10^{-11}
Cobalt	0.0003	^{60m}Co	5.6×10^{-13}	2.9×10^{-11}
		Total:	1.7×10^{-7}	2.3×10^{-7}

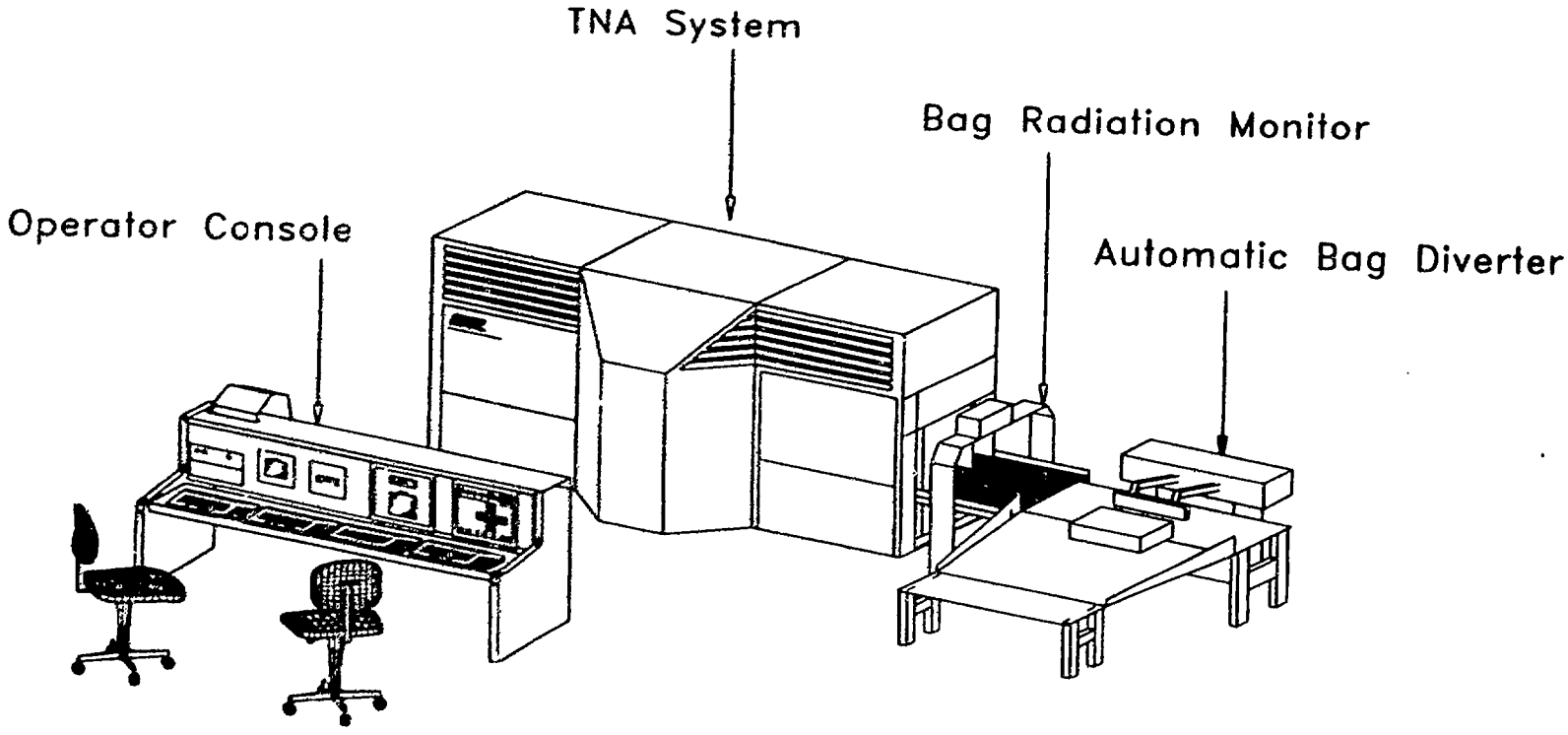


Figure 1. TNA and its Major Components

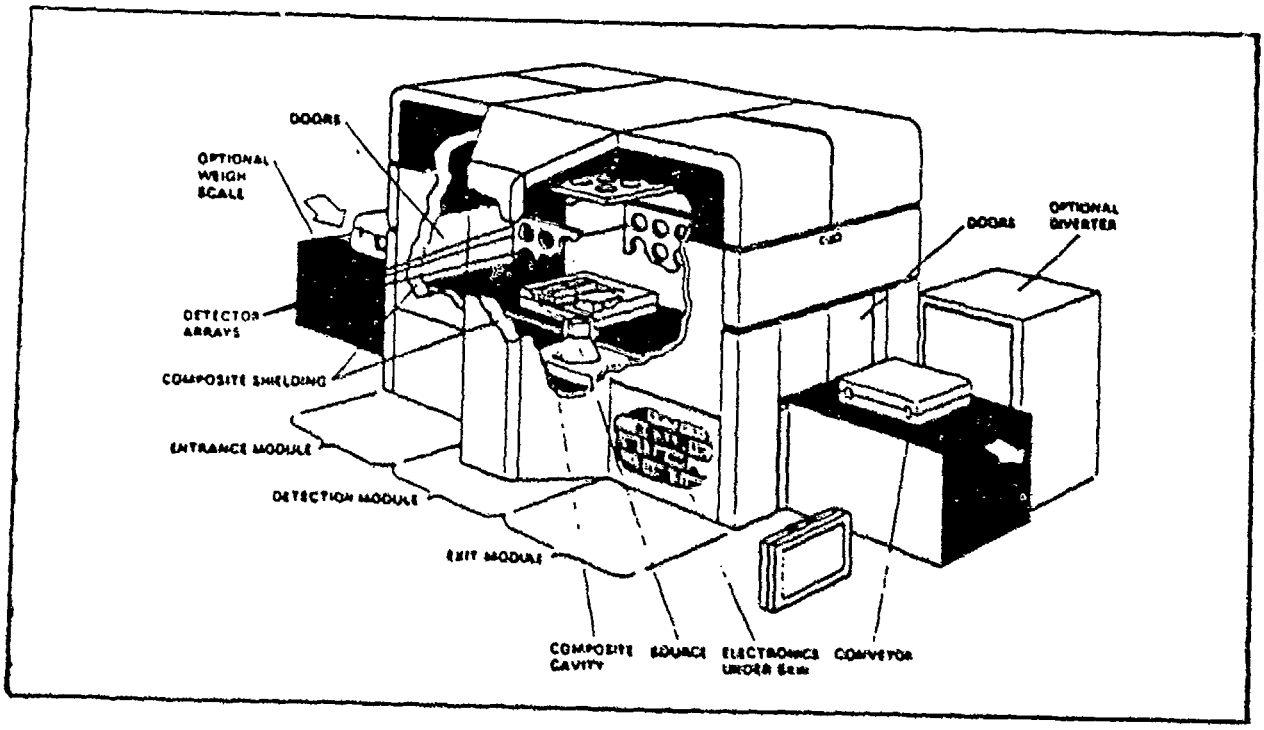


Figure 2. "See-Through" View of the System

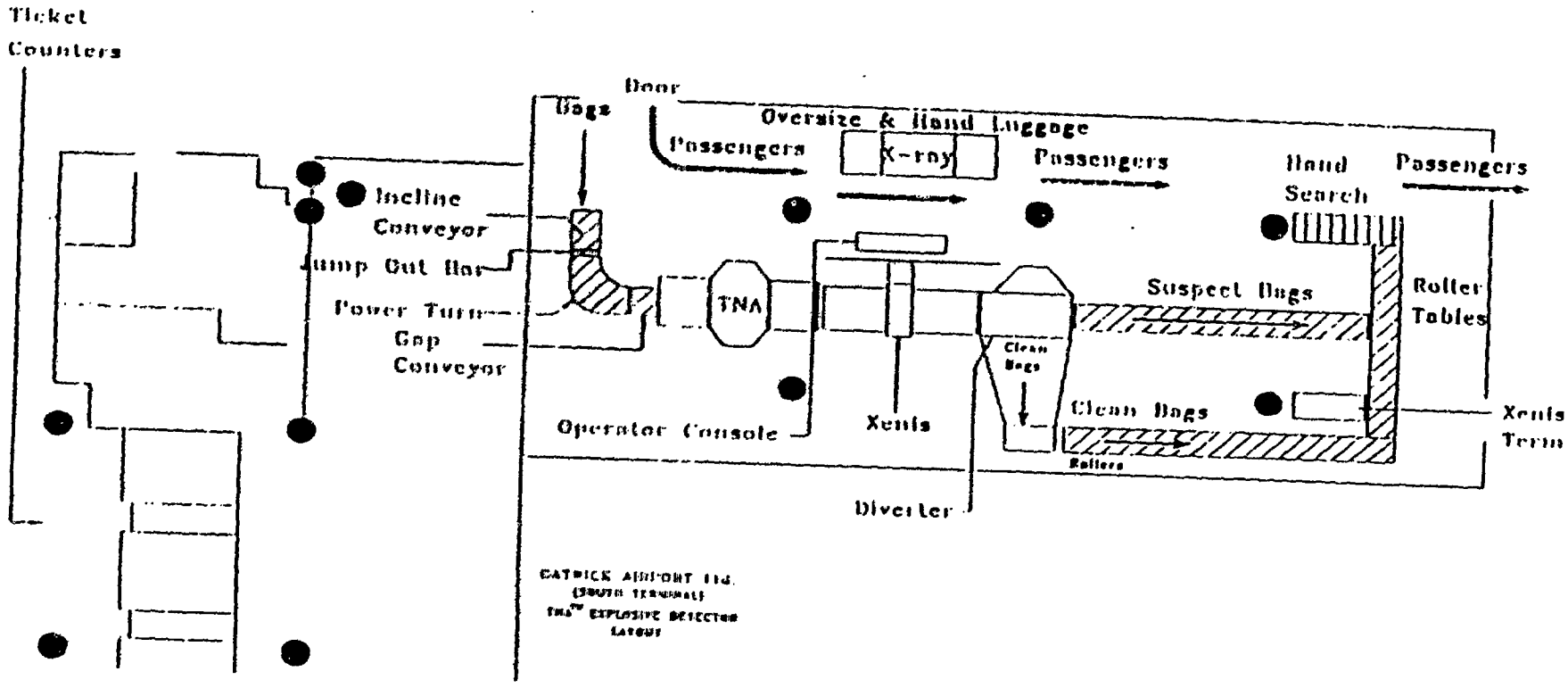
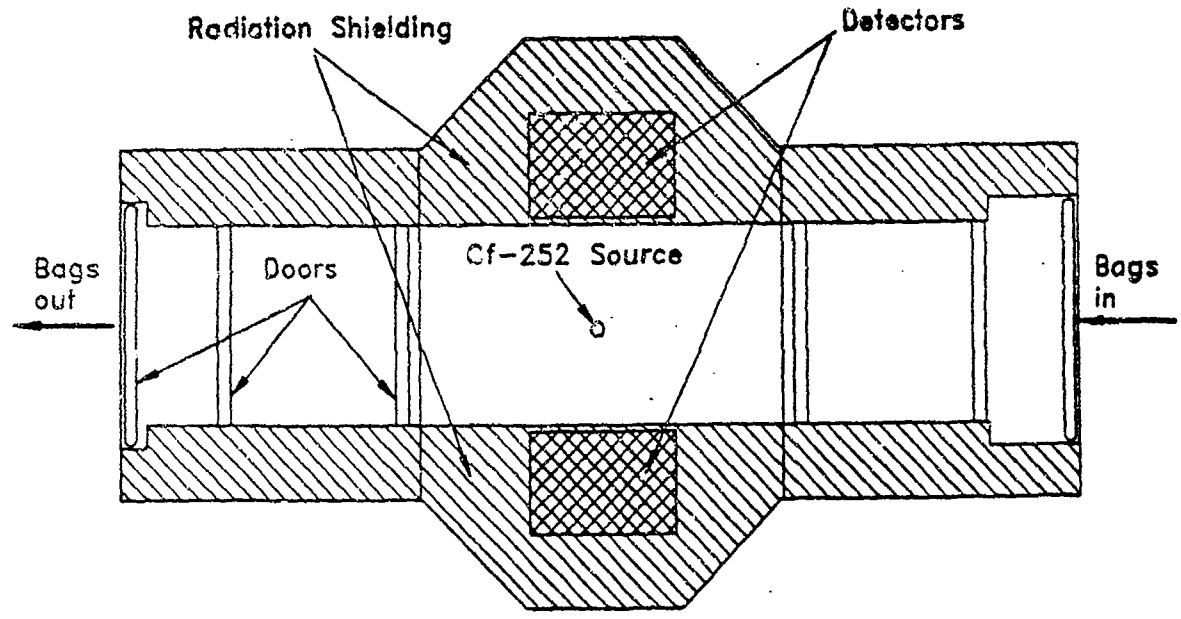
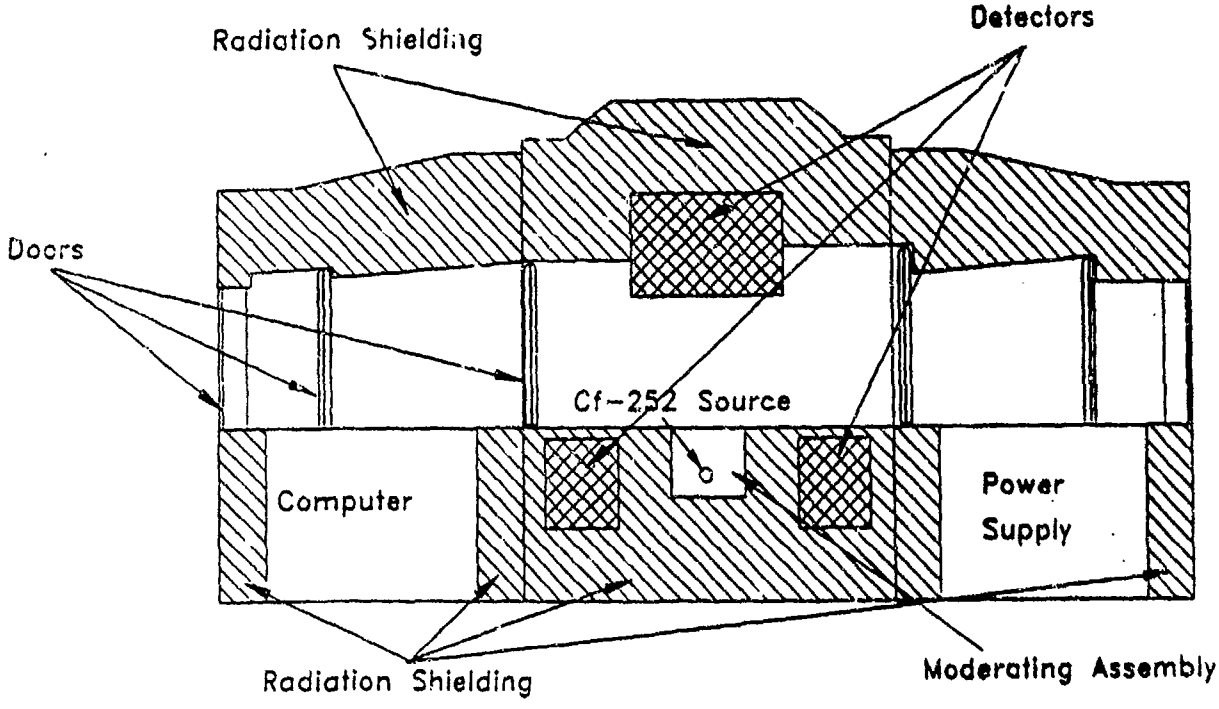


FIGURE 3. LAYOUT OF TNA INSTALLATION AT GATWICK AIRPORT
(Dark circles indicate structural columns)

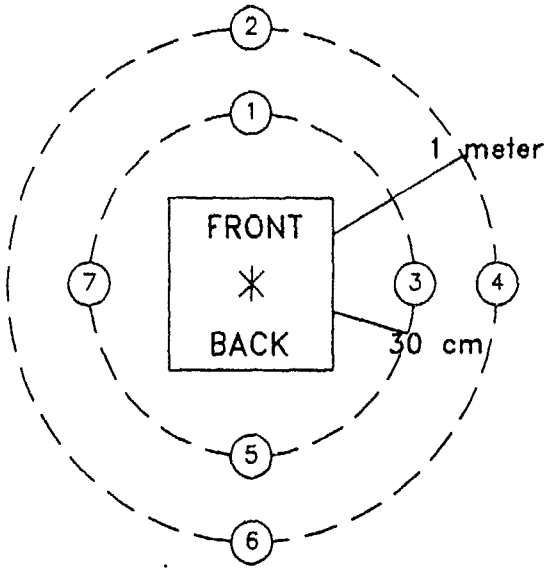


Top View



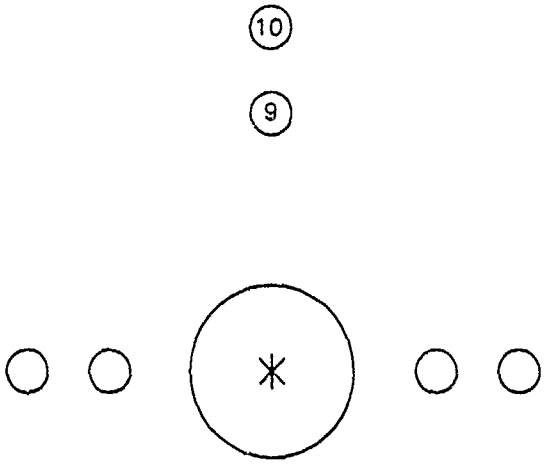
Side View

Figure 4. Top and Side Views of the TNA



TOP VIEW

	Dose Rate Neutrons (mSv/hr)	Gammas (mSv/hr)
1	0.065	0.03
2	0.018	0.009
3	0.08	0.04
4	0.018	0.01
5	0.03	0.02
6	0.006	0.005
7	0.08	0.04
9	0.075	0.04
10	0.011	0.011



END VIEW

Figure 5. TNA Source Shipping Cask Dose Rates

SAIC®
An Employee-Owned Company

RADIOLOGICAL SAFETY REGULATION AND LICENSING OF NUCLEAR-BASED EXPLOSIVE DETECTION SYSTEMS

P. Ryge, Ph.D., and I. M. Bar-Nir, Ph.D.
Science Applications International Corporation (SAIC)
Santa Clara, California

1. INTRODUCTION

The use of nuclear-based interrogation techniques for non-invasive explosive detection has several marked advantages over competing technologies. They employ neutrons or high energy gamma rays as probes. By analysing the products of the interactions of these probes with individual atoms in the inspected object, the presence of specific elements, characteristic of explosive materials, can be determined. These highly penetrating techniques can be made resistant to defeat mechanisms and are well suited to automatic operation -- the two key features required for any practical EDS.

However, the deployment and use of nuclear-based devices, especially in areas accessible to the public such as concourses of airports, raise concerns about potential radiation related hazards. It is necessary to address these issues in the design and manufacturing of such devices. In addition, it is necessary to deal with various regulatory agencies both on local and national levels and meet certain performance standards before these devices are permitted to be installed. The regulations regarding the use of radiation-based devices call for the implementation of certain procedures and safety measures. These have a direct bearing on the costs of operating such devices.

The safety issues and the general regulatory framework are discussed in section 2 below. Section 3 describes the path that has to be undertaken in the U.S. before one is authorized to install and operate a nuclear facility. Issues such as the responsibilities of the users and the manufacturers and the different regulatory bodies one has to deal with in different circumstances are discussed. Section 4 describes the situation in some foreign countries. The experience from the deployment of TNA systems is used as an example.

2. SAFETY AND REGULATION OF NUCLEAR-BASED EDS

Potential radiation safety issues raised by the use of nuclear-based explosive detection systems include the following:

- Radiation emitted by the system in the course of its normal operation and its environmental impact.
- Induced radioactivity in the contents of the inspected items caused by the neutron interactions.
- Potential radiation hazards in the event of a system malfunction (e.g., baggage jams or power failures) or emergencies (e.g. fire or a bomb exploding within the system).
- Shipping and handling of the radioactive source of the system, in particular, source loading and replacement.

Each of these issues must be addressed to the satisfaction of all the relevant authorities before such a system can be put into operation.

The nuclear industry may well be the most regulated in the world. Virtually every country has set up a regulatory framework incorporating various rules, regulations and guidelines that govern nuclear related activities. Before embarking on any such activity, licenses or permits have to be obtained from the relevant regulatory bodies. The procedures vary according to the particular regulations of each specific country. Sometimes they are straightforward albeit entailing considerable paperwork and sometimes delay, while in extreme cases the regulatory pathway effectively precludes the implementation of certain activities. Brief descriptions of the steps that have to be undertaken in various countries in order to install and operate a nuclear facility are provided in [1]. That document

is primarily oriented towards the nuclear power industry. The basic ground rules are similar, however, and it can serve as a good example of what is involved. In addition to the national bodies, there are a number of international bodies that deal with the uses of nuclear energy (e.g., the International Atomic Energy Agency - IAEA, the International Commission on Radiological Protection - ICRP or the World Health Organization - WHO). These bodies sponsor a wide variety of research activities as well as monitor the safety aspects of nuclear related activities. In particular, they issue recommendations and guidelines setting standards and upper limits for radiation exposures. Although these guidelines and recommendations are not legally binding, most countries incorporate them fully or in part into their laws. With few exceptions, when national regulations differ from the international recommendations, they are more stringent.

The basic approach to the use of nuclear technology is that "no practice involving exposures to radiation should be adopted unless it produces sufficient benefit to the exposed individuals or to society to offset the radiation detriment it causes."[2] The dire consequences of any successful bomb attack on an airplane make it of paramount importance to have an effective explosive detection in place. The use of nuclear based systems (e.g., TNA which at present is the only nuclear technique incorporated into a practical and tested EDS) for this purpose was found to satisfy these requirements.[3] Another dominating rule in the regulatory framework is that "the licensee shall use, to the extent practicable, procedures and engineering controls based upon sound radiation protection principles to achieve occupational doses and doses to members of the public that are as low as is reasonably achievable (ALARA)."[4] (See in this connection also [2]).

3. THE REGULATORY PATHWAY -- U.S.

3.1 The Regulatory Establishment

The Nuclear Regulatory Commission (NRC) is the primary regulating authority in the U.S. for all nuclear energy related matters. Its authority is derived from the Atomic Energy Act of 1954 and Atomic Energy Reorganization Act of 1974, which are concerned primarily with nuclear reactors and the nuclear power industry, not of concern here. The NRC regulates and licenses "byproduct material" -- radioactive sources produced in nuclear reactors (such as Cf-252, the neutron source used in TNA). The U.S. is divided into five NRC Regions, each administered by a Region office which issues licenses and conducts inspections. The NRC does not regulate X-ray or other radiation producing equipment such as particle accelerators, nor accelerator produced radioactive sources; these are subject to regulation by the individual states.

The NRC regulations are contained in Title 10 of the Code of Federal Regulations. Part 20 of Title 10, designated 10 CFR 20, is subtitled "Standards for Protection Against Radiation"; it is mostly but not entirely consistent with the recommendations of the ICRP.

The Atomic Energy Acts provide for "Agreement States." By agreement with NRC, these states license and regulate byproduct material themselves. Agreement states must maintain regulatory practices and standards at least as stringent as those of the NRC, and their programs are audited by the NRC. Approximately half of all the states are Agreement States.[1] In all other states, designated Non-Agreement States, the NRC regulates byproduct material. All states maintain radiation control programs which regulate other radiation matters such as accelerator-produced radioactive material.

The Conference of Radiation Control Program Directors, Inc. (CRCPD) is an organization whose members are representatives of radiation control related organizations, such as the NRC, state radiation control agencies, the USFDA, EPA, Department of Energy, military services, World Health Organization, etc. It publishes "Suggested State Regulations for Control of Radiation", used by states in running their radiation control programs. At the request of and with support from FAA, a special CRCPD task force on EDS produced "Regulatory Guidance for State Registration/Licensing of Explosive Detection Systems", covering both radioactive source and electronic neutron generator-based EDS.

The U.S. Food and Drug Administration (FDA) regulates X-ray baggage inspection systems under the regulatory category "cabinet x-ray systems." It also has jurisdiction over foodstuffs in commercial shipments ("interstate commerce") but not in personal baggage. Under FDA regulations, contained in Title 21 of CFR, radiation in food is an additive. In general, food additives are prohibited unless specifically permitted. Irradiation of foods is

permitted for certain specific applications, such as monitoring the moisture content in grains using neutrons. Since at present no regulation specifically permits irradiation for explosive detection purposes, it is not permitted currently; if it were deemed desirable, a regulation permitting TNA inspection could be made, since it can easily be shown to pose no health hazard.

3.2 Licensing

To possess and use a device containing a radioactive source, the user must obtain a radioactive materials license from the NRC or Agreement State, depending on the user's location. For a commercially distributed device such as SAIC's TNA, this is fairly straightforward because most of the burden falls on the manufacturer. The manufacturer is licensed as such, and, prior to commercial sale, the device must undergo a safety evaluation and be registered by the NRC or Agreement State (where the manufacturer is located). In addition, the source used by the device manufacturer is a "sealed source" sold by a licensed source manufacturer, in a sealed capsule which has undergone a separate safety evaluation and registration, according to a stringent quality control and test process.

For safety evaluation, the device manufacturer submits information such as source identification and quantity, description of the device and its safety features, measured radiation levels, prototype testing, the conditions for normal use, operating and emergency procedures, radiation warning posting and labeling, limitations and other conditions of use, and operator qualifications and training. The evaluation process results in issuance of a "device sheet" which is listed under the manufacturer's model number in the Registry of Sealed Sources and Devices. The Registry is issued to all Agreement States and NRC Region offices, administered by the NRC Washington headquarters office.

This evaluation process is typical of what is normally done for radiation-based industrial devices. For SAIC's TNA, there was an additional requirement. Because of the potential exposure of millions of members of the public, an Environmental Assessment was required to be performed. This process is required by the National Environmental Policy Act of 1963, and the implementing regulations for byproduct material licensing are described in 10 CFR 51. Two separate Environmental Assessments were done, for restricted access baggage handling area and for public concourse areas. These involved the submission to the NRC of extensive reports including:

- Description of use scenarios;
- Estimates of worst case individual radiation doses and collective doses to workers and members of the public;
- Dose pathways included direct radiation from the TNA, beta and gamma radiation from potential activation of baggage, external and internal (ingestion of foods in inspected baggage);
- Doses calculated for normal operation, installation, maintenance, clearing of possible baggage jams, extreme fire vaporizing the source and explosion of baggage within the TNA ;
- Cost/benefit analysis.

The NRC based its assessments on these reports as well as other information and in each case arrived at a Finding of No Significant Impact (FONSI). TNA units, manufactured by SAIC, are now approved for use in airport baggage handling areas and in public concourse areas, [4],[7].

As discussed, for a U.S. airline, airport or other organization to operate a TNA or other explosive detection system containing a radioactive source, a radioactive material license must be obtained. The applicant fills out a standard form and sends it with a fee to the NRC Region office or Agreement State; the amount of the fee varies with the jurisdiction but is generally in the range $1,000-10,000.

The application asks for the following:

- Organization, location, and contact person;
- Type and amount of radioactive source, and proposed use (e.g. in SAIC Model EDS-3 for inspection of baggage);
- Designation of Responsible Individual, usually called Radiation Safety Officer, and his qualifications. For TNA, a technical degree and a few-day radiation safety course are generally sufficient;
- Training for workers. Can be based on manufacturer-supplied training;

- Facilities and equipment, e.g. access control, nearby personnel and radiation monitoring instruments;

- Radiation safety program. Procedures (usually based on manufacturer's instructions and training), source leak test schedule, source loading, personnel radiation badging, record keeping, etc.

The NRC Region office or Agreement State looks up the device in the Registry of Sealed Sources and Devices and verifies that the proposed use and safety program are appropriate; if so, the license is issued.

The basic responsibility of the licensee is to operate safely and in compliance with the conditions of the license. In particular, this includes the following:

- Ensure that operating personnel are trained in radiation safety and the applicable procedures;

- Radiation badging as required (e.g. for TNA operators, not required for baggage handlers);

- Source leak tests (usually every 6 months); fairly simple procedure, can be done by trained operator or by manufacturer;

- Radiation instrument calibration (usually every 6 months);

- Posting and labeling of radiation warnings and signs;

- Security – control access of unauthorized individuals;

- Report exposure incidents, if any, to NRC or Agreement State;

- Keeping of records of license activity such as operator training, source leak tests, instrument calibrations.

The first generation TNA units are owned and have been deployed by the FAA. Although the FAA lends these units to individual carriers (TWA in JFK, Pan Am in Miami and United Airlines in Dulles), the FAA is the responsible organization and therefore is the licensee. At present, all TNA units are operated by specially trained SAIC personnel under contract with the FAA. This may change if an end user (a carrier or an airport) purchases a unit directly and installs and operates it on its own, though such an organization could also contract with SAIC for operation.

4. THE REGULATORY PATHWAY – OTHER COUNTRIES

It is beyond the scope of the present work to describe the regulatory situation worldwide. We shall present the situation in the UK, where a TNA unit has been in operation at Gatwick airport near London since July of 1990. We shall also include a brief description of the situation in France.

4.1 The United Kingdom

In the UK, the Health and Safety Executive (HSE) is the competent authority for regulating all nuclear or radiologically related activities. It is the primary authority in the issuance of licenses for the installation and operation of nuclear facilities. The HM Nuclear Installations Inspectorate (the Inspectorate) is the arm of HSE that ensures strict adherence to all statutory requirements regarding the safety of the workforce and the general public. Although both the HSE and the Inspectorate are to a large extent independent of any government department, they are ultimately answerable to the Secretary of State for Energy through the Health and Safety Commission. Another body which plays a key role in all nuclear related activities in the UK is the National Radiation Protection Board (NRPB). This is an independent body that acts in an advisory capacity primarily in nuclear safety related matters. It usually performs studies for the HSE to verify claims made in license applications for devices employing radiation.

The Health and Safety at Work Act places responsibility on the employer to operate safely. The enforcement agency is the Health and Safety Executive (HSE). The employer must notify HSE of intent to use radiation and designate a highly qualified Radiation Protection Adviser (RPA) (consultant-type arrangement). In addition, approval for possession of a radioactive source is required from the Department of the Environment. There is no generic device safety evaluation process like that in the U.S.

The regulations and rules that govern the installation, operation and, whenever applicable, eventual modifications of nuclear facilities in the UK, are summarized in "The Ionising Radiations Regulations" of 1985 (IRR 85), and their associated "Approved

Codes of Practice" (ACOP) for the protection of persons against ionizing radiation arising from any work activity, [8],[9].

Having to deal with a single body facilitates matters, and the regulatory procedures in the UK are rather straightforward. As is the case in the US, the user of the device must have his own permit to install and operate the device. It is his responsibility to see to the implementation of all the required safety measures and procedures on site as well as provide the appropriate personnel and necessary training. As regards the TNA, once the NRPB was satisfied (through its own measurements both in the factory and on site after the installation) that the safety of the systems conformed with the UK [radiation safety] standards they were very forthcoming and the whole licensing process could be completed with relative ease. The TNA at Gatwick is run by the Gatwick Airport Authority who is handling all security matters, and to whom the FAA has lent it. Again SAIC was subcontracted to operate the system with its personnel.

4.2 France

In France the regulatory situation is more complex primarily because there is no single body handling all nuclear activities. Rather, there are several authorities, each reporting to a different ministry. When applying for a license to install and operate a specific device, the circumstances determine to whom the application has to be submitted. Again, it is the user who must perform all the necessary activities (e.g., demonstrate the safety of the device, the adequacy of the facility, the implementation of appropriate measures and procedures etc.), and ensure compliance with all the regulatory requirements. The relevant rules and regulations are included in decrees 86-1103 and 88-521,[10],[11].

The Service Central de Protection contre les Rayonnements Ionisants (SCPRI) handles installations that employ electronic generators that produce ionizing radiation. The Commission Interministerielle des Radioéléments Artificiéls (CIREA) is the relevant authority for installations that use radioactive materials. When the operation of a facility might result in the exposure of foodstuffs to ionizing radiation, the ministry of agriculture and the office of the prime minister (through a special unit responsible for maintaining the integrity of foods) have a say as well. The Institut de Protection et de Sûreté Nucléaire (IPSN) which is an arm of the French atomic energy commission, has a role similar to that of the NRPB in the UK (i.e., it is usually called to perform studies and verify claims made by license applicants).

REFERENCES

1."Licensing Systems and Inspection of Nuclear Installations", Nuclear Atomic Energy Organization for Economic Co-Operation and Development (OECD), Paris, 1986.

2. "Annals of the ICRP", Vol. 21, No. 1-3, ICRP Publication 60, p. 71, Pergamon Press, 1991.

3. Federal Register/ Vol. 54, No. 156, pp. 33636 - 33639/ Aug. 15, 1989.

4. Federal Register/ Vol. 56, No. 98, p. 23396/ May 21, 1991.

5. "Applicant's Environmental Report: Use of Thermal Neutron Based Explosive Detection System for Checked Baggage Inspection in Airport Lobby Areas", NRC Control Number 111217, SAIC Report, December 1989.

6. "Quantitative Assessment of Induced Radioactivity in Baggage", D.A. Becker, Nuclear Methods Group, Center for Analytical Chemistry, National Institute of Standards and Technology, March 1989.

7. Federal Register/ Vol. 55, No. 41, pp. 7390 - 7393/ March 1, 1990.

8. "The protection of persons against ionising radiation arising from any work activity", The Ionising Radiation Regulation 1985, Accepted Code of Practice (ACOP), the Health and Safety Executive, HMSO Publications Centre.

9. "The Ionising Radiations Regulations 1985 No. 1333", HMSO Publications Centre, ISBN 0 11 057333 1.

10. "Décret 1986 no. 86-1103 relatif à la protection des travailleurs contre les dangers des rayonnements ionisants", Journal Officiel de la République Française, 12/10/1986 (modifié par le décret no. 88-652 du 6 mai 1988, Journal Officiel de la République Française, 8/5/1988).

11. "Décret 1988 no. 88-521 relatif à la protection du public contre les dangers des rayonnements ionisants", Journal Officiel de la République Française, April, 1988.

NOTE

1. Currently the Agreement States are: AL, AZ, AR, CA, CO, FL, GA, IL, IA, KS, KY, LA, MD, MS, NB, NV, NM, NY, NC, ND, OK, UT, RI, SC, TN, TX, and WA.

EXPERIENCE WITH EXPLOSIVE DETECTION SYSTEMS IN AIRPORTS

I. M. Bar-Nir, Ph.D., R. L. Cole, and D. Sumi
Science Applications International Corporation (SAIC)
Santa Clara, California

1. INTRODUCTION

Starting in 1985 the major threat to civil aviation shifted from hijacking to bombing (Air India flight from Montreal to London bombed, 329 killed). Although the number of highjacking attempts may be comparable or even higher than the number of bomb attacks, the consequences of bomb attacks in terms of the fatalities incurred are much more severe (see Figure 2 in ref. [1]). In response to the threat, the FAA stepped up its efforts to support the development of anti-terrorist technologies.

SAIC was selected in an open competition to develop and test operational prototypes of an Explosives Detection System (EDS). SAIC's approach was to utilize a known technology, thermal neutron analysis (TNA). Prototypes were developed and installed at San Francisco and Los Angeles International Airports. The testing demonstrated that the concept was feasible (details of the tests and discussion of their methodology can be found in [2]). Based on these tests, performance specifications were set by the FAA defining the types and amounts of explosives to be detected, as well as expected detection rates and alarm rates. Additional performance specifications defined the maximum sizes of baggage items to be inspected, the expected throughput (number of bags to be scanned in a given time unit) and the requirement for automatic decision by the system.

Again, SAIC was asked to complete the development process and prepare systems for testing at key airports. This latest development effort, which began in 1988, was accelerated in early 1989 in response to the Pan Am 103 bombing. Additional bombings that have occurred (e.g., the UTA and the Avianca planes) strongly suggest that more are quite possible. Presidential commission, congressional action, special interest groups, and intense media coverage have served to increase public awareness and concern.

At present, TNA is the only technology operational in airports and available commercially, that satisfies the FAA minimum contractual acceptance test standards: automatic decision making, acceptable rate of throughput, and meets minimum requirements for detection and false alarm rates. TNA systems have been installed and operated in JFK International Airport, Miami International Airport, Dulles International Airport, Gatwick Airport (UK) and in the Middle East during the Hadj period. Additional units will soon be installed in San Francisco International Airport. A detailed description of the TNA and its mode of operation is provided elsewhere ([2]).

This paper describes the integration of a high tech based EDS into the airport environment. In particular, the operational aspects are emphasized. The pros and cons of different installation scenarios (e.g., lobby versus tarmac) are discussed. Section 2 describes the operational experience of the TNA units in the various locations focusing on the installation and summarizing the performance results. Section 3 describes the operational logic of explosive detection in general and its implementation by the TNA. Conclusions are presented in Section 4. In an Appendix we discuss the performance of an EDS in terms of the relationship between its detection capabilities and its alarm rates.

2. OPERATIONAL EXPERIENCE

Upon completion of the primary R&D phase of the program, SAIC proceeded to build working units for the FAA. The next step was to incorporate these units into actual security systems. Once out of the lab, however, practical problems arose: 1 delivery and rigging the units in place; 2 locating the units so as to ensure smooth integration into the airport flow of operations; 3 interfacing with the existing security system and 4 handling suspect bags, to name a few. The introduction of high-technology large pieces of equipment, employing radioactive sources in public areas such as airport lobbies, turned into a bureaucratic challenge. In addition to addressing concerns about radiological safety and ascertaining

compliance with all the safety standards and regulations that govern the use of such devices, it was necessary to coordinate between different bodies each having jurisdiction over a different aspect of the program (e.g., airport management, airline, FAA, state and/or federal licensing authorities, foreign authorities to name a few). Figure 1 is a flow diagram of the process of getting a TNA unit into the field. The numbers in brackets present averages of the actual numbers of days required for each step in the different sites. The whole process, from the initial decision to start of routine operations, could take up to a year.

2.1 Installation

The overall weight of the TNA is approximately 28,000 lbs. The space requirements depend on the precise configuration installed. The TNA unit by itself requires an area of at least 20' x 15'. These requirements are a result of the massive shielding incorporated into the design of TNA to ensure that units can be safely installed and operated in areas accessible to the general public[2]. Space is at a premium in the airport, particularly in the ticketing areas. Moreover, in most airports the floor of the higher levels is usually not designed to withstand that type of weight. Thus, not only pure operational considerations affect the decision on the units placement, rather, additional mundane factors such as space availability, extra costs for site preparation or accessibility play an equally important role. To facilitate shipment, the TNA was designed so that it could be broken into smaller modules. However, the heaviest module weighs more than 10,000 lbs. which calls for careful planning of the access route and the method of transportation of the system to its designated location. None of these problems was insurmountable. Even in Gatwick, where the only direct access to the terminal is through a pedestrian footbridge, a solution was found enabling the whole installation and rigging process to be completed within one night. In the rest of this section we shall describe briefly each of the individual installations.

JFK TWA was the first airline volunteering to cooperate with the FAA in its program for installing EDS to protect civil air transportation. They offered to place a TNA unit at their facility in John F. Kennedy International Airport, New York.

Following the FAA's decision to let TNA screening substitute X-ray inspection of interline luggage, TWA opted to place the system on the tarmac where it could most easily be inserted into the normal flow of bags being transferred into the TWA system from other carriers. However, the TNA was not fully integrated into the overall TWA baggage handling system and luggage had to be routed specially to be fed into the system. As a consequence, the system throughput fluctuated widely since delays in domestic flight arrivals and adverse weather conditions frequently led to the system being bypassed.

Deciding to place the system out of doors meant that it was necessary to provide protection for the system and the operators. Figure 2 shows the layout of the JFK facility[3]. With the extreme weather conditions encountered in JFK, providing air conditioning and heating was mandatory. This was accomplished by getting a pre-fabricated building in place. However, after having the building in place and installing the system it turned out that the building which had been delivered from outside the state, did not meet the Port Authority and/or New York State building codes. Thus, the interior walls had to be torn down in order to redo the electrical wiring.

Miami In Miami the TNA system operated for a whole year without protective enclosure (it was located in the baggage make up area below concourse "F"). Like JFK, in Miami the TNA screened only interline luggage. In order to demonstrate the TNA capability to perform under adverse environmental conditions, no protective enclosure was built and the system was exposed to the high temperatures and humidity levels encountered in Miami. Apart from providing the necessary power nothing else was required. Unfortunately, the elimination of the need for a protective enclosure did not shorten the installation process. The airline would not allow the radioactive source on its premises until it got assurances from different bodies as to the safety of the device. On one day there were no less than 5 different representatives from federal, state, local and airport authorities examining the system with no problems cited. Additional issues were raised by the airlines that concerned liabilities and indemnification which led to further delays. The TNA ended up stored in a trailer in the FAA regional facility for three months before installation could start. The airline also insisted on having all personnel that might come in contact with the system undergo training in the basics of the system operation and emergency procedure. This amounted to about 700 employees,

and obviously took some time for sufficient classes to be held.

Gatwick, Dulles The next two units were installed in Gatwick Airport (UK) and Dulles International Airport (Washington, D.C.). Both are located on the concourse and do not need a special structure to protect the system. In both locations minor structural modifications were necessary to accommodate the system's weight (this was accomplished by providing a load spreading platform below the system). Partitions were built around the units, to limit access by the general public. In Gatwick, as mentioned above, the direct access route into the terminal was precluded by the system's weight, and a special crane was used to hoist the heavy modules of the system into the terminal through a window.

Gatwick was the first foreign installation and issues pertaining to sovereignty came up. The radiological safety of the device was checked and verified independently by the British authorities. Also, instead of the FAA lending the use of the machine to a specific carrier, the Gatwick agreement is between the FAA and the British Airport Authority (BAA). Since the UK Department of Transport (DTP) directs its airports with regards to aviation security requirements, they had to be consulted throughout the process and approved the bag screening procedures.

Dulles was the first domestic installation inside a main terminal not located on the ground level. Most of the installation time had to do with meeting the airport management requirements that the final system outside appearance blend into the terminal overall design. This was accomplished by having the system painted "Dulles gray", adding a power turn conveyor to feed the system and providing aesthetic covers for the various accessories (e.g., operator consoles, monitors, etc.) Liability and indemnification issues were raised here as well but with experience from previous installations, they did not result in significant delay.

One TNA unit was leased to the government of a Middle East country. It was used to screen luggage during the Hadj period in 1990 (June through August). It was again a lobby installation not requiring any special site preparations whatsoever apart from providing power. Since a major concern in that country was the smuggling of explosives into the country, the TNA was installed so that it could cover arriving flights as well as departures.

The two years of operating the TNA have shown that each installation is unique with its own problems. The program covered a diversity of environments, and demonstrated that in spite of large differences between specific scenarios (particularly between the requirements of lobby and tarmac installations) TNA systems could be adapted to fit into all environments with minor modifications. The suitability of the technology for use in a wide variety of operational scenarios was established.

2.2 Performance Results

There was concern expressed both by the airports and the airlines that the speed of the TNA would not be adequate and passenger delays or flight delays would result. Such has not been the case. As of October 31, a total of over 585,000 baggage items were inspected by TNA. Frequently, the TNA units were idle, waiting for luggage to be sent to it. The TNA units experienced practically no down time, since all trouble shooting and maintenance could be performed outside working hours. Hours of operation in the different sites were set so as to conform with the local flight schedules. Differences in operational logic between lobby installations and tarmac installations (see Section 3 for a more detailed discussion of this subject) resulted in substantial differences of throughputs at different sites.

The performance results of the systems at the different sites, during the 2 years covered in this report, are presented in Table 1. Differences in the implementation of TNA as well as differences in the approaches to security account for the diversity of the results. As an example, in one of the concourse installations the system was set to detect a moderate threat level (a smaller amount of explosives, see Section 3) at a higher detection rate with little regard to the resulting higher rate of alarms[4]. In addition, every bag that alarmed was opened and hand searched. In December of 1990 the TNA unit in Gatwick was recalibrated. The numbers in brackets reflect the performance of the unit for the period starting at January 1, 1991. No single flight was delayed due to usage of TNA.

Detection rate measurements were performed daily. Explosive simulants were attached to passenger bags at different locations and run through the system. Regulations prohibit the opening of the bags so the simulants were attached only to the outside of the bags. The decision process of the TNA is automatic, without any intervention from the operator, thus the

results are not compromised by the à priori knowledge of the presence of the simulants.

The TNA decision procedure is based on a "fail safe" philosophy, which means that whenever there is the slightest doubt about a given item it is marked as a suspect. Many of the raw TNA alarms are resolved by using a secondary method[5]. This is done automatically by the system (XENIS). Items that are not automatically cleared are dealt with by a security screener basing his/her judgment on the X-ray images together with the TNA additional information (see Section 3). In particular, the TNA generates composite images where the TNA information is imposed on the X-ray images clearly delineating the suspect items. So the security screener knows what to look for and where to look for it. In some cases the security screeners decided to have passengers open their bags and conduct a hand search[6]. Concerns that had been raised about "clogging the airport system" due to high number of alarms which result in having to conduct an "unacceptable" number of manual searches of bags[7] did not materialize. In fact, even where every alarm was manually searched, no delays resulted from the TNA usage.

The concerns about the throughput of the TNA resulted from the assumption that all international bags would have to go through the TNA. This is not the case. In a well designed comprehensive security system, a large part of the baggage load can be dealt with by alternative method(s) and/or various EDS configurations.

3. OPERATIONAL LOGIC

3.1 Detection and Alarm Rates

The performance of an EDS is usually expressed in terms of its detection rate (PD) and its alarm rate (PFA). These two parameters are not independent. The precise mathematical relationship may vary between systems, but the general characteristics are well described by the curves in Figure 3, which depicts the results of a given calibration of the TNA (the Appendix at the end provides a more detailed discussion of these curves). As can be seen, there is a "trade off" between the detection capability and the alarm rate. At high detection rates (e.g., above 90%), any incremental improvement in the detection rate comes at the price of a significant increase in the alarm rate. Several parameters affect the precise PD - PFA relationship (among others: the radioactive source size, the conveyor belt speed, the background distribution which is determined by the baggage contents and may vary seasonally). The most important parameter which affects the PD - PFA relationship, however, is the threat level (or the amount of explosives the system is set to look for[8]). From Figure 3 it can be seen that while an alarm rate of 3% is associated with a detection capability of 90% for a high threat level, one has to accept more than 4 times that value (13%) in order to maintain the same detection rate for a moderate threat level (a significantly smaller amount). At a detection rate of 95% the associated alarm rates are 6% and 25% for full and reduced threats respectively. Thus, when installing an EDS into the airport environment one faces a certain degree of a conflict of interest: a higher level of security (which requires a high detection rate with an associated high alarm rate) may result in a slow down of the flow of routine operations and delay flights. To mitigate this conflict of interest the TNA systems offer the flexibility of a varying set point on the PD - PFA curve. During periods of increased terrorist activity, or in response to intelligence information, one can raise the PD level and pay (temporarily) the price of a higher rate of alarms. This feature was used in Gatwick where the set point was changed on several occasions. Such changes were affected only with special authorization (by the ministry of transport or the home office). It goes without saying that such changes were not publicized.

3.2 Integrating TNA Into the Airport Security System

A most important aspect of an EDS operation is its capability of automatic decision making. A screening system which relies on human interpretation of its results is deficient (see in this connection p. 6 of [5]). In addition to the scope for human error, the large number of items involved will wear out even the best trained operators. TNA reliably clears the majority of inspected items without recourse to human judgment, and reduces the number of items that have to be manually inspected to a manageable size[9]. Any EDS that cannot operate in this manner will be impractical.

The effectiveness of any EDS depends to a large extent on its mode of employment. Differences in the attitudes to security had a large impact on the TNA usage (placement of the units in the lobby or on the tarmac, have all bags undergo inspection or use it on a selected sample only, how to handle the suspect bags, are but few of the issues that have to be

resolved). In both tarmac installations (JFK & Miami), it was intended to have all the interline luggage undergo TNA interrogation. However, operational considerations frequently interfered with this decision. For example, when inbound flights landed too close to their corresponding connection departure times, the ramp managers often decided to by pass the TNA inspection in order to avoid delaying the departures (required security standards were still met). In addition, the interline luggage constitutes only a small fraction of the total baggage load which resulted in both units being under utilized.

In the lobby scenario, on the other hand, one had to decide between having all passengers undergo inspection or pick up a sample only. Another decision to be made was whether the inspection should take place before or after check in. Figure 4 shows a schematic layout of the Gatwick TNA installation where the passengers check in before the TNA inspection. Only a selected sample of the passenger (composed approximately of 20% chosen according to a profile system and 10% picked at random), are sent to the TNA. The flow of passengers and luggage is indicated by arrows on the figure.

Another difference in the implementation of TNA stems from a basic difference between the US and the UK. Whereas in the US the responsibility for the implementation of security lies with the individual airlines, in the UK it is airport authorities together with the relevant ministries (e.g., the home office and the ministry of transport) that handle security matters. Thus, the TNA units installed in the US were allocated by the FAA to individual airlines (TWA in New York, Pan Am in Miami and United Airlines in Dulles). In the UK on the other hand, the TNA unit is operated by the Gatwick Airport Authority, and serves all US and international carriers flying to the US[10]. A similar approach will now be attempted in the new installations underway in San Francisco, where the TNA will be run by the airport for the benefit of all carriers using that facility. This mode of operation is likely to ensure higher system utilization.

3.3 Handling of Suspect Bags

The central issue in each of the scenarios described above is the handling of alarms. Obviously, there is a limit to what can be done by a machine and there is always a point at which the responsibility must pass to a human. As mentioned earlier, in Gatwick the approach was to have every alarm hand searched. At other sites it was left to a security screener to exercise judgment as to whether to clear a suspect bag or whether to conduct a hand search. In a lobby scenario, passengers are readily available and having them open their bags involves little inconvenience. In a tarmac scenario, on the other hand, getting a passenger to open his bag can be more complicated[11]. The reactions of passengers that were called, was positive. In most cases, the called passengers expressed their appreciation of this security measure.

In most European countries where methods of security are different, stopping and hand searching up to 40% of the passengers is quite common. Thus, having these 40% undergo TNA interrogation and hand searching only 35% of these (14% of the original total), presents a great improvement in terms of manpower and time requirements.

4. CONCLUSIONS

The experience gathered thus far from the TNA deployment clearly demonstrates that high tech based EDS can function effectively in a real airport environment without causing disruptions. Even the added complications emanating from the use of radioactive materials in the public domain did not affect the implementation. A lot depends on the actual method of implementation, and each of the scenarios described has its pros and cons. In particular, an additional benefit of the lobby scenario is the deterrent effect due to its very presence. The main argument raised against lobby installations is the scarcity of space.

As a last word of caution, one should bear in mind that any technology, TNA included, is only a tool. Like any tool, its usefulness and effectiveness are directly related to the way it is used. Judicious use of TNA as a part of a comprehensive security system based on a blend of a variety of independent methods, each compensating for the other's weaknesses, is probably the most effective way of achieving the goal of fool-proof security. A key feature that makes TNA an ideal candidate for such a system is its automated mode of operation (with no reliance on humans). This minimizes the likelihood for human error and, in view of the huge amounts of items to be inspected, turns an unmanageable problem into one that can be reasonably handled. In major airports, where the international traffic load is high (e.g., JFK, Heathrow or Miami) an EDS that

does not possess the capability of fully automatic decision making will be of limited use, regardless of its performance level. Rural airports, on the other hand, where the total number of international passengers is small, can cope well with security by manual methods, and are not likely to require automatic systems.

REFERENCES

1. "Aviation Security Remains a Top Priority", International Civil Aviation Organization (ICAO) Journal, July 1991, pp.45-46.

2. P. Shea, T. Gozani and H. Bozorgmanesh, "A TNA explosives-detection system in airline baggage", Nucl. Instr. & Meth. in Physics Research, A229, pp. 444-448, 1990.

3. Federal Register/ Vol. 54, No. 156, p. 33636/ Aug. 15, 1989.

4. Federal Register, March 1, 1990, p. 7390.

5. F.G. McGuire, "X-ray Technology, Marketing and Security", Security Intelligence Report (SIR), Vol. 6 No. 8, 1991, Published by Interests Ltd., Silver Springs, MD.

NOTES

1. Under "operational logic" we cover different facets of the TNA operation. Among others these include the following:
   - System placement (tarmac versus lobby)
   - Passengers selection process
   - Baggage processing
   - Handling of suspect bags
2. Extensive radiation safety evaluation of TNA both by the health authorities of the State of California, where the systems are manufactured, and by the Nuclear Regulatory Commission (NRC) ascertained the safety of TNA (see refs. [3],[4]).
3. Note that the JFK system, like all the EDS units ordered by the FAA, is augmented by an add on X-ray unit. The X-ray part, designed to help in resolving ambiguous cases, does not constitute an integral part of the basic TNA configuration. The overall area required by this system therefore, is significantly larger than that of a basic TNA.
4. The trade-off between detection and alarm rates has processing rate implications. Alarms must be examined and resolved. The resolution of alarms can be labour intensive (manual searches) or technology intensive (X-ray techniques involving sophisticated image processing). Europeans typically opt for manual techniques, whereas technology solutions are preferred in the USA. Costs, resulting disruption to passenger flow, and, of course, system efficacy all must be considered.
5. Early in the program it became apparent that a single technology based EDS would not suffice to cope with the threat. Rather, it was established that a comprehensive security system, employing a multi-technology based EDS as well as additional methods would be a better approach. TNA, although ideally suited to be at the center of such a system, cannot provide the ultimate answer by itself.
6. When time permitted, bags that had triggered the TNA alarm, were re-run through the system with the specific item that had been marked as suspect by the TNA removed. In all cases the alarm was not prompted during this additional pass. Since this entailed opening the bag, it was always done in the passenger's presence.
7. Every alarm must be regarded as a genuine threat and handled accordingly. Usage of the term "false alarm" which has been very popular in the media, could lead to complacency.
8. It should be stressed that setting the TNA to a given threat level does not mean that it will not be able to detect smaller amounts of explosive. It means that the unit is calibrated to obtain optimal results (in terms

of its PD and PFA) for this threat level. Setting a TNA unit for a different threat value without modifying the calibration at the same time, results in a less than optimal performance level.

In lab experiments, TNA successfully detected amounts of explosives less than one tenth of the full threat level as defined by the FAA at the start of the program.

9. It should be noted that by abandoning the "fail safe" approach mentioned earlier, one can reduce significantly the number of alarms. However, the consequences of missing a real threat, no matter how remote its likelihood is, are too severe to permit relaxing this requirement.

10. The following US carriers operate from Gatwick: American Airlines, Continental, Delta, NorthWest, TWA and UsAir. Although at the beginning TNA was used only to scan luggage of passengers of these carriers, this attitude changed in time. At present non-US carriers account for more than half of the bags inspected by the system.

11. Due to potential liability issues, the airlines personnel are reluctant to open passenger bags not in the presence of the owners. Also, in the event of a real bomb which may be booby trapped, it is safer to have the passenger handle his own luggage.

APPENDIX

EDS Performance, PD - PFA Relation

Derivation of PD - PFA curves like the ones shown in Figure 3 for an EDS is a straightforward procedure. The actual calculations though, may be quite involved, particularly when the decision algorithms used cannot be expressed in simple mathematical formulae. The curves of Figure 3 were obtained in the following way. A large number of bags were run through the system and the various features used by the decision algorithm were measured and recorded. The detection and the false alarm rates were then calculated with the threshold for distinguishing "suspect" bags from "clean" ones set at a given value. These calculations were repeated modifying these threshold each time. Each calculation produced one point on the curve. The bags used had been purchased from the "unclaimed bags" stock of different airlines. The bags' contents were left intact and explosive simulants were inserted into some of the bags. The use of real passengers' luggage ensures that the background encountered replicates the one expected in the real world. Different curves are produced by varying the sizes of the simulants used. Although there are differences between different EDS, the general characteristics are common to all systems:

- The alarm rate increases with the detection rate.
- At lower threat levels the alarm rate/detection rate deteriorates.

For a single-feature based EDS (e.g., X-ray devices that measure only the overall density), it is very easy to build a PD - PFA curve. Use of several features makes the calculations more complex, but there is more scope for fine tuning (calibrating) to obtain optimal performance from the system.

Table I

TNA Systems Performance Statistics

Site	Operating Days	Total # of Bags	Alarm Rate
JFK	745	135,000	<15%
Miami	275	68,500	<20%
Gatwick	427	286,000	<40%
Dulles	335	78,500	<10%
Saudi Arabia	35	17,000	<45%

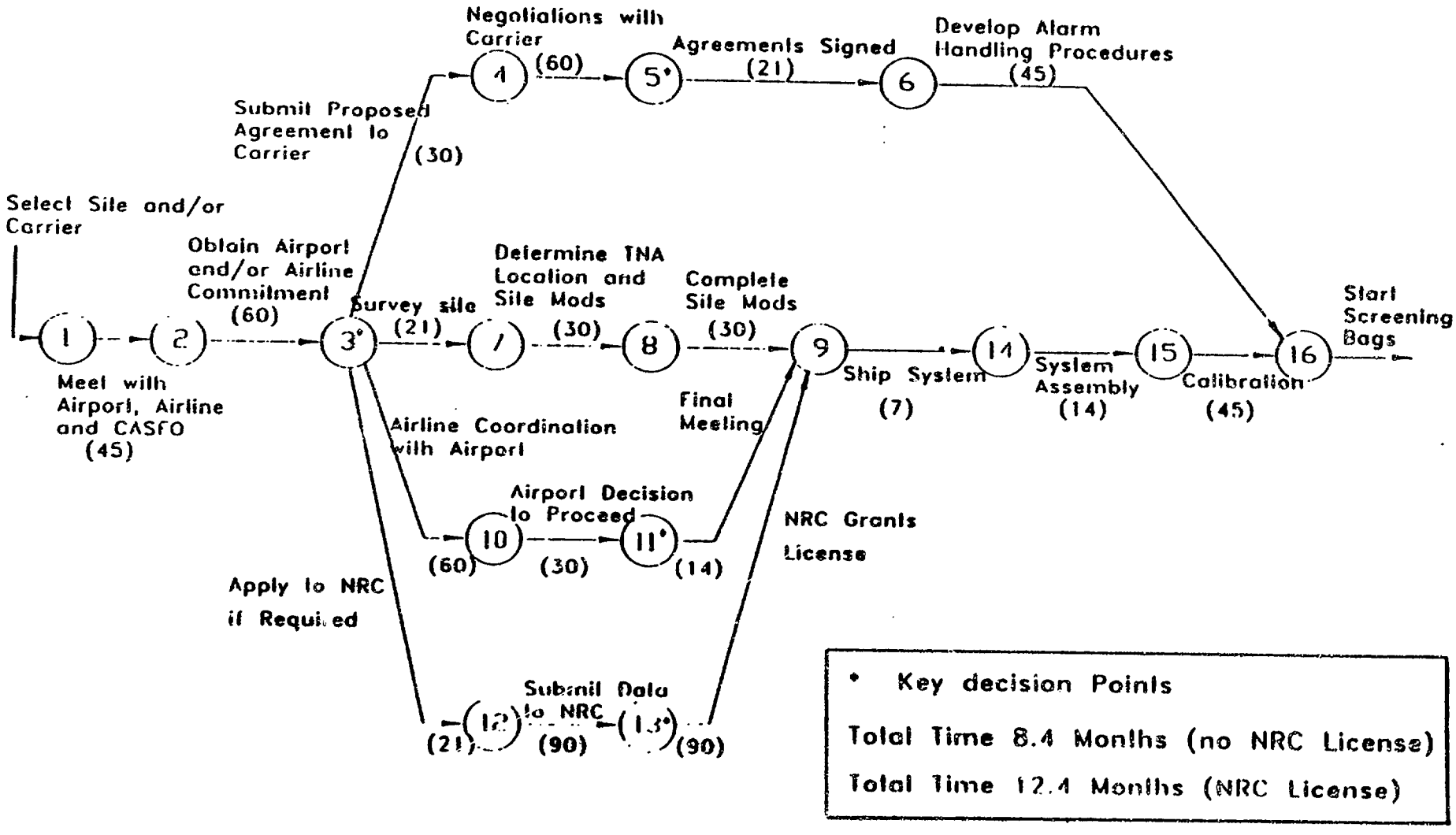


Figure 1. TNA Installation Flow Diagram

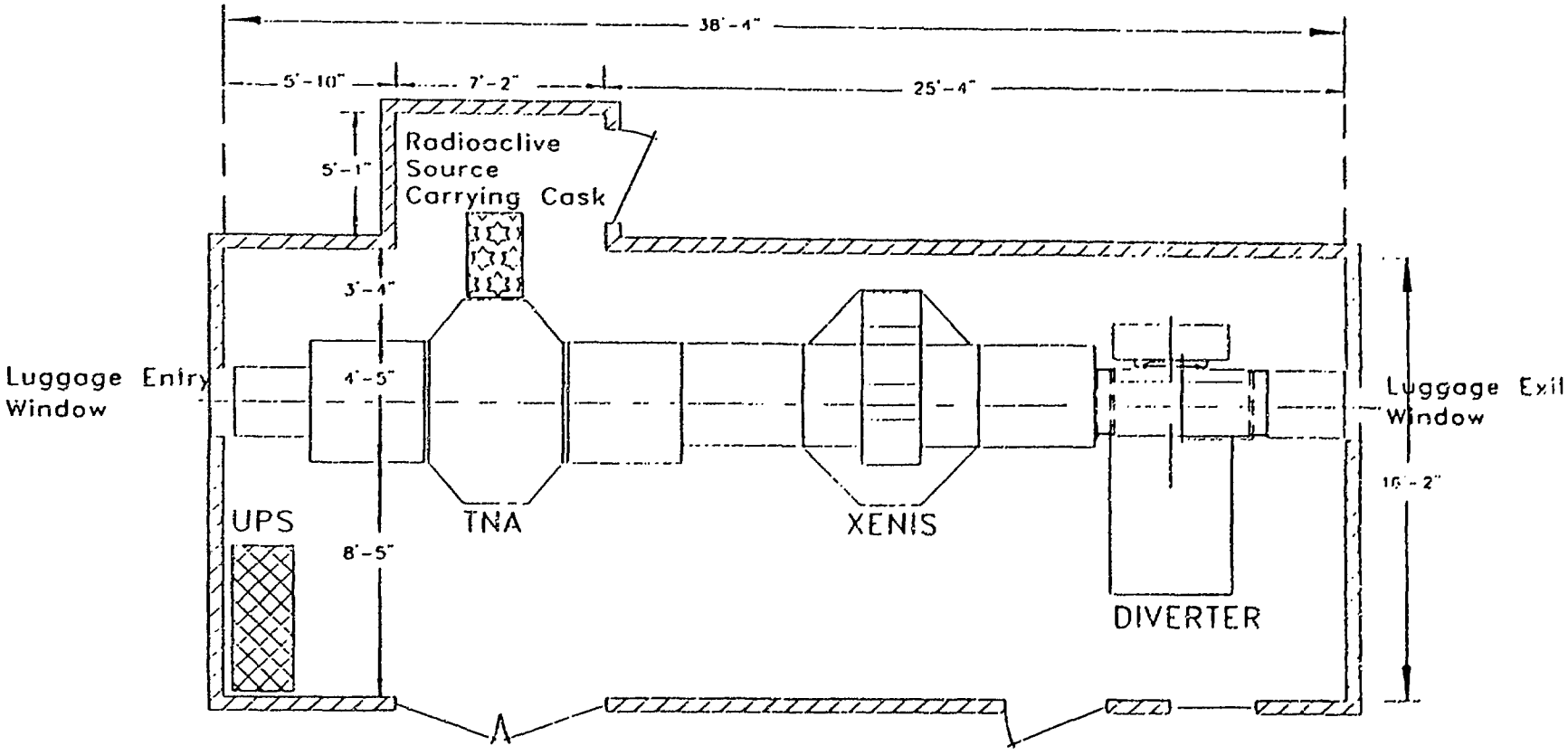


Figure 2. Layout of the TNA Installation at JFK International Airport (next to TWA Terminal "A")

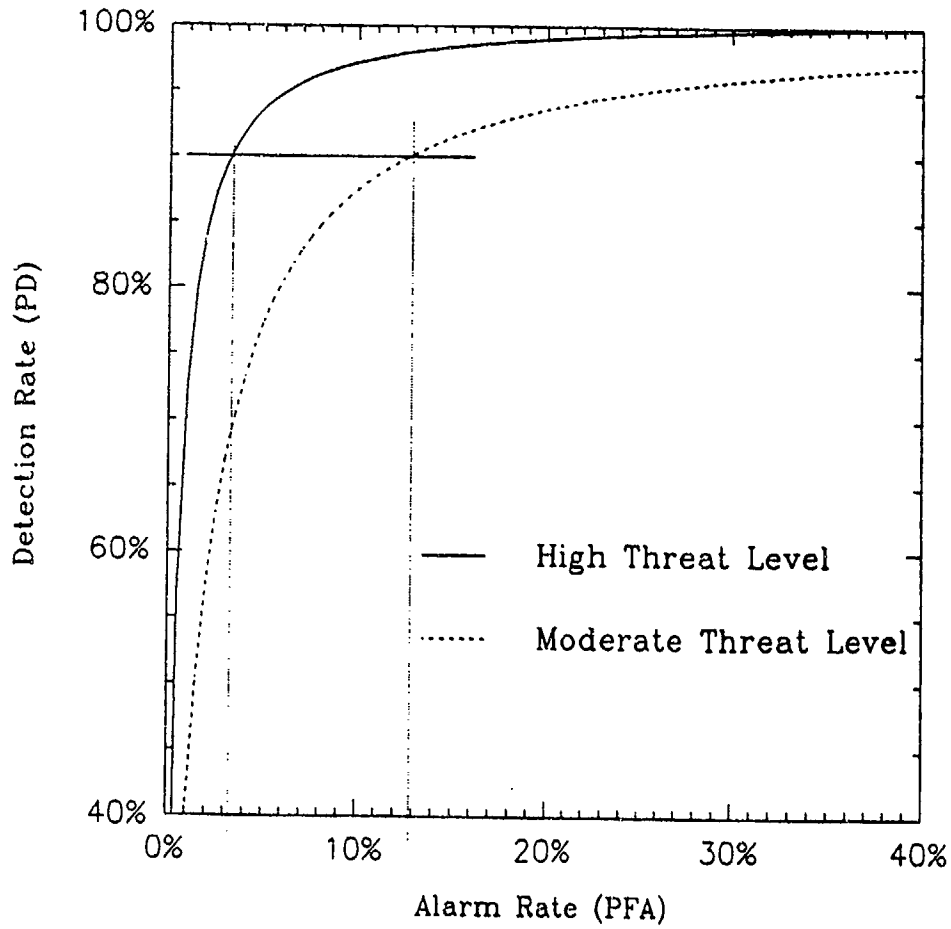


Figure 3. PD - PFA "Trade Off" Curves

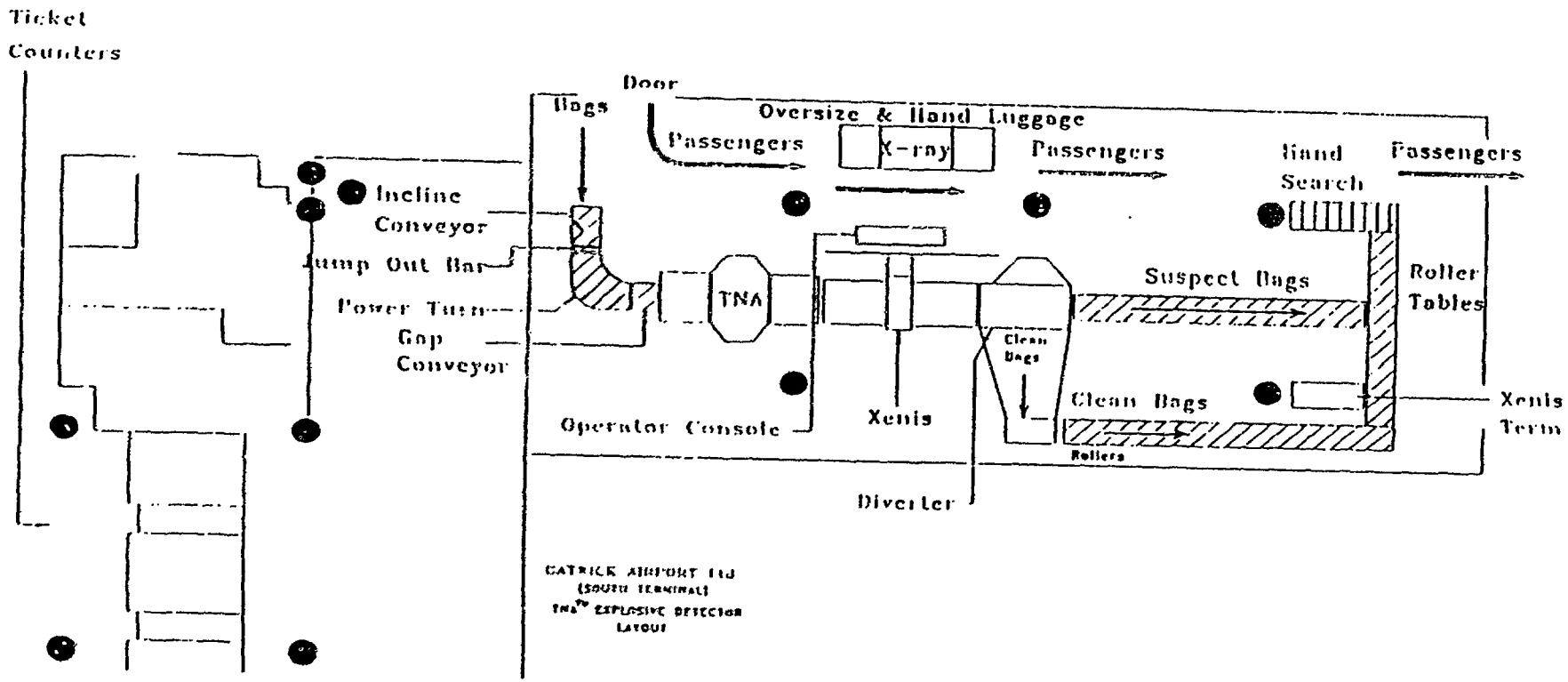


FIGURE 4. LAYOUT OF TNA INSTALLATION AT GATWICK AIRPORT
(Dark circles indicate structural columns)

SAMPLING EXPLOSIVES ON AIRLINE PASSENGERS

Eugene K. Achter, Gabor Miskolczy, and Freeman W. Fraim
Thermedics, Inc.
Woburn, MA 01888

Eugenie Hainsworth
Arthur D. Little, Inc.
Cambridge, MA 02140

John R. Hobbs
U.S. Dept. of Transportation
Cambridge, MA 02142

1. INTRODUCTION

Terrorist bombs have been planted in passenger compartments as well as luggage compartments of airliners. To guard against terrorist bombing attacks by this route, passengers as well as luggage should be screened for explosives. Under contract to the U.S. Department of Transportation, Thermedics has developed SecurScan, a prototype portal system for screening airline passengers for explosives, and has carried out limited airport testing. SecurScan is an integrated system consisting of a personnel sampling portal, a preconcentrator for explosives vapor, particulate, and aerosol, and a fast GC / chemiluminescence module for sensitive and selective detection and analysis of explosives. This paper discusses design considerations for efficient sampling of explosives from human subjects in an airport environment.

For the sampling portal, the essential functional criteria include sampling effectiveness, acceptable human factors, and passenger throughput. General design considerations and their specific implementation in the SecurScan portal system are discussed below.

2. GENERAL DESIGN CONSIDERATIONS

The sampling procedure must be performed on human subjects of varying size, sex, age, and clothing style. Explosive devices may be carried in pockets, or attached to the body and hidden under clothing.

Trace quantities of explosives must be extracted from the body or clothing of the subject and delivered to a chemical analysis system. In principle, this could be done with a hand-held probe. However, by analogy with metal detectors, this approach would be too slow, invasive, and labor-intensive for initial screening applications. Therefore, an automated portal screening system is the preferred approach.

In an air-coupled, automated portal system, the sample is collected without the need for physical contact with the body or clothing of the subject. The sampling process involves two essential steps: extraction of explosives from the subject into a sampling air stream, and transport to a collection device via the air stream.

When an explosive device is hidden underneath a subject's clothing, trace quantities of explosive are transferred from the explosive device to the air space near the device, and to adjacent cloth surfaces. The trace quantities released may be in the form of vapor, particulate, or aerosol. Evaporation is enhanced by temperature and by air movement. As clothing rubs against the explosive device during normal body movement, particulate is released by abrasion and electrostatic effects.

With time and normal body movement, traces of explosive in the form of vapor or particulate accumulate, either in the air space beneath the clothing, or adhering to hair, skin, or clothing. Passive transfer of traces of explosive into the sampling air stream occurs only slowly by diffusion and normal body movement. Active extraction techniques such as infra-red heating and air jet impingement must be used to enhance the rate of release into the air stream, and increase the effectiveness of the overall sampling process.

The sampling air stream receives the explosives released by the extraction process, and transfers this material from the immediate vicinity of the subject to a collection and pre-concentration device.

The extraction process and the sampling air stream must be designed to satisfy human factor and passenger flow requirements. Both processes must accommodate human subject variables such as subject size, type of clothing, and site of concealment of the explosive device. These processes must also be quick, taking only a few seconds, and must be acceptable in terms of human comfort, aesthetics, and safety. The air stream must transfer the sample to the pre-concentrator without major losses due to sticking of sample on duct walls.

3. SECURSCAN SYSTEM

The design approach for the prototype SecurScan portal is discussed in this section. A schematic view of the portal is shown in Figure 1. In operation, the subject stands in portal, and an array of infra-red heaters and air jets stimulates the release of traces of explosive into a sampling air stream. The air stream carries the sample through funnels and ducts to a pre-concentrator.

4. EXTRACTION PROCESS

Active extraction of explosives by infra-red heating and air jet impingement is discussed in this section.

Infra-red heaters are used to raise the temperature of the outer surface of the clothing, thereby increasing the vapor pressure of any explosives that may be present on the outer surface. A 20-degree rise in the surface temperature produces a 32-fold increase in the vapor pressure of PETN.(Dionne et. al., 1986) To minimize the perceptual impact on the subject, the heaters are designed to emit energy in the infra-red region, with little or no output in the visible region of the optical spectrum.

Air jet impingement extracts traces of explosive by a number of mechanisms. As the air jets agitate the clothing, particulate is shaken loose into the sampling air stream. The air jets cause a pumping action of the clothing that pushes air out from beneath the clothing, along with vapor and particulate contained in that air. Air jet impingement strongly enhances evaporation from surfaces of the explosive device, and from traces of explosive adhering to skin, hair, and clothing. A quantitative treatment of evaporative transport of RDX by air jet impingement appears in Fine & Achter, 1991.

5. SAMPLING AIR STREAM

The function of the sampling air stream is to carry traces of explosive from the subject to the preconcentrator. In principle, the air flow direction can be horizontal, vertically upward, or vertically downward. Vertical flow in either direction leads to a longer air flow path from the subject to the pre-concentrator. Upward flow causes the skirts of female subjects to billow. Downward flow can clog the pre-concentrator with excessive debris from shoes. Therefore, the horizontal direction was selected.

The portal is equipped with an array of air collection funnels. A suction blower mounted downstream of the pre-concentrator is used to pull room air past the subject, through the funnels, and through the pre-concentrator. At the flow rate of 380 liters per second, the air in the vicinity of the human subject is completely exchanged in about 2 seconds. The air flow pattern has been optimized so that vapor released near any part of the subject's body - front, back, waist, head, legs, - is swept into the funnels and collected.

The air flow pattern was studied by computer modeling using FLUENT, a general purpose program for fluid flow that solves continuity, momentum, and energy equations (Creare, Inc.). Figures 2 and 3 show computed air velocity contours for a small subject and a large subject, respectively. The air flow pattern is robust on the sides of the subject and along the walls of the enclosure. A stagnation zone at the front of the subject is broken up using the air jet puffers, which are not shown in the figures.

6. HUMAN FACTORS AND INDUSTRIAL DESIGN

The industrial design of the portal was developed in conjunction with Design Continuum, Inc. The objectives were to provide an aesthetic design that is attractive and looks like it belongs in an airport, and to minimize the negative impact of the heaters, puffers, and funnes, and problems associated with a small, confined space. A photograph of the portal is shown in Figure 4.

As the subject approaches the portal, a proximity sensor turns on some of the puffers to give the subject time to become accustomed to the sound of the puffers. When the subject enters the portal, photoelectric sensors measure the subject's height and turn off all puffers above shoulder height, to avoid puffing in the subject's face.

The funnels at the end of the portal may appear threatening. To hide them, the funnels and associated panels are painted black, and a light blue mesh is installed in front of the funnels. The perceptual effect is that the eye is drawn to the light colored mesh, and the black-painted structures behind the mesh are hardly noticed.

As part of the design study, the possibility of incorporating a metal detector was explored. Once the metal detector was considered, a design evolved in which an opaque metal detector arch opens into a transparent section near the back of the portal. The aesthetic effect is a light at the end of the tunnel that beckons and aesthetically draws a person into the portal. In design experiments, when the opaque roof of the metal detector was removed, or the metal detector section was removed entirely, the effect was lost and the portal became neutral rather than inviting.

7. TEST EXPERIENCE

In August and September 1988, laboratory tests at Thermedics demonstrated that the SecurScan system could detect a broad spectrum of explosives hidden under clothing. In October 1988, the SecurScan portal was installed at Boston's Logan Airport, and preliminary field testing was carried out. The purpose of this testing was to operate the equipment in a real-world environment for the first time, to test whether ambient background conditions associated with passengers, fuels, or engine exhaust would cause false alarms or serious maintenance problems, and to assess the willingness of the public to enter the portal.

People walking through the airport concourse were asked to enter the portal on a voluntary basis, and over 2000 tests were performed. The false positive rate for this testing was less than 0.15 %.

Public reaction to the portal was generally favorable. With few exceptions, people went into the portal smiling and came out smiling. There were frequent comments about the heaters. However, most people readily accepted the explanation that the heat helps to detect vapors, and generally found the heat only a minor nuisance.

There were no objections to the force of the puffing, although a number of people commented on the noise of the puffer solenoids - a problem that can be easily corrected in future designs.

People did ask whether the portal was safe, and almost everyone accepted the explanation that "you will feel heat and puffs of air. There are no x-rays or other harmful radiation, and the process is entirely safe."

Aesthetic reactions to the design were positive. People commented that the portal looked very nice and futuristic, and that it looked like it belonged in an airport. Frequent comments were: is that a teleportation booth, or the Orgasmatron from the Woody Allen movie?

After the preliminary field test at Logan Airport, additional research was performed to enhance the system's sensitivity to plastic explosives. The ability to detect plastic explosives hidden under clothing was demonstrated by extensive laboratory testing in 1989 and 1990.

8. CONCLUSIONS

The essential functional criteria for an explosives detection portal for airport use include effective detection of explosives, acceptable human factors, and acceptable throughput of passengers. Based on airport testing and laboratory testing, the prototype SecurScan system meets objectives for detection capability and human factors. Increases in passenger throughput are needed and can be achieved by engineering development.

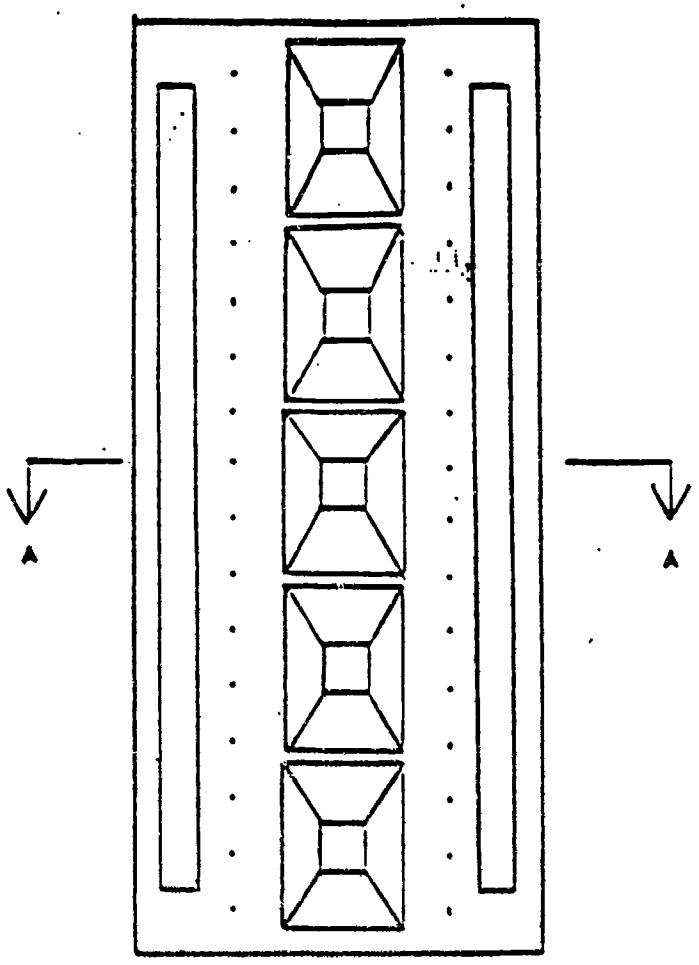
ACKNOWLEDGEMENTS

We would like to thank the Federal Aviation Administration and the U.S. Department of Transportation for their support under contract number DTRS-57-84-C under which most of the work described in this paper was performed.

REFERENCES

1. Dionne, B.C., Rounbehler, D.P.,Achter, E.K., Hobbs, J.R., and Fine, D.H., JOURNAL OF ENERGETIC MATERIALS 4, 1986, pp 447-472.

2. Fine, D.H., and Achter, E.K., in "Access Security Screening : Challenges and Solutions for the 1990's," ASTM Publication STP 1127, in press.



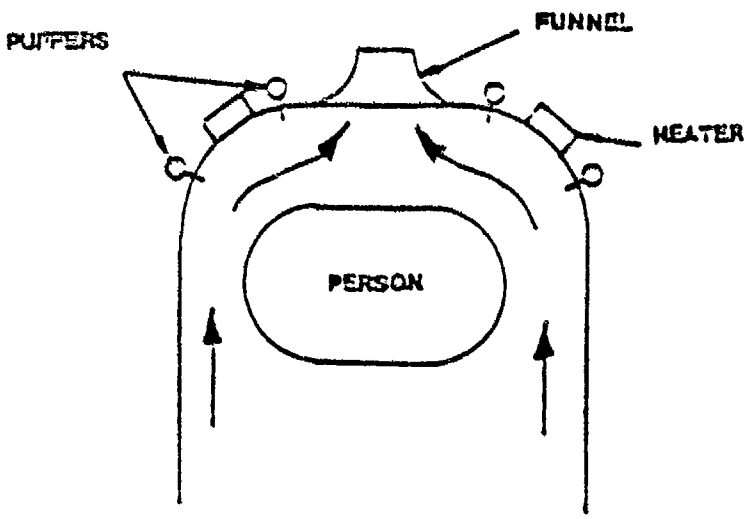


Figure 1 Portal Schematic.

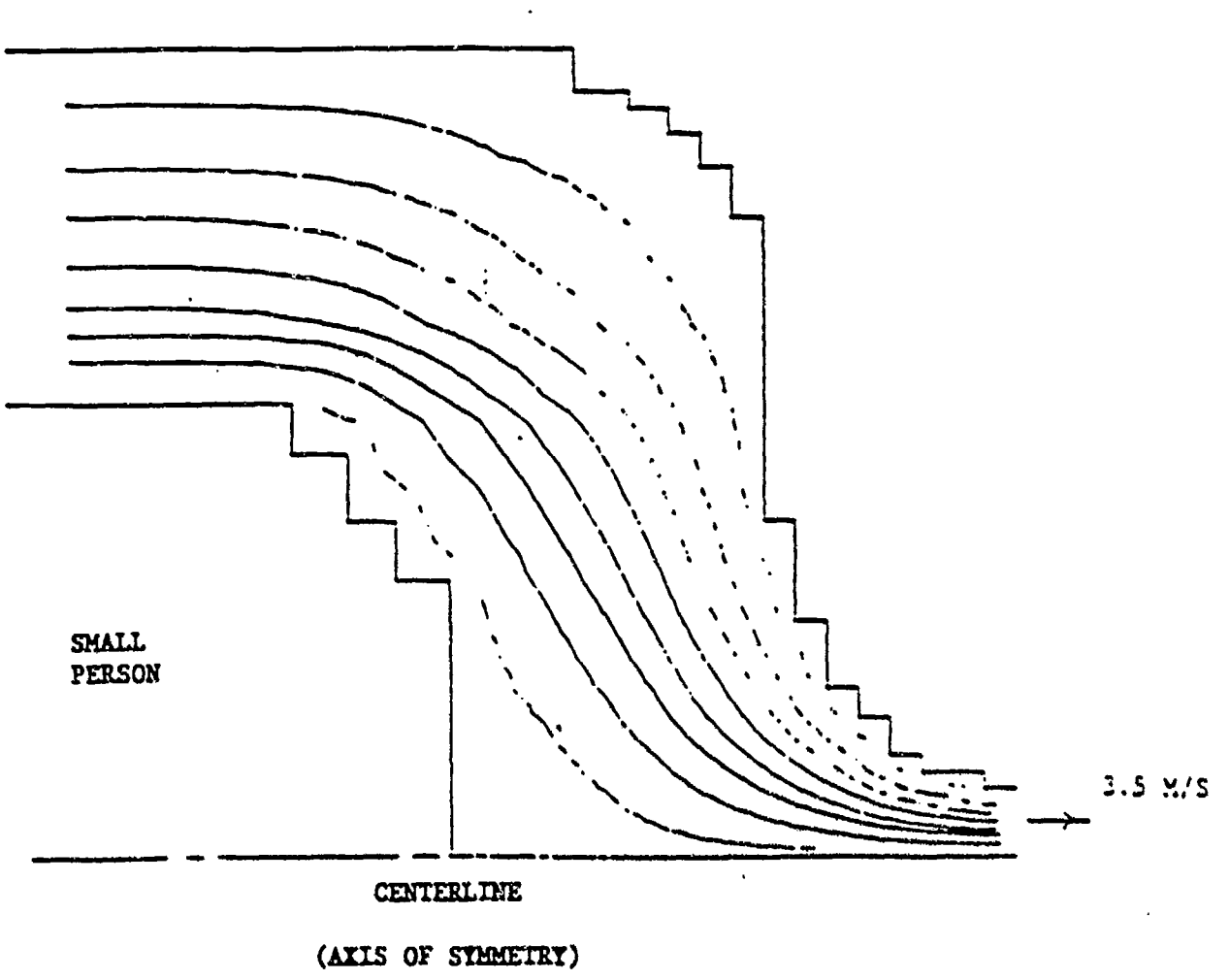


Figure 2 Computer Model of Flow in Portal showing computed air velocity contours for a small subject.

HORIZONAL SLICE: 2D MODEL

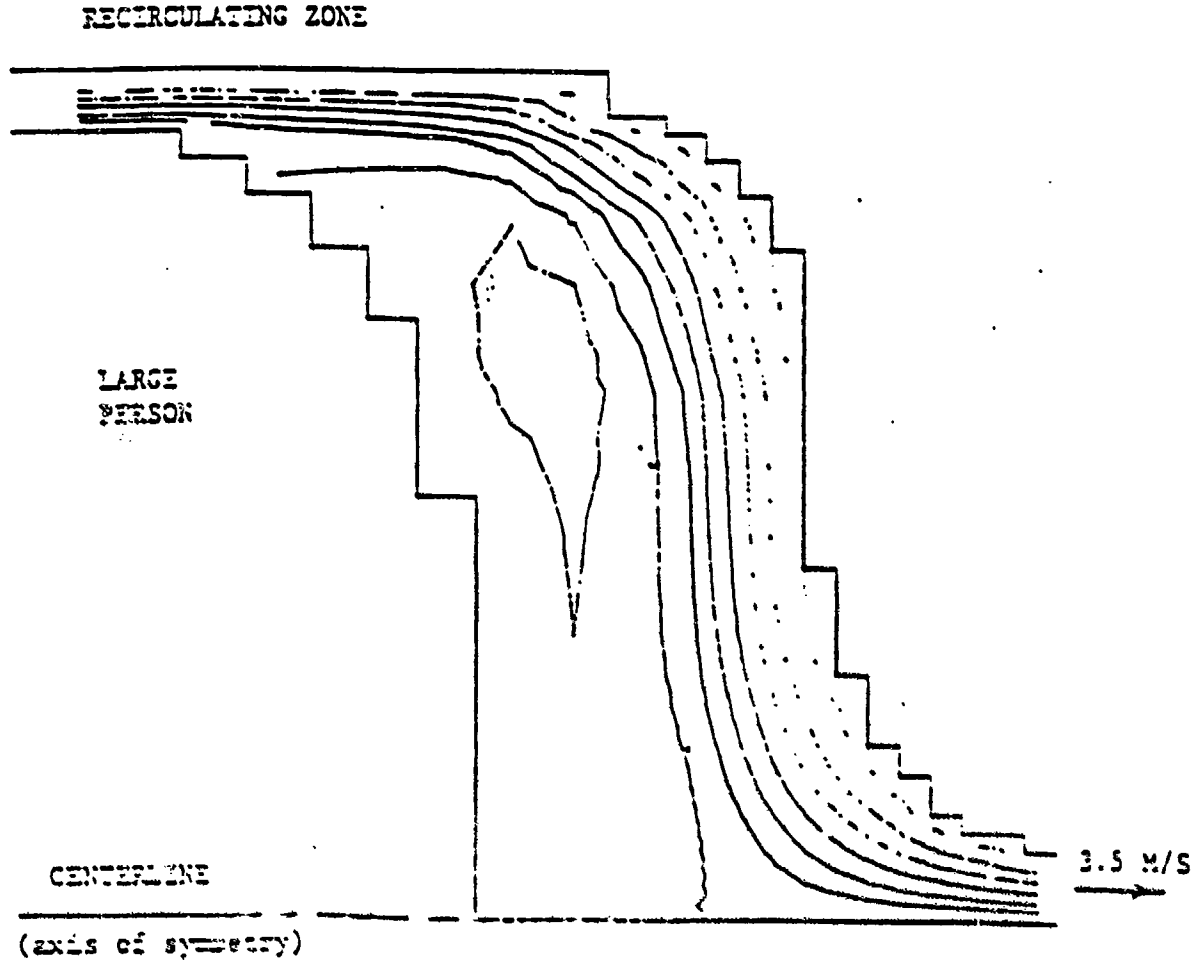


Figure 3 Computer Model of Flow in Portal showing computer air velocity contours for a large subject.

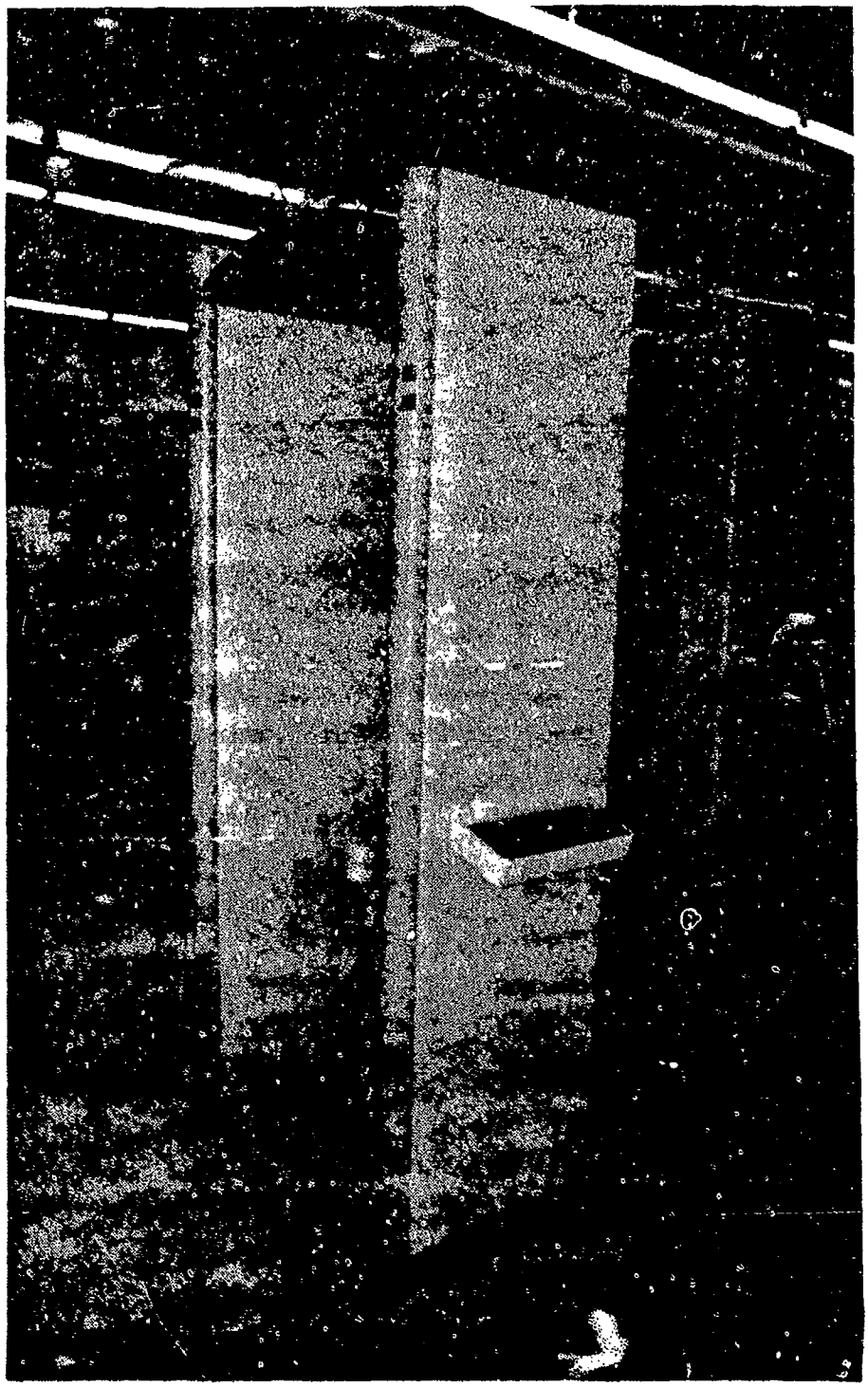


Figure 4 Portal Design

ELECTROMAGNETIC TECHNIQUES

EXPLOSIVES DETECTION BY PURE ^{14}N NQR

A. N. Garroway and J. B. Miller
Naval Research Laboratory, Chemistry Division, Code 6122,
Washington, DC 20375-5000

M. L. Buess
Sachs Freeman Associates,
Landover, MD 20785

1. INTRODUCTION

The goal of this project is to execute a proof-of-concept nuclear quadrupolar resonance (NQR) detection of explosives and, further, to explore NQR techniques in the laboratory in sufficient detail so that we can provide realistic design criteria for an NQR prototype fieldable at an airport. Experimental guidelines are the detection of sub-kilogram quantities of explosives within 6 seconds with a detection probability of 99% and false alarm rate no greater than 1% for RDX. We concentrate on RDX-based explosives since, on the basis of published data (1), RDX is (one of) the most favorable explosives to detect by NQR. Our primary focus is a detector for checked baggage, but we also consider NQR for potential application to examining people. For a suitcase size detector, the goal is detection of sub-kilogram quantities of explosives, and a lower detectable quantity for people scanning.

2. BACKGROUND

NQR is particularly attractive to the problem of explosives detection as the ^{14}N NQR absorption frequencies from crystalline materials are virtually unique and hence, by looking for the nitrogen signal at, say, the RDX NQR frequency, *only* those nitrogens in RDX will be detected. Hence we do not expect that systematic false alarms, due to 'interferences', will be a problem with an NQR explosives detector. A scan of the 10,000 compounds which have been examined by NQR fails to show any other NQR resonances sufficiently near to RDX. This specificity feature should be contrasted with nuclear-based techniques, for which *all* nitrogen cross-sections are the same, independent of the chemical composition of the material.

NQR would determine the presence of other classes of explosives (e.g., PETN) by examination at the corresponding PETN frequency. In principle, such examination could be performed essentially simultaneously with the RDX inspection, but implementation of such technical details is not a major goal of this project.

'Pure' NQR is the examination of nuclei with nuclear quadrupolar moments in the absence of a static magnetic field. Hence, in addition to its specificity, a second advantage of NQR is that no magnet is required, in contrast to nuclear magnetic resonance (NMR) methods. Hence damage to magnetically recorded material is avoided in NQR; there is no exposure of large, static magnetic fields to personnel; and, without the magnet, the costs are lower than for an NMR system.

There are some inherently unattractive features of NQR which must be addressed for a successful NQR explosives detector. NQR signals are weak and are generally below the level determined by the random electrical noise in the radiofrequency (RF) coil which detects the signal. The signal-to-noise ratio is increased by repeating the experiment as rapidly as possible and adding up the results: the signal-to-noise ratio improves by the square root of the number of repetitions. The maximum rate at which the experiment can be repeated is generally determined by the spin-lattice relaxation time, T_1, typically in the range 10 - 1000 ms for ^{14}N NQR. Hence, under a conventional approach, the maximum signal, corresponding to the equilibrium magnetization, is generated in a time greater or equal to T_1. We employ a particular RF pulse sequence, a strong, off-resonance comb (SORC) of pulses (2-3), which produces an NQR signal about equal to one-half of the equilibrium magnetization but in a time comparable to the spin-spin relaxation time, T_2, on the order of 1-10 ms.

We are also examining the potential of NQR as a people scanner. A very intriguing type of surface coil is the 'meanderline', for which the RF currents

meander back and forth in a regular linear array of conductors (4). We had earlier examined the meanderline RF coil and demonstrated for the first time its use in NQR (3). A particular advantage of the meanderline is that the RF field intensity falls off very rapidly away from the surface of the coil. We anticipate that an NQR people scanner could be constructed with a meanderline which has sufficient sensitivity to see an explosive on the human body, but does not deposit significant RF power into the body.

3. IMPLEMENTATION AND RESULTS

Figure 1 shows part of a full scale proof-of-concept NQR explosives detector for airline baggage that has been designed and built at the Naval Research Laboratory. The 300-liter (10 ft^3) radio frequency (RF) coil sits inside a screened cage. To the left of the cage are the RF amplifier and receiver; the PC-based controller and data system are at the far left. In a commercially built system the electronics can be constructed more compactly than in this laboratory version.

The contents of the suitcase in Figure 1 illustrate some advantages of NQR for explosives detection. No large magnetic field is required, so magnetic media (disks and credit cards) are not corrupted. The presence of ferromagnetic material (steel, electric shavers) does not interfere with the inspection. Electronics can be safely inspected. Due to the high chemical specificity of NQR, other nitrogenous materials, such as nylon, polyurethane or nitrile rubber, do not produce a signal.

We have not yet optimized either the hardware or the details of the NQR pulse sequence. We elected to freeze the implementation of the NQR explosives detector at a reasonable, though not optimal, operating condition and perform a series of benchmark tests to evaluate performance under laboratory conditions. Rather than challenging the system with thousands of different bags, each with different contents, we employed only one arbitrary suitcase geometry: no attempt was made here to look for systematic variations. Table 1 presents these abbreviated test results which indicate the capability of the NRL NQR explosives detector, but do not represent a definitive test of the technology or the system.

In Table 1 the 'Alarm/No Alarm' determination is based on a preset threshold value, set to give a 1% false alarm rate for the empty detector. The detection rate is reported as 99+ %; no missed detections were recorded for these tests. If the noise distribution were indeed strictly Gaussian, a detection rate of 99.99% would be *anticipated* from the signal-to-noise ratio under these conditions.

The performance of the detection system can be better understood by examining the distributions (Figure 2) of the actual intensities of the NQR signals under these four test situations: (a) empty; (b) RDX only; (c) suitcase and contents; (d) suitcase, contents and RDX. For each condition, the 6-second scan was repeated for either 400 or 1000 trials. For clarity, the areas of each distribution are normalized. Also shown is the threshold value, set to produce a 1% false alarm rate for the empty detector. This overall test examines only the random noise contribution to the detector: the variations seen in signal intensity in Fig. 2 reflect primarily the Johnson noise in the coil and preamplifier front end. Some further systematic 'noise' may be anticipated on examination of a large set of differing bags and contents.

In Figure 2 note that the signal profile for the empty detector (a) is substantially the same as for the suitcase and contents (c): there are *no* interfering NQR signals from benign baggage contents. Further note that the signal intensity distribution for RDX alone (b) is comparable to the response for the RDX *with* the suitcase and contents (d): the suitcase and contents do not mask the RDX signal. Finally, the substantial separation between the NQR signal response of the 'clean' and 'dirty' bags provides a very high detection probability and low false alarm rate.

4. SUMMARY

We have shown that nuclear quadrupolar resonance (NQR) provides a means for detecting RDX-based explosives in a full-size suitcase geometry.

Advantages of this approach include:

- Sensitivity: Sub-kilogram quantities of RDX-based explosives can be detected in suitcases.
- Specificity: Because the NQR resonance frequencies are highly specific to chemical structure, signals from other nitrogenous materials do not interfere.
- Throughput: An inspection time of 6 seconds is demonstrated in the laboratory.

- No magnets are required and therefore magnetic media will not be damaged.

- Radiofrequency (RF) field strengths are low, minimizing RF exposure to operators and allowing the possibility of examining people by NQR.

- An alarm is triggered when the NQR signal from a explosive *anywhere* within the NQR RF coil volume exceeds a preset threshold: operator intervention and interpretation are minimal.

- The apparatus is inherently simple, comprising RF electronics and a computer system.

This NQR approach has been demonstrated for RDX-based explosives in a laboratory setting. Extension to detection of other nitrogenous explosives carried in luggage, mail, small cargo or on a person is anticipated. The technology can be extended to detect certain drugs of abuse. As envisioned, such an NQR explosives detector could be useful in airport and other fixed site installations. The apparatus could be made portable.

FOOTNOTES AND REFERENCES

1. A.G. Landers, T.B. Brill, and R.A. Marino, J. *Phys. Chem.* **85**, 2618 (1981).

2. S. M. Klainer, T.B. Hirschfeld, and R.A. Marino, "Fourier, Hadamard, and Hilbert Transforms in Chemistry," pp. 147-182, (Plenum Press, New York, 1982).

3. M. L. Buess, A.N. Garroway, and J.B Miller, *Magn. Reson.* **92**, 348 (1991).

4. H. M. Frost, "Physical Acoustics: Principles and Methods", W.P. Mason and R.N. Thurston, eds., Vol.XIV, pp. 179-270 (Academic Press, 1979).

ACKNOWLEDGEMENTS

This work was supported in part by the Federal Aviation Administration. RDX specimens were kindly provided by the Indian Head Naval Ordnance Station.

TABLE 1

CONDITIONS

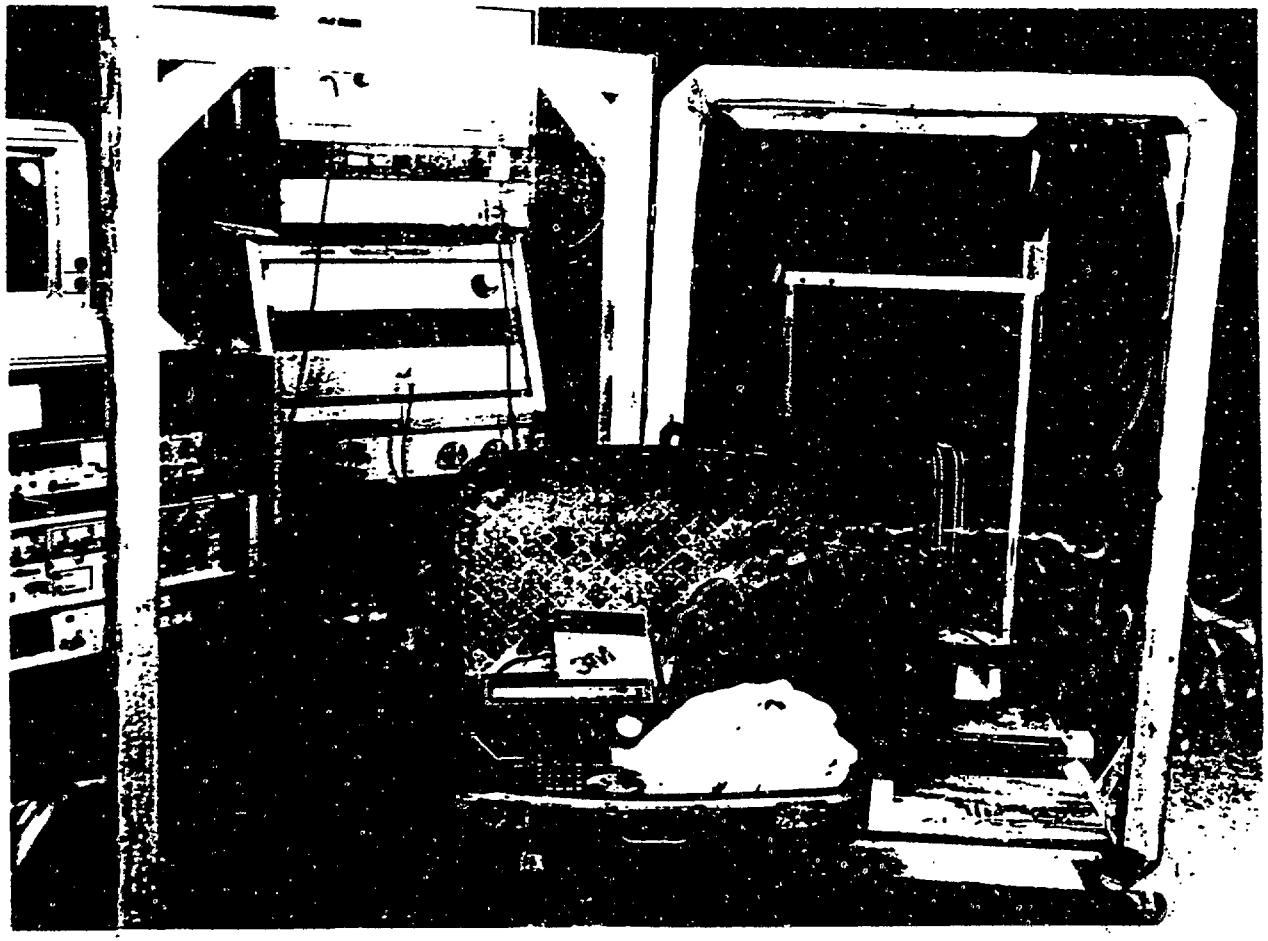
Scan time (data taking)	6 seconds
Quantity of RDX explosive	Sub-kilogram
Suitcase and contents*	35 pounds (16 kg) 2 ft^3 (60 liters)
NQR detector size	10 ft^3 (300 liters)

SUMMARY OF RESULTS

Specimen	*Number of Trials*	*Alarm*	*No Alarm*	*Detection Rate*	*False Alarm Rate*
Empty (no suitcase, no RDX)	1000	10	990	-	1.0%
RDX	400	400	0	99+%	-
Suitcase and contents*	400	3	397	-	0.75%
Suitcase, contents* and RDX	400	400	0	99+%	-

* Two small hardsided nylon lined overnight bags were used in place of a single large suitcase. Contents were:

2 hardcover books	computer diskettes	flashlight	polyurethane (400g) (125 g)
electric shaver	aerosol can	2 horseshoe magnets	man's windbreaker (polyester/cotton)
steel hammer	1 liter Perrier water	2 sweaters (75% wool; 50% ramie)	
$NaNO_2$ (2 kg)	1 liter methanol	electronic calculator	
hooded sweatshirt	nylon fishing line		
rubber soled shoes			



A full scale proof-of-concept Nuclear Quadrupolar Resonance (NQR) explosives detector for airline baggage has been designed and built at the Naval Research Laboratory. The 300-liter (10 ft³) radio frequency (RF) coil sits inside a screened cage. To the left of the cage are the RF amplifier and receiver; the PC-based controller and data system are at the far left.

The contents of the suitcase illustrate some advantages of NQR for explosives detection. No large magnetic field is required, so magnetic media (disks and credit cards) are not corrupted. The presence of ferromagnetic material (steel, electric shavers) does not interfere with the inspection. Electronics can be safely inspected. Due to the high chemical specificity of NQR, other nitrogenous materials, such as nylon, polyurethane or nitrile rubber, do not produce a signal.

In a commercially built system the electronics can be constructed more compactly than in this laboratory version

Figure 1

Naval Research Laboratory NQR Explosives Detector
Detection of RDX

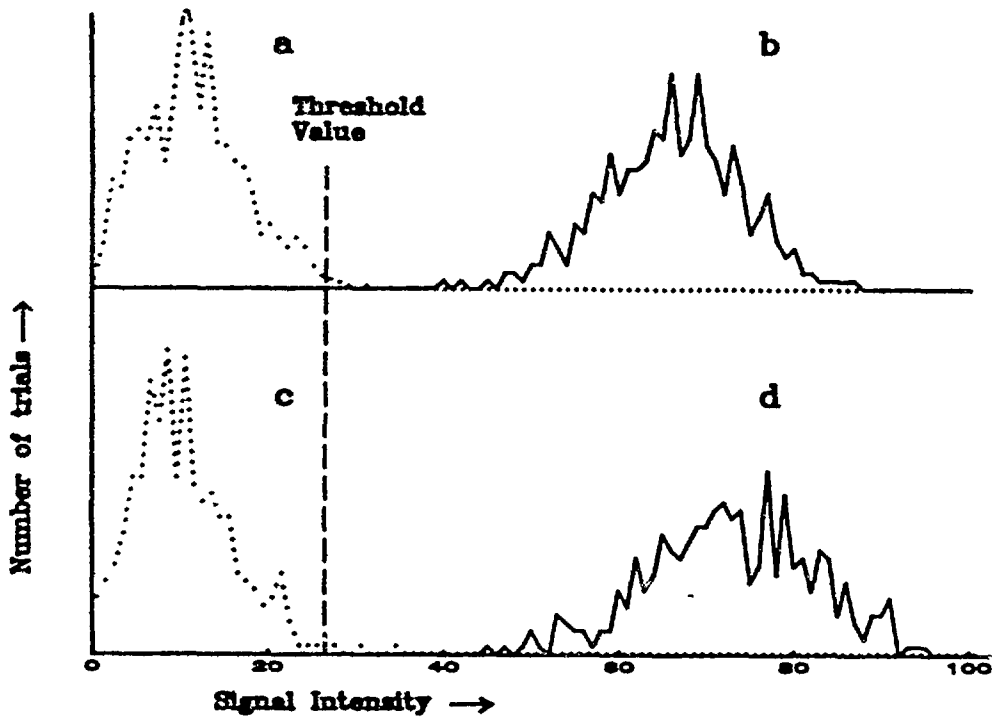


Figure 2

Shown are normalized distributions of NQR signal intensities under the following test conditions: (a) empty; (b) RDX only; (c) suitcase and contents; (d) suitcase, contents, and RDX. For each condition, the 6-second scan was repeated for either 400 or 1000 trials. The 1% false alarm rate threshold value is also indicated. This test examines only the random noise contribution to the NQR signal: some further systematic 'noise' may be anticipated on examination of a large set of differing bags and contents. Note that the NQR signal intensity profiles with (c, d) and without (a, b) the suitcase and contents are substantially the same: the benign baggage contents neither produce interfering NQR signals, nor do they mask the RDX signal. The substantial separation between the distributions for the 'clean' and 'dirty' bag provides the very high detection probability and the low false alarm rate.

EXPLOSIVE DETECTION USING DIELECTROMETRY

D. Clint Seward, President,
Spatial Dynamics Applications

T. Yukl, Technical Director,
Spatial Dynamics

1. DIELECTROMETRY TECHNOLOGY REVIEW AND DEFINITIONS

The dielectrometer detects using two parameters: dielectric constant and loss tangent. The basis for the technology and for the existing instruments is the patented antenna/lens combination described in the referenced patents[1,2]. The instrument establishes a standing wave of microwave energy in a fixed field configuration. For microwave users, it can be thought of as doing the work of a network analyzer without requiring waveguides or probes. As such it allows a wide range of non-contacting internal measurements. This technology forms the basis of existing instruments widely deployed.

As a brief review, the dielectrometer has an antenna/lens combination that establishes a fixed field of microwave energy in front of the instrument. Objects which enter the field will alter the field. The microwave energy penetrates non-metallic objects and produces a volumetric reflection coefficient. From the reflection coefficient can be calculated dielectric constant and loss tangent information. A picture of a typical dielectrometer is shown in Figure 1.

The dielectric technology can detect changes in chemicals and materials with a high degree of reliability. In many cases, such as finding cocaine dissolved in sealed bottles of wine and liquor, the detection of items and substances has proven to be a definitive GO/NO-GO tester.

Dielectric technology can also identify detected items on a limited basis at present, with the promise of improved identifications as the technology develops. This is possible because it utilizes two distinctly different parameters for detection; dielectric constant and loss tangent.

1.1 Definitions

1.1.1 Dielectric Constant (E'): the ratio of the strength of an electric field in a vacuum to that in a material under test for the same distribution of charge[3]. Phillipe Robert's work describes how dielectric constant is the summation of microscopic polarization effects from electronic, ionic, orientation, and interfacial factors[4]. Examples are air with E' = 1 and water with E' = 80.

1.1.2 Loss Tangent (D): (or dissipation factor) is the ratio of the loss current to the charging current in a material under test[5]. Robert's work describes in detail the difference between polarization dielectric loss and conduction dielectric loss[6]. Examples : lossless materials such as plastics have D close to zero. Metals are lossey and have an infinite loss tangent.

2. DIELECTRIC DETECTION OF DRUGS AND CONTRABAND: CASE HISTORIES

2.1 Summary of Detection Guidelines Based on Field Experience[7]

2.1.1 Water has a uniquely high dielectric constant of 80, and absorbs microwave energy very well. (This is why microwave ovens work so well). Any substitution for a water based item is an easy detection. All fruits, vegetables, flowers, meats, and drinkable liquids are water based, so anything substituted for them is easy to detect (drugs or explosives, for example, which have a low dielectric constant).

2.1.2 Metal reflects microwave energy very well. Thus it is easy to detect metal contraband items.

2.1.3 Dielectric constant is similar to density, so changes in density will be detected by dielectric changes.

loss tangent. Replacing them in part with drugs or explosives will enable an easy detection.

2.2 Best Detection Cases to Date

2.2.1 Drugs dissolved in beer, wine, whiskey and other water based fluids: when drugs are dissolved in a liquid, the microwave absorption is greatly changed, and can be used to make this detection. The M600 can be used as a GO/NO-GO tester for this application since the detection is so strong. There was a well publicized case in 1990 in Miami where the M600 was used to detect cocaine dissolved in bottles of imported soft drinks.

2.2.2 Liquid explosives in bottles: terrorists have carried liquid explosives in sealed wine bottles. Visually and by feel, the altered wine bottles look the same as normal wine bottles. Dielectric detection will always be able to tell the difference between a normal bottle and one filled with liquid explosive. The dielectric constant of petroleum based fluids is about 2, nitromethane is about 37 while water is 80. Testing has shown the microwave absorption change is so strong this is a GO/NO-GO detection.

2.2.3 Metal Contraband: drug runners recently hid cocaine in a metal container which in turn was hidden in the middle of a flatbed truck loaded with ceramic tiles. The M600 tested through the ceramic tiles and detected the metal. Metal is an excellent reflector of microwave energy and as such will give a strong response. This same detection ability enables the M600 to detect weapons hidden in any non-metallic articles due to the microwave absorption and reflection.

2.2.4 Drugs hidden in frozen blocks of fish and shrimp: Displacing ice or water with drugs will cause a strong change in microwave absorption.

2.2.5 Drugs hidden in fruits and vegetables: This is an easy detection since both the dielectric constant and the microwave absorption greatly change by this substitution.

2.2.6 Metal pipes, conduit, reinforcing bars: these can easily be detected since metal reflects microwaves so strongly. These can be found inside walls, inside concrete structures, underground.

2.2.7 Chemical Identification: Chemicals have different dielectric constants, as well as different properties can both be used at present to screen chemicals for further tests for absolute identification. This technique is being used to test 55 gallon plastic drums to ensure they are labeled properly. A data base of chemical responses is required and is obtained with simple tests.

3. SCREENING OF PEOPLE FOR EXPLOSIVES

Work has been done to demonstrate the proof of concept for detecting explosives and weapons carried by people under clothing. The theoretical considerations for this application will be discussed. Discussed will be the testing done to date, and the outlook of what needs to be done as a next step.

There are several reasons why the dielectrometer is attractive for the people screening application:

First, the use of low level microwave is safe. The dielectrometers operate at energy levels 1000 times less than government safety standards for leakage from kitchen microwave ovens[8]. Microwave energy is non-ionizing, and non-polluting.

Secondly, the lens/antenna combination of the dielectrometer allows for full penetration of clothing, even wet, heavy winter clothing.

Third, the dielectrometer detects items even if sealed in glass, plastic, or non-metal containers. It also detects all metal containers.

Fourth, no imaging or operator interpretation is required. Detection is made on the basis of dielectric effects Operation will be analogous to a present day metal detector which finds any undeclared metal above a threshold level. With the dielectrometer any undeclared object will be found, whether metal or non-metal. This method of operation potentially will keep traffic flow at today's rates, without increasing the number of operators.

A first prototype sensor has been built and tested with interesting initial results. This was done for Sandia National Laboratories. The antenna used has a patented, elongated parasitic array and operates at 5400 MHz. The sensor frequency was chosen as a tradeoff between the depth of penetration in clothing and the resolution of the detection.

Clothing tested was all easily penetrated including heavy winter coats and sweaters, and damp clothing. Sensitivity of the signal remained good even through the clothing. Detection of test objects was made through the clothing.

The purpose of the elongated parasitic array is to shape and project the microwave field and minimize reflections[9]. A field was designed for detection of the test objects under clothing in the range from 2" to 20". Testing confirmed that this is feasible.

The dielectrometer was designed to identify the test objects as well as to detect them. The objects chosen were:

Plastic: 2" square by 1/8" thick.
Metal: 2" square by 1/8" thick.

These test objects could be detected and differentiated from each other and from human skin at a range of 6" to 8". More testing needs to be done to collect data.

The above experimental sensor was delivered to Sandia National Laboratories for their tests and evaluation. Testing done was for the purpose of verifying proof of concept, and has been promising. Engineering work to move the technology forward has been defined as a result of this work.

The next step in the dielectrometry technology will be to build another sensor with improvements identified by the Sandia work. First, it will be necessary to measure distance to the target to avoid ambiguities. This effort appears to be straightforward. A second effort will be to add to the data base of responses of explosives and normal materials since there is little published information in this area. Finally, an array of sensors needs to be configured for a portal.

4. DETECTING EXPLOSIVES USING TIMED DIELECTROMETRY

A new extension of the dielectrometry technology has been patented to provide a method for internal searches of bulk materials and cargo. It utilizes the basic dielectrometer technology to measure dielectric effects. The technique adds the capability to measure in timed volumes. This allows searches by analyzing the object under test one small volume at a time. Thus, timed dielectrometry allows a three dimensional search and analysis from one side of an object under test[10].

4.1 Dielectrometer vs. Timed Dielectrometer

The Dielectrometer produces a microwave field which is shown schematically in Figure 2. Using timing circuits, the microwave field can be sliced and analyzed a piece at a time, as shown schematically.

4.2 Timed Dielectrometry: Description

A dielectrometer is used to transmit microwave energy in 1/2 wavelengths, starting and stopping at the zero crossings. During this transmission the receiver is turned off. At the end of the transmission, the receiver is turned on for 1/2 wavelength so the first portion of the reflection coefficient can be captured. The receiver is then turned off. The result is analyzed by computer.

Rest period: the dielectrometer is then turned off (see Figure 3) for a rest time of 5 wavelengths to allow the field to dissipate and the system to come to rest.

A second transmission is completed for two half wavelengths. This time the receiver is turned on at the end of the transmission for only 1/2 wavelength. This enables the capture of the second portion of the reflection coefficient. The result is stored in the computer and analyzed.

The process is repeated for successive transmissions and analyses until the entire object under test has been analyzed in timed slices. At that time the reflection coefficient of each slice will be known.

4.3 Timed Dielectrometry Specifications

Frequency: 600 MHz
Depth of penetration: 24 inches or more in baggage.
Wavelength: 20 inches in air, approximately 10 inches or more in baggage.
Resolution: Approximately 1 cubic inch.
Sensitivity: Approximately one ounce of cocaine or one ounce of explosive.

4.4 Responses of Materials to Timed Dielectrometry

4.4.1 Response of a homogeneous material: A homogeneous material will respond to a normal, untimed dielectrometer as shown in Figure 4. The homogeneous material will give the shown response to the dielectrometer as long as the material has a

in air for 600 MHz).

4.4.2 Response of different dielectric values: Figure 5 shows how the normal, untimed dielectrometer will respond to different materials. Different materials with different dielectric constants will have different responses as shown.

4.4.3 Response of a homogeneous material to timed dielectric interrogation: If a timed dielectrometer were to interrogate a known homogeneous material, each slice would be separately evaluated. A response would look like Figure 6.

4.4.4 Mixture of Materials: Response of a mixture of materials to a timed dielectric interrogation is shown in Figure 7. For ease of understanding, we assume one slice of the material under test is actually a higher dielectric constant material, and all the rest is a single material.

In this case, the actual response curve will parallel the response curve of the single material. However, the one slice of a different material will cause the response curve to displace as shown. It is this change in response that is measured and evaluated of successive interrogations.

4.5 Clarifications

4.5.1 Depth of analysis: the transmission is 1/2 wavelength. This allows for analysis of the material in 1/4 wavelength increments since time of two way travel must be considered. The 1/2 wavelength is an arbitrary selection and may be decreased to improve resolution.

4.5.2 X,Y resolution is enhanced by the addition of a matrix of receivers on one inch centers designed to provide analysis and identification in one cubic inch increments. Increased resolution will be provided in future configurations by reducing this spacing.

4.6 Timing Diagram for a Timed Dielectrometer

4.6.1 First measurement

4.6.1.1 First Transmission: At initial time T_1 a single transmission occurs. This is a 1/2 wavelength transmission (Figure 8).

transmission, the receiver is gated opened for 1/2 cycle. The receiver will get only information from the first part of the reflection coefficient.

4.6.2 First rest cycle: once the reception is complete, a rest period will occur until all reflections are ended. This is designed to be 5 cycles.

4.6.3 Computer Analysis: The received information is sent to a computer for storage and analysis. The reflection coefficient of the first reflection are calculated, then stored. In this way the first timed slice of the material is evaluated.

4.6.4 Second Measurement

4.6.4.1 Second Transmission: At initial time T_2, a transmission of two 1/2 wavelengths is completed.

4.6.4.2 Second Reception: At the end of the transmission the receiver is gated open for 1/2 cycle.

4.6.5 Second Rest Cycle: A rest period of 5 cycles is completed.

4.6.6 Computer Analysis: The received information is sent to a computer for storage and analysis. The reflection coefficient information of the first and second slices of the material under test are now known.

4.6.7 Successive Transmissions: In the same way, successive standard transmissions are made and analyzed. Each time a further 1/4 wavelength of data is captured.

5. DISCUSSION OF IDENTIFICATION USING DIELECTROMETRY

5.1 Identification

Initial testing confirms that classes of materials can be identified. Plastics, metals, and human tissue are three classes of materials which testing verifies have distinctly different responses.

Further testing is needed to determine other classes of identification. There is very little in the published technical literature to provide E' and D of any materials at the frequencies of interest. Testing to provide this information is not difficult, and could be accomplished quickly.

5.2 Dielectric Identification

Some field work has been done to indicate that screening and identification of chemicals using E' is possible. The "Handbook of Chemistry and Physics" lists approximately 1000 materials and chemicals by dielectric constant[11]. This is an indication that there is a wide range between the E' of chemicals and materials.

5.3 Loss Tangent Identification

This parameter also holds promise of screening and identification of materials. It is a separate parameter from dielectric constant.

5.4 Timed dielectrometry

This will initially provide screening and analysis for each individual cubic inch of an object under test. Testing a small volume at a time will improve sensitivity by at least 10x. Eventually, this test volume will be reduced further. With this information, it will be possible to screen substances and measure two separate parameters, improving the ability to identify.

6. CONCLUSION

Dielectrometry is a proven technology now in operational use for detecting contraband drugs. Testing has shown the technology can be useful for explosive detection. The new 5400 MHz sensor has been built and tested with promising results, and a plan to move forward has been established. Timed dielectrometry is a further extension of the technology, and has the promise of interrogating a volume in small, timed volumes.

BIBLIOGRAPHY

Garland, J.C. and Tanner, D.B. Electrical Transport and Optical Properties of Inhomogeneous Media. American Institute of Physics, 1978.

CRC Handbook of Chemistry and Physics CRC Press, 67th edition, 1986.

Microwave Cooking Handbook.
International Microwave Power Institute, 1987.

Robert, Phillipe. Electrical and Magnetic Properties of Materials. Artech House, Inc. 1988.

Seward, D.C. and Yukl, T. A Microwave Dielectrometer and its Applications. International Microwave Power Institute Symposium, Denver, CO, 1990.

Test Report: Drug Detector with US Customs at Miami, April 1990.
Spatial Dynamics Applications, Inc.

Skolnik, Merrill I. Radar Handbook. McGraw Hill Book Company. 1970.

Van Nostrand's Scientific Encyclopedia. Van Nostrand Reinhold. 1989.

Yukl, T. Patent 4,234,844: Electromagnetic Noncontacting Measuring Apparatus; Nov 18, 1980

Yukl, T. Patent 4,318,108: Bidirectional Focusing Antenna; March 2, 1982

Yukl, T. Patent 4,878,059: Nearfield/Farfiekd Transmission Antenna; October 31,1989

Yukl, T. Patent 4,912,982: Nonperturbing Cavity Method of Fluid Measurement; May 5, 1990

Yukl, T. Patent 4,947,848: Dielectric Constant Change Monitoring; March 26, 1990

Yukl, T. Patent 4,949,094: Nearfield/Farfield Antenna With Parasitic; April 1, 1990

Yukl, T. Patent 4,975,968: Timed Three Dimensional, Dielectrometry; June 1, 1990

NOTES

1. Yukl, T. Patent 4,234,844.
2. Yukl, T. Patent 4,318,108.
3. Van Nostrand, Vol.1, p 204.
4. Robert, P., p 307.
5. Van Nostrand, Vol.1, p 204.
6. Robert, P., p 321.
7. SDA Test Report, Miami, 1990.
8. IMPI Handbook, p 71.
9. Yukl, T. Patent 4,975,094.
10. Yukl, T. Patent 4,975,968.
11. Handbook of Chemistry and Physics, E49 - E57.

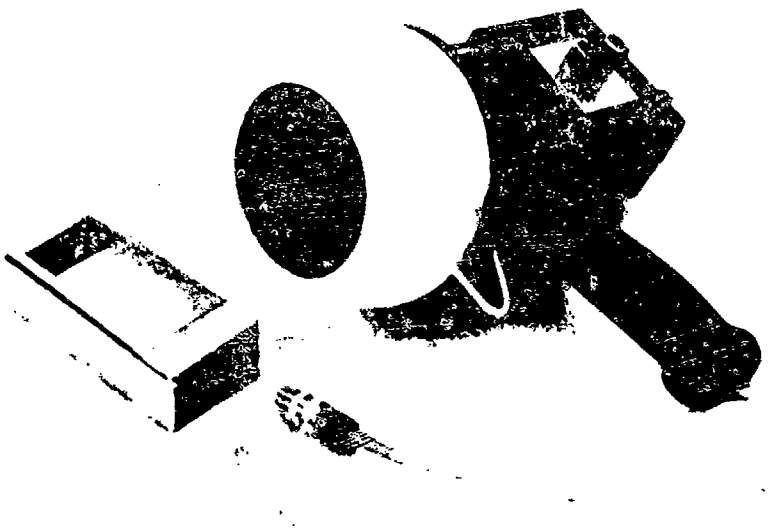


Figure 1. M600 Dielectrometer

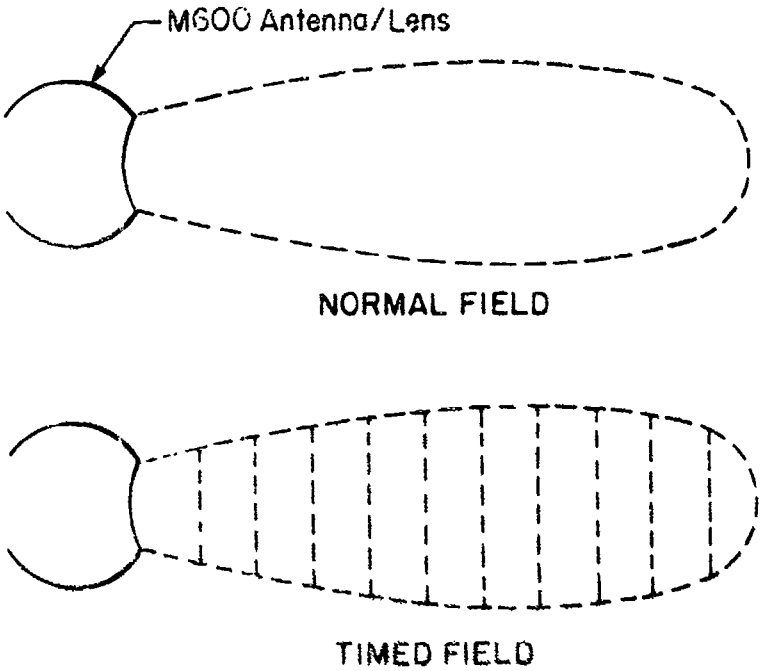


Figure 2. Normal Dielectrometer Field and Timed Dielectrometer Field

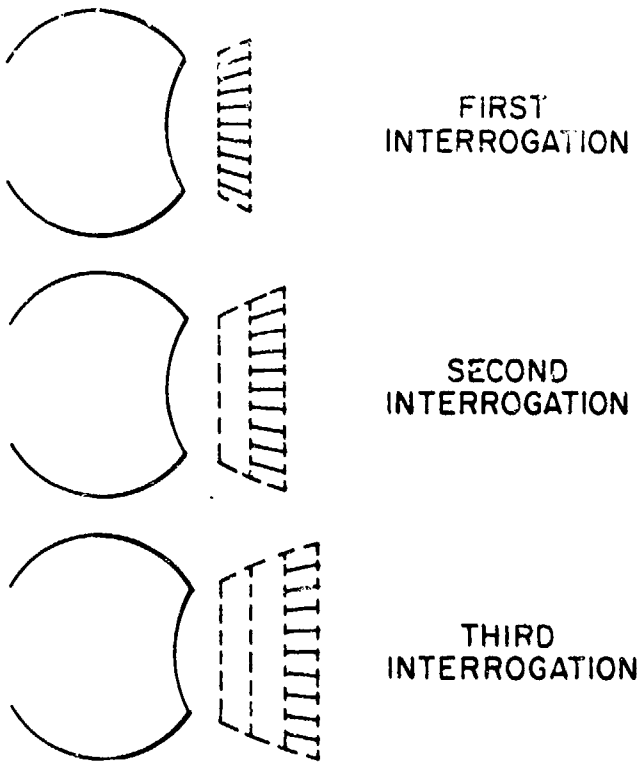


Figure 3. Successive Timed Interrogations

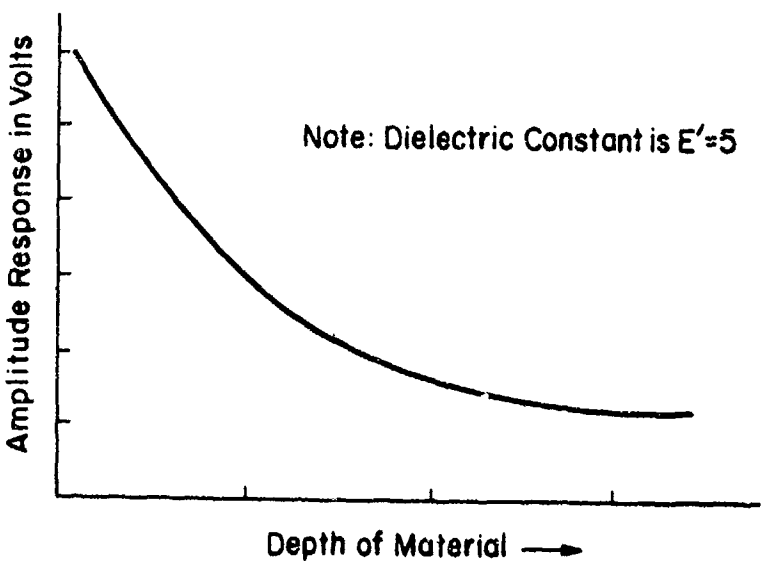


Figure 4. Response of a Homogeneous Material

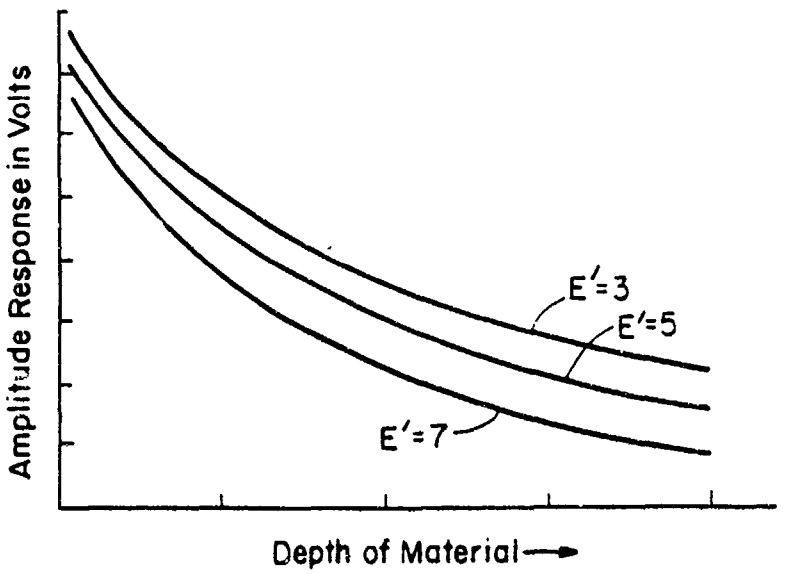


Figure 5. Response of Different Materials

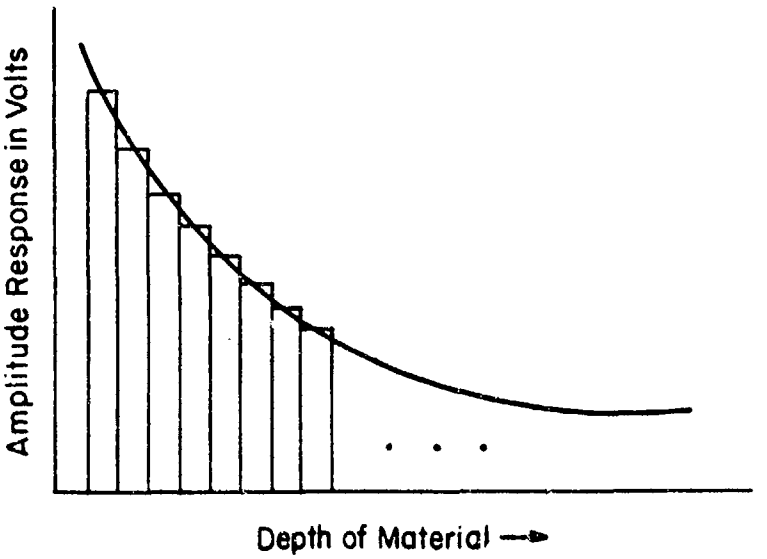


Figure 6. Response of a Homogeneous Material to Timed Interrogation

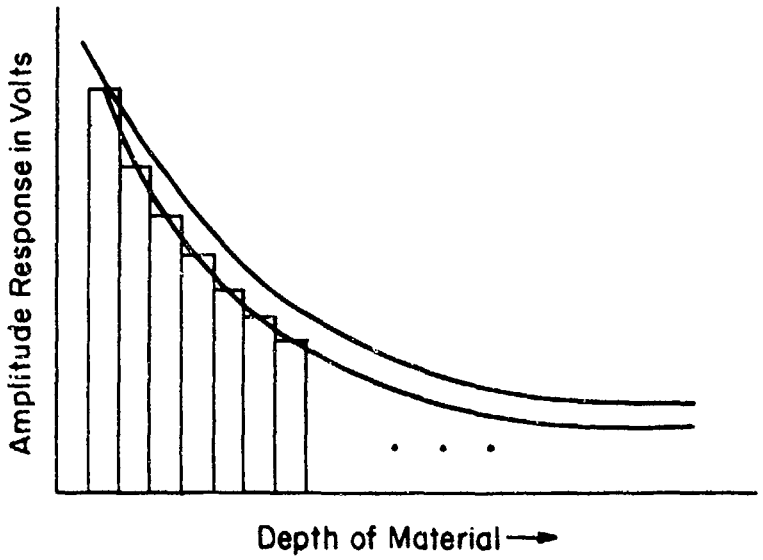


Figure 7. Response of a Mixture of Materials to Timed Interrogation

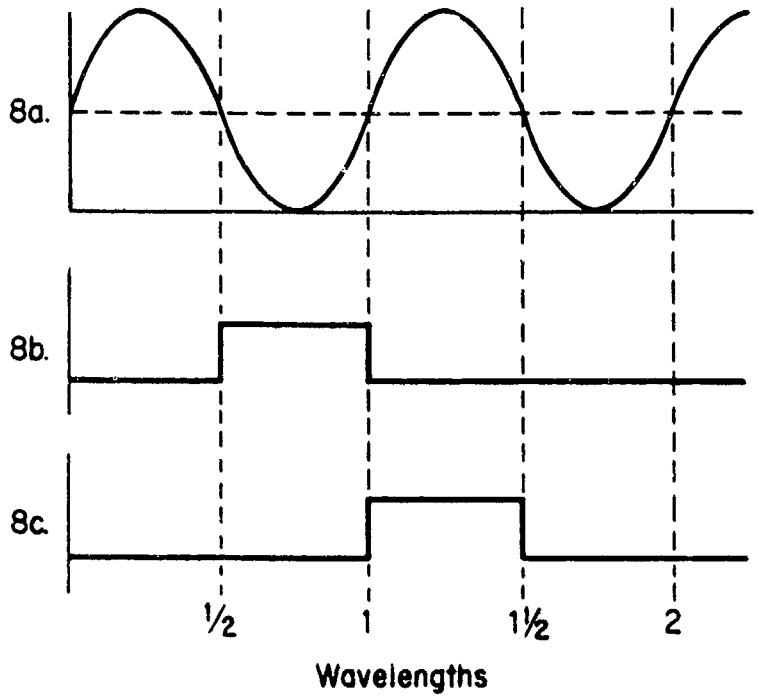


Figure 8. Timing Diagram

LIQUID EXPLOSIVES SCREENING SYSTEM

Dale R. McKay, Charles R. Moeller,
Erik E. Magnuson, and Lowell J. Burnett
Quantum Magnetics, Inc.
11578 Sorrento Valley Road, Suite 30
San Diego, CA 92121

1. INTRODUCTION

Nuclear Magnetic Resonance (NMR) techniques have been developed to verify the liquid contents of beverage containers commonly carried aboard aircraft, thereby detecting substitution of explosive liquids for the normal contents. The capability of NMR to distinguish between liquids is well known, but conventional NMR equipment is bulky and expensive. NMR systems generally require the application of an extremely strong and homogeneous magnetic field over the volume of the sample. The magnet used to generate this field largely determines the size and cost of the NMR system, particularly when large samples such as beverage bottles must be accommodated.

A detection strategy requiring modest magnetic field strength and homogeneity has been developed for distinguishing explosive liquids from alcoholic beverages. A surprisingly small magnet capable of applying such a field to common beverage containers has been designed, and a prototype has been built and tested.

The data gathered about a sample by the NMR system is extremely rich, with many parameters which can be measured, often simultaneously. Thus it is possible to construct several different types of signatures for any given set of samples. The system is designed to perform any of a number of NMR experiments under software control, thus providing the flexibility to respond to varying threat levels, and to adapt to new threats, without hardware modifications.

The system design readily accommodates information regarding bottle contents such as, for example, label or bar code information. Under this arrangement, the system would verify the legitimate contents of the container rather than looking for a particular explosive, so that few assumptions need be made as to the types of potential threat liquids which may be encountered. In addition, the system is designed to provide a "red light/green light" output, thus eliminating the need for operator interpretation.

2. TECHNICAL BACKGROUND

2.1 Nuclear Magnetic Resonance

Nuclear magnetic resonance (NMR) arises from the magnetic properties of atomic nuclei[1]. When immersed in a steady magnetic field, B_0, the nuclei align with the field and precess at a characteristic frequency given by

$$\nu_o = (\gamma 2\pi) B_o. \qquad (1)$$

This precession frequency is called the Larmor frequency, ν_o. The constant γ is called the gyromagnetic ratio and has a different value for each type of nucleus.

An externally applied pulse of radio-frequency (RF) field at the Larmor frequency causes the nuclei to tip away from their equilibrium position and, while still precessing, induce an NMR signal called a free induction decay (FID) into an adjacent pickup, or sample coil. A sketch of the envelope of a typical NMR FID signal is shown in Figure 1.

The magnitude of the NMR signal depends upon the magnitude of the nuclear magnetization at the time of the pulse. The equilibrium nuclear magnetization, M_0, in an applied field, B_0, is given by[2],

$$M_o = N\gamma^2 h^2 I(I+1)\, B_o / 12\pi^2 kT, \qquad (2)$$

where $I = 1/2$ for protons, γ is the proton gyromagnetic ratio, N is the total number of nuclei in the sample, h is Planck's constant, k is Boltzmann's constant, and T is the absolute temperature.

Both the nuclear magnetization and the Larmor frequency are proportional to the applied magnetic field and depend upon the type of nucleus immersed

in the field. For protons in a magnetic field of 0.1 Tesla (1000 Gauss), the Larmor frequency is 4.26 MHz. The strength of the signal is roughly proportional to the product of M_0 and ν_o.

2.2 Relaxation Times

The complex and detailed NMR spectral characteristics of molecules in solution have long been used as a powerful tool for the unique identification of chemical compounds. NMR spectral identification, however, requires very homogeneous and powerful magnetic fields. Spectra taken at low field strengths, or in less homogeneous fields, do not provide detailed chemical spectral details, yielding generally featureless NMR resonance lines.

Methods more appropriate to this study utilize NMR relaxation times, and related parameters. The two principal relaxation times used in the detection process are T_1 and T_2, defined below.

T_1: The spin-lattice relaxation time. This is the characteristic time for the nuclear spin system to come to equilibrium with its surroundings following a disturbance. Disturbances may be induced by an RF pulse or by a change in the applied field.

T_2: The spin-spin relaxation time. This is the characteristic time for the spin system to come to internal equilibrium following a disturbance. Also, it is the approximate decay time for the NMR FID signal in a perfectly homogeneous magnetic field.

In an imperfect field, the directly observed decay time is T_2^*, represented by

$$1/T_2^* = 1/T_2 + 1/T_{2m}, \qquad (3)$$

where T_{2m} is the rate at which the spins dephase due to the magnetic field inhomogeneity.

Note that the sample must be placed in the magnetic field and allowed to come to equilibrium for about one T_1 time before the experiment begins. If signal averaging is required to improve the SNR, then the spacing between experiments must also be about one T_1 time. In this case, the time to scan a given region will be nT_1, where n is the number of pulses required to produce an acceptable SNR.

Other parameters which can be measured by the Liquid Explosives Screening System include the following:

A: The Amplitude of the signal. This is a measure of M_0. It is usually measured as a relative number, determined by the initial signal strength in a given experiment. In that context, it varies primarily according to the number of spins in the volume of the sample to which the sample coil is sensitive. In most cases this volume is constant for different samples, so A represents the spin (hydrogen) density of the sample.

D: The Diffusion Constant. This is a measure of the mobility of the molecules in the sample. In the case of a simple fluid, it can be related to the sample's viscosity. Absolute measurements of D rely on knowledge of the magnet homogeneity, which is characterized by a parameter G, the magnetic field gradient.

J: The Spin-Spin Coupling Constant. This is the strength of the interaction between separate nuclear spins within individual molecules. It can be measured directly from an NMR spectrum, and can also be seen in some appropriately designed experiments intended primarily to measure T_2.

T_1 The longitudinal relaxation time in the rotating frame. This is similar to the T_1 which the sample would have in a much weaker magnetic field than that used to take the measurement: the SNR advantage of the higher field is retained in the experiment, and neither B_o or ν_o need be changed.

The effects of D can be readily observed in standard T_2 experiments on all of the samples measured in this study. J is visible in many, depending on the details of how the experiment is set up. In the Carr-Purcell experiment, for example, the experimental data has the form over time t of

$$\ln (M/M_o) = -t/T_2 - \gamma^2 D G^2 t^2 t/3, \qquad (4)$$

where G is a measure of the magnet inhomogeneity for the idealized case of a magnet whose field strength varies in a particular way, t is an adjustable experimental parameter, and the observed signal strength is M. Note that M_0 corresponds to A.

In addition, in experiments of this type, we may add a term for T_1, defining t' as the time between successive repetitions of the experiment, and one for an oscillating function dependant on the spin-spin coupling J. The data then takes the form

$$\ln (M/M_o) = -F_1(t',T_1) - F_2(t,T_2)$$

$$-F_3(t,D,G') - F_4(t,J). \quad (5)$$

In general, the sample may possess multiple components, so that the data is a super-position of several signals, each with the form of Equation (5). There would then exist more than one M_0, T_1, T_2, J, and D. In fact, we saw this with some of our samples.

For the purpose of establishing signatures for different liquids, there is no need to extract any of these parameters as individual numbers, though experiments and analysis techniques can be devised to do so. The actual time domain shape of the response of the sample to a particular experiment constitutes the signature.

2.3 NMR Instrumentation

The block diagram of a typical pulsed NMR system[3] is shown in Figure 2. The transmitter supplies RF pulses through a coupling network to the sample which is located in a steady magnetic field. A sensitive, low-noise receiver amplifies the resulting NMR signal, the FID, which is detected and then digitized.

Most modern NMR systems use a digital computer and computer controlled peripherals to control the transmitter, collect the digitized data, and perform various data analysis tasks. The size and cost of suitable computers, and of appropriate RF electronic building blocks, has declined substantially in recent years.

In most NMR applications, the NMR signal is very small. Low-noise, radio frequency engineering techniques are required to optimize the NMR signal-to-noise ratio. Since the signal is larger in stronger magnetic fields, the strongest field practical is used.

When the sample's T_2 is long, as for the liquids of interest in this study, the decay time T_2^* of the FID is dominated by T_{2M} (Equation 3). This means that the time available to collect the signal, and therefore the effective SNR of the experiment, depends on the homogeneity of the magnet.

The size, weight, and cost of the magnet used in an NMR system goes up rapidly with increased field strength, homogeneity, and sample volume. Thus the design of the magnet is critical to the success of an NMR design project.

Another detail, not shown in the figure, is a "lock" system, to maintain the relationship between M_0 and required by Equation (1). Some means must be provided to detect drift in the ratio of the two quantities and to adjust one or the other of them to hold that ratio constant.

3. DEVELOPMENT DETAILS

The development work proceeded in two phases. In the first, we took measurements in a general purpose laboratory NMR system. In the second phase, we built a prototype system and took additional measurements.

3.1 First Phase Results

In the first stage of this study, we used a laboratory system to measure the T_1's of a selected sample of explosive and benign liquids. We found that the T_1's of the explosives differed substantially from those of the beverages, thus providing a simple means of separating them. This early study was limited, however in two ways.

The laboratory system included a magnet which weighs several tons and yet is not big enough to accommodate ordinary beverage containers. This meant that serious efforts toward the design of a practical magnet were required, and that we could only estimate the performance parameters that might be expected from a deployable system. In addition, the range of samples was limited, and we did not attempt any measurements other than T_1.

4. ENGINEERING DEVELOPMENT

4.1 Magnet

We chose an electromagnet design for this system because its field strength can be varied and because, unlike a permanent magnet, it need not be temperature controlled. The temperature control system for a permanent magnet with a large, open pole gap would be no less cumbersome than the power supply and coils required for the electromagnet. In addition, an electromagnet can be

turned off. This is a safety issue, and is helpful during shipping and for portability.

The electromagnet in this system is unusual in that it generates a relatively weak field of 1200 Gauss, corresponding to a proton resonance of 5 MHz, but must do so over a substantial sample volume and allow for the placement of a large bottle such that at least part of the bottle is within that sample volume. Most NMR systems can accommodate samples of just a cubic centimeter or so. Systems which can accommodate larger samples are generally huge, and an order of magnitude too expensive for this application.

The solution was a traditional, open H-magnet design with a very untraditionally small ratio of magnet gap to pole diameter. An unusual pole face design compensates for the very poor homogeneity which would ordinarily be expected with a gap nearly as wide as the pole face diameter.

Figure 3 is an outline of the prototype magnet, which requires less than 150 Watts from the AC line. This magnet was intended to function as a very flexible test platform for what we expected would be a long, cut-and-try development process. Among other things, it is capable of generating a field twice as strong as required, and provides extra 'elbow room' for working within the gap region.

The magnet surprised us by working on the first try, delivering an effective field homogeneity of one part in 10,000 over the sample region. We expect the production version to draw a similar amount of power but to be about half the size of the prototype.

The lock system is realized in software. Whenever a sample is measured, the computer checks its center frequency and compares it to the desired value. If the difference exceeds a set limit, the magnet power supply is adjusted appropriately. At turn-on, or during periods of inactivity, the system would request that a standard sample be put in place so that it could maintain its ready status. Note that this system also constitutes a mechanism for continuously checking the system for faults.

5. RF ELECTRONICS

The RF electronics includes the transmitter/receiver board (RF Board), the preamplifier and multiplexer module, and the RF power driver and final amplifiers.

5.1 Coil/Preamp/Multiplexer

The Sample Coil, Preamplifier and Multiplexer are conceptually part of the RF Electronics but will be located within the magnet, in close proximity to each other.

Sample coils are usually designed so as to enclose the sample, but in this system that would require a very large coil which would show poor sensitivity with small samples, and would require an extremely powerful RF power amplifier. We therefore used a small, flat 'single-sided' sample coil oriented horizontally. The sample is conveniently placed directly on the coil.

The preamplifier is a conventional design with onboard regulation and active switching. It and the multiplexer are closely coupled at an impedance level of 2K ohms, rather than the usual lower impedance commonly used when a preamplifier must be fed from a coaxial cable.

Since recovery time is not a major concern in this system, the multiplexing scheme is passive, with discrete components. Time to full recovery is 100 microseconds. The system has a receiver Q of roughly 50 and a transmit Q of 5.

5.2 RF Board

A block diagram of the RF Board is shown in Figure 4. The transmitter section of the RF Board includes a divide-by-four phase shifting system followed by a phase selector / transmit gate. Its receiver section includes an IF amplifier, phase detectors, and video amplifiers. A frequency compensated crystal oscillator (TCXO) provides a fixed frequency clock. The transmitter's RF bandwidth is in excess of 20 MHz, with a transmitter output of approximately 12 dBm. Its video section has a quadrature bandwidth of more than 200 KHz, with a maximum output of 5 volts. It uses dc voltages of +5 and +/-15, and has on-board regulators which require an overhead of 3 volts.

The production version of the RF Board is expected to differ only in that it will plug directly into the CPU back-plane, and will incorporate the Pulse Width Generator and 8-bit port discussed below. The board was designed to facilitate the necessary connectoring changes.

5.3 RF Power Amplifiers

The RF power amplifier chain consists of two inexpensive solid state commercial modules with only minor modifications. It delivers 500 Watts of pulsed RF power, drawing only 125 Watts from the AC power line. It is a very rugged unit, operating at very short duty cycle at less than its full CW rating. It is inherently fail-safed, in that the power supply cannot deliver enough CW power to damage either the amplifier or any of its associated circuitry.

6. DATA ACQUISITION AND CONTROL ELECTRONICS

6.1 Central Processor

The data acquisition system is based on a ruggedized version of an ISA bus 80286 computer running Microsoft's MSDOS operating system. The production version will be essentially the same, but based on an 80486 to boost data processing speed.

6.2 Peripherals

The analog to digital convertor board (A/D) is a commercial unit which plugs into the CPU backplane. It features two fully independent channels, and anti-aliasing filters which can be configured under computer control. Its resolution is 16 bits. It can digitize, and DMA to the CPU memory, more than 50,000 complex points per second. In normal operation, the system runs at a bandwidth of about 5000 points/second, but the higher speed is available so that the lock can go into an extended capture mode to recover from being left without its standard sample by a careless operator.

The RF electronics are controlled by a pulse programmer, outlined in Figure 5, which consists of a commercial pattern generator board which plugs into the CPU backplane, and a pulse width generator/interface (PWG) board. The CPU controls the time between experiments, the commercial board determines the time between pulses and issues triggers to the A/D board, and the PWG sets the width of the pulses.

In the prototype unit, the PWG is free-standing. Its pulse width registers are loaded indirectly by a special 'pulse program' in the pattern generator board. In the production unit, the PWG will be incorporated with the RF board, on a plug-in board in the CPU, and its registers will be loaded directly from the CPU bus.

The magnet power supply is under digital control, with 16-bit resolution above an offset, via a simple 8-bit port which also plugs into the CPU. In the production unit, its bus interface circuitry will be used to control the RF/PWG board, and the 8-bit output to the magnet power supply will also come from that board.

6.3 Software

Most of the control software for the system, including the entire user interface, is written primarily in a commercial FORTH language extension called ASYST. The drivers for the A/D board and the pattern generator were supplied by the vendors and then modified and extended with their aid. An additional layer of code linking the drivers with ASYST was written in C. The C code for the A/D board is relatively simple, while that for the pattern generator constitutes an assembly language for pulse programming.

The ASYST language, which has numerous generic data analysis and presentation features built into it, was used to simplify and speed the development work. It will be retained in the production unit version only in that it will be available at the plant for test and maintenance purposes. The production unit's control software will retain only the drivers of the prototype system, with the higher level control, data analysis, and user interface functions re-written in C.

7. EXPERIMENTAL RESULTS

The experimental part of the project was set up as an iterative process, with the final goal being the collection of data for a wide range of beverages and explosive liquids, in actual beverage containers and using a signature expected to allow the unambiguous detection of explosives. To do this we started, in the first phase of the project, with a simple T_1 signature and a small range of samples in containers which could be accommodated by our general purpose laboratory electromagnet.

From this data we went on to develop other signatures, with which we accumulated more data. At the same time, we developed the hardware required to accommodate larger containers and to produce additional signature options. The process is by no

means complete. In addition, a new, longer list of both benign and threat liquids is being considered. If adopted, this will certainly necessitate additional testing, and may require the development of additional signatures.

We believe that the most efficient effective signature is a variation of the standard Carr-Purcell multiple pulse and acquisition sequence, in which the usual inversion pulses are replaced by 3-pulse composite sequences. This yields a signature such as that represented by Equation (5). The optimum tau time and number of inversions have not yet been determined. The choice of tau times affects the manner in which primarily the J and D parameters appear in the signature.

This sequence can be run, with sufficient signal to noise, in a single scan. The time required for the test is thus roughly one T_1, plus one T_2, plus the computation time. The longest part of the experiment is currently the computation time. We run a fast Fourier transform (FFT) of the data acquired after each inversion: this loads down the 80286 substantially. The production unit, using an 80486, is expected to be roughly 50 times as fast, at which point the computation time will no longer be significant.

Additional iterations will be required before this signature scheme can be considered finalized, however. More importantly, substantial analysis of the data already collected will be required in order to optimize the manner in which the signature is characterized and compared with the known signature of the labeled contents of the bottle being inspected. The characterization scheme will determine how the acquired data is ultimately converted to the go/no-go signal which must be delivered to the security personnel who use the system in the field.

8. COUNTERMEASURES

Given the richness of the NMR data available, the ability of the system to be configured in software to select from an almost arbitrarily wide range of signatures, and the fact that the liquid cannot be shielded from inspection, we know of no effective countermeasures to this technology.

9. CONCLUSIONS

It is possible to use a practical, field deployable NMR system to screen for liquid explosives packaged to be visually indistinguishable from ordinary sealed containers of alcoholic beverages. Such a system has been prototyped and is capable of meeting this goal.

Due to the unique magnet design, and the use of off-the-shelf components and sub-assemblies throughout the electronics, a production unit would be priced within the range of security systems currently in use. Because of this design strategy, it would generally be serviceable by ordinary electronics personnel. Due to the use of a general purpose digital computer for system control, data collection, and analysis, the system can be programmed to be operable in a "green light - red light" mode by ordinary security personnel with no special technical training or background.

The system can be operated in a mode where it verifies the labeled (or bar coded) contents of the container, rather than being sensitive to a particular explosive or class of explosive. Due to this characteristic, and because of the richness of the data which can be obtained from liquids by NMR, it is believed that any realistic technical countermeasures would be inherently ineffective.

NOTES

Support of this work by the Federal Aviation Administration through the SBIR program is gratefully appreciated.

1. Slichter, Chapter 1.
2. Abragam, Chapter 3.
3. Fukashima, Chapter 5.

REFERENCES

Abragam, A., The Principles of Nuclear Magnetism, Clarendon Press, Oxford (1961).

Fukashima, E., and Roeder, S.B.W., Experimental Pulse NMR, Addison-Wesley, Reading, MA (1981).

Slichter, C.P., Principles of Magnetic Resonance, 2nd Edition, Springer-Verlag, Berlin (1978).

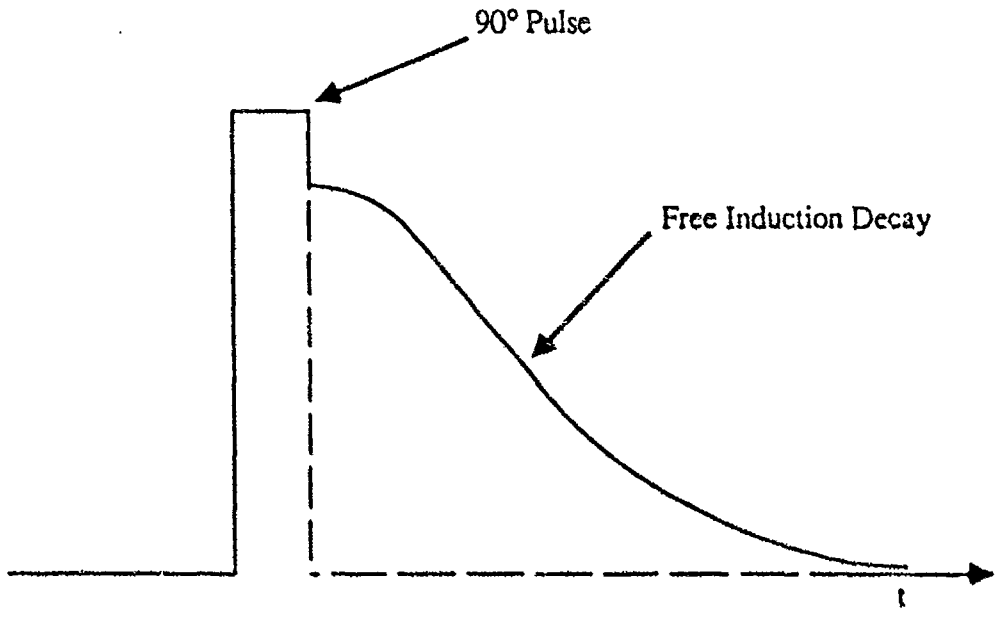


FIGURE 1. SKETCH OF AN NMR FREE INDUCTION DECAY.

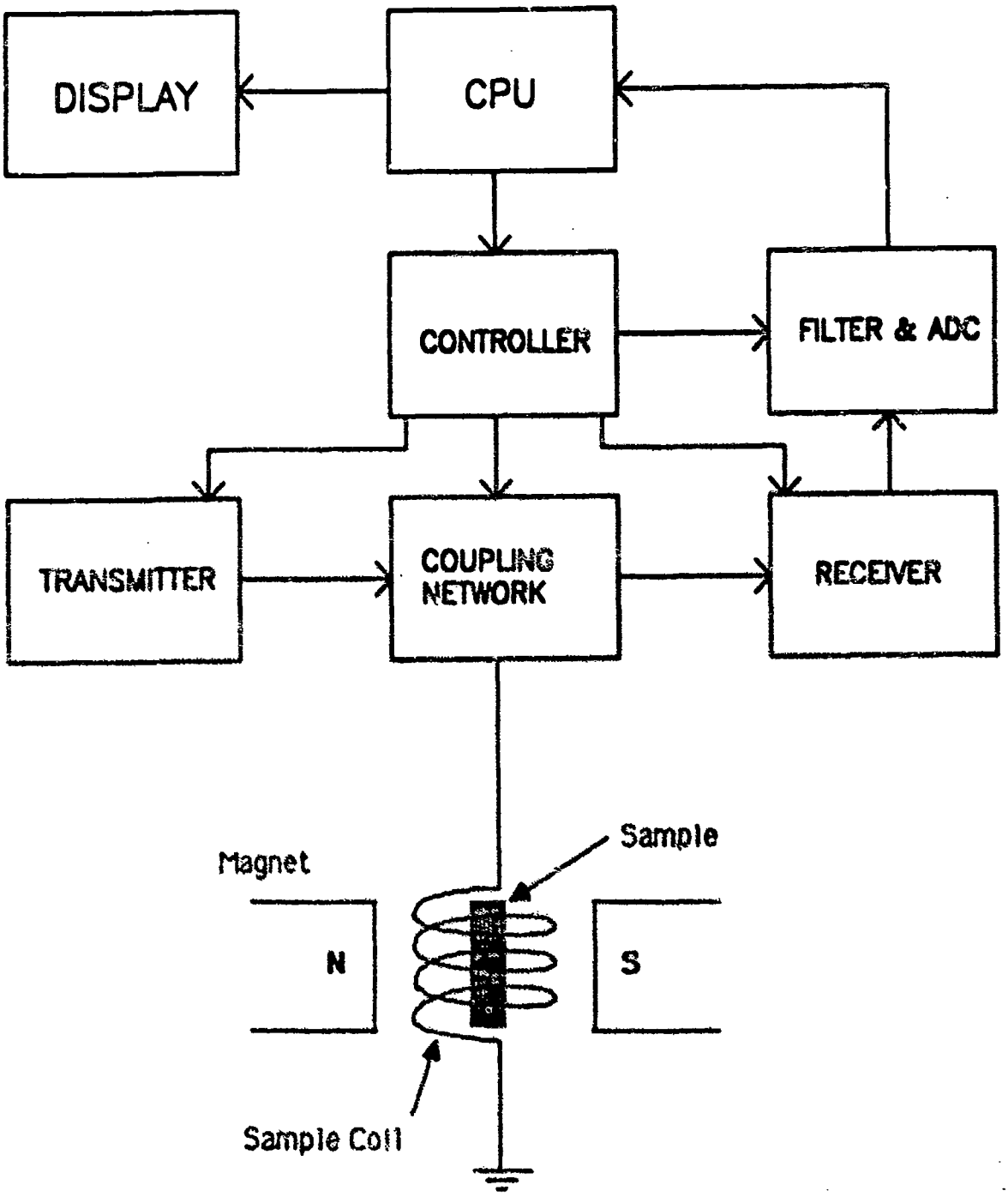
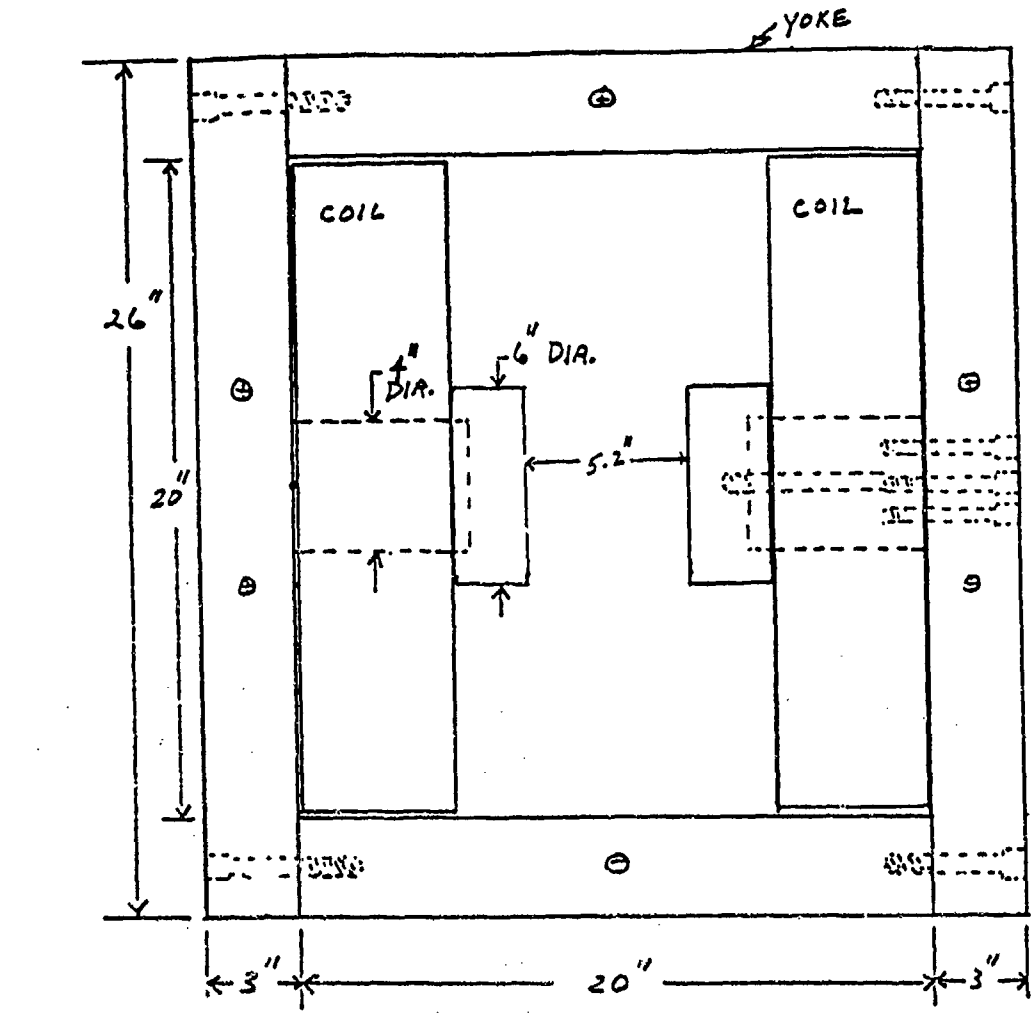
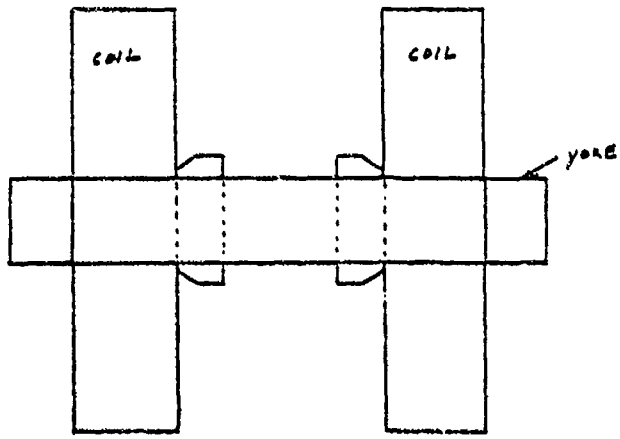


FIGURE 2. BLOCK DIAGRAM OF A TYPICAL PULSE NMR SYSTEM.





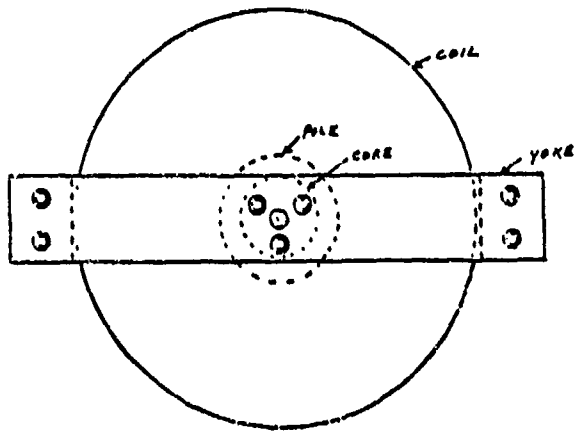


FIGURE 3. H-CORE ELECTROMAGNET.

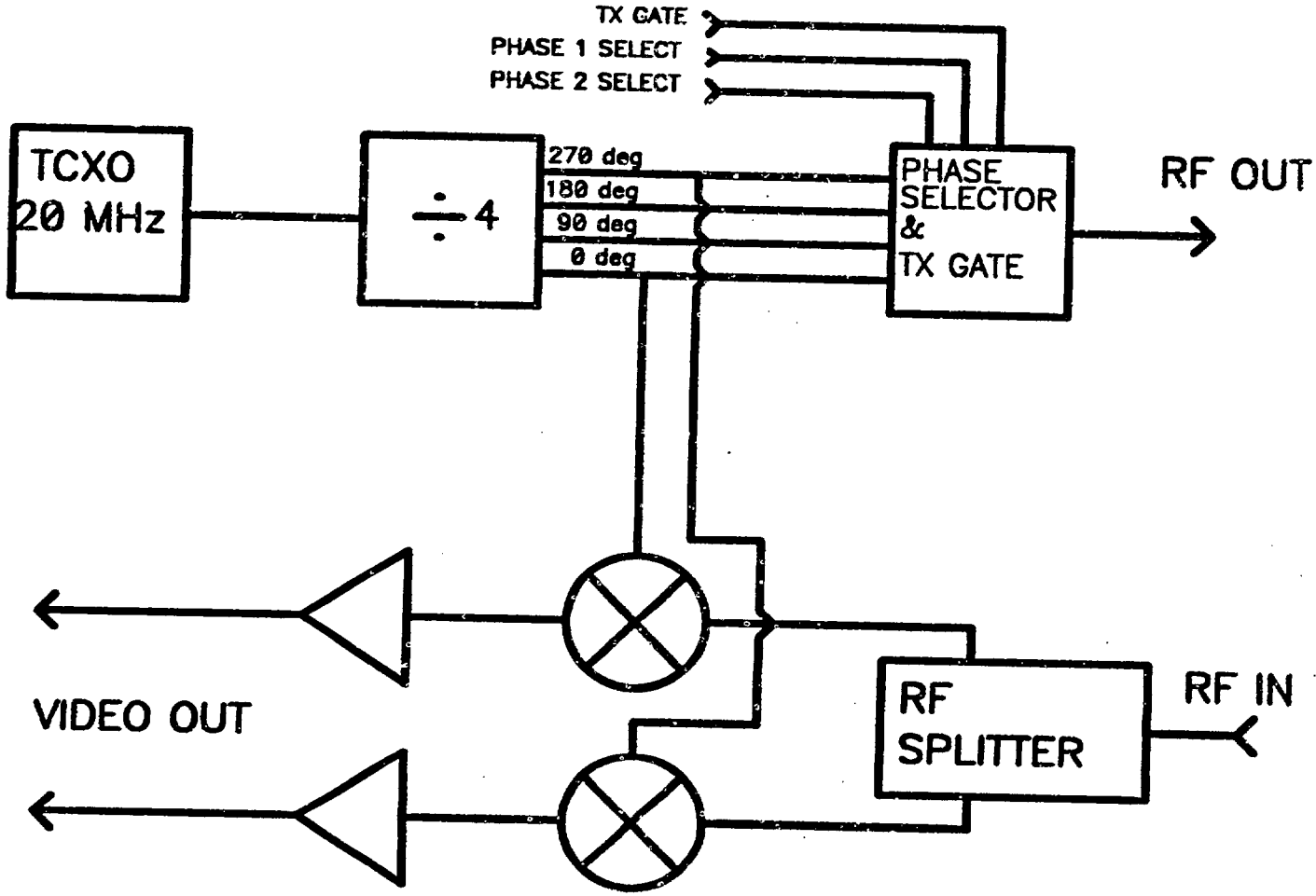


FIGURE 4. BLOCK DIAGRAM OF THE RF BOARD.

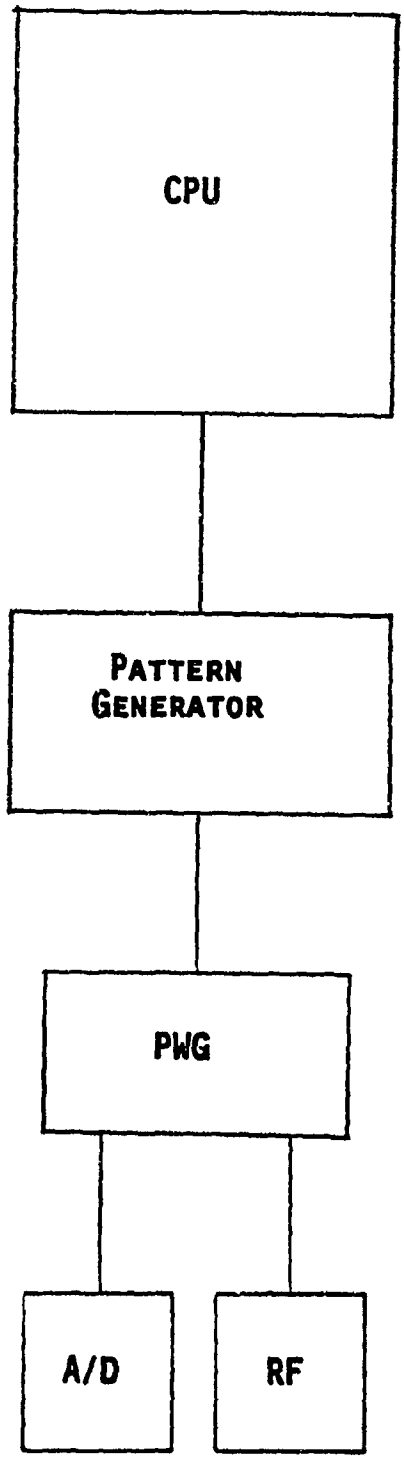


FIGURE 5. PULSE PROGRAMMING SYSTEM.

IMPROVED NMR SIGNATURES OF EXPLOSIVES

Lowell J. Burnett and John P. Sanders
Department of Physics
San Diego State University
San Diego, California 92182

1. INTRODUCTION

The work reported here is part of an ongoing program to identify unique proton NMR signatures for explosive compounds. In many explosives a significant fraction of the hydrogen nuclei (protons) are coupled to nitrogen nuclei. The energy level diagrams of these proton/nitrogen pairs contain both allowed and weakly allowed transitions. In the measurements reported here, weakly allowed transitions in the sample were irradiated with RF energy and the resulting effects on the proton NMR signal were recorded.

2. THEORETICAL BASIS

For an isolated nucleus in an applied magnetic field B_o, the interaction of the nuclear dipole moment with the field results in the following energy states[1],

$$E_m = -\gamma \hbar B_o m \qquad (1)$$

where γ is the gyromagnetic ratio of the nucleus.

Protons are spin-1/2 nuclei and possess only a dipole moment. Therefore, m in Equation (1) takes on one of the two values, -1/2 or +1/2. The resulting energy level diagram for protons is shown in Figure 1.

Nitrogen nuclei are spin-1 nuclei and possess both dipole and quadrupole moments. In high fields, the interaction of the dipole moment with the applied field produces three energy levels according to Equation 1 (corresponding to m values of -1, 0, and +1) and the interaction of the quadrupole moment with local electric field gradients perturbs these levels. The energy level diagram for nitrogen nuclei is also shown in Figure 1 with the quadrupole perturbation indicated by ω_q.

In high fields, when protons and nitrogen nuclei are coupled, six energy levels with 15 possible transitions result. These are also shown in Figure 1. Seven of these transitions correspond to changes in m of +1 or -1 and are, therefore, allowed. In a system of isolated spin pairs, the other eight transitions are strictly forbidden. However, the strong interactions present in many solids mix these states[2]. Therefore, the resulting energy levels are not pure states and the transitions are weakly allowed[3].

In low fields and zero field, the quadrupole interaction dominates, with the dipole interaction a perturbation. The energy levels for isolated nitrogen nuclei in zero field are determined by the quadrupolar interaction[4],

$$E_m^q = \frac{e^2qQ}{4}[3m^2 - 2] \qquad (2)$$

where e^2qQ is the quadrupole coupling constant and a zero asymmetry parameter is assumed[5]. Energy level diagrams for protons and nitrogen nuclei in zero field are shown in Figure 2.
In low fields, the dipole interaction perturbs the quadrupolar interactation through the relation[6],

$$E_m^d = -\gamma_n \hbar B_o m \cos\theta \qquad (3)$$

where γ_n is the gyromagnetic ratio for nitrogen and θ is the angle between the direction of the applied field and the symmetry axis of the electric field gradient. Energy level diagrams for protons and nitrogen nuclei in low field are shown in Figure 3 for a particular value of θ.

The data presented here were taken on polycrystalline samples at an intermediate value of field. That is, the angle θ takes on all values and the dipole and quadrupole interaction energies for nitrogen are comparable. This made it difficult to evaluate our results quantitatively.

Energy level diagrams for protons, nitrogen nuclei and coupled pairs in polycrystalline samples are

shown in Figure 4. It is important to note from Figures 3 and 4 that the maximum frequency of a weakly allowed transition is given by the sum of the proton and nitrogen Larmor frequencies and the zero-field NQR frequency.

3. EXPERIMENTAL DETAIL

Measurements were made on four compounds: TNT, PETN, the explosive simulant hexemethylenetetramine (HMT) and mannitol. The TNT and PETN samples were commercial grade.

HMT contains four nitrogen atoms, six carbon atoms and twelve hydrogen atoms per molecule. HMT has a proton spin-lattice relaxation time (T_1) of 58 seconds, as measured in our laboratory. HMT has a single nitrogen-14 quadrupole coupling constant and an asymmetry parameter of zero. At room temperature in zero field, HMT has a single NQR transition at 3.308 MHz[7].

Mannitol, a complex sugar, consists of a six-carbon linear chain with one hydroxyl group on each carbon. It contains no nitrogen atoms. The T_1 of mannitol at the frequency of these experiments is approximately 280 seconds.

The experiments were performed at a proton Larmor frequency of 19.14 MHz which corresponds to a nitrogen Larmor frequency of 1.38 MHz. A block diagram of the experimental apparatus is shown in Figure 5.

The pulse NMR spectrometer was a Spin-Lock Electronics Model CPS-2 used in conjunction with an Hitachi Model 6041 digital oscilloscope. The off-resonance irradiation electronics consisted of a PTS 160 frequency synthesizer, an Amplifier Research 150LA RF power amplifier, and a Diawa CL-680 impedance-matching circuit.

One method of acquiring data is shown in Figure 6. A series of 90 degree pulses, spaced time t_1 apart, is applied to the sample. The pulses disturb the proton magnetization from equilibrium and, between the pulses, the spin system relaxes back toward equilibrium. The NMR signal following each pulse determines the degree of proton polarization.

Off-resonance RF irradiation was applied to the sample in the time intervals between some of the 90 degree pulses in the series. If the frequency of the RF irradiation corresponds to a weakly allowed transition, then the return of the proton spin system to equilibrium is altered and the magnitude of the resulting NMR signal is reduced. This is also shown in Figure 6.

To acquire data, first an off-resonance irradiation frequency was chosen. Then the pulse sequence of Figure 6 was applied to the sample a number of times, with irradiation, and the results averaged. The sequence was then repeated without irradiation and the results averaged.

The averaged results obtained with and without irradiation were compared and the percentage decrease due to the effect of the irradiation was calculated. If the RF irradiation frequency corresponded to a weakly allowed transition, substantial changes in the proton polarization were noted. If not, then little or no change was noted. The effects were mapped out as a function of frequency by selecting a new off-resonance irradiation frequency and repeating the process.

4. RESULTS

The results for HMT are shown in Figure 7. As expected, the effects of RF irradiation are greatest near the proton Larmor frequency of 19.14 MHz due to the natural linewidth of the HMT resonance. However, significant effects are observable at frequencies far from the proton resonance frequency. These effects are much greater than experimental uncertainty. Below the proton resonance, significant effects occur near 16.8 and 17.4 MHz. Above the proton resonance, significant effects occur near 20.8, 21.2, 22.3, 22.7 and 23.8 MHz.

Definite zeros in the response to off-resonance irradiation occur at 21.7, 23.1 and above 23.9 MHz. The latter observation is in quantitative agreement with our expectations since the maximum weakly allowed transition frequency for a proton resonance frequency of 19.14 MHz in HMT (Figures 3 and 4) is 23.83 MHz.

The results for mannitol are shown in Figure 8. Again, the irradiation effects are largest near the proton Larmor frequency of 19.14 MHz. However, unlike HMT, there are no noticeable effects due to RF irradiation at frequencies more than a megahertz away from the proton Larmor frequency.

The lack of effects in the mannitol is attributed to the absence of nitrogen nuclei in the sample and, hence,

the absence of hydrogen-nitrogen couplings. The energy level diagram needed to explain these results is the simple two-level system characteristic of protons. There are no weakly allowed transitions available for off-resonance irradiation.

A plot of the percentage decrease in the proton NMR signal versus the RF irradiation frequency for PETN is shown in Figure 9. It is clear from these data that, compared to HMT, the effects of RF irradiation do not extend over as wide a range of frequencies.

However, the structure of the response may be as complex as in HMT. There is a pronounced effect at 20.2 MHz which is followed by an apparent zero in the response at 20.25 MHz. Similar behavior was observed on the low frequency side of the proton resonance.

In addition, there are clear non-zero responses near 17.8 and 20.6 MHz. No effects in PETN were observed above 21 MHz or below 17 MHz. The data are consistent with a symmetric response about the proton Larmor frequency.

The data obtained for TNT are shown in Figure 10. There is little or no response far from the proton Larmor frequency, though there appear to be small effects starting about one megahertz away from resonance, i.e., in the 20-21 MHz region.

The most striking feature of these data is that the TNT response appears to be asymmetric about the proton Larmor frequency of 19.14 MHz. At one-half megahertz above the proton Larmor frequency, the effect of RF irradiation is significant, i.e., between five and ten percent. However, one-half megahertz below the proton Larmor frequency, the response is clearly zero. These observations are well outside the range of experimental uncertainty.

5. CONCLUSIONS

This work demonstrates that it is possible to stimulate weakly allowed transitions through off-resonance RF irradiation and affect the proton polarization. It was found that changes in the amplitude of the proton NMR signal of the order of 10% could be produced in HMT with RF irraditation more than 4 MHz away from the proton Larmor frequency. The frequency dependence of the effect agrees qualitatively with expectations. No similar effects were observed in mannitol, a compound with similar proton NMR characteristics but lacking nitrogen nuclei.

NOTES

Support for this program was received from the US Federal Aviation Administration, EG&G Incorporated and San Diego State University. This support is gratefully acknowledged.

The present address of one of the authors (JPS) is: Southwest Research Institute, San Antonio, Texas 78228.

1. Slichter, Chapter 1.
2. Abragam, Chapter 9.
3. Wind and Yannoni.
4. Das and Hahn, Chapter 1.
5. Slichter, Chapter 10.
6. Das and Hahn, page 24.
7. Sanders.

REFERENCES

Abragam, A., "The Principles of Nuclear Magnetism", Clarendon Press, Oxford (1961).

Das, T.P. and Hahn, E.L., "Nuclear Quadrupole Resonance Spectroscopy", Academic Press, New York (1958).

Sanders, J.P., "Off-Resonance Pumping Effects in the NMR of Solids", M.S. Thesis, San Diego State University (1988).

Slichter, C.P., "Principles of Magnetic Resonance", 3rd Edition, Springer-Verlag, Berlin (1989).

Wind, R.A. and Yannoni, C.S., Journal of Magnetic Resonance 72, 108 (1987).

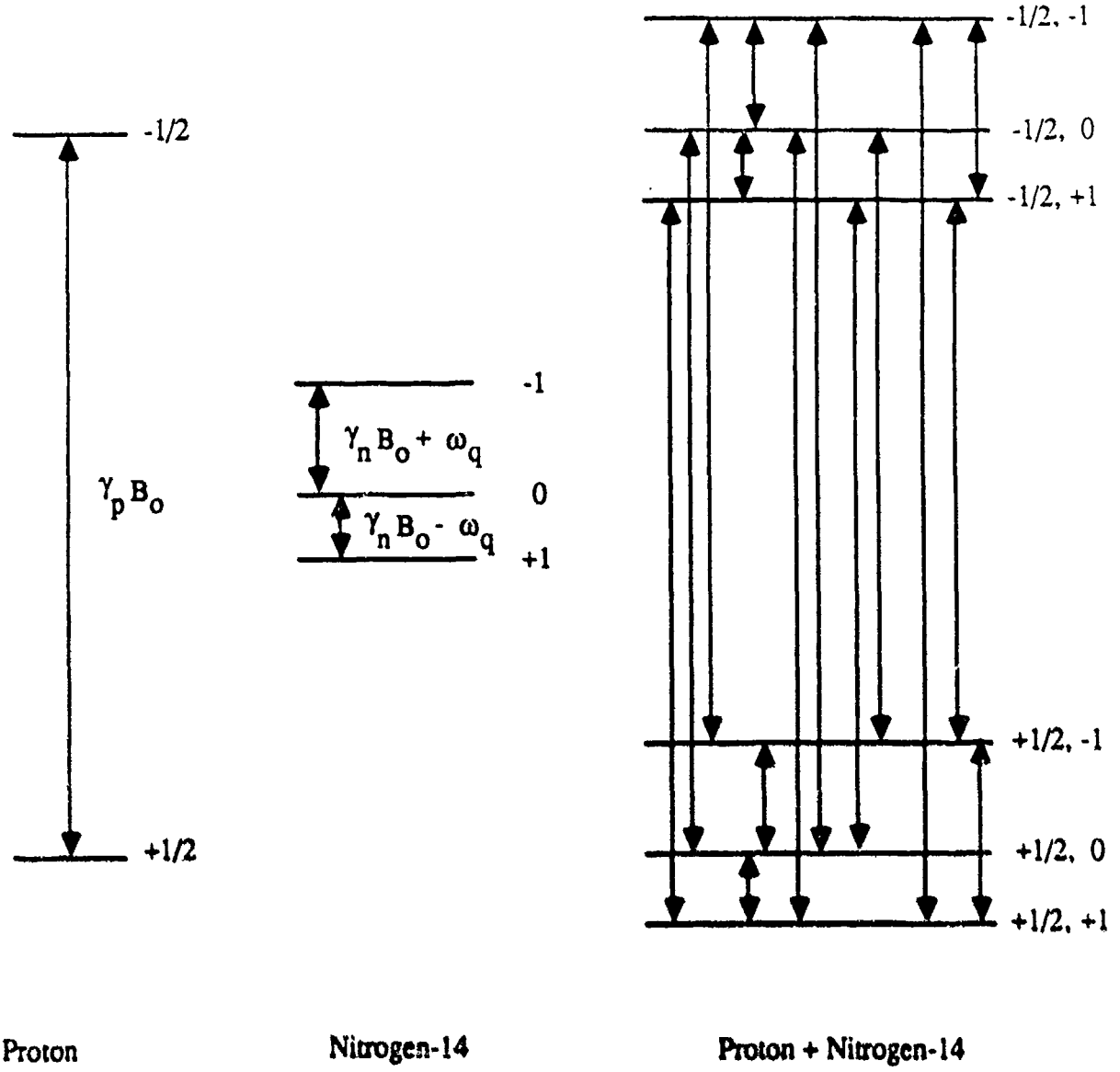


FIGURE 1. ENERGY LEVELS FOR PROTON, NITROGEN, AND COUPLED PROTON AND NITROGEN NUCLEI; HIGH FIELD CASE, QUADRUPOLE EFFECTS INCLUDED.

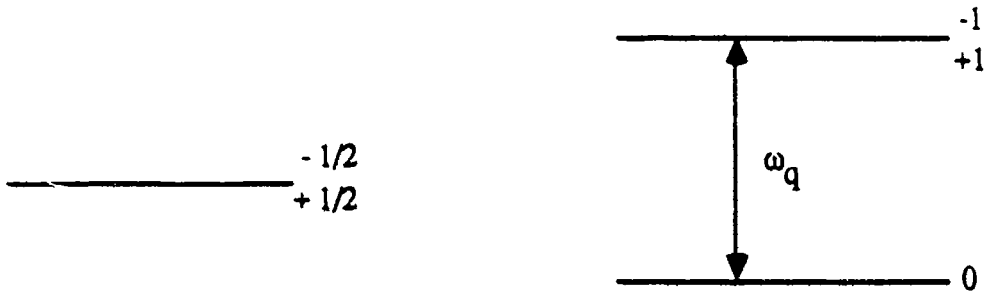


FIGURE 2. PROTON AND NITROGEN ENERGY LEVELS IN ZERO APPLIED MAGNETIC FIELD.

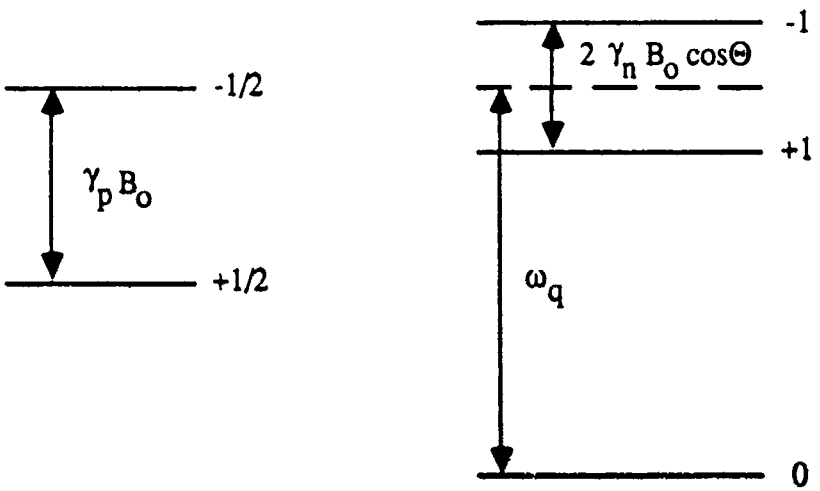


FIGURE 3. PROTON AND NITROGEN ENERGY LEVELS; LOW FIELD CASE; SINGLE CRYSTAL MATERIAL, QUADRUPOLE EFFECTS INCLUDED.

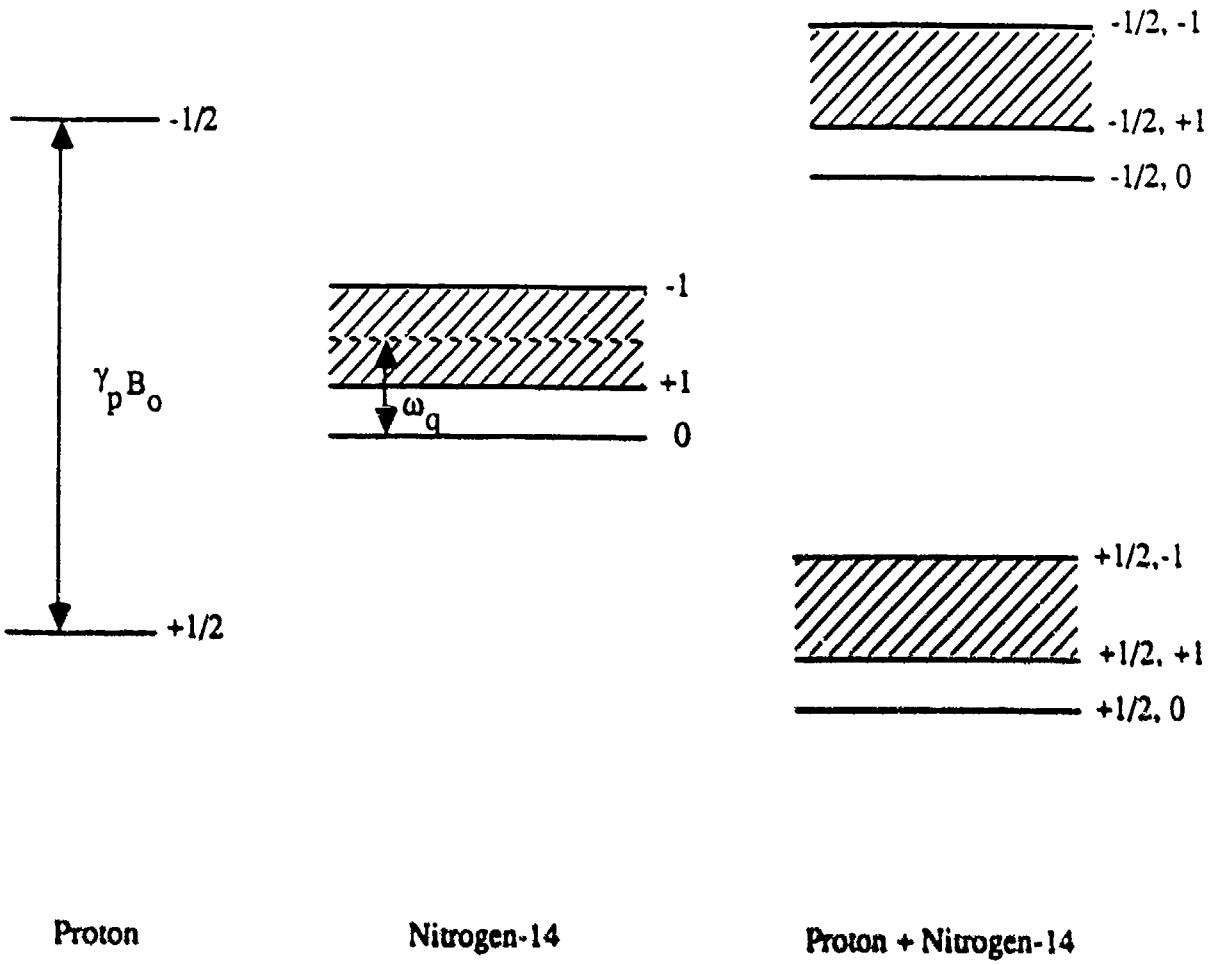


FIGURE 4. PROTON AND NITROGEN ENERGY LEVELS; INTERMEDIATE FIELD CASE; POLYCRYSTALLINE MATERIAL.

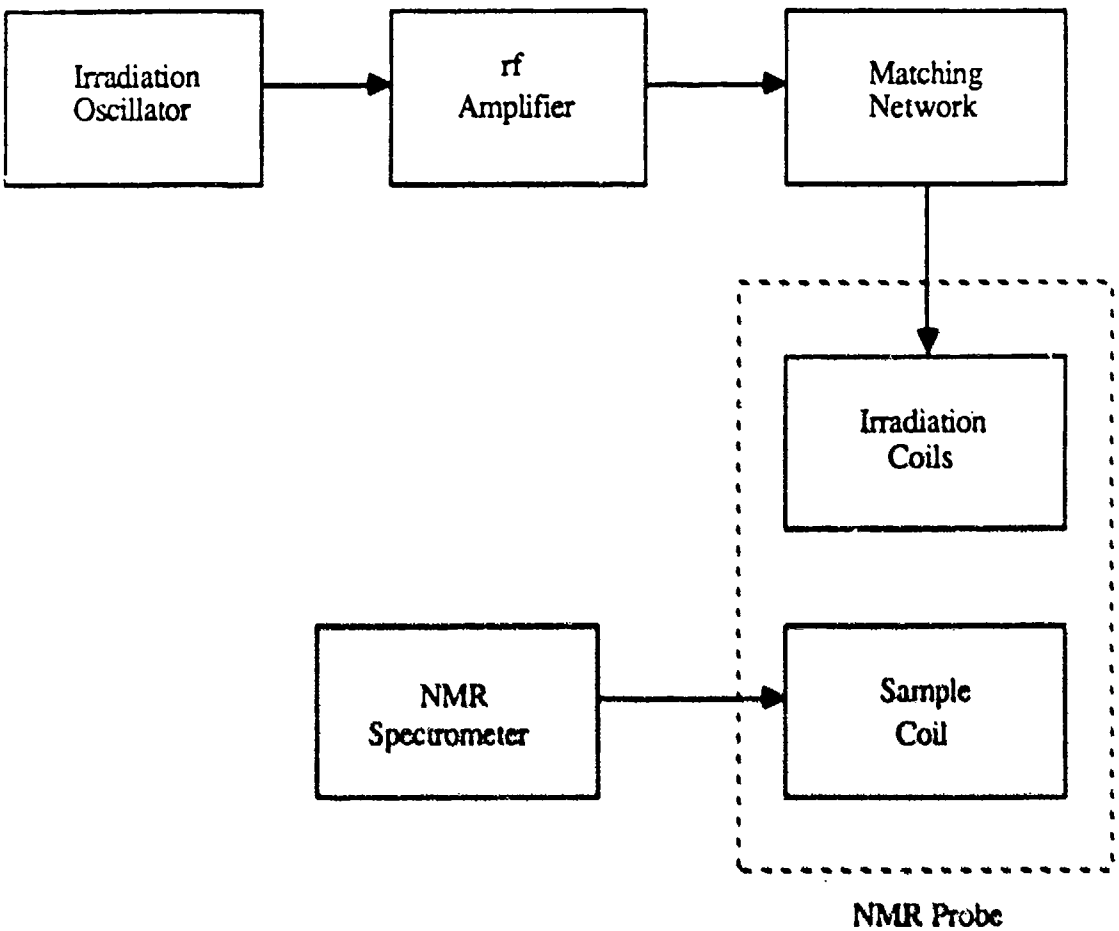


FIGURE 5. BLOCK DIAGRAM OF TWO-COIL DOUBLE IRRADIATION SYSTEM.

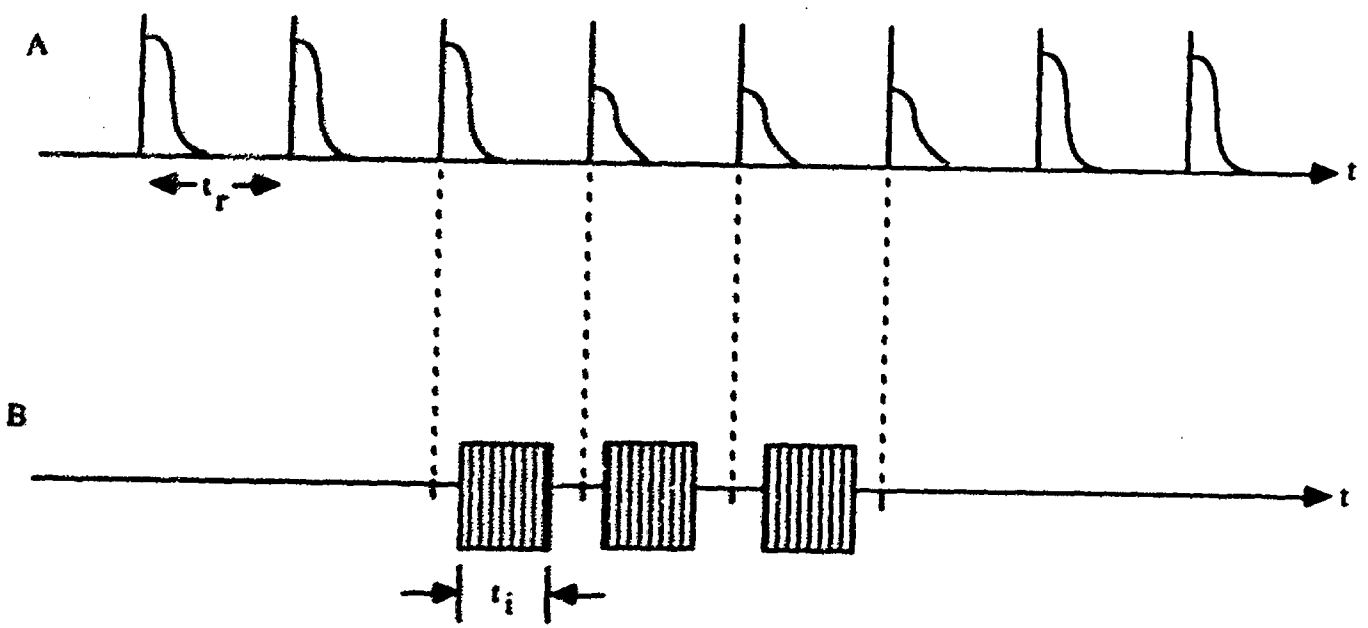


FIGURE 6. TIMING DIAGRAM FOR THE PULSE-TRAIN EXPERIMENT WITH CW RF PUMPING. A: PROTON FID; B: OFF-RESONANCE PUMPING.

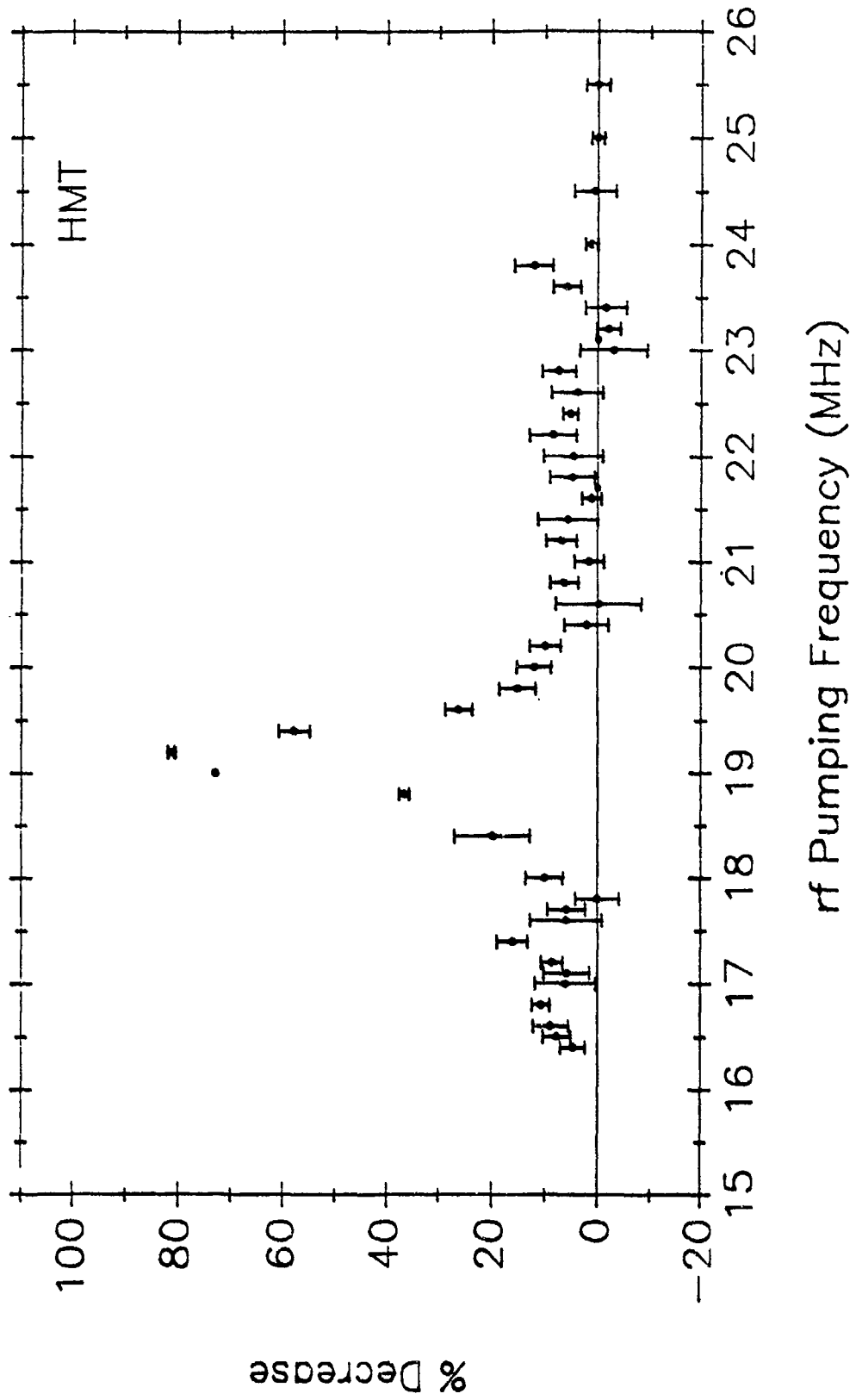


FIGURE 7. OFF-RESONANCE IRRADIATION EFFECTS IN HMT.

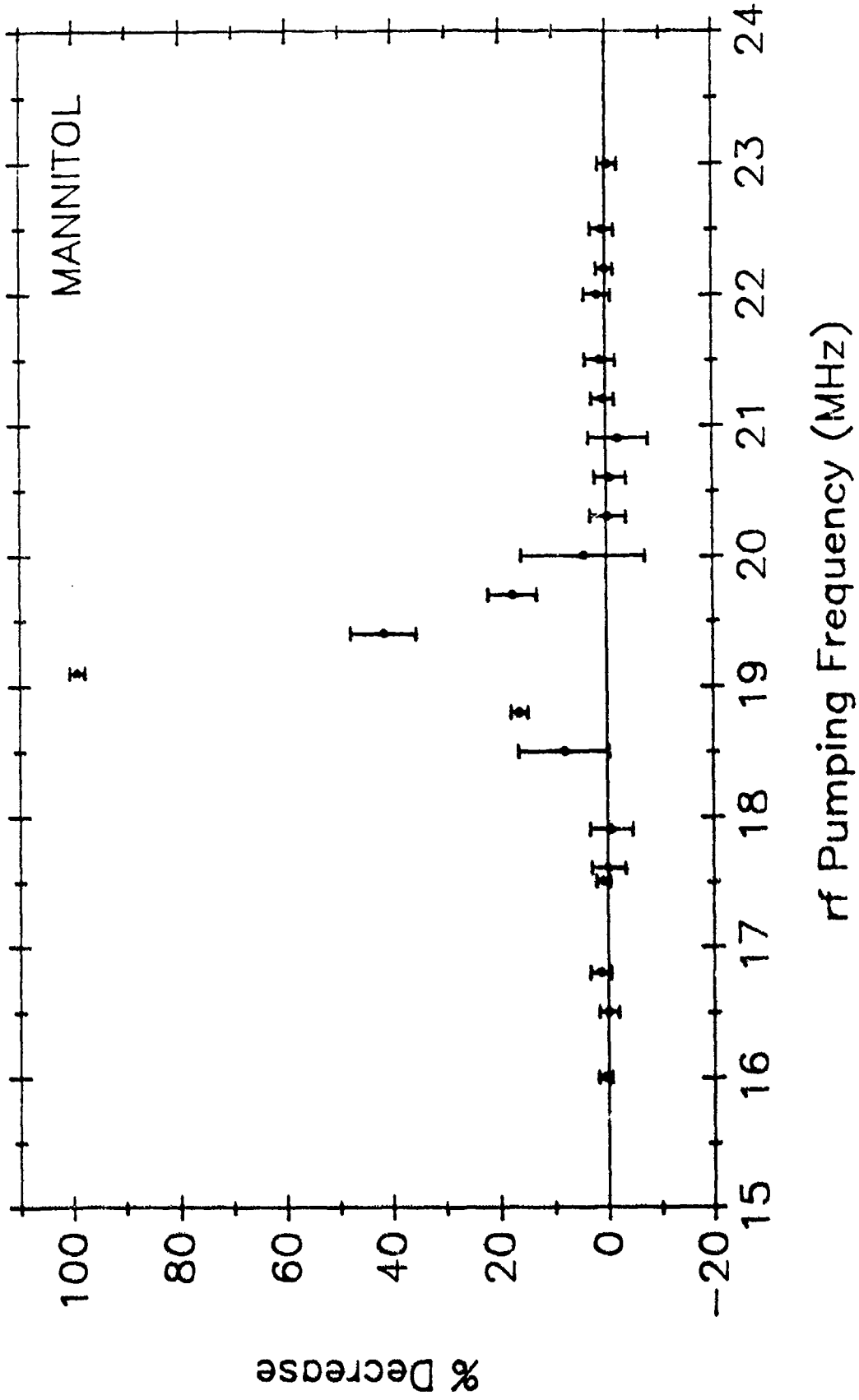


FIGURE 8. OFF-RESONANCE IRRADIATION EFFECTS IN MANNITOL.

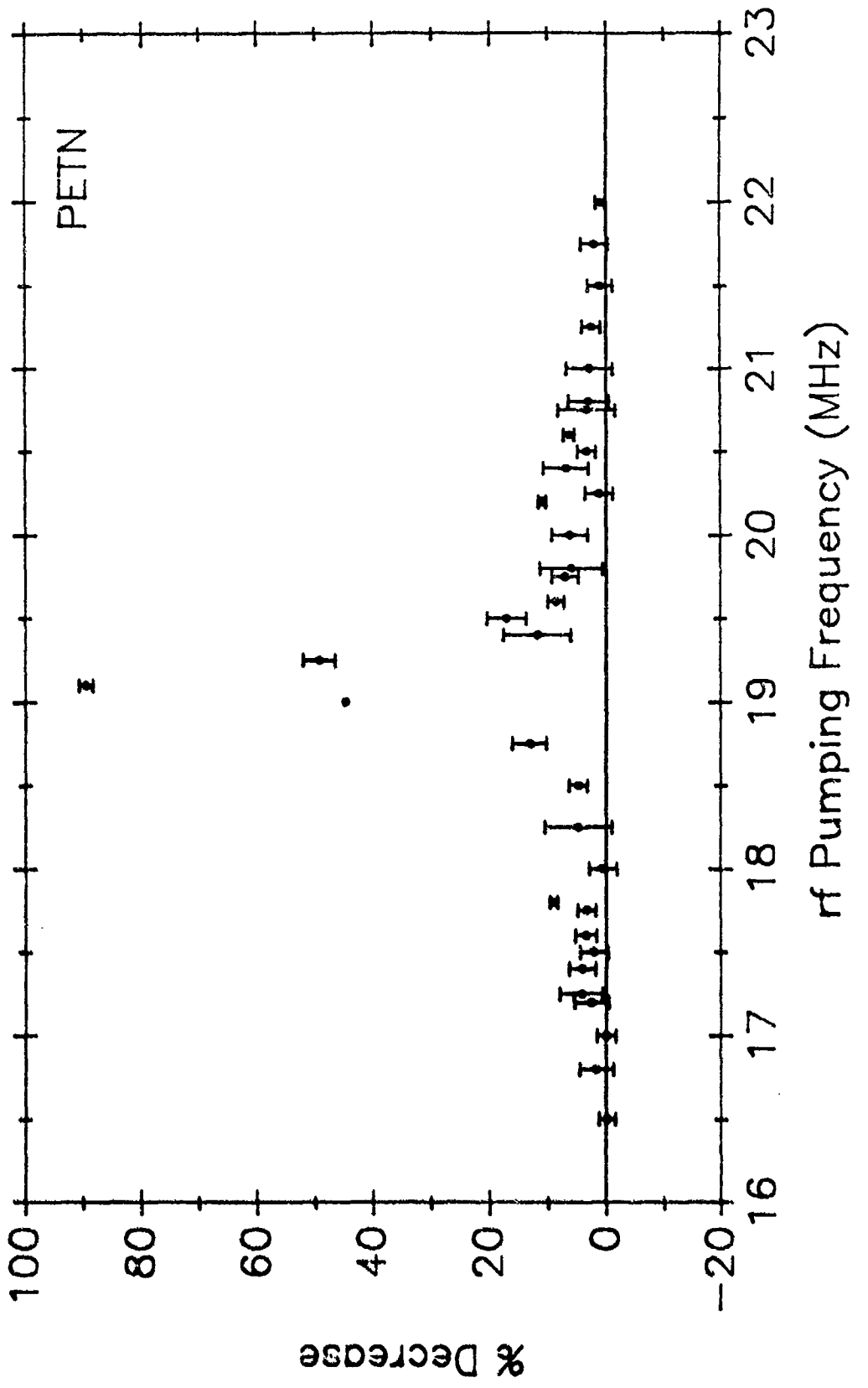


FIGURE 9. OFF-RESONANCE IRRADIATION EFFECTS IN PETN.

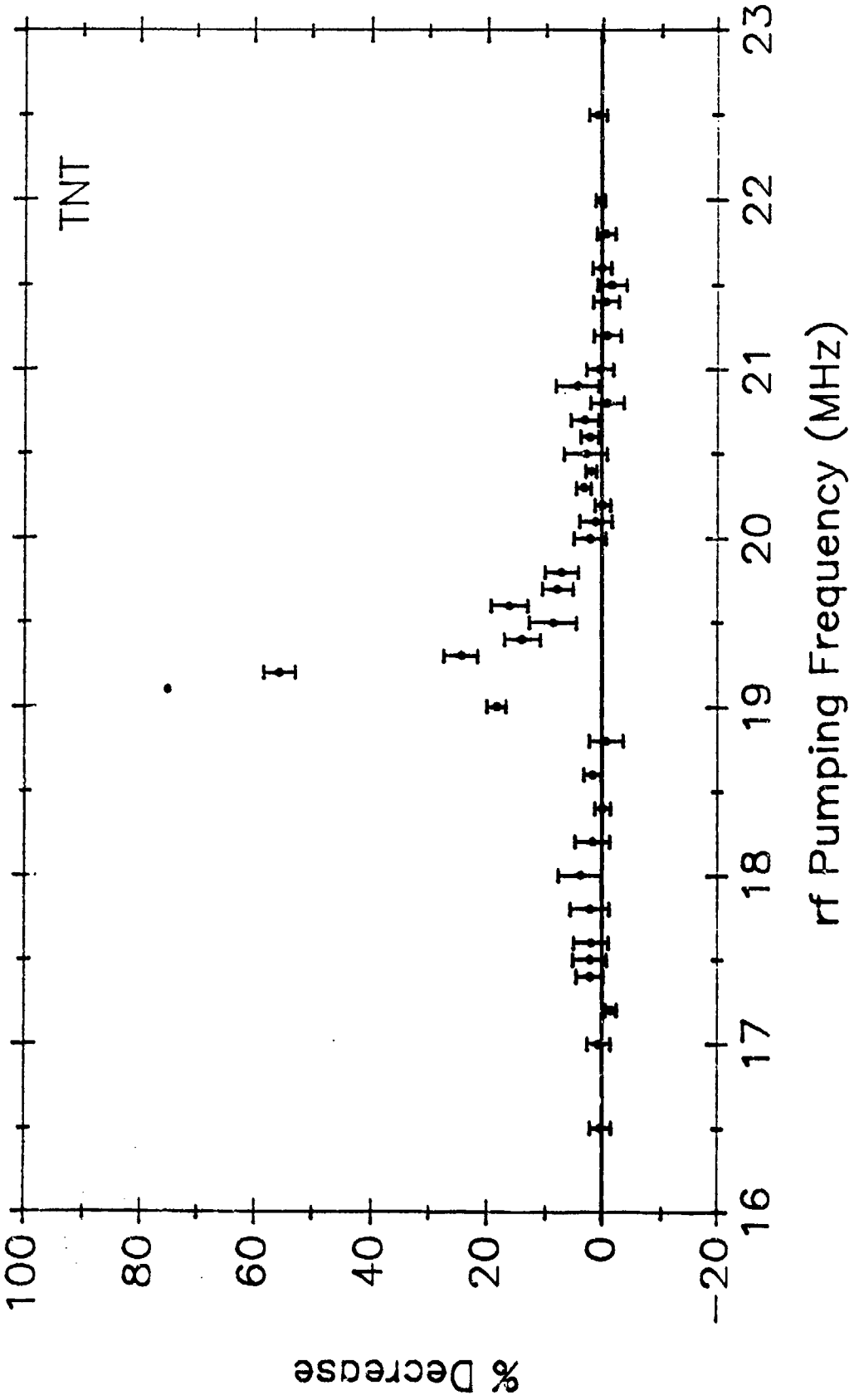


FIGURE 10. OFF-RESONANCE IRRADIATION EFFECTS IN TNT.

APPLICATION OF MAGNETIC RESONANCE TO EXPLOSIVES DETECTION

James Derwin King, Armando De Los Santos,
Colin I. Nicholls, and Williams L. Rollwitz
Southwest Research Institute
San Antonio, Texas

1. INTRODUCTION

An essential element in airport security is the inspection of all hand carried items and checked baggage to detect concealed explosives as well as weapons. An acceptable explosives detection system must be effective in the detection of all explosives that pose a threat to the safety of the passengers, crew and aircraft. It must rapidly and reliably distinguish between explosives and non-explosives and provide detection independent of explosive configuration and distribution. To avoid unnecessary delays the system must also provide rapid automated inspection and have as low a nuisance alarm rate as is consistent with operational and security effectiveness. In addition, the apparatus should not pose a health hazard to either the public or the operators nor damage baggage or contents. It should be reliable and friendly and should be economically affordable in initial cost, installation and operation. Development of the technology or combination of technologies needed to achieve these goals has posed a tremendous challenge to the scientific research and engineering communities. Radio Frequency Resonant Absorption Spectroscopy (RRAS) techniques were considered early in the efforts to find an acceptable solution to this inspection problem and these methods still provide features and capabilities that are largely unmatched by other technologies. Much of the work to successfully apply one of these techniques, hydrogen transient nuclear magnetic resonance (HTNMR), to the practical detection of explosives concealed in letters, parcels and baggage has been carried out by the authors and associates.[1-9,11-21]

HTNMR was first investigated for the detection of explosives nearly twenty years ago.[2] Early in our work it was discovered that explosives exhibited HTNMR signal relaxation properties that allowed the signals from these materials to be distinguished from those of most other materials. This feature is absolutely essential to the successful application of this method for inspection since the vast majority of non-metallic materials contain hydrogen and produce strong hydrogen NMR responses. In addition, ^{1}H-NMR to ^{14}N-NQR level crossing effects were found to be very effective in reducing the detection time for several explosives and also in providing a potentially useful selective signature[2-6]. Methods for implementing rapid detection of explosives based on hydrogen magnetic resonance properties were developed and first applied in an experimental apparatus for the detection of non-metallic land mines.[2,3,6,8,9] In the middle 1970's work was initiated to adapt this technology to the detection of explosives in letters (mail bombs) and, shortly thereafter, to the detection of bulk explosives in checked airline baggage. As part of this work the utility for baggage inspection of the various RRAS methods which includes Nuclear Magnetic Resonance (NMR), Nuclear Quadrupole Resonance (NQR),[1,10] Electron Spin Resonance (ESR), and Microwave Molecular Absorption (MMA) were evaluated.[7] ESR was found to be particularly suitable for detection of black powder, as was NQR for detecting a few of the explosives, notably RDX, while NMR was capable of detecting almost all of the explosives of interest at that time. This included the high energy military explosives as well as the more common commercial explosives such as dynamites and water gels used in civilian construction, excavation and mining activities. Microwave molecular absorption was determined to be of little value since it primarily responds only to selected materials in gaseous form. Based on these conclusions the nuclear magnetic resonance technology, in particular Hydrogen Transient Nuclear Magnetic Resonance (HTNMR), was selected for further study and for subsequent implementation in a form suitable for the inspection of checked airline baggage to detect concealed explosives.

To realize the baggage inspection objective, magnetic resonance apparatus much larger than anyone had ever attempted previously was needed. In addition the capability to provide sensitive, selective and rapid detection of all the explosives of interest while accommodating the wide variety of materials encountered in baggage structures and contents was essential. The capability to distinguish explosives from the non-explosive baggage contents was required to minimize

false alarms. These capabilities were first realized in an experimental system which was demonstrated and evaluated in the laboratory.[7,17] Following this success, the methods were applied to the development of an engineering model of a system suitable for testing in an airport environment (see Figure 1).[17] This objective was achieved and the first airport tests of the NMR baggage inspection technology were conducted in the spring of 1979. This initial series of tests allowed the general suitability of this technology for the inspection of checked airline baggage to be evaluated and a data base of HTNMR properties of checked airline baggage to be acquired. Secondarily the performance and limitations achieved to date in the apparatus could be assessed. The apparatus was found to operate quite well though some shortcomings were recognized where further work was required. In particular the sensitivity to materials inside the bag was lower than required. Subsequent series of airport tests were conducted in 1980, 1983, and 1984 to evaluate the effect of improvements that had been incorporated in the system during the intervening time periods. All of these tests were 6conducted with essentially the same basic apparatus. However, many minor modifications were incorporated to provide uniform detection sensitivity throughout the bag, to reduce spurious alarms, to improve the detection sensitivity and to incorporate additional signal criteria to eliminate false alarms from certain items of baggage contents. Additional modifications which could reduce spurious alarms and improve the detection probabilities were recognized and identified even prior to the last series of tests but these could not be accommodated within the mechanical configuration and frame work that was available in this initial model. Despite these limitations, and known possibilities for improvement, the performance achieved in this system were comparable to the best that has been achieved by systems based on any other technology to date.

HTNMR, like the other RRAS methods, does not use nuclear radiation, radioactive sources, x-rays nor any other form of ionizing radiation. Instead detection is accomplished through magnetic and electromagnetic fields used to sense the hydrogen contained within the materials of the bag and the baggage contents. By analyses and processing of this total hydrogen NMR signal, any contribution to the response produced by hydrogen in explosives can be separated from that produced by hydrogen in most other materials. Through processing of this total HTNMR response, NMR has been found useful for rapidly and selectively detecting nitroglycerine-based dynamites, water gel explosives, C-4 (plastic) explosives, RDX, TNT, PETN, smokeless powder and most other high-energy and commercial explosives and propellants. Results of several thousand tests have demonstrated the general suitability of the HTNMR method for baggage inspection and have shown a high detection probability and a low rate of false alarms. In the original implementation the system could not effectively inspect a small percentage of the bags but those were identified by the apparatus. As an additional limitations, it is advisable to remove magnetically recorded media prior to inspection to avoid possible erasure and liquid explosives were not selectively detected. Work currently underway is expected to greatly alleviate these limitations.

2. BASIC METHOD

Nuclear magnetic resonance is generated by interactions between the magnetic moment of atomic nuclei in materials being inspected and an externally applied magnetic field. The frequency of this resonance is typically in the high radiofrequency range and is dependent upon the intensity of the applied magnetic field and the specie of the nuclei. In the case of hydrogen the resonant frequency, f_o, is related to the magnetic flux density, H_o by

$$f_o = 42.57\ H_o \qquad (1)$$

where

f_o = frequency, MHz
H_o = Magnetic flux density, T (Tesla)

The choice of the frequency used for NMR is somewhat arbitrary but is based on tradeoffs between the improved sensitivity available at higher magnetic fields and the greater size, weight and cost of the required magnet structures and the increased potential for damage to baggage contents, as the flux density is increased.

Figure 2 illustrates the basic NMR detection concept. The item being inspected is located in a magnetic field of selected intensity, H_o, and tested with an electromagnetic field having a frequency, f_o, corresponding to the nuclear resonance. In the transient mode of operation as used for baggage inspection the electromagnetic field is applied in short pulses (RF bursts) of controlled width and amplitude. Detected NMR responses are in the form of transient radio frequency signals emitted by the excited nuclei following the burst of transmitted energy. The frequency of the emitted NMR signal is that for nuclear resonance in the applied magnetic field, H_o, and the peak amplitude is proportional to the number of nuclei contributing to the response. The transient, free induction decay (FID), signal following

a single transmitter pulse decreases in amplitude at a rate which, in a homogeneous magnetic field, is dependent upon the spin-spin time constant, T_2. This time constant is characteristic of the molecular structure and the state of the sample material as is the spin-lattice time constant, T_1, which sets the time required to detect an NMR response and the rate at which NMR tests may be repeated without signal degradation. Transient NMR for explosives detection makes use of multiple transmitted pulses of appropriate energy and spacing to aid in achieving selectivity to the time constants and to the ^1H-^{14}N cross coupling properties of the signal from explosives.

The block diagram in Figure 3 shows the basic components for a transient NMR system. The sequencer generates the pulses of appropriate widths and repetition rates to drive the radio frequency transmitter and to control the signal processing. Pulses of radio frequency energy applied to the sample coil through the coupling network produce the required pulsed electromagnetic (RF) field in the sample. The sample coil also senses the NMR response and connects the signal through the coupling network to the receiver where it is amplified and demodulated. After detection, the HTNMR signal is processed to extract the desired information and the results displayed, recorded or used for control.

3. APPLICATION TO EXPLOSIVES DETECTION

Any acceptable explosives detection system must rapidly inspect all bags, in "as received" condition, without causing damage and must reliably detect all explosives in quantities of concern regardless of the configuration and distribution and must produce a minimum of false alarms. These criteria can be realized only if the apparatus responds to a signature that is specific to explosives and which is not encountered in other materials commonly found in quantity in baggage. In addition the inspection apparatus must have sufficient sensitivity to produce a signal level from the smallest quantity of explosive of interest that is well above both the apparatus noise level and any clutter level which results from the baggage contents. This condition must hold even in the presence of the degrading effects of the bags and contents. These capabilities have been realized in magnetic resonance inspection apparatus through use of rather simple and un-sophisticated NMR techniques compared to those that are now available and common in analytical and imaging laboratories. However, these simple methods do work quite well in the practical environment encountered in airport baggage inspection.

In the HTNMR system the baggage passes through a polarizing magnetic field of selected intensity and then into the inspection magnet. Initially the bags moved continuous through the apparatus at a speed of about 2-feet/second. In this "continuous mode" the detection sensitivity was found to be acceptable but the "false alarm" rate was too high. To alleviate this problem the bags now pause for less than one (1) second in the inspection magnet while the HTNMR data required for inspection is acquired. The bag remains stationary for a short time while the computer processes the data and indicates "alarm", "pass" or "inadequate test". In the system previously implemented the inspection rate was 10 to 12 bags per minute but this can potentially be increased to near 30 bags per minute.

The HTNMR data required for processing is obtained in a set of multiple pulse sequences. These data allow HTNMR signals from materials having the characteristics of explosives to be recognized in the presence of the (typically) much larger HTNMR signals from the normal baggage contents. The processing algorithms are such that effects of the baggage and contents on the magnetic field intensity and homogeneity and on the sensor coil resonance characteristics are minimized. The result is that quantities of explosives greater than the threat level can be detected with a high probability while potential false alarms from much greater quantities of non-explosive materials are greatly suppressed. This is accomplished in essentially one test sequence without benefit of any signal averaging by making use of the T_1, T_2 and ^1H - ^{14}N level crossing characteristics of the HTNMR signals.

4. ENHANCED PERFORMANCE

There are several areas where enhanced performance could make magnetic resonance technology even more capable of meeting the needs for an operational explosive detection system. One of these is operation at lower magnetic field intensities to eliminate the need to remove recorded magnetic media prior to inspection and to enhance the capability to effectively inspect all bags.

The original work was directed toward detection of bulk (solid) explosives but developments over the past several years have shown the need to also detect liquid and emulsion type explosives. Means for adding this capability are known.

Improved specificity to explosives could produce substantial reduction in the false alarm potential and perhaps also extend the capability to detect smaller

quantities of explosives. Increased tolerance for the effect of the bag and contents could also potentially improve the detection probability and reduce the false alarm rates.

Of course, to be acceptable any or all of the foregoing enhancements must be achieved without substantially increasing the inspection time, the magnetic field intensity, or the size, weight and cost of the apparatus. The improvements must also cause no damage to the bag, be accomplished with acceptable baggage handling practices, and be tolerant of the effects of the bag and contents on the RF and magnetic field homogeneities and intensities. Current work of the authors is being directed toward practical achievement of enhanced capabilities in most of the identified areas.

REFERENCES

1. King, J.D., "Nuclear Quadrupole Resonance in Ammonium Chlorate and Ammonium Perchlorate," M.S. Thesis St. Mary's University, San Antonio, Tx. (May 1963).

2. King, J.D., Rollwitz, W.L., and Matzkanin, G.A. "Nuclear Magnetic Resonance Mine Detection, Part I," USAEERD Contract No. DAAK02-72-C-0467, Final Report, AD 5225380, October 1973.

3. King, J.D., Matzkanin, G.A., Shaw, S.D., and Squire, R.E., "Nuclear Magnetic Resonance Mine Detection, Part II," USAMERDC Contract No. DAAK02-72-C-0467, Final Report AD 52 709L, December 1973.

4. Gonano, R., Matzkanin, G.A., King, J.D., and Rollwitz, W.L., "Hydrogen-Nitrogen Cross Relaxation in Hexamethylenetetramine," presented at 3rd International NAR Conference, Tampa Florida, April 1975.

5. Gonano, R., Stewart, G.S., King, J.D., Matzkanin, G.A., and Rollwitz, W.L., "Concealed Explosives Detection by Means of Nuclear Resonance Techniques," Proceedings of the 1975 Carnahan Conference on Crime Countermeasures, Lexington, Kentucky. pp. 14-148, May 1975.

6. King, J.D., Rollwitz, W.L., and Matzkanin, G.A., "Nuclear Magnetic Resonance Techniques for Explosives Detection," U.S. Army Mobility Equipment Research and Development Center, Final Report, Contract No. DAAK02-74-C-0056, AD-C-003154, June 1975.

7. Rollwitz, W.L., King, J.D., and Shaw, S.D., and U.S. Department of Transportation, "Determining the Potential of Radiofrequency Resonance Absorption Detection of Explosives Hidden in Airline Baggage, Parts I and II," FAA Report No. FA-RD-75-29 October 1975.

8. King, J.D., De Los Santos, A., Rollwitz, W.L., "Nuclear Magnetic Resonance Techniques for Explosives Detection, Part III," U.S. Army MERADCOM, Final Report Part III, Contract No. DAAK02-74-C-0056, AD-B026059, Feb. 1977.

9. King, J.D., De Los Santos, A., Rollwitz, W.L., "Nuclear Magnetic Resonance Techniques for Explosives Detection, Part IV," U.S. Army MERADCOM, Final Report Part IV, Contract No. DAAK02-74-C-0056, AD-B026430, Fed. 1978.

10. Marino, R.A., "Detection and Identification of Explosives by Nitrogen-14 NQR," Proceedings of The New Concepts Symposium and Workshop on Identification and Detection of Explosives, Reston, VA., Nov. 1978.

11. King, J.D., Rollwitz, W.L., Gonano, J.R., "Applications of Nuclear Resonance Techniques to the Detection of Explosives," 1978 Carnahan Conference on Crime Countermeasures Lexington, Ky., May 1978.

12. King, J.D., Rollwitz, W.L., De Los Santos, A., Gonano, J.R. "Applications of Nuclear Magnetic Resonance to the Detection and Identification of Explosives," Proceedings of the 1978 New Concepts Symposium on the Detection and Identification of Explosives, Reston, VA., published April 1979.

13. King, J.D., Rollwitz, W.L., and Gonano, J.R., "Detection of Contraband on the Person by Means of Nuclear Magnetic Resonance," Proceedings of the 1978 New Concepts Symposium on the Detection and Identification of Explosives, Reston, VA, published April 1979.

14. Rollwitz, W.L., King, J.D., and Matzkanin, G.A., "Fundamentals of NMR for the Detection and Identification of Explosives," Proceedings of the 1978 New Concepts Symposium on the Detection and Identification of Explosives, Reston, VA, published April 1979.

15. King, J.D., "NMR Discrimination Apparatus and Method Therefor," U.S. Patent No. 4,166,972, (Sept. 4, 1979) Israeli Patent No. 58,168, Canadian Patent No. 1,130,631.

16. King, J.D., Rollwitz, W.L., and De Los Santos, A., "Advances in Magnetic Resonance for the Detection of Bulk Explosives," Proceedings of the 3rd International Conference on Security through Science and Engineering, Berlin, W. Germany, Sept. 23-26, 1980.

17. De Los Santos, A., King, J.D., Rollwitz, W.L., "Development and Evaluation of a Prototype Checked Baggage System--NMR Technique," U.S. Dept. of Transportation, Federal Aviation Administration, Final Report Contract No. DOT-FA77WA-3968, FAA-RD-8-46, Feb. 1981, also Addendums I, II, III, and IV.

18. King, J.D., Rollwitz, and De Los Santos, A., "Nuclear Magnetic Resonance for Explosives Detection," ASTM Symposium on Airport Security, Philadelphia, PA April 22, 1982.

19. Rollwitz, W.L., and J.D. King, "Radiofrequency Resonance Absorption Spectroscopy (RRAS) Methods for the Detection and Analysis of Explosive," Proceedings of the International Symposium on Analysis and Detection of Explosives, FBI Academy, Quantico, VA, March 29-31, 1983.

20. King, J.D., Rollwitz, W.L., and De Los Santos, A., "Magnetic Resonance Inspection Systems for Explosives Detection," ASTM Symposium on Explosives Detection for Security Applications, Philadelphia, PA., April 1983.

21. De Los Santos, A., et. al., "Baggage Inspection Apparatus and Method for Determining the Presence of Explosives," U.S. Patent No. 4,514,691 (April 30, 1985).

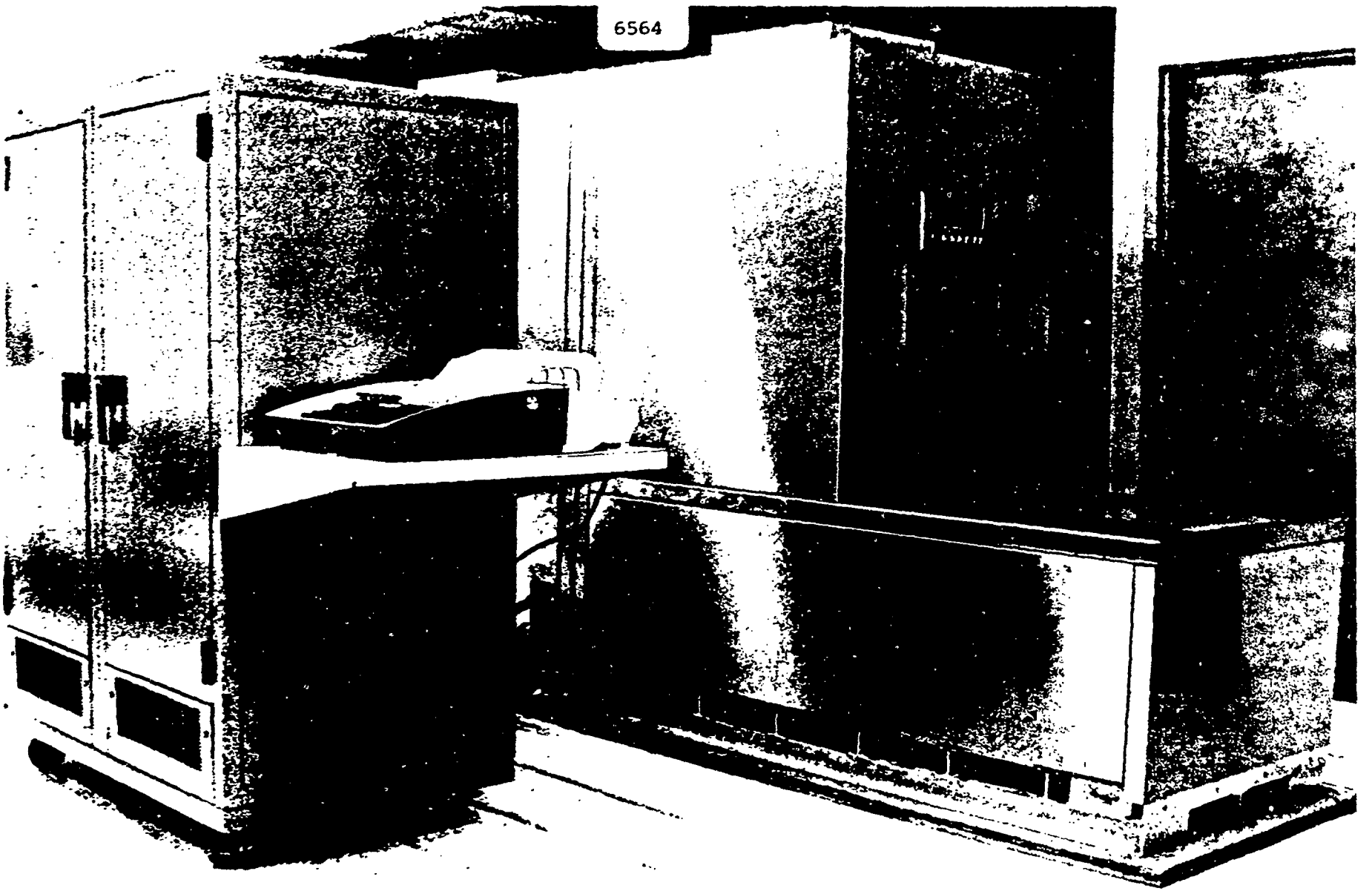


FIGURE 1. PROTOTYPE BAGGAGE SYSTEM

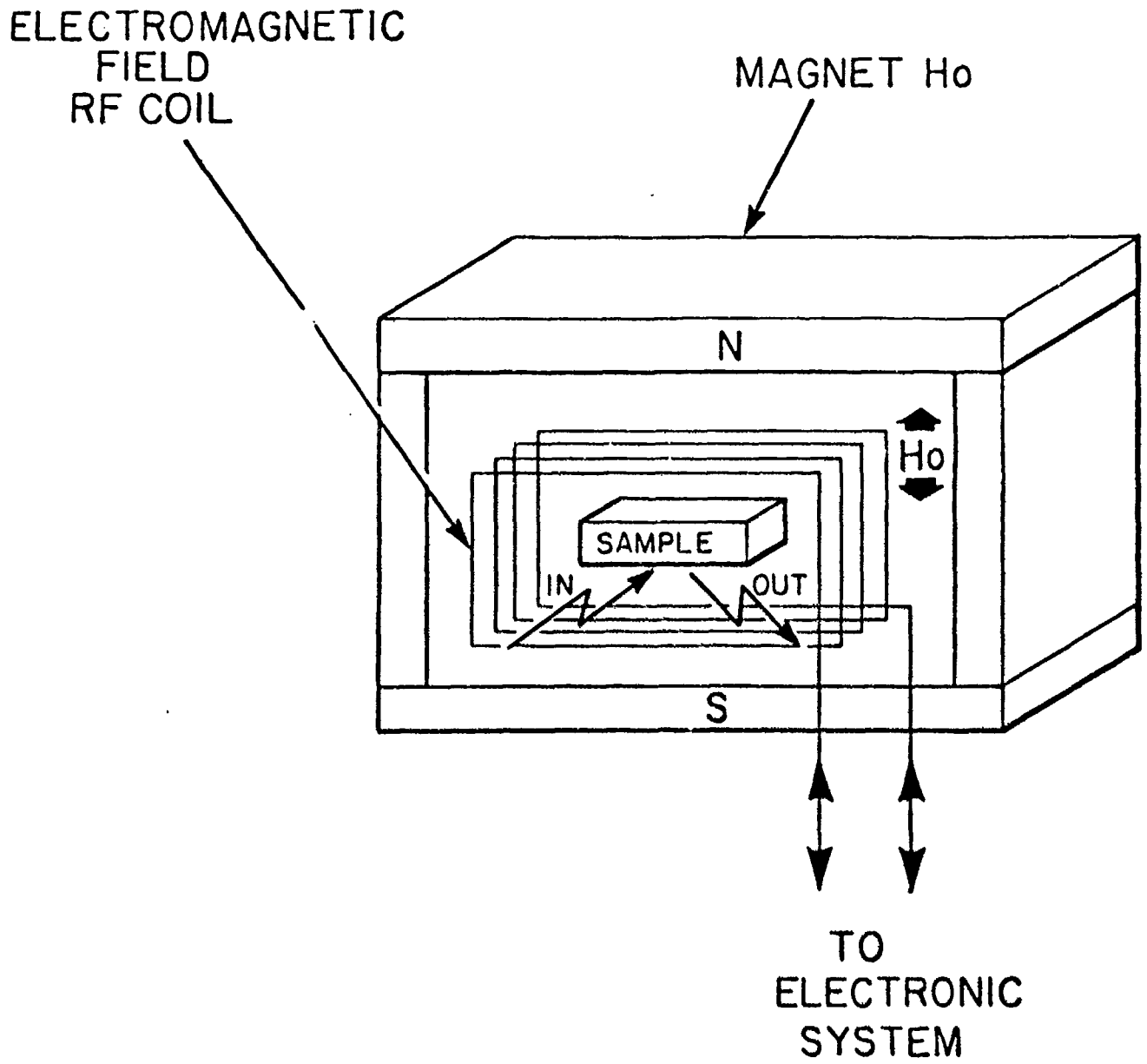


FIGURE 2. BASIC NMR DETECTION CONCEPT

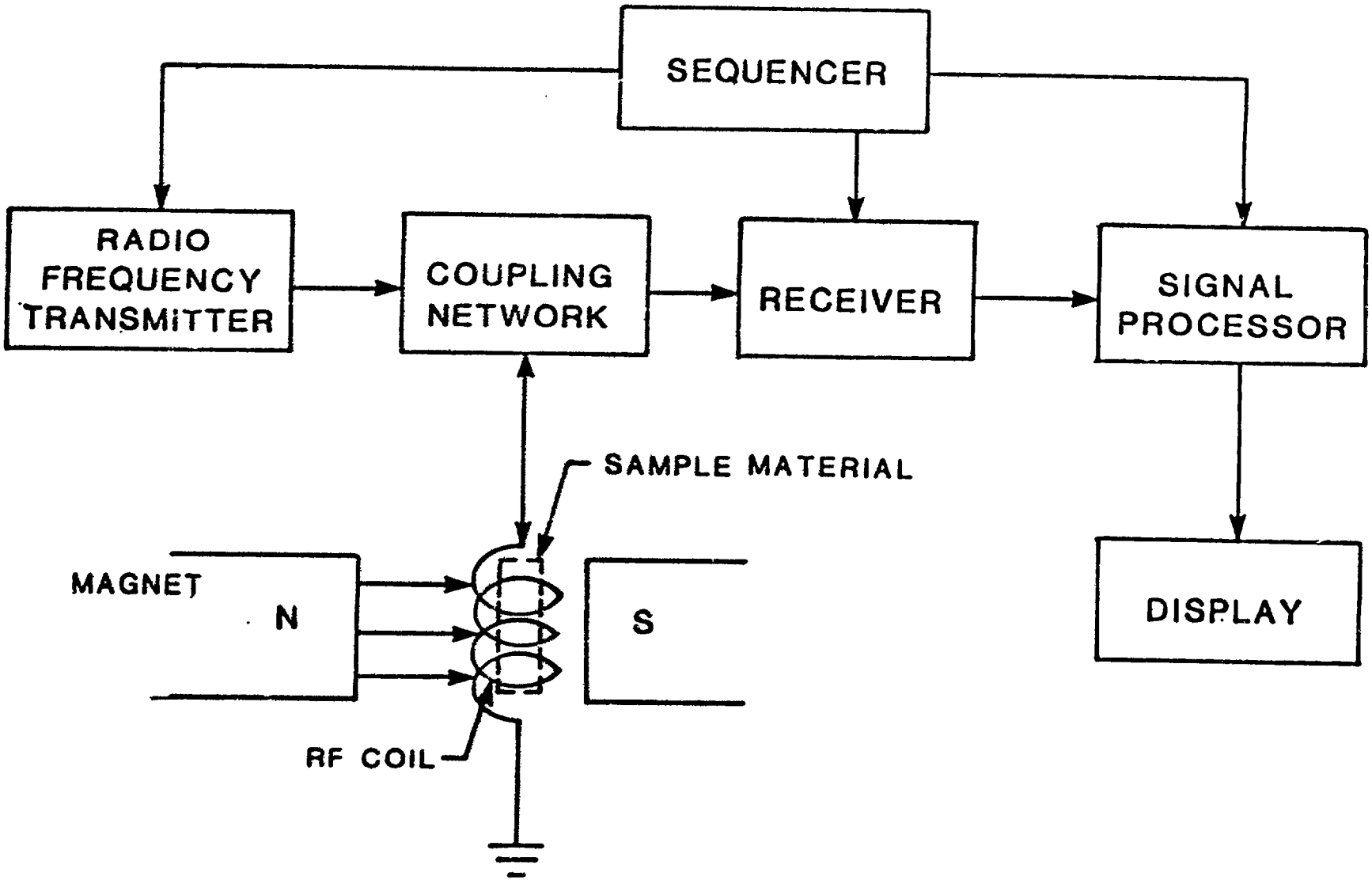


FIGURE 3. BLOCK DIAGRAM OF TYPICAL TRANSIENT NMR SYSTEM

EXPLOSIVE DETECTION USING MICROWAVE IMAGING

David G. Falconer, Ph.D., and David G. Watters, Ph.D.
Remote Measurements Laboratory
SRI International Menlo Park, CA 94025

1. INTRODUCTION

We have developed a microwave technique for detecting high-explosives (HEs), illegal drugs, and other contraband in checked airline luggage. Our technique detects chemical contraband by microwave radiation and measuring the magnitude and phase of the backscattered radiation with coherent receivers. From the collected data, we form a three-dimensional image of the checked luggage and its contents by means of pulse-synthesis and synthetic-aperature techniques. Special image-segmentation software isolates suspicious portions of the microwave image in preparation for spectroscopic analysis. We estimate the microwave spectrum of the isolated volumes using an inverse Fourier-transform algorithm. Suspicious chemicals are identified by examining the estimated spectrum for characteristic absorption lines and resonance structure.

We have demonstrated our inspection technique using simulants for both HE and cocaine. In particular, we have used our microwave anechoic chamber to illuminate and image a soft-sided suitcase containing both powdered sugar (our cocaine simulant) and ammonium sulfate (our HE simulant). We then segmented the suspicious portion of the microwave image. Using inverse algorithms, we returned our segmented data to the frequency domain and thereby obtained rough estimates of the microwave spectra of the suspicious regions. Finally, we have compared the estimated spectra with reference ones taken on bulk samples of the same materials and were readily able to differentiate the two simulants.

2. SPECTROSCOPIC MICROWAVE IMAGING

2.1 Microwave Imaging

Radio-frequency engineers use spatial and temporal diversity to form three-dimensional images of their microwave targets. Although implementations vary widely, the traditional approach to microwave imaging uses mechanical motion to scan the azimuthal coordinate, pulsed or frequency-swept illumination to obtain the range coordinate, and a receiver array to measure the elevational coordinate. The azimuthal scan, which can be almost arbitrary, is usually achieved by translating or rotating either the target body or the illuminating device. (Translational and rotational motions allow one to image the azimuthal coordinate with a fast Fresnel or Fourier transform, respectively.) The microwave illumination can also take many forms,including a sharp(nanosecond-type) pulse,a chirped (linear FM) emission, or sequenced (pseudorandom) illuminations. (In the latter two cases, analog or digital processing serves to synthesize a narrow pulse.) Although the elevational coordinate can be also be obtained with a mechanical scan, time and cost constraints usually favor receiver arrays that can gather the scattering data in some parallel fashion.

2.2 Microwave Spectroscopy

Microwave spectroscopy provides information about the molecular, as opposed to the atomic, structure of the test sample. In backscatter spectroscopy, one illuminates the test sample with microwave radiation of varying wavelength, measures the amount of backscattered radiation at each wavelength, and, using appropriate calibration data, computes the volumetric scattering cross section for the test sample as a function of wavelength. (Microwave spectroscopy is capable of measuring both the complex permittivity and permeability of the test sample, although unit permeability is often assumed.) Absorption and resonance bands, as well as the general scattering level, provide clues as to the chemical nature of the illuminated sample.

Microwave spectroscopy differs from atomic spectroscopy in that the absorption and resonance lines are highly broadened, i.e. have low Q values. Such broadening, which is traceable to coupling mechanisms, thermal agitations, and dissipative losses at the molecular bonds, reduces the discrimination capability of microwave spectroscopy. Microwave spectra are also subject to optical type effects, e.g.,

constructive and destructive interference. Such interference occurs when the radiation wavelength is comparable to the physical size of the test sample. The latter effects distort the recorded spectra and must be treated before identifying the resonance and absorption bands of the test chemical itself. When the test sample is heterogeneous, one must image the test sample, segment the microwave image into homogeneous regions, and finally apply the spectroscopic procedure to each region individually.

3. LABORATORY STUDIES

3.1 SRI's Rest Chamber

Figure 1 contains plan and elevational drawings of SRI 's REST Chamber. The transmit horn serves to illuminate the target zone; the receive horn measures the amplitude and phase of the backscattered radiation. An absorbing baffle between the two horns isolates the transmit horn from the receive horn. An HP 8510 network analyzer steps the transmit horn from 2-18 GHz in as many as 801 distinct steps. The microwave target sits atop a rotating inflatable or foam column and is illuminated by the transmit horn at the 100-mW level. As the target rotates, the HP 8510 measures and digitizes the backscattered radiation. The digitized measurements are then handed over to an HP Spectra computer, which forms a two-dimensional image of the scattering body. The imaging system is calibrated using an aluminum sphere. Miscellaneous reflections (range clutter) are suppressed with phasor-differencing techniques. Using a color graphics monitor, the system operator can segment the two-dimensional imagery with respect to its downrange and crossrange coordinates. Following segmentation, selected regions are inverse-transformed with respect to their downrange and crossrange coordinates, which yields each region's scattering cross section as a function of illumination wavelength.

3.2 Bulk-Sample Spectra

We have used our REST Chamber to develop approximate reference spectra for HE and cocaine simulants. In particular, we have illuminated a 6-oz cup of ammonium sulfate with microwave radiation between 2-18 GHz and then recorded the backscatter level at each illumination wavelength. The resulting recording, which is shown in the upper curve of Figure 2, indicates the general scattering level for this simulant. (The several scallops in the recorded pattern are not spectroscopic-type absorption or resonance lines, but rather interference effects associated with the size, shape, and contents of the 6-oz cup.) We have also illuminated a similar volume of two cocaine simulants, granulated and powdered sugar. Note that the microwave cross sections for these samples, shown as the lower two curves of Figure 2, are roughly 12 dB lower than that for the HE simulant. Note too that the maxima and minima of the two scattering patterns appear at different frequencies and with different periodicities, as would be expected with chemicals of differing refractive indices.

3.3 Microwave Image of Soft-Sided Suitcase

To illustrate our wall-penetration capability, we placed a 2 lb box of ammonium sulfate in a soft-sided suitcase and then imaged this target in our REST Chamber. A monochrome version of the microwave image is shown in Figure 3. The walls of the suitcase can be seen as a coarse outline, and the box of ammonium sulfate can be seen within the walls' outline. The downrange resolution ($c/2\Delta f$) for this imagery is governed by the band width (Δf) of the illuminating radiation, and the crossrange resolution ($\lambda R/2D$) by the radiation wavelength (λ), synthetic aperture (D), and target range (R).

3.4 Comparison of Reference and Estimated Spectra

To illustrate our concepts for detecting and identifying chemical contraband in checked luggage, we have manually segmented the image into its benign (walls) and suspicious areas (ammonium sulfate). We then discarded the benign portions of the microwave image and inverse-transformed the remaining portion, thereby obtaining the scattering spectrum shown in the dashed curve of Figure 4. When compared against the two bulk spectra (Figure 2), it is clear that the general level of the estimated spectrum is comparable to that for ammonium sulfate, but far stronger than that for granulated or powdered sugar. As noted above, the peaks and nulls of the microwave spectra shown in Figures 2 and 4 are related to the physical shape of their respective containers (cup or box), not to the absorption spectra of the chemicals themselves. Hence, the spectral details of the three curves are not directly comparable and thus provide no additional identifying information on the test sample.

4. CONCLUSIONS AND RECOMMENDATIONS

We find that microwave techniques are capable of penetrating and imaging the interiors of nonmetallic suitcases. With appropriate image segmentation, such techniques can estimate the general level of microwave scattering for each chemical compound within the suitcase. Under favorable conditions, the estimated spectra serve to identify the molecular character of each segment of the microwave image.

Our technique for detecting chemical contraband could benefit from operation at higher microwave frequencies, e.g., 30-100 GHz. Higher illumination frequencies would also provide better spatial resolution and a more productive spectral band for differentiating molecular compounds. However, higher-frequency illumination would penetrate suitcase walls less effectively and would thus require higher power (1-W) illuminators. Such illuminators are still safe and well within the microwave/millimeter-wave art.

Our discussion has neglected a number of technical issues special to the microwave imaging. In particular, we have set aside the second-order effects of beam attenuation and multiple scattering. These issues can be important ones, especially when imaging targets that fail the traditional assumption that the scattering body "represents tenuous or diaphanous medium." Microwave specialists, including SRI International, are currently devoting considerable time and energy to the management and treatment of these effects.

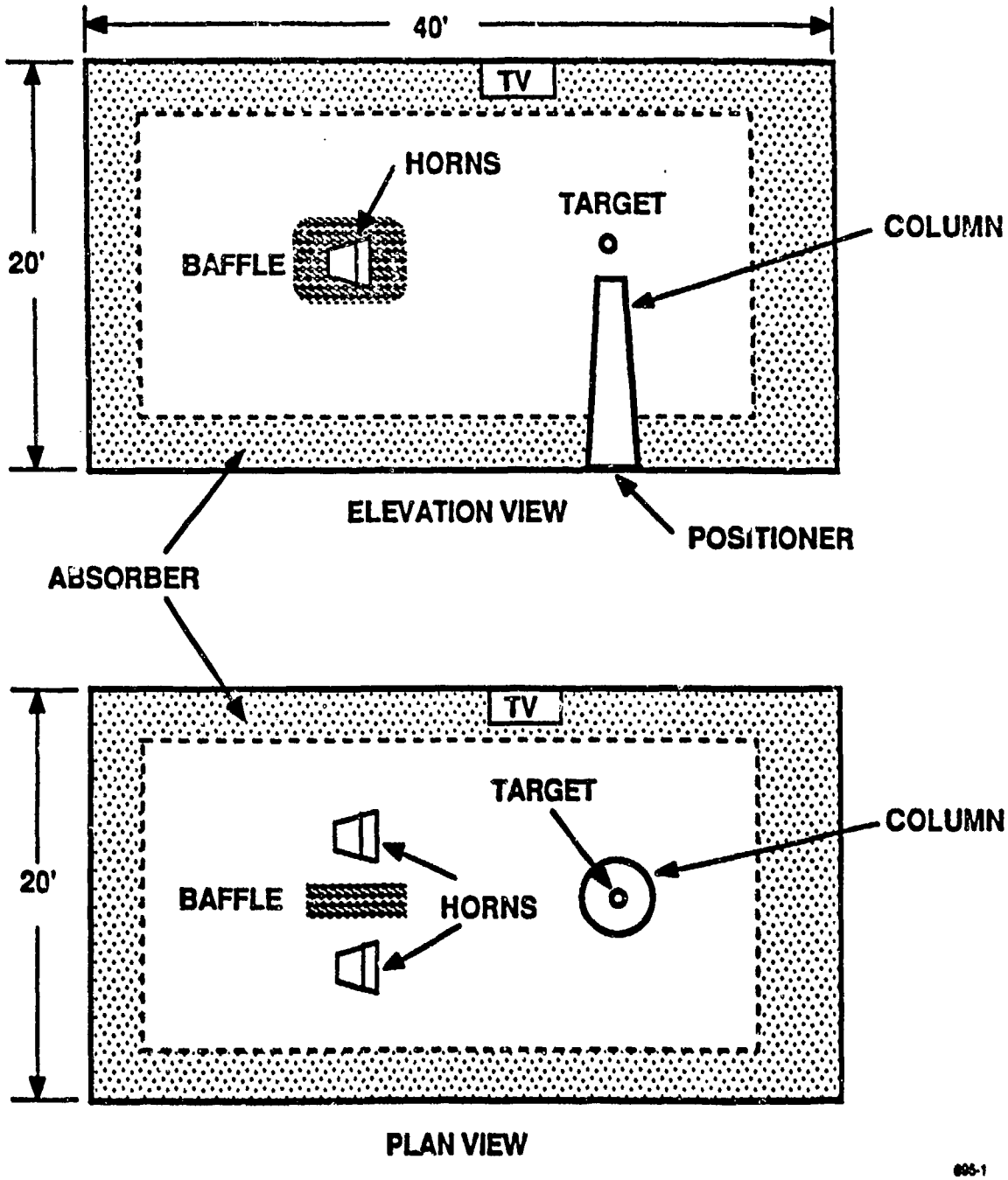


FIGURE 1 SRI'S REST CHAMBER. THE TRANSMIT AND RECEIVE HORNS ARE EFFECTIVE FROM 2-18 GHz.

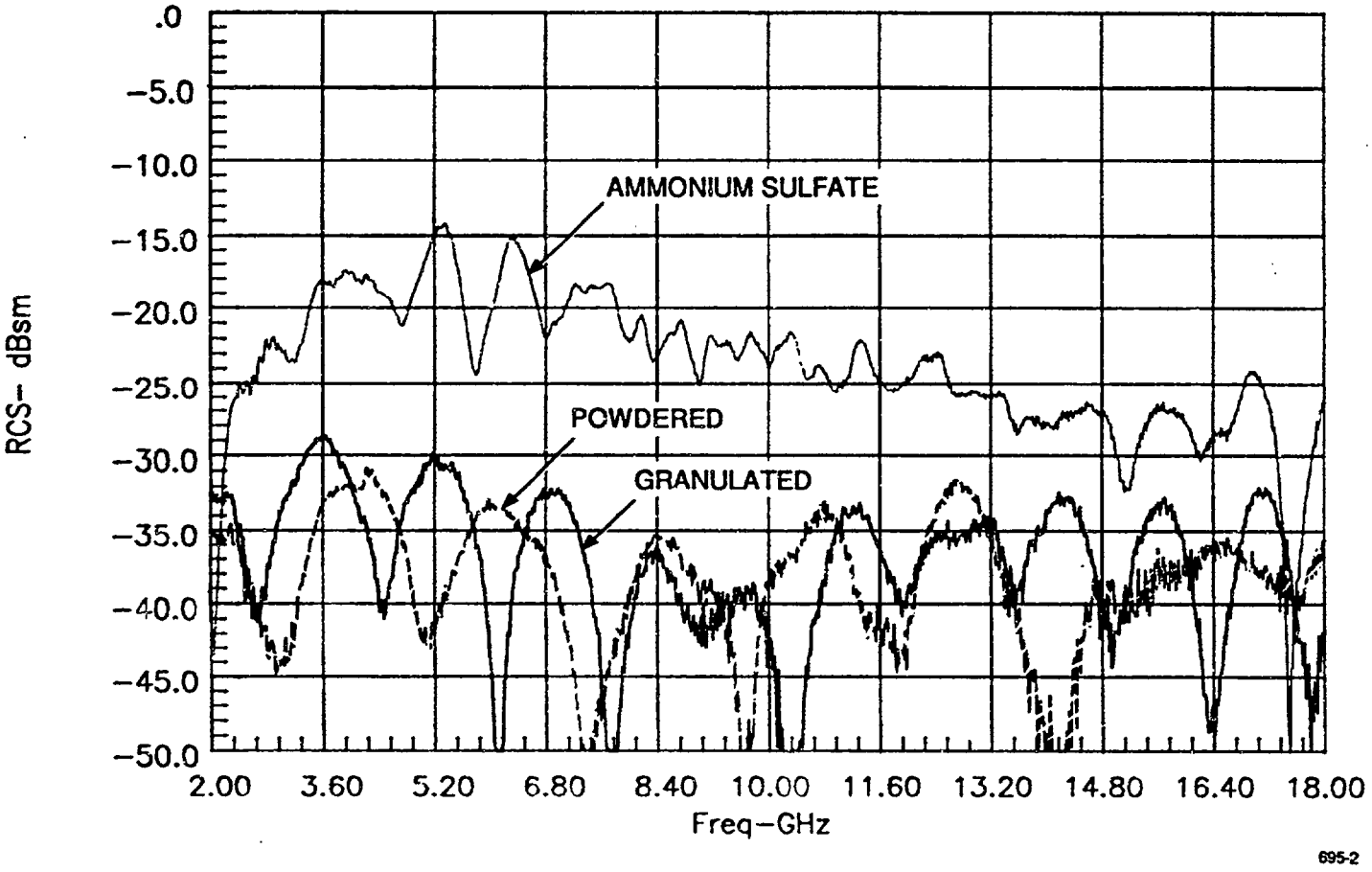


FIGURE 2 BULK SCATTERING SPECTRA FOR AMMONIUM SULFATE, GRANULATED SUGAR, AND POWDERED SUGAR

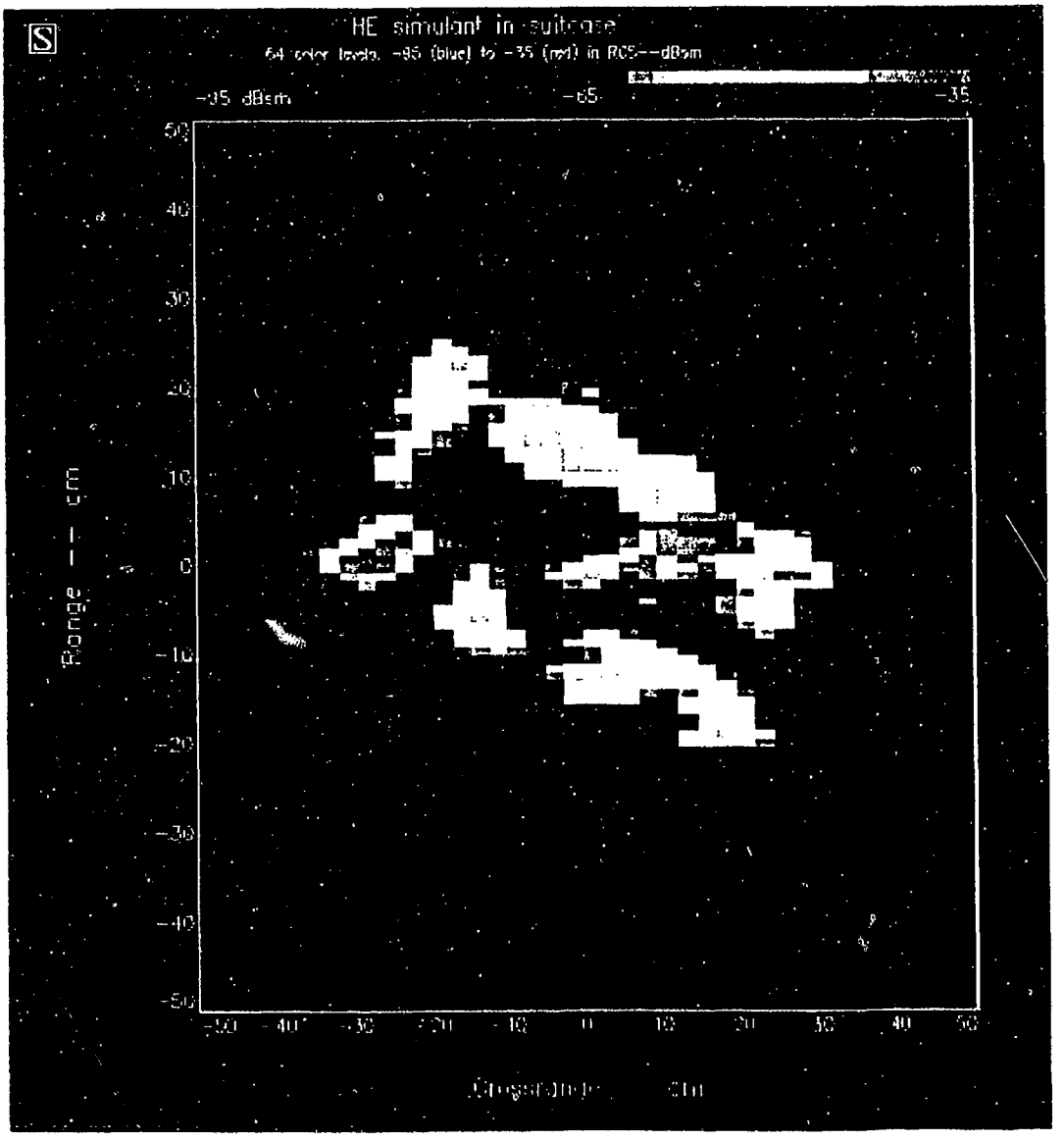


FIGURE 3 MICROWAVE IMAGE OF SUITCASE CONTAINING 2-lb BOX OF AMMONIUM SULFATE

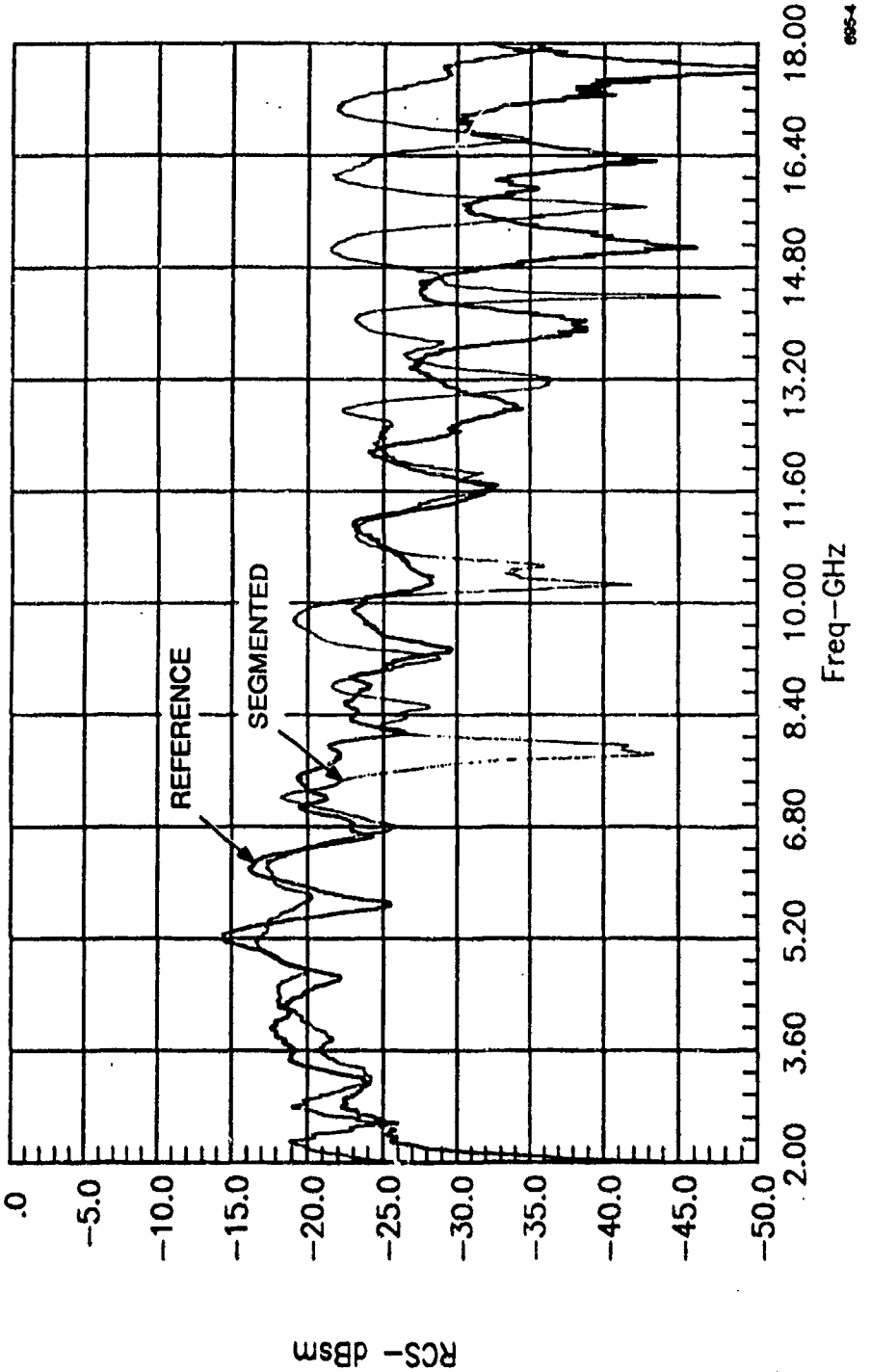


FIGURE 4 SEGMENTED AND REFERENCE SCATTERING SPECTRA FOR AMMONIUM SULFATE

CONSIDERATION OF UNTRIED MAGNETIC RESONANCE TECHNIQUES FOR POSSIBLE BAGGAGE ANALYSIS

E. H. Poindexter, H. A. Leupold, and R. H. Wittstruck
U. S. Army Electronics Technology and Devices Laboratory
Fort Monmouth, New Jersey 07703

G. J. Gerardi
Department of Chemistry
William Paterson College
Wayne, New Jersey 07470

1. INTRODUCTION

Magnetic resonance has been under consideration for nearly 20 years as a possible means to detect explosives in airline baggage, as described in several other papers in this present proceedings (Marino; Buess et al; McKay et al; Sanders and Barnett; King et al) and elsewhere (De Los Santos et al, 1981). In particular, nuclear magnetic resonance (NMR) has been subject to substantial test and evaluation via operational prototype apparatus. NMR is usefully limited to reliance on one resonant signal, viz., that of the hydrogen nucleus. This is the only nucleus present in adequate concentration in explosives for sufficient signal-to-noise ratio.

The NMR method is practically limited by several considerations to use of magnetic fields below 1000 Oe. This rules out any application of frequency- or field-dependent spectroscopic signatures, on which so much chemical research and analysis is based. Rather, discrimination is based on a rather unique combination of relaxation phenomena in explosives--viz., long T_1 and short T_2, which is in contrast to all expected substances likely to be found in baggage (including the luggage container). A further boon is the quadruple resonance (NQR) of nitrogen nuclei, which is field-independent. By tuning the NMR to the NQR frequency (requiring a field of about 800 Oe), a very efficient level-crossing energy transfer occurs, and both the sensitivity and uniqueness of the signature are greatly enhanced. Nonetheless, certain weaknesses and ambiguities of low-field NMR make it desirable to seek enhancements or operational alternatives. This paper presents limited results and discussion of some possible enhancements.

2. ELECTRON SPIN RESONANCE (ESR)

Electron spin resonance (ESR), also called electron paramagnetic resonance (EPR), is analogous to NMR, but relies on the Zeeman energy of unpaired electrons rather than nuclei. It is limited to the small proportion of materials which have free spins; but when applicable, it benefits from this uniqueness and an inherent sensitivity around 15000 times that of NMR. In practice, this advantage varies widely, depending on relative free-spin concentration, which seldom approaches that of hydrogen in materials of interest here, and ESR linewidth, which is generally larger than for NMR. However, despite all this, ESR is exceptionally sensitive to one major explosive--common black powder (De Los Santos et al, 1981), which is readily detectable with extremely high signal-to-noise (s-n) ratio.

A representative ESR signal from black powder is shown in Fig. 1. The sample quantity in this case was 18 mg, and the signal was detected in a commercial Bruker 300 spectrometer operating at X-band, 3000 Oe. The s-n ratio, not at all optimized, for a 1 g sample would be nearly 50000:1. Translated to 0.5 Kg of explosive at 800 Oe in a scaled-up, baggage-size "cavity", one could expect substantial s-n ratios. Alternatively, the field could be greatly reduced for a lesser but still useful signal.

Civilian baggage would not be expected to contain other materials which give a significant ESR signal, since most common organics and plastics are processed in ways which inadvertently or intentionally preclude free radicals (a fortunate circumstance, as they are generally highly carcinogenic). Another

consideration is that black powder is the oldest and most accessible explosive. Finally, black powder--being basically carbon (charcoal), sulfur, and potassium nitrate--contains no hydrogen, and therefore cannot be detected by NMR. In view of all this, it seems very desirable to evaluate the application of an ESR accessory to NMR detectors, for sensitive and interference-free detection of black powder in non-metallic luggage.

3. DYNAMIC NUCLEAR POLARIZATION (DNP)

In addition to the very strong inherent ESR signal from black powder, a number of explosives reveal smaller ESR signals from free-radical components. One such signal, from nitrocellulose pistol powder, is shown in Fig. 2. The s-n ratio here is much lower than for black powder, about 1000 times lower. The source of these paramagnetic impurities is not immediately known, as the material itself in principle has none. However, the occurrence of even small quantities of ESR-active centers suggests consideration of their possible useful interaction with hydrogen nuclei. Stimulation of the ESR of free-radical impurities can produce an enormous effect on NMR signals (Jeffries, 1963). A concentration of 0.001 M free-radical in a liquid sample, for example, can allow an enhancement of the proton NMR signal by a factor of up to nearly 300 × (Poindexter et al, 1967). In solids, an enhancement of up to 600 × is attainable (Jeffries, 1963), even with low spin-center concentration.

This seeming great boon for augmenting the s-n of NMR, however, is not practically realizable in a baggage inspection situation. The full enhancement requires enough RF power to saturate the ESR resonance. In a simple baggage-size low-Q resonator structure for ESR at 800 Oe, the paramagnetic center of Fig. 2 would require some 100 kW of power at 2.2 GHz. Not only is such power impractical, it would clearly be dangerous--even in application for only a few seconds. Fortunately, the strength of electron-nuclear interaction is so high that even a 1% saturation would yield an NMR signal gain of 2:1. Such a power level (1 kW) might be feasible for a few seconds. Examples of DNP enhancements in a laboratory test are shown in Fig. 3.

A 2:1 signal improvement might or might not be directly useful. However, its presence or absence offers another avenue for differentiation of NMR signals, presently based on relaxation or NQR phenomena. It seems modestly worthwhile to characterize in the laboratory all organic explosive materials for the possible DNP effect of included free radicals upon any aspect of trait of the hydrogen NMR signature.

4. PERMANENT MAGNET FIELD SOURCES

Many systems such as those of NMR require static magnetic fields for directional biasing. Traditionally, such fields are provided by horseshoe magnets, electric solenoids and similar primitive devices. Since the advent of high-coercivity, high energy-product materials, such fields are attainable with much more compact, convenient and elegant permanent magnet structures (Leupold et al, 1987).

Such structures have proven themselves to be so flexible as to make them readily adaptable to the production of an impressive variety of field strengths, distributions and directions. The fields can be longitudinal, such as those of the permanent magnet solenoids pictured in Fig. 4, or transverse, as in Fig. 5. These structures can be of round, square, rectangular or polygonal cross section. Fields can be very uniform or can vary with position, in both longitudinal and transverse directions. As can be seen from the flux plots in Figs. 6-8, excellent uniformity is attainable. A linear gradient of equal quality is readily feasible.

In principle, all of the structures of the longitudinal variety and the constant-field cases of the transverse type completely confine the magnetic flux to the working space and the interior of the magnetic structure. This, of course, obviates the inconvenience of large stray magnetic fields in the vicinity of the device and affords proximity with field-sensitive equipment if close-packing is desirable. In practice, architectural, fabricational, and financial considerations dictate compromises in manufacture that make flux confinement less than perfect. Nevertheless, order-of-magnitude leakage reductions are usually attainable without difficulty.

In the case of the transverse structures that employ no passively ferromagnetic pole-piece material such as iron, all fields produced by individual magnetic elements are additive, that is, the field produced by the structure is the vector sum of those produced by each of its components. This consideration suggests the possibility of a mechanically variable field source

such as that of Fig. 9. This structure consists of two nested cylindrical field sources, each of which produces the same field H_0 in its interior. Maximum field is produced when the polar axes of the two cylinders are aligned, and zero field when they are anti-aligned. If the cylinders are free to rotate with respect to each other, any field over the range $\pm 2H_0$ is available.

Design details and an extensive bibliography can be found in a recent technical report (Leupold and Potenziani, 1990).

REFERENCES

1. Buess, M.L., Garroway, A.N., and Miller J.B., these proceedings.

2. De Los Santos, A., King, J.D., and Rollwitz, W.L., Development and Evaluation of a Prototype Checked Baggage System--NMR Technique (U.S. Department of Transportation, Washington, 1981) 80 pp.

3. Jeffries, C.D., Dynamic Nuclear Orientation (Wiley-Interscience, New York, 1963) 177 pp.

4. King, J.D., DeLos Santos, A., Nicholls, C.I., and Rollwitz, W.I., these proceedings.

5. Leupold, H.A., and Potenziani, E. II, An Overview of Modern Permanent Magnet Design (Electronics Technology and Devices Laboratory, Fort Monmouth, New Jersey, 1990) 65 pp.

6. Leupold, H.A., Potenziani, E. II, Clarke, J.P., and Basarab, D.J., Mats. Rsch. Soc. Symp. Proc. 96, 279 (1987).

7. Marino, R.A., these proceedings.

8. McKay, D.R., Moeller, C.R., Magnuson, E.E., and Burnett, L.J., these proceedings.

9. Poindexter, E.H., Stewart, J.R., and Caplan, P.J., J. Chem. Phys. 47, 2862 (1967).

10. Sanders, J.P. and Burnett, L.J., these proceedings.

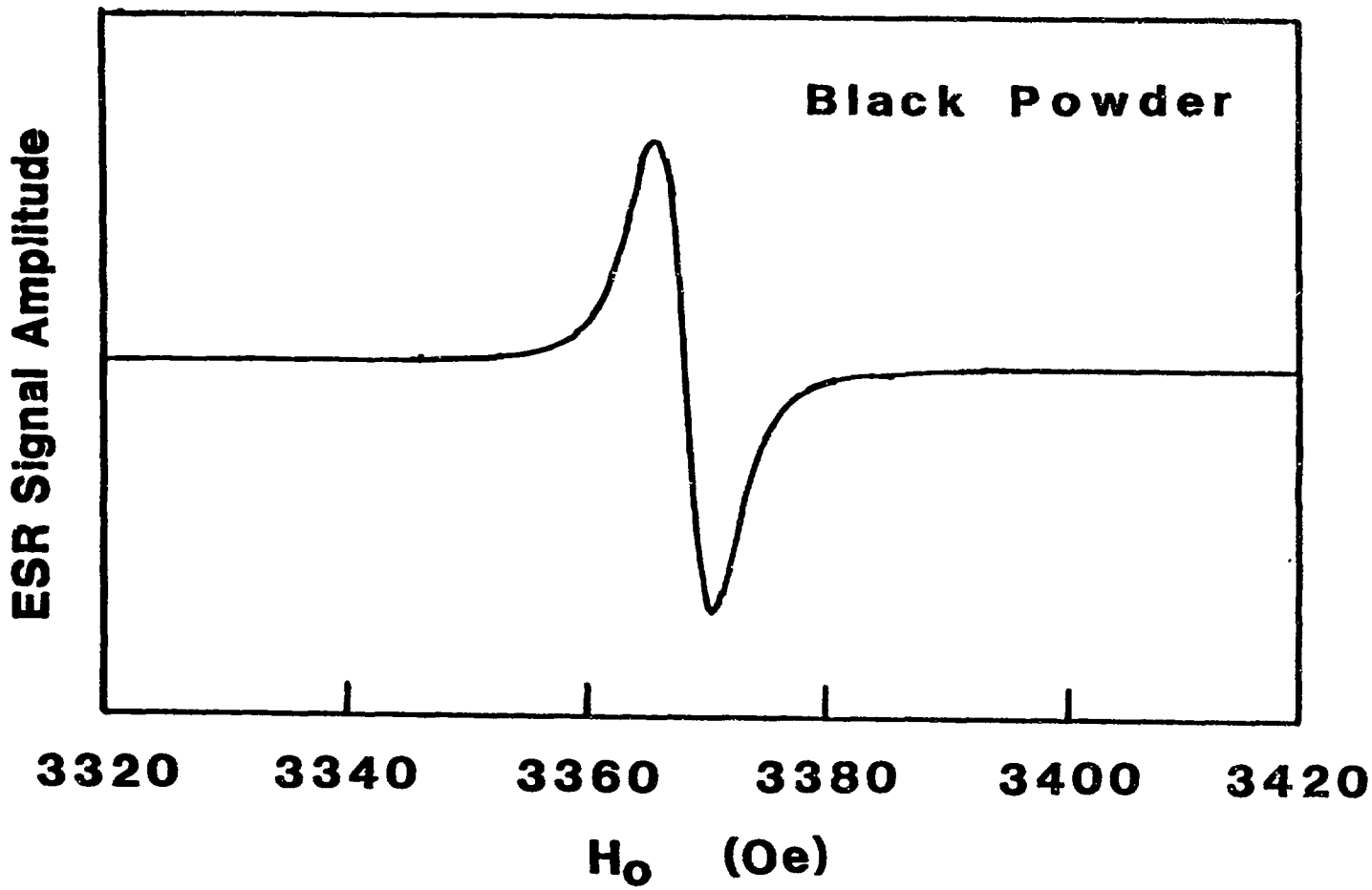


Fig. 1. ESR signal from 18.7 mg of black powder in a commercial laboratory spectrometer. Signal-noise ratio was determined by sample dilution to be about 50000:1 with 1 g of material, 1 s time constant, 2 Oe modulation, 10 mw RF (9GHz) power, sweep time 60 s.

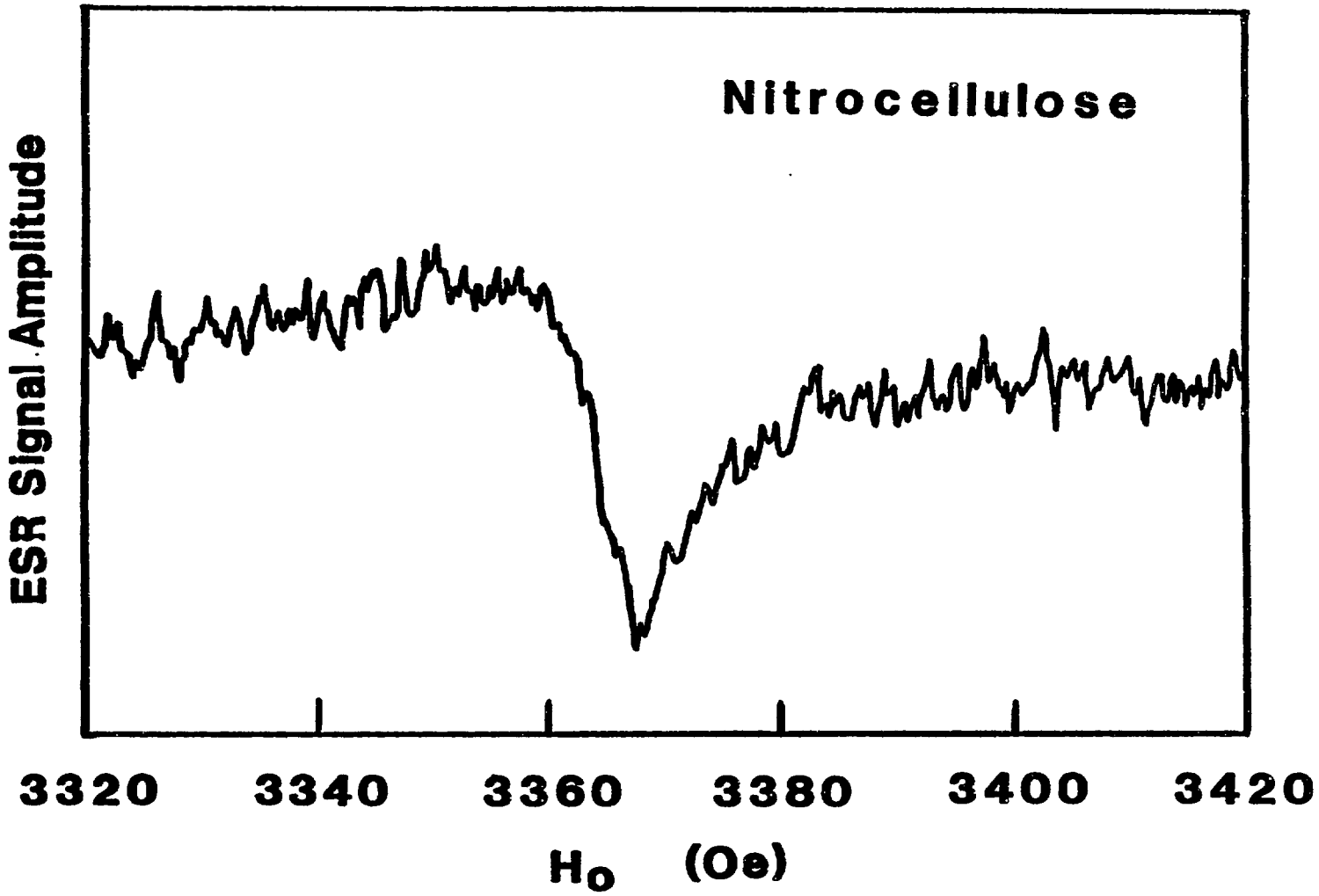


Fig. 2. ESR signal from 0.1 g of nitrocellulose pistol powder. Signal-noise ratio for same conditions as in Fig. 1 is about 10:1.

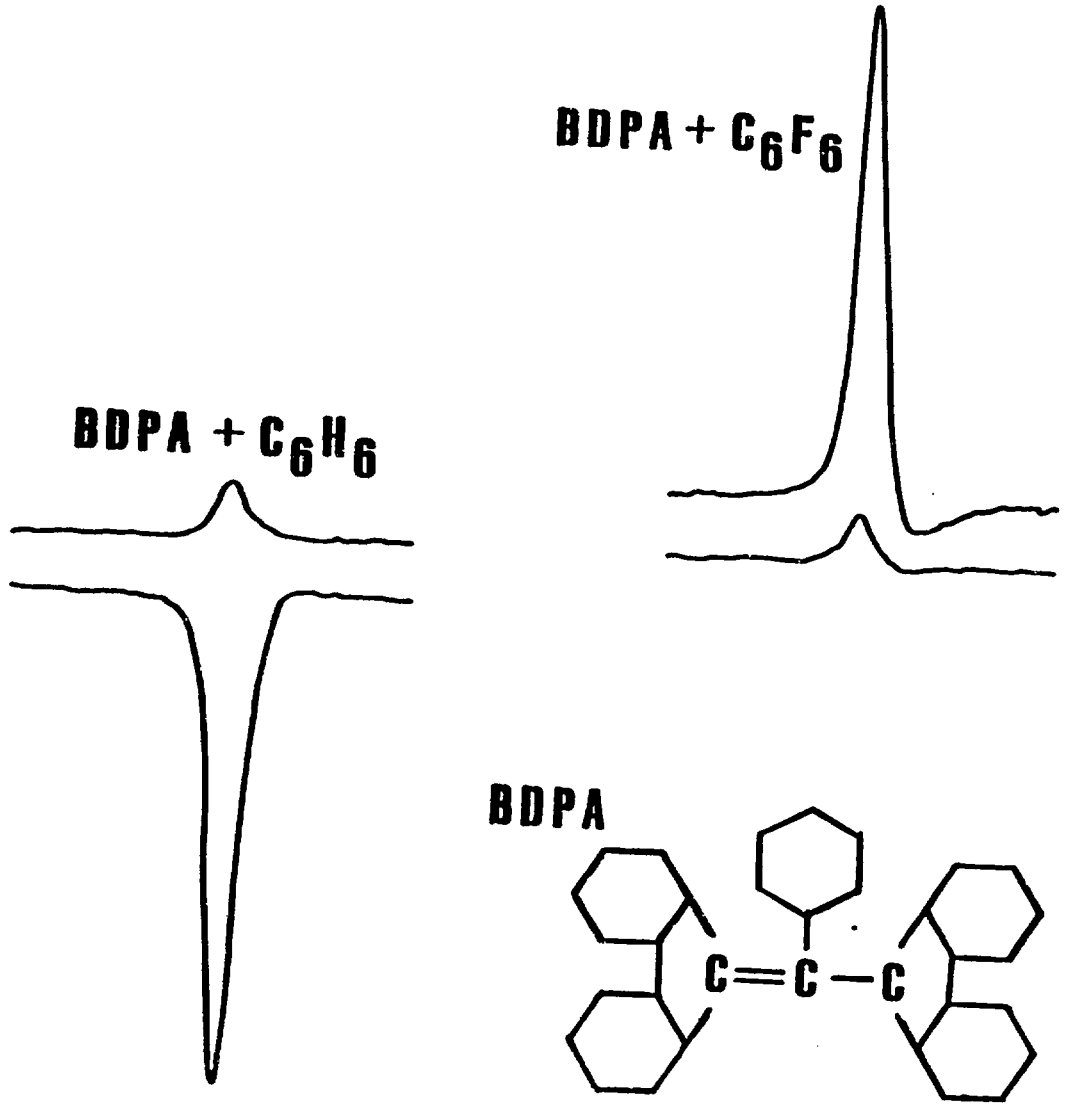


Fig. 3. Enhancement of NMR signals from free-radical solutions by DNP. Sample size: 10 cc; radical concentration, 0.01 M; H_0 = 75 Oe; γ_H = 320 KHz; γ_p = 301 KHz; γ_e = 211 MHz; RF power, 1.0 W; sample filling factor, 10%; sweep time 15 s.

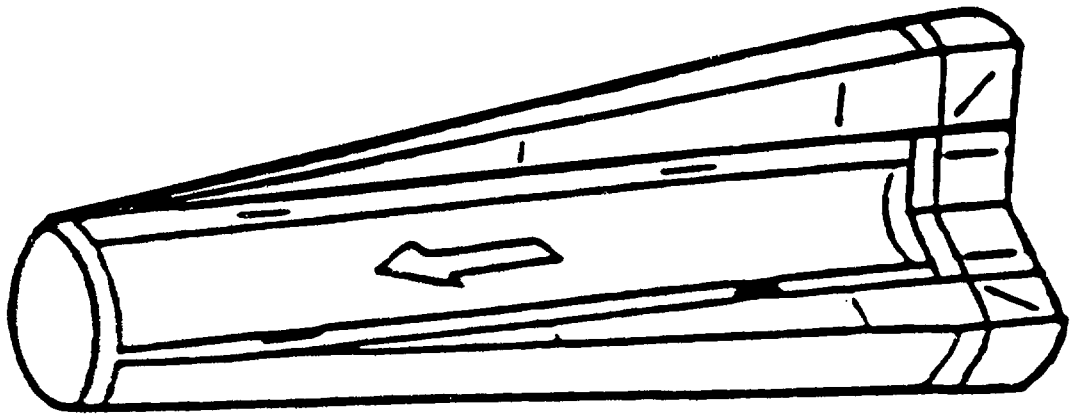


Fig. 4. Single-chambered Neugebauer structure. Left pole piece is taken as zero potential, and outer surface everywhere is lowered to the same potential by inward-pointing cladding magnets. Flux is thus confined to the interior.

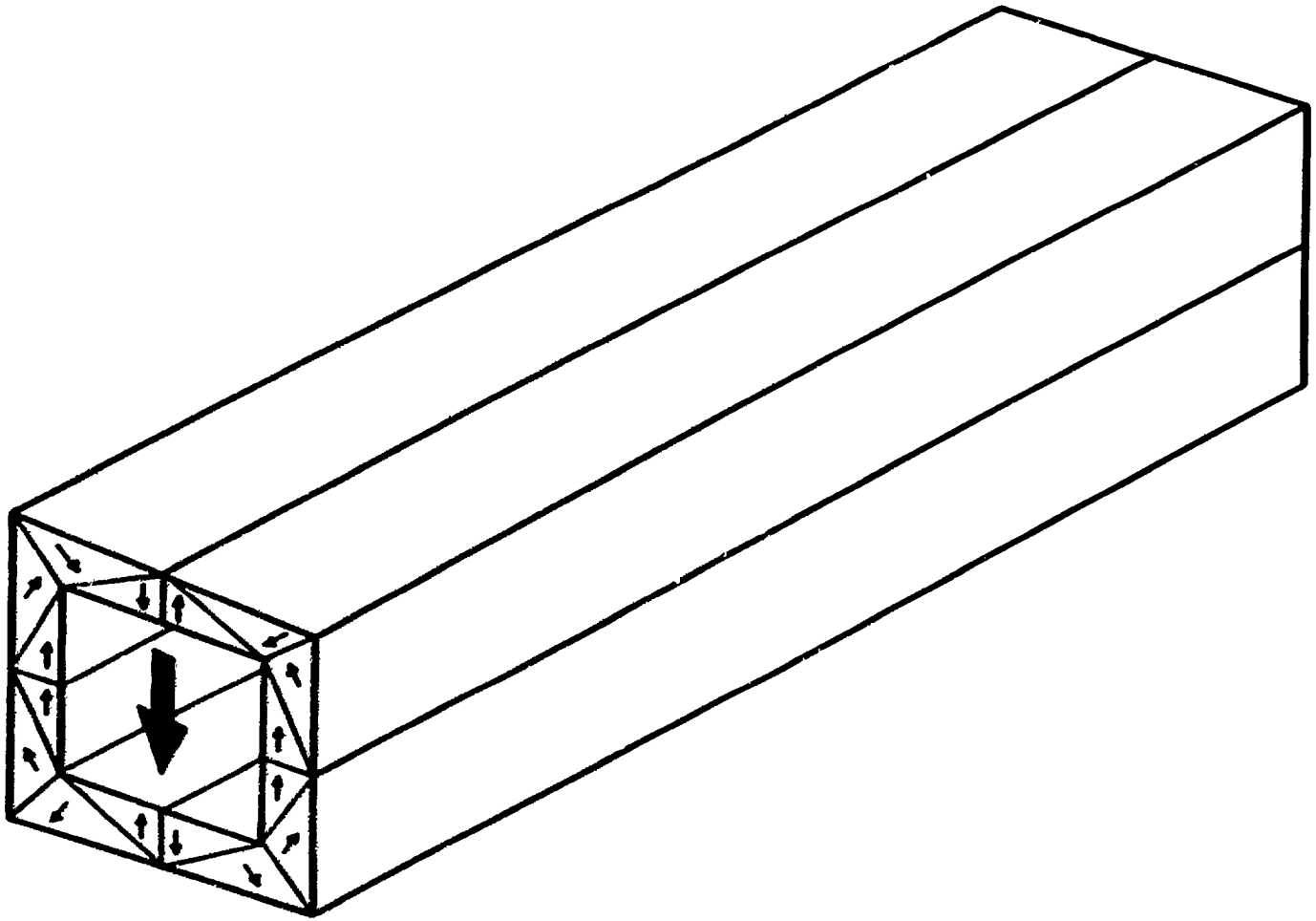
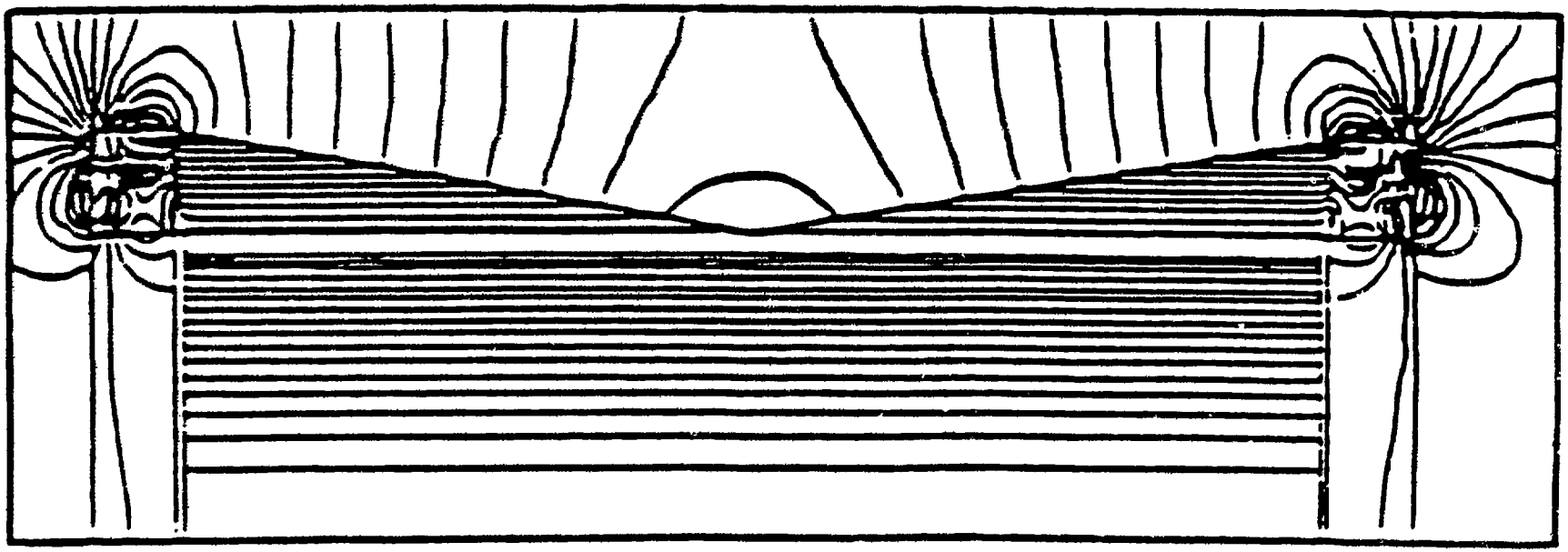


Fig. 5. A square permanent magnet structure. Flux is again confined to the interior. Field augmentation can be attained by sequential nesting.



AXIS OF ROTATION

Fig. 6. Magnetic field flux in permanent magnet solenoid in a refined version of that shown in Fig. 4. Note the great uniformity over the working space. Apparent flux crowding towards the edge is caused by each line's representing of a unit flux in an annular ring.

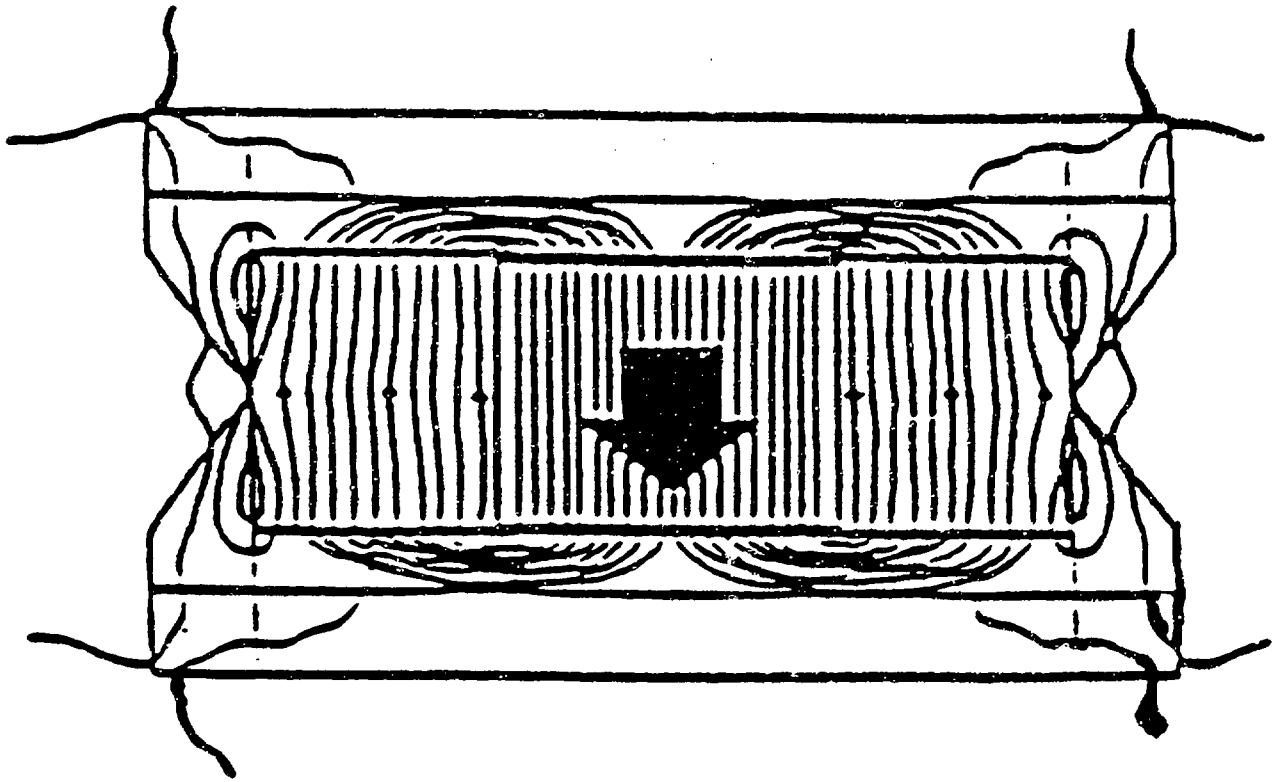


Fig. 7. Transverse magnetic field flux in a rectangular working space. The large arrow indicates the working field direction. A possible use is in an NMR imager.

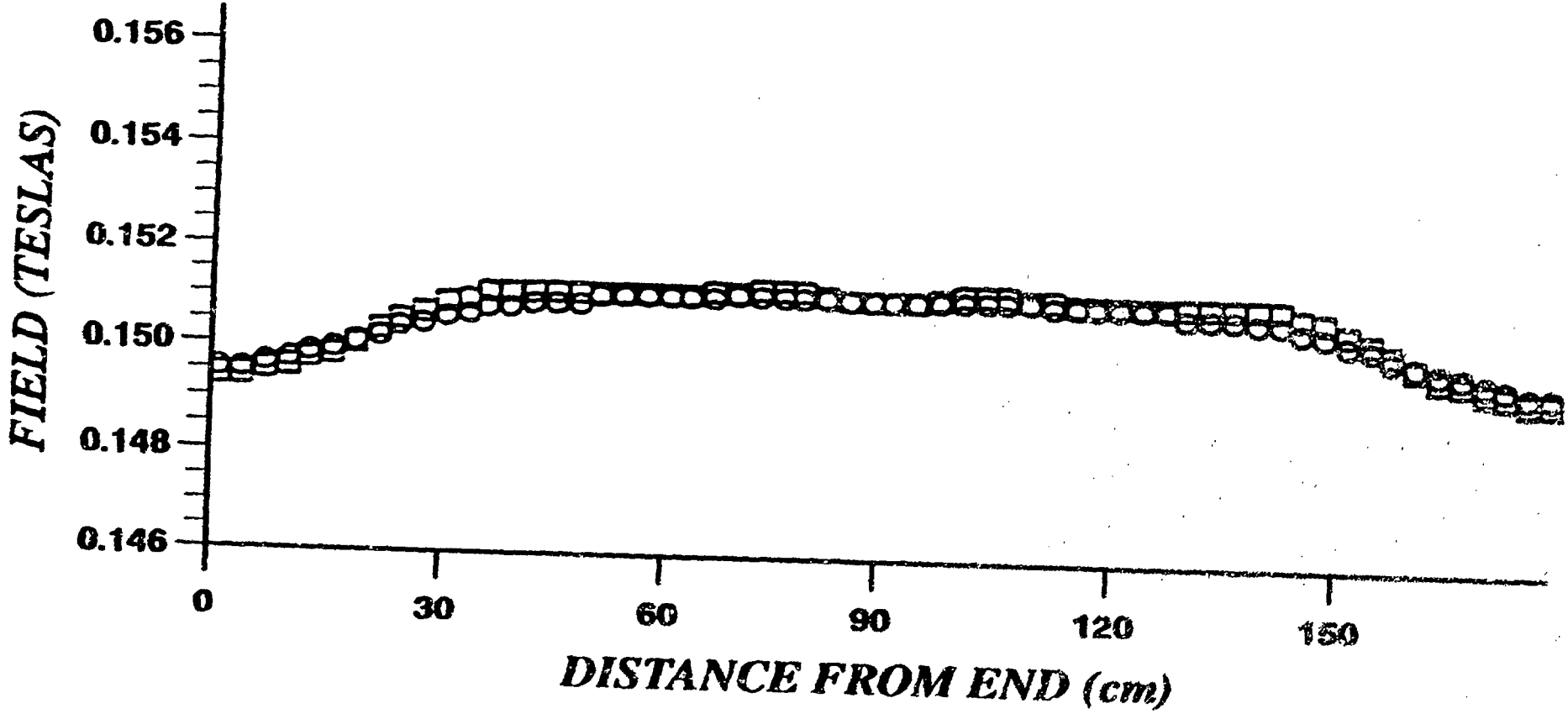


Fig. 8. Axial field profile in a solenoid similar to that in Fig. 4.

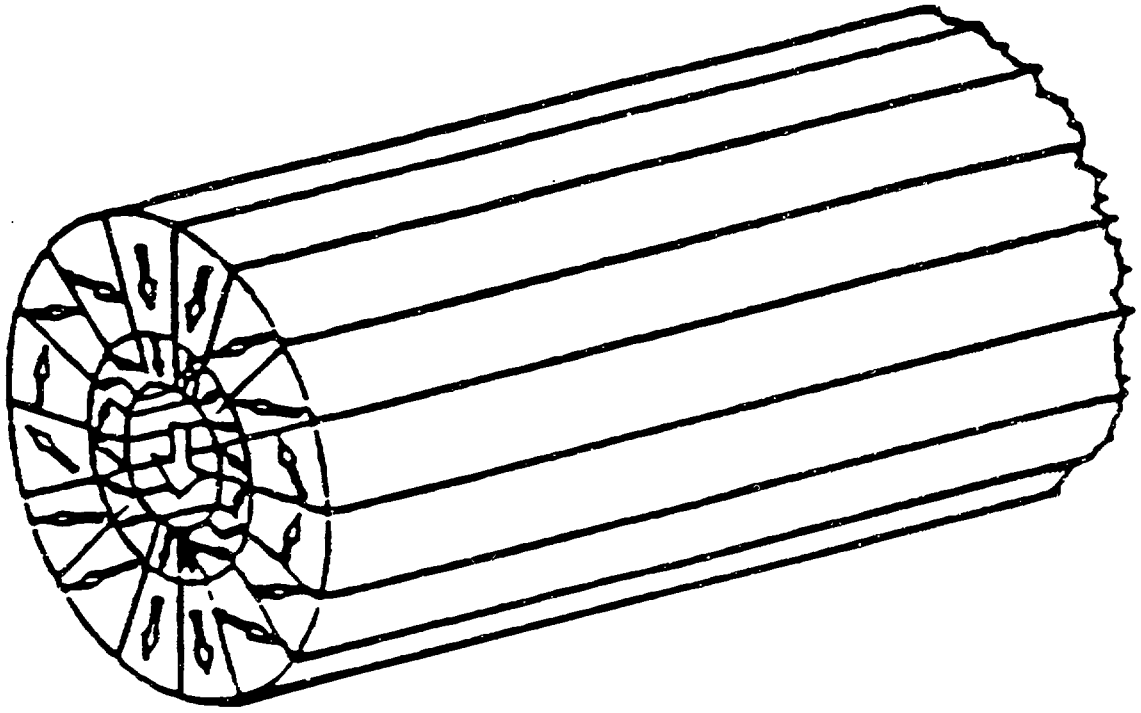


Fig. 9. Dual-cylindrical magnet shells which individually produce same field H_0 in the cavity. Rotation of the cylinders with respect to each other varies the field from zero to $\pm 2\ H_0$.

VAPOR DETECTION: GENERAL

DICHOTOMOUS KEY APPROACH FOR HIGH CONFIDENCE LEVEL IDENTIFICATION OF SELECTED EXPLOSIVE VAPORS

David H. Fine and David P. Rounbehler
Thermedics, Inc.
470 Wildwood St.
Woburn, MA 01888

and

William A. Curby
FAA Technical Center
Atlantic City International Airport
New Jersey 08405

1. INTRODUCTION

Explosive vapor detectors are chemical sensors which have been tuned to detect a few critical chemical compounds at very low concentrations, even when the explosive molecules are immersed in a sea of background material. Their performance and effectiveness are limited to how well they can be tuned to reject extraneous compounds and signals. While sensitivity is also important, selectivity is by far the dominant factor. For this reason, this paper focusses on detectability, which is an instrument's ability to discriminate between the analyte of interest and the background signal consisting not only of the summation of electronic and chemical noise, but also responses due to unknown chemical compounds in the sample matrix.

For an instrument to register a positive alarm for each chemical species, the signal strength, S, is defined as:

$$S = CR \tag{1}$$

and the minimum detectable signal, S_{ME}, as

$$S_{ME} = \sum_{e=1}^{m} C_e R_e + b \sum_{i=0}^{n} C_i R_i \tag{2}$$

where

C = concentration of the species

C_{ME} = minimum detectable concentration of explosives for i=0 and e=1

R = instrument response per unit concentration as if it were an explosive

b = signal to noise ratio for the machine to register an alarm (typically 5:1)

e = explosives species

i = interfering species

In a super-clean environment under ideal conditions, there are no interfering species present and i = 0. For this case, to register an alarm, for a single explosive species Equation 2 reduces to:

$$S_{ME} = C_{ME} R_E \tag{3}$$

C_{ME}, measured under ideal conditions, is often erroneously used as a figure of merit in comparing the performance of instruments of different types. Unfortunately, C_{ME} only has meaning under the ideal pristine conditions under which it was measured. In the real world, where there are n potentially interfering compounds whose identity and concentration are unknown to the user, the

summation term in Equation 2 dominates. Thus, C_{ME}, the minimum amount of explosive which can be detected under ideal conditions, is a meaningless quantity which serves only to distort reality and confuse would-be users.

2. FALSE POSITIVES

Under practical conditions, n > 0 and Equation 2 expands to:

$$S_{ME} = C_{ME} R_E + b (C_1R_1 + C_2R_2 \ldots C_nR_n) \quad (4)$$

where R_1, R_2 are instrument responses which are indistinguishable from an explosive, and therefore overlap with R_E. Under these conditions, the sea of potentially interfering compounds combine to moderate S_{ME}. The consequences are as follows:

First, if it was not known that the interferant(s) was(were) present in sample matrix or test environment, S_{ME}(for i>1) will be >b, and an apparent positive instrument response will be recorded, even though an explosive was not present. This condition is a false alarm, and the importance and magnitude depend on the concentration of the interferant species C_i, the response factor R_i, and on how common the interferant compound(s) are in the test environment.

If the technique cannot distinguish between the explosive compounds of interest, then every compound in the universe is a potential interferant, and the likelihood of the response being due to a compound which is not an explosive is high. A technique, such as Thermal Neutron Activation (TNA), for example, senses the Nitrogen (N) in all compounds and is unable to distinguish between the N in the different types of explosives or from the N in other innocuous materials such as clothing and foodstuffs; as a consequence, it suffers from an inherent high false alarm rate. Also, enhanced X-ray systems respond to all organic material and hence have great trouble distinguishing a bar of chocolate or a wax candle from a plastic explosive. Similarly, the earlier generation of explosives vapor detectors which identified explosives as a group and did not distinguish between the different types of explosives suffered from an inherently high and unacceptable false alarm rate. If, however, the technique can identify the individual explosives from each other, then only compounds which interfere with the particular explosive of interest can give a positive response. Positive chemical species identification greatly reduces the likelihood of false alarms and helps make the problem solvable.

Second, if it is known that the interferant was present in the test environment, then from Equation 4, C_{ME} must be increased for that environment.

Thus, if body sweat, for example, was found to be an interferant, then when sampling luggage and people, an unacceptable high number of false alarms would be recorded. In principle, false alarms could be reduced by decreasing the sensitivity of the machine, effectively increasing S_{ME}. However, increasing S_{ME} is effective only if the response to all interferences, R_I is very much less than the response to the explosive (R_E). Thus, even if the response to the explosive was one million times larger than the response to the interferant, $R_E > 10^6R_I$, the compound could still be a major one-for-one interferant if it was present in the test environment in a million fold excess compared to the explosive, $C_I > 10^6C_E$. In many situations, S_{ME} has to be increased so much to avoid the response from interferences that explosives can no longer be detected under realistic scenarios.

3. FALSE NEGATIVES

A second complicating factor arises because the response to an explosive R_E is not an independent variable, but rather depends on the type of detection technology and on the type and quantity of the n compounds in the environment:

$$R_E = f (technology) f\left(\sum_{i=1}^{n} C_i R_i \right) \quad (5)$$

Thus, in mass spectrometric and electron capture based systems, which rely on electron impact to ionize the compound of interest, other species can compete for the limited number of electrons, leading to a lack of ions of the compound of interest and hence a decreased response to the explosive R_E. In chromatographic systems, the liquid phase of the

columns can be temporarily overloaded, thereby causing peak retention times to shift. Other molecular species in the environment can even interact chemically with the explosive of interest. The result of these interactions is usually a decrease in response R_E, and a consequent increase in S_{ME}, which implies a loss in sensitivity to the explosive. In principle, the opposite could also occur, where the interactions lead to an enhanced sensitivity.

Again, there are two consequences:

First, if the matrix is a suitcase or a person, for example, where the chemical species which may be present are unpredictable or unknown, the response to the explosive R_E is decreased, causing S_{ME} to be increased to some value above the detection limit, resulting in a false negative response. This is the worst possible failure mode for an explosive detector since it should have detected the explosive, but failed to do so because the sea of compounds in the operating environment caused the detection threshold to be increased.

Second, if the problem is well documented and understood, the sensitivity of the instrument can be degraded from the ideal S_{ME}(for i=0), to take into account the anticipated problems. This is the approach which is normally taken, based on empirical data from a wide cross section of likely sample matrices.

4. GENERALIZED TESTING PROTOCOLS

The minimum detectable signal, S_{ME}(for i=0), under ideal pristine conditions, is generally evaluated using either vapor generators or dilute solutions of pure explosives. False positives are normally evaluated by exposing the instrument to likely compounds of interest at concentrations which may be encountered in the environment, and observing the response. False negatives, the most serious failure mode, are the most difficult to evaluate and understand, and are, as a result, often ignored.

In testing for false negatives, the machine must be exposed to a sample of the explosive at the detection limit C_{ME} together with the potential interferant. If the machine fails to give a response to C_{ME} in the presence of the potential interferant, then the experiment must be repeated using larger and larger amounts of explosive until the system gives a response. This new value of C_E, is the true minimum detection level in the presence of the test compound. Dust, dirt, tobacco smoke, cigarette ash, perfumes, body odors, etc. are typical compounds which severely stress an instrument's ability to reject false negatives. Although testing for false negatives is usually not carried out when evaluating different explosives detectors, we find it to be the single most important test of the practical usefulness of a particular technology. Many workers are content to accept C_{ME} as the detection limit, not realizing that the practical detection limit C_E in the real world can be many orders of magnitude greater, $C_E > C_{ME}$. It is a humbling experience indeed to learn how difficult it is to minimize false negative failures.

In trace level detection at the sub-nanogram level, great attention needs to be paid to all surfaces which come in contact with the explosives. A common flaw among explosives detectors which limits their usefulness under practical conditions is called "seeding". For a machine to be of practical use, it must analyze thousands of samples per day without ever coming into contact with an explosive. However, when an explosive at the practical detection limit, C_E level is presented to the machine, it must respond positively, without the material responsible for C_E being adsorbed or absorbed on active interior surfaces sites of the machine and as a consequence not reaching the detector. A machine which needs "seeding" may perform very well in a quick test where every second or tenth sample is an explosive, but may fail totally in an airport environment where only one in every hundred thousand samples may be an explosive.

The "seeding" effect can be tested by operating the machine for several hundred samples without exposing it to an explosive or calibration standard, and then determining whether the effective C_E has been compromised. While this effect is rarely, if ever, included in laboratory tests and acceptance protocols, a machine which needs frequent "seeding" is of little practical value. In the development of the Thermedic's high speed GC-chemiluminescence explosive detector, the avoidance of the "seeding" effect turned out to be the single most difficult and challenging technical problem which had to be overcome.

5. INTERFERENCES

As scientists succeed in lowering the minimum detectable concentration C_{ME}, the number of potentially interfering compounds is increased.

If the sensitivity of a machine is improved, say 100 fold, the likelihood of having a false alarm problem is thereby greatly enhanced. Unless the selectivity of the process is likewise enhanced, the increased sensitivity cannot be utilized. It is for this reason that selectivity considerations dominate questions of sensitivity, since the effective sensitivity of an instrument in the real world depends entirely on the ability of the system to reject false alarms. Another example of this problem occurs with TNA, where improved detection capability is not dependent upon the use of a more sensitive sensor for nitrogen, but rather on distinguishing between nitrogen in an explosive from nitrogen in the other compounds which are also present.

6. DICHOTOMOUS KEY

To boost selectivity (and thereby sensitivity), all modern explosives vapor detectors use a synergistic dichotomous key approach to help reject false readings. Instead of using a single selective filter, multiple filters are used to achieve a synergistic enhancement in detectability. In mass spectrometry - mass spectrometry (MS - MS), not only are the mass to charge ratios of the parent and daughter ions determined, but daughter ions are, in turn, subject to further mass spectrometric analysis and the granddaughter ions are also positively identified. In triple MS a third stage of filtration is used. In some ion mobility spectrometers, a positive identification is generally made only when multiple clusters of ions are correctly identified on the same sample. In the EGIS explosive detector, a string of 18 sequential filters is used before the machine can signal an alarm.

The 18 steps could be performed in a forensic laboratory to categorize a particular species where each test would be carried out on a separate set of apparatus. Modern computers allow the entire 18 step filter procedure to be carried out in less than 20 seconds.

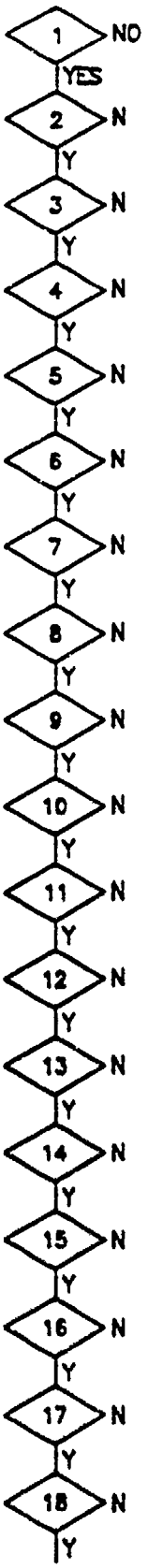
An example of the 18 sequential dichotomous keys which are needed to identify the plastic explosive, RDX, are shown in Figure 1. Some of the filters are general, particularly at the beginning of the sequence. Others are more specific. The first key is for RDX to be held on the concentrator. In key 2, the RDX is desorbed in an air stream and frozen out on a cold spot (key 3). The cold spot is then desorbed in a reducing environment (key 4) to release the RDX, which is then driven through a gas chromatographic column (key 5). On leaving the column, the RDX is decomposed under hydrogen gas to produce the nitrosyl radical, NO (key 6 and 7). The NO passes through a chemical trap (key 8), after which it is allowed to react with ozone (key 9) to produce electronically excited NO_2*. The NO_2* rapidly decays (key 10) to its ground state, giving an emission in the near infra red spectrum between 0.6 and 1.0 microns (key 11 and 12). The times of arrival at the detector 9 (key 13 and 14) are determined by the properties of the gas chromatograph. Narrow peaks due to extraneous photons are rejected (key 15) as are broad peaks (key 16). A peak shape algorithm is used by the computer to further reject extraneous signals (key 17). Finally, a signal to noise ratio of the right shape peak at the proper time of greater than five times noise is required for a positive identification (key 18).

While any single key of the dichotomous chain is relatively non-specific, taken together in the proper sequence, the entire dichotomous key becomes an extraordinarily selective filter. As a result, in most environments, the system's false positive and false negative responses are greatly reduced, even at concentrations approaching the level of C_{ME}. Thus, even though GC-chemiluminescence is not the most sensitive technique which has been tried, the performance under realistic conditions at airports is rarely degraded much from the C_{ME} level. This fact makes its full design sensitivity available for most applications.

A further extension of the dichotomous key approach is to use multiple detection technologies in an overall system approach to airport security. Thus, the performance of X-ray followed by vapor gives a further synergistic enhancement, wherein the performance of the combined X-ray-vapor system exceeds the summation of the performance of the two parts when used alone.

DICHOTOMOUS KEY

Fig. 1



EXPLOSIVE VAPOR EMISSION

B. T. Kenna, F. J. Conrad, and D. W. Hannum
Sandia National Laboratory
Albuquerque, NM 87185

1. INTRODUCTION

Emission rates of explosive vapors from explosive samples dictate whether a technique will provide a constant explosive vapor source for instrument evaluation. Indeed, emission rates determine whether a particular detection system is applicable directly for explosive vapor detection or if an initial "helping" step, such as preconcentration, is required.

Two questions facing explosives vapor detection are: (a) Is there sufficient explosive vapor from an explosive device to permit detection? and (b) Can an explosive vapor source be constructed which will provide a constant, known amount of explosive vapor to test explosive vapor detection systems? Many papers have been written regarding the first question. The most complete work on vapor pressure has been reported by Dionne, Rounbehler, Achter, Hobbs and Fine (1) and addresses the equilibrium vapor pressure as a function of temperature for various explosives, including TNT and RDX. T. A. Griffy (2) has developed a model to predict expected explosive vapor concentration for various scenarios.

2. STATEMENT OF PROBLEM

The second question, which is the primary subject of this paper, has not been investigated as thoroughly as the first. A possible reason is that it is somewhat more complex than just knowing the equilibrium vapor pressure. Rather, the amount of explosive vapor contained in a gas flow over the pure explosive surface at any flow rate, at any temperature, must be determined. The question is complicated further when the explosive is distributed throughout other materials, for example RDX in C-4. It is interesting to note that this latter point also impacts the first question.

3. DISCUSSION

One approach to the second question was suggested by Wm. Dennis (3). The ratios of equilibrium vapor pressure for TNT and DNT, for example, appear to be comparable to their respective emission rates in a gas flow. For example, at 20 C and at a flow of 20 cm/sec, their emission rate ratio is: $E_{TNT}/E_{DNT} = 3.9 \times 10^{-2}$ which is similar to their vapor pressure ratio, viz. 4.1×10^{-2}. Assume this relationship is also valid between TNT and RDX, i.e., $E_{RDX} = E_{TNT}[P_{RDX}/P_{TNT}]$. The vapor pressures for RDX and TNT can be obtained from the paper by Dionne, et. al., (1). E_{TNT} was obtained from the data by Dennis (3). Figure 1 demonstrates the vapor emission rates determined for TNT and calculated for RDX from pure TNT and RDX, respectively. Note that the curves begin to approach a constant emission rate above a flow rate of about 50 cm/sec. It is a logical step to extend this to explosive vapor emissions at higher temperatures, still utilizing the same assumption stated previously. This was done to provide Figure 2. Only RDX is shown, but TNT would give similar curves at higher emission rates.

3.1 Explosive Vapor Sources

One type of explosive vapor emission source is a coiled metallic tube, e.g., 10 ft x 0.125-in od, filled with 1-mm glass beads coated with pure RDX. The total RDX area calculated (inner tube surface plus bead surface) was 664 cm^2. This coil was operated at two temperatures (33 C and 45 C) at various flow rates and the total flow was directed into an IMS. The area of the peaks generated by RDX were determined. This data is compared to the calculated emission rate of RDX in Figure 3. The important point is not that the experimental data fall on or are close to the calculated curves (this is probably fortuitous), but that they approximate the shape, i.e., curvature, of the calculated curves. This is amplified in Figure 4 which compares the calculated pg RDX/cm^3 concentration with the concentration represented by the peak area.

A second type of explosive vapor generator contains RDX deposited on a wire screen which is in the path of a forced heated air flow, similar to a hair dryer. For this work, a #5 sieve screen was assumed (19.6 cm^2 area,, i.e., 4 mm sieve opening, 1.13 mm wire diameter, with 2 mesh per cm^2. The screen wire area was covered with RDX and was calculated

to be 31.7 cm^2. The estimated RDX vapor concentration as a function of temperature at a flow rate of 20 cm/sec for the screen is provided in Figure 5. Also shown in Figure 5 are the calculated concentrations from the 10-ft tube described previously, a corresponding 1-ft tube filled with RDX-coated 1-mm spheres, and the equilibrium vapor pressure of RDX as calculated using the equations developed by Dionne, et. al. (1).

Naturally, the vapor pressure cannot be more than the equilibrium vapor pressure. Therefore, Figure 5 is illustrating that the 10-ft and 1-ft tubes, filled with RDX-coated spheres, yield an output of saturated vapor. Each wire of the screen, on the other hand, would be similar to a 0.04 cm length tube, and provides a constant, but unknown, vapor pressure source. Both types of sources would have a definite place in testing instruments.

3.2 RDX in C-4

Dennis (3) has suggested the concept illustrated in Figure 6. Briefly, a pure RDX particle will possess an evaporation rate of about 33 fg RDX/cm^2-sec. However, in a material such as C-4, each RDX particle is coated with oil and plasticizer. The RDX particle is not open to the outside world; instead, a tiny fraction of the RDX is dissolved in the coating of oil and plasticizer. Raoult's Law states that the vapor pressure of a solute in solution is equal to the mole fraction of solute multiplied by the vapor pressure of the pure solute. Dennis (3) has shown that the solubility of RDX in the oil/plasticizer is low and perhaps on the order of 0.1 microgram per mL. Therefore, C-4 would have an RDX vapor pressure on the order of 3×10^{-6} fg per mL. If the original assumption pertains, i.e., that the rate of evaporation scales with partial pressure as in a pure substance, then the RDX evaporation rate from new C-4 would be on the order of 5×10^{-4} fg RDX/cm^2-sec. Of course, as the C-4 age increases and the oil and plasticizer concentration(s) decrease, the RDX vapor emission rate from C-4 should increase with time since more "pure RDX" would become available to the outside world. However, the point to be made is that RDX in C-4, particularly fresh C-4, may be difficult to detect.

3.3 Flow Sampling

One must realize that with any vapor source, two difficulties can exist. First, the total flow area of the vapor source cannot be left open, i.e., it must be totally directed into the inlet of a measuring instrument. The problem with not directing the total flow into a measuring device inlet is primarily that the RDX will deposit on the outside of the measuring instrument. At a later time, this RDX can desorb and perhaps produce erroneous reading(s) in the instrument, thereby providing false results.

The temperature of the vapor source must be considered the temperature of any instrument evaluation with that source. Thus, the distance between a vapor generator and the detection system must be held at the same or higher temperature as the vapor source.

4. SUMMARY

In summary, two types of vapor sources were discussed in this paper. One is a tubular coil filled with RDX-coated microspheres. It should provide an output of RDX saturated vapor. A second is a screen coated with RDX. This type would provide a constant RDX vapor source, but probably not a known RDX vapor concentration. Both stringent calculations and analytical experimentation would be required to define the amount of RDX vapor in the flow from any explosive vapor source.

It should be understood that whenever a pure explosive compound is not used, the vapor pressure observed may not be the true vapor pressure of the pure explosive compound. Rather, the emission rate, and therefore the available explosive vapor, would be that of the mixture containing the pure explosive. It could be dictated by the solubility of the explosive material in any "solvent" present.

REFERENCES

1. B. C. Dionne, D. P. Rounbehler, E. K. Achter, J. R. Hobbs and D. H. Fine, J. Energetic Matls., 4, 447 (1986).

2. T. A. Griffy, Proceedings Third Symposium on Analysis and Detection of Explosives, Mannheim, FRG, July 10-13, 1989, p. 38-1.

3. Wm. Dennis, Private communication with B. T. Kenna and F. J. Conrad, Albuquerque, NM, June 1990.

FIGURE 1. VAPOR EMISSION RATES OF TNT AND RDX FROM PURE TNT OR RDX SURFACES AS A FUNCTION OF NITROGEN FLOW VELOCITY ACROSS SURFACES.

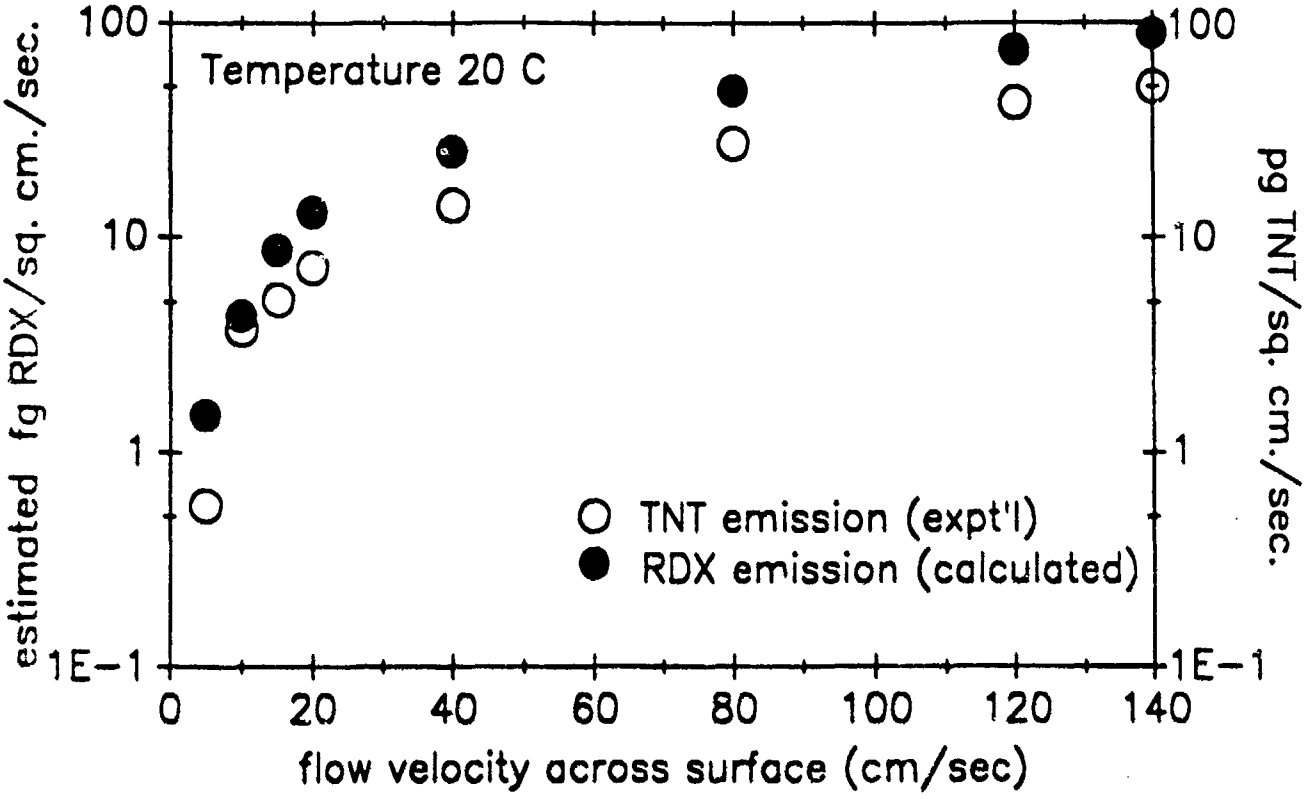


FIGURE 2. CALCULATED RDX VAPOR EMISSION RATES FROM PURE RDX AT VARIOUS TEMPERATURES AS A FUNCTION OF THE VELOCITY OF NITROGEN FLOWING ACROSS RDX SURFACE.

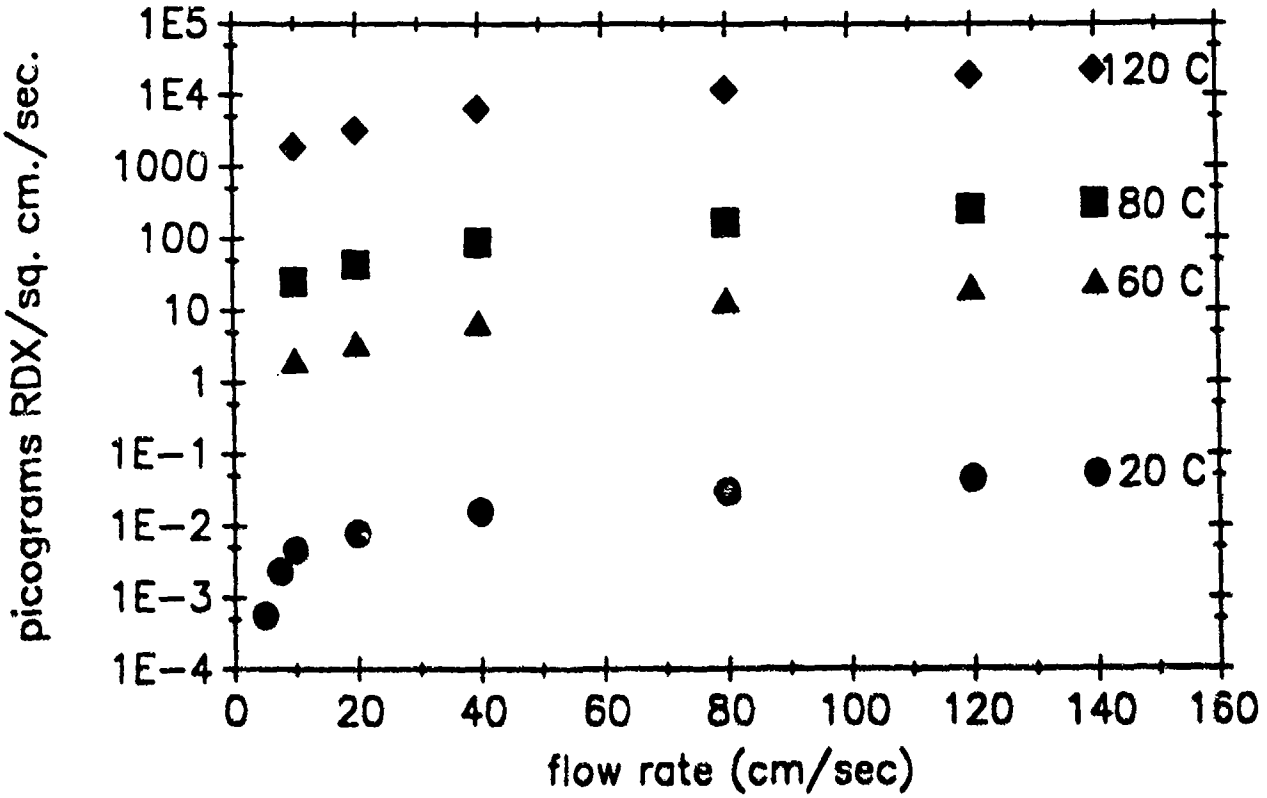


FIGURE 3. COMPARISON BETWEEN EXPERIMENTAL AND CALCULATED RDX EMISSION RATE FROM PURE RDX CONTAINED ON 1–MM BEADS IN METAL TUBE.

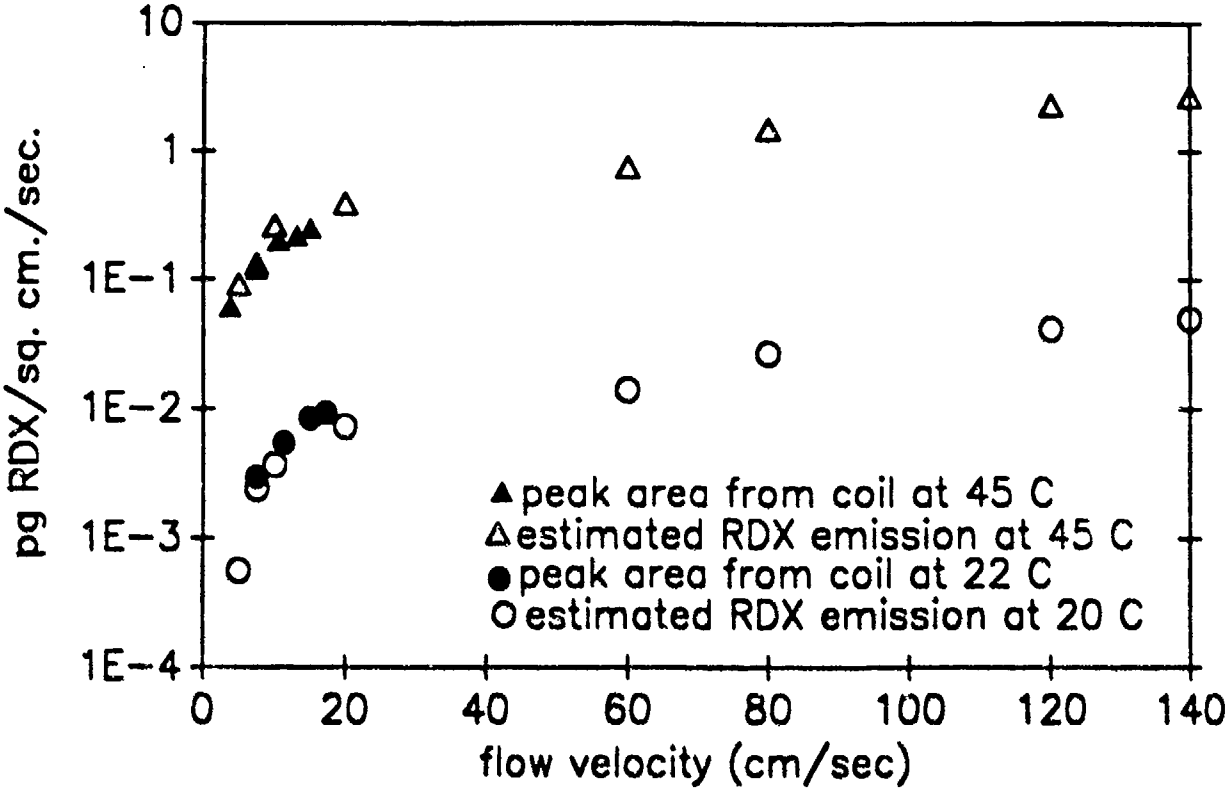


FIGURE 4. RDX VAPOR CONCENTRATION from 1/8-in O.D. 10-FT TUBE(.125-in) FILLED WITH PURE RDX-COATED BEADS: COMPARISON BETWEEN EXPERIMENTAL AND CALCULATED RESULTS.

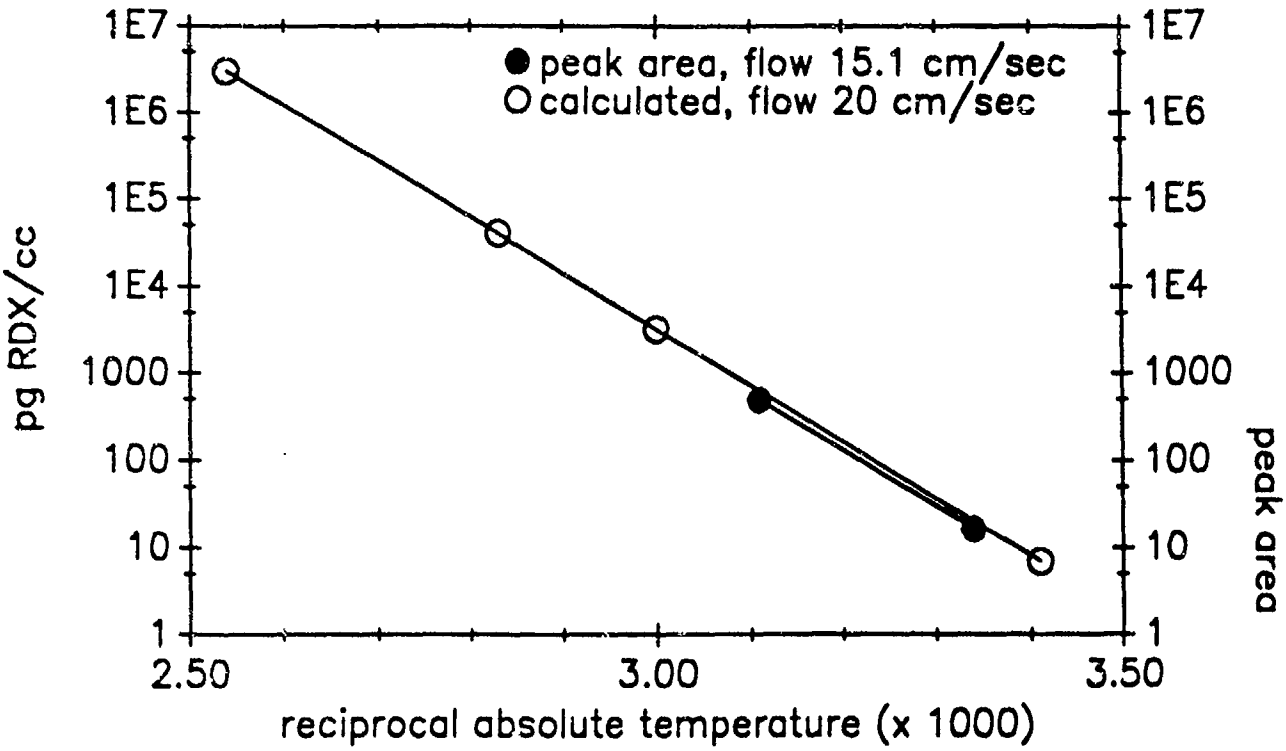
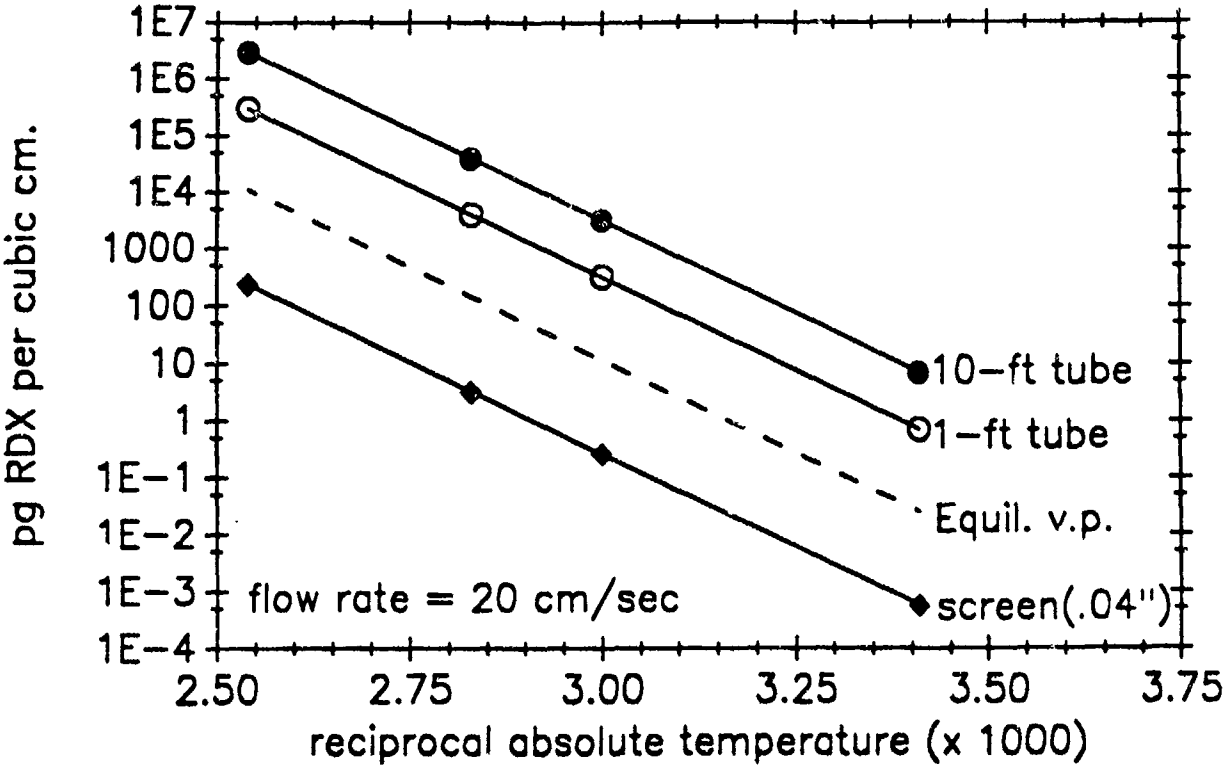


FIGURE 5. COMPARISON OF RDX EQUILIBRIUM VAPOR PRESSURE WITH RDX VAPOR EMISSION FROM VARIOUS PURE RDX SOURCES AS A FUNCTION OF TEMPERATURE.



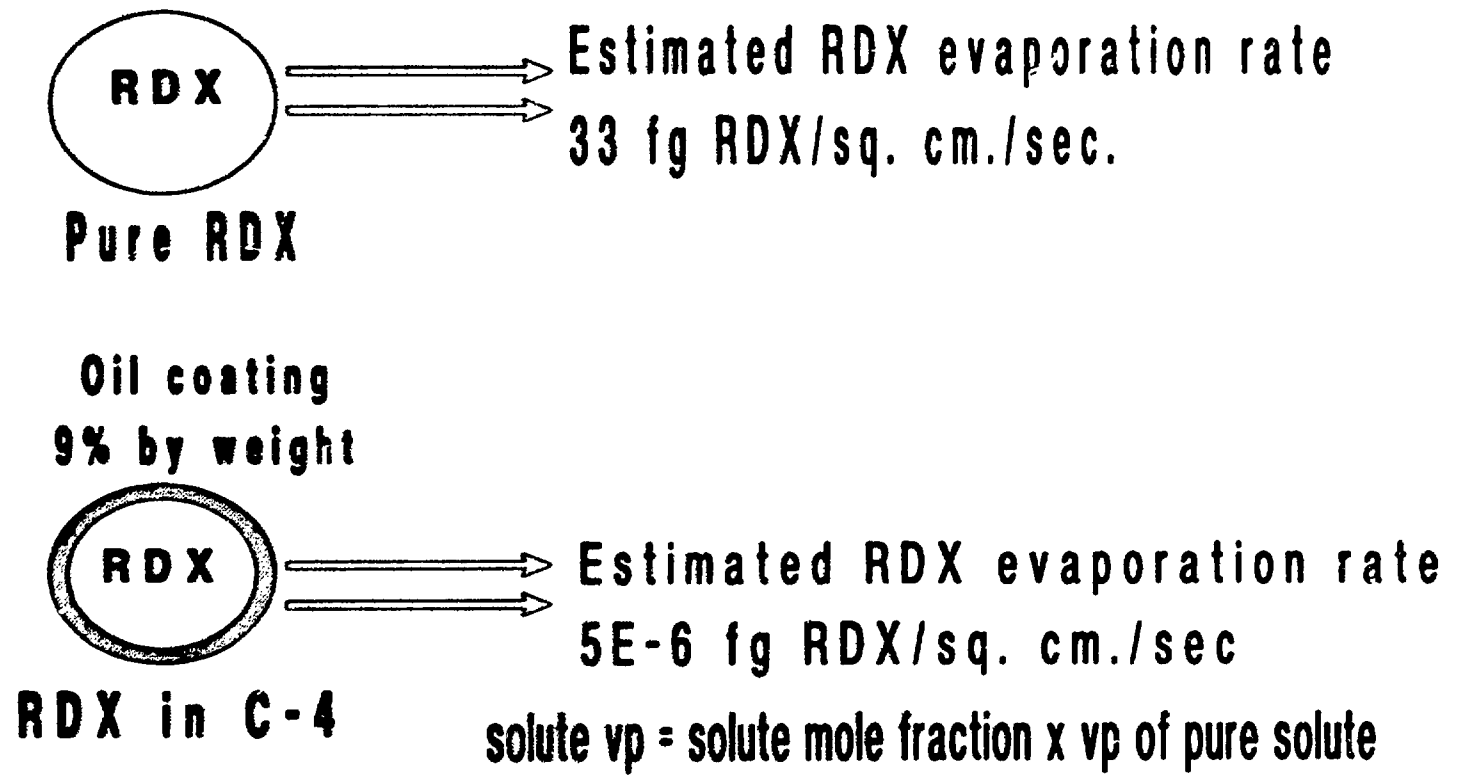


FIGURE 6. COMPARISON OF RDX EVAPORATION RATE FROM PURE RDX PARTICLE RELATIVE TO RDX PARTICLE IN C-4.

A THERMODYNAMIC STUDY OF THE VAPOR PRESSURES OF C-4 AND PURE RDX

W. McGann, A. Jenkins, and K. Ribeiro
Ion Track Instruments, Inc.
340 Fordham Road
Wilmington, MA 01887
(508) 658-3767

1. INTRODUCTION

One of the central requirements in the design of a chemical detection system is the understanding of the physical and chemical properties of the targeted compounds. In vapor detection systems for explosive compounds, the factor which ultimately limits the sensitivity is the amount of vapor available to the detector. Although this factor is a function of many variables including the efficiencies for vapor collection, transport, trapping and detection, it depends largely on the equilibrium vapor pressures of the compounds of interest. Of all the explosive compounds considered to pose a significant threat, RDX-based explosives exhibit the lowest vapor pressures.

The vapor pressure of RDX has been reported to be 4.6×10^{-9} mmHg [Dione, Edwards, Rosen]. This corresponds to a saturated vapor concentration of 6 ppt at room temperature. It is often the case that researchers gauge the sensitivity of their instruments in the laboratory with pure RDX in its native crystalline form. From the point of view of setting "benchmark standards" in the laboratory, this approach is highly recommended. However, it does not give a good indication of the systems ability to measure vapor from C-4 which is a solid solution of several organic compounds.

In this work, we report on the differences in the vapor pressure between pure RDX and C-4. The arguments presented are based on a series of experiments in the laboratory in which the signal response versus temperature of C-4 was measured and compared to pure RDX. Using the known literature values for the pure compound and a thermodynamic model based on the Clausius-Clapeyron equation, the vapor pressure of military grade C-4 has been determined. From these data, an estimate of the maximum amount of vapor available from C-4 can been made.

2. THERMODYNAMIC MODEL

The Clausius-Clapeyron equation provides a relationship between the temperature and pressure in a two-phase system at equilibrium (one phase being gaseous and the other condensed).

The relationship is cast as;

$$\frac{dP}{dT} = \frac{\Delta H}{TV}$$

where delta H is the enthalpy of the system, T is the absolute temperature and V is the molar volume of the gas. If one can assume that the molecules in the gas behave ideally, then substituting for V from the ideal gas law yields

$$\frac{dP}{dT} = \frac{P\Delta H}{RT^2}$$

Separating the variables and integrating gives rise to a particularly convenient and useful form of the equation

$$\int \frac{dP}{P} = \int \frac{\Delta H}{RT^2} dT$$

$$\log P = \frac{\Delta H}{2.303RT} + const.$$

Using this form of the equation, and the empirical value for the enthalpy, the change in vapor pressure at any given temperature can be directly calculated. For RDX, the equation reduces to

$$\log P = -\frac{6473}{T} + 22.5$$

3. EXPERIMENTAL DESIGN AND METHODS

3.1 System Description

The detection system used in this study was designed in partial fulfillment of an FAA contract for the development of a walk through vapor portal. The new detection system operates by transporting, trapping, separating, desorbing and detecting explosive vapors from atmospheres containing an abundance of pollutants. The design relies on a rotary trap and separator which provides a means of desorbing explosive vapor into an electron capture detector [Jenkins].

The design consists of a trap manufactured from a very thin stainless steel disc coated with a chromatographic liquid phase. The trap is supported by a structural element made from a non-porous machinable ceramic. The support element also serves to define the active surface area on the trap as well as the detection volume through the use of concentric seals between the trap and the support. Finally, the trap is temperature programmed to provide the desired trapping and desorption effects along the path of rotation.

In operation, air from the atmosphere is drawn into the system along a heated transfer line and is made to impinge on the trap surface at the sampling point. The sampled air is then drawn around the surface of the trap to the vacuum port which creates a pressure differential to provide an appropriate air flow.

The trap rotates from the sample inlet point through a region where all unwanted contaminants are separated from the system by the chromatographic effect of the warm carrier gas stream. From there, the remaining filtered explosive fraction of the sample passes into the desorption zone where the explosive vapors are stripped from the trap and swept into an electron capture detector. Finally, the traps rotates back around to the sample inlet position to repeat the cycle.

In the design of such a system there are many trade-offs which must be made in order to achieve the best compromise between sensitivity and selectivity for the system. For example, ideally the trap should be at the lowest temperature possible in order to provide high trapping efficiency; but at low temperatures many interfering pollutants will also be trapped and not removed by the separator. Similarly, at high trap temperatures, RDX may be trapped efficiently, but ethylene glycol di-nitrate (EGDN) vapor may be swept from the system by the separator and never be detected. The design of the system used in these studies, was based on the detailed understanding of these effects and resulted in a robust system which approached the theoretical limits of sensitivity for an electron capture system.

3.2 Sampling Technique

The experiments in this study were carried out by introducing quantitative amounts of pure RDX and C-4 vapor into the system by means of a vapor syringe. From previous work in the laboratory, we have shown that vapor samples from pure explosives can be introduced into a detection system from an all glass syringe. The vapor syringe is designed such that the entire length of the syringe barrel and the tip are maintained at a predetermined temperature. The temperature along the length of the syringe can be controlled and monitored with a temperature controlled heater and a thermocouple to within 1°C. Samples of explosive material are introduced into the syringe via an inert mineral wool plug saturated with the explosive compound. Figure 1 shows a drawing of the syringe used in this study.

The syringe was baked out for 48 hours at 200°C in a GC oven prior to assembly and tested for its vapor purity before loading it with explosives. This was accomplished by making a series of blank air injections at 80°C into the detection system. Figure 2 shows that no measurable response was obtained. Once the syringe was determined to be free from contamination, explosives were loaded and a series of injections were made to determine the linearity of the detector response with the volume of injected sample. The linearity of the detection system itself was greatly improved by operating the electron capture detector in the constant current mode. This experiment was performed in order to make sure that the explosive vapors are transported throughout the volume of the syringe without loss due to adsorption. The experiment was carried out using pure RDX heated to 50°C. Figure 3 shows that the signal response versus volume of injection is quite linear. A value for the linear correlation coefficient, R, was determined to be 0.98 and the best fit line is also shown in the figure. Note that the plot is scaled to 25°C down from 50°C. This was accomplished using the Clausius-Clapeyron equation described above.

3.3 Experimental Protocol

C-4 plastic explosive was obtained from the Massachusetts State Fire Marshals Office on loan and the pure RDX was purchased from Ensign-Bickford Chemical Corporation. These materials are believed to be of the highest purity. The C-4 was still contained in its original wrapping and no volatile impurities were detected by a conventional portable vapor detector capable of detecting $5x10^{-11}$ v/v RDX in air.

The goal of the experiments was to measure the detector response from quantitative injections of the RDX and C-4 as a function of sample temperature. Prior to performing these experiments, a series of injections were made to generate an equilibration time profile for each sample. These plots, shown in Figures 4 and 5, provided the crucial data pertaining to the soak time required to achieve saturated vapor in the syringe.

Once the soak times were determined, 1 ml sample injections of pure RDX and C-4 vapor were made at a series of temperatures and the responses were noted.

4. RESULTS

Figures 6 and 7 show the actual system response versus temperature for pure RDX and C-4. From these data, the signal response versus temperature profiles were constructed for each compound and compared (Figures 8 and 9). These profiles show conclusively that C-4 does indeed have a lower vapor pressure than pure RDX. To try to quantitate this statement, we have attempted to calculate the enthalpy of sublimation for C-4 based on these data. The approach taken involved performing a nonlinear least squares fit of an exponential function to the measured data [Bevington].

First, an exponential function was cast into a linear form.

$$Y = A_1 \cdot e^{-A_2 x}$$

$$Log\ Y = A_2 x + Log\ A_1$$

where Y, A_1, A_2 and x relate the Clausiuis-Claperyon equation as follows:

$$Log\ Y = Log\ P$$

$$Log\ A_1 = Constant$$

$$A_2 = \frac{\Delta H}{2.303 \cdot R}$$

$$x = \frac{1}{T}$$

The purpose of the least squares fit is to determine the coefficients A_1 and A_2 and relate them to their designated physical quantities. The solutions are obtained by minimizing Y with respect to the coefficients A_1 and A_2. This results in a set of nonhomogeneous linear equations whose solutions are derived from a secular determinant. These solutions consist of normalized differences of products of sums given by;

$$A_1 = \frac{1}{D}\left[(\Sigma y_i)\cdot(\Sigma x^2) - (\Sigma y_i x_i)\cdot(\Sigma x_i)\right]$$

$$A_2 = \frac{1}{D}\left[(\Sigma y_i x_i) - (\Sigma x_i)\cdot(\Sigma y_i)\right]$$

$$D = (\Sigma x_i^2) - (\Sigma x_i)^2$$

Once these parameters have been determined, one can predict the vapor pressure of C-4 or pure RDX at any temperature. The vapor pressure versus temperature plots for pure RDX and C-4 are shown in Figure 10. The only assumption invoked in the analysis was that the curve for pure RDX is defined by the parameters known from the literature. The physical meaning of the parameters obtained from the least squares fit is realized by recognizing that the shape of the curves is predicted by the Clausius-Clapeyron equation and on a logarithmic scale, the slope is equal to the molar enthalpy of sublimation. Therefore, the parameters A_1 and A_2 parameters from the least squares fit for pure RDX are tied to the known literature values determined empirically. Then, by relation to the fit for pure RDX, the A_1 and A_2 parameters for C-4 can be determined. The values A_1 and A_2 for RDX are reported to be 22.5 and -6473 kcal/mole respectively,

whereas the values for C-4 are calculated to be 15.5 and -4979 kcal/mole. This clear difference in the RDX and C-4 parameters translates into a difference in vapor pressure at room temperature of two orders of magnitude.

5. DISCUSSION

The results from the experiments performed and the data analysis clearly show that there is a significant difference in the equilibrium vapor pressures of pure RDX and C-4. These conclusions were drawn by fitting the empirical data to a known thermodynamic model for the vapor pressure versus temperature, namely, the Clausius-Claperyon equation. Although this model is known to be acceptable for pure RDX and any other pure compound in its standard state, it is less clear that the model holds true for the composition C-4. The difference is that C-4 is really more like a "solid solution" of RDX and a host of other polymeric binders and plasticizers such as polyisobutylene, di(2-ethyl, hexyl)sebacate and common motor oil. This being the case, it would seem more appropriate to define a different thermodynamic model for C-4. Such a model would be one derived from Henry's Law which states that the equilibrium vapor pressure of a solute in solution is directly proportional to the solubility of the vapor, or mole fraction in solution. This model makes more intuitive sense. Unfortunately, the form of the equations derived from this model to predict the vapor pressure versus temperature have precisely the same mathematical form as the Clausius-Clapeyron equation. Therefore, although the proper experiments have not been carried out to resolve this academic question, it is clear that the mathematical treatments and conclusions carried out within this body of work are valid.

Studies such as these have relevance beyond academic interest. Understanding the nature of materials targeted for vapor detection at both the physical and chemical level are crucial. This fundamental understanding helps to ensure that detection systems developed and tested in the laboratory work in an operational environment. For example, the conclusions from this study suggest that a vapor detection system for plastic explosives will require 100-fold greater sensitivity to detect C-4 as opposed to pure RDX. This fact will impact heavily on the system design all the way from vapor collection and transport to the choice of detector for the instrument.

ACKNOWLEDGEMENT

This work was supported by the FAA, Contract # DTFA03-87-C-00005.

REFERENCES

1. Bevington, P.R., "Data Reduction and Error Analysis for the Physical Sciences", McGraw-Hill, New York, 1969.

2. Dione, V.C., Roumbehler, D.P., Achter, E.K., Hobbs, J.R. and Fine, D.H., "Vapor pressure of Explosives", Journal of Energetic Materials 4, 447, (1986).

3. Edwards, G. Trans. Faraday Soc., 49, 152, (1953).

4. Jenkins, A., McGann, W.J., Ribeiro, K. and Napoli, J. "Feasibility Study For a New Portal Explosives Vapor Detection System", FAA #DTFA03-87-C-00005, (1991).

5. Rosen, J.M. and Dickinson, C., J. Chem. and Eng. Data, 14 No.1, 120, (1969).

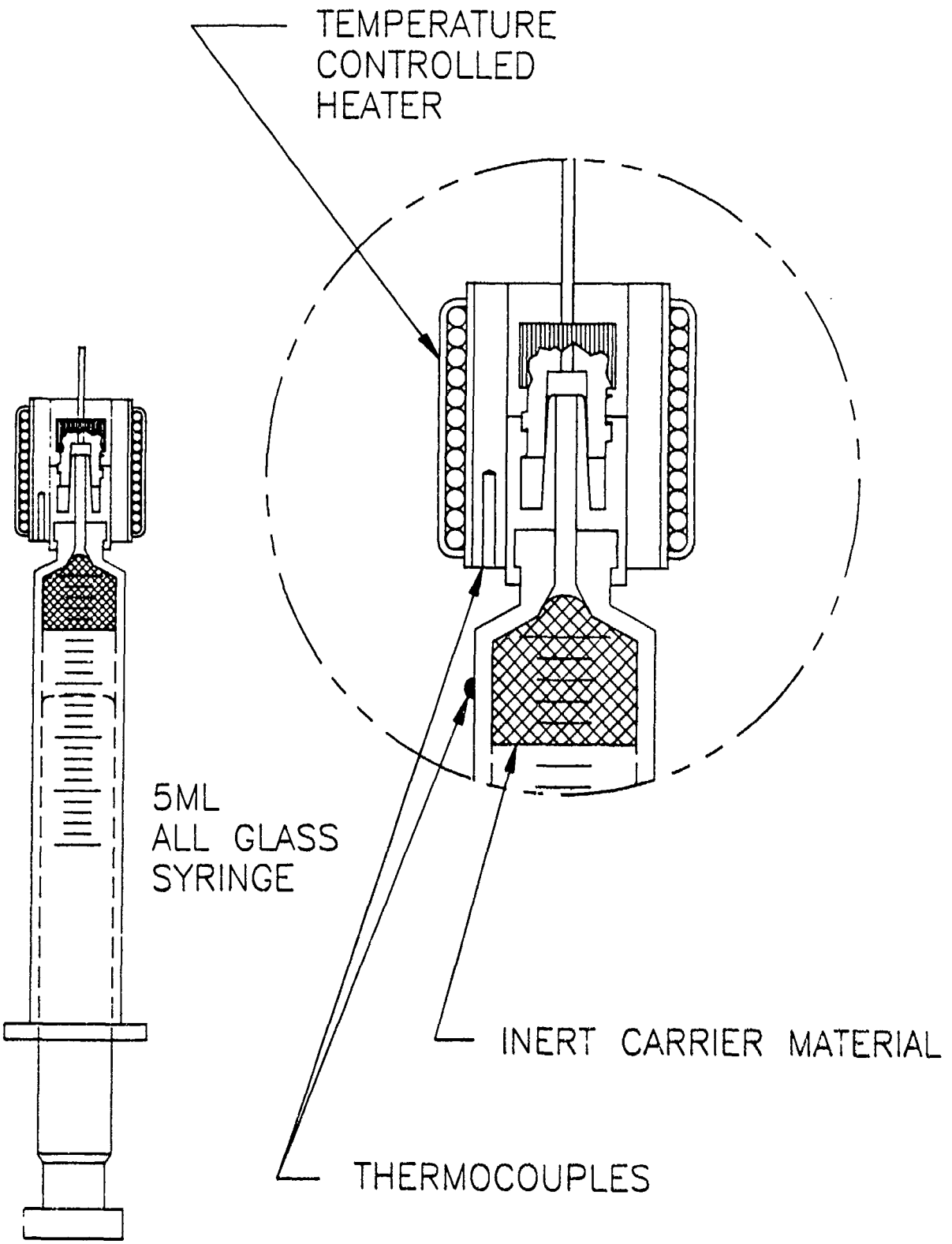


Figure 1. A diagrammatic illustration of the vapor syringe used to inject quantitative volumes of plastic explosive vapor into a detection system.

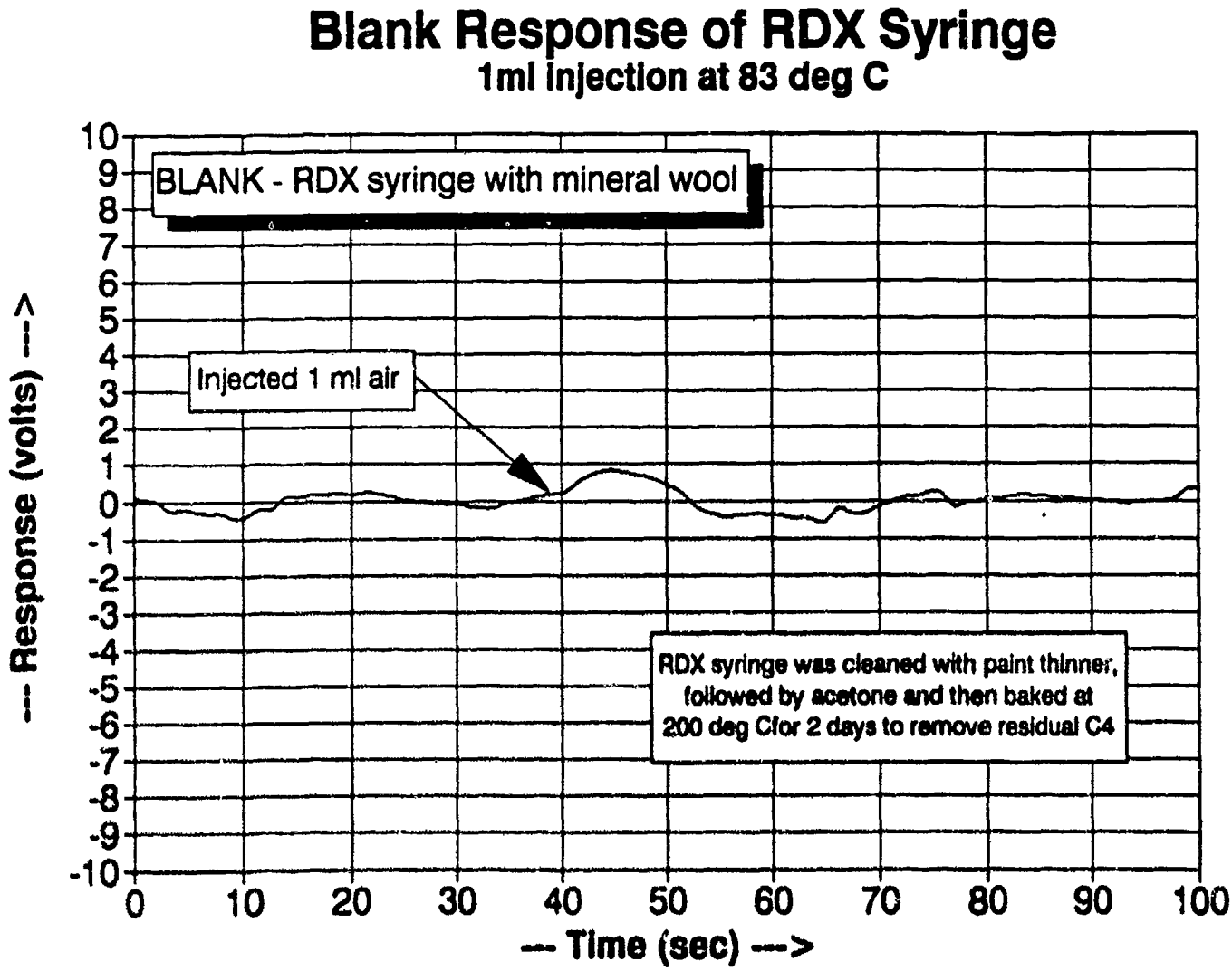


Figure 2. Shows the system response to an injection of air from a cleaned syringe prior to loading with explosives.

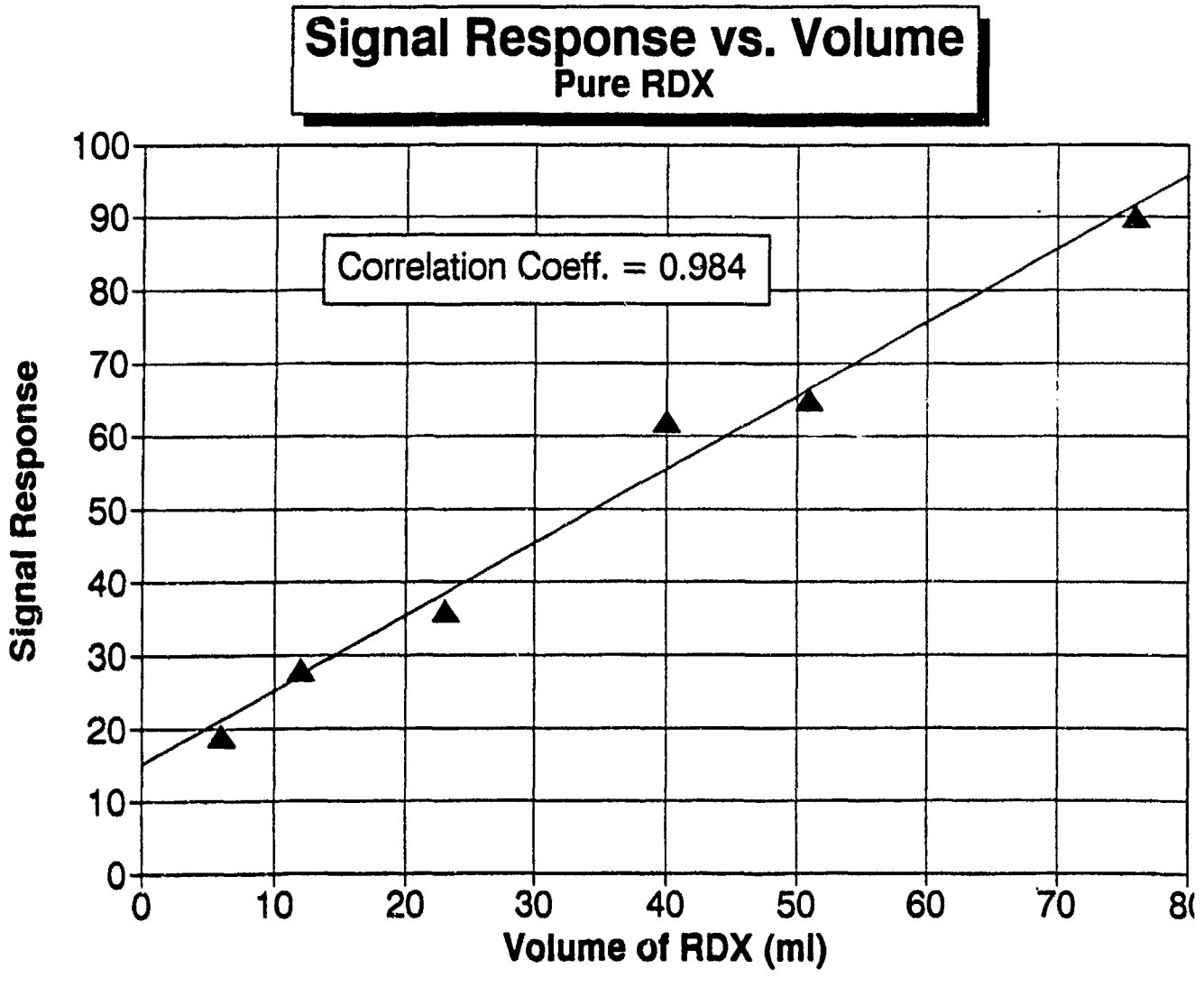


Figure 3. The signal response versus volume of injected RDX vapor at 50 °C. The purpose of the experiment was to determine the linearity of response of the system and of the syringe. A best fit line was drawn through the points from a linear regression analysis. The correlation coefficient is 0.984.

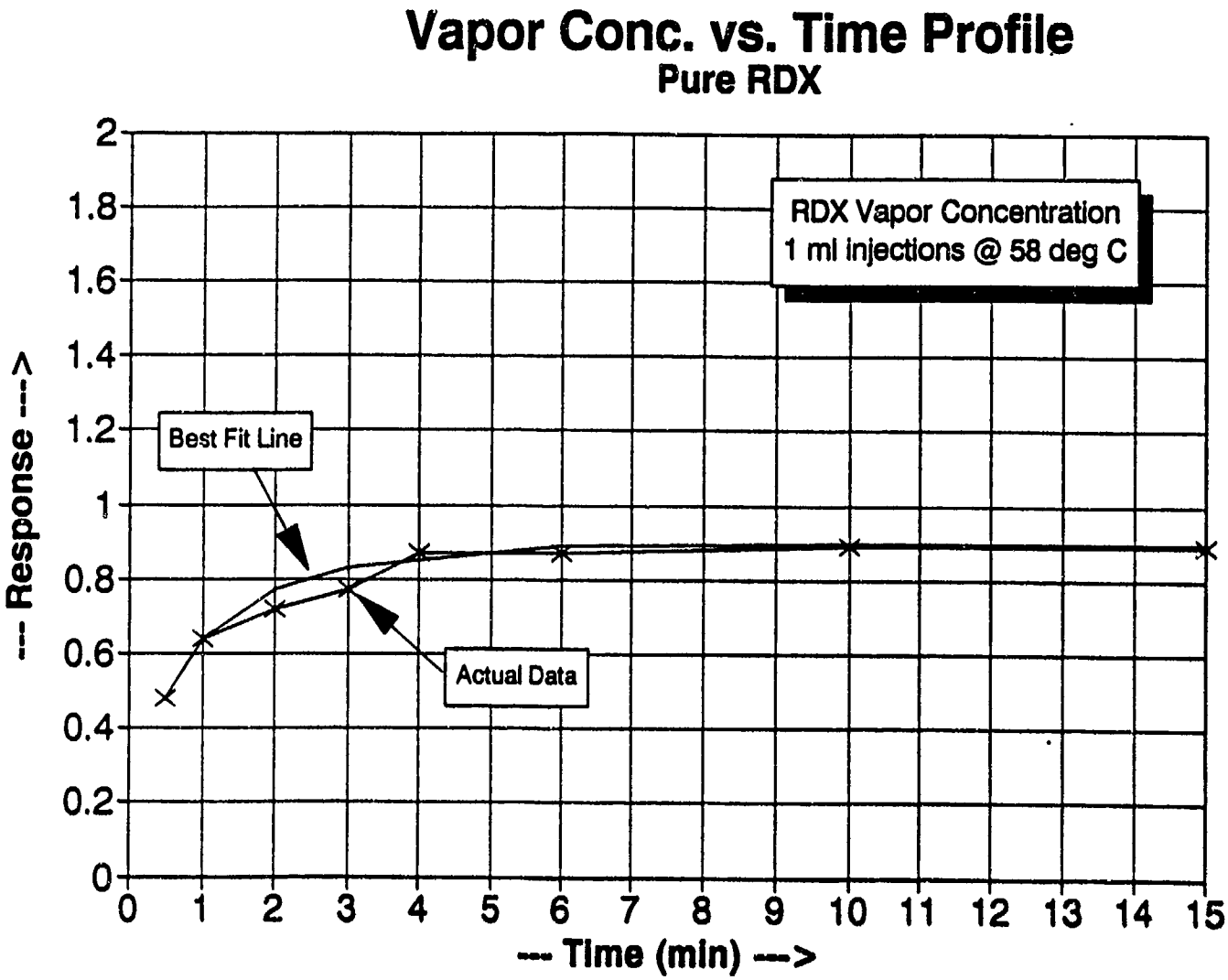


Figure 4. Shows a plot of RDX vapor concentration versus time at a fixed temperature of 58 °C. The experiments were carried out by making a series of 1 ml injections following different equilibration (soak) times. For pure RDX, equilibrium is achieved at this temperature in about 6 minutes.

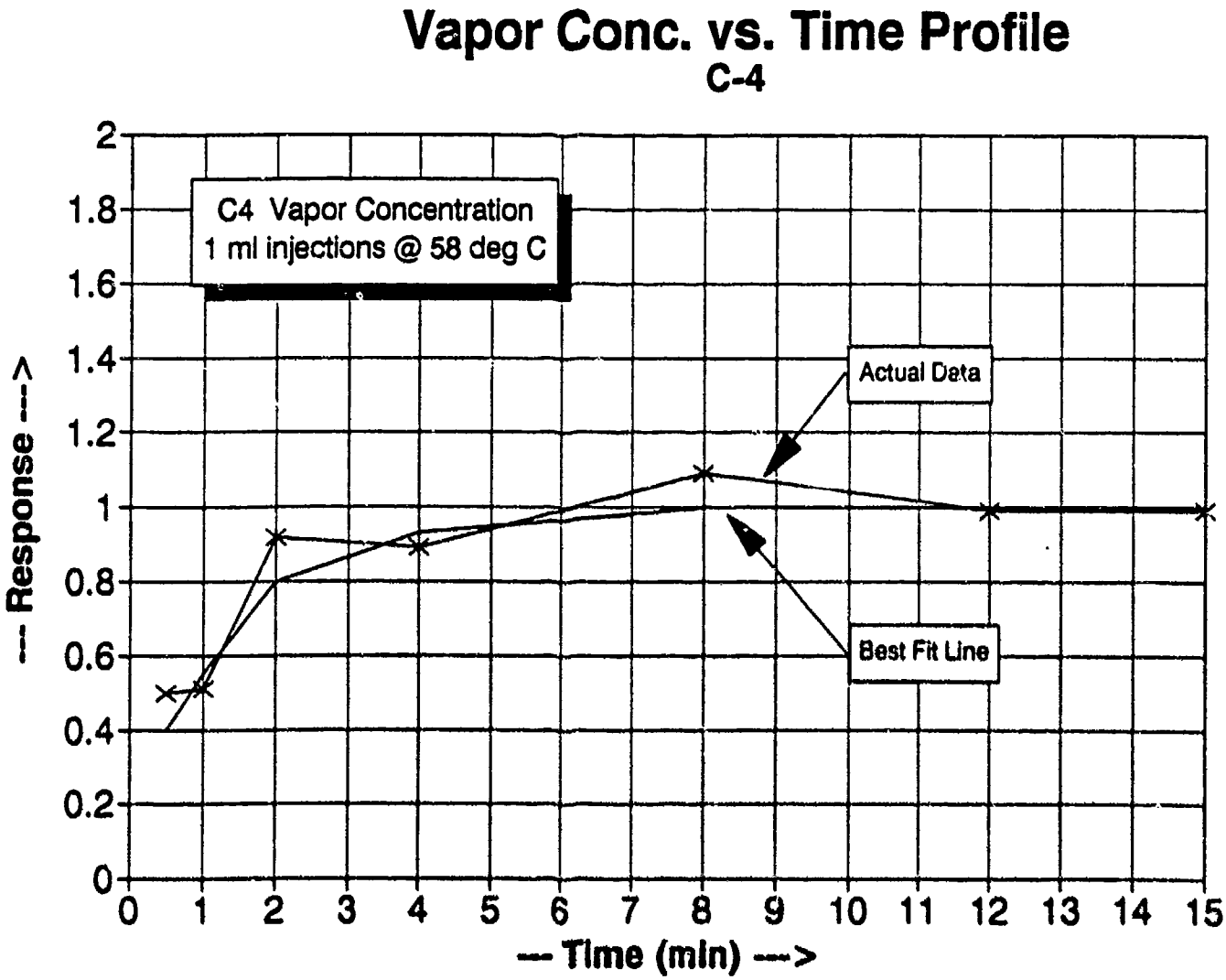


Figure 5. Shows a plot of C-4 vapor concentration versus time at a fixed temperature of 58 °C. The experiments were carried out as described in Figure 4. These data suggest that the soak time for C-4 is 12 minutes.

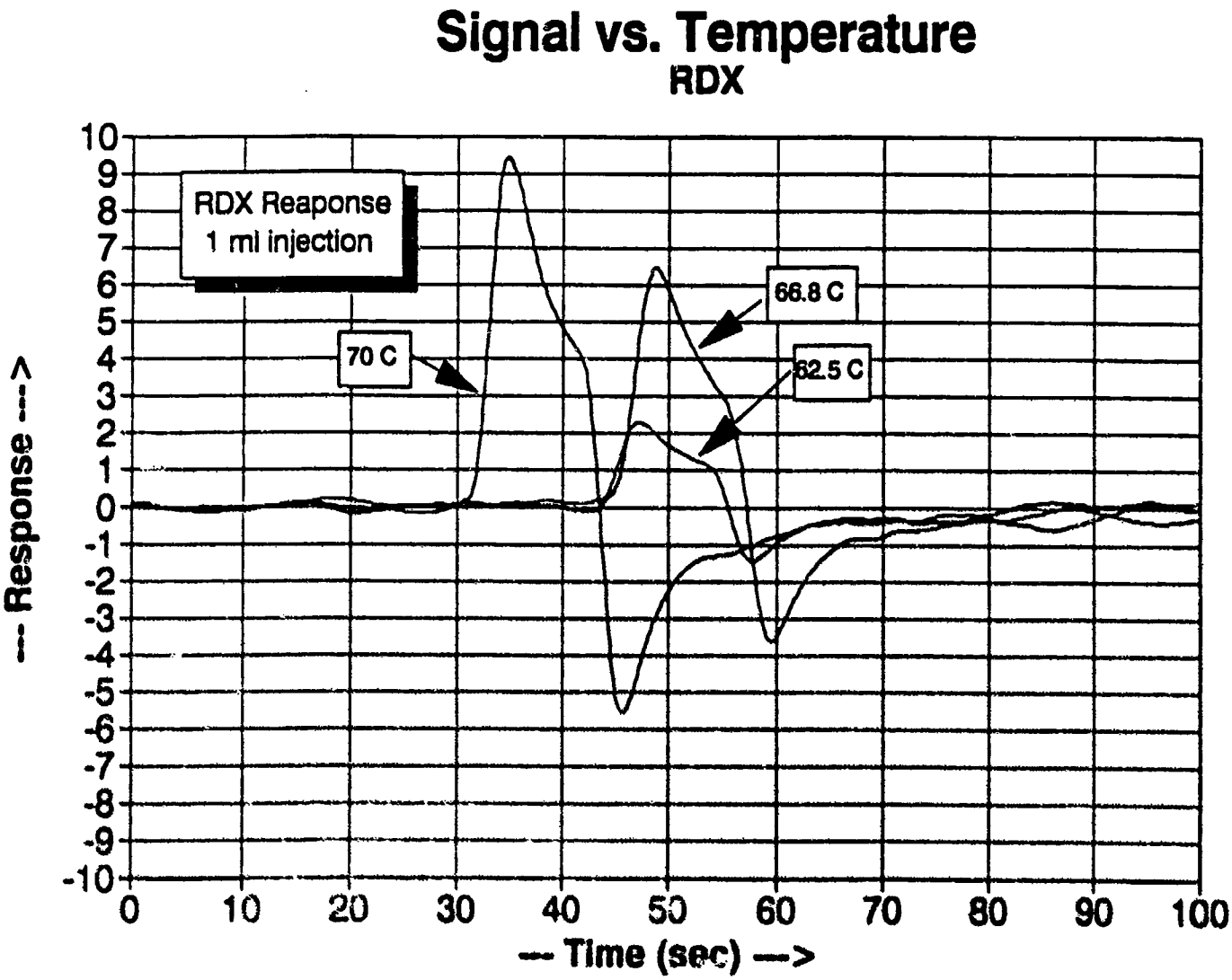


Figure 6. Shows the response of the ITI detection system to vapor from pure RDX as a function of temperature. To illustrate the response versus temperature, three traces are shown.

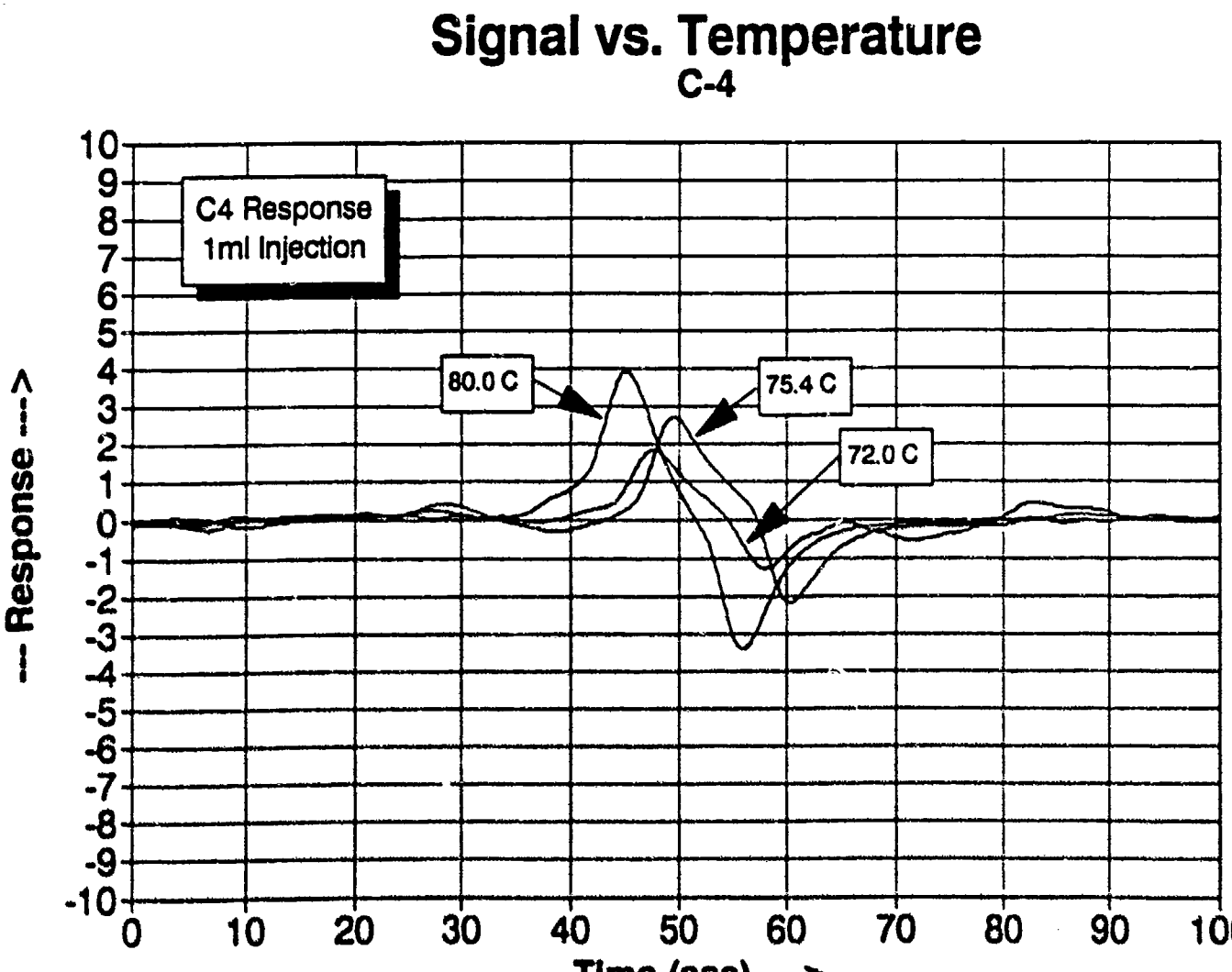


Figure 7. Shows the response of the ITI detection system to vapor from C-4 as a function of temperature. To illustrate the response versus temperature, three traces are shown.

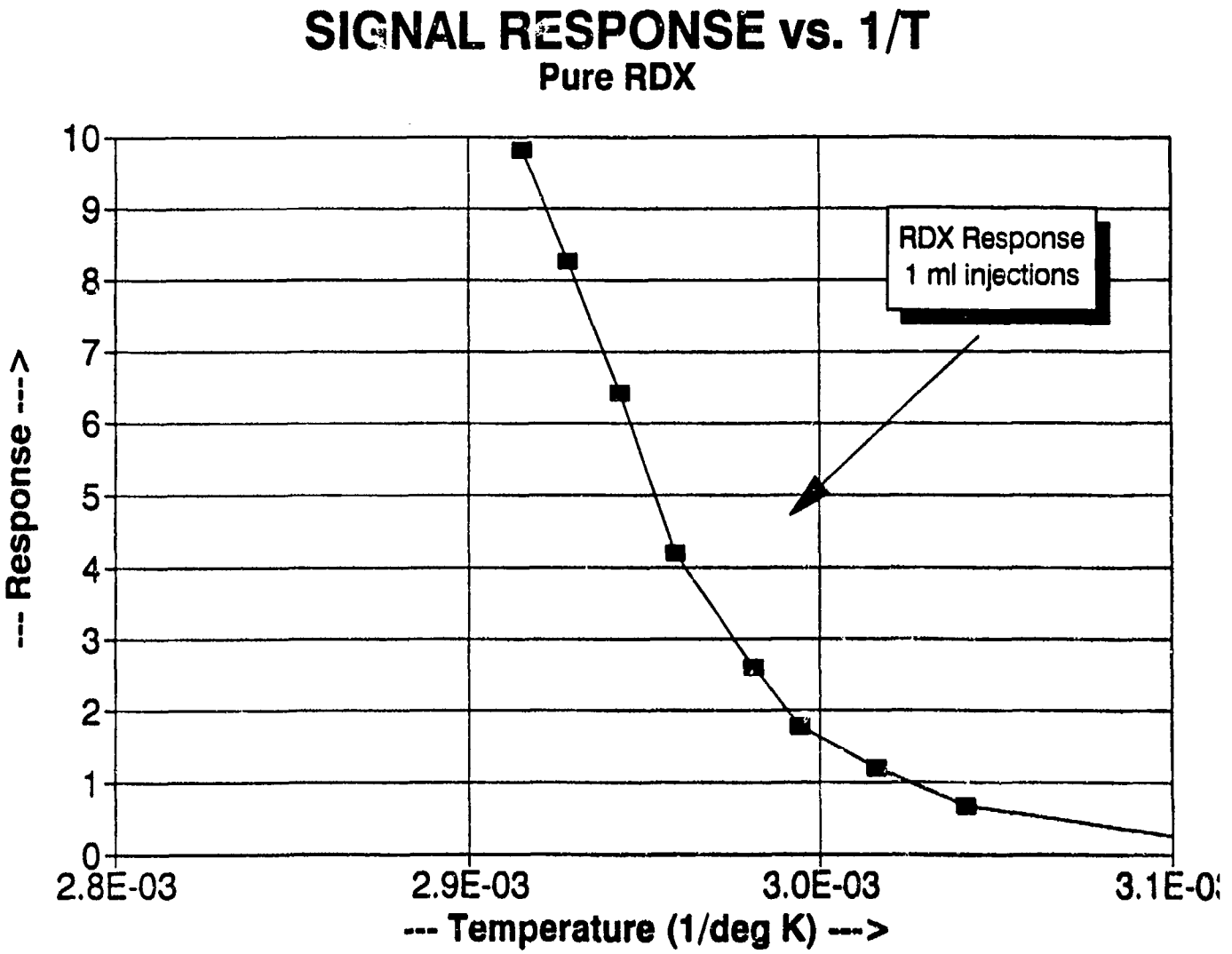


Figure 8. Shows the signal response versus temperature profile for pure RDX vapor. A series of 1 ml injections were made into the portal detection system at various temperatures and the integral response was measured and plotted.

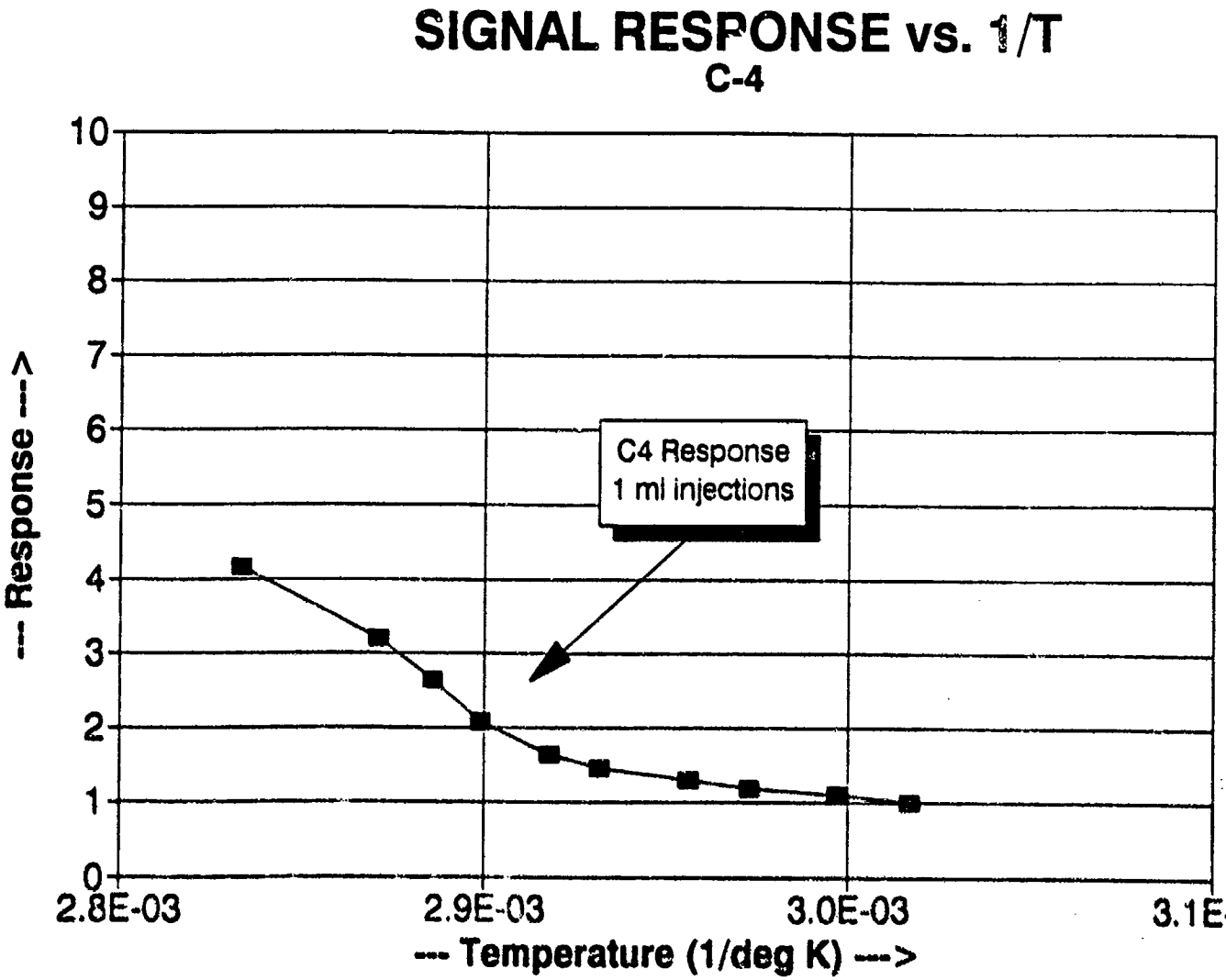


Figure 9. Shows the signal response versus temperature profile for C-4 vapor. The data was collected and plotted as described in Figure 8.

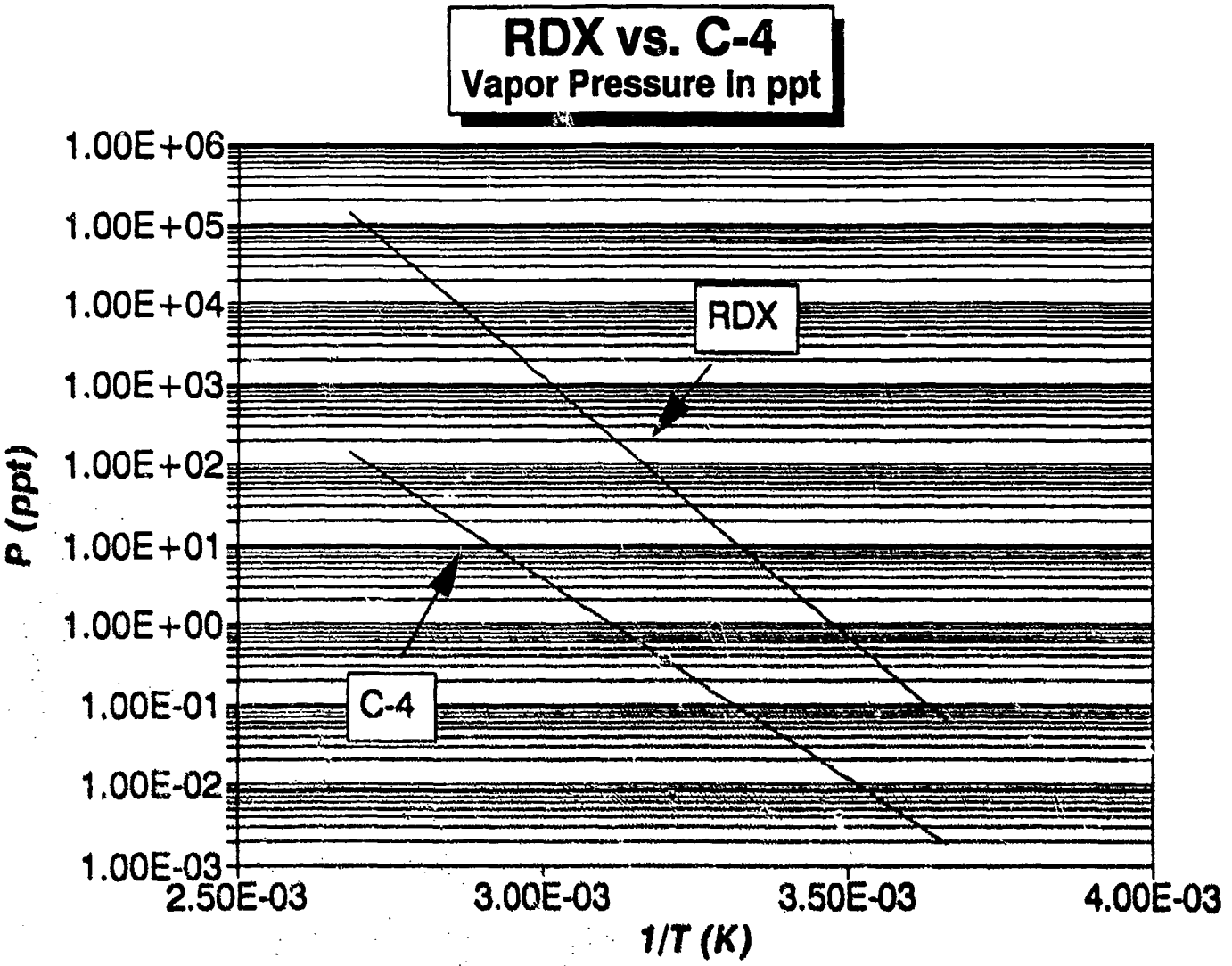


Figure 10. Shows the nonlinear least squares generated vapor pressure versus response curves for pure RDX vapor and C-4 vapor. These plots were generated from the measured data and the known literature values of the thermodynamic constants for pure RDX. The C-4 curve was then generated by relation to the curve from RDX.

EXTRACTION, TRANSPORTATION AND PROCESSING OF EXPLOSIVES VAPOR IN DETECTION SYSTEMS

A. Jenkins, W. McGann, K. Ribeiro
Ion Track Instruments, Inc.
Wilmington, Massachusetts 01887

1. INTRODUCTION

The perceived need for non-intrusive, hands off, detection systems for the detection of explosives on people and in baggage has heavily influenced the design of such systems. Ion Track Instruments has for many years designed and produced walk-through portal vapor detectors and hand held sniffers which sample the air around people and bags in order to detect the presence of explosives. Existing systems for portal detection of explosives such as the ITI 85 Entry Scan shown in **Figure 1** employ air curtain samplers which impinge on the body and sweep any entrained vapors into the trap of the detection system. Sampling flow rates in air curtains of portals have been variously employed by ITI and others at 25 l/s, 100 l/s and 250 l/s. In a typical test of six seconds duration, air volumes of between 150 and 1,500 liters have to be processed for one check. The detector used in such systems has typically less than 1 ml of internal volume. This means that for each test the volume containing the explosive molecules must be reduced by factors in the range from 10^4 to 10^6. We have shown that this is impossible to achieve without losing most of the explosive molecules which may have been sampled.

An alternative method is proposed which does not require high sample flow. This improves the sample trapping and processing efficiency but means that the air must be sampled intimately to clothing or bags in order to extract the available sample in as small a volume as possible. Low sample flows also pose problems of irreversible adsorption of low volatility explosives on the walls of the sample lines. These tubes are necessarily small bore in order to keep response times as low as possible and could pose greater problems than exist in the extremely high flows of air curtain samplers.

Several studies and experiments have been conducted to examine the feasibility and efficiency of low flow intimate sampling systems. The principle can be applied to both portal and baggage detection systems and design solutions for both scenarios have been proposed and tested.

1.1 The Trapping Process

In order to reduce the volume of the dilute sample and hopefully increase the concentration of explosive vapors, it is necessary to trap out the explosive vapor and desorb the vapor into a low flow carrier gas stream before transmitting to a detector. The choice of detector is limited by the extreme sensitivity and selectivity which is required to detect the sub-picogram amounts of explosive which may be available at the check point. The only commercially available detectors with sub-picogram capability are the electron capture detector, certain ion mobility detectors and a few specialized mass spectrometers. All these detectors optimally employ gas flowrates at or below about 1 atmospheric ml/s. It is also necessary to remove much of the interfering atmospheric contaminants in order to reduce false alarms, noise levels and suppression of real responses in the detector. Selective trapping is therefore an essential requirement for a successful system.

From a science and engineering point of view, there are several critical factors which must be understood and controlled in order to develop such a system. First, the trap must be very low volume and selective to explosive vapors.

Second, in order to meet engineering and speed requirements it must be very low thermal inertia. Third, to accommodate the sampling air flow of an air curtain for example, the trap must have low restriction to very high flows. Finally, in order to achieve high trapping efficiencies the trap should have high surface to volume ratio with reasonable residence time in the trap. These are all conflicting requirements on trap design and it is worthwhile to consider some theoretical limitations in order to achieve the optimal solution.

Consider the case of a tubular trap shown in **Figure 2** whose walls are constructed of solid absorber with extremely high affinity for explosive molecules. The best trapping efficiency possible would occur if there is a 100% probability of sticking on the wall when explosive molecules approach within one molecular diameter of the surface.

across a still boundary layer of 1mm thick from a saturated vapor over the surface of pure TNT explosive have been carried out by [Griffy]. The results show that the mean velocity of the diffusion is 3×10^{-3} m/s. Furthermore, the diffusion rate across laminar flow lines is expected to be similar for similar concentration gradients. This allows us to predict within an order of magnitude the rate at which explosive molecules strike the surface of the trap.

The theoretical maximum trapping probability becomes the statistical probability with which the average molecule will strike the wall of the trap.

Let the gas elution time in the trap be "t" seconds then

$$t = \frac{\pi R^2 l}{F} \qquad (1)$$

where F is the sample flow
R is the radius of the trap tube
l is the length of the trap

Let the mean drift velocity be V. Then the distance, d, which the average molecule diffuses across the laminar flow is

$$d = vt \qquad (2)$$

The probability of trapping p is given by the proportion of molecules that reach the surface to those which remain in the tube

$$p = \frac{d(2R-d)}{R^2} \qquad (3)$$

If $d << R$, then

$$p = \frac{2d}{R} \qquad (4)$$

substituting from (1) and (2) give

$$p = \frac{2\pi vRl}{F} \qquad (5)$$

Substituting some realistic values from a possible high flow trap of low restriction say 10 cm long by 2 mm diameter, the maximum theoretical trapping

2. In this example, the trap drops to about 50% efficiency at 4 ml/s. It would be preferable to maintain the trap volume no more than the free volume of the detector otherwise time delays and peak spreading will occur. For this purpose the trap volume should be maintained below 1 ml. The volume of a single tubular trap of dimensions quoted above is approximately 1/3 ml and so three parallel trap tubes could be used to make up a single trap assembly. This trap would have a maximum theoretical efficiency of 50% at a total flow of 12 milliliters per second. Contrasting this with the air curtain flow requirement of between 25,000 to 250,000 ml/second the maximum theoretical trapping efficiency would fall to between 0.025 and 0.0025%.

These efficiencies are typical of high flow trapping systems but clearly do not represent an acceptable solution to the trapping problem for plastic explosives vapor when so little vapor is available in the air stream. If one picogram is sampled by this (high flow) method then at the most, only 1/4 femtogram would be available at the detector. By contrast the low flow system would deliver 500 times more vapor to the detector. This model shows that a more creative approach to the trapping problem is required. Turbulent flow systems do improve the rate at which sample molecules are impinged on the surface of a trap but actual measurements have shown that less than one order of improvement is achieved.

Two further improvements have been successfully developed. The first is the shrinking trap, in which the volume of the trap at the point of trapping is very much larger than the volume of the trap at the point of desorption. This is achieved by a device known as the Rotary Pre-concentrator. Volumetric changes from twenty to one hundred fold have been achieved. The second is the development of the low flow intimate sampling system which extracts the vapor directly from the source in clothing or bags, and allows much lower flows to be employed.

1.2 The Rotary Pre-concentrator●

The rotary pre-concentrator was devised in response to the requirement to trap from high sampled air flows and deliver desorbed vapors of interest into low flow, low volume detection systems. The rotary pre-concentrator system also incorporates a continuous chromatographic scrubber which removes all unwanted volatile contaminants of the atmosphere and

delivers only the very low volatility and highly polar nitro compounds into the detection system. This reduces false alarms and interferences in the detection system.

The system is shown in **Figures 3 & 4** and a view showing the carrier and air flow patterns is shown in **Figure 5.** A ceramic plate carried two concentric seals which defined the sample, purge and carrier gas paths around the trap. These two 'o' ring seals shown as concentric rings in the figures seal against the face of the rotary disc trap. Deeper channels were provided in the ceramic around half of the backing plate for the flow of sampled air and purge air. In the other half, carrier gas is directed between the surface of the trap and the surface of the ceramic in a path whose depth is determined by the height of the seal above the ceramic surface. A depth between 0.25 and 0.50 mm is typical.

Air is drawn into the system down the heated Teflon® line and is caused to impinge on the trap surface at the sampling point. The sampled air is then drawn around the surface of the trap to the vacuum port which was in turn connected to a multi-stage turbine pump capable of pulling 40 mbar vacuum and up to 2 cubic meters/minute flow rate. An auxiliary air purge is added to the apparatus shortly before the sample inlet in order to cool the trap prior to the sample point.

The trap rotates from the sample inlet point through the pre-strip region where all unwanted contaminants are separated from the system by the chromatographic effect of the warm carrier gas stream. The temperature of the ceramic backing plate is maintained higher than the temperature of the disc to ensure all explosives and contaminants are carried by either the carrier gas or the trap and do not stick in the surface of the backing plate. In the pre-strip region the gas flows in the opposite direction to the trap rotation thus allowing the trap to carry the less volatile explosives into the desorption region in the opposite direction to the unwanted contaminants which are stripped continuously from the system.

The rotary trap carries the explosive fraction of the sample into the desorption zone where the trap temperature is increased rapidly to the strip temperature of 165°C. All explosives are expected to be desorbed at this temperature and are swept into the electron capture detector. A post strip position was designed for cleaning the trap before the next cycle but subsequent tests show that this is not necessary. The trap then rotates through the post strip region into the purge region where a flow of clean purge air is arranged to impinge onto the trap and cool the trap from 165°C back to within a few degrees of the ambient temperature.

2. RESULTS

2.1 Efficiency and Transport Measurements

The efficiency of the transport and trapping system was measured by a method of direct injections into the inlet of the trapping system and the inlet of the detector. The apparatus used for this test is shown in **Figures 6 and 7.**

In previous work, conducted in our laboratories, [Jenkins] it was shown that vapor samples from pure explosives can be introduced into a detection system from an all glass syringe containing the pure explosive within the barrel of the syringe as shown in **Figure 6.** Samples of pure TNT and pure RDX were prepared on inert mineral wool by evaporation from solution in acetone. The responses to blank injections from syringes containing the support material alone were first obtained. Unfortunately the flow changes induced in the carrier stream provided significant responses in the detector. This was eliminated by adding two syringes back to back as shown in **Figure 7.** As the syringe containing the explosive was depressed the connecting syringe was drawn back by exactly the same amount. The syringes were operated many times until a steady reading was obtained. Blank results were obtained for both the mineral wool and the glass wool supports. The syringe containing the explosives was then injected into the carrier line as shown in **Figure 7** and again the tandem syringes were worked many times to remove all residual oxygen and atmospheric contaminants. The temperatures of the syringe needle and body were recorded. The syringes were drawn back and then depressed by 0.5ml each time at increasing intervals. This would show whether a saturated vapor level was achieved.

The injection apparatus was then removed and the rotary trap replaced in the apparatus. The operating conditions were set and allowed to stabilize. The same syringes were used at the same temperature to inject metered amounts of explosive into the sample inlet. The responses were recorded by a laboratory

data acquisition system and the results are shown in **Figures 8 and 9.** The response peak produced from the air injections is much more diffuse than the direct injection but the total integrated response showed that in an air flow of 50 ml/s a trapping and release efficiency of 27% was achieved for RDX vapor.

These results encouraged us to engineer the rotary

trap system into an intimate portal sampling system for plastic explosives.

2.2 Intimate Sampling

We have taken great care to design a portal sampling system which although samples from actual contact with the clothing is also nonintrusive to the subject. **Figure 10** is an illustrators depiction of an intimate portal sampler in use alongside an x-ray and metal detector at an airport security check. The test model is shown in the photograph **Figure 11** and a drawing showing the sampling panels against subjects of differing height is shown in **Figure 12.** The panels are provided with heated Teflon® sampling lines in order to intimately extract air from within the clothing.

Previous work conducted in our laboratory showed that RDX vapor and all other higher volatility vapors can be transported down heated Teflon® lines without attenuation at temperatures over 70°C. A Teflon® extrusion was designed which comprised a cylindrical bore with four small holes in the wall cross section in which heater wires were threaded. Four fins were extruded on the outside of the Teflon® tube to provide thermal insulation and aid assembly into the door cavity shown in **Figure 13.** A thermocouple was assembled into the door cavity below the heated Teflon® line. This was incorporated in a temperature control circuit that maintained the heated Teflon® line at constant temperature within the test range from 60 to 90°C.

A groove for the heated Teflon® line was milled in each door as shown in **Figures 13.** The wall of the Teflon® sampling tube was drilled to provide several input ports along the edge of the door as shown in **Figure 14.** Preliminary testing on a two panel system was conducted. Samples of pure plastic explosives obtained from the laboratories of Ensign Bickford were placed in a temperature controlled all glass syringe as previously described. A range of vapor volumes were injected into the door panel in the air stream. Responses for RDX and PETN were obtained and recorded and are shown in **Figures 15 and 16.**

2.3 Vapor Emission Stimulation and Extraction

The level of vapor emissions was increased by the application of infra-red irradiation of the subjects clothing and by direct warming by the door panels. Further mechanical stimulation is achieved by the action of the door panels on the subjects clothing as seen in **Figure 11.** These methods of stimulation increase the amount of available vapor from hidden plastics explosives. The results unfortunately cannot be published here but the system was shown to exhibit a potent level of detection to plastics explosives containing PETN or RDX.

The instrument cycle allowed for two seconds of heating before directing the subject to walk through the door. Any vapor sampled was carried into the detection system in less than one second and a further four seconds were taken to process and detect the sample in the detection system. The total testing time was between six and seven seconds to provide a result.

3. CONCLUSION

We have shown that intimate sampling at low sample flows provide far more sample delivery efficiency than high flow air curtain samplers. The problems of sample absorption at low flow were overcome by employing heated Teflon® lines at or above 70°C. An efficient rotary trap was designed which can accommodate the high temperature sample gas stream and trap RDX vapor with 27% efficiency. An intimate sampling walk through portal detector was designed and tested which responded to sub picogram quantities of RDX vapor in six seconds.

REFERENCES

1. Griffy, T.A. Proc Manheim Conference on Explosives Detection, 1989.

2. Jenkins, A., McGann, W.J., Ribeiro, K. and Napoli, J. "Final Report", FAA DTFA-03-87-C-00005 (1991)

ACKNOWLEDGEMENT

This work was supported by the FAA, Contract No. DTFA03-87-C-00005.

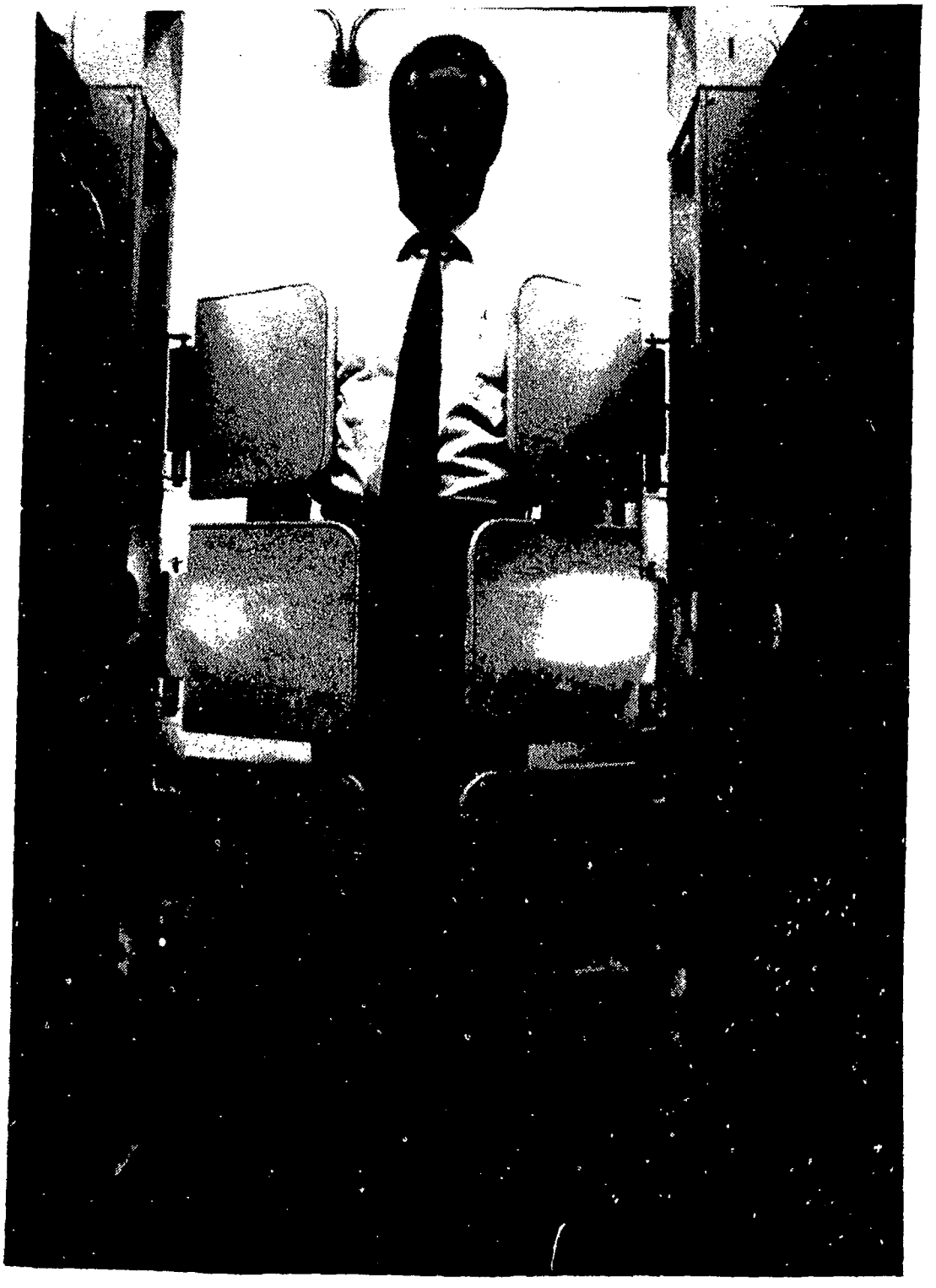


Figure 1 ITI 85 Entry Scan Walk Through Explosives Detector

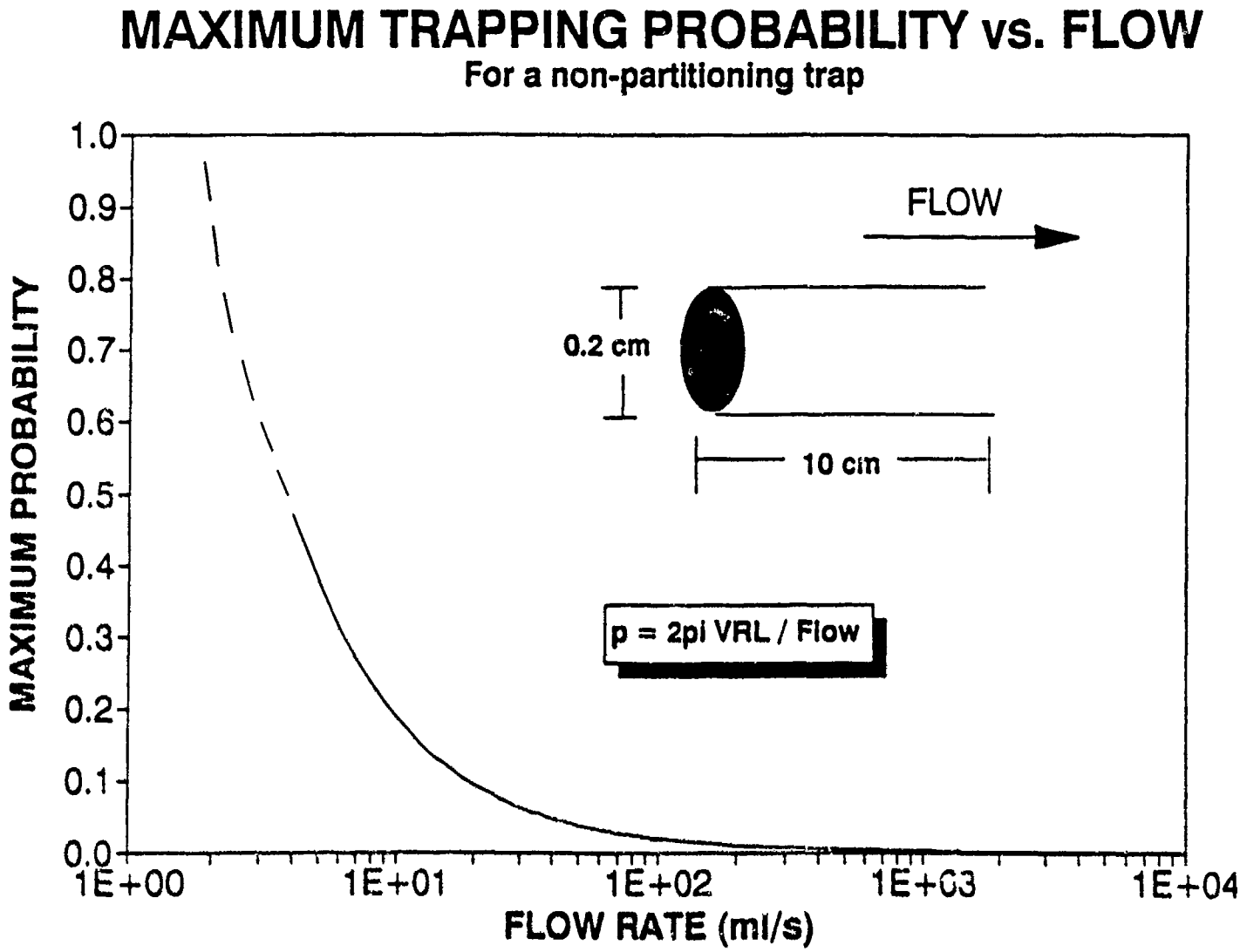


Figure 2 Theoretical trapping probability in a tubular trap.

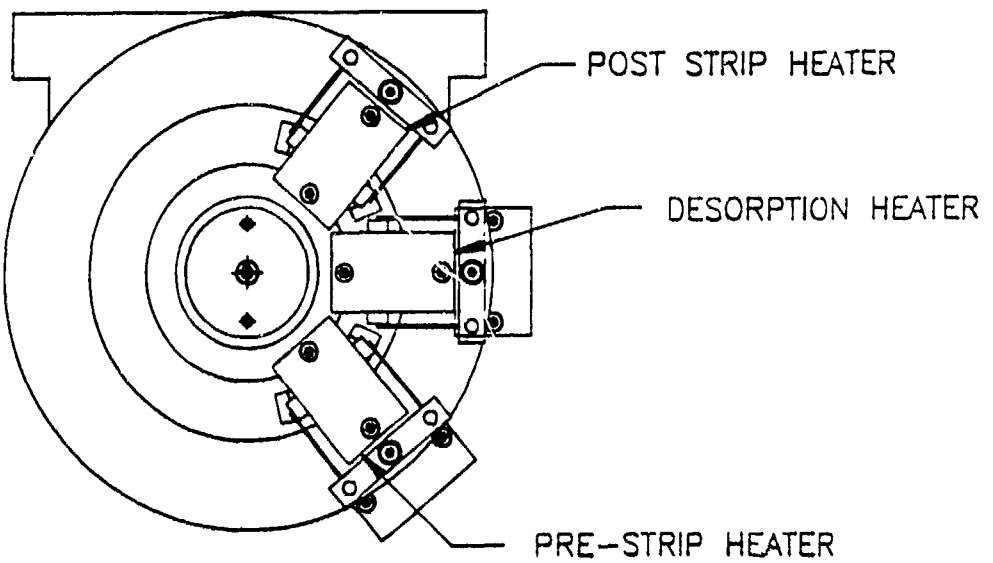


Figure 3 Top view of the rotary trap showing the heaters.

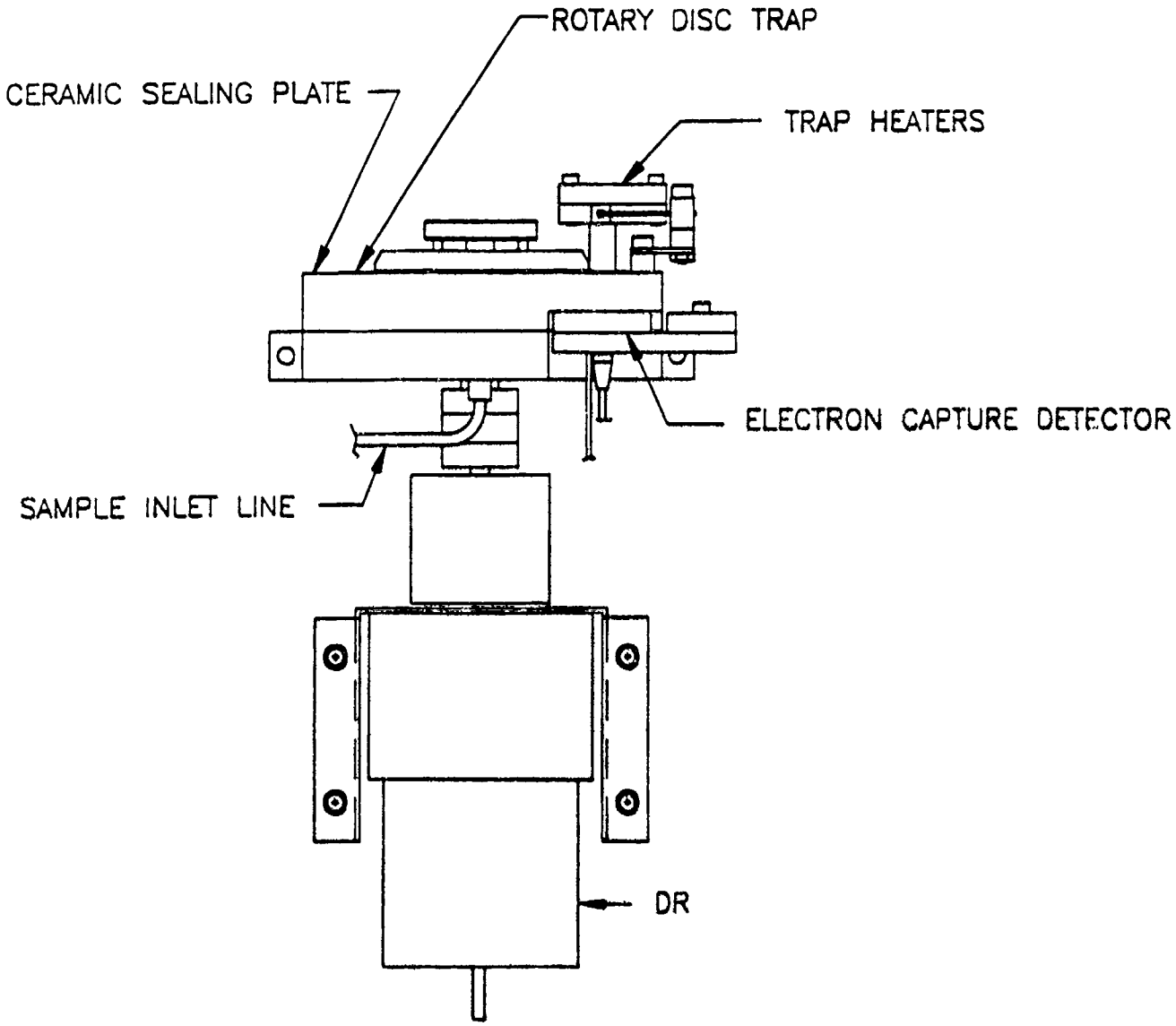


Figure 4 Side view of the rotary trap.

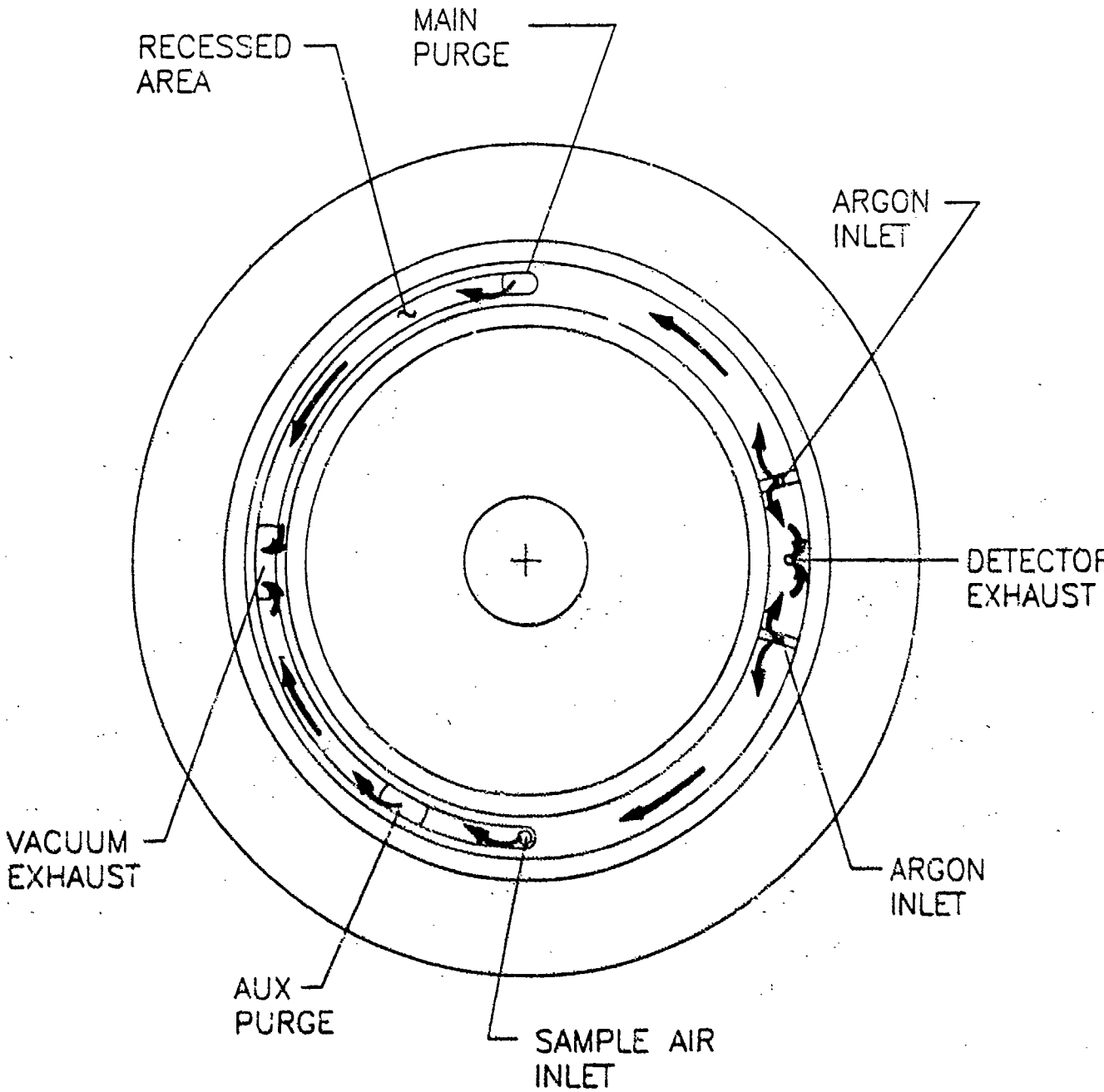


Figure 5 View of the rotary trap showing the carrier and air flow patterns.

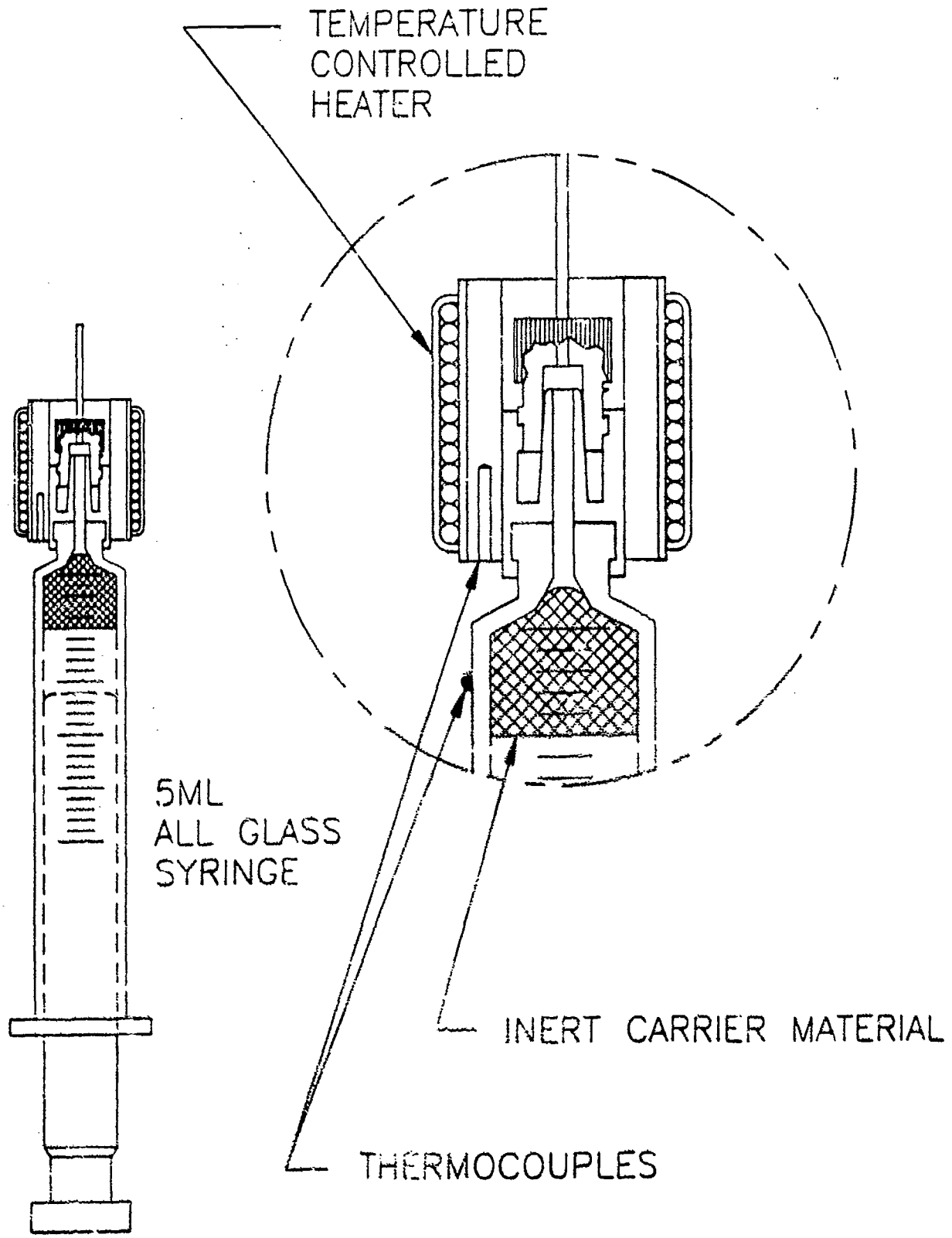


Figure 6 All glass syringe with detail of the heater and inert carrier material.

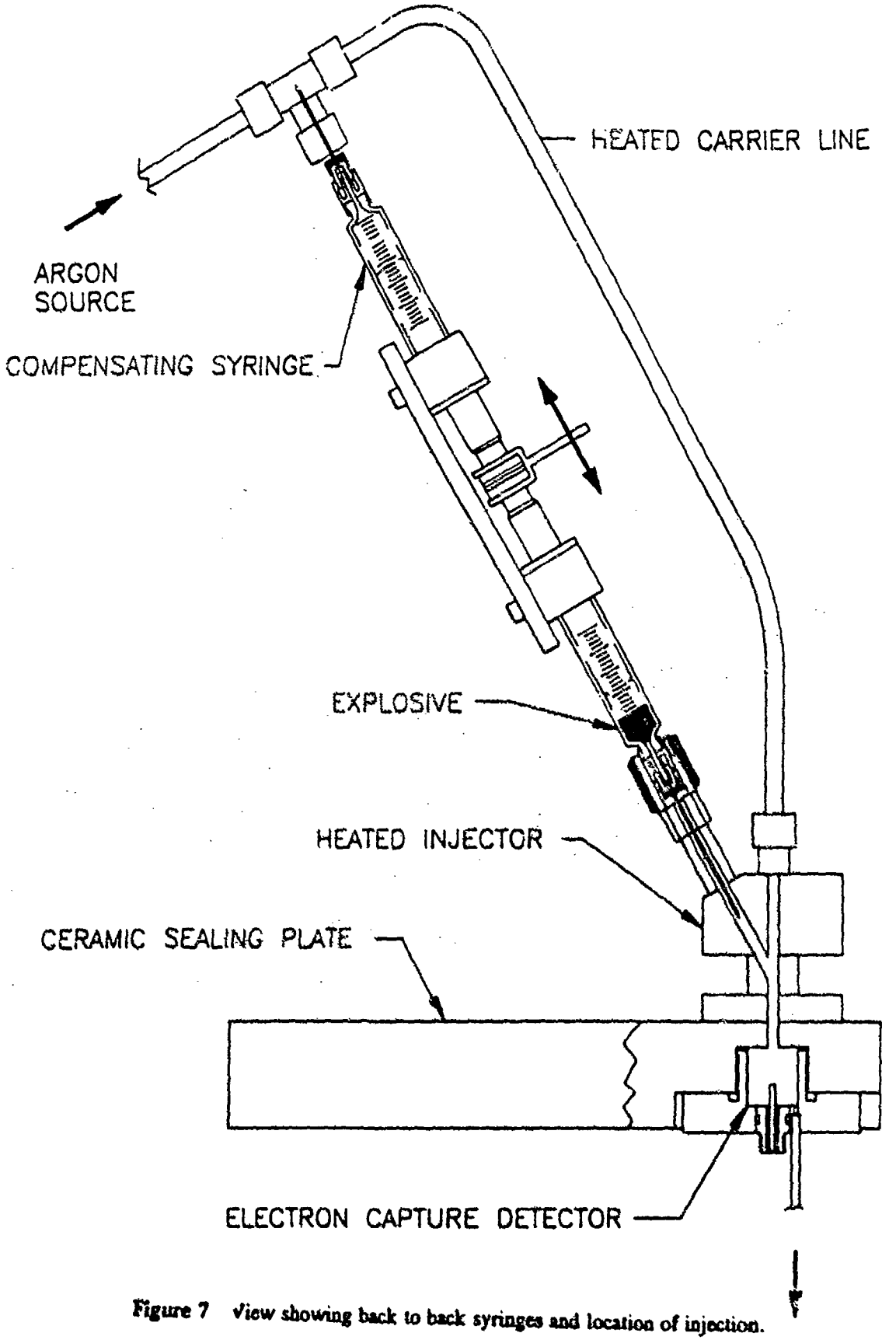


Figure 7 *View showing back to back syringes and location of injection.*

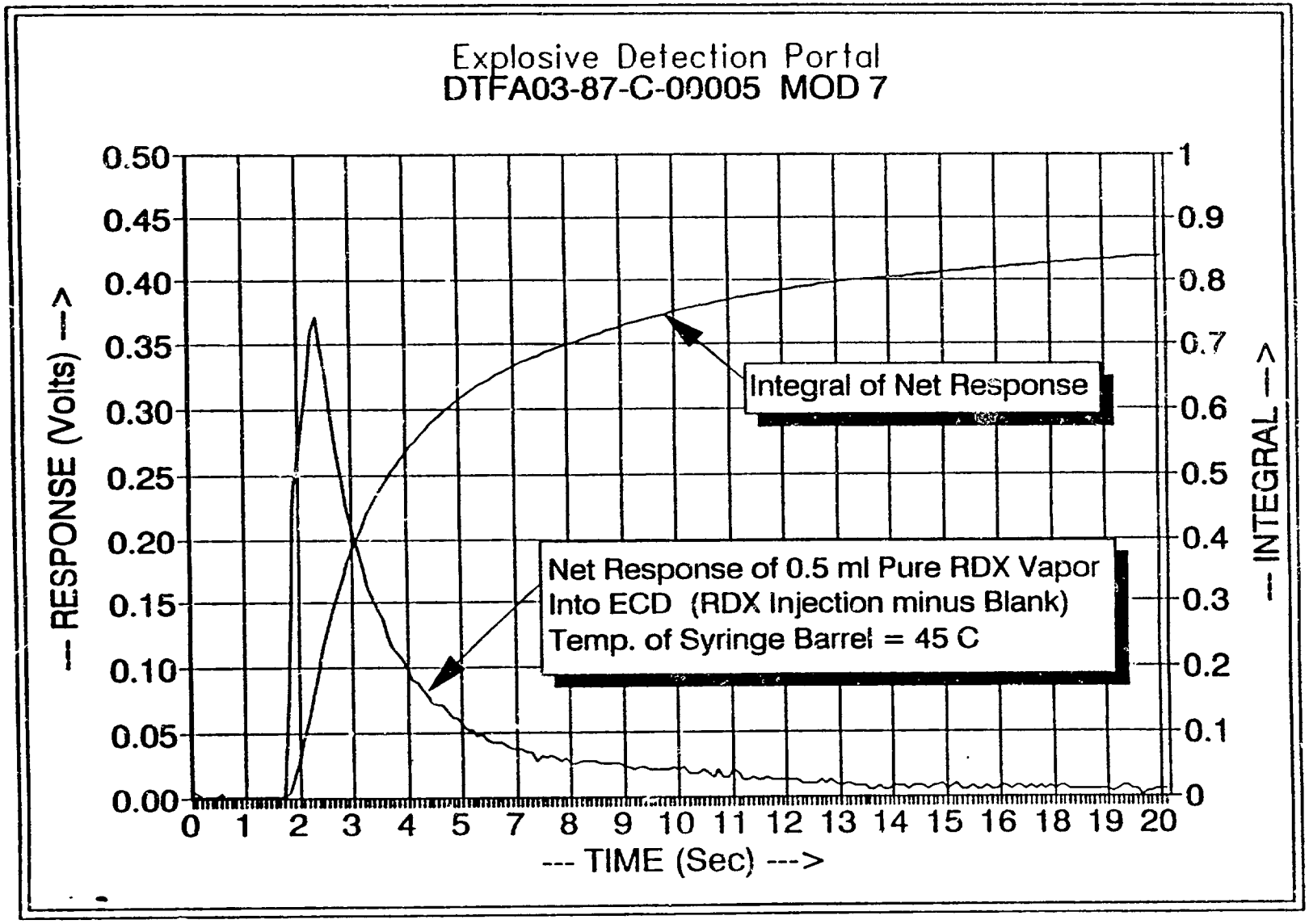


Figure 8 Response to direct injection of RDX vapor into the ECD showing net response of 0.5 ml pure RDX vapor into ECD at a syringe temperature of 45° C.

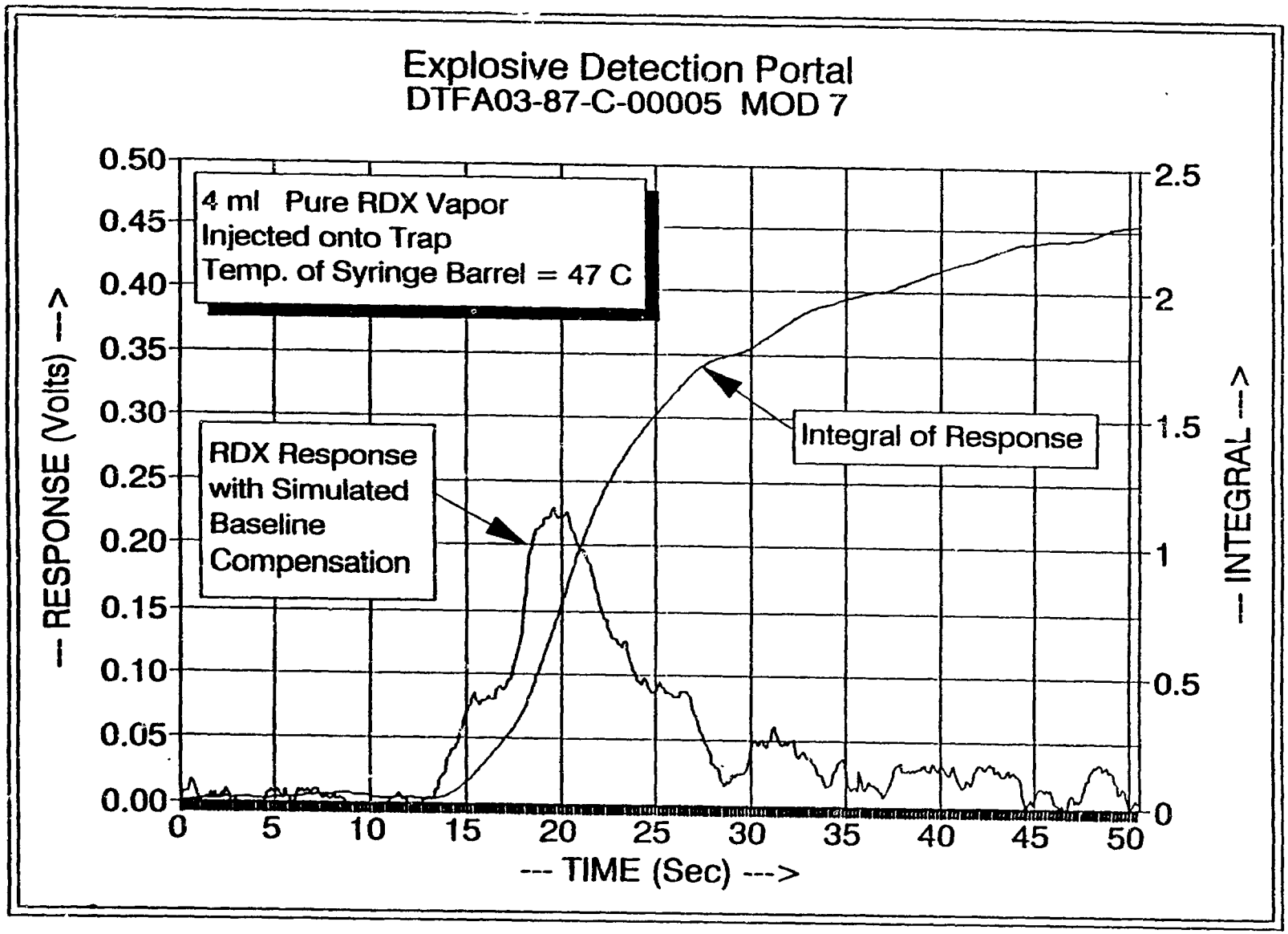


Figure 9 Response to injection of RDX vapor into the air inlet showing response of 4 ml of pure RDX vapor injected onto the trap at a syringe temperature of 47° C.

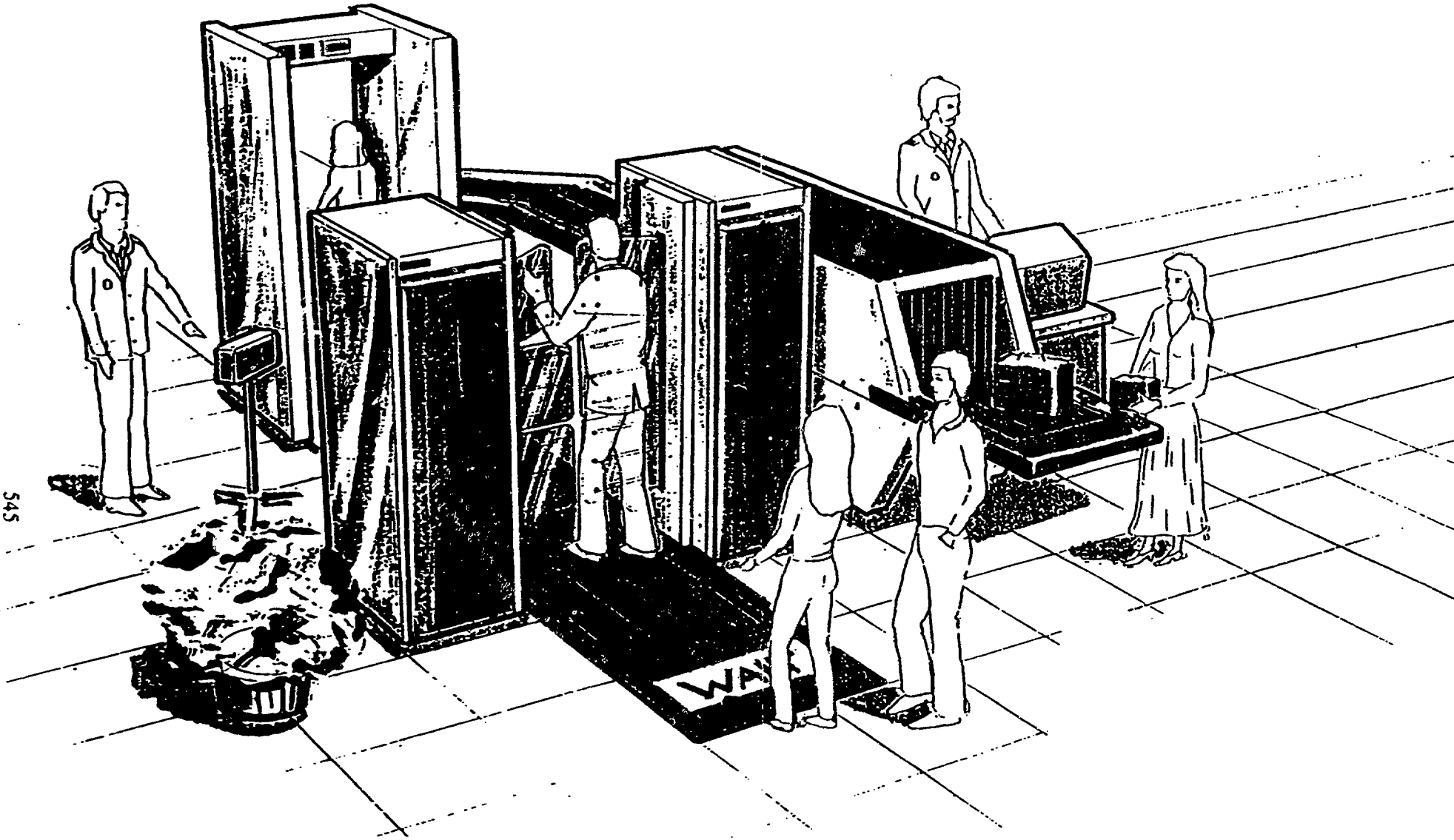


Figure 10 Illustrators depiction of an intimate portal sampler in use alongside an x-ray and metal detector at an airport security check.

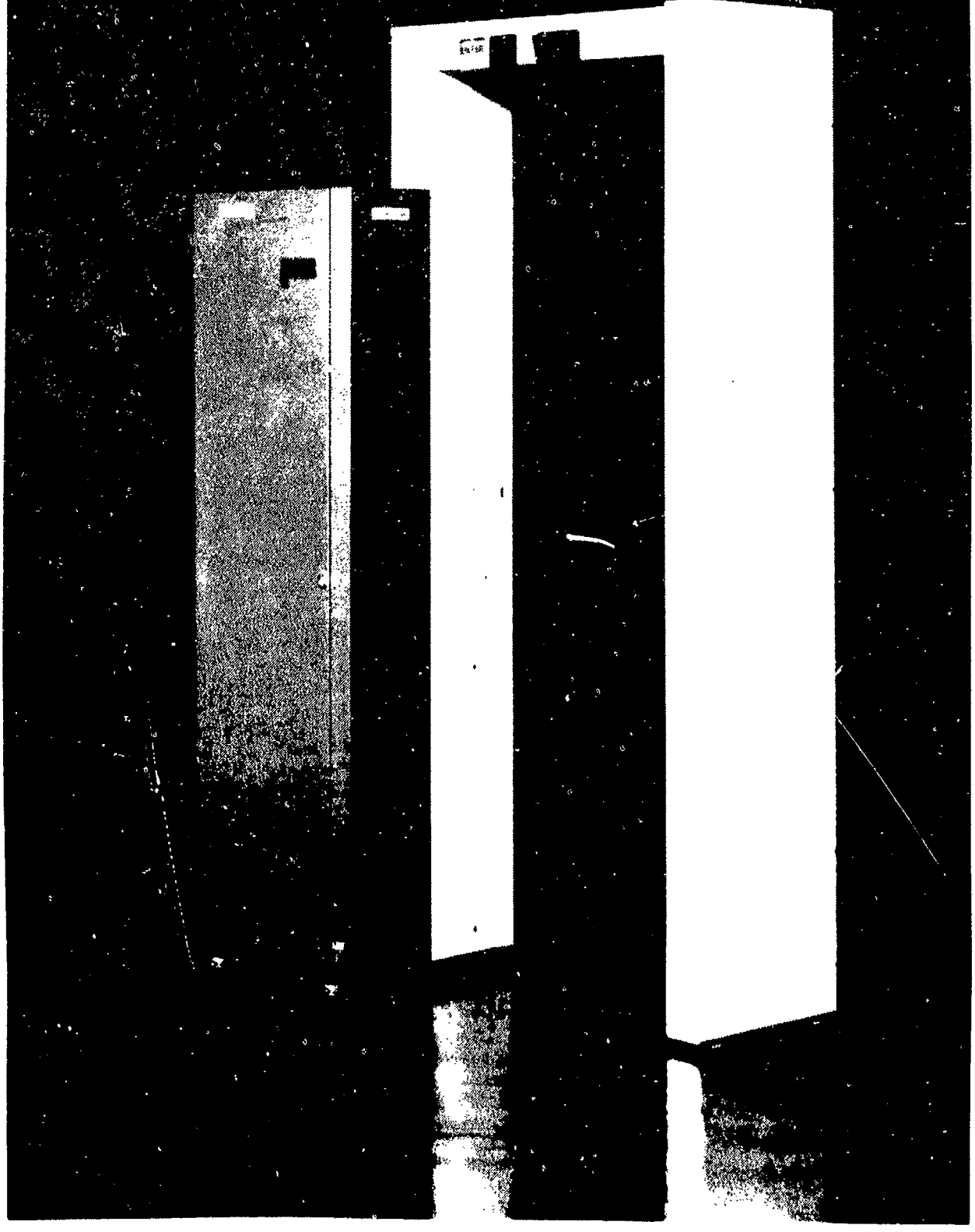


Figure 11 Test Model of Portal Explosive Detector

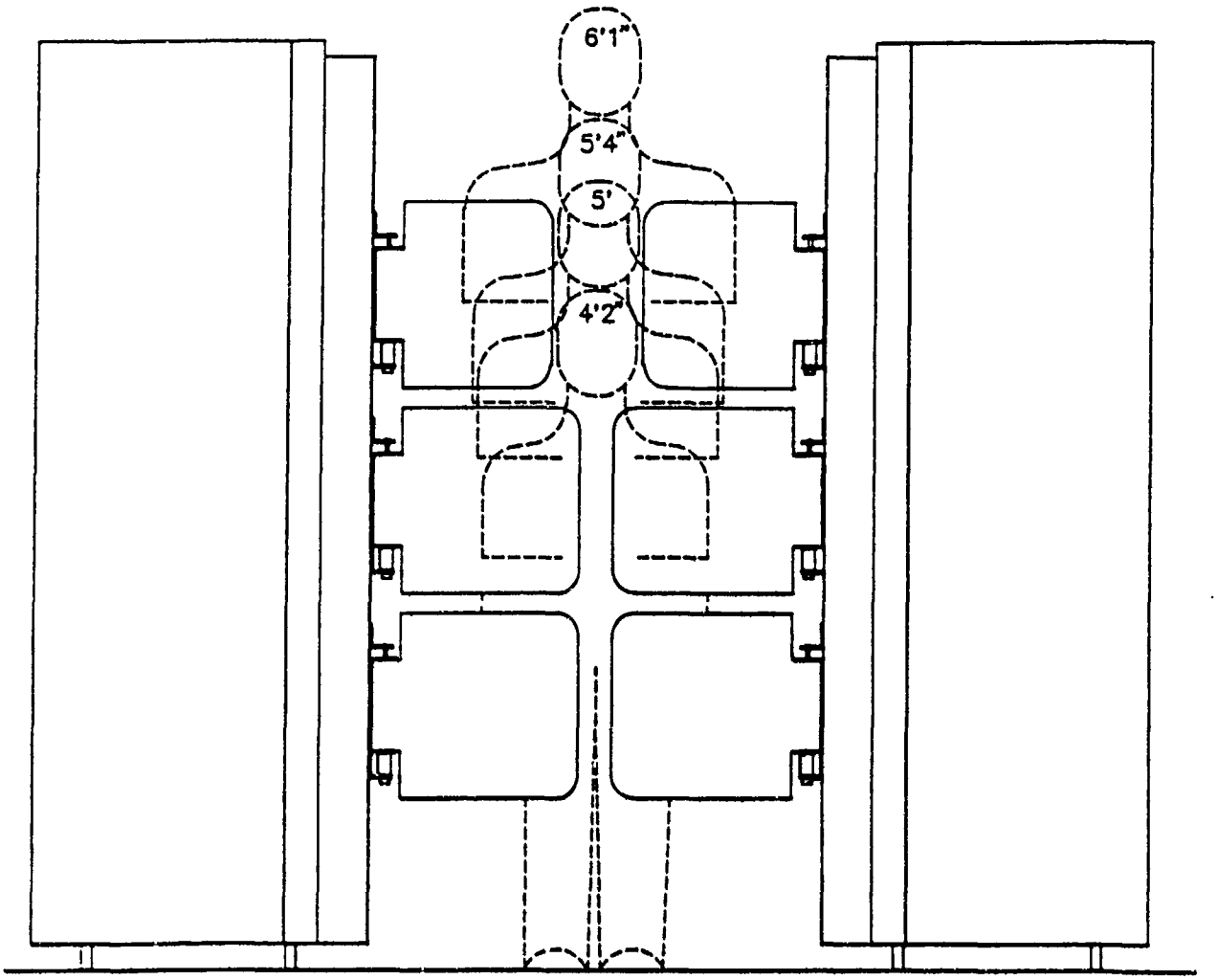


Figure 12 View showing the sampling panels against subjects of differing heights.

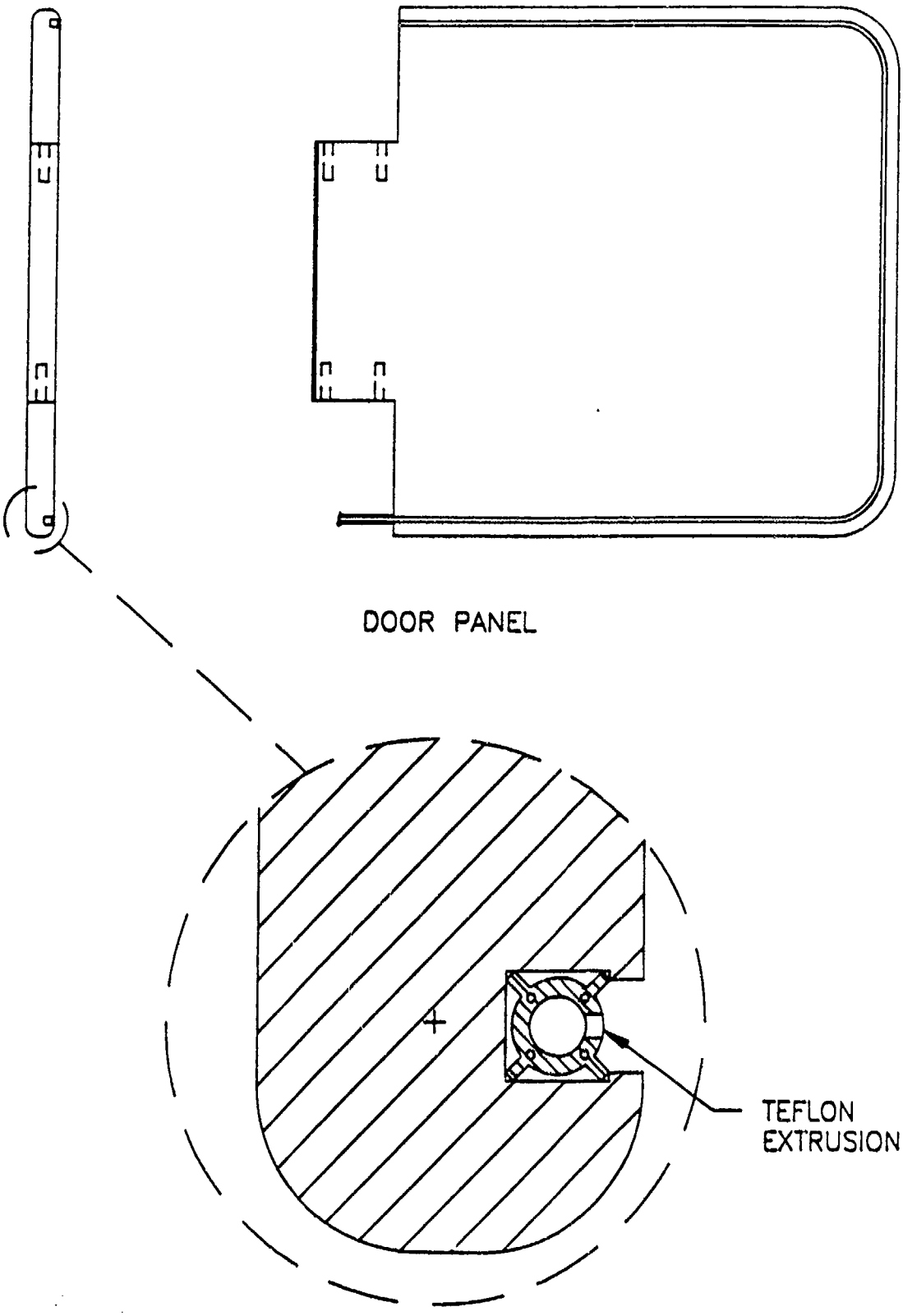


Figure 13 View showing door section with detail of the inlet line

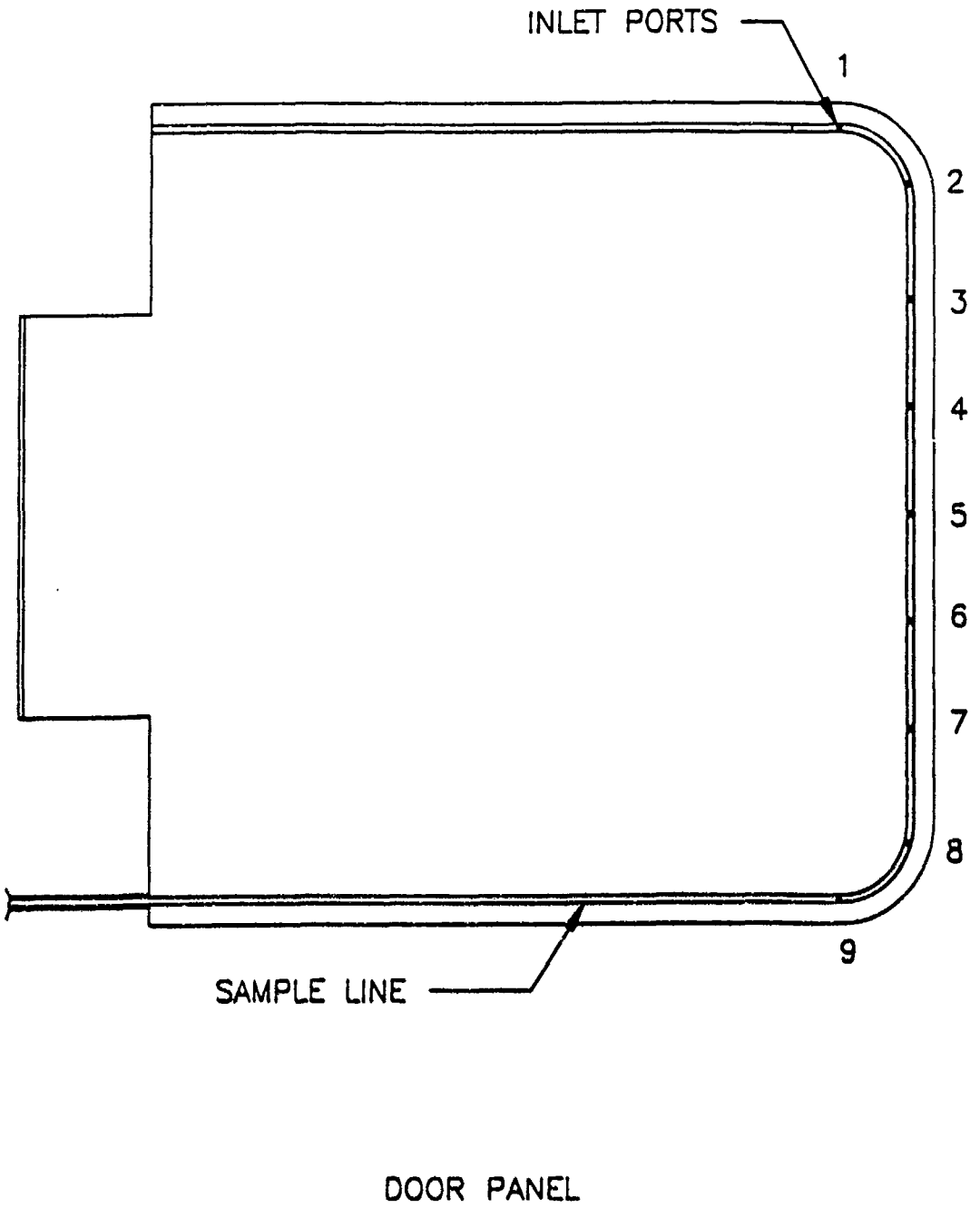


Figure 14 View showing input ports along the edge of the door.

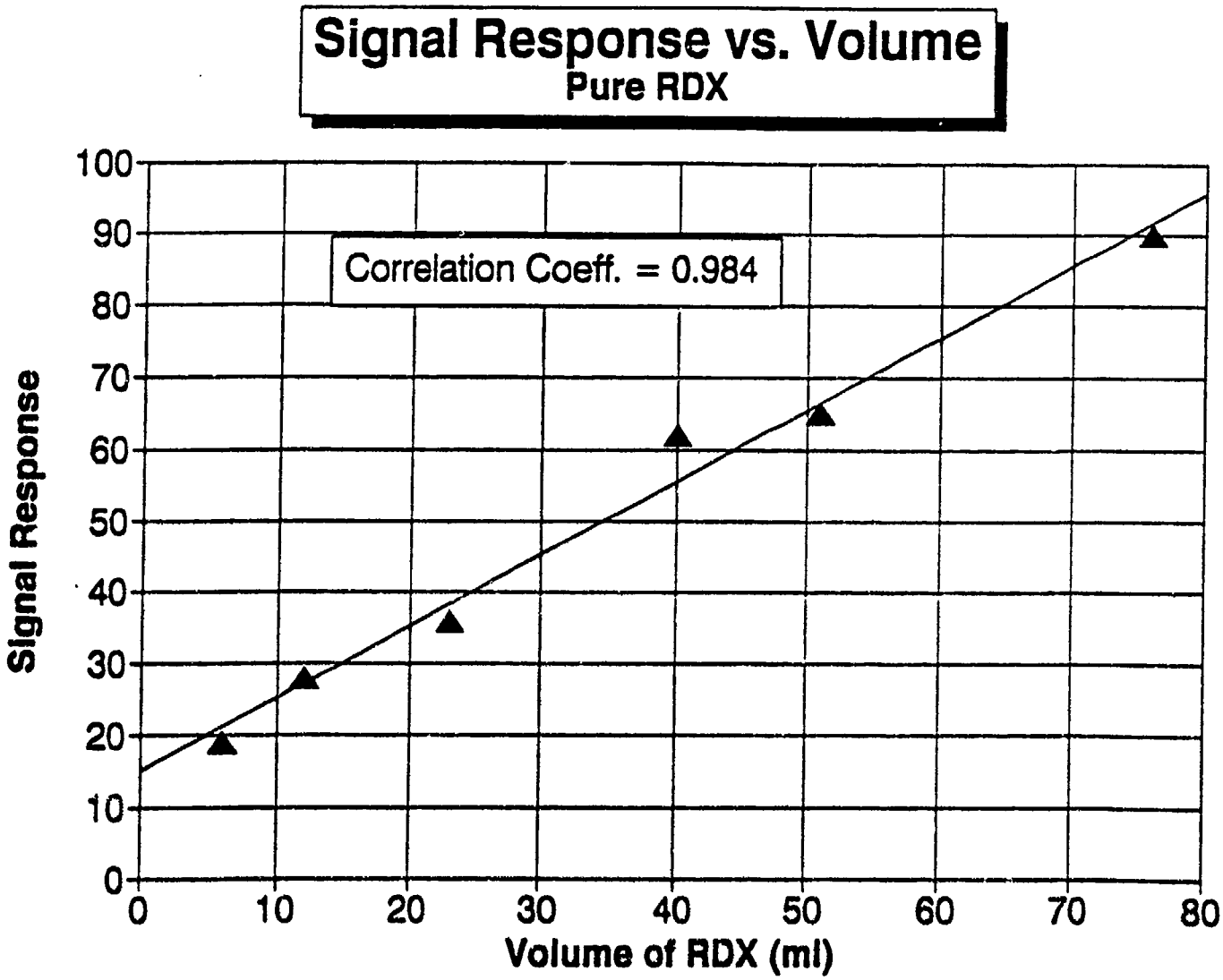


Figure 15 Signal response versus volume of injection of pure RDX at 25 °C.

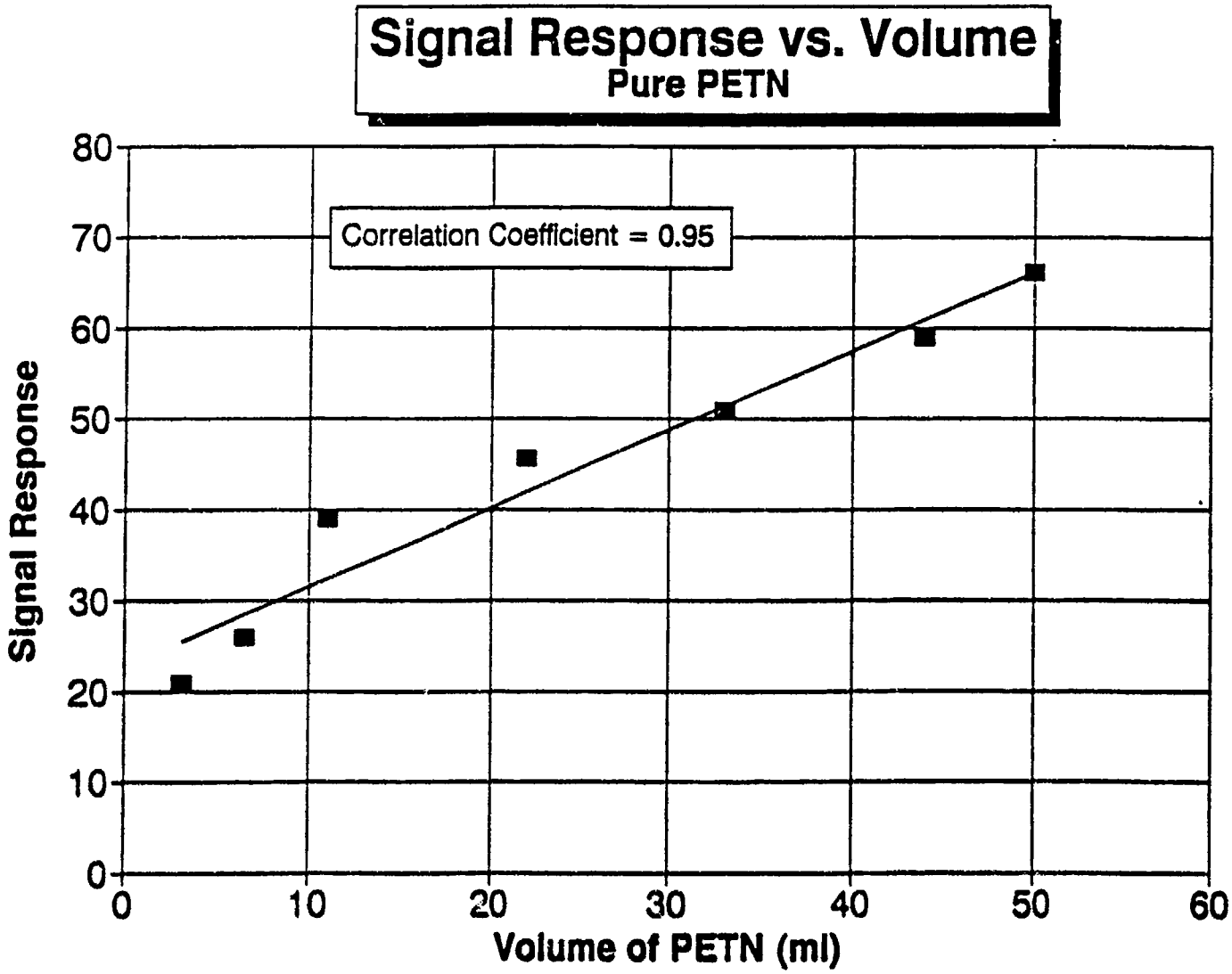


Figure 16 Signal response versus volume of injection of pure PETN at 25 °C.

VAPOR SAMPLING USING CONTROLLED HEATING

Edward E. A. Bromberg, A. Lindsay Carroll,
Freeman W. Fraim, and David P. Lieb
Thermedics, Inc.,
470 Wildwood Street
Woburn, MA 01888

1. INTRODUCTION

In the typical use of a vapor explosive detection system, explosive devices hidden by a terrorist in a package, suitcase on a person etc, are being searched for. While the practical sensitivity required to alarm on 99+ % of the potential devices is not known, it is recognized that the more sensitive the system is the higher is the probability of detection. For most vapor explosive detection systems there are at least two major sections, the sampling section and the analysis section. The analysis section itself can often further be broken down into major sub-components. In order to increase the total sensitivity, one could increase the sensitivity of one or all of the components. In this paper we will focus on increasing the sensitivity of the sampling device. The important issue of increasing the sensitivity of the analysis device, or the equally important issue of selectivity, will not be addressed.

Figure 1 summarizes the vapor pressure data of Dionne *et al*[1] for some of the important explosives of interest. As seen from this figure an increase of temperature by 10C will typically increase the vapor pressure by a factor of 3 - 10. Clearly, increasing the temperature of the device being sampled will increase the vapor pressure, and thus increase the probability of the sampling device capturing the vapors for later analysis. While it may not be practical to increase the temperature of the complete device being sampled in a short period of time (of the order of seconds,) it is possible to heat sections of the surface quickly. In designing such a device the following criterion were considered:

A) Heating the surface quickly to the desired temperature.
B) Not burning the surface while trying to achieve the desired temperature.
C) Integrating a reliable temperature measuring device if required.
D) Low power consumption so as to operate with batteries.
E) Safe to operate.
F) Be relatively lightweight and portable.

It was based upon these considerations that the sampler of Figure 2 was designed. This device consists of an infra-red heat source (a projection lamp), a temperature measuring device (infra-red pyrometer), the concentrator (described in a accompanying paper by L. Carroll et al[2]), a vacuum blower system to suck the vapors across the collection device, rechargeable and replaceable batteries, and the internal micro-computer system and electronics to operate the device.

2. HEATING

Many methods of heating of the surface were considered. Some were eliminated as not practical, for example ultra-sonic heating; or not acceptable from a safety point of view, for example lasers or microwaves. Two methods were evaluated, hot air and infra-red energy from a projection lamp.

One technique that was evaluated and eliminated was that of using heated air. The air would be heated by blowing ambient air over a resistively heated element. Since this is a battery operated unit, the heating element would be off, until required. It would typically take a few seconds for the resistively heated element to achieve the desired temperature. Additionally, unless the source temperature was significantly higher than the target temperature, it would take a long time for the surface to come to the target temperature since the heating rate is a function of temperature difference. Finally, the hot air would be sucked into the sampling collector area, increasing the temperature of the collector, and thus decreasing its collection efficiency. It was also found that the

infra-red heating described below was more power efficient and faster.

The second heating method evaluated, and finally chosen was a modified 24V 250 Watt quartz halogen projection lamp. In order to increase lamp life, and to increase battery life, the lamp is operated at 21 or less volts, and thus does not operate in the halogen cycle mode. With this lamp typical times to achieve the target temperature of about 80C ranges from a fraction of a second for plastic and paper, to about 4 seconds for painted metal. Highly polished metal, as for example polished chrome, reflect most of the infra-red, and thus hardly increase in temperature.

3. TEMPERATURE CONTROL

The projection lamp chosen is effective in heating the surface area of about 10 centimeters square of most materials. In fact, if there is no control, for many materials the temperatures rise could be high enough to damage, and even cause the material to burn. In order to avoid any damage, the surface temperature is measured, and the power to the lamp is controlled so that once the set point temperature is achieved, the temperature is held constant at the set point. This is achieved by measuring the temperature remotely using an infra-red pyrometer specifically configured for this application. Since the emissivity cannot be calibrated for each material, a wavelength was chosen for which the emissivity of most materials is similar. Table 1 summarizes the emissivities of a sample of different materials[3]. Looking at table 1, one sees that assuming an emissivity of .92 for most materials using a pyrometer sensitive in the 10 micrometer range, will lead to a proper measurement. It is only for highly polished metals that the error will be significant. Further, the error will be in the safe region with respect to overheating of any of the surfaces.

The control loop between the lamp and the pyrometer is microprocessor controlled. In actual use, the lamp is initially turned on at low power and the temperature rise as a function of time is measured for a few tenths of a second. Based upon this temperature rise, the algorithm of the processor can determine if the surface being heating is one that heats up fast or slow. If it is a fast heating surface, the processor continues power to the lamp at a reduced voltage, so that the heating process is performed at a rate that the loop can control. If the surface is heating slowly, the algorithm will command the lamp to go on to full power and will turn the power off when the set point temperature is reached. Once the set point temperature is reached, the lamp goes into control and the voltage is reduced to the point that the set point temperature is maintained. For safety reasons, there is also a "time out" that will shut the lamp off after 10 seconds under all conditions. The reason that the power starts off reduced, is that it has been found that for certain materials, such as dark vinyl, at full power the end point temperature is reached so quickly that the controller does not have time to respond before the temperature overshoots and damage may occur. Further since it is fast heating surfaces that are typically more delicate, the algorithm can change the set point within a range of temperatures based upon the heating rate.

It should be pointed out that while the pyrometer and the software algorithm together form a sophisticated system that is seldom fooled, it is possible for it to occasionally over heat surfaces. For this reason the use of the heating lamp on people is not recommended. Also when using the device on delicate and expensive materials, it is recommended that a test sample be taken. It should further be noted that the pyrometer is measuring the average temperature of its field of view. The field of view is smaller than the heating area of the system. Thus the average temperature may be below the set point, and thus the system continues heating, while actually some areas may be cold, while others are being over heated. Two extreme examples of this would be a checker board pattern, with sections alternatively white and black. The black surface will heat up much faster. Since for most surfaces the emissivity is independent of the perceived color in the visible, the pyrometer will read the temperature of each section properly, but if an average is being reported, the black portion will be overheated while the white portion may still be quite cold. A second example would be a surface such as a carpet. In this case the fibers sticking out may be singed, while the main portion of the carpet remains quite cold. Experience has shown that it is straight forward to train the user to use the sampler so as not to damage virtually all samples that will be checked.

4. PERFORMANCE

Figure 3 shows the heating rate of different surfaces as a function of time for the sampler with the projection lamp. In running these experiments, the lamp was operated without control from the

ml to computer, while the output of the pyrometer was used to measure the surface temperature. Prior to these experiments, the materials were put on a hot plate heated to the different temperatures with the temperature being measured by both a small thermocouple and by the infra-red pyrometer to calibrate the different responses. The agreement in worse case was +/- 10°C. The power used for the vinyl sheet was about 100 watts, while the power used in heating the black painted stainless steel sheet was about 200 watts. Even with the reduced power for heating of the vinyl sheet, the sheet was heated from ambient to about 100°C in about one second. In the same one second period the stainless steel sheet was heated from ambient (25°C) to about 50°C, a significant increase, and an increase that would significantly increase the probability of detection.

Tests with explosives were performed with absorbent paper impregnated with explosives dissolved in solvents, the solvent was allowed to evaporate, and the paper was sampled with the sampler. While the exact detailed response to the explosives is classified it can be stated that when the paper was sampled at ambient temperatures without heating, the response of the unit was to detect at about the alarm level. When the sample was heated there was an increase of signal of a few orders of magnitude. These test were also repeated with similar results using a stainless steel plate and placing a known solution of explosives on the plate, allowing the solvent to evaporate, and then sampling the plate.

A mode of operation that has been found to be effective is to operate the sampler in a "panning" mode. In this mode, the sampler is held up on the surface being sampled and slowly moved across the surface at such a rate that the lamp can maintain the set point temperature of the surface. The fact that the lamp can maintain the temperature is indicated by the lamp flickering off and on. If the lamp is full on, the user is moving too fast, if the flicker rate is slow, the user is moving too slowly. It has been found that the typical user gets the feel for the proper panning speed quickly.

In addition to sampling directly with the sampler described, it has also proven to be effective to sample using different types of wipes. When wipes are used, the wipes, typically paper or cloth, are used to wipe the surface being checked. The explosives are then transferred from the wipes the pre-concentrator of the sampler by using the controlled heating system of the sampler, increasing the probability of detection.

5. CONCLUSIONS

It has been shown that by using an infra red source for heating and an infra-red pyrometer it is possible to design and build a system to heat different surfaces in a controlled and non-destructive manner. This sampling system can be used to effectively raise the surface temperature of the sample being checked for explosives to increase the probability of detection. This sampler has been designed to enable successful use by guards at the different security check positions with a minimum of training.

ACKNOWLEDGEMENTS

We would like to thank the United States Department of State for its support under contract number 2038-563371 under which most of the work described in this paper was performed.

REFERENCES

1. B. C. Dionne, D. P. Rounbehler, E. K. Achter, J. R. Hobbs, D. H. Fine, "Vapor Pressure of Explosives," *Journal of Energetic Materials*. 4 (1986), pp. 447-472.

2. F.W. Fraim, E.K. Achter, A.L. Carroll, E. Hainsworth, "Efficient Collection of Explosive Vapors, Particles and Aerosols", to be published in proceedings of The firstInternational Symposium on Explosive Detection Technology, November 13-15, 1991.

3. G. G. Gubareff, J. E. Janssen, R. H. Tsorborg, *Thermal Radiation Properties Survey*, 2nd ed. (Minneapolis: Honeywell Research Center, Minneapolis-Honeywell Regulator Company, 1960).

TABLE 1 - EMISSIVITIES OF DIFFERENT MATERIALS[2]			
	WAVELENGTH, MICRONS		
MATERIAL	10	3.6	.6
MARBLE	0.95		0.46
PLASTER	0.93		
QUARTZ	0.89		
WHITE PAPER	0.95	0.82	0.28
OAK, PLANED	0.91		
POLISHED STEEL	0.08	0.14	0.45
PAINTED STEEL	0.91		

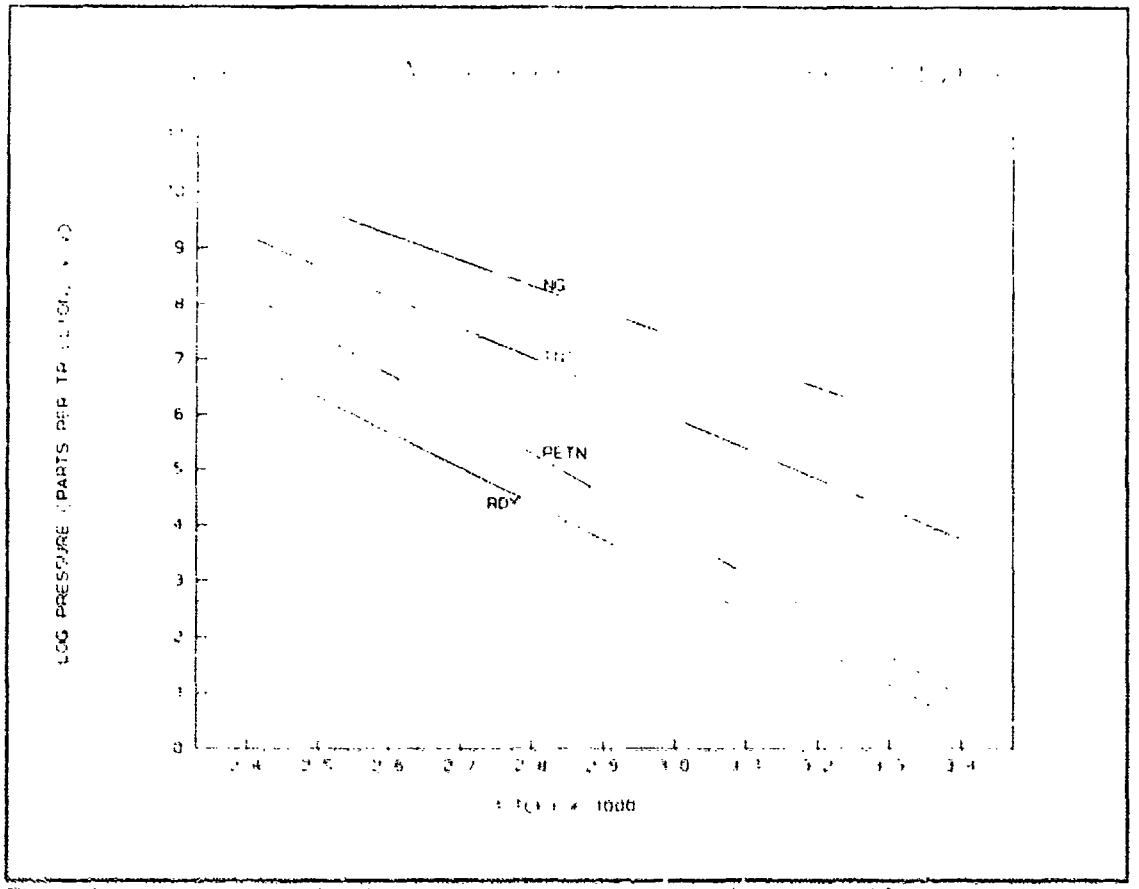


Figure 1 - Vapor pressure of explosives versus temperature The data presented here is based upon the data of Dionne et al[1].

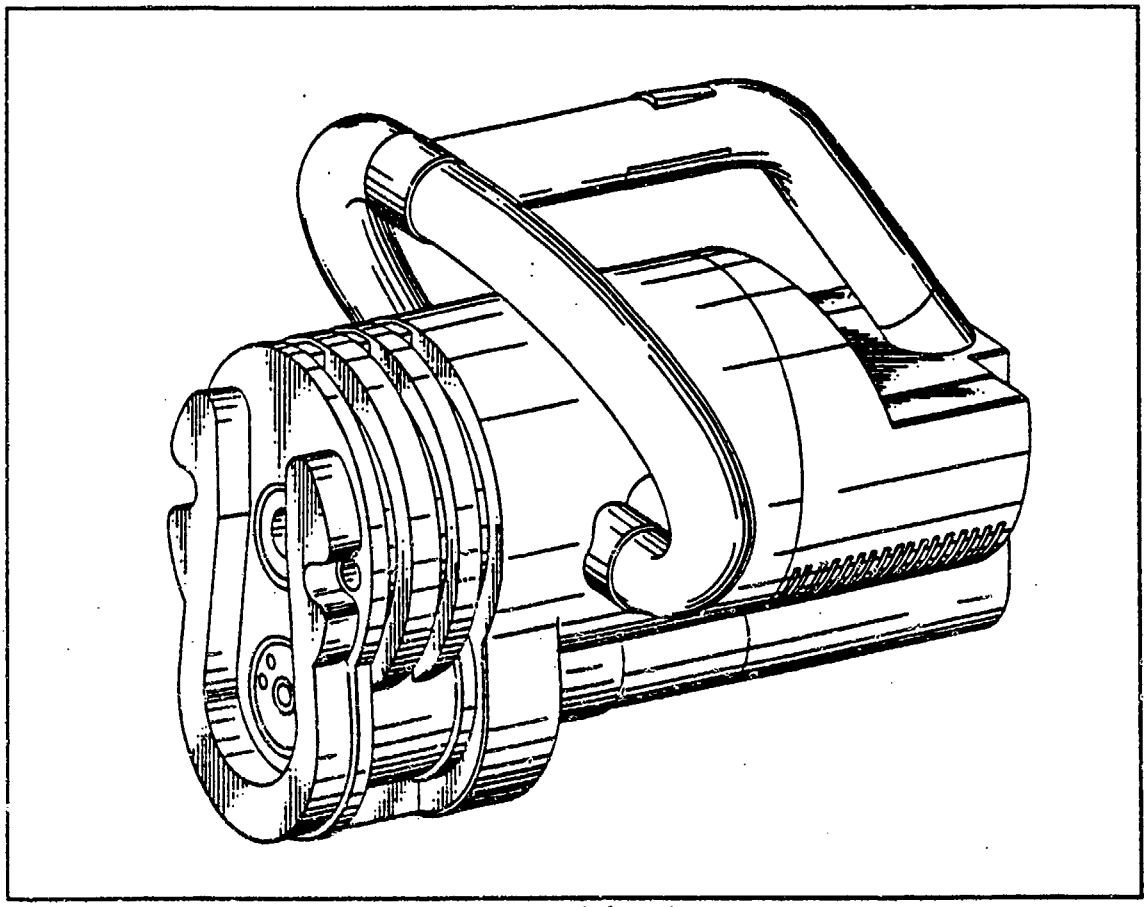


Figure 2 - Sampling device with integral heater and infra-red pyrometer.

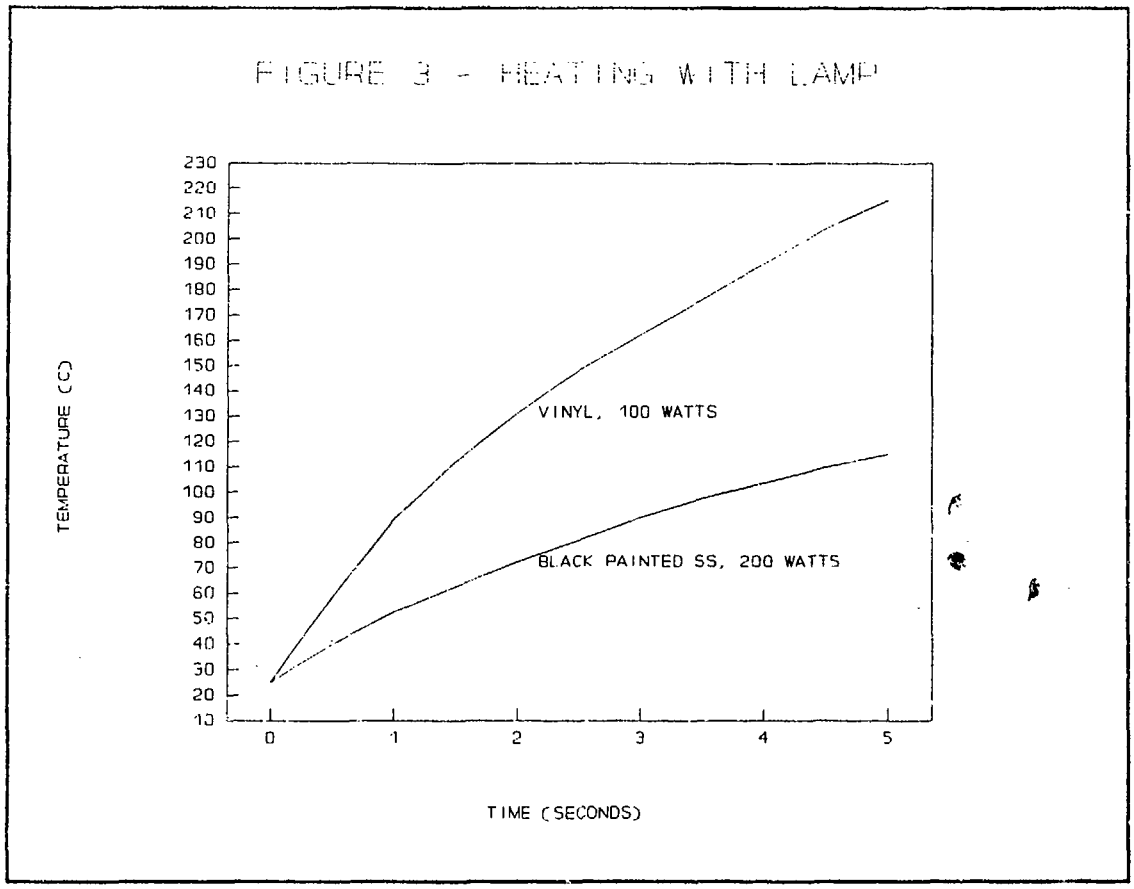


Figure 3 - Heating rate as a function of time using the projection lamp for heating.

EFFICIENT COLLECTION OF EXPLOSIVE VAPORS, PARTICLES AND AEROSOLS

Freeman W. Fraim, Eugene K. Achter, and A. Lindsay Carroll
Thermedics, Inc.
Woburn, MA

Eugenie Hainsworth
Arthur D. Little, Inc.
Cambridge, MA

1. INTRODUCTION

Many explosive detection applications require the collection of explosive vapors, or fine particulates from air samples. In applications such as detecting explosives from airline passengers or their luggage, the air volume that has to be sampled is quite large because of the size of the item sampled, or in the case of passengers because it is not possible to confine them in a small sampling space. In these applications, the task is to extract the explosives present from a large air sample. This can be done either by sampling a portion of the total air sample, hoping that the whole sample is well mixed so that the explosives are present in the extracted sample, or by sampling the entire air volume. The disadvantage of the former approach is obviously that the quantity of explosives in the portion sampled is reduced by the fraction of the whole sample that is taken, assuming that the entire sample is well mixed. The disadvantage of the second approach is that it becomes difficult to efficiently sample a large air volume in a practical time frame, typically five to ten seconds.

ThermedeTec's approach for sampling a large volume has been to sample as much of the total sample as possible. The reduction in effective sensitivity if only a small portion is sampled is felt to be too large a sacrifice in sensitivity, resulting in an impractically high limit of detection. Thus the main design task has been to develop a collection means that can handle large air volumes at high flow rates and achieve good collection efficiency.

2. SAMPLING METHODOLOGY

A sampling device for large air volume sampling has to accomplish three things: efficiently collect the explosive vapors from the air stream, retain the collected vapors throughout the entire sampling period, and efficiently release the vapors when the sampling device is called on to do so to allow analysis of the sample. For a sampling device to operate effectively it has to accomplish these three operations as efficiently as possible, while ideally having a small size, and simple design. The following discussion describes the approach that ThermedeTec has taken to accomplish these objectives.

2.1 Sample Collection

The sample collection process involves trapping the explosive vapors and fine particulates present in the air being sampled for later release into a detection system. The design goal of the collection process is to trap as much of the vapor present in a large air volume as possible. Many trapping systems have been employed, including volume traps such as charcoal beds, and surface traps such as membrane filters, and solid surfaces. The volume traps are efficient, but difficult to desorb quickly. Many types of surfaces can be used for a surface filter, a typical one is a porous membrane or filter through which all of the air being sampled is drawn. Membrane filters are very efficient collectors, but have the problem that the pore size required for efficient collection results in a high pressure drop to obtain the flows required. This means a large sampling pump. Also a membrane is a difficult media to release the collected vapors from quickly, a problem similar to the volume trap. Heat is usually needed to release the collected vapor. It is difficult to quickly heat a membrane; as a result, the analysis time for this collection approach is slowed by the time required for heating. For these reasons, we have concentrated on a surface collector design, utilizing a metal surface that can be quickly heated for fast release of the sampled explosives, designed to have a high collection efficiency.

A solid surface collector operates by passing the sampled air across the surface, rather than through it. To collect the explosive vapors the air stream has to be in intimate contact with the surface for sufficient time that the explosive molecules can be transported to the surface where they are retained. The mechanisms involved in this process are almost identical to those in the equivalent heat transfer process. Therefore, the approach has been to view the collection process as being a heat transfer/mass transfer problem. Typically in heat exchanger designs one wants to transfer the maximum amount of heat possible in the smallest possible volume, and do it with as low a pressure drop as possible. Because there is a direct correlation between heat transfer and mass transfer processes, (1-6), the procedures used for heat exchanger design can also be used to design a system for optimum mass transfer. Basically then the design task is to design an efficient mass "heat" exchanger.

For collecting explosive vapors the most appropriate heat exchanger geometries are either tube bundles, or parallel plate systems. For a variety of reasons involving simplicity of construction, and speed of the desorption process, a parallel plate system was selected. This is shown schematically in Figure 1. The air to be sampled flows through passages between parallel plates. Vapors and fine particulate in the stream will diffuse to, or be transferred to the walls by turbulent flow eddies. Once the vapor molecule reaches the surface it will be trapped on the surface. Because the processes involved are identical to heat transfer processes, all of the knowledge of heat exchanger design can be applied to optimize the geometry for efficient vapor collection. The section following on the Analytical Approach describes the calculations involved.

2.2 Sample Retention

The model just described assumes that if a vapor molecule reaches the collection surface it will be trapped, and not reenter the air stream. Obviously for the collector to work efficiently it has to have the proper trapping characteristics. Ideally the surface will retain the materials of interest, but not materials that interfere with the detection process. We have developed surfaces to accomplish this function using proprietary techniques. The result is a treated metal surface optimized to retain a wide variety of explosive vapors.

2.3 Sample Release

The third important element of the design is the efficient release of the sampled vapors into the detection system. Since the collector surface retains the vapors under sampling conditions, to release them requires an elevated temperature. A typical example of this type of collection and release is an activated charcoal tube collector. Once a sample is collected, the tube is heated, and a carrier gas is used to purge the sample from the sample tube. In the case of the flat plate collector, if it is constructed with metal plates then these can be electrically heated to heat the surface which releases the sampled vapors.

3. DESIGN APPROACH

The previous discussion has described the design approach ThermedeTec has taken to develop efficient vapor collectors. From heat transfer principles a flat plate heat exchanger produces the desired results. The question is how to turn this basic design concept into practical collectors. The approach that has been taken is shown in Figure 2. The flat plates geometry is achieved by spiral winding a ribbon. This geometry is very common in heat exchanger applications such as for flame arrestors where the energy in a propagating flame front is transferred to the arrestor structure quenching the flame. The spiral design is very convenient because a large plate surface area can be achieved in a small size with good rigidity, and since the ribbon is continuous it is easy to electrically heat.

The specific design parameters for a spiral wound collector will depend on the volume of the sample to be taken, the efficiency required of the sampling process, the acceptable pressure drop across the collector while sampling, and the acceptable physical size of the device. The next section describes the analytical model that has been used to develop spiral collector designs, and illustrates its use by calculating the performance for a particular application.

4. HEAT TRANSFER/MASS TRANSFER MODEL

A correlation between heat transfer thermodynamics and mass transfer through diffusion has been demonstrated by theory and empirical testing by many investigators in the field. Some of the more prominent authorities on the subject are T.H. Chilton and A.P. Colburn[1], T.K. Sherwood and R.L. Pigford[2], W. Jost[3] and others. Many textbooks on

this subject have been published which expand on these principles such as: Heat, Mass and Momentum Transfer[4], Mass Transfer in Heterogeneous Catalysis[5], and Transport Phenomena[6].

This technology can be applied to the design of a vapor collection device by substituting a mass transfer factor (J_m) for the heat transfer factor (J_H) and utilizing geometric and flow parameters from heat transfer to predict collection performance. The corresponding fluid property in mass transfer becomes Schmidt Number (N_{sc}) as contrasted with Prandtl Number (N_{pr}) in heat transfer behavior.

An examination of the fundamentals which govern collector performance can be made by reviewing the early work of Chilton and Colburn[1] sometimes referred to as the "Colburn Relation", given as follows:

$$J_H = \frac{H}{C_p G}(N_{pr})^{2/3} = J_m = \frac{K_g}{G_m}(N_{sc})^{2/3} = f(N_{re})$$

J_H , J_m - *Heat and mass transfer coefficients*

H - *Heat transfer coefficient BTU/Hr-FT²-°F*

C_p - *Specific Heat (Air) BTU/LB - °F*

G - *Flow Stream Mass Velocity LB/HR - FT²*

N_{pr} - *Prandtl number (air)* $\frac{C_p u}{K}$

K_g - *Mass transfer coefficient LB moles/sec-ft²-mole fra*

G_m - *Flow stream mass velocity LB moles/sec -FT²*

N_{sc} - *Schmidt number* $\frac{\mu}{\rho D_v}$

D_v - *Mass diffusivity FT²/HR.*

μ - *Viscosity LB/HR - FT*

ρ - *Density - LB/FT³*

$\dot{m}$ - *Mass Flow Rate LBS/SEC.*

One example of the correlation between mass transfer and heat transfer from empirical testing is shown in Figure 2 from the works of J.M. Coulson and J.F. Richardson[7]. This test shows the results of evaporation of various liquids from plane surfaces into an air stream. The test points are plotted as a dimensionless group analogous to Schmidt Number versus Reynolds Number. The correlation to heat transfer is shown by the solidtrace generated from a dimensionless group relating to Prandtl Number (N_{pr}).

5. APPLICATION OF TECHNIQUE TO ONE GEOMETRY

Development work on a spiral ribbon collector involved developing the analytical model based on these principles, and tests to substantiate the empirical coefficients used to predict the collection efficiency, and flow pressure drop. The resulting correlation developed has been used to design a whole family of collectors for a variety of applications.

The following example describes the analytical process in detail for a collector design to handle a

flow rate of 70 liter/sec. This particular design is of interest because a considerable amount of testing was performed with it to verify the model.

The collector design is of the spiral construction described above. It has an annular body into which a thin metal ribbon is wound. The spiral shape is maintained by way of orthoganol struts which pierce the ribbon radially. Spacer washers separate the turns of the spiral, and are held in place with the struts. A diagram of the device is shown in Figure 3.

To follow through a typical calculation it is first necessary to clearly describe the collectors geometric properties, and fluid characteristics used in the analysis. This information is given below:

Geometric Properties

A_{ff}	-	Free flow area (open frontal area) - FT^2
A	-	The total heat transfer area - FT^2
L	-	Length of collector (in direction of flow)- FT (.0313) (Fig. 1)
b	-	Free spacing between fins - FT (1.25×10^{-3}) (Fig. 1)
δ	-	Fin thickness - FT ($.83 \times 10^{-4}$) (Fig. 1)
r_h	-	Hydraulic radius - FT
D_1	-	Collector outer diameter - FT (.104)
D_2	-	Collector hub diameter - FT (.063)
d	-	Support strut diameter - FT (7.8×10^{-3})
N	-	Number of ribbon layers or turns (16)
n	-	Number of supporting struts (8)
α	-	Fin proportionality factor
N_{re}	-	Reynolds Number through collector
l	-	ribbon length (unwound)
p	-	collector foil pitch - FT. (1.33×10^{-3})
Q	-	no. of ribbon revolutions - radians

The flow media is basically air with very small concentrations of explosive vapor; therefore, the appropriate air properties to be used are as follows:

C_p	=	0.24 BTU/LB °F
N_{Pr}	=	0.70
ρ	=	.075 LB/FT^3
D_v	=	.27 FT^2/HR.
N_{re}	=	2.17
K	=	.015 BTU/HR FT °F
μ	=	0.044 LB/HR-FT.

6. CALCULATION OF COLLECTOR GEOMETRIC PARAMETERS

(See Figure 3 for Dimensional Reference).

The various collector geometric parameters are calculated using these relationships:

Flow Thru Area

$$l = Q\left(R_S + \frac{p}{4\pi} \cdot Q\right) = 32\pi\left(.39 + \frac{.016}{4\pi} \cdot 32\pi\right) = 4.27$$

$$A_{ff} = \left[\frac{\pi}{4} \cdot (D_1^2 - D_2^2)\right] - \left[n \frac{(D_1 - D_2)}{2} \cdot d\right] - [l \cdot \delta] = 3.81 \times 10^{-3}$$

where

$$R_s = R_2 + b$$

Heat Transfer Area

$$A = \left[l \cdot L - 16 \cdot n \cdot \frac{\pi}{4} d^2\right] \cdot 2 = .255\ FT^2$$

Hydraulic Radius

$$r_h = \frac{A_{ff}}{A} \cdot L = \frac{3.81 \times 10^{-3}}{.255} \cdot .0313 = .47 \times 10^{-3}\ FT$$

Because the collector design is an annular design with a spiral ribbon foil, it is necessary to convert this geometry to an equivalent rectangular heat exchanger with fins in order to use classic heat exchanger performance data.

Assume that the heat exchanger rectangular width will be equivalent to the mean collector circumference C_m.

$$C_m = \pi \left[\frac{D_1 + D_2}{2} \right] = .26\ FT\ (X)$$

The fin height Y can be calculated from collector flow area (A_{ff}).

$$(Y) = \frac{3.81\ x\ 10^{-3} FT^2}{.26\ FT} = 14.7\ x\ 10^{-3} FT$$

The number of fins (N') can be calculated from collector ribbon length L

$$N' = \frac{l}{(C_m)} = \frac{4.27}{.26} = 16.4$$

and fin spacing becomes:

$$b = \frac{Y}{N'} = \frac{14.7}{16.4}\ x\ 10^{-3} = .896\ X\ 10^{-3}\ FT$$

solving for α (fin proportionality)

$$\alpha = \frac{C_m}{b} = \frac{.26}{.896\ x\ 10^{-3}} = 290$$

7. COLLECTOR EFFICIENCY CALCULATION

In heat collector design practice, it is convenient to use the term N^{TU} (number of units transferred) so that an efficiency or "figure of merit" can be determined independently from actual heat transfer rate.

For a collector design we will determine efficiency without having the need to know the actual moler concentration from a moler balance relationship as follows:

The rate of outlet concentration to inlet concentration for the collector is given by:

$$e - \left[\frac{K_t\ A}{6_m \cdot A_{ff}} \right]$$

If we express this exponential power

as N_{TU} (number of transfer units)

$$\left[\frac{K_t \cdot A}{6_m\ A_{ff}} \right]$$

it is then possible to express an efficiency equation as:

$$COLLECTION\ EFFICIENCY(E) = 1 - e^{-N_{TU}}$$

To calculate the collector's efficiency, we must determine the operating conditions of the collector with respect to mass flow rate, and Reynolds Number from which the mass transfer factor (J_m) can be estimated (see Figure 4).

Assuming a 20 liter/sec flow rate through the collector a few more parameters must be calculated before we can enter Figure 4 and estimate (J_m).

MASS FLOW RATE

$$th = 20\ l/s \cdot 3.53x10^{-2}\ FT^3/l \cdot 0765\ LB/FT^3 = .054\ LB/S$$

UNIT MASS FLOW

$$G = \frac{\dot{m}}{A_g} = \frac{.054}{3.81x10^{-3}} = 14.2\ LB/SEC\text{-}FT^2\ (51.0x10^3\ LB/HR\text{-}F$$

REYNOLDS NUMBER

$$N_{RE} = \frac{4r_h G}{\mu} = \frac{4 \cdot .47\ x\ 10^{-1} \cdot 51.0\ x\ 10^3}{0.044} = 2179$$

PROPORTIONALITY CONSTANT

$$\frac{L}{4\,r_h} = \frac{.031}{4 \cdot .47 \times 10^{-3}} = 16.5$$

From Figure 4, $J_m = .005$ f = .019

EFFICIENCY

$$N_{tu} = \frac{L \cdot J_m}{N_{sc}^{2/3} \cdot r_h} = \frac{.0313 \cdot .005}{2.17^{2/3} \cdot .47 \times 10^{-3}} = .20$$

$$E = 1 - e^{-N_{tu}} = 1 - e^{-.20} = .181\ (18.1)\%$$

8. PRESSURE DROP CALCULATION

Pressure drop across the collector can be calculated from the friction factor (f) at the specified unit mass flow rate G.

$$\Delta P = \frac{G^2 \cdot f}{2_t} \frac{A}{A_f \cdot \rho} = \frac{(14.2)^2 \cdot .014 \cdot .255}{64.4 \cdot 3.81 \times 10^{-3} \cdot .075}$$

$\Delta P = 53.08\ LB/FT^2 \sim 10.2\ IN.W.C.$

9. CORRELATION WITH TEST RESULTS

To verify the analytical model against actual performance, both heat transfer and pressure drop measurements were performed on this particular design. Actual collection efficiency was also shown to correlate with theoretical performance, subject to a greater spread in test repeatability due to the difficulty in generating exact vapor concentrations presented to the collector.

10. VERIFICATION OF HEAT TRANSFER FACTOR

The heat transfer coefficient was verified by establishing a steady state flow rate through the device, and heating the metal ribbon to a steady temperature above ambient. Using the flow rate, ambient air temperature, ribbon temperature, and the electrical power required to maintain the elevated temperature, the actual heat transfer factor was calculated as follows:

$FLOW = 20\ LITERS/SEC \sim 51.0 \times 10^3\ LB/HR\text{-}FT^2$

$INPUT\ POWER = 582\ WATTS \sim 1979\ BTU/HR$

$MAINTENANCE\ TEMPERATURE \cdot 155.3°F$

$AMBIENT\ TEMPERATURE \cdot 68°F$

HEAT TRANSFER COEFFICIENT

$$H = \frac{Q}{A\ (\Delta T)}$$

HEAT TRANSFER FACTOR

$$J_H = \frac{H\ (N_{PR})^{2/3}}{C^P\ G} \left(\frac{BTU}{R\ FT^2 - °F}\right) \left(\frac{LB - °F}{BTU}\right) \left(\frac{HR\ FT^2}{LB}\right)$$

Combining these expressions,

$$J_H = \frac{Q\ \ (N_{PR})^{2/3}}{A \cdot \Delta T\ C_p\ G} = \frac{1979\ (.71)^{2/3}}{.255\ (87.3)\ (.24)\ 51.0 \cdot 4 \times 10^3} = .(\ldots$$

Compared to,

$J_H = .0060$ *FROM FIGURE* 4

11. VERIFICATION OF PRESSURE DROP

Figure 5 presents measured values of pressure drop (ΔP) as a function of flow rate through the collector. Measurements were made for both a fully assembled collector and a collector housing without the spiral-wound collector, to obtain the net pressure drop, (ΔP_{net}). ΔP_{net} is the portion of the pressure drop due to frictional interaction between the flowing air and

the spiral-wound ribbon. At 20 liters/second, the observed value of ΔP_{net} is 12 in. w.c., in good agreement with the value of 10.2 in. w.c. obtained using Figure 4.

12. CONCLUSION

The use of the correlation between heat and mass transfer allows the principles of heat exchanger design to be applied to the design of surface type collectors for explosives vapors. The availability of such a powerful set of design tools allows a very thorough parametric design analysis to be done for surface type collectors. Together with fluid flow considerations, this model allows any collection requirement to be modeled, and optimized. This paper has concentrated on a flat plate spiral ribbon design, however, the same principles can be used for any geometry of surface type collector.

ACKNOWLEDGEMENTS

We would like to thank the United States Department of State for its support under contract number 2038-563371 and the Federal Aviation Administration, U.S. Department of Transportation for its support under contract number DTRS-57-84-C under which most of the work described in this paper was performed.

REFERENCES

1. Chilton, T.H., and Colburn, A.P., Ind Engineering Chemistry 26, 1183, 1934.

2. Sherwood, T.K., and Pigford, R.L., "*Absorption and Extraction*", 2nd Ed., NY: McGraw Hill Book Company, Inc., 1952.

3. Jost, W., *Diffusion*, Academic, NY: 1952.

4. Rohsenow, W. M., and Choi, H. Y., *Heat, Mass, and Momentum Transfer*, Englewood Cliffs, NJ: Prentice-Hall, 1961.

5. Saherfield, Charles, *Mass Transfer in Heterogeneous Catalysis*, Department of Chemical Engineering, Mass Institute of Technology.

6. Bird, R. Byron, Stewart, W.E., Lightfoot, John, *Transport Phenomena*, NY: John Wiley and Sons, Inc.

7. Coulson, J.M. and Richardson, J.F., Chemical Engineering, 1, 2 Ed. (New York : McGraw Hill Book Company, Inc., 1952), p. 257.

8. Kays, W.M. and London, A.L., "Convection Heat Transfer and Flow Friction Behavior of Small Cylindrical Tubes - Circular and Rectangular Cross Sections Trans", ASME, 74, No. 7, 1952.

FIGURE 1

GEOMETRY OF A FLAT PLATE COLLECTOR FOR EXPLOSIVES

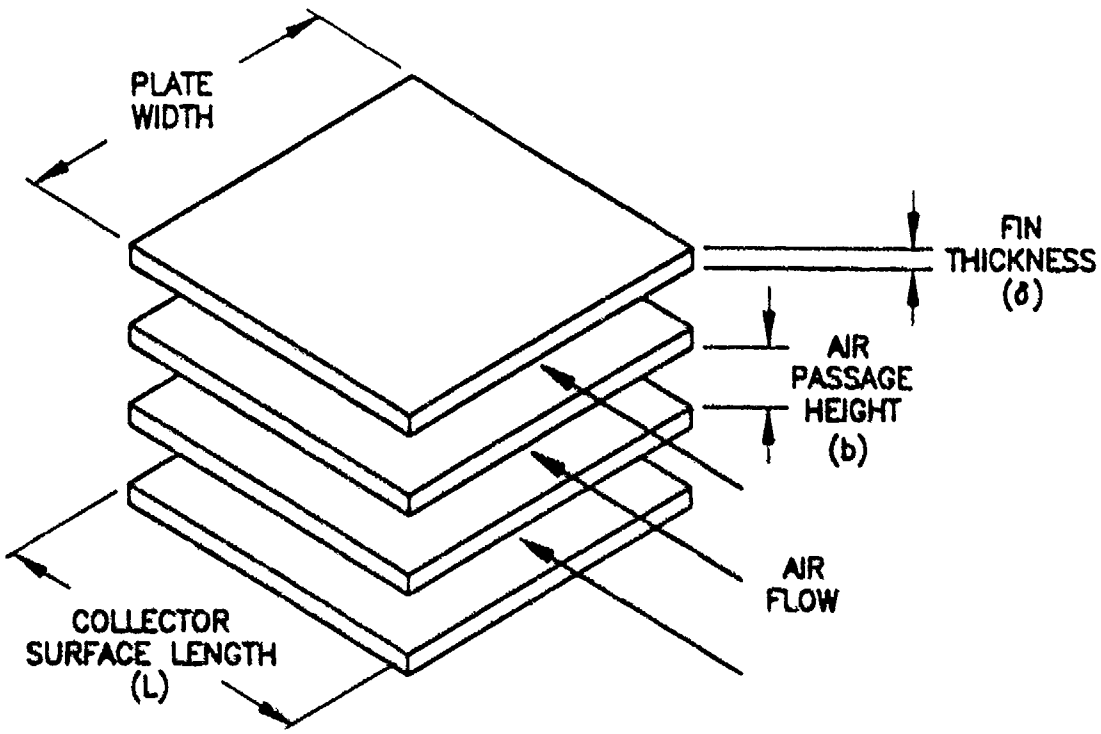
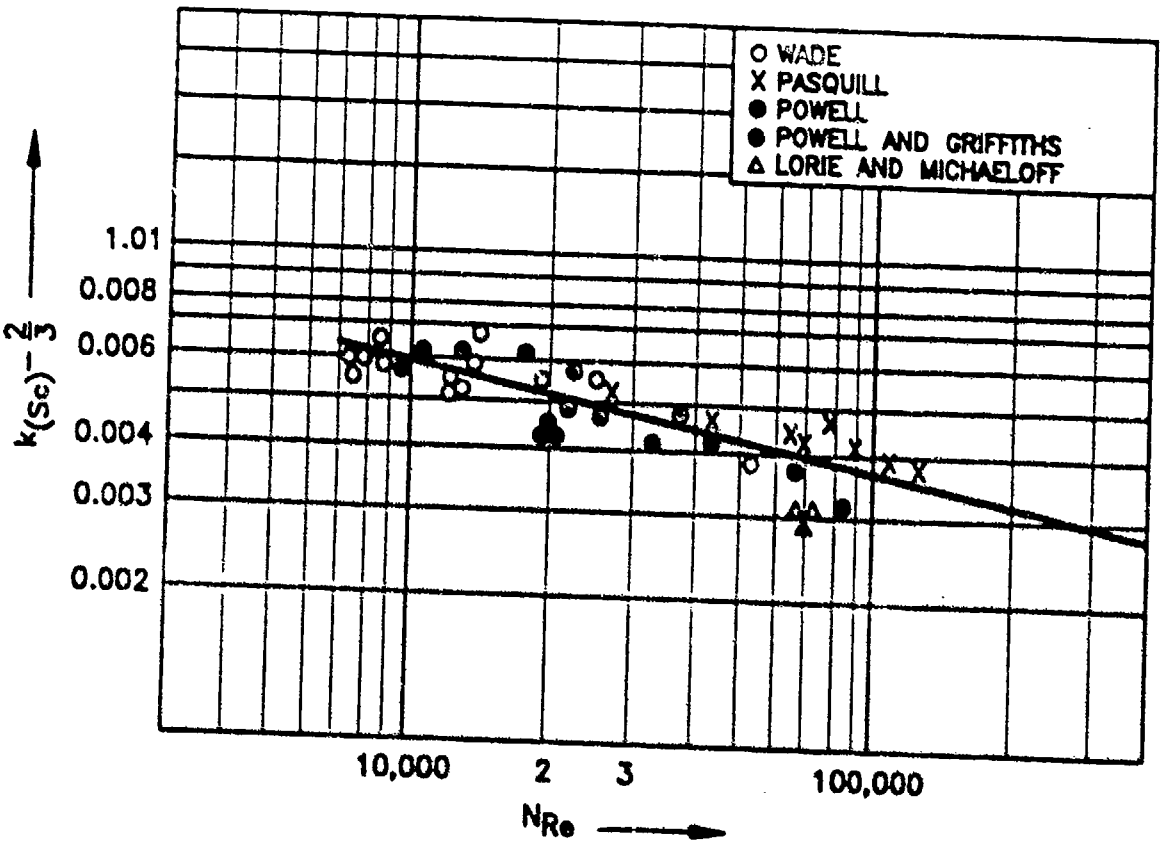
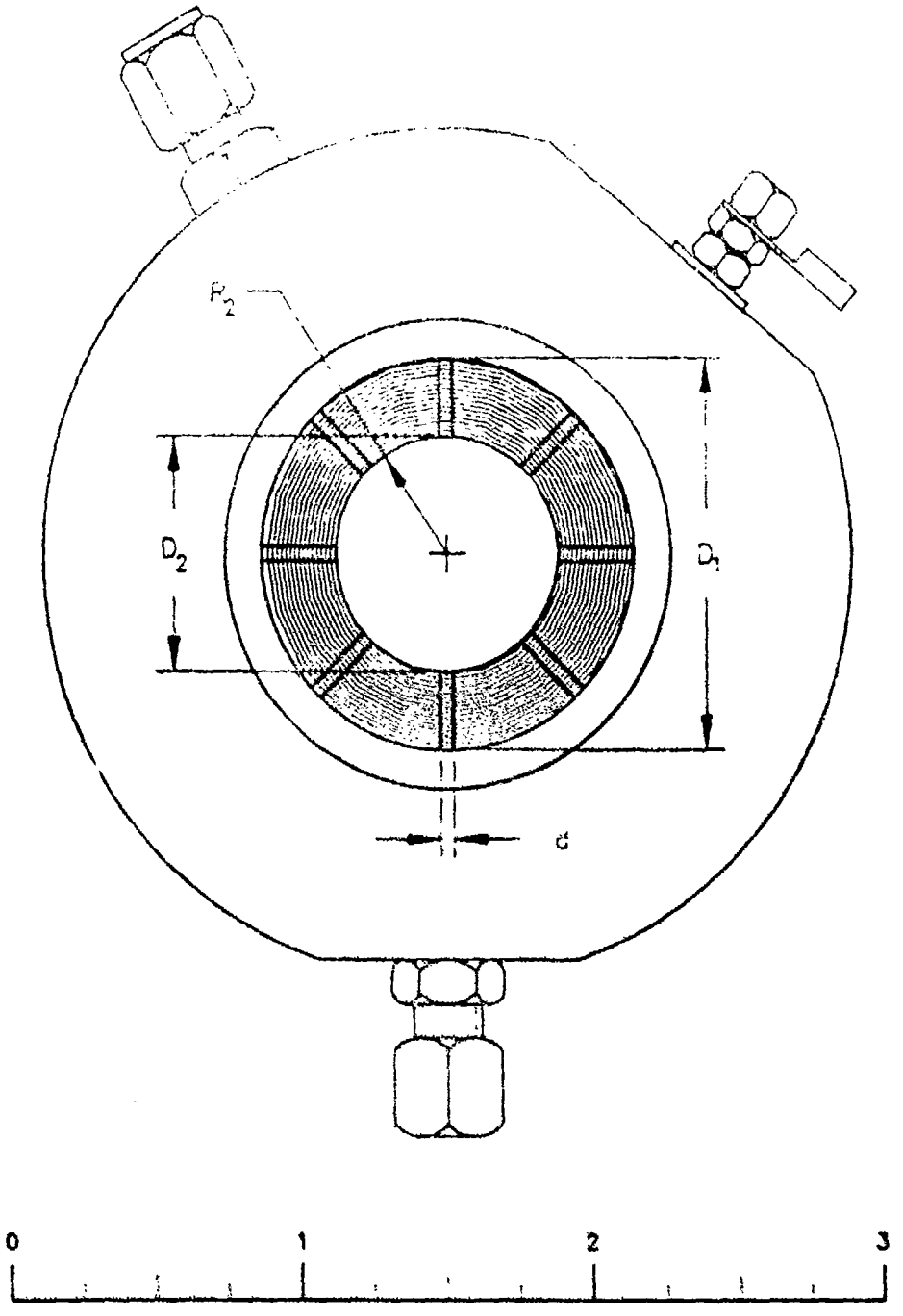


FIGURE 2



EXPERIMENTAL VERIFACATION OF ANALOGY BETWEEN HEAT AND MASS TRANSFER FROM COULSON & RICHARDSON. ⑦

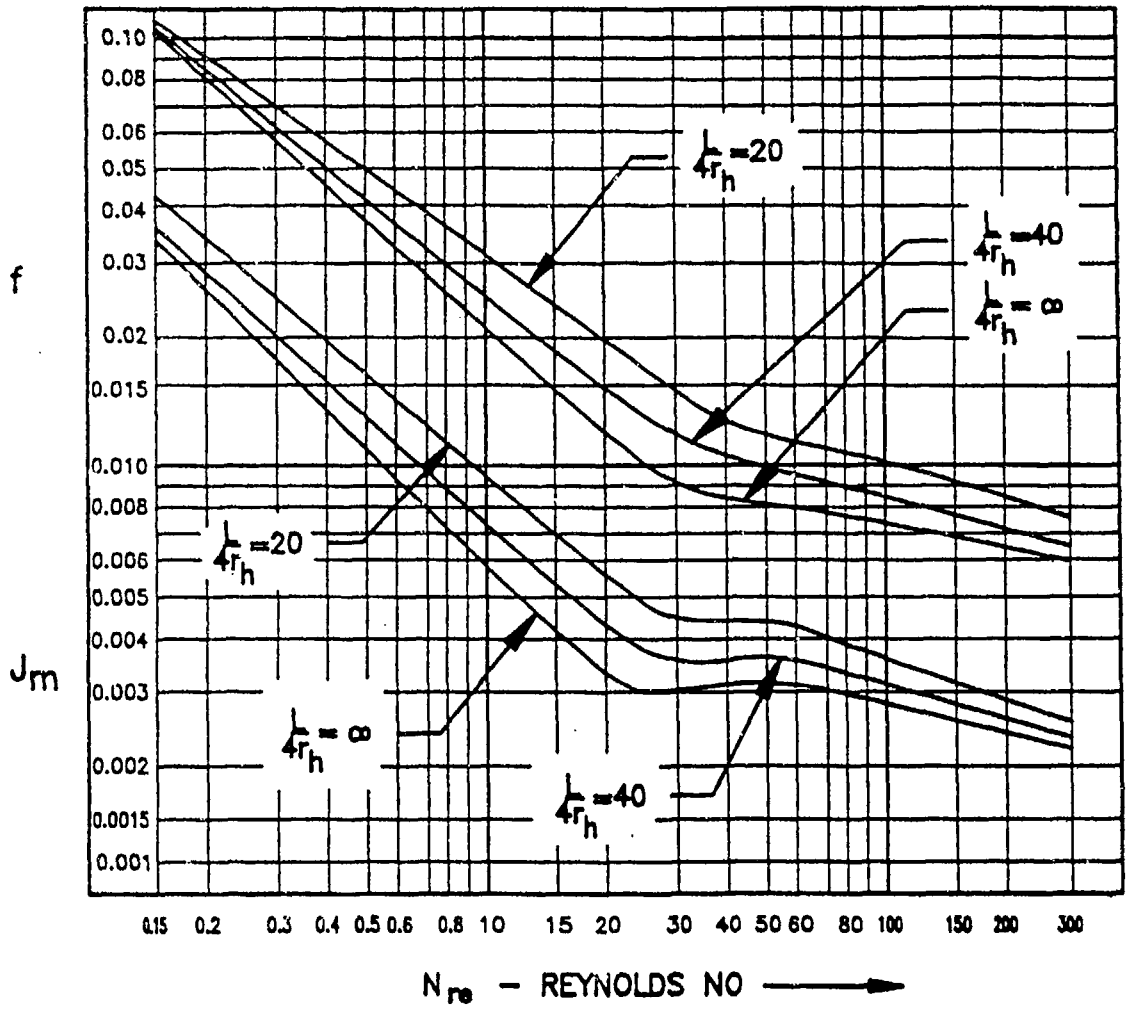
FIGURE 3



20 LITER PER SECOND VAPOR COLLETOR

GEOMETRY DETAILS

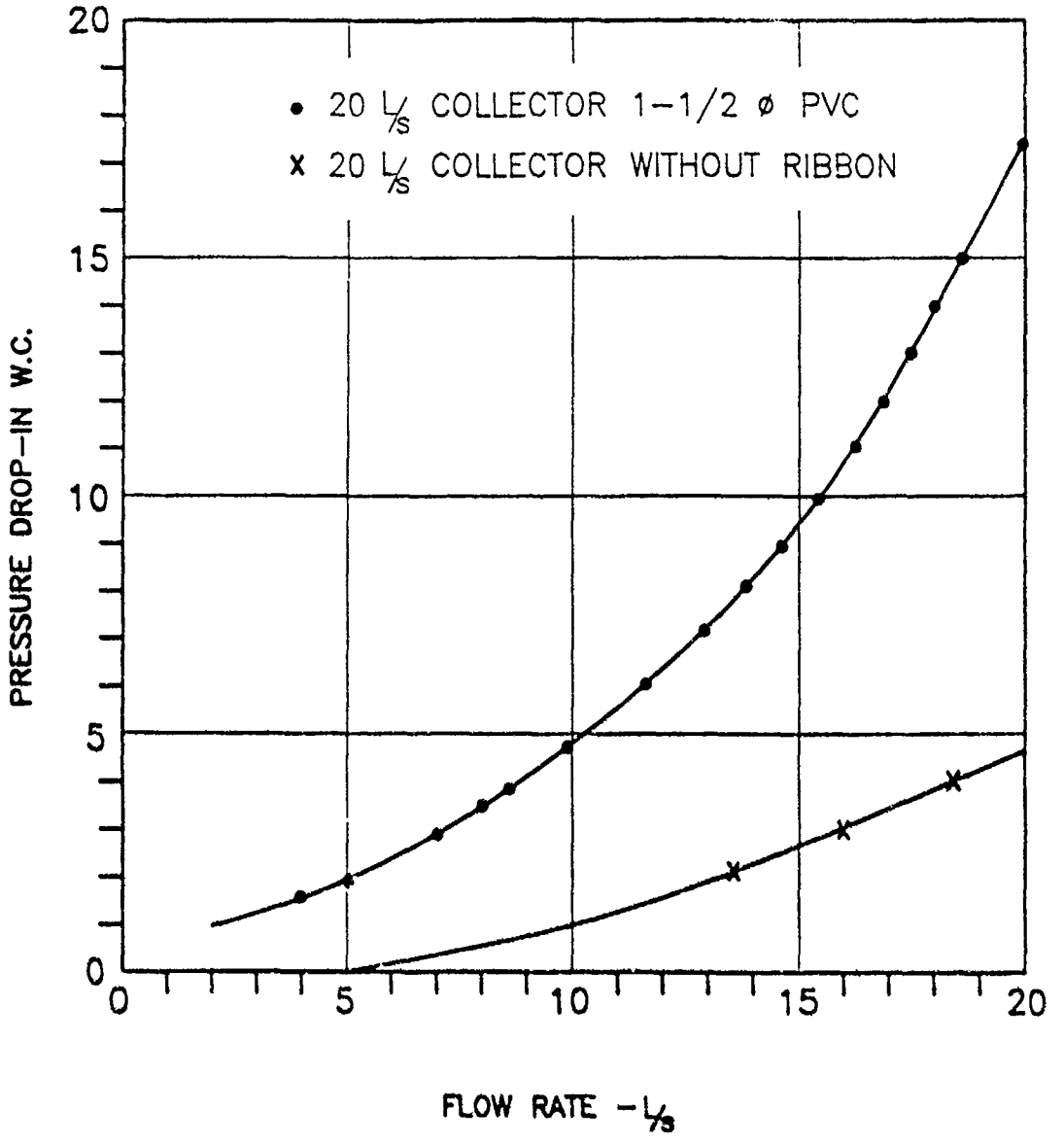
FIGURE 4



FRICTION FACTORS (f) AND MASS TRANSFER FACTOR (J_m) VERSUS REYNOLDS NUMBER FOR VARIOUS PROPORTIONS ($\frac{L}{4r_h}$)

GAS FLOW INSIDE RECTANGULAR TUBES WITH ABRUPT CONTRACTION ENTRANCES. A SUMMARY OF EXPERIMENTAL AND ANALYTICAL DATA FOR FIN PROPORTIONALITY (2) OF 8 OR GREATER FROM THE WORKS OF W.M. KAY AND A.L. LONDON.

FIGURE 5



PRESSURE DROP VERSUS FLOW FOR 20 L/s COLLECTOR
WITH AND WITHOUT RIBBON SECTION

NEGATIVE-ION FORMATION IN THE EXPLOSIVES RDX, PETN, AND TNT USING THE REVERSAL ELECTRON ATTACHMENT DETECTION (READ) TECHNIQUE

A. Chutjian, S. Boumsellek, and S. H. Alajajian
Jet Propulsion Laboratory, California Institute of Technology
Pasadena, CA 91109

1. INTRODUCTION

In the search for high sensitivity and direct atmospheric sampling of trace species, techniques have been developed such as atmospheric-sampling, glow-discharge ionization (ASGDI) (McLuckey *et al.* 1988, 1989, 1989a), corona discharge (Lee and Lee 1991), atmospheric pressure ionization (API) (Huang *et al.* 1990), electron-capture detection (ECD) (Lovelock 1982, Conrad and Peterson 1978), and negative-ion chemical ionization (NICI) (Daugherty 1981) that are capable of detecting parts-per-billion to parts-per-trillion concentrations of trace species, including explosives, in ambient air. These techniques are based on positive- or negative-ion formation *via* charge-transfer to the target, or electron capture under multiple-collision conditions in a Maxwellian distribution of electron energies at the source temperature. Subsequent detection of the ion-molecule reaction products or the electron-attachment products is carried out using time-of-flight, quadrupole, magnetic-sector, ion trap or analog current measurement methods.

One drawback of the high-pressure, corona- or glow-discharge devices is that they are susceptible to interferences either through indistinguishable product masses, or through undesired ion-molecule reactions. The ASGDI technique is relatively immune from such interferences, since at target concentrations of less than 1 ppm the majority of negative ions arises *via* electron capture rather than through ion-molecule chemistry (McLuckey *et al.* 1989). A drawback of the conventional ECD, and possibly of the ASGDI, is that they exhibit vanishingly small densities of electrons with energies in the range 0-10 millielectron volts (meV), as can be seen from a typical Maxwellian electron energy distribution function at T=300K. Slowing the electrons to these subthermal (less than 10 meV) energies is crucial, since the cross section for attachment of several large classes of molecules -- including the explosives, chlorohalocarbon compounds and perfluorinated carbon compounds -- is known to increase to values larger than 10^{-12} cm^2 at near-zero electron energies (Orient *et al.* 1989, Chutjian and Alajajian 1985, 1985a). In the limit of zero energy these cross sections are predicted to diverge as $\epsilon^{-1/2}$, where ϵ is the electron energy. This is a direct consequence of the Wigner threshold law for electron attachment (Orient *et al.* 1989, Wigner 1948). The READ concept is, in fact, the molecular-physics analog of the same quantum-mechanical threshold law operative in the Thermal Neutron Analyzer (TNA) (Chutjian 1991).

In order to provide a better "match" between the electron energy distribution function and attachment cross section, a new concept of attachment in an electrostatic mirror was developed (Orient *et al.* 1985). In this scheme, electrons are brought to a momentary halt by reversing their direction with electrostatic fields. At this turning point the electrons have zero or near-zero energy. A beam of target molecules is introduced, and the resultant negative ions extracted. This basic idea has been recently improved to allow for better reversal geometry, higher electron currents, lower backgrounds, and increased negative-ion extraction efficiency (Bernius and Chutjian 1989, 1990). We present herein application of the so-called reversal electron attachment detector (READ) to the study of negative-ion formation in the explosives molecules RDX, PETN, and TNT under single-collision conditions. The technique exploits the fact that these molecules are known, indirectly through results in the ECD (Conrad and Peterson 1978), to attach thermal-energy electrons. Present results provide the first direct verification that explosives molecules attach zero-energy electrons, and offer the dissociative attachment fragmentation pattern for each target.

Unlike the ASGDI, API, corona-discharge, ECD, or NICI techniques, negative-ion generation by reversal

electron attachment is also able to access resonances at $\epsilon > 0$, beyond the range of thermalized energies. This feature has been demonstrated by shifting the location of the electron turning point with respect to the target beam (Bernius and Chutjian 1989). While one would require zero-energy electrons for attachment to the nitrogen containing explosives RDX, PETN, TNT, and EGDN, there is yet another class of energetic peroxy-explosives, containing no nitrogen, whose attachment cross sections may peak beyond the range of electron energies present in a plasma discharge (Fetterolf and Clark 1991). The variable-energy READ would find additional use for such molecules, as well as for narcotics (known to be undetected in the ECD). Also, because measurements are carried out under single-collision conditions, there is no ion-molecule chemistry in READ to speak of. Finally, since one is detecting product masses, the READ method is capable of identifying one or more "signature" ions in the attachment process. In applications where time is not critical, one can envisage the use of several mass detectors to detect products in coincidence. This would mitigate strongly against interferences, and could even serve to identify which type(s) of explosives were being detected.

However, a sobering problem awaiting "in the wings" with the READ, and with any single-collisions technique, is that of sample introduction from atmosphere to vacuum. This work is currently underway in our laboratory.

2. READ INSTRUMENT DESCRIPTION

A schematic diagram of the READ apparatus is shown in Fig. 1, and details of its operation have been given elsewhere (Bernius and Chutjian 1989, 1990). READ consists of an indirectly-heated cathode F from which electrons are extracted, accelerated by a five-element lens system, and focused into an electrostatic mirror. The mirror decelerates the electron beam to zero longitudinal and radial velocity at the reversal plane R (Fig. 1). The electron beam is square-wave modulated by fast switches S_1-S_3 with a nearly 50% duty cycle. These switches are power MOSFET-based to ensure fast (50 nsec) risetimes between full-floating lens voltages (Bernius and Chutjian 1989a, 1990a).

Electron attachment to the explosives target takes place at R during one half of the pulse cycle. The resulting negative ions are extracted during the second half (electron beam pulsed off), then focused, deflected by a 90° electrostatic analyzer (ESA) to ensure the sign of charge, and further focused onto the entrance plane of a quadrupole mass spectrometer (QMS). Ion counts are recorded in a multichannel scaling mode using an Ortec 7100 multichannel analyzer interfaced to an Extrel quadrupole mass controller. Spectra are obtained by scanning the masses transmitted by the quadrupole; and are recorded in 1024 channels with a dwell time of 0.1 sec/channel.

3. EXPLOSIVES HANDLING

Because of the low vapor pressure of the explosives targets, and their tendency to adsorb to most surfaces, special care had to be taken to transport the target into the reversal region, and to ensure that there was no contamination amongst the RDX, PETN, and TNT measurements. Each solid target was placed in a pyrex bulb P (Fig. 1) inside the vacuum chamber. The vapor pressures at 300K of RDX, PETN, and TNT are quite low: 8.5×10^{-7} Pa, 2.7×10^{-6}, and 1.3×10^{-3} Pa, respectively (Dionne *et al.* 1986). And hence the bulb had to be heated, with nichrome wire wound around the outside body. The resulting vapor was conducted to R through a heated stainless-steel tube.

4. EXPLOSIVES ATTACHMENT RESULTS

Negative-ion mass spectra of RDX, PETN, and TNT are presented in Figs. 2-4, respectively. Several spectra, taken on different days, were recorded for each molecule. For each spectrum, a recording time of 0.5-2 h was needed to scan 200-300 amu with a resultant signal/background of 50-150. Spectra were obtained with a mass resolution of Δm = 0.9 amu (FWHM), using low extraction voltages in the ion lens system and low acceleration voltages in the quadrupole rods (0-10 V). In order to (a) focus the incident electron beam at the reversal plane, (b) check the calibration of the mass scale, and (c) monitor the spectral lineshapes, one first observed the zero-energy electron attachment products in CCl_4, c-C_6F_6, and c-C_5F_8. Electron attachment in CCl_4 leads via dissociative attachment to form only the isotopes $^{35}Cl^-$ and $^{37}Cl^-$. The targets c-C_6F_6 and c-C_5F_8 form only the molecular ions c-$C_6F_6^-$ and c-$C_5F_8^-$ at m/e = 186 and 212, respectively. These ions served to calibrate the entire range of the mass scale.

The fragmentation pattern ("signature") of each explosives molecule was recorded between mass 30

and the mass corresponding to the molecular ion. Spectra are not reported below mass 40. This region, during blank runs, contained the two peaks at m/e = 35 and 37 due to persistent CCl_4 adsorbed on the optics surfaces. In addition, there was a strong, continuous background, starting at m/e = 20 and extending towards m/e = 1, which was assumed to arise from scattered and extracted electrons from the gun.

Each of the three explosives spectra shows an abundance of the NO_2^- ion at m/e = 46. This is in agreement with methods using a multiple-collision, high source-pressure (NICI) environment (Yinon 1982). It is useful to point out that, unlike in NICI (Yinon 1980, 1982), no masses greater than the parent ion mass can be observed in this work, since one is in a single-collision regime, with crossed (or just touching!) beams of electrons and target. Further discussion of differences among the three spectra can be found in Boumsellek et al. (1992).

5. INCREASING THE ELECTRON CURRENT IN READ

The original READ (READ I) electron gun lens system has been redesigned to allow for greater electron currents at the reversal region R. With the use of a spherically-shaped electron emitter and an added "shim" electrode in the cathode region, currents as large as 1 ma have been focused at R (Boumsellek and Chutjian 1992). This is approximately two orders of magnitude greater than with the planar emitter in the original READ I design. Electron trajectories, computed with a sophisticated space-charge limited code, are shown in Fig. 5.

The new detection sensitivity of READ II has been measured using the technique of standard dilutions (Willard et al. 1981). The test mixture was varying concentrations of CCl_4 in N_2, and c-C_6F_6 in N_2. Results of this test are shown in Fig. 6. As one would expect from the increased electron current in READ II, the present detection sensitivity exceeds that of READ I. For example, at a common concentration of 10 pptr, READ II has approximately a factor of 25 greater signal rate than READ I (see Fig. 3 of Bernius and Chutjian 1990). Moreover, from Fig. 6 (CCl_4) one may easily extrapolate to a count rate of 13 kHz at a mixture of 1 pptr, and to a count rate of 7.5 kHz at a mixture of $1{:}10^{13}$.

6. THE GRIDDED (MINIATURE) ELECTRON REVERSAL IONIZER

As noted above, there are several types of glow-discharge and corona-discharge ionizers capable of accepting a sample of the explosives molecules directly from atmospheric pressure, and ionizing it in the plasma. A portion of the plasma is then focused into suitable detector, such as a quadrupole mass analyzer. While such devices have a low ionization efficiency, their advantage lies in the simplicity, ease of use, and ruggedness of the ionizer. Cleaning is only infrequently required, and there are no filaments to replace.

Given this simplicity, one may naturally ask if there is a configuration to the present READ device which may have a comparable simplicity, yet retain the essence of the reversal idea. Shown in Fig. 7 is one conception of the reversal ionizer, together with a photograph of the constructed miniature READ. Here, zero-energy electron current and precise control of the reversal trajectories are sacrificed for simplicity of design. Basically, electrons are emitted from a filament F which is wrapped around or placed adjacent to a conical, gridded structure C. Within C is a second gridded or porous cylinder G through which the sample is introduced. Potentials V_C, V_G and V_F are arranged so that electrons are accelerated from F towards C. A simulation of this system using the SIMION code indeed showed electron trajectories reflected at the surface of the porous cylinder G. And hence attachment to the explosives molecules will take place along the length of G. A typical set of voltages is V_F = 0v, V_C = 150v, and V_G = 12v. For extraction A1 = 0v, A2 = 500v, and A3 = 50v.

Between C and G the electrons are decelerated to near zero energy. Negative ion formation through the zero-energy or low-energy attachment resonances in the explosives (or drugs) molecules occurs here. By symmetry, and due to the conical shape of C, there exists a radial electric field E^-_r, as well as an axial field E^-_z, which weakens towards the extraction aperture A1. Negative ions generated in the immediate region about G are then accelerated towards A1 by E^-_z. At A1, the penetrating fields of the shaped electrodes A2 and A3 extract, focus and accelerate the ions to several hundred eV towards the detector entrance window W (which may be a quadrupole mass analyzer, ion trap, etc.). The device operates continuously, with no pulsing or grids or lens elements required. The sample entrance may

be, as with the READ case, a leak valve, or a rotary trap.

7. THE ENERGY DEPENDENCE OF THE ATTACHMENT PROCESS

It was apparent, although not proven, that electron attachment to explosives molecules should have a maximum cross section at or near zero electron energy. While the performance of the conventional electron-capture detector (ECD) is based on this phenomenon, it was not until the recent results of Boumsellek et al. (1992) that this was demonstrated experimentally.

There is practically no information on the explosives molecules of basic attachment properties such as electron affinities, dissociation energies, rate constants, cross sections, or energy dependence of attachment. In the course of previous READ work lineshape measurements were carried out on nitrobenzene, an explosives simulant, with JPL's photoionization apparatus. Attempts to measure lineshapes for TNT failed due to the relatively low vapor pressure of TNT, and the limited sensitivity of that apparatus.

JPL is currently assembling a new type photoionization apparatus based on our earlier krypton photoionization idea (Chutjian and Alajajian 1985, 1985a). In the new technique, vacuum ultraviolet (VUV) photons will be generated from a pulsed laser (see Fig. 8 schematic). These photons will photoionize a mixture of xenon atoms and the explosives target in a beam. The electrons will attach to the target, and the resulting negative ions will be extracted and detected by a quadrupole mass analyzer. The VUV photons will be generated by a unique method consisting of (a) doubling the 1064 nm Nd:YAG laser line to 532 nm, (b) exciting a dye cell with the 532 nm line to generate 548 nm, (c) mixing the 532 and 548 nm wavelengths to generate 270 nm radiation, (d) tripling, in vacuum, 270 nm to 90 nm radiation, (e) ionizing a mixture of Xe and RDX (say) to generate the attachment spectrum of RDX, and (f) extracting the negative ions and focusing them into a quadrupole mass analyzer. Calculations based on the laser manufacturer's specification of 6 mj/pulse at 270 nm shows that RDX should give a total attachment signal (all masses) of 120 ions/pulse. This is a large and easily detectable signal, with a very small expected contribution from backgrounds. The expected resolution and sensitivity of the laser ionization apparatus will be factors of 20 and 100 greater, respectively, than in JPL's previous work.

Using this technique, the electron energy dependence of the attachment process in the explosives molecules will be determined. Initial tests will be made on TNT and RDX. Moreover, methods will be explored of converting the energy dependence to attachment cross sections.

The laser and associated equipment (doubler, dye cell, mixer, computer, and table) were purchased under a $95,000 grant to this project from the JPL Capital Equipment Fund, at no cost to the DoT/FAA Technical Center. The apparatus is currently being assembled, and portions of it (vacuum chamber, quadrupole mass analyzer and electronics) will also be used for testing the miniature READ device described in Sec. 6 above.

ACKNOWLEDGEMENTS

We thank Dr. J. Hobbs for many helpful discussions. This work was carried out at the Jet Propulsion Laboratory, California Institute of Technology, and was supported by the Department of Transportation, Transportation Systems Center through agreement with the National Aeronautics and Space Administration.

REFERENCES

1. Bernius, M. T. and Chutjian, A. 1989 J. Appl. Phys. 66, 2783.

2. Bernius, M. T. and Chutjian, A. 1989a Rev. Sci. Instr. 60, 779.

3. Bernius, M. T. and Chutjian, A. 1990 Anal. Chem. 62, 1345.

4. Bernius, M. T. and Chutjian, A. 1990a Rev. Sci. Instr. 61, 925.

5. Boumsellek, S., Alajajian, S. H., and Chutjian, A., 1991 First International Symposium on Explosive Detection Technology (abbreviated herein as FISEDT) (Atlantic City, NJ 13-15 Nov.) Abstract P-10.

6. Boumsellek, S., Alajajian, S. H. and Chutjian, A. 1992 J. Am. Soc. Mass Spectrometry 00,000 (in press).

7. Boumsellek, S., and Chutjian, A., 1992 Unpublished Results.

8. Chutjian, A., 1991 invited talk at the XVIIth Int. Conf. Physics Electron. Atom. Collisions (Brisbane, Australia July, 1991) in press.

9. Chutjian, A. and Alajajian, S. H., 1985 Phys. Rev. A 31, 2885.

10. Chutjian, A. and Alajajian, S. H., 1985a J. Phys. B: At. Mol. Phys. 18, 4159.

11. Conrad, F. J. and Peterson, P. K., 1978 in New Concepts Symp. and Workshop on Detect. Ident. Explosives (NTIS Publ. PB-296 055) p. 277.

12. Daugherty, R. C., 1981 Anal. Chem. 53, 625A.

13. Dionne, B. C., Rounbehler, D. P., Achter, E. K., Hobbs, J. R. and Fine, D. H. 1986 J. Energetic Materials 4, 447.

14. Fetterolf, D. D. and Clark, T. D. 1991 FISEDT, Abstract E-2.

15. Glish, G. L., McLuckey, S. A., Grant, B. C. and McKown, H. S., 1991 FISEDT, Abstract C-7.

16. Huang, E. C., Wachs, T., Conboy, J. J. and Henion J. D., 1990 Anal. Chem. 62, 713.

17. Lee, M. L. and Lee, E. D., 1991 FISEDT, Abstract C-4.

18. Lovelock, J. E., 1982 in Appl. Atom. Coll. Phys. (eds. H.S.W. Massey, E. W. McDaniel and B. Bederson, Academic, NY) Vol. 5, p. 1.

19. McLuckey, S. A., Glish, G. L., Asano, K. G. and Grant, B. C., 1988 Anal. Chem. 60, 2220.

20. McLuckey, S. A., Glish, G. L. and Asano, K. G. 1989 Anal. Chim. Acta 225, 25.

21. McLuckey, S. A., Glish, G. L. and Grant, B. C. 1989a Proc. 3rd Symp. Anal. Detect. Explosives (Mannheim, Germany, July).

22. Orient, O. J., Chutjian, A. and Alajajian, S. H. 1985 Rev. Sci. Instr. 56, 69.

23. Orient, O. J., Chutjian, A., Crompton, R. W. and Cheung, B., 1989 Phys. Rev. A 39, 4494.

24. Wigner, E. P. 1948 Phys. Rev. 73, 1002.

25. Willard, H. H., Merritt, L. L. Jr., Dean, J. A. and Settle, F. A. Jr., 1981 Instrumental Methods of Analysis, 6th Ed. (Van Nostrand, NY) Ch. 29.

26. Yinon, J. 1980 J., Forensic Sciences 23, 401.

27. Yinon, J. 1982 Mass Spectrom. Revs. 1, 257.

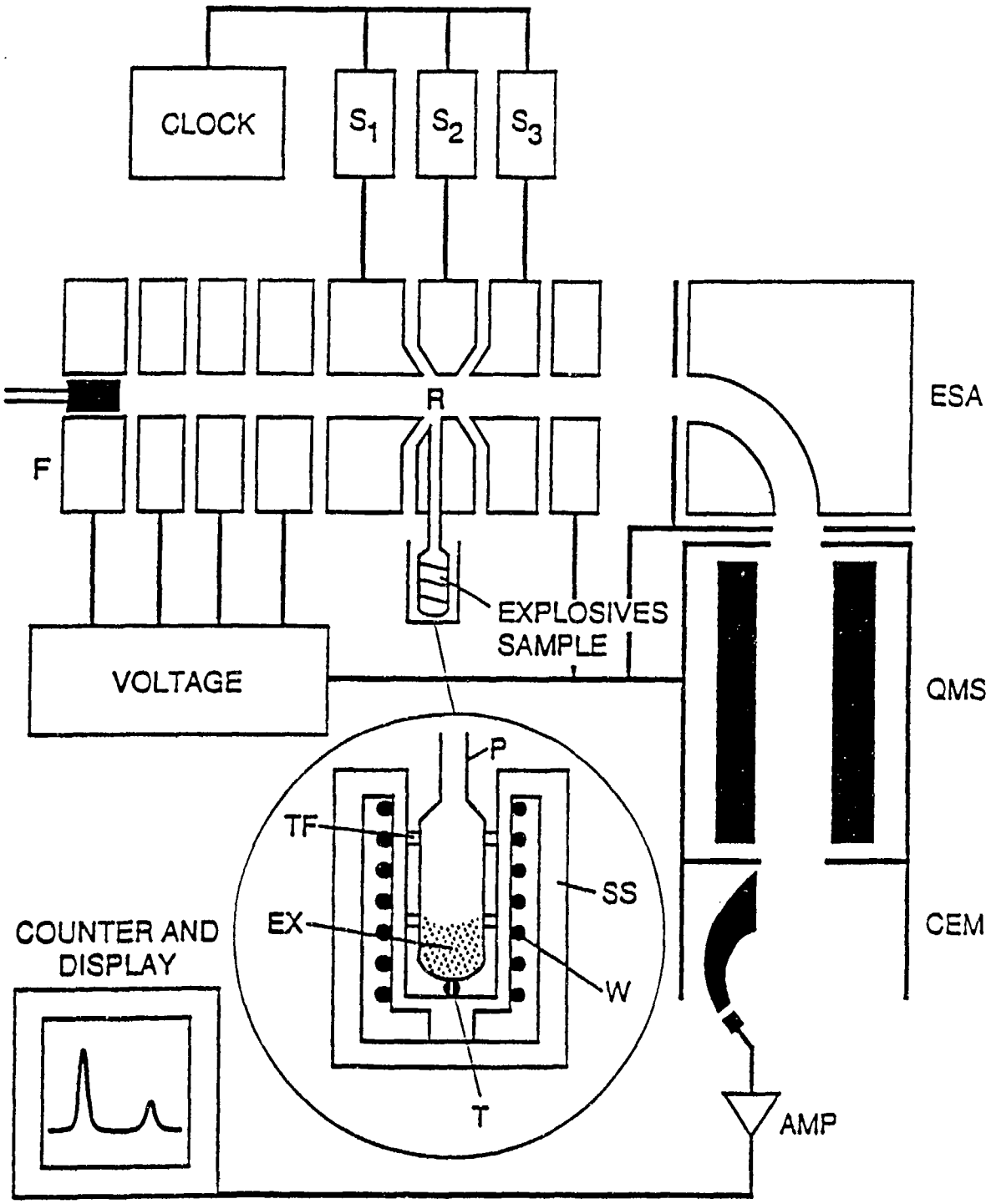


FIGURE 1: Schematic diagram of the READ apparatus, with detail of the explosives sample tube. Electrons are generated at the filament F, accelerated into the reversal region R where attachment takes place. Fast switches S_1-S_3 pulse electrons during one half cycle, then pulse negative ions out towards the electrostatic analyzer (ESA) during the second half. Ions are focused into the quadrupole mass spectrometer (QMS), detected at the channel electron multiplier (CEM), amplified and counted. Detail shows the heated tube (P), sample (EX), heater wires (W) thermocouple (T), teflon spacer (TF), and stainless-steel outer heat shield (SS).

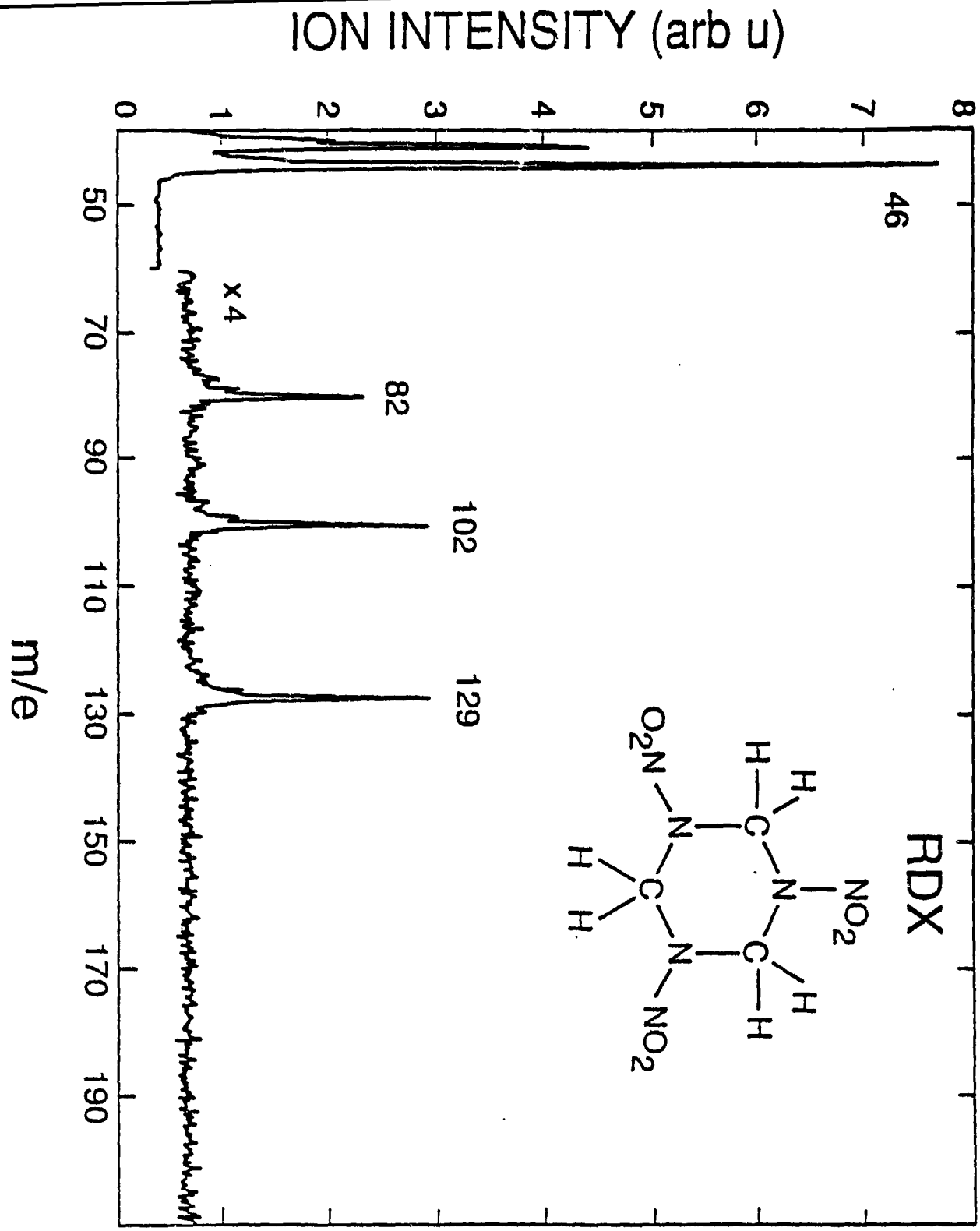


FIGURE 2: Negative-ion mass spectrum of RDX formed in zero-energy electron attachment.

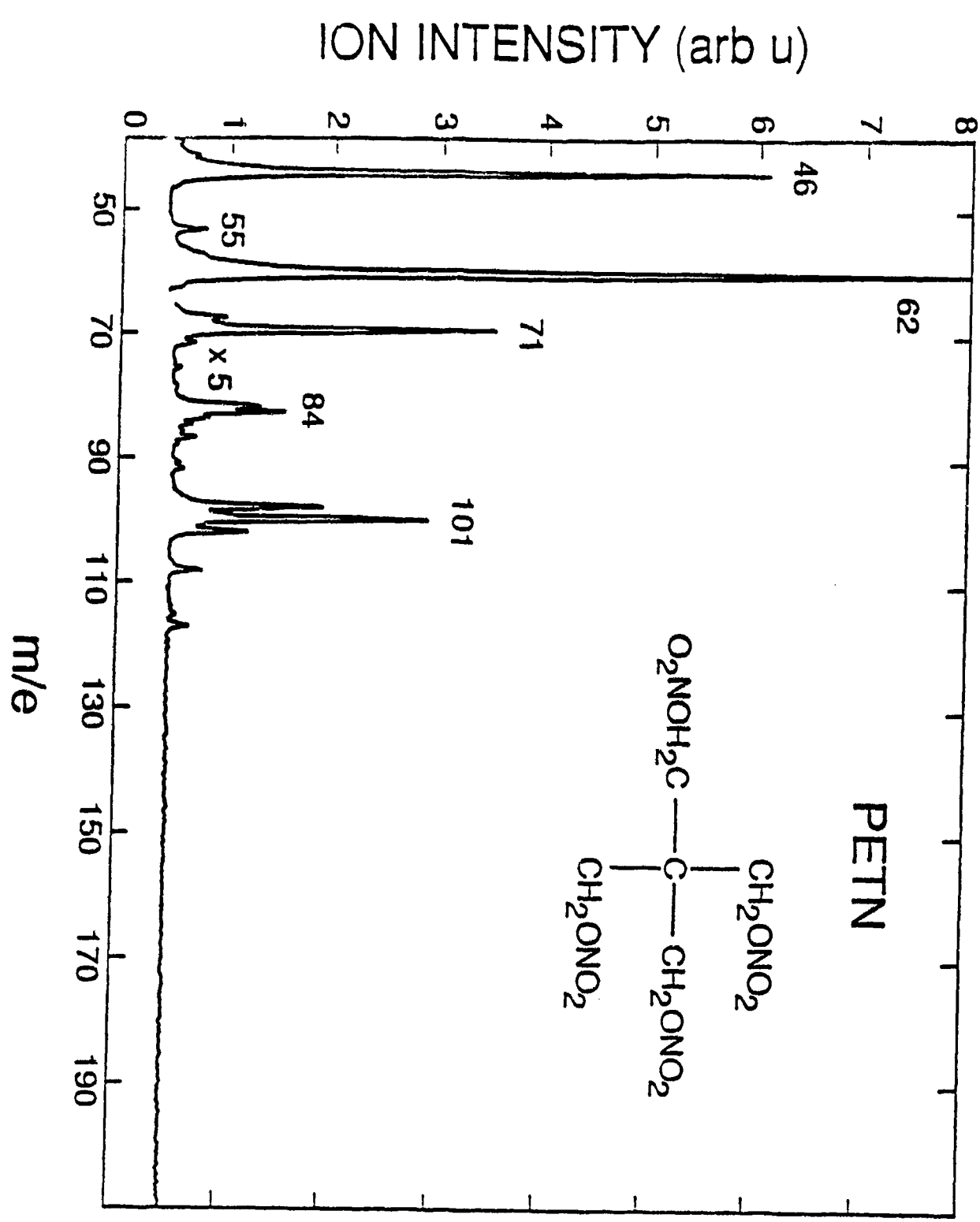


FIGURE 3: Negative-ion mass spectrum of PETN formed in zero-energy electron attachment.

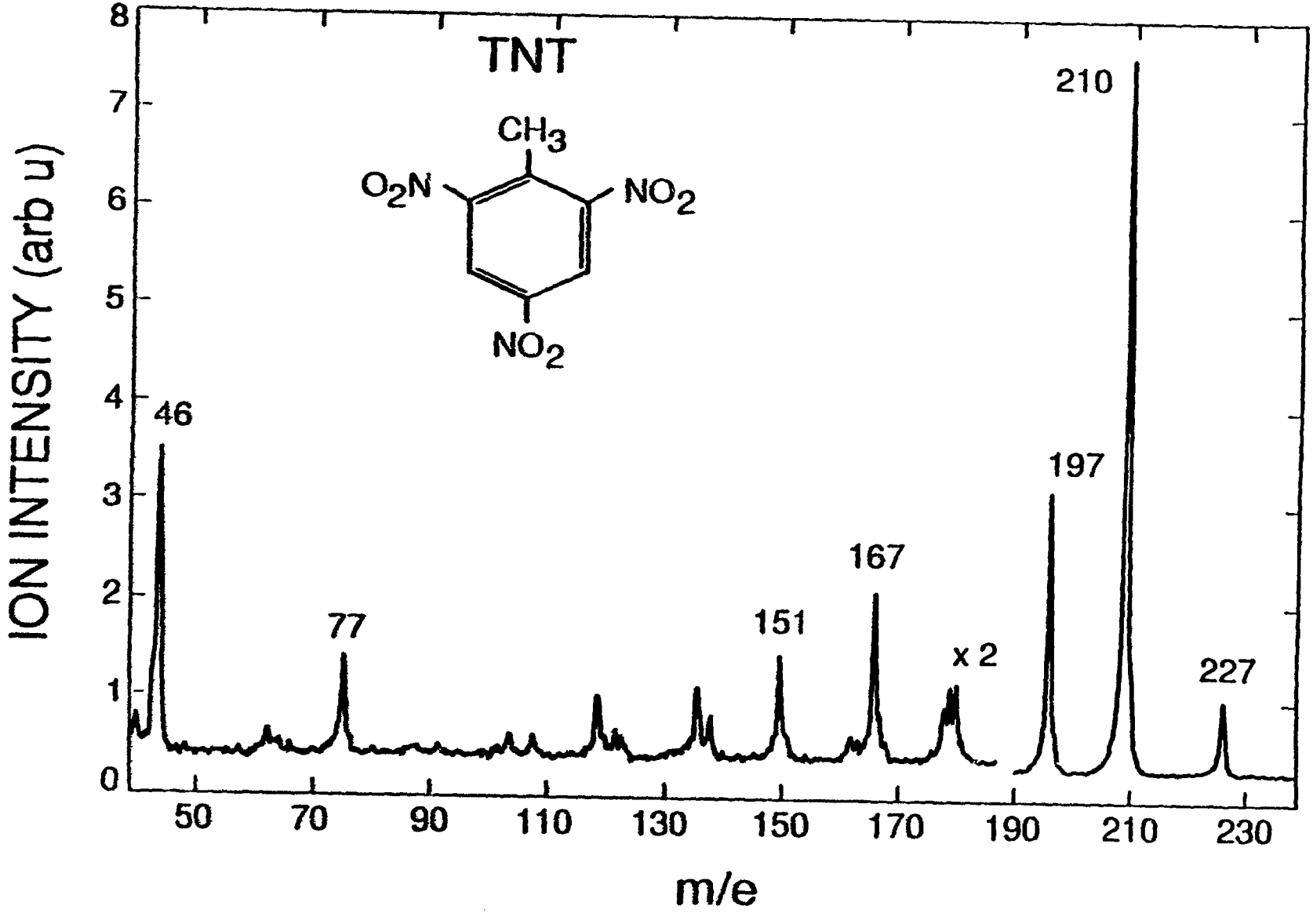


FIGURE 4: Negative-ion mass spectrum of TNT formed in zero-energy attachment.

READ ELECTRON TRAJECTORIES USING A SPHERICAL CATHODE (I_{em} = 1 mA)

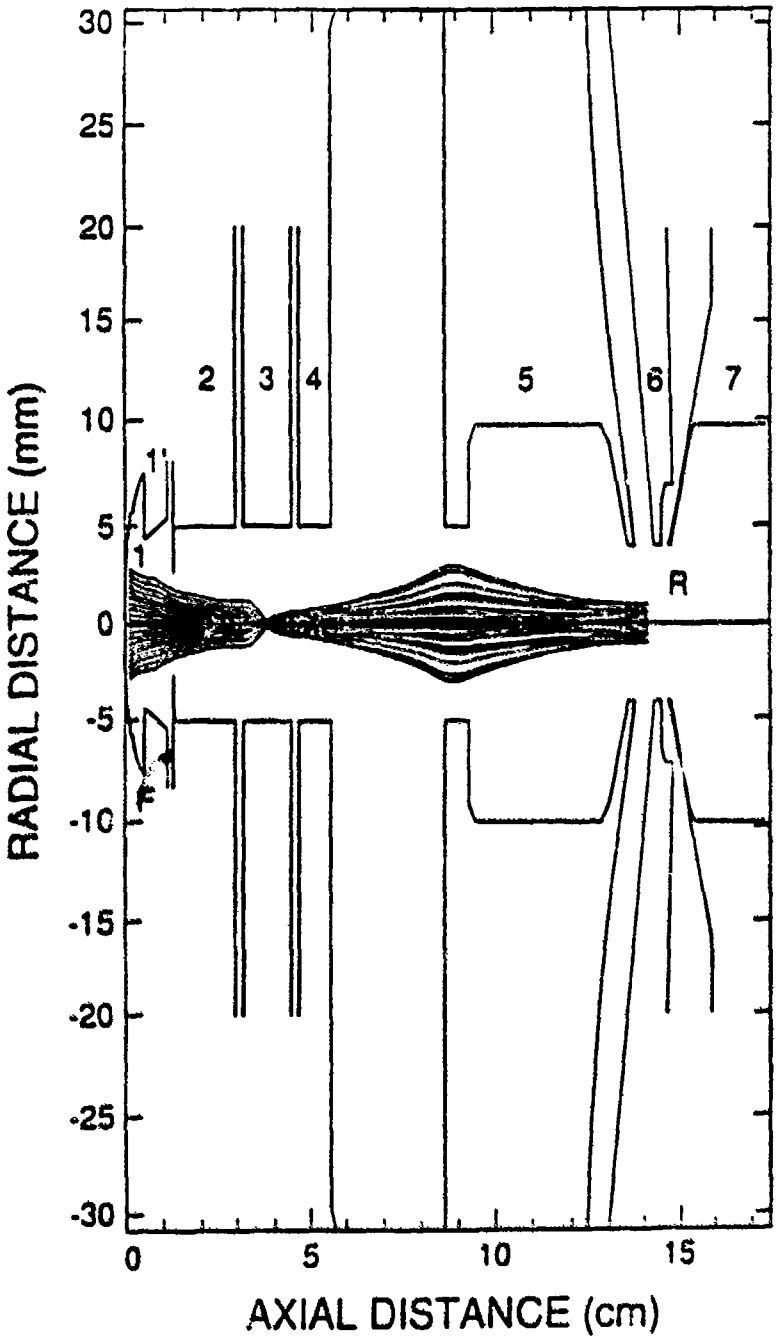
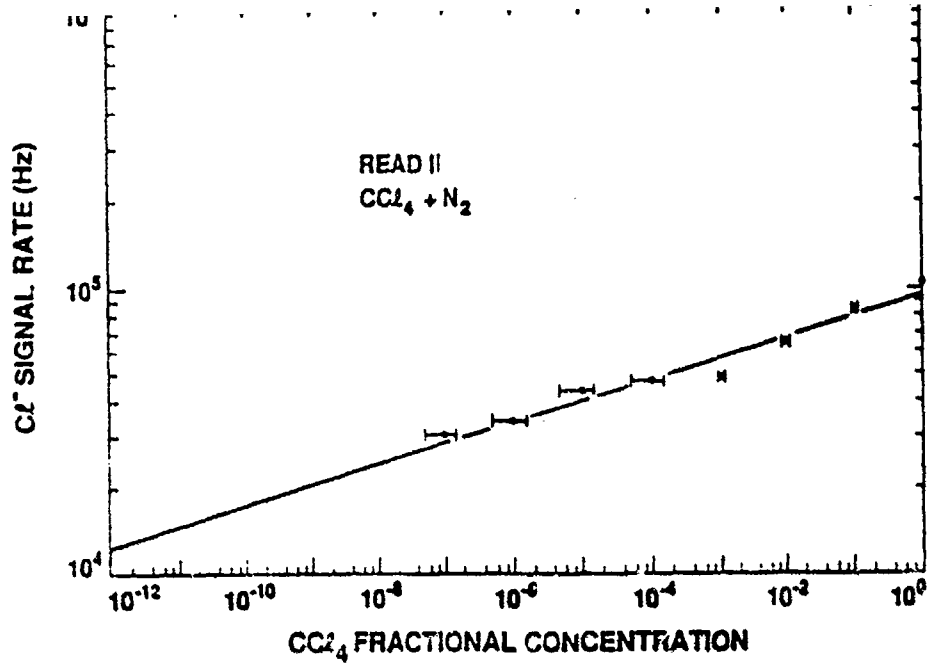


FIGURE 5: Schematic diagram and electron trajectories of the spherical-cathode READ II device, showing the electron gun, electron reversal, and ion extraction lens systems. The indirectly heated spherical electron emitter is denoted as F, the reversal region and collision center by R, and the entrance window to the subsequent mass analyzer (not shown) by W.



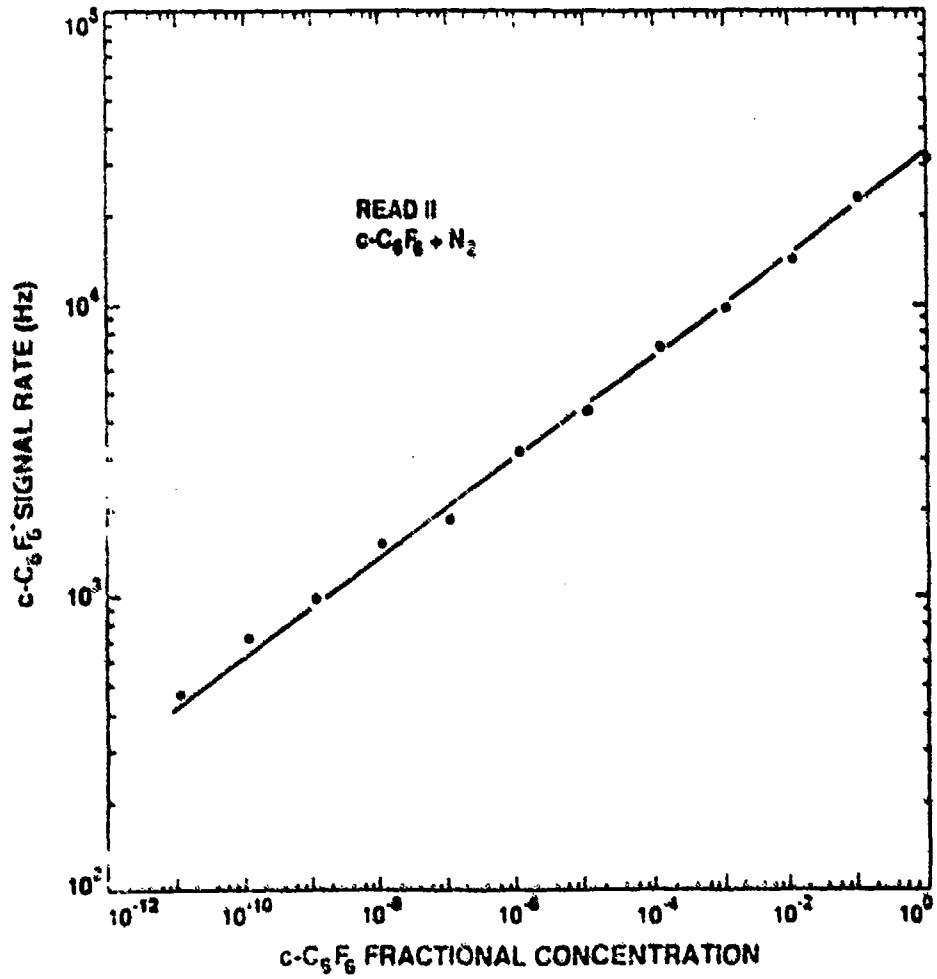
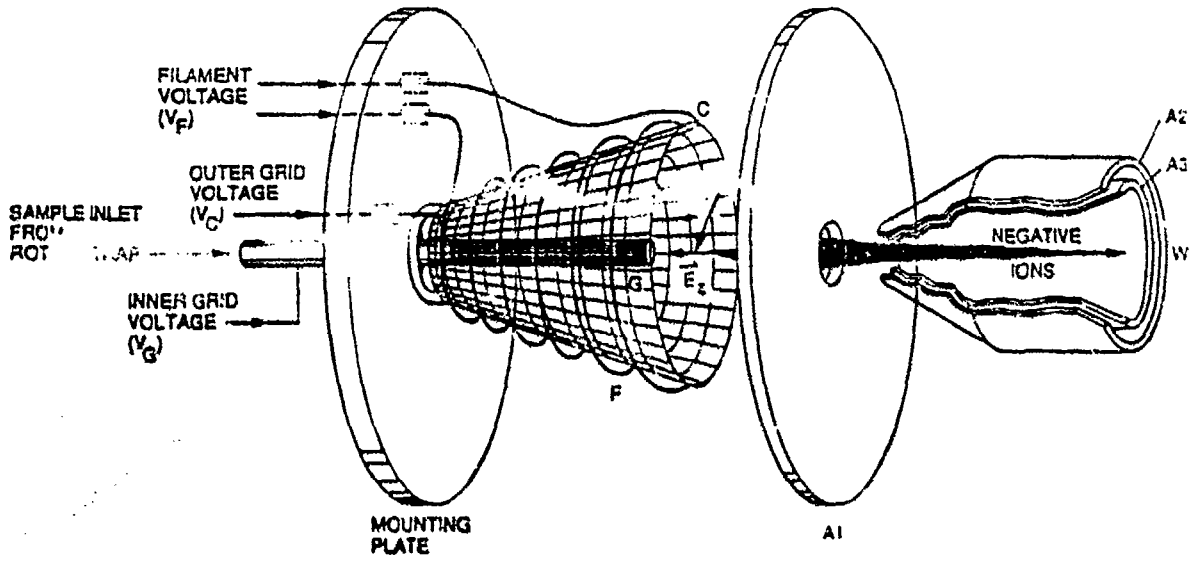


FIGURE 6: READ II sensitivity evaluation using the standard additions analysis for various concentrations of CCl_4 in N_2 (top) and c-C_6F_6 in N_2 (bottom). The solid lines represent a least-squares fit to the data, and extrapolates in CCl_4 to a count rate of 13 kHz at a concentration of 1 pptr, and 7.5 kHz at $1{:}10^{11}$. The count rate at 10 pptr is a factor of 25 greater than previous results reported to READ I (Bernius and Chutjian 1990).

GRIDDED (MINIATURE) REVERSAL IONIZER



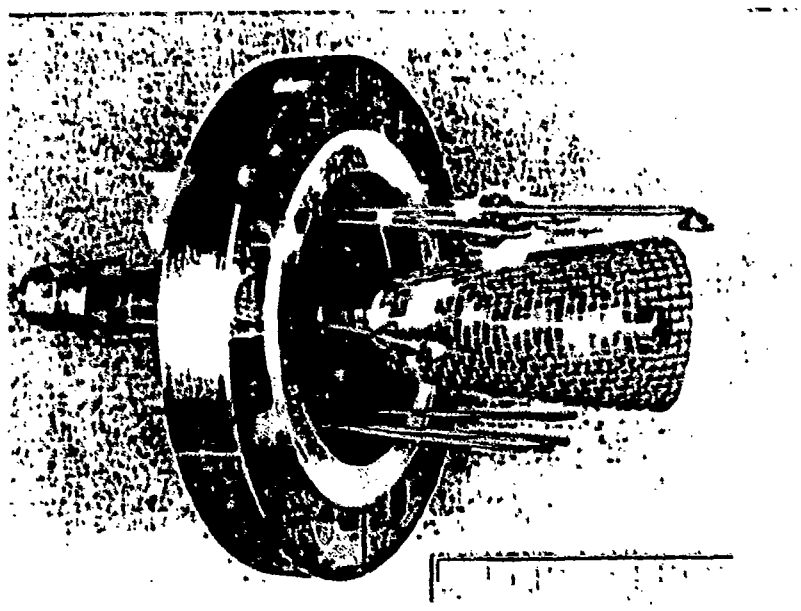


FIGURE 7: Schematic diagram of the gridded, miniature, electron-reversal ionizer (top). Electrons from filament F are accelerated through C and decelerated to zero energy at G where they attach to the target molecules. Extraction is *via* the weak axial electric field E_z, and penetrating potentials of apertures A1-A3. Final focusing is made onto the entrance plane W of a suitable detector which could be, for example, a quadrupole mass analyzer. (Bottom) Photograph of the constructed miniature READ ionizer.

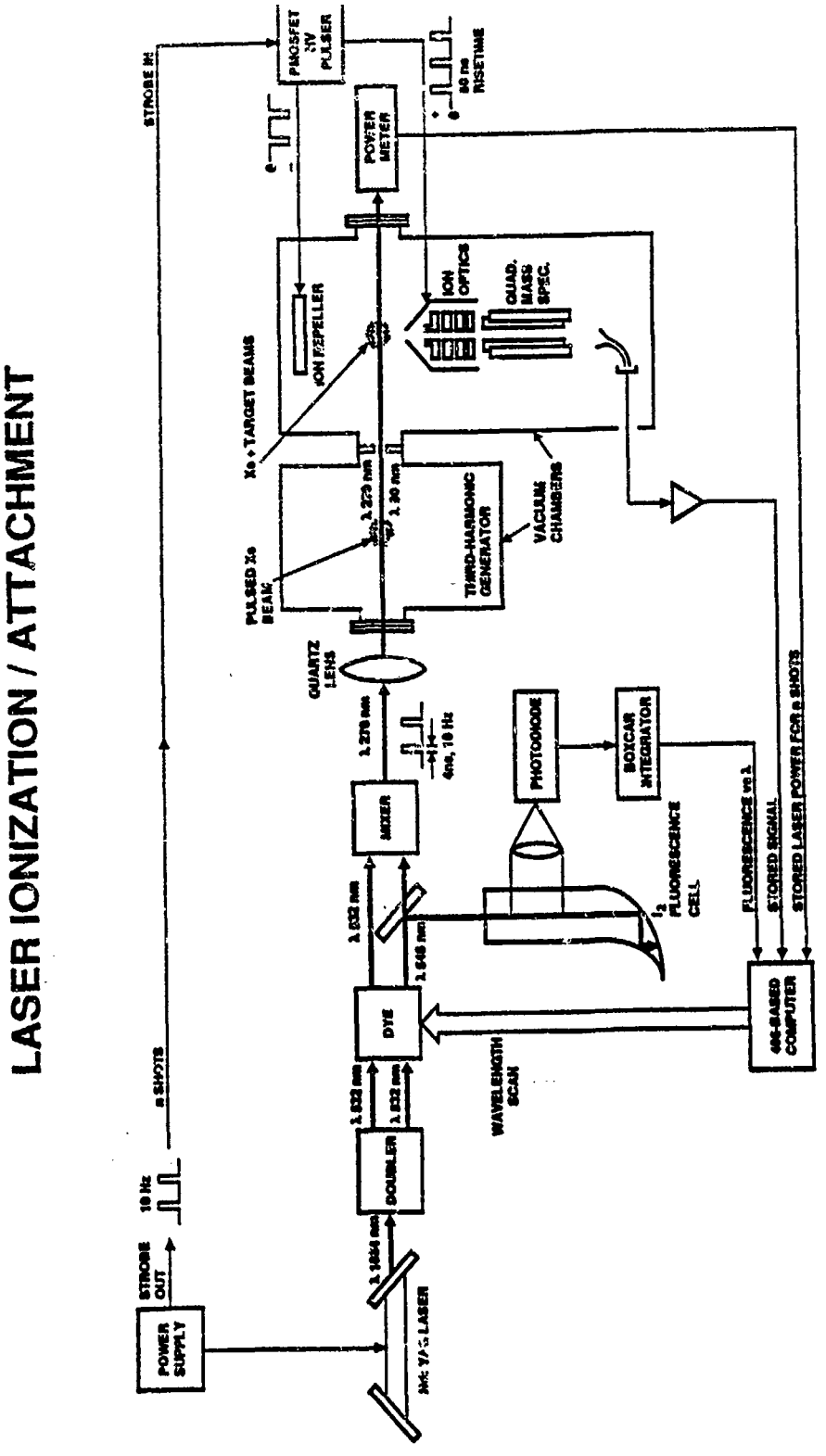


FIGURE 8: Schematic diagram of the laser ionization apparatus. Low-energy electrons are generated by vacuum ultraviolet (VUV) ionization of Xe. The VUV photons are generated by (a) doubling the 1064 nm Nd:YAG laser line to 532 nm, (b) exciting a dye cell with the 532 nm line to generate 548 nm, (c) mixing the 532 and 548 nm wavelengths to generate 270 nm radiation, (d) tripling, in vacuum, 270 nm to 90 nm radiation, (e) ionizing Xe in a mixture of Xe and RDX (say), (f) allowing the electrons to attach to RDX, and (g) extracting the negative ions and focusing them into a quadrupole mass spectrometer. The I_2 cell is used to calibrate the laser wavelength.

CALIBRATION METHODS FOR EXPLOSIVES DETECTORS

Stephen J. MacDonald and David P. Rounbehler
Thermedics Inc.
470 Wildwood Street
Woburn MA 01888

1. INTRODUCTION

Airport security has become an important concern to cultures in every corner of the world. Presently, efforts to improve airport security have brought additional technological solutions, in the form of advanced instrumentation for the detection of explosives, into use at airport terminals in many countries. This new generation of explosives detectors is often used to augment existing security measures and provide a more encompassing screening capability for airline passengers.

The application of a new technology to address problems encountered in the real world environment is a complex process. The technology must be designed into rugged, easy-to-operate systems that can successfully interact with a myriad of situations that are seldom anticipated during initial R&D phases. Once explosives detection systems are implemented, they are routinely operated by personnel who are more focused on the overall security provided by the screening procedure than on the intricacies of the instrumentation employed. In this context, an explosives detection system must allow for rapid verification of performance by untrained personnel with minimal interruption of normal screening procedures.

Because of the broad spectrum of technologies currently being used to address explosives detection, it would be difficult to implement an industry wide doctrine governing the inclusion of calibration steps into normal operating procedures. Factors such as the frequency and extent of calibration required to ensure proper operating performance depend on the underlying technology of the detection scheme. In general, calibration procedures should provide accurate information regarding system performance. Additionally, a well designed calibration procedure also provides diagnostic information when the system malfunctions. This type of information enables corrective action to be quickly initiated and downtime minimized. Calibration procedures should also be fast, relatively easy, inexpensive, and should not require the use of specialized equipment. Simplicity and speed are important characteristics of a successful calibration procedure because system operators usually have very limited experience with the instrument. Furthermore, any time devoted to system calibration represents time lost for explosives screening.

Another factor that affects system performance is the sampling protocol employed. The sampling protocol interfaces the detection technology with real world samples, therefore, the calibration procedure should closely resemble the sampling protocol used during routine explosives screening. It is also important that the calibration procedure include real explosives to accurately test the entire screening procedure. Technologies that require dangerous amounts of material for detection render the use of real explosives impractical due to public safety concerns. In these cases a suitable explosive simulant, if available, should be included in the calibration sample.

This paper describes two calibration procedures used for the Thermedics' EGIS explosives detectors. The systems were designed to screen people, electronic components, luggage, automobiles, and other objects for the presence of concealed explosives. The detectors have the ability to detect a wide range of explosives in both the vapor state or as surface adsorbed solids, therefore, calibrations were designed to challenge the system with explosives in each form.

Because the false alarm rate during routine daily operation is low, it is easy for system operators to become complacent. For this reason calibration procedures should be designed to evaluate each facet of the analysis, from the sampling step to analysis and detection. As described below the two calibration procedures, one for adsorbed solids, another for vapors, provide accurate data concerning the performance of the EGIS instrument, do not require any specialized equipment, and are quickly and easily performed at minimal cost.

2. EXPERIMENTAL

2.1 Equipment

An EGIS explosives detector (Thermedics Inc., Woburn, MA) was used to evaluate the calibration procedures for adsorbed solids and vapors. A hand-held sampler collects explosives in either the vapor state or as solids adsorbed on particulate matter by drawing a sample stream across a collection/preconcentration device. The sampler is then plugged into an analyzer unit which contains automatic sample processing hardware, a high speed gas chromatograph, chemiluminescence detector, and on-board computers.

2.2 Calibration Solution

The calibration solution contained representative explosives whose vapor pressures spanned more than six orders of magnitude. Calibration data is presented for ethylene glycol dinitrate (EGDN), trinitrotoluene (TNT), and hexogen (RDX). Individual concentrations were less than 1 X 10^{-7} moles per milliliter, in acetone, and the solution was stored in a tightly sealed amber glass vial.

2.3 Adsorbed Solids Calibration Equipment and Procedure

Wooden craft sticks were used as a substrate on which to apply trace amounts of individual explosives for the construction of a calibration sample or bomb surrogate which contained explosives adsorbed on its surface. They measured 5.5" X 0.375" X 0.033", roughly the dimensions of a popsicle stick. The craft sticks were "loaded" by dipping them into the calibration solution, immediately removing them, and allowing the solvent to evaporate.

The Adsorbed Solids Calibration Procedure was designed to resemble the real world sampling protocol. It is performed by first loading a wooden craft stick with the explosives of interest. Next, the loaded craft stick is wiped repeatedly with a cloth material to collect adsorbed explosives. The cloth is then sampled with the hand-held sampler which is subsequently connected to the analyzer to determine the presence of explosives.

2.4 Vapor Calibration Equipment and Procedure

For the Vapor Calibration Procedure, 8.5" X 11" sheets of paper were used as the substrate surface. A 50 microliter aliquot of the calibration solution was placed onto a targeted area of the paper which was suspended by a ring shaped spacer to prevent wicking of the solution to secondary surfaces. A simple calibration platform was built to hold the paper and sampler such that the targeted sample area was reproducibly aligned with the hand-held sampler.

The Vapor Calibration Procedure was designed to challenge the systems ability to collect explosive vapors emanating from surfaces. Once the surrogate surfaces were prepared and placed in the alignment platform, the hand-held sampler applied heat to the paper surface and swept the resulting explosive vapors across the collection/preconcentration device. The sampler was then connected to the analyzer for explosives determination.

2.5 Experimental Design

Twenty five repetitive trials were performed for the Adsorbed Solids Calibration Procedure, ten trials were performed with the Vapor Calibration Procedure. The average response and the amount of variability inherent in each calibration procedure was determined. All of the experimental work was performed by a person with limited EGIS experience. The calibrations described in this text were designed to challenge the detection system at levels approaching the detection limit, therefore, relative standard deviations (RSD) of 50% or less were targeted as acceptable.

3. RESULTS AND DISCUSSION

3.1 Variability of the Adsorbed Solids Calibration Procedure

The Adsorbed Solids Calibration was performed twenty five times to determine the inherent variability of the procedure. Data from the twenty five trials is shown in Table I. The average (AVG) values obtained for each explosive are also listed along with the standard deviation (STD DEV) and the relative standard deviation (RSD). The RSD values were 30% for EGDN, 43% for TNT, and 41% for RDX, this amount of variability was satisfactory for the purpose of field calibration.

3.2 Variability of the Vapor Calibration Procedure

The Vapor Calibration was performed ten times in order to determine the inherent variability of the

overall procedure. The data is shown in Table II. The RSD values were 36% for EGDN, 28% for TNT, and 46% for RDX. Again, these values were acceptable for field calibration purposes.

3.3 Sources of Variability

The sources of variability associated with the calibration procedures include operator error, as well as the original amount of explosives transferred from either the craft stick or the paper surface to the sampler. These experiments were performed by an inexperienced technician given minimal instructions. Further experiments employing different technicians would reveal the significance of individual technique in performing the calibrations.

The effect of vapor pressure for the individual explosives while the acetone is allowed to evaporate would contribute to the variability as well. The individual explosives contained in the calibration sample were selected to represent a mixture with a wide range of vapor pressures, therefore, the behavior of individual components would be expected to be significantly different.

4. CONCLUSIONS

The overall data indicates that these calibrations provide accurate data reflecting the performance level of the system. As expected, the RSD values indicate that there are many sources of inherent variability associated with the procedure. These would reflect the variability of the sampling method as well as operator error. The calibration procedures were demonstrated to be well suited for explosive detectors that are designed to determine the presence of trace levels of materials in a highly complex sample matrix.

The calibrations are simple and straightforward because they mimic their respective sampling protocols. Each procedure can be performed in approximately two minutes and the only equipment required is the standard explosives solution and wooden craft sticks for the Adsorbed Solids Calibration and a simple alignment platform for the Vapor Calibration. The procedures are inexpensive to perform and cause minimal interruption in the normal screening procedures.

TABLE I

ADSORBED SOLIDS CALIBRATION DATA
FOR TWENTY FIVE REPETITIVE TRIAL

TRIAL #	SIGNAL INTENSITY (arbitrary units)		
	EGDN	TNT	RDX
1	792	1277	1040
2	646	699	600
3	1156	1309	1117
4	1055	1357	1590
5	815	1017	1007
6	1142	1045	1059
7	738	735	674
8	1210	1683	1647
9	1376	1376	1229
10	1325	978	1018
11	1437	942	935
12	1155	1210	1177
13	850	692	679
14	638	385	385
15	1679	2266	2186
16	616	553	864
17	563	310	330
18	1555	1195	1235
19	808	1230	1312
20	939	987	908
21	975	664	572
22	1076	828	910
23	908	785	811
24	833	1165	1279
25	681	338	440
AVG	999	1001	1000
STD DEV	301	430	414
RSD	30	43	41

TABLE II

VAPOR CALIBRATION DATA
FOR TEN REPETITIVE TRIALS

Trial #	Signal Intensity (arbitrary units)		
	EGDN	TNT	RDX
1	1619	1050	950
2	599	722	660
3	910	848	581
4	1303	704	663
5	840	1390	2097
6	617	957	1176
7	951	933	1012
8	929	743	581
9	727	1108	1214
10	1502	1543	1056
AVG	1000	1000	999
STD DEV	358	283	455
RSD	36	28	46

VAPOR DETECTION USING SAW SENSORS

G. Watson, W. Horton, and E. Staples
Amerasia Technology, Inc.
2248 Townsgate Road, Westlake Village, CA 91361

1. INTRODUCTION

There is a need to detect low concentrations (nanogram to femtogram levels) of TNT, DNT, C4, PETN and other explosive materials. The development of SAW vapor detectors has been reported previously [Ref. 1-3], however none offer high selectivity, specificity or high sensitivity. Previous SAW sensors have been limited to nanogram sensitivities because they utilize relatively large area and low Q SAW delay lines to detect condensing vapors. The need to coat the entire path of the SAW delay line requires that considerable mass be condensed and hence results in low sensitivity when attempting to detect and classify extremely small amounts of an unknown material. The problem is compounded by the presence of other unknown materials in even larger concentrations than that of the target explosive materials.

Reported here are SAW sensors for detecting explosive material vapors at picogram (1×10^{-12}) and even femtogram (1×10^{-15}) concentrations. These SAW sorption sensors utilize a physical area no larger than the smallest quartz capillary column. In effect, the sensor is on the head of a pin. Using a SAW resonator structure operating at 500 MHz, a nearly 4 order increase (10,000) in scale factor is achieved [Ref. 4].

2. SAW CHROMATOGRAPHY SENSOR

The sensors studied consisted of SAW resonators operating at 500 MHz. Electrodes were photo-lithographically generated in aluminum films followed by plasma etching of reflective grooves at either end of the structure (Ref. 1). Typically, unloaded resonator Q's of 10,000 are achieved.

In the SAW based GC system the SAW resonator crystal is exposed to the exit gas of a GC capillary column by a carefully positioned and temperature controlled nozzle as shown in Figure 1. When condensible vapors entrained in the GC carrier gas impinge upon the active area between the resonator electrodes (nicknamed the sweetspot of the resonator) a frequency shift occurs in proportion to the mass of material condensing on the crystal surface. The frequency shift is dependent upon the mass and elastic constants of the material being deposited, the temperature of the SAW crystal, and the chemical nature of the crystal surface. The narrow beam of gas exiting the column has been mapped by traversing the gas stream with a minute thermocouple (Figure 2). This narrow beam maintains its geometry well beyond the distance to the SAW surface which assures that the deposition spot matches the sweetspot. The gas jet also causes a localized heating of the SAW surface due to the hot carrier gas, which creates a thermal gradient within the surface of the SAW resonator. The heating effects of the carrier gas are compensated for by the presence of a thermoelectric cooler placed immediately beneath and in thermal contact with the back side of the SAW crystal.

The thermoelectric cooler maintains the SAW surface at sufficiently low temperatures to ensure >95% trapping efficiency for explosive vapors. The surface can be rejuvenated (adsorbed vapors boiled off) by reversing the drive voltage polarity to the thermoelectric cooler allowing it to heat up. Currently temperatures over 120oC are achieved within seconds to rapidly return the SAW to its initial operating frequency. Thus the temperature of the SAW crystal acts as a control over sensor specificity based upon the vapor pressure of the species being trapped. This feature is particularly useful in distinguishing between relatively volatile materials and "sticky" explosive materials [Ref. 5].

Exposing the system to controlled vapor concentrations has allowed scale factor data to be obtained. A vapor generator [Ref. 6] was used to deliver controlled amounts of explosive vapors. To date the best scale factors observed for the SAW resonator system operating at 500 MHz when exposed to TNT and RDX are as follows:

TNT: 9600 Hz/ng @ 500 MHz

RDX: 14,460 Hz/ng @ 500 MHz

When operating at 500 MHz the noise floor of a SAW resonator controlled oscillator is typically 1 Hz or better, hence the minimum detectable mass is 104 and 69 femtograms for TNT and RDX respectively. The higher scale factor for RDX is offset by its much lower vapor pressure which reduces the amount of actual material which can be collected and deposited onto the sensing crystal.

Work with SAW crystals operating at near 1GHz (1000 MHz) frequencies indicate that the scale factors are higher by at least the ratio of the operating frequencies squared.

3. SAW BASED GC SYSTEM

A SAW based GC system for explosive materials has been constructed. A primary design goal was to produce a system which could screen ambient vapors for the presence of explosives in under10 seconds and which would be able to operate with minimum support equipment or electrical power. In addition, achieving other system goals such as low cost and ease of manufacture were also important.

The current SAW based GC system is schematically illustrated in Figure 3. During the sample sequence (A), vapor samples are drawn through the inlet from a preconcentrator (not shown), are pumped through a 6 port GC valve and pass through a cryo-trap. The cryo-trap is a metal capillary which is held at a low enough temperature to trap explosive vapors while allowing more volatile vapors to pass through to the pumpwhere they are exhausted.

After trapping the low vapor pressure materials on the cool cryo-trap loop, the GC valve is actuated and the flow path containing the cryo-trap loop is connected in series with another flow path containing a flow controller, filter, GC column, SAW detector, and another metal capillary loop termed the cryo-focus (B). At this time a short duration (< 2 millisecond) pulse of electrical current is passed through the cryo-trap loop causing rapid heating to approximately 200oC. This causes the vapors trapped to be released and pass through the GC valve to the cryo-focus loop where they are again trapped. The cryo-focus acts as an on-column injector and is directly attached to the GC column. After transfer is completed, the GC valve is reset to its original position and the GC cryo-focus is considered armed and ready for on-column injection.

On column injection is achieved by another short (<2 milliseconds) electrical pulse of heating current (C). An injection time of less than 25 milliseconds and >95% release of trapped vapor isachieved. The injected vapors pass through the GC column (J & W, DB-5) and are separated in time by normal column operation. As the constituent vapors exit the column they are collected and selectively trapped on the surfaceof the SAW crystal where they cause a frequency shift proportional to the amount of material collected. To achieve ashort analysis time (<10 seconds), a short 1 meter length of DB-5 (0.18 mm I.D.) capillary column is used. The column is operated isothermally at a temperature of approximately 175oC. A photograph of the explosive detector system is shown in Figure 4. Figure 5 shows a photograph of the SAW sensor module including its oscillator circuitry.

4. EXPERIMENTAL RESULTS

The current operation and timing of the explosive detection system is controlledby a microprocessor and the resulting chromatograms are displayed on a color monitor. Software provides a user friendly interface from which all temperatures and timing sequences can be selected. Of particular importance is control over the SAW temperature which enables the user to control the degree of specificity based upon the vapor pressure. By selecting a relatively low SAW detector temperature of 0oC, most effluents, even volatile vapors, are trapped on the SAW crystal surface.

Shown in Figure 6 and 7 are typical computer displayed chromatograms. Four areas of the screen are used to display the SAW sensor frequency vs time, the derivative of frequency vs time, user notes regarding test conditions, and a listing of detected peaks with time and total frequency change for each peak. In addition system conditions such as timing settings, gas flows, and column temperatures are displayed along the bottom of the screen.

In Figure 6 a chromatogram of laboratory air without explosives is shown. The actual output of the SAW detector is displayed in the upper left display area. Each "step" indicates the presence of an eluting material sticking to the SAW surface. While a typical chromatographic detector requires that the output be integrated to determine the peak area, the SAW sensor gives the peak area directly and the

signal must be differentiated to allow for the observation of "peaks". The presence of "system" and "background" material peaks is normal.In Figure 7 a chromatogram of nitrogen containing TNT vapors is displayed. In this case the first five peaks (derivative of SAW sensor frequency) are system background peaks while peaks 7 through 10 are due to the introductionof the sample. Peak #8 at 3.25 seconds is DNT and peak #9 at 5.78 seconds is TNT. In this instance a relatively large sample was injected (540 pg) and the 11,386 Hz step response for the TNT peak at 5.78 seconds is shown inthe upper plot of SAW frequency vs time (integrated output). In this chromatogram the SAW temperature was 5oC and the flat line at the base of each step indicates that the material remained trapped on the SAW surface.

Shown in Figure 8 is a plot of system response vs sample size for TNT. The slope of the data indicates a system scale factor of 6500 Hz per nanogram for TNT. Because the transmission efficiency of the system is not perfect, detected frequency changes are not always as large as might be expected from sample injections derived from calibrated vapor generators. The sampling valve can act as a cold spot by holding up the sample during the transfer from the trap to the focus. In addition, the cryo-trap and cryo-focus do not give do not have 100% release, hence the scale factor (Hz/nanogram) for the system is less than that of the SAW detector itself.

5. SAW DESORPTION CHARACTERISTICS

The SAW GC detector operates as a true integrating device and as such provides information on the adsorption and desorption characteristics of each material which exits from the GC column. Shown in Figure 9 is a series of six chromatograms showing the direct and differentiated SAW detector response for the case of sampling TNT headspace vapors. The presence of DNT at approximately 4.9 seconds and TNT at 8.5 seconds is clearly shown in each chromatogram. Of note is the slope of the integration line immediately following each step in the upper curves. If the material desorbs from the SAW crystal surface, the rate of desorption is the slope of the integration line. It is clear from Figure 9 that DNT desorbs more rapidly from the SAW sur-face at any given temperature than TNT.

The desorption information is more clearly displayed in the expanded series of chromatograms shown in Figure 10. Here the time scale is lengthened and the negative portion of the derivative expanded so that the desorption characteristics are clearly shown as a function of SAW substrate temperature. The deposited material causes an initial sharp drop in the SAW frequency followed by a somewhat linear return to the original SAW frequency as the material desorbs from the surface of the crystal. The derivative measurements indicate that the slope of the desorption curve is nearly constant until the material is totally desorbed from the SAW crystal surface.

Desorption characteristics for all materials are not the same. Plotting the information contained in Figures 9 and 10 as the logarithm of the desorption slope vs the reciprocal of temperature in degrees Kelvin results in the plot shown in Figure 11. The curves follow straight lines which implies, not surprisingly, that the desorption rate is also a measure of the vapor pressure. No attempt has been made to relate the equilibrium vapor pressure to the rate of desorption in this work. This data can be used, however, to determine at what temperature and for how long the SAW should be heated to remove a sample of explosive vapor during the heating of the thermoelectric cooler. It is of interest to note that the slopes or activation energies for DNT and TNTare not the same.

6. CONCLUSIONS

The performance of a high speed SAW based gas chromatography system for the detection of explosive materials has been demonstrated. The current system is able to perform a complete analysis in 10 to 15 seconds. The SAW sensor is an integrating GC detector with selectivity resulting from the surfaceadsorption and desorption characteristics of explosive materials. Desorption also allows the SAW sensor to be easily cleaned in-situ and this allows the integrating detector to operate for extended periods without replacement. Specificity to explosive materials is enhanced by controlling the sorption/desorption characteristics of the SAW crystal surface.

The detection of explosive material vapors at femtogram levels is possible usingsurface acoustic wave sensors. Scale factors of 20,000 Hz/ng and above can be achieved by using very high frequency SAW resonators and by confining the depositions to only the active area of resonators. The physical size of theSAW detector is well matched to small diameter GC capillary columns and results in a very small dead volume GC detector.

In order to successfully apply SAW sensing technology, a full understanding of the many physical and chemical principles which are involved is necessary. Besides detecting explosives there are many other applications which may benefit from the use of this new sensor technology. Beyond achieving high sensitivity there is always a need for higher specificity. Future advances are certainly possible using material specific chemical coatings applied to the SAW GC detector.

REFERENCES

1. H. Wohltjen and R. Dessy, "Surface acoustic wave probe for chemical analysis: I. Introduction and instrument description; II. Gas chromatography detector, III. Thermomechanical polymer analyzer," Anal. Chem. Vol 51, pp.1458-1475, August 1979.

2. D. Ballantine and H. Wohltjen, "Use of SAW Devices to Monitor ViscoElastic Properties of Materials,", Proceedings 1988 Ultrasonics Symposium, pp.559-562.

3. R. Lec, J. Vetelino, R. Falconer and Z. Xu, "Macroscopic Theory of Surface Acoustic Wave Gas Microsensors," Proceedings 1988 Ultrasonics Symposium, pp. 585-588.

4. G.W. Watson and E.J. Staples, "SAW Resonators as Vapor Sensors," Proceedings 1990 Ultrasonics Symposium, pp. 311-314, 90CH2938-9.

5. B.T. Kenna and F.J. Conrad, "Studies of the Adsorption/Desorption Behavior ofExplosive-Like Molecules, "Sandia Report, SAND86-0141.UC-501, Oct. 1989.

6. B.C. Dionne, D.P. Rounbehler, E.K. Achter, J.R. Hobbs and D.H. Fine, "Vapor Pressure of Explosives," Journal of Energetic Materials, vol. 4,447-472 (1986).

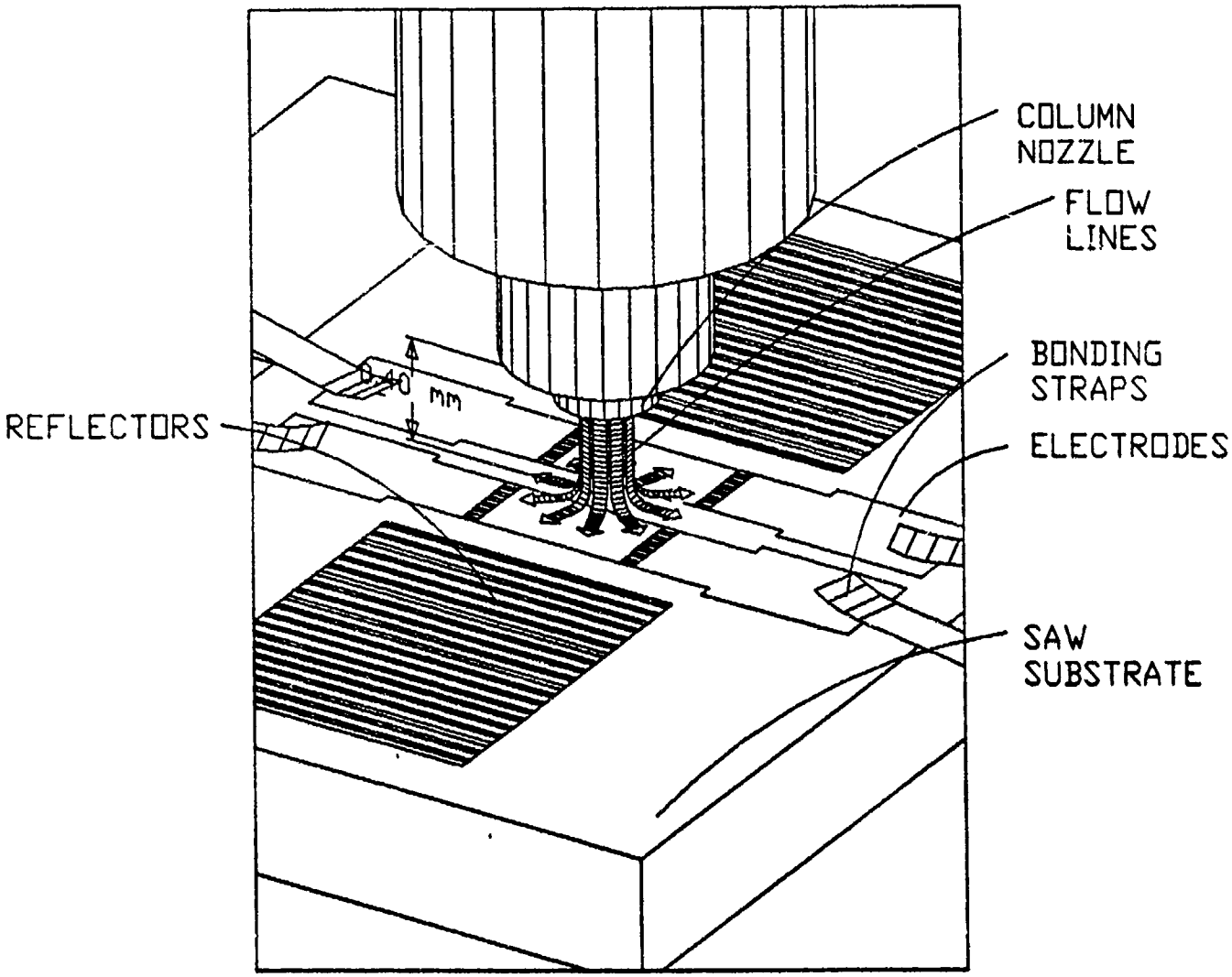


Figure 1- Surface acoustic wave (SAW) resonator gas chromatography (GC) sensor.

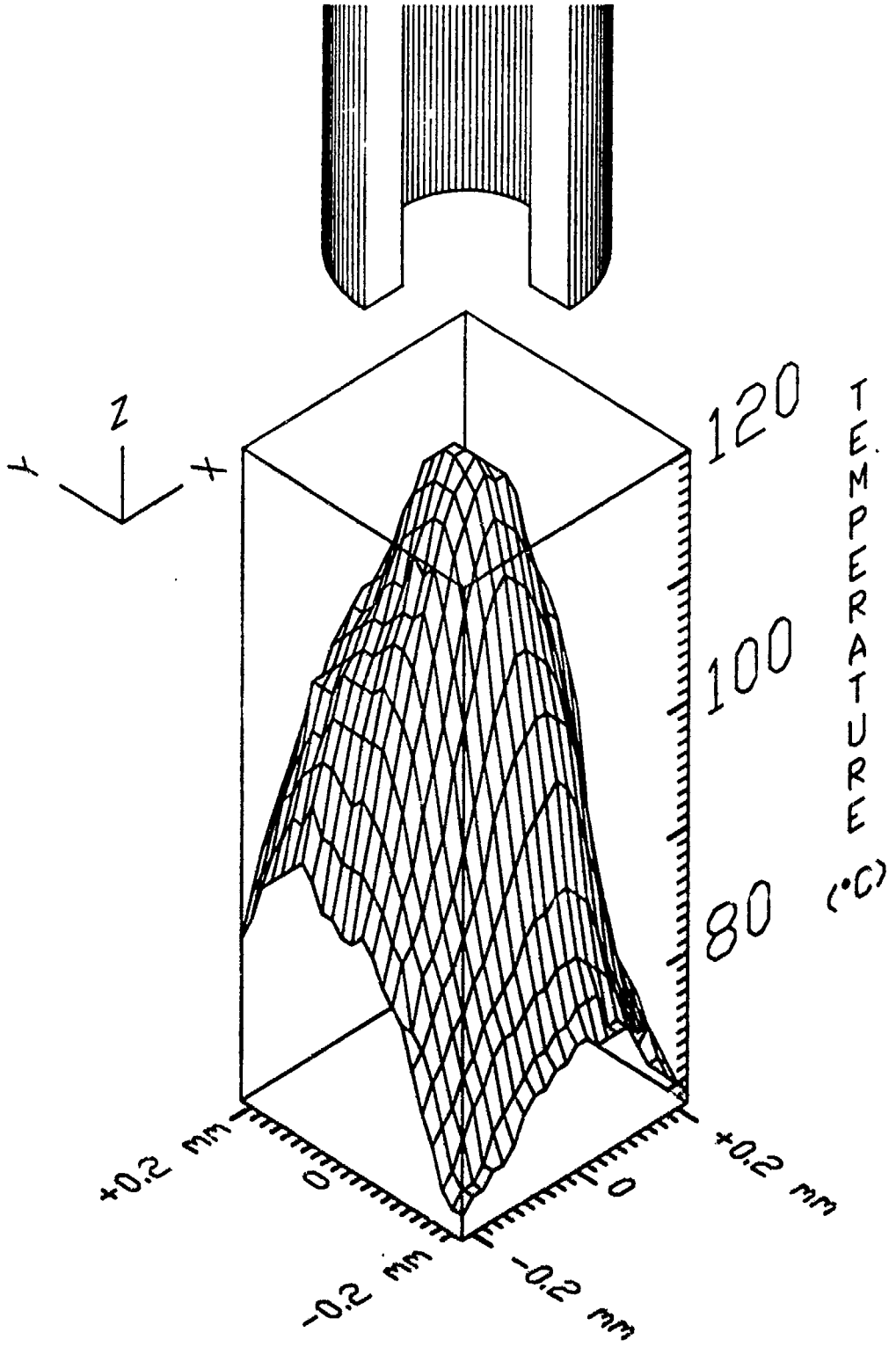
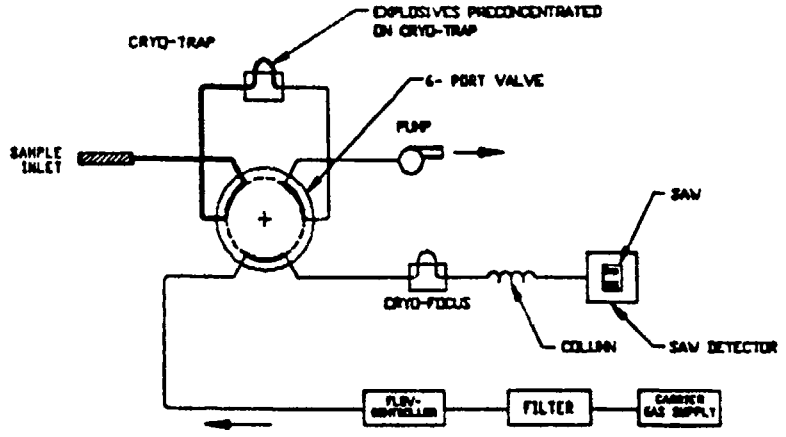
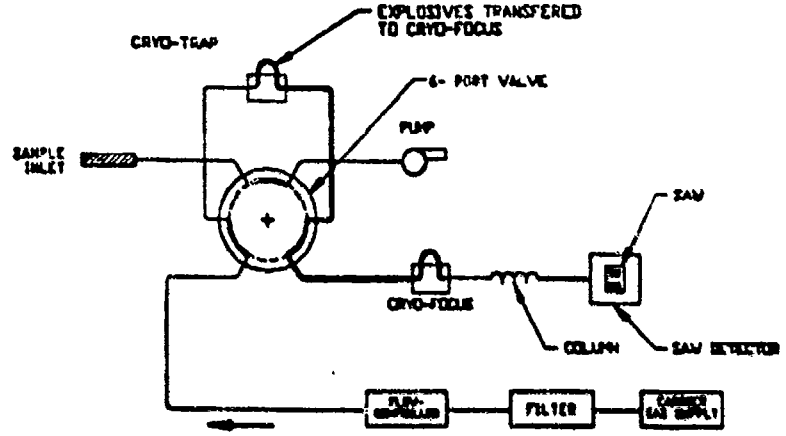


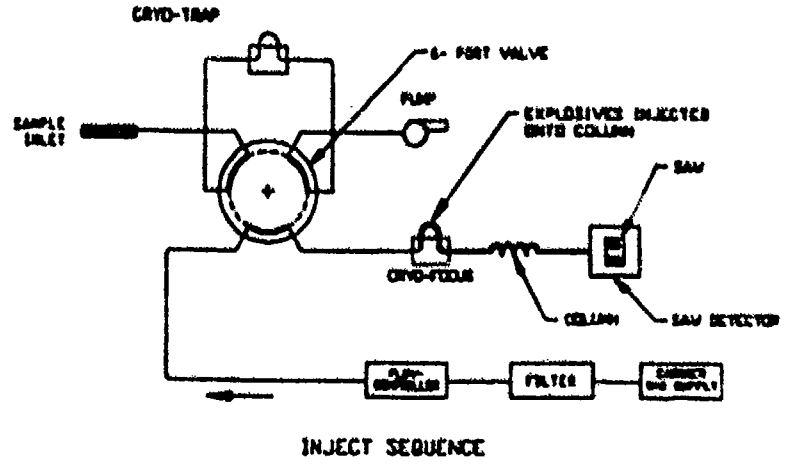
Figure 2- Temperature distribution resulting from carrier gas exiting capillary column.



(A)



(B)



(C)

Figure 3- System diagram showing sampling valve, cryotrap, cryofocus and the major elements of the SAW based GC detection system. The sample sequence is shown in (A), the transfer sequence in (B), and the inject sequence in (C).

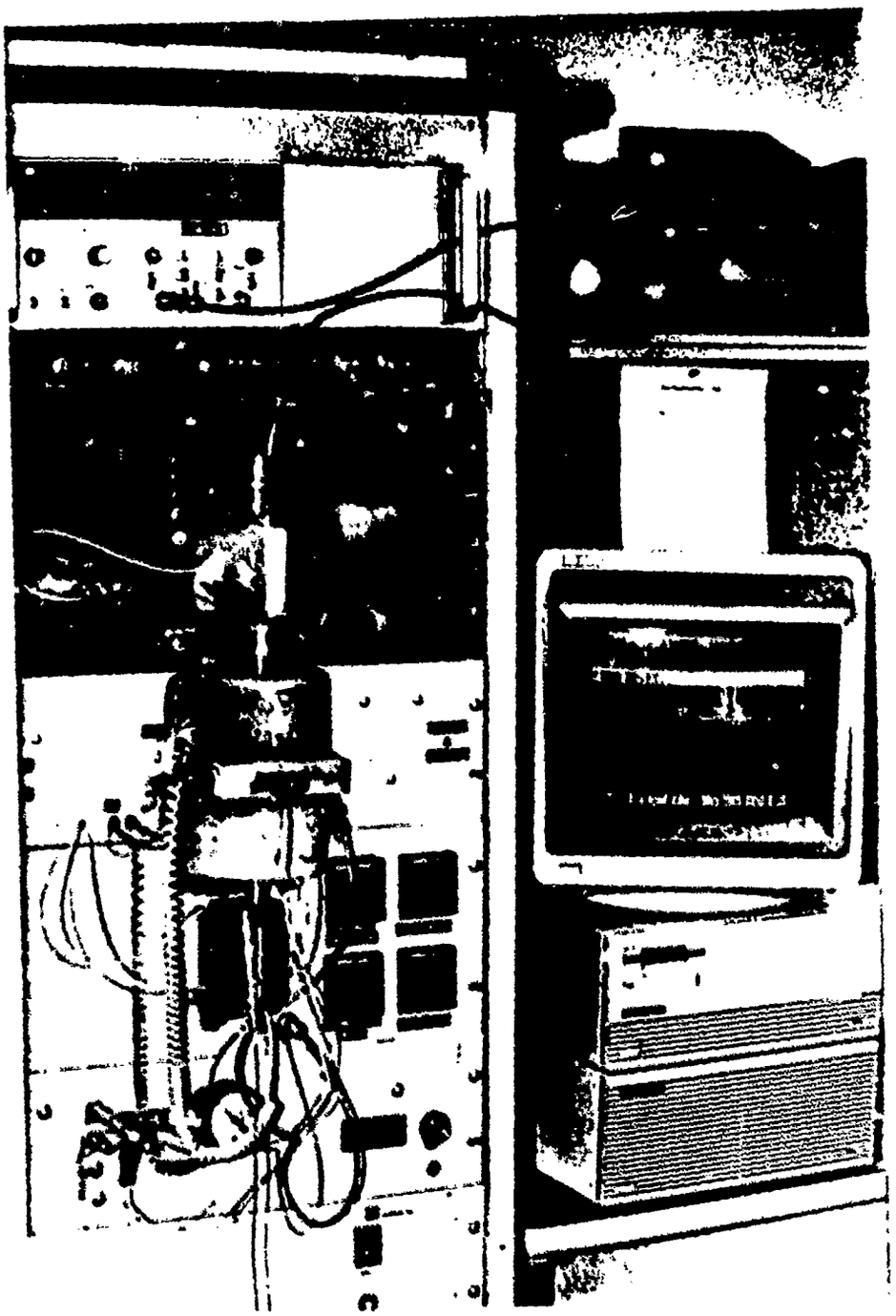


Figure 4- Photograph of Prototype Explosive Detector System.

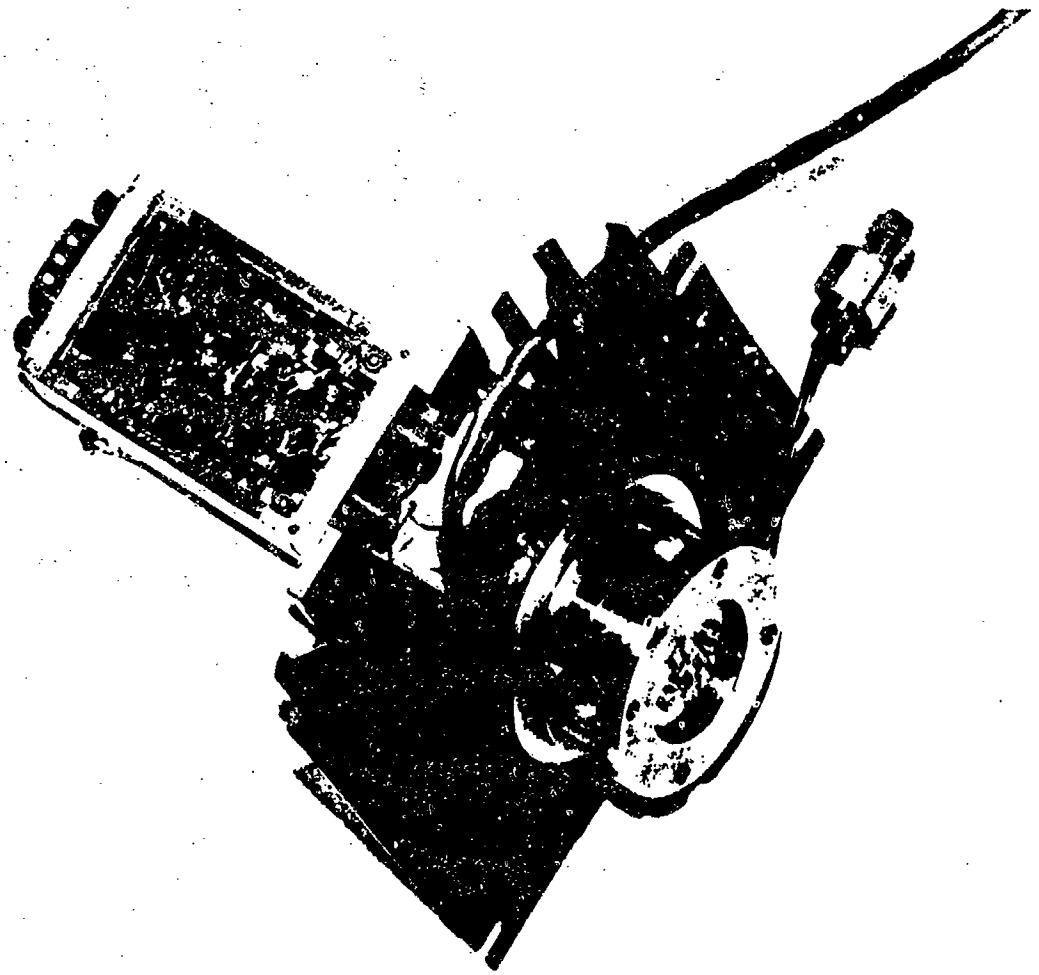


Figure 5 Photograph of SAW sensor module.

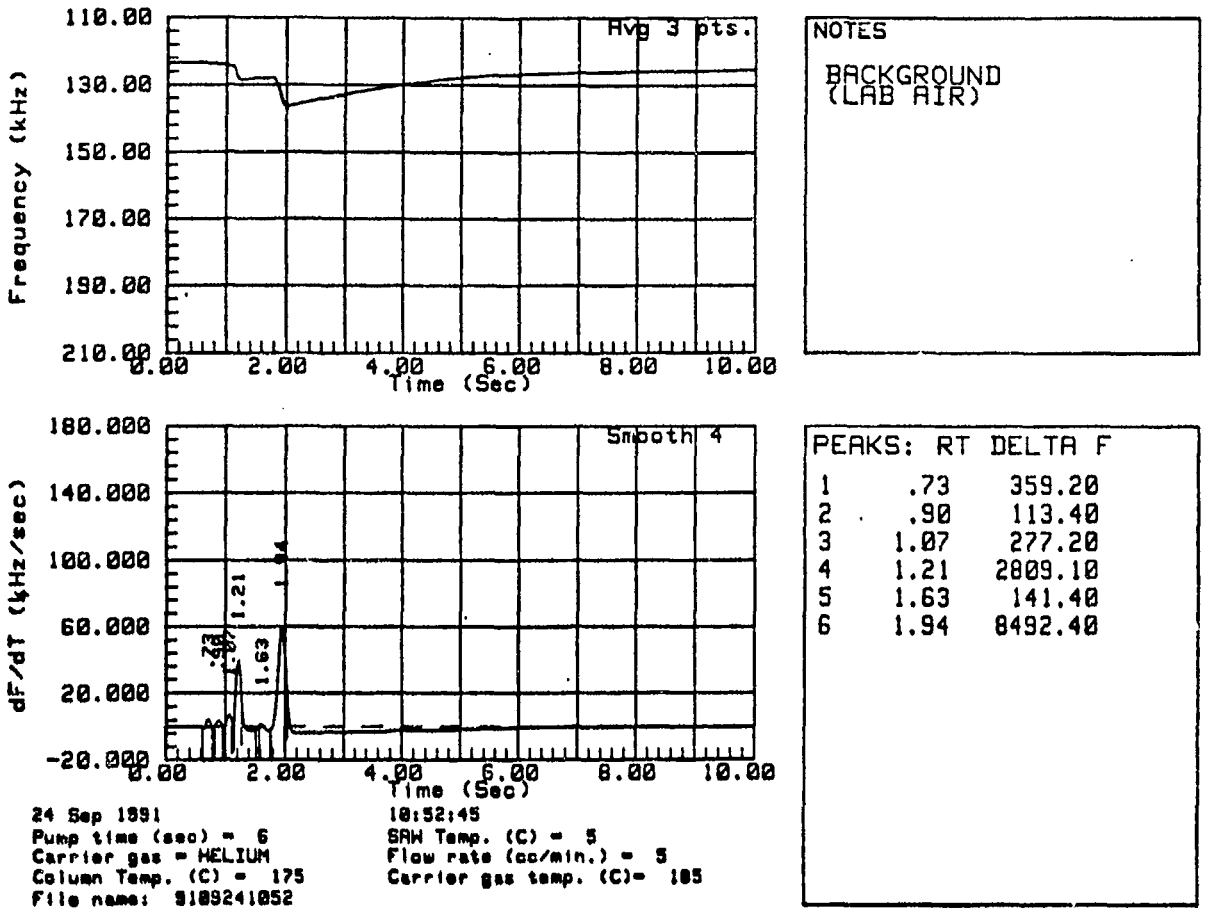


Figure 6- Computer generated chromatogram showing analysis of laboratory air.

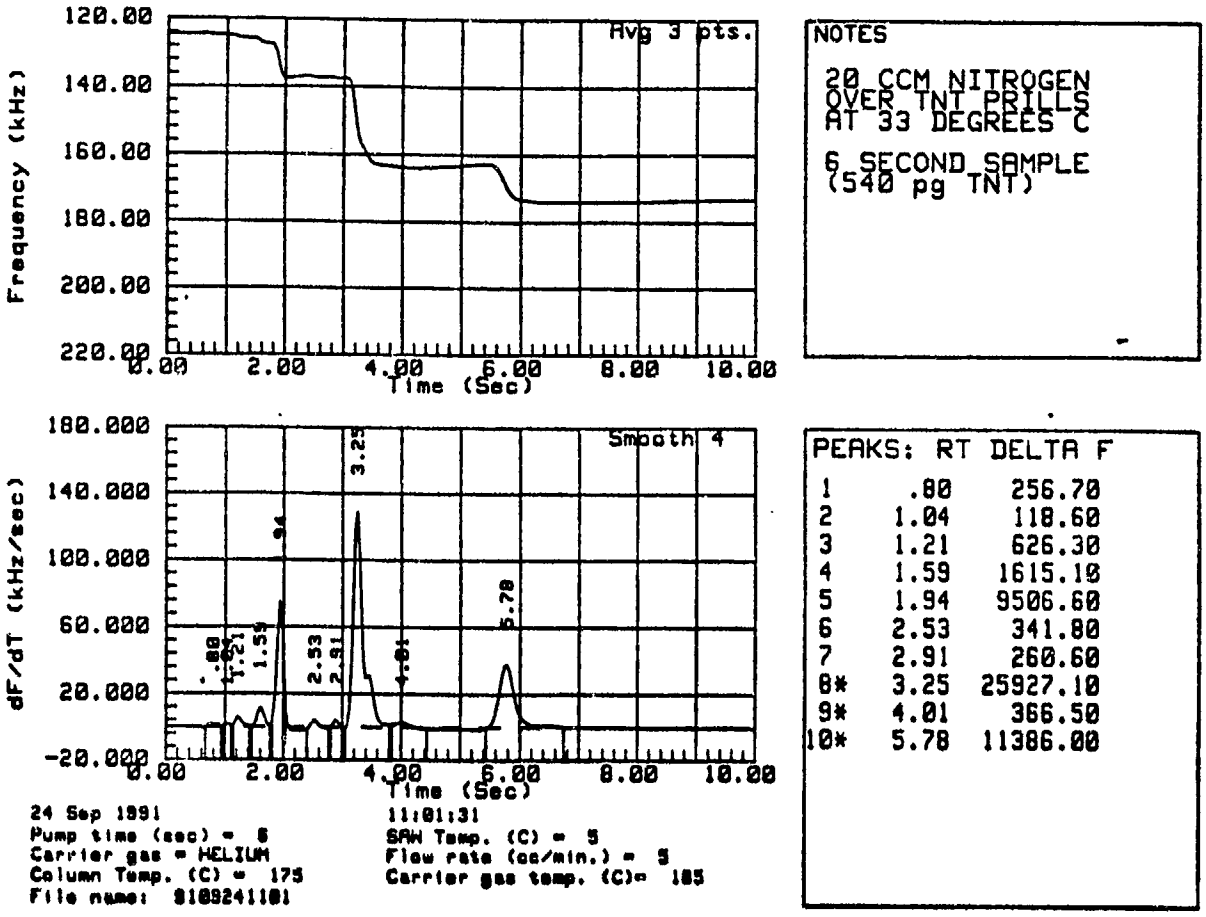


Figure 7- Computer generated chromatogram showing analysis of TNT prills.

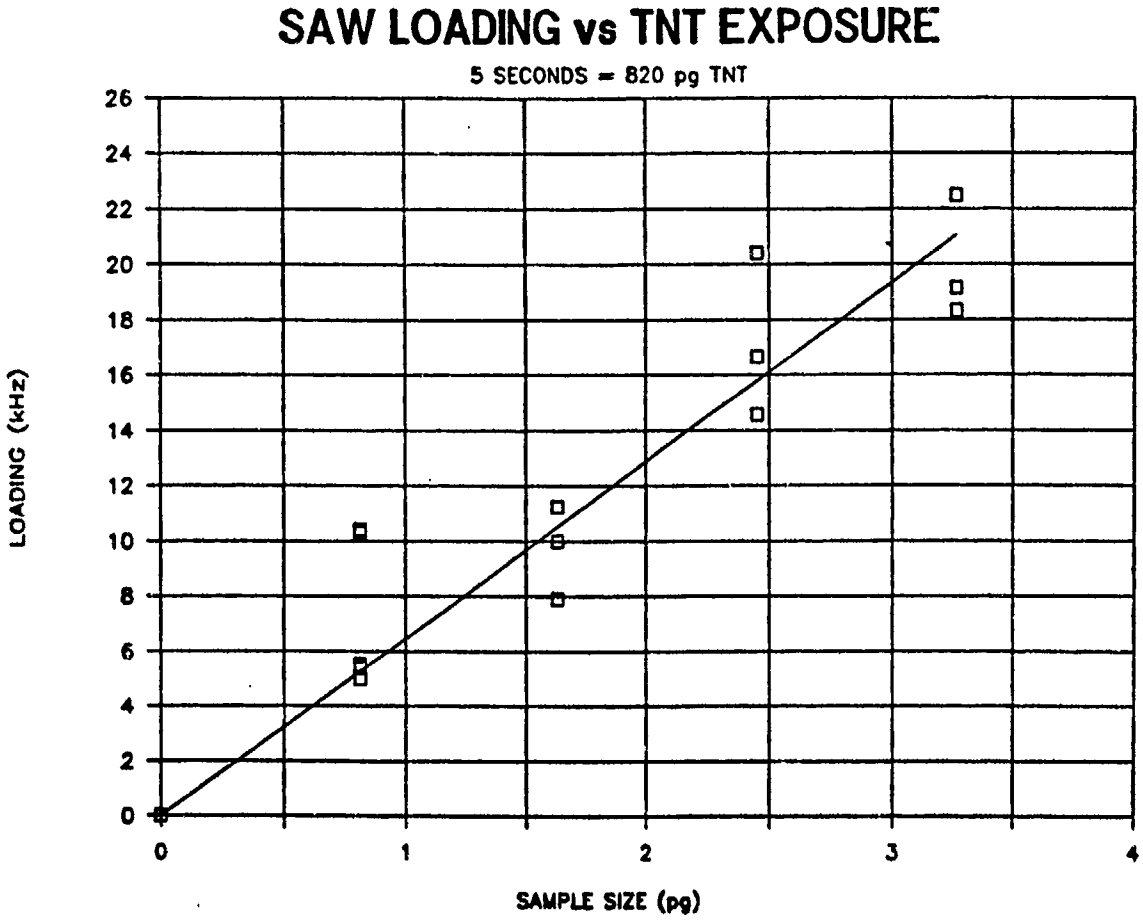


Figure 8- System response vs sample size for TNT.

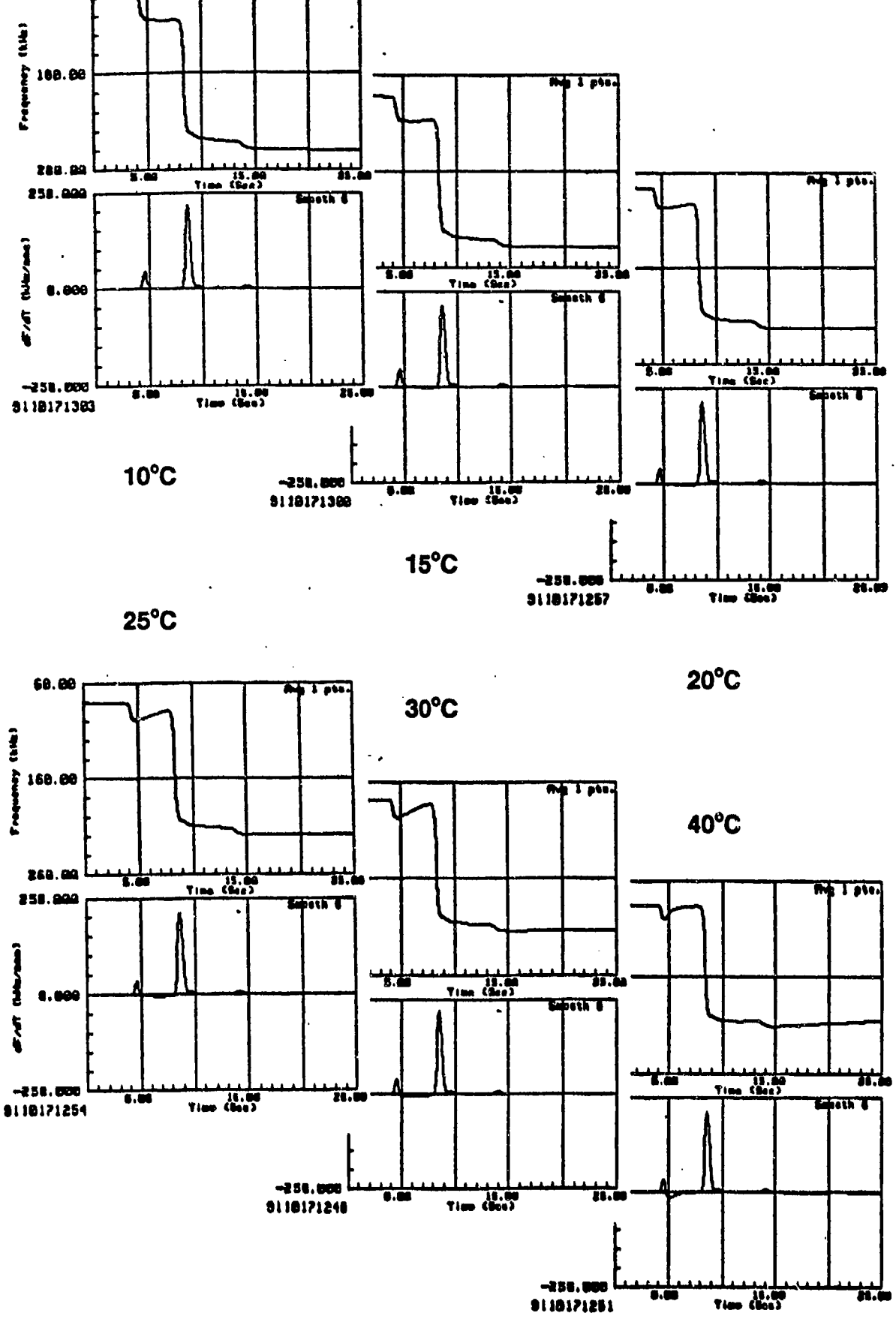


Figure 9- Six chromatograms of TNT Prills showing the effect of different SAW crystal temperature.

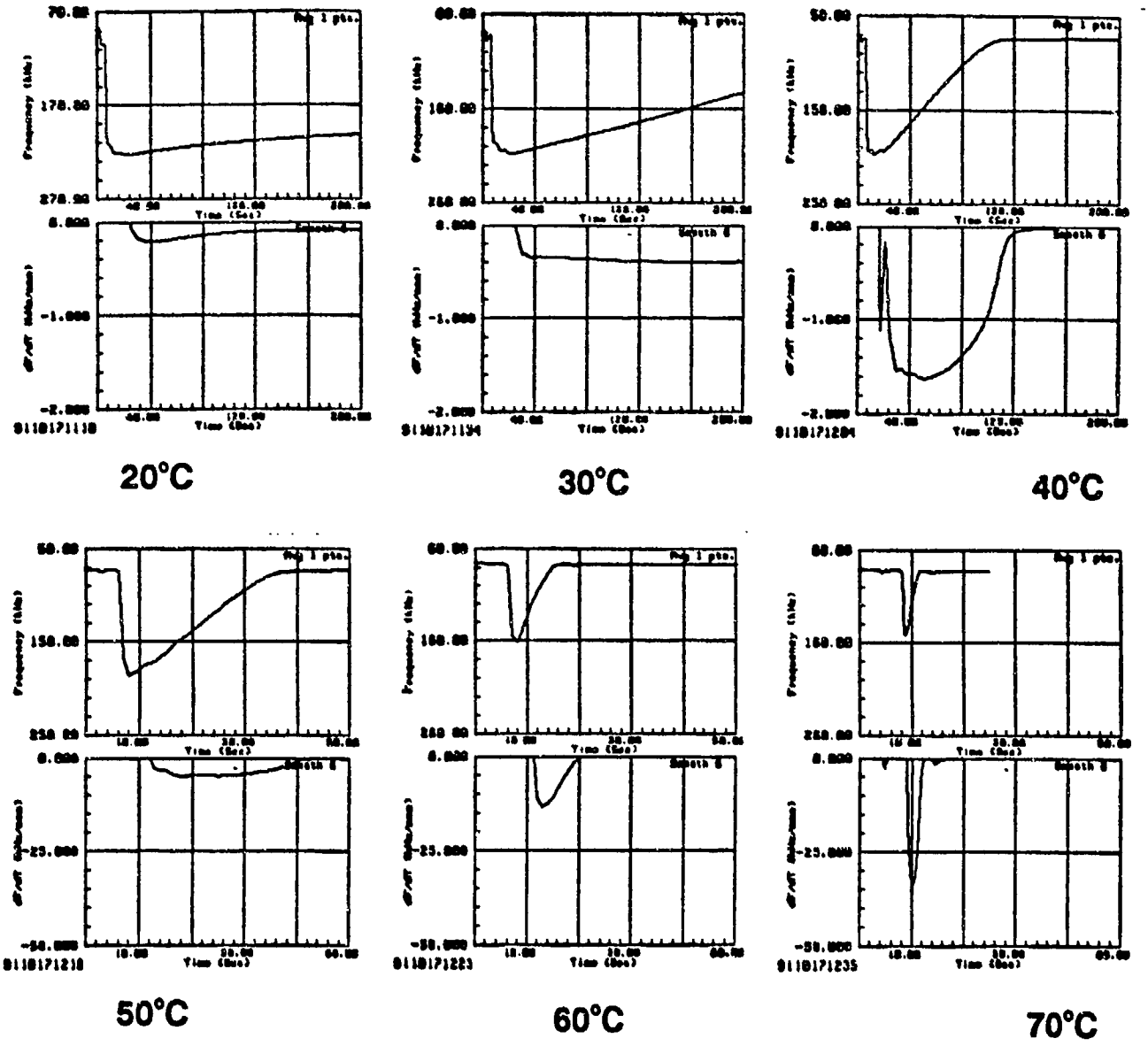


Figure 10- Six chromatograms of TNT Prills showing the the effects of SAW crystal temperature upon desorption.

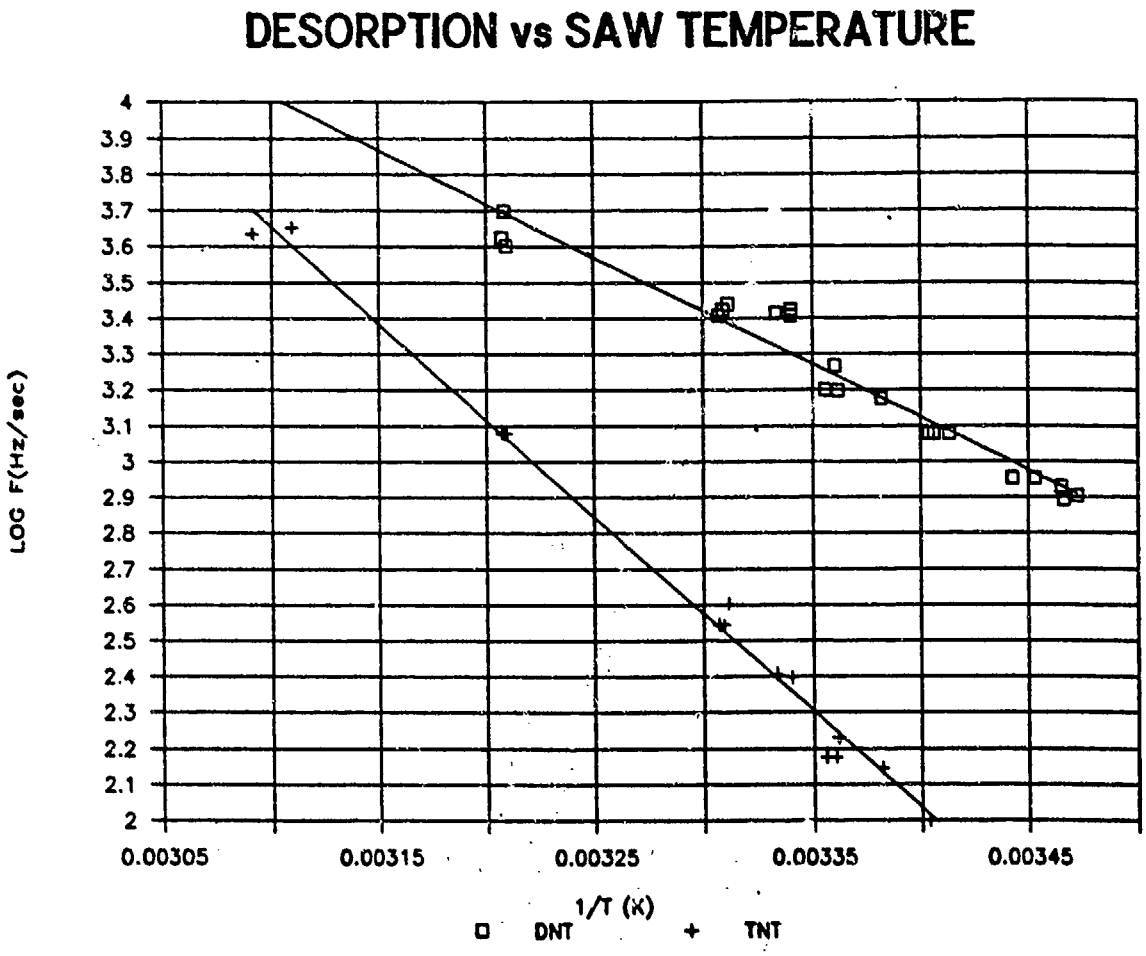


Figure 11- Plot showing logarithm of desorption rate vs reciprocal of temperature (^{0}K).

FOURIER-TRANSFORM INFRARED SPECTROSCOPY APPLIED TO EXPLOSIVE VAPOR DETECTION

D. O. Henderson and E. Silberman
Physics Department
Fisk University
Nashville, TN 37208

F.W. Snyder
FAA Technical Center
Atlantic City International Airport, NJ

1. INTRODUCTION

The infrared part of the electromagnetic spectrum extends from 10,000 to 5 cm^{-1}. This broad spectral range is further classified into the near-IR (10,000-5000 cm^{-1}) mid-IR (5000-200 cm^{-1}) and the far-IR (200-5 cm^{-1}). It is the interaction of this radiation with matter which is responsible for exciting vibrational transitions. In the near-IR, harmonics and combination transitions are typically observed, while in the far-IR, phonons in crystals, and rotational transitions in the gas phase are commonly observed. In the mid-IR, transitions associated with fundamental molecular vibrations may be measured and is often referred to as the fingerprint region. It is this part of the spectrum which is of interest with regard to explosive materials. In particular, since many explosives have the $-NO_2$ group in common, absorptions due to this group serve as signature in the infrared spectra of explosives.

The energy levels of a harmonic oscillator are given by

$$E_v = h\nu(v+\frac{1}{2})$$

where v is the vibrational quantum number and h is Planck's constant. The classical frequency is related to the force constant, k and the reduced mass μ by

$$\nu = \frac{1}{2\pi}\sqrt{k/\mu}$$

A molecular vibration is said to be active in the infrared if the displacements of the nuclei involved in the vibration produce a change in the dipole moment, the transition moment is given by

$$R_v = (\frac{d\rho}{dx})_e \int \psi_1^* x \psi_2 dx$$

where ρ is the dipole moment, X is an internal coordinate, and the Ψ's are the vibrational wavefunctions for the lower and upper states in the transition. At this point, it is worthwhile to mention that the absorptions corresponding to the $-NO_2$ group vibrations, besides having well defined group frequencies, are the strongest in the infrared spectra of explosives. Because of the common presence of the $-NO_2$ group in explosive materials, its group frequencies, large oscillator strengths, and its chemical reactivity, it is very useful to investigate by infrared spectroscopy the interaction of this functional group with preconcentrator materials. Consequently, we present here, in some detail the infrared spectra of explosives measured using selected sampling techniques, and in some cases describe the interaction of explosives with metal oxide substrates in which they are adsorbed.

2. EXPERIMENTAL

The typical instrument [Griffiths] used in modern infrared spectroscopy is a Fourier transform infrared (FTIR) spectrometer. The instrument used in the studies descibed here has a resolution of 0.02 cm^{-1} and a specrtral range of 5000 to 5 cm^{-1}. The signal to noise factor in a typical spectrum is controlled by the number of scans selected for that given measurement. In most cases single beam or raw spectra of a reference material are recorded and ratioed with the

raw spectrum of the sample to produce transmittance, reflectance, or diffuse reflectance spectra depending on the sampling technique employed.

2.1 Transmission and Absorption

Transmission or absorption measurements of solids are usually made by mixing the material of interest with a matrix material, such as KBr, which is transparent in the mid-IR. The KBr and sample mixtures are then pressed into solid pellets under the pressure of a hydraulic press. The self supporting pellets may then be introduced into the spectrometer for analysis. The raw spectrum of the pellet is ratioed with the raw spectrum of an undoped KBr pellet to give a transmission spectrum. For far-IR measurements, a support matrix of high density polyethylene is used instead of an alkali halide and is heated under pressure to form a low scattering pellet.

2.2 Attenuated Total Reflectance [Harrick]

In this technique, a transparent, high refractive index material (KRS-5, Ge, ZnSe) is used as an internal reflection element. Radiation incident on the reflection element undergoes total internal reflection. When a sample is placed in contact with the reflection element, the radiation penetrates a finite depth into the sample which absorbs some of the radiation. The penetration depth, d_p depends on the refractive indices of the sample, n_2, and the reflection element, n_1, the extinction coefficient of the sample, k_1, the angle of incidence, ϕ, and the wavelength, λ and is given by

$$d_p=(\lambda/2\pi)\left[\frac{\sqrt{A^2+B^2}+C}{2}\right]^{-1/2}$$

where

$$A=n_1^2\sin^2\phi-n_2^2+k_1^2$$

$$B=2n_2k_1$$

and

$$C=n_1^2\sin^2\phi-n_2^2+k_1^2$$

Inspection of the equation for penetration depth reveals that the concentration profile of an analyte dispersed in a subtrate may be studied by varying the angle of incidence. This type of measurement should be useful for determining diffusion rates of an explosive concealed in packing materials such as saran. Some preliminary results of this type of measurement are presented in Section 3.

Attenuated total reflectance is also very well suited for pliable materials like DETA-sheet, semtex and C4 which do not mix well with KBr powder to form a pellet. All that is required is to bring the sample in contact with the reflection element to within the penetration depth of the light and the spectrum may be measured. Also, reflection elements may be coated with thin films (10-100 Å) and adsorption of explosives on these films may be investigated.

2.3 Diffuse Reflectance [a. Fuller, b. Burger]

When radiation strikes the surface of a solid, two types of reflection may occurr. Front surface or specular reflection, where the angle of incidence equals the angle of reflection, is most common and diffuse reflectance where a solid angle of light is reflected from the surface. Diffuse reflectance ocurs when the reflection is from a matte surface or a powder. In diffuse reflectance, radiation passes into the bulk of the sample and undergoes reflection, refraction, scattering and absorption before re-emerging from the surface. Kubelka and Munk developed a theory for diffuse reflectance in which they relate a function R_∞ to an absorption coefficient, k, and a scattering coefficient, s, in the following way

$$f(R_\infty)=\frac{(1-R_\infty)^2}{2R_\infty}=\frac{k}{s}$$

where R_∞ is the ratio of the diffuse reflectance from a sample to that of a non-absorbing reference powder which is infinitely deep compared to the penetration depth of the radiation.

The absorptivity, a, and concentration, c, are related to the absorption coefficient by

$$k=2.303ac$$

Then,

$$f(R_\infty)=\frac{2.303ac}{s}=k'c$$

This shows that the concentration varies linearly with the diffuse reflectance and can be used in quantitative applications.

We have used metal oxides as substrates in diffuse reflectance studies to monitor adsorption and desorption kinetics of EGDN on their surfaces. This allowed for a direct *in situ* measurement of the interaction of the explosive with the surface. Materials other than metal oxides could be used as substrates for adsorption/desorption studies and any materials which are potential candidates for preconcentrators could be studied using this technique.

2.4 Reflection-Absorption [Hayden]

Reflection-absorption infrared spectroscopy, (RAIRS), which is used for investigating molecules adsorbed on a metallic surface, is based on the surface selection rule which states that only molecular vibrations with a finite component of their dynamic dipole perpendicular to the surface on which they are adsorbed are observable. This arises from the fact that at grazing (~85°) incidence only the p-component of the incident radiation can interact with the adsorbed molecule. A variety of metal substrates (Cr, Cu, Au, Ag, Fe, Ti, Ta, Ni, W, etc) may be used in these measurements, as well as alloys or other metal compositions which are used as preconcentrator elements. Temperature controlled measurements are also possible and could be used to investigate adsorption and desorption phenomena of explosives on metal surfaces as well as surface phase transitions.

3. RESULTS AND DISCUSSION

3.1 Absorption

Figure 1 shows the absorption spectra of several explosives. The most two intense absorptions near 1250 and 1650 cm^{-1} may be assigned to the symmetric and antisymmetric NO_2 stretching vibrations. Their frequencies are listed in Table 1. Inspection of the table shows that the frequencies can be grouped into two classes, those belonging to nitrate-esters like EGDN, PETN and those belonging to nitro groups. Since absorption spectra are generally free of artifacts, they serve as a data base for interpreting more complex IR measurements which are important for explosive vapor investigations.

3.2 Attenuated Total Reflection

In this section, the application of the attenuated total reflectance technique to monitor the diffusion of DETA-sheet and Semtex in commercially obtained saran (12 μm thick) is discussed.

All our measurements were made with a Harrick ATR accessory equipped with a germanium reflection element adjusted to an angle of incidence of 45°. Reference spectra of a clean germanium prism were recorded by coadding 200 interferograms in a Bomem MB100 IR spectrometer. Sample spectra consisted of two types: saran and saran backed by a sheet of explosive. The sample spectra were ratioed with the reference spectra to give absorbance. Difference spectra were obtained by subtracting the spectra of the saran from the saran plus explosive. Detection of absorption features due to explosives would confirm that the explosive had diffused through the saran film. Such absorptions were observed for Semtex and are shown in Figure 2. This spectrum was measured 30 days after Semtex was placed in contact with saran. Also shown in the figure are the spectra of saran and the difference spectra. Four bands appear in this spectrum which are attributed to diffused semtex and are indicated by the vertical lines. Several other bands are observed which are due to saran which were not fully compensated in the spectral subtraction.

Figure 3 shows the spectra PETN, DETA-sheet, saran+DETA-sheet and saran. In this experiment, DETA-sheet was placed in contact with saran for 15 days and the spectrum was recorded. Absorptions appear in the trace for saran+DETA-sheet near 1150 and 1250 cm^{-1}. These absorptions do not belong to PETN, but correspond to the elastomer material supporting PETN in DETA sheet. These results indicate that diffusion of the elastomer in DETA-sheet occurs before that of PETN. It is therefore

likely that efforts to detect samples of DETA sheet concealed in saran or another polymeric material will result in strong interferences from the elastomer.

3.3 Diffuse reflectance

Diffuse reflectance was used to follow the adsorption and desorption of ethyleneglycol dinitrate (EGDN) adsorbed on zinc oxide powder as a function of dosing time. Inhomogeneous broadening of the NO_2 antisymmetric stretching band was found to be dose dependent. Through non-linear curve-fitting techniques [Morgan] the sum of three component bands were found to reproduce the inhomogeneously broadened envelope and are attributed to three types of adsorbed EGDN. The adsorbed EGDN species were characterized in terms of their absorption kinetics.

The diffuse reflectance studies were performed using a Harrick high vacuum accessory fitted into a Bomem DA3.02 spectrometer. This accessory was equipped with ZnSe windows and a thermocouple positioned at the base of the sampling pedestal. Gas inlets and outlets were connected to the body of the cell for dosing the substrate with EGDN vapor. Single beam spectra of the clean ZnO were recorded and used as a reference for subsequent measurements. The ZnO substrate was dosed with EGDN for periods up to 22 minutes. Single beam spectra of dosed ZnO were recorded as a function of dosing time and ratioed with the spectra of the clean ZnO to give transmittance spectra. The transmittance spectra were transformed to diffuse reflectance spectra through the Kubelka-Munk equation.

Representative spectra of EGDN adsorbed on ZnO for different dosing times are shown in Figure 4 in the region of the antisymmetric NO_2 stretching vibration. For low doses (3 and 4 minutes), the band contour is symmetric, indicating the molecule is adsorbed on one site. At higher doses, new features appear on the high and low frequency sides indicating the presence of two other adsorption sites occupied by EGDN. These features have been resolved using non-linear curve-fitting techniques. Typical curve fits for dosing times of 3 and 13 minutes are shown in Figure 5. Similar results were obtained for the other dosing times and plots of the band area vs. the dosing time are shown in Figure 6. From the plots shown in the figure, it is clear that there are three different rates of adsorption of EGDN, corresponding to three sites where EGDN is adsorbed on the ZnO surface. These rates correspond to different enthalpies of adsorption and should therefore reflect the performance of this material as a potential preconcentrator. Further information was obtained from the desorption studies which were carried out at 40° C and are shown in Figure 7. These spectra show not only a decrease in the intensities of the absorption due to antisymmetric NO_2 stretching band, but the appearance of new bands near 1575 and 1610 cm^{-1}. The appearance of the new bands must be due to decomposition of EGDN on the ZnO surface. The desorption curves are shown in Figure 8. It is clear from these plots that there are three rates of desorption, the most populated site having the fastest.

The kinetic information obtained from these studies and future investigations on preconcentrator elements should provide a basis for characterizing preconcentrators and add to the fundamental knowledge required for understanding the physicochemical interactions of an explosive with a preconcentrator or other surfaces of interest.

4. CONCLUSIONS

Fourier spectroscopy is a valuable analytical tool for characterizing explosives. Moreover, the surface techniques of diffuse reflectance, attenuated total reflectance, and reflection-absorption provide means of studying explosive-preconcentrator interactions. An understanding of explosive-surface interactions will provide essential criteria for the development of useful preconcentrators.

ACKNOWLEDGEMENTS

This work was performed under the auspices of the Federal Aviation Administration, Contract No. DTFA01-87-00042.

REFERENCES

Burger, A., Henderson, D. O., Morgan, S. H., Silberman, E., J. Crystal Growth, 109, 304 (1991).

Fuller, M. P. and Griffiths, P. R., in *Advances in Infrared and Raman Spectroscopy*, Vol. 9, Chap 2. (1982).4.2

Griffiths, P. R. and de Haseth, J. A., *Fourier Transform Infrared Spectrometry*, John Wiley & Sons (1986).

Harrick, N. J., *Internal Refelcction Spectroscopy*, Wiley-Interscience (1967).

Hayden, B. E. in Vibrational Spectroscopy of Molecules on Surfaces, Vol. 1, Chap 7, (1987).

Kubelka, P. and F. Munk, Z. Tech. Phys. 12, 593 (1931).

Morgan, S. H., Henderson, D. O., and Magruder, R. H., J. Non-Cryst. Solids, 128, 146 (1991)

Table 1. Symmetric and Antisymmetric NO_2 Stretching Frequencies for Selected Explosives.

EXPLOSIVE	ANTISYMMETRIC NO_2 STRETCH (cm^{-1})	SYMMETRIC NO_2 STRETCH (cm^{-1})
EGDN (v)	1678	1281
EGDN (l)	1668	1279
p-NITROTOLUENE	1511	1351
m-DINITROBENZENE	1544	1352
TNT	1537	1353
PETN	1653	1285
RDX	1596	1267
SEMTEX	1656, 1644, 1594, 1573	1271

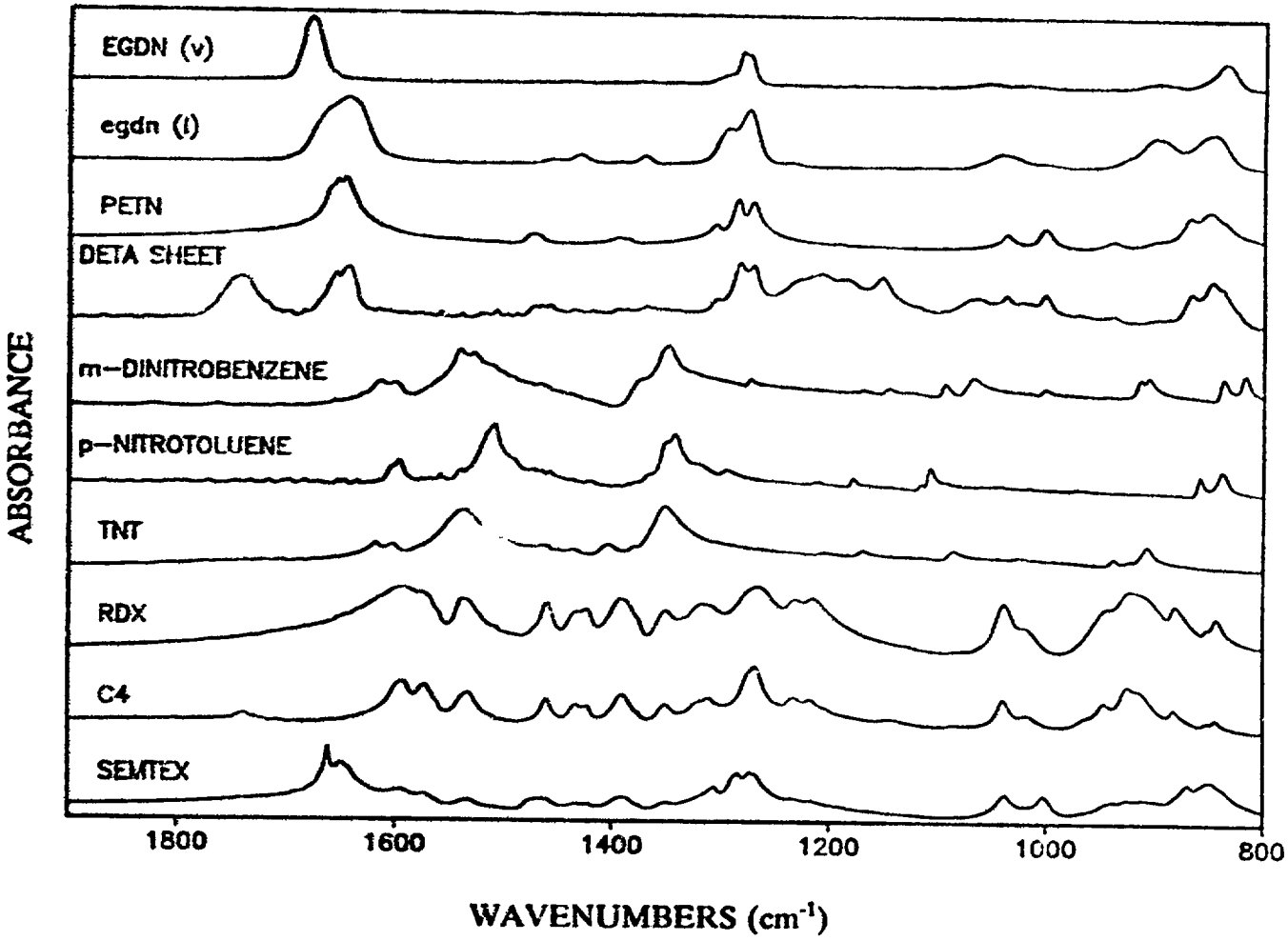


Figure 1. Absorption spectra of various explosives.

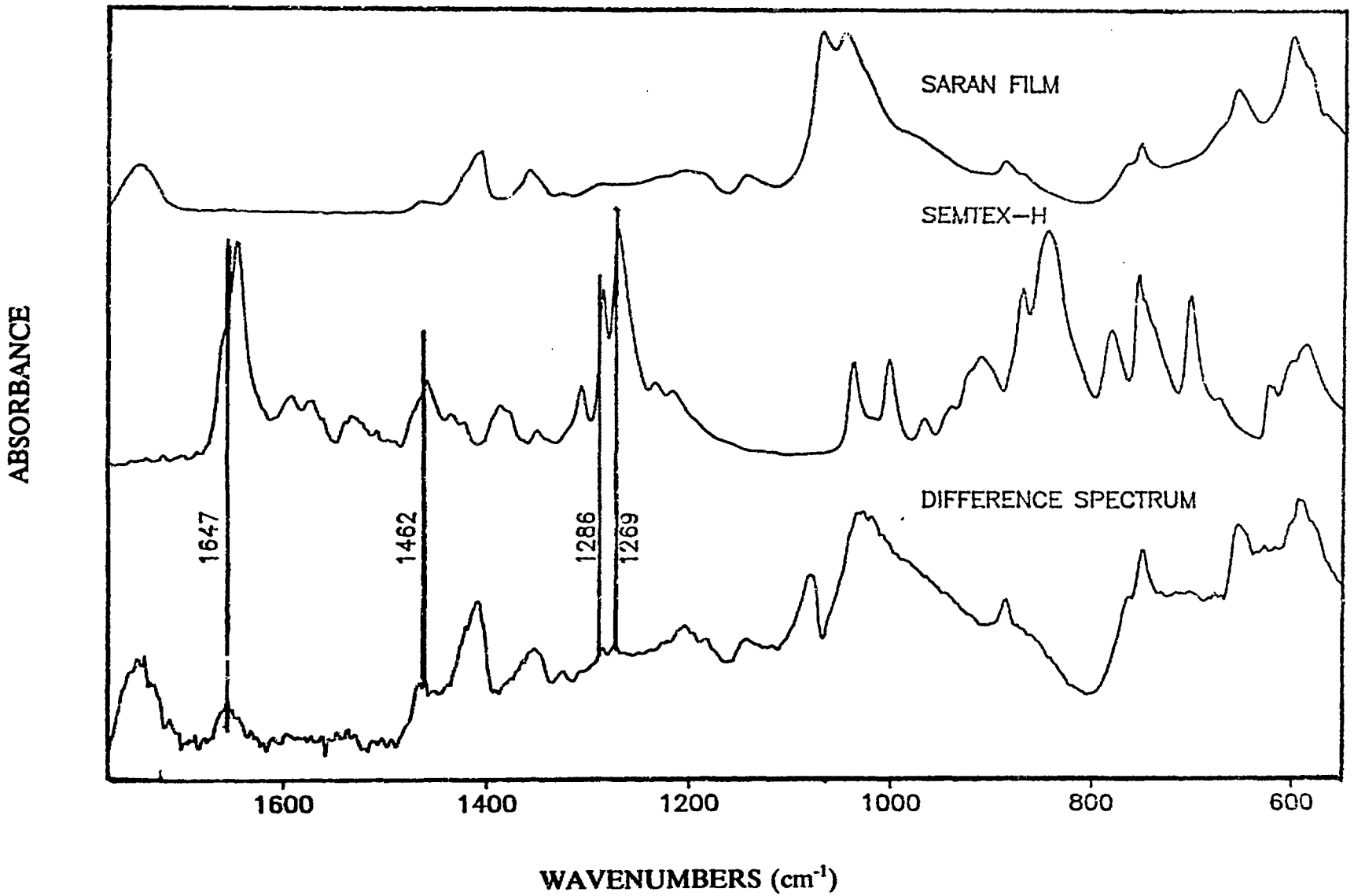


Figure 2. Attenuated total reflectance spectra saran film, semtex-H, and their difference spectrum. The vertical lines indicate absorptions of semtex-H diffused in saran.

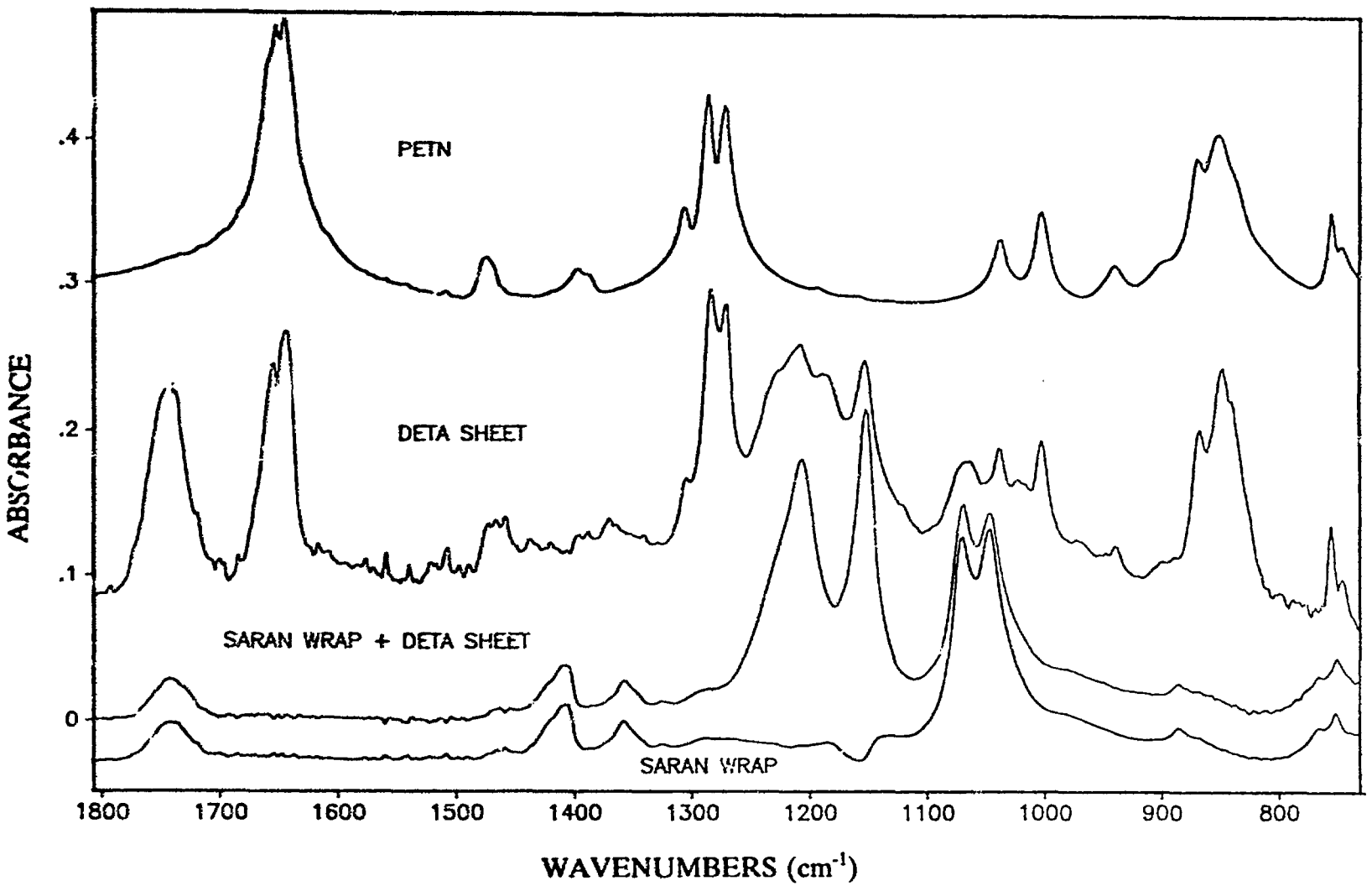


Figure 3. Attenuated total reflectance of PETN, Deta sheet, saran, and saran backed by a layer of Deta sheet.

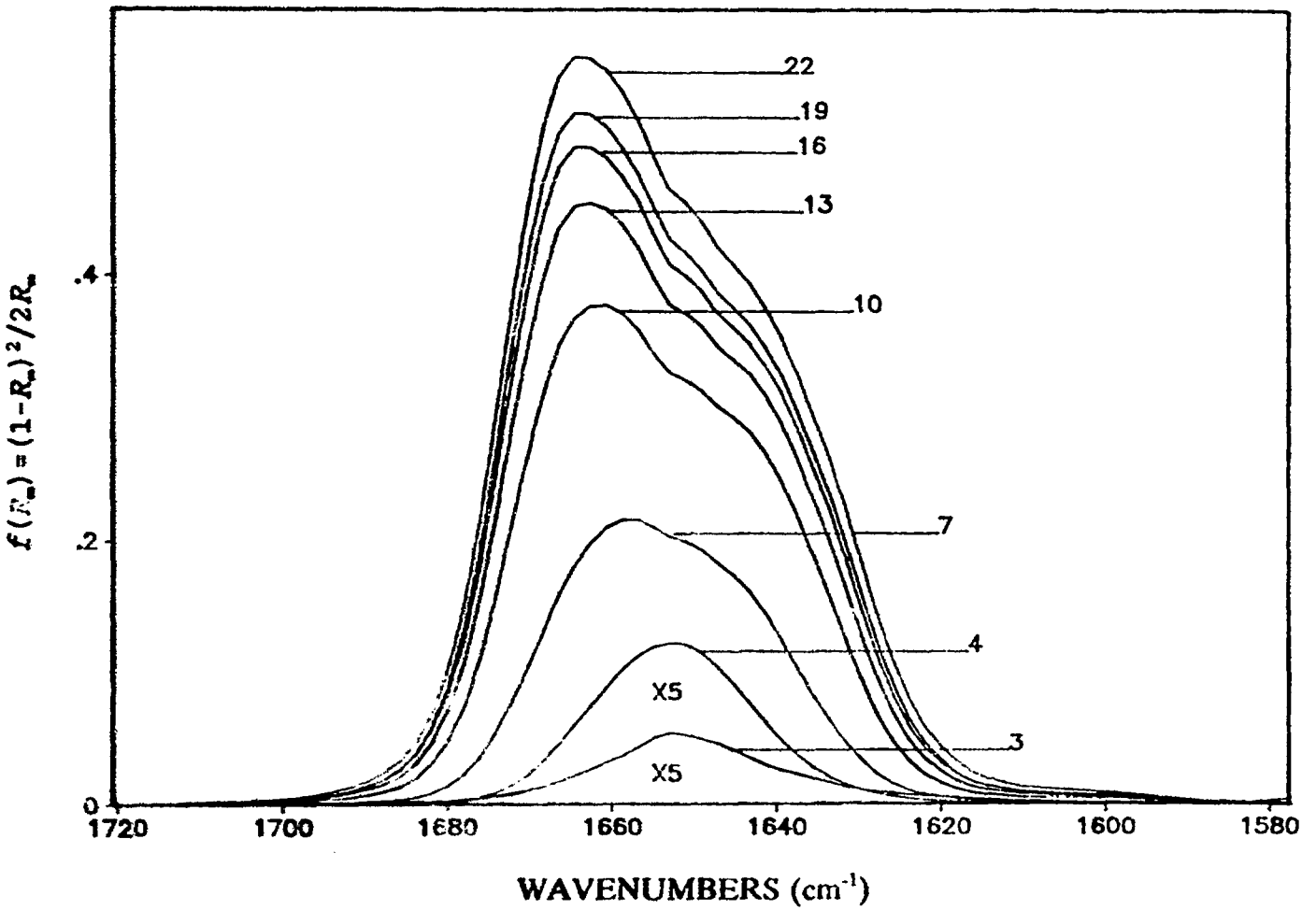


Figure 4. Diffuse reflectance spectra of EGDN adsorbed on zinc oxide as a function of dosing time. The ordinate scale for the 3 and 4 minute doses is expanded by a factor of 5 for clarity.

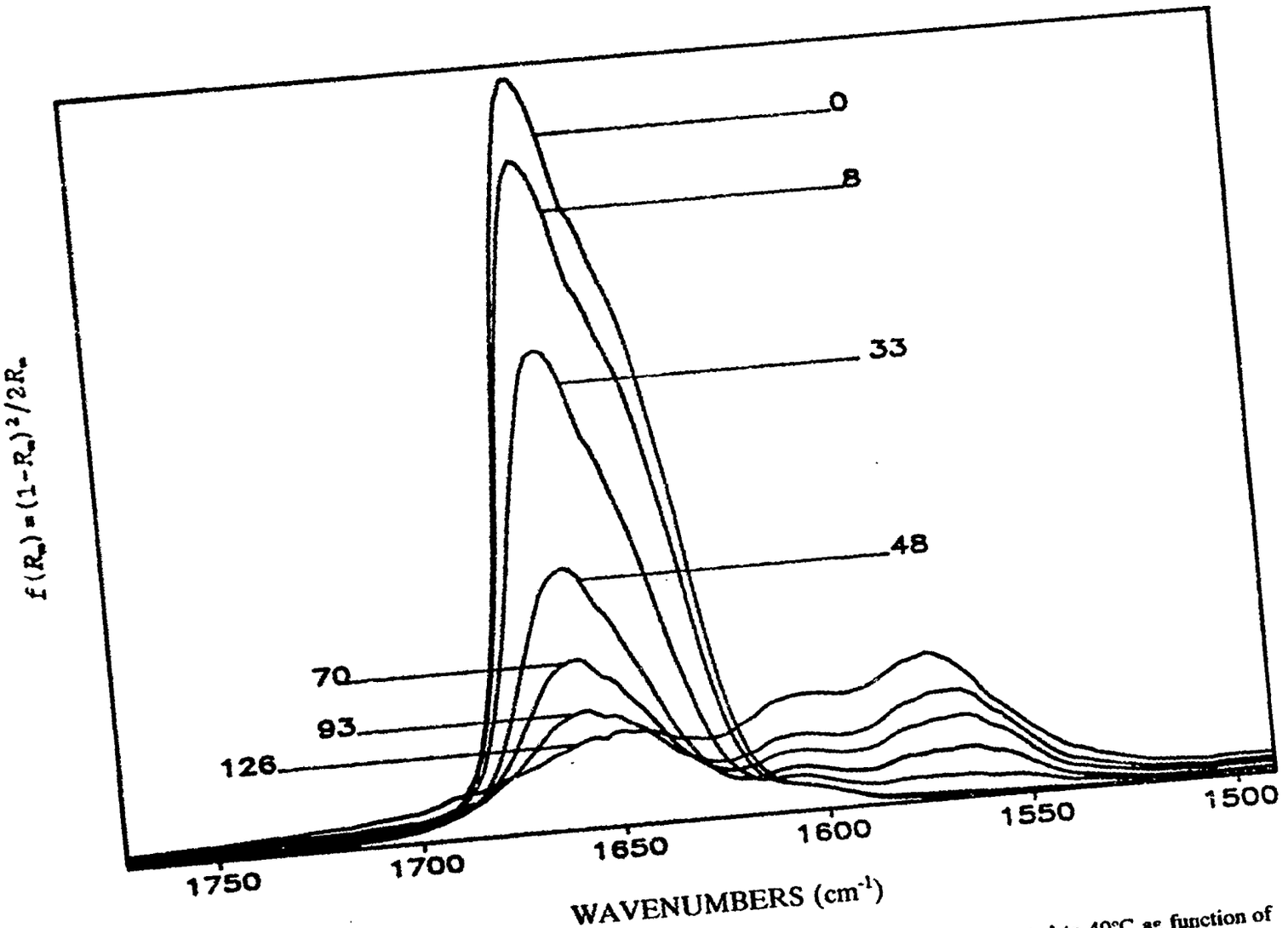


Figure 5. Diffuse reflectance spectra of EGDN desorbing from a zinc oxide surface heated to 40°C as function of time.

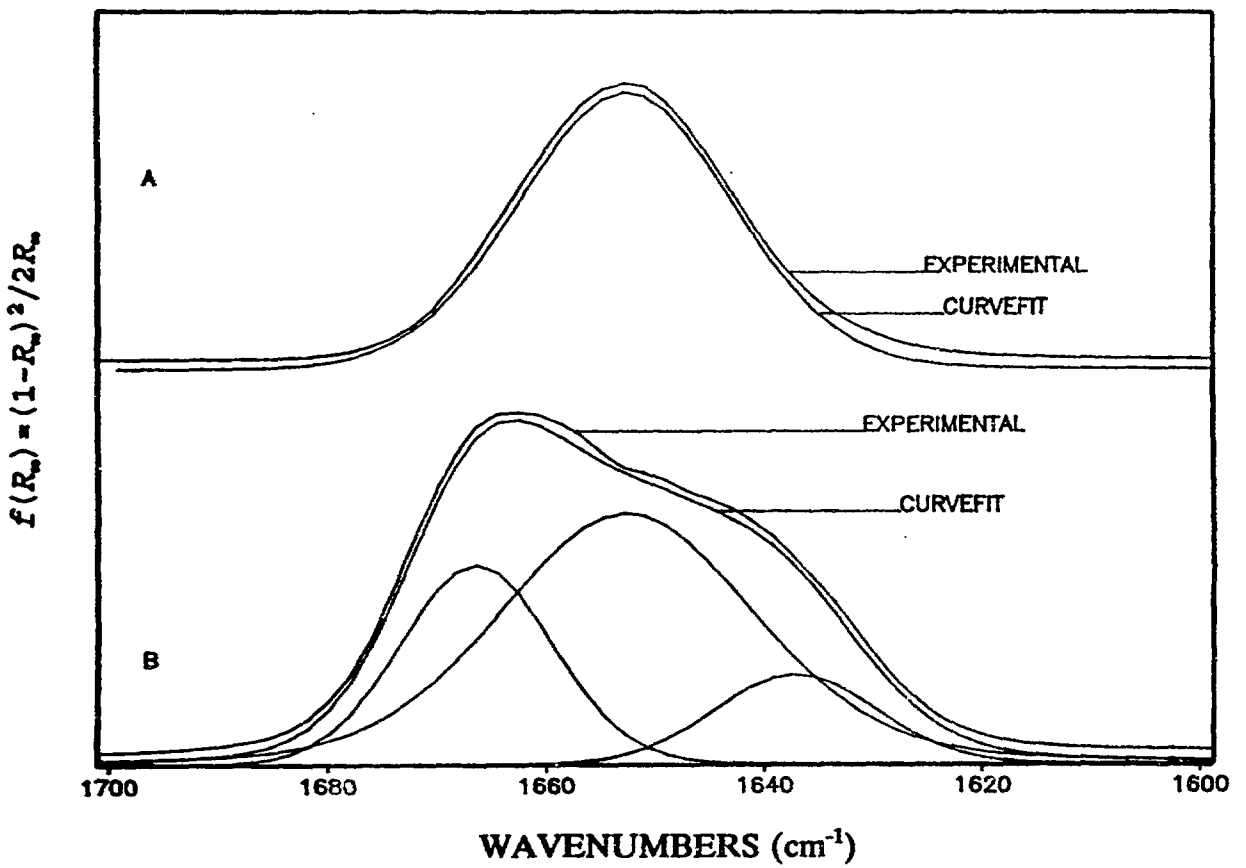


Figure 6. Curve fit of the antisymmetric NO_2 stretching absorbtion for A) 4 minute dose, and B) a 13 minute dose. The experimental spectrum is offset from the curvefit for clarity.

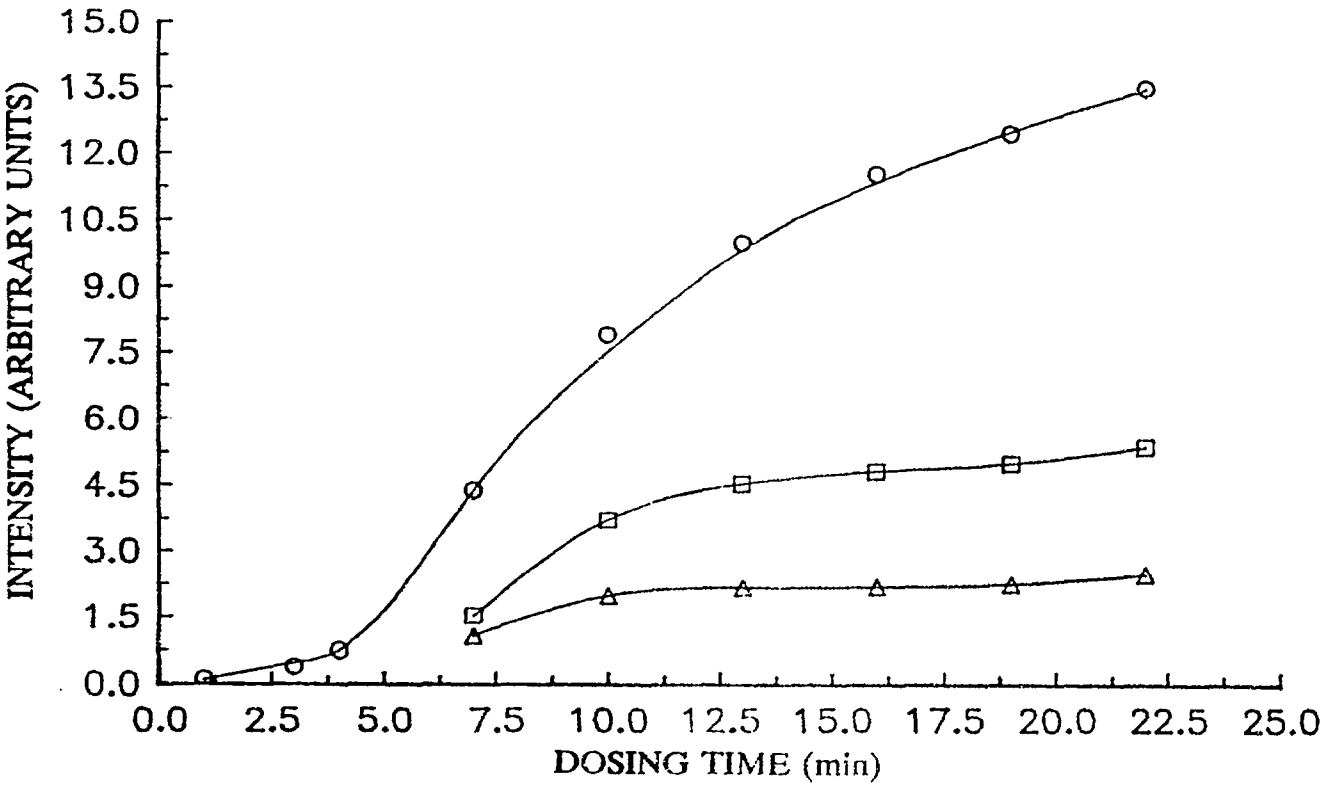


Figure 7. Plots of intensity for the three component bands obtained from the curevfit for adsorption vs. dosing time, where ○, □, and △ are the data for the three component bands with center frequencies at 1651 cm^{-1}, 1666 cm^{-1}, and 1636 cm^{-1}, respectively.

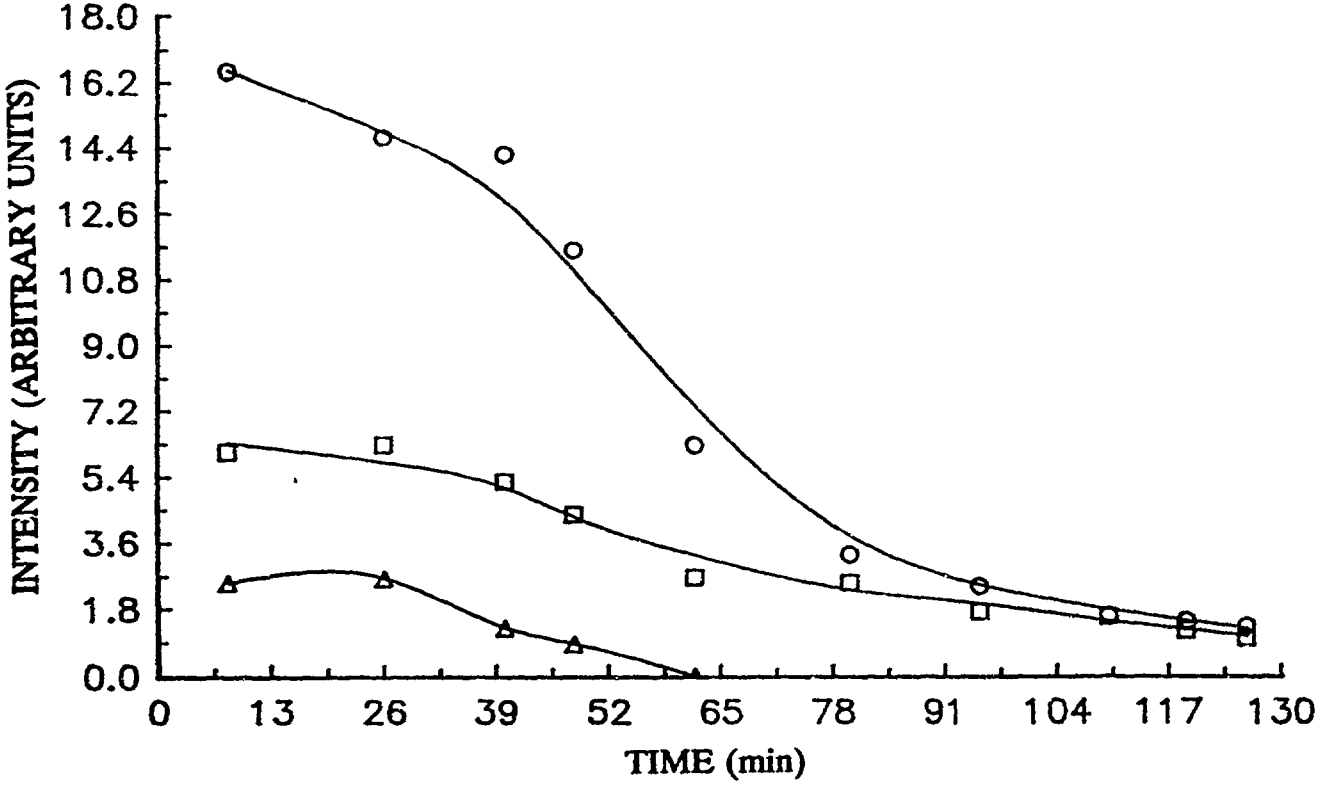


Figure 8. Plots of intensity for the three component bands obtained from the curvefit for desorption EGDN on zinc oxide vs. time where O, □, and △ are the data for the three component bands with center frequencies at 1651 cm^{-1}, 1666 cm^{-1}, and 1636 cm^{-1}, respectively.

MASS AND ION MOBILITY SPECTROSCOPY

ATMOSPHERIC PRESSURE IONIZATION TIME-OF-FLIGHT MASS SPECTROMETER FOR REAL-TIME EXPLOSIVES VAPOR DETECTION

Harold G. Lee, Edgar D. Lee, and Milton L. Lee
Department of Chemistry
Brigham Young University
Provo, Utah

1. INTRODUCTION

There are two types of explosives chemical detectors: bulk (condensed phase) and vapor (gas phase) detectors. A bulk explosive detector identifies explosives by bombarding the suspicious material with radiation such as X-rays, gamma rays, neutrons, or beta particles (electrons), and analyzes the reflection, diffraction, and/or absorption of the radiation by the explosive material. Vapor detectors, on the other hand, identify an explosive by chemically analyzing its vapor molecules.

For the detection of explosive vapors, several proposed technologies involving electron capture (ECD), nitrogen-phosphorus (NPD), chemi-luminescence (CD), ion mobility (IMD), and mass spectrometry (MS) have been evaluated (Nyden, 1990). In the ECD, a radioactive foil generates beta particles or electrons. The electrons are captured by the explosive, which must have a high affinity for electrons. The capture of electrons results in a measurable loss of current. In the NPD, a thermal source is used to remove electrons from nitrogen or phosphorus atoms in the explosive. The current produced is proportional to the number of nitrogen and phosphorus atoms present. In the CD, nitro groups are converted to nitric oxide. The nitric oxide reacts with ozone to form nitrogen dioxide. Energy liberated in this reaction is given off as light, which is measured by a photomultiplier.

The atmospheric pressure ionization (API) source is used in both IMD and MS. The API source uses either a corona discharge or a ^{63}Ni β-source, which emits electrons. An air sample containing the vapor of the substance to be analyzed is drawn into the ion source. Ionization is initiated by the production of ions of the most abundant species, in this case, nitrogen gas in the air. These ions become involved in a series of ion reactions. Eventually, so-called reactive ions are formed. The reactive ions, as they come in contact with the molecules in the sample, impart a charge to them, creating ions. In an IMD, the explosive vapor ions are separated by their mobility in an electric field. A mass spectrometer separates and distinguishes the explosive vapor ions by their mass-to-charge ratios.

The ECD and the NPD do not exhibit a high degree of selectivity. As a result, they are usually coupled with gas chromatographs, which separate the components of the sample. A chromatograph, however, can take from 30 seconds to several minutes to process a sample. An IMD is more selective (but less sensitive) than a stand alone ECD or NPD. Therefore, IMD vapor detectors are often used without chromatography. A mass spectrometer is, on the other hand, inherently both very sensitive and very selective.

Analyses by gas chromatography have revealed the presence of many different compounds in samples of common explosive materials. These include nitro-organic compounds, nitrate salts, and flammable liquids (which are frequently used as explosive fillers). The commercial ECD, CD, NPD, and IMD vapor detectors can only detect a limited range of nitro-organic compounds. They are not sensitive or versatile enough to detect the very low vapor pressure nitro-organic explosives and explosive components that do not contain nitro-organic groups. For example, one commonly used ECD is programmed to detect only three explosive compounds (Nyden, 1990). In comparison, a mass spectrometer can be used to detect a wide range of organic compounds.

A detector must be used correctly to be effective. All else being equal, easy-to-use detectors clearly have an advantage over complicated instruments.

Looking for explosives can be a stressful activity, and operators should not have to be burdened with complicated and/or temperamental instruments.

In this study we report a high-sensitivity, easy-to-use chemical analyzer for the detection of trace volatile explosive chemicals in ambient air, based on a time-of-flight mass spectrometer (TOFMS) with an API source. Because of its unique design, it is much more sensitive than other mass spectrometers; subfemtogram ($< 10^{-15}$g) detection limits are possible. As with other mass spectrometers, the TOFMS separates ions according to their mass-to-charge ratio and thus gives the best selectivity among all other non-MS based detectors. The ultrahigh sensitivity obtained in TOFMS precludes the use of a preconcentration stage. The mass resolution is approximately 500. Simultaneous analyses for up to 16 compounds can be accomplished within 200 microseconds.

2. EXPERIMENTAL

2.1 Description of the Instrument

In operation, air containing the substance to be analyzed is drawn into the atmospheric pressure ion source, where a corona discharge ionizes the molecules at ambient pressure. The ions are adiabatically expanded into a vacuum chamber through an orifice, forming a supersonic beam perpendicular to the direction of acceleration. The internal and kinetic energies of the ions in the beam are equalized through numerous two-body collisions. Ions are pulsed from the supersonic ion beam into a perpendicular field-free drift tube. Since all ions receive the same energy from the pulse, the specific ions in each pulse travel the length of the drift tube at velocities dependent on their masses. To a first approximation, the arrival time of an ion at the detector is proportional to the square root of its molecular weight. The instrument is equipped with a data acquisition system that monitors up to 16 masses simultaneously.

A schematic diagram of the API TOFMS system is shown in Figure 1. The vacuum chamber is divided into two compartments by a skimmer. The chamber is differentially pumped by a rotary pump and a He-cooled cryogenic pump. The ion source is a corona discharge needle, which is placed in front of an orifice called the nozzle. The nozzle separates the vacuum from the ion source which is at one atmosphere. The nozzle and skimmer lead to pressures of 0.5 torr and 2×10^{-5} torr in the first and second compartments, respectively. The nozzle is insulated from the source housing so a voltage can be applied for ion focusing. The flight tube is housed in the second vacuum compartment perpendicular to the nozzle/skimmer axis. A repeller plate is positioned below the nozzle/skimmer axis. A grounded focus grid at the bottom of a cylindrical enclosure is suspended above the nozzle/skimmer axis. Inside this enclosure, a metal tube with a second grid is positioned. This second grid is located above the focus grid. The metal tube (drift tube) is 50 cm long. A final grid is placed at the end of the drift tube. The repeller plate, the focus grid, and the second grid are electrically insulated from one another. The area bound by the second grid, the drift tube, and the final grid form the field-free drift region. The electric pulse applied to the repeller plate is provided by a 300-V fast pulse generator. The rise time is 3 ns for a 300-V pulse. The pulse width is 2 μs. The discharge current can be regulated between 0 and 25 μA. A dual microchannel plate detector is used to detect ions as they exit the flight tube.

The ions produced in the ion source expand supersonically into the first vacuum compartment through the nozzle. A small voltage (10-150 V) is applied to the nozzle to focus the ions toward and through the skimmer. The supersonic ion beam expands into the acceleration region between the repeller plate and the focus grid. The repeller plate is at ground potential before the pulse. During the pulse, ions are repelled upward past the focus grid. They then experience a pull from the second grid which is used to separate the field-free region from the ground potential on the focus grid. The second grid and the drift region are set at approximately -2000 V. After passing the second grid, the ions enter the field-free drift region. The use of a double acceleration arrangement before the field-free region minimizes peak broadening caused by the finite width of the ion jet. The ions exit the field-free region through the final grid at the end of the flight tube and are accelerated toward the microchannel plate detector.

2.2 Measurement of Sensitivity and Detection

Samples were introduced into the ion source of the mass spectrometer by two different methods. The first approach was to place one gram of TNT into a balloon and fill the balloon with dry (99.999%) nitrogen gas. The TNT was allowed to equilibrate

for 24 h at 25°C. After the 24-h period it was assumed that the gas within the balloon was saturated with TNT vapor. One of two different internal diameter stainless steel capillaries was inserted into the balloon. The diameters of the capillaries controlled the flows to 100 mL min^{-1} and 400 mL min^{-1}. The exit end of the capillary was positioned one cm from the discharge electrode in the API source. This arrangement is illustrated in Figure 2. Spectra were recorded using a LeCroy 9410 digital storage oscilloscope. All spectra were recorded as single, nonaveraged scans, plotted using an HP 7470 plotter. The spectra in Figure 3 show typical results obtained at two flow rates. These spectra correspond to 136 and 34 fg of TNT per scan, respectively.

The second method of sample introduction used a thermal and pnuematic nebulizer as shown in Figure 4. The nebulizer was constructed from a stainless steel capillary which was heated to 200°C at the exit end by a 50-W heater. The other end was connected to a tee. Dry nitrogen gas was introduced into the tee perpendicular to the stainless steel capillary. A 70-μm i.d. fused-silica capillary was inserted into the opposite side of the tee and through the entire length of the stainless steel capillary. The exit end of the fused-silica capillary extended 0.5 mm past the end of the stainless steel capillary. The front end of the capillary was connected to a 1-μL loop injector. A syringe pump was used to deliver acetone to the injector at a flow rate of 2 μL min^{-1}. Standard solutions of TNT in acetone were injected into the acetone stream and single-shot spectra were collected using the digital storage oscilloscope.

3. RESULTS AND DISCUSSION

3.1 Atmospheric Pressure Ionization

Atmospheric pressure ionization (essentially atmospheric pressure chemical ionization, CI) is operated with the source chamber at atmospheric pressure. The API source uses either a ^{63}Ni β-source that emits electrons in the energy range of several KeV, or a corona discharge. An API source produces ions through ion-molecule reactions (Carroll et al., 1981; Good et al., 1970; Keharle and Hogg, 1965; Shahin, 1966); Siegel and Fite, 1976). As in CI, ionization is initiated by the production of ions of the most abundant species, in this case, nitrogen gas. Eventually, as shown below, water cluster ions are formed:

$$N_2 + e^- \rightarrow N_2^+ + 2e^-$$
$$N_2 + 2N_2 \rightarrow N_4^+ + N_2$$
$$N_4^+ + H_2O \rightarrow H_2O^+ + 2N_2$$
$$H_2O^+ + H_2O \rightarrow H_3O^+ + OH$$
$$H_3O^+ + H_2O + N_2 \rightarrow H_3O(H_2O)^+ + N_2$$
$$H_3O(H_2O)_{n-1}^+ + H_2O + N_2 \rightarrow H_3O(H_2O)_n^+ + N_2$$

In the positive ion mode, these water cluster ions play an important role in the production of positive ions, and the major mechanism is proton transfer:

$$H_3O(H_2O)_n^+ + R \rightarrow RH(H_2O)_m^+ + (n - m)H_2O$$

This occurs if the proton affinity of the species, R, is greater than that of $H_3O^+(H_2O)_n$. More generally, any sample species in the carrier gas that is a stronger gas phase base than $H_3O^+(H_2O)_n$ will be ionized to form RH^+ and $RH^+(H_2O)_m$. The final ions leaving the ion source will have reached equilibrium and will seldom give fragment ions. The efficiency of API can reach 100% for trace species (Carroll *et al.*, 1981).

Negative ionization proceeds through electron attachment:

$$RX + e^- \rightarrow R + X^-$$

The dominant reactive ions for negative ionization in ambient air are the "superoxide" O^-_2 and its monohydrated adduct, $O^-_2(H_2O)$. The electron affinity of O^-_2 is only 0.44 eV, and thus it can undergo charge transfer with compounds of higher electron affinity. However, proton transfer reactions occur more often than charge transfer reactions in the negative ion mode:

$$RH + M^- \rightarrow MH + R^-$$

The O^-_2 ion has a proton affinity of 350 kcal mol^{-1} (15.2 eV) and will accept protons from acids whose corresponding anions have lower proton affinities.

Since an API source operates at atmospheric pressure, it is most suitable for direct air monitoring. Air is drawn into the ion source at a very high flow rate (>2 mL min^{-1}) to prevent molecules from adsorbing onto the chamber and to reduce any memory effects.

3.2 Time-of-Flight Mass Spectrometry

Time-of-flight mass spectrometry has been described

previously (Price, 1984; Sin et al., 1991; Wiley, 1955). In a TOFMS, charged masses separate according to the times needed for them to reach the electron multiplier. Assuming that singly charged ions are formed, and that they attain equal kinetic energies after they leave the acceleration region, the flight time, T, of each is proportional to the square root of its mass, M. The flight time can be approximately calculated by the following equation

$$T = L\left(\frac{M}{2eV}\right)^{1/2}$$

where L is the length of the field-free drift region, and V is the total potential drop across the acceleration region.

An important parameter for this instrument is the maximum detectable m/z value. Since there is a horizontal velocity component for the ions going up the drift tube, larger ions may hit the wall before they are detected. Table 1 shows the flight times of different m/z ratios and their horizontal displacements. These values were calculated with an acceleration potential gain of 2100 V. Also, in the acceleration region, the width of the electric repelling pulse determines the limit for m/z ratio of the ion that can pass the focus grid. Table 2 shows the ion residence times within the region between the repeller plate and the focus grid, and the corresponding horizontal displacements for ions of different sizes. An electric pulse that lasts longer than the residence time is needed to detect the corresponding ions. The displacement within the acceleration region is less than 10% of the total displacement. The total displacement for a mass of 5,000 amu is about 2.5 cm. Thus, the problem of horizontal displacement is easily solved by using a flight tube of larger diameter (e.g., 6 cm). On the other hand, longer pulse width or higher pulse voltage is needed to move ions of higher masses across the gap between the repeller plate and focus grid.

3.3 Conditions Affecting Sensitivity Measurements

All substances emit vapor molecules at any temperature above absolute zero. At some point in time, equilibrium is reached in which the number of molecules being emitted from the substance is equal to the number being re-absorbed by the substance. Given enough time, vapor molecules eventually equilibrate throughout the enclosure to a vapor pressure that is characteristic of the substance and dependent on the temperature. As these vapor molecules move around, they may collide with the probe of an explosives detector. An explosive can only be detected if there are enough collisions with the detector to trigger a response. The number of collisions is proportional to the number of molecules, which is, in turn, proportional to the vapor pressure. Unfortunately, most solid explosives have extremely low vapor pressures (St. John, 1975). Furthermore, the actual concentration of vapor in the atmosphere of an enclosure depends strongly on factors such as air flow and on the hindering effect a container holding the explosive may have on the vapor molecules leaving the container. These concentrations are usually only a very small fraction of the actual vapor pressure. It is likely in a real situation that the vapor will be concentrated near its source and localized in other areas that are determined by air circulation.

The TOFMS is a mass-sensitive detector as opposed to a concentration-sensitive detector. This means that the response of the instrument is a function of the mass of the analyte that flows through the instrument per unit time. For a mass-sensitive detector, the detection limit is the minimum mass flow rate of analyte that elicits a measurable response from the detector. Different detection limits can be obtained by increasing or decreasing the velocity of air pumped through the detector. If the mass flow through the instrument is increased, the detection limit is improved. For a concentration-sensitive vapor detector, the detection limit is the minimum concentration of analyte in the gas flow into the detector that elicits a measurable response from the detector. For comparisons of different vapor detectors, a better measurement of detection is the minimum detectable quantity. This is the minimum amount of analyte that elicits a measurable response from the detector. This measurement characterizes the instrument itself. It places all vapor detectors on the same basis, whether they are mass-sensitive or concentration-sensitive, or whether the sample is preconcentrated or taken directly from the ambient air.

3.4 Factors Affecting Detector Sensitivity

Due to its high sensitivity for trace components, API has become an important ionization method in mass spectrometry. The ionization efficiency of API is two to three orders of magnitude greater than other forms of ionization. For trace species, the ionization efficiency can approach 100% (Carroll et al., 1981).

The use of a perpendicular supersonic ion beam in a TOFMS provides more sensitivity than an axial configuration (Sin, et al. 1991). In an on-axis arrangement, ion pulses can only be produced by deflecting the ion beam. Since the ion peak width depends on the "on" time during which ions are allowed to pass, very narrow pulses are needed to maintain a reasonable mass resolution. These narrow pulses result in a very low duty cycle of less than 0.2%. In a perpendicular configuration, however, the ion peak width is determined by the rise-time of the repelling pulse rather than the actual pulse "on" time. When the electric pulse reaches its maximum, no additional ions can be admitted into the acceleration region. The ions subsequently pulsed into the drift region are those already inside the acceleration region. Thus, the ion packet width is only determined by how fast the repelling plate is brought to its maximum potential. Therefore, the electric pulse can be as long as needed to maximize the number of ions entering the drift tube. If the ion beam velocity, the width of the grid, and the pulsing frequency are represented by v, d, and f, respectively, then the duty cycle is f x d/v.

The beam velocity is about 3 x 10^4 cm s^{-1}. If the maximum frequency (i.e., 6 kHz) is used, the duty cycle of the system is about 50%. It should be noted that this frequency can still be used for an ion of 5,000 amu, because the flight time is only 76 μs. Allowing for a 50% ion loss to the grids and walls during the flight time, the overall efficiency is 25%, which is much higher than those obtained from on-axis TOFMS configurations and quadrupole mass spectrometers (Sin et al., 1991).

The main reason for the high throughput of this instrument is that in a perpendicular arrangement, ions within the acceleration region are simultaneously pulsed into the drift tube. This is depicted in Figure 5, which compares the two different ways of creating ion pulses. In the axial orientation, ions enter the drift region sequentially, whereas in the perpendicular orientation, all ions along the repeller plate are introduced at the same time.

The open configuration of a TOFMS enhances sensitivity due to its high transmission efficiency (Glish et al., 1987). Unlike a quadrupole, whose ion transmission efficiency decreases for heavier ions (Watson, 1985), a TOFMS has an unlimited mass range (provided the heaviest ions arrive at the detector before the next pulse begins).

A calibration plot of TNT at three levels in triplicate was generated. The three data points represent 33 fg, 330 fg, and 3.3 pg of TNT for each spectrum aquired (Figure 6). The sensitivity for TNT was determined to be 3.5 x 10^{-3} mV fg^{-1}, and the minimum detectable quantity was 10 fg of TNT at a signal to noise ratio of 3.

3.5 Factors Affecting Detector Selectivity

The API source produces a supersonic ion beam, because the ions are formed at one atmosphere and adiabatically expanded into the vacuum chamber through an orifice. Since the diameter of the orifice is much greater than the mean free path of the gas molecules, numerous two-body collisions occur and energy transfer is facilitated. Both the translational and internal energies (kinetic energy) are transferred into a directed mass flow. Any molecules or ions seeded in this gas jet experience a similar effect. If the pressure downstream is low enough to prevent the formation of a shock wave, ions and molecules in this supersonic beam eventually travel at similar velocities. The energy and velocity distribution is narrowed, and the mass resolution is greatly improved.

Historically, TOFMS has been limited by its low resolution (about 300). The innovative feature of the TOFMS reported here is the use of a supersonic ion beam at right angles to the flight tube. As a result of supersonic expansion, the initial energy spread of the ions is minimized and the mass resolution is improved to more than 500, comparable to current quadrupole mass spectrometers. Since this technique does not use a reflectron or an electrostatic sector to focus the ion energy, sensitivity is not compromised. Ions are pulsed from the supersonic ion beam into a perpendicular flight tube. The mass resolution of a TOFMS is influenced by the temporal width of the ion packets produced by the pulse. The spatial differences and initial kinetic energy spreads of the ions being pulsed from the source contribute to the peak widths. Since all of the ions do not start moving toward the drift region from the same position at the start of each pulse, a spatial distribution results. A double field acceleration region is used to compensate for these spatial differences. Another advantage of having the flight tube perpendicular to the ion beam is that the energy spread eliminated in the direction perpendicular to the drift tube.

resolution. For example, the potential applied to the nozzle may add energy spread to the ion beam. Because the pressure in the first chamber is quite high (0.5 - 1.0 torr), the additional energy spread is less likely to be observed due to cooling through two-body collisions. This potential field is necessary to focus the ions into the skimmer. If the applied potential is less than 10 V, no ion peaks are observed. Other important factors include the homogeneity of the accelerating fields, the flatness of the grids, and the overall alignment of the flight tube.

3.6 Factors Affecting Speed of Analysis

In a TOFMS, ions are separated in space in the field-free drift region, allowing them to exit and hit the detector at different times. To a first approximation, the arrival time of an ion is proportional to the square root of its molecular weight. TOFMS is unique in that it can produce a complete mass spectrum in less than 200 microseconds.

An important characteristic of API is its "soft" ionization nature; usually, the majority of ions produced are molecular ions. This performance makes API very suitable for environmental monitoring since the target compounds can be easily identified by their molecular masses without going through tedious mass spectral matching. Other forms of ionization used in mass spectrometry are more energetic and produce a high percentage of fragment ions. Because of little fragmentation interference, API can be used for direct analysis of complex samples without pretreatment of the sample.

4. SUMMARY

A high-sensitivity, high-speed API TOFMS system has been developed for explosives vapor detection. The advantages of this system include:

4.1 Sensitivity

The high ionization efficiency of API and the high transmission efficiency and duty cycle make this mass spectrometer 100 to 1000 times more sensitive then any existing mass spectrometer system. The minimum detectable quantity for TNT was measured as 10 fg using this system. Minor modifications are expected to increase the sensitivity to 0.1 fg.

4.2 Speed of Analysis

A complete mass spectrum can be acquired in less than 200 microseconds.

4.3 Selectivity

This system has a resolving power of 500 at 450 amu. For example, it can distinguish a compound of mass 450 from a compound of mass 451. Unlike most mass spectrometers, there is no tradeoff between sensitivity and resolution since the resolution is defined by the supersonic expansion and not by the instrumentation.

4.4 Simplicity

The TOFMS is the simplest type of mass spectrometer and requires very little optimization compared to other mass spectrometers. Simplicity of design also means less downtime and less maintenance.

4.5 Range of Compounds Detected

This system can detect a broad range of compounds, including non-nitro-containing explosives and flammable liquid explosive fillers, as well as nitro-organic explosives. Illegal drugs can also be detected at the same time.

4.6 Robustness

The API/TOFMS instrument can be easily moved or transported. It can be mounted in a vehicle. There are few moving parts, and the only moving voltage is the pulsing voltage. There are very few restrictive environmental requirements.

REFERENCES

1. D.I. Carroll, I. Dzidic, E.C. Horning, and R.N. Stillwell, Appl. Spectro. Rev. 1981, 17, 337.

2. G.L. Glish, S.A. McLuckey, and H.S. McKown, Anal. Instrum., 16, 191, 1987.

3. A. Good, A. Durden, and P. Kebarle, J. Chem. Phys. 1970, 52, 212.

4. P. Kebarle and A.M. Hogg, J. Chem. Phys. 1965, 42, 668.

and G.J. Milnes, Int. J. Mass Spectrom. Ion Phys. 1984, 60, 61.

6. M.M. Shahin, J. Chem. Phys. 1966, 45, 2600.

7. M.W. Siegel and W.L. Fite, J. Phys. Chem. 1976, 80, 2871.

8. C.H. Sin, E.D. Lee, and M.L. Lee, Anal. Chem., in press.

9. G.A. St. John, J.H. McReynolds, W.G. Blucher, A.C. Scott, and M. Anbar, Forensic Sci. Internat. 6, 53, 1975.

10. J.T. Watson, Introduction to Mass Spectrometry (Raven Press, New York, NY, 1985), Chapter 4.

11. W.C. Wiley and I.H. McClaren, Rev. Sci. Instrum. 1955, 26, 1150.

Table 1. Calculated flight times and horizontal displacements for ions of different m/z ratios[a].

m/z	Flight Time (μs)	Horizontal Displacement (mm)
100	10.8	2.0
250	17.0	5.1
1,000	34.0	10.2
2,000	48.1	14.4
5,000	76.0	22.8

[a]The horizontal velocity was 3 x 10^4 cm s^{-1}. Total acceleration voltage was 2,100 V. The flight tube length was 60 cm.

Table 2. Calculated residence times and horizontal displacements for ions of different m/z ratios in the acceleration region between the repeller plate and focus grid[a].

m/z	Residence Time (μs)	Horizontal Displacement (mm)
100	1.0	0.3
250	1.6	0.5
1,000	3.2	1.0
2,000	4.4	1.3
5,000	7.0	2.1

[a]A pulse voltage of 300 V was used.

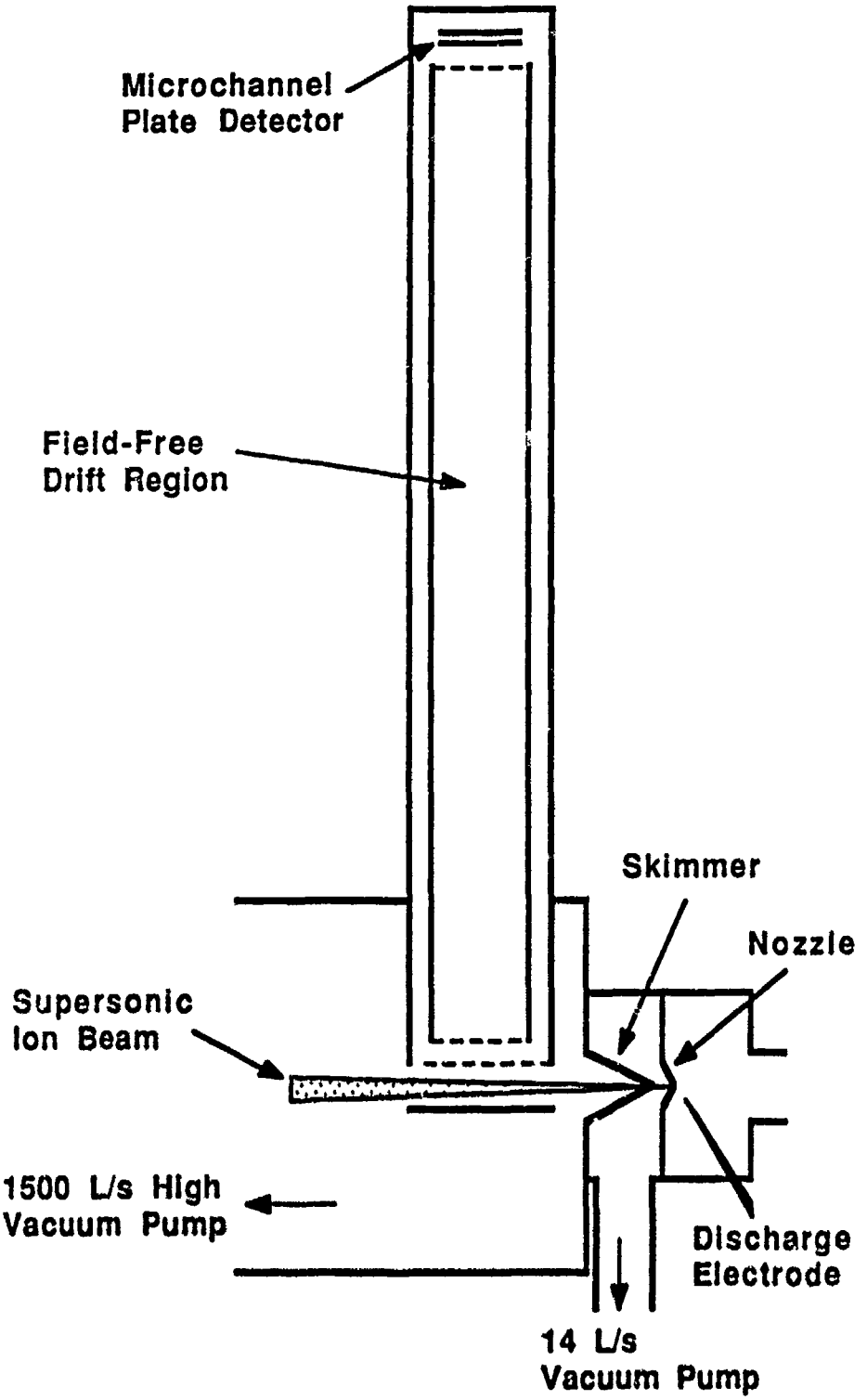


Figure 1. Schematic diagram of the API/TOFMS vapor detector showing the API source and TOF mass analyzer.

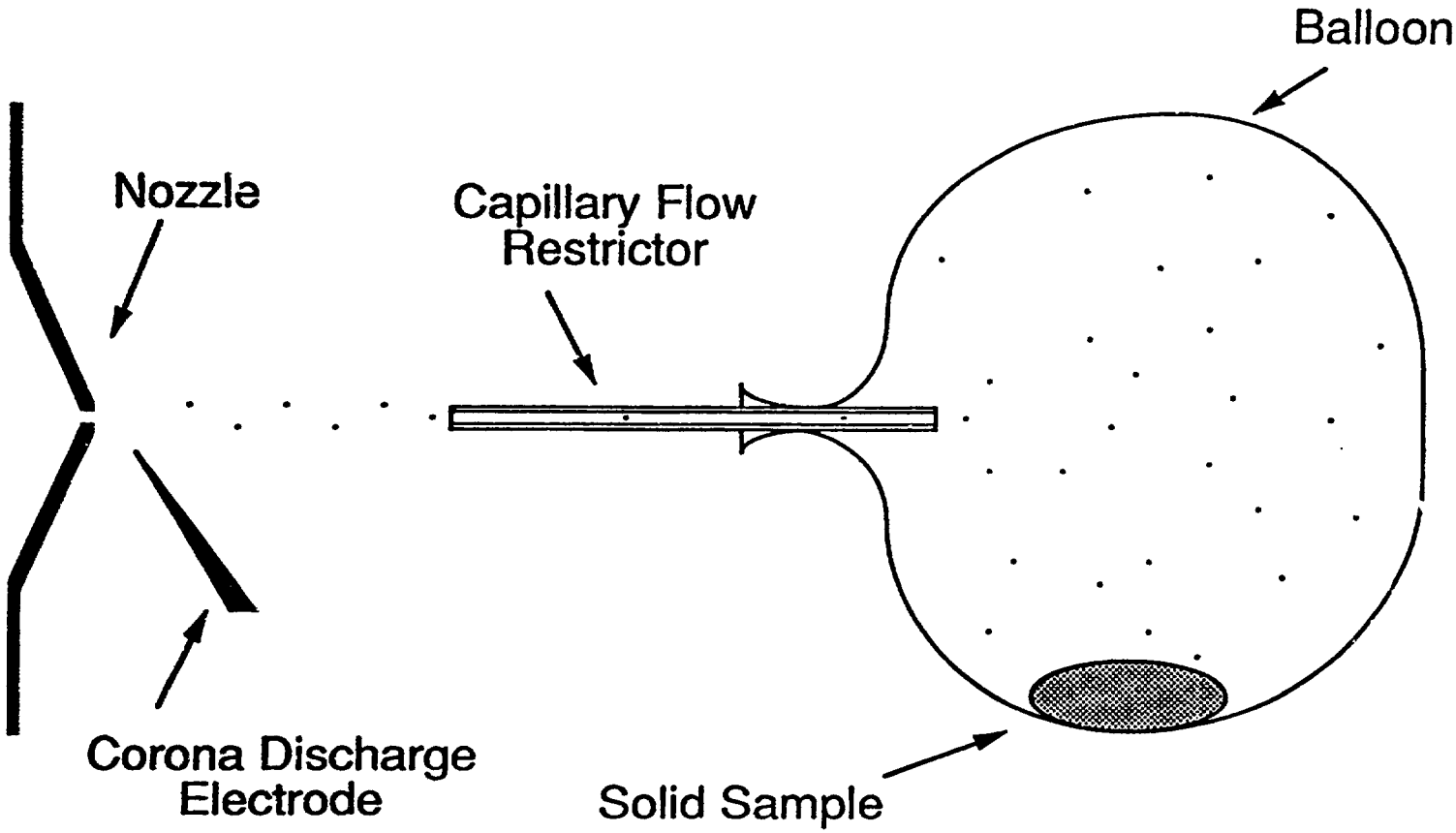


Figure 2. Diagram of a simple explosives vapor generator.

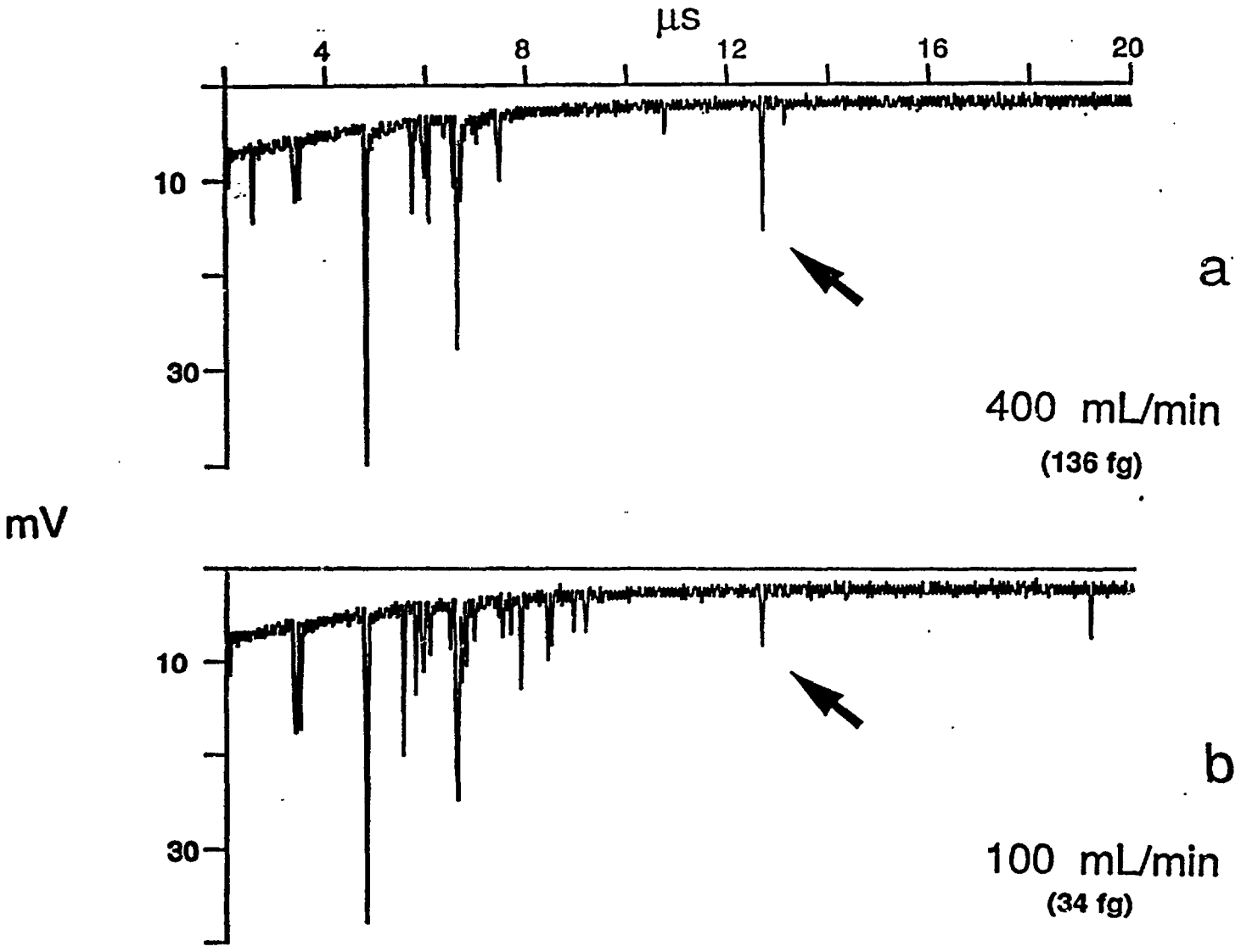


Figure 3. Detection of TNT vapor from a simple explosives vapor generator. Flow rate of (a) 400 mL/min representing 136 fg of TNT vapor per scan and (b) 100 mL/min representing 34 fg of TNT vapor per scan.

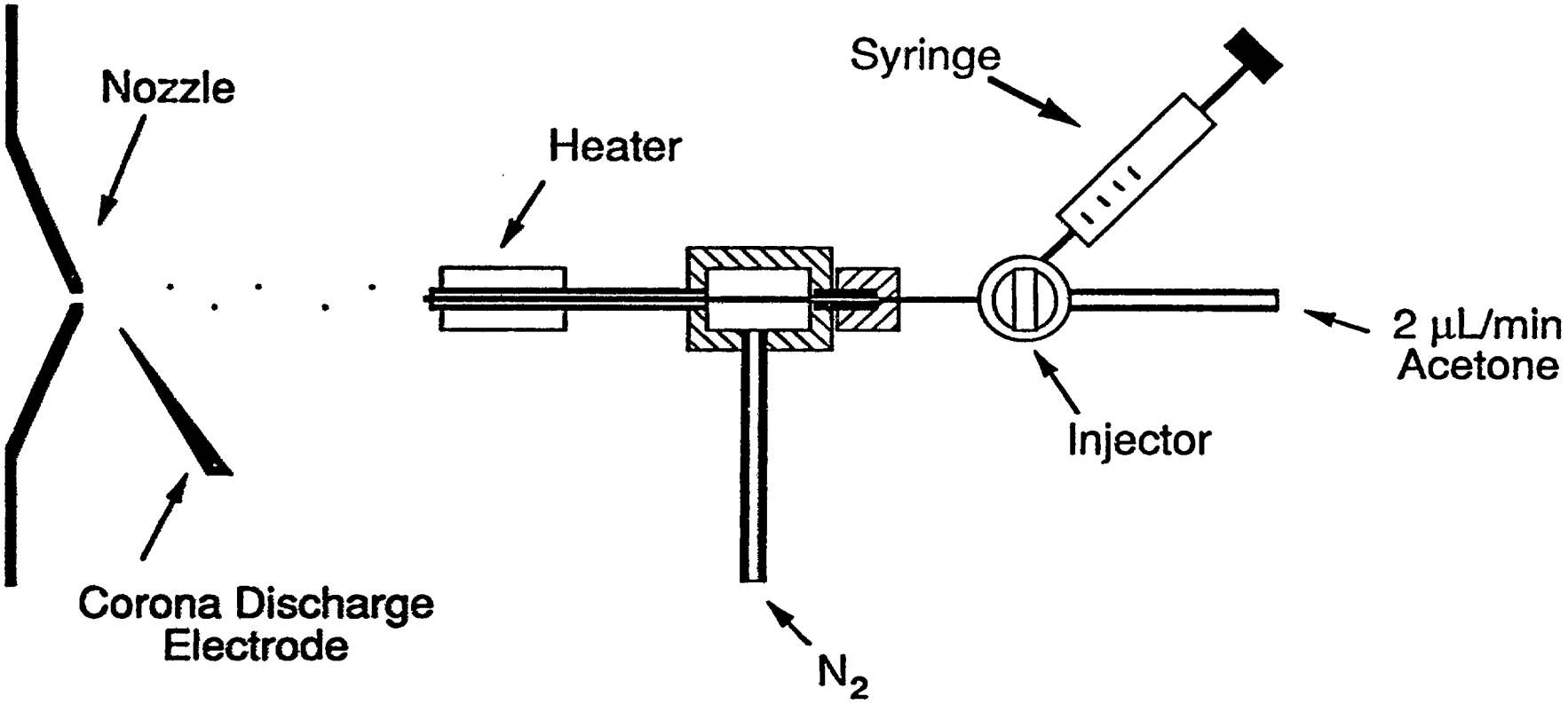


Figure 4. Diagram of a controlled flow sample delivery system.

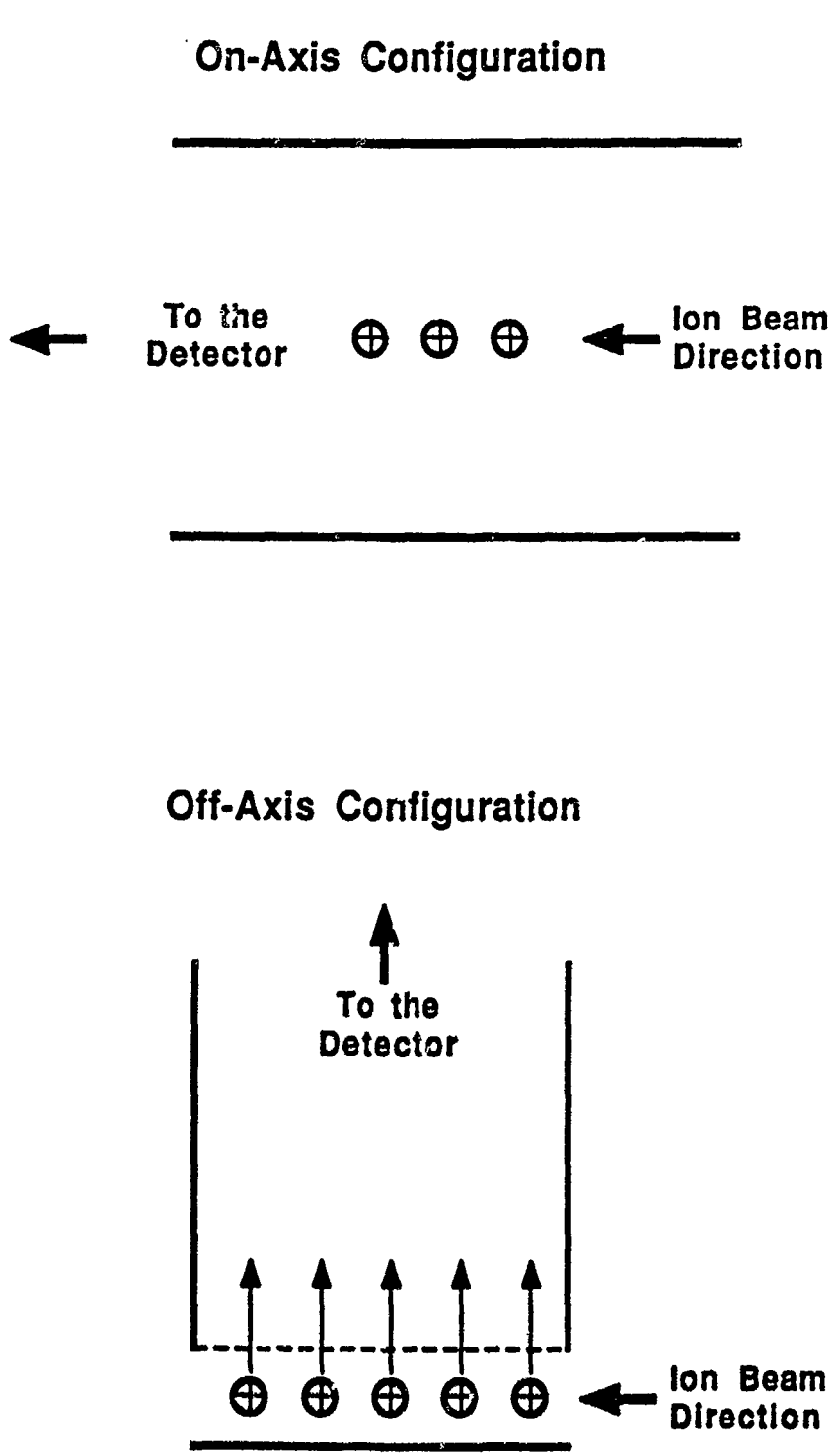


Figure 5. Schematic diagram showing ion throughput from pulsing by (a) a deflection plate and (b) a repeller plate perpendicular to the direction of acceleration. More ions are detected per pulse in case (b).

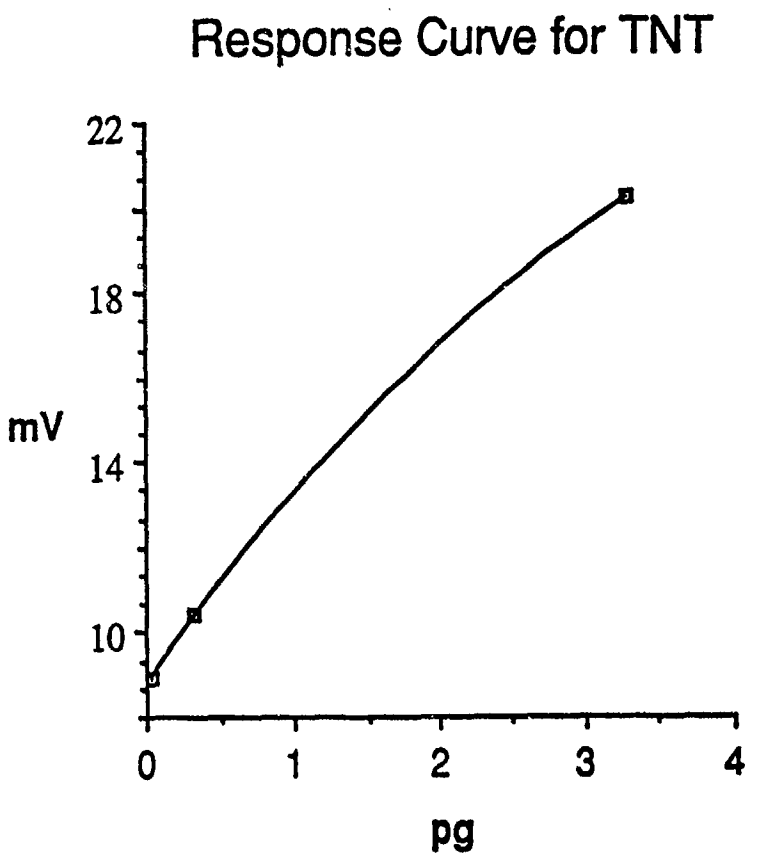


Figure 6. Signal response curve for TNT samples delivered by a controlled flow sample delivery system.

AND COLLECTION SYSTEMS FOR USE WITH THE ATMOSPHERIC PRESSURE IONIZATION TIME-OF-FLIGHT MASS SPECTROMETER

M. Marx Hintze
Byron L. Hansen
Scientech, Inc.

Dr. Russell L. Heath
Consultant

1. INTRODUCTION

This paper is a companion document to the Atmospheric Pressure Ionization Time-of-Flight Mass Spectrometer (API TOFMS) presentation (Lee, et al., 1992). Two significant technical challenges related to design and implementation of vapor collection systems are addressed. They are: a. Freeing deposited or trapped explosive material particles or vapor; and b. Transportation of sample specimen from the pickup point to the detector.

Addressed in this dissertation will be both hand-held collection and air shower booth accumulation.

Detection of low concentrations of explosive material, (one femptogram (fg) or less range), is now a technical accomplishment (Lee, et al., 1992). These low trace quantities can be missed, lost, absorbed, diluted below recognition, or destroyed in the collection system.

In nature, the collection systems of the blood hound and polar bear have carefully positioned detectors at the point of pickup, which is just inside the nostril openings. An ideal man-made system would employ the detector also at the opening or adjacent to the orifice in which the vapor sample first passes. The design methods for a man-made collection system which would satisfy a one fg sensitivity are complex and employ components that are not readily miniaturized or packaged at the sample intake orifice.

Therefore, preconcentration is required accompanied with secondary injection to the detector.

2. GENERAL DISCUSSION

The collection system, which includes the sample acquisition through the purging of preconcentration media, must be separated from the detection system for discussion or specification purposes.

The detector system, an API TOFMS, is an instrument which detects and distinguishes compounds by mass (Sin, et al., 1990).

Explosive compounds gathered by a vapor must be swept from the air or near emission sources, such as luggage, people or dislodged by agitation/vacuuming.

The hypothetical, unofficial specification for detecting a 1.0 fg or less sample does not equate or relate to a dispersed explosive vapor air mixture (ppq).

The collector system can deliver a certain weight of sample to the detector after combing it from the area, item or person in question. Parameters of importance are air flow rates, collector efficiency, media desorption efficiency and overall processing time required. Detection processing time, after the collection system purges the media, is not a problem since the API TOFMS can display the spectrum in micro seconds (Lee, et al., 1992).

3. HAND-HELD (AIR-SUCTION) COLLECTION

In theory, hand-held sample collection offers the best chance for success since it closely follows nature by placing a pseudo-detector close to the vapor source. Implementation of hand-held collection has several inherent conflicts or tradeoffs. For instance, if a

high vacuum, large air-volume is employed, the suspect vapors or particles will be removed satisfactorily, but would deteriorate from dilution and preconcentration uncertainty which would make detection difficult. A low vacuum, small air-volume, on the other hand, reduces the probability of dislodging any substances at all, and again makes detection unlikely. Assuming that an optimum vacuum/air-flow can be attained, any significant distance for a one (1.0) fg or less sample to travel, from pickup point to detector, will present a risk of reduction or even loss due to adherence, or absorption.

With these constraints, it is state-of-the-art to collect and preconcentrate adjacent to the pickup point. A two-step process, collect and purge, is required to present the sample at the detector.

Some added enhancement can be accomplished with the pickup head, the media for preconcentration storage and the purge/sample removal technique. Six candidate pickup-head design configuration concepts for enhancing sample collection are postulated (See Figure 1). They are: 1. regular inlet flow employing no improvements; 2. inert gas hydraulic stimulus positioned at the nozzle tip; 3. ultrasonic emission at the tip; 4. low frequency pulsed air piston at the tip; 5. rotating beaters or flails at the tip; and 6. infrared radiation emitted from the tip. Hand-held collection is already implemented in certain commercial vapor collection systems and promises to be one of the most effective methods of gathering trace amounts of explosive compounds.

4. AIR-SHOWER (BOOTH) COLLECTION

Booth or walk-through collection must take into consideration an "air-exchange" sweep, concentration to a point, media temporary sample retention, and purge to the detector. Imposing an arbitrary time of six (6.0) seconds per person and assuming a conventional booth of approximately two hundred (200) cubic feet with a walk-through transit time of three (3) seconds, an air shower/removal period of three (3) seconds, design criteria for the collection system can be formulated. One important trade-off will be the air-velocity at the collection media. For a three (3) inch diameter media, the air velocity for the above criteria, would be twice the speed of sound through the preconcentration. This is, of course, unacceptable. Another consideration is the air collected in the booth with respect to the air loss due to natural walk-through pumping of the transiting individuals. Storage/purge efficiency or desorption of the preconcentration media is of prime importance. Budgeting the losses and efficiencies might have the following profiles: a. 50% for air collected vs air lost to the walk-through pumping; b. 50% for sample collected to sample actually deposited on the preconcentration media, and c. 80% for storage/purge efficiency to the detector. With these losses in mind, a one (1.0) fg sample at the detector translates to five (5) emitted or off-gassed or otherwise acquired during the booth transit. Booth collection is fraught with problems. A dynamic model of all components is needed to finalize the design or demonstrate theoretical feasibility.

5. SUMMARY

Vapor detection, by definition, is dependent upon sample mass quantity being delivered to the detector. At a one (1.0) ppq density of TNT vapor, the air volume quantity containing one (1.0) fg would be approximately 108 ml. Noting the gross inefficiencies and uncertainties of mixing and sampling in an Air Shower (Booth), significant challenges exist for that method of credible vapor detection. Hand-held acquisition (vacuuming) follows nature the closest by placing a pseudo-detector next to the source. Air sampling of a large area by sweeping with adequate time to collect and preconcentrate from large air volumes is feasible. Finally, it is generally recognized that the challenge of detecting vapors is real and attainable. The bigger question is: what is the specification and its respective breakdown parts for vapor detection?

REFERENCES

H. G. Lee, E. D. Lee, and M. L. Lee, Atmospheric Pressure Ionization Time-of-Flight Mass Spectrometer for Real-Time Explosives Vapor Detection, These proceedings, 1992.

C. H. Sin, E. D. Lee, and M. L. Lee, Atmospheric Pressure Ionization Time-of-Flight Mass Spectrometry with Supersonic Ion Beam, 1990.

Probe Tip Concepts

Configuration 1
Straight Suction

Configuration 2
Suction with CO_2 Sweep Gas

Configuration 3
Suction with ultra-sonic Pulse Emitter

Configuration 4
Suction with low Frequency High-Volume Pulser

Configuration 5
Suction with Rotating Surface Agitators

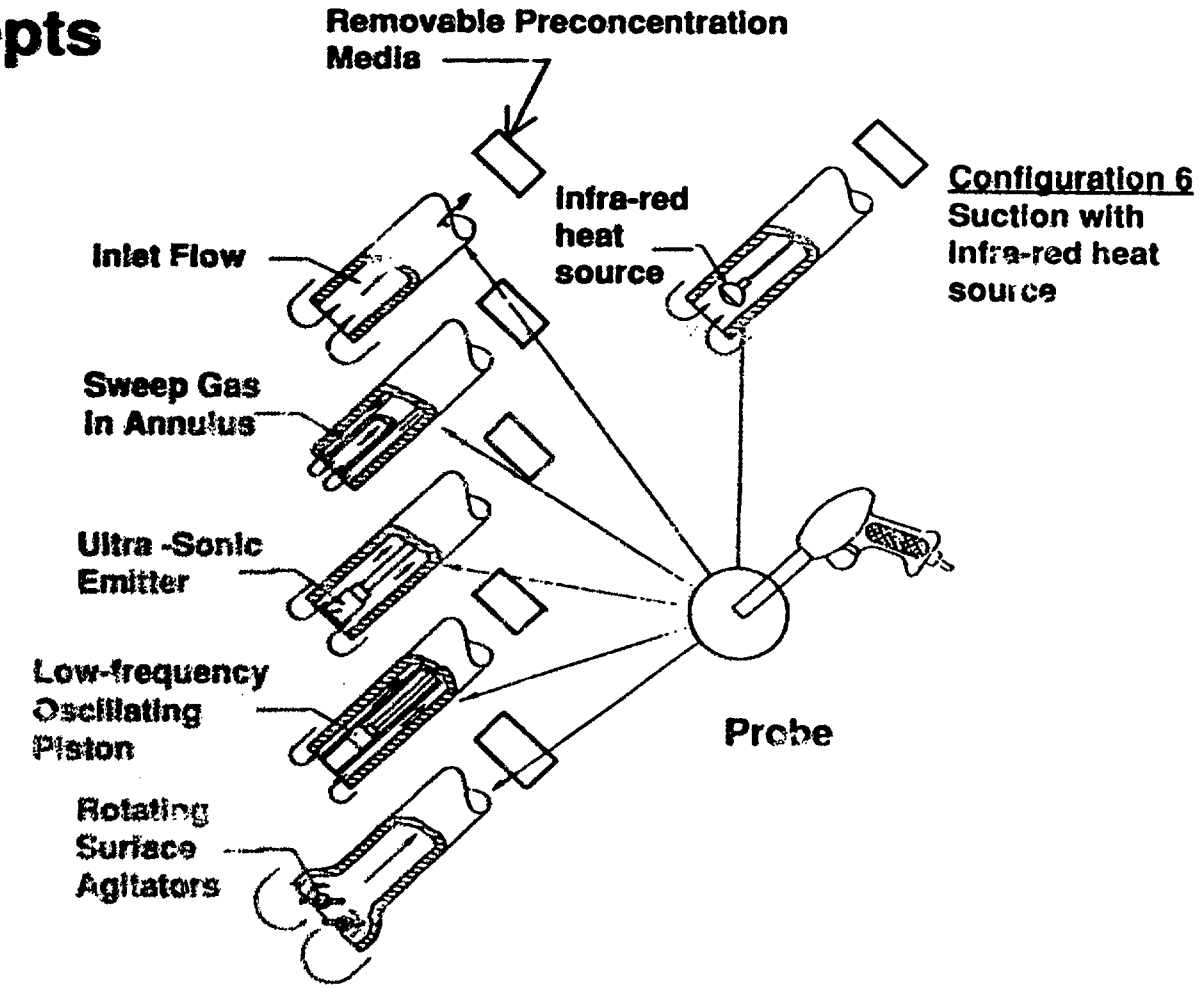


Fig. 1 - Probe Tip Concepts

DETECTION OF EXPLOSIVES MATERIAL ON SINGLE MICROPARTICLES

W. B. Whitten, J. M. Dale, and J. M. Ramsey
Analytical Chemistry Division
Oak Ridge National Laboratory
Oak Ridge, TN 37831-6142

1. INTRODUCTION

Some of the explosive materials with very low vapor pressure such as RDX or PETN are most likely to be encountered either as solids or adsorbed on solids. We are developing a new technique for the chemical characterization of explosives-bearing microparticles based upon the use of electrodynamic traps. The electrodynamic trap has achieved widespread use in the mass spectrometry community in the form of the ion trap mass spectrometer or quadrupole ion trap (March, 1989). Small macroscopic particles (microparticles) can be confined or levitated within the electrode structure of a three-dimensional quadrupole electrodynamic trap in the same way as fundamental charges or molecular ions by using a combination of ac and dc potentials (Wuerker, 1959). Our concept is to use the same electrode structure to perform both microparticle levitation and ion trapping/mass analysis. The microparticle will first be trapped and spatially stabilized within the trap for characterization by optical probes, i.e., absorption, fluorescence, or Raman spectroscopy. (We have previously shown that such spectroscopic probes can be extremely sensitive, e.g., a detection limit of one molecule of Rhodamine-6G has been determined in the case of fluorescence spectroscopy (Whitten, 1991.) After the particle has been optically characterized, it is further characterized using mass spectrometry. Ions are generated from the particle surface using laser ablation or desorption. The characteristics of the applied voltages are changed to trap the ions formed by the laser with the ions subsequently mass analyzed. The work described here focuses on the ability to perform laser desorption experiments on microparticles contained within the ion trap. Laser desorption has previously been demonstrated in ion trap devices by applying the sample to a probe which is inserted so as to place the sample at the surface of the ring electrode (Heller, 1989, Glish, 1989). Our technique requires the placement of a microparticle in the center of the trap. Our initial experiments have been performed on falling microparticles rather than levitated particles to eliminate voltage switching requirements when changing from particle to ion trapping modes. Such experiments have also been reported by Sinha (Sinha, 1984) and by McKeown et al. (McKeown 1991).

2. THE EXPERIMENTS

Figure 1 shows a schematic diagram of our current apparatus for performing these experiments. The ion trapping device is a modified Finnigan MAT Model 800 Ion Trap Detector (ITD). The trapping electrodes were removed from the ITD vacuum chamber and placed in a 6-inch cube with the rotational symmetry axis of the trap oriented vertically. The cube is attached to a 4-inch oil diffusion pump. The rf voltage from the ITD was reattached to the ring electrode by extending the transformer tap wire to a high-voltage vacuum feed-through mounted on one of the side ports and retuning the transformer for resonance. The ITD was operated with nominally 1 mtorr of He buffer gas as usual. The ion lens assembly normally used for electron-impact ionization was removed from the top end cap and a particle dropping device was installed. The particle dropper consisted of a funnel-shaped container with a 450-μm spout. A 300-μm wire attached to a 6-mm rod normally rests in the spout. The rod exits the vacuum chamber through an o-ring sealed fitting. Particles of interest are placed in the container and dispensed by moving the wire attached to the rod. The other three side ports were fitted with 6-inch pyrex windows while the bottom port was covered with a flange mounted with the channeltron electron multiplier. A 5-mW HeNe laser beam is focused into the trap through the windows and opposing 3-mm holes drilled in the ring electrode. The HeNe beam is positioned ≈ 1 mm above the center of the trap. The second harmonic laser radiation from a pulsed Nd:YAG laser (Quanta-Ray DCR-2A) propagates in the opposite direction

through the trap and is focused by a 1-m lens at the trap center.

Collection of a laser desorption mass spectrum requires synchronization of the Nd:YAG laser with the falling particle and the ITD. The ITD runs continuously through its normal scan sequence of trapping and mass-selective particle ejection. The ITD can have a trapping-mode duty cycle of ≈ 40% if appropriate scan settings are used. When particles are dropped they pass through the HeNe probe beam scattering light that is detected by the photodiode. The photodiode signal is converted to TTL, then ANDed with the electron gate signal from the ITD. If a light scattering signal is detected when the ITD is in the trapping mode, the Nd:YAG laser is fired after an adjustable delay time. The laser trigger delay allows for the spatial displacement between the HeNe and Nd:YAG beams. Particles can be reliably illuminated with the 10-ns pulse from the Nd:YAG laser after proper alignment.

Silicon carbide particles (nominal 125-μm diameter) coated with various materials were used in our initial studies. Particles were coated with various quaternary ammonium or phosphonium salts or with TNT by dissolving the analyte (in methanol for the quaternary salts, toluene for TNT), combining with a given mass of particles and evaporating the solvent. Compounds investigated include besides TNT, trimethylphenylammonium chloride, triethylphenylammonium iodide, tetrabutylammonium iodide, and tetraphenylphosphonium bromide. All experiments were performed with pulse energies of ≈ 1mJ (10^9 W/cm^2) except where noted. Ions were reliably produced from dropped particles with yield correlating with the intensity of the 532-nm light scattered by the particle as detected by the photodiode. The quality of the mass spectra varied primarily due to what appears to be space charge effects. Mass spectra of the quaternary ammonium or phosphonium salts all produced intact cations and expected fragment ions. The mass spectra compare favorably with those of Glish et al. (Glish, 1989) and SIMS data on the same particles. The mass spectrum of TNT was obtained by detecting negative ions with a supplementary conversion dynode biased at +3000 V. The spectrum was in good agreement with results obtained by chemical ionization in the ion trap (McLuckey, 1987).

Figure 2 shows a mass spectrum for a single SiC particle coated with tetraphenylphosphonium bromide irradiated with a single pulse of 532-nm radiation for the Nd:YAG laser. The intact cation peak is observed at m/z 339. Peaks were also observed that correspond to loss of 2 benzene units and loss of 3 phenyl groups at 183 and 105 m/z respectively. The loss of a single phenyl group results in an odd electron ion and is occasionally observed at low abundance. This mass spectrum is representative of the better spectra observed. Spectra of this quality are observed with ≈ 50% of the particles. The other 50% of the experiments are either of low ion yield due to poor overlap of the Nd:YAG laser beam with the particle or too high an ion yield resulting in poor mass resolution from space charge effects in the ion trap. The minimum particle loading that was tried corresponded to 133 femtomoles or 8 x 10^{10} molecules on a 125-μm SiC particle.

In addition to the above coated SiC particles, uncoated particles of SiC, Fe, and Nb were also investigated. The uncoated SiC particles yielded Na and K ions presumably due to surface contamination. No ions were observed that would be associated with SiC even at intensities of 10^{10} W/cm^2. The iron and niobium particles required slightly higher energies (≈ 3mJ/pulse) to yield ions as would be expected. The iron spectra included the iron isotopes in addition to showing a copper impurity. The Nb spectra also indicated some iron contamination.

3. CONCLUSION

Improvements in the current apparatus promise to yield good sensitivity for materials on the surface of microparticles. Submonolayer sensitivities have already been achieved. Excess ion production leading to space charge effects in the trap is currently more of a problem than lack of signal. Combining particle levitation with ion trapping may allow multiple desorption experiments to be performed on a single particle and thus permit signal averaging.

ACKNOWLEDGEMENTS

The authors would like to express their appreciation to Thomas Rosseel and Werner Christie for obtaining SIMS data on the particles investigated, to Peter Todd for interpretation of some of the mass spectra, and to Gary Glish and Doug Goeringer for suggesting and providing the quaternary salts. Research sponsored by U.S. Department of Energy under contract DE-AC05-84OR21400 with Martin Marietta Energy Systems, Inc.

REFERENCES

G. L. Glish, D. E. Goeringer, K. G. Asano, and S. A. McLuckey, Int. J. Mass Spectrom. & Ion Proc. 94, 15 (1989).

D. N. Heller, I. Lys, R. J. Cotter, and O. M. Uy, Anal. Chem. 61, 1083 (1989).

P. J. McKeown, M. V. Johnston, and D. M. Murphy, Anal. Chem. 63, 2073 (1991).

S. A. McLuckey, G. L. Glish, and P. E. Kelley, Anal. Chem. 59, 1670 (1987).

R. E. March and R. J. Hughes, Quadrupole Storage Mass Spectrometry, Vol. 102, "Chemical Analysis", J. D. Winefordner, Ed., Wiley-Interscience, New York, 1989.

M. P. Sinha, Rev. Sci. Instrum. 55, 886 (1984).

W. B. Whitten, J. M. Ramsey, S. Arnold, and B. V. Bronk, Anal. Chem. 63, 1027 (1991).

R. F. Wuerker, H. M. Goldenberg, and R. V. Langmuir, J. Appl. Phys. 30, 441 (1959).

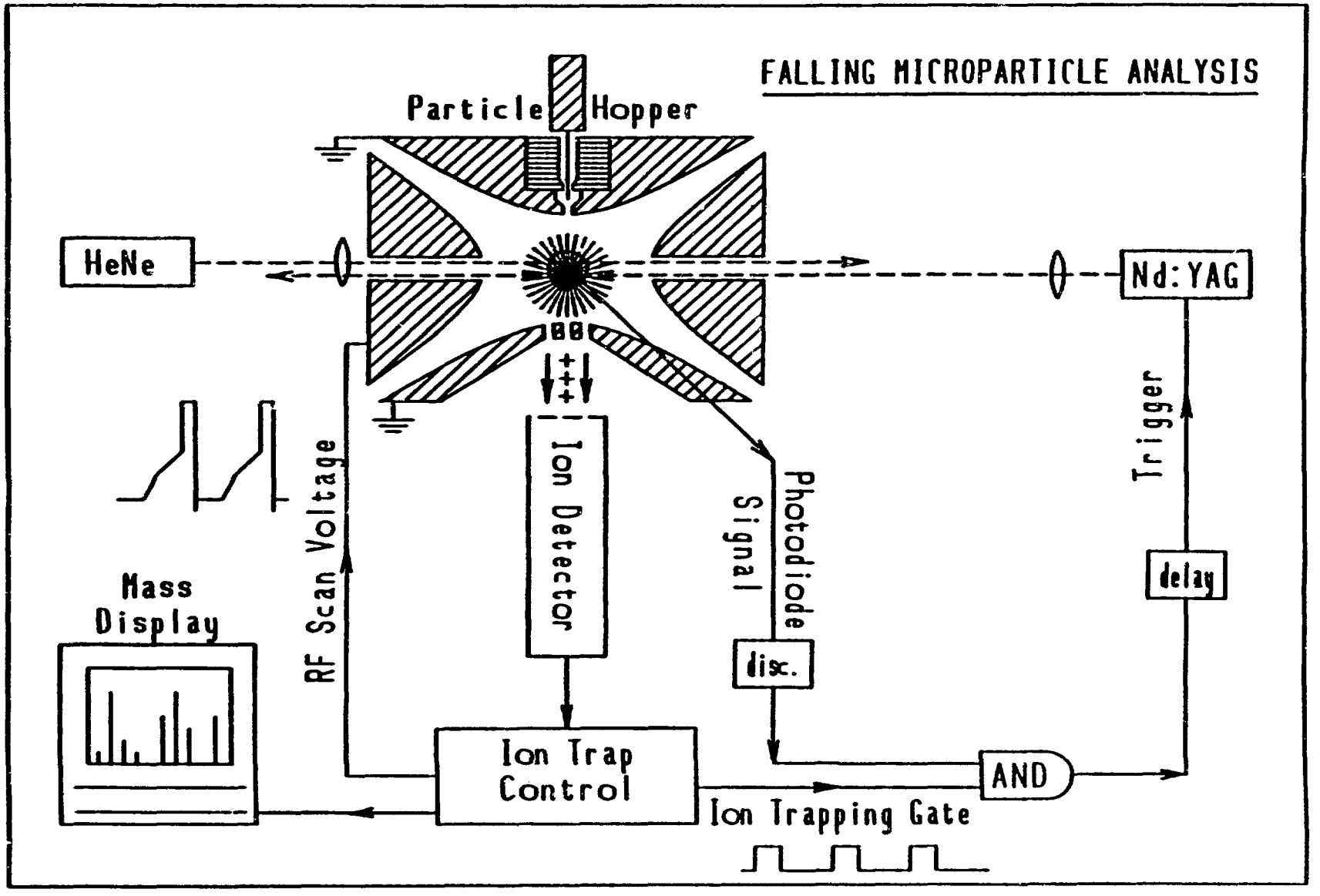


Figure 1. Schematic Diagram of the ITD

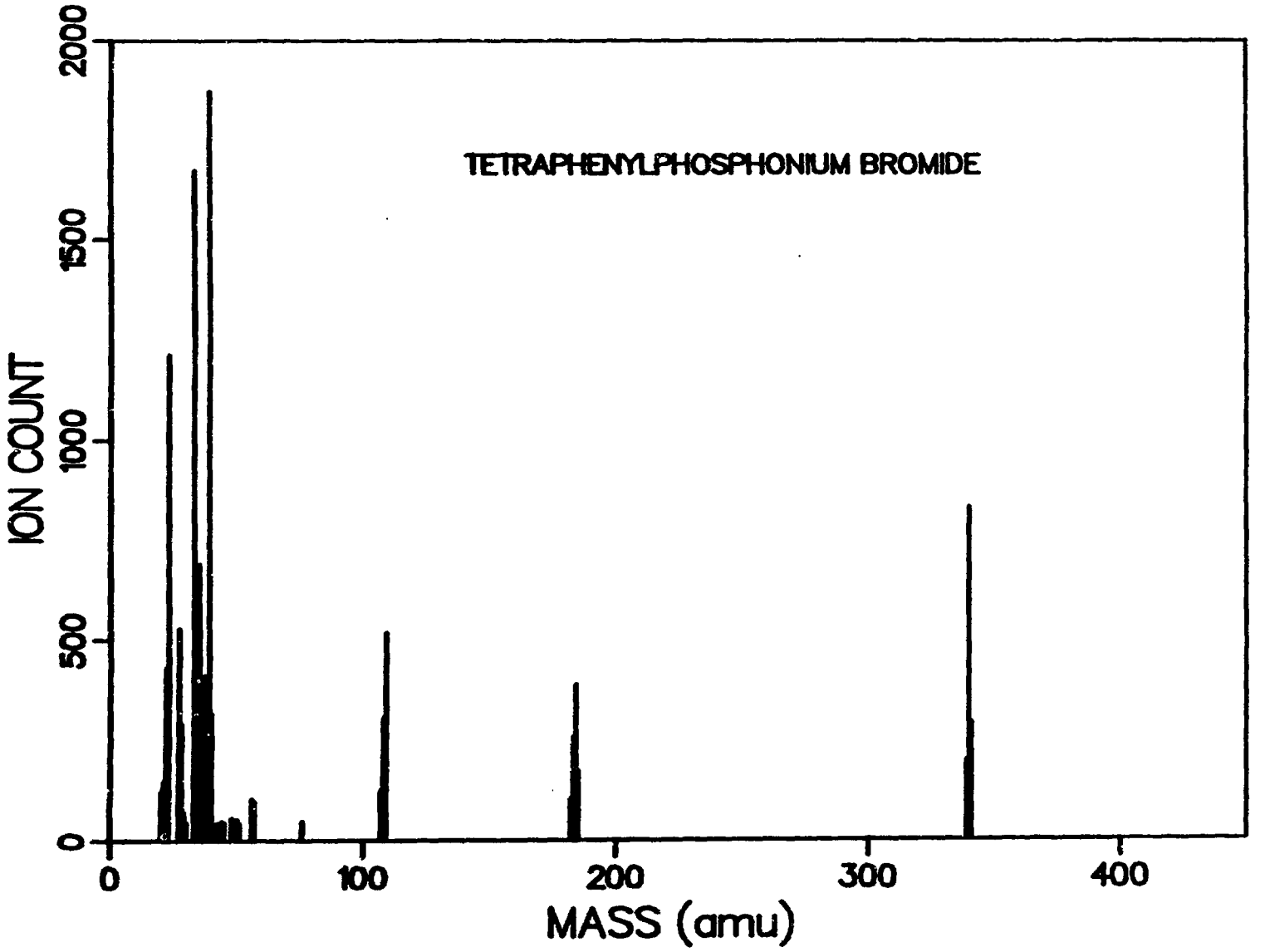


Figure 2. Mass Spectrum for a Single SiC Particle Coated with tetraphenylphosphonium Bromide

TANDEM MASS SPECTROMETRY FOR EXPLOSIVES VAPOR DETECTION

G.L. Glish, S.A. McLuckey, B.C. Grant, and H.S. McKown
Analytical Chemistry Division
Oak Ridge National Laboratory
Oak Ridge, TN 37831

1. INTRODUCTION

Atmospheric sampling glow discharge ionization (ASGDI) has been shown to be a highly sensitive ion source for the detection of explosive compounds in air (1,2). We first interfaced this ion source with a home-built quadrupole/time-of-flight (QT) instrument (3). A second MS/MS instrument, a Finnigan ion trap mass spectrometer (ITMS), was then modified extensively to adapt the ASGDI source (4). We have recently interfaced an ASGDI source with a Finnigan TSQ 700 tandem quadrupole instrument. Part of the rationale behind this work was to adapt ASGDI in a very simple and inexpensive manner to a widely available state-of-the-art tandem mass spectrometer. The purposes of this paper are to describe the modification to the TSQ 700 and to show illustrative data obtained with the ASGDI/TSQ 700 combination. To provide a context for the TSQ 700 results we also present data acquired with equal analyte levels with the two other tandem mass spectrometers.

2. TSQ 700 MODIFICATION

An ASGDI ion source geometry was designed that would adapt directly to the TSQ 700 ionization region vacuum manifold. A side-view schematic of the ASGDI source as it is positioned in relation to the TSQ 700 ion source lens stack is shown in Figure 1 (vacuum manifold not shown). The modifications to the TSQ 700 include:

- Removal of the normal EI/CI ion source and solids probe flange and replacement with the ASGDI source,
- Addition of a 1 cm tube extension to the first lens element for ion extraction,
- Addition of a 10 L/s roughing pump to evacuate the ASGDI source to 0.8 torr, and
- Addition of a DC power supply to provide the -400 V, 10 mA for the discharge.

3. EXPERIMENTAL

All data shown here were acquired in the negative ion mode using -350 to -400 V on the cathode (A1 of Figure 1) which results in a discharge current of 4 to 8 mA. Mass spectra were acquired with the TSQ 700 by scanning the second quadrupole. Various approaches to acquiring MS/MS data were made and are described with the relevant data. Samples were admitted either as room temperature head space vapors or by placing a few crystals in a capillary tube and placing the capillary in a heated quartz tube leading to the inlet aperture of the ASGDI source. Details of the procedure for acquiring data with the QT and ITMS have been described (3,4).

4. RESULTS AND DISCUSSION

We have focussed our attention on the negative ion performance of the ASGDI/TSQ 700 system since the analysis of explosives is most readily performed using this polarity of ion. Figure 2 shows the background ASGDI negative ion mass spectrum from laboratory air. This spectrum shows the normal background peaks ordinarily observed with the ASGDI sources on the other instruments. The prominent peak at m/z 46 arises from NO_2^- formed in the ion source from the oxygen and nitrogen in air.

4.1. Mass Spectra of Explosives

Figure 3 shows negative ion mass spectra of several explosives of interest, obtained with the ASGDI/TSQ 700. They include TNT and the commonly encountered plastic explosives PETN and RDX. These mass spectra are virtually identical to those obtained on the other instruments. TNT, for example, gives the molecular anion almost exclusively whereas the plastic explosives yield

fragment ions as the base peaks in the spectra. The high mass ion used for MS/MS identification of RDX appears at m/z 176 and corresponds to the loss of a nitro group from the molecular anion. The high mass ion used for PETN identification appears at m/z 240 and corresponds to the loss of CH_2ONO_2 from the molecular anion.

4.2. MS/MS Spectra of Explosives

Figures 4-6 provide the MS/MS spectra acquired for each of the three explosives from each of the three ASGDI/tandem mass spectrometers. Although the mass spectra acquired from the three instruments are similar, the MS/MS spectra show some significant qualitative differences due to differences in analyzers and collisional activation conditions. Collisional activation conditions are similar for the TSQ 700 and the QT but the analyzers (MS II) differ (Q vs. T). Of particular note is the inferior resolution provided by the QT. The collisional activation conditions provided by the ion trap differ significantly from those of the TSQ 700 and the QT. Similar high mass product ions are observed but very little NO_2^-, which constitutes the most abundant product under some conditions in the beam-type instruments, is observed in the ITMS.

4.3. Energy Resolved Mass Spectrometry of TNT

MS/MS spectra are, of course, dependent upon a number of conditions. From the analytical point of view, it is sometimes desirable to maximize the charge in particular product ions. Such a situation is usually desirable for the "targeted product ion" mode of operation (5). In this mode, the first quadrupole is operated as a high pass filter (e.g., passing only ions of m/z > 150) and scanning the second analyzer to detect any product ions characteristic of a compound class. The product ions NO_2^- and NO_3^-, for example, are characteristic of nitroaromatics and nitrate esters, respectively. It is therefore desirable to maximize NO_2^- from the MS/MS of M^- of TNT for application of the targeted product mode of operation. Figure 7 shows an ERMS plot acquired with 20% parent ion beam attenuation. Under these conditions, laboratory collision energies of about 40 eV constitute the best compromise between transmission and NO_2^- production.

4.4. Comparison of MS/MS Performance

The performances of the three ASGDI/tandem mass spectrometers were compared under different MS/MS operating modes. In all cases an equal and constant flux of TNT was admitted into the instrument (maximum concentration estimated to be 1 ppb) and data were collected for two seconds. This normalized the analyte quantity sampled by each instrument. A quantitative measure of "signal/background" for each experiment was taken as the analyte signal (minus background signal) divided by three times the standard deviation of the background signal. For the beam-type instruments, the NO_2^- product ion was used as the analyte signal whereas the product ion at m/z 210 was used for the ITMS data.

Table I summarizes the "signal/background" results acquired under various MS/MS operating modes. The various operating modes establish compromises between signal/background and specificity via the normal trade-offs between resolution and transmission, duty cycle and scan length, etc. The most direct comparison to evaluate signal/background at equal specificity comes from the data acquired with MS I resolution > 400 and MS II resolution maximized. For the TSQ 700 and the ITMS, MS II resolving powers are comparable. However, the resolution of MS II of the QT is at least an order of magnitude lower. The TSQ 700 provides slightly better signal/background than does the QT and with much superior specificity. The ITMS, however, provides roughly an order of magnitude greater signal/background with specificity at least as good as that of the TSQ 700. At the cost of specificity, however, the beam-type instruments can come closer to the performance of the ITMS. This is apparent in the numbers obtained using various forms of parent ion resolution degradation, including the targeted product ion mode. The TSQ 700 can approach the performance of the ITMS in the targeted product ion mode with a narrow scan (to improve duty cycle) over the m/z 46 product ion. An analogous procedure is not available for the QT.

5. CONCLUSIONS

The TSQ 700 can be fitted with an ASGDI source simply and with minimal expense (hardware costs < $10k). This preliminary ASGDI/TSQ 700 data indicates that this instrument provides performance superior to that of the QT instrument both in terms of specificity and signal/background (which should translate to lower limits of detection). The ASGDI/ITMS currently provides the best performance of the three instruments in terms of specificity and signal/background. However, at

degraded specificity the ASGDI/TSQ 700 can provide performance in MS/MS signal/background comparable to that of the ASGDI/ITMS.

REFERENCES

1. S.A. McLuckey, G.L. Glish, K.G. Asano and B.C. Grant, Anal. Chem., 60 (1988) 2220.

2. K.G. Asano, S.A. McLuckey, G.L. Glish, Spectros. Int. J., 8 (1990) 191.

3. G.L. Glish, S.A. McLuckey and H.S. McKown, Analyt. Instrum., 16 (1987) 191.

4. S.A. McLuckey, G.L. Glish, and K.G. Asano, Anal. Chim. Acta, 225 (1989) 25.

5. S.A. McLuckey, B.C. Grant, and G.L. Glish, Anal. Chem., 62 (1990) 56.

NOTES

Research sponsored by the Federal Aviation Adminstration and by U.S.D.O.E. Office of Safeguards and Security under contract DE-AC05-84OR21400 with Martin Marietta Energy Systems, Inc.

Table 1. Comparison of various MS/MS operating modes for three different instruments

OPERATIONAL MODES		MS/MS "Signal/Background"		
MS I	MS II	TSQ700	QT	ITMS
m/Δm>400	m/Δm>400, Full Scan	30	-	200
m/Δm>400	m/Δm=50, Full Scan	-	20	-
RF only, m/z>180	m/Δm>400, Full Scan	75	-	-
RF only, m/z>180	m/Δm=50, Full Scan	-	75	-
RF only, m/z>180	m/Δm>400, Narrow Scan	150	-	-

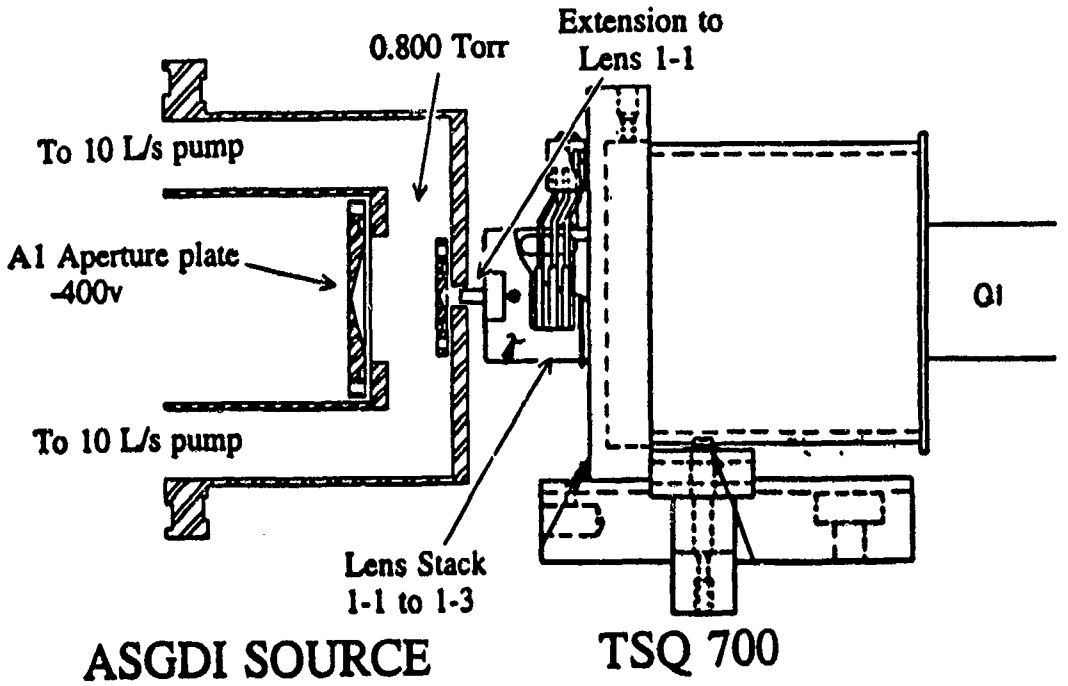


Figure 1

Schematic drawing showing the coupling of the ASGDI source to the TSQ 700.

ASGDI TSQ700 Background MS

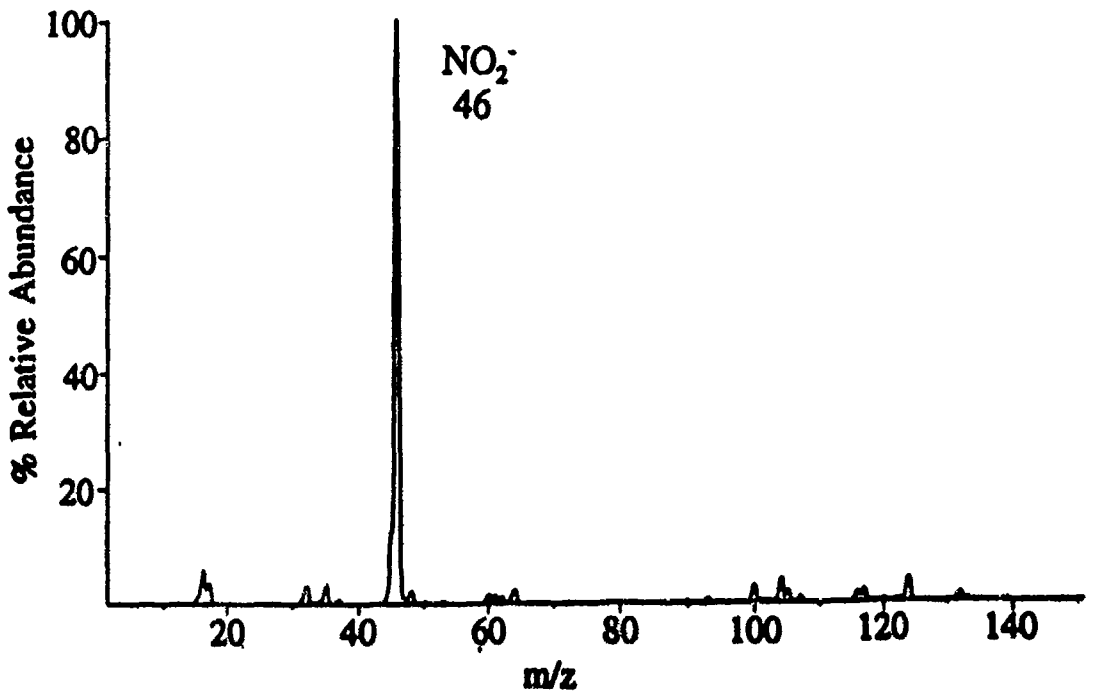


Figure 2

ASGDI/TSQ 700 background mass spectrum.

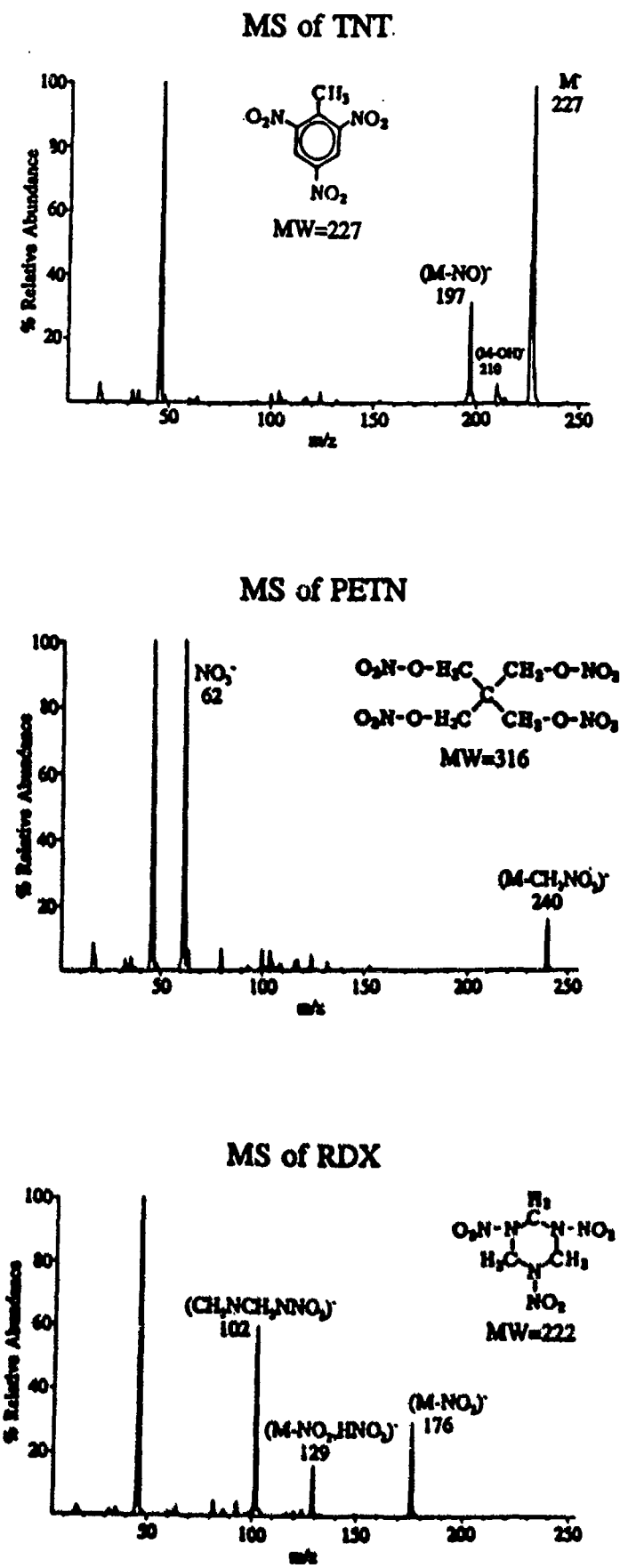


Figure 3. ASGDI/TSQ 700 mass spectra of TNT, PETN, and RDX.

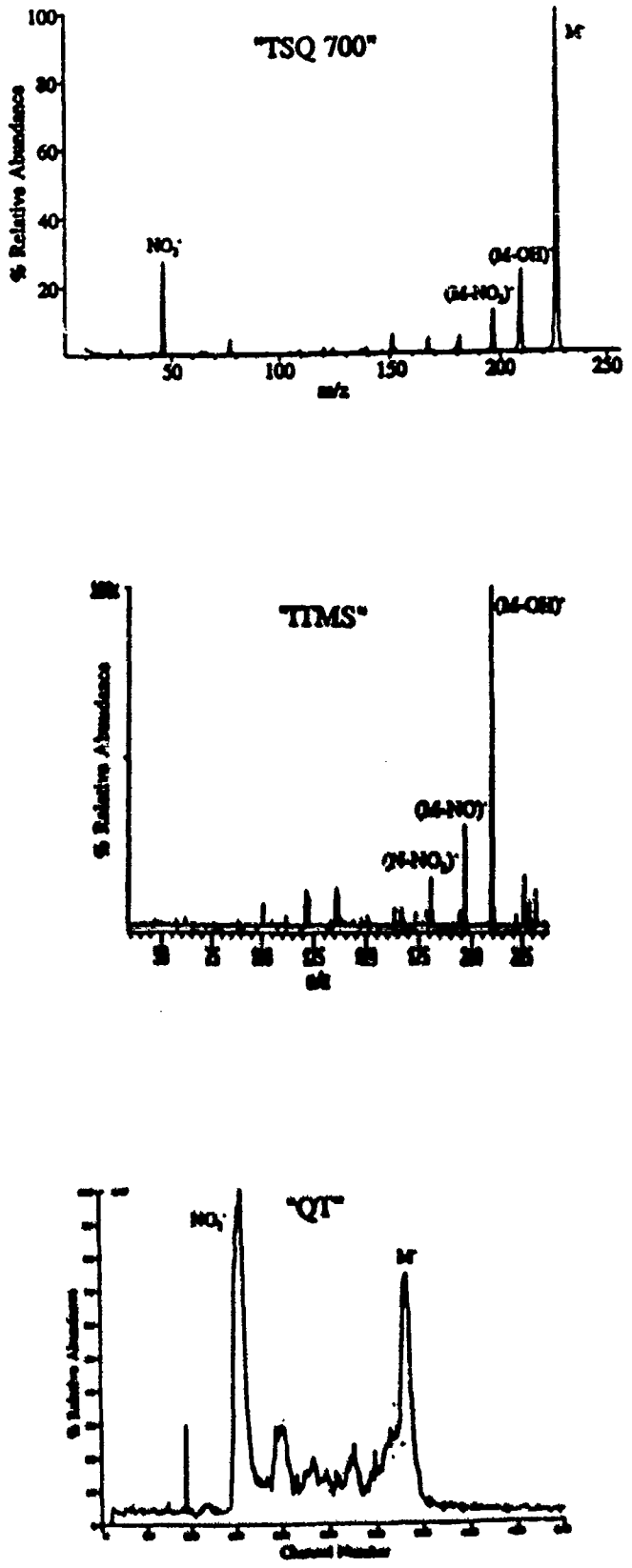


Figure 4. MS/MS of TNT (m/z 227) on the TSQ 700, ITMS, and QT instruments.

MS/MS of PETN (m/z 240) vs Instrument

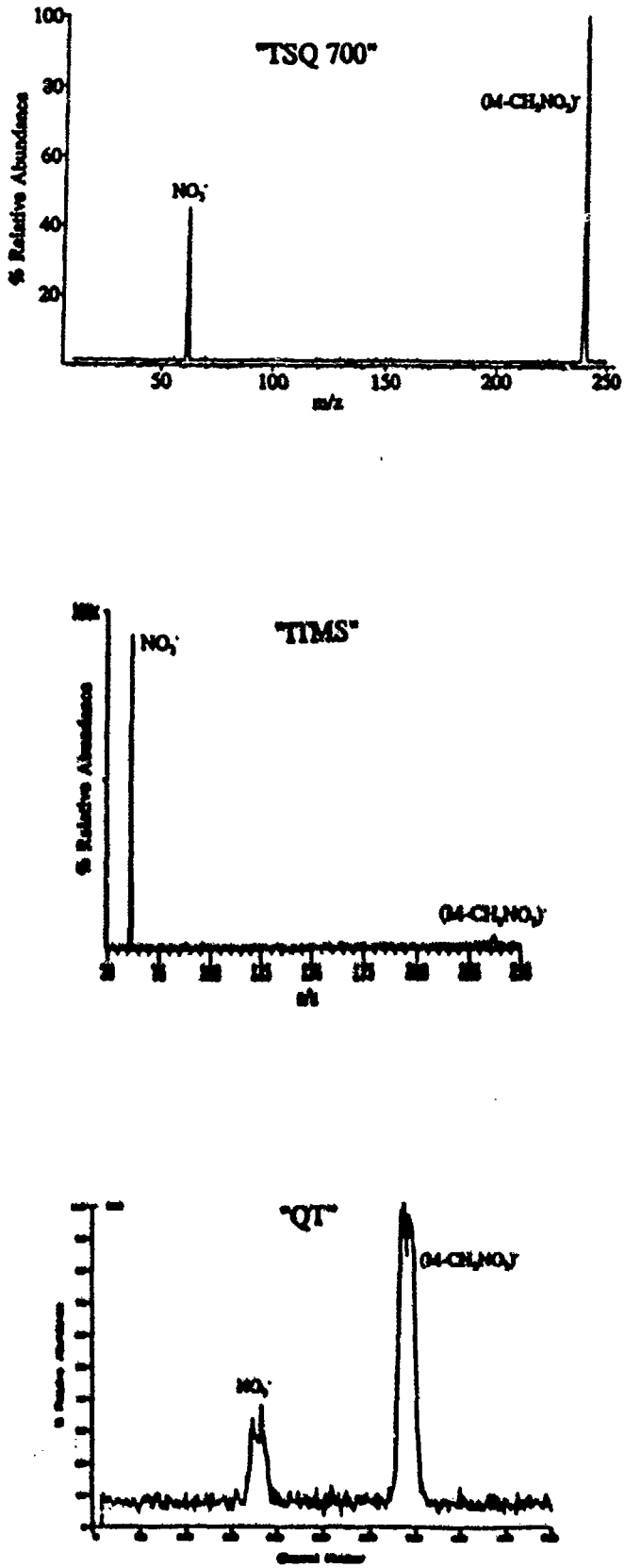


Figure 5. MS/MS of PETN (m/z 240) on the TSQ 700, ITMS, and QT instruments.

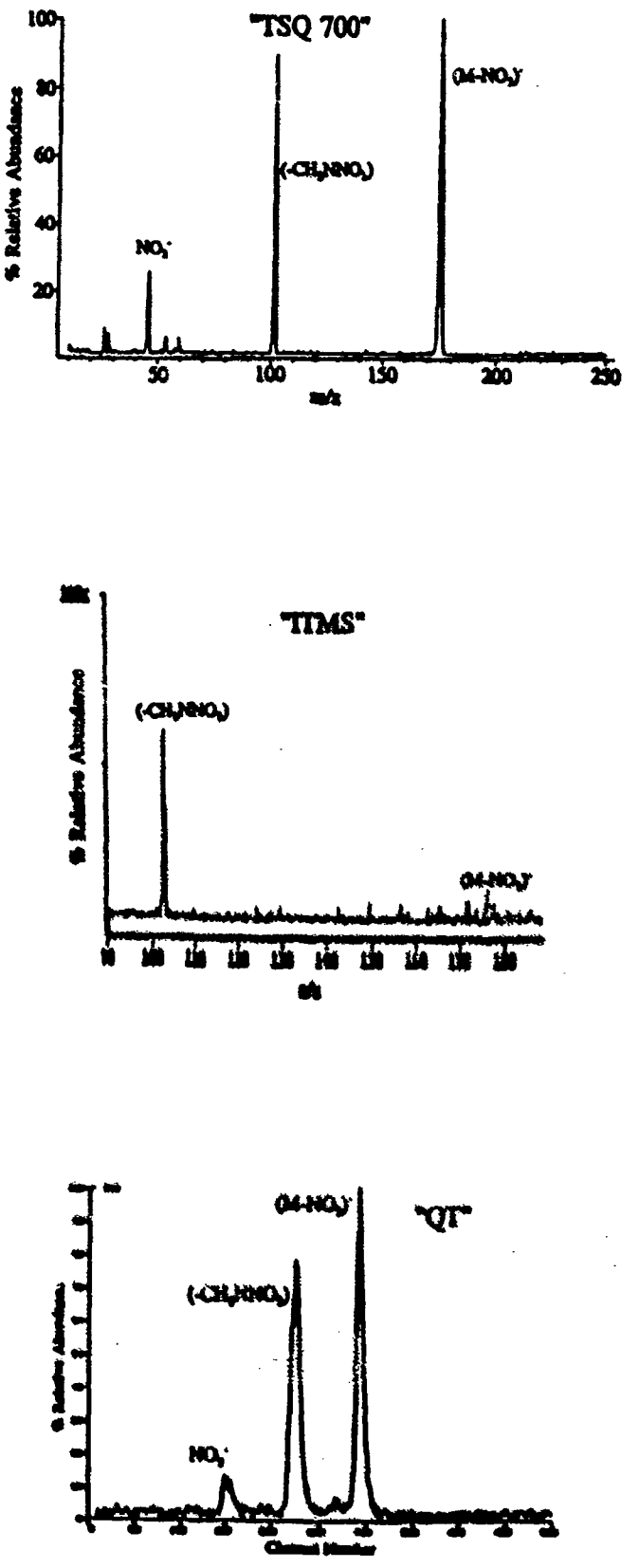


Figure 6. MS/MS of RDX (m/z 176) on the TSQ 700, ITMS, and QT instruments.

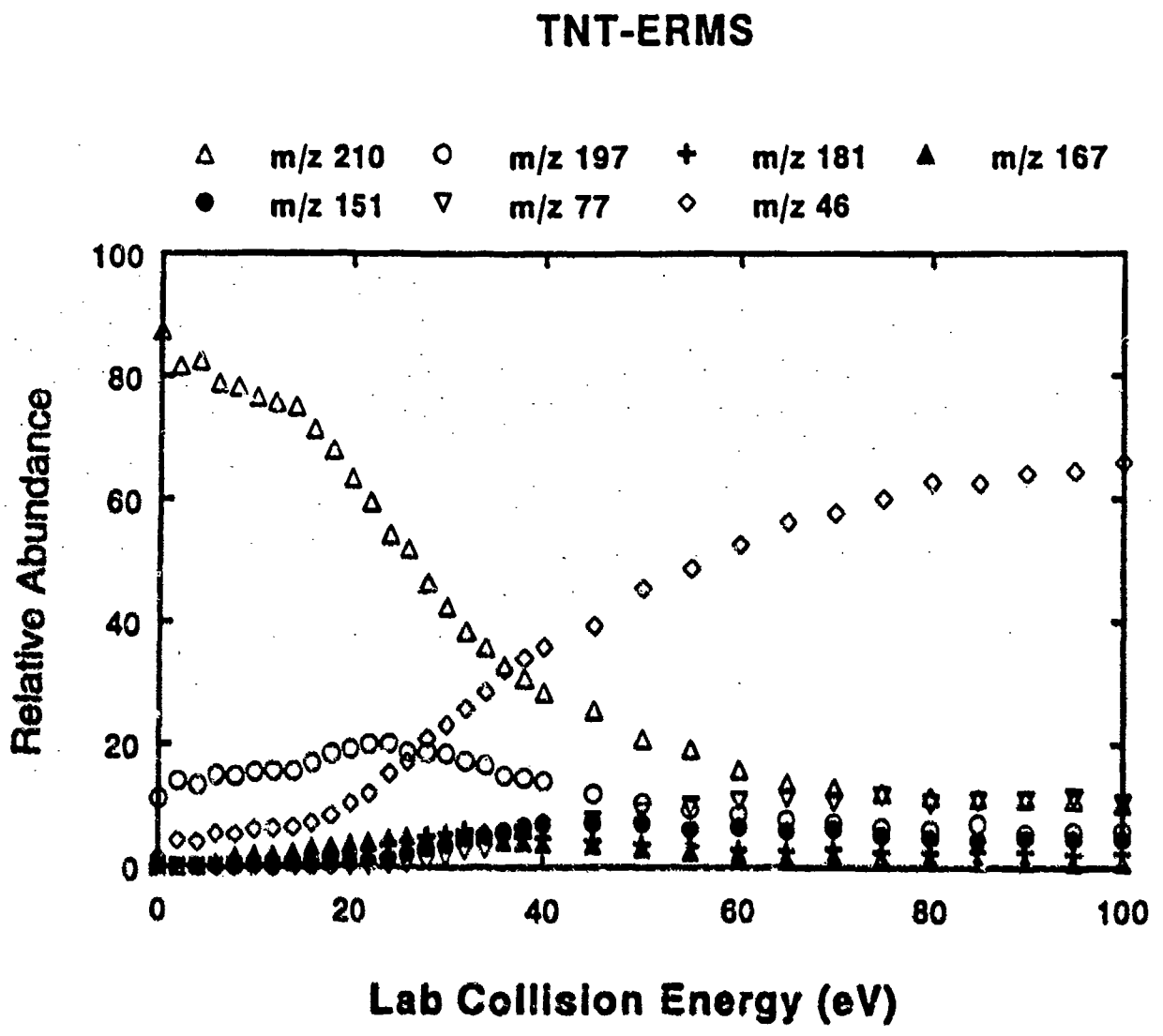


Figure 7

Plot of product ions from m/z 227 (TNT) as a function of collision energy

MODIFICATONS TO THE IONIZATION PROCESS TO ENHANCE THE DETECTION OF EXPLOSIVES BY API/MS/MS

William R. Davidson, Bruce A. Thomson,
Takeo Sakuma, and William R. Stott
SCIEX

Alan K. Akery and Richard Sleeman
British Aerospace Security Systems

1. INTRODUCTION

Atmospheric pressure ionization (API) is presently widely used in trace residue detection equipment, including the British Aerospace/SCIEX CONDOR tandem mass spectrometry (MS/MS) system, and the Barringer Ionscan ion mobility spectrometer (IMS) [Danylewych-May, 1991]. Both these devices modify the normal API reaction mechanisms by adding chemical reagents to increase the potential of detecting explosives.

Ionization at atmospheric pressure is the most efficient method of ionizing molecules that have the appropriate chemical features (eg., strong acids, strong bases, or compounds that are highly electrophilic). In addition, because of the selective nature of the ionization process, common potential background interferences, such as hydrocarbons, do not form ions under atmospheric conditions, and are thus not observed by techniques that utilize ionization detectors.

Due to the presence of nitro or nitrate groups, most explosives are generally highly electrophilic. Electrons are readily attached to the explosive molecules and are not readily released. The resulting explosive ion can then be detected. However, in many instances, the explosive anion decomposes on ionization to form ions such as the nitrite or nitrate anions, both of which can be formed from several other sources. Modifications to the ionization process can be used to alter the chemistry and provide a more selective product ion.

Since IMS operates completely at atmospheric pressure, the resolution of the spectrometer is much lower than that of mass spectrometers which operate under vacuum. Detection schemes based on the observation of one ion under IMS conditions, can lead to a significant incidence of false alarms. The ionization process for several explosives can once again be altered to provide several specific ions relating to the explosive, and thus increase the overall specificity of the IMS detector. A similar technique could also be implemented in an MS/MS approach to increase the selectivity to an even higher level.

2. NEGATIVE IONIZATION AT ATMOSPHERIC PRESSURE

Most devices which form ions at atmospheric pressure use either a corona discharge, or a radioactive foil, most often a beta emitter such as ^{63}Ni, to initialize the ionization process. Although these techniques utilize significantly different methods to initialize the ionization process, the general ion chemistry is identical. Corona discharge systems operate at much higher ion currents than do the radioactive systems, but their reaction times are much shorter. The overall sensitivity of the two approaches for a particular chemical species is similar, but the dynamic range of the corona discharge approach is much broader due to the initial higher concentration of reagent ions [Siegel, 1979].

Reagent ions are formed via a fairly complex series of chemical reactions as illustrated in Figure 1. The major reagent ion at atmospheric pressure in the negative ion mode of operation is O_2^- and its hydrates, $O_2^-[H_2O]_n$. The four pathways for the ionization of explosives can be summarized as follows:

2.1 Charge Transfer

An electron is transferred from the reagent ion to a molecule with a higher electron affinity (ie., more

electrophilic):

$$O_2^- + M \rightarrow M^- + O_2 \qquad (1)$$

The resulting ion, M^-, has a molecular weight identical to that of the original molecule. For example, TNT reacts with the superoxide anion, O_2^-, to form an ion at mass 227, the molecular weight of TNT.

2.2 Proton Transfer

A proton is transferred from the target molecule to the reagent ion. The target molecule is considered a strong acid.

$$O_2^- + M \rightarrow [M\text{-}H]^- + HO_2 \qquad (2)$$

The detected ion, $[M\text{-}H]^-$, would have a molecular weight one mass lower than the original molecule. For example, TNT undergoes this reaction to form a product ion at mass 226.

2.3 Addition or Clustering

A reagent ion, generally NOx- or COx-, clusters with the target explosive molecule.

$$NO_3^- + M \rightarrow [M \bullet NO_3]^- \qquad (3)$$

The resulting ion has a molecular weight equal to the sum of the reagent ion and the target molecule. Nitroesters such as EGDN readily undergo such addition reactions.

2.4 Dissociative Charge Transfer

In many instances, a target molecule will dissociate upon ionization to form a very stable negative anion such as Cl^- or NO_x^-.

$$O_2^- + MNO_3^- \rightarrow NO_3^- + M + O_2 \qquad (4)$$

No molecular weight information about the parent ion is available. Nitroesters and cyclic nitramines, such as RDX, are highly susceptible to these reactions.

3. CHLORIDE ATTACHMENT REACTIONS

For explosives such as the nitroesters, and cyclic nitramines, the normal ionization processes described above are not suitable for use in a reliable explosive detector. The variation in the composition of traces in the ambient air, result in ambiguities in the reagents ions for addition reactions (3), and the intensity of any ions which can be related to the molecular weight of the explosive is low due to dissociation reactions such as reaction (4). However, an additional reagent gas (or gases) can be introduced to overcome these difficulties.

An ideal reagent ion for the detection of explosives is the chloride ion, Cl^- [Thomson, 1980]. It is a very weak base, corresponding to the complementary very strong acid, HCl, and does not readily extract protons from potential interfering compounds in the ambient air. The chloride radical also has a very high electronegativity, and thus, the corresponding chloride ion will not charge transfer to many compounds found at trace levels in ambient air.

One additional, and highly desirable, feature of the chloride ion is its ability to form stable clusters, or addition products with compounds of similar acidity to HCl [Davidson, 1980]. Clusters are also formed from molecules that may chelate with the chloride ion to form a stable addition product. In particular, the chloride ion forms stable clusters with nitroesters such as EGDN, NG, or PETN, as well as nitramines such as RDX and HMX [Tanner, 1983]. The two stable isotopes of the chloride ion, $^{35}Cl^-$ and $^{37}Cl^-$ lead to the formation of cluster ions which are separated by two mass units. For example, for RDX which has a molecular weight of 222, two product ions are formed via chloride addition at masses 257 and 259:

$$^{35}Cl^- + RDX \rightarrow [M \bullet {}^{35}Cl]^- \qquad (5)$$
$$(m/z=257)$$

$$^{37}Cl^- + RDX \rightarrow [M \bullet {}^{37}Cl]^-$$
$$(m/z=259)$$

The chloride ion is formed in the CONDOR tandem mass spectrometer by adding methylene chloride at fairly high concentrations (hundreds of parts per million) to form the chloride reagent ion. The high concentration of chloride is beneficial in reducing the formation of potential interferences from extraneous compounds which may be found in the sampling environment. For example, Figure 2 shows the spectrum in the mass range of 200 to 260 with and without the presence of chloride. Although the ions formed from the butylated hydroxytoluenes (BHT's) are not direct interferences for any explosives, their removal in the presences of chloride is indicative of a wide range of compounds which could potentially interfere.

The chloride also reduces the inherent baseline chemical noise, as can be noted in Figure 2. Since detection limits are based on signal to noise ratios, any reduction in chemical noise will lead to more favorable detection limits.

The rapid reaction to form the chloride ion as the reagent ion, inhibits the dissociative charge transfer reaction (reaction 4) which would otherwise occur if O_2^- were the reagent ion. That is, the very favorable reaction:

$$O_2^- + MCl \rightarrow Cl^- + M + O_2 \qquad (6)$$

acts as a scavenger for the O_2^- and thus minimizes the probability of reaction (4) occurring. This effect, coupled with the formation of chloride addition products for nitroesters and nitramines increases the formation of specific products ions, as opposed to the formation of non-specific fragment ions such as the nitrate ion.

The resulting increase in sensitivity is shown for the detection of EGDN in Figure 3. The ion intensities for the normal parent ion formed in via charge transfer, labelled (a) in the figure, and the chloride addition product, labelled (b), are monitored with respect to time. At approximately 0.2 minutes, EGDN vapor is added to the system and both the monitored ions increase significantly over background. The chloride adduct is formed from residual methylene chloride present in the system. At 0.55 minutes, methylene chloride is introduced into the system, and the chloride ion adduct increases substantially over the M^- parent. The overall increase in sensitivity, due to the presence of the chloride ion, is approximately a factor of 4.

A more dramatic effect is shown for RDX in Figure 4. The thermal desorption profile of the chloride adduct of 1 ng of RDX is shown in box (a) of the figure, versus the M^- parent in the absence of chloride ion in box (b) for a similar 1 ng desorption. The increase in sensitivity is approximately a factor of 100. The major product ion for RDX when no chloride is present is mass 46, a totally non-specific ion.

4. MS/MS OF CHLORIDE ADDUCTS

Although the formation of chloride adducts is specific as an ionization process, additional specificity is achieved by fragmenting the original chloride adduct parent ion (see [Davidson, 1991] for a description of the MS/MS operation of a CONDOR). The true key to the success of this approach is the fact that the chloride adducts tend to be covalent rather than electrostactic clusters. Fragmentation of the parent results in specific fragments, which relate to the structure of the target compound, rather than just the original free chloride.

The fragmentation, or daughter ion, spectrum of the parent chloride adduct of RDX is shown in Figure 5. Although this is a fairly simple spectrum, the fact that a nitrite ion, m/z=46, is formed is fundamental to the specificity of the process. Only ions that

- undergo chloride addition,
- contain a nitrite group, and
- have a molecular weight of 222

will give rise to a mass 46 daughter ion from both the 257 (^{35}Cl adduct) and 259 (^{37}Cl adduct) parent ions. Both these ion pairs are monitored during a normal screening of samples for the presence of RDX-based explosives.

A much more dramatic fragmentation spectrum results from the chloride adducts of HMX, as shown in Figure 6. A series of daughter ions are observed, corresponding to the consecutive loss of $-CH_2N-NO_2$ groups, a neutral loss of 74 mass units. It is interesting to note from the ^{35}Cl and ^{37}Cl spectra, boxes (a) and (b) in Figure 6, that the chloride ion is maintained in the resulting daughter ions, strongly supporting the formation of a covalently bonded complex. This is such a specific fragmentation pattern, that it is highly unlikely that there would ever be a misidentification giving rise to a false alarm.

5. SUMMARY

In systems which are dependent upon the formation of ions through chemical processes, great gains in both sensitivity and selectivity can be achieved through modifications to the reagent ions. In particular, for nitroesters and cyclic nitramines, adding the chloride ion as a reagent can increase the detection capability of an ion-based analytical system, such as the CONDOR MS/MS, by over an order of magnitude.

As demonstrated by the results presented in this paper, the higher probability of detection is a combination of higher sensitivity for the formation of mass-related parent ions, lower chemical background,

and highly specific fragmentation patterns for the resulting chloride addition reaction products.

REFERENCES

Danylewych-May, L.L; Presented at the First International Symposium of Explosive Detection Technology, Atlantic City (1991).

Davidson, W.R.; Nacson, S.; Lane, D.A.; Thomson, B.A.; Proceedings of the 73rd Annual Meeting of the Air Pollution Control Association, p 80-39.8-1, Montreal (1980).

Davidson, W.R.; Stott, W.R.; Akery, A.K.; Sleeman, R.; Presented at the First International Symposium of Explosive Detection Technology, Atlantic City (1991).

Siegel, M.W. and Fite, W.L.; *J.Phys.Chem.*,80,2871,(1976)

Tanner, S.D.; Davidson, W.R.; Fulford, J.E.; Proceedings of the First International Symposium on Analysis and Detection of Explosives, FBI Academy, Quantico, VA, p 409 (1983).

Thomson, B.A.; Davidson, W.R.; Lovett, A.M., *Environ. Health Perspectives*, 36, 77 (1980).

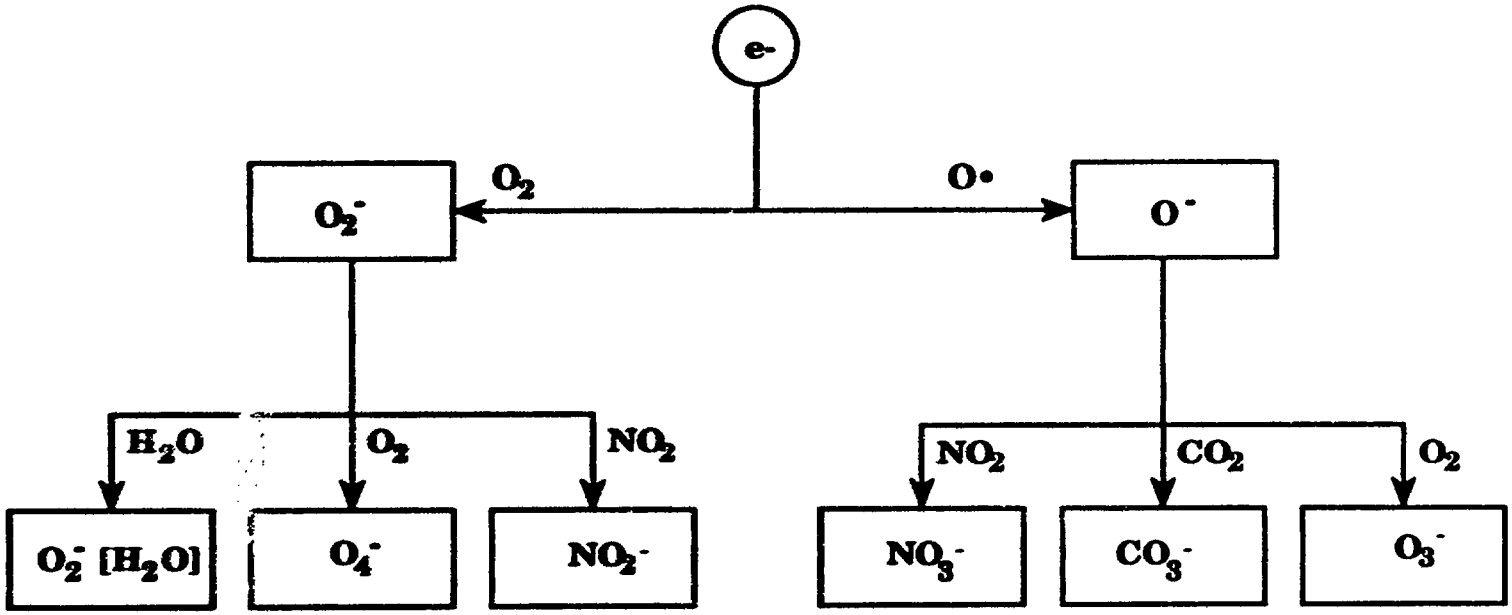


Figure 1 A simplified reaction scheme for the formation of reagent or terminal ions under Atmospheric Pressure Ionization [API] conditions. For simplicity the formation of higher molecular weight water clusters, eg., $O_2^-[H_2O]_n$ in the ionization region is not included.

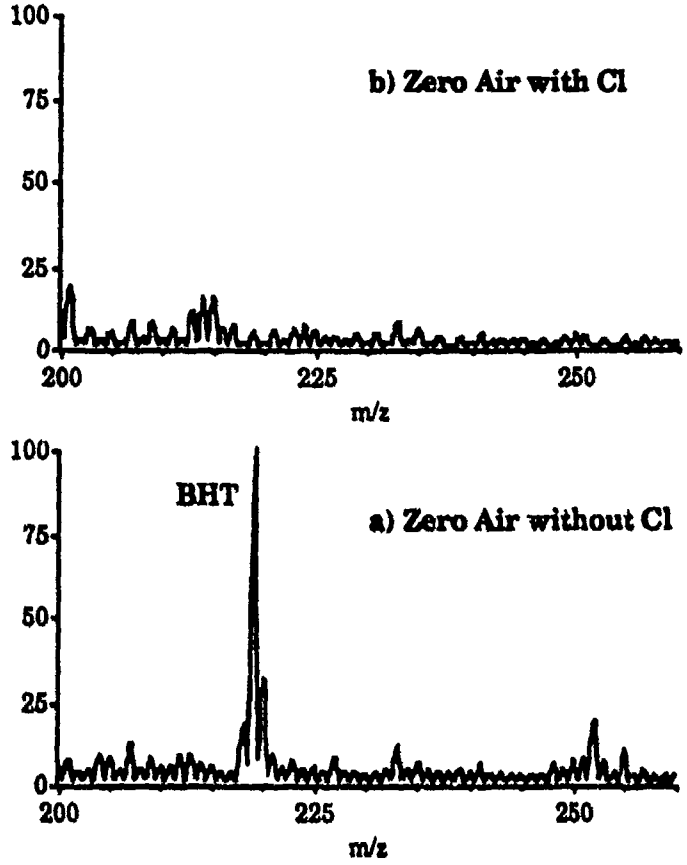


Figure 2 The background spectrum of parent ions in the mass range 200 to 260 with (b) and without (a) the presence of chloride ions. Zero air is an artificial mixture to nitrogen and oxygen at concentrations identical to those found in normal air. BHT refers to the cluster of peaks centered at mass 219 which are formed from butylated hydroxytoluenes.

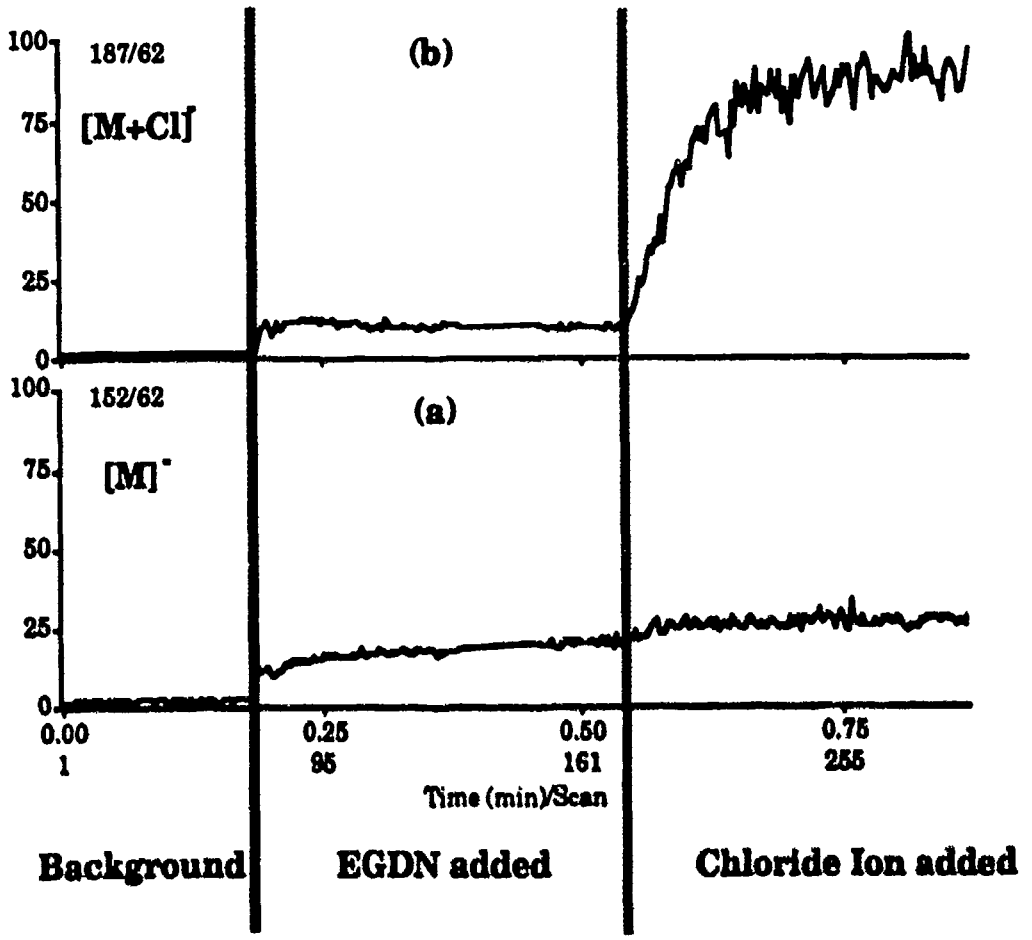


Figure 3 The ion intensities of the standard parent ion (a), and chloride adduct ion (b) are plotted versus time. EGDN vapors are added at 0.2 minutes, and the chloride ion is added to the ionization region at 0.55 minutes.

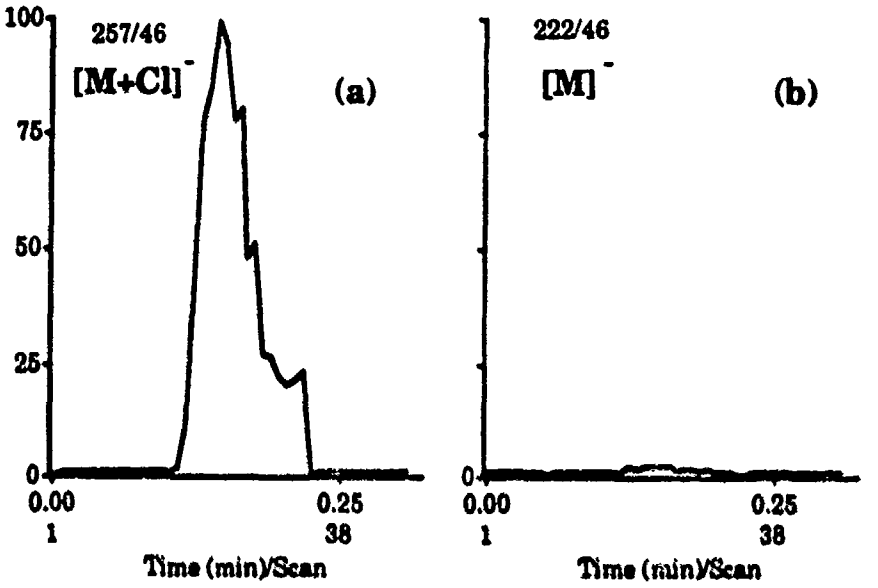


Figure 4 The thermal desorption profiles, intensity versus time during the desorption of a sample, for the chloride ion adduct (a), and standard parent ion (b) for RDX. One nanogram of RDX was thermally desorbed in each case.

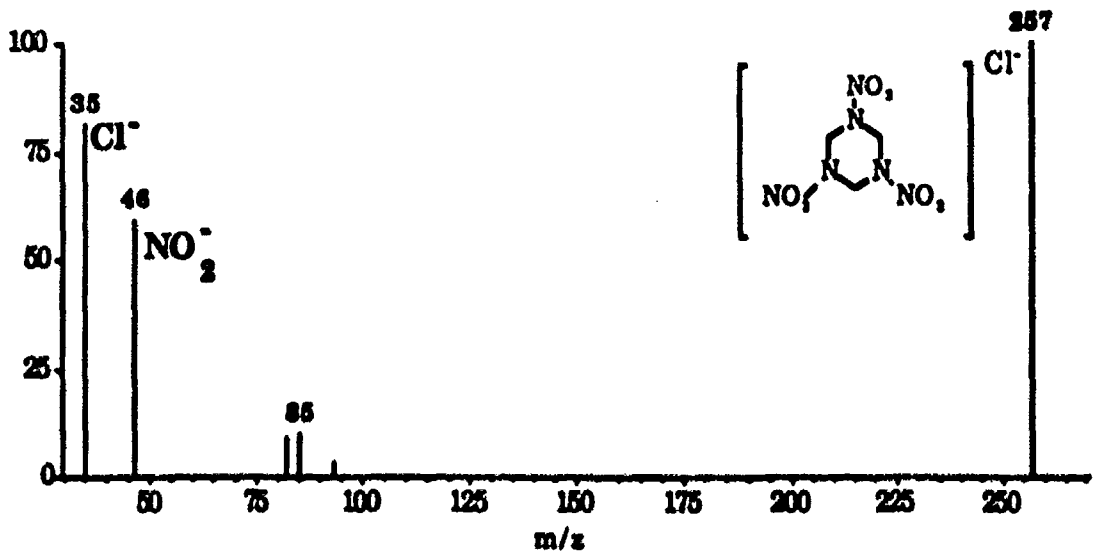


Figure 5 The fragmentation, or daughter ion, spectrum of the ^{35}Cl adduct of RDX. The parent ion has a molecular weight of 257.

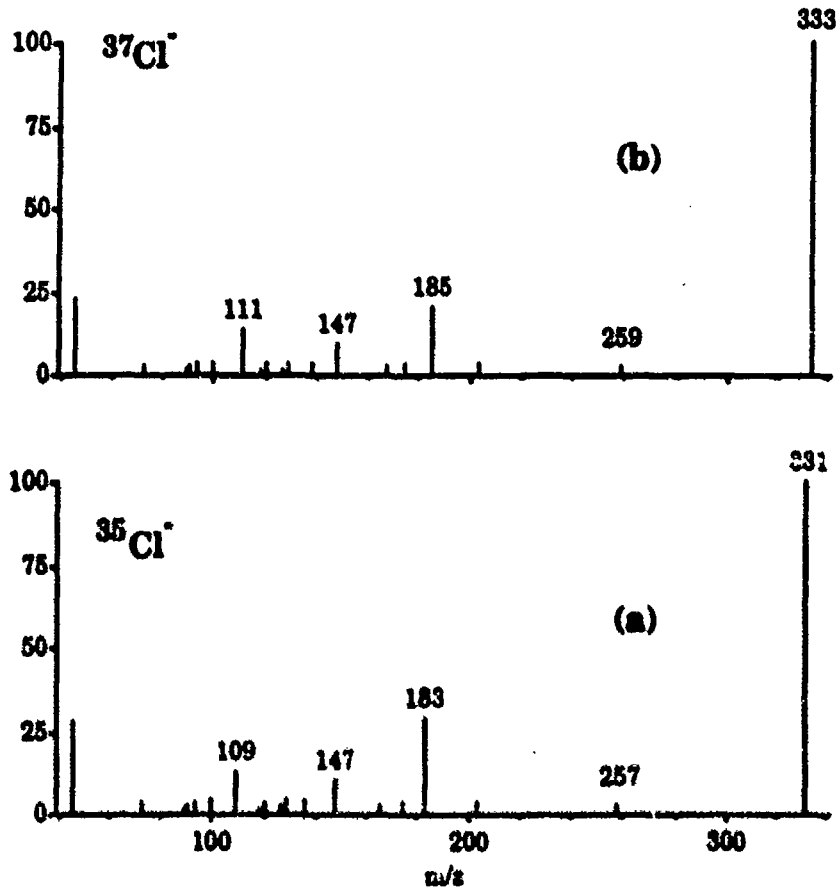


Figure 6 The fragmentation spectrum of both the ^{35}Cl (a), and ^{37}Cl (b) chloride adducts of HMX. Multiple losses of mass 74 correspond to consecutive losses of -CH_2N-NO_2.

THE ROLE OF MASS SPECTROMETRY IN THE DETECTION OF EXPLOSIVES

William R. Davidson and William R. Stott
SCIEX

Alan K. Akery and Richard Sleeman
British Aerospace Security Systems

1. INTRODUCTION

Mass Spectrometry is considered as one of the most sensitive and selective analytical techniques. Over the years, it has played an ever increasing role in the detection of explosives, with the major emphasis on forensic applications [Yinon, 1991]. However, the increasing need for the benefits of mass spectrometry in combating terrorist activities has led to the development of commercial products which are presently in use throughout the world. These benefits include high sensitivity (detection of picogram levels of explosives), high selectivity (ability to detect explosives in highly complex matrices), and the potential for high-speed analysis.

The major differences between the use of a mass spectrometer in a forensic application and the use in the detection of hidden explosives relates mainly to the speed of analysis. In a forensic approach, the major role of the mass spectrometer is to determine the identity of the explosive which has been used in a clandestine activity. This generally occurs after the fact, in an evidence gathering mode, and does not require instant feedback. However, in instances where luggage is being screened for explosives at an airport, the results on each analysis must be available to security officials instantaneously.

To gain the selectivity required for most applications, some separation technique is generally added to the mass spectrometer. Where time is not critical, this is most often a gas or liquid chromatograph. However, analyses under these separation devices may take up to 25 minutes or more, and are thus not suitable for rapid screening applications.

Tandem mass spectrometry [for a review see McLafferty, 1983] or MS/MS offers the ideal solution for rapid screening of luggage or cargo for the presence of explosives. In this case, the separation technique is a mass spectrometer itself, and the separation and complete analysis can be completed within a second or two.

2. HISTORICAL REVIEW

Mass spectrometers were first introduced into the detection of hidden explosive field in the 1970's as modified residual gas analyzers [Yinon, 1981]. In general, air was introduced into the electron impact ion source via a membrane. Overall, these systems were never considered practical since the sensitivity was poor (part per billion) and the selectivity was marginal since no high resolution separation techniques were used.

In the late 1970's, SCIEX introduced a mass spectrometer based on the principles of atmospheric pressure ionization (API) [Buckley, 1978]. Samples could be introduced directly into the ionization region of the mass spectrometer without the complications of membranes. The sensitivity of the SCIEX system was adequate (part per trillion), but it had inherently poor selectivity since only one ion was formed from each explosive, and little structural information was available. Additional separation techniques were required.

The advent of triple-quadrupole tandem mass spectrometry [Yost, 1979] was fundamental in the progress of mass spectrometry applications in this area during the 1980's. SCIEX expanded the capability of their single MS product by adding the separating power of an additional MS [Tanner, 1983]. This system was soon further developed with British Aerospace and introduced as a commercial product in the Middle East in 1986 (the CONDOR Contraband Detection System). The original system was directed towards the detection of explosives and drugs in ISO cargo containers and in the cargo compartments of vehicles. Unlike mass spectrometer systems in use elsewhere, the system was geared towards operation by fairly unskilled operators.

Tandem mass spectrometry was also the key approach followed by other workers in this area, in particular the group at Oak Ridge [McLuckey, 1988, 1989]. They have investigated the use of a glow discharge ion source coupled with MS/MS system comprised of quadrupole/time-of flight, triple quadrupoles, and ion traps.

The major advances for mass spectrometry in the 1990's will likely be oriented towards lowering the cost of the systems and minimizing the complexity of operation. Research and development activities will likely be aimed towards sampling and collection techniques, rather that on the mass spectrometer itself. Reliability and ease-of-use will be critical issues to resolve over the next few years.

3. THE CONDOR TANDEM MASS SPECTROMETRY

The CONDOR system is based on the rapid analysis of complex samples (for example, air cargo vapors and residual dust particles) for the presence of trace levels of contraband material using atmospheric pressure chemical ionization (APCI) coupled with tandem mass spectrometry (MS/MS). The two key areas which separate it from other methods of contraband detection are the sample acquisition network and the method of analysis.

A sample is acquired either by introducing it directly into the ion source of the mass spectrometer or by collecting involatiles or particles on a collector cartridge which is in turn thermally desorbed to provide a vapor sample for analysis. The ions which are formed from the various items in the sample are first separated according to their molecular weight using a quadrupole mass filter. To gain structural information about the selected ions, they are introduced into a fragmentation region where the original ions are broken down into a series of specific fragment ions (or daughter ions). These daughter ions are then mass analyzed using a second mass filter. The resulting ion stream is then measured using a detector, and the output intensity is fed into the data system for a comparison with expected values. The output results (pass/fail) are then fed to a printer and to the touch-screen terminal which acts as the operator interface.

3.1. Sample Acquisition

Sample acquisition is critical in the detection of contraband. The most sensitive instrument will not be able to detect contraband unless the sample is presented to the analyzer. The present methods used by the CONDOR are a direct air analysis technique which is appropriate for volatile signatures of explosives (generally impurities or by-products of the manufacturing process), and collection/desorption techniques which are suitable for the detection of picogram levels of less volatile vapors (eg, nitroglycerine and TNT) and particles which have been left on surfaces during the concealment of the explosives (eg. RDX and PETN).

The CONDOR sample acquisition equipment is presently optimized for both methods of sample acquisition in an air cargo environment. A sampling probe is fitted with a specially designed brush head which in turn is connected to a cartridge housing which holds the collection medium (presently a "T"-shaped device which contains three treated quartz mesh elements). Air is drawn through the sampling probe during the analysis sequence at a rate of 25 l/sec. All the sampled air passes through the collection medium, and explosive vapors and particles are trapped on the quartz mesh elements. A small fraction of the air is passed directly into the ion source region of the MS/MS system where it is analyzed instantaneously for the presence of volatile explosive signatures (for example, MNT and EGDN). The sampling takes place by passing the brush head directly over all available air cargo surfaces within a container or on a pallet. For a typical air pallet the time required to sample all surfaces is about 30 seconds. At the completion of this 30 seconds, the collection cartridge is removed from the sampling probe and inserted into a desorption carousel which is attached to the ion source of the CONDOR.

A second method of collecting involatiles and particles is often used in situations where a suspect cargo is located at a considerable distance away from the CONDOR unit. A self-contained hand-held sampler, complete with an internal battery pack and air pump, is used by a security officer to sample the surfaces of the cargo. The collector cartridge, which is housed in the sampler, is returned to the CONDOR and thermally desorbed in an identical manner as described above for samples taken using the internal CONDOR pump.

3.2 Sample Analysis

The direct air analysis is very straightforward since all the incoming air is in vapor form. However, the

collected particles and less volatile vapors must be desorbed (vaporized) before the analysis can take place. The three quartz elements of the collection cartridge are rotated, in turn, to a desorption position. In that position, a hot-air blast is used to vaporize the particles on the mesh and pass the resulting vapors into the ion source of the system.

The ionization process occurs at atmospheric pressure. This eliminates any need for membranes and/or other transfer methods into an ion source at lower pressure. The advantages to this technique are higher sensitivity, higher reliability (minimal contamination of the vacuum system), higher specificity of ionization (lower false alarms) and faster throughput. For explosives such as those based on RDX, the major ion is a chloride ion complex, which is formed in the ion source from all the species available in the incoming sample. All parent ions formed in the ionization region are fed into the vacuum chamber of the instrument for separation and subsequent analysis.

A schematic diagram of the ion source and mass spectrometer is shown in Figure 1. A series of molecules from a sample are brought into the corona discharge region of the source. Molecules with certain chemical characteristics are ionized (as indicated by the dashed circles). The majority of the molecules in the air stream (for example hydrocarbons) are not ionized and are removed from the source via a suction pump. This leads to a first stage of selectivity in separating out unwanted potential interfering compounds. The ions which were formed are then focussed through an atmospheric pressure to high vacuum interface region into the first region of the tandem mass spectrometer (Q1). In general, explosives are monitored as negative ions. For several of the explosives, eg. RDX and nitroesters, a chloride ion is used to "cluster" with the explosive and provide a specific complex [Thomson, 1980]. This increases the selectivity of the ionization process and increases sensitivity.

The tandem mass spectrometer provides a method of rapidly separating parent ions of a particular mass (using the first of two quadrupole mass filters), fragmenting the selected parent ions (in a collision chamber) and then separating out specific fragment ions which are specific to the explosives of interest using a second mass filter. That is, many other compounds have a parent ion of mass 257 (the chloride complex of RDX), but none are known to fragment to form the same series of daughter ions (fragments) as RDX. The first quadrupole is tuned to mass 257, and only ions which have a molecular weight of 257 are allowed to pass into the fragmentation region (Q2). The impact of the 257 ions with a collision gas results in the breakup of the 257 parent ion into a series of daughters, for example 35, 46, 129 for the chloride complex of RDX. The second mass analyzer (Q3) is then tuned for the specific daughter ions of RDX. Only those ions which start as mass 257 parents and then fragment to the specific RDX daughter ions reach the detector.

The total system is under computer control and several parent/daughter ion pairs can be monitored simultaneously (in fact the analysis is sequential, but the cycle time is extremely rapid). The measured intensities of the various daughter ions, which are formed from the selected parent ion masses and detected on the electron multiplier, are fed into a computer for subsequent data analysis.

3.3 Data Analysis

The selection of the proper ion pairs for each explosive species is critical. The daughter ions must be present at high intensity levels to maximize sensitivity, but they must also be specific to maximize selectivity (or reduce false alarms). Ideally, the higher the number of daughter ions monitored for each explosive of interest, the more selective the analysis. However, the rapid vaporization of the collected explosive vapors or particles does put constraints on the number of ion pairs which can be included in any single desorption of a mesh element. In general, two or three ion pairs are sufficient to produce optimum detection criteria.

Detection is based on a comparison of the observed intensities of all ion pairs versus a threshold value which is based on background readings. The threshold is generally set to minimize false alarms while maximizing the detection of explosives. False alarm rates vary with the application, but units presently in the field are oriented towards a 0.1% false alarm rate for a specific contraband item (false alarm rates are defined as the number of false detections versus the number of cargos examined). For example, although the system has a detection limit of less than a picogram of RDX when dealing with pure standards, the thresholds are set to about ten picograms in normal operations.

3.4 An Example Result

The thermal desorption profile of one of the early, but critical, results obtained using the approach described above, is shown in Figure 2. In 1985, when this data was obtained, it was believed that all explosives could be detected using vapor techniques if instrument sensitivity and sample collection methods could be improved. A sample of the air in an automobile trunk was sampled four hours after 2 Kg of a PETN-based explosive (Hydromex) was placed in the trunk. PETN was readily detected (as can be seen by the high intensity reading for the two ion pairs in Figure 2.) after that short incubation period. This result could not be explained based on the vapor pressure of PETN, and indicated that some trace particles of PETN must have been collected as opposed to vapors. Further testing supported this hypothesis, and sampling techniques were modified to emphasize the collection of trace particles.

4. REAL-TIME SAMPLING

The normal operation mode of the CONDOR is oriented towards the examination of ISO cargo containers. The methods of sampling and data analysis are aimed towards a throughput of approximately 20 containers per hour. A modified version of this approach has been used in the airport environment in various trials, where pallets or air containers were sampled in a batch mode. Although this approach provided the required throughput of baggage, it was not possible to rapidly identify the particular suitcase which contained contraband. That is, if a pallet indicated the presence of contraband, it either required a manual search of all luggage to determine which was the suspect item, or required several secondary samples taken in a binary search technique.

The Real-Time Sampler (RTS) was conceived to overcome the difficulties in batch mode analysis and to orient the overall system more to the needs of baggage examination. The sensitivity and selectivity of the RTS mode is identical to the conventional CONDOR approach, but the RTS offers significant throughput advantages. The system is designed to sample up to 20 items per minute, but has a recommended throughput of 12 items per minute, or 720 per hour. Several sampling stations can be multiplexed to increase the throughput, e.g. three sampling stations would provide an examination rate of over 2000 items per hour for a single CONDOR system.

The Real-Time Sampler consists of a sampling head, sampling line, collector and desorption unit, and a monitor which displays the output analysis results in a histogram format. The sampling head contains a rotating brush to maximize the removal of trace residues for the exterior of baggage or other items. Rapid air flow through a 20 meter smooth bore sampling line minimizes particle loss within the tube and provides a response time of approximately 1 to 2 seconds.

The collection and desorption unit of the RTS is shown in Figure 3. The sampled particles removed from a suitcase, or a similar item, are decelerated as they approach a continuously moving collector (belt) to maximize the collection efficiency of the device. The collected particles are transported along the belt and enter a desorption region where the particles are vaporized. The volatilized sample is then introduced into the ion source of the CONDOR unit where it is ionized and analyzed for the presence of contraband. Non-volatilized material is removed from the belt in a cleaning unit.

The display on the monitor is an output of the relative intensities of the signatures for various explosives or drugs. If all the signatures for a particular target compound exceed threshold, then an alarm is triggered (audio and/or visual).

Feasibility testing of the RTS approach was carried out at Pearson International Airport[1]. A time-based output for the screening of air cargo for RDX-based explosives is shown in Figure 4. Five suitcases were seeded with trace levels of C-4 explosives by touching the outer surface with contaminated hands. Four fingerprints were place on each of the suitcases in locations that would be likely contaminated in real-life situations. The sample throughput was 1 suitcase every three seconds, which meant that only 2 of every 3 items of luggage could be sampled. Of the five suitcases which were seeded, three were sampled directly on one of the fingerprints, one was sampled several inches from a fingerprint, and one suitcase was not sampled at all. The RDX was detected in the four situations where the suitcase was sampled.

5. SUMMARY

The major performance requirements of equipment used in the detection of explosives are sensitivity, selectivity, and speed of analysis. Mass spectrometry, and in particular, tandem mass spectrometry, readily meets all of these requirements.

At present, the complexity and cost of mass spectrometry based systems limit the market application to "high risk" situation. However, it is anticipated that more reliable, and more cost effective systems will allow for the extension of the technique to a much broader market.

REFERENCES

1. Buckley, J.A.; French, J.B.; Reid, N.M.; Proceedings of the New Concepts Symposium and Workshop on Detection and Identification of Explosives, NTIS: Springfield VA, p 109 (1978).

2. McLafferty, F.W.,ed.; *Tandem Mass Spectrometry*, John Wiley & Sons: New York (1983).

3. McLuckey, S.A.; Glish, G.L.; Asano, K.G.; Grant, B.; *Anal. Chem.*, 60, 2220 (1988).

4. McLuckey, S.A.; Glish, G.L. Asano, K.G.; *Anal. Chim. Acta*, 225, 25 (1989).

5. Tanner, S.D.; Davidson, W.R.; Fulford, J.E.; Proceedings of the First International Symposium on Analysis and Detection of Explosives, FBI Academy, Quantico, VA, p 409 (1983).

6. Thomson, L.A.; Davidson, W.R.; Lovett, A.M., *Environ. Health Perspectives*, 36, 77 (1980).

7. Yinon, J.; *The Analysis of Explosives*. Pergamon: Oxford (1981).

8. Yinon, J.; *Mass Spectrometry Reviews*, 10, 179 (1991).

9. Yost, R.A.; Enke, C.G.; *Anal. Chem.*, 51, 1251A (1979).

NOTE

1. The trials were carried out during November and December of 1989. A report is available to authorized agencies from Transport Canada or Canada Customs.

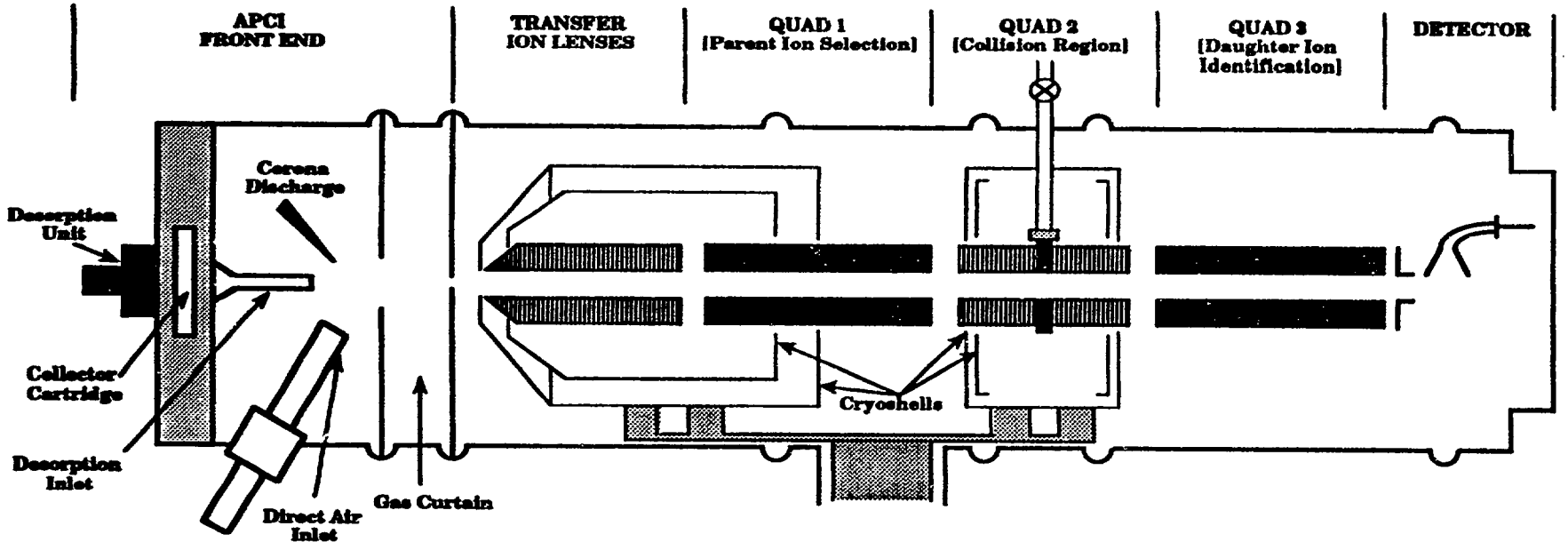


Figure 1 A Schematic Diagram of the Ion Source and Analysis Region of an API-based Triple Quadrupole Mass Spectrometer.

Figure 2 Thermal Desorption Profile from a Sample Obtained in an Automobile Trunk Which Housed 2 Kg of Hydromax, a PETN-based Explosive.

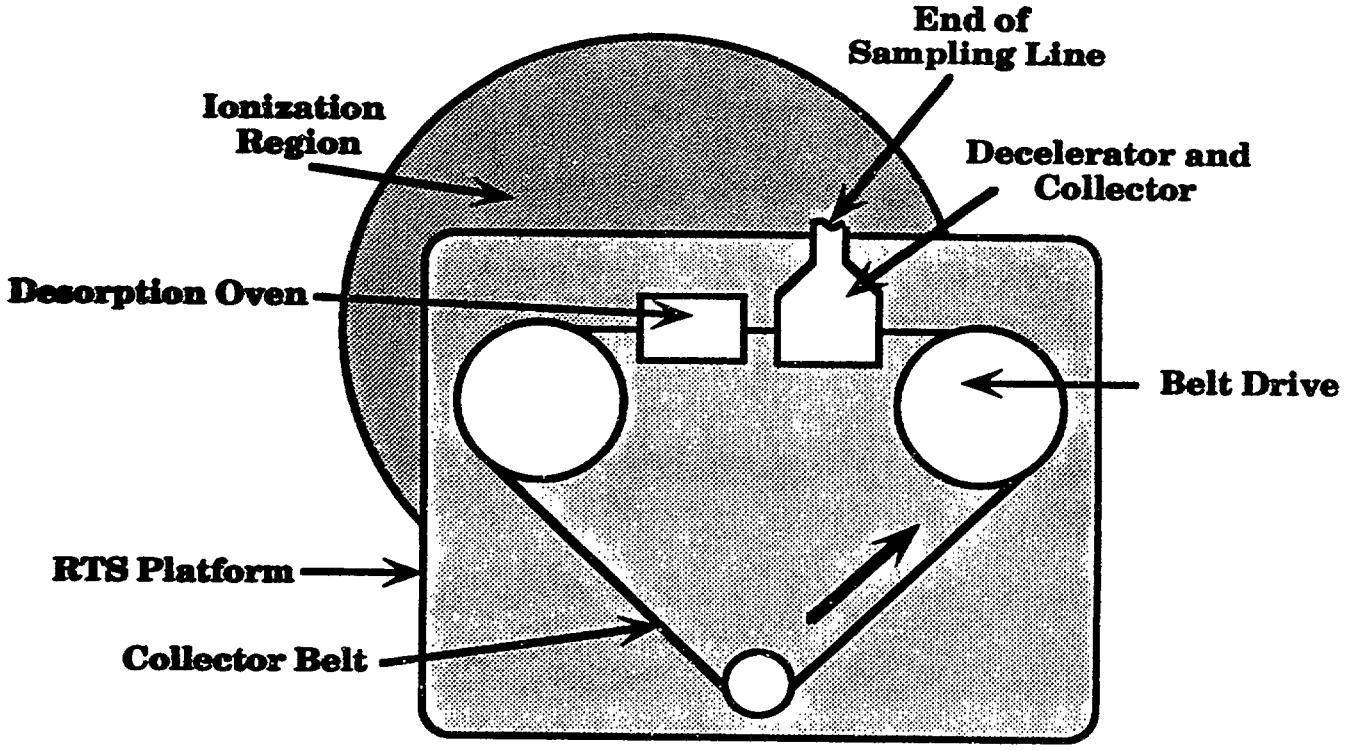


Figure 3 A Schematic Diagram of the Sample Collection/Desorption Region of a Real-Time Sampler.

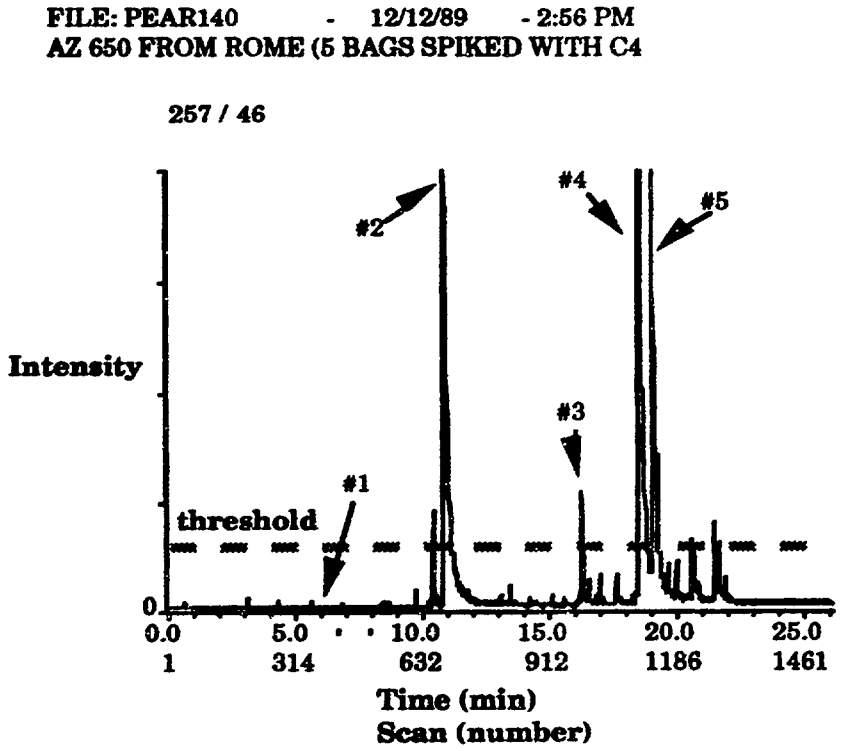


Figure 4 Signal versus Time Profile for RDX Obtained During the Screening of Air Cargo. Five suitcases (labelled #1 through #5) were seeded with residues of C-4. Suitcase #1 was not sampled due to throughput limitations, suitcase #3 was sampled several inches away for the site of the C-4 residue.

MODIFICATIONS TO THE IONIZATION PROCESS TO ENHANCE THE DETECTION OF EXPLOSIVES BY IMS

Lucy L. Danylewych-May
Barringer Research Limited
304 Carlingview Drive
Rexdale, Ontario, Canada

1. INTRODUCTION

The ionization of trace compounds at atmospheric pressure in plasma chromatography is accomplished by ion-molecule reactions. The nature of the ions formed depends on the type of reactant ions generated by the ionization source in the reaction region and the operating temperature in the ionization and drift tube regions.

Using ^{63}Ni as an ionization source and air as drift and carrier gas the free electrons are converted to primarily $(H_2O)m.O_2^-$ ions. The ion chemistry in the IONSCAN can easily be modified by changing reactant ion through introduction of a suitable dopant to facilitate formation of molecular ions and molecule-ion clusters from trace compounds. The types of ions formed from several explosive substances and taggants of interest are discussed here.

2. IONSCAN PRINCIPLE OF OPERATION

A commercially available instrument from Barringer Inc., shown in Figure 1, is based on an ion mobility spectrometer (IMS) as a detector. The basic principle of IMS operation is well reported in the literature (Carr) and will not be dwelt on here. The major differences between the IONSCAN and other commercially available units are the flexibility in temperature controls in three regions: sample desorption, sample transfer line which is connected to the reaction chamber, and the drift tube.

The type of reactant ion can also be easily changed from one to another. An independent temperature control of the desorber and ease with which either liquid, solid or preconcentrated vapour samples can be introduced into the IMS ionization chamber allows great flexibility in studying different compounds of interest.

Results from IONSCAN analyses were stored on a PC for further data evaluation and hard copy record. The relevant IMS operating conditions are summarized in Table 1.

Stability of formed molecular-ion clusters can be improved for some compounds by lowering IMS operating temperatures.

Formation of multiple ions from a molecular species enhances selectivity in the identification of a particular substance in the presence of contaminants.

3. IONIZATION PROCESSES

The IMS detector is operated in the negative mode since all explosives of interest form stable negative ions.

The important ionization processes in the negative mode are:

- Dissociative electron transfer
- Proton transfer (proton abstraction)
- Ion-molecule attachment

3.1 Dissociative Electron Transfer

The major reactant ion in the ionization region, when air is used as a drift gas, is the hydrated O_2^- ion. Upon introduction of a chlorinated hydrocarbon, dissociative electron transfer takes place:

$$O_2 + MCl_n \rightarrow Cl^- + MCl_{n-1} + O2 \qquad (1)$$

3.2 Proton Transfer

Most organic compounds do not readily undergo direct charge transfer reactions, especially in the presence of an ion with high proton affinity. Proton transfer reactions are more common in the negative mode than charge transfer. Proton transfer (or a proton abstraction) reactions are based on gas phase

acidities. The ion-molecule reaction proceeds as,

$$M + Cl^- \rightarrow (M-H)^- + HCl \qquad (2)$$

3.3 Ion-Molecule Attachment

Several small ions, and especially halide ions, can undergo a clustering reaction with a trace compound. Theoretically, halide attachment reactions should occur with almost all organic compounds. However, not all cluster ions can survive at high temperature and pressure. If the ion attachment product is weakly bound, it will fall apart in the drift region before it reaches the collector. A strongly bound ion-molecule cluster is formed due to covalent sharing of the acidic hydrogen. When interaction is strictly electrostatic the cluster will not normally survive. Decreasing the operating drift tube temperature improves stability of weakly bound ion-molecule clusters.

4. EXPLOSIVE ION IDENTIFICATION

The analyses of the explosive compounds were carried out on the IONSCAN manufactured by Barringer. The explosives and proposed taggants investigated were: dinitrotoluene (DNT), mononitrotoluene (MNT), trinitrotoluene (TNT), cyclonite (RDX), pentaerythritol tetranitrate (PETN), ethyleneglycoldinitrate (EGDN), nitroglycerin (NG), tetranitramine (HMX), trinitrophenylethyl nitramine (tetryl), and dimethyldinitrobutane (DMDNB). The explosive analytes used for the study were pure analytes supplied by Standard Analytical Reference Materials (SARMs). The IMS operating conditions are summarized in Table 1.

Although the IMS operating temperature was varied between 290°C and 50°C, results from only three temperatures will be reported here (50, 100 and 260°C).

4.1 High Operating Temperature

At 260°C single molecular ions were observed from DNT, RDX, TNT and HMX. Based on ion identification for TNT and DNT reported in literature and reduced mobilities of Cl^- and NO_3^- (Asselin, 1978, Wernlund, 1978, Spangler, 1976) the ions formed from the above explosives are believed to be $(M-H)^-$ ions. At high operating temperature no changes in reduced mobilities were observed by replacing Cl^- reactant ion with O_2^- ion.

EGDN, PETN and NG were detected only as NO_3^- ion. Results from these studies are summarized in Table 2.

4.2 Medium Operating Temperature

At an operating temperature of 100°C all of the explosive substances tested were detected as proton abstracted molecular ions. In addition to the proton abstracted molecular ion, ion-molecular clusters were also formed for all explosive substances investigated. However, for TNT and DNT, an ion-molecule cluster was detected only at high concentration (nanogram concentration).

A typical plasmagram for RDX is shown in Figure 2. RDX gives rise to four different ions. The ion denoted by peak 5 is due to proton abstraction, while peaks 2 and 3 are molecule-ion clusters with chloride and nitrate ions, respectively. Peak 4 becomes prominent at higher concentration and the ion is believed to be clustering of an RDX molecule with an $(RDX-NO_2)^-$ ion. When O_2^- is used as a reactant ion a peak 2 shifts to longer drift time and it would appear to be due to $RDX.(H_2O.O_2)^-$ ion cluster.

To confirm the origin of peak 3, chloride reactant ion was replaced with NO_3^- reactant ion. Under these conditions the only peak observed from RDX is peak 3 as is seen in Figure 3.

Similar ion formation patterns were observed for NG, PETN, HMX and Tetryl. In the case of Tetryl an additional peak was detected with an ion mass corresponding to $(M-NO_2)^-$.

When commercial explosives are examined, the peak associated with the NO_3^- clustering is much more prominent than for the pure analyte; this is especially true for explosives containing PETN. This is due to partial decomposition of PETN resulting in NO_3^- ion presence in the reaction chamber and thus enhancing the formation of the ion-molecule cluster associated with the NO_3^- ion. An example of the above is shown in Figures 4 and 5.

An RDX-based plastic explosive, such as C-4, appears to be more stable and very little NO_3^- ion is observed, although more than in pure analyte.

4.3 Low Operating Temperature

At an operating temperature of 100°C the two proposed explosive taggants, EGDN and DMDNB, could not be detected. By lowering the IMS

operating temperature to 50°C the two taggants were easily detected. All other explosives previously mentioned showed the same basic ion pattern observed at 100°C.

The two peaks observed for EGDN are associated with chloride and nitrate ion attachment to the EGDN molecule. The intensity of the nitrate peak is about one third of that of EGDN.Cl^- ion when pure EGDN is used. The EGDN plasmagram is shown in Figure 6. Traces of NG (peaks 8 and 9) are observed in this record.

Increasing traces of the NO_3^- ion concentration in the reaction chamber enhances EGDN.NO_3^- formation; however replacing Cl^- reactant ion with NO_3^- ion resulted in almost complete disappearance of both EGDN ions. Similar results were obtained with NG at 100°C and 50°C IMS operating temperatures.

The ions observed from DMDNB are proton abstracted ions, and chloride and nitrate ion attachment. The effect of the NO_3^- ion concentration in the reaction chamber was similar to that of EGDN and NG.

4.4 Ion Mass Identification

The inferred chemical identity of the ion formed from different explosives or explosive taggants was based partially on previously identified ions in the literature using IMS/MS and by enhancing peak intensity by changing the reactant ion in the ionization chamber. In addition to the above a plot of drift time as a function of ion mass was used to infer mass of other ions that could not be identified otherwise. The drift times at different temperatures were normalized to the drift time of $(TNT-H)^-$ at 100°C. Reduced mobilities were also calculated based on measured drift times and assumed reduced mobility for $(TNT-H)^-$ to be 1.450 $cm^2V^{-1}s^{-1}$. This value of reduced mobility was arrived at from calculations at high temperature (260°C) and assuming $(K_o)NO_3^- = 2.44$ and $(K_o)Cl^- = 2.74$ $cm^2V^{-1}s^{-1}$.

From the original theory by McDaniel the ion mobility is given by:

$$K = \frac{3e}{16N}\left\{\frac{1}{m} + \frac{1}{M}\right\}^{1/2}\left\{\frac{2\pi}{kT}\right\}^{1/2}\frac{1}{\omega_D} \quad (3)$$

where K - ion mobility, and determines the drift time for a given drift distance, temperature (T), pressure (gas density, N), electrostatic field (e - the charge on the ion)

M - is the mass of the neutral drift gas molecules

m - is the ion mass

ω_D - is the average collision cross section

From the above equation a non-linear relationship is seen between ion mobility and mass.

A semilogarithmic plot of reduced mobility as a function of ion mass should produce a straight line. A semilogarithmic plot of K^{-1} as a function of M/Z did not result in a straight line. However, a plot of K^{-1} or t_D as a function of ion mass produced a reasonably straight line over a wide range of ion mass. The breakdown appears to occur at mass around 100 Daltons and also for very large ions. For very large ions there is some doubt as to their identity.

Ion drift time data and the related reduced mobilities calculated from the equation (4) are summarized in Table 2 for a number of explosives and explosive related compounds.

The reduced mobility can be calculated from the measured drift time as follows:

$$K_o = \frac{d\,T_o\,P}{E\,T_d\,P_o T\,t_D} \quad (4)$$

where K_o - is the reduced mobility ($cm^2V^{-1}s^{-1}$)

d - is the drift tube length

T_o, P_o - standard temperature and pressure 273°K and 760 torr respectively

P - is the operating pressure, which is the atmospheric pressure at the time of plasmagram generation

E - is the electric field strength in the drift tube (V/cm)

t_D - is the measured drift time from the middle of the gating pulse in seconds

T - is the drift tube temperature.

Some variations in the reduced mobility with IMS temperature have been observed for some compounds. Almost no variation was observed for $(TNT-H)^-$ ion (about 1 %) throughout the temperature range studied. Variations observed were random and probably are due to inaccuracies in the drift tube temperature reading rather than the reduced mobility itself. Based on IMS operating conditions and the drift tube length the reduced mobility for the $(TNT-H)^-$ ion was found to be 1.590 $cm^2V^{-1}s^{-1}$. In column 5 of Table 3, reduced mobilities, calculated from the equation (4) using measured drift times, drift tube length and the operating parameters are given for a number of ions observed in this study.

5. CONCLUSIONS

A thorough understanding of the physics of plasma chromatography requires further fundamental research work into the nature of the ion molecule reactions and development of an ion mobility theory. If one deals with compounds of similar structure and properties, a direct relationship, to a first degree of approximation, between inverse of reduced mobility, or drift time, and ion mass can be assumed.

In the drift region, ions may undergo a variety of reactions with molecules of the drift gas and trace impurities introduced with air and sample. The types of ion-molecule clustering processes that may take place in the drift tube region are also influenced by the operating temperatures. Change in drift tube temperature may emphasize some interactions and reduce others, resulting in either totally different ions or the same ion but with a slightly different drift time. For example, traces of water in the drift gas affect reduced mobilities of some compounds more than others. Hence, it is usually impossible to identify the ions that are collected at the end of the drift tube with certainty unless an auxiliary mass spectrometer is used.

In cases where multiple ions are formed from one molecular species, the ion's identities may be inferred using a number of approaches. Using literature values for the species as a starting point, the ion chemistry can be modified using different reactants giving rise to preferential formation of one or more of the other ions, and thus identity may be inferred from the pattern of ion formation. In addition, literature values of related compounds, similar in structure, and properties can be utilized. Finally, a plot of drift times or inverse reduced mobilities as a function of M/Z is very useful in estimating ion masses.

By adjusting operating IMS parameters and by modifying ion chemistry (changing reactant ion) it is possible for many compounds to form more than one type of ion from the same parent molecular species. Although this inherently reduces sensitivity, the specificity for identification of a particular compound in the presence of impurities improves greatly.

REFERENCES

1. Asselin, M., Proceedings: New Concepts Symposium and Workshop on Detection and Identification of Explosives, Reston, VA, 177 (1978).

2. Carr, T.W., "Plasma Chromatography", Plenum Press, New York (1984).

3. McDaniel, E.W., Collision Phenomena in Ionization Gases, John Wiley, N.Y. 426 (1964).

4. Spangler, G.E. and Collins, C.I., Anal. Chem., 48, 612 (1976).

5. Wernlund, R.F. et al, Proceedings: New Concepts Symposium and Workshop on Detection and Identification of Explosives, Reston, VA, 185 (1978).

TABLE 1
IMS OPERATING PARAMETERS

Gate	200 μs
Single scan duration	24 ms (26 ms for 50°C)
Sample desorber temperature	210°C
Transfer line temperature	50°C to 290°C
Data acquisition interval	25 μs
Carrier and drift gas	prepurified room air
Drift tube T ° C	50° to 290°C
Drift tube length	7.0 cm
Drift field	180 to 230V/cm

Table 2
Ions Generated in IMS at Three Different Temperatures and with Chloride Reactant Ion

Ion	50°C	100°C	260°C
(m-MNT-H)$^-$	minor	minor	
m-MNT.Cl$^-$	major	major	not tested
m-MNT.NO_3^-	minor	minor	
(DNT-H)$^-$	major	major	major
DNT.Cl$^-$	trace	trace	—
(TNT-H)$^-$	major	major	major
TNT.(TNT-NO_2)$^-$	at high conc.	at high conc.	not observed
(DMDNB-H)$^-$	minor	not	not
DMDNB.Cl$^-$	major	detected	detected
DMDNB.NO_3^-	minor		
EGDN.Cl$^-$	major	not	detected
EGDN.NO_3^-	minor	detected	as NO_3^-
(NG-H)$^-$	minor	minor	detected
NG.Cl$^-$	major	major	as NO_3^-
NG.NO_3^-	minor	minor	
(RDX-H)$^-$	trace	trace	—
RDX-Cl$^-$	major	major	major
RDX.NO_3^-	minor to major	minor to major	trace
RDX.(RDX.Cl)$^-$	at high conc.	at high conc.	—
(Tetryl-NO_2)$^-$	trace	trace	—
Tetryl.Cl$^-$	major	major	major
Tetryl.NO_3^-	minor to major	minor to major	—
Tetryl.			
(Tetryl-NO_2)$^-$	at high conc.	at high conc.	—
(HMX-H)$^-$	trace	trace	—
HMX.Cl$^-$	major	major	major
HMX.NO_3^-	minor to major	minor to major	—
(PETN-H)$^-$	minor	minor	detected
PETN.Cl$^-$	major	major	as NO_3^-
PETN.NO_3^-	minor to major	minor to major	
PETN.ClO_3^-	minor	minor	

Table 3a

Drift Times and Reduced Mobilities for Explosives and Taggants

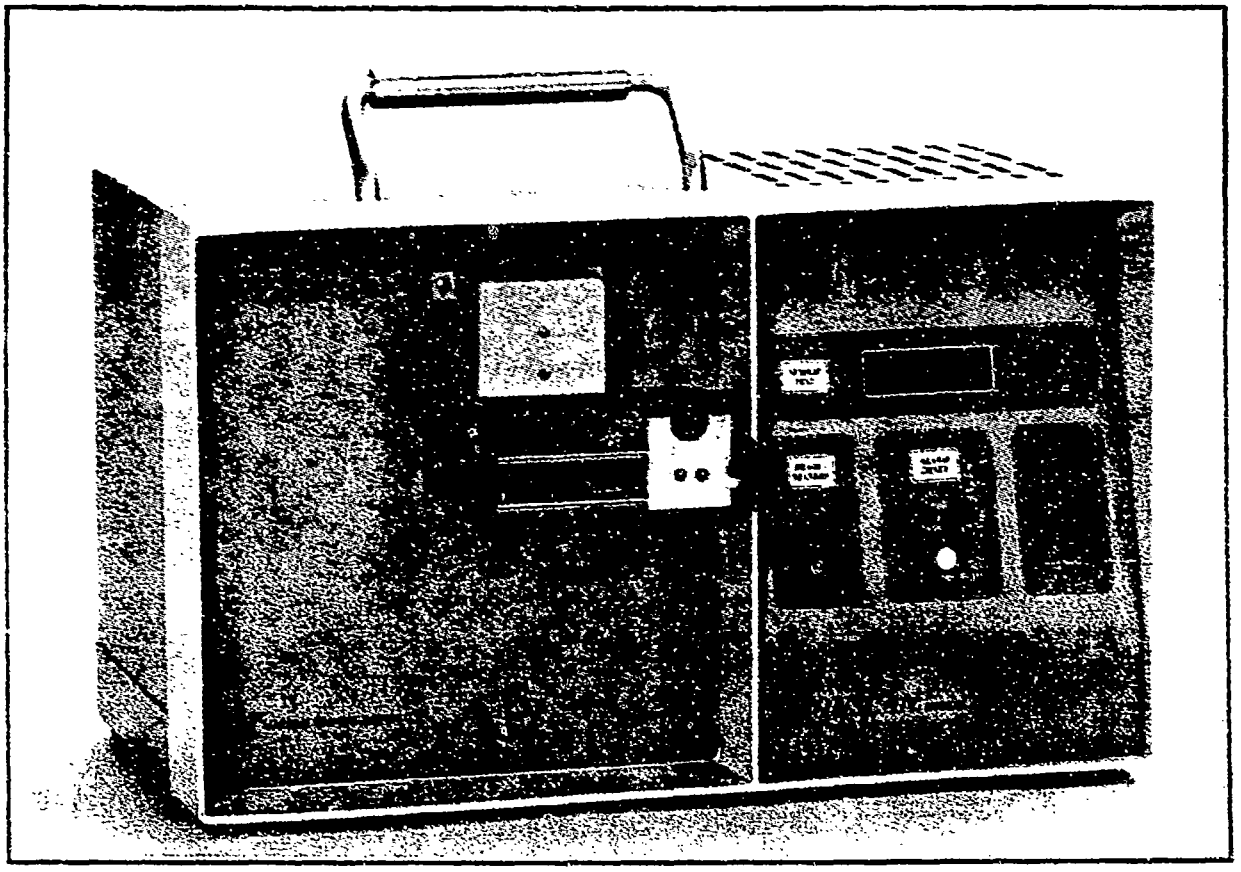
Ion	M/Z Daltons	[1]T_D (ms)	[1]K_o ($cm^2V^{-1}s^{-1}$)	[2]Ko $cm^2V^{-1}s^{-1}$
Cl^-	35	6.77	2.743	3.007
Cl_2^-	70	9.03	2.223	2.437
$H_2O.Cl^-$	53	7.99	2.513	2.755
[3]NO_3^-	62	8.23	2.440	2.675
$H_2O.O_2^-$	68	9.16	2.194	2.406
ClO_3^-	82	9.54	2.107	2.310
$H_2O.NO_3^-$	100	10.98	1.935	2.012
(m-MNT-H)$^-$	136	12.66	1.587	1.740
m-MNT-Cl^-	172	13.67	1.470	1.612
m-MNT.NO_3^-	199	14.56	1.380	1.513
(DNT-H)$^-$	181	12.80	1.569	1.672
DNT.Cl^-	216	13.97	1.438	1.577
[4](DMDNB-H)$^-$	176	13.14	1.556	1.706
DMDNB.Cl^-	211	13.85	1.450	1.590
DMDNB.NO_3^-	238	14.47	1.388	1.522
[5]EGDN.Cl^-	187	13.14	1.528	1.675
EGDN.NO_3^-	214	13.93	1.438	1.597
(NG-H)$^-$	227	13.85	1.450	1.590
NG.Cl^-	262	14.94	1.345	1.475
NG.NO_3^-	289	15.66	1.283	1.407
(TNT-H)$^-$	227	13.85	1.450	1.590
TNT.(TNT-NO_2)$^-$	410	18.61	1.070	1.173

1 Based on TNT (t_D = 13.85 ms, Ko = 1.45 $cm^2V^{-1}s^{-1}$)
2 Calculated from instrument and operating parameters
3 Observed at high drift tube temperature
4 Observed at low drift tube temperature

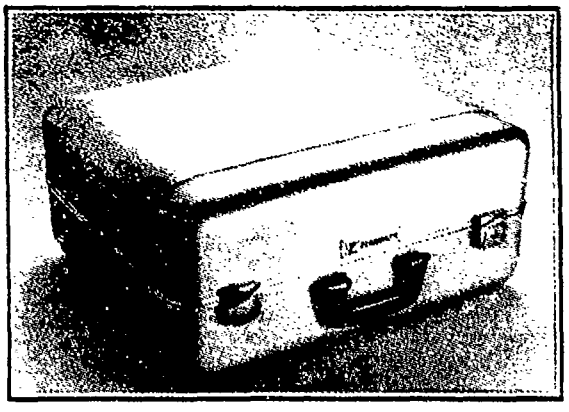
Table 3b
Drift Times and Reduced Mobilities for Explosives and Taggants

Ion	M/Z Daltons	^1t_D (ms)	^1K_o ($cm^2V^{-1}s^{-1}$)	^2Ko $cm^2V^{-1}s^{-1}$
$(RDX-H)^-$	221	13.48	1.490	1.634
$RDX.Cl^-$	257	14.45	1.390	1.524
$RDX.(H_2O.Cl)^-$	272	14.70	1.475	1.618
$RDX.NO_3^-$	284	15.28	1.315	1.442
$RDX.(RDX.Cl)^-$	479	21.15	0.950	1.042
$(Tetryl-NO_2)^-$	240	14.55	1.385	1.518
$Tetryl.Cl^-$	322	16.32	1.231	1.350
$Tetryl.NO_3^-$	349	16.84	1.193	1.308
$Tetryl(Tetryl-NO_2)^-$	537	23.06	0.871	0.955
$(HMX-H)^-$	294	15.28	1.316	1.443
$HMX.Cl^-$	331	16.10	1.248	1.368
$HMX.NO_3^-$	358	16.82	1.194	1.309
$(PETN-H)^-$	316	16.44	1.222	1.340
$PETN.Cl^-$	351	17.42	1.153	1.264
$PETN.NO_3^-$	378	18.20	1.104	1.210
$PETN.ClO_3^-$	401	18.77	1.063	1.666

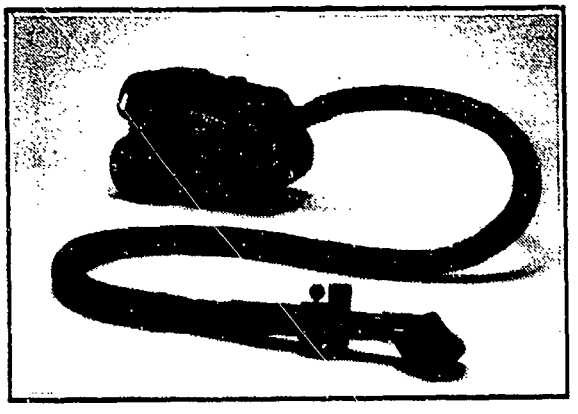
1 Based on TNT (t_D = 13.85 ms, Ko = 1.45 $cm^2V^{-1}s^{-1}$)
2 Calculated from instrument and operating parameters



Detector Unit



Pump / Power Supply Unit



Remote Sample Collector

Figure 1. The ion mobility spectrometer, IONSCAN, with pump/power supply unit and remote sample collector manufactured by Barringer Inc.

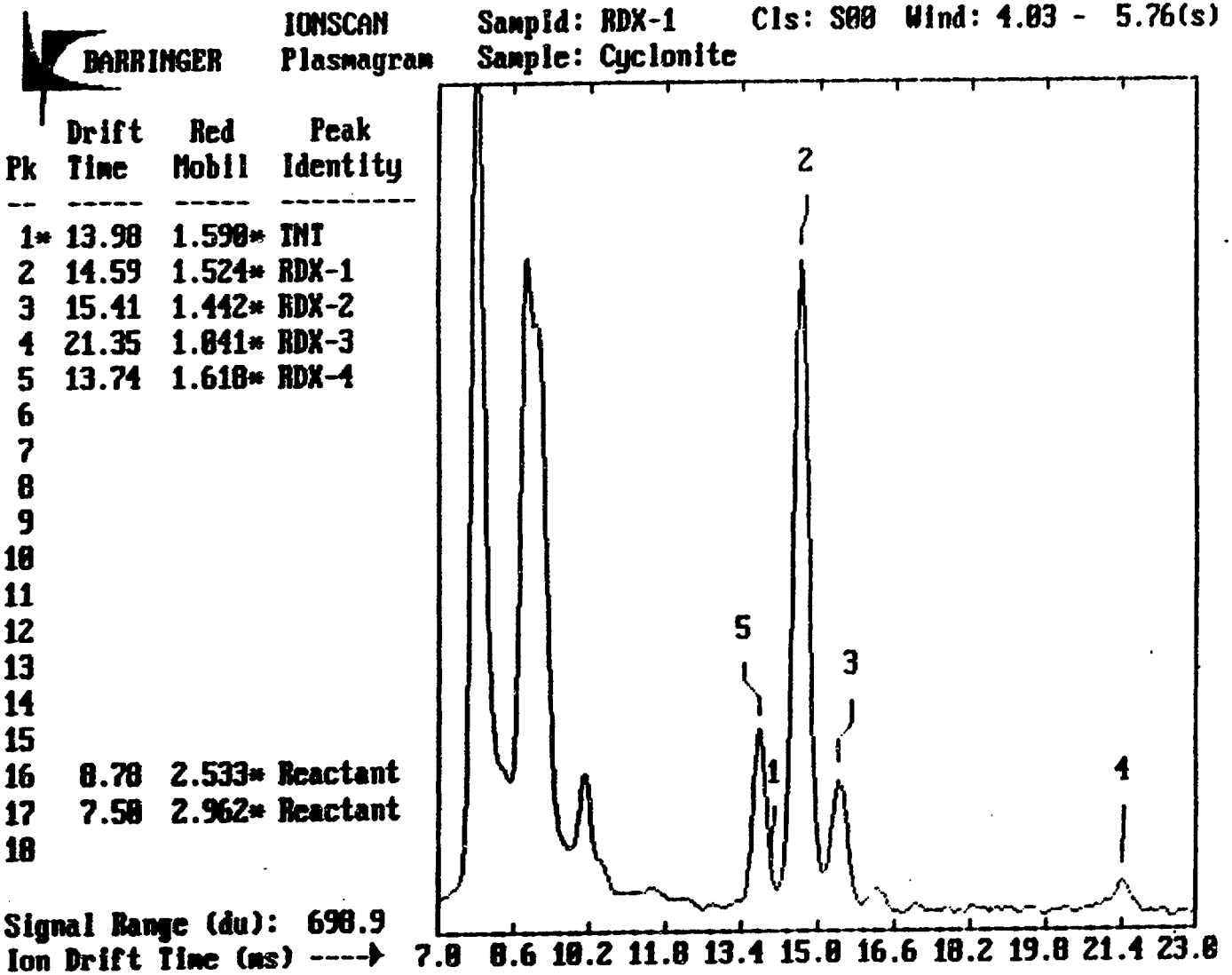


Figure 2 Plasmagram of RDX with chloride as a major reactant ion and IMS operating temperature of 100°C.

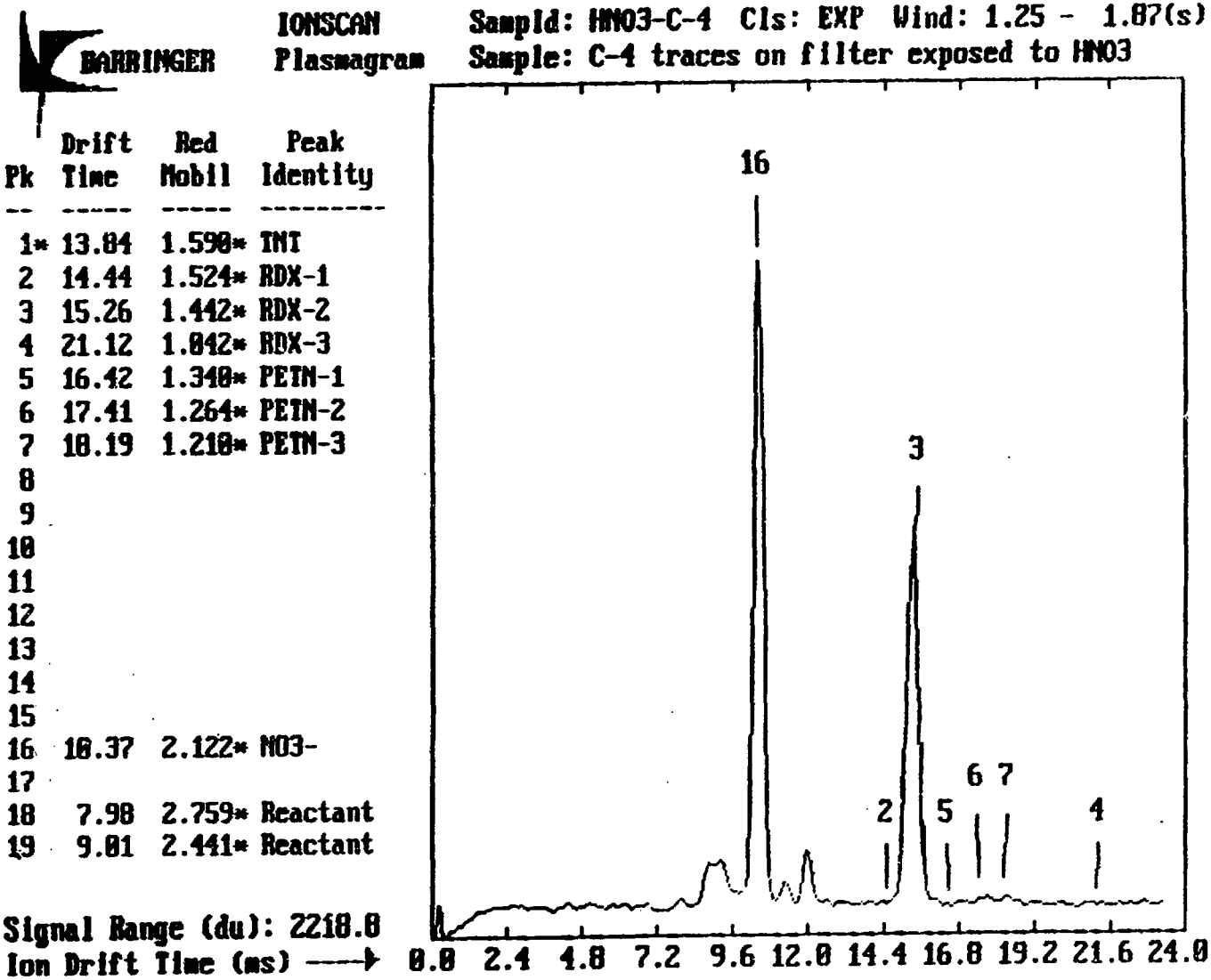


Figure 3 Plasmagram of RDX with nitrate as a major reactant ion and IMS operating temperature of 100°C.

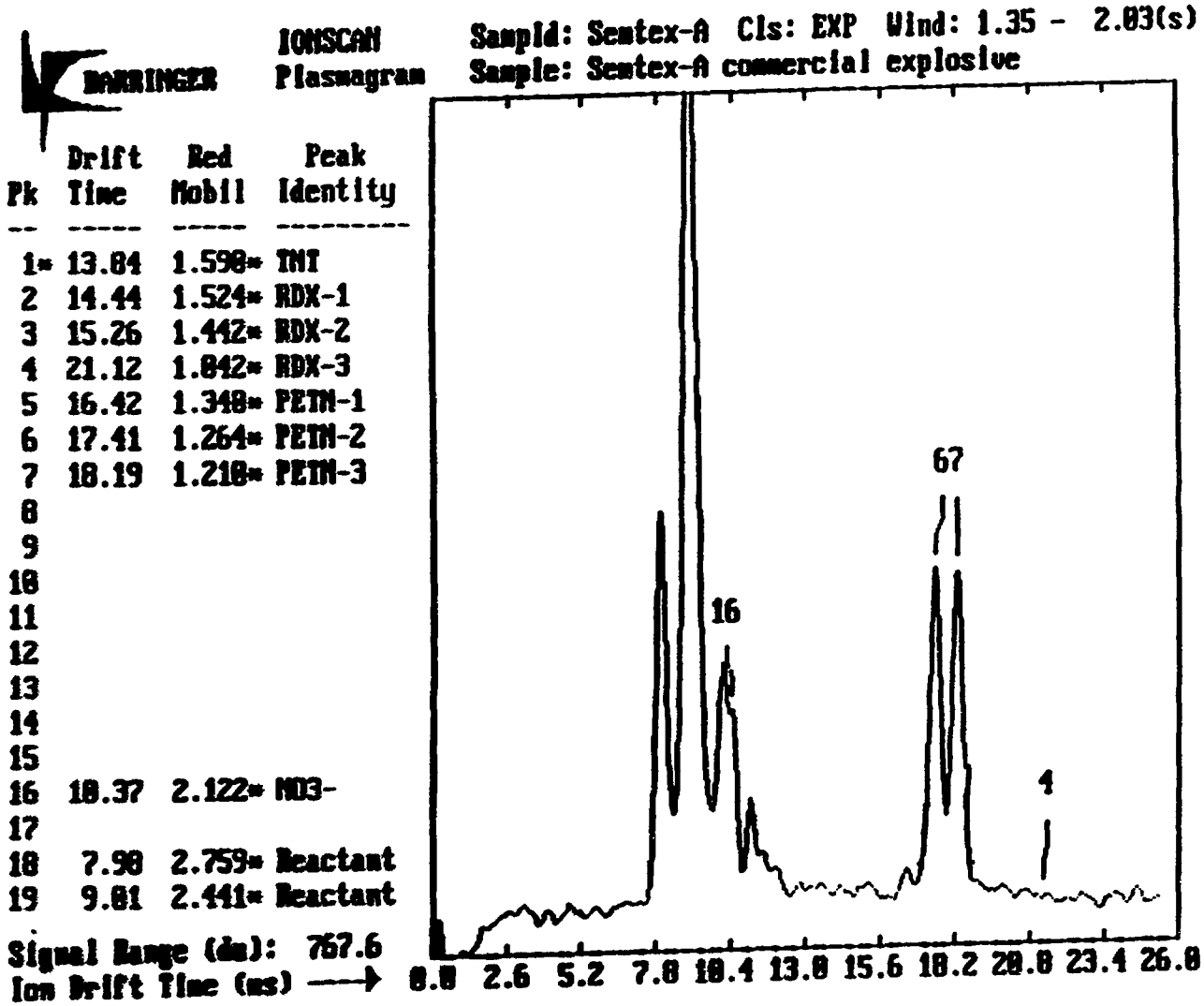


Figure 4 Plasmagram of Sentex-A with chloride as a major reactant ion and IMS operating temperature of 100°C.

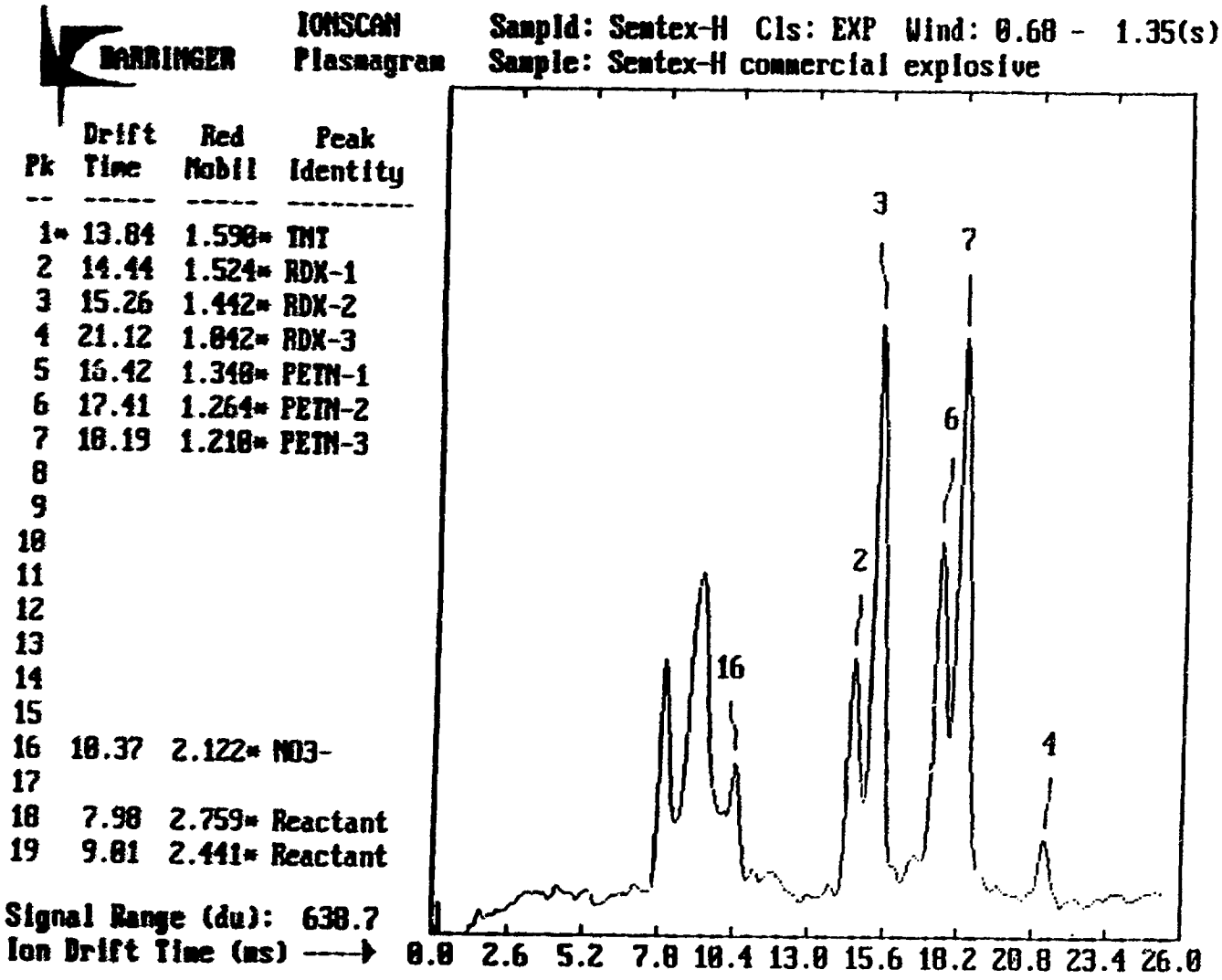


Figure 5 Plasmagram of Semtex-H with chloride as a major reactant ion and IMS operating temperature of 100°C.

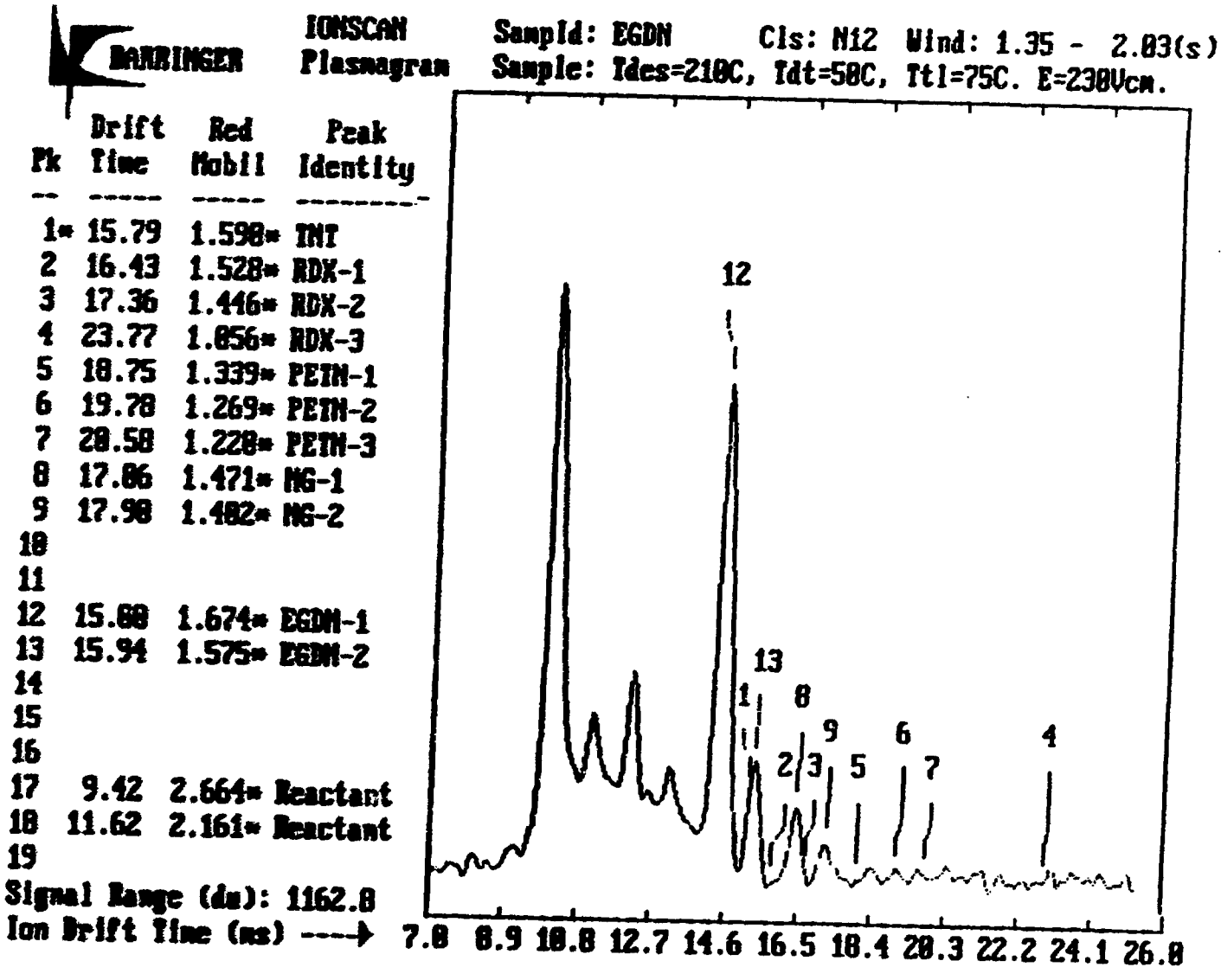


Figure 6 Plasmagram of EGDN with chloride as a major reactant ion and IMS operating temperature of 50°C.

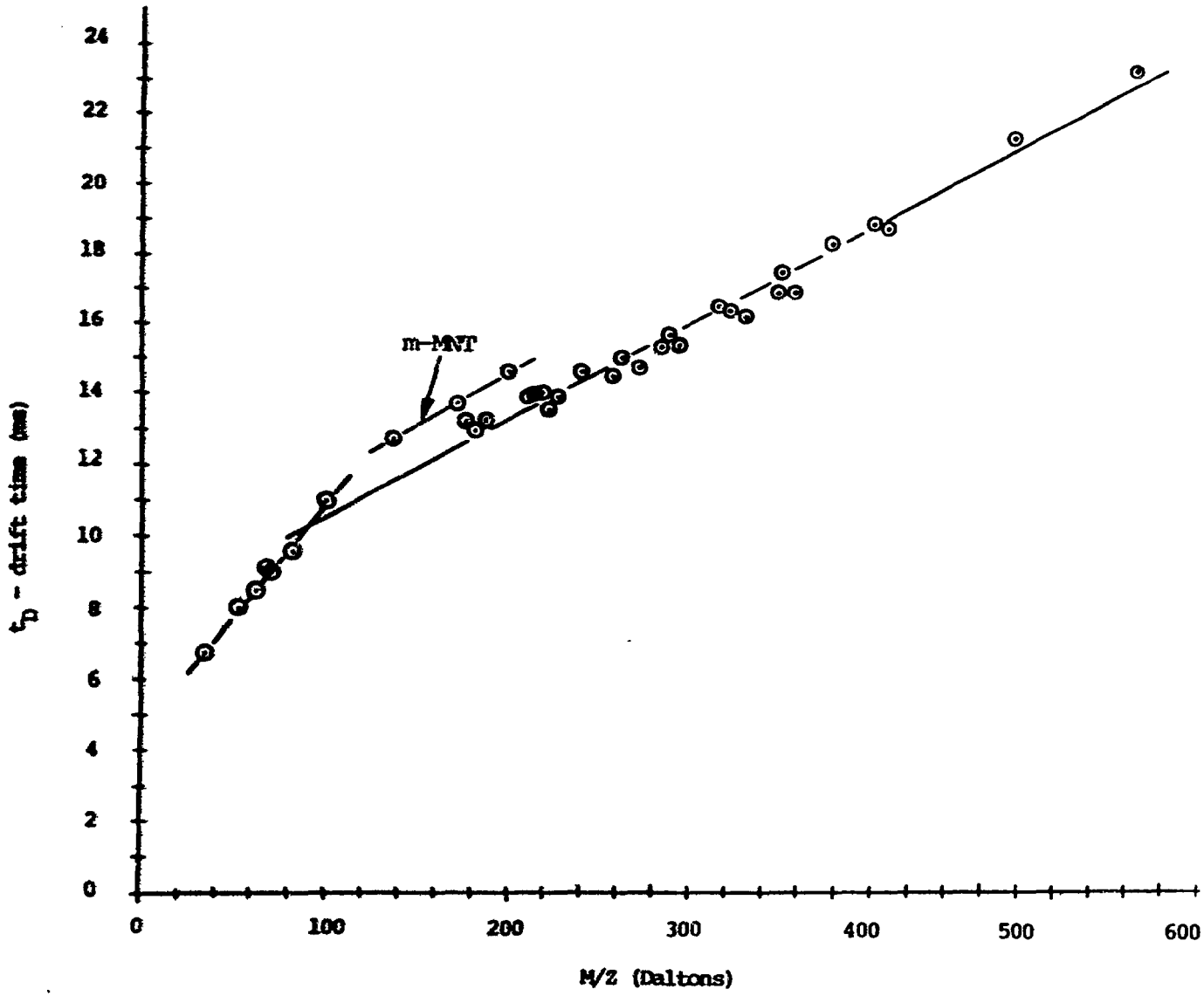


Figure 7 Plot of ion drift time as a function of ion mass.

FOURIER TRANSFORM ION-CYCLOTRON RESONANCE (FT-ICR) MASS SPECTROMETRY OF RDX, PETN AND OTHER EXPLOSIVES

C.S. Giam
M.S. Ahmed
R.R. Weller
Texas A&M University
Galveston, TX

jennelle Derrickson
Federal Aviation Administration
Atlantic City International Airport, NJ

1. INTRODUCTION

Previous investigations of explosives by conventional mass spectrometry using electron impact (EI) ionization have shown that the explosives underwent extensive fragmentation and did not provide molecular weight information (Bulusu et al, Schulten et al, Yinon et al, and Zitrin et al). We wish to present the Fourier Transform Ion-Cyclotron Resonance-Mass Spectrometry (FT-ICR-MS) investigations of RDX (1,3,5-trinitro-1,3,5 triazacyclohexane), PETN (Pentaerythritol tertranitrate) and TNT(1,3,5-Trinitro toluene).

The theory, instrumentation and methodology of FTMS have been described in detail elsewhere (Lehman et al, Wanczek et al, Parisod et al, Ghaderi et al, Johlman et al, and Weller et al).

All experiments are carried out using an Extrel FTMS-1000 equipped with a Tachisto 215G pulsed CO_2 laser and a 5.08 cm cubical cell. EI and self-chemical ionization (SCI) spectra are obtained at 50 eV electron energy; electron capture (EC) spectra at 0.2 eV. A delay of 3 ms, 500 ms and 200 ms was allowed between ion excitation and detection in EI, SCI and EC respectively. In laser desorption ionization (LDI) a delay of 5 seconds was introduced to allow most of the neutrals to be pumped away. The laser pulsed at 10.6μ m with repetition rate of 2 per second delivering approximately 10^8 Watts/cm^3 in 45 ns. Other details may be found in our earlier publication (Weller et al).

2. RESULTS AND DISCUSSION

Positive ion electron impact mass spectrum of RDX from FT-ICR-MS is similar to those from previous reports (Bulusu et al). Under EI conditions, RDX undergoes extensive fragmentation giving little (<5%) or no molecular ion peak intensity. The electron capture (EC) mode spectrum was found to contain less fragmentation; (EC) was more sensitive than EI.

FT-ICR-MS switches easily from EI to EC, to chemical ionization or to laser desorption ionization modes. An unique feature of FT-ICR-MS is that SCI does not require external reagent gas. Positive ion SCI spectrum of RDX gives a base peak of pseudomolecular ion, $[M+H]^+$; thus the identity can be established by the molecular mass.

Soft ionization mode such as LDI is desirable for compounds like RDX, PETN and TNT that are thermally labile. Positive ion LDI/FT-ICR-MS spectrum of RDX gives pseudomolecular ions, $[M+Na]^+$ and $[M+K]^+$. Negative ion LDI of RDX gives mono and dimeric adduct peaks at m/z 268 ($[M+NO_2]^+$) and m/z 490 ($[2M+NO_2]^+$). LDI of TNT and PETN also gives characteristic pseudomolecular ions. With relative ease of switching from +ve to -ve mode, the combination of EI, EC, and LDI modes provides an excellent method to study the decomposition temperature of RDX. Thus, from -45° C to 0° C , no vapor of RDX was detected by EI and EC modes. However, the presence of frozen RDX can be indicated by its LDI spectra. RDX vapor began to appear at temperatures higher than 0° C as indicated by the presence of

characteristic peaks at m/z 46, 102 and 129 in the EC spectrum. At temperatures higher than 100° C, RDX appeared to decompose, as indicated by the increase of peak intensity at m/z 46 (NO_2).

Preliminary studies of PETN and TNT gave similar observations; thus FT-ICR mass spectrometry is one desirable method of characterization of trace amounts of RDX, PETN and RDX.

REFERENCES

1. Bulusu S., Axenrod T., and Milne, G.W.A., Organic Mass Spectrometry, 1969, 3, 13.

2. Ghaderi, S., Kulkarni, P.S., Ledford, E.B., Wilkins, C.L., and Gross, M.L., Anal. Chem., 1981, 53, 428.

3. Gills, R.G., Lacey M.L., and Shannon, J.S., Organic Mass Spectrometry, 1974, 9, 359.

4. Johlman, C.L., White, R.I., and Wilkins, C.L., Mass Spectrom. Rev., 1983, 2, 389.

5. Lehman, T.A., and Bursey, M.M. "Ion Cyclotron Resonance Spectrometry", Wiley-Interscience, New York, 1976

6. Parisod, G., and Comisarow, M.B., Adv. Mass Spectrom., 1980, 8, 212.

7. Schulten, H.R., and Lehmann, W.D., Analitica Chimica Acta, 1977, 93, 19.

8. Wanczek, K.P., Int. J. Mass Spectrom. Ion Process., 1964, 60, 11.

9. Weller, R.R., Mayernik, J.A., and Giam, C.S., Biomed. Environ. Mass Spectrom., 1988, 15, 529.

10. Yinon, Y, J. of Forensic sciences, 1980, 25, 401.

11. Zitrin, S., Organic Mass Spectrometry, 17, 74 (1982).

DETECTION OF TRACE EXPLOSIVE EVIDENCE BY ION MOBILITY SPECTROMETRY

Dean D. Fetterolf
Research Chemist
Forensic Science Research Unit
FBI Academy
Quantico, VA 22135

Tracy D. Clark
FBI Honors Intern
Department of Chemistry
Southwest Missouri State University
901 S. National
Springfield, MO 65804

1. INTRODUCTION

Many nations, including the United States, have been prime targets of international terrorism for many years. The bombings of the U.S. Embassy and the U.S. Marine Barracks in Beirut in 1983, and the destruction of Pan American Flight 103 over Lockerbie, Scotland in December, 1988 are grim reminders of terrorism in recent years. These criminal acts have prompted the need for the development of innovative methods of explosives detection. As part of an ongoing research effort, the FBI Laboratory has been evaluating new technology and the innovative adaptation of existing technology for use in counterterrorism and counternarcotics investigations.

Ion mobility spectrometry (IMS), first introduced in 1970 (1) is currently experiencing a resurgence of interest as a specific purpose detection system. Because of the exceedingly low vapor pressure of explosives (ppm to ppt) (2), the detection of plastic explosives by vapor methods alone has been difficult. We have been examining the application of an Ionscan Model 200 by Barringer Instruments, Inc. (South Plainfield, NJ), in detection of modern explosives in a variety of scenarios of forensic interest by collecting particulate matter.

The IMS has many of the advantages of conventional laboratory instruments such as good sensitivity, selectivity, speed, size, and ease of use. This ease of use and portability permit operation in real world situations.

Forensic applications of IMS technology from 1970 to 1989 have been thoroughly reviewed by Karpas (3). Much of the earlier work on the forensic applications of IMS technology focused on the laboratory feasibility. Recently, an IMS detection system has been used to test for drug micro-particulates on evidentiary material (4,5) and in customs scenarios (6). Explosives detection by IMS on evidentiary materials (7,8) has been presented.

1.1. Technique

The IMS (Figure 1) consists of two main areas: the reaction region and the drift region. In the reaction region, atmospheric pressure carrier gas (purified air), hexachloroethane (C_2Cl_6), the reactant gas and 4-nitrobenzonitrile, an internal calibrant are ionized by a ^{63}Ni beta emitter to form Cl^- ions. The reactive Cl^- ions or reactant ions then undergo ion/molecule reactions with an explosive molecule (M):

Electron Attachment:
$M + Cl^- \longrightarrow M^- + Cl$

Proton Abstraction:
$M + Cl^- \longrightarrow (M-H)^- + HCl$

Chloride Attachment:
$M + Cl^- \longrightarrow (M+Cl)^-$.

The explosive molecules also undergo other ion forming reactions such as adduct formation and dissociation reactions. The exact nature of the species formed in the IMS under these conditions is still under investigation and can only be decisively

determined using an IMS/MS combination. Karpas has reviewed the ionization of explosives in IMS under a variety of operating conditions (3). For routine use however, under a given set of instrument conditions, the resulting spectra are reproducible. From a practical standpoint, the negative ionization provides a high degree of specificity because only electronegative compounds are ionized.

Under the influence of an electric field, the mixture of reactant and product ions reaches a shutter grid that separates the reaction region and the drift region. The shutter grid is made of sets of thin mesh wires with a voltage bias between them. When the shutter grid is "on" (with bias voltage applied), the ions are attracted to the gating grid and lose their charge. For a brief amount of time the grid is turned "off". Ions are then transmitted into the drift region of the cell.

In the drift region an electric field gradient is applied. The ions migrate through the electric field, but at the same time are hindered by the countercurrent drift gas. The smaller, compact ions have a higher mobility than the heavier ions, and therefore traverse the region and collide with the electrometer plate in a shorter time. With the aid of a microprocessor, a plot of ion current intensity versus the time elapsed from the opening of the shutter grid gives the mobility spectrum (plasmagram).

1.2. Theory

The drift velocity, v_d,(cm/s) of an ion traversing through an electric field, E, (V/cm) is as follows:

$$v_d = KE$$

where the proportionality constant, K, is the mobility of the ion.

If t is the required time (sec) for the ion to travel the drift region length (cm), d, at this velocity, and the drift velocity is the drift length divided by the drift time, then

$$K = d/(Et)$$

In general, for a given temperature, T, (Kelvin) of the drift gas and pressure, P, (torr) the mobility is given as reduced mobility, K_o, in the form of

$$K_o = [d/(Et)] (273/T) (P/760)$$

With a given set of electric field gradient, temperature, and pressure conditions, the product of the reduced mobility and the drift time of an ion, $K_o t$, is a constant. When reduced mobilities are calculated, the internal calibrant is used to calibrate the plasmagram. A channel ratio of the sample mobility versus the mobility of the calibrant corrects for any drift. The instrument conditions for our experiments are shown in Table 1.

2. RESULTS AND DISCUSSION

2.1. IMS Spectra and Limits of Detection

Standards with concentrations of 1 ng/μL and 100 pg/μL were prepared of TNT, RDX, PETN, NG, and NH_4NO_3, and placed on the teflon membrane filter with a microliter syringe. The appearance of the ions and their limit of detection for these five common explosive components are shown in Table 2. They were found to range from 200 pg to 80 ng. The plasmagram for RDX and PETN are shown in Figures 2 and 3, respectively. To reduce the chance of false alarm two of the three peaks for RDX, PETN and NG must be detected before the audible alarm will sound.

2.2. Hand and Surface Contamination

Contamination of the hands has been shown to occur after handling commercial and military explosives (9). The persistence of these explosives on hands and evidence of contact transfer is well documented in forensic sciences (10,11). IMS can be used to identify explosives on suspects or on their belongings. This evidence can provide probable cause for a search warrant, help identify a potential terrorist, and locate concealed explosives.

For this experiment a subject touched C-4 (RDX). He then enacted several normal stages in operating a car, including: opening and closing the hood, the driver side door, the trunk and handling the steering wheel, gearshift and keys.

Samples were collected before and after the contact transfer from each of the touched areas of the car and from the subject's hands by vacuuming onto a membrane filter disk. Each disk was then placed over the desorption heater (Figure 1) and thermally desorbed into the IMS for analysis.

Careful procedures were followed to ensure that no cross contamination occurred by changing the sample nozzle and verifying that the sample disks and the IMS were clear of explosives before sample collection.

As shown in Table 3 the car surfaces and hands were negative for RDX prior to touching the explosive. After contact, all touched areas showed easily detectable RDX residue. In a separate experiment, after handling C-4, eight consecutive hand washings with soap and water were required before the IMS could no longer detect the RDX.

2.3. Post Blast Residue

With increased terrorist activities, improved and accurate analysis of postblast residues has become vital in bombing investigations. The first question often posed by an investigator following a blast is, What was the explosive? The analysis may provide the link between a suspect and the type of explosive used. Yelverton has demonstrated the detection of post-blast RDX vapor using a quartz tube pre-concentrator and IMS (12). Because it has portability, the IMS can be taken to the location of the bombing for preliminary analysis to aid law enforcement investigators.

We conducted a series of postblast residue experiments the results of which are summarized in Table 4. Samples were collected by a vacuum, and the IMS was cleared between samples by running a blank.

Four improvised explosive devices, pipebombs, were prepared. The pipes contained Hercules Green Dot and Scott Royal double-based smokeless powder, Pyrodex (a black powder substitute) and black powder. Following detonation, fragments of the pipes were recovered for analysis. Both pipes containing the double based smokeless powder alarmed positive for nitroglycerine. Figure 4 shows the NG plasmagram from a segment of the pipe which contained Green Dot double-based smokeless powder. The fragments of pipe from the pyrodex and black powder devices were negative.

The second experiment involved postblast steel plates. Semtex (PETN and RDX), C-4 (RDX), Deta Sheet (PETN), Powermax (an Atlas Powder emulsion explosive), and Trenchrite (a Dupont water gel) were placed on top of five clean steel plates on the ground and detonated in the open atmosphere. Samples were collected vacuuming the plates.

The Ionscan alarmed for PETN from the Deta-Sheet steel plate, and for ammonium nitrate on the Trenchrite plate. The lack of explosives on three of the plates could have been because of the high heat of the blast and the lack of available material in the environment for condensation of explosives vapor or trapping particles. This explanation seems reasonable considering the following experiment involving C-4 in a closed suitcase full of clothing.

One demolition block of C-4 was placed in a suitcase containing ten clothing items. Before the blast, the clothing and suitcase were clear of explosives. The C-4 was detonated and the post blast debris was collected. Postblast RDX residue was detected on all articles of clothing using the vacuum sample method.

Figure 5 shows the plasmagram for the detection RDX on pieces of a pair of blue jeans. Pieces of cardboard from the liner of the suitcase also alarmed for RDX, as did metal pieces of the rim. The clothing was placed in heat sealed polyester bags and is being stored for later reanalysis.

Lastly, a portable cassette/radio containing SEMTEX was detonated. Figure 6 shows the post-blast RDX and PETN residue on a speaker magnet. RDX and PETN were detected on a piece of plastic and the metal nameplate.

3. CONCLUSION

In our evaluation of the Ionscan 200, laboratory measurements of sensitivity and experiments involving practical law enforcement scenarios were presented, including contact transfer and postblast residue.

The IMS proved to be a reliable and simple detector to use. The ease of sample collection with a vacuum, 5 second analysis, sensitivity of 200 pg for most explosives, selectivity (lack of false alarms in real world scenarios) and the capability for on-site explosives detection demonstrate the value of this analytical instrument.

Microprocessor controlled, lightweight, portable ion mobility spectrometers offer forensic scientists, law enforcement, and security personnel a powerful new tool in trace explosives detection.

REFERENCES

1. Cohen, M. J., Karasek, F. W. *J. Chrom. Sci.*, 1970, 8, 330-337.

2. Dionne, B. C., Rounbehler, D. P., Achter, E. K., Hobbs, J. R., Fine, D. H., *J. Energetic Materials*, 1986, 4, 447-472.

3. Karpas, Z. *Forensic Science Review*, 1989, 1, 104-119.

4. Fetterolf, D. D., Donnelly, B., Lasswell, L. "Detection of Heroin and Cocaine Residue by Ion Mobility Spectrometry", Proceedings of the 39th ASMS Conference on Mass Spectrometry and Allied Topics, Nashville, TN, May 19-24, 1991.

5. Fetterolf, D. D., Donnelly, B., Lasswell, L. "Detection of Heroin and Cocaine Residue by Ion Mobility Spectrometry", Presented at 12th International Mass Spectrometry Conference, Amsterdam, The Netherlands, August 26-30, 1991.

6. Chauhan, M., Harnois, J., Kovar, J., Pilon, P., *Can. Soc. Forens. Sci. J.* 1991, 24, 43-49.

7. Fetterolf, Whitehurst, F. W., "Detection of Explosives Residue by Ion Mobility Spectrometry", Proceedings of the 39th ASMS Conference on Mass Spectrometry and Allied Topics, Nashville, TN, May 19-24, 1991.

8. Fetterolf, Whitehurst, F. W., "Detection of Explosives Residue by Ion Mobility Spectrometry", Presented at 12th International Mass Spectrometry Conference, Amsterdam, The Netherlands, August 26-30, 1991.

9. Twibell, J. D., Home, J. M., Smalldon, K. W., Higgs, D. G. *Journal of Forensic Science.* 1982, 27, 783-791.

10. Jane, I., Brookes, P. G., Douse, J. M. F., O'Callaghan. *Proceedings of the International Symposium on the Analysis and Detection of Explosives.* 1983, 475-483.

11. Lloyd, J. B. F. *Journal of Forensic Science Society.* 1986, 341-348.

12. Yelverton, B. J., *J. Energetic Materials*, 1988, 6, 73-

Table 1. Operating Conditions for Explosives Detection

Parameter	Setting
Drift Temperature	95 C
Inlet Temperature	215 C
Desorber Temperature	235 C
Desorption Time	4.3 s
Shutter Grid Pulse	200 μs
Scan Cycle Time	24 ms
Drift Flow	350 ml/min
Sample Flow	300 ml/min
Exhaust Flow	650 ml/min

Table 2. K_o and limit of detection values for common explosives

Substance	$K_o(cm^2volt^{-1}sec^{-1})$	L.O.D.
TNT	1.451	200 pg
RDX-1	1.387	200 pg
RDX-2	1.314	800 pg
RDX-3	0.948	1 ng
PETN-1	1.213	80 ng
PETN-2	1.145	200 pg
PETN-3	1.104	1 ng
NG-1	1.339	50 pg
NG-2	1.275	200 pg
NO_3	1.927	200 pg

Table 3. Contact Transfer of C-4 from Hands to Automobile Surfaces

Car Area	Before Touching	After C-4 Transfer
Hood	-	+
Door Handle	-	+
Hatch Back	-	+
Steering Wheel	-	+
Gear Shift	-	+
Keys	-	+

Table 4. Post Blast Residue Analysis Results

Item/Explosive	Explosive Detected
PIPE BOMBS	
Green Dot Double Based Smokeless Powder	NG
Scott Royal	NG
Pyrodex	-
Black Powder	-
STEEL PLATES	
Deta Sheet	PETN
C-4	-
Semtex	-
Trenchrite	NO_3
Powermax	-
SUITCASE (C-4)	
10 items of clothing	RDX
Cardboard liner	RDX
Metal Rim	RDX
Cassette/Radio (SEMTEX)	
Speaker Magnet	RDX/PETN
Plastic Piece	RDX
Name Plate	RDX

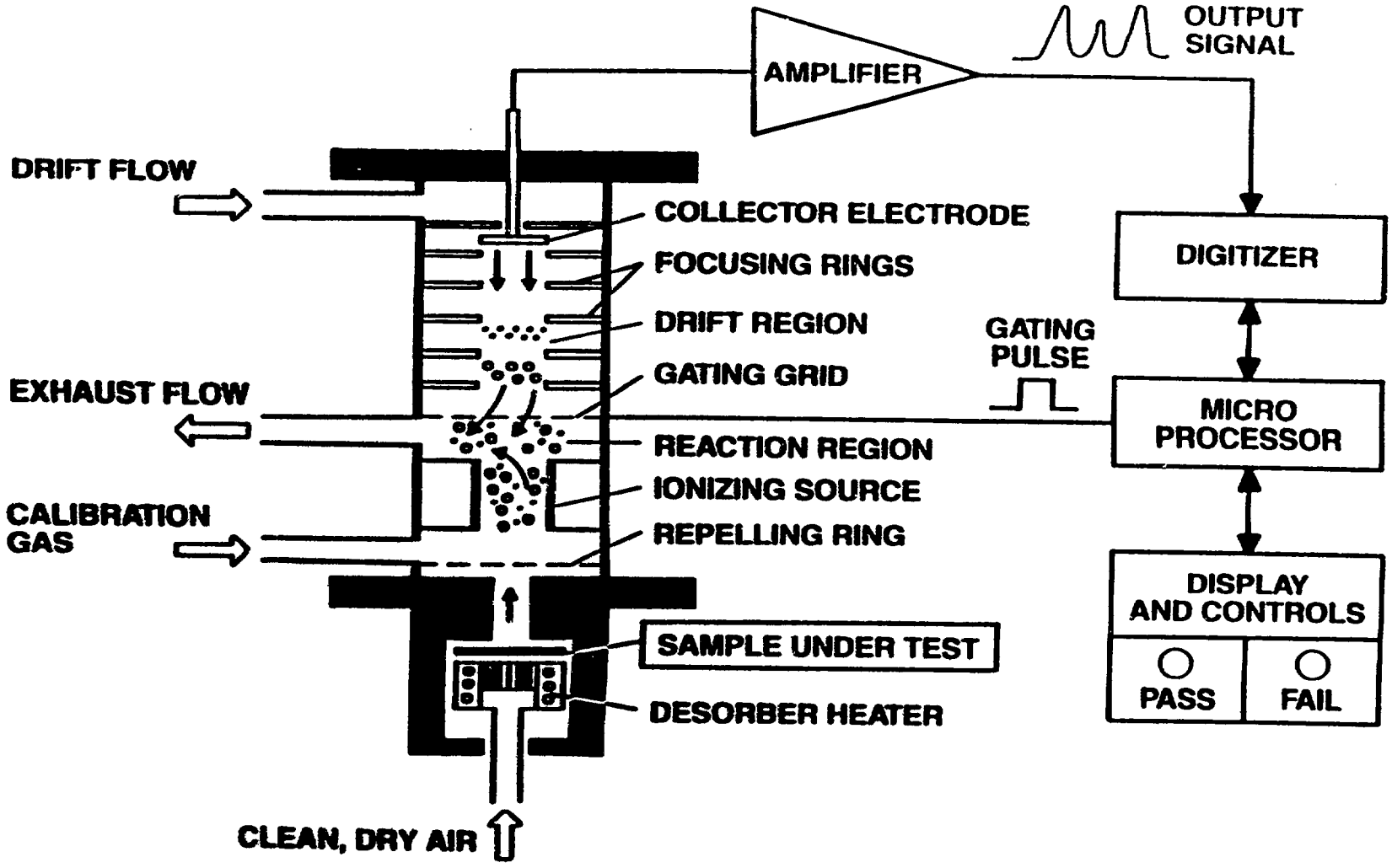


Figure 1. Regions of the Ion Mobility Spectrometry (IMS)

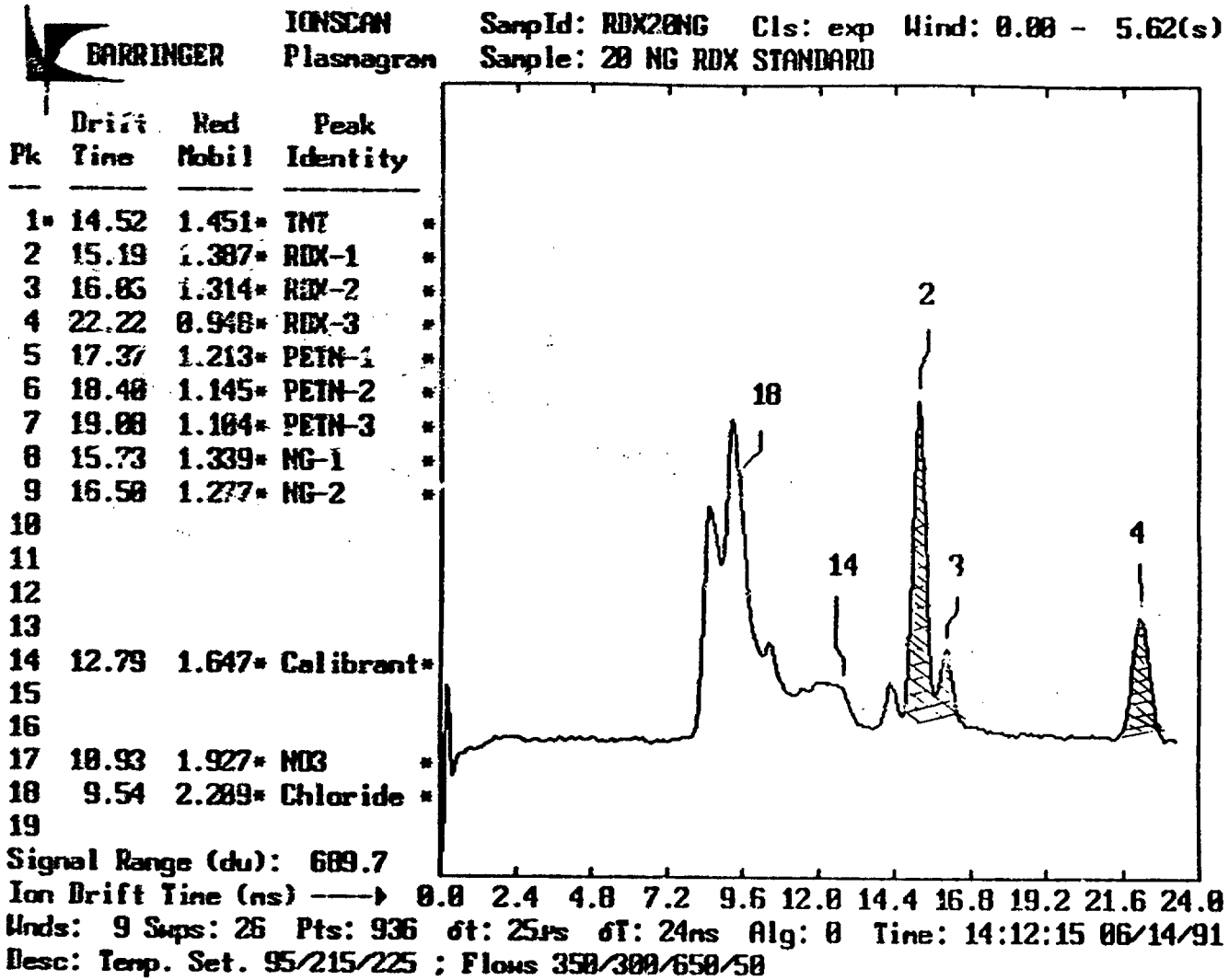


Figure 2. Plasmagram for RDX

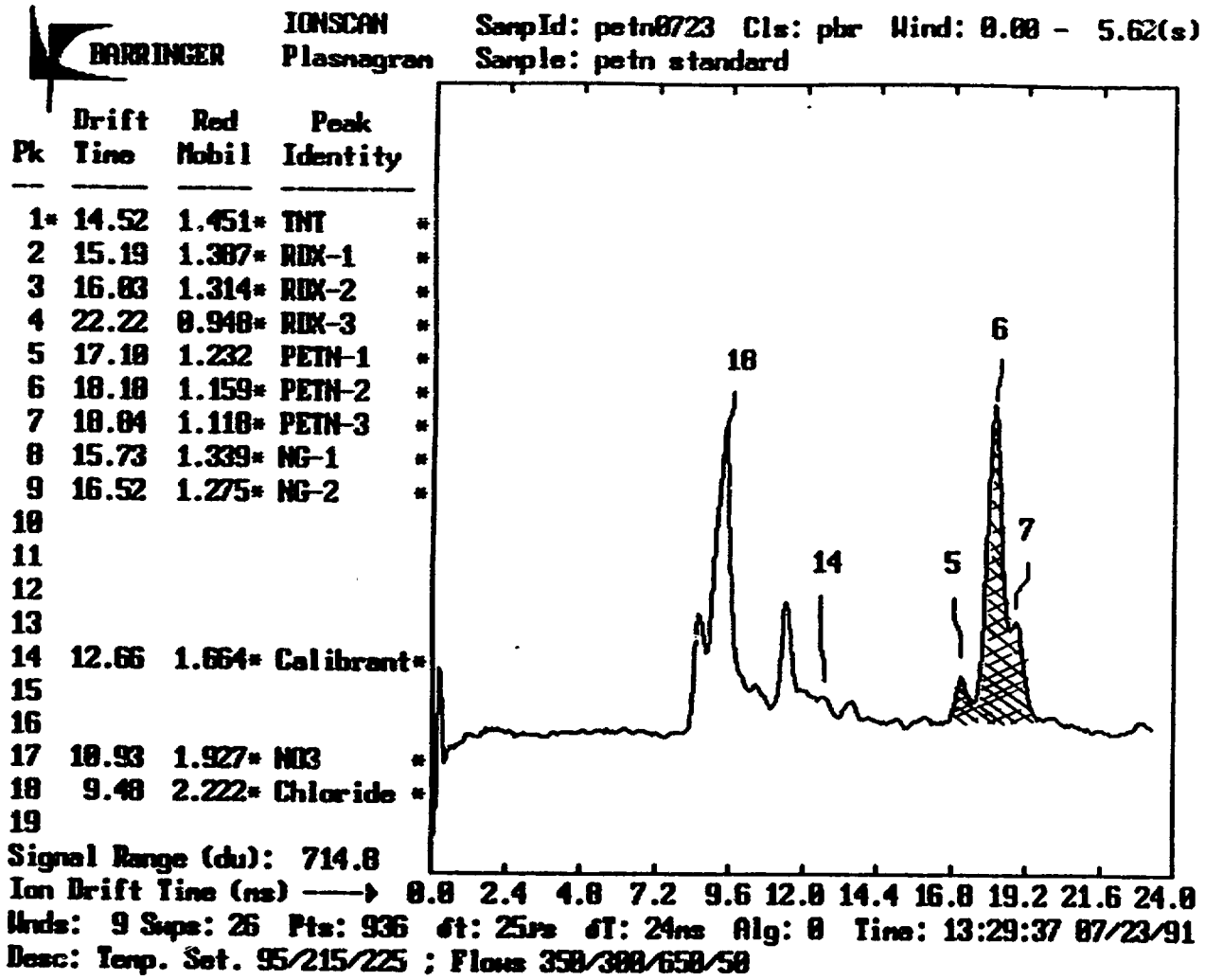


Figure 3. Plasmagram for PETN

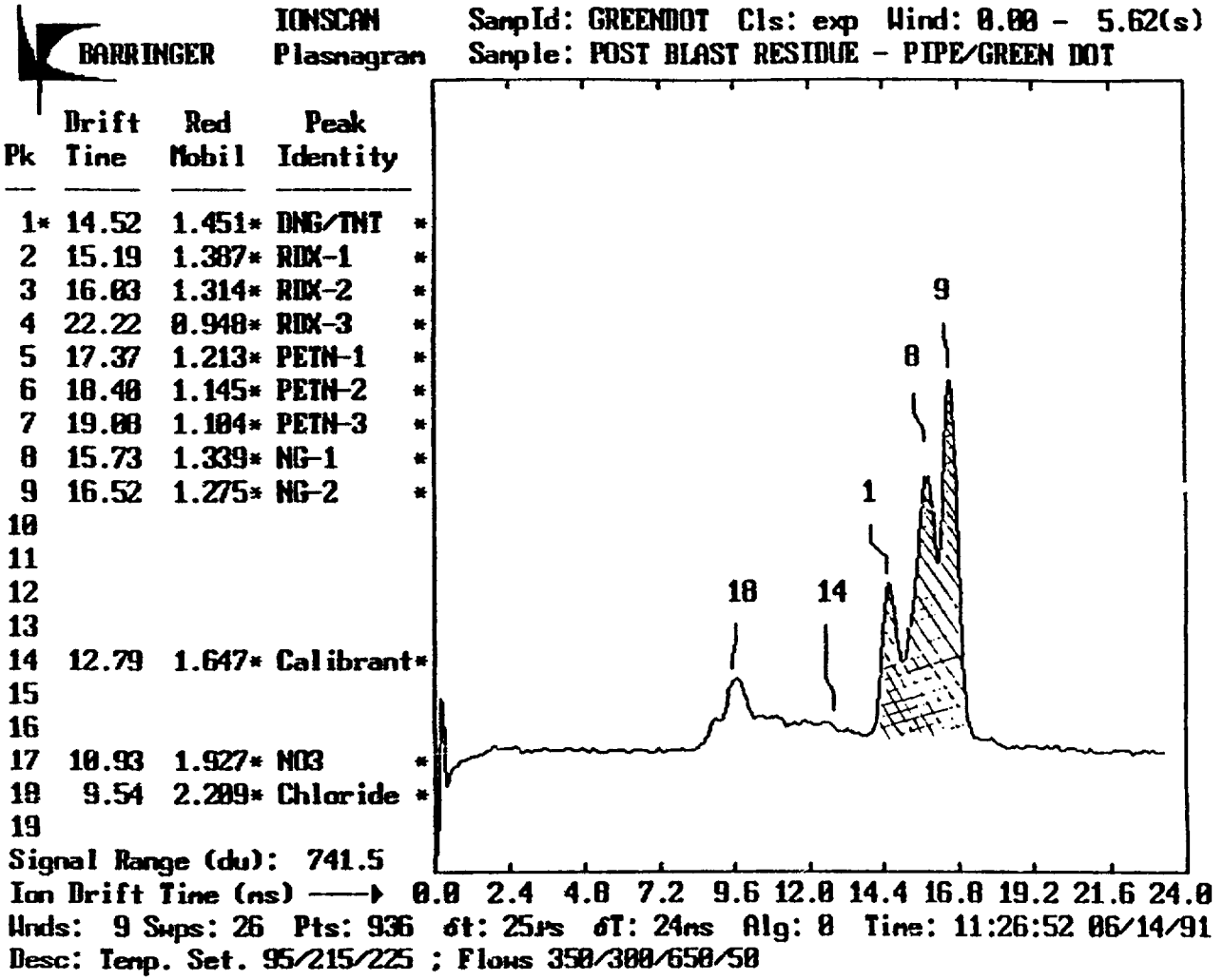


Figure 4. Plasmagram for NG

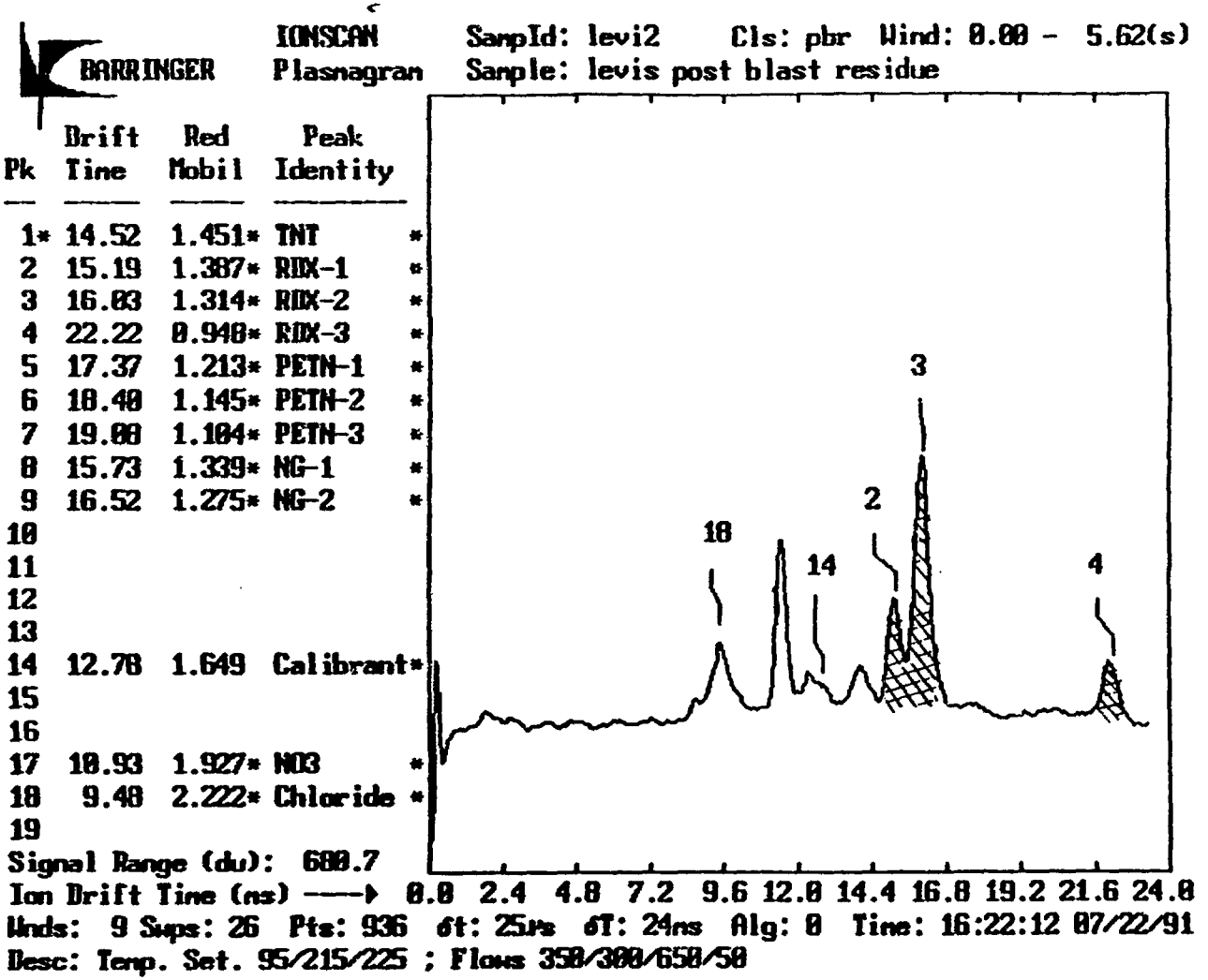


Figure 5. Plasmagram for the Detection of RDX on a Pair of Blue Jeans

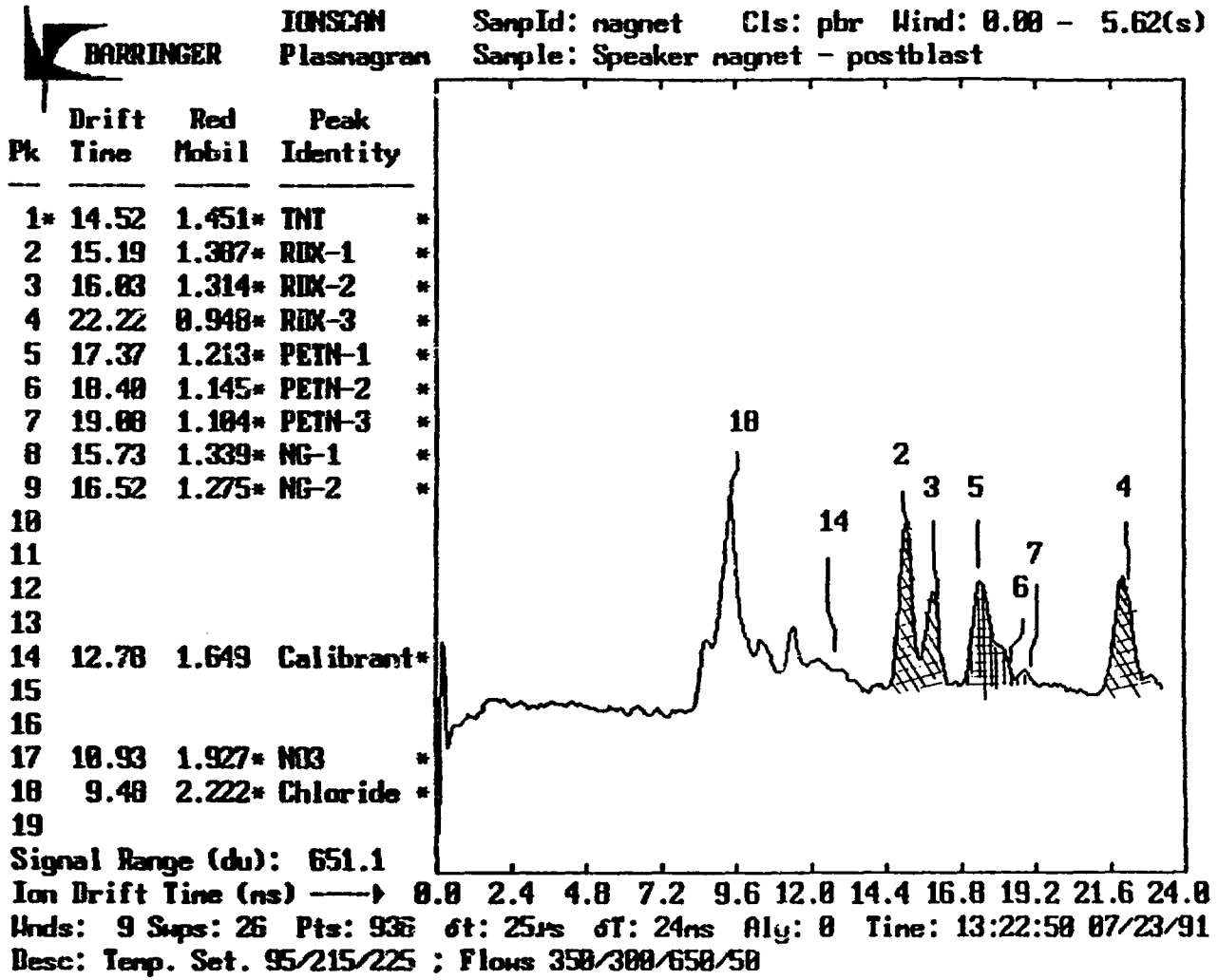


Figure 6. Post-Blast RDX and PETN Residue on a Speaker Magnet

GAS CHROMATOGRAPHY

ANALYSIS OF EXPLOSIVES USING HIGH SPEED GAS CHROMATOGRAPHY WITH CHEMILUMINESCENT DETECTION

David P. Rounbehler, Stephen J. MacDonald,
David P. Lieb, and David H. Fine
Thermedics, Inc.
470 Wildwood St.
Woburn, MA 01888

1. INTRODUCTION

The use of gas chromatography (GC) with detection by chemiluminesence (CL) has been described for the analysis of explosive compounds such as nitrite esters (R-O-NO2) [1], nitramines (R-N-NO2) [2], and c-nitro compounds (R-NO2)[3] and has been used since 1975 for the detection of N-nitroso compounds [4]. The primary reason for using gas chromatography chemiluminescence (GC /CL) for the detection of these compounds is its inherent specificity and high sensitivity[2,5]. For trace analysis of explosives in complex environmental matrices such as samples obtained from people or their luggage, high specificity and sensitivity is essential. Furthermore, when sampling for explosives in an airport setting, or when time does not permit for sample cleanup, specificity and sensitivity become an absolute requirement of any explosives detector. Other detection methods have been demonstrated to be highly sensitive for explosives, however, if they are not also highly specific then they may not be able to achieve their rated detection limits. Interfering components or increased background noise due to other environmental components generally limit the performance of these detectors. Often this aspect of specificity is overlooked when testing explosives detectors. It is one thing to detect trace levels of explosives, it is, however, quite another thing to do so in the presence of environmental contaminants.

Using the GC/CL analytical technique, it has been found that picogram levels of explosives can be detected without interference in the presence of high levels of other non-nitro compounds [2]. In a comparison study of four sensitive and selective detectors for nitroaromatics [5] which included, the Hall electrolytic conductivity detector (HECD), the thermionic detector(TSD), the electron capture detector (ECD), and the Thermal Energy Analyzer (TEA) chemiluminesence detector, solvent extracts of biosludge containing added nitroaromatics were examined. The nitroaromatic compounds used in this study were nitrobenzene, 2,4-DNT and 2,6-DNT. The biosludge was from an active chemical waste treatment plant and was reported to contain 10- 15% other organic soluble material. The added levels of nitroaromatics were from one part per million to as low as 50 parts per billion. The spiked extracts were then analyzed by GC using the optimum conditions for the four detectors. The results of this study clearly indicate that the specificity and sensitivity of the GC/TEA chemiluminesence detection method was superior to the other three detectors. The chromatograms obtained using the three other selective detectors all contained many interfering compounds that eluted on or near the retention times of the nitroaromatics. In contrast, the GC/TEA chemiluminescence detector responded only to the test nitroaromatics and was also able to achieve its detection limit.

This ability to detect explosives and nitro compounds, even in the presence of complex environmental matrices and still maintain its sensitivity, is why GC/CL is an ideal technique for the detection of environmentally occurring explosive vapors and/or particles. Originally, the only serious drawback of the method was the time required to effect a chromatogram. Using standard GC techniques, a typical analysis could take up to 30 minutes. Other faster techniques still required 3 to 5 minutes to complete [2]. These analysis times may be satisfactory for a laboratory setting, but they were too slow for use in screening airline passengers and their luggage for explosives.

2. HIGH SPEED GC/CL EXPLOSIVES DETECTOR

In order to utilize the potential of GC/CL for a practical explosive detector, it was necessary to increase the speed of analysis. To overcome this limitation, a two column temperature programmable high speed gas chromatograph (HSGC) was developed at Thermedics Inc (Egis 3000). This instrument was designed specifically for the high speed GC separation and detection of explosive compounds. The Egis 3000 explosive detection system consists of two temperature programmed high speed gas chromatographic columns coupled to a nitric oxide (NO) chemiluminescence (CL) detector [Figure 1]. Also included is an electrolysis gas generator and an on-board computer. The electrolysis gas generator is used to produce both hydrogen for the HSGC and oxygen to make ozone. The on-board computer is used to control all of its functions including the analytical HSGC/CL system, data handling and display. The computer also monitors all operations for self diagnostics.

Using the HSGC/CL instrument it is possible to analyze environmental samples for explosive compounds such as ethyleneglycol dinitrate (EGDN), nitroglycerine (NG), dinitrotoluene (DNT), trinitrotoluene(TNT), pentaerythrol tetranitrate (PETN), hexogen (RDX), and other explosive compounds with no sample cleanup and with complete chromatographic separations in under 10 seconds [Figure 2]. While only one of the two HSGC columns is needed to effect a separation, the two columns are used together in an arrangement that differentiates between compound classes of explosives. This aspect of the HSGC/CL will be further discussed in the section on gas chromatography.

3. CHEMILUMINESCENCE

The chemiluminescence principle used in the HSGC/CL explosives detector is based on the detection of infrared light emitted from electronically excited NO2*. The electronically excited NO2* results from the reaction of nitric oxide (NO) with ozone (O3). In a CL detector, this reaction generally takes place in an evacuated reaction chamber maintained at a pressure of about 3 torr [Figure 3]. A photomultiplier situated behind a red light filter is used to detect the infrared light emitted from the NO2*. The red filter is in place to block any light with a spectral frequency higher than the near-infrared. The signal output from the photomultiplier is directly proportional to the amount of NO present in the reaction chamber. It is this signal that is used to detect the presence of explosives in a CL system. The following illustrates the important reactions taking place in an NO/CL detector:

1. NO + O3 ------> NO2* + NO2 + O2

2. NO2* ------> NO2 + infrared light (600-1800 nm)

3. NO2* + M -----> NO2 + M*

The actual light emitting reaction (reaction 2) is due to NO reacting with ozone (reaction 1) to produce the excited NO2*. Reaction 3 is due to the excited NO2* transferring its energy to a third species (M). This is not a light producing reaction but it is, however, the predominant one. Operating the CL reaction chamber at reduced pressures helps to minimize this reaction such that more of the excited NO2* releases its energy as infrared light. While these reactions can be used to detect NO, any NOx containing compounds, with the exception of nitrous oxide (N2O), can also be detected by this method provided they can be made to release NO. An example of this is the detection of NO2. NO2 can be converted to NO by pyrolysis as shown in equation 4:

4. NO2 + heat ---(catalyst, 180 C- 600 C)---> NO

This reaction (reaction 4) is used in NOx detectors to monitor ambient air levels for NO2. Other nitrogen containing compounds can also be detected by pyrolysis followed by CL. The temperatures used, however, to decompose NOX containing compounds to produce the needed NO for detection will depend upon their thermal stability. The following are examples of classes of NOX containing compounds and the approximate temperatures needed to decompose them:

5. N-nitrosamines ----------> NO + R2-N (350 C)

6. Nitramines
----------> NO +RS-N
(350 C)

7. Nitrite esters
---------> NO + fragments
(350 C)

8. C-Nitro and Nitroaromatic
compounds ------> no effect
(350 C)

9. Nitroaromatics
---------> NO + Fragments
(800 C)

10. C-Nitro compounds
---------> NO + Fragments
(800 C)

Reactions 5, 6 and 7 show that N-nitrosamines, nitramines and nitrite esters all decompose at a temperature of 350 C to release NO. C-nitro compounds,including nitroaromatics require higher temperatures for decomposition. Reaction 8 shows that heating C-nitro compounds to 350 C does not result in NO being released. However, when these compounds are heated to higher temperatures (reactions 9 and 10) NO is produced. Examples of nitro compounds, and the number of NO molecules released from each, can be seen in Figure 4. As can be seen in Figure 4, decomposition of these compounds results in the molar release of the bound NO. The temperature differences needed to decompose the various explosive compounds to NO is exploited in the design of the two column HSGC/CL instrument.

4. HIGH SPEED GAS CHROMATOGRAPHY

The construction of the HSGC/CL is shown in Figure 1. The two HSGC's which are labeled SE-1 and SE-2 consists of two separate capillary columns. These HSGC columns are operated in series with a 350 C pyrolyzer (PYRO-1) located between them. A second, 800 C pyrolyzer(PYRO-2),is located at the end of SE-2. At the entrance to SE-1, the device labeled CS-2 is a temperature programmed re-focusing cold spot that is used to inject the sample on to the HSGC system. The HSGC hydrogen gas flow used in both columns is about 40 cc / minute. All of the HSGC operations are controlled by the on-board computer. Using the computer, the temperature programing rate of the SE's can be controlled at up to 100 C / second to within 2 C. The CS-2 sample injector operates in a similar fashion and it also is temperature programmed.

The HSCG design and configuration results in all of the explosives passing through SE-1 and PYRO-1 before they enter SE-2. At the 400 C temperature of PYRO-1, all of the nitrite esters and nitramines will decompose to produce NO. The NO gas produced from the 400 C pyrolysis becomes part of the carrier gas and pass through SE-2 without retention. The NO gas from SE-1 will be detected by the CL detector and then displayed as the SE-1 chromatogram. Since C-nitro compounds do not decompose at 350 C they will pass through PYRO-1 to SE-2. SE-2 at this point in the analysis is maintained at a low temperature, any C-nitro compounds entering it will condense in its GC phase. At a preselected time after SE-1 has completed its temperature program, SE-2 is then temperature programmed to separate any C-nitro compounds present. At the exit of SE-2 the C-nitro compounds pass through the 800 C PYRO-2 where they are decomposed. The NO produced from this pyrolysis is detected as a separate chromatogram from the first SE-1 column. Figure 5A is an example of a typical chromatogram resulting from the separation of a mixture of explosive compounds. The added dotted line in the center of the chromatograph shows the time separation between SE-1 and SE-2. The explosives shown in Figure 5A are 1 (EGDN), 2 (NG), 3 (PETN), 4 (RDX), 5 (DNT) and 6 (TNT). Figure 5B demonstrates the effect of lowering the temperature of PYRO-2 to 450 C. At this temperature, none of the DNT or TNT shows up in the resulting chromatograph of the same test sample of explosives shown in Figure 5A.

5. SAMPLE ANALYSIS

The types of samples examined by the Egis 3000 usually consist of vapors and particles vacuumed from the surfaces of objects like luggage or clothing. When such environmental samples are gathered there are few clues, if any, as to what they may contain. Any other material that the sampled object had previously been in contact with could also contribute to the sample. Whether or not any sampled material will produce a false explosives signal, or will contain material that interferes with the detection of an actual explosive can't be known for all possible combinations of samples. For these reasons the HSGC/CL system has been, and continues to be, tested extensively under realistic conditions with the

actual explosives. The use of surrogates, or explosive simulants, may produce data which suggests whether a detection method will or will not work, but it cannot simulate the real condition. Negative interferences, for example, can only be tested with actual explosives. An example of the kind of testing the HSGC/CL system was subjected to can be seen in Figures 6A and 6B. Figure 6A is an analysis of a vapor and particulate sample taken from the hands and clothing of a person who is a smoker and who had just finished eating a lunch of three different pizzas. The test subjects clothing included a laboratory jacket that had been used for 2 weeks without cleaning. The sample was taken by vacuuming vapors and particles from the subjects hands and clothing on to a metal foil sample probe at a rate of 2 liters / second for a total of 20 seconds. This sample also consisted of 40 / L of ambient air and an added amount of explosives injected on to the sample probe. The amount of explosives added were less than 5 picomoles each and consisted of EGDN (1), NG (2), DNT (3), TNT (4), PETN (5), and RDX (6). Figure 6B is a chromatogram of a sample taken from the same subject without the added explosives.

During an analysis, the sample which had been collected on the sample probe is thermally desorbed into the analytical system by a rapid resistance heating of the collector coil while simultaneously forcing air through it. In this fashion, all of the collected sample is converted to a vapor which is then separated from the non-volatile matrix. The vapors from the sample are subsequently recondensed onto a sub-ambient cold spot for later analysis as described above. The time required to complete an analysis is 18 seconds. The 18 seconds includes sample desorption, signal processing and the time needed to complete the two column chromatographic separation. The results of an analysis are presented as either "clear " or "alarm". In the event of an alarm, the system indicates the specific explosive or combination of explosives that were responsible by lighting a vertical array of red lights on the display panel. The number of red lights indicates the relative amount of each explosive detected. In addition to the alarm display, the system can also display the complete chromatogram of an analysis.

6. SUMMATION

Chemiluminescent detection has been demonstrated to be both sensitive and specific for the detection of explosives. The previous speed of GC analysis ha: been increased by over 2 orders of magnitude sucl that it is now practical for use for the detection o explosives in airport settings. The end result of th two column HSGC and pyrolysis is that there are nc C-nitro compounds detected in that part of th chromatogram containing the nitrite esters or th nitramines. The main benefit of the 2 colum separation technique is that, C-nitro compound cannot interfere with the detection of plasti explosives. This has made a highly specific detectior system even more specific. This increase ir selectivity is important since there are several widel used C-nitro compounds found in perfumes, paints, dyes and other products. These compounds can alsc be found as pollutants in ambient air and, perhaps, or objects such as luggage.

ACKNOWLEDGEMENTS

We would like to thank the United States Department of State for its support under contract number 2038-563371 and the Federal Aviation Administration, U.S. Department of Transportation for its support under contact number DTRS-57-84-C which most of the work described in this paper was performed.

REFERENCES

1. Lafleur, A.L., Morriseau,B.D., *Anal. Chem. 1980*, 52, 1313.

2. Douse, J.M.F., *Journal of Chromatography*, 410 (1987) 181-189.

3. Hansen, T.J., Archer, M.C., Tannenbaum,S.R., *Anal. Chem. 1978*, 51, 1526.

4. Fine, D.H., Rufeh, F., Lieb, D., Rounbehler, D.P., *Anal. Chem. 1975*, 47, 1188.

5. Phillips, J.H., Coraor, R.J., Prescott, S.R., *Anal. Chem. 1983*, 55, 889-892.

6. Fine, D.H., and Rounbehler, D.P. (1975) *J. Chromatogr.*, 109, 271.

7. Lafleur, A.L., Mills, K.M., *Anal. Chem. 1981*, 53, 1202.

8. Rounbehler, D.P., Bradley, S.J., Challis, B.C., Fine, D.H., Walker, E.H., *Chromatographia* Vol. 16 Sept. 1982.

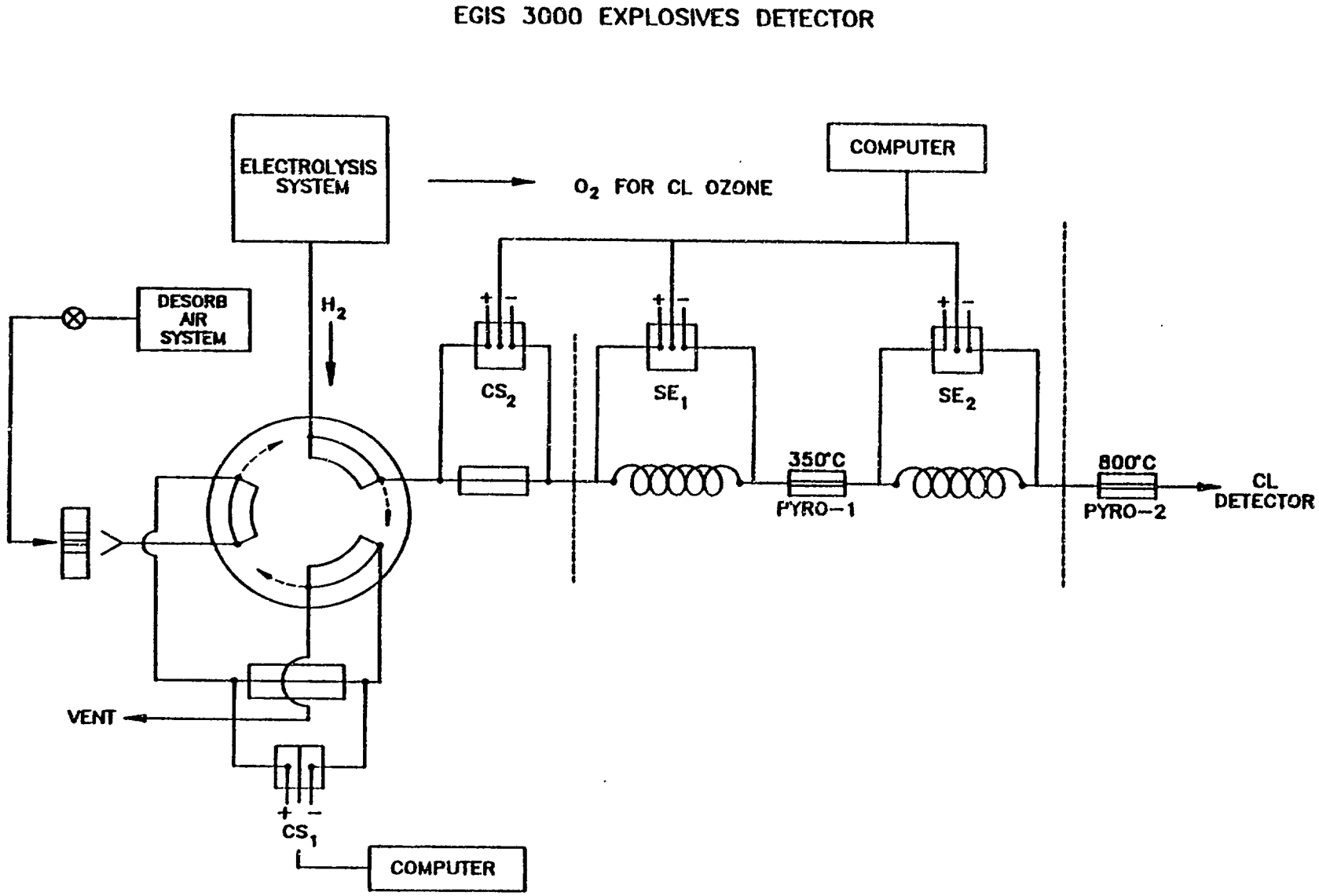


FIGURE 1 Schematic diagram showing the 2 column high speed gas chromatograph used in the

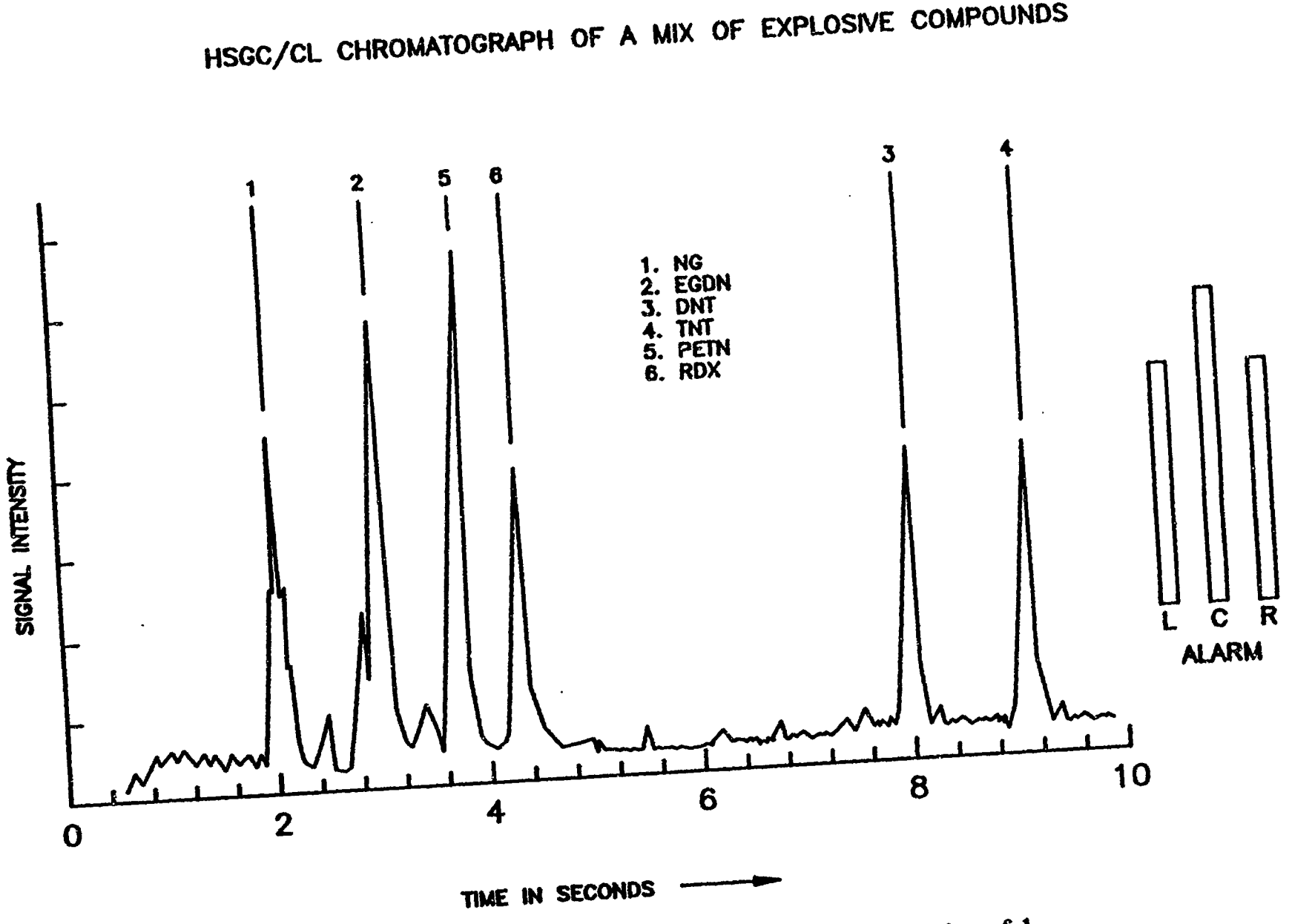


FIGURE 2 HSGC/CL chromatogram of a mixture of explosives compounds consisting of 1 (EGDN), 2 (NG), 3 (DNT), 4 (TNT), 5 (PETN) and 6 (RDX).

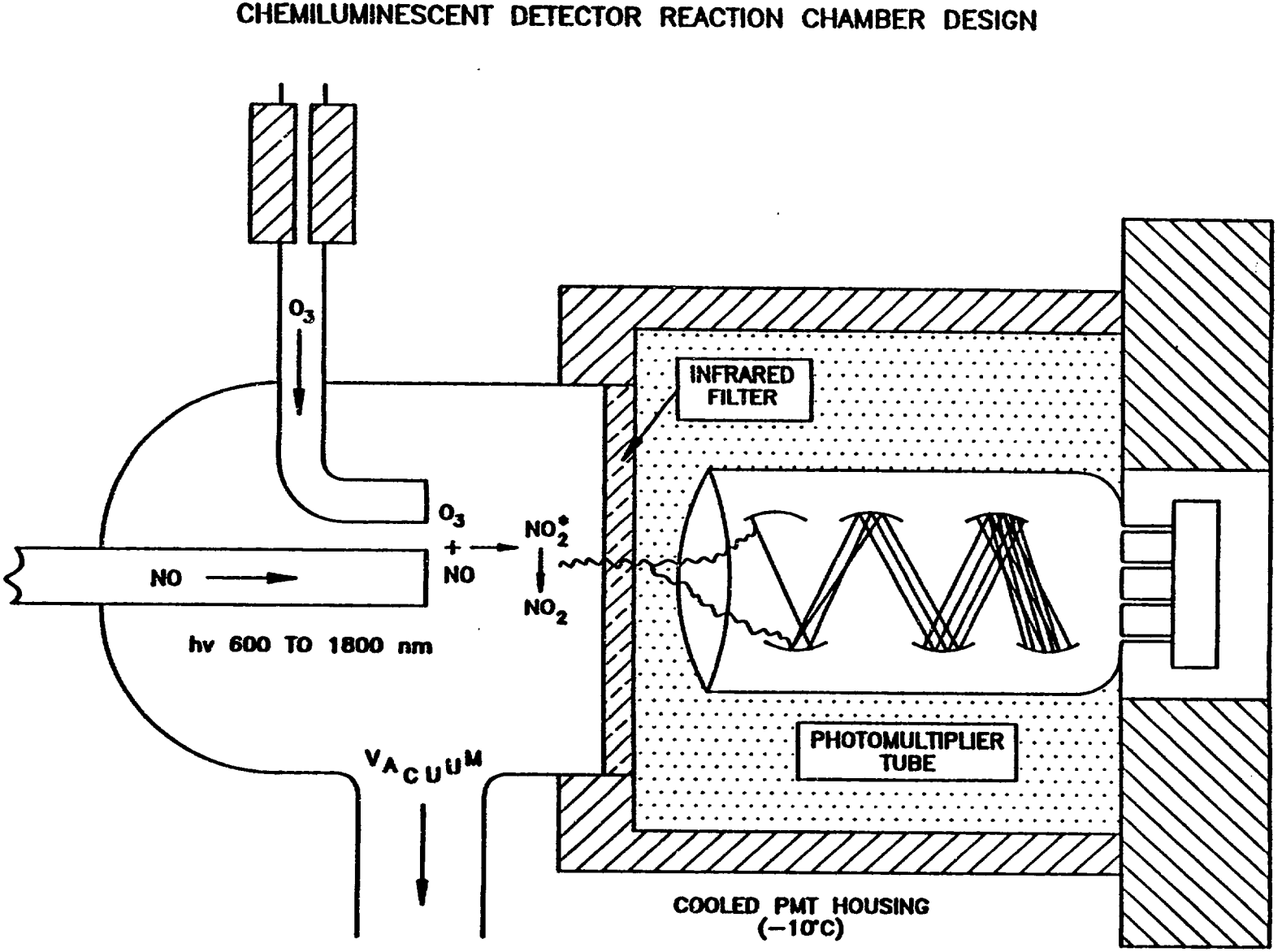


FIGURE 3 Schematic of a chemiluminescence reaction chamber and photomultiplier detector.

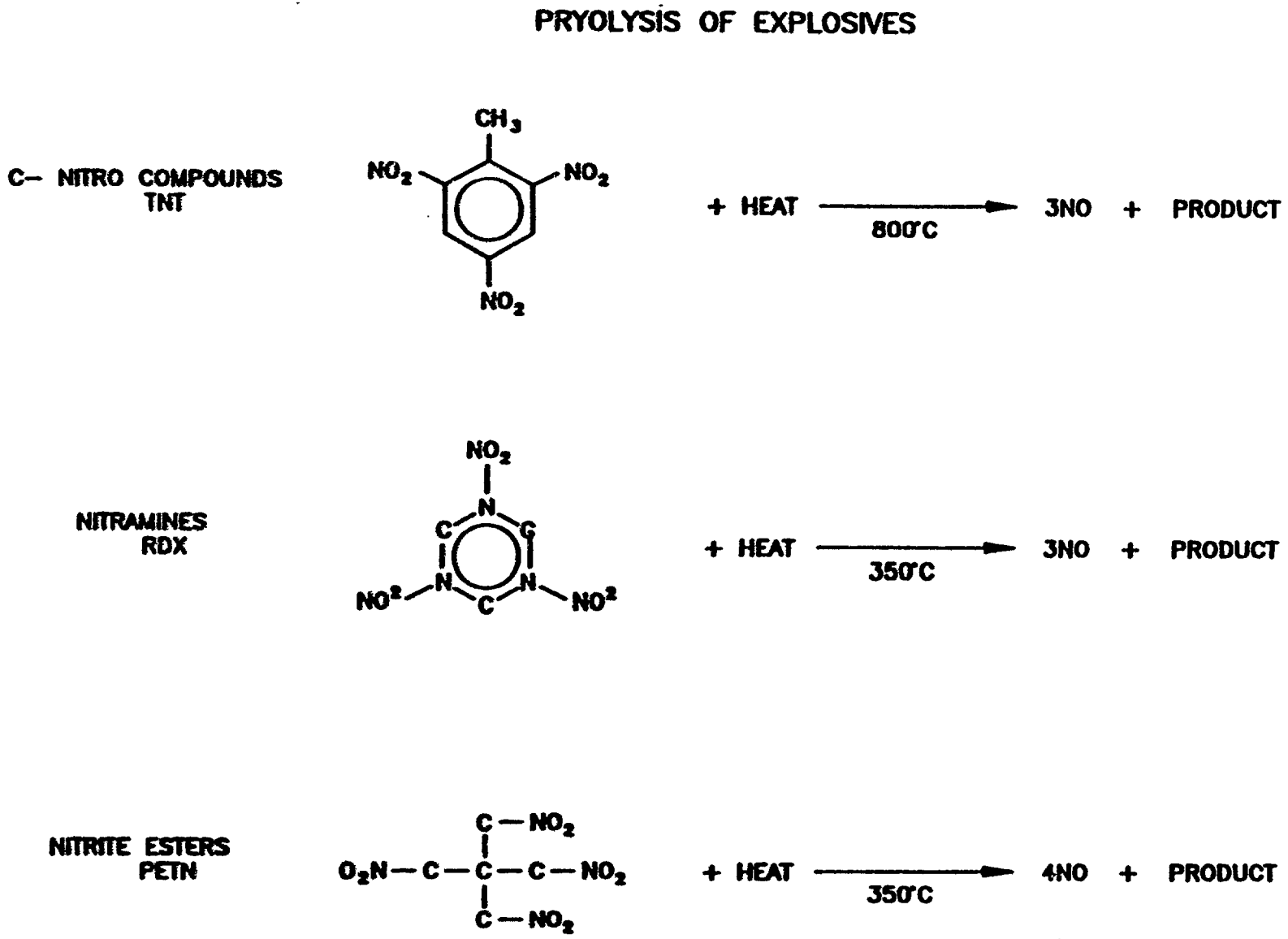


FIGURE 4 **Examples of explosives that can be pyrolized to produce nitric oxide (NO).**

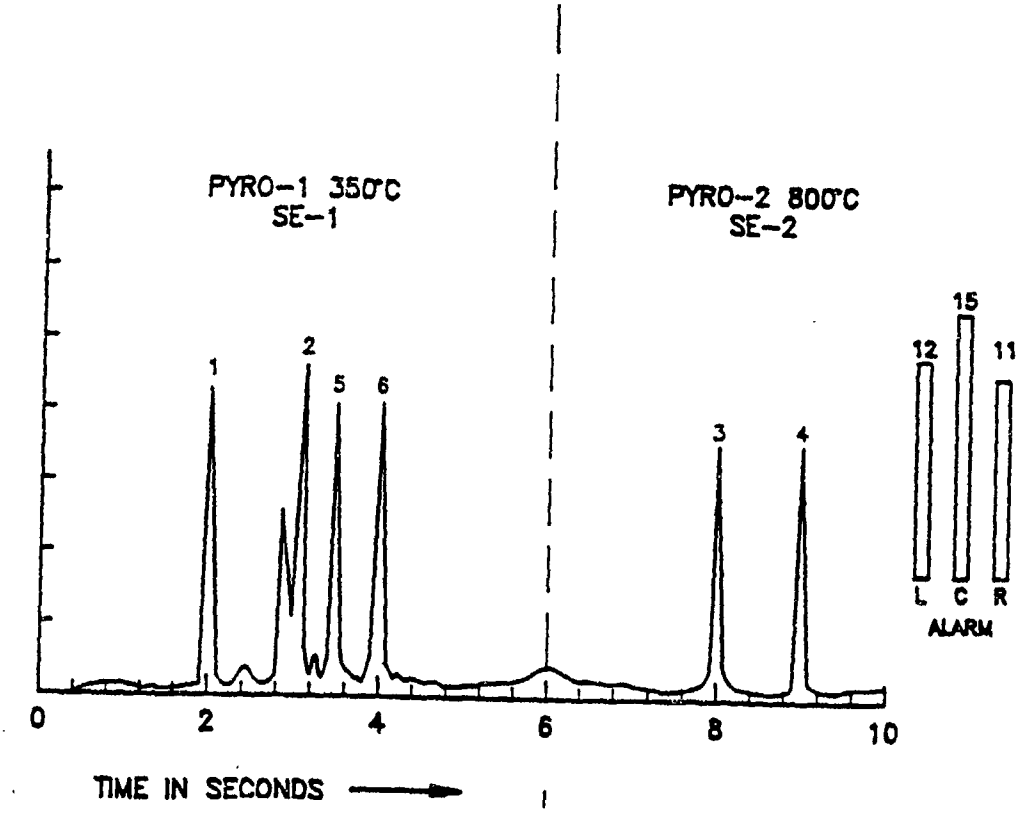


FIGURE 5A Chromatogram of explosives showing the SE-1 and the SE-2 regions. The explosives in the SE-1 region are 1 (EGDN), 2 (NG), 5 (PETN) and 6 (RDX). The others in the SE-2 region are 3 (DNT) and 4 (TNT). The added line indicates the time separation between the SE-1 and SE-2 regions.

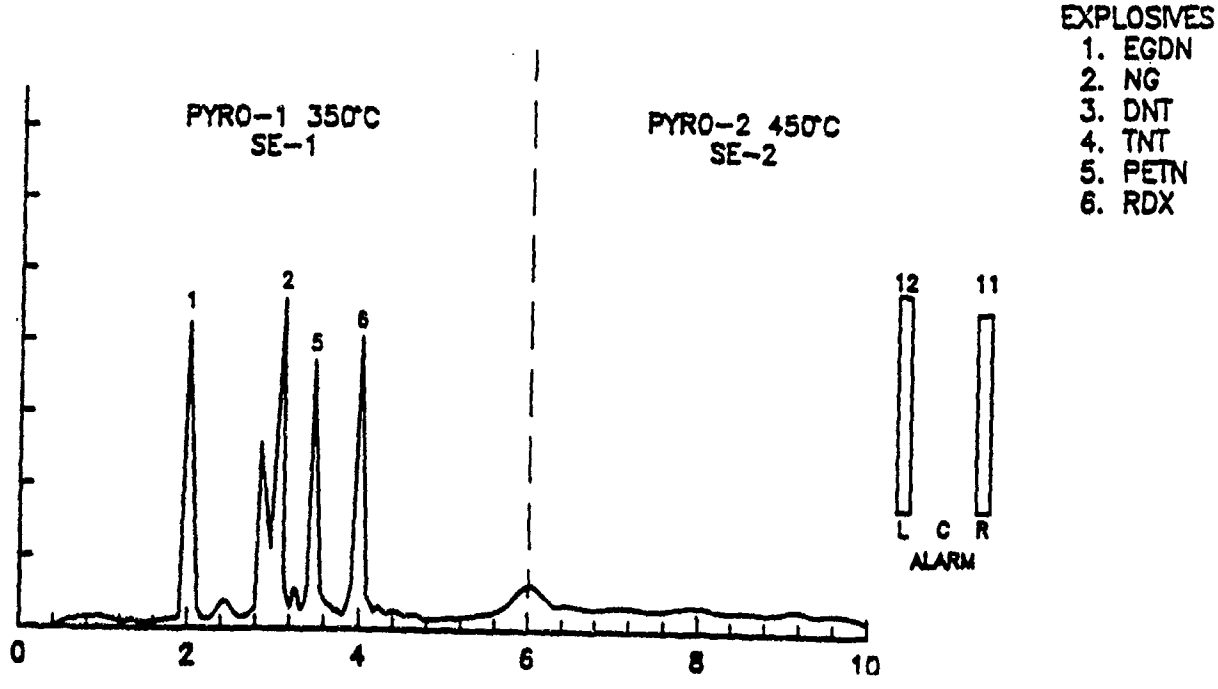


FIGURE 5B This chromatogram is similar to the one shown in 5A except that the SE-2 pyrolyzer (Pyro-2) has been reduced in temperature from 800 °C to 450 °C. The result of this temperature reduction is that there is no DNT or TNT detection in the SE-2 region of the chromatogram.

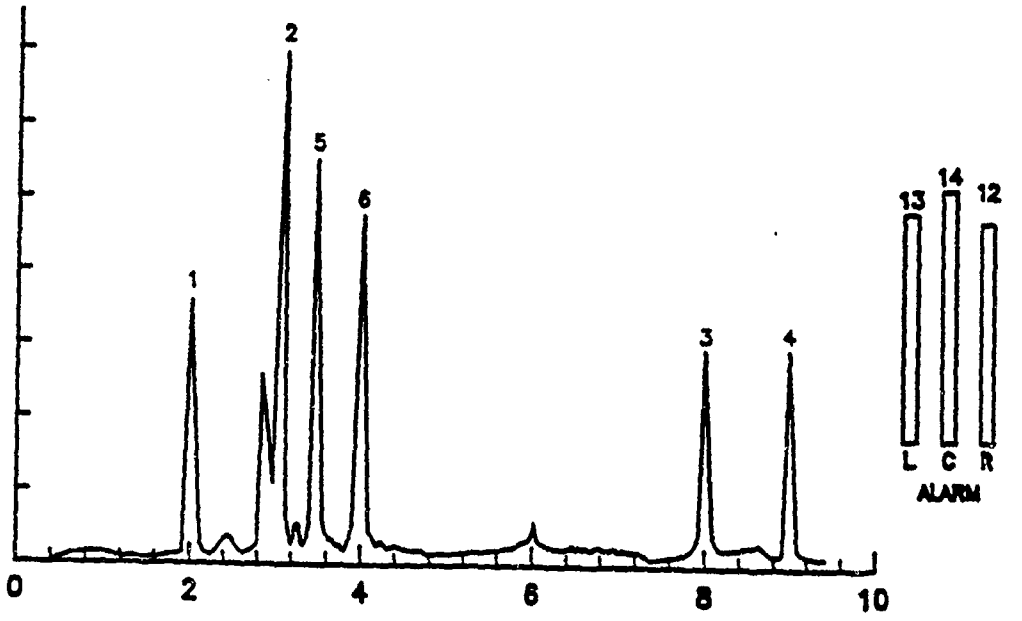


FIGURE 6A Chromatogram of vapor and particulates samples from a human test subject. Less than 5 picomoles each of the same explosive compounds shown in Figure 5A were spiked onto this sample.

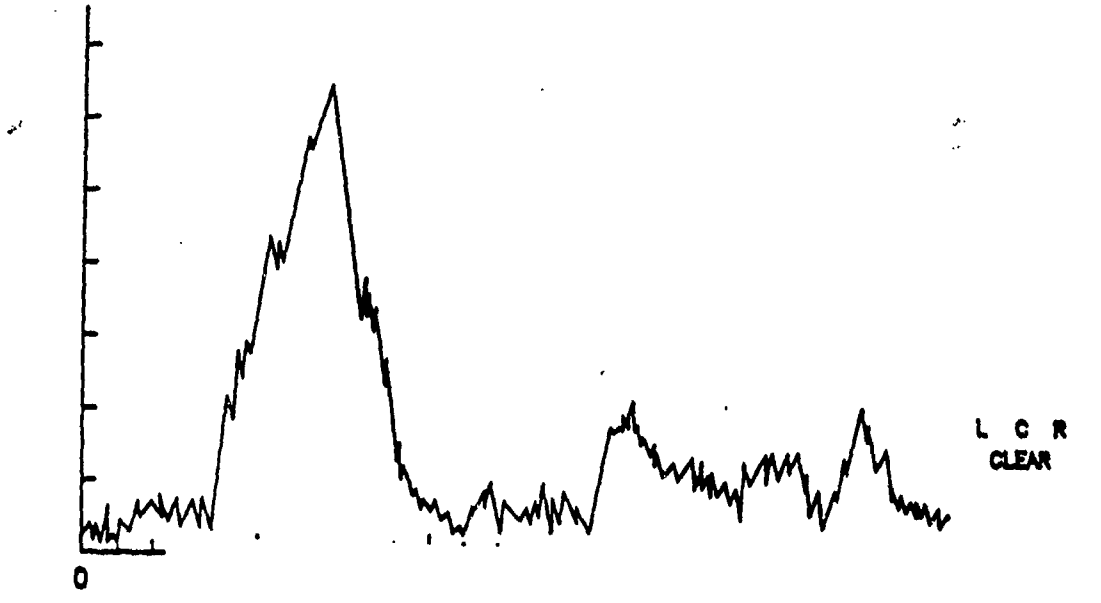


FIGURE 6B Chromatogram of the sample shown in Figure 6A except no explosive compounds were added.

A GC/ECD APPROACH FOR THE DETECTION OF EXPLOSIVES AND TAGGANTS

Dr. S. Nacson, Bob Mitchner, Otto Legrady
Tony Siu, Dr. S. Nargolwalla
SCINTREX LIMITED
222 Snidercroft
Concord, Ontario
L4K 1B5 Canada

1.INTRODUCTION

Since its introduction to the market some 6 years ago, the EVD-1 has achieved an enviable reputation as an explosive detector due mainly to its sensitivity, specificity and durability. This paper is intended to report on the expanded capabilities of the EVD-1 for the detection of all proposed ICAO taggants in addition to the conventional type of explosives (NG, DNT). Most interesting is its ability to detect PETN from plastic explosives.

The EVD-1DC unit is a 2 component system consisting of a battery-powered hand-held sampling unit and an analyzing unit, which can be AC or battery operated. The analyzer unit consists of a desorber, dual chromatographic columns and an ultra sensitive ECD detector. A block diagram of the system is shown in Fig. 1.

The sample collection tube (containing the adsorbed vapour or collected particulates) is placed in the continuously heated desorption unit of the analyzer. Desorption time is roughly 2-3 seconds under a purge gas of pure nitrogen. The vapour sample then enters the analyzer unit into a secondary adsorber, which serves the purpose of reducing sample contamination prior to introduction into the analytical columns. Separation of both volatile and relatively non-volatile explosive molecules takes place on the dual analytical columns terminating to a single ECD detector. A microprocessor software algorithm decides whether there is a signal within preset retention time windows corresponding to an explosive peak or a set of overlapping explosive peaks. The results are then sent to an LCD.

2. INSTRUMENT PERFORMANCE

The EVD-1DC response to an injection of a standard solution mixture of MNT, EGDN and DMNB (50-100 pg of each component) is shown in Figure 2. Background response of the solvent injection is shown in the left side of Figure 2.

Injection of a PETN standard solution produced two hits on windows A & C. These peaks shown in Figure 3 were attributed to the PETN parent peak (channel C) and fragment peak (channel A). The minimum detection limit for PETN is about one nanogram producing an average of 10 counts of peak area.

Total analysis time per sample is roughly 60 seconds, which includes, thermal desorption of the 1st adsorber tube, pre-cleaning step, chromatographic separation, detection and data processing/reporting.

Direct air sniffing of the head-space vapour of Semtex H and C4 (U.S. made) plastic explosives produced positive hits in channels A, B and C for the Semtex explosive and only channel B for the C4 (Fig. 4) explosive. A few grams of Semtex H explosive was placed in a glass bottle of approximately 120 cubic meters at room temperature. The same was done with the C4 explosive. From the equilibrium vapour pressure data of PETN (0.018 ppb at room temperature Ref. 2) and the equation governing the rate of evaporation of PETN from a solid, it is estimated that the amount of PETN expected to be collected on the 1st adsorber tube is roughly 16 nanograms. Laboratory sniffing of the head-space vapour of a small piece of Semtex H showed roughly over 20 ng of PETN. It is important to mention that other ingredients present in the Semtex sample may

contribute to the obtained signal. These ingredients were not characterized, but their presence confirmed using head-space vapour injections on a 15 meter capillary column connected in a Varian 3400 G.C. equipped with an ECD detector.

The signals obtained in channels A & B are from organonitrates, which the plastic explosive (e.g. C4) was contaminated with, either during manufacturing, transport or storage. The EVD-1DC dual column system is not set for detection of RDX, although the RDX peak appears at a later retention time, unacceptably long for a routine security checking operation.

Further improvements of the unit may involve a third G.C. column and possibly a separate ECD detector for detection of the RDX peak at a reasonable analysis time. It is also important to mention that with the high volume sampler, trace residual plastic explosives are readily transported onto the 1st adsorber cartridge. However, it is preferred to perform sampling as close to the suspected surfaces and possibly to touch the surface, in order to increase the probability of particulate transfer into the sample tube.

Other sampling methodology, not reported in details in this paper, involve direct surface swabbing with a fibre glass paper and subsequent close sampling of the swab with the EVD-1 sample tube.

Sampling of head-space vapour of crystallized commercial TNT sample produced positive hits on channels A & B with the parent TNT peak appearing late in the chromatogram (Fig. 5.). Further investigation of this sample revealed presence of 0-MNT, and P-MNT, and 2,4 DNT which are readily detected in channels A & B, respectively.

3. TEST EXPLOSIVES RESULTS

Head-space vapours of small samples of each of the test explosives were collected using the EVD-1 high volume sampler. Great care was taken to prevent sucking particulates onto the sample tube. The results of sampling the test explosives are shown in Table I.

Laboratory air and the production assembly area produced positive hits of roughly 20-40 counts in Channel A. Interferant results with a long list of men's/women's toiletries, household chemicals, smoking materials and common laboratory chemicals have revealed that Channel A was susceptible to false alarms on the men's/women's toiletries, producing an alarm in the 10-400 counts range. Recent EVD-1DC evaluation in Germany have produced similar false positives on Channel A using certain perfumes. This however, does not exclude the presence of the ortho-mono nitrotoluene as a trace contaminant in these products. Channel A could be blanked or disregarded as desired by the EVD-1 user.

4. CONCLUSION

A commercially available Explosive Vapour Detector EVD-1DC was modified to allow faster sample analysis without compromising sensitivity and selectivity of the device and provided additional capabili-ties to allow detection of all ICAO plastic explosive taggants in addition to the traditional organonitrate EGDN, NG and DNT. Finally, the ability to detect PETN as an overlapping peak with the DMNB taggant at Channel C was also demonstrated.

Future efforts will be focused in improving sampling methodo-logy, faster analysis and expanding the instrument capability to detect RDX.

REFERENCES

1. T.A. Griffy, Proceedings Third Symposium on Analysis and detection of explosives, Fraumbfer-Institut fur, Chemische Technologie July 10-13, 1989 pg. 38-2.

2. Rudolf Meyer "Explosives" 2nd edition, Verlag Chemie Weinheim, Derfield Beach, Florida Basel 1981

SUMMARY TABLE 1
OF
EXPLOSIVES DETECTION WITH THE MODIFIED EVD-1DC UNIT

EVD-1DC DETECTION WINDOW (+/-HIT)				
TYPE OF EXPLOSIVE/TAGGANT	A	B	C	APPROXIMATE DETECTION LIMITS
Explosive Semtex plastic	+	+	+	1 ng for PETN
C4 U.S. made plastic	-	+	-	<5pptv*
DMNB taggant	-	-	+	5ppt
O-MNT taggant	+	-	-	1ppt
P-MNT taggant	-	+	-	1ppt***
m-MNT taggant	-	+	-	1ppt
EGDN	-	+	-	1ppt
EGMN	-	+	-	5ppt
MMAN	-	+	-	5ppt
NG	-	+	-	5ppt
DNT	+	+	-	1ppt*
TNT	+	+	-	5ppt
Detonator cord	-	+	-	5ppt*
Plater U.K. made	-	+	-	5ppt*
Double base propellent	-	+	-	5ppt**
Black powder	-	+	-	5ppt*
Ammonium nitrate (commercial)	-	+	-	1ppt*
PETN	+	-	+	zx1 ng
Background room air	-	-	-	
Sniffing lab air	+	-	-	
Sniffing assembly room	+	-	-	
Blank run	-	-	-	
Machine shop	-	-	-	

* Organonitrates contamination or from MNT
** From NG
*** Always includes the P.MNT isomer

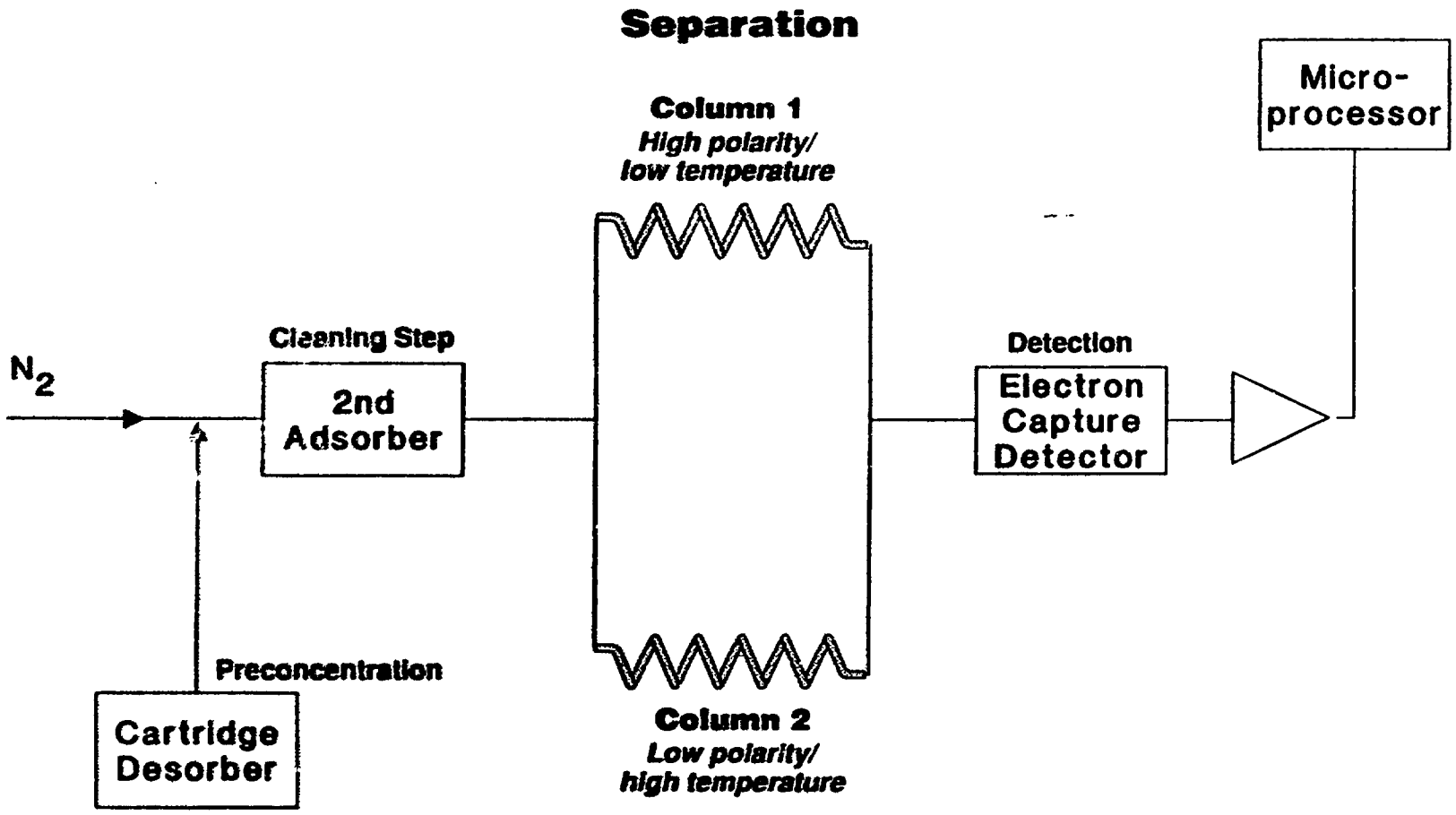
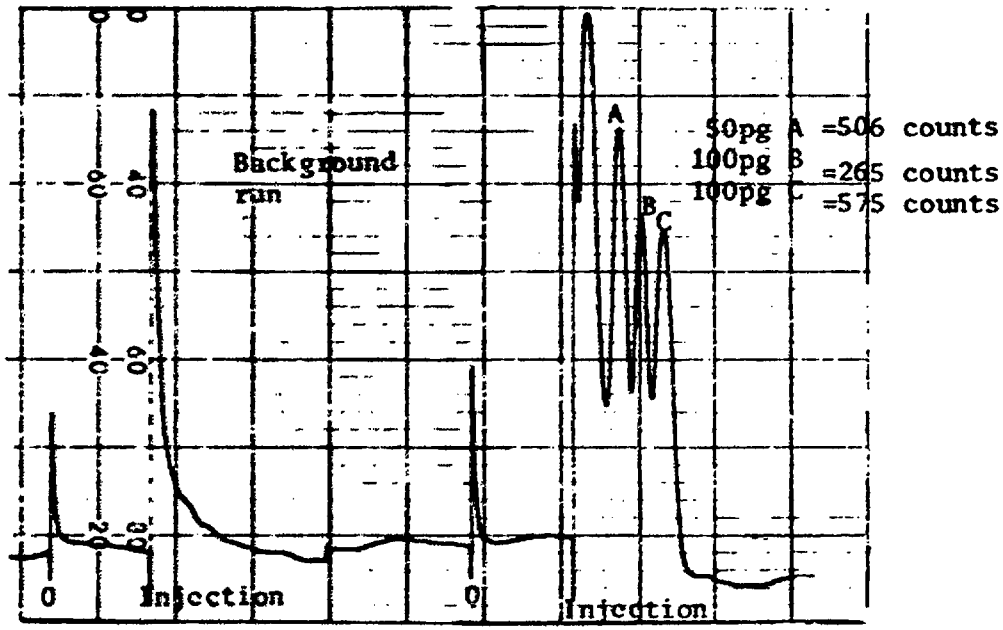


Fig. 1 **Block Diagram of EVD-1DC Unit**

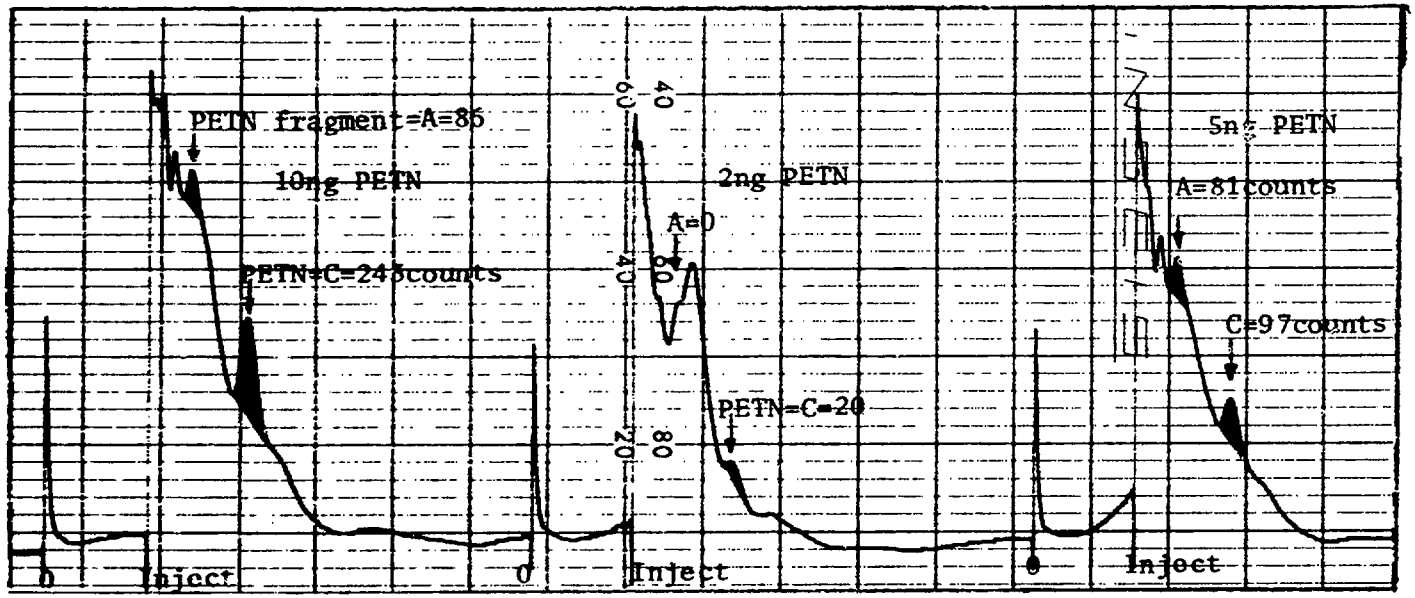
Fig. 2 **EVD-1DC Response to Liquid Injection of Standard Solutions of 0-MNT, EGDN and DMNB.**



Target Explosives

A = 0-Mono Nitrotoluene, PETN fragment
B = EGDN, MMAN, EGMN, P-MNT, NG and DNT
C = DMNB, PETN

Fig. 3 **Testing and Evaluation of New Software Package for Multi-Detection Windows. Detection of PETN Plastic Explosive in Window A and C.**



Injection of liquid standard solution of PETN onto the Tenax 1st adsorber tube.

Fig. 4 **New Software Evaluation and Testing EVD-1DC Unit .**
Head Space Sampling of Semtex H and C4 Plastic Explosives.

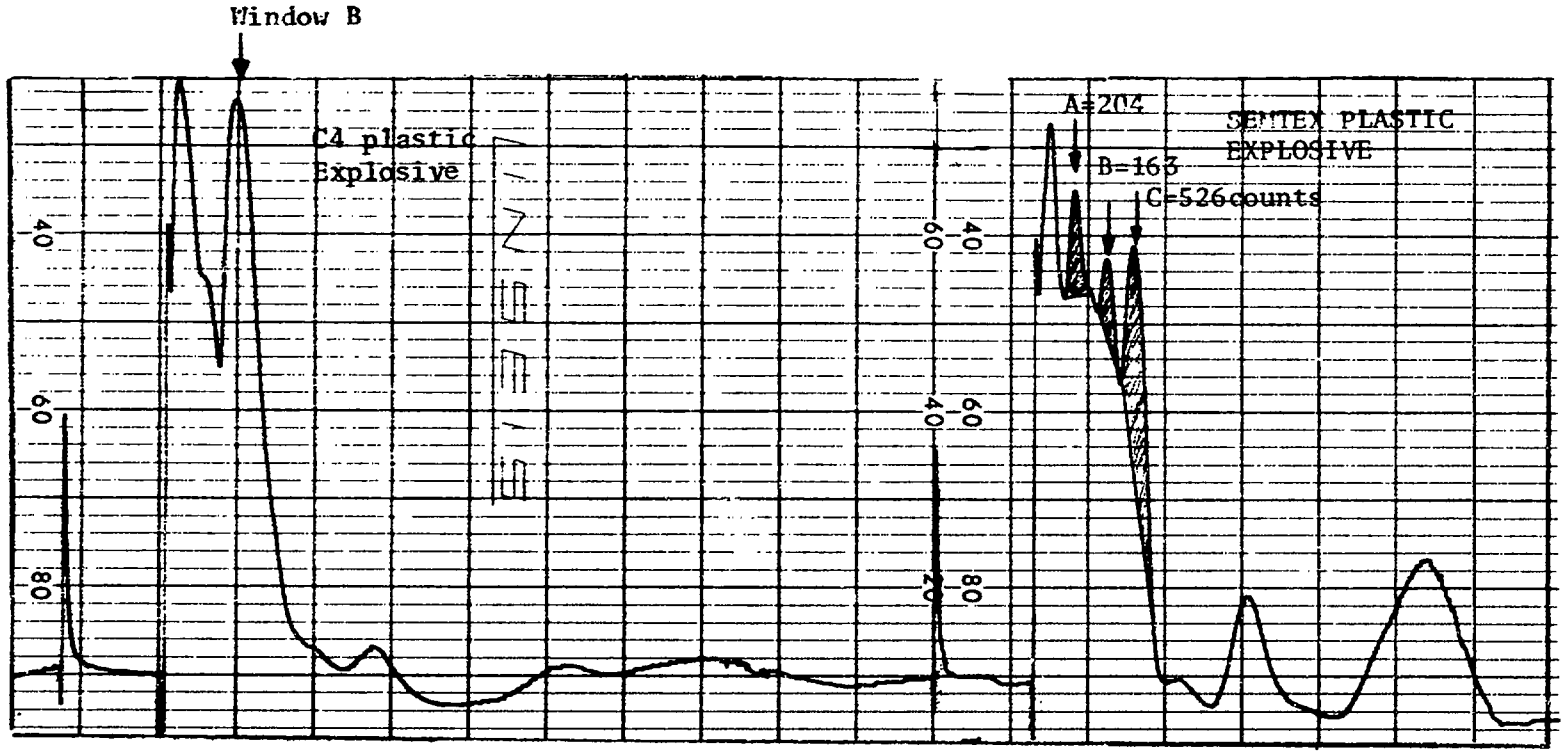
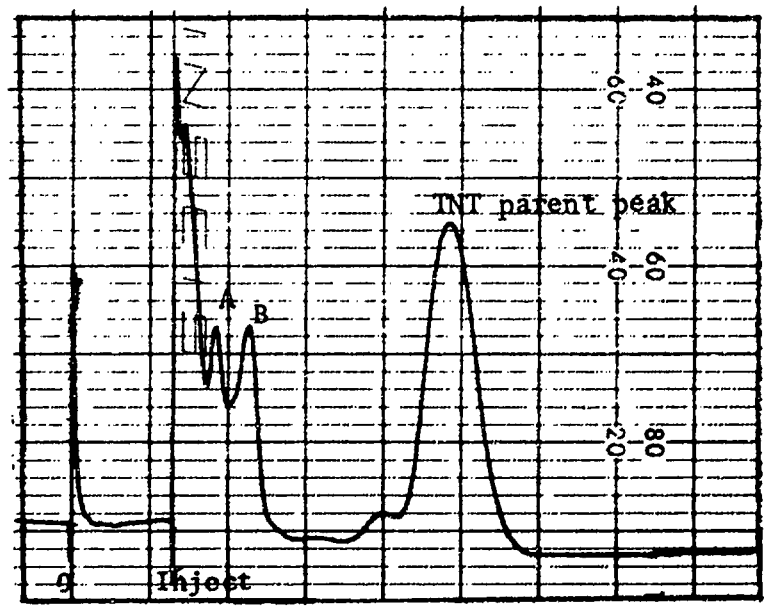


Fig. 5 **Head Space Vapour Sampling of Commercial TNT Sample for 5 Seconds.**



TAGGING

MARKING OF GERMAN PLASTIC EXPLOSIVE FOR THE ENHANCEMENT OF VAPOR DETECTION

Dr. Peter Kolla
Forensic Scientist
Bundeskriminalamt, Germany

1. INTRODUCTION

Explosive vapor detection is one of the most successful methods to discover hidden explosive devices. For the correct operation of this method, there must be an evaporation of molecules from the explosive. The detection limit of most of the equipments available, the so-called explosive vapor detectors (EVD's) (1), (2), requires at least in the range of 1-5 1012 molecules (trillions of molecules) to be collected and introduced into the machine. That seems to be a high amount and it is. All the molecules must be at the outside of the sampled container and must be in a collectable form e.g. not adsorbed at the surface. Presuming the above number as an example and sampling one litre of air directly above the pure explosive substance, PETN and RDX with vapor pressures in the range of 10 ppt (3) can just be detected. Under real conditions the searched explosive is covered with several layers of different material and is placed in any kind of container. The vapor from the explosive is retarded and the amount of collectable molecules is much lower. Experience shows, that ingredients with vapor pressures lower than TNT are not detectable. Reliable detection is only possible for explosives that contain explosive oils such as EGDN or NG. Pure vapor detection i.e. without any mechanical transfer of particles is impossible when plastic explosives are hidden. Main constituents of plastic explosives are PETN and RDX with very low vapor pressures. Therefore the tagging conception was created and the addition of easy evaporating substances to plastic explosives shall enable vapor detection.

2. RESULTS AND DISCUSSION

In Germany only one plastic explosive is produced, SEISMOPLAST. The main constituent is PETN. In contrast to many other plastic explosives from other countries, the plastifier in the German plastic explosive is silicon oil. This composition leads to several problems in the production procedure if a taggant has to be added. In Germany the taggants still in question are o-mononitrotoluene, p-mononitrotoluene and dimethyl-dinitro-butane. No decision could be found until today on the selection of one. The problem for the manufacturer is that none of the three is soluble in silicon oil to easy mix them into the plastic explosive. Additionally during the manufacture water has to be removed under slight vacuum at about 60° C. Consequently it will be very difficult to adjust a defined amount of tagging substances in the final plastic explosive.

A very important point, which influences the selection of a substance is the injuriousness to health. The two nitrotoluenes are believed to be carcinogenic and the manufacturer as well as the user want to avoid this risk.

During such discussions the essential criterion, why taggants are added, is often forgotten. The enhancement of the detectability of plastic explosives depends not only on the compatibility of the taggant with the explosive but also on the response behaviour in the detector. The marking agents in discussion have molecular structures that should enable most of the commercially available EVD's to detect them. That statement considers only the function principle e.g. IMS, GC-ECD or chemoluminescence. The operational conditions of all devices have to be adopted to all taggants in question. This additional recognition criterion for at least three substances simultaneously with six explosive compounds is a very difficult problem. First, you must have a high separation efficiency with a peak capacity (spectroscopic and chromatographic) of nine peaks and more in one run. It must also be possible to set the corresponding nine windows for recognition. Second, the false alarm rate will consequently increase to a much higher number than before, because much more interferences are possible. The increase of the false alarm rate may lead to chaotic conditions for the operation of the detection method in the real security control.

The investigations, that have been made in Germany comprise the detection as well as the stability field. The addition of o—MNT, p—MNT and DMNB to small amounts (50 g) of the plastic explosive was done by intensive kneading by hand.

3. DETECTION WITH THE ICAO BOX

The detection experiments in Germany were performed with the chemoluminescence based EGIS equipment (4). It was selected because of its superior selectivity and separation efficiency compared to all other EVD's (Figure 1). The sampling procedure of the EGIS supports a good mechanical transfer of particles into the detector. That is especially important for the detection sensitivity in real baggage checking.

The experiments were made with the prepared explosives following the ICAO proposal. The explosive was put into a polythene bag, wrapped into cotton-wool and packed with newspapers in a paper box. Measurements were performed after several hours up to three days and the height of the signal was recorded (Table Ia and Ib). The measure for the amount of taggant outside the box was the peak height in the chromatogram. Distinct signals were depicted if peaks were higher than five peak height units. The relation of the total amount of substance in the sampled air volume is approximately as follows: 1 peak height unit of the nitrotoluenes corresponds to 20 pptv, 1 peak height unit of the DMNB is related to 10 pptv. The measurements were performed with and without burping by sampling twice with the sampling device (14 s; 2 l/s). The approximation of the concentrations was performed with regard to a collecting efficiency of 10 % of the substance to be adsorbed on the collector coil.

The o-MNT in a concentration of 0.5 % could already be detected after 1 hour with burping, whereas under the same conditions the p-MNT was detectable not before 3 hours. Time for the first detection was nearly doubled at a concentration of 0.1 % (Figure 2). Without burping detectability of the MNT's was worse, but the o-MNT gave still acceptable results. The p-MNT could not be detected before 24 hours. The widely discussed DMNB showed a different behaviour. It was only detectable when sampling was performed with burping. The 0.5 % sample took 24 hours for the first signal and the 0.1 % sample was detectable only after 2 days. All results correspond to the differences in vapor pressure (5). The o-MNT is the best evaporating substance with a vapor pressure, that is roughly 100 times higher than the vapor pressure of DMNB. Measurements of the vapour pressure showed an approximate linear decrease with dilution in the explosive (Table 2).

4. SUITCASE EXPERIMENTS WITH MONO-NITROTOLUENES

For these experiments the nitrotoluenes were selected, because they were believed to be the best marking agents at that time. The o-MNT and the p-MNT were mixed 0.5 % in plastic simulators consisting of paraffins.

A hardcover suitcase was cleaned with acetone at the outer surface and the simulators with the tagging substances were put into the suitcase. Shortly after the closure of the suitcase, no substances could be measured at the outside. After 16 hours three new measurements were taken and each time a distinct signal was obtained for the two nitrotoluenes with a slightly higher signal for the ortho isomer. The suitcase had overlapping slots and seemed to be fairly tight.

The second experiment was done with a usual bag with a zipper at the upperside. Already after 30 minutes clear peaks were obtained from o-MNT and p-MNT with similar peak heights. The sampling was done by moving the device twice along the zipper. The simulators were layed without special covering about ten centimeters below the closed zipper.

Another suitcase of imitation leather and a zipper was used because it seemed to be more tight than the bag. The simulators were put into the middle upperside of the suitcase, which also contained clothes. The zipper was closed and 25 minutes afterwards the first measurement was performed. No signal was seen in the detector. After 3 hours a small peak arose from o-MNT, the peak of p-MNT was in the range of the detection limit. After 4.5 hours the signals for the substances had increased with a clear peak for o-MNT and a poor peak for p—MNT (o-MNT 3 times higher than p—MNT). The sampling was done by sniffing twice along the zipper.

The last suitcase was a hardcover one again. But the simulators were packed into polythene bags each and then put in the upper middle region of the suitcase. The suitcase was filled up with clothes. The outside

of the closed suitcase was sampled after 70 hours (a weekend). Only very small peaks just above the detection limit were observed for the two taggants. The peak height was similar. After opening the suitcase and sniffing at the clothes, that were in a layer at a distance of about 10 cm from the packed simulators, big peaks were obtained with a peak height of p-MNT twice of the o-MNT. That shows that the para isomer tends to be adsorbed more strongly.

Nitroaromatic compounds, such as the tagging substances discussed in this paper, tend to be strongly adsorbed at several surfaces, because of polar interaction as well as partition effects. The vapour pressure of the substances, when they are adsorbed is strongly decreased, so that often above the surfaces no vapour can be detected. In order to look for an adsorption effect, the inner surface of the hardcover suitcase was sampled 3 hours after the removal of the simulators. Very big peaks of each component were found. Two polythene bags were put into the same suitcase, without samples in it. The first bag was removed after 3 hours and its surface was sampled. Distinct peaks of o-MNT and p-MNT were observed. The second bag was removed after 8 hours and both bags were exposed to clean air for 70 hours. After that long time, there were still signals observed, but they decreased by a factor of ten. If the taggants are adsorbed, they stick very fast especially at plastic surfaces.

After the removal of the simulators from the imitation leather suitcase, it was opened for half an hour and then the surface of the clothes was sampled. Big peaks of each taggant were observed, showing that the clothes, which are exposed to the taggant vapour, are strongly contaminated with these substances. The same observation was made at the surface of a briefcase, that had never been handled directly with the taggants in before. It was standing near the preparation place. On its surface small amounts of o-MNT as well as p-MNT were measured by a single sniffing experiment.

5. STABILITY OF THE MARKING AGENTS

The stability of the taggents in the plastic explosive was investigated by analytical measurements after one year of storing. The marked explosives were formed to small balls and laid at a well ventilated place without any wrapping. After one year, samples were taken from the center of the ball and the outer surface. The samples were analyzed by HPLC and GC-MS to quantify the amount of the remaining tagging substance (Figures 3 and 4). Analysis of the DMNB marked ball gave a 2 times higher concentration in the sample from the center compared to the surface sample. A possible explanation for that big difference is the relatively slow diffusion velocity compared to the evaporation from the surface. It is believed, that such an effect may reduce the detectability considerably. The o-MNT and the p-MNT could only be analyzed as very low amounts by overloading the HPLC, quantification or calculation of ratios was not possible. In GC-MS analysis none of the two substances were found in the explosives that were stored without wrapping. Samples of the same explosives that were stored in a closed bottle gave clear signals for both taggants. It seems that the mononitrotoluenes are lost by the one year of unpacked storing. To get a final conclusion it is necessary to repeat such experiments with bigger amounts of explosives formed to different shapes (plates, balls, blocks).

6. CONCLUSION

The detectability of German plastic explosive is considerably enhanced with addition of the tagging substances. The best results were obtained by marking with o-mononitrotoluene but the evaluation of stability investigations shows, that both nitrotoluenes are lost very fast by storing the unwrapped explosives. Additionally, the carcinogenic properties of the nitroaromatic taggants may prevent their usage. Dimethyldinitrobutane shows a moderate detection behaviour, but it seems to stick for a longer time in the plastic explosive. Some serious doubts exist about the routine checks of real baggage. Because the existing vapour detectors have to be extended with additional detection windows for all the possible taggants, the false alarm rate may increase to a very high value. Especially the nitrotoluenes have very similar polarities and vapour pressures to a lot of odorous substances. Some experiences in recent EVD tests in Germany showed possible interferences between nitroaromatics and perfumes. If false alarm rate only rises in the range higher than 1 %, the usage of the method may be impractical.

REFERENCES

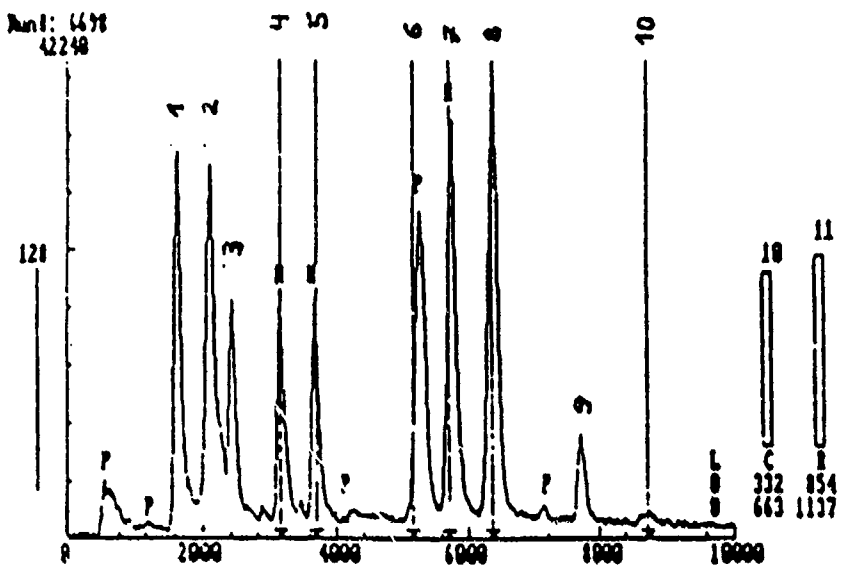
1. L. Elias, P. Neudorfl, Proc. 3rd Symp. on Analysis and Detection of Explosives, 43-1, Mannheim, Germany, 1989.

2. D. Fetterolf, Proc. 3rd Symp. on Analysis and Detection of Explosives, 33-1, Mannheim, Germany, 1989.

3. B.C. Dionne, D.P. Rounbehler, E.K. Achter, J.R. Hobbs, D.H. Fine, J. of Energetic Materials 4 (1986) 447.

4. R.Jackson, E.E.A. Bromberg, Proc. 3rd Symp. on Analysis and Detection of Explosives, 42-1, Mannheim, Germany, 1989.

5. Handbook of Chemistry and Physics, 63rd Edition, 1982-83, CRC press.



Calibration of the EGIS with six explosives and three taggants

1. EGDN; 2. DMNB (A); 3. NG; 4. PETN; 5. RDX; 6. o-MNT;
7. p-MNT 8. DMNB (B); 9. DNT; 10. TNT

Figure 1

Tests with the ICAO standard box (1)

measure: peak heights after x hours

	o-MNT0.1	p-MNT0.1	DMNB0.1	o-MNT0.5	p-MNT0.5	DMNB0.5
with burping						
0	-	-	-	1.4	-	-
1	-	-	-	21.7	-	-
2	3.4	-	-	x	x	x
3	x	x	x	26.0	2.8	-
5	13.9	1.2'	-	x	x	x
24	36.4	7.8	-	99.0	31.2	1.9
48	44.3	7.8	1.8	195.0	175.0	5.1
72	70.0	26.0	4.2	144.0	235.0	6.7

p-MNT0.1: 0.1% w/w p-mononitrotoluene in plastic
x: not measured 1.2': after 7 hours

Table 1a

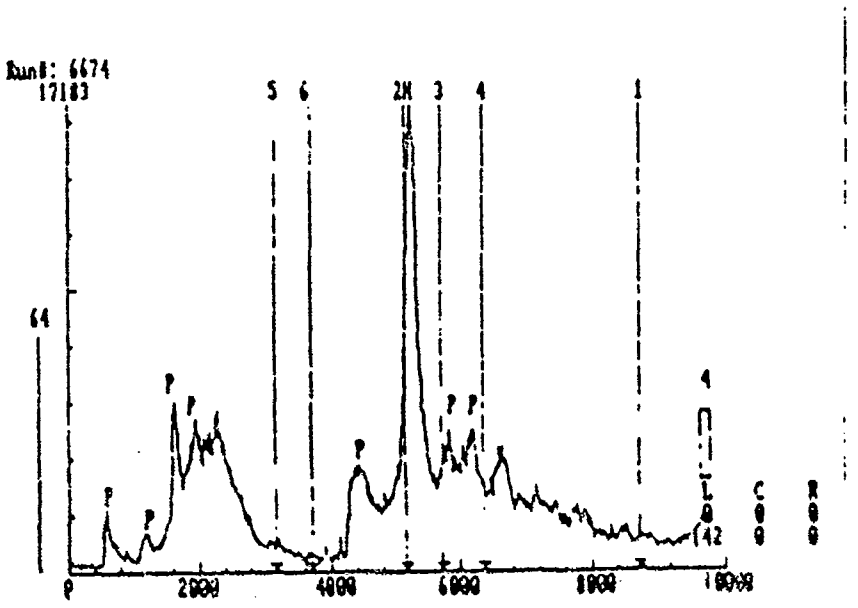
Tests with the ICAO standard box (2)

measure: peak heights after x hours

	o-MNT0.1	p-MNT0.1	DMNB0.1	o-MNT0.5	p-MNT0.5	DMNB0.5
without burping						
0	-	-	-	1.4	-	-
1	-	-	-	9.8	-	-
2	2.8	-	-	x	x	x
3	x	x	x	15.0	-	-
5	5.1	-	-	x	x	x
24	33.0	2.1	-	56.5	20.2	-

p-MNT0.1: 0.1% w/w p-mononitrotoluene in plastic
x: not measured 1.2': after 7 hours

Table 1b



Test with the ICAO standard box: Sampling o-MNT0.1 after 24 hours without burping

Figure 2

Vapour pressure of the substances above the marked German plastic explosive (Seismoplast)

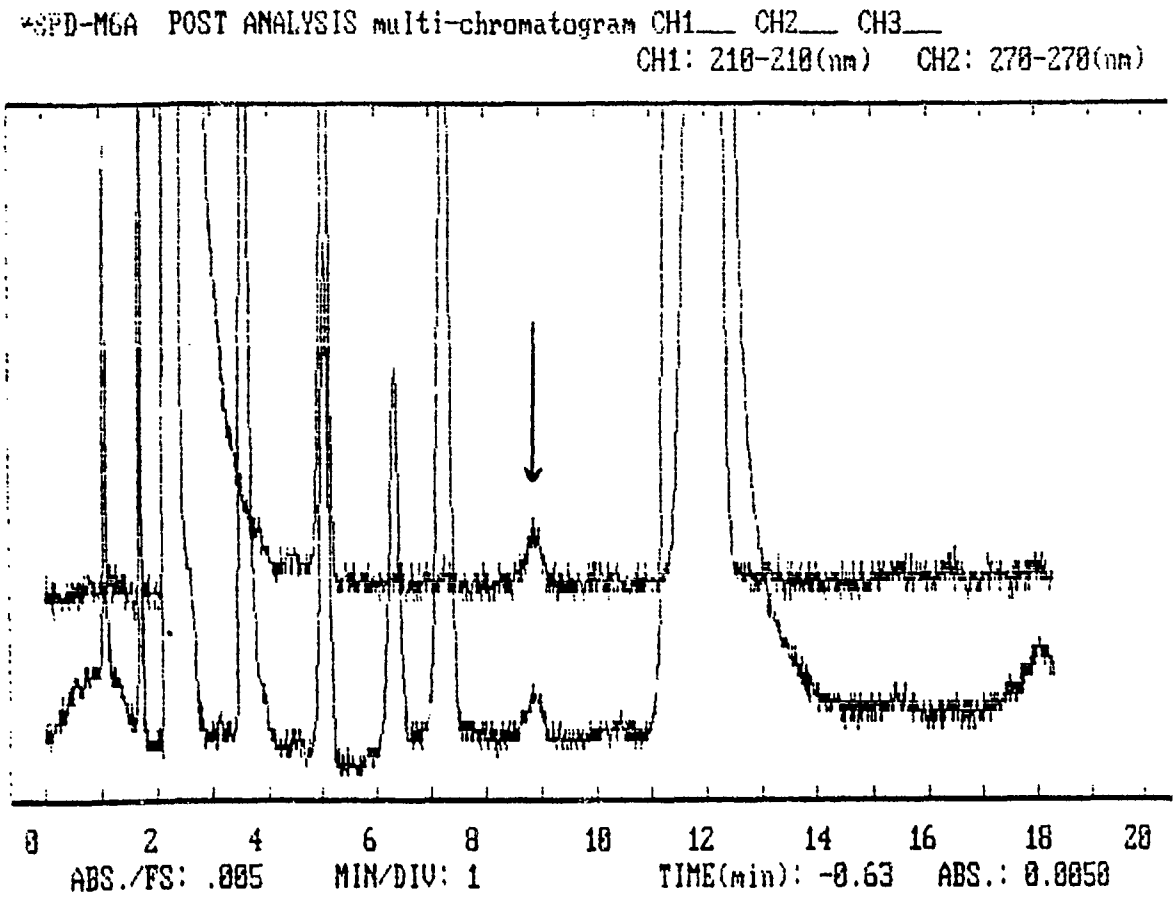
Plastic + 0.1% o-MNT = 100 ppbv

Plastic + 0.5% o-MNT = 460 ppbv

Plastic + 0.1% p-MNT = 50 ppbv

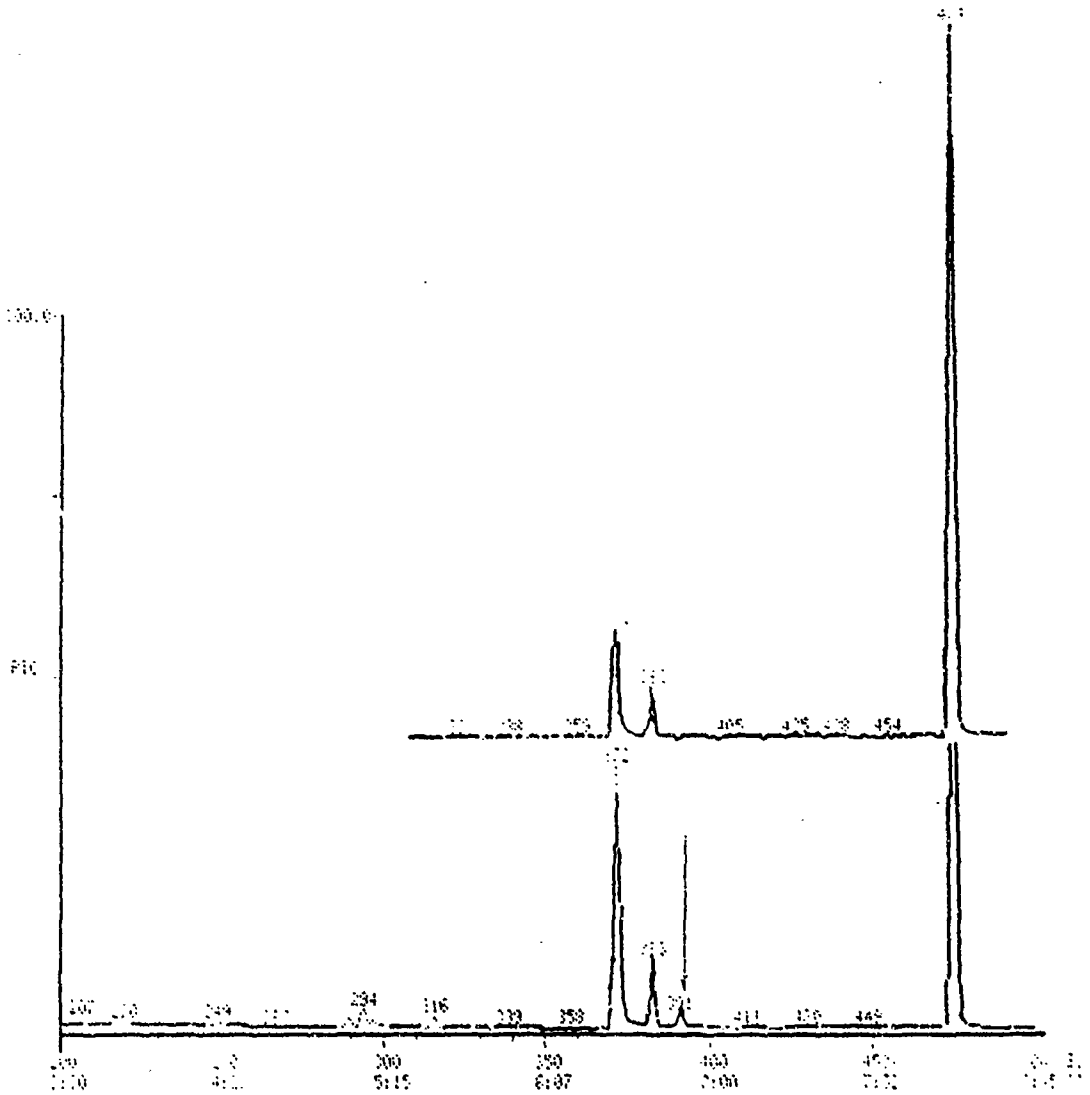
Plastic + 0.5% p-MNT = 200 ppbv

Table 2



HPLC overloading analysis of p-MNT 0.5 after one year storag

Figure 3



GC-MS analysis of o-MNT 0.5 after one year storage

1. Explosive stored in a closed bottle
2. Explosive stored without wrapping

Figure 4

PROGRAM TO TAG MILITARY PLASTIC/SHEET EXPLOSIVES

Sarah Eng, Joseph Lannon, and Carolyn Westerdahl
U.S. Army Armament Research Development and Engineering Center
Picatinny Arsenal, NJ

1. INTRODUCTION

Although there have been efforts by private and Government investigators to tag explosives for more than 20 years as evidenced by the establishment of the Advisory Committee on Explosives Tagging in 1973, this effort took on renewed urgency in response to the PAN AM 103 tragedy in December 1988. The International Civil Aviation Organization, a United Nations Committee, pursued an international convention which requires the tagging of all plastic explosives (including flexible sheet explosives) with an ingredient that will make the explosives detectable with existing, commercial explosive vapor detectors.

The United States Government participated in the diplomatic conference which ratified the convention in February, 1991. This convention requires all manufacturers, including the government, to begin tagging all plastic explosive production after 1 January, 1994 and to ensure that no untagged inventory of unincorporated explosive remains after that date for civilian use, or after 1 January 1997 for military use.

The Department of State was the U.S. lead for negotiating the international agreement. Within the Department of Defense the U.S. Army has been given the technical lead to plan and implement the negotiated convention. The Armament Research, Development and Engineering Center, ARDEC, has provided the technical support from the onset of Army involvement.

2. OBJECTIVES

The first objective of this program was to identify candidate taggants which: are reliably detectable by commercial vapor detectors with minimal false alarms; are compatible with the explosives with which they come in contact; do not degrade other materials with which they are packaged; do not degrade the performance or safety of the plastic explosive in which they are incorporated; have an acceptable lifetime within the explosive; and can be safely manufactured and stored.
After identifying the most promising taggant this program has the goals of: carrying out all necessary health and safety tests; ensuring that the explosive and the related items can be produced; identifying all items within the DoD which use plastic explosives; testing and requalifying them as necessary; managing the inventory so the minimum amount needs to be disposed of in 1997.

3. APPROACH

ARDEC began work on this project in FY 90 with money provided by The Department of State. A candidate taggant was identified, and several preliminary tests were conducted in the plastic explosive Composition C-4. This is the only plastic explosive manufactured by DoD. The program schematic is depicted in Figure 1. Phase 1 of this program was the identification of candidate taggants through literature search and knowledge of explosive characteristics using the above Objectives. There was extensive interaction with the scientific community of other nations who are interested in this effort.

Phase II had two parts. There was small scale testing of the candidate taggant to determine compatibility, sensitivity, performance, detectability, and toxicity. There was also consultation with the other services and other parts of the Army to identify concerns; e.g. which items incorporate plastic explosives and may need requalification.

Phase III has 5 main parts: Full scale toxicity and environmental testing; manufacture and qualification of Composition C-4; testing for degradation of neighboring materials; manufacture and qualification of selected end items; and management of inventory. The last part is not handled by ARDEC.

3.1 Full scale toxicity and environmental testing has begun at the Army Environmental Hygiene Agency. These tests will determine if particular care is required in the manufacture and handling of the

tagged material.

3.2 One of the primary concerns in the manufacture of tagged plastic explosive is ensuring the uniform distribution of the taggant. Experiments are planned using colored material to monitor the dispersal in the mixer. After a large batch of the tagged material is manufactured, the distribution will be tested, the required performance and safety tests will be conducted, then all documentation will be modified.

3.3 A testing program has been outlined to determine the effect of the taggant on the non-energetic components in the end items. These are things like plastic sheets, adhesives, and plastic parts. These will be aged at elevated temperatures and high humidity with the tagged and untagged explosives, then be examined for degradation.

3.4 Not only the basic explosive but also key armament items made with the explosive will be requalified i.e. have the performance and safety testing. The documentation for all items using plastic/sheet explosives will be changed and new National Stock Numbers will be issued. This includes not only items made with Composition C-4 but also those made with commercial sheet/flexible explosive.

3.5 Stockpile management is a tri-service effort which is coordinated from the Office of the Single Manager for Conventional Ammunition.

4. STATUS

The following work has been carried out on batches of tagged Composition C-4 made in the laboratory at Holston Army Ammunition Plant. Many of the tests will be repeated with the material from the full scale manufacture.

4.1 The taggant's detectability was measured with the International Civil Aviation Organization (ICAO) suitcase using five different commercial explosive vapor detectors. This gave guidelines as to the minimum concentration of the taggant which could be used.

4.2 Accelerated aging tests are being conducted at several temperatures to determine the loss of taggant from the Composition C-4 with the objective of predicting an overall lifetime for the taggant in the explosive.

4.3 Sensitivity and performance tests such as compatibility, impact sensitivity, detonation velocity and plate dent were carried out on material produced in the laboratory to compare the tagged and untagged C-4.

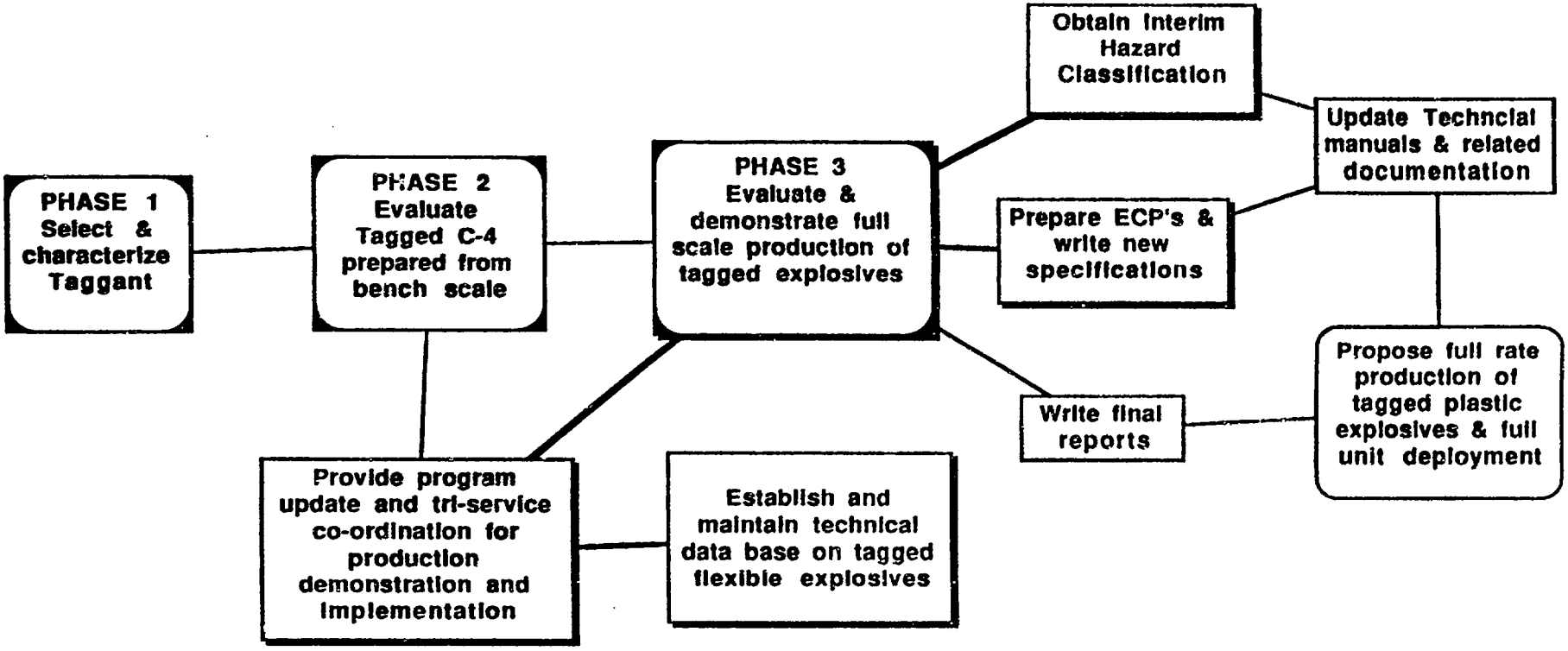
4.4 Mechanical property tests compared the tagged and untagged C-4.

4.5 The pure taggant was used in in-vitro and in-vivo toxicity tests for mutagenicity and carcinogenicity, as well as, oral LD50 tests for the Swiss-Webster mouse.

5. CONCLUSION

There has been extensive tri-service co-ordination on this program and that continues. Large scale toxicity tests have begun and environmental tests are scheduled. The Workplan and schedule for the remaining tests have been finalized. It appears that the Department of Defense will be able to meet the deadline for incorporating taggant into plastic explosives.

FIGURE 1. PROGRAM SCHEMATIC FOR VAPOR TAGGANT PROGRAM October 1991



AN IMPROVED VAPOR TAGGANT DETECTOR

T. H. Chen
U. S. Army Armament Research, Development, and Engineering Center
Picatinny Arsenal, New Jersey 07806-5000

1. INTRODUCTION

An international effort in the tagging of plastic explosives with vapor taggants culminated in the signing of an international convention this year. As part of this effort, we conducted the detectability of a vapor taggant in concealed modified Composition C-4 using several off-the-shelf portable commercial explosive vapor detectors.

One detector was found to perform quite well. However, this detector which is based on GC/ECD, has a turnaround time of approximately two minutes. This is, of course, too long for passenger screening purposes. Furthermore, the retention windows are fairly wide which could lead to potential false alarms. In addition, the hand-held sampler does not lend itself for automated sampling applications. The ion mobility spectrometer (IMS) type detectors were found to be quite unsatisfactory for the detection of the taggant.

The objective of this paper is to briefly spell out the general requirements for optimizing various important parameters such as the turnaround time, sensitivity and selectivity of detection, and the sampling protocol.

2. EXPERIMENTAL

2.1 Apparatus

A portable explosive vapor detector of GC/ECD type with dual packed columns was used in the improvement of an international sampling protocol.

3. RESULTS AND DISCUSSION

The vapor taggant detector for passenger screening applications requires a very short turnaround time (about 10 seconds). I believe that a low-cost, rapid response portable vapor taggant detector based on GC/ECD, or gas chromatograph/mass spectrometer (GC/MS) or MS alone, or gas chromatograph/chemiluminescence detector (GC/CLD) could be built. The discussion in this paper will be limited to the GC/ECD type.

Experimentally so far, we have only examined the taggant sampling protocol (see our paper in this volume on the detection of taggant in modified Composition C-4). We feel that we have made a significant improvement in the existing international detection protocol and concluded that an effective sampling protocol must incorporate a sampling device and procedure to enable sampling of taggant vapor from inside the suitcase with minimum sampling of outside air from around the sampling area. We are currently working on a device incorporating our latest findings for sampling taggant vapors from the "real world" suitcases.

To my knowledge, an efficient sample concentrator properly interfaced to the portable GC/ECD, or GC/MS for automated analysis is not available at present. This device is quite important in the overall scheme of taggant detection. It must be capable of concentrating the taggant vapor and delivering a concentrated slug of taggant to the separation columns very rapidly and automatically.

In order to shorten the analysis time, increase the sensitivity and specificity and thus reduce the false alarm rate, use of short, rugged high resolution columns is essential. These columns became available only recently. The multicolumn approach will obviously enable the identification of taggants with greater confidence.

Use of ECD should be satisfactory for taggant detection although other taggant-specific detectors should be carefully examined.

In order to achieve the very short overall turnaround time, the dead-volume and the heat sink throughout the entire detection system should be eliminated, or minimized.

Finally, the detector should be designed for rugged automatic operation and be as "user friendly" as possible.

4. SUMMARY

The general system requirements for a low-cost, rapid response portable vapor taggant detector based on GC/ECD, which is suitable for passenger screening as well as other applications, have been briefly discussed.

PLANT LABORATORY SCALE PREPARATION AND COMPLETE CHARACTERIZATION OF MODIFIED COMPOSITION C-4 CONTAINING A TAGGANT

T. H. Chen, C. Campbell, R. Reed, W. F. Ark, J. Autera,
D. A. Wiegand, and M. S. Kirshenbaum
U. S. Army Armament Research, Development, and Engineering Center
Picatinny Arsenal, New Jersey 07806-5000

1. INTRODUCTION

An international effort in the tagging of plastic explosives with vapor taggants which culminated in the signing of an international convention this year. As part of this effort, modified Composition C-4 *homogeneously* tagged with 1 and 0.1 wt % vapor taggant were prepared at plant laboratory scale and a complete characterization of the modified Composition C-4 was conducted. The objective of this paper is to evaluate all parameters which are crucial in the detection of concealed tagged plastic explosives, performance of tagged explosives, and safety. Preparation of homogeneous specimens is critical to obtaining valid conclusions.

The parameters investigated include homogeneity, detectability, life-time, stability, compatibility, performance, sensitivity, mechanical properties, and toxicity.

This paper will briefly describe the comprehensive studies conducted and discuss the conclusions obtained.

2. EXPERIMENTAL

2.1 Apparatus

A ternary high performance liquid chromatograph was used in the analysis of the taggant. Several off-the-shelf commercial portable explosive vapor detectors and a portable particulate explosive detector were used in the quantitative detectability evaluation of the chosen taggant in the concealed tagged Composition C-4 using an international protocol. A differential scanning calorimeter was used in the stability and compatibility studies. Other physico-chemical tests were conducted in accordance with standard military specification methods.

3. RESULTS AND DISCUSSION

In order to simulate a situation as close as possible to the "real world", the modified Composition C-4 tagged with the taggant at nominally 1.0 and 0.1 wt. % concentrations was prepared using a two-pound scale manufacturing plant equipment. A total of 50 pounds, i.e., 25 batches, each of control (untagged), tagged at 1.0 wt. %, and tagged at 0.10 wt. % compositions, were prepared.

A total of five cored samples were obtained from each of the 50 pound cubic blocks of tagged Composition C-4 containing approximately 1.0 and 0.10 wt. % taggant to determine the homogeneity of taggant distribution. The five samples represent the center-top, center-middle, and center-bottom along the vertical axis, left-side, and the right-side along the horizontal central axis. The samples were analyzed by the high performance liquid chromatographic method (HPLC) developed for this work.

The samples were found to be homogeneous within the experimental error and the concentrations were identical to the nominal values. Thus, the simple mixing process and equipment used enabled the preparation of homogeneous specimens without taggant loss.

Among the five detectors tested, only two detected the taggant in concealed Composition C-4 tagged at the 1.0 and 0.1 wt. % levels. One is capable of producing reproducible quantitative detector response for the taggant with a detection limit of approximately 5 picograms and the detection time of approximately 2 minutes. The response of the other is nonquantifiable and this detector sometimes detected the taggant as a halogenated compound, a false response. Although incapable of detecting the

taggant, the particulate detector tested was excellent in the detection of 1,3,5-trinitro-1,3,5-triazacyclohexane (RDX) from both outside and inside of the suitcase contaminated with Composition C-4.

The life-time studies have not been completed. However, the results obtained so far indicate that the life-time of the taggant in Composition C-4 will meet the requirement.

The results of both the standard compatibility test and the differential scanning calorimetry (DSC) study on the tagged Composition C-4 were indistinguishable from the untagged control Composition C-4 within the experimental error. The compatibility between the taggant and pentaerythritol tetranitrate (PETN) was also tested and they were found to be compatible. Other plastic explosives containing PETN are therefore likely to be compatible with the taggant. Furthermore, the taggant was found to be very stable. In fact, it is more stable than RDX.

The results of the impact sensitivity test, shock sensitivity test, detonation velocity measurements, and the plate dent test, an output test, showed no significant differences between the tagged and the control Composition C-4 within the experimental error.

The results of *in-vitro* and *in-vivo* short-term toxicity tests indicate that the taggant is neither mutagenic, nor carcinogenic. The oral LD50 for the Swiss-Webster mouse was estimated to be similar to that of RDX for rat. Since RDX constitutes the main component of the Composition C-4, the toxicity of the taggant at the 1.0 wt. % or lower levels is acceptable unless the results of additional long-term tests, which are being conducted, indicate otherwise.

The results of mechanical property tests by compression measurement of cylindrical samples showed no significant difference between the tagged Composition C-4 and the control within the experimental error.

4. CONCLUSIONS

A *homogeneously* tagged Composition C-4 can be prepared by a simple procedure at the plant laboratory scale. It is anticipated that in the large scale manufacture of the modified Composition C-4, only a minor change is needed in the current manufacturing process.

The results of the comprehensive studies on the physico-chemical properties of the modified Composition C-4, tagged with 1.0 and 0.1 wt. % taggant selected, established that the properties of Composition C-4 are unaffected by the taggant.

The selected taggant meets all critical requirements for tagging of plastic explosives.

DETECTION OF TAGGANT IN MODIFIED COMPOSITION C-4 TAGGED WITH A TAGGANT

T. H. Chen, C. Campbell, and R. A. Reed
U. S. Army Armament Research, Development, and Engineering Center
Picatinny Arsenal, New Jersey 07806-5000

1. INTRODUCTION

In the comparative evaluation of the detectability of vapor taggants from concealed plastic explosives, it is absolutely essential to develop a standard detection protocol which is capable of obtaining reproducible results. The current protocol is grossly inadequate for yielding such data. Thus, the recent comparative studies by international experts on the comparative evaluations of the detectability of vapor taggants from concealed plastic explosives have been unsatisfactory.

The aim of this paper is to examine various parameters of the detection protocol and devise a scheme including design and sampling procedure changes to obtain reproducible detector response.

The improvement strategy essentially involves redesign of the sampling slit and sampling procedure which ensure sampling of vapors from inside the suitcase.

2. EXPERIMENTAL

2.1 Apparatus and Reagents

A Varian 5500 High Performance Liquid Chromatograph and a Scintrex EVD1-DC Explosive Vapor Detector were used in the analysis and detection of the taggant from the standard suitcase, respectively. The mobile phase solvents employed in the high performance liquid chromatography (HPLC) were the HPLC Grade.

3. RESULTS AND DISCUSSION

In order to simulate a situation as close as possible to the "real world", the modified Composition C-4 tagged with a taggant at nominally 1.0 and 0.10 wt. % concentrations was prepared using a two-pound scale manufacturing plant equipment. A total of 50 pounds, i.e., 25 batches, each of control (untagged), tagged at 1.0 wt. %, and tagged at 0.10 wt. % compositions, were prepared.

A total of five cored samples were obtained from each of the 50 pound cubic blocks of tagged Composition C-4 containing approximately 1.0 and 0.10 wt. % taggant to determine the homogeneity of taggant distribution. The five samples represent the center-top, center-middle, and center-bottom along the vertical axis, left-side, and the right-side along the horizontal central axis. The samples were analyzed by the HPLC method developed for this work. The blocks containing nominally 0.11 and 1.1 wt. % taggant were found to contain 0.107 ($n = 10$, RSD = 15 %) and 1.108 wt. % ($n = 10$, RSD = 5.69 %) taggant. The samples are homogeneous within the experimental error of the method developed.

The International Civil Aviation Organization's (ICAO) standard suitcases were used in the improvement of the ICAO's detection protocol. Our previous work as well as those of other nations were not reproducible and thus a meaningful quantitative comparative evaluation of the detectability of taggants in concealed plastic explosives employing portable off-the-shelf commercial explosive vapor detectors could not be made. Furthermore, our use of thermocouples imbedded in the suitcases for temperature measurement and substitution of newspaper with a specified newsprint to eliminate print inks still did not improve the results. We have therefore concluded that the slit design and the sampling protocol might be the principal causes of non-reproducibility of detector response.

In the ICAO's standard suitcase, the slit made by a razor blade or a narrow-blade knife on the corrugated cardboard is not rigid. Furthermore, the slit width is undefined. We feel that "burping" should not be used in any quantitative studies as it would distort the cardboard slit in a non-reproducible manner. To eliminate this undefined parameter, a slit (0.38 ± 0.04 mm)(slit width) x 100 mm (length), was fabricated on an aluminum plate with a dimension of 15.24 cm (L) x 7.62 cm (W) x 0.16 cm (T). This plate was attached to the side of the suitcase, with the

original slit enlarged to the width of 5 mm, so that the center axis of the new slit was directly above that of the enlarged original slit.

However, the results obtained were not sufficiently reproducible. We attributed this to imprecise sampling of taggant vapor from inside the suitcase. Therefore, the metal slit was further modified to eliminate the possibility of sampling air from around the slit area. Figure 1 shows the detail of the slit. The length of the latter is confined to within the inner diameter of the o-ring groove. Proper sampling requires pressing of the outer-end of the absorption tube vertically and squarely on the o-ring, i.e., lining up the central axis of the tube with that of the o-ring while exerting sufficient pressure on the o-ring to avoid sampling of air from around the o-ring.

Figure 2 shows a strip chart recording of the sample taken using the new slit and sampling procedure from inside ICAO's standard suitcase containing all materials specified *except* tagged C-4. This test is conducted to rule out the use of contaminated suitcases. The arrow indicates the retention time of the taggant. It should be noted that only one absorber tube was used throughout this study. Furthermore, the tube was put through the "clean" cycle of the detector after each sampling to remove any possible memory effect. The signal in Figure 1 is identical to that of a typical air sample, establishing the suitcase to be uncontaminated.

Figure 3 shows the signal from the suitcase containing C-4 tagged with 0.1 wt. % taggant at the 78-minute mark after the placing of the explosive in the suitcase and the sealing off of the suitcase with a specified tape. The taggant signal is quite strong and easily detectable at 78 minutes.

Figure 4 displays the signal of 20.84 picograms of taggant to show the sensitivity of the detector used. The latter is capable of detecting about 5 picograms of the taggant.

In Figure 5, the calibration curve for taggant quantitation is shown. As can be seen from the figure, the electron capture detector of the detector is quite non-linear. Thus, the linear range extends only from about 100 to about 400 picograms (see the Insert). Since the chart paper was not provided with an electronic integrator, the area integration of the signal was performed by cutting and weighing the paper, which is not a very satisfactory quantitation method. However, at 62.52 pg taggant level, the RSD was 7.7 % (n = 6), a reasonably good number (see the error bar in the Insert).

Figures 6 and 7 show the quantitative detector response in pg as a function of time of taggant samples taken from two ICAO standard suitcases up to about 3000 and 500 hours, respectively. Samples were not taken between about 500 to 2800 hours. The temperatures at the time of sampling varied from 22.2 to 24.0 °C. The suitcases contained Composition C-4 tagged with 0.1 and 1.0 wt. % taggant, respectively. Considering that the sample flow rate of the hand-held sampler was not calibrated and the crude integration method was employed, the results are quite acceptable.

The reason for the apparently somewhat faster response from the suitcase containing C-4 tagged with 0.1 wt. % is not clear at this time. The random packing of the crumpled newsprint may have played a role. This parameter will be examined in our future efforts. The relative response times of the concealed C-4 tagged with 0.1 and 1.0 wt. % taggant will be closely studied because significantly different values will have obvious important implications in airport security. It may be noted that the taggant was detected within 20 minutes at about 23 °C. The reproducibility of this observation will be carefully examined in our future efforts.

In order to demonstrate the importance of appropriate sampling procedure, the lateral distance, perpendicular to the slit, between the center of the slit, i.e., the center of the o-ring, and the central axis of the sampling tube, as well as the vertical distance between the center of the plane of the outer-end of the absorption tube and the center of the slit, were carefully changed very slightly prior to sampling and the effects of these parameters on the taggant detectability were examined.

Figure 8 illustrates the dramatic decrease in the taggant detection sensitivity from an ICAO's standard suitcase containing 50 grams of concealed modified Composition C-4 tagged with about 0.1 wt. % taggant after approximately 500 hours (see Figure 6). By moving the absorption tube away directly above the slit only about 0.2 mm, the sensitivity dropped by essentially an order of magnitude. It may be noted that the vertical distance is a much more critical parameter than the lateral one. The results very strongly suggest that the improper slit design and

imprecise and faulty sampling procedure are the prime causes for the unreliable results obtained in the past.

4. CONCLUSION

This work very strongly suggests that improper slit design and imprecise and faulty sampling procedure are the prime causes for the unreliable results obtained in the comparative evaluation of the detectability of various taggants in concealed plastic explosives employing various off-the-shelf commercial explosive vapor detectors conducted by the U.S. and other nations.

The key to obtaining reproducible results is direct leak-tight vapor sampling from inside the suitcase to prevent sampling of outside air from around the slit area.

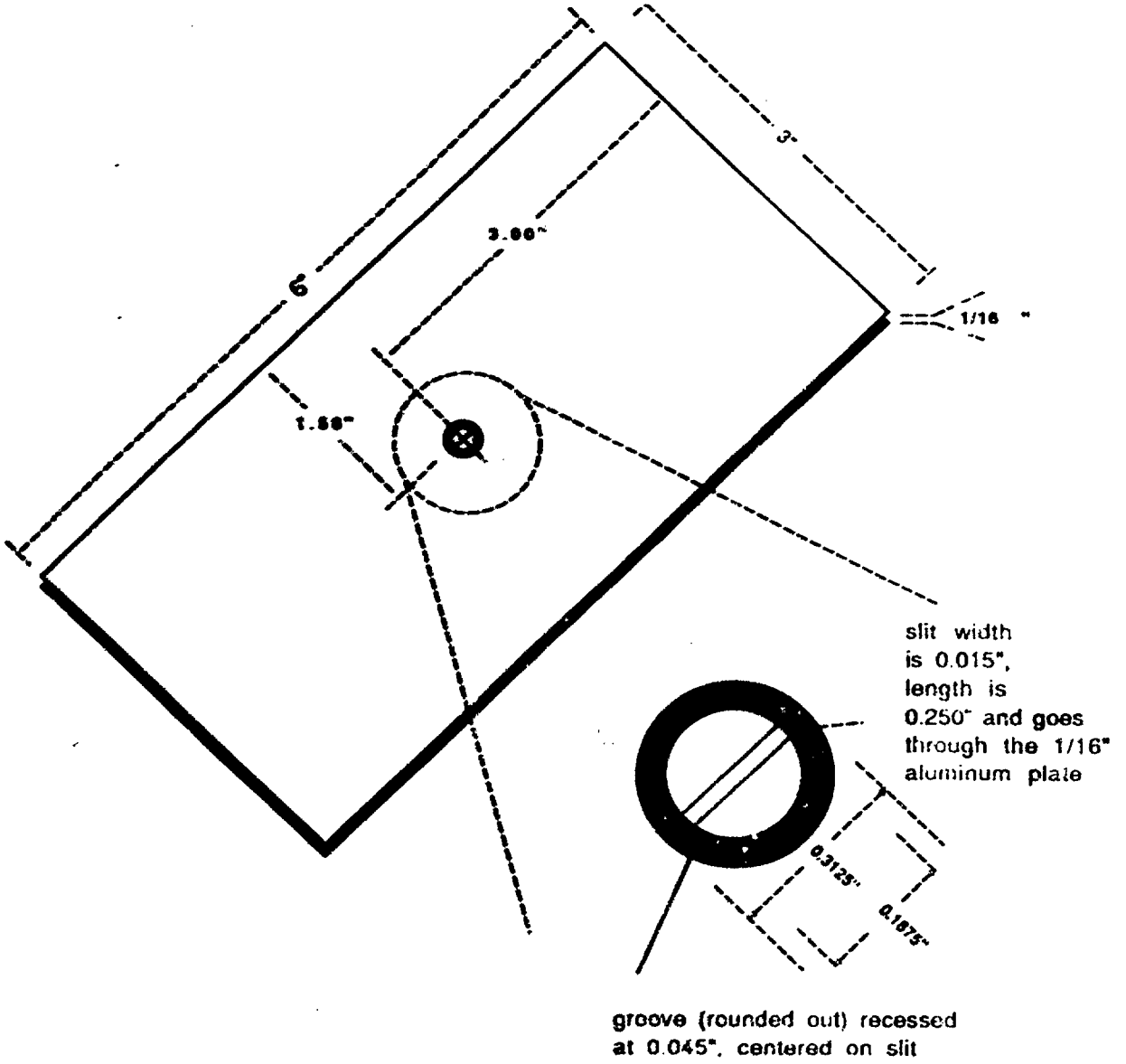


Figure 1. Modified Slit for ICAO's Standard Suitcase

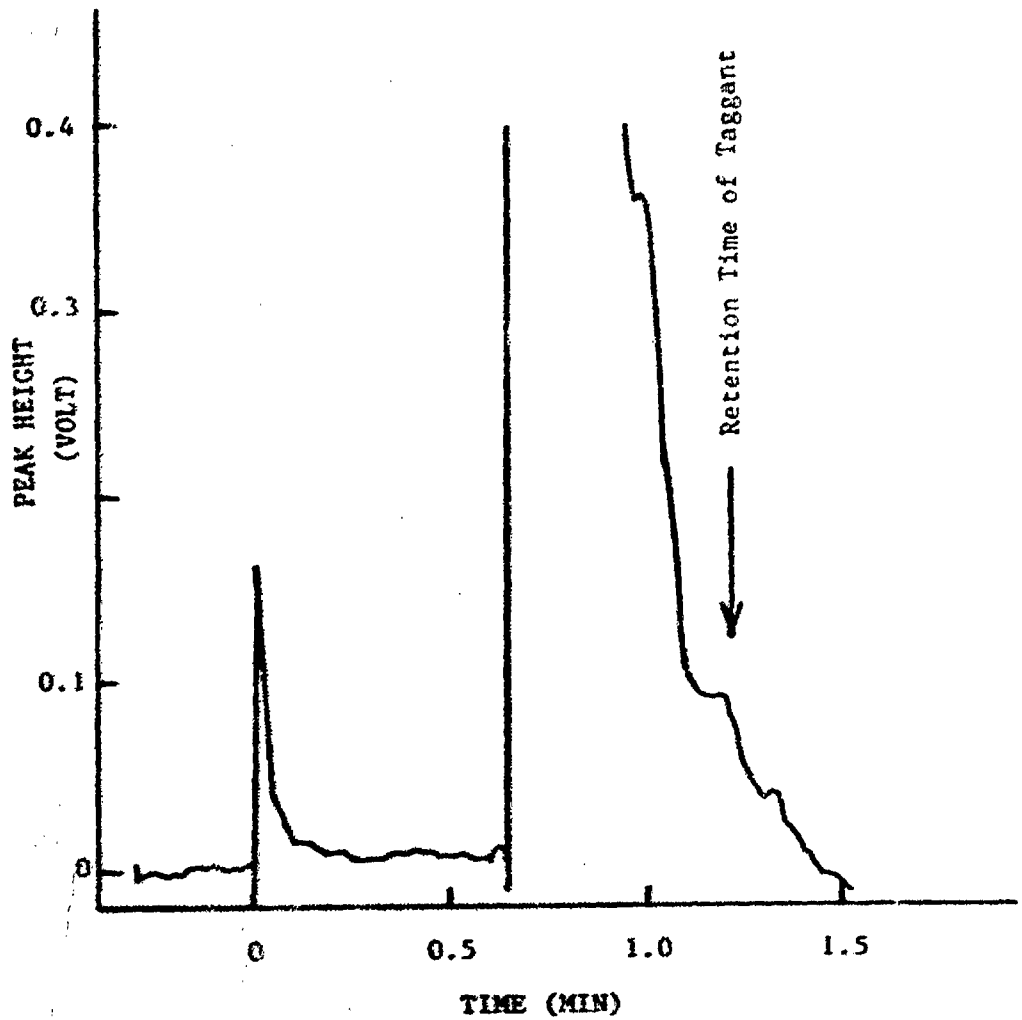


Figure 2. ICAO's Standard Suitcase Without C-4

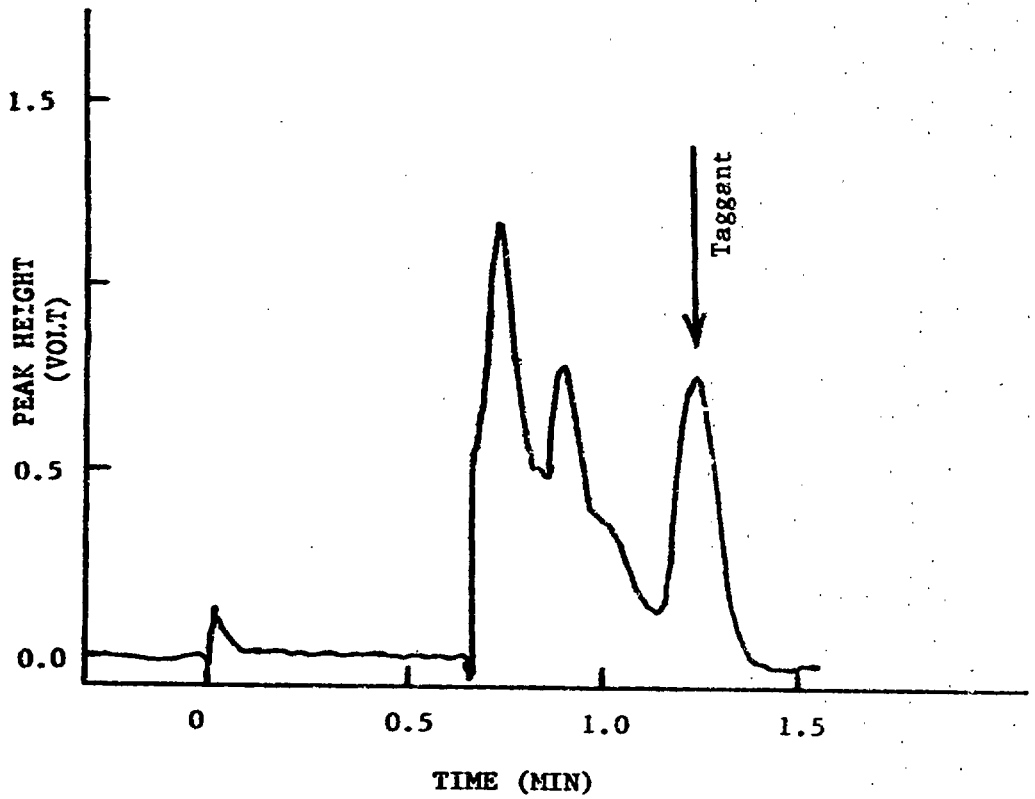


Figure 3. Taggant Detection at the 78-Minute Mark from the Suitcase with C-4 Containing 0.1 Wt. % Taggant

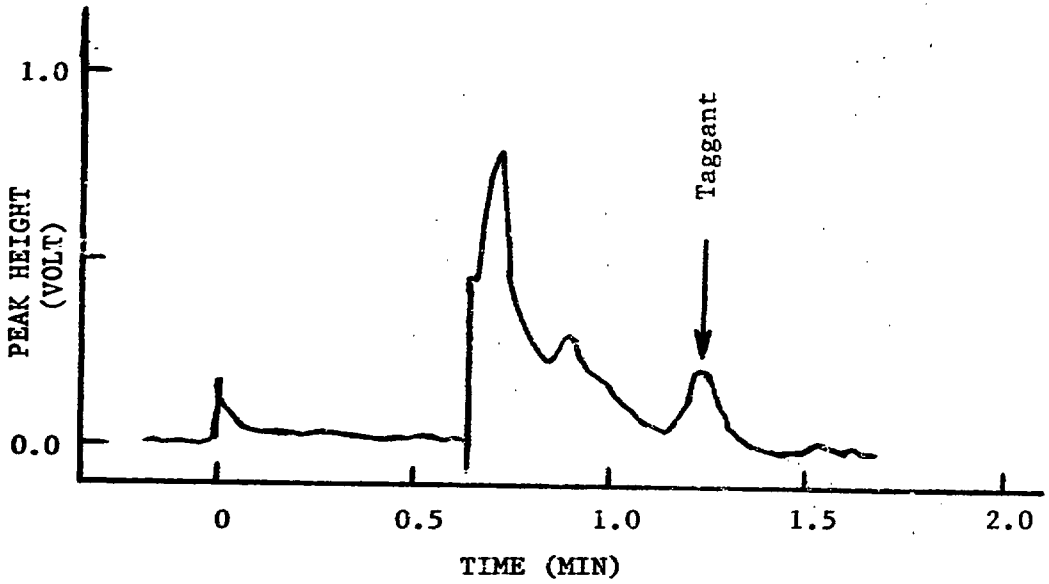


Figure 4. Detection of 20.84 pg Taggant

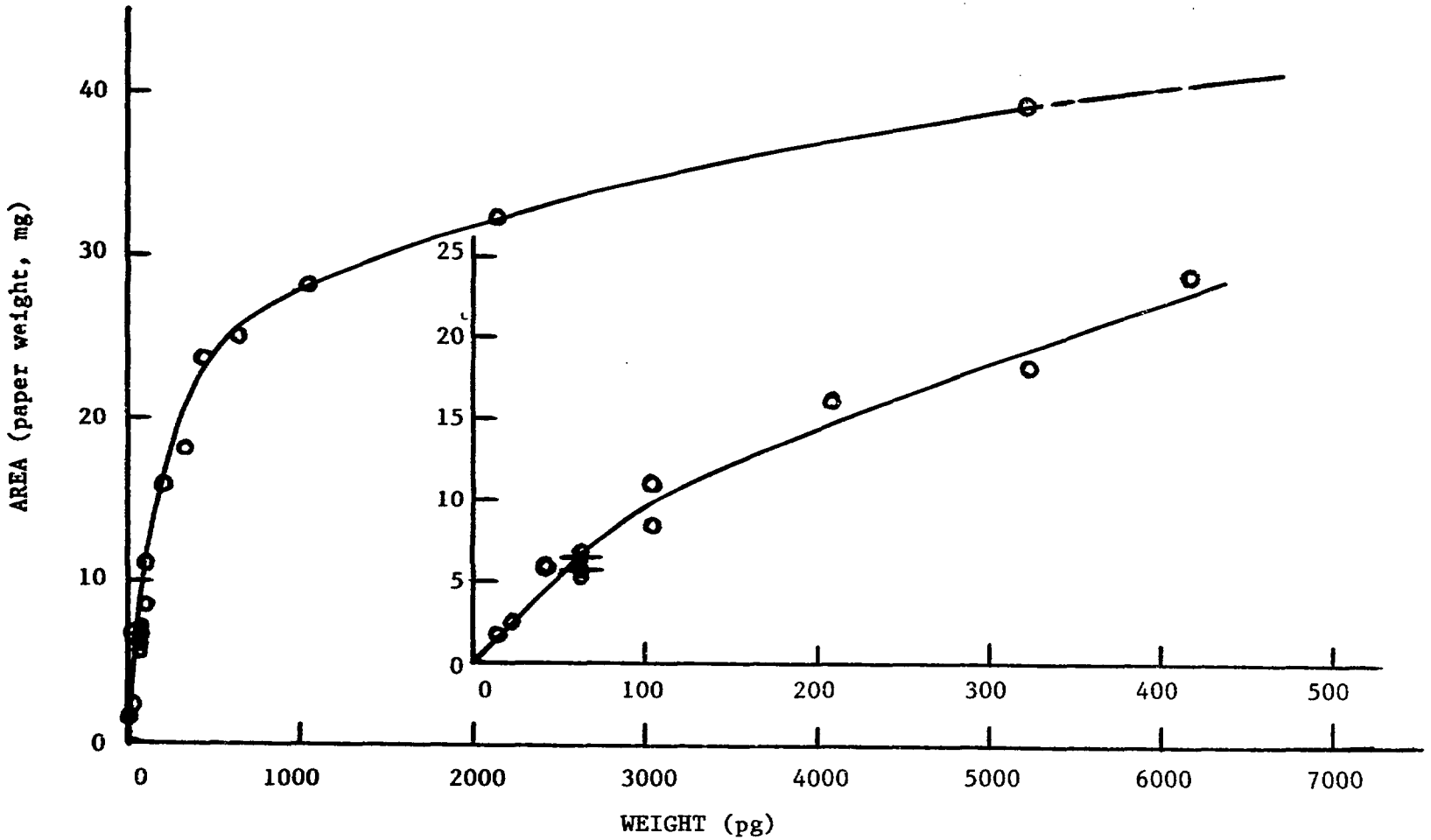


Figure 5. Calibration Curve for Taggant Detection

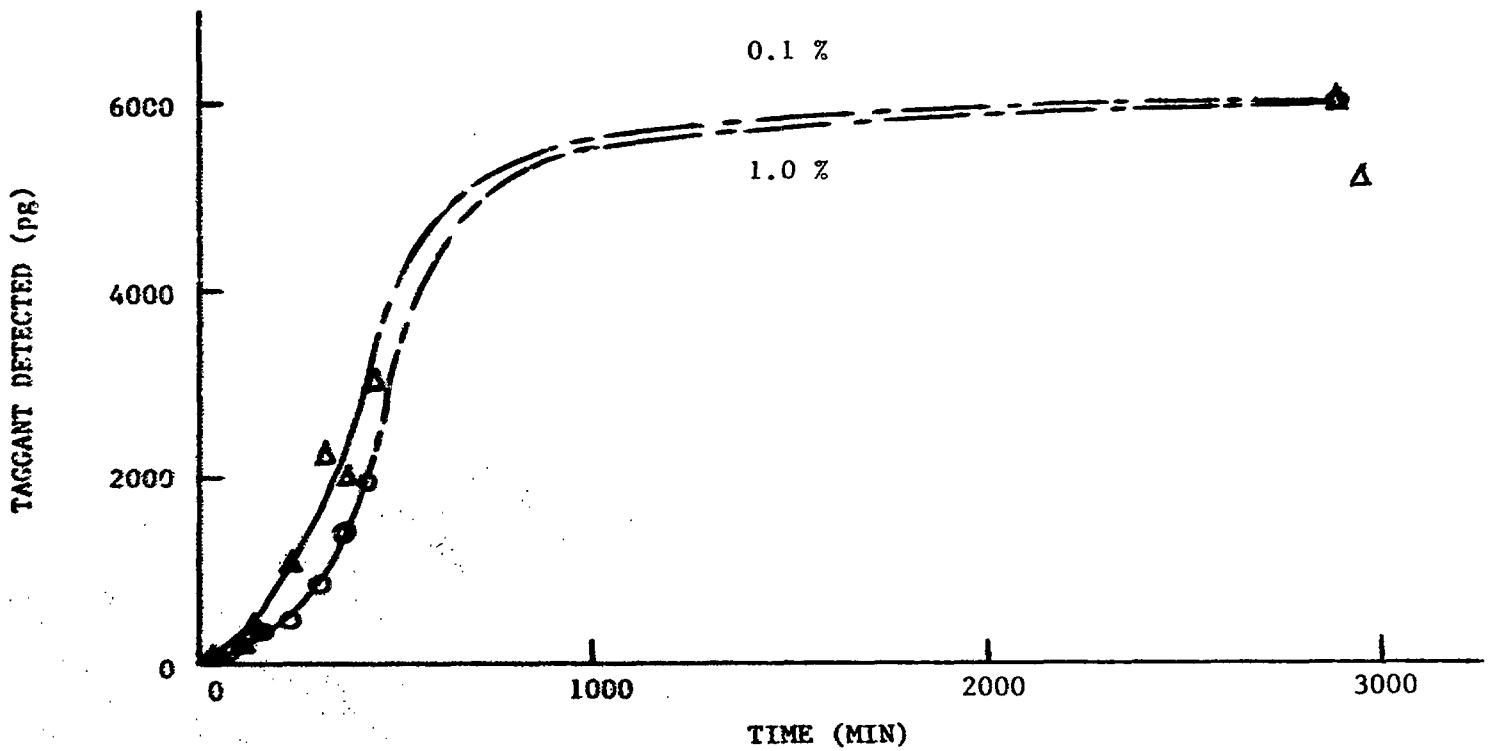


Figure 6. Detector Response for the Taggant from ICAO's Standard Suitcase as a Function of Time

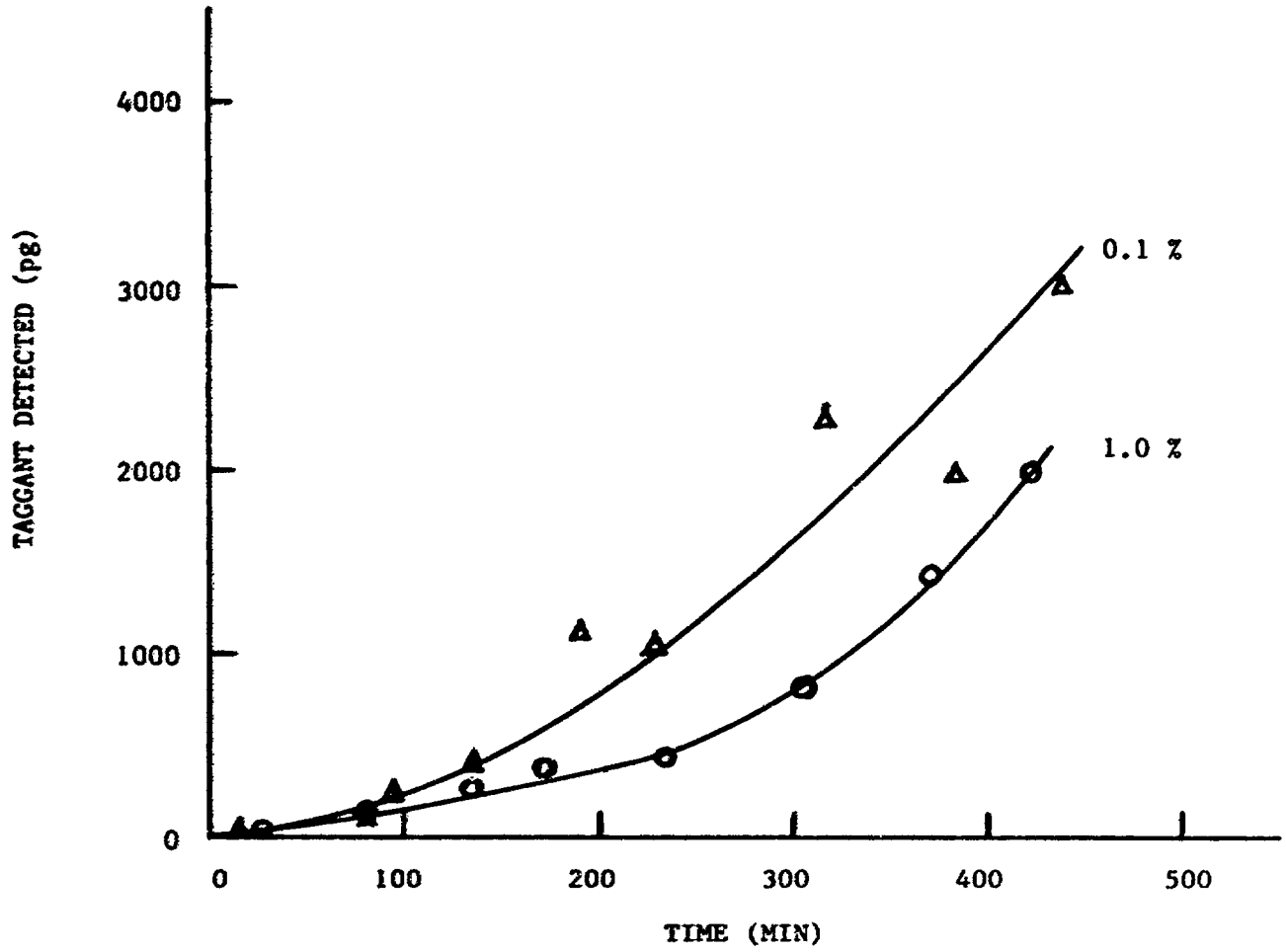


Figure 7. Detector Response for the Taggant from ICAO's Standard Suitcase as a Function of Time

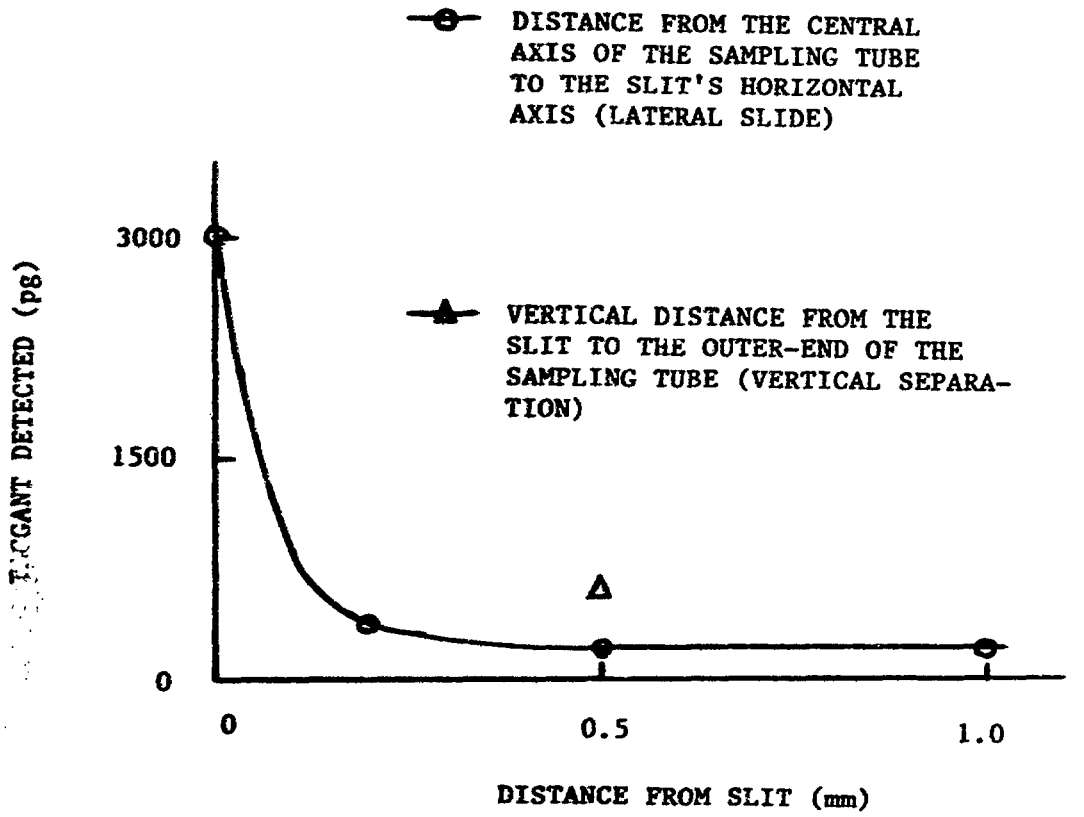


Figure 8. Effect of Detector Response as a Function of Time

BIOSENSORS

DRY IMMUNOCHEMICAL SENSOR FOR THE DETECTION OF PETN VAPOR

H.R. Lukens, Ph.D.
Diametrix Corporation

1. INTRODUCTION

Giaever (1973) showed that an indium semi mirror coated with a monolayer of a substance would undergo reduced optical reflectance after incubation with a solution of the substance's antibody. He was able to see the effect with the naked eye. Lukens and Williams (1977) reversed the process by first attaching the target substance's antibody to the semi-mirror, after which the device would show a decline in optical density when exposed to a solution of the target substance. Lukens and Williams (1982) subsequently found that the device could also be used as an immunochemical film badge (IFB) to detect an airborne target substance.

Early efforts to develop the IFB for the detection of airborne substances were plagued by such a high degree of performance variability that there were doubts in some quarters that an airborne target substance could bind to its antibody until Lukens (1990) demonstrated such binding in experiments with radiolabeled cocaine and morphine.

Recently improved semimirrors and densitometry have been obtained and have led to improved performance of IFBs. As shown in this paper, IFBs can now be constructed that detect PETN vapor in a few seconds.

2. MATERIALS AND EQUIPMENT

Semimirrors, prepared by deposition of evaporated indium on 22mm x 22mm x 0.16mm glass microscope slide covers, were obtained from Thin Film Technology, Inc. (Buellton, CA). Their optical densities (ODs) were in the range of 0.7 to 0.8, but each semimirror had a highly uniform OD across its surface. TEM photographs show that the indium on the semimirrors exists as islands of approximately 60 nm diameter separated from each other by about 40 nm.

Antibody toward PETN was developed in rabbits via injection of an immunogen produced in our laboratory. The immunogen was constructed, with the help of Dr. G. Leung, of San Diego, by conjugating pentrinitrol (obtained courtesy of Warner-Lambert, Pharmaceutical Research Division) with TGB (thyroglobin, bovine). The conjugation procedure began by refluxing 55 mg of pentrinitrol for 20 minutes with 46 mg of chloroacetic acid and 2 ml of 9M NaOH, in order to substitute the acetic acid moiety for the hydrogen of the hydroxyl group of pentrinitrol. The solution was then adjusted to a pH of 7.5 with HCl. Then 4.3 ml of the solution was adjusted to 5 ml with 0.1M phosphate buffer (PB), pH 7.6, and 200 mg of 1 ethyl -3(3-dimethylaminopropyl)carbodii-mide was added to activate the carboxylic acid group of the substituted pentrinitrol. The resulting solution was added dropwise, with stirring, to 10 ml of 0.01M PB containing 100 mg of TGB. The solution was stirred one hour at room temperature and 8 hours at 4° centigrade, after which it was dialyzed against 0.01M phosphate buffer (pH 7.6) for 2 days at 4° centigrade with 5 changes of buffer. The dialyzed solution contained the immunogen.

The immunogen was sent to the commercial antibody facility of Dr. Leung for mixing with Freund's adjuvant and injection into rabbits followed by booster injections. Blood was taken from the rabbits at intervals, and the blood serum, which contained polyclonal antibody toward PETN (anti-PETN), was frozen and delivered to this laboratory.

Antibody toward bovine serum albumin (anti-BSA) was obtained from Sigma Chemical Company for use as a control on the IFB.

Each IFB was prepared by deposition of 75 microliter aliquots of dilute solutions of anti-PETN and anti-BSA at defined, adjacent, but separate, positions on the indium side of a semimirror and incubating for 10 minutes. The aliquots, each of which contained about 4E14 molecules of protein, were lifted off with a pipet and the antibody positions were rinsed with a stream of deionized water. The IFB was then allowed to dry in air at room temperature overnight. The

procedure resulted in a sensor area and a control area, each about 0.4 cm in diameter. Each area was covered with a monolayer of protein molecules and was noticeably darker than the untreated area of the semimirror.

The area of the IFB containing anti-PETN is referred to as the target sensor; i.e., the area that senses the target substance. The area containing anti-BSA is referred to as the interference sensor, or control, since it serves to respond to general environmental variables, such as dust and changes in humidity, which will affect both sensor areas equally. Thus, the control serves to compensate for general variables.

A two-channel prototype portable IFB reader was constructed to our specifications by C. Pepper, an independent contractor in San Diego. The reader splits a common light source, via light pipes, to the target sensor (anti-PETN in the present case) and control (anti-BSA) areas of the IFB. On the other side of each area is a phototransistor, two stages of amplification, an analog-to-digital convertor, and a three decimal read-out of transmitted light intensity. A third circuit computes the ratio of light intensity through the sensor area to the light intensity through the control area and displays the ratio to three decimal places. There is also an analog circuit to adjust and stabilize the lamp intensity.

Plastic frames to hold IFBs for placement in the reader were designed and manufactured by 4Ward Tech, Inc., of San Diego. The reader's sample slot was constructed to hold the frames snugly for purposes of constant positioning.

Wheaton screw cap Coplin staining jars (10 slide capacity, 3.5 inches tall, 66 ml volume), each containing 4 mg of PETN in an open, one dram vial, were used to expose IFBs to PETN vapors.

3. EXPERIMENTAL

Separate rooms were used for preparing and exposing IFBs. No PETN was present in the laboratory used for preparing and measuring the IFBs in order to avoid premature exposure to the target vapor. The laboratory was climate controlled to the ranges of 21 to 23°C and 59 to 61 percent relative humidity. The reader was not brought into the room where IFBs were exposed to PETN vapor.

The room in which the exposure to PETN vapor was carried out was also climate controlled, and the air replacement rate was one room volume every 30 minutes. The motion of air in the room could be felt on the skin.

Measurements with the reader were carried out by insertion of the framed and unexposed IFB in the sample slot and obtaining nine readings of W, the sensor/control light transmission ratio. W was measured in the same fashion after each of a series of timed exposures to PETN vapor in a Coplin staining jar. Seventeen IFBs were prepared and tested in this fashion with exposure times ranging from one minute to 1400 minutes.

The mean and standard deviation of the mean, s(m) of each set of nine readings was calculated. The percent relative difference, D, between the pre-exposure value of W and each post-exposure value was calculated, and the standard deviation of the difference, s(d), was obtained by taking the relevant s(m) values in quadrature. Student's t-test for the difference between means was applied at the 95 percent level of confidence. Given sets of nine measurements, the difference is considered significant if t, where $t = D/s(d)$, is at or above 2.306.

The average s(m) among the 109 sets of nine readings in this work was 0.018 percent relative, and the average s(d) was 0.025. Hence, in these laboratory conditions, detection at the 95 percent level of confidence may be said to have occurred, on the average, when D reached a value of 0.058 percent, relative.

In order to estimate the likely value of D required for detection in the field, a single IFB was measured many times with frequent removal from, and reinsertion into, the reader, and the reader was moved several times between rooms. From 87 readings under these conditions it was estimated that on the average, for sets of 9 readings, detection in field conditions would occur when D reached 0.152 percent relative.

A quantity R, which is related to the rate of change of D, was obtained by dividing D by the time of exposure, T: i.e.:

$$R = D/T \qquad (1)$$

In the case of each IFB tested, the relationship between R and minutes of exposure was found to be

represented by the power model,

$$R=a * T^{(n)} \quad (2)$$

For convenience, the expression was modified to relate T and 1000R as follows:

$$1000R = b * T^{(m)} \quad (3)$$

and the value of b and m was found for each IFB.

The constants, b and m, were obtained for each IFB from experimental data. The performance of the 17 IFBs is summarized in Table 1, wherein the values of b and m shown are used in Eq.(3) to estimate the minutes required for each IFB to detect PETN under simulated field conditions (time for D to equal 0.152 percent relative). The standard deviation, s, of the observed values of 1000R about the calculated curve for each IFB is also given.

4. DISCUSSION

An IFB prepared with antiserum has about 2E11 to 4E11 binding sites per square centimeter (Lukens, 1990). PETN has a vapor pressure of 5.4E-6 torr, according to McReynolds et al (1975). Thus, at saturation, there are about as many molecules of PETN per ml of air (2E11 1) as there are binding sites per square centimeter of IFB. Since the Coplin jar volume is 66 ml and the sensor area is 0.5 square centimeter, there are about 100 times the number of PETN molecules required to saturate the sensor area's binding sites.

As seen in Table 1, the time to reach D of 0.152 percent relative and, thus to detect PETN vapor, is estimated to be less than one minute for 10 out of the 17 IFBs. The detection threshold was not reached for 19 minutes or more in 5 of the 17 IFBs, and two IFBs reached the threshold in between 1 and 10 minutes. On this basis, it could be argued that 59 percent of the IFBs were fast to very fast, 12 percent were of medium speed, and 29 percent were slow. In this sense the speed of the IFBs exhibited a bimodal distribution. Four of the five pairs of IFBs behaved the same: i.e., either both were fast to very fast or both were slow. Only one pair split with respect to speed of response.

Table 1 shows that the data fit the calculated curve for each IFB fairly well. It is worth noting that the observed 1000R values from IFBs 2-10 fit a general power curve with b=247. 1 and m=-0.9694 with a standard deviation of $\pm$45 percent relative. The data and curve are shown in Figure 1. Similarly, for IFBs 11-17, the slow IFBs, the fit is $\pm$35 percent relative to the power curve with b=83.5 and m=-0.7664. These results show considerable improvement over earlier, unpublished results wherein the observed 1000R values had a standard deviation of :$\pm$156 percent relative about the calculated power curve.

The calculated response times of the three fastest IFBs are not explicitly given in Table 1, because of the extent of extrapolation beyond the range of actual exposure times.

The large spread in response times argues against diffusion as the rate limiting factor in all cases. In fact, since the air in the jar is disturbed when the IFB is inserted to begin an exposure, it is unlikely that any of the observed responses were limited by the diffusion rate of PETN molecules. In the absence of diffusion limitations, it might be expected that the large excess of airborne PETN molecules in the Coplin jar over the binding sites on the IFB sensor area would result in pseudo-first order kinetics. However, the fact that the data fit a power model indicates that such is not the case.

One possible explanation for the observed decline in rate of response with time is that not all of the binding sites are equally accessible to the PETN molecules, but rather that there is a gradient of accessibility of binding sites. Variability in accessibility of binding sites could also be an important part of the explanation for the observed differences in responses among the 17 IFBs. Thus, learning to optimize binding site availability is important to the production of uniformly fast IFBs.

A key factor relative to the variation in times to detect PETN with the seventeen IFBs appears to be the age of the semimirrors. Eleven and six old (>10 months) and new (<2 months) semi mirrors, respectively, were used to make the IFBs. The seven IFBs with threshold detection times of over 1 minute were all made with old semimirrors.

Freshness of the antibody solution used to prepare an IFB may be an important factor, since three of the slow IFBs were made with day-old antiserum solutions, whereas all of the fast IFBs were made with fresh solutions. Also, there are data to suggest that the level of trace moisture in the IFB sensor areas is important. Relevant to this point are the

facts: 1) IFBs don't work when the relative humidity drops to 1 percent, and 2) IFBs work best when the relative humidity is high (Lukens, 1991). Since the target sensor and control areas are prepared in the same fashion, beginning with the same concentrations of their respective proteins, it is expected that they will contain equal quantities of trace moisture. Thus, the control will compensate for changes in trace moisture in the sensor; but it is possible that, in the field, IFB response will be faster under conditions of high humidity.

Variation in semimirror wettability has also been observed, and the relationship between this and IFB performance is under investigation.

As more is learned of the factors that govern IFB performance, the proportion of IFBs produced with fast responses to the target compound will improve.

REFERENCES

1. Glasover, I (1973), "The Antibody-Antigen Reaction--A Visual Observation," J.Immunol., vol.110, p.144.

2. Lukens, H.R. and C.B.Williams (1977), "A Solid Substrate Immunological Assay for Monitoring Organic Environmental Contaminants," EPA Report EPA-600/1-77-018.

3. Lukens, H.R. and C.B.Williams (1982), "Method for Detecting Organic Vapors," U.S.Patent 4,353,886.

4. Lukens, H.R. (1990), "Binding of Airborne, Radiolabeled Haptes Controlled Substances to 'Dry' Immobilized Antibody," J.Radioanal.Nucl.Chem., Letters, vol. 144, pp.223-228.

5. Lukens, H.R. (1991), "An Immunoassay Film Badge Detector of Trace Substances in Air," Diametrix Corporation Report 77031-A16.

6. McReynolds, J.H., G.A.St.John, and M.Amber (1975), "Determination of Concentration of Explosives Vapors from Parcels and Letters," SRI Final Report, U.S.Postal Service Contract 74-00810; January.

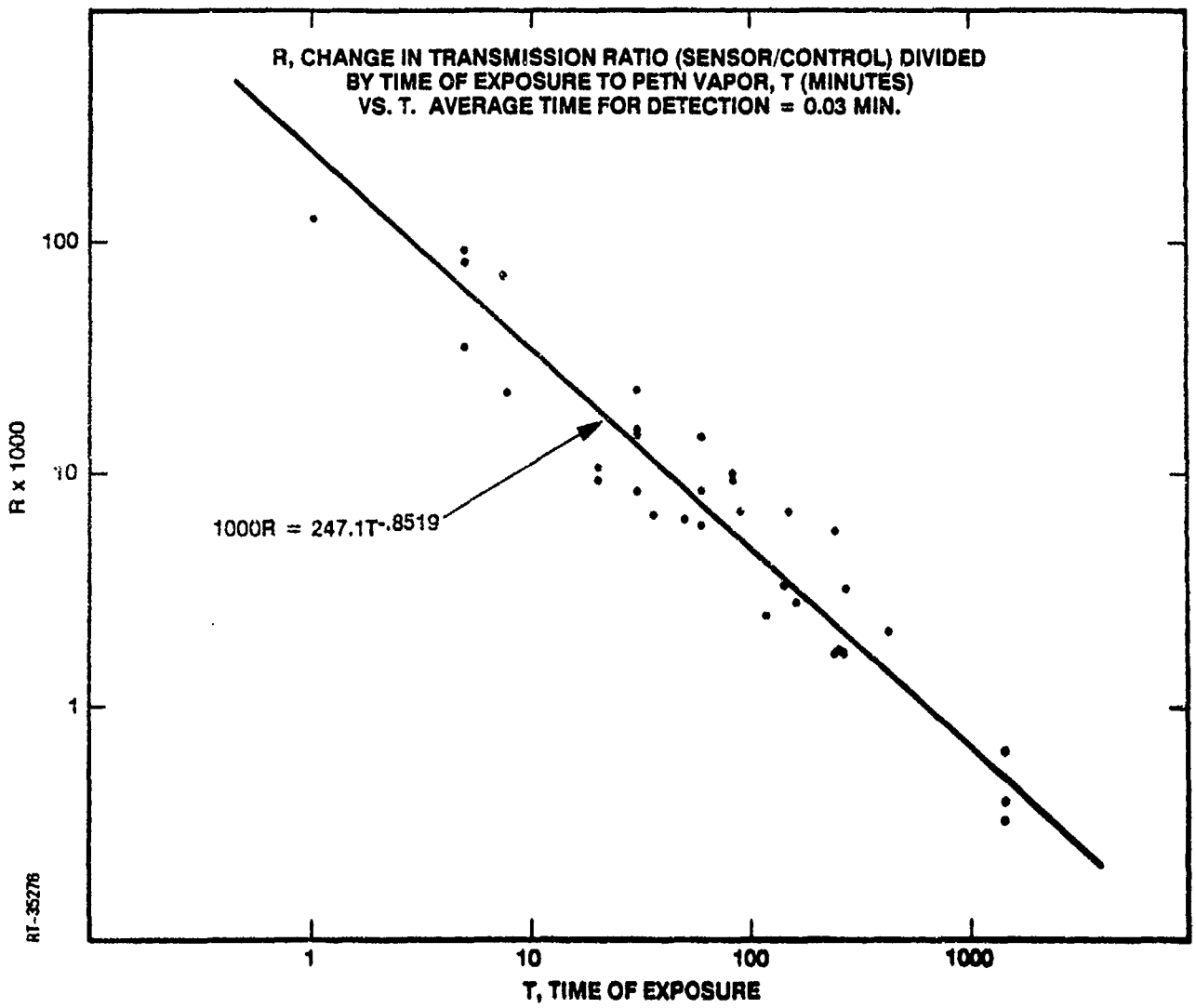


Figure 1. Nine fast IFBs for detecting PETN

Table 1. Performance of Seventeen IFBs for Sensing PETN,
In order of increasing time for detection

IFB	Eq. (3) Parameters b	m	Minutes to Sense PETN (a)(b)		s, %rel. (±)(c)
1	1544	-0.9175	<0.01	(1)	10.8
2	191.0	-0.9808	<0.01	(1)	29.7
3	286.1	-0.9149	<0.01	(2)	1.6
4	275.8	-0.8348	0.03	(3)	24.8
5	290.5	-0.8034	0.04		22.2
6	274.4	-0.7735	0.08	(3)	11.8
7	214.3	-0.7959	0.19	(4)	17.7
8	180.0	-0.8599	0.30		12.6
9	183.1	-0.8427	0.31	(2)	15.1
10	162.2	-0.6528	0.83		37.2
11	114.0	-0.7474	3.2		25.9
12	97.08	-0.7703	7.0		2.6
13	53.88	-0.6471	19		16.7
14	114.2	-0.9099	24	(4)	13.1
15	45.32	-0.6148	25		14.6
16	25.48	-0.5169	41	(5)	19.9
17	56.77	-0.7614	62	(5)	6.1

(a) Time, per Eq.(1), to reach D=0.152.
(b) Pairs of IFBs prepared at the same time are indicated by matching numbers in parentheses.
(c) Standard deviation of observed 1000R about the calculated curve for the IFB.

THE CHALLENGE OF BIODETECTION FOR SCREENING PERSONS CARRYING EXPLOSIVES

Curt Weinstein, M.A., and Sidney Weinstein, Ph.D.
Western Connecticut State University
Danbury, CT

Ronald Drozdenko, Ph.D.
NeuroCommunication Research Laboratories, Inc. (NCRL)
36 Mill Plain Road, Danbury, CT

1. INTRODUCTION

Only vapor detection is safe enough to be used to screen persons for carrying explosives into airline terminals, ball games, controlled-access political gatherings, corporate buildings, bus terminals, etc. Although there are many vapor detection techniques available, none, as yet, surpass the following parameters, which are based on a biodetection model--a specific animal model developed at NCRL. Thus, this biodetection technology becomes the benchmark with which other detection technologies may be judged. See Table 1. The parameters reflect those of NCRL's SYS-5(tm).

The 12 parameter model is very general; one expression is NCRL's SYS-5 in which 5 detecting elements are employed in simultaneous independent detection. The detecting element is the rat, a specially prepared rat. Following is information about the detection behaviors of this detecting element, considering both clean and explosively dirty environments.

1.1 An Experiment with the Detecting Element in an Explosive-Dirty Environment

Introduction. Although much work has been performed using trained animals to detect the presence of explosive vapors, few attempts have been made to determine performance as a function of explosive-vapor concentration in an explosive-dirty environment. In our earlier work (Nolan, Weinstein & Weinstein, 1978a: 1978b), rats were successfully prepared to detect military-grade TNT with a high level of confidence. A typical example is rat-00-76 which detected military grade TNT with a statistical confidence level of better than 99.9%. Subsequent to that work, rats were shown to be able to detect pure TNT, black powder, RDX, and any one of the three. See Figure 1, which shows for these explosives the average percentages of detection and false alarm, employing detecting units with a single detecting rat. In more recent work with highly-pure TNT we collected samples of the test air and control air during measurements of rat performance to see how the rat would perform in an environment contaminated with explosive vapors. We called the control air that was contaminated with explosive vapors the explosive-dirty environment. The task for the rat was to detect explosive vapors greater than the environmental levels. The concentration of TNT in test and control air streams was measured by gas chromatography (GC). One rat was selected for demonstration purposes. We investigated the ability of this rat (79-88) to differentiate between concentrations of pure TNT.

Background. Rat-79-88 was trained to press a bar when TNT-laden air was delivered, and to refrain from pressing a bar when nonTNT-laden air was delivered using NCRL's training technique. The test apparatus was under computer control, and was used to deliver varying concentrations of TNT vapor. The computer additionally scored the rat's performance, controlled reinforcement contingencies, and controlled the air-sampling pumps for the GC.

Preceding results. Before the experiment to measure rat performance concurrently with TNT concentration, experiments were conducted to insure that the rat was indeed responding only to the presence of TNT, and not to some concomitant cue. In one series of experiments, the arms of the test apparatus that were used to deliver TNT or control air to the rat were switched. The rat responded to the delivery of TNT and not to the control air. In another series of experiments, the TNT source was removed from the test apparatus. For the first 50 trials, the rat detected TNT as if the source was still intact. For the second 50 trials, performance fell

appreciably. Finally, during the last series of 50 trials, performance stopped. Because the reinforcement contingencies remained enabled, the rat could have received its reinforcement if it could have solved the detection task by alternate means. However, it did not, thus indicating that TNT vapor was the controlling stimulus. Detection during the first 100 trials was evidently due to residual TNT in the source chamber. In this manner, we verified that the rat responded only to the presence of TNT.

Procedure. The experiment to measure performance as a function of concentration in an explosive-dirty environment was conducted by measuring TNT concentrations by GC concurrently with the rat's performance. Both the test air and the control air were sampled concurrently during each session. The samples of air for GC analysis were collected from the same area that the rat sampled so that an accurate measure of what the rat was sampling would be obtained. Rather than training the rat to specifically detect low levels of TNT, the rat was trained to detect saturated levels, and performance testing took place during titration of the concentration of TNT in the test air. During the titration experiments (600 trials), this rat evidenced 96% correct detection when challenged with TNT in the range of 2 to 3 ng/L; simultaneously, there were only 1% false alarms (3 in the 309 challenges with control air). Before titration, the rat averaged 95% correct behavior. Table 2 provides data from the last three sessions.

Results and discussion. Results are presented in Table 2. First note from Table 2 that "performance" is a very strict measure of the ability to perform the task. Errors of both detection and false alarms subtract from 100% performance. Not only do specially prepared rats have excellent performance, but also they are able to maintain that performance for over a thousand trials over a period of up to eight hours. Second, note that performance falls for this naive rat when the difference in concentrations of test to control air fall below 1 ng/L. When the concentration difference was .93 ng/L performance fell to 95%, and when the difference fell to .70 ng/L performance fell to 60%. Note that the decrement in performance concomitant with titration was probably not due to fatigue, because the rat had a history of responding to up to 1171 trails in a few hours. That high work level was not exceeded during these experiments. Whereas, the experiment demonstrated the performance level of one rat in an explosive-dirty environment, SYS-5(tm) performance is not limited to the performance of a single rat, even though the rat is used as the detecting element. The use of multiple detecting units enhances performance.

1.2 Use of Multiple Detection Elements

SYS-5 outperforms a single detecting element by employing majority logic, which causes the detection rate to be enhanced and the false-alarm rate lowered. Because each detecting element performs an independent simultaneous evaluation for explosives vapors, the following equation can be used to relate the proportional detection for one active element to the proportional detection of the system employing majority logic of five active elements:

Key:

D(ml5) = proportional detection of a majority logic system of five active elements (NCRL trade name: SYS-5)

p = proportional detection of one active element (all have the same specifications for this demonstration)

$$D(ml5) = 6p^5 - 15p^4 + 10p^3$$

Because the above formula is derived solely from probability theory, it also relates the proportion of false alarms for the majority logic to that of each active element. One result of employing majority logic based on five active elements is that detection rates increase while false alarm rates fall. For example, consider the specifications given in Table 3, for an incompletely trained rat. Notice that the rates of detection and false alarm are quite deficient. Yet even under these conditions, the system response is very good, having a 93% performance.[1] Detection rates of 81.1% or greater by each of the active elements combine for a system detection rate of 95% or better. Further, false alarm rates of 13.5% or less by each active element become a system false alarms rate of less than 2%. Actually, NCRL specially prepared rats obtain much better performance than indicated here (see Tables 1 and 2).

2. POTENTIAL APPLICATION

2.1 Airport Passenger Screener (APS)

Overview. The 12-parameter biodetection model

permits application to an APS that is capable of screening individuals at the rate of 600/hour for bombs that contain many high explosives (including RDX). The external appearance of the NCRL APS resembles a revolving door (see Figures 2, 3, and 4) abutting the control center (at the stationary hub). Persons to be screened enter the revolving door singly at rates up to 10 each minute. The person pushes a bar which activates the revolving door, causing it to rotate at a fixed rate. Jets of slightly moisturized air gently scrub the person as he/she walks while temporarily sealed in the door's chamber. Meanwhile, the moist air is sampled and analyzed in real time. If no detection occurs, the person exits the revolving door; however, if a detection occurs, the person is locked in the revolving door, while security personnel are alerted. A brief discussion of the APS functional details follows.

Redundancy. The sample, collected from within the revolving door, is delivered to each of five detecting elements (e.g., SYS-5). Each detecting element is capable of detecting at least picogram levels of explosives molecules. The APS employs these active elements in a majority-logic response system. When at least three of the five active elements respond, a detection occurs. The advantage of employing 5 active elements in the APS is that performance is increased markedly over one active element.

Manufacturing ease. Even though NCRL rats are produced that perform at better than 95% detection with less than 2% false alarms, it is not necessary to produce such "high performers." A five-element majority-logic system, if employed, could use active elements that perform at 81.1% detection and 13.5% false alarms. It is not that such high performers are not desirable, but just not necessary for a good system response, hence facilitating quick production.

Active element. The active element, of which there are 30 in each APS, is the NCRL prepared rat. The NCRL rat is a specially prepared and controlled rat. Hardware placed into the rat allows it to be controlled by electrical brain currents from external computers. When prepared as such, the active element will operate for long periods of time (e.g., up to 8 hours) and at high rates of screening without a significant performance decrement.

Verifiable. In order to demonstrate continually that the APS is functional, sets of 10 active elements are on call at any one time. Of these ten active-elements, 5 are employed for screening persons, while the other 5 are being verified for operational performance. The remaining 20 are off duty, 10 just having completed an 8 hour shift with the remaining 10 waiting for the start of an 8 hour shift. Of the ten active elements at any one time, only five are actually used for screening purposes in a majority-logic program. The remaining five active-elements are tested by the random introduction of explosives vapors. The testing continues at ten screens per minute for a period of two minutes. After each two minute test, the tested-true active elements are switched (logically) with the screening active-elements (no physical switching is necessary--just switching of the actual samples and test-samples). In this manner, the active-elements which are testing the sample have always been freshly verified as operational within the preceding two minute period. In the unlikely case of impairment of an active element, reserve elements from the 10 waiting to be used would be logically substituted. Therefore, the APS is always using freshly tested and verified active elements. The low cost of active elements makes this procedure of providing tested and verified active elements a feasible approach.

Maintenance. Maintenance is simple, because the active units are contained in modules. Feeding and waste disposal is by enclosed modules--black boxes, in the engineering sense. If an active element ceases to perform, replace the module: unplug the defective active-element module and plug in the replacement. Currently, active elements are effective for six months, but with the inclusion of newly developed hardware into the rat, active elements may be effective for a year or more.

2.2 Criteria Met

The following criteria were suggested for an airport personnel screening device, and are met by NCRL's APS design. First, the APS averages 10 screenings per minute. Second, it is harmless to people. Third, it is reliable (and reliability is verified). Fourth, it is maintainable (assembly-line features). Fifth, it is operable by unskilled labor. Sixth, it is cost effective, because the active elements are very inexpensive. In addition, the APS is designed to have met the parameters of the 12-parameter model, including the following criteria: Detect at better than 98%. False alarm rate of less than 2%. Rejection cycle at 5 seconds/sample. Detection cycle at 10 seconds/sample. Detects several explosives species.

Does not confuse similar molecules with target molecule.

3. CHALLENGE

The challenge to do better than these values has been made. We believe that this challenge is difficult to meet with current technology. Finally, NCRL is ready to transfer this technology for its use in detecting explosives.

NOTE

1. Performance, a technical term, is defined as the difference in percentage of detection and false alarm.

REFERENCES

1. Nolan, R.V., Weinstein, S. and Weinstein, C. (May, 1978a). Neurophysiological, operant, and classical conditioning methods in rats in the detection of explosives. Presented at 3rd Annual Meeting of Role of Behavioral Science in Physical Security.

2. Nolan, R. V., Weinstein, S. and Weinstein, C. (October, 1978b). Electroencephalographic studies of specifically-conditioned explosives detecting rats. Presented at New Concepts Symposium and Workshop on detecting and Identification of Explosives.

Table 1. PARAMETERS OF NCRL BIODETECTION MODEL

Parameter Name	Description of Parameter	NCRL SYS-5
Detection Rate	The probability that the device will indicate detection when explosives are present.	95% for TNT
False-Alarm Rate	The probability that the device will indicate detection when explosives are not present.	1% for TNT
Performance	The difference between the rates of detection and false alarm.	94% for TNT
Time to Detect	The time from presenting a sample until a detection decision is made.	4.0 seconds for TNT
Detection Frequency	The number of detection decisions per minute. This frequency includes the total time from sampling initiation through detection decision.	4.0/minute for TNT
Duty Cycle	The number of working hours per day.	8 Hours
Warm-up time	The number of minutes necessary before specifications are obtained.	1 minute
Detector Life	The number of working hours before the detector has a 50% chance of failing to perform as specified.	624 Hrs (est.)
Minimum Weight of Sample	The smallest amount of explosives detectable under the most favorable conditions.	0.015 ng for TNT
Count	The percentage of explosives, from the following list, that are detectable at specifications. DNT, TNT, RDX, Dynamite.	100%
Confusability	The percentage of items from the following list that yield a false positive. Nitrogen fertilizers, tuna, bologna, protein powder, powdered milk.	0%
Volume	The volume of air needed to sample.	3 ml (est.)

Table 2. PERFORMANCE AT CONCENTRATION LEVELS

						Test	Control	
Sess.	**Trial.**	**%Corr.**	**%Det.**	**%FA.**	**PERF.**	**ng./L**	**ng./L**	**Tst.-Con.**
11.	50.	100.	100.	0.	100.	2.44	0.37	2.07
12.	50.	98.	95.	0.	95.	1.32	0.39	0.93
13.	100.	80.	60.	0.	60.	1.07	0.37	0.70

KEY:

1. Sess. identifies the ordinal set of trails.
2. Trail. is the number of challenges presented.
3. %Corr. is the percentage of correct decisions.
4. %Det. is the percentage of detections.
5. %FA. is the percentage of false alarms.
6. PERF (performance) is the difference between the percentages of detection and false alarm.
7. TEST presents the concentration of TNT vapors (ng./L) in the test air.
8. CONTROL presents the concentration of TNT vapors (ng/L) in the control air (which is background noise).
9. Tst.-Con is the difference of concentrations of TNT in test air to control air listed.

Table 3. SYSTEM RESPONSE CONVERSION

Each Active Element		System Response	
Detection	False Alarms	Detection	False Alarms
81.1%	13.5%	95.0%	2.0%

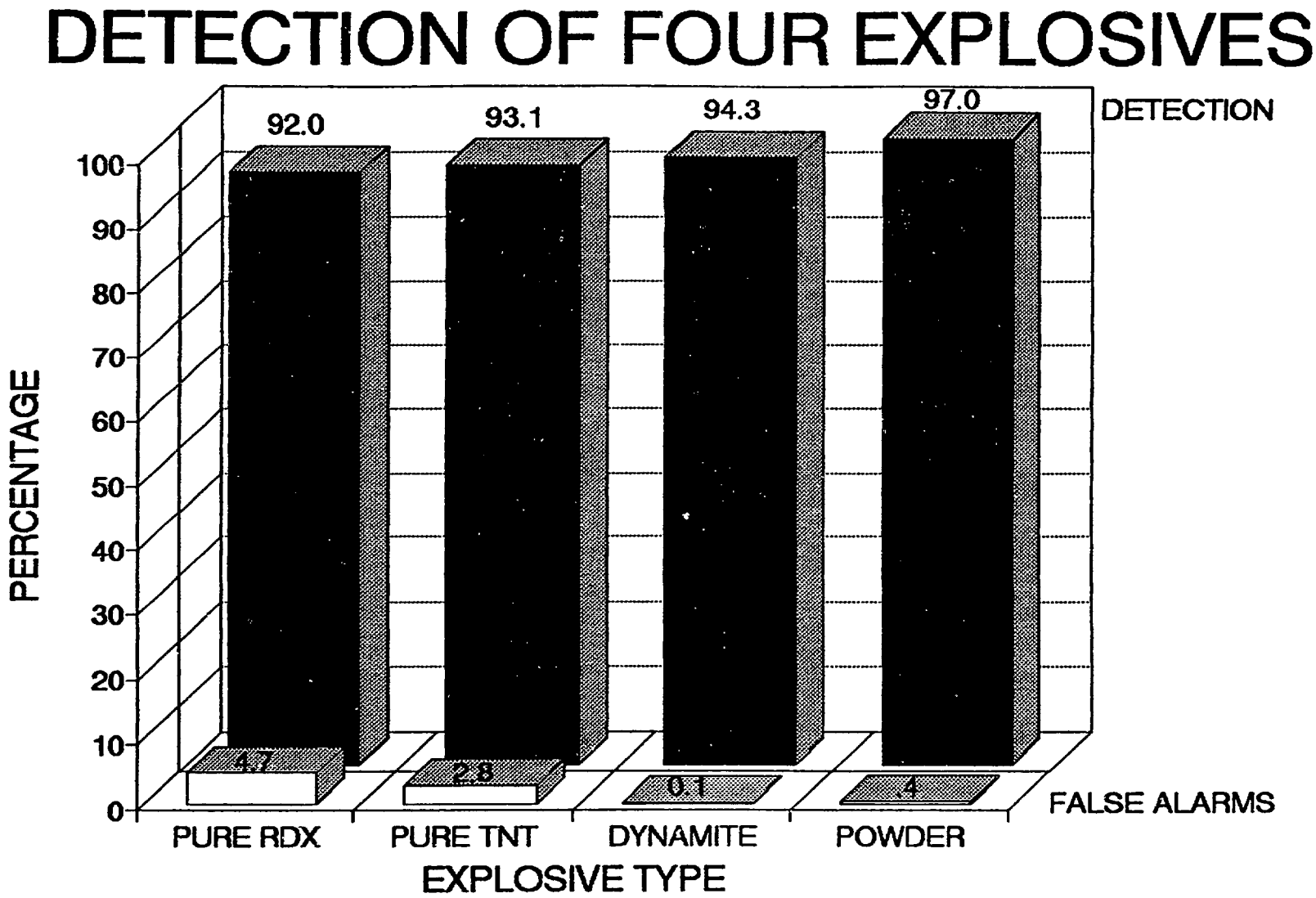


FIGURE 1. SINGLE DETECTOR PERFORMANCE

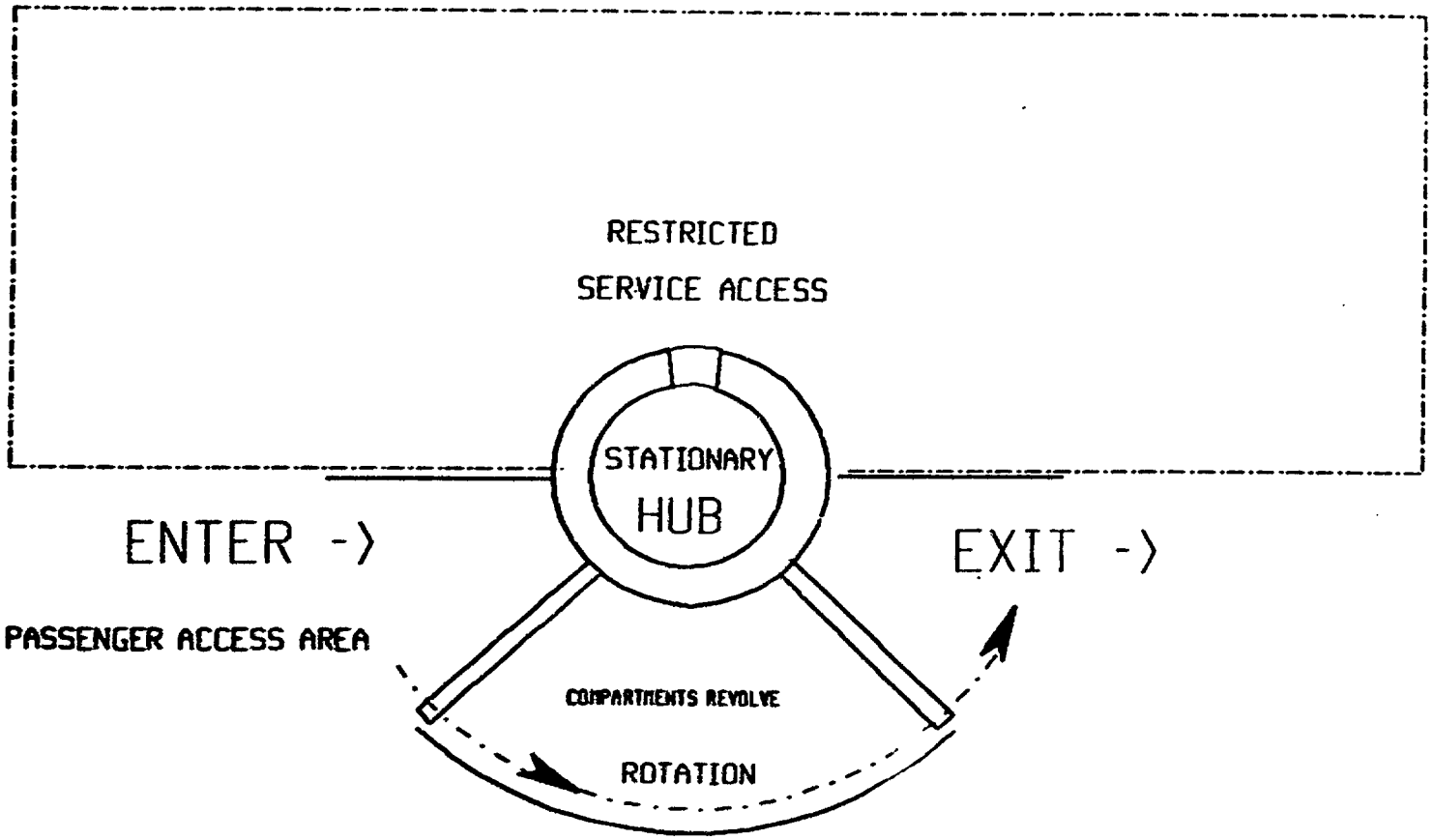


FIGURE 2. AIRPORT PERSONNEL SCREENER (APS) SCHEMATIC (TOP VIEW)

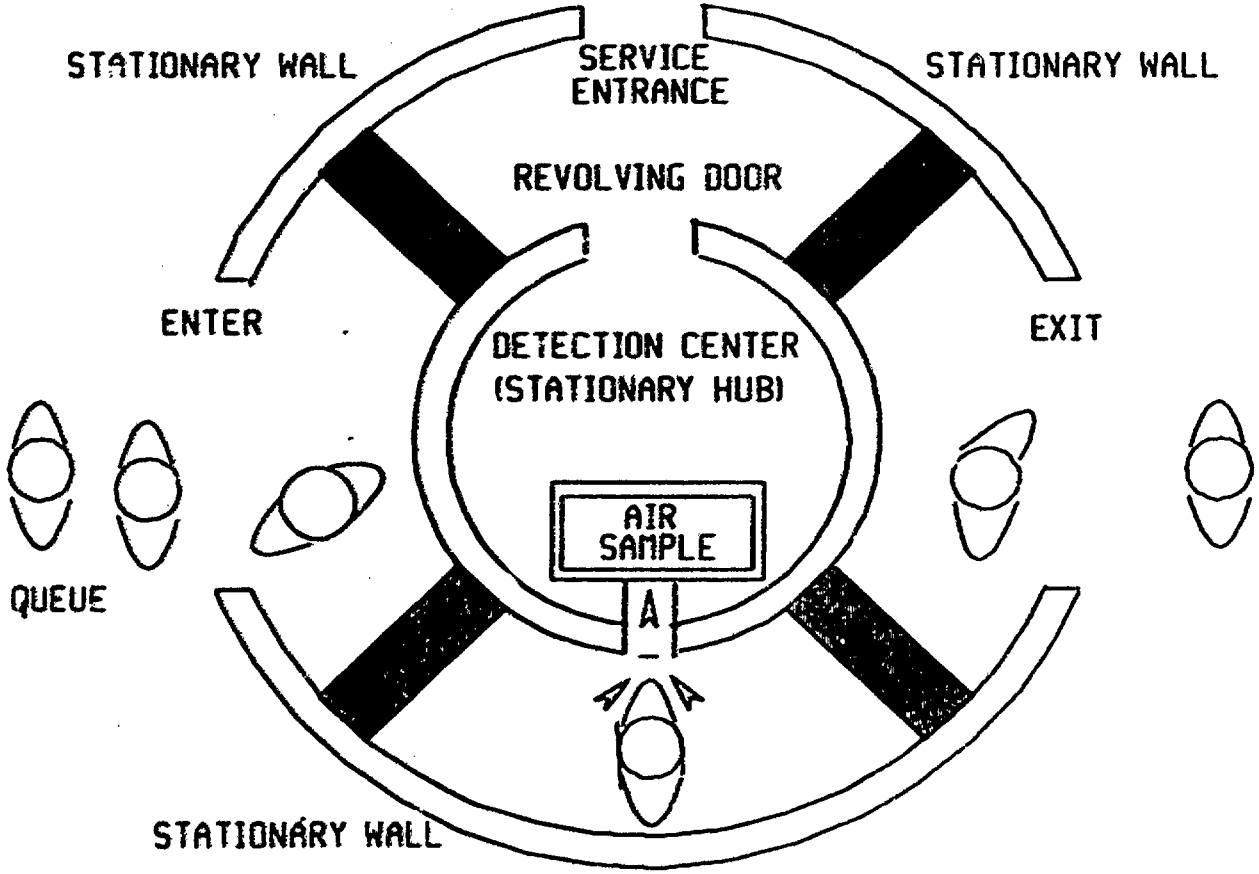


FIGURE 3. APS TOP VIEW

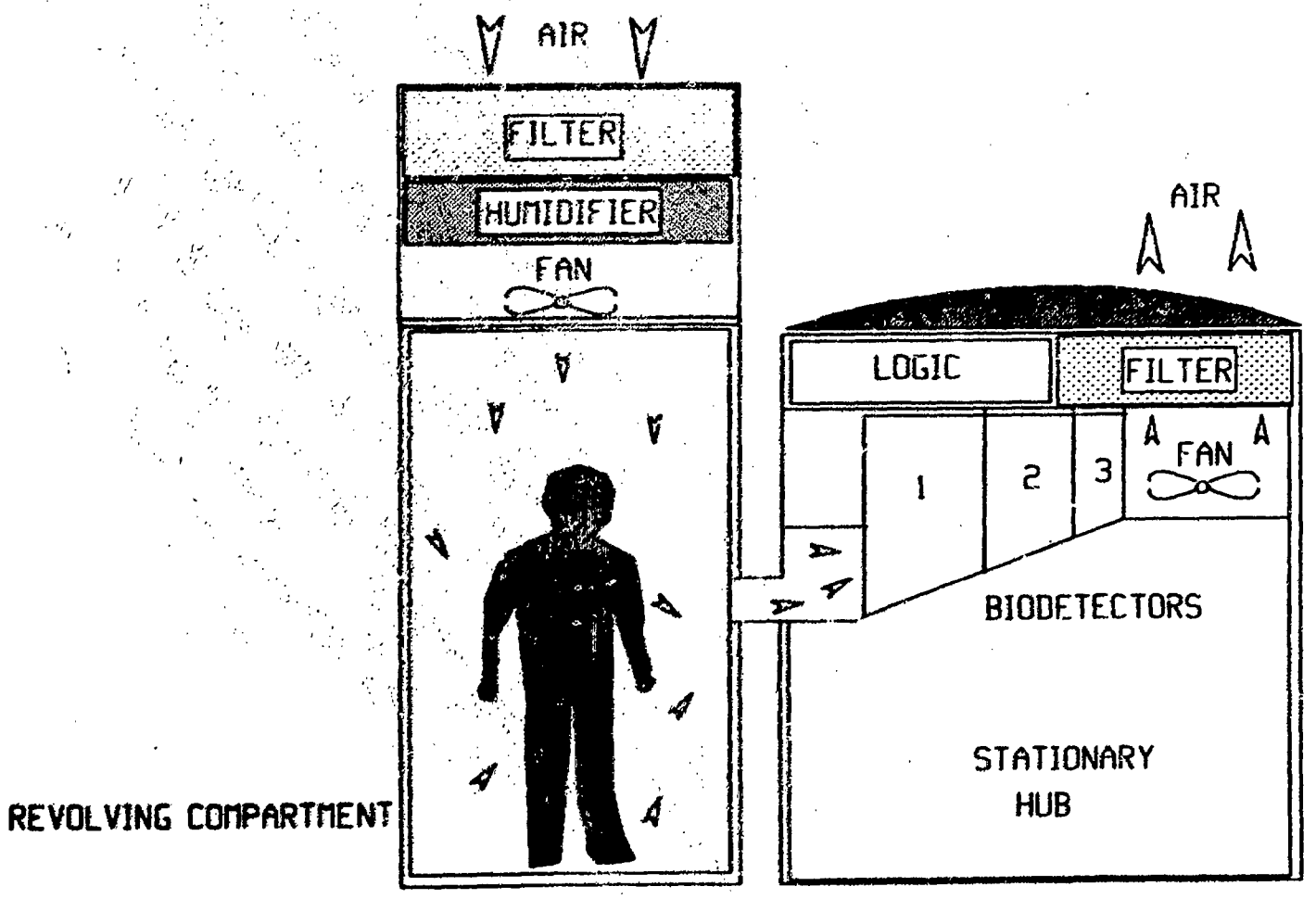


FIGURE 4. APS SIDE VIEW CROSS-SECTION

THE FLOW IMMUNOSENSOR: AN ANTIBODY-BASED SYSTEM FOR EXPLOSIVES DETECTION

Anne W. Kusterbeck
Frances S. Ligler
Center for Bio/Molecular Science and Engineering, Code 6090,
Naval Research Laboratories, Washington, DC 20375-5000

James P. Whelan
Geo-Centers, Inc., Washington Operations,
Fort Washington, MD 20744

1. INTRODUCTION

A dramatic need exists in the transportation industry for a rapid detection system which can readily differentiate explosive materials in complex environments. This need for explosives detection was the major impetus for development of a biologically-based detector (biosensor) at the Center for Bio/Molecular Science and Engineering at the Naval Research Laboratories in Washington, D.C. Designed to minimize analysis time and provide a means to examine multiple samples rapidly, the continuous flow detection system relies on an immobilized antibody molecule for its high specificity and high sensitivity. Unlike traditional antibody-based assay systems (1,2,3) the flow immunosensor does not require long sample incubation periods.

In addition to the immobilized antibody, the prototype system consists of fluorescent target molecules, a portable, off-the-shelf fluorimeter, a laptop computer, a small peristaltic pump, and the associated tubing and hardware (Figure 1).

Proof-of-principle for the system was demonstrated previously utilizing an antibody specific for dinitrophenol (DNP) and a DNP-fluorescein conjugate as the labelled analyte (4). With only slight modifications, the same system has been adapted to detect TNT by analogous means. Briefly, anti-trinitrotoluene (anti-TNT) monoclonal antibodies were experimentally selected for their ability to bind to TNT with high affinity and then attached to a matrix of support beads in a flow column. These immobilized antibodies are subsequently saturated with signal explosive molecules that have been coupled to a fluorescent marker or tag. An aqueous flow stream is then established through the column into which samples are introduced. Because antibody interactions are reversible, TNT molecules in the test samples displace labelled signal molecules, which are detected downstream in a spectrofluorimeter. Using a flow rate of 0.5 ml per minute, this system produces a positive signal down to the low parts per billion range in less than a minute.

2. METHODS

Labelled antigen (trinitrobenzene-cadaverine-fluorescein isothiocyanate - (TNB-CV-FITC)) was prepared by reacting trinitrobenzene sulfonic acid (Aldrich) with cadaverine-fluorescein (Molecular Probes) in borate-buffered saline (BBS) at pH 8.6-9.1 overnight at 4°C while rocking. Synthesis of product was monitored by thin-layer chromatography in methanol:chloroform (1:3). Reaction proceeds to near completion under these conditions. Monoclonal anti-TNT antibody (11B3) was coupled to tresyl chloride-activated Sepharose 4B by standard methods. Mass of antibody bound was determined by using a Coomassie Blue procedure (5). Immobilized antibody was saturated while rocking with TNB-CV-FITC at a molar ratio of antigen to antibody of 100:1 for several days at 4°C. Analyte-saturated Sepharose was stored at 4°C in this solution with 0.1% sodium azide (v/v). Bed volumes of 0.2-0.5 milliliters were prepared in disposable microcolumns (ISO-LAB) for use in the flow sensor. A continuous flow stream of phosphate-buffered saline, pH 7.4, containing 0.1% Triton-X-100 is established through the column into a downstream Spectrofluorimeter (Model 821, Jasco). Signal above background from each sample was determined by integration of millivolt output signal from the spectrofluorimeter utilizing an Hewlett-Packard Integrator (model 3396B).

3. RESULTS

After establishing a stable baseline reading, a standard curve can be determined employing known dilutions of TNT. Under the conditions of antigen density, bed volume and flow rates described here the linear range for TNT is in the 10-600 ng/ml range (Figure 2). Specificity of the system is confirmed since no signal is detectable when either lysine or phenylalanine are tested at 8 μg/ml or 5 μg/ml concentrations (data not shown). In addition to TNT, dinitrotoluene (DNT) gives a signal in the system (Figure 2). Integrated area values for DNT are 62 $\pm$ 5% (mean $\pm$ S.E.M.) the values for TNT over this concentration range.

4. DISCUSSION

The continuous flow immunosensor has been shown to be able to detect TNT in the nanomolar range in less than two minutes. Further increases in sensitivity may be possible by utilizing different fluorophores or multiple fluorophores coupled to the analyte of interest. Although a finite amount of antibody and signal molecule limits the useful life of each column, tests indicate that columns can be used for several days without a loss of sensitivity. Replacement of columns is necessary only after multiple large positive TNT samples are introduced. An additional advantage to the flow immunosensor is the limited amount of reagents required for operation. Since the chemistry of the system is confined to the small in-line column, it is not necessary that numerous reagents be available. Both the fluorophores and the antibody are contained in the column. Prepared columns are stable for at least several months and continuous 8 hour operation requires only 500 ml of buffer. Using the current system, we are currently addressing questions such as repetitive sampling, detection limits and analysis time.

Despite the extreme specificity of antibodies, cross-reactivities to other molecules due to structural similarities can be fortuitous, as in the case of DNT. The DNT molecule is a significant contaminant in commercial grades of TNT and has a vapor pressure twenty times higher than TNT. Thus, for purposes of explosive detection, DNT sensitivities are desirable.

Finally, two major advantages of the flow immunosensor are its ease of use and its adaptability for detecting a wide range of different molecules. Additional explosives can be monitored by using the analogous experimental design with antibodies specific for other explosive molecules.

REFERENCES

(1) Smith, D.S., Al-Hakiem, M.H.H., and Landon, J. (1981) *Ann. Clin. Biochem.* 18: 253-274.

(2) Warden, B.A., Allam, K., Sentissi, A., Cecchini, D.J. and Giese, R.W. (1987) *Annal. Biochem.* 162: 363-369.

(3) Lee, S.R. and Liberti, P.A. (1987) *Annal. Bichem.* 166:41-48.

(4) Kusterbeck, A.W., Wemhoff, G.A., Charles, P.T., Yeager, D.A., Bredehorst, R., Vogel, C.-W., and Ligler, F.S. (1990) *J. Immunol. Meth.* 135:191-197.

(5) Ahmad, H., and Saleemuddin, M. (1985) *Anal. Biochem.* 148:533-541.

NRL FLOW IMMUNOSENSOR

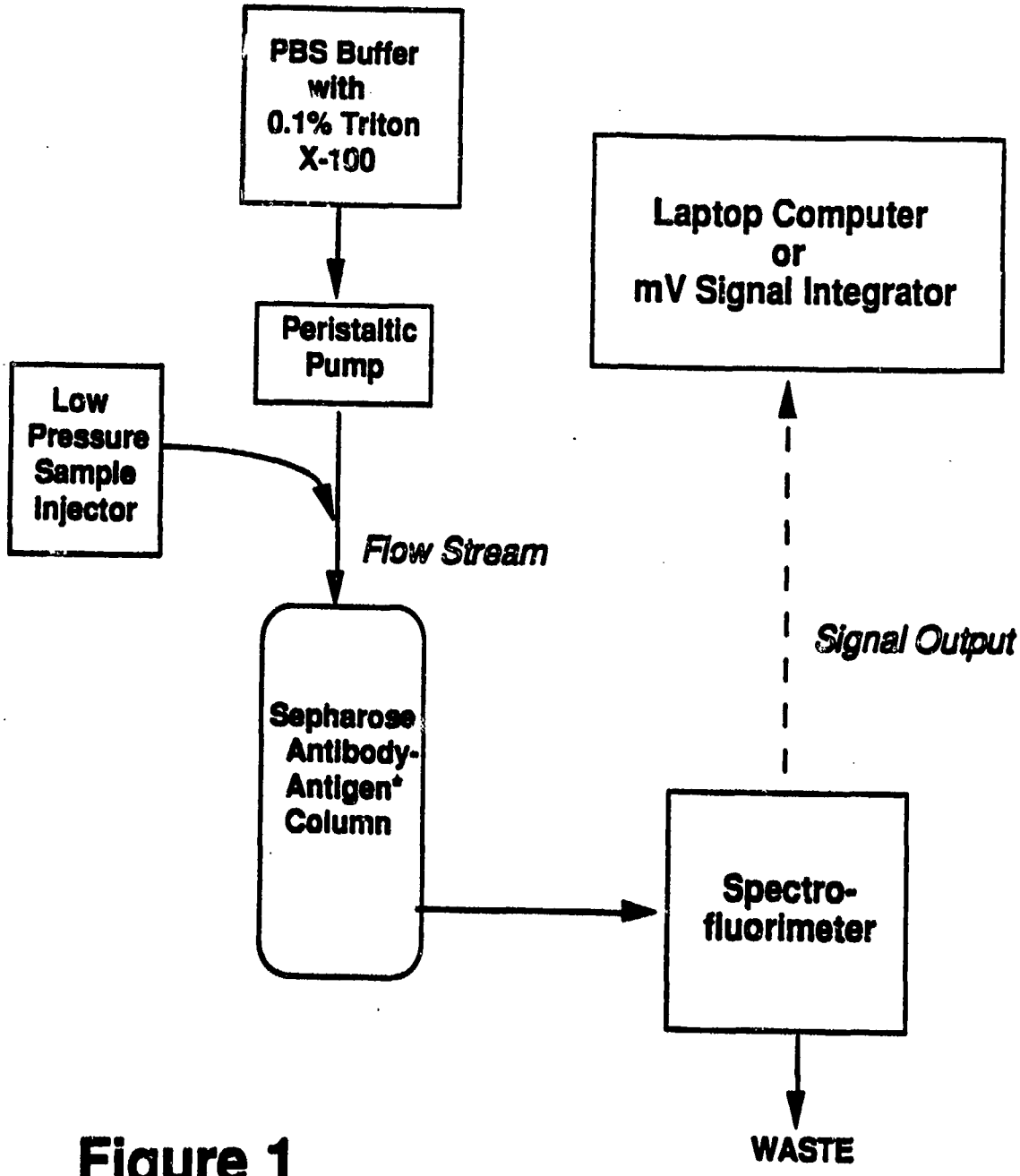
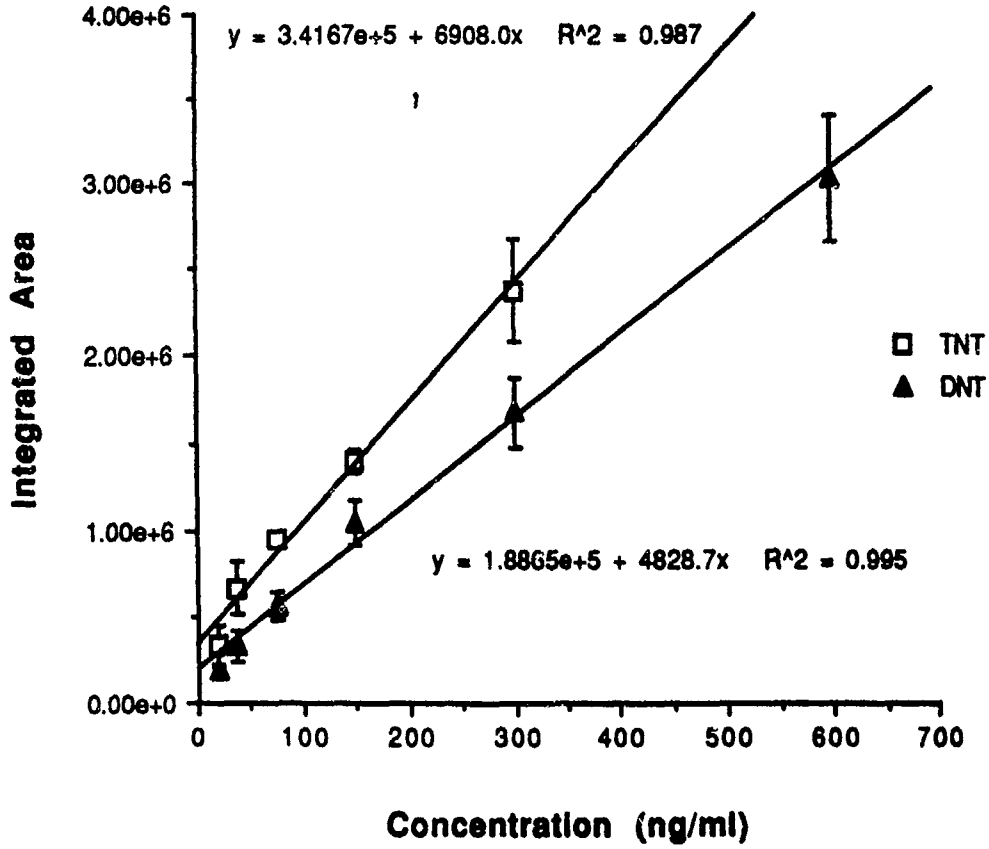


Figure 1

Diagram of Continuous Flow Immunosensor.
The current prototype model of the flow sensor comprises a low pressure sample injector, peristaltic pump, antibody-antigen column, fluorimeter and signal processor. Placement of the pump can be placed any munber of lovations in the flow stream path, however, placement as shown minimize's tuving lenght and comcomittantly, analysis time.

Figure 2- TNT and DNT Standard Curves
11B3 MoAb-Sepharose



Standard Curves of Trinitrotouluene and Dinitrotoluene Signals obtained in the Flow Sensor.

Integrated area from fluorimeter output signals are graphed verses sample concentration. Sample size coulum bed size, and flow rate were 100μl, 200 μl and 400 μl/min respectively. Best fit linear regression lines are shown. Each point is the mean of three determination $\pm$ S.E.M.

EXPLOSIVES SEARCH DOGS

S. Lovett
Defence Research Agency
United Kingdom

1. INTRODUCTION

Dogs are superb detection equipments, capable of detecting hundreds or thousands of molecules of explosive vapours, very user friendly and mobile, they do not need a power source except a reasonable supply of biscuit and meat. They can not only find explosives but can find drugs, weapons, crossbows, money, mines, ammunition, people and empty or full terrorist weapon hides, to name but a few. The detection rate of this excellent detector is in excess of 70% when trials are run using known amounts of hidden explosives. Considerable difficulty is experienced if attempts are made to determine the mean failure rate in active service as we cannot ascertain the number of misses. False alarms due to items of, for example, attractive food, are not recorded by dog handlers. I have asked several dog users from the police and Customs Authorities about the failure rate but no sensible answer has been given - there is the possibility to be considered that handlers do not wish to admit his dog failed in its duty! The irritating thing about the detection ability of the dog is that we are very uncertain how the animal achieves this extraordinary olfactory success. Extraordinary is perhaps not a strong enough word because dogs have been able to detect explosives and drugs in the presence of very odorous materials such as farmyard manure, diesel fuel or domestic bleach.

2. TRAINING

In the UK the breeds used for detection are: German Shepherd, Labradors, Springer Spaniels and Collies. Dogs cannot be trained to find explosives on their own; the handler and the dog must be trained together. This normally takes two months or more depending upon the natural ability of the dog and a rigorous test of the pair must take place to ensure their ability to carry out their work. In the UK the pair are re-tested every year to ensure that they are still competent to carry out search work. This is a very reasonable requirement considering that the discovery of explosive placed by a terrorist could lead to the saving of many lives. A good search dog can have a knowledge of at least 14 different types of odour. This list could include drugs, human odours and explosives.

3. THE DOGS' DETECTION EQUIPMENT

Dogs have three systems which can be used to detect odours. These are: the olfactory epithelium situated under the forehead, the vomeronasal organ which is located under the muzzle and receives stimuli through vessels which terminate under the upper lip, and the trigeminal system which consists of many nerve endings in several locations in the mucus membranes within the nose. The latter system seems to be able to detect certain chemicals, for example, benzaldehyde, acids and alkaline vapours but has not been studied to a great extent. The vomeronasal system requires a liquid stimulus and is used by the dog to detect substances in urine which might indicate oestrus in bitches. (The presence of the organ is very obvious in horses as shown by the curling of the upper lip of a stallion when testing mares urine) Most studies on canine olfaction have been directed to the olfactory epithelium. This organ is quite large and is easily recognised on dissection by its yellow/orange colour in contrast to the pink/red colour of the respiratory epithelium. The olfactory epithelium is convoluted and has a large surface area - in the German Shepherd this area is approximately 100 sq cm as against about 3 sq cm for a human. The surface of the organ is covered in cilia which are bathed in a layer of mucus which is only a micron or less in thickness. The cilia are attached to neurones in the upper layer of the olfactory epithelium and the base of the neurone is connected by a nerve fibre which passes through the cribriform plate to the olfactory bulb where the signals are processed before being sent to the brain. Odours dissolve in the mucus and trigger a transduction system within the cilia which results in an electrical signal being generated within the neurone which in turn passes to the olfactory bulb. The electrical signal can be detected and measured with a suitable electrode system to obtain an electro-olfactogram (EOG) which provides a

measure of the ability of the olfactory epithelium to detect an odour. Generally, this technique is applied to the olfactory epithelium exposed by a sagittal section of the head of an experimental animal but it is possible to apply the electrodes to the organ of an anaesthetised animal.

However, it is desirable to use methods which do not involve vivisection and in the UK we are funding research into the detection of explosives which will enable a measure of the sensitivity of dogs to explosive vapours to be determined by behavioural methods. The research is being conducted under a Ministry of Defence Research Contract. Trained sniffer dogs are allowed to search for a sample of explosive contained in a plastic container which is placed under a metal mesh cover to prevent access by the dog. Twenty identical containers each under mesh covers are used and are placed in rows in a large room. The handler may conduct the search with the dog running free or on a leash. The proceedings are recorded on video. The test can be repeated as often as required and the explosive sample can be placed in any of the locations. The arena and the mesh covers can be washed to remove any contaminating odours. The plastic containers can be easily replaced. The containers loaded with explosive can be left in position for as long as desired to allow the vapour to diffuse out. There are few draughts in the room and air movements occur principally when people or dogs move around. Different pairs of handler and dog can be easily assessed for effectiveness. The concentration of explosive vapour will be estimated by collection on Tenax adsorbent followed by desorption and determination using a gas chromatograph. To obtain a reasonable measure of the ability of any dog to detect the explosive the search can be conducted several times. Appropriate statistical analysis may then be applied to obtain the probability of the detection of a particular explosive at a given confidence level.

SIGNAL PROCESSING AND SIMULATION

BOMB/NO BOMB: FROM MULTIVARIATE ANALYSIS TO ARTIFICIAL NEURAL SYSTEMS

Patrick Shea, Felix Liu, and Barak Yedidia
Science Applications International Corporation
Santa Clara, CA

1. BACKGROUND

Systems for the detection of explosives hidden in checked airline baggage have been under development at Science Applications International Corporation (SAIC) for the Federal Aviation Administration since 1985. In May of 1987, the first prototype was fielded for testing at San Francisco International Airport. In 1989 the first production unit was fielded at JFK Airport in New York. Since then, over 550,000 bags have been screened by SAIC units around the world.

2. DESCRIPTION OF THE SYSTEM

The system uses thermal neutron activation (TNA) to detect the presence of explosives. In this technique a suitcase on a conveyor belt moves past a source and an array of detectors. Neutrons from the source easily penetrate the luggage, and are absorbed by all of the materials present. Different elements will emit different energy gamma rays after absorbing these neutrons (much like fluorescence). These gamma rays are of a high enough energy that they easily penetrate the luggage, and are detected by a detector array which surrounds the cavity enclosing the suitcase and conveyor belt. The detectors record the number of gamma rays observed at each energy. The number of gamma rays of a "characteristic" energy which are observed depends on the amount of the element present, its location, the number of neutrons present, and the probability that the element will capture a thermal neutron and emit that gamma ray. Since this probability is a known constant for any particular element, and the number of neutrons present and the number of characteristic gamma rays are measured, the amount of each element and its location can, in theory, be determined from the array of signals.

Commercial and military explosives, such as are used by terrorists, have several characteristics which distinguish them from most objects in luggage. One of these characteristics is a high density of nitrogen.

3. DECISION ALGORITHMS DESCRIPTION

A simple approach to distinguishing a bag with an explosive from an ordinary passenger bag is to threshold the total number of nitrogen gamma rays captured in the detectors. Figure 1a shows a histogram of bags with and without simulated explosives placed within the bags. The x-axis is an arbitrary scale showing the relative nitrogen signal from the bags and the y-axis represents the number of bags in the sample. The separation is not good. A "feature" which provides better separation can be generated with some pre-processing of the signal to filter for more "useful" gamma rays as is shown in Figure 1b. But the separation is still poorer than is desirable.

This feature and others are produced by combining the signals from the detectors and correcting for all of the effects understood by physicists (interferences, pileup and the like). The features have different statistical properties; those features which average over many detectors have smaller statistical fluctuation but lose some spatial and elemental resolution.

A large number of these features that use raw signals in various combinations generate a multi-dimensional space populated by bags with and without explosives. It is the job of the decision algorithm to select the best set of features and produce the best performance. While no single feature will provide good separation, a combination of features may be separable by a hyperplane, a multidimensional equivalent of a line.

The basic technique used in the automated decision analysis is linear discriminant analysis. A discriminant value is computed by a linear combination of the values of a set of features

measured for a bag. If the discriminant value is greater than zero, the bag is classified as containing a threat; otherwise, it is cleared. Geometrically, the features are axes which define the classification hyperspace. The measurement of any particular suitcase can be plotted as a point in this space. The points for suitcases without threats cluster separately from those with threats. The hyperplane which best separates the two clusters is the dividing surface which results from the linear discriminant function; in fact, the computed discriminant value is just the normal distance to the hyperplane from the point which represents the bag, the sign representing which 'side' of the hyperplane the point is on.

Application of Fischer's Criteria (the usual least squares technique) to the problem results in the dividing hyperplane being perpendicular to the line that joins the centers of the two clusters. This plane is also 'halfway' between the two centers, if the distance is measured after normalization by the covariance matrix. The overlap between the two clusters determines the possible tradeoff between detection and false alarm rates. By moving the dividing hyperplane along the line joining the two centers (equivalent to changing the threshold the discriminant value has to exceed) this tradeoff can be set to any level, from 0 false alarm rate (and a low detection rate) to 100% detection and a commensurately higher false alarm rate. In addition, the value of the discriminant implies a "sureness" for the decision. This value can be used in some kind of Bayesian analysis or can simply map onto the tradeoff curve as the PD/PFA point that would result if the threshold were set at that value.

4. ANS

An artificial neural system (ANS), however, is not limited to hyperplane separation in classifying luggage. It is possible that an ANS can discover a curved decision surface resulting in a much better classification.

The ANS paradigm that is currently used is called Back Error Propagation (BEP). The BEP is a supervised learning technique based on the Generalized Delta Rule. The Generalized Delta Rule is a steepest descent method of computing the interconnection weights that minimize the total squared output error over a set of training vectors. The standard BEP is a multilayered fully connected feed forward network. It consists of an input layer, any number of hidden layers and an output layer. In a simple two-layer network the outputs are computed directly from the inputs through the connections or *weights* between the two layers. Every unit in the output layer is connected to every unit in the input layer. Figure 2 is an example of a two-layer network.

The outputs generated by the network are compared with the desired or target outputs. Errors are computed from the differences, and the weights are changed in response to these *error signals* as dictated by the Generalized Delta Rule. Thus, a BEP network learns a mapping function by repeatedly presenting patterns from a training set and adjusting the weights. Each pass through the training set is called a *cycle*.

Input patterns that are similar to each other produce output patterns that are similar because of the direct mapping of inputs to outputs in a two-layer network. Unfortunately, this prevents a two-layer network from learning mappings which have very different outputs from very similar inputs. In particular, a two-layer network cannot learn the exclusive-OR function. In order to learn such arbitrary mappings, the network must have more than two layers. In a network with more than two layers, the intermediate layers are called the *hidden layers*. Figure 3 is an example of a network with a hidden layer.

The activations of the units in the hidden layers constitute an internal "representation" of the input patterns. These hidden units learn to encode features that are not explicitly present in the input patterns. By applying the Generalized Delta Rule, a multi-layer network can learn to develop whatever features are necessary to perform the desired mapping.

The activation of each unit in the hidden and output layers is computed by the sigmoid activation function and is shown in Figure 4.

Here, O_i is the activation value for each unit, net_i is the sigmoid activation function used to modify each weight, Θ_i is the bias for unit i, and w_{ij} is the weight to unit i from unit j. (The biases are learned in the same manner in which the weights are learned.)

The Generalized Delta Rule guarantees continuous descent in the total root mean square (RMS) error. This measure is computed by summing the square of the target minus the output for every output unit and for every pattern, averaging this, then taking the square-root.

5. ON-LINE EXPERIENCE

On test data, the ANS performed better than discriminant analysis, i.e., at a lower false positive rate with the same detection rate. Consequently, the FAA decided to proceed with the testing of the ANS in the six units it was purchasing for deployment. The first step was to install the unit at the airport and operate it to gather data. The ANS would then be trained and would work in parallel with the standard analysis, and, if the results were still better, it would be used on-line. At the first installation at Trans World Airlines at JFK International Airport, the system was installed, the standard analysis was calibrated and the performance was demonstrated in the month of October 1989.

Typical operation at the airport involves measuring some bags with simulated explosives and most without. These data are shipped back to the SAIC facility in Santa Clara for processing. All calibration and training is done at the Santa Clara facility, and thus only the feed-forward network needed to be encoded in the explosive detection system. The data which had been accumulated during operations through early October were split into two parts. The fist part was used for calibration, the second for testing.

During the week of October 21 through 26, the ANS was tested in parallel with the standard analysis. During this week, the ANS performed at an equal or higher level than the discriminant analysis every day.

Since these on-line results demonstrated similar performance improvements to those shown during the testing phase, the ANS was installed as the decision algorithm. It has been in operation in all units since then.

It is sometimes desired to set the operating point of the system at different levels. For example, during high threat times very high detection rates might be required; otherwise, it may be desired to minimize the false positive rate. The different PD and PFA operating points at which the system can be set determines the "tradeoff" curve. A sample tradeoff curve is shown in Figure 5. Note that while the ANS curve is superior to the standard analysis curve in the range of interest, there are ranges over which this is not true.

6. DECISION SURFACES

The full decision analysis uses a number of features. Consequently, it is very difficult to portray decision surfaces in only two dimensions. In order to view sample surfaces, a small set of data was abstracted from the data set. A few hundred bags were used, all of which were similar in gross terms (size, destination, etc.). The number of features used was also reduced to five. This reduced set of data was used to train a network using these five features. Figure 6 shows the projection of the calibration data onto a plane passed through the decision space. Each of the two axes are features used in the network. The decision surface is obtained by fixing the values of the three features not used as axes and finding the locus of points which form the boundary between the "bomb" and "no bomb" decision.[1]

This is a strongly curved decision surface. Under these conditions (fixing the three other features) the discriminant analysis surface would be a straight line on this graph. Figure 6 implies that an ANS using only the two features can correctly separate the data in the calibration set, while a straight line (i.e., discriminant analysis) could not.

It is probably possible to find a nonlinear transformation of the features which could produce a more linear response of the ANS (i.e., straighten the line). However, the network training that gave this result used the information contained in the collected data, without operator intervention. Examination of similar curves for other groups of bags shows that differing degrees of curvature are required. In fact some groups of bags will have little difference between linear discriminant analysis and an ANS. Whatever else it does, ANS provides a consistent and effective algorithm for developing these nonlinear combinations.

7. SUMMARY

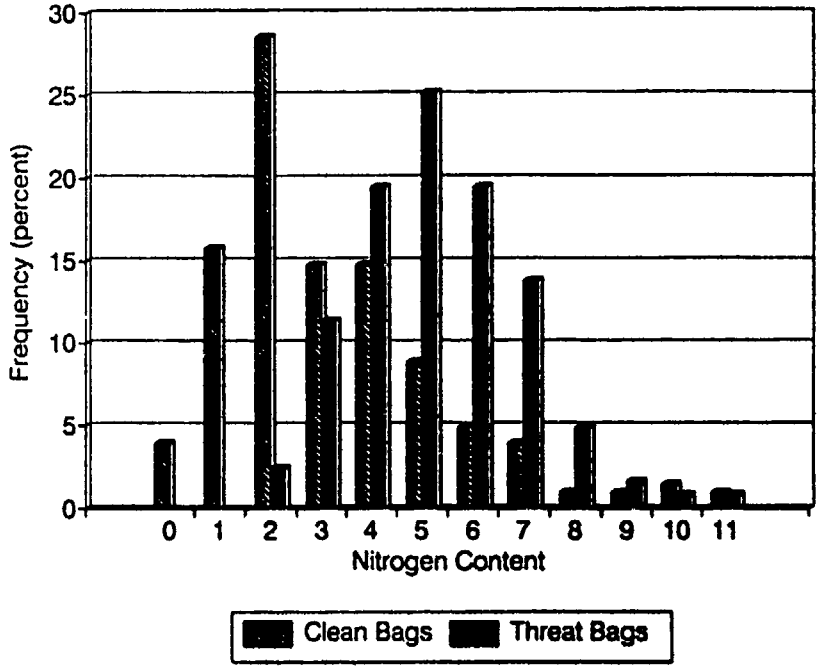
The complexity of the distribution of suitcases makes a decision analysis a difficult problem. While some features of bags make good decisions, and linear combinations of these features do even better it takes the nonlinearity of an artificial neural system to make the most effective decisions.

ACKNOWLEDGEMENTS

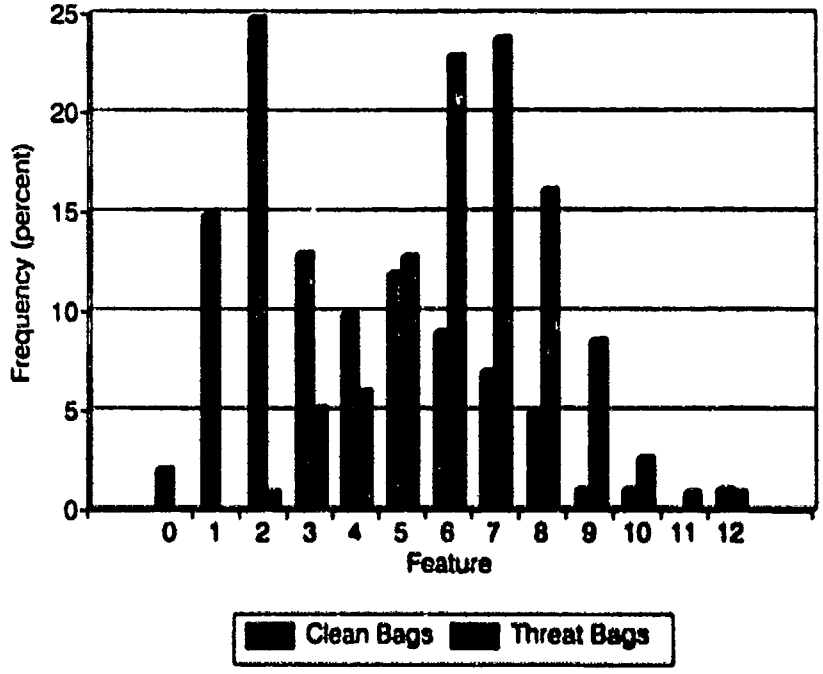
This work has been supported by the FAA Technical Center under various contracts as a part of the work on the TNA explosives detection system. The authors would like to thank the contract monitors involved, Mr. Chris Seher, Mr. Hector Daiutolo, Mr. Carmen Munafo and Mr. Lok Koo for their continued interest and support of this work.

NOTE

1. As should be clear from the figure, a number of points on the separating surface were found, and a smooth curve was passed through them. There are not likely to be any small scale fluctuations which are missed, due to the small number of training points and restricted training times.



(a)



(b)

Figure 1 **Distribution of bags versus the total nitrogen signal and a processed feature. While the separation provided by the feature is superior, it is still insufficient for discrimination of clean bags from threat bags.**

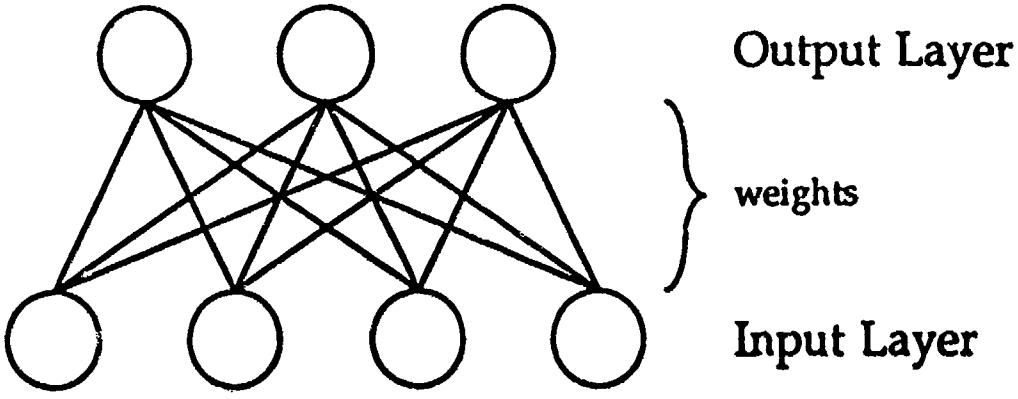


Figure 2 **Two-Layer Network**

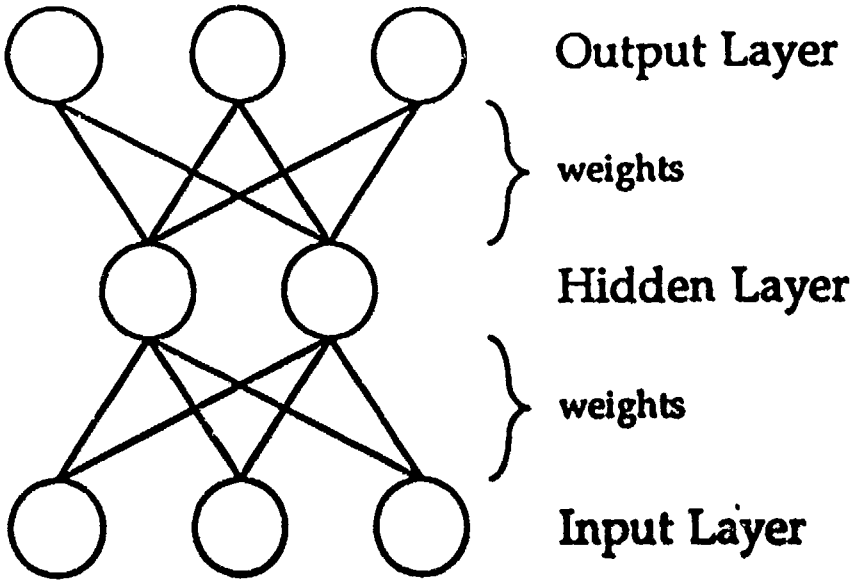


Figure 3 **Network with Hidden Layer**

$$o_i = \frac{1}{1 + e^{-net_i}} - 0.5 \qquad net_i = \theta_i + \sum_j w_{ij} o_j$$

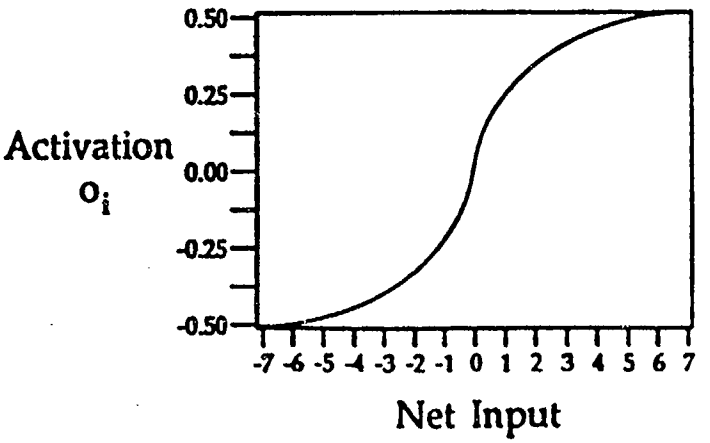


Figure 4 Sigmoid Activation Function

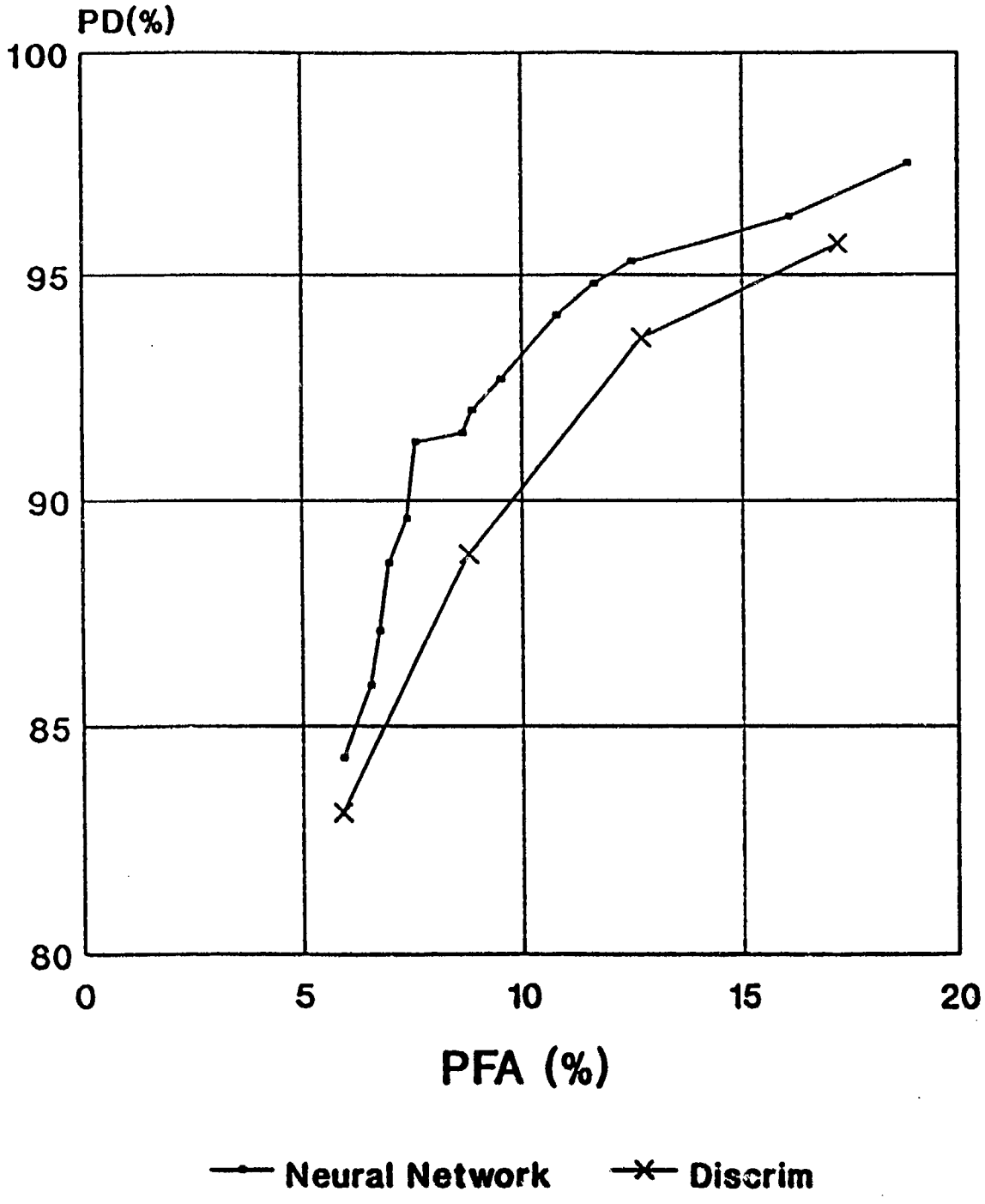


Figure 5 PD/PFA Trade-Off Curve

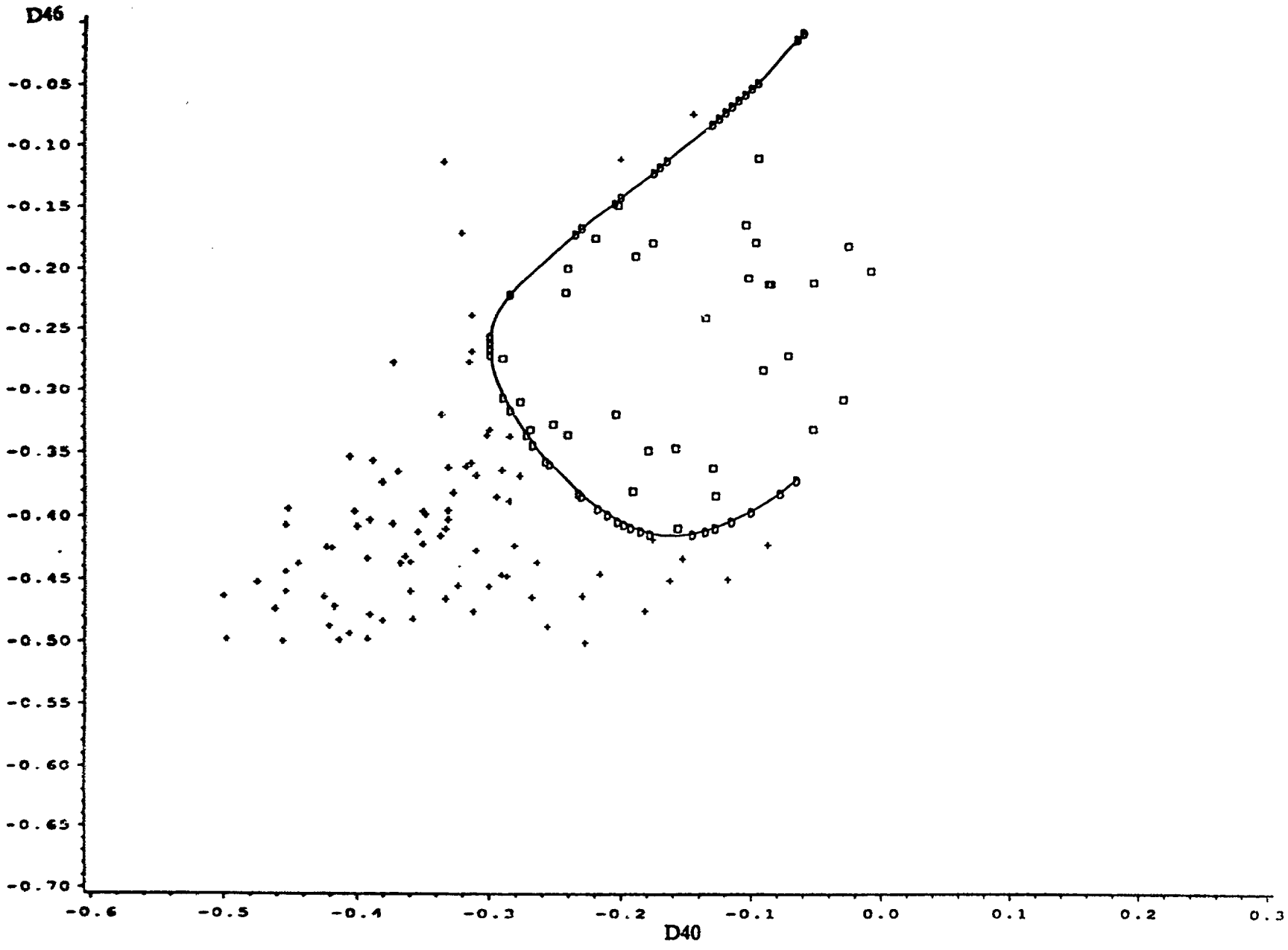


Figure 6 Cross Section Group 6

A NOVEL APPROACH TO DESIGN OPTIMIZATION OF NUCLEAR-BASED EXPLOSIVE DETECTION SYSTEMS

E. Greenspan
Department of Nuclear Engineering
University of California
Berkeley, CA 94720

J. Bendahan and T. Gozani
Science Applications International Corp.
Santa Clara, CA 95054

1. INTRODUCTION

The Explosive Detection Systems (EDS) under consideration use neutron or photon sources for probing the explosive material. For the sake of abbreviation we shall refer explicitly only to EDS driven by neutron sources. The design optimization methodology to be described is applicable, nevertheless, to EDS driven by photon sources, as well as by a combination of photon and neutron sources.

The design of an EDS is a complicated multidisciplinary process. The present paper focuses on the nuclear design discipline. The goals of the nuclear design are defined in Section 2. Section 3 reviews the conventional approach to the nuclear design of EDS while Section 4 describes the novel design approach we are proposing to develop. A limited number of illustrations of the usefulness of the proposed optimization method are presented in Section 5. A program plan for the development of a powerful three-dimensional nuclear design optimization capability is outlined in Section 6.

All of the illustrations presented pertain to simplified EDS because: (1) The limitation of the presently available optimization code to one dimensional problems, and (2) The commercial sensitivity of the details about the design and composition of the EDS and their subsystems.

2. GOALS OF THE NUCLEAR DESIGN

The interaction of the source neutrons with one or more of the constituents of the explosive material creates a characteristic signal (of gamma rays or neutrons). This signal leaves the enclosure of the explosive and reaches the detectors of the EDS. Also reaching the detectors will be neutrons and photons that do not carry the explosive characteristic signal. This background radiation can come from the source neutrons interaction with (a) the explosive material which do not result in the emission of characteristic radiation; (b) constituents of the explosive enclosure (such as luggage); and (c) constituents of the EDS, including the detectors of the EDS. The background radiation can also come from the interaction of the characteristic signal with the medium it has to transverse before reaching the detectors. The background radiation can mask the signal and thus reduce the EDS sensitivity; i.e., the probability that the EDS will identify an explosive of a given size.

Once the performance requirements of an EDS are given: namely, probability of detection and false alarm for specified amounts and range of contiguous sizes of the explosives, the goals of the nuclear design of an EDS can be set as follows: For a given source (could be a number of sources) strength, maximize the amplitude of the signal and minimize the amplitude of the background radiation which reaches the detectors. The above stated goals may not be simultaneously attainable for every EDS. An alternative design goal is to maximize the signal-to-background ratio. The exact definition of the signal and of the background for the purpose of the design optimization may be EDS dependent.

Another goal of the nuclear design is to provide an adequate shield for the neutron source (or sources) so that the dose rate on the outer surface of the EDS will not exceed the permissible level. The acceptable radiation level is to be achieved with a shield of minimum cost. Under certain circumstances it might be desirable to minimize the shield thickness.

Generally speaking, the closer to optimal is the nuclear design of an EDS, the higher could be its sensitivity. Moreover, with all other subsystems (such as detectors, data collection and data analysis systems) being the same, the nuclear design optimization could minimize the cost of the EDS. Consequently, a good nuclear optimization capability could be highly beneficial for the development of improved EDS. In certain circumstances the nuclear design will be the bottleneck to the EDS sensitivity improvement; going to a more sophisticated (and expensive) data collection and data analysis systems will not be effective if the nuclear design will not provide a higher signal and/or a higher signal-to-background ratio.

3. THE COMMON APPROACH TO NUCLEAR DESIGN OPTIMIZATION

The most efficient approach to the nuclear design of EDS, in terms of the resources and time needed, is a well balanced theoretical/experimental program. The theoretical effort should involve a numerical simulation of the host of nuclear phenomena which take place in the EDS. The nuclear simulation tool should be used for studying the effect of different variations in the EDS design parameters on the nuclear performance of the EDS. The ultimate purpose of the theoretical effort is to identify the design of the EDS that will optimize its nuclear performance, as defined by the goals stated in Section 2.

The experimental part of the nuclear development program is to validate the results from the numerical calculations, which often involve different assumptions and approximations.

In reality one encounters situations in which the developers of EDS (as well as other nuclear systems) do not use numerical simulation at all. One selects the constituents of the different components and decides on the dimensions of these components based on general considerations and intuition. Then a mockup is constructed in which the signal and background radiation levels are measured. These measurements are repeated for a number of design variations before a final design is selected. For such an approach to lead to a real optimal design, the experimental study is likely to be prohibitively expensive. This is because the large number of material combinations, component geometries and dimensions that need be studied. Thus, in practice, such an approach is not likely to lead to an optimal nuclear design. In any event, it can never tell the developers, or the sponsors of the development, how close to the optimal their design really is.

When numerical simulation of the EDS nuclear performance is undertaken, it usually uses a trial-and-error approach. In this approach the system (either the entire EDS or one or more of its components) is divided into Z number of zones; each zone having a uniform composition. Assigning a certain composition to each of the zones, the transport equation for neutrons and photons is numerically solved. From this solution one can deduce the amplitude of the signal and background radiation which reaches the detectors (or, even, counted by them). The spectrum of the signal and background radiation reaching the detectors is obtained as well. The solution of the transport equation can be done using one of the well developed discrete-ordinate or Monte-Carlo codes [Bendahan et al., 1991].

The composition of different zones is then changed and the transport equation is solved again to provide the signal and background radiation for the modified composition. This process is being repeated many times until what appears to be an optimal composition is identified.

Even though this numerical simulation process is significantly less expensive and less time consuming than a comparable experimental simulation, it is a long and tedious process; if C different constituents are to be considered for each of the system zones, the total number of transport solutions that need be obtained in order to cover all the possible permutations of Z zones and C constituents is, usually, prohibitively large (in terms of the required time and resources). In practice, the designer will apply his intuition and prior knowledge to reduce the number of transport calculations that need be performed. Nevertheless, even then it is not practical to cover all the parametric space of relevance. As a consequence, the best design identified by this trial-and-error approach is not necessarily the real optimal design. Even when the trial-and-error approach leads to a near optimal design, the designer (and the sponsors of the development) have no way to know how close is the design to the real optimum.

4. A NOVEL APPROACH TO NUCLEAR DESIGN OPTIMIZATION

The novel approach proposed here for the optimization of the nuclear design of EDS involves three new ingredients:

(a) The calculation of material "effectiveness functions",

(b) The use of these effectiveness functions to help identifying the most promising constituents, and

(c) The use of these effectiveness functions to guide an automated search of the optimal distribution of the selected constituents.

The effectiveness function of a given material gives the change in a Figure-Of-Merit (FOM) due to the addition of a small quantity of this material to a given zone. Thus, the Material Effectiveness Function pertains to a given FOM and a given reference EDS design. Usually, the addition of a given material to a given zone can be done only at the expense of removing the equivalent volume of one (or few) of the existing constituents. Thus, in practice, one needs to consider the Substitution Effectiveness Function (SEF). The SEF of material i for material j gives the change in the FOM due to the substitution of a small quantity of material i for the same volume of material j in a particular zone in the EDS.

The SEF are calculated using perturbation theory formution [Greenspan, 1976]. The perturbation theory calculation of the SEF requires the solution of the transport equation and of a corresponding adjoint equation for the EDS. The transport equation and the numerical method used for its solution are the same as required for the numerical simulation of the EDS, as described in Section 3. The solution of the adjoint equation can be done using the same numerical simulation codes. For each FOM to be considered one needs to solve a corresponding adjoint equation (For details see Greenspan, 1976).

In summary, our approach to the optimization of the nuclear design of EDS works as follows:

(a) Based on prior experience, define a reference design for the EDS (or of one of its subsystems). The reference design specifications include the system geometry, type and location of the neutron sources, type and location of the detectors, type of constituents of all the subsystems and their distribution across the EDS.

(b) Solve the neutron and/or photon transport equation for this reference design.

(c) Solve the corresponding adjoint equation for each FOM that is to guide the design optimization.

(d) Calculate the SEF for each of the system constituents as well as for candidate constituents. Get a set of SEF for each FOM.

(e) Guided by the SEF information, decide whether to make a change in the constituents of the EDS (relative to the constituents of the reference design).

(f) Apply an iterative optimization algorithm to find the optimal distribution of the selected constituents.

(g) Calculate the SEF for candidate constituents, now pertaining to the optimized EDS composition. By examining these SEF decide whether a significant enough gain can be expected by adding one or more other constituents to the EDS, possibly instead of an existing constituent.

(h) Repeat the optimization procedure (Steps "b"-"d" and "f").

(i) At the end of this process, estimate how far is the FOM calculated for the optimized system from its absolutely optimal value -- the value it would have assumed had we carried the optimization process to very close to complete convergence. This estimate can be done using the SEF values.

(j) The optimal EDS composition identified with the above outlined procedure may call for a zone-wise variation in composition. Based on this optimal material distribution, work out a design that is practical to implement and yet closely matches the performance of the semi-continuously varying design.

A computer code called SWAN was developed already in the early seventies [Greenspan, 1973] to perform all the above listed functions. Thus, details about the theoretical basis for the above outlined optimization procedure as well as on the practical implementation of this procedure can be found in the SWAN literature [Greenspan, 1973; Greenspan et al., 1973; Greenspan, 1976].

SWAN was originally developed for the optimization of the nuclear design of fusion reactor components which are exposed to the 14 MeV neutrons originating from the D-T fusion reaction.

Throughout the years SWAN was successfully applied to the optimization of a large variety of nuclear design optimization problems. Illustrations of optimization studies carried with SWAN can be found in [Greenspan et al., 1974; Gilai et al., 1977; Gilai et al, 1983; Gilai et al, 1984; Greenspan et al, 1985a; Greenspan et al., 1985b; Kinrot et al., 1985; Greenspan et al., 1986; Greenspan et al., 1987; and Karni et al., 1989]. In many of these optimization studies the optimal nuclear designs identified with the help of SWAN were found to offer a better performance (i.e., to be more optimal) than corresponding designs arrived at using conventional nuclear design approaches (as described in Section 3). In fact, this was the case almost whenever a comparison was attempted between the SWAN and the conventional approaches to the optimization of the nuclear design of a given system. Following is a brief summary of three of the comparisons.

In one of the studies [Gilai et al., 1983] SWAN was applied to search for the optimal design of a shield the major constituents of which are stainless steel and water. The reference shield was designed by a team of highly experienced professionals. It was found that the dose rate behind the optimal shield identified with SWAN was lower than the dose rate behind the reference shield by a factor of 20!, when both shields were of the same thickness. Moreover, SWAN found that by a proper addition of boron to the shield, the dose rate can be reduced by a factor of nearly 100 below the dose rate predicted using the conventional design approach!

Another study [Kinrot et al., 1985] illustrates the usefulness of the SEF information generated by SWAN for identifying the most effective constituents for radiation shields and their best location within the shield. Conventional design practices applied by a shield design expert led to the conclusion that boron containing materials are preferable shield constituents than hydrogen containing materials. SWAN, on the other hand, revealed that titanium hydride is more effective than the borides. A certain combination of titanium hydride and boron carbide was found to be better than either one of these constituents. These findings would have been extremely difficult to come by even for highly experienced nuclear design specialists without a tool like SWAN. Also found by SWAN is that a tungsten-copper composite material makes a more effective shield constituent than tungsten having 90% of its theoretical density. Overall, the radiation induced heating rate beyond the SWAN optimized shield was only about 60% that arrived at by careful and professional optimization but using the conventional design approach.

In another study [Greenspan et al., 1987] SWAN was applied to make a systematic comparison of the effect of the tritium breeding material on the blanket thickness that is required to provide a given tritium breeding ratio. A specific question addressed was whether the remarkable difference (of over a factor of 3) in the thickness of three different blankets designed by three different groups of experts using conventional design practices, is due to the different lithium compounds used or to non-optimal nuclear designs. SWAN easily found that the latter was the case. As a by-product, SWAN showed how to distribute the different constituents across the blanket in order to obtain the desired tritium breeding ratio using a minimum thickness blanket.

The optimal compositions identified with SWAN throughout the years for a large variety of systems also led to the invention of new composite materials which offer improved performance. An illustration of such composite materials and their expected performance can be found in [Greenspan, 1991]. One of the new materials is polynated tungsten. The total dose rate behind a 40 cm thick shield of a californium-252 neutron source was found [Greenspan, 1991] to be nearly 20 times lower than the dose rate behind a comparable shield which is made of the conventionally used commercial borated polyethylene! Another new material is polynated titanium-hydride. The Cf-252 neutron leakage out from a 40 cm thick shield made of this material was found to be an order of magnitude lower than the neutron leakage from the same thickness shield made of the commonly used borated polyethylene. These new composite materials might enable a significant improvement in the design and performance of EDS.

Even though so far SWAN was applied to primarily the nuclear design optimization of problems pertaining to fusion reactor systems, it can as readily and efficiently be applied to the optimization of the nuclear design of any kind of source-driven nuclear system (i.e., a system which is exposed to a neutron and/or photon source). An illustration of nuclear design optimization problems encountered in the development of EDS which can be addressed with SWAN are presented in the following sections.

However, presently SWAN can only be applied to nuclear systems which can be simulated by a one-dimensional stationary transport equation (in

either spherical, cylindrical or slab geometries). Fortunately, the methodology for the calculation of the SEF and for the system composition optimization developed for SWAN can be directly applied to two- and three dimensional problems. A program plan for the development of a three-dimensional optimization capability is outlined in Section 6.

5. NUCLEAR DESIGN OPTIMIZATION OF EDS

The ultimate goals of the optimization of the nuclear design of EDS were defined in Section 2. In practice it is helpful to optimize the nuclear design of selected components of an EDS before embarking upon an overall EDS optimization study. In Sections 5.1 and 5.2 we will briefly define a number of component optimization studies that are useful to undertake in the course of the development of a Thermal Neutron Analyzer (TNA) and of a Fast Neutron Analyzer (FNA). In Sections 5.3 and 5.4 we shall illustrate the application of the one-dimensional SWAN to the optimization of one component of the TNA and one component of the FNA under development by SAIC.

5.1 TNA Optimization Problems

Figure 1 is a highly simplified schematic illustration of an EDS that has many features in common with the TNA. The "thermal neutron source system" of this EDS consists of one or more Cf-252 spontaneous fission sources. The explosive detection mechanism is based on thermal and epithermal neutron captures in one of the constituents of the explosive material. The characteristic photons emitted as a result of the neutron capture reactions in the specific constituent are to be detected by the detector or detectors of the EDS. The explosive material is usually surrounded by other materials which are either a part of the "target" or adjacent to it. The detector needs to be shielded from neutrons and photons which do not originate from the target. A biological shield is needed to assure that the dose rate at the outer boundary of the EDS will not exceed the permissible level.

5.1.1 Optimization of the neutron source assembly

One optimization problem is to maximize the probability that a source neutron will be captured in the proper constituent of the target (to be referred to as the target constituent). The optimization variables are the constituents of the neutron source system and their spatial distribution. When more than one neutron source is to be used, the location of the different sources can also be a variable of the optimization.

An even more general (and more complicated) optimization problem is to maximize the probability (per source neutron) of the emission of characteristic photons from the target constituent in the direction of the detector. There are situations in which the optimal source system design arrived at using the couple of optimization goals defined above will be different. The latter criterion is the more general of the two, but the former one is more universal.

5.1.2 Optimization of the detector shielding

In many applications it is desirable to locate the detector as close as possible to the neutron source, so that it will "see" the target constituent at the largest possible solid angle. The largest the solid angle, the higher is the detection probability. Thus, it is desirable to design the detector shield (See Figure 1) against neutrons and photons which come out from the source system (See path "2" and path "3", Figure 1) as compact as practical.

A related problem (that is not illustrated in Figure 1) is the optimization of a protection cover and/or of a collimator for the detector. The task of these components is to increase the signal-to-background ratio, although not without penalty. The penalty will be a reduction in the amplitude of the signal. A very intriguing optimization problem is to maximize the signal-to-background ratio under the constraint that the signal should not be reduced below a given level.

5.1.3 Optimization of the detector design

The optimal size of a detector of the TNS can also be a subject for an optimization study. Too small a detector volume will penalize the detection efficiency and, hence, will detect a smaller signal. Too large a detector volume (and surface area) may lower the effectiveness of the collimation and shielding against background radiation, thus increasing the background count rates.

5.1.4 Optimization of the biological shield

The biological shield can have a significant impact on the size, weight and cost of the EDS. It might also effect the background radiation level, as illustrated in Figure 1 (Path "3"). For many applications the

design goal will be to minimize the cost of the biological shield (and EDS structure) without significantly increasing the background radiation level, while meeting the constraint on the permissible surface dose rate.

5.2 FNA Optimization Problems

Figure 2 is a simplified schematic illustration of a FNA. Fast neutrons emitted from the source are to reach the target through a collimator. The interaction of these neutrons with certain constituents of the explosive located in the "target" is to cause the emission of characteristic photons. These photons are to be detected by the detectors of the FNA. The entire EDS need be surrounded by a biological shield.

5.2.1 Collimator optimization

The collimator is designed so as to maximize the number of energetic neutrons to reach a predetermined area on the surface of the target that points towards the source. At the same time, the collimator contribution to the background radiation reaching the detector needs to be small enough. Path "2" of Figure 2 illustrates one way for the contribution of the collimator to the background radiation. The variables of the collimator design optimization include the collimator shape and the materials which are located adjacent to the collimator walls.

5.2.2 Optimization of the collimator shield

One function of the "shield" (Figure 2) is to reduce the probability that energetic and other neutrons (and photons) will reach the target not through the collimator aperture to an acceptable level. Another function of this shield is to shield the detectors from neutrons and photons that do not come from the target (Such as from those which come via path "1" of Figure 2). The closer a given source can be to the target, the larger will be the number of neutrons reaching a unit surface area of the target and the more sensitive the FNA could be. Hence, it is highly desirable to minimize the thickness of the "shield".

5.2.3 Optimization of the detector shielding

It is desirable to protect the detector from neutrons and photons which stream through the collimator and then are scattered into its direction (as, for example, in Path "2" of Figure 2). The detector protection may consist of a special collimator and/or a protection layer (not shown in Figure 2). The optimization variables should be the geometry and the composition of these detector protection measures.

5.2.4 Optimization of the detector design

This optimization problem is similar to that described in Sec. 5.1.3.

5.2.5 Optimization of the biological shield

This optimization problem is similar to the one described in Sec. 5.1.4.

5.3 The Application of SWAN -- Illustration I

Referring to the EDS system depicted in Figure 1, the question addressed is how to design the detector shield so as to minimize the background radiation reaching the detector via path "2". The thermal neutron source system is assumed to be of a fixed design. The detector shield is taken to be 20 cm in thickness. The FOM to be minimized is the total flux of photons in the volume of the detector. The problem is represented in spherical geometry, with a Cf-252 neutron source at the center. The 56 group coupled neutron - photon cross-section library FLUNG [Roussin et al, 1991] is used for the calculations.

Figure 3 shows the optimal composition of a 3 - constituent shield identified with SWAN, while Figure 4 shows one possibility for implementing this optimal composition in practice. The total amount of constituent D in the layered shield arrangement of Figure 4 is the same as in the SWAN optimized shield of Figure 3. The location of the layers of constituent D is guided by the distribution of this constituent in Figure 3.

Next let us examine the SEF distributions calculated by SWAN for a candidate constituent -- boron carbide in which the boron is at its natural isotopic composition. Figure 5 shows the B_4C SEF pertaining to the shield composition of Figure 3. The B_4C is to be substituted for constituent A. The SEF data of Figure 5 provide us with a couple of important messages: (a) The addition of some B_4C to the shield will reduce the FOM (Notice that the SEF values shown in Figure 6 are negative), and (b) The most effective locations to add B_4C are right near by the neutron source system, and in the vicinity of the peak in the D distribution. By making use of this

guidance, SWAN finds the optimal composition of the 4 - constituent shield to be that depicted in Figure 6.

An estimate of the magnitude of the reduction in the FOM due to the substitution of a small amount of B_4C for constituent A can be obtained as follows: Multiply the SEF pertaining to a given zone by the zone volume to be occupied by the B_4C, and sum over all the zones.

Notice that the optimal amount of B_4C called for by SWAN is very small. Moreover, no B_4C is needed in more than half of the volume of the shield. The common practice in shield design is to use borated materials (such as borated polyethylene or borated paraffine) whenever the base materials (i.e., polyethylene etc.) are to be used. Such a practice can often impair the shield performance, as the addition of boron comes on the expense of removal of a more effective constituent. It is only with a code like SWAN that it is possible to know where in the system it is desirable to add a given constituent and where it is not desirable to have this constituent.

The reduction in the FOM reached by the addition of B_4C turned out to be few percent only. The small contribution of the B_4C is attributed to the negative effect on the FOM associated with the displacement of the major shield constituents caused by the introduction of the B_4C. This displacement effect compensates for most of the positive effect of neutron capture by boron. Thus, the next question SWAN was applied to was to find out to what extent concentrating the B-10 isotope in the boron used could improve the shield performance. The SEF data from SWAN indicated that it should have a significant effect.

Figure 7 shows the optimal composition of a $^{10}B_4C$ containing detector shield identified with SWAN. The amount of boron-carbide now called for is significant; the overall shield composition is quite different from the optimal shield composition when natural boron is used (Figure 6). The photon flux behind this shield is 65% that behind the shield of Figure 6. Studying the SEF calculated by SWAN for other candidate constituents revealed that none of them could reduce the photon flux level below that achieved with the shield of Figure 7.

Having identified the lowest level of photon background radiation attainable with shields limited to 20 cm in thickness, SWAN was than applied to search for a practical shield design. The practical design is to be at least as effective as the shield of Figure 7, and to be simple and relatively inexpensive to construct.

Guided by the optimal composition of the shield of Figure 7 and by consultations with Reactor Experiments Inc. (a shielding material manufacturer), a new composite material specifications were defined. SWAN was then applied to identify the optimal detector shield composition that uses this composite constituent. Figure 8 shows the optimal composition identified. Figure 9 shows how we propose to translate the shield of Figure 8 into practice. The performance of these two shield designs is practically identical to each other, and is as good as the performance of the shield of Figure 7.

It ought be realized that without a tool like SWAN it would have been extremely difficult and time consuming for a shield designer to arrive at the optimal designs presented above. Even more difficult (almost impossible) would it be for the designer to know how far his design is from the real optimum. Also impractical would it be for the designer to conceive of new composite shielding materials which enable to simplify the shield design and to make it less expensive, while providing the best performance attainable using existing commercial materials.

It ought also be realized that the above described shield compositions are not necessarily the optimal shields for the real EDS. Limited by the one-dimensionality of the present SWAN, the above illustration of the optimization capability of SWAN did not account for the contribution, to the detector background, of neutrons and photons which bypass part of the shield. One bypassing pathway is via the biological shield, such as illustrated by path "3" in Figure 1. Another bypassing pathway is through scattering from the target system. A three dimensional optimization capability is needed in order to properly account for these effects. In addition, the ultimate optimization of the detector shield will have to be done interactively with the optimization of the thermal neutron source system (See Figure 1). It will have also to account for the detailed interaction of the leaking radiation with the detector. Cost considerations may also affect the optimal shield design.

5.4 The Application of SWAN -- Illustration II

Referring to the simplified FNA system shown in

Figure 2, the question addressed is how effective a 90 cm thick collimator can be designed to be. This collimator is to minimize the background radiation reaching the detector via path "1", i.e., not accounting for the effect of streaming through the collimator aperture and for the effect of scattering from the target. The source is an accelerator that generates neutrons in the 7 to 8 MeV range. Two FOM have been considered: (a) the total flux of neutrons, and (b) the total flux of neutrons and photons in the volume of the detector which is located beyond the collimator. A 1.5cm B_4C layer (using natural boron) is located between the collimator and the detector. The 56 group coupled neutron - photon cross-section library FLUNG [Santoro et al., 1981] is used for the calculations.

Consider, first, FOM "a". The first constituents considered for the collimator are iron and polyethylene -- conventional constituents for the design of collimators. Figure 10 shows the optimal composition of the iron-poly collimator identified with SWAN. The background radiation behind this collimator is found to be 4 times lower than the background behind a similar collimator made out of a uniform distribution of iron and polyethylene, each occupying 50% of the volume. Relative to a uniform collimator made of only polyethylene or only iron, the SWAN optimized collimator offers a reduction in the background level of, respectively, 28 and 13,430!

Figure 11 shows the SWAN calculated effectiveness function for the substitution of B_4C for iron in the optimal shield of Figure 10. It is seen that further reduction in the background level is attainable by the addition of B_4C to the collimator zones near by the detector. However, the magnitude of the possible background reduction estimated from the SEF data of Figure 11 was found to be rather small.

Next we studied the SEF for alternative candidate collimator constituents calculated with SWAN for the optimal collimator of Figure 10. A number of candidate materials were found to offer a lower FOM. Figure 12 shows the optimal collimator design identified with SWAN when the iron was replaced by one of these promising constituents. The corresponding FOM is lower than that of the optimal iron - polyethylene collimator (Figure 10) by a factor of 50! Additional FOM reduction by a factor of 2.5 was found possible by the use of an additional constituent. However, this added constituent is presently not available commercially.

Consider, next, the "b" FOM. Figure 13 shows the optimal composition obtained with SWAN when using the same constituents as in the collimator of Figure 12. It is seen that the change in the FOM can have a significant effect on the optimal collimator composition.

The shield compositions presented in this section are not exactly the optimal for the real FNA. In order to identify the real optimal design, it is necessary to account for (a) the detailed interaction of the neutrons and photons with the detector, and (b) for three dimensional effects, notably, the streaming through the collimator.

6. SWANTORT DEVELOPMENT PLAN

The methodology for the calculation of material effectiveness functions and the methodology for the identification of the optimal system composition developed for SWAN are directly applicable to multi-dimensional problems. Two developments which took place since the development of SWAN make practical the extension of SWAN to two-, and even three - dimensional systems: (a) The development of powerful 2-D and 3-D transport codes for the solution of the neutron and/or photon transport equation, and (b) The advancement in the computational capability of modern computers, and the development of novel computer architectures, such as parallel processing. Hence, it appears that this is the proper time to benefit from the advancements in software and hardware development over the last couple of decades and to embark upon the development of a 2-D and a 3-D version of SWAN.

Specifically we propose to use the 2-D transport code DORT [Rhoades, 1982] and the 3-D transport code TORT [Rhoades, 1987] as the basis for multi-dimensional general purpose shield design optimization codes SWANDORT and/or SWANTORT. DORT and TORT were developed at the Oak Ridge National Laboratory by the same group that developed the 1-D transport code ANISN [Engle, 1967] which makes the transport (and adjoint) calculations for the present version of SWAN. Both DORT and TORT have undergone extensive series of tests and are considered highly reliable. In fact, DORT is now incorporated as a special module of TORT, so that, in practice, the development of SWANTORT will give us both a 3-D and a 2-D optimization capability.

The proposed SWANTORT will be able to address all the nuclear design optimization problems that will be encountered in the process of the development of EDS based on the use of neutron and/or photon sources. These include all the problems defined in Sections 5.1 and 5.2 in addition to the optimization of the nuclear design of the EDS as a whole.

Based on the experience gained from the application of the 1-D SWAN to the optimization of a large variety of nuclear systems, it is expected that the development of SWANTORT will contribute to the development of improved EDS based on nuclear techniques. Expected specific contributions of SWANTORT include, but is not limited to, the following:

(a) Improving the sensitivity of the EDS developed so far.
(b) Guiding the nuclear design of new generations of EDS.

In summary, it appears to us that the availability of a tool like SWANTORT will assure that the potential of any EDS concept that is based on neutron and/or photon sources will be exploited to the utmost, as far as the nuclear design is concerned. Specifically, SWANTORT will enable the designers to get the best signal (signal-to-background ratio etc.) from the EDS. It will also enable the designers or the sponsors of the development to reliably compare different design concepts. In addition, it will enable the developers of EDS and their sponsors to examine the consequences of new ideas and of design modifications on the nuclear performance of the EDS. Furthermore, SWANTORT will enable to efficiently determine how far from the optimal the design of an EDS becomes as a result of a change in the detection goal (such as the introduction of a new type and/or different amount of explosives). Overall, SWANTORT is likely to improve the benefit-to-cost ratio of the development program of EDS which use radiation sources.

REFERENCES

1. Bendahan, J., Pentaleri, E., Elias, E., Shayer, Z., and Pierre, J., 1991, "Computer Simulations and Performance Predictions for Explosive Detection Systems," These Proceedings.

2. Engle, W.W., Jr., 1967, "A User's Manual for ANISN -- A One Dimensional Discrete Ordinates Transport Code with Anisotropic Scattering," Oak Ridge National Laboratory Report K-1693.

3. Gilai, D., Greenspan, E., Levin, P., and Price, W.G., 1977, "Optimal Iron-Water Shields for Fusion Reactors," Proc. 5th Int. Conf. Reactor Shielding, CONF-770401, pp. 731-738.

4. Gilai, D., Greenspan, E. and Levin, P., 1983, "On Optimal Shields for Fusion Reactors," Proc. 6th Int. Conf. on Radiation Shieldings, Vol. II, pp. 646-654, Tokyo, Japan.

5. Gilai, D., Greenspan, E., Levin, P., and Karni, Y., 1984, "Optimal Shields for Fusion Reactors," Proc. Amer. Nucl. Soc. Top. Mtg. on Reactor Physics and Shielding, Chicago, IL.

6. Greenspan, E., 1973, "A Method for the Optimization of Fusion Reactor Neutronic Characteristics," Proc. Conf. on Mathematical Models and Computation Techniques for Analysis of Nuclear Systems," Princeton Plasma Physics Laboratory Report MATT-981.

7. Greenspan, E., Price, W.G., and Fishman, H., 1973, "SWAN: A Code for the Analysis and Optimization of Fusion Reactor Nucleonic Characteristics," Princeton Plasma Physics Laboratory Report MATT-1088.

8. Greenspan, E., and Price, W.G., 1974, "Tritium Breeding Potential of the Princeton Reference Fusion Power Plant,"Princeton University Plasma Physics Lab. Report MATT-1043.

9. Greenspan, E., 1976, "Developments in Perturbation Theory,"Advances in Nuclear Science and Technology, Vol. 9, 181-268, Academic Press, Inc.

10. Greenspan, E., 1982, "New Developments in Sensitivity Theory," Advances in Nuclear Science and Technology, Vol. 14, 313-361, Plenum Publishing Co.

11. Greenspan, E., Levin, P. and Kinrot, A., 1985, "Optimal Blanket Concepts for D-T Fusion Reactors," Proc. 6th Amer. Nucl. Soc. Top. Mtg. on the Technology of Fusion Energy, San-Francisco, CA.

12. Greenspan, E., Levin, P. and Kinrot, A., 1985, "Optimal Shield Concepts for Experimental Fusion Devices," Proc. 6th Amer. Nucl. Soc. Top. Mtg. on the Technology of Fusion Energy, San-Francisco, CA.

13. Greenspan, E., and Karni, Y., 1986, "Neutronic Optimization of Li_4SiO_4/Be/He/SS Blankets and Shields for NET," Fusion Technology, 10, 1605-1610.

14. Greenspan, E., and Karni, Y., 1987, "helium Cooled Beryllium Blanket Thickness Dependence on Tritium Breeding Material,"Trans. Amer. Nucl. Soc., 55, 124-126.

15. Greenspan, E., 1991, "High Effectiveness Shielding Materials and Optimal Shield Design," Proc. Symp. on Radiation Shielding for the 21st Century, Atlantic City, N.J. To be published in the Journal of Testing and Evaluation of the ASTM, Jan. 1992.

16. Karni, Y. and Greenspan, E., 1989, "Minimum Thickness Blanket - Shield for Fusion Reactors," Fusion Eng. and Design, 10, 63-69.

17. Kinrot, A. and Greenspan, E., 1985, "Borides vs. Hydrids for Minimizing Fusion Reactor Shield Thickness," Trans. Amer. Nucl. Soc., 49, 441-442.

18. Rhoades, W.A., and Childs, R.L., 1982, "An Updated Version of the DOT 4 One- and Two-Dimensional Neutron/Photon Transport Code," Oak Ridge National Laboratory Report ORNL-5851.

19. Rhoades, W.A., 1987, "The TORT Three-Dimensional Discrete Ordinates Neutron/Photon Transport Code," Oak Ridge National Laboratory Report ORNL-6268.

20. Santoro, R.T., Roussin, R., and Barnes, J.M., "FLUNG: Coupled 35-Group Neutron and 21-Group Gamma Ray P_1 Cross Sections for Fusion Applications", Oak Ridge National Laboratory Report ORNL/TM-7828.

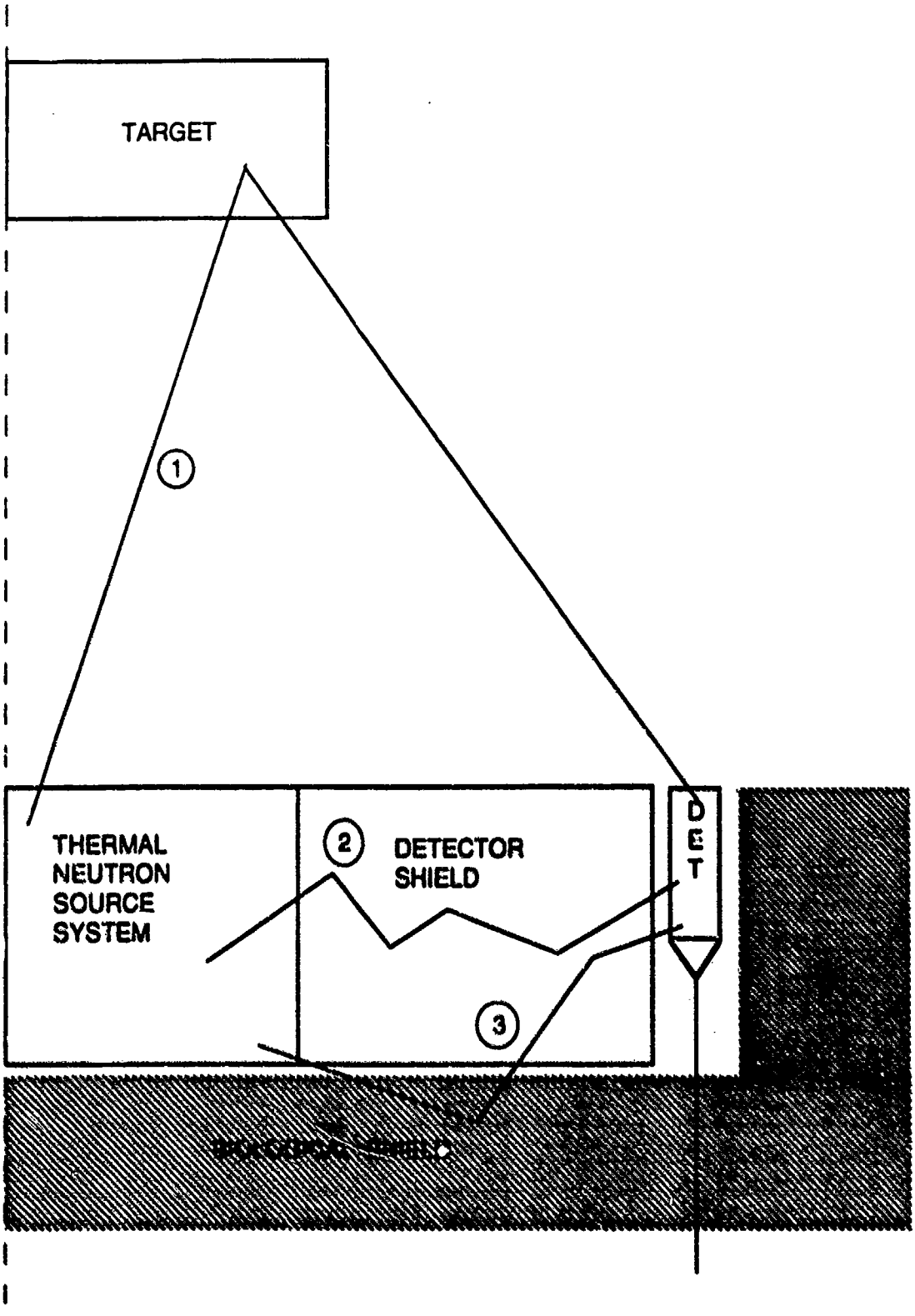


Figure 1 **A simplified schematic illustration of an EDS based on thermal neutron interactions.**

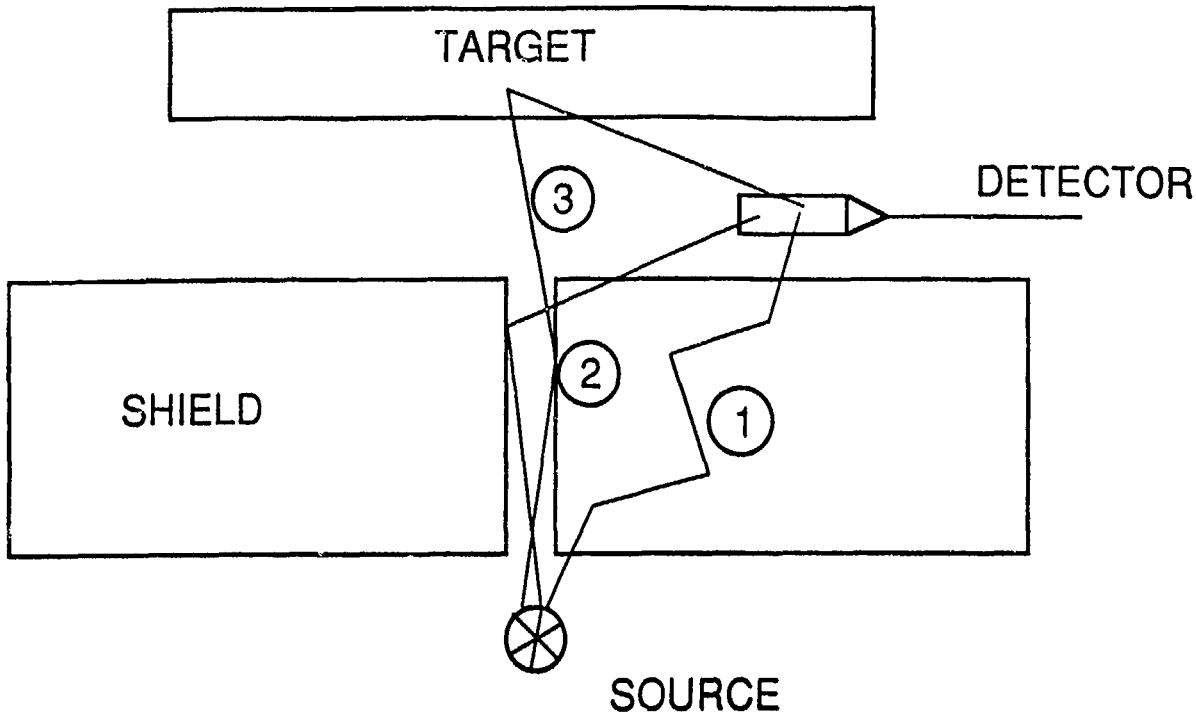


Figure 2 **A simplified schematic illustration of an EDS based on fast neutron interactions.**

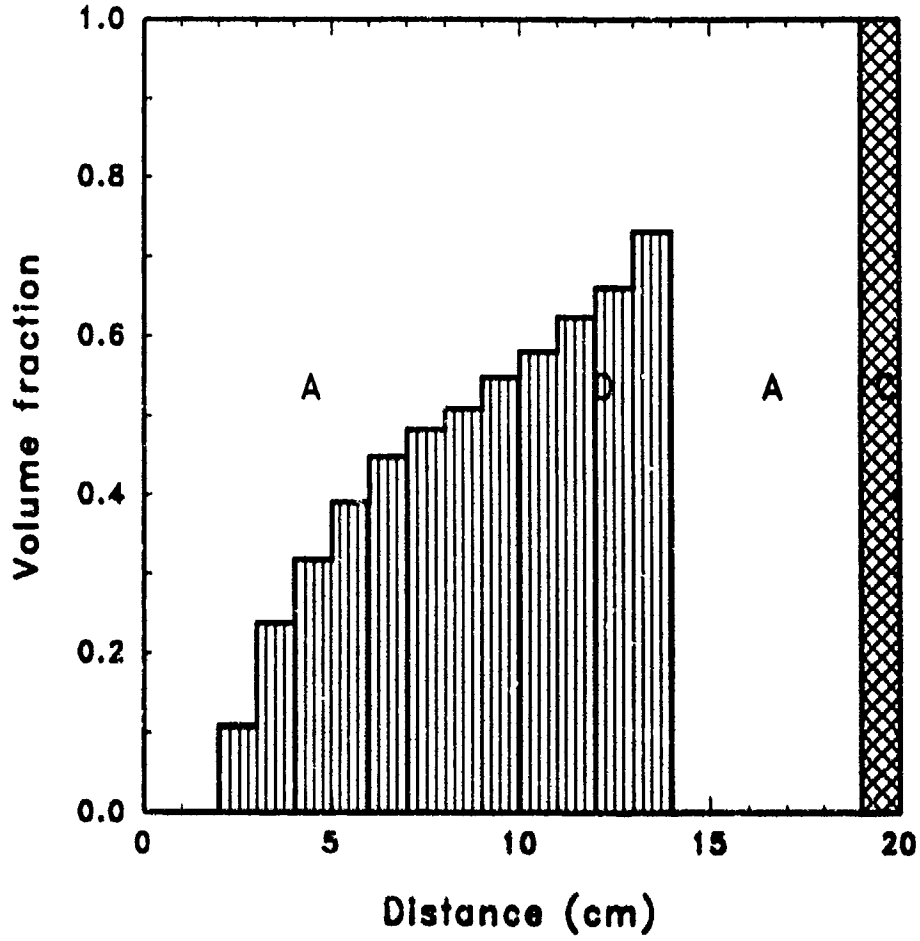


Figure 3 **Optimal composition of a 3-constituent detector shield as obtained with SWAN.**

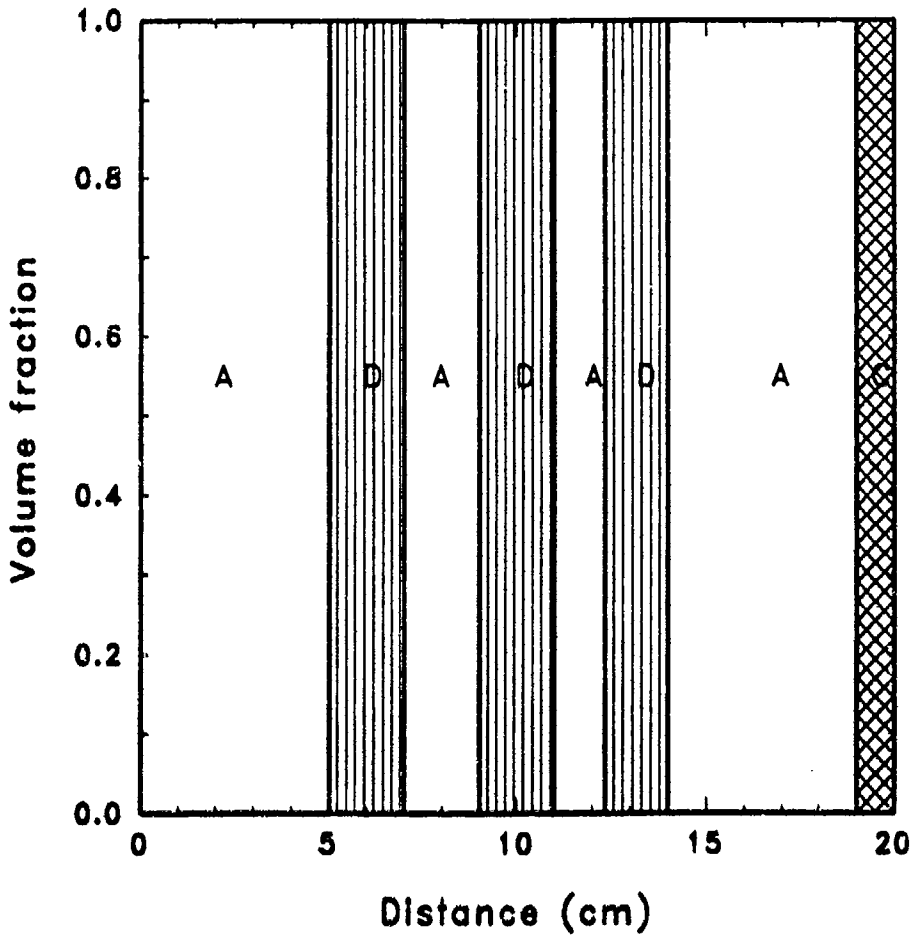


Figure 4 **A practical 3-constituent detector shield design which closely approximates the performance of the shield of Figure 3.**

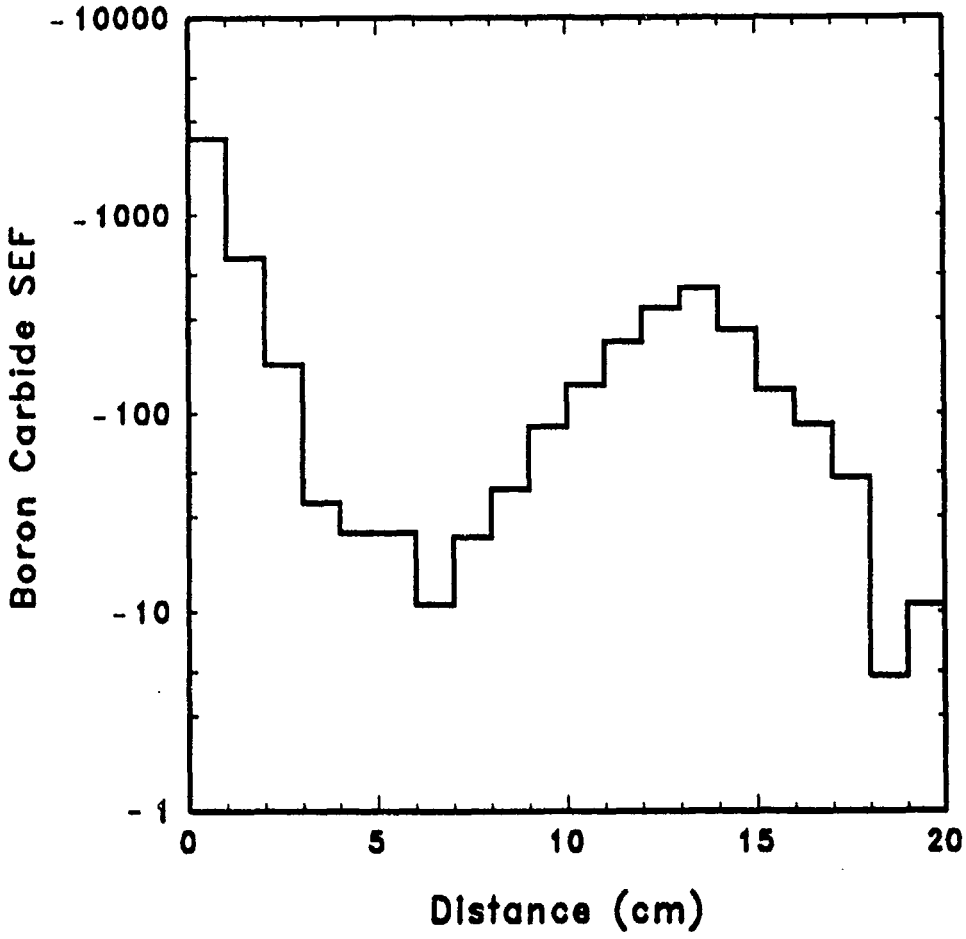


Figure 5 **The effectiveness function for substituting B_4C for constituent A in the optimal shield of Figure 3.**

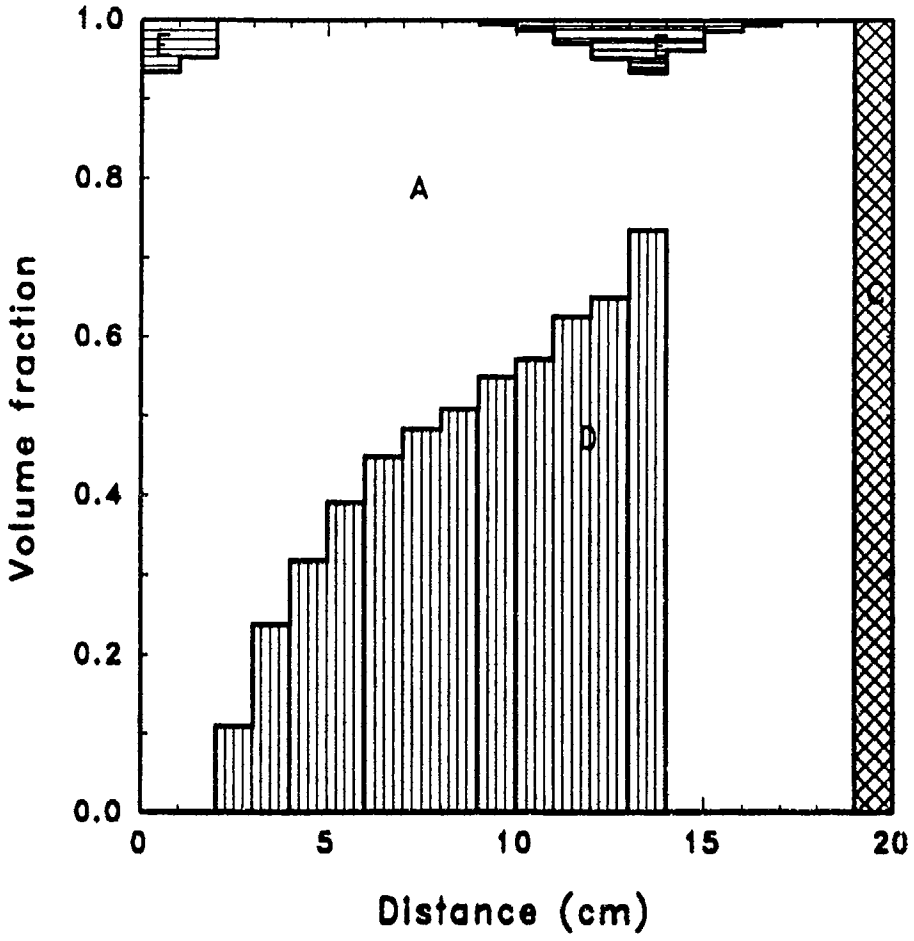


Figure 6 **Optimal composition of a 4-constituent detector shield as identified with SWAN. The added constituent (E) is B_4C featuring natural boron.**

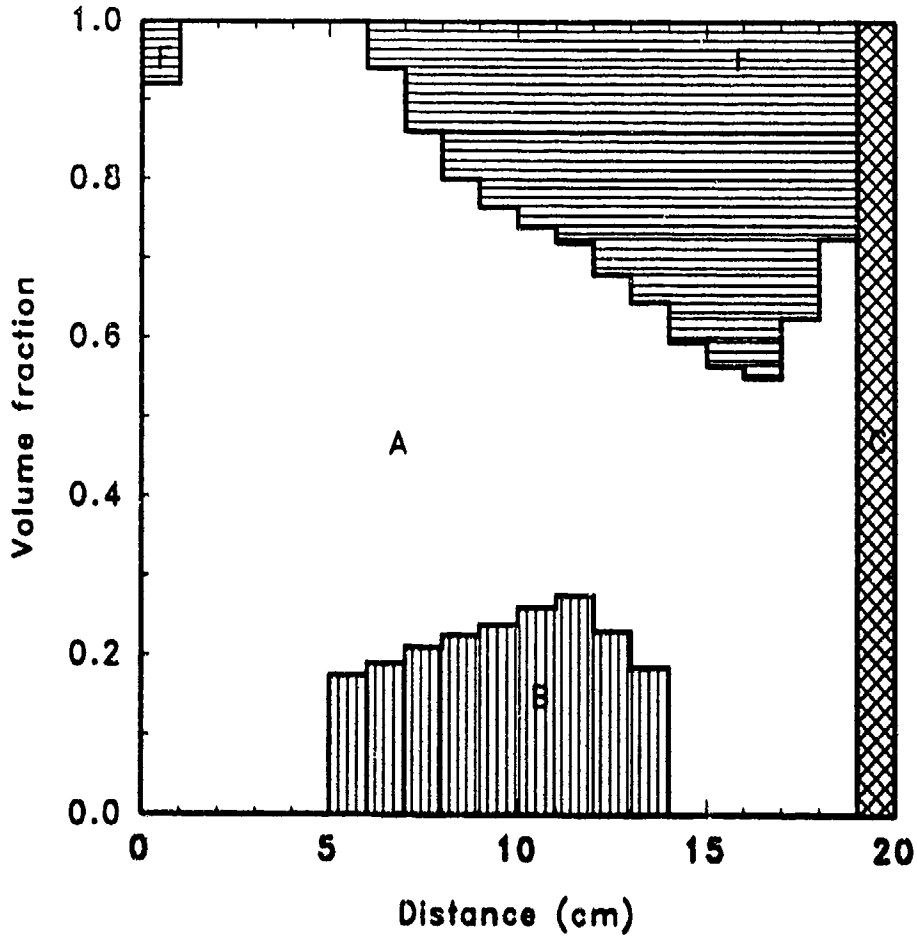


Figure 7 **Optimal composition of a 4-constituent detector shield as identified with SWAN. The added constituent (F) is $^{10}B_4C$.**

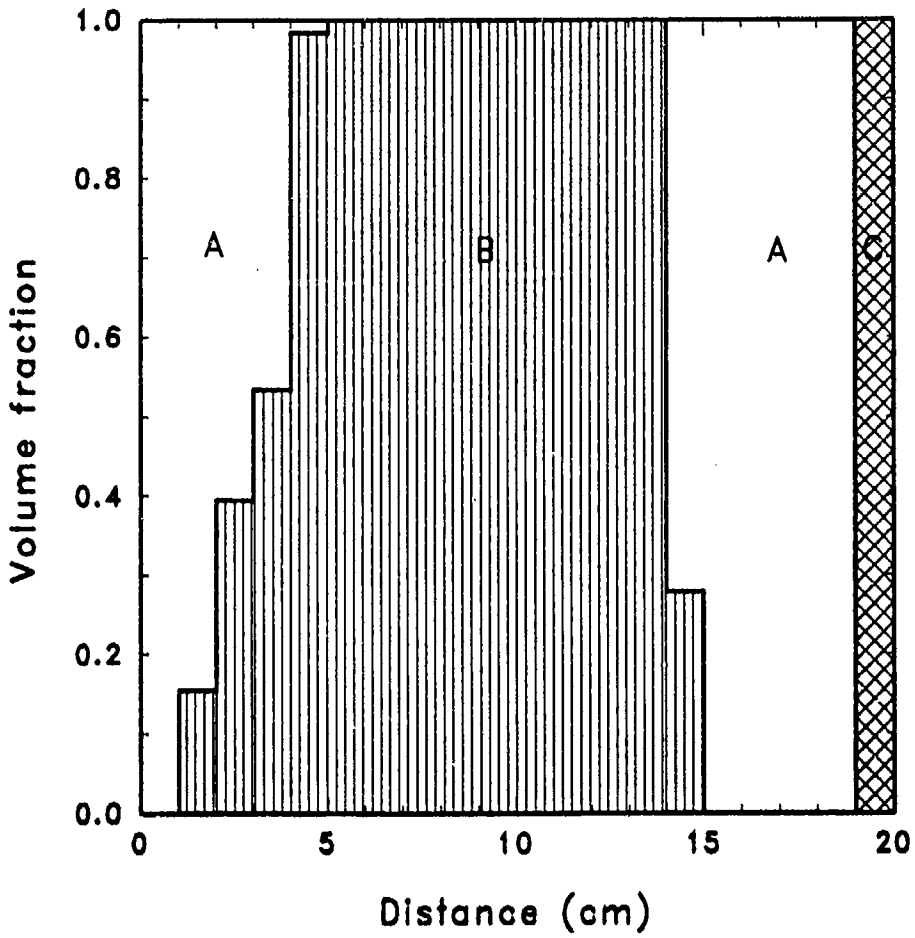


Figure 8 **Optimal composition of a 3-constituent detector shield featuring a novel composite material (B), as identified with SWAN.**

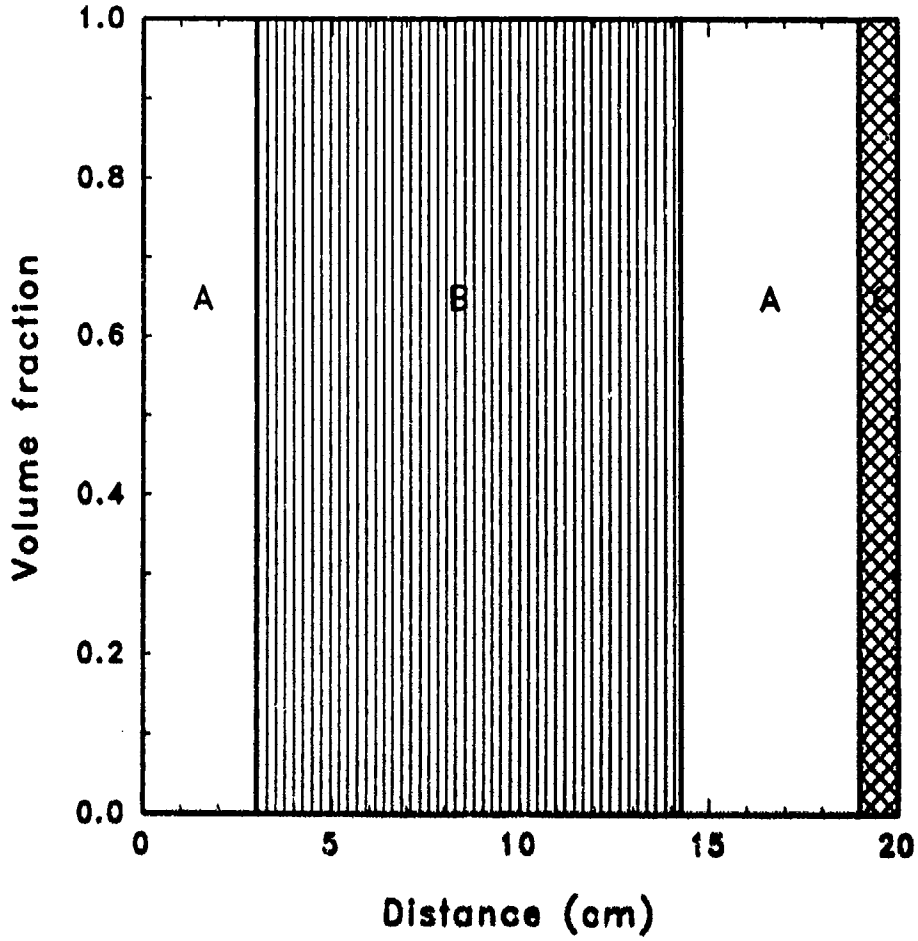


Figure 9 **A Practical 3-constituent detector shield design which closely approximates the performance of the shield of Figure 8.**

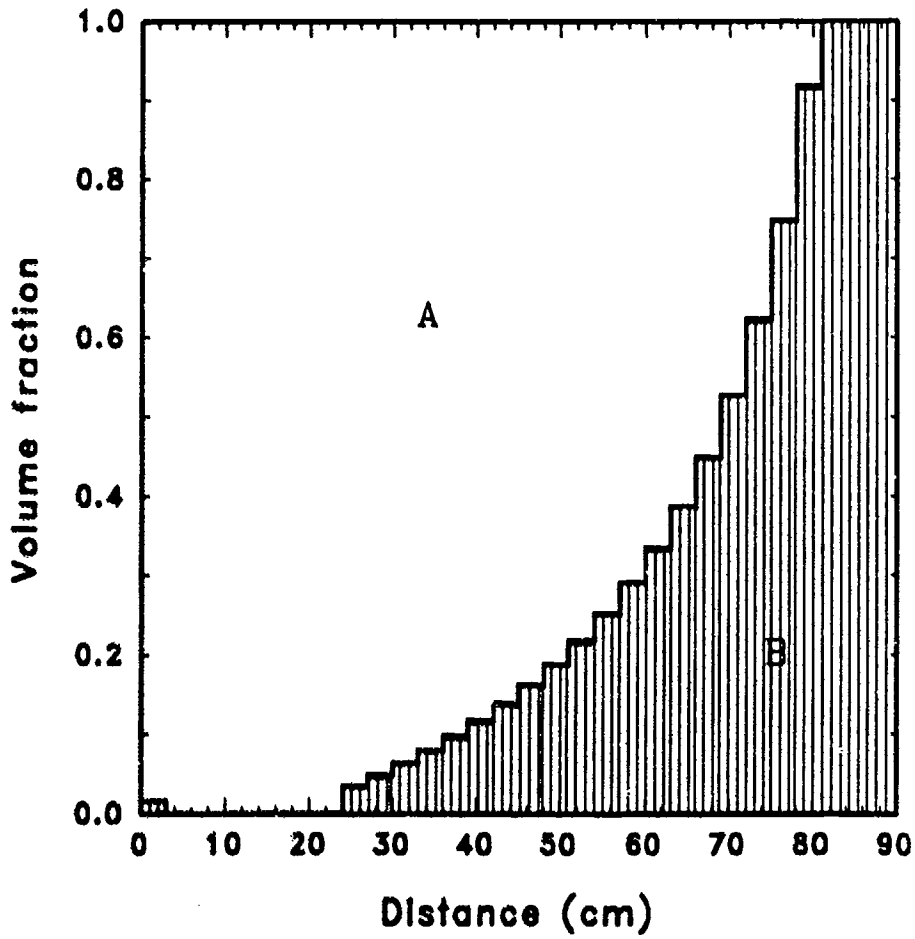


Figure 10 **Optimal composition of a collimator made of iron (A) and polyethylene (B) as calculated with SWAN when the FOM is the total neutron flux in the detector region. Following the shield is a 1.5cm B_4C layer.**

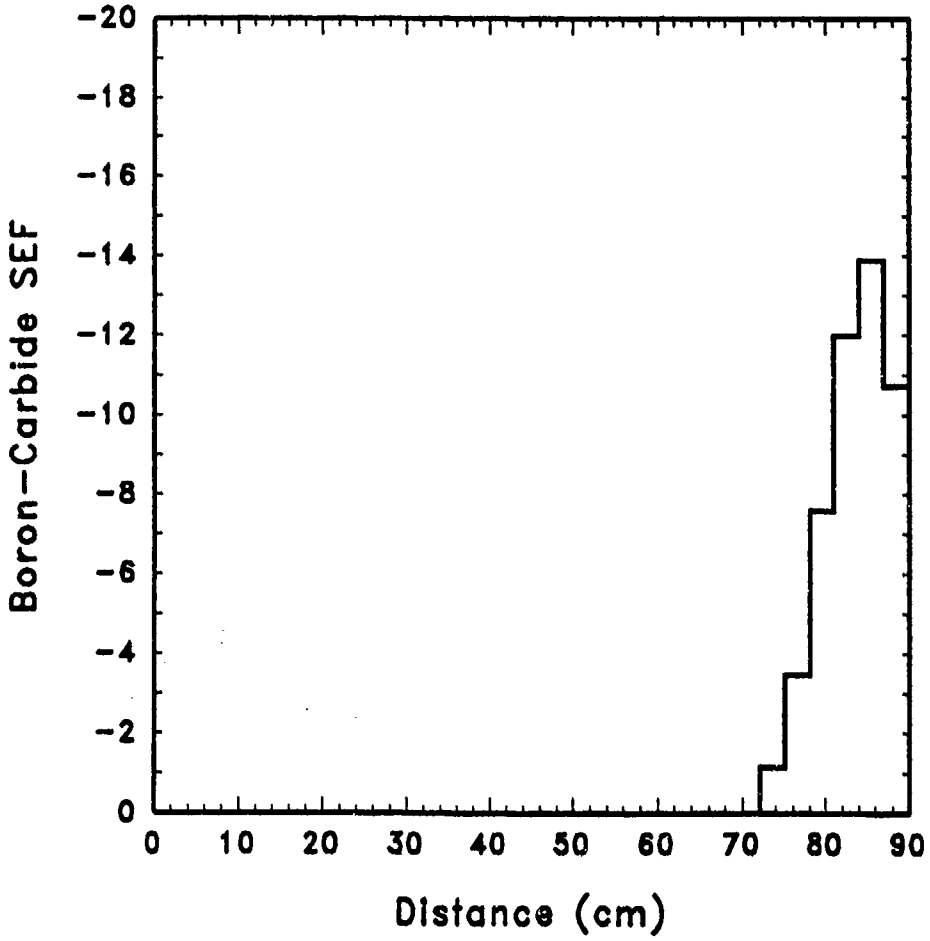


Figure 11 **The effectiveness function for the substitution of B_4C for iron in the shield of Figure 10.**

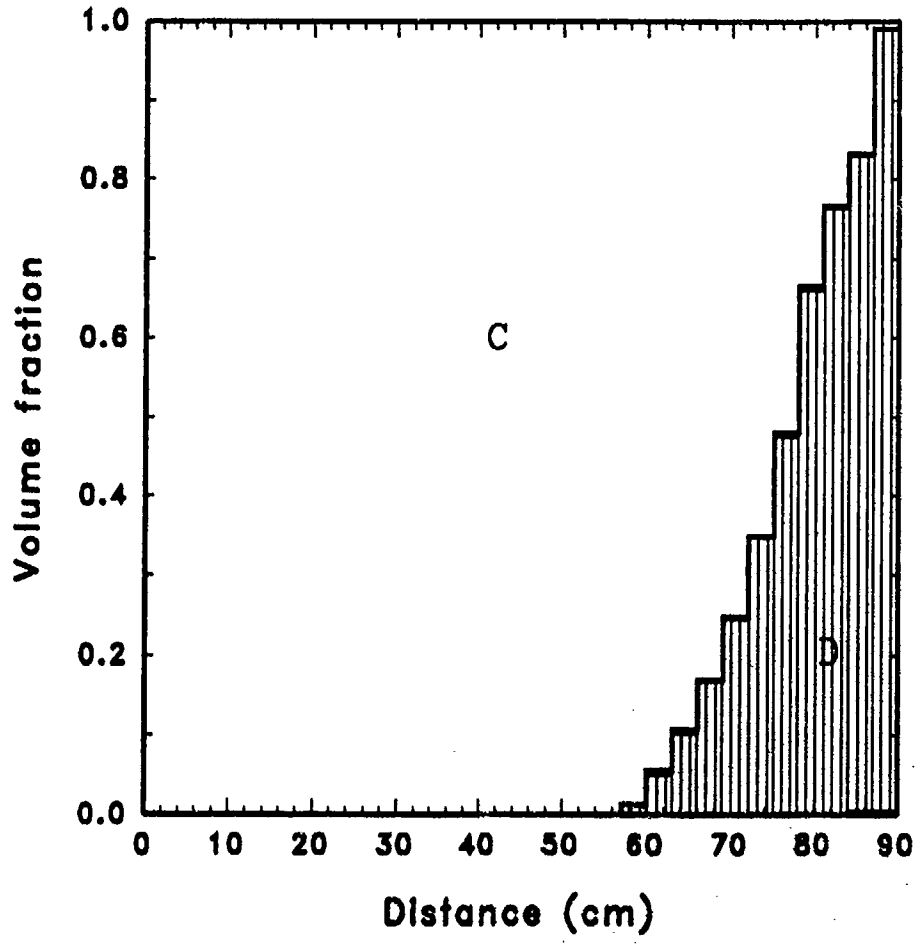


Figure 12 **Optimal composition of a collimator made of effective constituents identified by SWAN when the FOM is the total neutron flux in the detector region. Following the shield is a 1.5cm B_4C layer.**

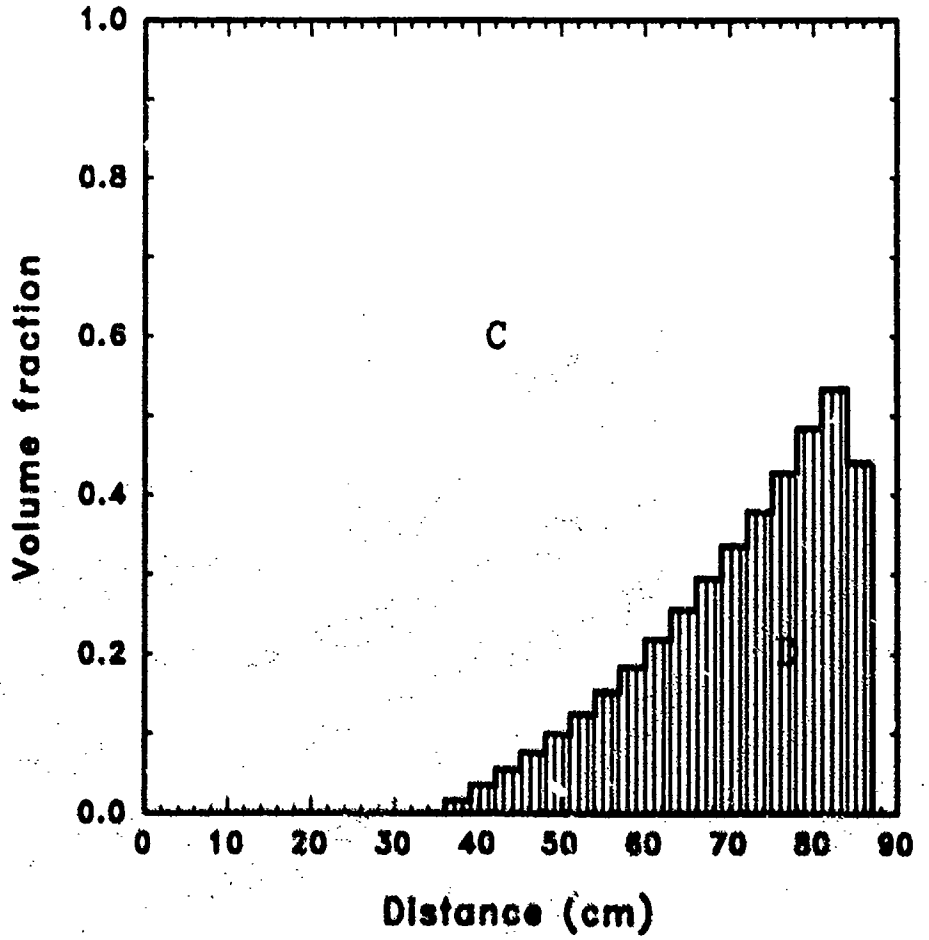


Figure 13 Optimal composition of a collimator made of effective constituents identified by SWAN when the FOM is the total neutron and photon flux in the detector region. Following the shield is a 1.5cm B_4C layer.

ASSESSING THE OPERATIONAL IMPACTS OF CHECKED LUGGAGE SCREENING

Steve Wolff
Imatron Industrial Products, Inc.
373 Vintage Park Drive
Suite D
Foster City, California 94404

1. INTRODUCTION

Several technologies are currently under development to more reliably detect explosives and speed up the inspection of checked luggage. However, the operational effects and benefits of equipment selection and deployment are still under debate.

The computational model described in this paper provides insights into security operations by analyzing the entire passenger luggage security screening process. In this way it is possible to determine parameters that will be important in selecting technologies and configurations to improve security while minimizing operational impact. Additional work that links the cost (both in terms of equipment investment and on-going operational costs) of security measures is under way but is not discussed here.

This paper presents the theory behind the computational model, briefly discusses the data used and presents two examples to illustrate how the model can evaluate the impact of different security strategies and novel scanning technologies.

2. THEORY OF COMPUTATIONAL MODEL OPERATION

There are two distinct parts to evaluating a security process.

- Evaluation of the maximum baggage processing rate for the security configuration itself with no emphasis given to the rate of arrival of luggage at the security area;
- Assessment of the ability of a given security process to handle the actual baggage arrival rates, determined from the airline departure times, aircraft size, load factors and the baggage arrival profile.

For ease of use, we implemented the model on Excel 3.0 which can be run on either 386-PC or Macintosh® personal computers.

3. QUEUING MODEL TO DETERMINE MAXIMUM BAG PROCESSING RATE OF SECURITY PROCESS

The most useful operational parameter to determine the efficiency of a security process is the baggage processing rate (BPR). This is the rate at which luggage moves through the entire screening process, including:

- Passenger interview;
- Baggage scanning;
- Secondary screening (e.g., hand search);
- Check-in/ passport check;
- Any other special measures in place.

Note that the BPR is not the time required to scan luggage based on scanner belt speed. This is a small part of the overall security process. Passenger interviews, secondary screening and check-in are events that typically take several minutes per bag and may limit the BPR.

Figure 1 shows a block diagram of a typical security screening process located at the check-in counter. This method is used by many U.S. carriers for international flights. Because of the time required to process passengers, this four stage process currently requires a two hour advanced check-in for international passengers.

This process can be described mathematically as follows.

3.1 Interviewing

Interviewing is usually the first step in the security process. Usually, there are several interview stations. The average time taken per passenger processed through the interview stage is:

$$t_1/N_1$$

where:
t_1 = Time required to interview one passenger at each station
N_1 = Number of interview stations

3.2 Primary Screening

For primary screening, if Nb is the average number of bags carried by each passenger, then the mean time taken per bag is:

$$\langle t_{bs} \rangle = \frac{Nb.t_1}{N_1}$$

Similarly, the mean time taken per bag for the scanning process is:

$$\langle t_{bs} \rangle = \frac{1}{Q_s N_2}$$

where:
Q_s = Scanning speed (average # of bags/ hour)
N_2 = Number of scanners in operation.

3.3 Secondary Screening

Secondary screening occurs on a fraction, x, of the total number of bags scanned. The parameter, x, can be the alarm rate from the scanner or the random search fraction, depending on the method implemented by the airline. The methods used to resolve threats also vary from airline to airline and sometimes from flight to flight. Regardless, the mean time taken per bag for secondary screening is:

$$\langle t_v \rangle = \frac{x.t_3}{N_3}$$

where:
t_3 = Time required to clear one bag
N_3 = Number of secondary screening stations

3.4 Passenger Check-in

Passenger check-in is the final stage in this process. The mean time per passenger through the check-in process is:

$$\frac{t_4}{N_4}$$

where:
t_4 = Time required to check-in one passenger at one station
N_4 = Number of check in stations

The mean time per suitcase through the check-in process is:

$$\langle t_{ck} \rangle = \frac{N_b.t_4}{N_4}$$

The baggage processing rate through the entire security process is related to each of these individual mean processing times by the following relationship:

$$BPR = \frac{1}{\langle t_{bs} \rangle + \langle t_{bs} \rangle + \langle t_v \rangle + \langle t_{ck} \rangle}$$

The values of N_1, Q_s and x depend on the specific application being analyzed. Once basic data have been collected for these variables, this relationship allows the maximum throughput of bags through different security processes to be determined easily. We discuss the data collection methods and results later in this paper.

4. OPERATIONAL IMPACT OF A SECURITY PROCESS

In practice, baggage arriving at the airport is closely tied to flight departure times. The functional form of this baggage arrival distribution for a single flight has previously been determined by least squares fit to observed passenger arrivals for departing flights [1]:

$$F_p = \frac{a}{a + e^{b t_d \cdot t}}$$

where F_p is the cumulative percent of bags that have arrived by time, t, for a flight with a departing time, t_d. Parameters a and b are determined from least squares fit to actual arrival data. We found that the values for these parameters determined by the authors,

a = 515,
b = 0.108,

were inconsistent with the more recent two hour advanced check-in requirements for international flights. We obtained new values based on more recent data supplied by Pan Am. Figure 2 compares the predicted arrival profile with the final form of this distribution (a = 214, b = 0.0596).

The computational model uses the baggage arrival function to predict the number of bags arriving within a time interval (ten minutes) for all flights in a data-set. The data-set usually consists of one airline at a given airport. However, if several airlines are sharing one security station, all the flights from each airline can be included in the data-set to determine the overall arrival profile of luggage at the security station. The model presents the results graphically and in tabular form.

5. ACCUMULATION OF DATA USED IN THE MODEL

Data for these models come from several sources:

- Measurements and observations made during airport visits;
- Airline schedule data;
- Operational data supplied by airlines.

5.1 Airport Visits

Security configurations and times required for each stage of the screening process were obtained from visits to several airports worldwide. We collected data on personnel allocations, types of equipment, and procedures used for all phases of the screening process. We also measured the time taken to pass through each stage of security. Table 1 shows the results, averaged over all the data collected. The model allows any of the separameters to be easily changed to reflect a specific security process.

An average load factor of 0.68 was assumed for each flight and the aircraft baggage capacity was obtained from a table supplied by the Reed Travel Group [2].

5.2 Airline Schedule Data

Worldwide air traffic data were supplied by the Reed Travel Group in ASCII form, directly readable by Excel 3.0. Data were stored initially by airport code. We distilled the individual airlined at a from the airport data-set. The flow diagram shown in Figure 3 outlines the entire analysis process.

6. RESULTS OF ANALYSIS

One of the specifications that has been important in developing requirements For explosives detection systems (EDS) is the baggage capacity (belt speed). Specifications of between 600 and 1000 bags/hour have been targets for many manufacturers. We have studied the effect of varying baggage capacity for both primary and secondary screeners to determine the effects on the overall baggage processing rate (BPR).

Case Study 1: Effect of an EDS's Baggage Capacity (Primary Scan Rate) on BPR

Figure 4 shows the effect of varying the baggage capacity of the primary screener only. Secondary screening was set at 6 minutes/bag. This is equivalent to a moderate (but not exhaustive) hand search. The graph clearly shows the sensitivity of the BPR to the secondary screening diversion rate.

Case Study 2: Effect of Changes in Secondary Screening Time on BPR

Figure 5 shows the effect of variations in the secondary scan (or threat resolution) time have on overall BPR. A constant primary scanning speed of 600 bags per hour was used. These data show that a considerable reduction in luggage processing occurs even if only a small fraction of luggage is diverted to secondary screening if this process takes more than one minute per bag.

Case Study 3: Baggage Processing Rate Dependence on Number of Check-in and Security Stations

The check-in process severely limits the ability to maintain a high BPR. International check-in currently takes 5.5 minutes per travelling party (which contain, on average, approximately two people per party). As a result, one security station can be shared by several check-in counters. Figure 6 shows the variation of BPR as a function of number of check-in counters and the primary screening rate. Secondary screening was set at 6 min/bag on 5% of the bags.

Case Study 4: Evaluation of a Security Operation: United Airlines at London Heathrow Airport, Terminal 3

Figure 7 shows the layout of United Airlines' checked luggage security at London Heathrow Airport in operation during May 1991. This information can be distilled down into data used by the model, shown in Tables 2 and 3. Assumptions were made regarding aircraft load factors and no attempt was made to determine the fraction of interline passengers; for the purposes of the case study we assumed that all passengers on each flight went through security at LHR. The output from the model (Figure 6) shows the baggage arrival profile throughout the day and the predicted maximum baggage processing rate of the existing security system based on the input parameters.

With these parameters and departure times, the model predicts the ability of the security process to handle the arrival rate of passengers at check-in. Figure 8 shows the baggage arrival profile and the security system's capacity based on the existing configuration at the check-in counter.

Whenever the baggage arrival rate exceeds the BPR, a queue develops. Only when the baggage arrival rate drops below the baggage processing rate (from 10 am until noon) will the queue diminish. The number of passengers in queue at any time can be predicted by integrating the difference between the BPR and the baggage arrival rate at any point in time. Figure 9 shows the estimated passenger line size for the above scenario.

7. CONCLUSIONS

These results yield several important conclusions regarding baggage processing rates through airport security.

Slow secondary scan rates (greater than 1.5 minutes per bag) significantly reduce the overall BPR for high throughput primary scanners; even for less than 2% diversions.

The only ways currently to improve BPR are to install more secondary screening stations or develop faster methods for secondary screening.

Aside from space and personnel considerations, the ability of an EDS to perform both primary and rapid secondary screening functions is more important than operating the primary screener at a higher belt speed.

Baggage processing rates are reduced significantly by check-in (and interview) processes. This can be improved only by increasing the number of check-in stations or speeding up this phase of the process.

In the UA-LHR scenario, the model clearly demonstrates the inability of the security process to keep up with the flow of departing passengers. From the data shown, the security process is continuously overloaded between 6:30 am and 3:00 pm.

8. RECOMMENDATIONS FOR FUTURE WORK

There are several additional directions that this work will take. In addition to streamlining the analysis, we are investigating ways to predict the operational cost of the security process in place at any given terminal. This will allow the security process to be analyzed in terms of operational cost for different security procedures and equipment.

These tools will allow analysts to understand the impact of different security configurations, EDS performance, and deployment of security personnel both in terms of operational impact and cost.

ACKNOWLEDGEMENTS

The author would like to thank Dr. Fred Roder of Imatron Federal Systems, Inc. for his guidance and encouragement during this paper's preparation. In addition, many thanks to Joel Blumenthal and the staff at Reed Travel Group for supplying the critical data for parts of this study.

REFERENCES

1. Robuste, F., "Analysis of Baggage Handling Operations at Airports", PhD Dissertation, August 1988, Inst. of Transportation Studies, University of California, Berkeley.

2. Reed Travel Group, "Summarized Airport Report" and supplementary data.

Table 1: Range of Values Used in Computational Model

Parameter	Description	<Value>
t_1	Interview time	1.3 min/person
t_3	Secondary screening time	6 - 10 min/bag
t_4	Check-in time	2.7 min/person
N_b	# bags/ passenger	1.6 (check-in) 3 (check-in + carry on)

Table 2: Data from United Airlines' LHR Security Process Used in the Model

Security Process rate Scenario:		LHR United Airlines	
# X-ray Scanners Operating	3	Time-profiling (min/per)	1.3
# Secondary screening Stations	3	Time-Check-in (min/per)	2.7
# Interview Stations	6		
# Check-in Stations	4		
# bags/ passenger	3		
Primary Scan Rate (bags/hr)	600		

Table 3: United Airlines Departure Flight Schedule from LHR

Flight #	Aircraft Code	Load Factor	Departure Time
901	763	0.68	9:55
903	74L	0.68	13:10
906	72A	0.68	10:25
918	72A	0.68	9:30
919	747	0.68	11:30
934	72A	0.68	7:55
935	742	0.68	13:30
907	74L	0.68	11:10
900	72A	0.68	8:25
915	72A	0.68	8:40
920	72A	0.68	13:10
1930	72A	0.68	10:25
1931	742	0.68	14:15

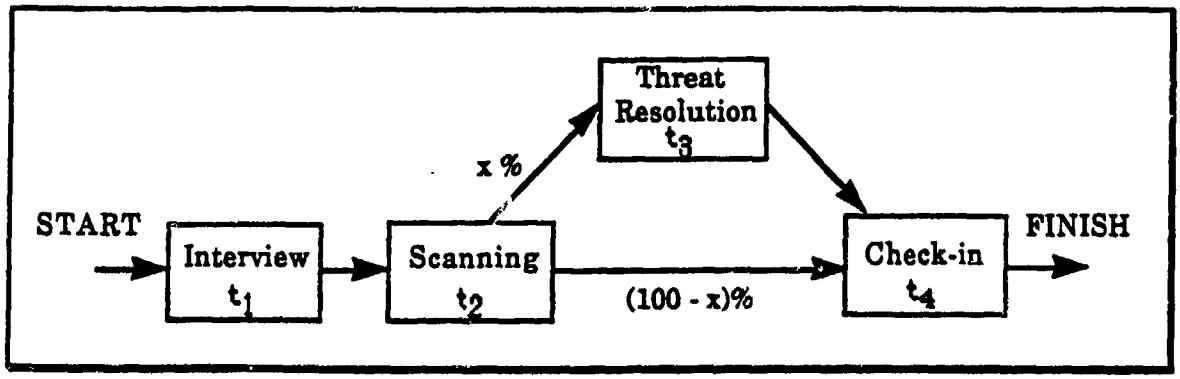


Figure 1: Schematic of a Typical Security Screening Process

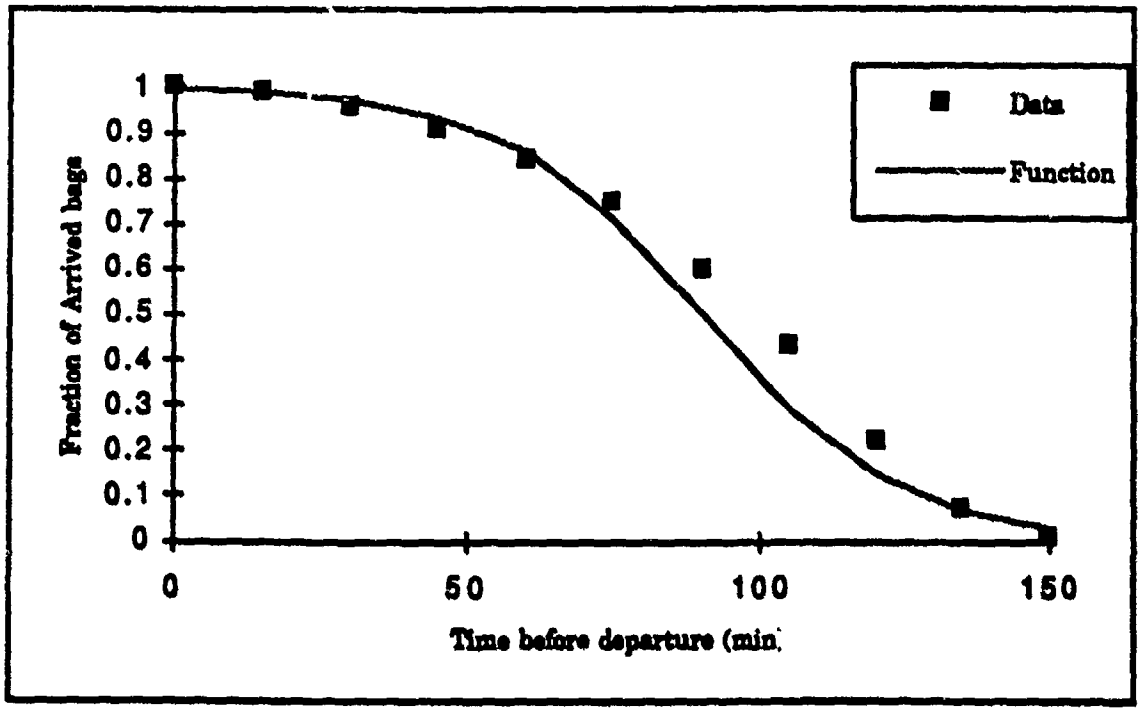


Figure 2: Comparison of Calibrated Baggage Arrival Function and Actual Arrival Data

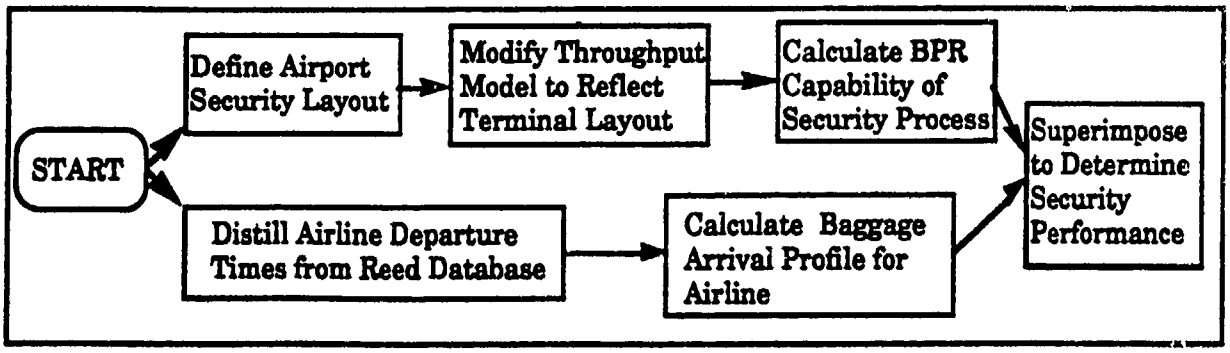


Figure 3: Flow Diagram of Analysis Process

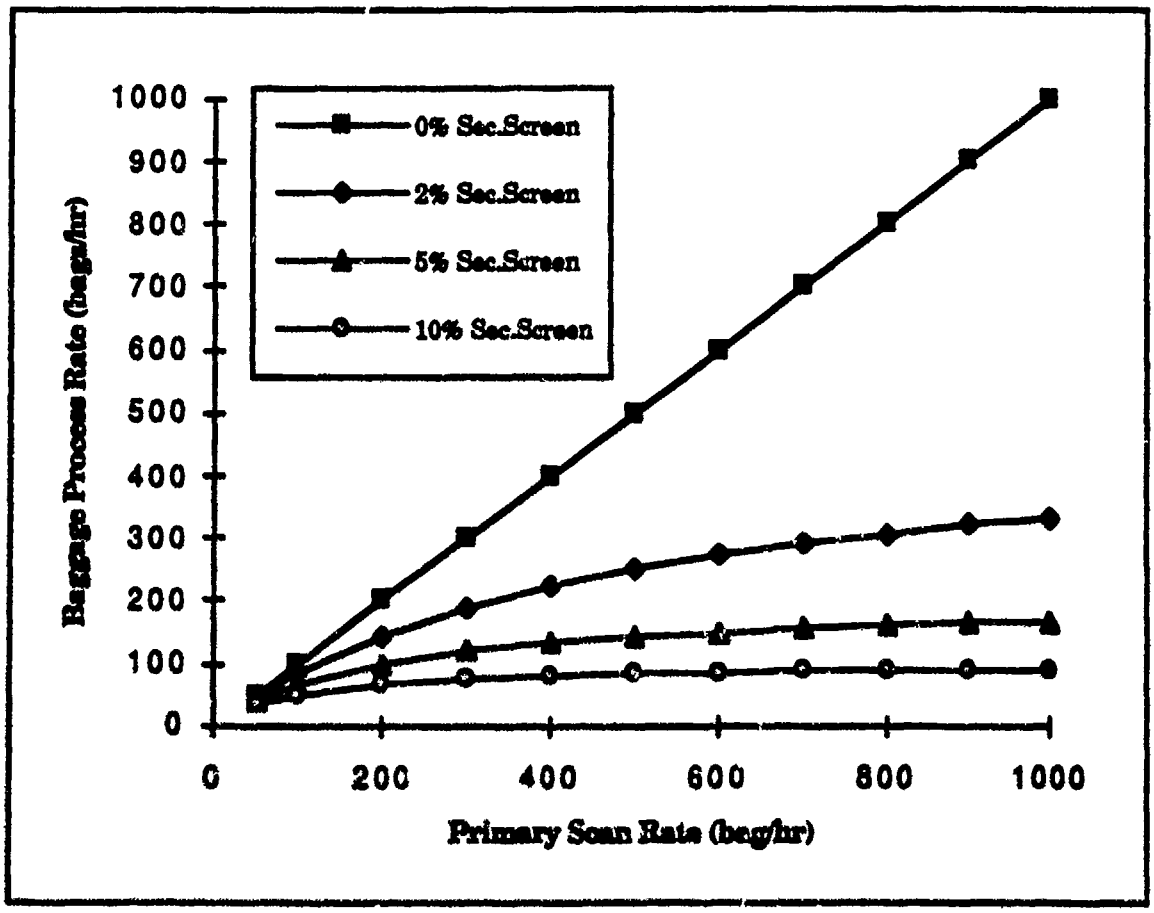


Figure 4: Effect of Primary Scan Rate on Overall Baggage Processing Rate

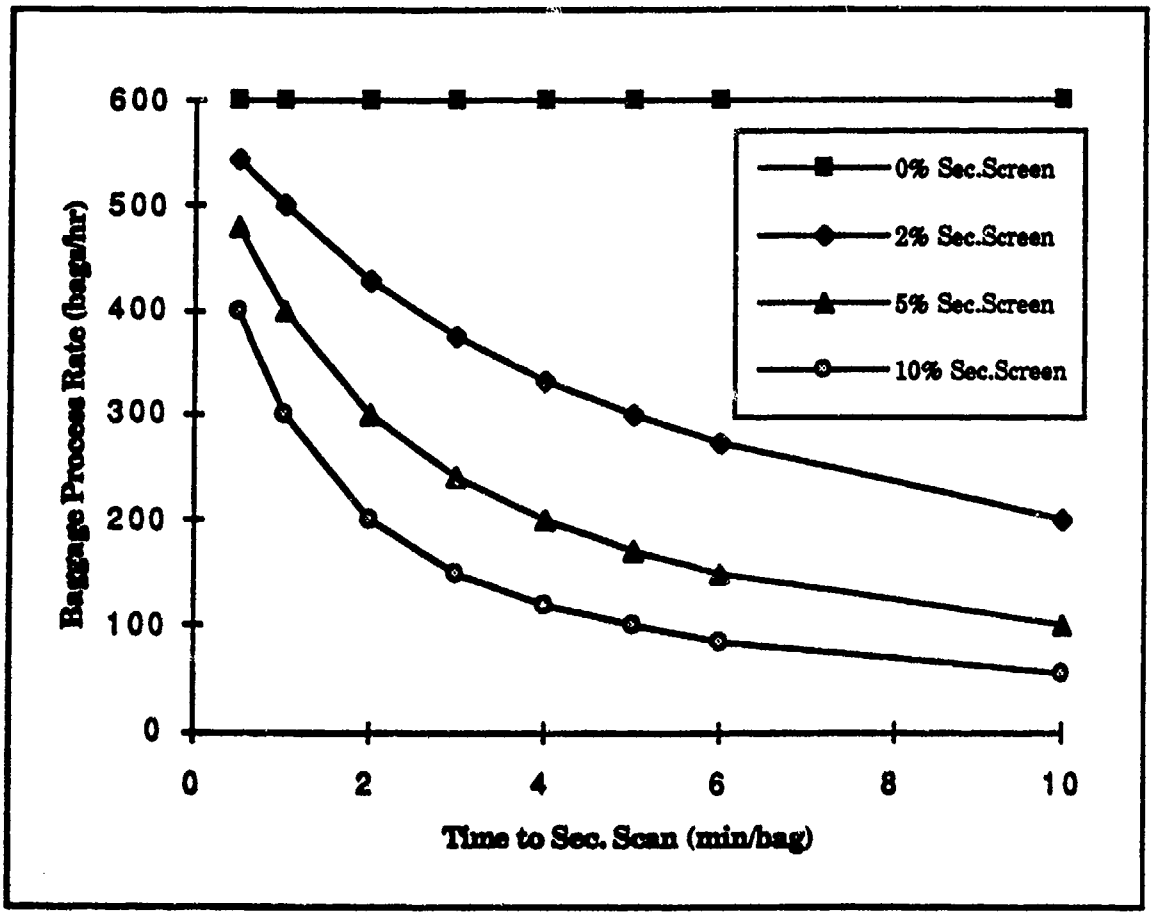


Figure 5: Effect of Secondary Scan Time on Overall Baggage Processing Rate

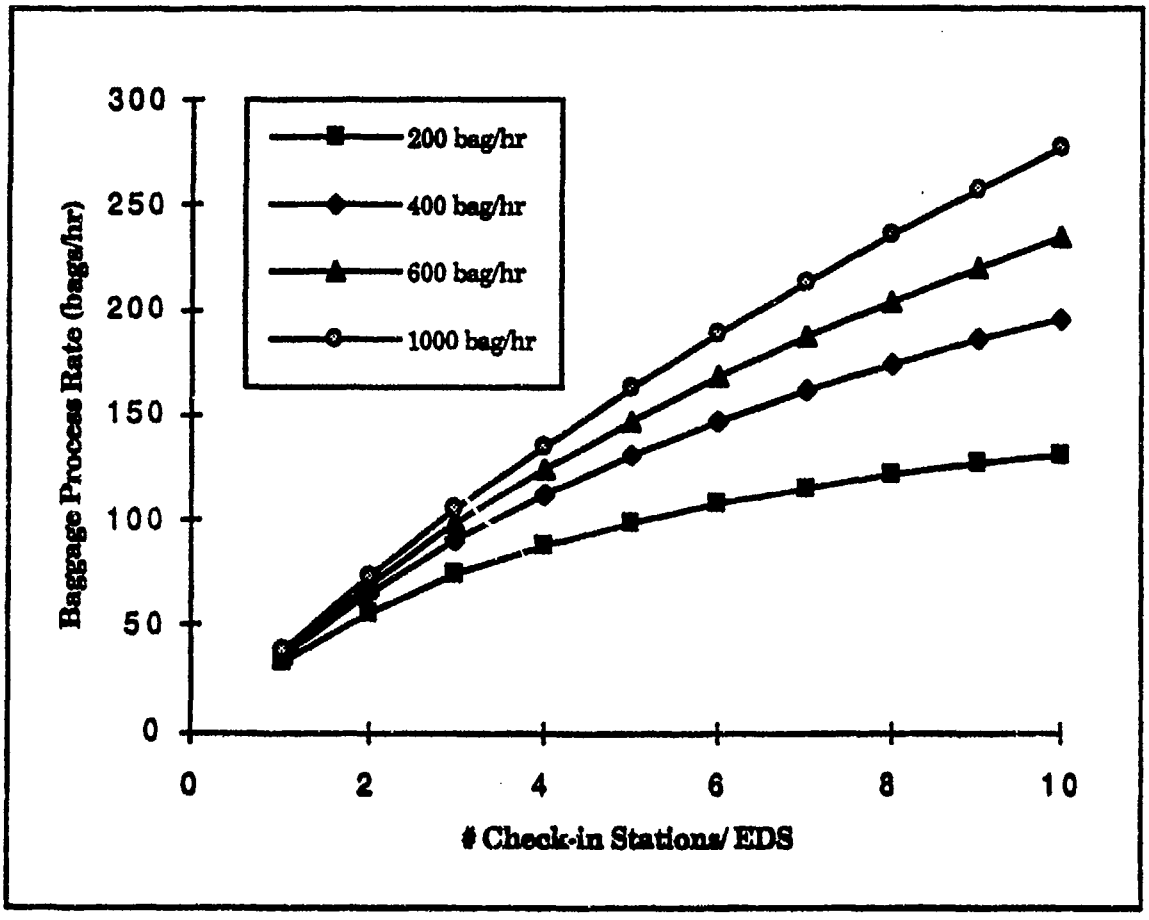


Figure 6: Variation of Overall Baggage Processing Rate with Number of Check-in Counters

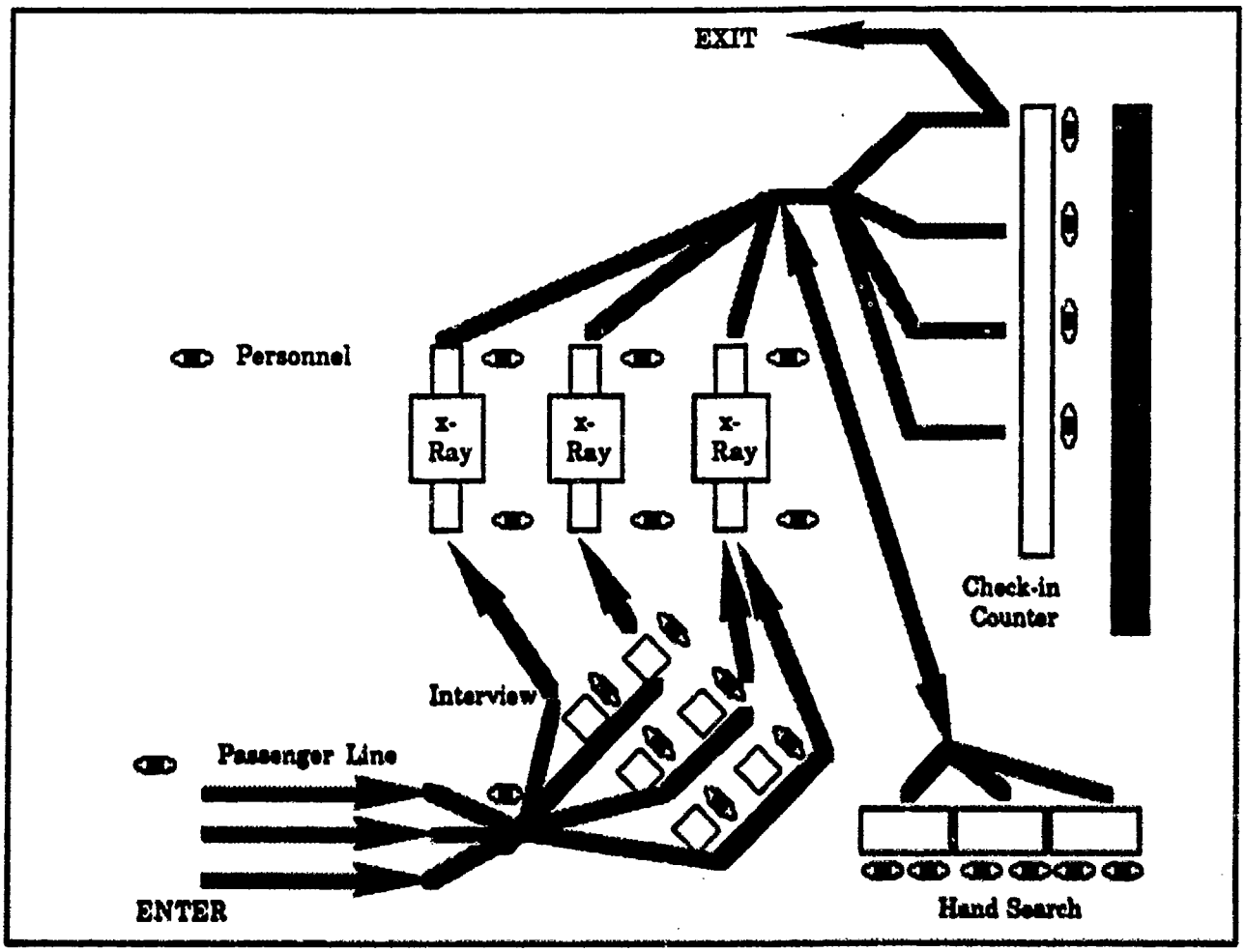


Figure 7: Operational Layout of United Airlines Security at LHR during May 1991

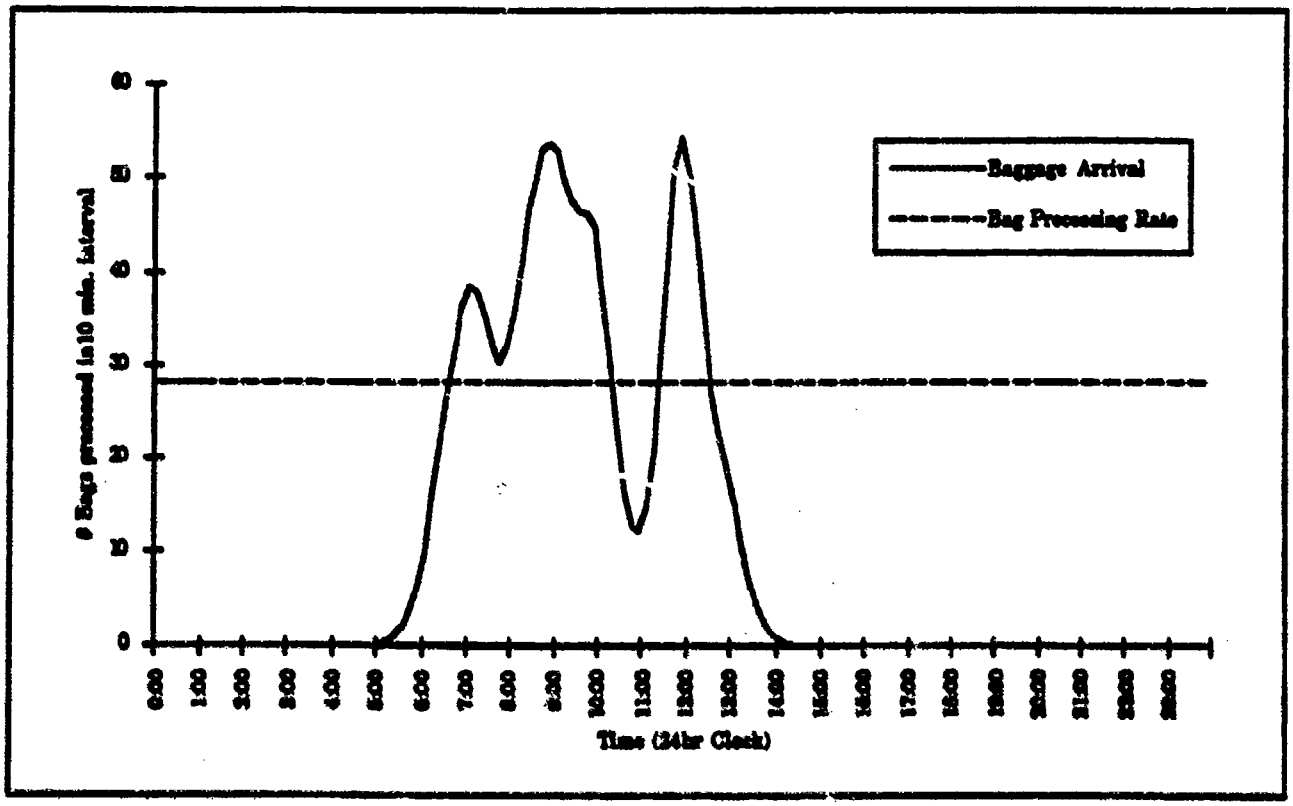


Figure 8: Baggage Arrival Profile and BPR for United Airlines at LHR

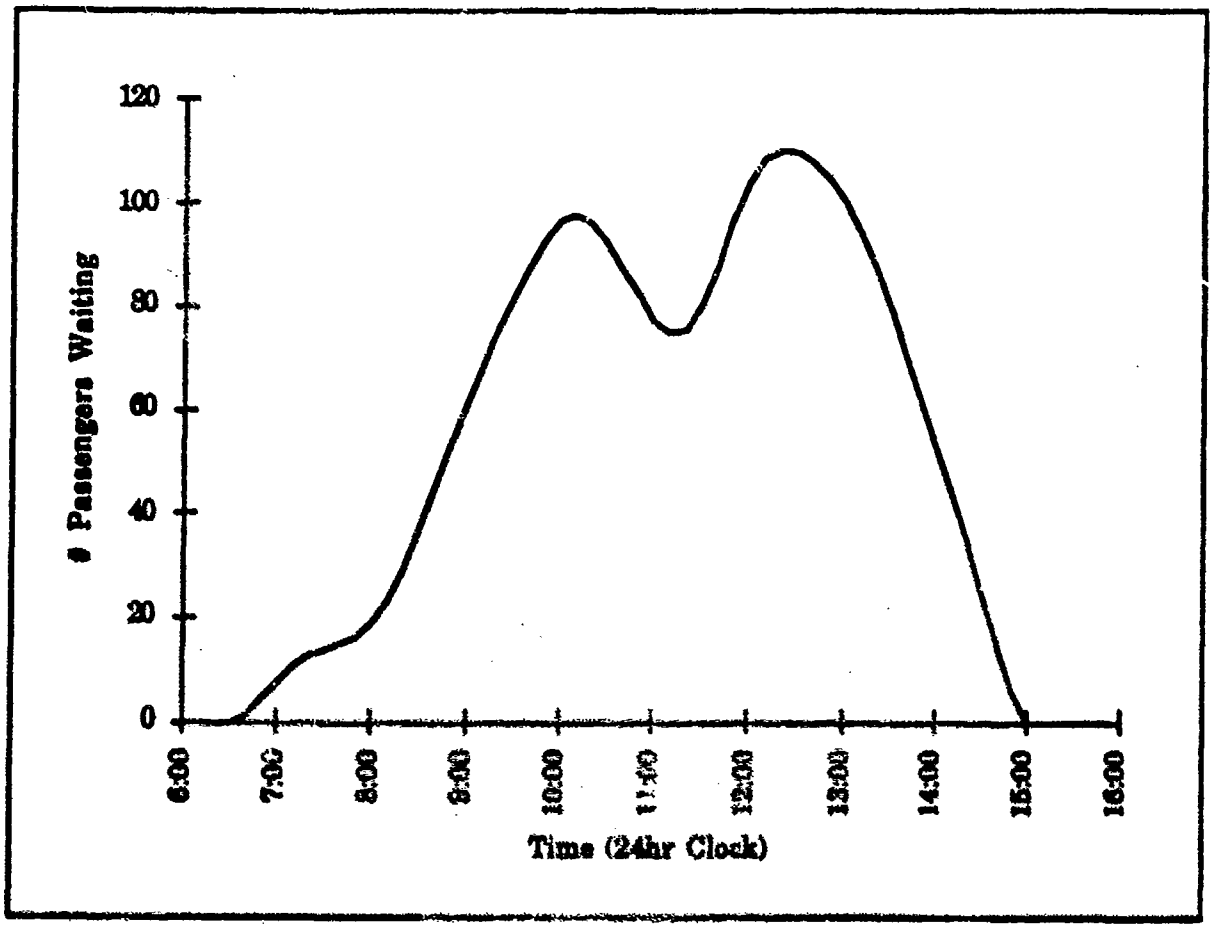


Figure 9: Predicted Passenger Line Length at Security/ Check-in: United Airlines, LHR

FAST NUCLEAR SPECTROSCOPY FOR EXPLOSIVE DETECTION SYSTEMS

P. Ryge, R. Benetti, A. Patel, and E. Chou
Science Applications International Corporation (SAIC)
Santa Clara, California

1. INTRODUCTION

The requirements for rapid and precise analysis in nuclear-based explosive detection systems pose special spectroscopy problems. Sufficient data must be acquired so that adequately low statistical errors are obtained in a sufficiently short time to meet inspection throughput requirements. In practice, this generally means that these systems employ many detectors, each having very high signal rates. Complex signal processing in each of many channels requires careful design attention to reliability considerations so that inspection system availability demands can be met.

In the Thermal Neutron Analysis (TNA) system, the primary information is a very low rate, high energy gamma ray (10.8 MeV) combined with a high rate at lower energies, producing a pile-up background at the energy of interest. This background is one of the principal factors limiting system performance. Several authors have recognized this problem of pile-up in prompt capture gamma ray spectroscopy using NaI(Tl) detectors [1,2,3,4].

Because the relative number of counts of interest is so small, it is critical that in the signal processing:

- Very few valid pulses are lost
- Background is minimized.

A valid pulse can be lost if it arrives while the acquisition system is busy ("dead") processing a previous pulse, preventing the following pulse from being observed. To minimize this problem, a fast gated system can be used to select relevant pulses on a fast time scale, so that the slower parts of the electronics are not tied up. This reduces the event rate for the fully processed pulses and as a result, system dead time losses are minimized.

Interfering background can come from the high energy tail of a peak at slightly lower energy or from pile-up. The former is minimized by assuring that good energy resolution is maintained through the signal processing. Pile-up is the more important effect in the TNA application, and it is mitigated by a two-pronged approach, pile-up suppression and pile-up rejection.

To overcome these problems, a high counting rate signal processor utilizing time variant filtering was developed [7, some of the following is from this reference]. Since the more common counting mode pile-up rejector did not improve the pile-up characteristics of the system significantly, a more effective pile-up rejector based on pulse length inspection was used.

2. PRINCIPLES OF OPERATION

The amplifier is composed of a time-invariant delay-line differentiator and time-variant gated integrator. A trapezoidal weighting function is realized by convolution of the roughly gaussian pulse shape with the rectangular function of the gated integrator [5,6]. This serves to gate and filter the signal, and produces an output compatible with the ADC following. A separate logic channel generates the gating signal.

The photomultiplier anode signal pulse is passively shortened to reduce (suppress) the pile-up rate which is proportional to the pulse width. The roughly exponential light pulses from the NaI(Tl) detector have a duration at the baseline of approximately one microsecond. Due to the non-exponential decay components of the NaI(Tl) signal, simple delay line clipping is not sufficient and a residual tail occurs on the output pulse. This is removed by a single bridged T-filter. Fast recovery to the baseline of the shaped pulse is critical for proper function of the pile-up rejector.

Fig. 1a shows for a single gamma ray the signal directly from the detector and the shortened pulse following the filter. Fig. 1b demonstrates the pile-up suppression: two gamma rays separated in time by about 250 nanoseconds are not resolved directly from the detector but are nicely separated after being shortened.

Pile-up rejection is based on inspecting the signal level just before and after the pulse. Pile-up results

in the pulse being wider at the baseline, and, for such events, no gate signal to the gated integrator is produced.

Figure 2a, 2b, and 2c show the input signal from the detector and the gated integrator output signal for three cases:

- Single gamma ray,
- Two gamma rays separated sufficiently that the shortened version (internal to the ASP) of the first is not contaminated by the second and therefore not rejected. The second gamma ray is lost,
- Two gamma rays so close that they are both rejected -- no output occurs.

Two energy thresholds at different levels are used. All gamma rays above the higher level are of interest, and their rate is low. The lower threshold triggers on intermediate energy gamma rays; a fraction 1/N of these produce a gate signal, where N is a jumper selectable multiple of two. These gamma rays are used for secondary corrections and energy calibration, and their rate is much higher so that statistically adequate information can be obtained from the fraction. By thus reducing the output rate to the following multichannel analyzer, a higher system throughput is maintained.

Only the shaped pulses with amplitude above the energy threshold levels and free of pile-up are integrated by the gated integrator. The rise time of the output signal is determined by the width of the input gaussian function, and the width of the flat top is determined by the difference between the integrator gate width and the width of the gaussian function at its base.

3. FUNCTIONAL DESCRIPTION

The pulse processor block diagram is shown in Fig. 3. Basic pulse shaping is performed by the delay line differentiator and gated integrator. In addition, the processor contains a baseline inspector, pile-up rejector and a circuit to allow acquisition of a fraction of the spectrum at lower energies, as described above. The timing reference comes from a constant fraction discriminator circuit (CFD) on the delay line shortened signal. The output from the CFD is relatively walk free; the time walk is less then 1 ns for a range of input signal amplitudes of 1:100. The baseline discriminator inspects the signal level shortly before the start of the pulse to verify that any residue of another pulse is below a low threshold. The same baseline discriminator inspects the signal level after the pulse to verify that the signal level is below the baseline threshold, i.e., that the pulse has not been extended by the addition of a pile-up pulse.

The timing signal is combined with other logic signals in the control unit which generates signals for the gated integrator and the linear gate. Other inputs to the control unit come from the base-line inspector, pile-up rejector and counter-divider for reducing the processed low energy gamma ray rate by a factor 1/N.

If the above requirements are met, the pulse is accepted as not being piled up. The linear gate will be opened in the time interval $(0,T_i)$, and the signal integrated in the gated integrator during that time interval. The integrator holds the integrated amplitude for an extension time (T_e-T_i) to allow the ADC time to sample accurately. The integration time is approximately the same as the interval between the before- and after-pulse baseline inspection. The input linear gate cannot be opened again until the output pulse has been completed, preventing pile-up within the hold time of the integrated amplitude.

The determining parameters in the above pile-up detection that can be optimized are pulse shape and baseline inspector threshold level. The pulse shape determines the minimum time interval between pre-signal inspection and pulse as well as time interval from pulse to post-signal inspection. The first time interval is defined by signal rise time and the latter by signal baseline recovery. The baseline threshold level is set just above the noise level to detect the smallest signals.

A signal delay in the system is necessary because of the delay in the timing and inspection logic functions.

The pulse processor has been implemented using standard components: IC linear amplifiers, fast buffers and high speed comparators, tapped lumped constant delay lines, and 74S series IC's. Two channels of the pulse processor have been packaged into a single width NIM module, Fig. 4.

4. EXPERIMENTAL RESULTS

The pulse shortening by delay line clipping results in

loss of net signal, and, since the energy resolution is dominated by the electron statistics, the resolution becomes worse with the reductior of clipping time. A compromise must be made between resolution requirements and pile-up effects. The resolution of the system as a function of clipping time for different gamma ray energies was measured. Fig. 5 shows the relative deterioration of the resolution as a function of gamma ray energy and clipping time. The resolution deterioration due the pulse shortening becomes less important as the energy increases and other contributors to the resolution become dominant.

The effect of random pulse pile-up also was evaluated by measuring the number of "background" counts in the high energy region. Since the real background is very low at this energy (only due to cosmic rays), almost all of the observed counts are due to pile-up. Fig. 6 shows the relative effect of pile-up as a function of the total count rate using a 100 ns delay line for pulse shaping, with and without pile-up rejection. The pile-up rejector incorporated in the processor has reduced the number of pile-up background more than a factor of three, while losing less than 10% of the valid counts. Fig. 7 shows the net number of counts under a high energy peak of interest (signal) to background ratio for different delay line clipping times. It can be observed that the signal to background ratio when the pile-up rejector was enabled is almost constant for different delay line clipping times, from 50 ns to 200 ns. This indicated that the pile-up rejector was more effective when the pulse was differentiated with longer delay lines. This is reasonable since the noise amplitude varies inversely with the shaping time. When short shaping times are used, to avoid excessive noise triggering, the baseline inspector threshold level must be raised, so pile-up of low amplitude pulses is not sensed as efficiently by the inspection channel.

Fig. 8 shows a spectrum of the 10.8 MeV neutron capture gamma ray of nitrogen, collected from a melamine sample irradiated by thermal neutrons, obtained by moderating the output of a Kaman A711 neutron generator. The total average count rate from the detector was 300,000 cps. For comparison, a low count rate measurement is shown in the same figure. The ASP functions efficiently in count-rates of range 500,000 to close to 1,000,000 cps, depending on the shape of the measured spectrum.

5. EXPERIENCE

Since the original development of the ASP [7], modifications were made and procedures developed to expedite set-up and adjustment on a production basis. With the improved set-up procedure, pile-up rejection reduces the background by 30-50% with losses of signal less than 5%.

240 units have been built and used in TNA systems over a 2.5 year period. A total of 2.1 million ASP hours experience have been accumulated, over a total of six TNA system-years. During this time, two ASP failures occurred, both during the first two system-years. The ASP mean time between failure (MTBF) is thus about one million hours.

6. CONCLUSION

The ASP was developed to address the nuclear spectroscopy problems that typically occur in nuclear-based explosive detection systems. Using it, the TNA met its design specifications, and operating experience with hundreds of units over several years has been good, with very few failures.

REFERENCES

[1] C. Brassard, "Fast Counting with NaI Spectrometers", Nucl. Instr. and Meth., vol. 94, pp.301-306, 1971.

[2] T. Gozani, "High Counting Rate Gamma Spectroscopy", American Nuclear Society Transaction, vol. 15, no.2, pp. 951-952, 1972.

[3] D. Vartsky et al., "Fraction Charge Collection Technique for Pile-Up Reduction - Counting Low Intensity Radiation in Presence of Intense Gamma-Ray and Neutron Background," Nucl. Instr. and Meth., vol. 145, pp. 321-329, 1977.

[4] J. H. McQuaid et al., "High Rate Spectroscopy for On-Line Nuclear Coal Analyzer," IEEE Trans. on Nucl. Science, vol. NS-28, no.1, pp. 304-307, February 1981.

[5] V. Radeka, "Trapezoidal Filtering of Signals from Large Germanium Detectors at High Rates," IEEE Trans. on Nucl. Science, vol. NS-19, pp. 412-428, February 1972.

[6] N. Kurlovac and T. V. Blalock, "Resolution and Count Rate Characteristics of the Gated Integrator Nuclear Amplifier," IEEE Trans. on Nucl. Science, vol. NS-22, pp. 452-456, February, 1975.

[7] V. R. Drndarevich, P. Ryge and T. Gozani, "A Signal Processor for High Rate Gamma Ray Spectroscopy with NaI(Tl) Detectors," IEEE Trans. on Nucl. Science, vol. NS-35, pp.222-225, February, 1988.

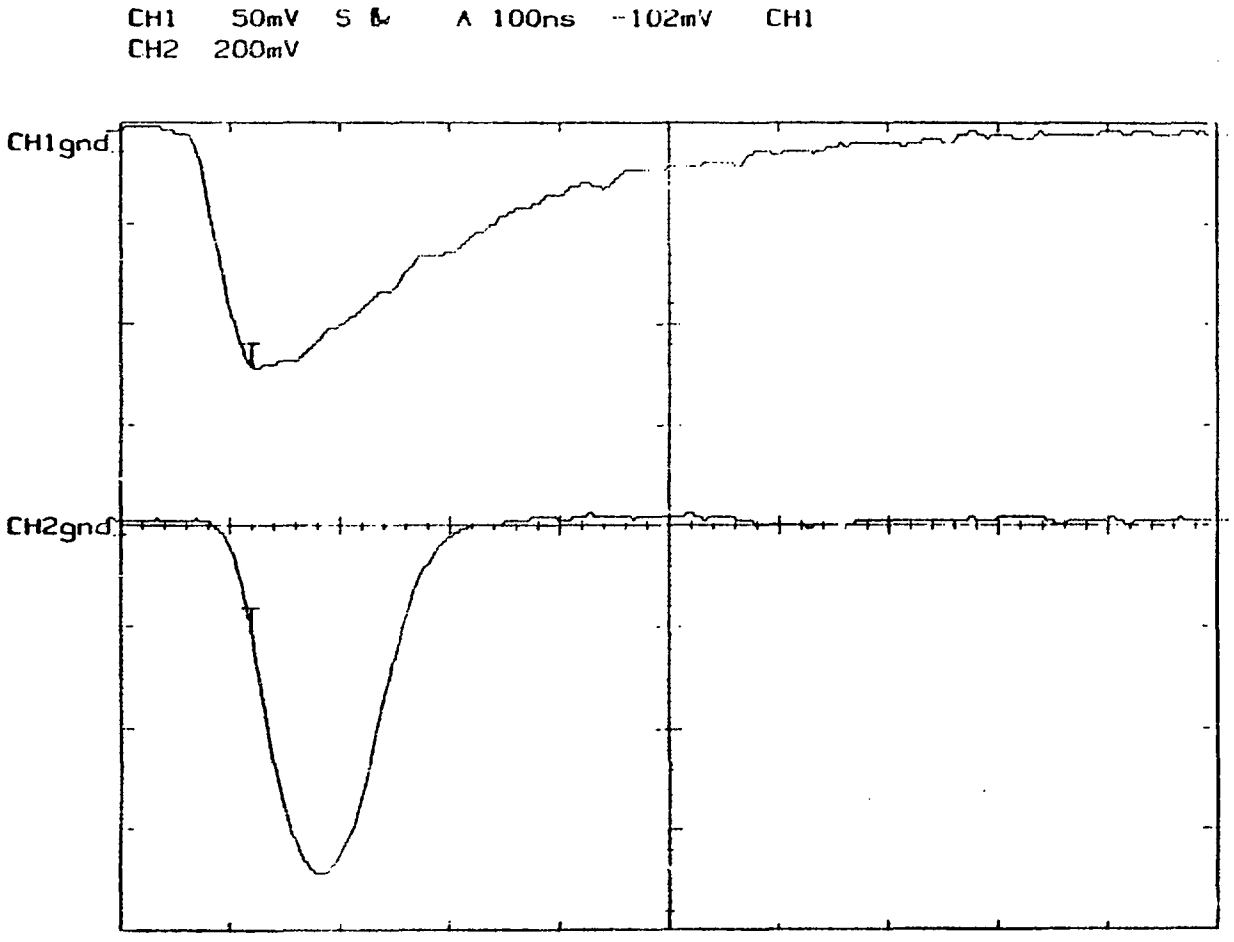


Figure 1a **Gamma ray signal direct from detector and after delay line shortening and tail removed by filter for a single gamma ray.**

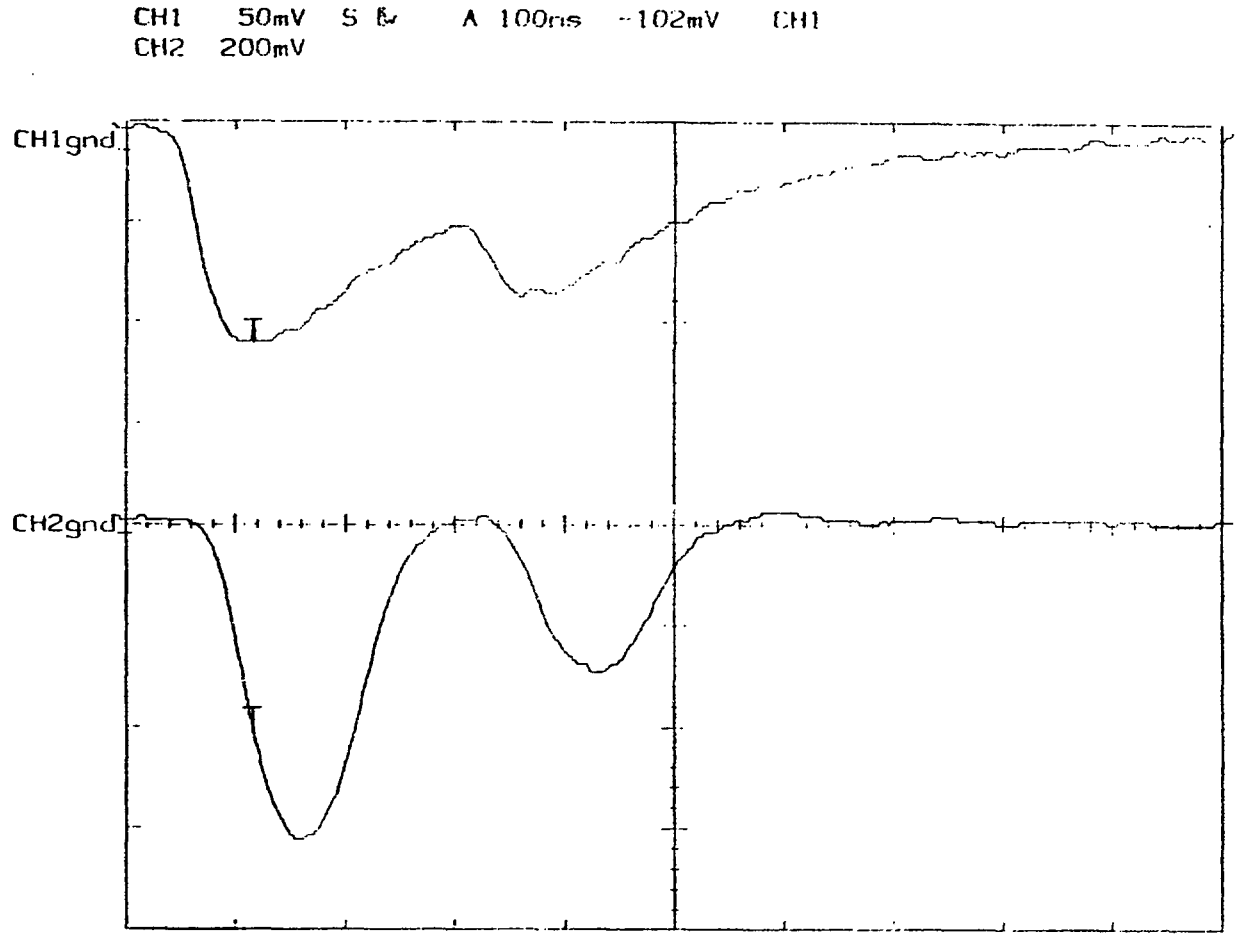


Figure 1b **Gamma ray signal direct from detector and after delay line shortening and tail removed by filter for two gamma rays 250 nanoseconds apart showing direct pulses unresolved but shortened pulses well separated.**

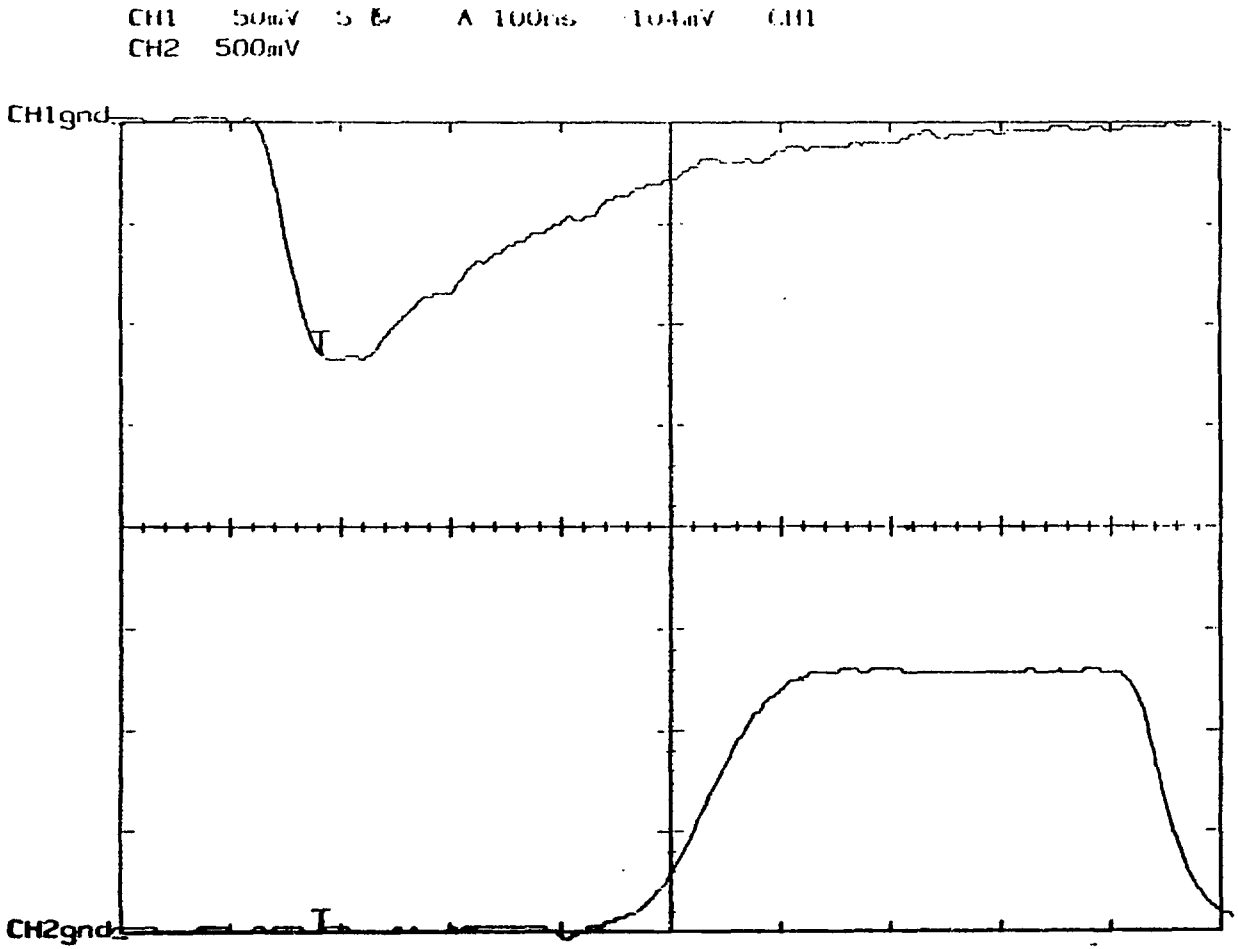


Figure 2a **Input signal from the detector and output from the gated integrator output signal for single gamma ray.**

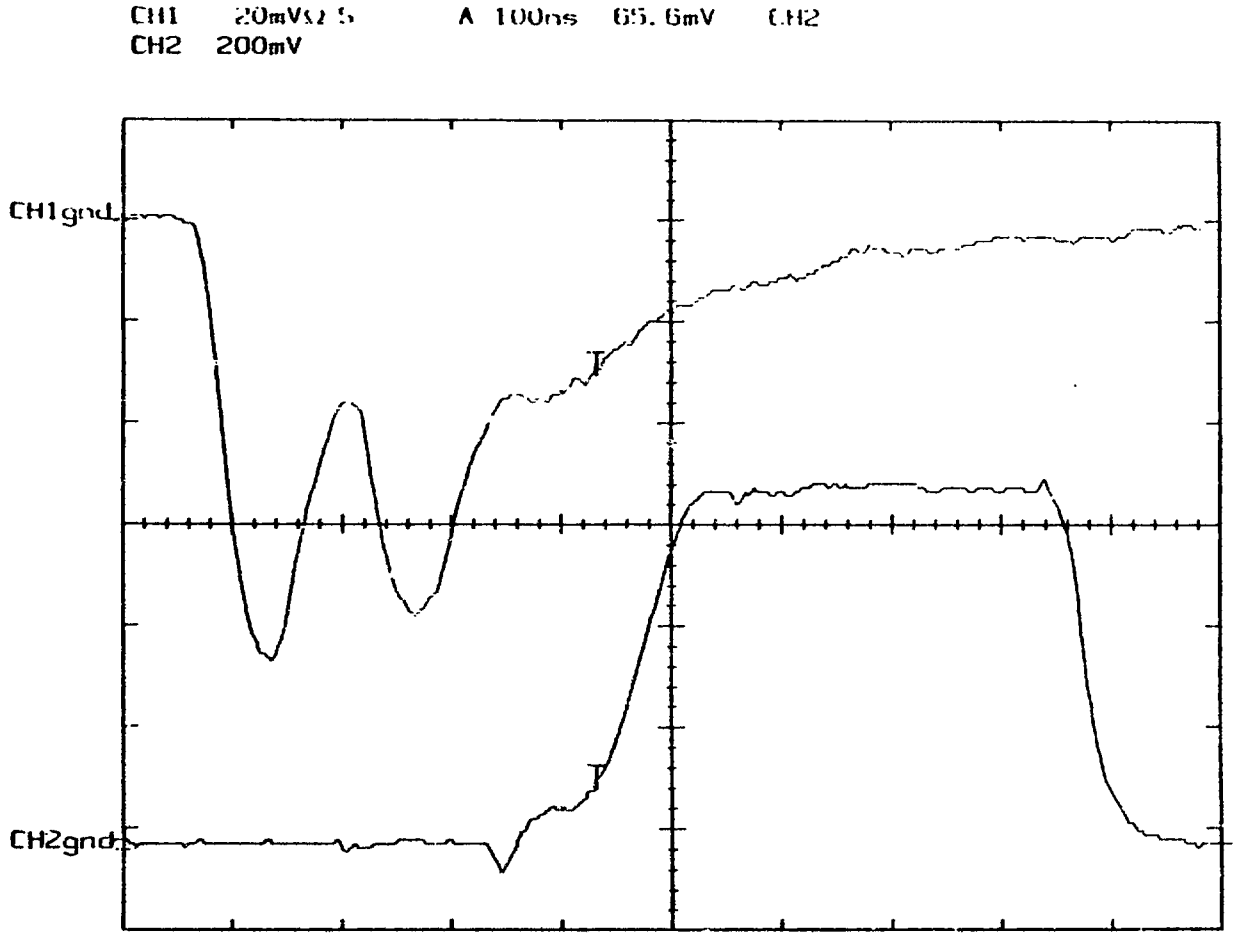


Figure 2b **Input signal from the detector and output from the gated integrator output signal for two gamma rays which overlap at the input but are separated sufficiently to not be rejected.**

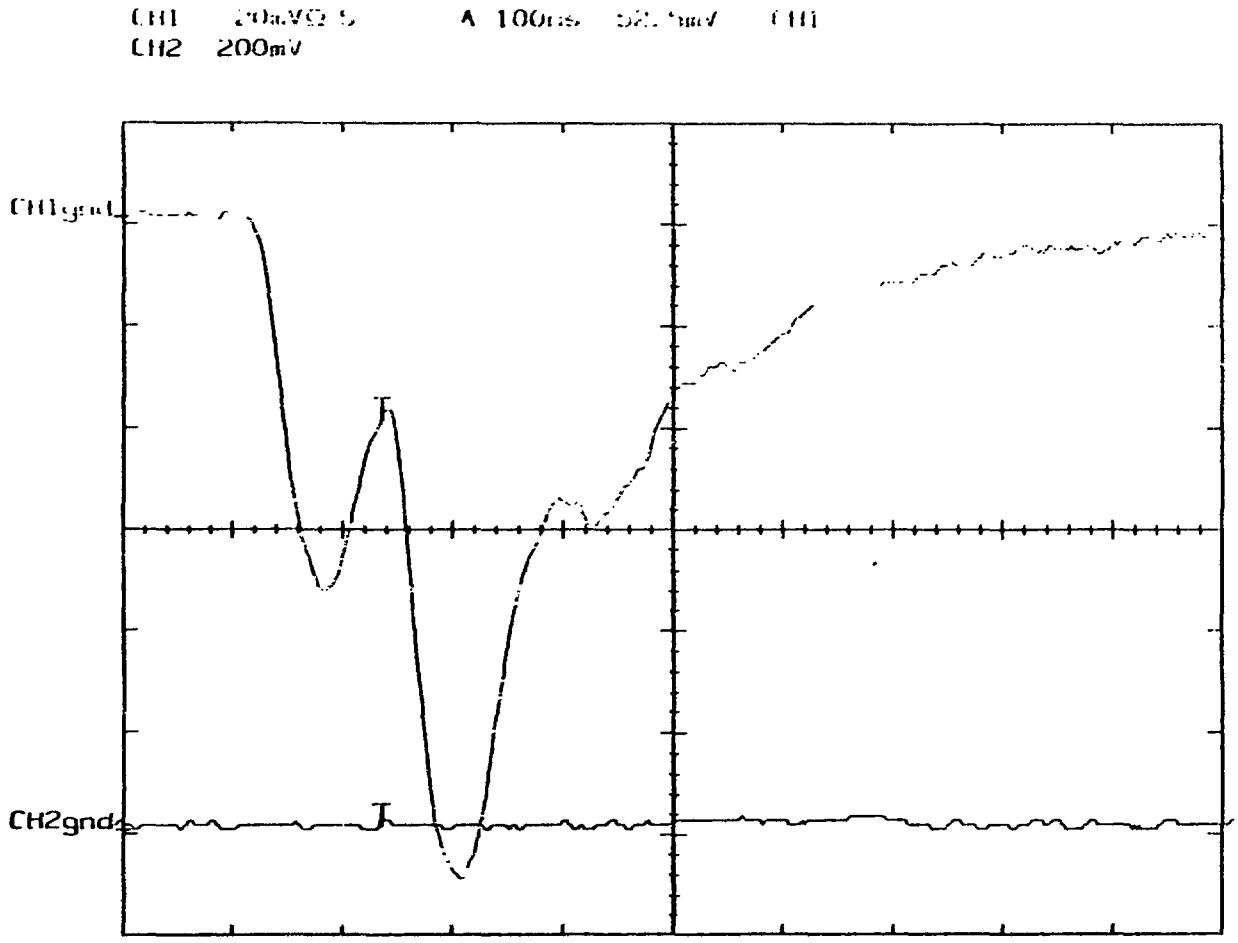


Figure 2c **Input signal from the detector and output from the gated integrator output signal for two gamma rays so close that they are both rejected, no output is seen.**

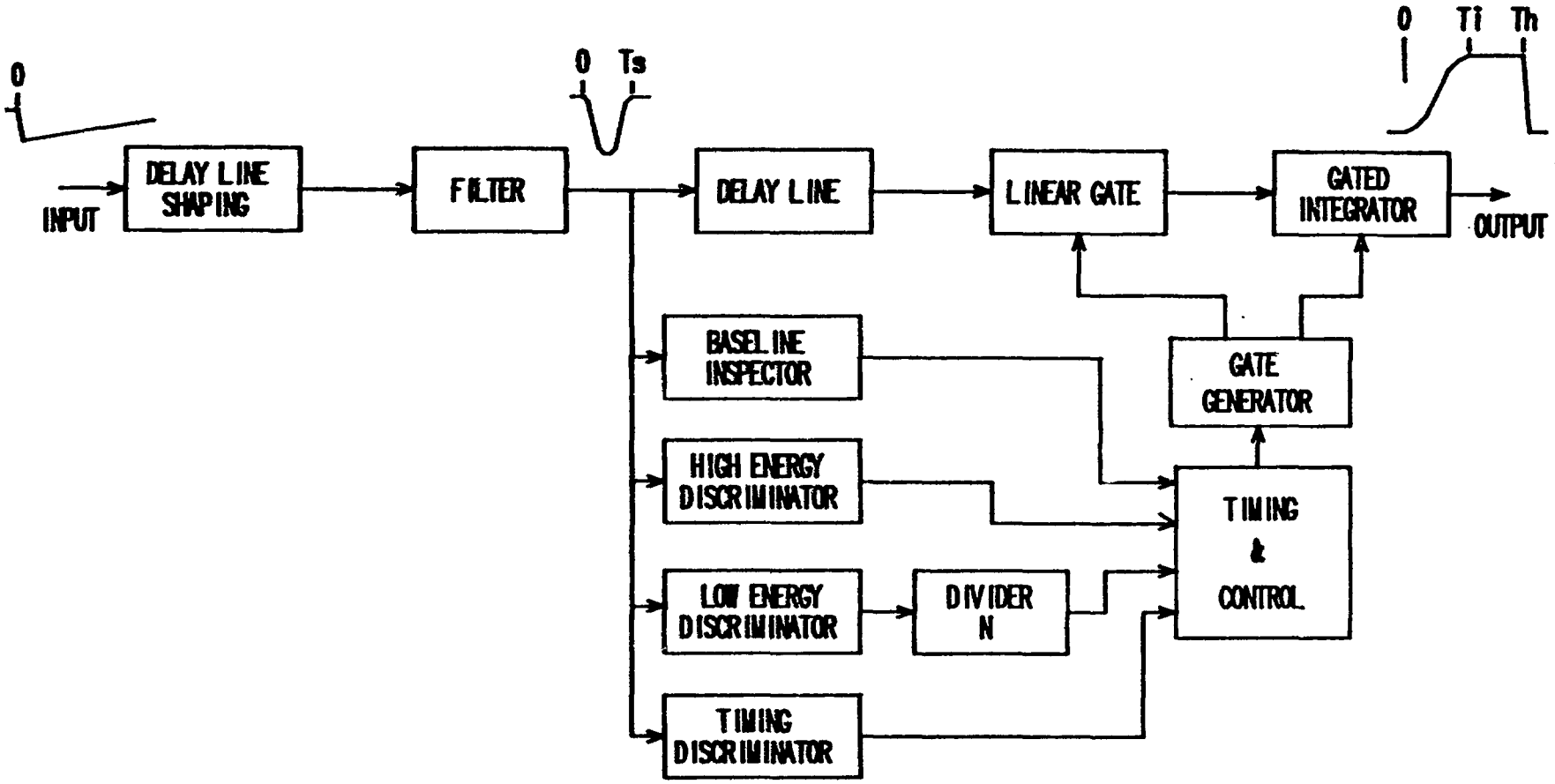


Figure 3 Analog Signal Processor block diagram.

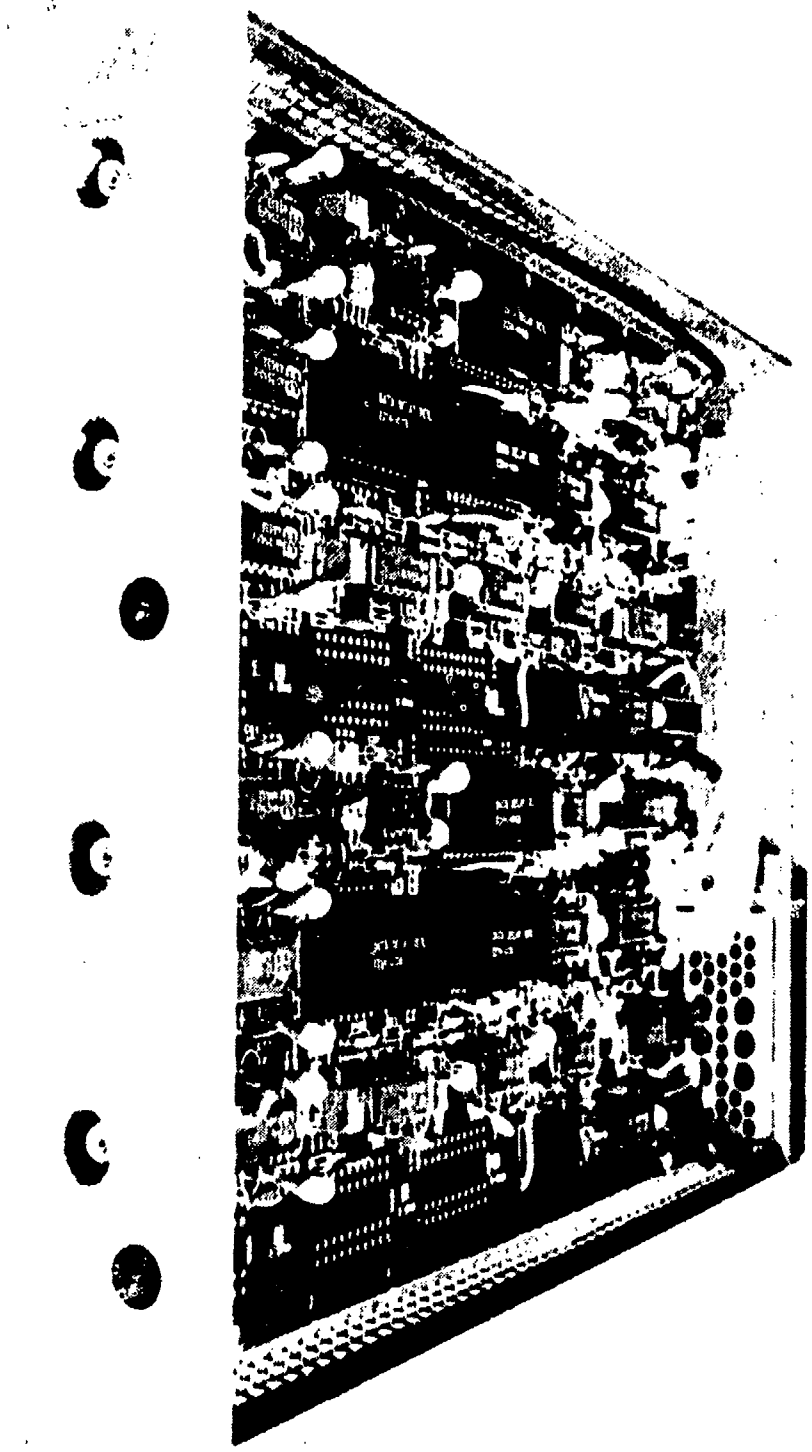


Figure 4 **Photo of NIM module containing two processor channels.**

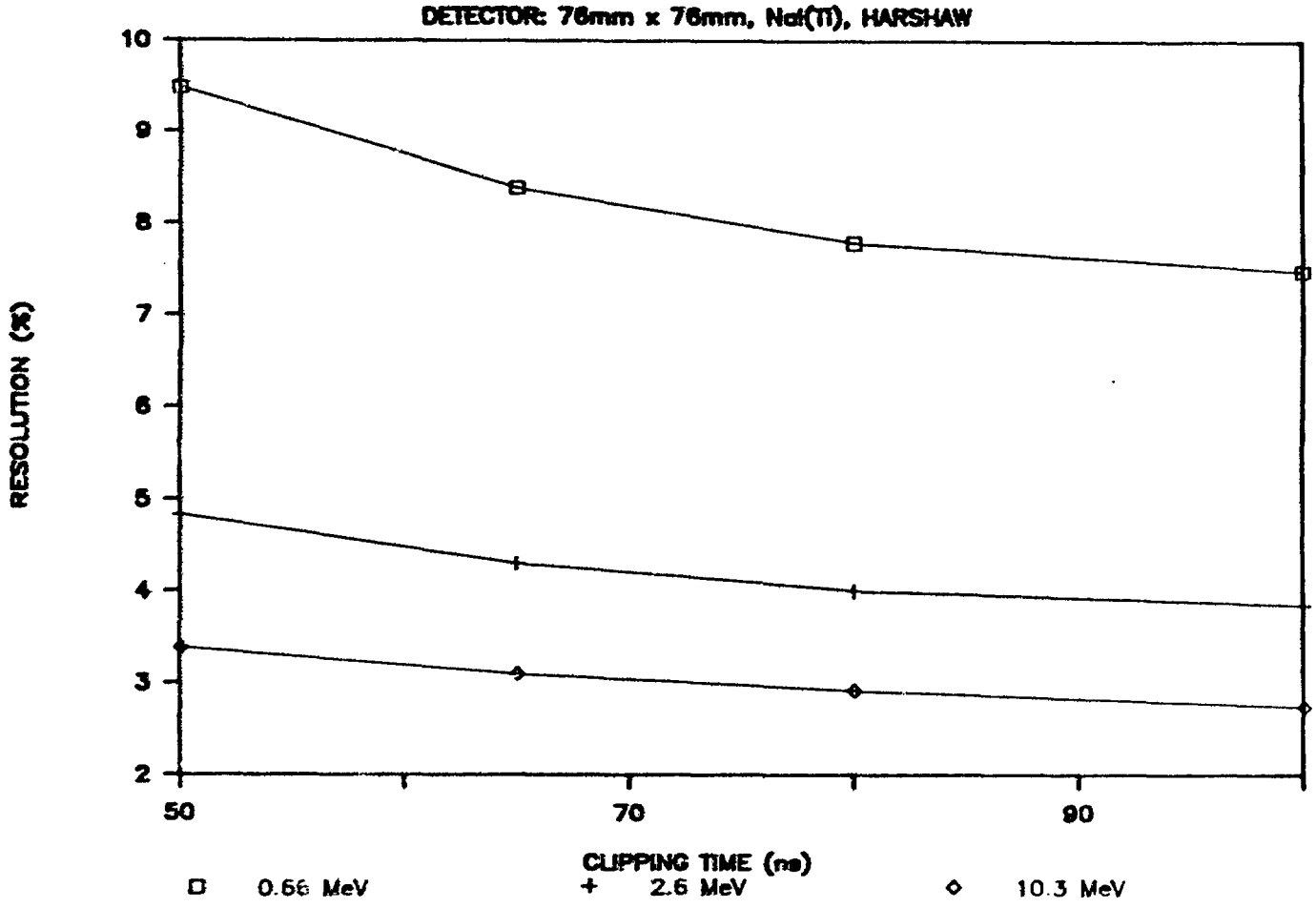


Figure 5 **Resolution as a function of shaping delay line length and energy.**

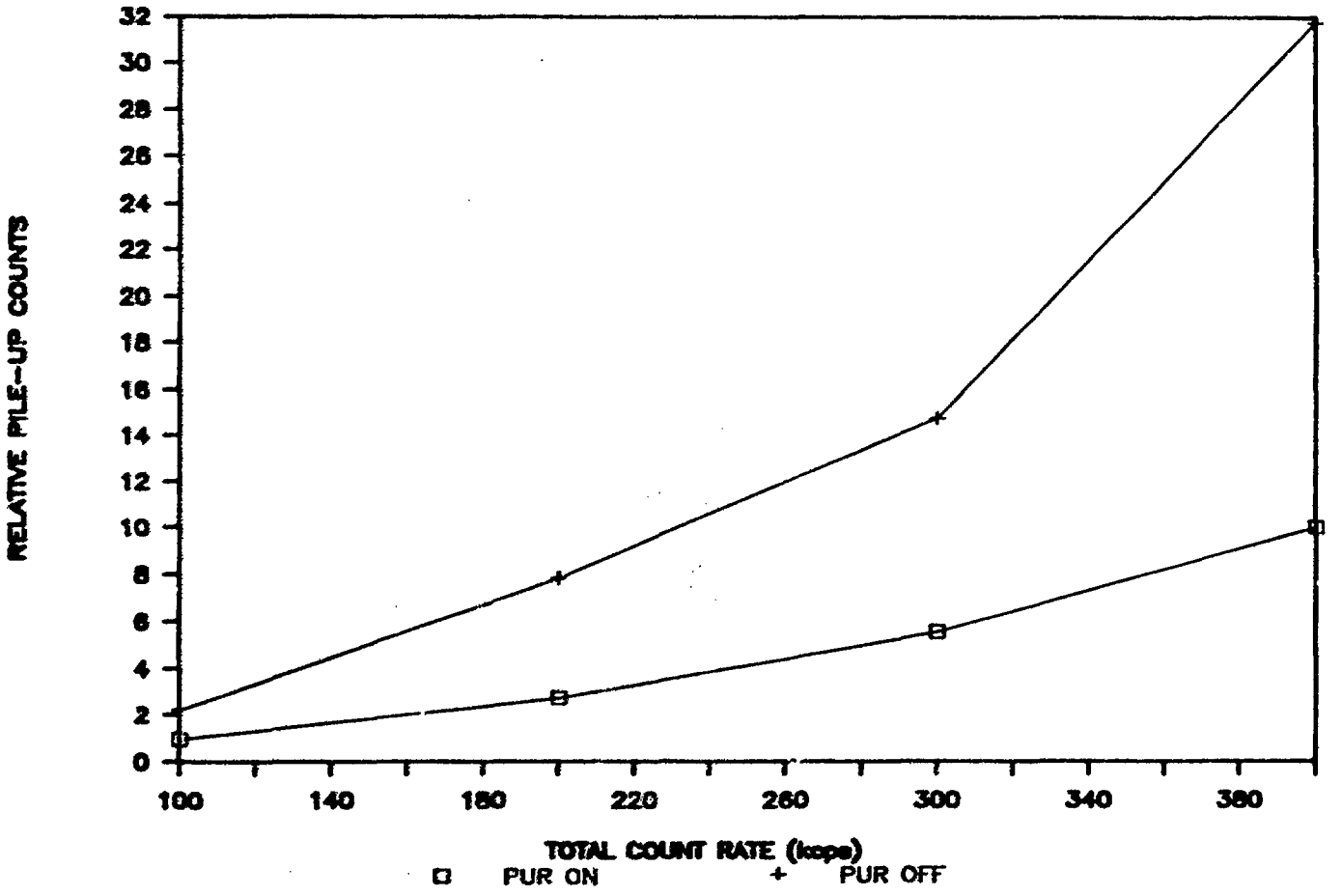


Figure 6 **Count rate in high energy pile-up region as a function of total input rate, with and without pile-up rejections.**

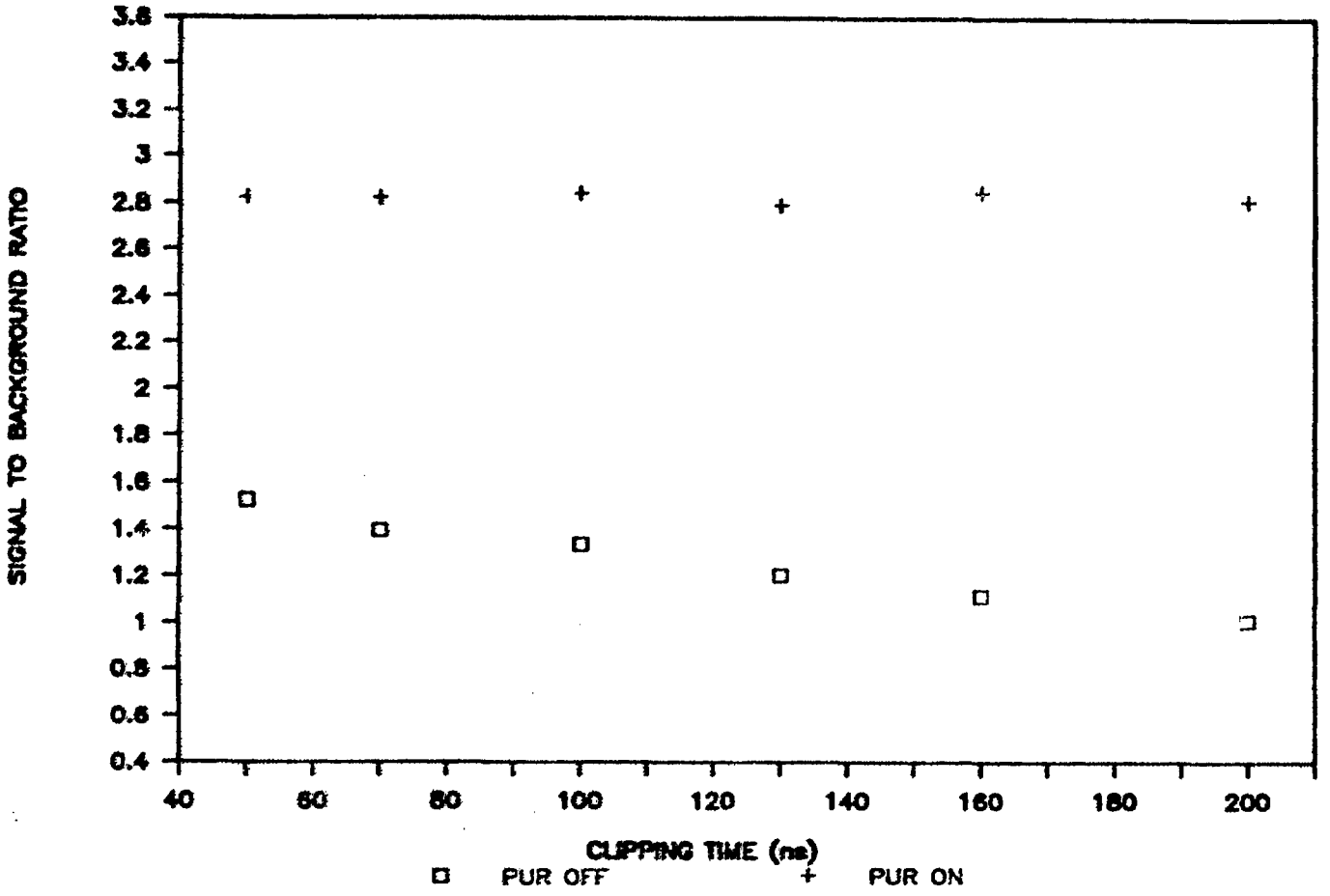


Figure 7 **Signal to background ratio as a function of shaping time, with and without pile-up rejection, for a high energy peak in typical PGNAA spectrum at 300,000 Kcps.**

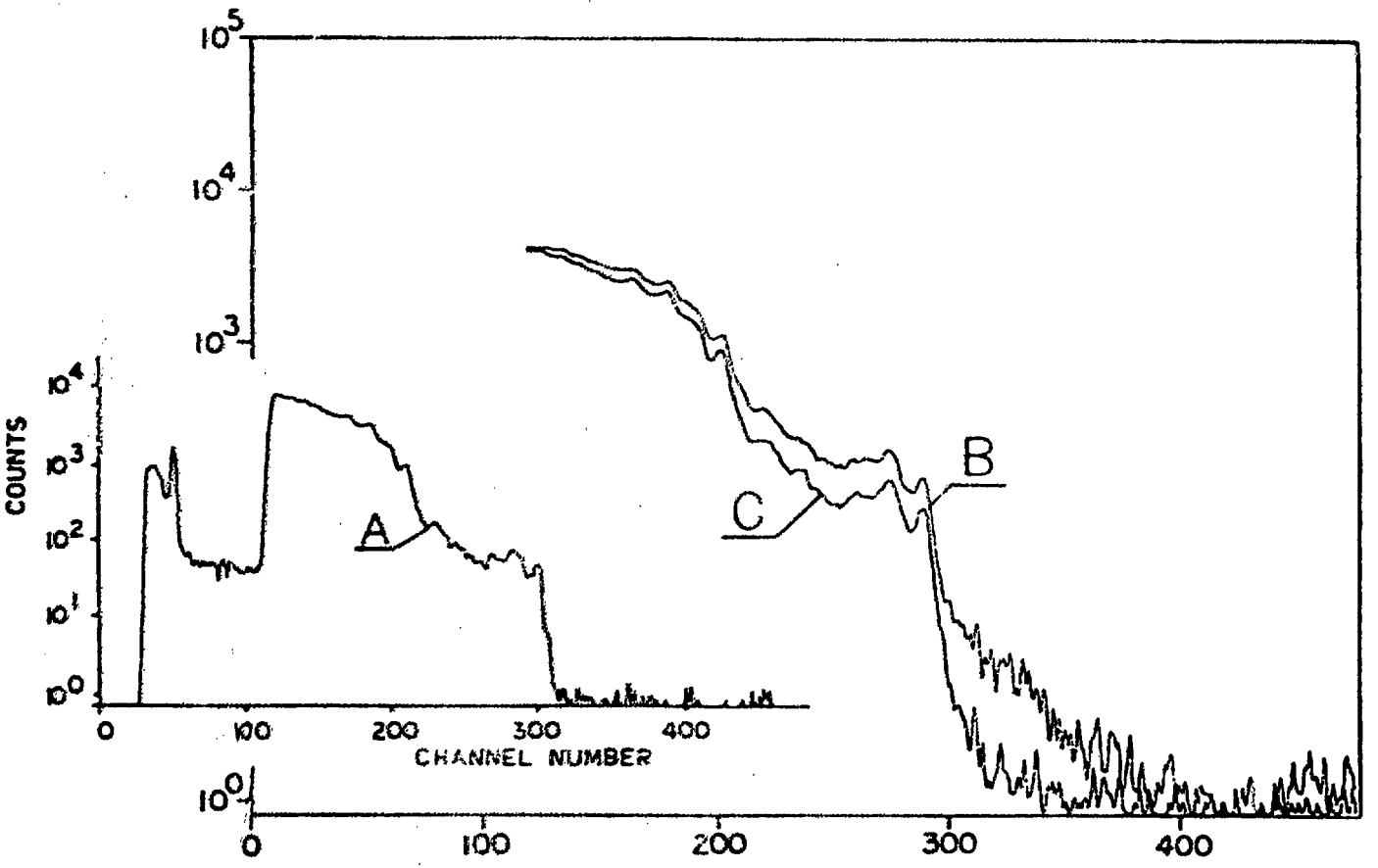


Figure 8 **PGNAA spectra of a melamine sample showing the 10.8 MeV nitrogen full energy and escape peaks. A. Whole spectrum inset showing effect of two level thresholds, N = 128. B. 10.8 MeV region without PUR and C. with PUR.**

COMPUTER SIMULATIONS AND PERFORMANCE PREDICTIONS FOR EXPLOSIVE DETECTION SYSTEMS

Joseph Bendahan, E. Elias, Z. Shayer, J. Pierre,
E. Altschuler, and T. Gozani
Science Applications International Corporation
2950 Patrick Henry Drive
Santa Clara, CA 95054

1. INTRODUCTION

In the design of nuclear based explosive detection systems (EDS) optimization techniques play an important role. These assist in the design of a system with maximum performance at a minimum cost, size and weight.

A complete and validated model is required to efficiently probe the large parameter space of possible EDS designs, and to quantify the ultimate explosive discrimination performance for changes in system parameters. The objective of such a model is to calculate a large number of design tradeoffs and to quantify the impact on performance of each design configuration without the need for a full experimental verification. This considerably reduces the extent and cost of the design, and makes possible the production of a highly optimized explosive detection system.

For nuclear systems based on neutrons as the probing radiation, the neutron flux in the interrogation area should be optimized to yield a maximum figure of merit (FOM). The selection of detector type, size, location and other parameters should also be modeled and optimized to improve the imaging capabilities, and ultimately the overall system performance.

In this paper, the tools and procedures employed by SAIC for optimizing its EDS based on neutron irradiation (TNA and PFNA) are presented.

2. THERMAL NEUTRON ANALYSIS (TNA)

For TNA applications, the luggage moves on a conveyor into the interrogation region containing a high thermal neutron flux. The neutrons penetrate the bag where some of the nuclei present absorb them and emit gamma-rays. Every element has a characteristic gamma ray signature, and by monitoring the emitted gamma ray spectrum the content of a bag can be determined. The explosive detection system searches mainly for nitrogen by detecting its characteristic 10.82 MeV gamma- rays. The determination of an object with high nitrogen density would indicate the presence of explosives.

A similar technique is utilized to detect land mines. In this application a vehicle equipped with a TNA system runs on a land mine field. The detection of an increased nitrogen signal (and other features) indicate the presence of a mine.

In both applications, the thermal neutrons are generated by the slowing down of ^{252}Cf source neutrons or those produced by d-D or d-Be reactions. An important goal of the simulation effort is to design the moderator assembly to provide a maximum thermal neutron flux in the interrogation area.

There is a variety of codes available which can be utilized for these optimizations (see Table I). The MORSE code has been used extensively to simulate the thermal neutron flux and lately DORT and TORT. The results of the calculations have been verified against experiments obtaining an agreement within 15%.

TABLE I

Codes utilized to simulate the transport of neutrons and gamma rays at SAIC - Santa Clara

- ANISN : 1D discrete ordinate
- DORT,TORT : 2D and 3D discrete ordinate
- MORSE : Oak Ridge Monte Carlo Code
- MCNP : Los Alamos Monte Carlo Code
- SWAN : 1D optimization code.

In Figure 1 MORSE calculations are shown for various moderator configurations. The simulations allow selection of configuration A to obtain a

maximum yield without the need of lengthy and costly experimentation. This type of calculations also allows determination of the effect of suitcase density and the effect of the explosives in a TNA cavity. In Figure 2 the neutron flux is shown for three suitcases with cellulose densities of 0.1, 0.2 and 0.3 g/cc. The thermal flux increases with suitcase density. Figure 3 shows the thermal flux when C4 and TNT explosives are positioned in the center of the suitcase for various densities. Observe that the flux is depressed in both cases, with C4 having a larger effect. This is attributed to a larger hydrogen weight fraction of C4 (3.2%) compared with TNT (1.8%).

This optimization process is very important to ensure a minimum source strength and therefore a smaller, lighter and cost effective EDS.

One of the most efficient ways to calculate shielding and deep penetration problems is by utilizing the solution of the linear version of the deterministic transport equation (discrete ordinate codes). Before accepting these codes for optimization we need to have confidence that the code will solve the required types of problems with sufficient accuracy. Few benchmark cases were calculated. In the first series of calculations the energy dependent neutron flux in a D_2O sphere with a Cf source at the center was determined. The results of ANISN, MORSE and MCNP are shown in Figure 4; there is a very good agreement at all energies. In order to verify the DORT code, a finite cylindrical polyethylene block with a point Cf source was run (see Figure 5). The results are compared with MCNP in Figure 6. There is a good agreement with differences of about 10%, mainly attributed to the different cross section libraries. It is important to note that MCNP took 130 minutes to complete the calculation, with a 2-3% statistical error, while it took DORT 8 minutes to obtain similar results.

In addition to the neutron flux, detector responses were also modeled. EGS4 (Electron Gamma Shower) was utilized to generate the detector response for a variety of detector types and sizes, in the presence of various shielding materials. In Figure 7 the detector responses are compared for three detector types : NaI(Tl), BaF_2 and BGO at 10.82 MeV.

Another important issue is the detector shielding. A large number of neutrons and gamma-rays originating at the source and scattered by the surrounding materials interact with the detectors. An optimization code, SWAN, has been utilized to reduce this background while keeping the amount of shielding and signal loss to a minimum. In Figure 8 the results of an optimization to reduce the number of gamma-rays arriving and induced in the detector for a Cf system is shown. Figure 8 gives the optimal volume fraction as a function of thickness. Unfortunately the SWAN code can only be used for simple cases where the configuration can be approximated by a one dimensional geometry. Implementation of SWAN in 2D and 3D would allow a fast and cost effective optimization of shielding, flux maximization, etc. for complex geometries.[1]

The 10.82 MeV gamma-ray is the highest energy produced by any element following thermal neutron capture. Except for a few gamma-rays interfering with the nitrogen region, the main source of high energy background is the pileup. Pileup is produced when two or more events overlap in time with combined energy falling in a higher energy region. The reduction of total count rate results in a reduction of pileup. This effect has been modeled for arbitrary gamma ray spectra, pulse shape and counting rate.

In order to perform a systematic analysis and design tradeoffs in the large parametric space of TNA design, a computer code, TNASIM, has been written and implemented. TNASIM includes an extensive knowledge of neutron fluxes, detector response, backgrounds, gamma and X-ray imaging, discriminant analysis and/or neural network decision process. This code is a front-end TNA simulator that models from the generation of realistic luggage sets, the passage of individual bags through the TNA and X-ray environments. TNASIM was developed by SAIC to the following specifications: (1) fast, in order to generate large data sets; (2) parametric and modular, in order to understand, modify and calibrate; (3) modifiable, through input files, to represent all hardware modifications; and (4) verifiable, by producing simulated data that is statistically similar to observed data. With FAA support, TNASIM has been further calibrated and tested, and is being used to upgrade the existing TNA system.

3. PULSED FAST NEUTRON ANALYSIS (PFNA)

FNA techniques utilize fast neutrons as the radiation probe. The neutrons interact with various materials and produce gamma-rays characteristic to the element

being irradiated. In particular, the signatures of oxygen, carbon and nitrogen are of special interest since explosives can be distinguished from benign materials by the high oxygen and nitrogen and low carbon densities.

Compared to TNA, PFNA is a more powerful, but more complex technique. A large set of new parameters to be simulated are required: more elemental signatures, neutron attenuation, neutron and gamma ray timing, etc. Since, the position resolution is obtained with TOF (time-of-flight) techniques, time dependent simulation codes are required. The standard time dependent coupled neutron-gamma ray code used for this purpose is MCNP (Monte Carlo Neutron Gamma). MCNP includes nuclear libraries which contain the compilations of the most important experimental results.

DORT has been also utilized to study the transport of fast neutrons and gamma rays. The neutron collimator shown in Figure 9 was modeled and the results are compared in Figure 10 with experiments. There is good agreement within the experimental errors.

In order to carry out tradeoff studies and performance predictions, large numbers of signal sets resulting from the irradiation of a variety of target materials and configurations are required. Although MCNP is accurate, it is relatively slow for the amount of data that should be generated. SAIC has developed a computer code, PFNASIM, which produces approximate results in shorter times and allows the performance of design trades. PFNASIM is a result of hundreds of man hours of development and contains the most important effects taking place during a pulsed fast neutron irradiation in an arbitrary geometry. These include:

1. Angular and energy distribution of the generated neutrons. These were taken from Nuclear Data Sheets.

2. Energy dependent cross sections for $(n,n'\gamma)$ reactions for the elements of interest. Most cross sections were taken from ENDF-V and ENDF-VI evaluations.

3. Angular distributions of neutron and gamma-rays. Angular distributions of neutrons were obtained by running MCNP. Angular distributions for gamma-rays were determined experimentally. For some transitions there are no evaluations and for other the evaluations show major discrepancies with the experimental results.

4. Energy dependent neutron and gamma ray attenuations. The neutron attenuation and buildup have been parameterized for a variety of materials using MCNP. The gamma ray attenuation were taken from Nuclear Sata Rables.

5. Detector responses as a function of energy, angle and distance from gamma ray source. The detector response was obtained by running EGS4. It includes the effect of shielding materials and attenuation through neighboring detectors.

6. Detector response to fast neutrons. The response to neutrons was determined experimentally. Simulations were not carried out because of the lack of $(n,n'\gamma)$ cross sections for the detector materials. Partial data can be found in the literature.

PFNASIM has been utilized to optimize the neutron source and detector locations, and other parameters required for the design of an explosive detection system. Under FAA support, a variation of the PFNASIM code will be utilized to simulate the passage of realistic luggage sets in a PFNA based system.

4. SUMMARY

Performance optimization can only be obtained through a systematic engineering and design approach using coordinated experimental measurements, data analysis and modeling efforts. TNASIM and PFNASIM codes, developed at SAIC, are the key to performing design trades, developing accurate decision algorithms and projecting the performance of TNA and PFNA based systems. Their utilization ensures the designing of a well balanced optimized and cost effective explosive detection system.

REFERENCE

1. Refer to the paper "A Novel Approach to the Optimization of Nuclear Design of Explosive Detectors Using Radiation Sources" presented in this proceeding.

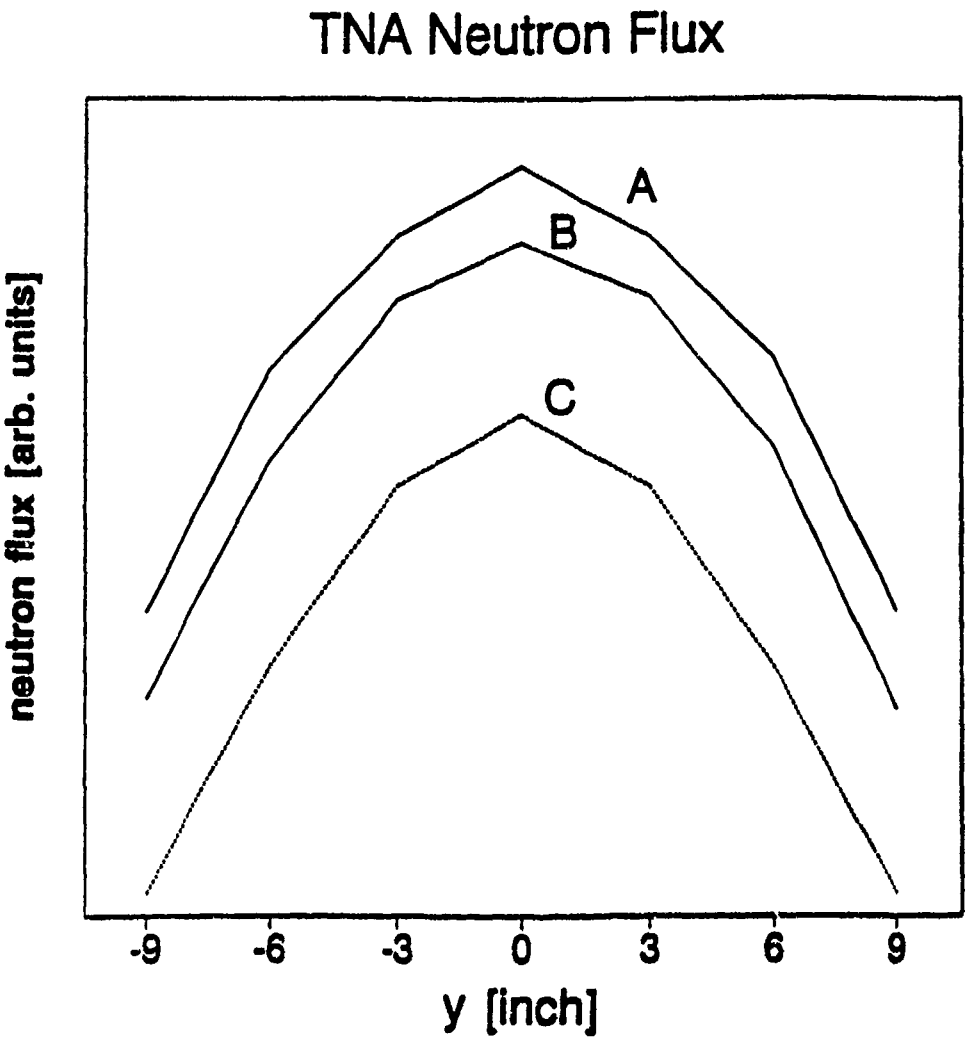


Figure 1 Comparison between the neutron flux for three different moderator configurations. Configuration A shows maximum neutron flux for the same source strength.

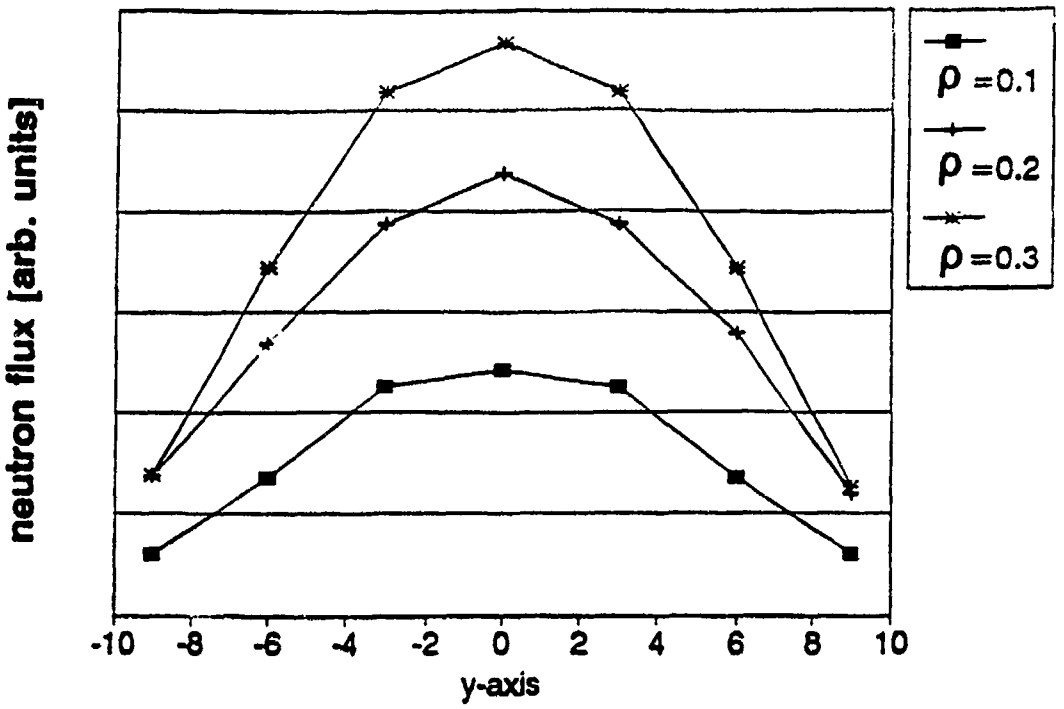


Figure 2 Neutron flux as a function of suitcase density.

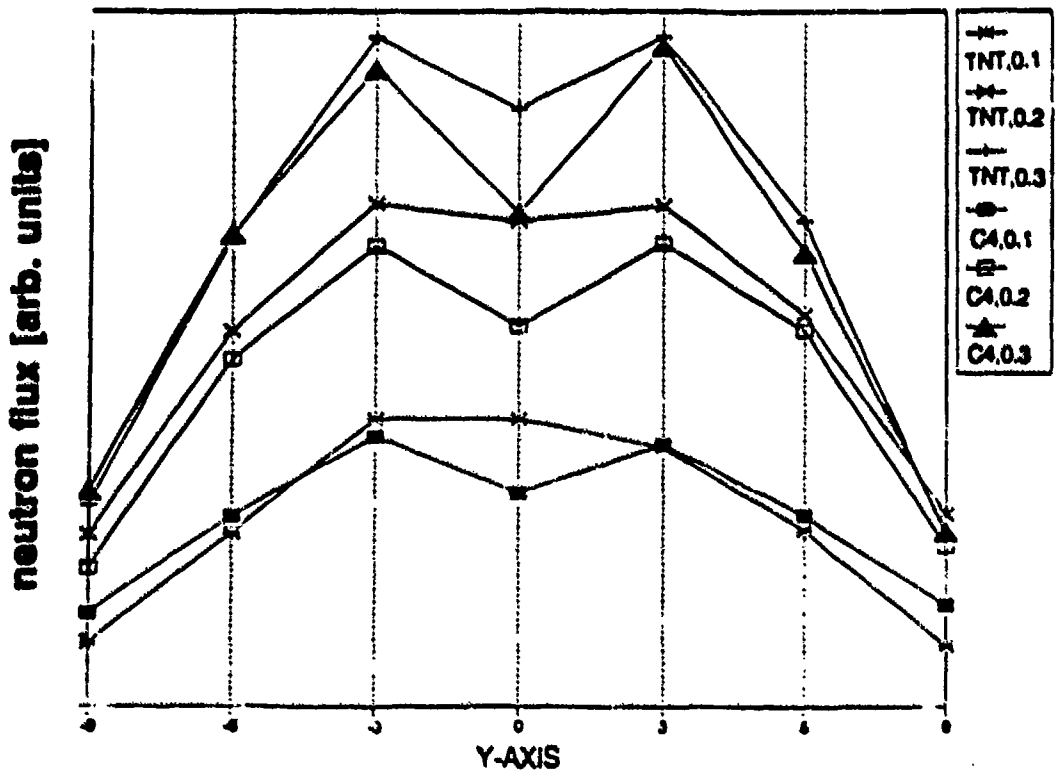


Figure 3 MORSE output comparison - TNT vs C4.

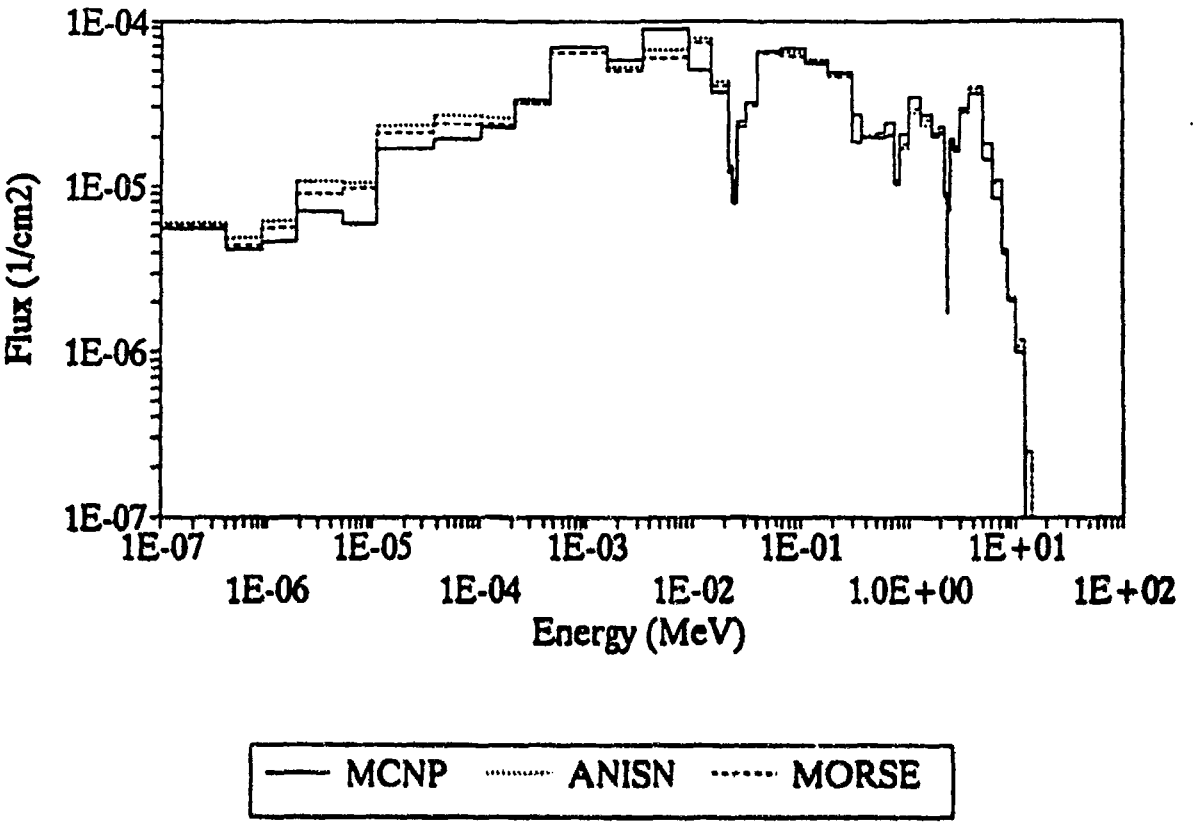


Figure 4 Energy dependent neutron flux at a surface of a 10cm D_2O sphere obtained with MCNP, ANISN and MORSE. There is a good agreement at all energies.

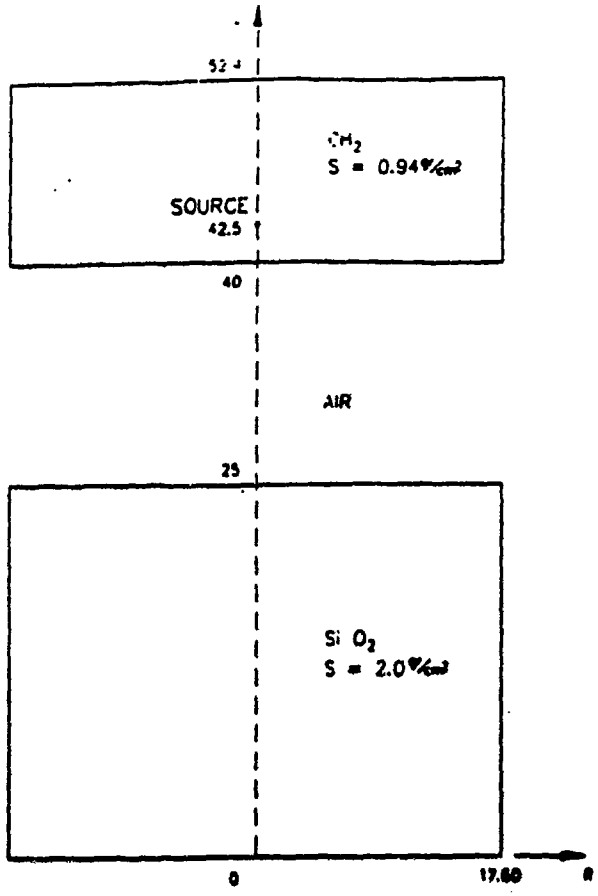


Figure 5 Benchmark geometry used to compare MCNP and DORT Codes.

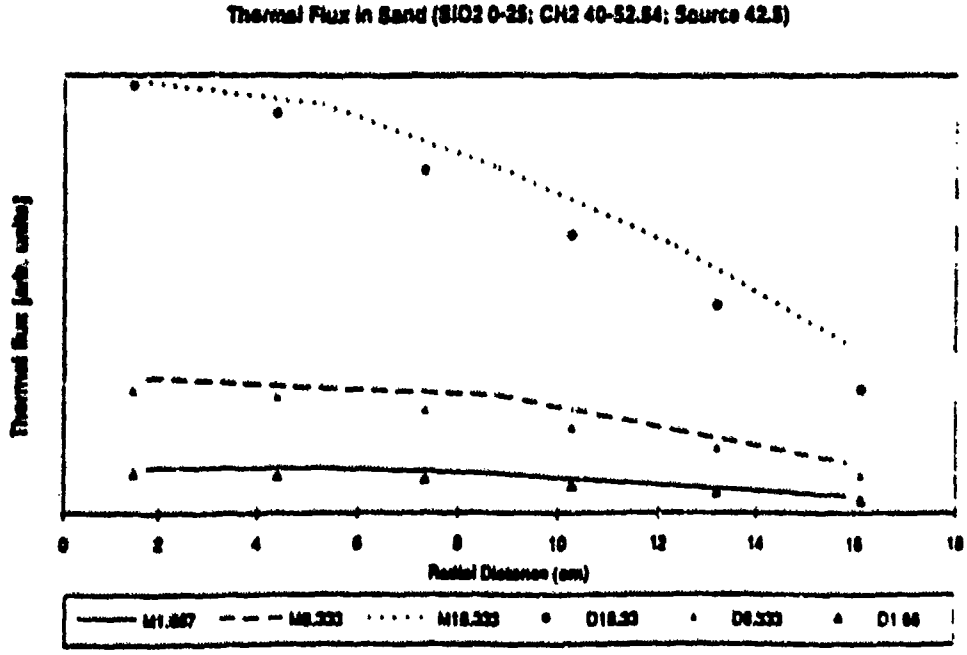


Figure 6 Thermal neutron flux distribution at different distances (M = MCNP, D = DORT).

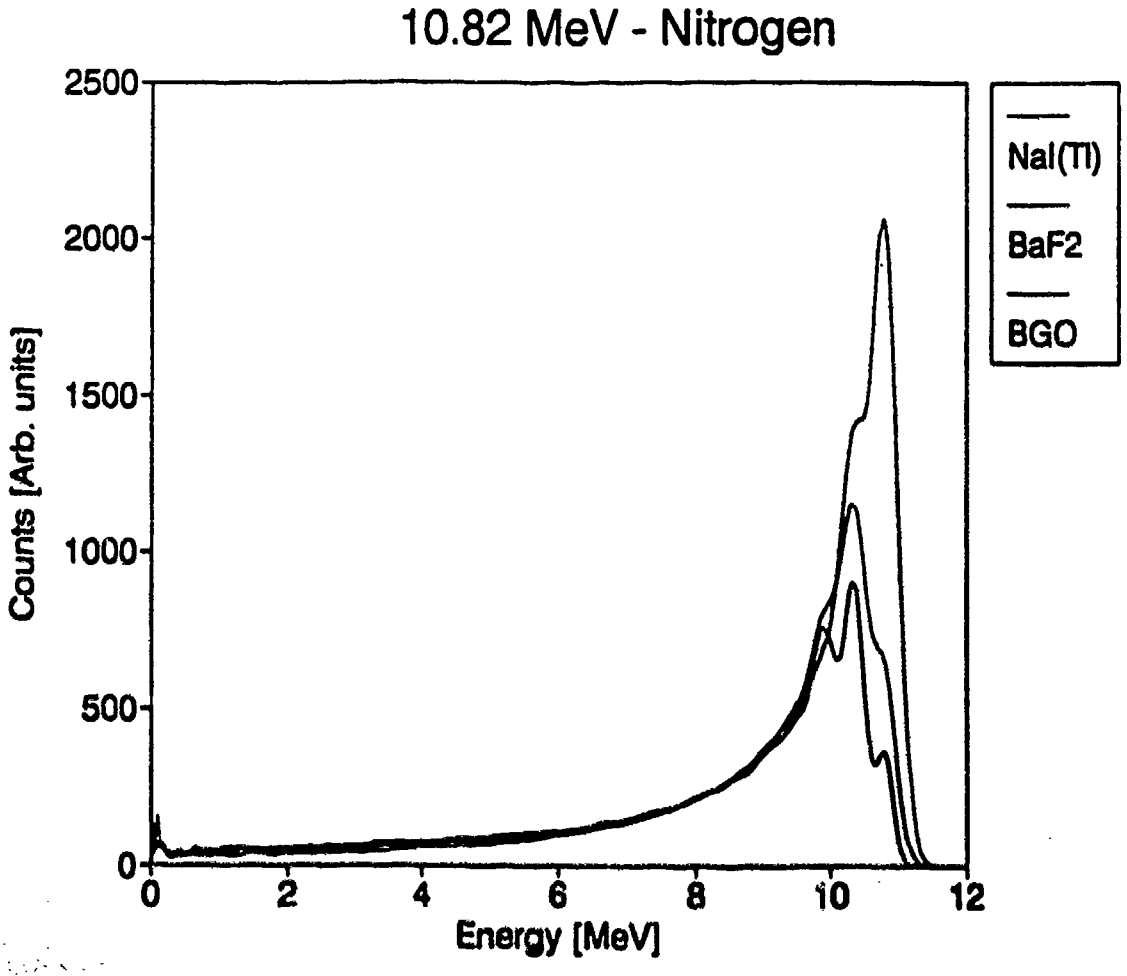


Figure 7 Detector response comparison for 3"x3" NaI(Tl), BaF_2 and BGO at 10.82 MeV obtained with EGS4 code. Observe the significant larger efficiency of the BGO detector.

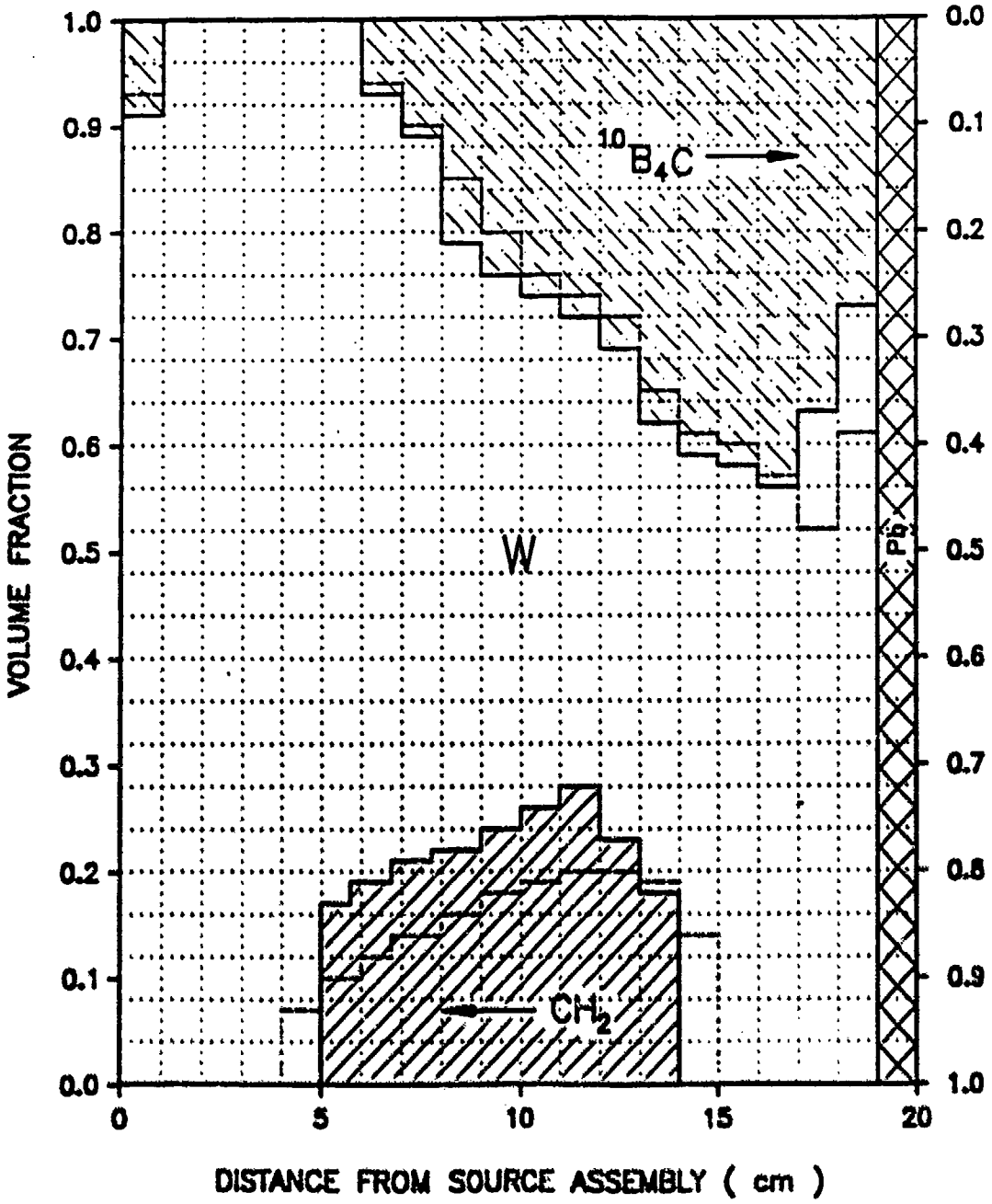


Figure 8 Results of the SWAN optimization code in reducing the number of gamma rays, arriving and induced in the detector, for a Cf system. The constituents of the shields are expressed in volume fraction.

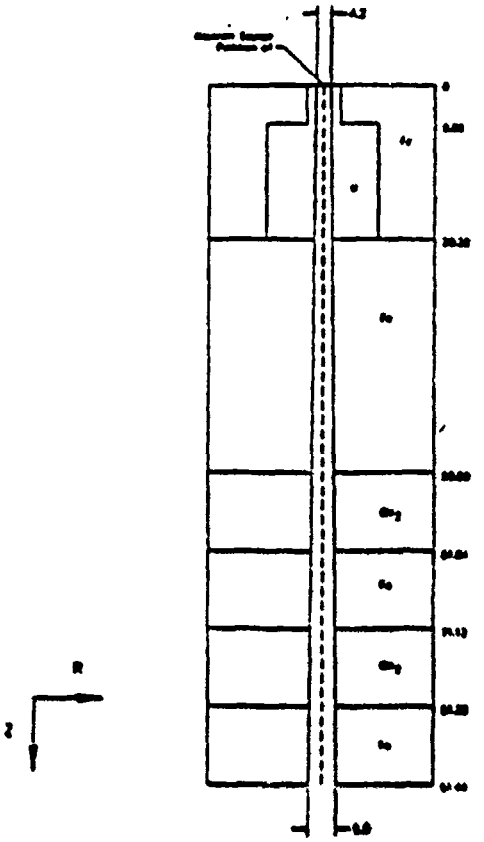


Figure 9 The R-Z computational model of experimental collimator.

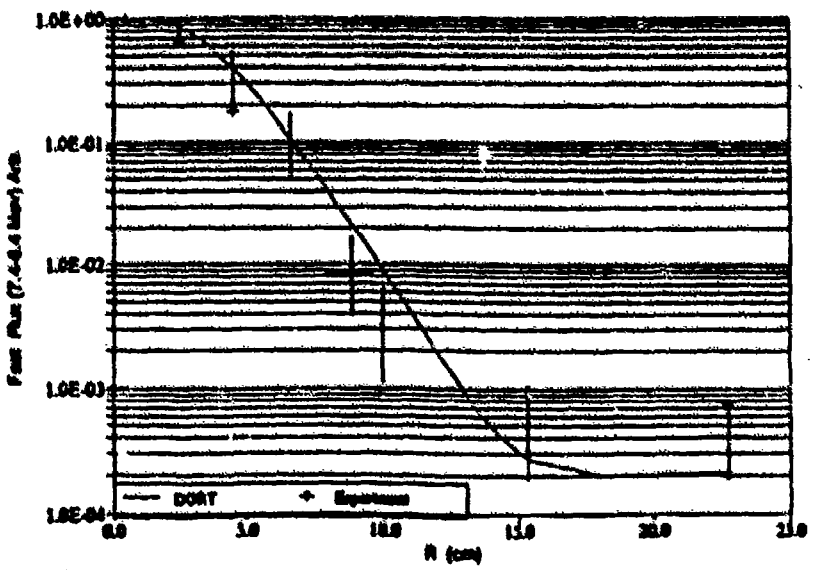


Figure 10 Experimental and simulated fast neutron flux for the configuration shown in Figure 9.

RECOGNITION OF PARTIALLY OCCLUDED THREAT OBJECTS BASED ON HYBRID HOPFIELD NEURAL NETWORK

Jung H. Kim, Ph.D.
Department of Electrical Engineering
North Carolina A&T State University

E. H. Park, Ph.D and C. Ntuen, Ph.D.
Department of Industrial Engineering
North Carolina A&T State University

Shiu M. Cheung, Ph.D.
FAA Technical Center

1. INTRODUCTION

Recognition of partially occluded objects has been an important issue in the fields of industrial automation and military application, because occlusion causes significant problems in identifying and locating an object in the workspace of the robot, baggage inspection in airport, etc.. Occlusion occurs when two or more objects in a given image touch or overlap one another. In such situations vision techniques using global features to identify and locate an object may fail because descriptors of part of a shape may not have any resemblance with the descriptors of the entire shape. local-feature-based methods have been developed in an effort to solve the occlusion problem instead of a global descriptor, [1-4]. More reliable features are needed to recognize occluded objects since false features in addition to features of occluded parts accelerate mismatching of objects. A polygonal approximation method, [5-6], which has been widely used, may not provide reliable features because it may not produce unique break points which are necessary for reliable matching. Researchers, therefore, are burdened to compensate for phantom segments as well as an occlusion problem. In this paper, the unique boundary segmentation is obtained by using a constrained regularization technique, [9]. As the result of the unique segmentation, a graph matching technique [7-8] based on neural network will be presented.

The inherent parallelism of Neural Networks allows rapid pursuit of many hypotheses in parallel with high computation rate. Moreover, they provide a great degree of robustness or fault tolerance comparative to conventional computers because of the many processing nodes, each of which is responsible for a small portion of the task. Damages to a few nodes or links thus do not impair overall performance significantly. For this reason, Hopfield style neural network is proposed to solve graph matching problems for partially occluded objects. Hopfield neural network has been used for solving NP-complete optimization problems and has been applied to pattern recognition area, which can be cast into a combinatorial optimization problem,[10-11]. Some researchers apply Continuous Hopfield Network to three-dimensional object matching problem, [12]. However, CHN takes much computational time in simulating a differential equation while it provides good solutions. Discrete type Hopfield Network has been used for the two-dimensional objects matching problems, [13]. However, DHN is an approximation method and gives only rough solutions resulting in mismatching on occasions. In this paper, Hybrid Hopfield Neural Network, which has the advantage of both CHN and DHN is proposed to obtain reliable solutions and reduce computational time. Unlike the traveling salesman problem implemented by Hopfield Neural Network, the matching problem is handled by normalizing features made by a fuzzy function which gives distinguishable values to a connectivity matrix. HHN is derived from estimating behavior of neurons as time evolves based on the distinguishable value of a connectivity matrix. The method reduces the amount of simulation time and provides the better solutions than CHN does.

2. FEATURE EXTRACTION AND GRAPH FORMATION

In boundary based approach, corner points are

important since the information of the shape is concentrated at the points having high curvatures. We use these kinds of features such as a local feature of an angle between neighboring corners and relational features of distances from all the other corners. These two features which are invariant under transnational and rotational changes are used for the robust description of shape of the boundary. Corner points are usually detected in a curvature function space by capturing the points whose curvature values are above a certain threshold value. We developed a new corner detection algorithm which provides reliable and invariant corners for a matching procedure in the early study, [9]. A graph is constructed for a model object using corner points as nodes of graph. Each node has a local feature as well as relational features with other nodes. In the matching processing, a similar graph is constructed for the input image which may consist of one or several overlapped objects. Each model graph is then matched against the input image graph to find the best matching subgraph.

3. MATCHING BASED UPON HYBRID HOPFIELD NEURAL NETWORK

3.1 Discrete Hopfield Networks (DHN)

DHN is a original model of Hopfield style neural network and has a merit that it is simple to implement and it is fast. A two dimensional array is constructed to apply matching problem to neural network. The columns of the array label the nodes of an object model, and the rows indicate the nodes of an input object. Therefore, the state of each neuron represents the measure of match between two nodes, one from each graph. Matching process can be characterized as minimizing the following energy function:

$$E = -\frac{A}{2}\sum_{i}\sum_{j}\sum_{k}\sum_{l} C_{ijkl}V_{ik}V_{jl} + \frac{B_1}{2}\sum_{i}\sum_{k}\sum_{l\neq k} V_{ik}V_{il} + \frac{B_2}{2}\sum_{k}\sum_{i}\sum_{j\neq i} V_{ik}V_{jk} \qquad (1)$$

where V_{ik} is a binary variable which converges to 1.0 if the ith node in the input image matches the *kth* node in the object model; otherwise, it converges to 0. The first term in (1) is a compatibility constraint. Local and relational features which have different measures are normalized to give tolerance for ambiguity of the features. The last two terms are included for enforcing the uniqueness constraint so that each node in the object model eventually matches only one node in the input image and the summation of the outputs of the neurons in each row or column is no more than 1. Some papers concerning a matching problem with Hopfield style Neural Net have used $\Sigma\Sigma(1-V_{ij})^2$ as a uniqueness constraint. This term implies global restriction. However, matching of occluded objects will not guarantee that every row or every column has only one active neuron. Therefore the energy function of the occluded matching problem excludes the global restriction condition like Eq.(1). In a traveling salesman problem, coefficients B_1, B_2 are more emphasized than the coefficient A because B_1, B_2 contribute yielding valid solutions. However, in the matching of occluded objects conditions of valid solutions are indefinite. In addition, C_{ijkl} is normalized by a fuzzy function so that it helps us obtain good solution. Therefore the coefficient A is supposed to be more emphasized in the matching problem. Eq.(1) can be cast into a Hopfield style energy function as follows:

$$E = -\frac{1}{2}\sum_{i}\sum_{j}\sum_{k}\sum_{l} T_{ijkl}V_{ik}V_{jl} - \sum_{i}\sum_{k} I_{ik}V_{ik} \qquad (2)$$

$$T_{ijkl} = AC_{ijkl} - B_1\delta_{ij} - B_2\delta_{kl} + (B_1 + B_2)\delta_{ij}\delta_{kl}$$

where $\delta_{ij} = 1$ when $i = j$, otherwise $\delta_{ij} = 0$. Hopfield proved that the energy function is a Liapnov function. Thus the energy function converges to a local minimum as the states of neurons converges to stable states, [13].

3.2 Mapping DHN to HHN

DHN gives an approximate solution of the problem so some neurons might have unexpected final stable states, which may cause mismatching of the objects. On the other hand, CHN gives a near optimal solution since it seeks a solution in a continuous domain. HHN combines the above two types of Hopfield Neural Network. The principal concept of HHN is that output of DHN is used as input of CHN since the configuration of output of DHN is very close to stable states of desired output of CHN. After running DHN, the output is adjusted by an analyzing procedure based upon CHN theory. In fact, adjusting neurons is accomplished without iterations so that running time of HHN is as fast as that of DHN. This method is different from the assumption of Wei's method, which are constraint $\Sigma\Sigma V_{ij} = N$ is valid for initial states, since occluded objects can lose a lot of segments of the original, [12]. Let us consider the adjusting procedure beginning with CHN. Matching process of CHN can

be characterized by the same energy function as that of DHN. Only the integral term is added to the energy function as follows :

$$\sum_i (1/R_i) \int_0^{V_i} g_i^{-1}(V) dV \qquad (3)$$

This term comes from the point of view that u_i will lag because of existence of capacitance in an analog electrical circuit . Thus, there is a resistance-capacitance charging equation, called the equation of motion that determines the rate of change of u_i, [14]. It is the first order differential equation. As explained in the previous section, simulation of the differential equation requires a lot of computations. we solve the equation of the motion in a small interval to reduce computational time caused by the equation of the motion. The equation of the motion is as follows :

$$\frac{du_i}{dt} = -u_i/\lambda + \sum T_{ij}V_j + I_i \qquad (4)$$

First, a sigmoid function is linearly modeled in HHN:

$$g(u_i) = au_i + b \qquad (5)$$

where $t^- < u_i < t^+$ otherwise $g(u_i)=0$. Therefore, a modified motion equation is as follows:

$$\frac{du_i}{dt} = -u_i/\lambda + T_{ik}(au_i + b) + \sum_{i \neq j} T_{ij}V_j + I_i \qquad (6)$$

In a small interval, $\Sigma T_{ij}V_j$ $(j \neq i)$ can be considered as a constant in synchronous / asynchronous neural system, so the behavior of the input state u_i in eq.(8) is:

$$u_i(t) = (u_{ini} - K_1)e^{-k_2 t} + K_1 \qquad (7)$$

where $K_1 = (b + \Sigma T_{ij}V_j + I_i) / (1 - aT_{ii})$ and $K_2 = (1 - aT_{ii})$. As shown in Eq.(7), $u_{ik}(t)$ is decreasing exponentially with small change of time Δt. Deciding the range of Δt with constant $\Sigma\Sigma T_{ij}V_j$ depends on initial states, interactions of unstable states, which causes fluctuation of the change ΔE in the function E. In our algorithm, almost all of the initial states of neurons u_{ini} are close to stable states and only few neurons would be unstable. It is therefore possible that one can estimate future behavior of each neuron from Eq.(7). For example, if u_{ini} is greater than K_1, u_{ik} will monotonically decrease, so input of the ikth neuron will close to K_1; Input state get closer to K_1 as the transien part is exponentially decreasing. K_1 is not a constan but time-varying behavior of inputs of a neuron as tim evolves. Suppose that M is the number of columns an N is the number of rows in a neural structure. W might have mismatched neurons as initial states o CHN. Let active neurons in initial state be $N' + \epsilon$ where N' is the number of exactly matched neurons an ϵ is the number of mismatched neurons at the fina stage of DHN, then the number of inactive neurons i $NxM-(N'+\epsilon)$. Let us assume that T_{ij} is α ($\alpha > 0$ for the positive support and $-\alpha$ for the negative suppor for simplification. Now $K_1(t)$ is calculated and the fina output of each neuron can be analyzed and predicted a follows :

(1) For the neuron to be unmatched

$$K_1(t_0) = \Sigma T_{ij}V_j + I_i + b = -\alpha(N' + \epsilon) + I_i + b \qquad (8)$$
$$K_1(t_f) = \Sigma T_{ij}V_j + I_i + b = -\alpha N' + I_i + b$$
$$V_{final} = sigmoid(u_{final}) = sigmoid(K_1(t_f)) = sigmoid(K_1(t_0)),$$
$$if\ K_1(t_0) = -\alpha(N' + \epsilon) + I_i + b < t^-$$

(2) For the neuron to be matched

$$K_1(t_0) = \Sigma T_{ij}V_j + I_i + b = \alpha(N' - \epsilon) + I_i + b \qquad (9)$$
$$K_1(t_f) = \Sigma T_{ij}V_j + I_i + b = \alpha N' + I_i + b$$
$$V_{final} = sigmoid(u_{final}) = sigmoid(K_1(t_f)) = sigmoid(K_1(t_0)),$$
$$if\ K_1(t_0) = \alpha(N' - \epsilon) + I_i + b > t^+$$

As indicated in Eq.(8), (9), a final output state of a neuron can be predicted by an initial output state because value of $K_1(t_0)$ between a matched neuron and an unmatched neuron are distinguishable. For a neuron to be unmatched, $K_1(t_0)$ is always negative support because $-\alpha(N'+\epsilon) << -1$ and I_i+b is not more than 1 (b is set to 0.5). The restriction therefore is always satisfied. For a neuron to be matched, if ϵ is less than $N' - 1/\alpha(t^- - I_i - b)$, then it makes the matched neuron active, otherwise mismatching occurs. This condition requires that DHN give an approximate solution as an initial states of neurons. If violation of the restriction for the neuron to be matched occurs, all neurons to be matched will be inactive so that one can find the procedure goes to wrong way and can correct the situation by beginning again at the first stage of the algorithm. After running DHN, $K_1(t_0)$ is calculated

with output state of DHN and final output state of HHN is directly obtained from $K_1(t_0)$.

Few neurons might have similar local features which have a fuzzy function to make a false decision because of robustness of features and tolerable threshold levels of a fuzzy function. When the neurons have correspondences of relational features of some neurons to be matched, the neurons remain unstable or cause mismatching in DHN. Once obtaining output stable states of neurons of DHN, we can more emphasize relational features to adjust the states of the neurons because those are related to both a distance and order of all positions of active neurons. It therefore gives more confidence to the theory of HHN and can even improve the performance of CHN.

4. EXPERIMENTAL RESULTS

HHN gives exact matching results between a model object and an input image. Matched nodes have corresponding active neurons. Several images are generated for two different purposes of experiments. Experiments are conducted by increasing the number of occluded segments of an input image to see the bound of matching score while a model object is identified. Our algorithm shows that a model object is identified from a heavily occluded object (for example, more than half of segments are lost). The other experiments are conducted by using many kinds of model objects and input images to see performance of the algorithm. Performance of DHN, CHN, HHN is compared. As shown in Table-1, results of DHN have many mismatched segments which might result in fault decisions. On the other hand, HHN gives almost perfect matching in the experiments. CHN produced good results as HHN did, but running time of CHN which used the Runge-Kutta method to simulate the equation of motion, was five times as much as that of HHN. Coefficients of energy function in Eq.(1) A, B_1, B_2 are chosen as 1.0, 0.5, 0.5. External bias I_i is set to 0.5. The results of HHN are shown in Figures 1 to 4. Model objects shown in the figures are a handgun, a hammer and a couple of pliers. Experiment-1 and Experiment-2 shows that all nodes are preserved. Only one nodes is lost in Experiment-3. In the Experiment-4, even if almost half segments are lost, the results of HHN shows the robustness of the algorithm. All the figures show perfect matching.

5. DISCUSSION

A method for recognizing occluded objects based on neural network approach has been presented. Features such as angle and distance which are invariant under a rotational and translational changes are used for the robust description of the shape. Experimental results show that HHN gives a reliable matching of the corresponding segments between two objects. The method eliminates possibility of matching for a part of an object to be matched to similar segments in a different object by finally adjusting states of neurons. We conclude that HHN is a robust approach to solve the two-dimensional occlusion problems.

REFERENCES

1. B. Bhanu and O.D. Faugeras, "Shape matching of two-dimensional objects," *IEEE Trans. Pattern Anal. Machine Intell.*, PAMI-6, pp. 137-155, 1984.

2. W.K. Chow and J.K. Aggarwal, "Computer analysis of planar curvilinear moving images," *IEEE Tran. Comput.* C-26, pp. 179-185, February, 1987.

3. J.L. Turney, T.N. Mudge and R.A. Volz, "Recognizing partially occluded parts," *IEEE Trans. Pattern Anal. Machine Intell.*, PAMI-7, pp. 410-421, 1985.

4. R.C. Bolles and R.A. Cain, "Recognizing and locating partially visible objects: the local-feature-focus method," *Int. J. Robot.* Res. 1, pp 57-82, 1982.

5. Mark W. Koch and Rangasami L. Kashyap, "Using polygon to recognize and locate partially occluded objects," *IEEE Trans. Pattern Anal. Machine Intell.*, PAMI-9, No. 4, pp. 483-494, 1987.

6. Bir Bhanu and John C. Ming, "Recognition of occluded objects: A cluster-structure algorithm," *IEEE Pattern Recognition* vol. 20, No. 2, pp. 199-211, 1987.

7. R. C. Bolles and R. A. Cain, "Recognizing and locating partially visible objects: The focus feature method," *Int. J. Robotics Res.*, vol. 1, No. 3, pp.36-61, Fall 1982.

8. W. S. Rutkowski, "Recognition of occluded shapes using relaxation," *Computer Graphics Image Processing*, vol.19, pp. 111-128, 1982.

9. Kwanghoon et al. "Optimal curvature estimation using constrained regularization technique" *25th Asilomar on SSC*, 1992 (In press).

10. J. J. Hopfield and D. W. Tank, "Neural computation of decisions in optimization problems," *Biolog. Cybernet.*, vol. 52, pp. 141-152, 1985.

11. J. J. Hopfield and D. W. Tank, "Computing with Neural circuits: A model," *Science*, vol. 233, pp. 625-633, 1986.

12. W. Lin, F. Liao, C. Taso, and T. Lingutle, "A hierarchical Multiple-view approach to three-dimensional object recognition," *IEEE Tras. on Neural Net.* vol. 2, pp. 84-92, 1991.

13. W. Li and M. Nasrabadi, "Object recognition based on graph matching implemented by a hopfield-style neural network," *Int. J. Conf. Neural Networks.*, *II* , pp. 287-290, June 18-22, 1989.

14. J. J. Hopfield, "Neurons with graded response have collective computational properties like those of two-state neurons" *Proc. Natl. Acad. Sci. USA* vol. 81, pp 3088-3092, May 1984.

15. Rafael C. Gonzalez, *Digital Image Processing* Addison - Wesley Publishing Co., 1987.

Table 1. Comparison of Results

Type	Experiment	# of desired Matched Neurons	# of Matched Neurons	# of Unmatched Neurons	# of Mismatched Neurons
DHN	Experiment #1	10	9	1	4
	Experiment #2	10	10	0	2
	Experiment #3	6	7	1	4
	Experiment #4	7	7	0	1
HHN	Experiment #1	10	9	1	0
	Experiment #2	10	10	0	0
	Experiment #3	6	6	0	0
	Experiment #4	7	7	0	0

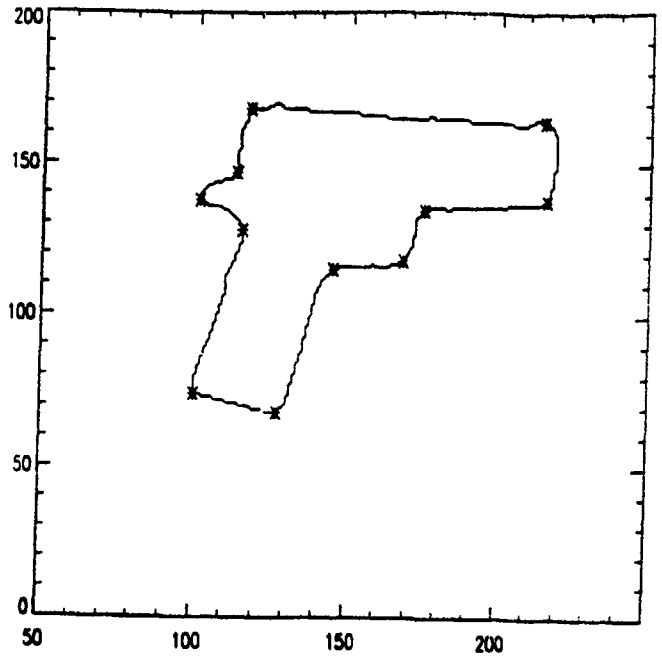


Fig. 1a. Boundary of a Model Object

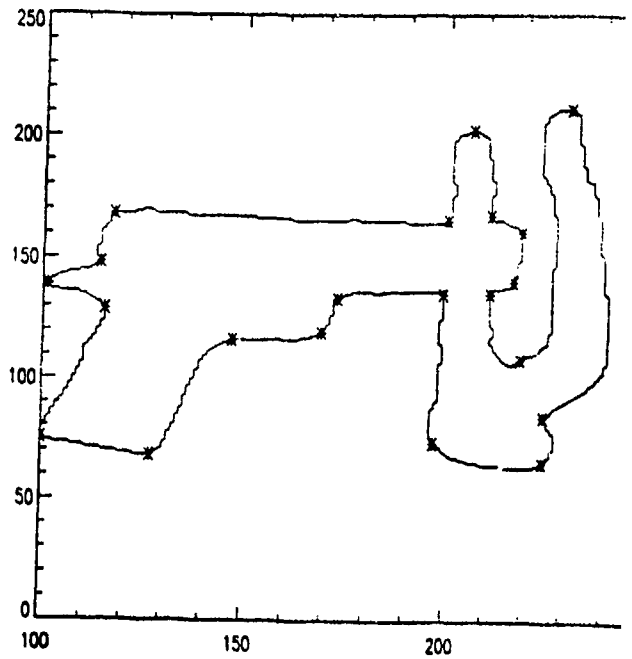


Fig. 1b. Boundary of an Input Object

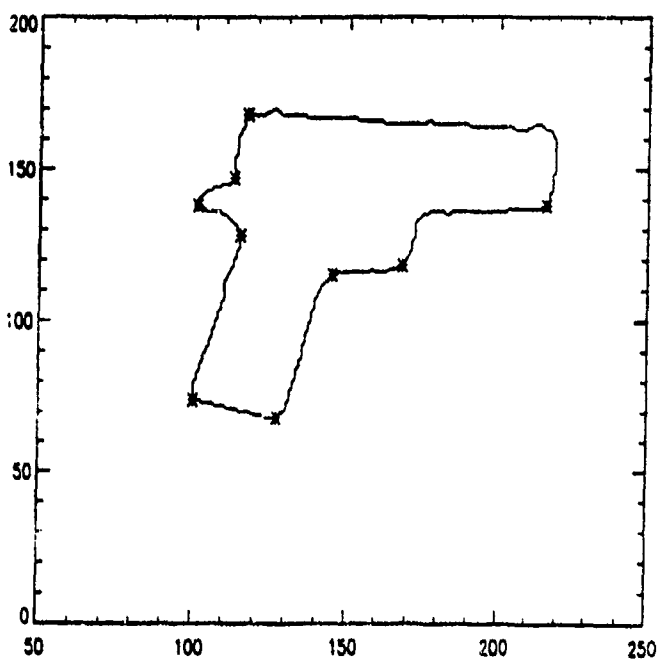


Fig. 1c. Matched Nodes of a Model Object

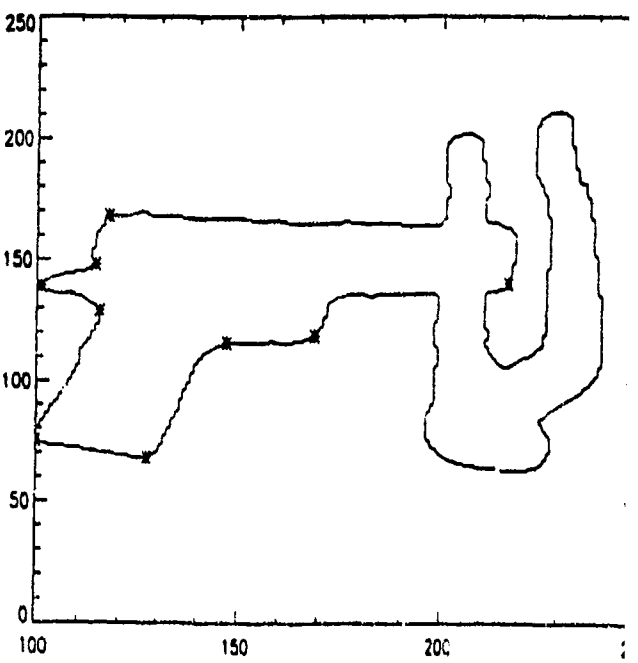


Fig. 1d. Matched Nodes in an Input Object

Fig. 1: Experiment - 1 (a Handgun and a Plier)

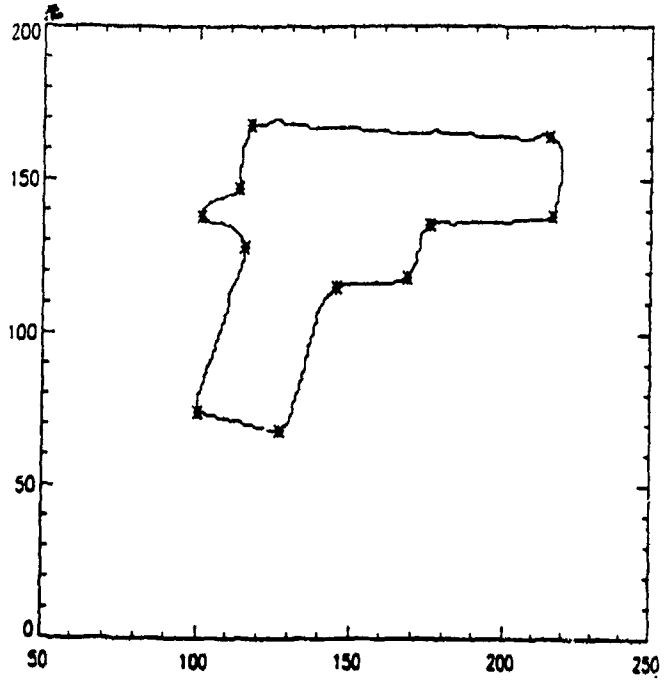


Fig. 2a. Boundary of a Model Object

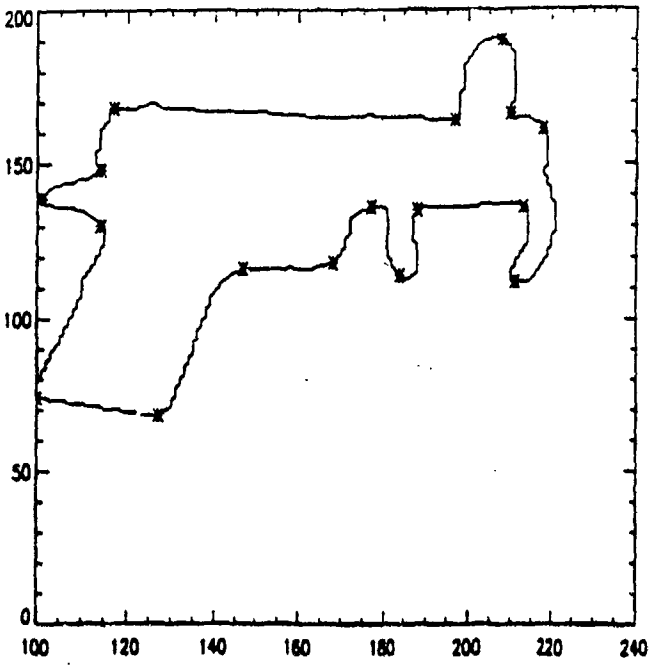


Fig. 2b. Boundary of an Input Object

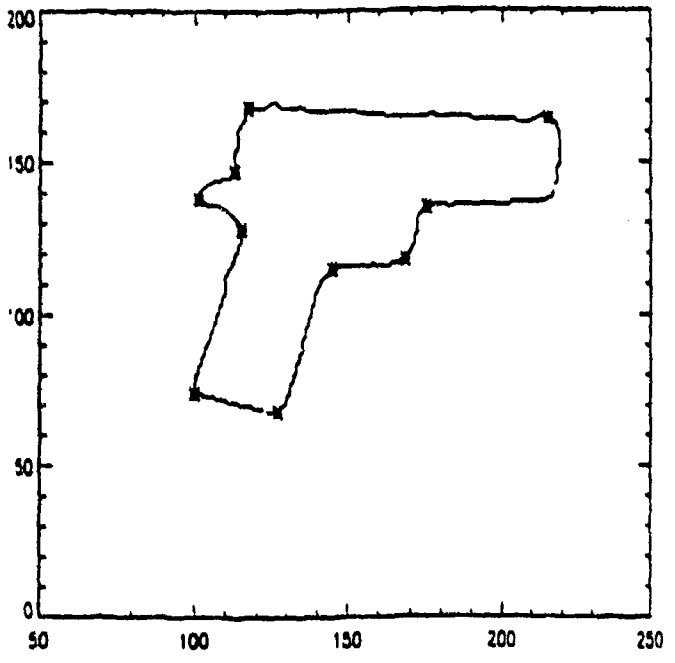


Fig. 2c. Matched Nodes of a Model Object

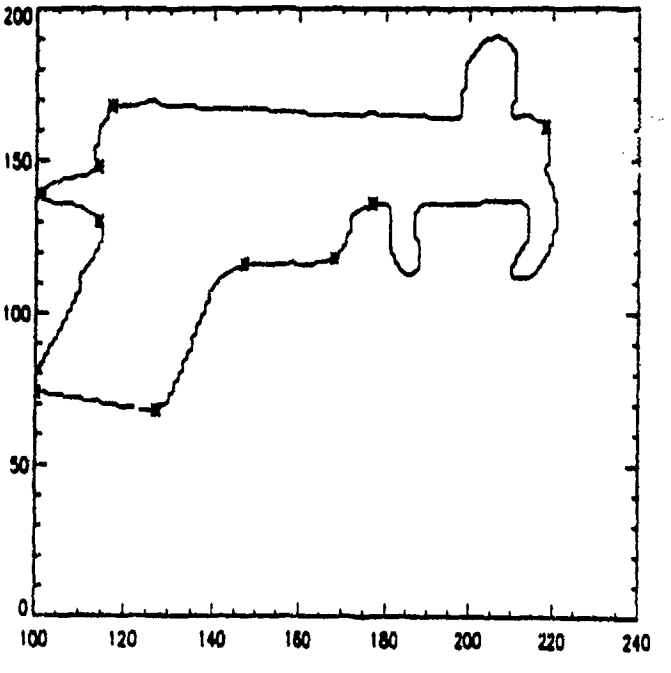


Fig. 2d. Matched Nodes in an Input Object

Fig. 2: Experiment - 2 (a Handgun and a Plier)

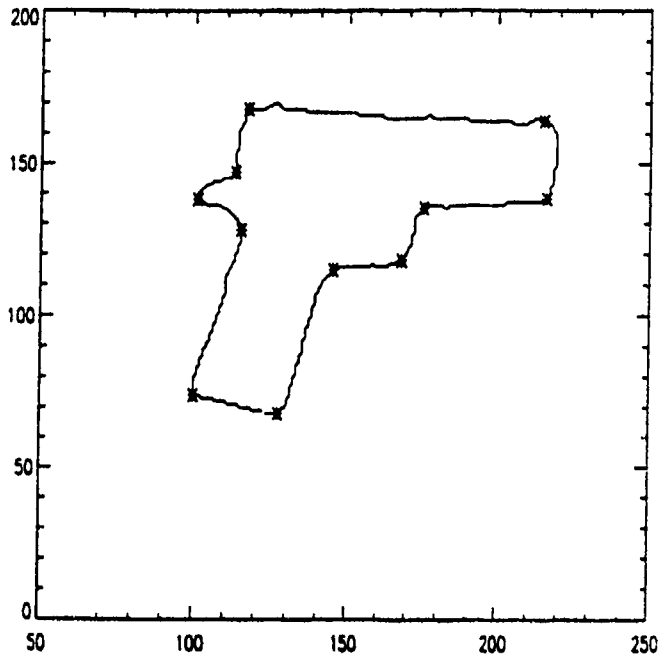


Fig. 3a. Boundary of a Model Object

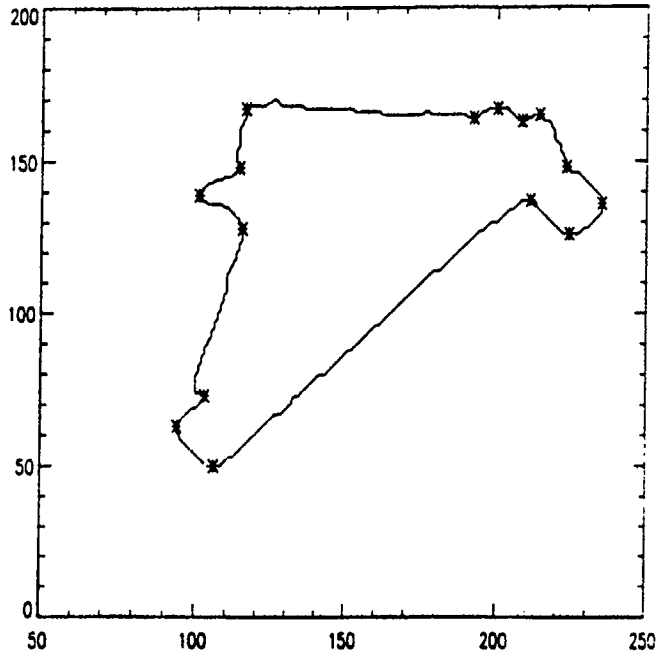


Fig. 3b. Boundary of an Input Object

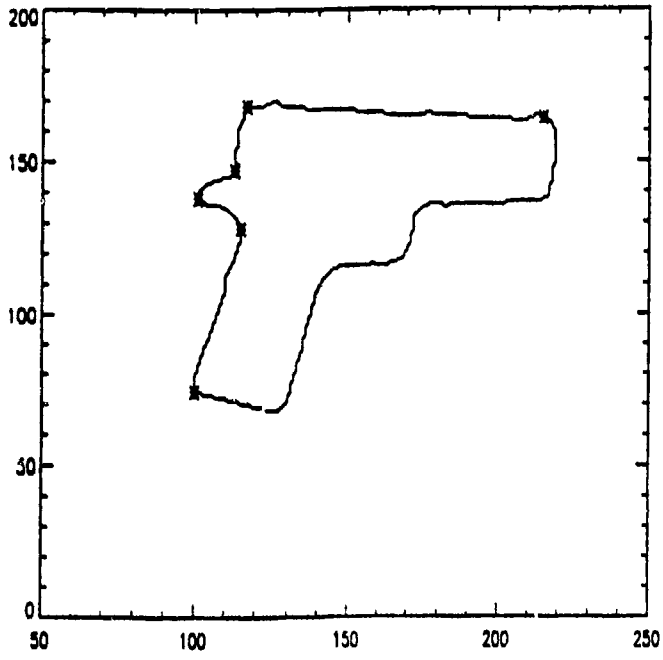


Fig. 3c. Matched Nodes of a Model Object

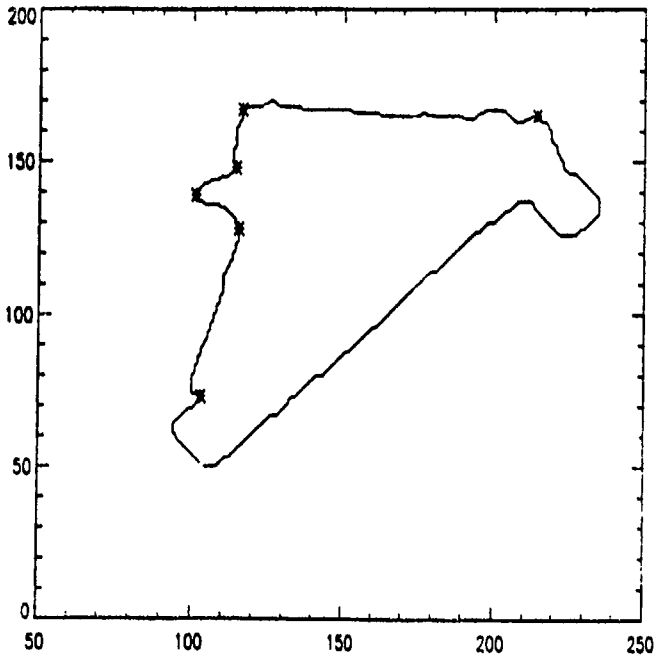


Fig. 3d. Matched Nodes in an Input Object

Fig. 3: Experiment - 3 (a Handgun and a Hammer)

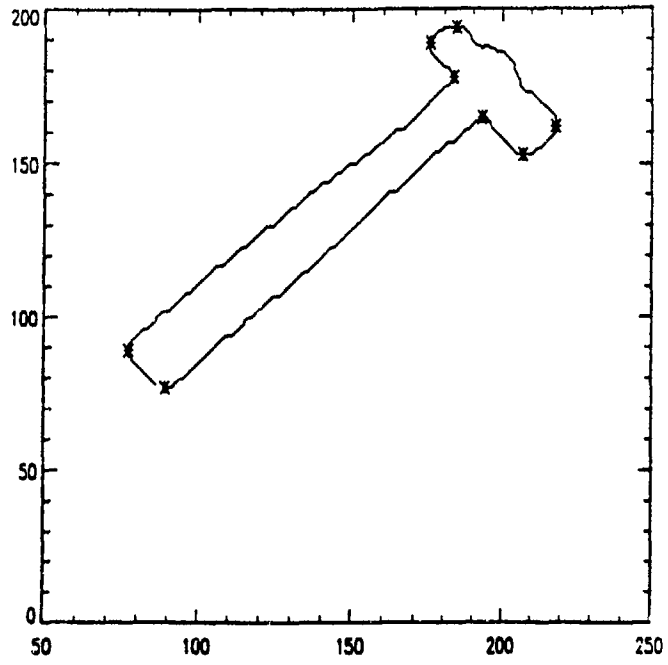


Fig. 4a. Boundary of a Model Object

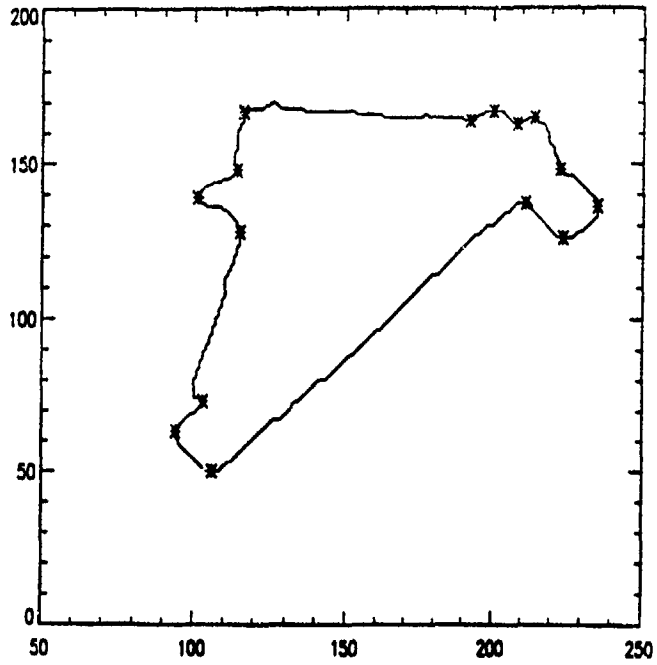


Fig. 4b. Boundary of an Input Object

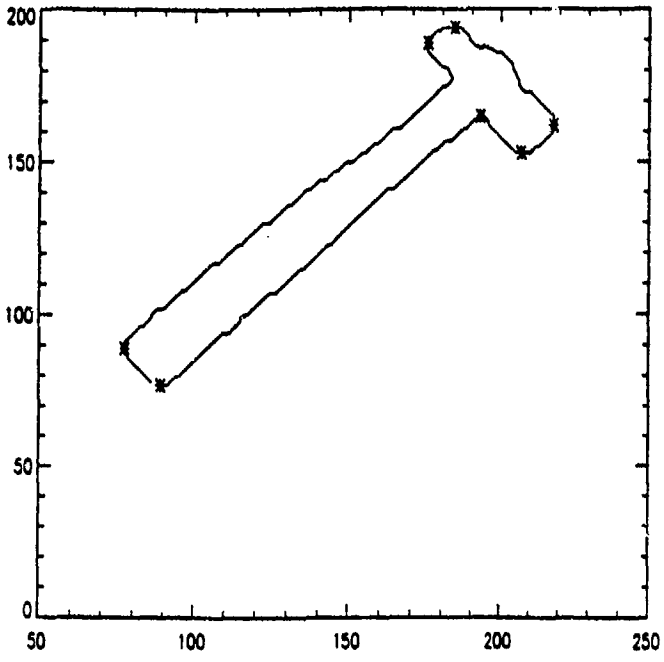


Fig. 4c. Matched Nodes of a Model Object

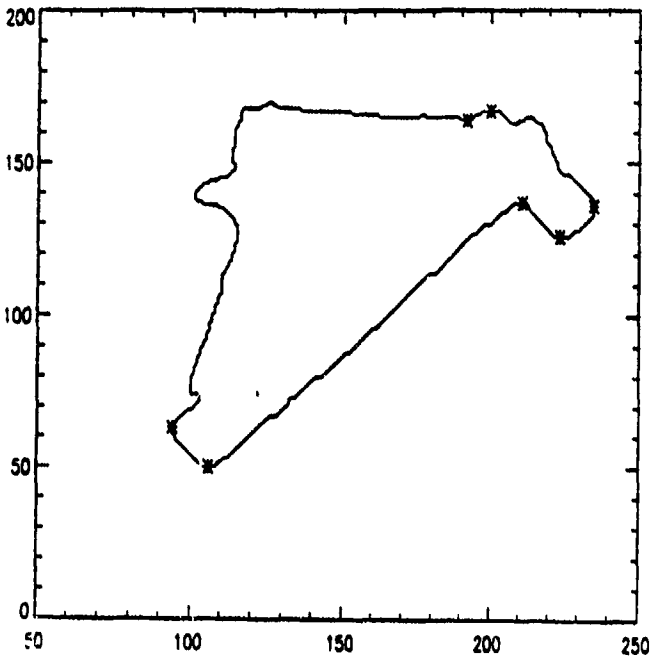


Fig. 4d. Match Nodes in an Input Object

Fig. 4: Experiment - 4 (a Hammer and a Handgun)

SEGMENTATION OF X-RAY IMAGES USING PROBABILISTIC RELAXATION LABELING

Tan Q. Thai
Sandia National Laboratories
Albuquerque, NM 87185

1. INTRODUCTION

One of the most important tasks of an image analysis system for contraband detection using X-ray images is to separate objects or regions of interest from their background or other objects in the image. The segmentation problem can be stated as follows: Given an X-ray baggage image and some limited a-priori knowledge about the image characteristics of a contraband item, we want to label all pixels in the image into two classes: one class has similar image characteristics of the contraband and the other does not. Although segmentation of an image can be done with many different methods, there are three general approaches to the problem: 1) pixel-based approach, 2) region-based approach, and 3) model-based approach.

Pixel-based algorithms segment an image using information such as grey level, gradient magnitude or color of each pixel independently from its neighboring pixels. The pixels' information can then be used in a cumulative fashion as in histogram thresholding [3] or thresholding based on the degree of membership of the image pixels using fuzzy set concept [7]. Region-based approach takes into consideration the information of the neighboring pixels and their relations with the examined pixel. A pixel is assigned to the same region (class, cluster, etc.) if it has similar properties to its neighbors. One method of region-based approach is region growing [6]. Using this method the image is first divided into atomic regions of constant grey levels, then similar adjacent regions are merged sequentially until the adjacent regions become sufficiently different. Examples of region-based algorithms are the K-means clustering [12], the split-and-merge [6] and morphological segmentation using watershed transform with markers [4]. Unlike the pixel-based and region-based approaches that make no assumption about the image content and its noise, the model-based approach attempts to model both the image content and the image noise. Markov random field is often used to model the local properties and dependencies among neighboring pixels of regions in an image and Gaussian noise is assumed as the image noise mode [1,5].

Probabilistic relaxation labeling (PRL) segmentation is an iterative algorithm that labels each pixel in an image by cooperative use of two information sources: the probability that a pixel belongs to a class and the degree of certainty of its probability supported by the neighboring pixels. PRL algorithm can be considered as a hybrid approach of both region-based and model-based algorithms because of the dependency of each pixel to its neighbors in the labeling process and the assumption that each pixel can be assigned a probability index.

Details of the PRL algorithm are shown in Section 2. Practical implementation of the PRL segmentation algorithm is discussed in Section 3. Its application to X-ray baggage images and a comparison of the results with other methods are presented in Section 4.

2. PROBABILISTIC RELAXATION LABELING SEGMENTATION

The idea of cooperative use of two sources of information in pixel classification through the mechanism of probabilistic relaxation was first developed by Rosenfeld et al. [11]. In essence the basic concept of the method is to iteratively reduce local ambiguities by optimizing a probabilistic index associated with a pixel in classifying a pixel using local contextual information of the neighboring pixels. The method, however, does not guarantee a unique optimal solution but rather seeks a practical suboptimal solution.

The relaxation labeling process is defined as the "best" assignment of a set of pixels $A = \{a_1, a_2, \ldots, a_N\}$ to a set of labels (or classes) $\Lambda = \{\lambda 1, \lambda 2, \ldots, \lambda M\}$ where N is the total number of pixels in the image and M is the total number of labels (classes). Initially each pixel a_i is given a probability that it

belongs to a label λ_l, $p_i(\lambda_l)$. These probabilities must satisfy the following constraints:

$$0 \le p_i(\lambda) \le 1 \quad \text{and} \quad \sum_{l=1}^{M} p_i(\lambda_l) = 1$$

For each pair of neighboring pixels a_i, a_j and each pair of labels λ_k, λ_l, we assume that there exists a measure of compatibility (compatibility coefficient) that $a_i \in \lambda_k$ and $a_j \in \lambda_l$. This measure of compatibility, denoted as $r_{ij}(\lambda_k, \lambda_l)$ has the following properties:

a) $-1 \le r_{ij}(\lambda_k, \lambda_l) \le 1$

b) If the assignment of pixels a_i, a_j to labels λ_k, λ_l is compatible then $r_{ij}(\lambda_k, \lambda_l) > 0$

c) If the assignment of pixels a_i, a_j to labels λ_k, λ_l is not compatible then $r_{ij}(\lambda_k, \lambda_l) < 0$

d) If the assignment of a_i to λ_k and a_j to λ_l is independent of each other then $r_{ij}(\lambda_k, \lambda_l) = 0$

The iterative update process of the image pixels incorporates the information of both the pixel's initial probability and the influence of neighboring pixels based on the compatibility coefficients. One heuristic update process [10,11] is given as follows

$$p_i^{m+1}(\lambda) = \frac{p_i^m(\lambda)\,(1 + q_i^m(\lambda))}{\sum_{l=1}^{M} p_i^m(\lambda_l)\,(1 + q_i^m(\lambda_l))} \qquad (1)$$

where

$$q_i^m(\lambda) = \sum_{j=1}^{K} w_{ij} \sum_{l=1}^{M} r_{ij}(\lambda, \lambda_l)\, p_j^m(\lambda_l). \qquad (2)$$

m is the iteration number, K is the total number of neighboring pixels, w_{ij} are the weighting coefficients for the contribution of the neighboring pixels j in the labeling process to pixel i, and M is the total number of labels (classes).

The update rule is simply a product of both p_i, the pixel probability and q_i, the degree of certainty of its probability, supported by the neighboring pixels. Since the range of r_{ij}'s is [-1, 1], 1 is added to q_i to ensure that $p_i^{m+1}(\lambda)$ is always in the range of [0, 1]. The denominator of the update rule, which is a normalizing factor, ensures that the probability of pixel i is summed to 1 for all possible M labels.

Given the update rule, how can we determine the initial probabilities of all image pixels? What is a good number for the neighboring system in the update rule? How do we select the compatibility coefficients r_{ij}'s? Although different answers to these questions can lead to slightly different results in evaluating the relaxation update rule, the overall relaxation update should consistently reduce the ambiguity in the labeling process. Fekete et al [2] suggested two criteria to measure the performance of the probabilistic relaxation process: the rate of change between consecutive updates

$$R(m) = \frac{1}{N} \sum_{i=1}^{N} \left[\sum_{l=1}^{M} \left[p_{il}^{m+1} - p_{il}^{m} \right]^2 \right]^{1/2} \qquad (3)$$

and the entropy of the pixel probabilities evaluated at each iteration

$$H(i, m) = -\sum_{l=1}^{M} p_{il}^{m} \ln p_{il}^{m} \qquad (4a)$$

$$H(m) = \frac{1}{N \ln M} \sum_{i=1}^{N} H(i,m) \qquad (4b)$$

where N is the number of pixels in the image, M is the total number of labels and m is the iteration index. In general, the rate of change and entropy between updates should be decreased in the relaxation update process. The measures, however, are not true indicators of the performance measures because they tell us nothing about the correctness of the segmentation results. Therefore, instead of using them as performance measures, we only use them as convergence criteria for the update process.

2.1 Assignment of Initial Labeling Probability

Most commonly the image's histogram is used to assign the initial labeling probability to each pixel in the image. A histogram represents the relative frequency of occurrences of the grey levels in the image.

$$p(x_i) = \frac{n(x_i)}{N}, \qquad i = 0, 1, \ldots, L-1$$

where L is the number of grey levels, $n(x_i)$ is the number of occurrence of pixels with grey level i in the image, and N is the total number of pixels in the

image. This assignment, however, doesn't take into consideration the a-priori knowledge about the classes that we want to segment the image into. In our application of segmenting X-ray baggage images, the a-priori knowledge can be the average grey level of the X-ray images of a certain type of contraband that we want to extract from the input image. Since the a-priori knowledge is only an estimate, it is more appropriate to model the assignment of the initial probability by the S function [13, 7] which is defined as

$$S(x; a, b, c) = \begin{cases} 0, & x \le a \\ 2\left(\frac{x-a}{c-a}\right)^2, & a \le x \le b \\ 1 - 2\left(\frac{x-c}{c-a}\right)^2, & b \le x \le c \\ 1, & x \ge c \end{cases} \quad (5)$$

with $b = \frac{a+c}{2}$ and $a \le b \le c$. Figure 1 shows an example of the S function with the same crosspoint b for different values of a's and c's. If the crosspoint b is an estimate of the average grey level of an X-ray contraband image, then the S function defines the membership function corresponding to a fuzzy set "grey level x is similar to the contraband average grey level". The "spread" of the S function which controls by the distance (c - a) is a measure of fuzziness (uncertainty) in associating a grey level x to the contraband average grey level. As (c - a) approaches zero, the S function becomes a simple thresholding function about the crosspoint value b.

2.2 Selection of Compatibility Coefficients

The compatibility coefficients are the measures of how much the labeling of a pixel is compatible with what its neighbors "think" that labeling ought to be. There are many ways to select these coefficients according to different definitions of compatibility functions [9].

The simplest selection of compatibility coefficients is to restrict them to the extreme values -1 and 1

$r_{ij}(\lambda,\lambda') = +1 \quad$ if $\lambda = \lambda'$

$r_{ij}(\lambda,\lambda') = -1 \quad$ if $\lambda \neq \lambda'$

This assignment does not take into consideration the fact that a pair of labels can spatially co-occur in the image. To account for these co-occurences, one way to estimate the coefficients is using conditional probabilities. Let $p_i(\lambda)$ be the initial estimate of the probability that a pixel i having label λ, then the probability of all pixels in the image having label λ is given by

$$p(\lambda) = \frac{1}{N} \sum_{i=1}^{N} p_i(\lambda)$$

The joint probability of a pixel pair having label λ at pixel i and λ' at pixel j relative to i (e.g. pixel j is one pixel on the south side from i) is estimated as follows

$$p_{ij}(\lambda,\lambda') = \frac{1}{N} \sum_{i=1}^{N} p_i(\lambda)\, p_{i+j}(\lambda')$$

Given the above probabilities, the conditional probability is given by

$$p_{ij}(\lambda \mid \lambda') = \frac{p_{ij}(\lambda,\lambda')}{p(\lambda')} = \frac{\sum_{i=1}^{N} p_i(\lambda)\, p_{i+j}(\lambda')}{\sum_{i=1}^{N} p_i(\lambda')} \quad (6)$$

Note that the estimate of the compatibility coefficients using conditional probabilities are global estimates because it is computed only once for a given neighboring configuration system. Once computed the coefficients are kept constant during the update process. The estimates only reflect the overall dependencies among neighboring pixels of the entire image; therefore, they may not be good estimates for local dependencies. For images with different textural details, local dependencies can be preserved by using a different estimate that applies only to local neighboring pixels. Such estimates can be computed by simply replacing N (total number of pixels in the image) with K (total number of pixels in the neighboring system). One drawback, however, is the significant increase in the overall computation of the algorithm. If conditional probabilities are used for compatibility coefficients, the relaxation update rule can be reformulated using Bayesian probability theory [8] with the assumption that the probability of pixel i given its label is λ is independent of its neighboring pixel's label. The relaxation update scheme is now given by

$$p_i^{m+1}(\lambda) = \frac{p_i^m(\lambda)\, q_i^m(\lambda)}{\sum_{l=1}^{M} p_i^m(\lambda_l)\, q_i^m(\lambda_l)} \quad (7)$$

where q_i is in the same formulation as in Eq. (2). The update rule is basically the same as Eq. (1); the only difference is the elimination of 1 because the compatibility coefficients are now in the range of [0, 1] instead of [-1, 1] as before.

Experimentally we find that one set of compatibility coefficients does not work well for X-ray baggage images because the estimate is done globally. For example, if a bag is small and the background level is dominant then the estimated compatibility coefficients tend to bias toward the background. To compensate for the bias in the estimate, we propose the use of two update passes using two different sets of compatibility coefficients. The first set of coefficients can be viewed as estimates from images with more background than baggage details; while the second set is the estimates from images with cluttered baggage details. The biggest advantage of this method is that the compatibility coefficients do not have to be computed on-line for each image but they can be "learned" off-line from a number of different images.

3. ALGORITHM IMPLEMENTATION

Because the compatibility coefficients can be calculated off-line, the implementation of the PRL algorithm becomes very simple for the two-class segmentation problem. Recall from Eq. (2), the local dependency information in the labeling process for the two-class problem is given by a vector. (For notation convenience, from now on $q_i(\alpha)$ is written as $q_{i\alpha}$.)

$$\begin{bmatrix} q_{i\alpha}^n \\ q_{i\beta}^n \end{bmatrix} = \begin{bmatrix} \sum_{j=1}^{K} w_{ij}\, q_{j\alpha}^n \\ \sum_{j=1}^{K} w_{ij}\, q_{j\beta}^n \end{bmatrix} \qquad (8)$$

where

$$\begin{bmatrix} q_{i\alpha}^n \\ q_{i\beta}^n \end{bmatrix} = \begin{bmatrix} r_{ij}(\alpha,\alpha) & r_{ij}(\alpha,\beta) \\ r_{ij}(\beta,\alpha) & r_{ij}(\beta,\beta) \end{bmatrix} \begin{bmatrix} p_{j\alpha}^n \\ p_{j\beta}^n \end{bmatrix}$$

with α and β as the two classes. Let

$$c1 = r_{ij}(\alpha,\alpha)$$
$$c2 = r_{ij}(\alpha,\beta)$$
$$c3 = r_{ij}(\beta,\alpha)$$
$$c4 = r_{ij}(\beta,\beta)$$

then

$$q_{i\alpha} = c1 \sum_{j=1}^{K} w_{ij}\, p_{j\alpha} + c2 \sum_{j=1}^{K} w_{ij}\, p_{j\beta} \qquad (9)$$

since $p_{j\alpha} = 1 - p_{j\beta}$ and $\sum_{j=1}^{K} w_{ij} = 1$, we have

$$q_{i\alpha} = (c1 - c2) \sum_{j=1}^{K} w_{ij}\, p_{j\alpha} + c2 \qquad (10a)$$

Similarly,

$$q_{i\beta} = (c3 - c4) \sum_{j=1}^{K} w_{ij}\, p_{j\beta} + c4 \qquad (10b)$$

Therefore (7) becomes

$$p_{i\alpha}^{n+1} = \frac{p_{i\alpha}^n\, q_{i\alpha}^n}{p_{i\alpha}^n\, q_{i\alpha}^n + (1 - p_{i\alpha}^n)\, q_{i\beta}^n} \qquad (11)$$

Theoretically, the range of pixel values in a PRL should be [0.0, 1.0]; however, for display purposes the pixel values must range from [0, 255] for an 8 bit image. The mapping from real values to integer values is simply done as follows

$$p'^{n}_{i\alpha} = \mathrm{ceil}(p_{i\alpha}^n * 255.0)$$

where p' is a displayed pixel value and ceil(x) is a function that returns a smallest integer which is greater than or equal to x. If we neglect the round off errors in the mapping, Eq. (11) can be implemented with a 64K integer look-up-table (LUT). The 64K size of the update rule LUT is used to account for all possible results in the product of p's and q's. Figure 2 shows the block diagram of the PRL algorithm for two-class problem. All computations for the initial probabilities, update rule, and the convergence criteria can be implemented using LUTs and a convolver. Because both the LUT and convolution (especially with 3x3 and 5x5 kernels) can be executed in real-time (30 frames/second) in many inexpensive image processing hardware, each iteration of the PRL can be completed in less than 100 ms.

4. EXPERIMENTAL RESULTS

The experimental results are based on X-ray images that are taken from a local airport. The image size is 512 x 512 with 256 grey levels. In this paper, we only show the results from two X-ray baggage images using four different methods: PRL, adaptive histogram thresholding, constrast intensification using fuzzy set concept [7] and Iterated Conditional Modes (ICM) [1, 3]. The adaptive histogram thresholding is a simple, one pass segmentation using an adaptive threshold which is defined as the peak of the image's histogram that falls within the segmenting class' variance and has a certain height. (The peak height is used for size discrimination purpose.) The peak is found using the top-hat transformation [4]

$$\text{Peak} = H - O(H)_n$$

where H is the image histogram and $O(H)_n$ is the opening of H by a line structure element of n pixels long. The opening operation is defined by an erosion followed by a dilation.

The contrast intensification using fuzzy concept is an iterative algorithm which attempts to assign individual pixel values into different classes based on their initial membership function. The assignment is done recursively with the following operation

$$T(x) = \begin{cases} 2[T(x)]^2, & 0 \le x \le 0.5 \\ 1 - 2(1 - T(x))^2, & 0.5 \le x \le 1.0 \end{cases}$$

Details of the algorithm can be found in [7].

The ICM algorithm is a model-based method. In its simplest form, the method iteratively minimizes the following energy function

$$U = \frac{1}{2}\ln(\sigma_\alpha^2) + \frac{(x-\mu_\alpha)^2}{2\sigma_\alpha^2} + \sum_{r=1}^{c} \beta_r [1 - J(\alpha, \alpha_r) + 1 - J(\alpha, \alpha_{-r})]$$

where α is the class label, σ_α^2 and μ_α are the variance and mean of class α, respectively, β_r is the clique' parameter, and J(a,b) is the spatial interaction among the clique neighbors.

4.1 Test Parameters

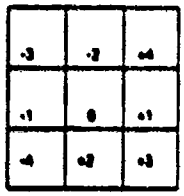
All parameters of the four tested algorithms[2] are fixed during the entire segmentation process. They are the following.

- Adaptive histogram thresholding:
  Structure element = {1, 1, 1, 1, 1}
  Minimum peak height = 800
  μ_1 = 15 (average grey level of class 1)
  σ_1 = 6.5

- Contrast intensification with fuzzy set:
  μ_1 = 15
  Fe^2 = 2

- Iterated conditional modes:
  J(a, b) = 1 if a = b
  = 0 if a ≠ b
  μ_1 = 15
  μ_2 = 60
  $\sigma_1 = \sigma_2$ = 6.5
  β_r = 1.5 for all r

c = 4 and the relative neigborhood configuration (r's) is as follows:



- Probabilistic relaxation labeling:
S function parameters:
  a = 0.0, c = 25.0
Compatibility coefficients for pass 1:
  r_{00} = 0.62; r_{01} = 0.38; r_{10} = 0.57; r_{11} = 0.43
Compatibility coefficients for pass 2:
  r_{00} = 0.49; r_{01} = 0.51; r_{10} = 0.45; r_{11} = 0.55
3x3 convolution mask = {1, 1, 1, 1, 2, 1, 1, 1, 1}

Except for the adaptive histogram threshold, the other three methods are iterative. The iteration loop is fixed to 7 for those methods.

4.2 Results and Discussion

Figures 3 and 8 show two original baggage X-ray images. The results of adaptive histogram threshold method are shown in Fig. 4 and 9. Only the final results from the last iteration are displayed for each iterative algorithm. Fig. 5 and 10 are the results of PRL segmentation. These images are taken from the second pass of the algorithm. The results of the contrast intensification using fuzzy set concept are shown in Fig. 6 and 11. Finally, Fig. 7 and 12 are the results from the ICM algorithm. Although the high density and cluttered areas in the test images can

be segmented out with all four methods, the results from the PRL method are much cleaner. For example in Fig. 5 we can detect the objects from the cluttered areas in the two bags easier than with the results from other methods.

Although the results from the PRL method are visually better than those of the other methods, assigning a "measure of performance" to their results is not a trivial task. The rate of change between consecutive updates and the entropy measurements proposed by Fekete et al. [2] do not guarantee the correctness of the segmentation results. For example, among the iterative algorithms, the rate of change between updates and entropy of the Iterated Conditional Modes method decreases faster than other methods; however, by visual inspection, one can conclude that its results are poorer than those of other methods. Using "true map" (a known segmentation result) then computing a deviation (e.g. mean square error) from the segmented results and the true map is also not a valid measure of performance because different parameters in the algorithms can give different results. Therefore, a fair comparison must not only be done with various possible combinations of the algorithms' parameters but also over a large number of data.

After testing the four different algorithms on a number of X-ray baggage images, the PRL is selected over other methods based on the following considerations:

1) Good and consistent performance (based on visual inspection).

2) Extendable to multiple classes and image characteristics other than grey level based such as color, texture, volume density, shape and size.

3) Processing time is suitable for real-time baggage checking applications.

5. CONCLUSION

The paper presents a method of segmenting X-ray baggage images using probabilistic relaxation labeling (PRL). To compensate for the bias in estimating the compatibility coefficients, we propose the use of two different sets of coefficients for two update passes. These coefficients can be estimated off-line from a number of baggage images instead of on-line from the examined image as proposed in various literature. For a two-class problem it is shown that all computation of the PRL method can be implemented with look-up tables and a convolver. Using a real-time convolver that processes at a rate of 30 image frames/second, the PRL process can be done under one second. In addition, the algorithm can also be extended to segment contrabands based on other features such as color, texture, volume density, shape and size.

REFERENCES

1. J. Besag, "On the statistical analysis of dirty pictures", J. Roy. Statist. Soc. B., vol. 48, no. 3, pp. 2181-2197, 1984.

2. G. Fekete, J. Eklundh, and A. Rosenfeld, "Relaxation: evaluation and applications", IEEE Trans. on PAMI, vol. 3, no. 4, pp. 459-469, July 1981.

3. K. V. Mardia and T. J. Hainsworth, "A spatial thresholding method for image segmentation", IEEE Trans. PAMI, vol. 10, pp. 919-927, 1989.

4. F. Meyer and S. Beucher, Morphological Segmentation, Centre de Morphologie Mathematique, School of Mines, Tech. Report, Apr. 1990.

5. T. N. Pappas and N. S. Jayant, "An adaptive clustering algorithm for image segmentation", IEEE Second International Conf. on Computer Vision, pp. 310-315, 1988.

6. T. Pavlidis, Algorithms for Graphics and Image Processing, Computer Science Press, 1982.

7. S. K. Pal and R. A. King, "Image enhancement using smoothing with fuzzy sets", IEEE Trans. Syst., Man, Cybern., vol. SMC-11, no. 7, pp. 494-501, July 1981.

8. S. Peleg, "A new probabilistic relaxation scheme", IEEE Trans. on PAMI, vol. 2, no. 4, July 1980.

9. S. Peleg and A. Rosenfeld, "Determining compatibility coefficients for curve enhancement relaxation processes," IEEE Trans. Syst., Man, Cybern., vol. SMC-8, no. 7, pp. 548-556, July 1978.

10. A. Rosenfeld, "Iterative methods in image analysis," Pattern Recognition, vol. 10, pp.181-187, 1978.

11. A. Rosenfeld, R. A. Hummel, and S. W. Zucker, "Scene labeling by relaxation operations," IEEE Trans. Syst., Man, Cybern., vol. SMC-6, pp. 420-433, 1976.

12. J. Tou and R. Gonzales, Pattern Recognition Principles, Addison-Wesley, 1974.

13. L. A. Zadeh, K. S. Fu, K. Tanaka, and M. Shimura, Eds., Fuzzy Set and Their Applications to Cognitive and Decision Processes, Academic, 1975.

NOTES

1. A clique is a set of points that are neighbors of each other.

2. See Reference [7] for explanation of the algorithm's parameters.

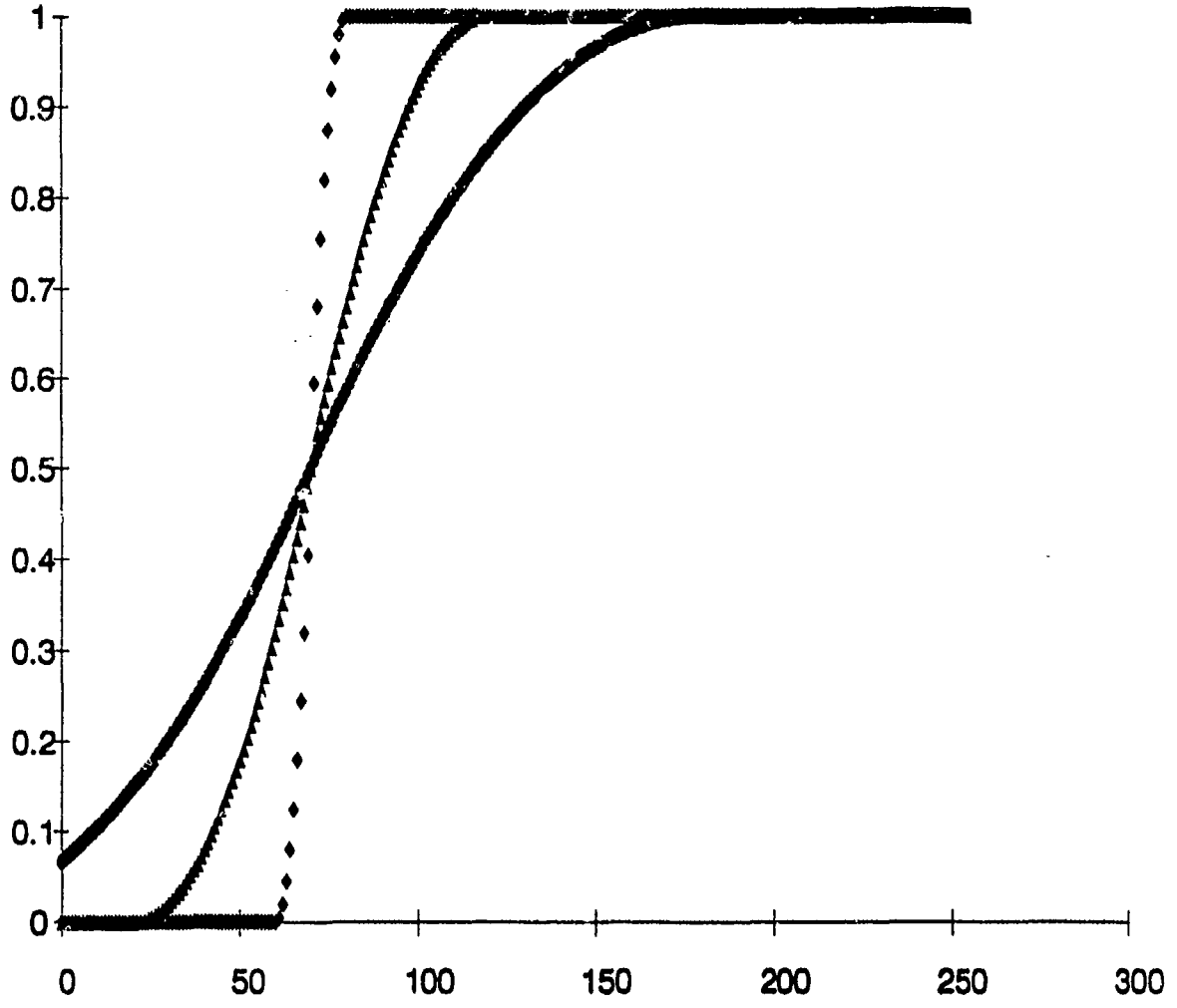


Figure 1: S function with different parameters

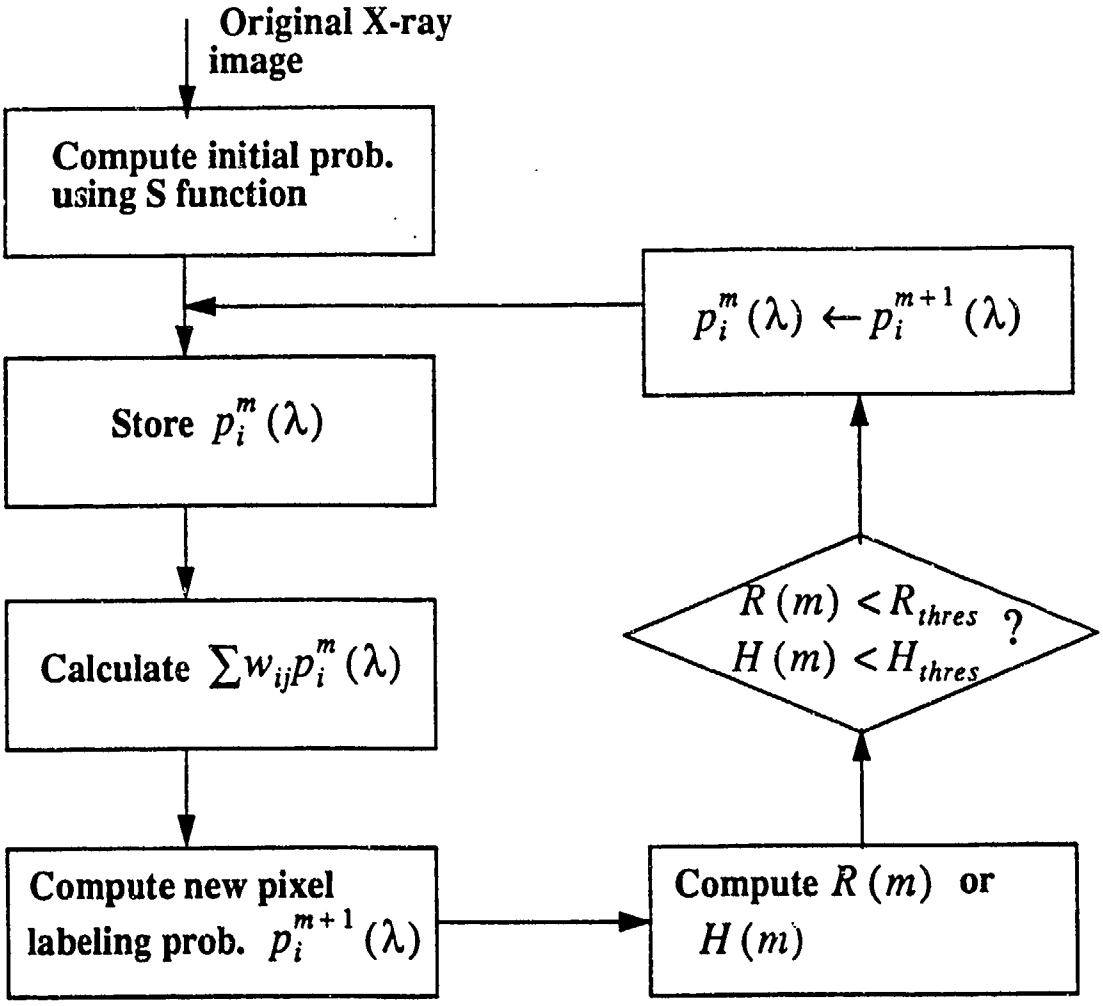


Figure 2: Implementation of PRL algorithm for two class problem

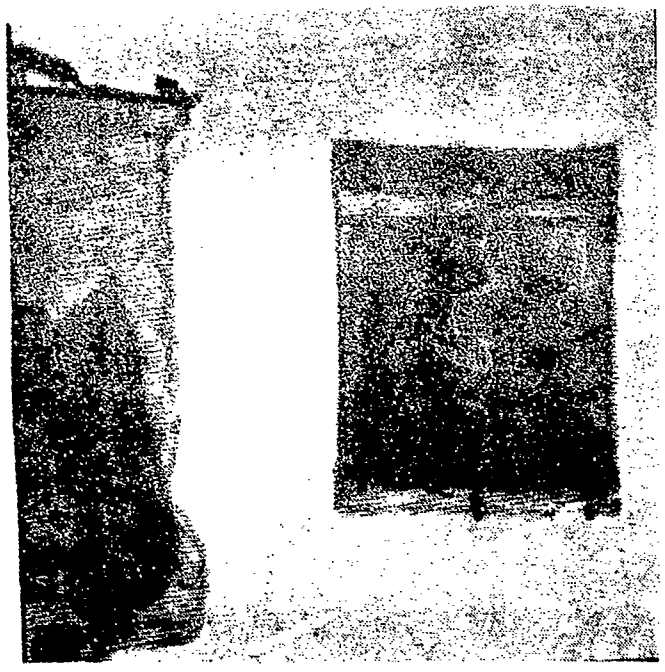


Figure 3: Original X-ray image 1

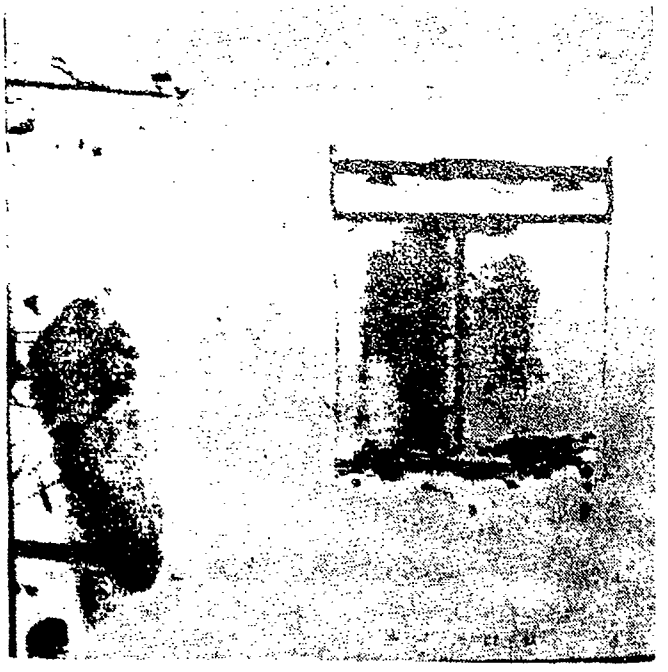


Figure 4: Result from adaptive histogram threshold on image 1

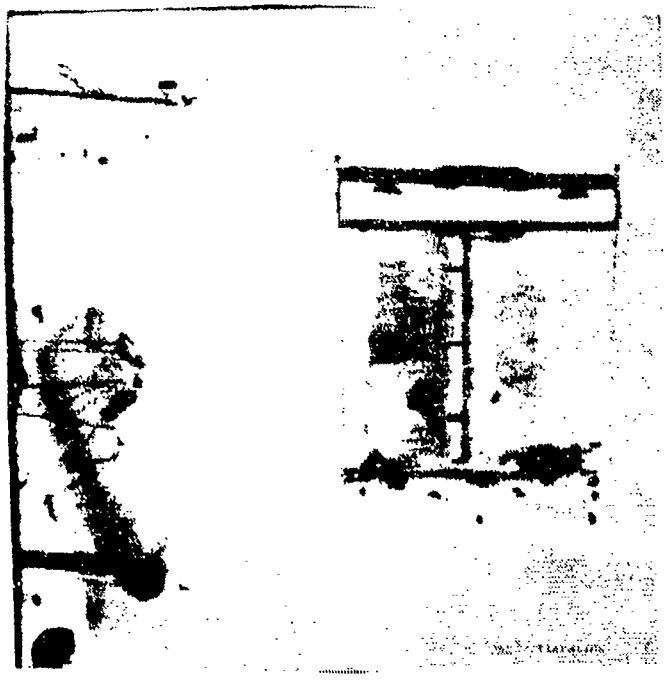


Figure 5: Result from PRL method on image 1

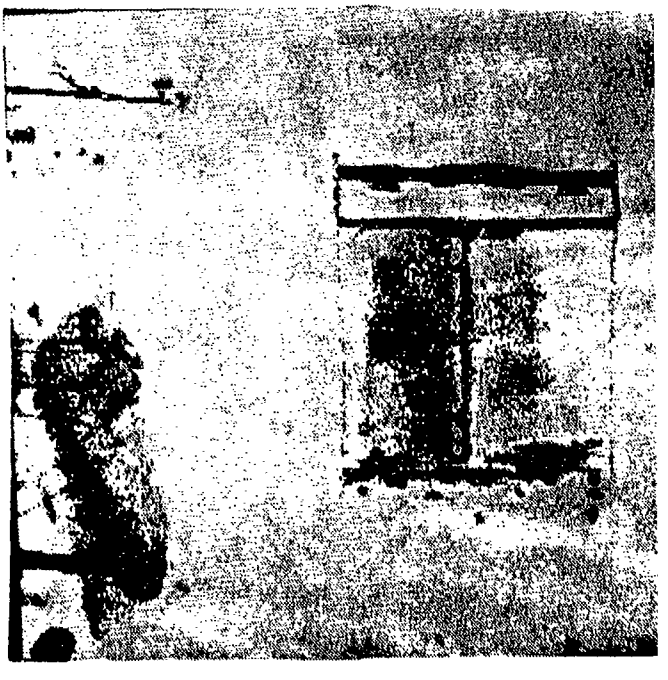


Figure 6: Result from constrast intensification on image 1

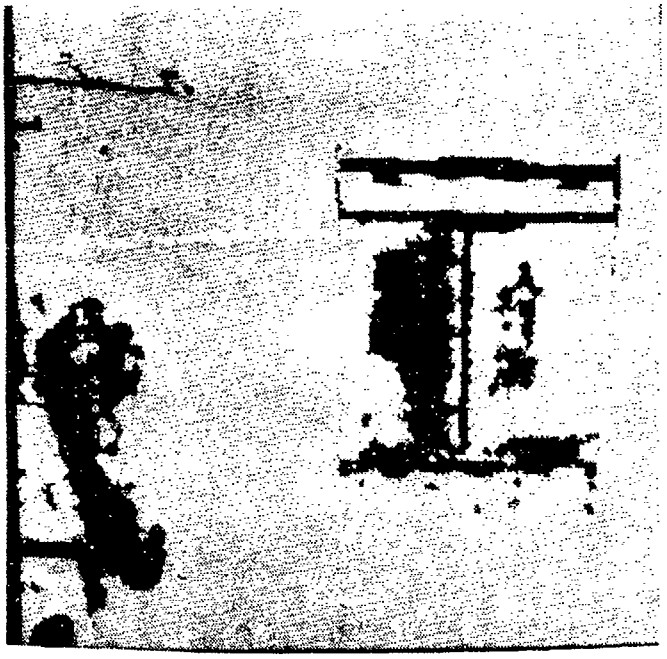


Figure 7: Result from the ICM method on image 1

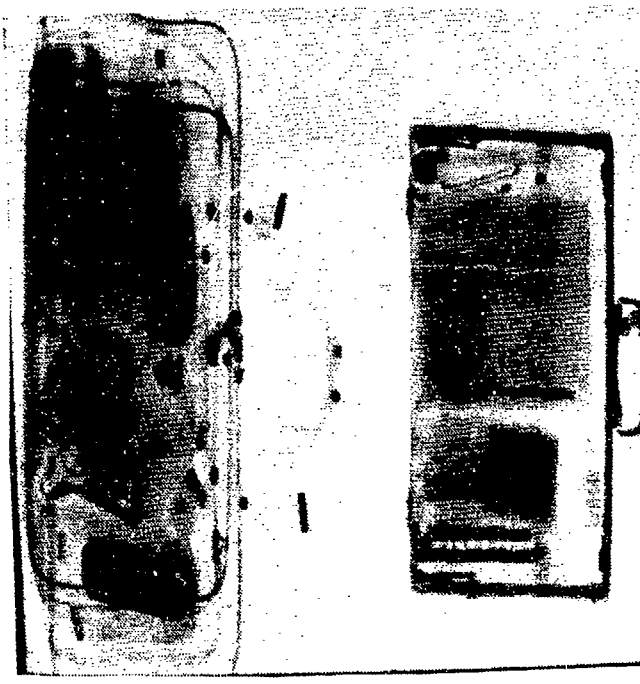


Figure 8: Original X-ray image 2

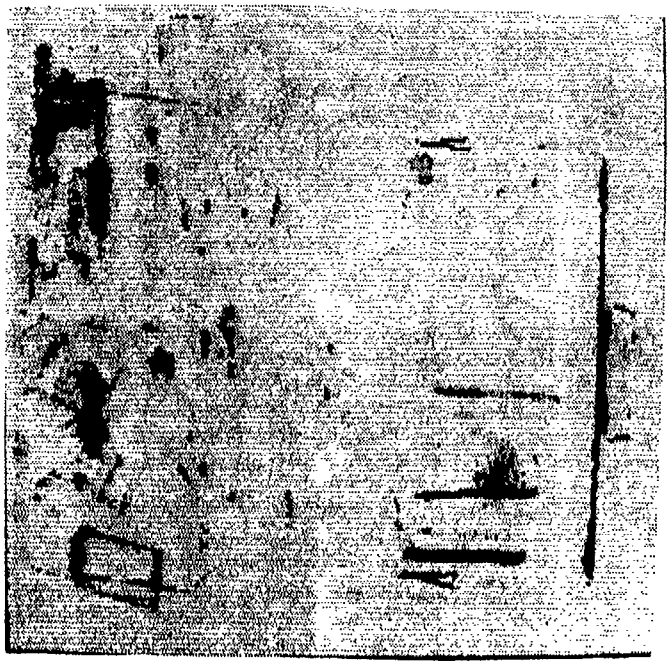


Figure 9: Result from adaptive histogram threshold on image 2

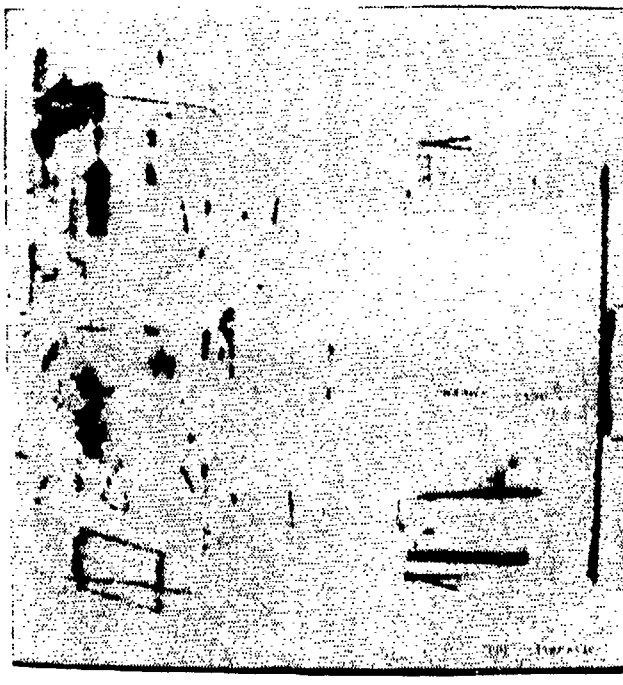


Figure 10: Result from the PRL method on image 2

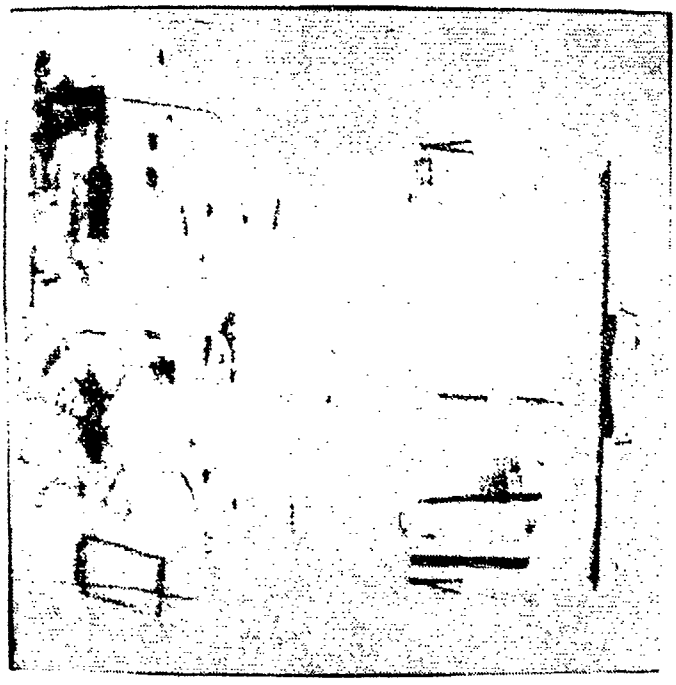


Figure 11: Result from constrast intensification on image 2



Figure 12: Result from the ICM method on image 2

SYSTEMS INTEGRATION

ROBOTICS SYSTEMS FOR DEPLOYMENT OF EXPLOSIVE DETECTION SENSORS AND INSTRUMENTS

M.W. Siegel
The Robotics Institute, School of Computer Science

A.M. Guzman and W.M. Kaufman
Carnegie Mellon Research Institute
Carnegie Mellon University
Pittsburgh, PA

1. INTRODUCTION

Methods for intercepting explosive devices in commercial aviation by directly detecting the explosives fall into two categories: vapor (or sometimes particulate) detection and bulk detection. Vapor (or particulate) detection (for example, gas or plasma chromatography) is inadequate because all such methods are child's play to evade by packaging the explosive component or the entire device in plastic bags, metal cans, etc. In contrast, several bulk detection instruments have been demonstrated to have enough sensitivity, selectivity, probing range, and immunity to evasion to be practical explosives detectors. The most promising methods appear to be neutron activation and x-ray backscattering. However, radiation-based methods are unsuitable for passenger screening, and the present generation of these instruments are neither portable nor flexible. Radiation safety requirements limit the intensity of the source that can be used, forcing design compromises that reduce the sensitivity. Hand carried instruments that might be envisioned fundamentally suffer from functional problems such as low throughput, spotty coverage, and inconsistent interpretation.

In this paper we outline a program whereby instruments based on a bulk detection method that uses penetrating radiation that is hazardous to enforcement personnel, can nevertheless be used safely and effectively. Several methods that use penetrating radiation are feasible in theory and in the laboratory, but hand-held instrument designs sacrifice sensitivity to meet safety requirements. These degraded instruments nevertheless have been shown, in contexts such as contraband drug detection, to be viable in the hands of some especially knowledgeable and enthusiastic inspectors who have developed and begun to use effective operating protocols. In the context of these facts, we propose a five point program:

1) Deploying existing instruments via robotic machines that would operate at the skill level of the most expert inspectors. Thus we would improve the effectiveness of existing instruments by:

- applying a consistently high level of operating expertise equivalent to the level now practiced by the most capable human inspector now in the field;
- improving throughput, inasmuch as robots work with unfailing consistency without taking off for meals, sleep, sickness or vacation;
- increasing acceptability to the inspection work force by essentially eliminating exposing them to radiation.

2) Optimizing instrument sensitivity for deployment by robotic machines:

- instrument design compromises previously made to minimize radiation exposure to the operator of a hand-held instrument would be removed;
- the instruments would be designed for maximum effectiveness in explosives detection;

- safety interlocks would ensure that these high dose instruments would cease to emit radiation any time humans were in their vicinity.

3) Augmenting the primary detection method with complementary sensing technologies and "sensor fusion" data handling methods for disambiguation:

- other bulk solid sensing modalities to reduce the false alarm rate, resolve borderline detections, etc., all in the general category of "disambiguation";

- vapor detecting sensor modalities for situations in which penetrating radiation based bulk detection is unsuitable, e.g., for endpoint searching by hand, for sniffing the garments of suspected offenders, etc.;

- a suite of navigation, location, and manipulation sensors, coupled with machine vision systems to provide a multi-sensor modality image and interpretation of the baggage under inspection.

4) Providing a picture- and graphics-oriented interface through which the inspectors would remotely supervise the robotic machines and instruments, thus improving interdiction system performance by:

- depicting the primary data in a natural form amenable to rapid and accurate interpretation by people and computers;

- providing an integrated representation of multiple data types synergistically contributing to a high interdiction rate and a low false alarm rate;

- taking optimum advantage of the respective unique strengths of people, machines, and people and machines working together.

5) Developing state-of-the-art database management and statistical analysis tools to aid inspection personnel:

- in making strategic and tactical decisions about deployment of finite human and machine resources;

- in interpretation of instrument responses;

- in identifying the most suitable strategies and tactics for physical seizure of explosives and other contraband.

Taking into account knowledge of container materials and construction, physical properties of the anticipated explosives types, and the operating methods employed by terrorists, we can select the instrument source radiation energy or spectrum, the instrument detector physical and electronic filtering, and other engineering parameters to maximize overall instrument effectiveness in the context of the application. If a dual technology instrument is employed, "sensor fusion" methods allow synergistic operation wherein the whole becomes, effectively, greater than the sum of the parts.

2. ROBOTIC DEPLOYMENT

The purpose of this paper is to outline the concept that the functional and safety shortcomings of existing instrumentation can be overcome by using remotely operated machinery to separate the inspector from the instrument. We also suggest that at the same time the functional problems can be overcome by using computer control of the machinery to automate the boring, uncomfortable, time consuming and error prone aspects of the inspector's job. We believe that some supporting basic research will be required to accomplish these goals: mobile robots similar to those that will be required in this application (with respect to mechanical complexity, remote controllability, and degree of local autonomy) are already in use in other applications. The flexibility and extensibility of the robotic approach will permit systems built along these lines to keep up with evasive maneuvers that will emerge in terrorists' bomb construction and deployment technologies as the interdiction technology improves.

Robotic approaches to deployment of established detection technology would wisely be the first step of a broad program to make systematic improvements in the effectiveness of counterterrorism activities in commercial air transportation. These might include, in addition to explosives, substances such as chemical and biological weapons, guns and ammunition, special nuclear materials, and various forms of "currency" including narcotics, cash, and securities. The application of the same level of technology to a variety of similar problems, each with unique features that need to be individually addressed in a common context, presents an opportunity in breadth.

The machines would be integrated with a suite of proven detection and sensing technologies, using established observation and context based procedures for path planning, guidance, and world model building. A combined color TV and computer graphic human interface would report the instrument's findings via contour maps, special symbols marking suspicious areas, with printed numerical data and appropriate highlighting superimposed on live images of the actual container under inspection. In our operational scenario a supervisor, working at the display, dispatches inspectors to suspicious pieces of baggage or passengers who may have explosives concealed on their persons. The inspectors carry color prints of the display, guiding them rapidly, by images and coordinates, to the suspicious artifacts or people. They proceed with their own familiar methods of inspection and interrogation. If they want more detail from the instrument, they request it. The immediate localization to a specific locality enhances by a hundred or more the throughputs and the seizure rates that are credited to the inspectors. The machines are doing what machines do best: the tedious, uncomfortable, and dangerous work. The inspectors are doing what intelligent people do best: flexibly exercising human judgment.

The unpredictable and open-ended jobs of final inspection, seizure, and apprehension of the terrorist cannot be automated with off-the-shelf technology. To automate these tasks would take large scale, expensive, risk laden research programs outside the pragmatic boundaries dictated by the present perceived need to rapidly deploy a practical explosive devices interdiction system.

Practical constraints will also limit the number of instruments that can be deployed in a pilot program that must produce real results. The most technical and cost-effective solution will therefore be achieved by the most intelligent deployment of a small number of machines. Intelligent deployment means being able to predict which objects and people are most likely to be concealing explosives, and concentrating the machines and the inspectors there. The inspection technology that we conceive incorporates electronic command, communications, and computing components that, for program evaluation, will automatically build a performance database. It would be useful, although not essential, to combine this program with research toward improving the statistical and heuristic (artificial intelligence) methods available for using the database to guide resource deployment decision making.

3. METHODS SELECTION

Contraband detection technologies that have been considered are divided, in some arenas, into *physical, chemical,* and *biological,* and in other arenas, including (at least recently) explosives detection, into *vapor (and particulate)* collection based means and *bulk interrogation.* The latter grouping is the most relevant in the deployment systems context.

The vapor (or particulate) based group, which includes techniques like mass spectrometry, ion mobility spectrometry (a.k.a. plasma chromatography), gas and liquid chromatography, chemiluminescence, antibodies, and others, require the evaporation or removal of a portion of the contraband material from its hiding place, and its introduction into the instrument. There is generally at most one opportunity to interrogate each molecule before it is buried in the walls of the instrument, dissolved in the vacuum pump oil, or otherwise lost. Vapor (and particulate) techniques have generally been demonstrated on the relatively large quantities of material found in particulate suspensions, e.g., airborne dust. Whether any of them have adequate sensitivity to detect and discriminate dilute vapors in real world environments is still under intense study. But these studies and debates aside, vapor barriers (plastic film, metal containers, etc.) are just too cheap and too effective for any air sampling technology to be considered seriously as a sole interdiction technology against explosive-containing packages.

On the other hand vapor detection must continue to be pursued as it is one of the few available alternatives (along perhaps with magnetic resonance methods) for inspecting people; fortunately encapsulation of explosives carried on the person is more difficult than encapsulation of explosives in a package, and body temperature aids volatilization and thus detectability.

In contrast, potential bulk detection methods, which include x-rays, acoustics, neutron interrogation, neutron and x-ray backscatter, nuclear magnetic resonance, microwave attenuation, and others, are applicable *in situ.* They are in some cases (especially neutron interrogation) difficult to shield, and they more than compensate for modestly low sensitivity by being able to work with the order of 10^{12} times the number density of molecules that are available in vapor sniffing. They provide the opportunity,

because they are not destructive, to improve signal-to-noise by interrogating each molecule an arbitrarily large number of times. For these reasons we consider the bulk detection technologies to be the only serious contenders for screening of baggage, cargo, mail, galley supplies, etc.

Both single-sided and through-the-container implementations, both with and without imaging, are more or less feasible for most of the identified bulk interrogation technologies. Our advocated methodology, the combination of existing (optimized for the new deployment method) detection instruments with robotic mobility, is flexible and extensible with respect to these choices. The five component program we have outlined describes a pragmatic evolutionary path.

The weakness of these instruments, in a scenario where the threat is constantly evolving in evasion of detection apparatus, is their inflexibility because of their marginal suitability for deployment as hand-held instruments. There are two essential reasons:

- they expose the inspectors to radiation; and
- to use these instruments effectively the inspector has to develop an unlikely "rapport" with the instrument, given the hazard to his (or her) health.

However the possibility of robotic deployment opens up several areas of dramatic improvement:

- the existing instruments, remotely deployed in a computer-aided and partially automated scenario, become much more attractive because the health hazard is immediately and virtually completely removed;
- the instruments can be optimized, e.g., source strengths increased, and therefore signal to noise ratio improved, once the operational scenario has the inspector at a remote location;
- whether or not the instruments actually are optimized for robotic deployment, the systematic nature of the automated robotic inspection process will decrease both the miss rate and the false alarm rate.

In addition, throughput will be substantially improved:

- automated or semi-automated machines operate steadily and continuously;
- one inspector can simultaneously direct multiple robots;
- inspectors will work primarily in an endpoint search mode, with a very high hit rate per person-hour, in contrast to the present situation where they spend most of their time looking for suspicious looking passengers and baggage.

There are numerous additional technical possibilities, for example, differentiation of robotic deployment machines into those specializing in volume inspection through the container and those specializing in single-sided or outside surface inspection. In particular, volume inspection could be facilitated by:

- placing source(s) and receiver(s) on two limbs of one machine; or
- by coordinated movement of two or more robotic machines working different faces of the baggage or container.

4. DETECTION REQUIREMENTS

The required, or at least the desired, attributes of a contraband explosives detection system include:

- sensitivity -- the ability to detect quantities well under 1 kilogram on a person or in baggage and perhaps just a few kilograms in cargo;
- specificity -- the ability to discriminate explosives from legitimate baggage or cargo contents;
- portability and transportability -- we regard it as essential, against an ever changing threat, that the instrument can be carried to the suspected baggage or cargo, not vice versa;
- low false alarm rate -- despite some evidence that a modest level of false alarms keeps inspectors "on their toes," the high cost of manual inspection dictates a requirement for a very small false alarm rate;

- safety -- e.g., both ionizing and laser radiation present personnel problems;
- simple to operate -- inspectors are not trained in instrumentation;
- "in the flow" -- the instrument must not introduce additional delays into the already objectionably slow inspection process, nor can it significantly disrupt current procedures;
- reliable -- down times must be short and infrequent.

The semi-automated robotic deployment scenario makes a positive contribution to each of these requirements:

- sensitivity of any instrument deployed robotically is enhanced by the systematic and untiring nature of the process, which improves signal-to-noise ratio by decreasing the noise associated with procedural inconsistency and increases the signal by permitting uniform scans at rates that are automatically adapted to the situation pertaining at any moment;
- sensitivity is further enhanced if the opportunity is taken to optimize the instrument for machine deployment, e.g., relaxation of radiation source strength restrictions;
- specificity is enhanced by improved signal-to-noise, facilitating signature analysis, as well as by the ease of incorporation of auxiliary sensors and sensor fusion approaches to disambiguation;
- portability and transportability become fundamental features of the approach, i.e., in the robotic deployment scenario the instrument is inherently and integrally part of a mobile machine designed at every level to bring the instrument to the baggage, cargo container, or passenger, and most effectively to scan the subject with the instrument;
- a low false alarm rate is assured both by the improvements to the physical detection process per se, and even more by the filtering, reliability checking, consistency and context cross checking, disambiguation, etc, provided by the computer modeling, analysis, and reporting system;
- safety is assured, for detection modalities involving penetrating radiation, by the physical separation of man and machine, and by conservative programming of the man/machine interaction with numerous software implemented interlocks and limit switches;
- simplicity of operation is inherent in the semiautonomous nature of the system;
- all the interactions with the humans are at a natural language communication level, and are thus, from the human perspective, inherently simple;
- throughput is enhanced, not because robots are fast (in fact, in the short run they are usually slower than skilled people), but because the competition almost always turns out to be a tortoise-and-hare story in which the robot's perseverance and untiringly systematic methods win out, statistically, over the human's "sprints" of wisdom or intuition;
- reliability is assured by conservative design, and by the relatively low cost of redundancy.

5. SYSTEM ARCHITECTURE

Our approach is not an instrument but rather a method of deploying existing and future instruments to maximize interdiction rate and minimize interdiction cost. We take it as given that there are several existing instruments that, with specifiable constraints, can detect explosives. The design phase for a practical system would include assessment of sensitivity, selectivity, false positive rate, false negative rate, and related technical parameters, in a realistic context subject to the constraints of the commercial air travel scenario. By using automatic and semi-automatic robotic machines to transport and operate one or more instruments, system functionality, throughput, and safety will raise one or more detection technologies to the realm of practical feasibility.

The system we envision is comprised of four subsystems: *measurement*, *manipulation*, *mobility*, and *monitoring*, integrated in a system that delivers adequate sensitivity, discrimination, reliability and throughput:

- *measurement: primary* sensing technologies, e.g., neutron activation, interact with the baggage *per se*, cargo containers, and any suspected contraband; *secondary* sensing technologies, e.g., magnetometers, discriminate effects relating to the container from effects relating to its content; *knowledge based interpretation* integrates sensor data into the explosives interdiction context;

- *manipulation:* precise navigation and motion control relative to the dimensions of the baggage piece or cargo container are essential to localization of suspect regions; scanning is generally autonomous, but an inspector or supervisor can intercede to target suspect pieces or areas; a knowledge base of baggage and container types will aid navigation by facilitating landmark recognition, and it aids discrimination by maintaining sensitivity to anomalies, e.g., backscattering from structural regions that should be empty;

- *mobility:* it is crucial that the inspection equipment move to the subject person, piece of luggage, or cargo container wherever its location; the alternative of bringing these to a central inspection station is unacceptably disruptive to the normal flow of activities; however there is little impetus to make this activity autonomous, and there would be much technological risk in attempting to do so; mobility is thus directed by inspection personnel, either locally or by teleoperation;

- *monitoring:* high level control and command, including data-driven dispatch of inspectors, is effected via a high quality visual interface; interaction between a supervisor, the robotic inspection equipment, and the human inspection staff is based on color TV images of subjects with automatic overlaid mapping of sensory data, computer highlighting of automatically detected suspect areas, and the option of the supervisor designating other areas as suspect based on his or her interpretation of the data in context.

6. DEPLOYMENT STRATEGY

We suggest that in contraband interdiction it is a more valuable skill to be expert about when and where to inspect than it is to be expert, with or without "high tech" instruments, at conducting the inspection *per se*. Present inspection target selection methods rely on heuristics whose effectiveness are unmeasured. Were inspection resources unlimited, targeting effectiveness would not be an issue. But the real situation is that there are too few inspectors to physically examine more than a small fraction of the targets. Under these circumstances, *flawed heuristics may be worse than no heuristics*. Powerful statistical and analytical methods could be brought to bear on at least two components of the contraband interdiction deployment problem: verifying and improving existing heuristics (a sampling program), and systematizing inspection targeting practice in the context of knowledge of the heuristics (an operations research program).

7. CONCLUSION

We have described a concept for using robotic systems to deploy and to evaluate objectively the effectiveness of sensors and instruments for detection of contraband explosives, particularly as they might be employed by terrorists against commercial aviation. The system architecture divides the problem into four levels: *measurement*, *manipulation*, *mobility*, and *monitoring*.

The *measurement* level is a suite of existing or adapted sensors and instruments that report the presence of material with chemical or physical properties that suggest the presence of explosives.

The *manipulation* level is a family of fine motion devices that, with the aid of secondary sensors, automatically deploys the explosive detecting sensors and instruments.

The *mobility* level is a family of virtually unlimited motion platforms that transport the manipulators and their sensor suites to appropriate inspection locations.

The *monitoring* level is the computer, interface, and display that, in response to strategic requirements articulated by the human operator, carries out an appropriate sequence of inspection, interpretation,and sensor fusion tasks, and notifies the operator of exceptions that require human attention. The monitoring function particularly benefits from access to a variety of sensor inputs and a historical database. These in concert substantially enhance the abilities of the monitoring system to discern and call to the operator's attention small but potentially significant departures from nominal, and to resolve ambiguities due to sensors with high sensitivity but imperfect selectivity.

We developed this model as a flexible approach to the general problem of making difficult observations in difficult environments. In commercial aviation, our concept is now being realized via an FAA sponsored program through which we are applying it to aging aircraft inspection. The systems integration concepts and technology we are developing in the aging aircraft program have direct counterparts in the explosive detection program. We look forward to being able to apply what we learn in the first context to the problems of the second context.

A SYSTEMS APPROACH TO THE EXPLOSIVE DETECTION PROBLEM

Michael C. Smith and Roger L. Hoopengardner
Science Applications International Corporation
1710 Goodridge Drive
McLean, Virginia

1. INTRODUCTION

Science Applications International Corporation (SAIC) has been involved in research and development (R&D) of Explosive Detection Systems (EDS) for baggage inspection since the mid-1980's when the U.S. Federal Aviation Administration (FAA) funded SAIC to develop the Thermal Neutron Analysis (TNA) system. After the tragic bombing of Pan Am Flight 103, the FAA accelerated research efforts, leading to early fielding of TNA systems. TNA is currently being used on a trial basis in airports in both the United States and Great Britain. While TNA met the initial FAA specifications, evidence from the Pan Am 103 bombing indicates that smaller amounts of explosive than originally specified must be detected. However, TNA testing for smaller amounts of explosives yields higher than desirable false positive rates. Most experts agree that TNA is currently the only true explosive detection technology available, but, to provide an effective system with acceptable false alarm rates, TNA may need to be supplemented with other detection devices, methods and procedures.

Recently, the FAA Technical Center began considering different combinations of technology and procedures that could provide acceptable detection and false alarm rates. Since most people agree that TNA is likely be a part of any system fielded, SAIC elected to take an overall systems approach to the problem, seeking to develop a method or procedure to evaluate "systems of systems" comprised of TNA and other technologies and procedures. The authors of this paper studied the problem; developed logical measures of effectiveness (MOE); designed, constructed, validated, and exercised an EDS simulation model; and briefed results to the FAA Technical Center's Aviation Security Research Service. The resulting PC-based computer simulation model was designed to be simple to understand, logically correct, and capable of providing meaningful visual displays of the results.

Figure 1 shows the operational analysis approach needed to fully evaluate EDS alternatives. The approach begins with a clear statement of requirements in the form of security system objectives (e.g., specific threats and the required detection probability) and operational requirements (e.g., throughput, space available). The analytical framework prescribes the scope of the analysis effort, the system measures of effectiveness and the relevant trade-offs. The simulation model discussed here falls in the "Identify or Develop Tools" and "Apply Analysis Tools" boxes. It is an example of one of the tools that could be used in an operational analysis of the process for detecting explosives in baggage.

Our compressed schedule required that security objectives and baseline operational parameters be assumed as given. Data for the analysis were generally obtained from internal SAIC sources or from available literature and are adequate to demonstrate the utility of the approach and the model. We have not developed specific options for evaluation and testing but have provided an analytical tool that could assist in the evaluation and have demonstrated it using notional data the approximates what is likely to be experienced using available technologies and procedures.

This paper describes the computer simulation that was developed. The paper also suggests some enhancements that could be made to increase the fidelity of the simulation and other ways to use a systems analysis approach to improve security.

2. SIMULATION DESCRIPTION

The purpose of the simulation model described here is to assist in developing and assessing various systems alternatives for achieving security system design goals for screening checked baggage in airports. A simplified logical model of the simulation is shown in Figure 2.

The stimulation model requires a number of run parameters that describe the operational environment of the EDS. These parameters include:

- the total number of passengers to be processed;
- the time during which passengers arrive;
- the peak passenger arrival time;
- the average number of checked bags per passenger;
- the probability that a passenger is carrying a bag that contains an explosive;
- the fraction of passengers that will be profiled through interrogation ("manual profiling") or through electronically compiled data (automatic profiling"); and
- the first device or procedure used to screen checked bags.

In addition to these run parameters, each EDS technology and procedure is characterized by a set of parameters. These parameters are:

- the probability of detecting an explosive when an explosive is present;
- the probability of a false alarm (i.e., indicating the presence of an explosive when there is none);
- the time required to process a checked bag or, in the case of passenger screening, a passenger; and
- the next station for bags and/or passengers if not cleared (i.e., an alarm, detection, or positive screening result).

The model begins with the arrival of passengers in the security screening area according to the arrival pattern specified through model parameters. The model uses a triangular distribution to reflect the gradual rise and fall in passenger arrivals as an aircraft departure approaches. The triangular distribution is divided into fifteen minute intervals. The model computes the mean interarrival time for each interval and passenger arrivals occur exponentially within each fifteen minute interval.

Attributes are assigned to passengers randomly as they arrive. Attributes include the number of bags the passenger wishes to check and whether or not one of the passenger's bags contains an explosive. The model permits the analyst to select any combination of EDS technology and procedures and configure them in series, parallel, or recycle patterns. This modeling flexibility facilitates analysis of options where bags have to clear two or more EDS technologies or procedures before being placed on the aircraft. The model logic flowchart shows how, once a passenger or bag is "Cleared," the passenger or bag may be routed to the aircraft ("To A/C") or to another inspection station. Generally, if a passenger's bag fails to clear an inspection, the bag is sent to another device or procedure and, ultimately, to a hand search station for final resolution. If an explosive is suspected, the bag is sent to a holding area for explosive ordinance disposal.

The simulation model produces a number of metrics that can be monitored throughout the simulated period and at the end of each simulation run. The measures we routinely report are:

- **Sensitivity.** The percentage of bags that contain explosives that are detected by the system.
- **Specificity.** The percentage of bags that do not contain explosives that are correctly cleared for boarding.
- **Time to Clear.** The total elapsed time from the arrival of the first passenger until the last passenger is cleared through the system.
- **Maximum Passengers in the System.** The single largest number of passengers that were in the system at any one time during the simulated period.

In addition to these measures reported by the simulation, we compute a rough order magnitude cost for each configuration considered. Cost estimates include initial acquisition cost (including training) and the annual operating cost, including costs for personnel and support. A total five-year cost is computed comprised of the initial cost and five times the annual cost. No discounting is used in these estimates.

The simulation model is implemented in the GPSS-PC simulation language and runs under MS-DOS on a 386 platform with a VGA monitor. This configuration provides real-time interactive modeling capability as well as dynamic graphic color graphics displays of the simulation in progress. Typical run times for processing 1200 passengers and their checked bags are 2-3 minutes, depending upon the amount of interaction that occurs during the simulation run.

3. INITIAL ANALYSES

One of the most difficult tasks in developing and demonstrating the simulation model was finding reasonable data to characterize the EDS technologies and procedures. Except for the TNA System, no hard performance data exist. In fact quantification of performance data of many of the available techniques is quite difficult to obtain and significant effort will be required to obtain it. Because of the short time frame for our work, we tuned to SAIC experts for descriptions of technologies available and for initial rough estimates of the required parameters. We focused our efforts on currently or soon to be available technologies and procedures. These included both manual and automated profiling, TNA with X-ray (or XENIS -- X-Ray Enhanced Neutron Inspection System), vapor detectors ("sniffers"), enhanced X-ray, focused hand search (where the inspector knows a specific area of the bag to examine based on information from a previous device) and unfocused hand search (where the inspector has no prior information about the bag). Initial parameter estimates used are shown in Table 1.

Our reasons for limiting our initial work to available technologies and procedures were (1) to be able to use reasonable parameter estimates and (2) to facilitate examining test-bed configurations that the FAA is considering for field testing. No matter how valid the simulation logic may be, without field testing of the devices to validate the parameter values and provide accurate estimates, the simulation cannot provide reliable results. However, the simulation will assist analysts in determining which proposed configurations of systems make sense to field test and which are obviously less attractive from the very beginning. After field test data are available to refine parameter estimates, the simulation model can be used to evaluate other configurations that might prove too costly or have too great an operational impact for operational testing.

After determining which technologies and procedures to include, we selected configurations to use in our initial analyses. We briefly reviewed how the TNA devices are being used in New York's Kennedy Airport and London's Gatwick Airport, and how El Al handles security checks in Tel Aviv. We visited Washington's Dulles Airport to observe how United Airlines is using the TNA system. Finally, we conducted a brainstorming session to identify potential configurations that employed other technologies and procedures. We began our work with eleven possible configurations, reducing them to eight important configuration. Figure 3 shows an example configuration based on a highly simplified view of how XENIS is employed at Gatwick.

Based on historical data from Gatwick, we used the model to determine the number of stations that would be needed to handle approximately 1,200 passengers arriving over a three hour time period for a flight. We wanted to have enough stations to process all the passengers in as close to three hours as possible. By monitoring the simulation as it ran, we could observe where queues were building and then estimate the number of stations needed. We tried to reduce the maximum number of people in the system at any one time to a number that we felt was reasonable. Once we had a reasonable configuration, we ran the simulation a number of times to obtain average results and then computed a rough order of magnitude cost estimate for the system.

Summary graphs of the eight initial cases evaluated are shown in Figure 4. Table 2 shows the actual configuration of the devices used in each case. In each case, the number of devices or stations was chosen to ensure that the 1200 arriving passengers were processed in a reasonable time. Figure 4(b) shows the delay after the last passenger arrived until all passengers cleared the EDS. Note that configuration "A" with manual profiling resulted in the greatest delay, clearing the last passenger about 14 minutes after the last passenger arrived. Configurations "F", "G", and "H" use parallel rather than sequential logic. That is, if either device or procedure alarms, the bag must be hand searched. As would be expected, the Sensitivity (see Figure 4 (a)) for these configurations is high, but additional hand search stations are required to clear false alarms (see Table 2). In all other cases, as soon as the passenger or bag clears one procedure or inspection device, the bag is cleared for boarding. Cases "D" and "E" are identical except that case "E" has one additional automatic profiling station. Note the resulting

reduction in delay time and maximum passengers in the system.

The results of these runs are interesting, but one must remember that the values used were for illustrative purposes only. The real benefits of this modest effort are the demonstration that a more vigorous quantitative analysis approach can provide insights and different ways to look at the problem, and that using a computer-based simulation offers a viable method for examining system metrics that cannot be easily calculated because of the synergism of various components. This simple simulation is, by no means, the answer or tool to solve the EDS problem. However, there are a number of ways that this approach can be used in examining the explosive detection problem, and a higher resolution simulation could and should be developed to help in this systems approach.

4. POTENTIAL USES OF THE SIMULATION

As the FAA continues to grapple with the air travel security problem, it faces the dilemma of whether to call for fielding of imperfect systems or to wait until a new technique or device can be evaluated to see if it is the "answer." A simulation such as the one described above can be used to examine various system combinations in an operational environment. This provides a low-cost method for assessing proposed techniques or equipment, thus allowing more than one configuration to be tested with a minimal change to the overall site. This allows the FAA to begin a testing program of the currently available detection devices while other EDS programs continue in the R&D mode.

Naturally, as test-beds are designed, testing procedures must also be developed for use at the test sites. The design of operational tests is a difficult and time consuming process that carries significant ramifications not only in terms of safety for millions of travelers, but also in financial implications for the airlines and the EDS designers and manufacturers. As a prerequisite for designing detection devices and the operational tests, the operational requirements that the systems must meet must be determined and announced. More sophisticated simulation models could be used by the FAA to assist in determining operational parameters and in validating test results. The importance of developing valid tests cannot be over stressed because of the safety and financial significance such tests have. Simulations can help uncover flaws in the tests that may not be discovered until after the expense of conducting the test has been incurred. The use of such a tool is also likely to develop an increased sense of confidence in the tests and their ability to determine the capabilities of a specific EDS.

Development and use of a simulation tool such as this has added benefits that may not be readily apparent. As the simulation is run, questions or observations will surface that allow systems developers and funding agencies to identify areas where additional research is needed. This allows the FAA and others to focus R&D efforts and to apply limited R&D funds more efficiently. Simulations also point out areas that require better data and greater analytical emphasis. For instance, the simulation may indicate that a number of bags will be awaiting additional inspection, but developers are not certain how much space is available in a specific airport for holding bags. The model would help determine the amount of space needed so that data could be gathered concerning available space for baggage storage and passenger waiting at the airports being considered for the test-bed activities. These types of analyses help make analysts more aware of the ramifications of the total system and more knowledgeable about the total impact that their recommendations may have.

Another possible use of this model would be to use it in conjunction with other models used to assess the explosive detection problem. One model, developed at the Institute for Transportation Studies (ITS) at the University of California at Berkeley, examines the operational impacts on airlines of using some type of explosive detection device to screen all international baggage throughout the U.S. The two models could form a type of hierarchical structure with the SAIC model providing inputs for ITS model to examine delays in airline flights or quantities of bags that miss their flights due to the time needed to screen them. Such a combination offers a comprehensive examination of potential system configurations and airport layouts without incurring the expense of actual system purchases. It could help save money by allowing airlines and security personnel to estimate the number of people needed during peak hours of the day.

5. CONCLUSIONS

The authors were originally challenged to find some system measures of effectiveness that were different from the individual detection devices' MOE. In the

course of examining this large problem of baggage screening, a computer simulation has been developed that, if imaginatively applied, can assist in the examination of a wide variety of operational problems. We have demonstrated that a simple computer tool can be quickly, yet effectively, applied to a seemingly very difficult problem to provide insights to the interaction and synergism of several components of an overall system. Complex problems, such as this problem of insuring that unaccompanied baggage is safe to load on the aircraft, must be examined in their total operational context in order to make wise decisions about solutions. Tools such as the computer simulation discussed here help provide the decision maker with a better understanding of the operational consequences of decisions and help develop sound and rational choices.

BIBLIOGRAPHY

1. Committee on Aviation Security, National Materials Advisory Board, ***Reducing the Risk of Explosives on Commercial Aircraft***, National Academy Press, Washington, DC, 1990.

2. Fotos, Christopher P., "Aviation Security Act Puts TNA Buy on Hold", ***Aviation Week & Space Technology***, March 25, 1991.

3. Gosling, Geoffrey D. and Mark M. Hansen, ***Practicability of Screening International Checked Baggage for U.S. Airlines***, Research Report UCB-ITS-RR-90-14, Institute of Transportation Studies, University of California at Berkeley, July 1990.

4. Henderson, Breck W., "FAA Stays Undecided on Deploying TNA Amid Conflicting Views and Test Results", ***Aviation Week & Space Technology***, March 25, 1991.

5. Hughes, David, "Explosive Detection Equipment Firms Develop Enhanced X-ray and Vapor Technologies", ***Aviation Week & Space Technology***, March 25, 1991.

6. MacKenzie, F.D., J.W. O'Grady, P.W. Rempfer, L. Frenkel, and J.E. Kuhn, ***Aviation Explosives Security, Analysis of the Checked Baggage System***, U.S. Department of Transportation, Research and Special Programs Administration, Final Report No. FAA-RD-79-30, April, 1990.

7. Ott, James, "Airlines, FAA Bolster Research Efforts to Intensify Detection of Aircraft Bombs", ***Aviation Week & Space Technology***, March 25, 1991.

8. ***Report of the President's Commission on Aviation Security and Terrorism***, Washington, D.C., May 15, 1990.

9. Yeaple, Judith, "The Bomb Catchers", ***Popular Science***, October 1991.

Table 1. Parameter Estimates Used in Initial Analyses

Inspection Technique	Input P_d	Input P_{fa}	Time Per Unit
Automatic Profile	.750	.200	30 seconds per passenger
Manual Profile	.950	.100	300 seconds per passenger
Focused Hand Search	.999	.001	200 seconds per bag
Unfocused Hand Search	.950	.001	300 seconds per bag
TNA with X-Ray (XENIS)	.900	.200	6 seconds per bag
Vapor Detector	.600	.100	30 seconds per bag
Enhanced X-Ray	.750	.200	20 seconds per bag

Key:

P_d: Probability of detection
F_{fa}: Probability of false alarm

Table 2. System Configurations for Initial EDS Analyses

System Configuration*	Automatic Profiling	Manual Profiling	Hand Search	TNA with X-Ray	Vapor Detector	Enhanced X-Ray
A		50	8			
B	5		20			
C			20	2		
D	4		3	1		
E	5		3	1		
F	5		30	2		
G			15	2	8	
H			25	2		5

* Table entries are numbers of stations required to achieve results shown in Figure 4.

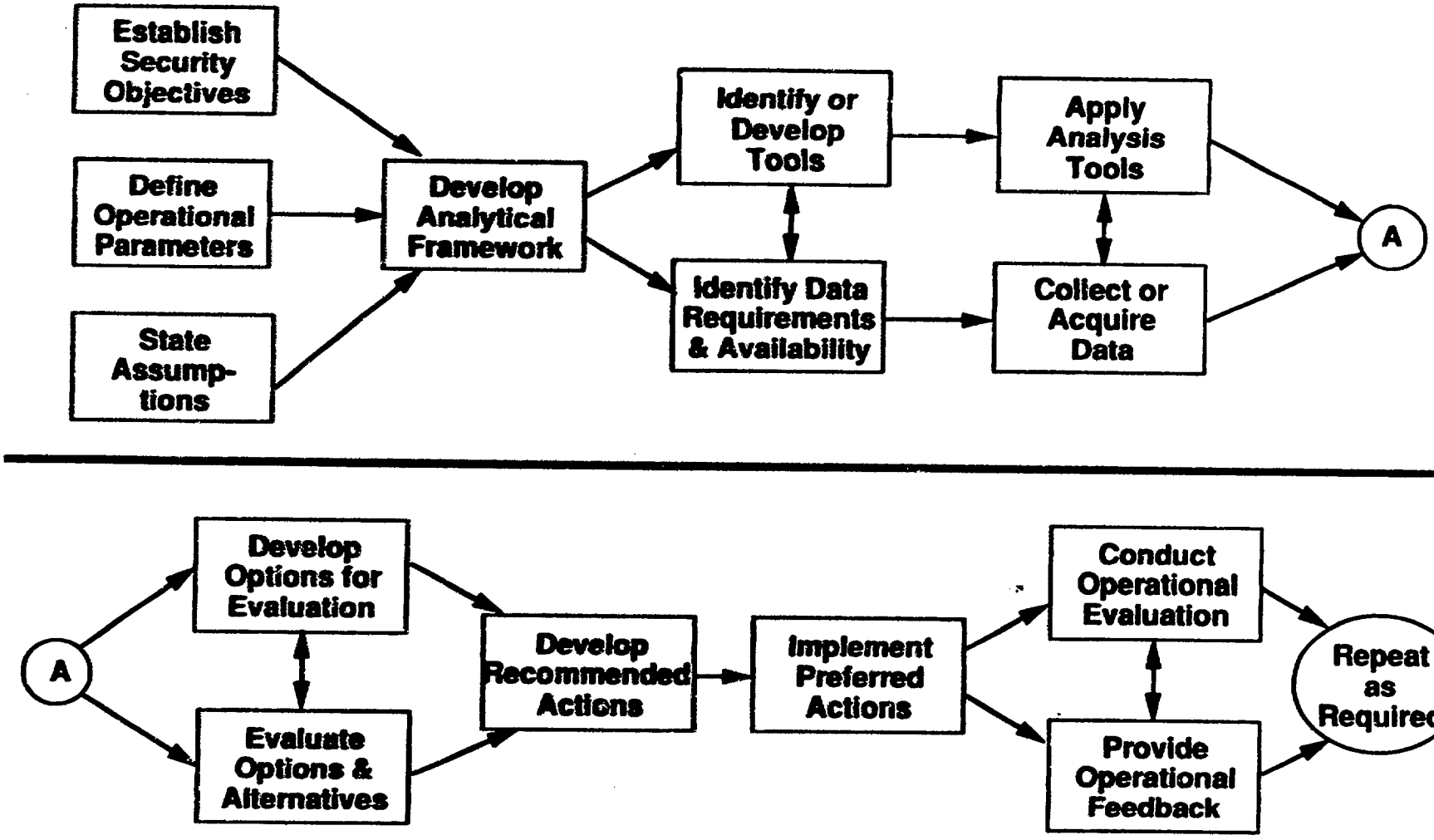


Figure 1. Approach for EDS Operational Analysis

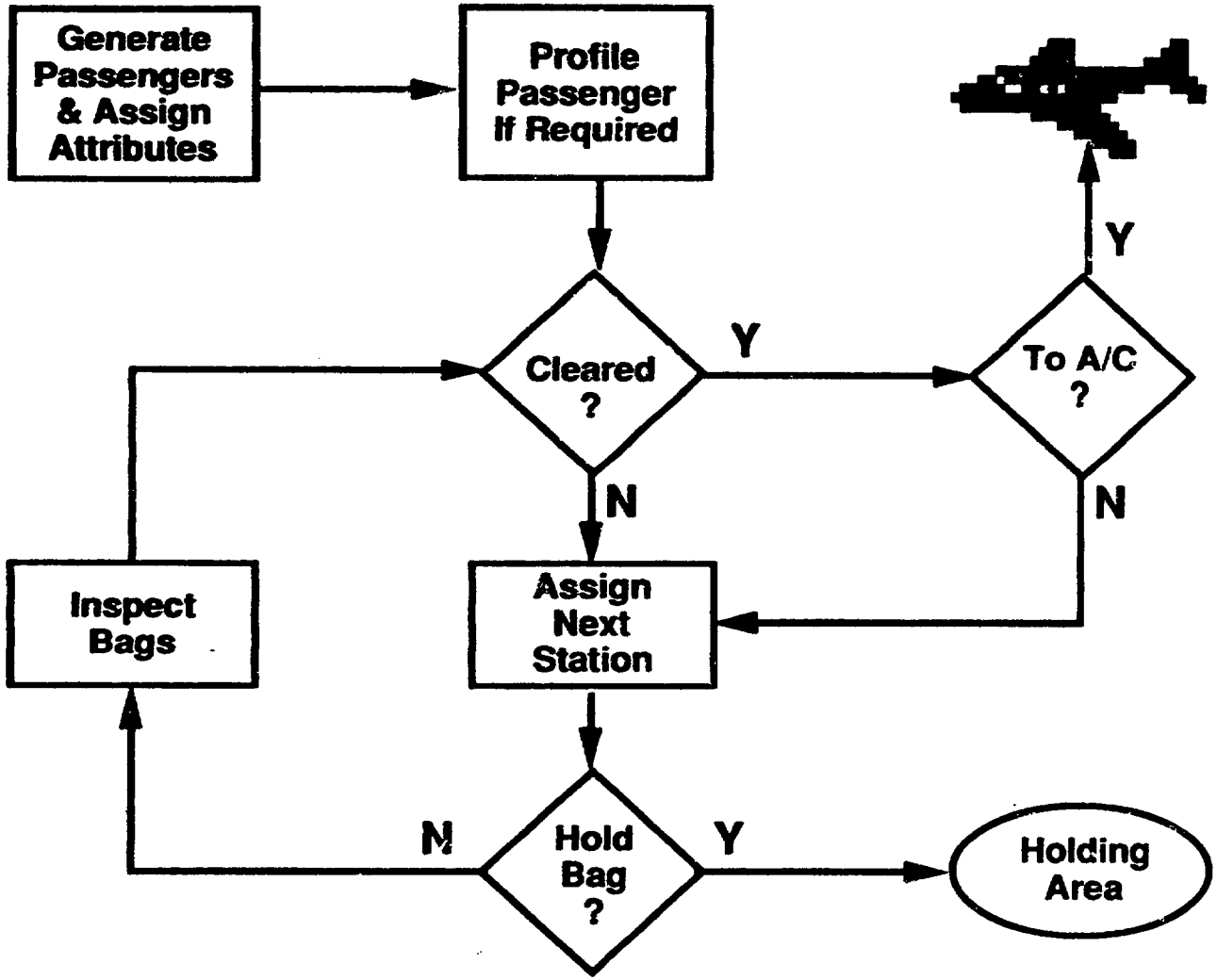
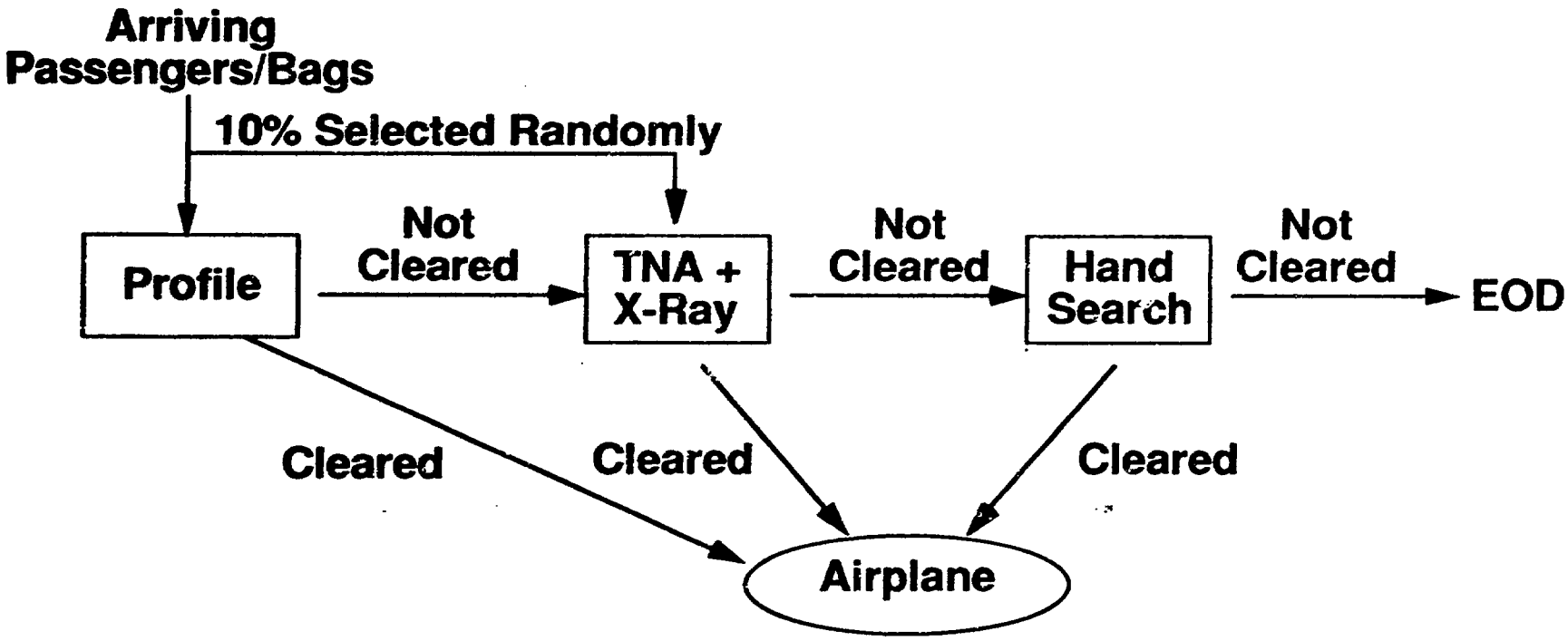


Figure 2. Simplified View of Simulation Model Logic



688

Figure 3. EDS Configuration Based on Gatwick Airport (Cases D and E in Figure 4)

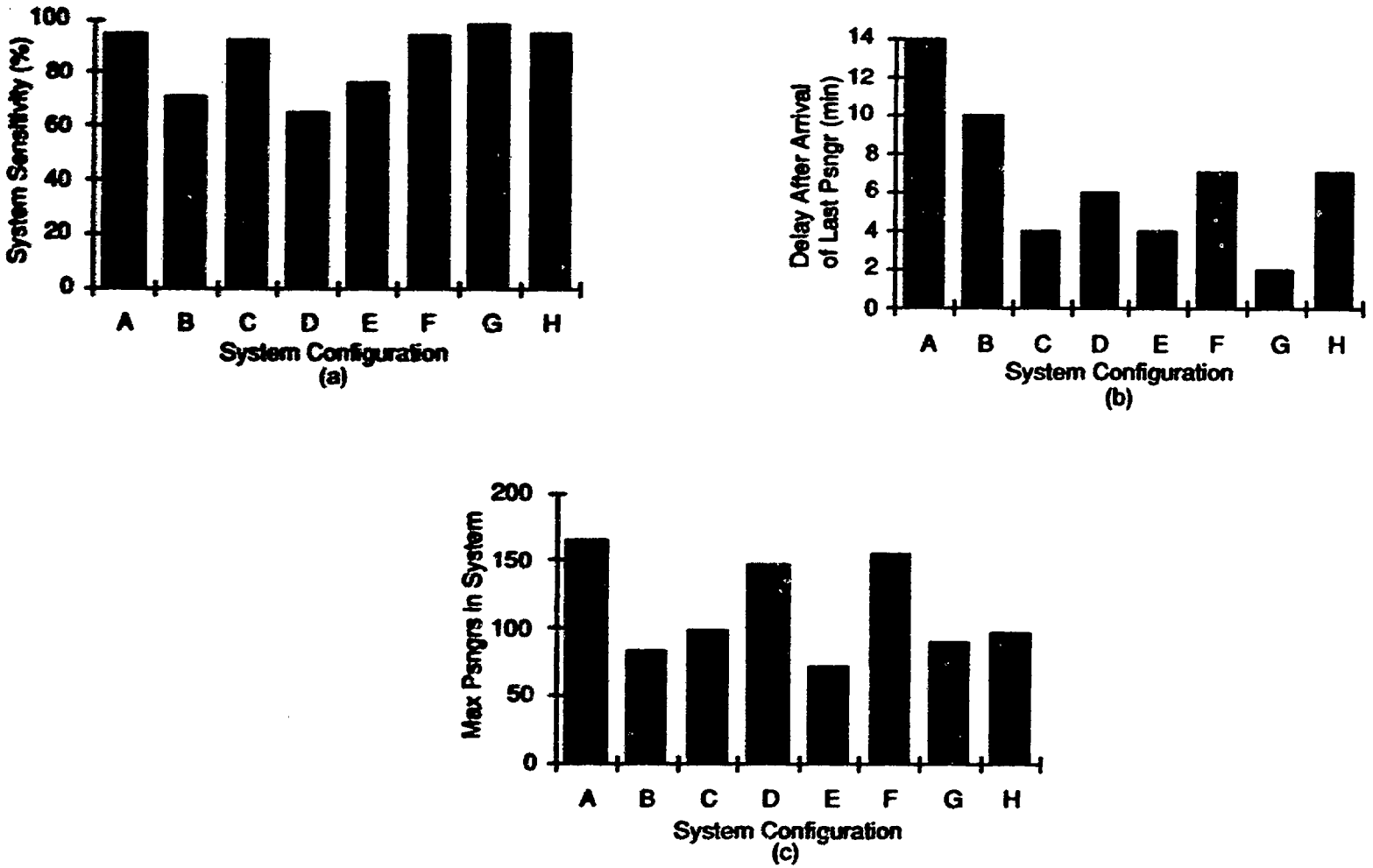


Figure 4. Results from Selected Cases Based on Initial Analysis

INTEGRATION OF THE HUMAN, CANINE, MACHINE INTERFACE FOR EXPLOSIVES DETECTION

J.W. Ternes, Ph.D.
Philadelphia VA Medical Center

A.M. Prestrude, Ph.D.
Virginia Polytechnic Institute and State University

1. INTRODUCTION

The technology of terrorism has outpaced airport security. A recent review of airport bomb detection technologies (Yeaple, 1991) indicated that the metal detecting and x-ray devices currently in place are not capable of detecting plastic explosives. Though there is a new generation of devices which promise to significantly improve detection of explosives, many of these devices are still in development and prototype stages. Further, most of these devices are large, fixed-base and expensive. There is however, a "technology" which is mobile, relatively inexpensive, and has been field tested under a wide variety of conditions for many years. That, of course, is the dog/human-handler explosives detector team.

In our modern world, technology has provided mechanical devices to fulfill functions formerly provided by humans and animals, but the dog's combination of sensory acuity, mobility, and bond with humans leaves it uniquely qualified as a tracker and detector for which there is no mechanical surrogate. In addition to its continued use in hunting and locating missing persons, dogs are currently being used in a wide variety of other search tasks, all presumably depending on olfactory sensitivity. For example, in the United Kingdom dogs have been used to locate and retrieve parts from crashed aircraft at the RAF Farnborough base (Boorer, 1969) and by the police to locate unknown, but suspected burial sites (Lewis, 1991). Of course, detecting contraband items at major airports and ports of entry has been and remains one of the detector dog's primary functions. The U.S. Customs Service (Francis, 1990 a,b,c), the Department of Agriculture (Eastwood, 1990), and the Federal Aviation Administration regularly employ dogs to detect drugs, contraband food and plants, and explosives at ports of departure and entry.

There is extensive precedent for the use of dogs as explosives detectors. The U.S. Army has funded several projects (e.g., Carr-Harris and Thal, 1970; Nolan and Gravitte, 1977) which have demonstrated the dog's ability to detect mines, trip wires, and tunnels. These capabilities were subsequently tested in the war in Viet Nam. Based on the U.S. experience in Viet Nam, the government of Thailand, beginning in 1970, developed 300 teams of mine-detecting dogs and their handlers to locate and remove mines left by various insurgent groups (Francis, 1991a). In 1989 the Thias sent 14 trained mine-detecting dogs to be used in Afghanistan (Francis, 1991b). The Soviets left 50,000,000 mines in roadways, airstrips, and towns. Commerce was at a standstill. Many mines were buried too deeply to be detected by metal detectors. Mine clearing by teams using only metal detectors proceeded at 200 meters of highway per day whereas dog teams averaged 2 to 4 kilometers of highway clearance per day. These 14 dog teams cleared 2,473 mines from 636 kilometers of road and two airstrips. No dogs or humans were lost or injured. There are now 50 dog teams at work in Afghanistan, the remainder trained under the auspices of USAID.

More specific to airport security, the FAA has trained handlers and dogs to be deployed as explosives detectors at major airports throughout the U.S. where they are used to search aircraft, vehicles, and freight and baggage areas in the event of an alert. U.S. Customs and the Department of Agriculture have extensive training programs for "sniffer" dogs to detect contraband drugs and food and plant items.

Until recently, most of the "evidence" for the dog's keen sense of smell was anecdotal. Comparative anatomical studies, however, indicate that dogs have a highly developed olfactory apparatus The shape of the skull and the air passages are particularly appropriate for warming, moistening, and moving air over the olfactory epithelium. That olfactory epithelium is large (30 times larger than that of humans) and convoluted and contains a large number

of receptors (20 to 40 times as many as humans). Each of those receptors contains 6 - 16 cilia (twice the number of human receptors). Since the dog's nares are completely separated by a septum, it essentially has a bilateral separation of olfactory stimuli which allows it to detect the direction and/or location of an odorant source similar to directional hearing or auditory localization.

Both laboratory and field studies, varying in procedures and precision, all agree that the dog's absolute sensitivity for a given chemical is considerably greater than that of humans. Psychophysical studies of canine olfactory sensitivity suggest that dogs can detect chemicals in molar concentrations 3 - 4 log units less than those detected by humans. Table 1 summarizes some observations from several studies about the thresholds of dogs to a variety of odorants.

Not much is known about the dog's differential sensitivity to odor intensity, but the alleged ability of the dog to track an individual in the correct direction suggests that it is discriminating a fine gradient in odor intensity. The successes of dogs in tracking and in detecting contraband items and explosives suggests that they are capable of ignoring distractors and attending to the signal odorant. The detector dog training program at Lackland AFB has demonstrated that dogs can be readily trained to respond to each of several members of a class of odorants while ignoring a variety of distractors. A recent study by Craig (Personal Communication) analyzed the training of 82 drug detector dogs in the Lackland Detector Dog Training School. German Shepherds, Belgian Malinois, German Shorthaired Pointers, Beagles, English Pointers, Labrador Retrievers and Cairn Terriers were trained to detect marijuana, hashish, cocaine, and heroin. The dogs were trained to search warehouses, occupied and unoccupied buildings, aircraft, vehicles, theaters, open areas (woods or fields) and luggage. They attained a 90 to 95% proficiency level within twelve weeks.

There is often a tradeoff between sensitivity and selectivity in designing electronic detectors. As the device becomes more sensitive it brings in more signals and cannot select between them. Consequently, the target signal becomes lost in the noise of the other signals. The usual remedy is to reduce the sensitivity. The dog seems to be an olfactory detector with a high degree of sensitivity which, by training, can also be made highly selective without loss of sensitivity.

The current machine technology is almost exclusively fixed-base, and most machine detectors are still in the developmental stage. Several of the larger systems are still in the prototype stage and won't even be available for testing until 1994 to 1996. The cost of dog-handler team training is a mere fraction of the cost of current bomb detection devices. Dog teams are mobile and reliable within known training limits. They also enjoy a reputation for accuracy such that the deterrent and public relations aspects of detector dog technology is an important psychological factor which cannot be over estimated.

A current problem with detector dogs is that the dogs frequently exhibit a decline in performance over time after deployment to the field which requires checking and constant retraining. Additionally, when performing a search task dogs become tired after approximately 30 to 120 minutes of work which suggests the need for two or more dogs in each location, the number depending on the size of the airport and the number of machine detectors in operation. Of course, the machine detection devices also require regular checking and recalibration.

Several federal agencies have dog teams in place and have their own training facilities, e.g., the Customs facility at Front Royal, VA. The Department of Agriculture also trains its own dogs. FAA contracts the training to the U.S. Air Force which trains the FAA's dogs at Lackland AFB.

Recently, Public Law 101-45 mandated that the FAA review its explosives detection procedures and initiate research to evaluate various forms of explosive detection technologies including the explosives detector dog teams. This paper reviews that technology and suggests research which would allow its integration with machine technologies.

2. A BRIEF EVALUATION OF EXPLOSIVES DETECTOR DOG TEAM TECHNOLOGY

When crude order of magnitude calculations to estimate the mean concentrations of various explosives chemical cues in the field are compared with the upper bounds for reported laboratory dog olfactory thresholds, it appears that the number of molecules that could be emitted from a concealed explosive are large enough to be detected by a canine's sense of smell (Caine, Mason & Morton 1985). It is also quite possible that chemical cues of low volatility may be transported to chemical sense organs such as the dog's vomeronasal system via dust

particles or water droplets, particularly from targets that have been concealed for a long period of time. The aerodynamics of odorant dispersal over short ranges suggests that the distribution of odorant in the atmosphere usually consists of pockets (or plumes or filaments) of high concentration comingled with pockets of air that contain virtually no odorant. Odor detection under these conditions requires a sampling strategy that optimizes the likelihood of sampling an odorant containing filament. This implies that the sensor must be properly oriented with respect to the prevailing wind and that the positions of eddies (or odorant plumes) be located. Dogs invariably orient their noses downwind from possible odor sources and their vibrissae are exquisitely sensitive to air currents. Thus dogs are able to maximize the number of molecules reaching their noses through any instantaneous advection. This gives the dog a substantial advantage over artificial detectors, because it can move its nose to sample eddies in a nonrandom fashion. There is no convenient way for humans to visualize these eddies; therefore, an optimal strategy for sampling with a hand held detector device would be random sampling unless otherwise directed by a canine.

2.1 Specificity

Dogs can search for contraband concealed both on the person or in bags or packages carried by a passenger and can do so effectively even in areas where there are large numbers of people in close proximity. Dog/handler teams are mobile search units which are particularly well suited for searches of areas such as aircraft, vehicles, cargo, baggage lockers, warehouses and terminals. Well trained explosive detector dog teams offer mobility, speed and accuracy which cannot be matched by current artificial detector technology. Portable machine systems may augment or complement the detector dog teams' effectiveness, however in certain environments such as in aircraft searches and in time-critical tasks prior to explosive ordinance disposal (EOD) operations the dog team has no competition. Finally, the detector dog teams' reputation as a highly reliable contraband detection technology has powerful psychological value both as a deterrence to potential terrorist activity as well as for maintaining the public's confidence in airport security measures against terrorism during periods of international tension or social unrest.

2.2 Sensitivity

The training program at Lackland AFB demonstrates that a variety of dog breeds can be trained to correctly detect all of the nine major explosives on at least 95% of the test trials prior to certification. Higher performance levels of 98% or 99% correct detections are also possible but are not cost effective under current training protocols. Maintenance of these high proficiency levels following deployment of the detector dog to the field is a significant problem which has not been adequately addressed to date. A human factors task analysis of the handler/dog interface is a necessary first step to developing improved handler and dog selection and training procedures. Research to determine the dog's absolute thresholds for the nine major explosives and investigations of various methods for enhancing sensitivity are long overdue. Thus the physiological limits of the detector dog technology have not as yet been defined. We believe that new behavioral and pharmacological strategies could be utilized to produce a superior explosives detector dog/man/machine system.

2.3 Cost

Currently the cost of training a detector dog and a handler at Lackland AFB is approximately $18,000. The yearly salary of the handler who is responsible for the care and maintenance of detector dog's skills varies depending on the agency which supports the team as well as the handler's experience and years of service. Ideally, multiple dog teams should be deployed to all Category X airports in the USA. However, significant problems in maintaining the skill and proficiency of certified dog teams after deployment to the field have been consistently identified. Research to study methods to remedy these problems and to improve the dogs' performance should be funded.

2.4 Relation of Detector Dog Teams to Other Methods and Possible Systems Interactions

Machines usually must sacrifice some degree of sensitivity for selectivity in order to avoid losing the target signal among the noise of other signals whereas dogs can be trained to be highly selective for the nine explosives without loss of sensitivity. All available information indicates that detector dog teams are potentially reliable, the current problems with

maintaining their skills after deployment not withstanding. Detector dogs which are in place at all major airports are certified 95% correct at time of deployment. Dogs don't need to be recalibrated during a search if their skills are appropriately maintained. They could be utilized in conjunction with a variety of machine explosive detector technologies to reduce the false alarm rate following a potential detection by a mechanical device. They also offer mobility, speed and a known level of accuracy. When a time-critical search for explosives must be made within a closed space like an aircraft, only the dog can indicate where to focus a physical search by the EOD. And only a dog can then be used in that same closed space following the disposal of the first bomb to search for a second explosive device.

In other instances, a portable machine explosives detector device could be used to complement the detector dog team during the search of a warehouse or luggage locker by indicating a general area to be subsequently searched by the dog team. Dogs have a time limited search capacity in that they can only be motivated to work effectively for periods of 30-120 minutes at a time without a break. Once on line, a machine will work for a period of 20 hours or more without maintenance or recalibration. Using a portable ED machine to limit the length of the dog's search by indicating specific areas to be examined would assist the dog to maintain sufficient motivation to work efficiently and to conserve its energy during a time-critical search in areas where machine EDs would be less effective or unable to set up and operate.

Potentially a detector dog team could also be used to back up a machine baggage examination system such as a mass spectrometer using batch sampling techniques for screening pallets or cargo containers. The required throughput speed of baggage handling could be preserved if a detector dog team could be held in reserve to search if the machine indicates the presence of explosives in a container. Ordinarily this requires a manual search of all baggage to determine which one contains contraband, or it requires several secondary samples be taken in a binary search technique. Both of these are prohibitively time consuming and costly. However, a dog specifically trained for this purpose could rapidly identify the particular item of baggage containing the explosive when the pallet or container is unloaded thus avoiding the physical search of most of the baggage and saving at least 80% of the time which otherwise would be necessary to physically search each bag. We are not proposing that dogs be used to screen all bags but rather to use them as a back up. This would utilize the best aspects of both systems.

The major problem for deployed detector dog teams is the decline in performance over time following assignment to the field. This implies a need for procedures for maintaining readiness of the dog at an acceptable level of proficiency through regularly scheduled retraining and proficiency testing. Portable machine detectors could also assist dog handlers during training and retraining to guard against contamination of search areas by training aids, and to avoid contamination of the dog's coat by training aids.

It is also important to maintain the efficacy of the motivating reinforcer by means of appropriate scheduling of reinforcement following deployment to the field. Examples are feeding dogs 10-15% less than normal so that they will be motivated to work for food reinforcers or avoiding making the dog a pet and taming it so that chasing a ball will be reinforcing. Then giving training which systematically reinforces correct performance. Many dogs live at the homes of their handlers. This may have both positive and negative features (e.g., weight gain or access to reinforcers such as too much play, taming, etc.) Handlers must be alert to any decline in performance and aware of the consequences of any retraining procedures or to any possible extraneous influences or factors which could result in unexpected performance decrements. The handler must also be capable of taking appropriate remedial action if this occurs. The recent recertification procedures for FAA detector dog teams, which had an unacceptably high failure rate, suggests that the selection, training, and supervision of handlers following deployment needs serious scrutiny.

2.5 Current Status

Several federal agencies have dog teams in place and either have their own training facilities, or contract the whole operation to private contractors who provide the dog-handler teams to a variety of consumers e.g., FAA dogs trained at Lackland AFB. However, although detector dog teams are currently in place at major facilities across the country we are not sure how well their skills are being maintained. Public Law 101-45 mandates that the FAA review its explosives detection procedures. Unfortunately, as of this date in late '91 no research effort to accomplish

this for the detector dog technology is in progress. A research effort should be initiated to study the multiple possibilities for utilizing dogs as explosives detectors both as primary first line detection systems and/or as back up systems. This should include investigations of methods of improving the training and the sensitivity of dogs as well as the selection, training, and supervision of handlers.

2.6 Research

The methods to be described in this section are technologically and behaviorally complex. They are sketched here to indicate that the behavioral methodology for measuring sensitivity and the technology for measuring the physical stimulus are currently available. However, their use would be unwise if not impossible for anyone who has not had advanced training in psychophysics and behavioral science. We believe that the detector dog technology is good; however, no one knows how good. We also believe that methods exist to improve it as well. Since the dog teams are currently in place and functioning it makes sense to investigate how good they currently are, how good they could become, and ways to integrate them with other technologies. The thesis of this paper is that it is currently possible and economically feasible to develop a superior explosives detection system for airport security which integrates dogs, men and machines. However, in order to achieve this goal several basic and applied research projects need to be accomplished.

2.6.1 Evaluation of Current Detector Dog Team Skills

At the time of deployment detector dogs trained on all nine major explosives odors are certified to be capable of 95% correct detections. However, their performance frequently deteriorates following deployment to the field. Whether this is due to their original training (e.g. with contaminated training aids) or to poor skill maintenance or to mismanagement by the handler is at present undetermined. Therefore, an empirical evaluation of currently deployed dog/handler explosives detector teams in a standardized field trial needs to be performed by an objective and independent research team. We need to evaluate currently deployed detector dog/handler teams in a well controlled and entirely novel test environment in order to assess their ability to detect pure uncontaminated explosive vapors; to assess their abilities to detect standard training aids (contaminated by handler or dog smells as well as by naturally occurring masking elements), and to compare these results with the detection of "pure" vapors of explosives. We also need to make direct comparisons with a variety of vapor and particle detector devices.

2.6.2 Determination of Canine Olfactory Detection Thresholds for the Nine Major Explosives

Absolute detection thresholds for explosives vapors need to be determined in order to establish the theoretical limits of the dog's olfactory explosive detection abilities. We also need to study both sexes and a variety of breeds to determine if there are important breed and sex differences in the dog's explosives detection abilities. This will allow the selection of the best breeds for training relative to both chemosensory sensitivity and operational requirements. Finally, comparisons should be made to mechanical explosive detectors to determine whether the dog can do a better job, or could be used in conjunction with or to back up a machine detector. Even if the dog is more sensitive, but unable to sustain high performance levels for more than 30 minutes, it may still be an effective back up for a machine with lower sensitivity in order to reduce the false alarm rate to an acceptable level.

2.6.3 Measurement of Olfactory Thresholds in Canines

Over the past 40-50 years there has been a consistent effort by researchers in olfaction to measure the responses of animals and humans to different concentrations of a wide variety of odorants. The single most commonly generated measure from these studies is the absolute threshold. Although there are a variety of definitions of this term (see Engen 1971 for an excellent review of this topic as it relates specifically to olfaction), it is generally taken to mean the lowest concentration of odorant that can be detected. Concentrations higher than this are required for odor identification. Concentrations lower than threshold cannot be identified through the olfactory receptors. They may be identifiable on the basis of some other attribute such as their ability to act as irritants to the nasal or ocular systems.

Progress in the study of olfaction in dogs has improved with the advent of the olfactometer so that odors can be presented in a more controlled way. Trial characteristics and odor concentrations can now be accurately specified. Modern procedures for

measuring thresholds with animals (animal psychophysics) involve conditioning techniques to establish different behaviors in the presence and absence of odor. Once this training is complete, the concentrations are lowered until no evidence of detection is seen. The ability to respond differently to odor and clean air declines in an orderly manner with decreases in concentration and supports the interpretation that a complete absence of this ability indicates the absence of odor sensations. More practically, threshold measurements in a given species provide an estimate of the minimum concentration required in order for particular odorant to influence behavior in the natural environment. The most straightforward means of comparing different animals or different species for odor sensitivity is to examine their thresholds for the same compounds. Powerful animal psychophysical procedures, such as conditioned suppression brings behavior under precise control for psychophysical measurements. This allows the investigator to more precisely define the "edge" of the detection threshold. While it is relatively easy to demonstrate that dogs can make use of airborne chemical cues, it is far more difficult to maintain odor stimulus control when stimulus concentrations approach the limits of a dog's sensory capacity. A variety of procedures have been developed to accomplish this. Most have used reinforcement techniques coupled with either response lever or body placement (e.g., nose positioned in the correct odor port) to register a response. The method of conditioned suppression combines both appetitive reinforcement and aversive conditioning (see Smith 1970 for a review of this procedure).

Systematic comparative research is needed to determine which canid species is better at judging intensity differences and how this ability may be influenced by nonolfactory factors such as nasal irritation and respiration (sampling rate). This research is predicated on the use of newly developed olfactometers, newly developed control techniques and reliable psychophysical methods in order to obtain more reliable detection thresholds and make direct comparisons of different canid species.

Walker (1989) has pointed out the need for adequate controls of stimulus concentration and purity, as well as the need to avoid psychological "impurity" (the perception of irritation as well as odor) and the use of procedures which avoid biasing subjects to either over-report or under-report odor stimulation. Walker has also reported that total volume of air breathed increases as an inverse function of concentration of odorant in air. His data suggest that even when there is no psychophysical evidence of detection of suprathreshold concentration of an odorant, e.g. in an anosmic subject, there are respiratory changes to odor stimuli at concentrations within the range of the psychophysical thresholds of normals. These data provide strong evidence that one or more nonolfactory systems are stimulated by odorants at concentrations at least as low as the psychophysical threshold for normals. These changes occur in several aspects of respiratory behavior and appear to be due to stimulation of the trigeminal receptors on the surface of the cornea and in the nasal cavity. Thus it seems essential to record psychophysical, physiological and behavioral measures in order to characterize an animal's chemosensory detector capabilities.

An automated system designed and recently patented by J.C. Walker is available for the measurement of the psychophysical, physiological, and behavioral responses of dogs to odorant stimulation of the nose. All aspects of the generation and production of odor stimuli from explosive molecules, the recording of physiological and psychophysical responses of the subjects and the storage of data are managed by an Apple IIe computer. The nasal olfactometer is based on electronic mass flow controllers which are used to control the ratio of volume flow rates of clean and odorant-saturated air. The output of the olfactometer is measured by a photo-ionization detector. Odor stimuli are delivered to fitted face chambers that allow stimulation of nose through teflon (rtm) flow valves. A video camera and a pneumotechograph, in combination with a pressure transducer records changes in respiration and behavior. A nose key is used to enter the dog's operant responding for water reinforcement directly into the computer. Odorant and control stimulus presentations are controlled by the computer which presents equal numbers of each during periods of operant responding which are matched for response and reinforcement rate and density.

3. AN EXAMINATION OF THE PROCEDURES FOR THE SELECTION AND TRAINING OF NEW TEAMS AND FOR THE REHEARSAL OR RETRAINING OF DEPLOYED DETECTOR DOG/HANDLER TEAMS

We need to examine the practices and procedures for selection, training and skill maintenance of detector dog/handler teams by means of human factors task

analysis of the man/dog interaction in detector team training. If as we suggest a portable ED is to be added to the dog team it would be important to perform the task analysis of the three-way man/dog/machine interaction.

3.1 Task Analysis

The purpose of a task analysis is to evaluate a procedure by identifying its components and determining how these individual components integrate into an efficiently functioning entity. Typically, a task analysis is used to match human operators to complex jobs requiring the use of equipment. The ability and training required for an optimum match among operator-equipment-outcome can be identified and the conditions and criteria for subsequent evaluations and modifications can be specified. Task analyses are routinely done to match humans and equipment. The present situation presents a unique opportunity to optimize a three-way match among dogs, humans, and equipment.

The strong probability exists that airport security can be maximized by the integration of the dog-handler explosives detector team with the newly developed machine detection technologies. The task analysis procedure can identify those responsibilities which are best allocated to the dog handler team and those which can be most effectively done by machine technology. Furthermore, a task analysis can tell us when and where the two systems can best supplement and complement each other.

The process of task analysis has four main parts. They are: identifying tasks, determining system structure, developing a functional task description which can take any one of several forms, e.g. a flow chart, and defining work modules (Bailey, 1982). Task analysis must not only consider the characteristics of tasks, but also of people and work settings (Guion, 1981). A completed task analysis logically leads to the identification of performance based criteria, preparation of instructional materials and training procedures, and development of evaluation techniques.

Identifying tasks essentially focuses on the information, skills, and performance levels that need to be developed in order for humans (and, in this case, dogs) to perform the tasks as described (McCormick, 1976). This requires that the system analysis consider such factors as current knowledge and skills required in related work systems, skill level categories and task complexity, redundancy among tasks, and integration of the tasks in meeting the overall purpose of the work system. Task identification often proceeds by successive approximation, repeating several times until the integration of the system and its work force are thoroughly understood.

System structure refers to the relative complexity of the various tasks involved in a piece of work. It describes the work system in regard to the proportions of simple, moderately complex, and highly complex tasks it contains. This description suggests the level of experience required of individuals entering training, the extent to which previous experience will transfer into the system, and how quickly one should master the training. Functions are statements of required work which incorporate tasks with similar requirements and levels of complexity. The structure of an already extant system can be identified and compared with that of an "ideal" system suggested by the task identification process above.

A task description in the form of a task level flow chart is then developed to illustrate the integration and interdependence of the tasks which make up the work system. This stage provides a check on the previous stages, identifying omissions and unnecessary redundancies. When this stage is completed, the work modules can be defined.

A work module is a basic unit of work (Bailey, 1982). It is the set of tasks that the worker must accomplish in completing a part or all of the work system. Work modules, however, can be made up of tasks from several different functions (see system structure above). A function is a statement of required work, but a work module is a description of the work (task set) to be accomplished by a specific person.

A description of the work system in terms of tasks, functions, and modules must include the characteristics of the work settings and of the people to do the work (Guion, 1981). Work settings are typically described by work space, organizational, managerial, and social variables. Work space variables include descriptions of areas, structures, vehicles, barriers, numbers of people, and condition such as temperature, lighting, noise, and humidity. Organizational variables deal with the chain of command and managerial variables describe the management policies and communications within that

chain of command. Social variables consider the work climate; e.g., attitudes of confidence, cooperation among colleagues, competitiveness, stress, etc.

Characteristics of people are the individual difference variables which qualify one for training and placement in the work system. They can include physiological responses, sensorimotor capability, task proficiency, task related knowledge, information processing, personality or temperament, and attitudes.

Once the task description has been completed, the system structure, as it currently exists can be evaluated for efficiency and any improvements identified and instituted. Subsequent procedures would be directed at revising training procedures, producing training aids, and developing field test and evaluation techniques and methods for maintaining the proficiency of the dog/handler teams in the field.

4. BASIC RESEARCH ON ENHANCING ODOR SENSITIVITY AND IMPROVING ODOR DETECTION TRAINING

Data from drug detector dogs trained at Lackland AFB Detector Dog School (Craig, Personal Communication) indicate that the average dog will learn to detect an odor at any of four locations and respond fifteen consecutive times correctly in six days. They will learn to discriminate subsequent odors to the same criterion in two days. Positive transfer of training occurs when dogs are trained on more than one odor since the number of trials required to learn the subsequent odors decreases. These data also indicate that task sequence, sex, and breed are not important, at least with present training and selection procedures. Final certification averages 35 training days with a standard deviation of 14 days.

Although we understand how dogs are currently trained to discriminate odors, there are several pharmacological and behavioral techniques for sensitization, potentiation, and enhancement of detection techniques which need to be evaluated for their applicability to the detector dog training procedures.

4.1 The Influence of Selected Drugs on Measures of Olfactory Sensitivity

The degree to which olfactory sensitivity can be enhanced by pharmacologic agents has received little attention, although recent studies suggest that some drugs can enhance or depress the odor detection performances of rats. For example, at very low doses (.2 mg/kg), amphetamine enhances detection performance of rats to the odorant ethyl acetate, whereas at slightly higher doses (1.2 mg/kg) this drug depresses such performance, without significantly altering motor performance, per se (Doty & Ferguson-Segall, 1987). Recent data suggest that these effects may be due to differential stimulation of dopamine D-1 and D-2 receptors. Thus, the dopamine D-1 agonist SKF 38393 enhances detection performance, whereas the dopamine D-2 agonist quinpirole depresses such performance (Doty, Li, Pfeiffer & Risser, 1990).

Despite such observations, it is important to note that a number of drugs which adversely alter odor-guided behaviors in the field have, in fact, little influence on olfactory sensitivity, per se (e.g. fluprazine hydrochloride; Doty, Li & Risser, 1990). Thus, rigorous psychophysical evaluation of not only the effect of a drug on olfactory sensitivity but of other related factors is needed; for example, some drugs may alter olfactory function via sharpening of the signal to noise ratio in a complex signal or by altering odor memory. Studies should explore the influence of a number of pharmacologic agents, including catecholanergic, serotonergic, and cholinergic agonists, on tests of olfactory detection, odor discrimination, and odor memory.

4.2 A New Behavioral Technology for Biosensation

A new behavioral strategy for the detection of flavors (compounds of taste and odor in solution) that, until recently has been used primarily for the study of ingestional learning, recently has been brought to bear on the problems of improving odor discriminations in animals. It has proved extremely successful in the learning of discriminations between various flavors. This technique involves presentation of a flavor for a brief period of time (e.g., 10 min) prior to administration of a malaise-producing chemical, lithium chloride. Aversions to the flavor are produced after only one pairing of the flavor and lithium chloride. This technique has allowed the examination of the retention of flavor aversions across time and the behavioral mechanisms of flavor memory.

4.3 Retention of Flavor Memory

Recent investigations have demonstrated that a flavor aversion appears to be stronger as many as 21 days after the flavor was originally paired with lithium chloride than it was 1 day after this pairing. Since flavor aversions are known for their strength, it is surprising to observe that these aversions were weaker 1 day after they were learned than they were as much as 3 weeks after they were learned.

When a complex flavor is consumed and followed by internal malaise, the aversions established to the various components of this flavor are often weaker than they are when the elements are conditioned separately. For example, when a strong bitter taste such as denatonium saccharide and a weaker sweet taste such as saccharin are paired with lithium illness (conditioned), the aversion to denatonium is weaker than when conditioning occurs only to denatonium alone if both tests for conditioning are performed one day after the taste illness pairings. This diminution of learning is known as **overshadowing** but could also be thought of as the effort of **masking**. However, when sweet saccharin and bitter denatonium are conditioned in compound and tested three weeks later, aversions to the saccharin are greater than when conditioning occurs only to the sweet saccharin element. This enhancement of flavor aversion is called **potentiation** and, at least empirically, is the opposite of overshadowing. The context (environment) of both the conditioning and of the testing has been found to influence the manifestation of flavor memories in the following way: The novel taste and the malaise experienced during flavor aversion conditioning sensitizes the contextual stimuli present on this occasion. If these contextual stimuli are not further familiarized or extinguished before the flavor is tested in the presence of these contextual stimuli, they will interfere with the retrieval of the flavor memory. This retrieval interference is more likely to occur if the flavor aversion is tested 1 day after conditioning than 21 days after conditioning because the conditioning environment will not have been rehabituated or extinguished. Flavor aversions to the saccharin were stronger if animals spent the interval between conditioning and testing in the conditioning context (in other words, if the conditioning occurred in the home cage).

These findings have significant importance for the training of explosive detector dogs in the following ways: First, the effectiveness of an odor as a training stimulus can be increased through manipulation of the interaction with taste. Second, retention of an odor memory can be improved with time if the novelty of the background cues in the testing environment is reduced through repeated exposure or familiarization. One determinant of how readily a flavor memory can be retrieved is the presence of contextual stimuli which can interfere or compete with the retrieval of a flavor memory. To prevent retrieval competition at the time of a test, the contextual stimuli around which the test occurs should be familiar and any contextual stimuli that were present during conditioning should be refamiliarized. This implies that an unbiased objective test of a dog team's potential explosives detection skills should actually be conducted in an entirely novel and unfamiliar environment (simulating the real world). On the other hand, training and actual searching would benefit from presenting stimuli which were present during the initial training (reminders).

Applications of these findings could be brought to bear on the training of dogs to detect explosives in the following ways:

1) This method should allow the rapid acquisition of conditioned responses to explosives vapors. We believe dogs could be trained to detect target odors presented in taste/odor compounds (flavors in solution) in only a few trials. Using this method, one could reliably produce both conditioned aversions to taste-in-solution and conditioned preferences to odors-in-solution. Additionally, a conditioned inhibition methodology could be employed. The conditioned inhibition procedure makes target stimulus B one which predicts a period of safety in the context of danger to stimulus A. Stimulus B could be the odor of the explosive to be detected which would be appetitively conditioned by pairing it with recovery from illness (conditioned preference) while stimulus A could be an aversively conditioned taste. Taste A could then be administered at the beginning of a search to provide a mildly aversive excititory context (the dangerous context) to set the occasion for performance of the task of detecting (the safety signal) odor B. The administration of this reminder (taste A) in the field should facilitate the performance of a search for explosives vapors.

2) This new method should yield high resistence-to-extinction of the conditioned responses. A persistent problem in bomb-detecting dogs is that their behavior deteriorates over time. Conditioned odor preferences in rats have persisted (failed to extinguish) for as long as they have been measured. Therefore, by implication, this new training method should avoid the rapid deterioration of performance currently occurring with present training techniques. Theoretically, once established, these conditioned responses should be relatively permanent. Dogs trained using the conditioned inhibition procedures should need minimal, if any, retraining in the field.

3) Sensitivity enhancement. Conditioned inhibitory procedures theoretically should sharpen discriminations for target odors. Animal psychophysical methods used to measure odor thresholds could in theory be improved if conditioned inhibition procedures were incorporated into the animal training regimen.

5. FUTURE DIRECTIONS

The dog's history as a domesticated animal and its sensitivity to most odors makes it ideal to train as an explosives detector. Although data on vapor phase chemical cues for explosives suggest they may not be powerful odorants, careful psychophysical determinations of olfactory thresholds for explosives need to be accomplished on representative samples of canines in order to establish whether dogs can reliably detect the vapors of explosives at the low pressures emitted from concealed sources. We are aware that vapor phase chemical cue estimates of homogeneous transport suggest that the impurities in explosives are more likely to provide a basis for olfactory detection than the explosives vapors themselves. However, if dogs can be shown to detect pure explosives at these low vapor pressures, a behavioral technology now exists which can train the dogs to perform reliably. An immediate research effort is needed to obtain this vital information as well as to integrate new machine based technology with the current detector dog team technology. These technologies could be complementary and supplementary and will provide the redundancy necessary in a system which must have the level of fail-safes that airport security requires. This integration would also help to minimize passenger delays due to baggage inspection. The mobility of the dog and the speed with which it can sweep a given area to identify the general location of a bomb or bombs is a quality that no mechanical device, fixed base or portable, can yet duplicate. The determination of explosives detection thresholds for dogs, the human factors analysis of the training procedures, the actual field testing, and the subsequent study and improvement of recertification and retraining procedures is of great importance. This information will make it possible to have dog teams functioning on-site more quickly, to deploy them more widely and at a far lower cost than the current machine technologies development promise. When improved machine technologies do come on line and are integrated with the new detector dog team technology, airport security will be even further improved.

REFERENCES

1. Bailey, R. W. (1982). Human performance engineering: A guide for system designers. Englewood Cliffs, NJ: Prentice-Hall.

2. Barker, L. M., Herbert, L., and Bowman, M. Conditioning the Odor of Alcohol by Pairing Cocktails with "Getting Well." Presented at the 31st Annual Meeting of the Psychonomic Society. New Orleans, LA: 1990.

3. Barker, L. M., & Weaver, C. A., Conditioned flavor preferences in rats: Dissecting the 'medicine effect'. 1991. Learning and Motivation., 22, 311-328.

4. Barker, L. M., Chalhoub, A., Bowman, M., and Herbert, L. Concurrent conditioning of odors: evidence for a conditioned inhibition interpretation. To be presented at the 3rd Annual Meeting of the American Psychological Society, Washington, D.C., May 1991.

5. Barker, L. M., Chalhoub, A., Bowman, M., and Herbert, L. Concurrent conditioning of odors: evidence for a conditioned inhibition interpretation. (Ms. in preparation).

6. Batsell, W. R., & Best, M. R. Variations in the retention of taste aversions: Evidence for retrieval competition. Animal Learning & Behavior, in press.

7. Batsell, W. R., & Best, M. R. Retention of taste aversions. Poster to be presented at the 32nd Annual Meeting of the Psychonomic Society, San Francisco, November 23, 1991.

8. Boorer, W. (1969). The world of dogs. London: The Hamlyn Publishing Group Ltd.

9. Cain, W. S., Mason, J. R., & Morton, T. H. (1986?). Use of animals for detection of land mines and other explosives: A review and critique of prospects. US Army Mobility Research and Development Command, DAAK70-84-K-008.

10. Carr-Harris, E. & Thal, R. (1970). Mine, booby-trap, tripwire and tunnel detection. Technical Report No. LWL-CR02B67 & 01B68, US Army Limited War Laboratory, Aberdeen Proving Ground, MD 21005.

11. Chao, E. T. (1977). Olfaction in dogs: A critical review. Unpublished paper, Florida State University.

12. Craig, D. J. (Personal Communication) Training Drug Detector Dogs. Manuscript in preparation.

13. Doty, R. L., Ferguson-Segall M. (1987). Odor detection performance of rats to ethyl acetate following damphetamine treatment. Psychopharmacology 93:87-93.

14. Doty R. L., Li C, Pfeiffer C. Risser J. (1990). Enliancement of odor detection performance by the dopamine D-1 agonist SKF 38393. Psychopharmacology, submitted.

15. Doty R.L., Li C, Risser J. (1990). Influence of fluprazine hydrochloride on the odor detection performance of male rats to ethyl acetate. Pharmacology, Biochemistry and Behavior 35:699-703.

16. Doty R. L., Risser J. (1989). Influence of the D-2 dopamine receptor agonist quinpirole on rat odor detection performance before and after administration of spiperone. Psychopharmacology 98:310-315.

17. Eastwood, B. (1990). Beagles beg contraband foodstuffs. Dog World, 75, No. 8, 10, 144-149.

18. Engen, T. (1971) Olfactory psychophysics. In Beidler L. M. (Ed) Handbook of Sensory Physiology, Springer-Verlag NY p 216-244.

19. Francis, C. (1990a). Drug dogs go maritime. Dog World, 75, No. 9, 14, 125.

20. Francis, C. (1990b). The making of a sniffer dog. Dog World, 75, No. 11, 16-17, 58-60.

21. Francis C. (1990c). U.S. Customs opens doors to canine sniffers. Dog World, 75, No. 7, 12, 62-64.

22. Francis, C. (1991a). Sniffers in Afghanistan. Dog World, 76, No. 5, 13-14.

23. Francis, C. (1991b). Mine-detecting dogs secure Afghanistan. Dog World, 76, No. 6, 14-18.

24. Guion, R. M. (1981). Problems of measurement in organizational psychology. In J. A. Sgro (Ed.), Virginia Tech symposium on applied behavioral science. Lexington, MA: Lexington Books.

25. Lewis, S. (1991). Body dogs. Dog World, 76, No. 7, 54-61.

26. McCormick, E. J. (1976). Human factors engineering. 4th ed., New York: McGraw-Hill Book Co.

27. McCormick, E. J. (1979). Job analysis: Methods and applications. New York: AMACOM.

28. Nolan, R. V. & Gravitte, D. L. (1977). Mine detecting canines. Report No. 2217, US Army Mobility Equipment Research and Development Command, Ft. Belvoir, VA.

29. Passe, D. H. & Walker, J.C. (1985). Odor psychophysics in vertebrates. Neuroscience & Biobehavioral Reviews, 9, 431-467.

30. Smith, J. C. Conditioned suppression as an animal psychophysical technique. In: Animal Psychophysics: The Design and Conduct of Sensory Experiments, edited by W. C. Stebbins. New York: Appleton- Century-Crofts, 1970.

31. Walker, J. D., Reynolds, J. H., Warren, D. W. and Sidman, J. D. (1989). Responses of normal and anosmic subjects to odorants. In G Green, B.G., Mason, J. R., Kare, J. R., Chemical Senses Vol 2 Irritation, Marcel Dekker, NY p 95-121.

32. Yeaple, J. (1991). The bomb catchers. Popular Science, 239, No. 4, 61-65, 98, 102, 104.

Table 1. Canine thresholds (in molecules/cc) for various odorants. (after Caine, Mason, & Morton, 198)

Odorant	Thresholds
acetic acid	5×10^{5}, 6×10^{12}, 2×10^{18}
amyl acetate	1×10^{5}, 2×10^{11}
butyric acid	1×10^{4}, 3×10^{9}, 3×10^{16}
caproic acid	4×10^{4}, 2×10^{10}, 2×10^{17}
caprylic acid	5×10^{4}, 5×10^{8}, 3×10^{16}
formic acid	3×10^{14}, 2×10^{19}
haptanoic acid	8×10^{16}
heptylic acid	3×10^{8}
isobutyric acid	4×10^{9}
propionic acid	3×10^{5}, 1×10^{11}, 1×10^{17}
valeric acid	4×10^{4}, 9×10^{10}, 3×10^{17}

LOGISTICS AND THE "ILITIES" REQUIREMENTS FOR EXPLOSIVE DETECTION SYSTEMS

Russell L. Cole and Gerald V. Brown
Science Applications International Corporation
2950 Patrick Henry Drive
Santa Clara, CA 95054

1. INTRODUCTION

For purposes of this paper, Explosive Detection Systems (EDS) will include Thermal Neutron Analysis (TNA), Fast Neutron Analysis (FNA), Pulsed Fast Neutron Analysis (PFNA), and Gamma Resonance. These techniques, either by virtue of demonstrated performance or from their promise based on preliminary findings, are all accepted explosive detection techniques. These techniques all share common characteristics. They are expensive, both to acquire and to operate. They are large. They incorporate complicated technology. The technology they use is unique.

These characteristics taken as a whole are a recipe for high costs. Economies of scale are limited. Availability of trained personnel is non-existent. The limited application resulting from the cost factor results in higher support costs. Qualified suppliers are scarce. Lead times are long. Volume production is not feasible. Development is costly, so prototypes often move directly into production.

Further exacerbating this difficult situation, system requirements are demanding. EDSs must be available, reliable, accurate, maintainable, supportable, and safe. Levels of performance, thought to be acceptable only a matter of months ago, are in a state of flux.

How then, in the face of these seemingly insurmountable challenges, do we design and develop systems and equipment that meet our needs as companies, agencies, governments, and as a people? The answer lies not in panaceas or miracle cures. This paper will offer, at least as a partial solution, an approach utilizing proven methods across a broad spectrum of techniques and a recognition that the success of these efforts lies in your individual creativity and ingenuity.

2. LOGISTICS AND THE "ILITIES"

A story has been told, and attributed to Werner Von Braun, of the early days of rocket development in Germany. It seems that a requirement for a highly reliable pump, with high capacity, low weight, and high availability was identified. Scientists and engineers carefully specified and debated the trade-offs between various design parameters. When the dust settled, a crack team was put to work on designing the pump. Nearly two years later, at enormous cost of time and effort, the pump was ready for testing. It worked. When the pump was in the process of being integrated into the first manufacturing run, a worker asked why a standard pump, currently in use on fire engines (which, incidentally, met all the design criteria), had not been used. There was no credible answer. Two precious years were lost because certain types of knowledge were thought to have little or no value to the task at hand. Anecdotes abound, all with a similar message, early involvement by those not traditionally thought to be a part of the design process can pay unexpected dividends.

Fundamental to the approach we are recommending is the concept of interdisciplinary teams. Interdisciplinary teams bring fresh insights and new strengths to bear. Their efficacy has been demonstrated time and again. They can when skillfully used, make contributions not normally anticipated. Careful selection of the makeup of interdisciplinary teams can produce positive results.

3. TECHNIQUES AND AREAS OF APPLICATION

Logistics, the "ilities", system engineering, design to cost, operations research, and concurrent engineering, to name a few, are techniques of great promise. Their potential for contribution is limited only by the imagination of a given program manager and the practical constraints applied to the program i.e.,

schedule and budget. In order to fully develop our argument for the application of these techniques we will first define the techniques we wish to recommend and the specific areas where they are best applied.

Logistics according to the Society of Logistics Engineers (SOLE)[1], is 'the art and science of management, engineering, and technical activities concerned with requirements, design, and supplying and maintaining resources to support objectives, plans, and operations'.

Availability is the probability that a system or equipment will be capable of operating at or above a specified level of performance if called upon to do so at a random point in time.

Reliability is an inherent characteristic of a design. In simple words, this means that when the design is complete you cannot improve its reliability without altering the design or its operating environment. It is defined by Jones[2] as 'the probability that an item of equipment will perform its intended mission without failing, assuming that the item is used within the conditions for which it was designed'.

Maintainability is also an inherent design characteristic and, like reliability, 'what you see is what you get'. Without altering the design or its operating environment, you cannot change the maintainability of a system or product. According to Blanchard[3], 'it pertains to the ease, accuracy, safety, and economy in the performance of maintenance actions'.

Manability embraces the disciplines of human factors engineering and safety engineering. It deals with such items as personnel requirements, the accomplishment of analyses and trade-offs dealing with human-machine relationships, equipment design functions, the determination of training requirements, and the test and evaluation of the human being in the system. And yes, you guessed it, it too is an inherent design characteristic.

Supportability is a term, introduced with MIL-STD-1388-1A, Logistics Support Analysis, that defines the degree to which a system or product, when placed in its intended operating environment and already established support system, can be economically supported[4].

Concurrent Engineering Meredith and Blanchard offer[5] the following definition '...a systematic approach to the integrated, concurrent design of products and their related processes, including manufacture and support. This approach is intended to cause the developers, from the outset, to consider all elements of the product life cycle from conception through disposal including quality, cost, schedule, and user requirements.'

Life-cycle cost According to Blanchard[3], '...in addressing the economic aspects of a system, one must look at total cost in the context of the overall life cycle, particularly during the early stages of conceptual design and advanced system planning. Life-cycle cost, when included as a parameter in the systems engineering process, provides the opportunity to design for economic feasibility.'

4. APPLICATION

Techniques applied to the wrong areas are not likely to result in beneficial results. Application of the 'ility' techniques is most appropriate in the 'development' areas. The following definitions are offered to further limit the area of application.

The National Science Foundation (NSF) uses the following definitions of R & D in its resources surveys:

1. Basic research has as its objective "a fuller knowledge or understanding of the subject under study, rather than a practical application thereof."

2. Applied research is directed toward gaining "knowledge or understanding necessary for determining the means by which a recognized and specific need may be met."

3. Development is the "systematic use of the knowledge or understanding gained from research directed toward the production of useful materials, devices, systems or methods, including design and development of prototypes and processes."

It is evident from an examination of these definitions that the areas defined in 2 and 3 will be the most appropriate for logistics and the "ilities". These areas are where product development takes place.

Blanchard reports[3] that 41 percent of all scientists and engineers are engaged in applied research, development, and the management of research and development. This numbers more than one million individuals and does not include those performing R & D related functions through consulting, teaching, professional services, and others. Blanchard also states[3] that national expenditures for R & D by character of work reveal that the greatest portion is related to the early life-cycle activities of applied research and development. Of the total dollars expended in 1989 for R & D activities, 86% was directed toward applied research and development.

5. MAXIMIZING THE BENEFICIAL EFFECTS

When?

Isn't there a point beyond which the application of interdisciplinary teams have a negative effect? Won't this approach slow things down in the early stages? The answer to these questions is, of course, yes. But on the other hand, waiting too long can also have a negative effect as evidenced by the following:

1. Blanchard offers[3] 'Experience has indicated that a large portion of the total cost for many systems is the direct result of activities associated with the operation and support of these systems, while the commitment of these costs is based on decisions made in the early stages of the system life cycle.'

2. Again citing Blanchard[3] 'The costs associated with activities such as research, design, testing, production or construction, operations, consumer use, and support have been isolated and addressed at various stages in the system life cycle, and not viewed on an integrated basis.

3. Blanchard also reports[3] '...costs of operating and maintaining systems already in use are increasing at alarming rates.' This is due primarily to a combination of inflation and cost growth from causes such as:

    a. Engineering changes occurring throughout the design and development of a system or product (for the purposes of improving performance, adding capability, etc.).

    b. Changing of suppliers in the procurement of system components.

    c. System production and/or construction changes.

    d. Changes in the logistic support capability.

    e. Initial estimating inaccuracies and changes in estimating procedures.

    f. Unforeseen problems.

It has been noted on occasion that cost growth due to these various causes has ranged from 5 to 10 times the rate of inflation over the past several decades.

The obvious message here is to apply the techniques as early in the development process as possible, while there is still time to have maximum favorable cost impact on the design.

6. THE IMPLEMENTATION PROCESS

6.1 Change

Volumes have been written on how to implement change. This paper would not presume to offer anything other than a few observations by the authors and recommendations for further reading on the subject of change and how to implement it.

6.2 Getting Started

Do a "lessons learned" analysis of a recently completed project and extract the items that might have been avoided if the 'ilities' had been applied or applied differently.

Integrate logistics and the 'ilities' into your next project planning session. Let them raise issues and voice concerns. Better to deal with them when there is an opportunity to design problems out/improvements in than to attempt costly fixes later on.

7. THE PROCESS

Commencing with a definition of a "need", identify the characteristics desired by the user when the system is deployed in the users environment. These include, but are not necessarily limited to:

a. Functionality - Specifically identify

what, how much, when and where the system will perform.

b. Availability - Identify the minimum time the user demands the system be operational and what if any degradation can be tolerated.

c. Physical limitations - Identify space, weight, power consumption, configuration dimensions, and environmental maximum/ minimum requirements.

d. Manability - Clearly define the human interface.

e. Cost - Identify all cost limitations and cost factors. This is not just to define tolerable initial procurement cost, but to look at life-cycle costs all of the way to system retirement.

Once these factors have been addressed, a team of subject element experts is assembled to begin concept exploration and definition. This team should be planned to remain active on the project until the system is turned over to the customer for his use. The team is drawn from the required disciplines of science and engineering, but must also include experts in logistics and 'ilities.'

Working within the customer defined constraints, a system concept is developed that includes functional and characteristic allocations that meet the "need" and the customer imposed limitations. This is the most important phase of a system development program. As allocations of functions, availability, physical limitations, human factors and cost are made, the customer should be educated on the trade-offs that were made to reach these allocations and why these trade-offs were chosen. The customer should be an "active" member of the design team. This strategy minimizes surprises!

Once the customer has provided the desired system characteristics and imposed his limitations, a systematic process of allocations begins. Each step in this process involves analysis, trade-offs, and re-analysis. Systems Engineering is not a clear-cut science. Many disciplines must be called upon for inputs, opinions, and contributions. In the case of Explosive Detections Systems, physicists, chemists, psychologists, civil engineers, safety engineers, electrical engineers, mechanical engineers and others are called upon to conceptualize and develop the functionality of the systems.

But there's more than just the function - namely; "How long will the system function without failure?" and "How much will it cost - both to procure and to operate?"

These areas require to use another group of specialists. Reliability engineers, maintainability engineers, support specialists, logisticians, mathematicians, human factors analysts are just a few of the supporting engineering disciplines required to field a successful EDS.

8. UTILIZING SUPPORTING DISCIPLINES

While functional allocations are being derived by the science and engineering staff, the availability analysis should commence. An operational availability requirement or desire was obtained from the customer. This requirement may be so simple as to merely state "I want the system to work 98% of the time." Or it may be much better defined with such elements as mission time, through-put, maximum down-time, mean down-time, minimum reliability provided.

Regardless of the level of detail, it is necessary to obtain or develop information such that requirements and allocations can be made in such a language that the required system parameters may be defined in a classical way by all participants in the systems engineering process.

9. APPLICATION NOTES

9.1 Operational Availability

Using the term operational availability requires returning to the classical definition which was previously provided in words but is expressed mathematically as

$$A_o = \frac{MTBF}{MTBF + MDT}$$

Where:

A_o = Operational Availability

MTBF = Mean Time Between Failure

MDT = Mean Down Time

a customer's availability requirement, a trade-off must be made between MTBF and MDT.

The customer may have provided minimum requirements for either one or both of these parameters. In the case of MTBF, a relationship to reliability must be made.

$$R_t = e^{-\lambda t}$$

Where: R_t = Reliability

λ = Failure Rate

= 1/MTBF

t = Mission Time

10. RELIABILITY CALCULATIONS

A very useful application of the fundamental reliability equation, is to answer the question, 'what is my probability of being in operation "x" hours after beginning operations?'

$$R = e^{-\lambda t}$$

Given $\lambda = 0.0005$

λ = failures per hour

t = 24 hours

R = .988 or 98.8% probability of operating for 24 hours without failure

Obviously you can manipulate this equation to solve for any of the variables. It is quite often instructive to do so. For instance, suppose that you wish to know what failure rate will give you a 90% probability of operating for a 24 hour period.

Again, $R = e^{-\lambda t}$

and $\lambda = -\frac{\ln .9}{24}$

= 0.0044 failures per hour

If one takes the reciprocal of the failure rate (λ) you obtain the time between failures, normally presented as the MTBF or mean time between failures. Thus for the system described in reliability terms above,

1/0.0044 = 228 hours

Is this acceptable to you and your customer? Yes, then pass on this requirement to your designers and get on with it. If not, work with the parameters until you have an acceptable set. Note: It's not uncommon at this point to discover that you have a situation that is unacceptable from a cost standpoint, i.e., you have met the customers stated requirements, but the cost may be unacceptably high. This must be resolved and mutually acceptable parameters agreed upon.

11. RELIABILITY ALLOCATION

Reliability allocation allows one to take the individual elements of a system and provide each with an equitable share of the available system reliability. One may start with a very simple block diagram. The block diagram is expanded element by element with the reliability of the parent being allocated to the children. This provides both targets for designers and tracking points for management. Expect the allocation process to bring forth "screams of agony". These conflicts must be resolved in either of three ways, (a) rob peter to pay paul; (b) redesign; or (c) changed requirements. Figure 1 depicts a typical iterative allocation process. Figure 2 shows, in a different format, the results of the allocation process.

12. HOW NOT TO

Certainly, we would be remiss if we did not offer some 'words to the wise' regarding the pitfalls associated with applying the specialty engineering disciplines.

Do not be discouraged if your expectations are not met. Re-examine the expectations, the techniques, how they were applied, and develop new approaches. Remember you are tinkering with a process and as long as you are improving the process your efforts are justified.

Do not use fear or threats. Use positive motivation. Note: its ok to use the lessons learned and negative results to get peoples attention, but using those same items in a jawboning fashion can result in destructive backlash effects.

REFERENCES

1. Arsenault, J. E. and Roberts, J. A., Reliability and Maintainability of Electronic Systems, Computer Science Press, Inc., Potomac, Maryland, 1980.

2. Blanchard, Benjamin S., System Engineering Management, John Wiley & Sons, Inc., 1991.

3. Dhillon, Balbir S., Reliability Engineering in Systems Design and Operation, Van Nostrand-Reinhold Co., New York, New York, 1983.

4. Hammer, Willie, Product Safety Management and Engineering, Prentice-Hall, Inc., Englewood Cliffs, New Jersey, 1980.

5. Michaels, Jack V. and Wood, William P., Design to Cost, John Wiley, New York, New York, 1989.

6. National Science Foundation, National Patterns of R & D Resources, Final Report NSF 89-308, Washington, D.C.: 1989.

NOTES

1. Blanchard, Benjamin S., Logistics Engineering and Management, 3rd edition, Prentice-Hall, Inc., Englewood Cliffs, New Jersey, 1986.

2. Jones, James V., Integrated Logistics Support Handbook, Tab Professional and Reference Books, Blue Ridge Summit, Pennsylvania, 1987.

3. Blanchard, Benjamin S. and Fabrycky, Wolter J., Systems Engineering and Analysis, 2nd edition, Prentice Hall, Inc., Englewood Cliffs, New Jersey, 1990.

4. Specialty Engineering Primer, SAIC, 1991.

5. Meredith, Joe W. and Blanchard, Benjamin S., Concurrent Engineering: Total Quality Management in Design, Logistic Spectrum, Vol 24 Issue 4 Winter 1990, Journal of the Society of Logistics Engineers.

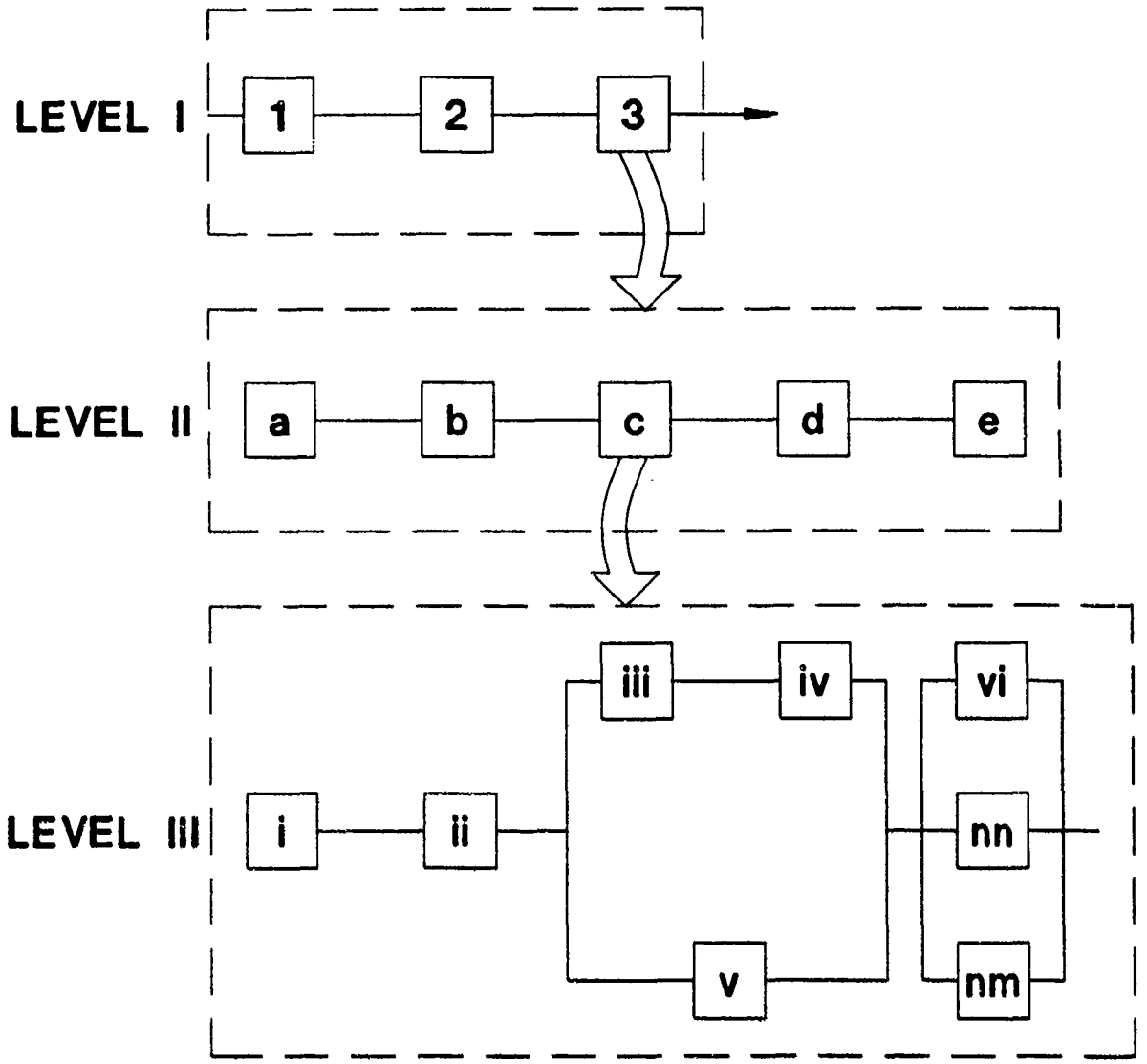


Figure 1. Reliability Block Diagram

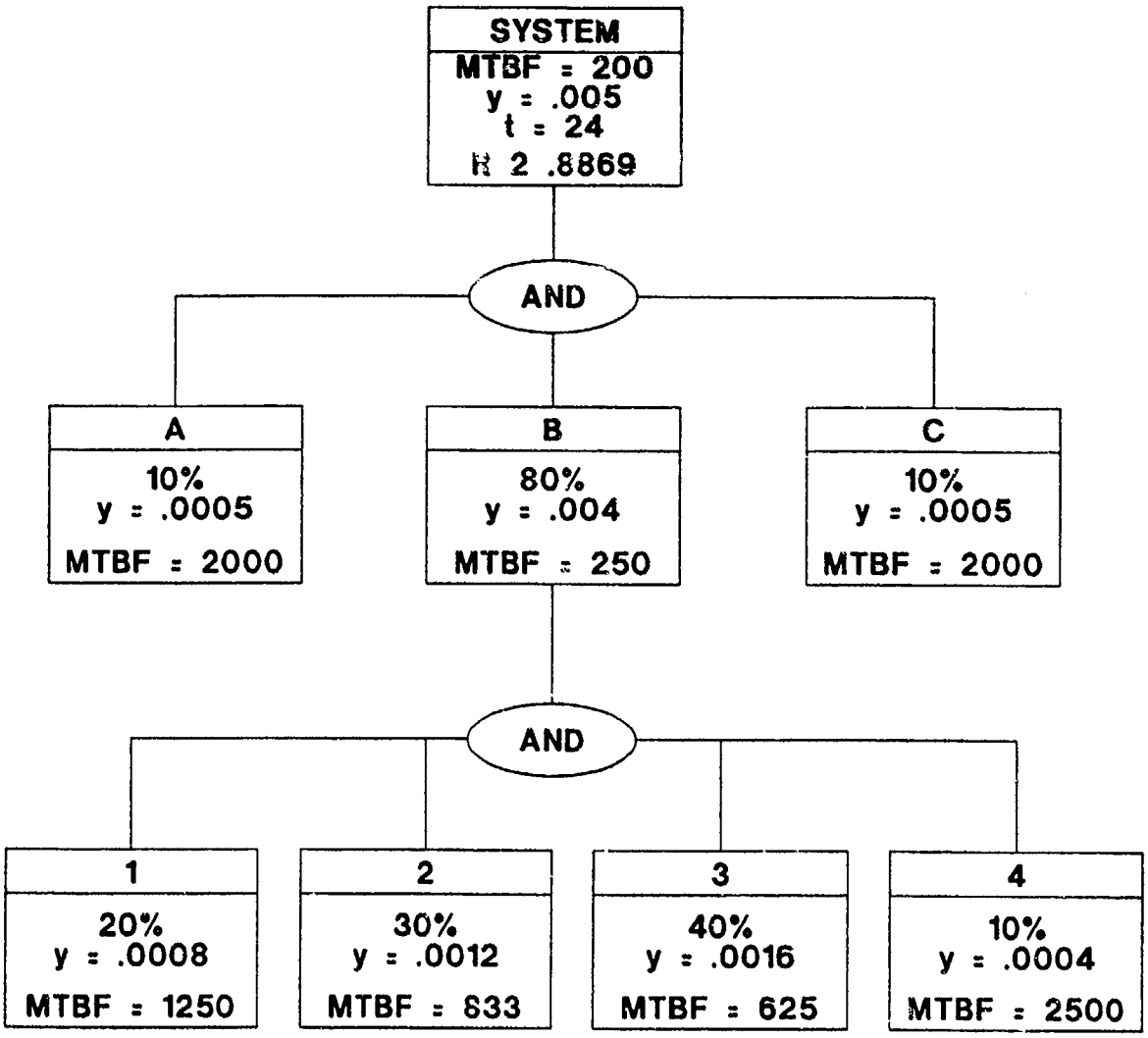


Figure 2. Allocation of Reliability Requirements

IMPACT ON THE AIR CARRIER OF EXPLOSIVE DETECTION SYSTEMS

Diane Hsiung, Patrick Shea, and Mala Sivakumar
Science Applications International Corporation
2950 Patrick Henry Drive
Santa Clara, CA 95054

1. INTRODUCTION

The addition or improvement of security screening measures will have an impact on air carrier operations. This impact must be at least planned for, and preferably evaluated to optimize the choice of systems and procedures to be used. In order to do this, an economic model has been constructed which allows for the comparison of different technologies and procedures on a common basis.

This paper describes the application of this model to one specific case. In this case, different X-ray technologies are compared to see which ones are most useful as a "secondary" screening for explosives in checked luggage. The different X-ray technologies are placed between a Thermal Neutron Analysis (TNA™, the "primary" screening system) and an arbitrary "tertiary" screening system (here taken as hand searching of the luggage). All of the alternative X-ray systems are operated at the same detection rate; and system performance information is used to predict how many bags are rejected to the tertiary screening for final examination. Note that this is just the specific case under study; the same modeling techniques can be applied to combinations of other systems to lead to a coherent evaluation of the relative merits.

The different systems being evaluated have quite different technologies for inspection, and thus will have very different strengths and weaknesses. The purpose of the economic model is to systematically compare these very different X-ray systems and determine the operational and economic impact that each imposes on the air carrier. There are many systems on the market or in advanced development with a wide range of size, performance and costs. Some systems are expensive with excellent performance while others are less expensive with moderate performance. To achieve an overall understanding of the cost and performance benefits that a system offers, it is important to consider all characteristics of a system. All of these systems are evaluated only on those bags which are rejected by the TNA as needing further inspection. Also, all of those systems are followed by a tertiary process which may include human intervention or destructive testing. While the cost of the tertiary process is relevant to the study, the method of this technique need not be well defined.

2. MODEL INPUTS

The economic model analyzes system and rate parameters. The system parameters describe unique characteristics of a particular unit (e.g., footprint or unit cost). These parameters originate from field tests, manufacturer's literature, or extrapolation from lab tests.

The following are system parameters (per month) and default values used in the study:

a) Footprint (per square foot): The floor area of a unit.
b) Utility (per kilowatt hour): The power needed to operate a unit for an hour.
c) Unit cost ($)
d) Operator fee: The cost of an operator to run a unit, if applicable.
e) Installation (Default: $4,000): An initial, one-time fee to install a unit.
f) Maintenance (Default: 10% of unit cost): The cost to maintain operations of a unit.

The rate parameters describe cost rates (e.g., floor space rental rate per month) and are determined from outside sources. They are influenced by the location and individual specifications of the airports; thus, rates will vary from site to site. The following are rate parameters (per month) and default values used for the study:

a) Rental space (Default: $2.00/square foot)
b) Utility (Default: $56.00/KW month)
c) Radiation License (Default: $175/year)

The study is not limited to the system and rate parameters listed above. Additional parameters could be added as required. The system and rate parameters combine to form an expense parameter. For example, combining the footprint with the floor space rental rate per month yields the floor space expense parameter. The summation of expense parameters reveals the cost to run a particular system.

Since this is a model, assumptions were made based on research conducted to produce realistic default values for the study. It is important in this kind of modeling to see how the various parameters and assumptions influence the cost to process a bag through a particular X-ray unit, that is, establish the sensitivity of the model results to these inputs. To accomplish this, rate parameters were analyzed with values greater and less than the default value. By evaluating each system under the same operational scenario, the relative costs of the systems can be determined as a function of the parameter values. Furthermore, graphing these results allows visual comparison of the different systems to each other over a range of parameter values. Intersections of two graph lines represent equal performance of two systems and a pivotal change in the choice of the superior system. Large slopes indicate a 'sensitive' parameter, that is, a parameter that notably effects the rating of one system against another. For example, at some parameter value x the cost per bag through system A may be the lowest. At parameter value y, however, the cost per bag through system B may be the most efficient. Thus, the evaluations and conclusions are influenced on the particular value of these 'sensitive' parameters.

Each system is evaluated under identical economic conditions and base assumptions. A Thermal Neutron Analysis (TNA)-Explosive Detection System is assumed to be operating on about 2000 bags per day, at a 10% false alarm rate. This means that 200 false alarm bags per day need to be cleared by a combination of the secondary technique (the X-ray systems discussed here) and the tertiary technique. The secondary and tertiary techniques are both assumed to be set at nearly 100% relative PD; that is, if the TNA alarmed on a bag with a threat, it must be found by all of the following systems. Thus, the level of security is fixed by the TNA detection rate and the choice of bags fed into the TNA. The tertiary technique is here represented only by a cost of handling any bag which alarms the secondary system; if an X-ray system is better at clearing false alarms, fewer bags will be sent to the tertiary clearing process and thus the cost of clearing TNA alarms will be reduced. Thus, the economic model is one consistent way for comparing different technologies if the performance of the different units can be estimated, and if the other 'mundane' parameters like floor space, capital cost, etc. can be determined. Figure 1 illustrates the baggage screening process as 2000 bags pass through the TNA, X-ray and tertiary system.

3. ECONOMIC METHODOLOGY

This study utilizes a net present value equation,[1] which computes the difference between "income" and cost of a system. The income term is determined by the flow of secure bags passing through the system. Secure bags refer to bags which are cleared by the TNA and X-ray. The 'benefit' of the system is the cleared bags which can be loaded onto the plane. The cost term is the total sum of expenses needed to operate a system (e.g., utilities, floor rental space). These terms were introduced in the previous section as the expense parameters. Equating the monetary input of the expense with the output (cleared bags) results in a cost per bag to provide the fixed level of security (determined by the fixed detection rate). This can be achieved by setting the net present value to zero and equating the income and cost terms.

The following is the basic formula used for the economic model.

$$NPV = \underbrace{\sum_{t=1}^{N} \frac{P1*B1}{(1+I)^t}}_{\text{Income}} - \underbrace{\sum_{t=0}^{N} \frac{C_t+P2*B2}{(1+I)^t}}_{\text{Costs}} \quad (1)$$

The following variables are used to solve the net present value equation and can be set by the user to satisfy any desired economic scenario:

Y = Number of Years this model spans (default: 3 years)
P = Time Period (Annually, Semi-Annually, Quarterly, etc.)
N = Total time (Y*P)
I = Interest rate (default: 5.00%)

B0 = Initial Number Bags through TNA (default: 2000 bags)
B1 = Number of bags through Secondary
B2 = Number of bags through Tertiary
P1 = Cost per bag through Secondary (Desired variable.)
P2 = Cost per bag through Tertiary (default: $5.00)
C_t = Total Cost of all expenses needed to run XENIS
TNA PFA = Percentage of false alarm of the TNA (default: 10%)
SECONDARY PFA = Percentage of false alarm of the Secondary Unit

The total cost, C_t, includes the capital cost incurred in time period t = 0; so the second sum starts at t = 0; t = 1 is the first period the system is used. The first step in solving the economic model is to balance all costs with total income. This is accomplished by setting the NPV = 0.

$$0 = \sum_{t=1}^{N} \frac{P1*B1}{(1+I)^t} - \sum_{t=0}^{N} \frac{C_t+P2*B2}{(1+I)^t} \qquad (2)$$

The key variable in this model is P1, the cost to process a bag through the secondary system.

Solving and isolating P1 yields the following equation:

$$P1 = \frac{\sum_{t=0}^{N} \frac{C_t+P2*B2}{(1+I)^t}}{\sum_{t=1}^{N} \frac{B1}{(1+I)^t}} \qquad (3)$$

The software for this economic model uses this reduced form of the net present value equation to solve the cost of processing a bag through a given system.

4. RESULTS

The following graphs show how variations of certain parameters affect the processing cost per bag. Recall that parameters with unusual effects on the cost per bag are the 'sensitive' ones most important to any conclusions drawn from this study. It is through these graphs that one can visually observe unusual activity. The graphs compare the following five systems and two alternative techniques:

1) XENIS (Astro Physics System 5) - an integration of the TNA™ image with a two-view X-ray system.
2) American Science and Engineering 101Z
3) Heimann Hi-Scan 5170 DV
4) Heimann Hi-Scan 5170 TS
5) Imatron CTX 5000
6) Laminography/Laminar Tomography
7) Custom two-view X-ray system

These systems are "typical" of their class, where such exists.

Figure 2 shows how the cost per bag is affected by the power needed to operate a system. The y-axis displays the cost per bag and the x-axis displays the Kilowatt-Month Rate. This rate ranges from $30 to $80 in increments of $5. Notice that as the power rate increases, the cost per bag only slightly increases. The cost per bag calculated at a rate of $30 is comparable to the cost at $80. This indicates that the cost per bag is not significantly affected by the cost to power a system.

Figure 3 shows how the cost per bag is affected by the space requirements of a system. The monthly rent is calculated by multiplying the footprint of a system by the monthly rent which is set by the airport. The y-axis displays the cost per bag and the x-axis displays the monthly Rental Space Rate/Square Foot. This rate ranges from $0.00 to $5.00 at increments of $.50. This graph behaves very similarly to that shown in Figure 2. As the rental rate increases, the cost per bag only slightly increases. Again, this indicates that the cost per bag is not significantly affected by the rent rates at the airport.[2]

Figure 4 shows how the cost per bag is affected by the cost to process a bag through the tertiary unit. The y-axis displays the cost per bag and the x-axis displays the tertiary cost per bag. This tertiary cost ranges from $0.00 to $10.00 at increments of $1.00. This graph displays some very unusual activity. Notice that the Imatron system is initially much more expensive than the other four systems, which have roughly the same costs at $0.00.[3] When the tertiary cost is $5.00, the Imatron system begins to intersect

with the cost of the other systems. This indicates that the Imatron system starts to cost the same or less than that of the others. When the tertiary cost reaches $9.00 the Imatron system is the cheapest system. This graph clearly displays a 'sensitive' parameter. Depending on the value of the tertiary cost, the Imatron system will either be the most practical alternative or the most expensive choice.

In Figure 5 the number of bags through the TNA unit is varied which in turn varies the number of bags processed through the X-ray; the effect on the cost per bag is shown. Recall that the probability of false alarm (PFA) for the TNA unit is set at 10% for this study; therefore, running 2000 bags per day produces 200 bags for the XENIS to process. Initially, the Imatron system is more costly than the others. It costs over $7.00 while the others fall in a range from $3.40 to $4.30. As the number of bags through the TNA increases, however, the Imatron demonstrates the most dramatic reduction in cost per bag. At running 1900 bags, the Imatron system matches the cost of the HS 5170 TS. As the number of bags increases, it slowly surpasses all of the other systems and at over 3400 bags, it becomes the cheapest alternative. Note that the AS&E system is the most inexpensive system to run when the number of bags range from 1000 to about 3400. This would be the best alternative to handle a moderate flow of bags. Like Figure 4, Figure 5 displays a "sensitive" parameter. Depending on the number of bags run through the TNA, the Imatron can be the most expensive or the most cost efficient alternative X-ray system.

Lastly, the projected cost per bag incurred with alternative X-ray techniques can be compared to other systems. Based on the projected specifications, the cost per bag for the custom two-view X-ray system and the laminographic system are shown compared to the present XENIS system, the Imatron and AS&E systems in Figure 6. It is seen that although the initial capital cost of the custom systems are higher than the XENIS or AS&E 101ZZ system that due to the better performance, the cost per bag is lower than the XENIS at a tertiary cost of around $1.00 - $2.00 per bag. The cross over point with the AS&E 101ZZ is around $6.00 per bag. It should be noted that the cross over points are very sensitive to the assured performance numbers.

5. CONCLUSION

From the economic analysis presented above some basic conclusions can be drawn. Two sensitive parameters were found, the tertiary cost per bag and the number of bags through the TNA. This means that the values chosen for these parameters greatly influence which system performs best under the given scenario. Over reasonable ranges of these parameters, the AS&E 101ZZ System was significantly lower on a cost per bag basis than the present XENIS or other alternatives. As the cost per bag was increased over $8.00 per bag or the system load exceeds 3400 per day, the assumed high performance of the expensive Imatron system makes it the most cost effective choice.

NOTES

[1]The net present value takes into account the cost of money by decreasing the future value of money by the discount rate.

[2]Changes in this rate may affect the cost of the tertiary screening system, which may be more space intensive. See below for the impact of the cost of the tertiary system.

[3]Note that at $0 for the tertiary cost, it no longer makes sense to use a secondary system.

BAGGAGE SCREENING SYSTEM

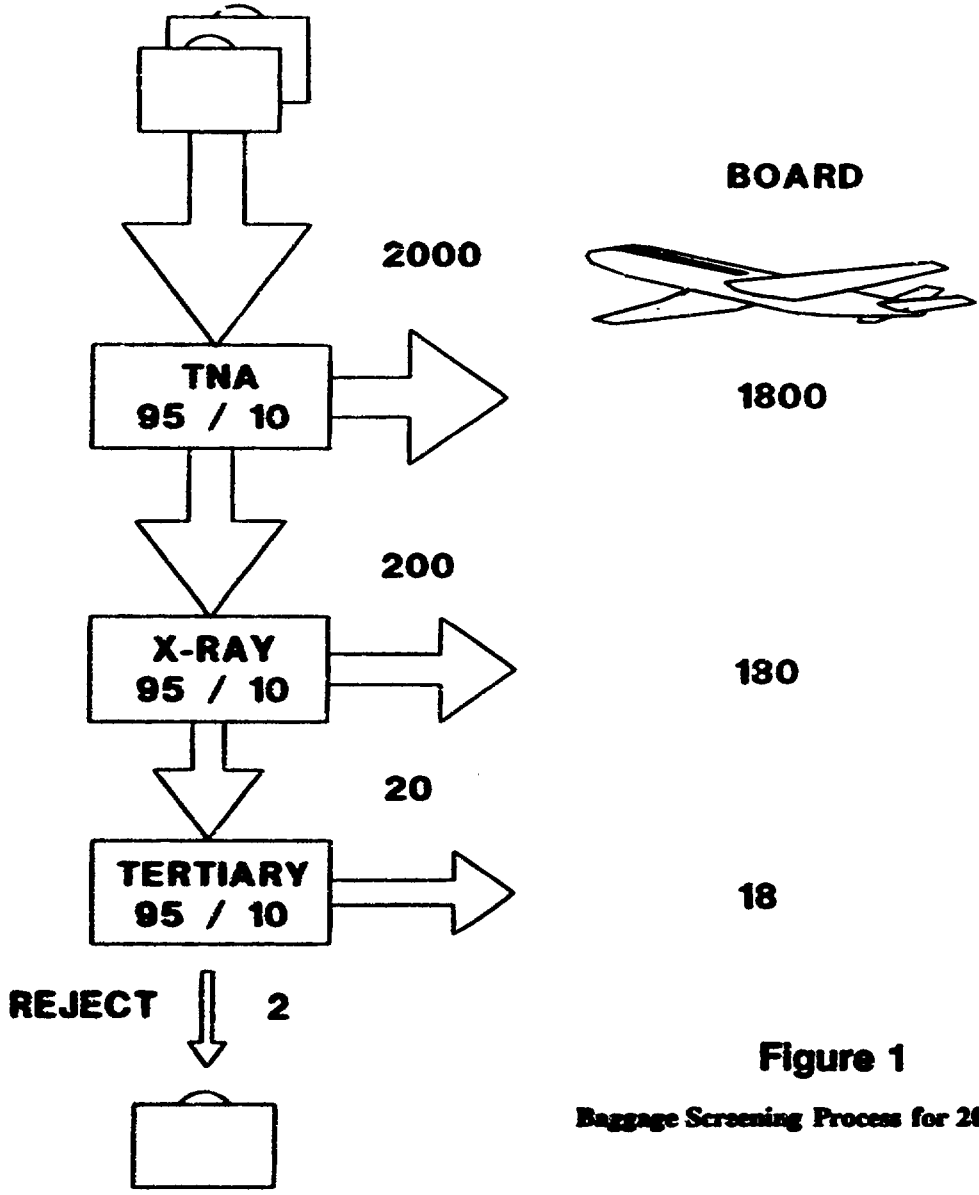


Figure 1

Baggage Screening Process for 2000 Bags.

ALTERNATIVE X-RAY
VARIATION OF KW MONTH $ RATE

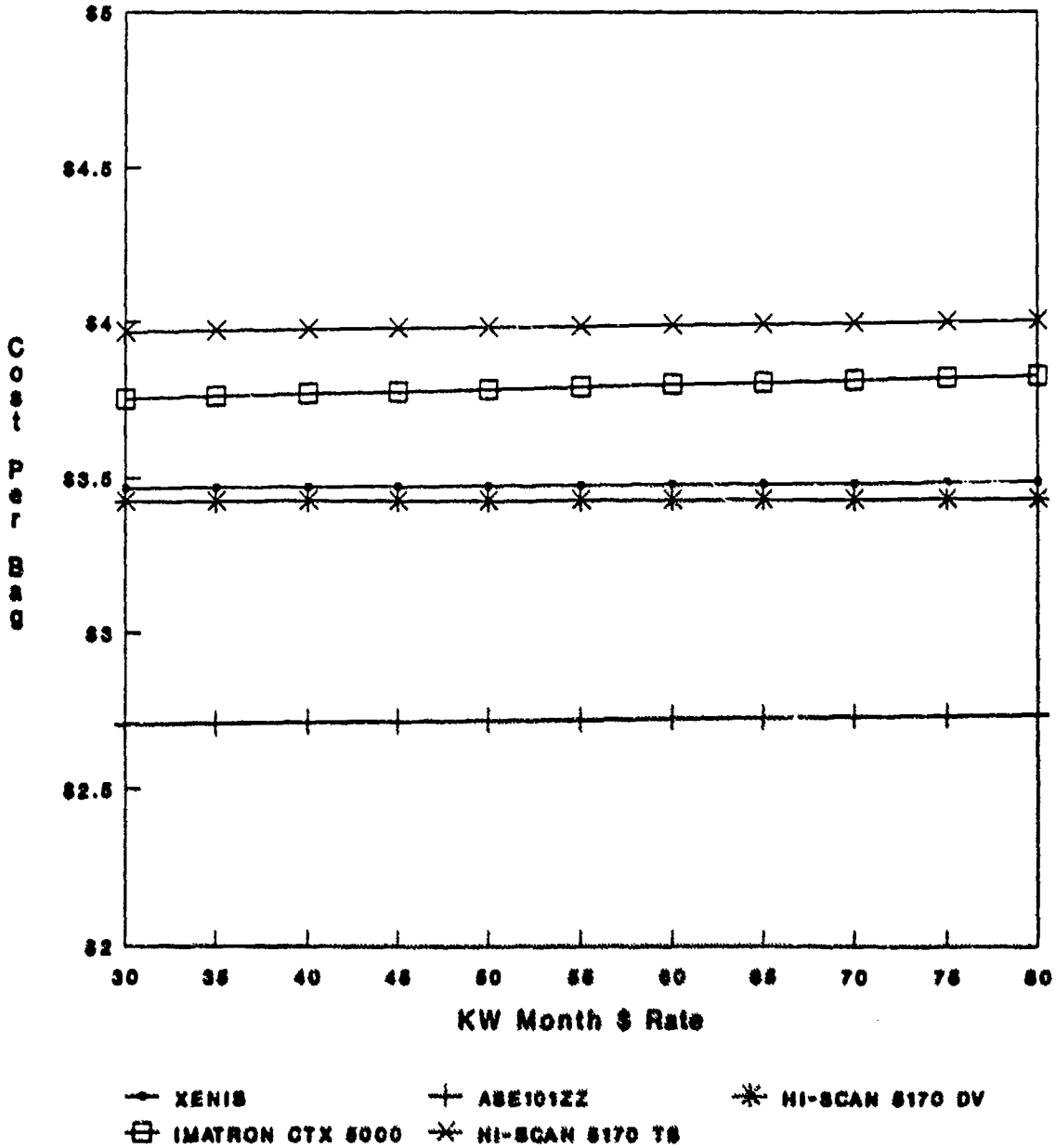


Figure 2 This graph shows that the cost per bag is not affected by varying the kilowatt month rate. The cost per bag is basically constant at each step.

ALTERNATIVE X-RAY
VARIATION OF RENT $

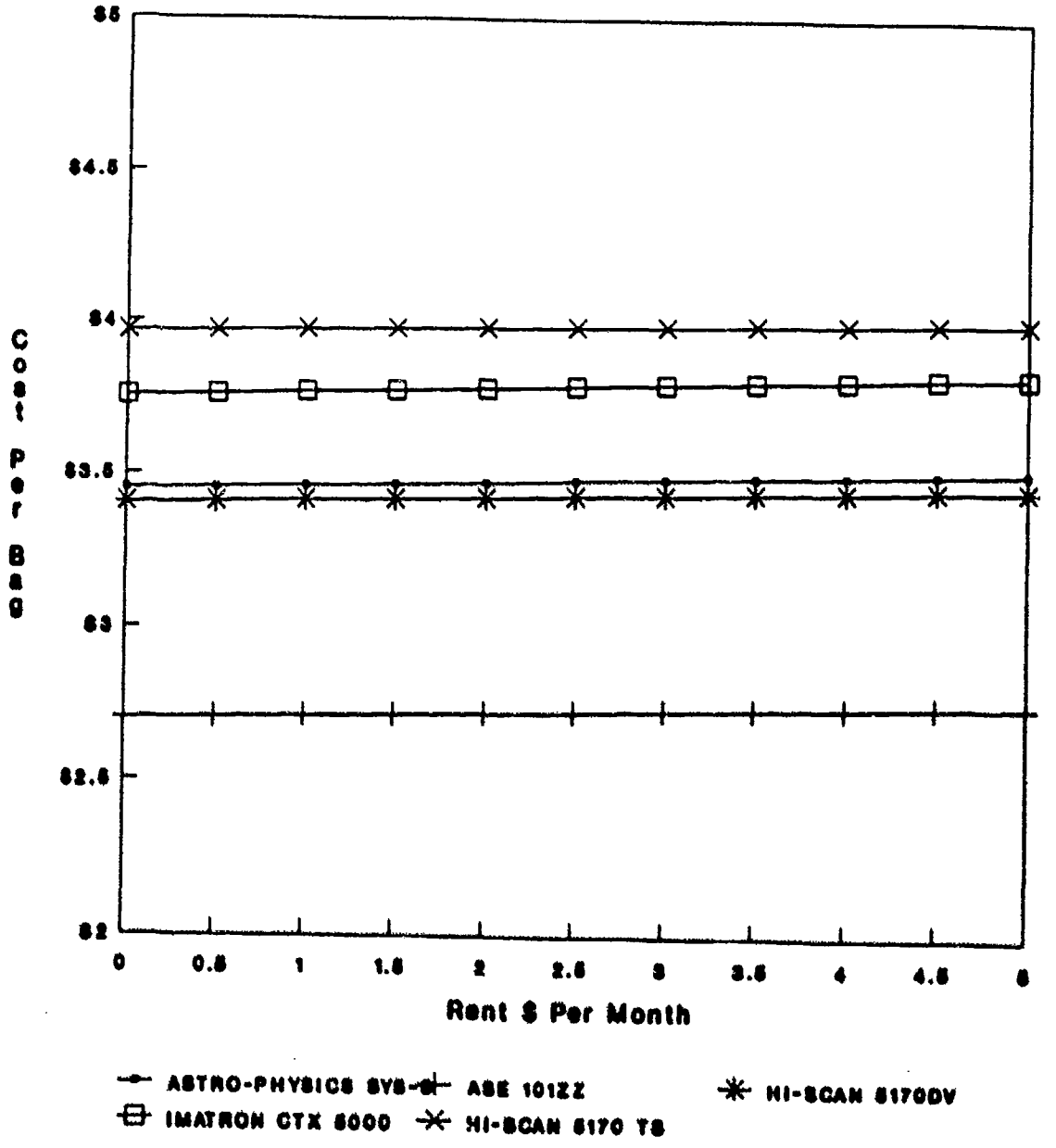


Figure 3 This graph behaves like Figure 2. The cost per bag is basically constant at each step. Thus, it is not really affected by varying the space rental rate.

ALTERNATIVE X-RAY
I VARIATION WITH TERTIARY COST

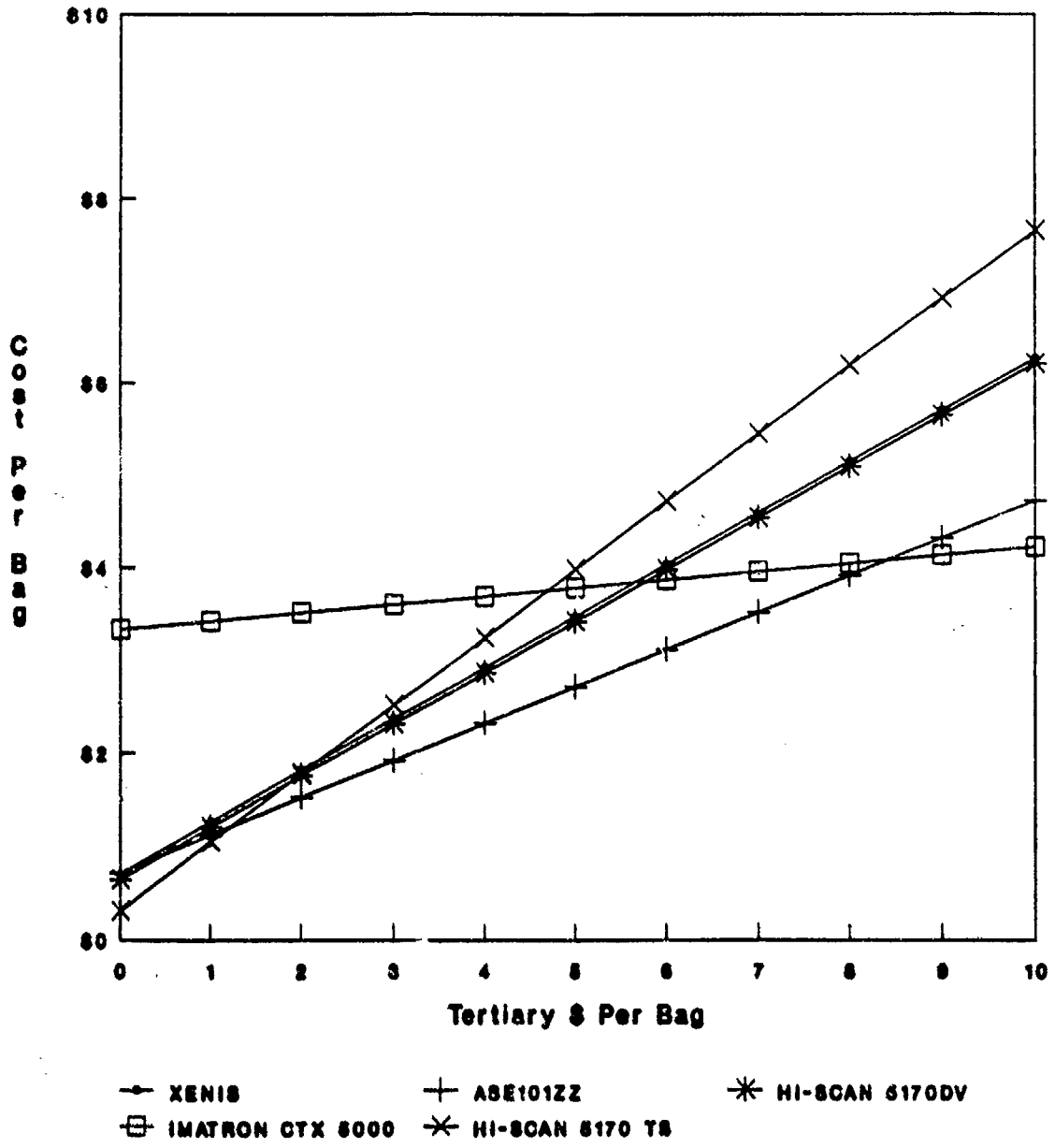


Figure 4 This graph shows how the tertiary cost per bag affects the cost per bag through a given system. Notice the sensitivity of the Imatron system. Initially, it is the most expensive, but as the tertiary cost increases, it gradually becomes cheaper and eventually the cheapest.

ALTERNATIVE X-RAY
VARIATION OF BAGS THRU TNA

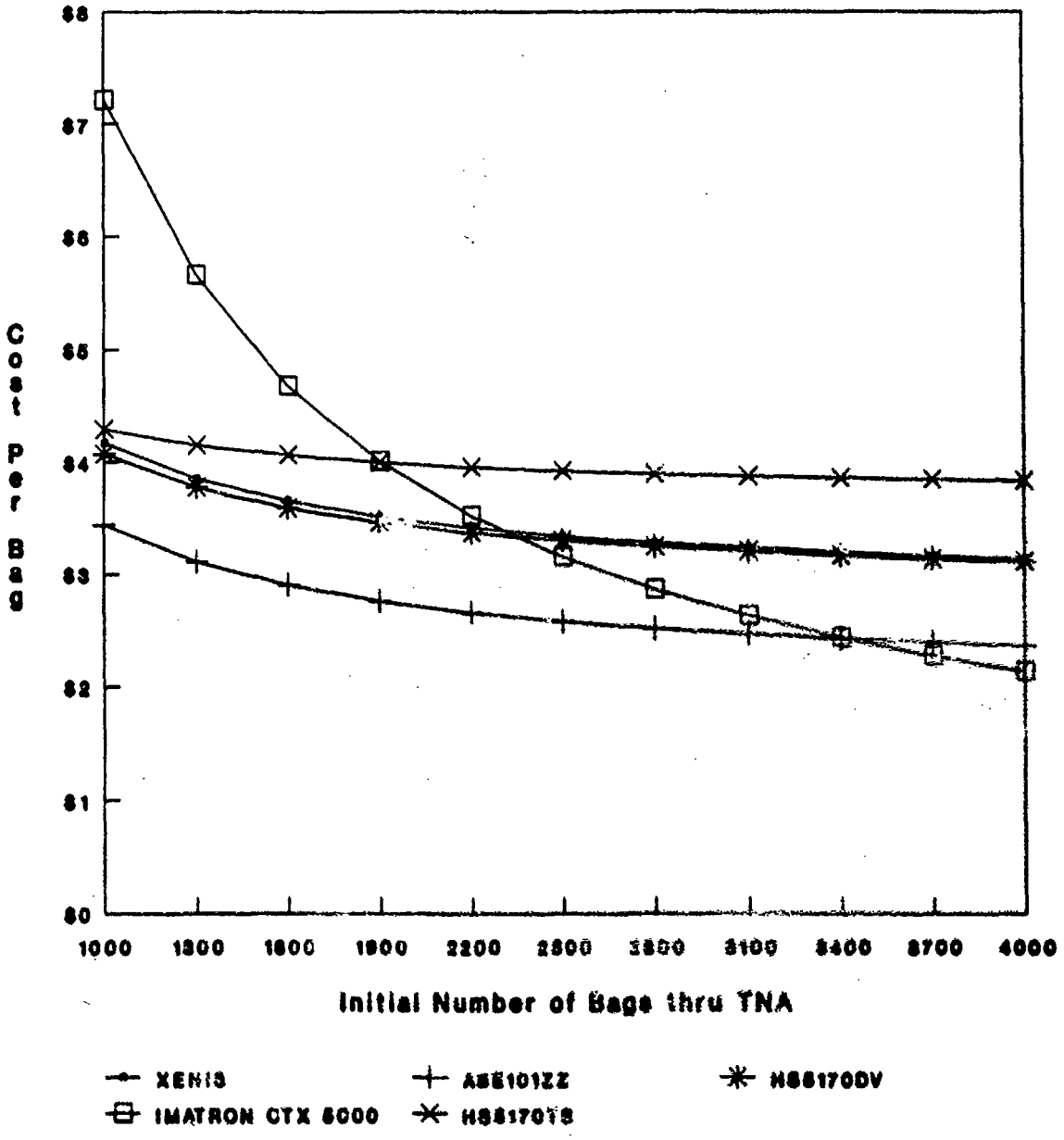


Figure 5 This graph shows how the number of bags through the TNA affects the cost to process each bag through each X-ray system. As in Figure 4, we see the sensitivity of the Imatron system. It is initially the most expensive to run, but as we increase the number of bags run, it eventually becomes cheaper than all the other systems.

ALTERNATIVE X-RAY
II VARATION OF TERTIARY COST

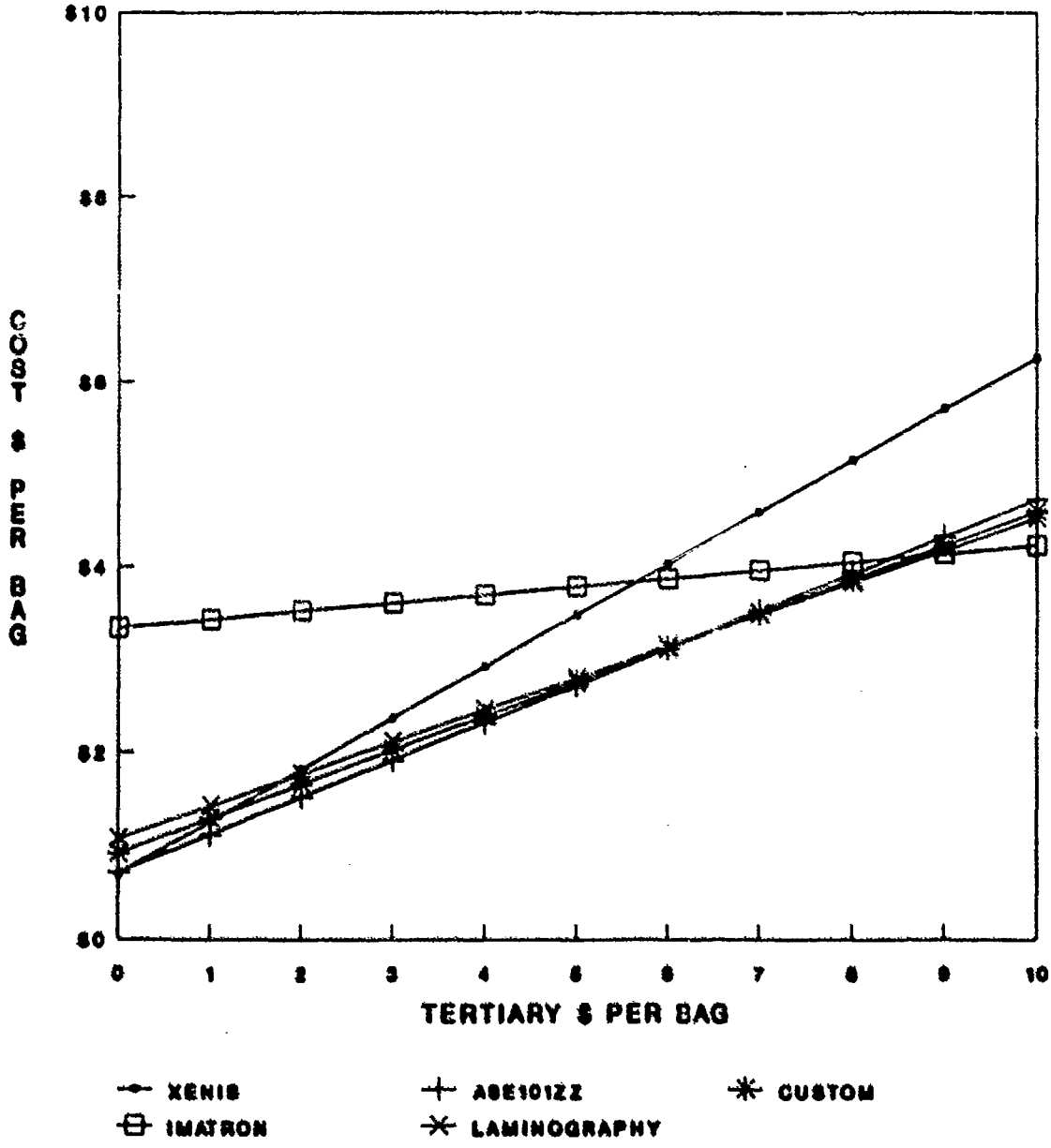


Figure 6 This graph varies the tertiary cost like Figure 4, but analyzes a different set of systems.

APPENDICES

APPENDIX A

List of Attendees at the First International Symposium on Explosive Detection Technology

Achter, Eugene K.
Thermedics, Inc.
Woburn, MA

Adelman, Stephen
S. Adelman Associates
Vienna, CA

Akery, Alan Keith
British Aerospace Security Systems
Bristol, ENGLAND

Alonso, Jaime Juan
Multi-Alarm Security
Caguas, Puerto Rico

Amar, Patrick
DGAC
Paris, FRANCE

Annecchini, Frank C.
Special Technologies Lab
Santa Barbara, CA

Appolony, Andrew
FBI
Newark, NJ

Atkinson, Dale B.
DOD/OSD
Springfield, VA

Aubas, Jean-michel
DGAC
Paris, FRANCE

Bach, Pierre H.
SODERN
Limeil - Brevannes, FRANCE

Baer, Richard T.
Bowie, MD

Baker, Holly
FAA Technical Center
Atlantic City, NJ

Balch, Joseph W.
Lawrence Livermore National Lab
Livermore, CA

Bannister, William W.
University of Massachusetts
Lowell, MA

Bao, Qingcheng
SilverDow Corporation
Tempe, AZ

Bar-Nir, I.M.
SAIC
Santa Clara, CA

Barnett, Arnold
MIT
Cambridge, MA

Barrington, Alfred E.
DOT/RSPA/VNTSC
Cambridge, MA

Bell, Curtis
FAA Technical Center
Atlantic City, NJ

Bendahan, Joseph
SAIC
Santa Clara, VA

Bergamo, Frank R.
MF Physics Corporation
Colorado Springs, CA

Berkowitz, Stuart J.
Array Systems Computing, Inc.
Downsview, Ontario - CANADA

Berman, Barry L.
Georege Washington University
Washington, DC

Bermbach, Rainer
Heimann
Wiesbaden, GERMANY

Bertozzi, William
MIT
Cambridge, Mass.

Beyerle, Albert C.
EG&G
Santa Barbara, CA

Black, Michael L.
Rutgers University
Piscataway, NJ

Blackwood, Michael Edward
SAIC
Aiken, SC

Boubli, Bernard B.
Eurotunnel Security
London, ENGLAND

Boumsellek, S.
California Inst. of Technology
Pasadena, CA

Bouyett, Gil
Naval Ordinance Station
Indian Head, MD

Bowen, Daniel A.
U.S. Deptartment of Defense
Ft. Meade, MD

Bowers, Williams Dale
Femtometrics
Costa Mesa, CA

Brady, Dennis Carl
U.S. Department of Defense
Ft. Meade, MD

Brandenstein, Albert E.
DARPA
Arlington, VA

Brauckmann, Walter Joseph
Westinghouse Electric
Baltimore, MD

Brenner, Marty
FAA Technical Center
Atlantic City, New Jersey

Bromberg, Edward A.
Thermedics
Woburn, MA

Bruckheim, Arthur Jay
Bethseda, MD

Brzosko, Jan S.
Stevens Institute of Technology
Hoboken, NJ

Buchmann, Lothar Rainer
Triumf
Vancouver, BC - CANADA

Buchsbaum, Steven Bruce
SAIC
San Diego, CA

Bunting, Basilyn D.
FAA Technical Center
Atlantic City, NJ

Burnett, Lowell J.
Quantum Magnetics, Inc.
San Diego, CA

Burnett, Robert F.
U.S. NRC
Washington, DC

Bush, Stirling
Lorac Atlantic, Limited
Nottingham, ENGLAND

Campbell, C.
U.S. ARDEC
Picatinny Arsenal, NJ

Cantu, Antonio
U.S. Secret Service
Washington, DC

Caprio, Gianfranco
FAA
Newark, NJ

Carney, Ritche L.
U.S. Department of Energy
Damascus, MD

Carr III, Baxter Chamblan
U.S. Postal Inspection Service
Washington, DC

Carroll, A. Lindsay
Thermedics, Inc.
Woburn, MA

Carroll, Chris
FAA Technical Center
Pittsburg, PA

Carson, Raymond Larry
U.S. Capitol Police
Washington, DC

Cartwright, Nick
Royal Canadian Mounted Police
Ottawa, Ontario - CANADA

Casper, Robert
Hughes Aircraft
El Segundo, CA

Chapman, Harry Payne
Apex Technology
Arlington, VA

Chapman, Jeffrey Allen
Martin Marietta
Oak Ridge, TN

Chawla, M.S.
System Planning Corp.
Arlington, VA

Chen, Tung-Ho
U.S. ARDEC
Picatinny Arsenal, NJ

Cheng, Gartung
U.S. Army ARDEC
Picatinny Arsenal, NJ

Cheung, Shiu
FAA Technical Center
Atlantic City, NJ

Chian, Hui-Chen
China Airlines, Ltd.
New York, NY

Chutjian, Ara
California Institute of Technology
Pasadena, CA

Clifford, Jerome R.
TITAN
Albuquerque, NM

Coggiola, Michael J.
SRI International
Menlo Park, CA

Cohen, Martin Joseph
PCP, Inc.
West Palm Beach, FL

Cole, Russel
SAIC
Santa Clara, CA

Collier, John A.
Varian Canada
Georgetown, Ontario - CANADA

Colombani, Pasce P.
Schlumberger Industries
Montrouge Cedex, FRANCE

Colon, Francisco
U.S. Secret Service
Washington, DC

Congedo, Thomas Vincent
Westinghouse Electric Corp.
Churchill, PA

Connelly, James
FAA Technical Center
Atlantic City, NJ

Connelly, Joseph C.
Atlantic City Police
Atlantic City, NJ

Conrad, Frank J.
Sandia National Laboratories
Albuquerque, NM

Cooper, David Eugene
SRI International
Menlo Park, CA

Corby, James E.
FBI
Washington, DC

Coughlin Jr., Frank
ASEC
Burlington, MA

Coulomb, Herve
DGAC
Leclerc, FRANCE

Cowan, Alvin Ethelbert
FELCORP and TECHNICA, Inc.
Orlando, FL

Crewson, Walter
Universal Voltronics
Mt. Kisco, NY

Crossley, Peter Anthony
Schlumberger
Austin, TX

Curby, Bill
FAA Technical Center
Atlantic City, NJ

Dahlgren, Matthew
Ion Track Instruments, Inc.
Wilmington, MA

Daly, John B.
U.S. Department of Transportation
Washington, DC

Danylewych-May, Lucy L.
Barringer Research
Rexdaly, Ontario - CANADA

Daubner, Ludo Robert
Barringer Research
Rexdale, Ontario - CANADA

Davenport, James
Davenport & Associates
McLean, VA

Davidson, William R.
SCIEX
Thornhill, Ontario - CANADA

Davies, John P.
EG&G Idaho
Idaho Falls, ID

DeMoulpied, David Sargent
EG&G Astrophysics
Long Beach, CA

Dennis, William H.
CIA
Braddock Heights, MD

Derickson, jenelle
FAA Technical Center
Atlantic City, NJ

Devigili, Lew A.
SAIC
San Diego, CA

DiDonato, Loretta T.
FAA Technical Center
Atlantic City, NJ

Dickason, Phil Harris
Eldyne, Inc.
Arlington, VA

Dolan, Kenneth W.
Lawrence Livermore National Lab
Livermore, CA

Dolev, Shalom
Magal
Yahod, ISRAEL

Doney, Richard H.
UK Department of Transport
London, ENGLAND

Drew, Jim
FAA Technical Center
Atlantic City, NJ

Drost, Ronald
Amsterdam Airport Schiphol
Amsterdam, NETHERLANDS

Duggan, Ruth A.
SNL
Albuquerque, NM

Duong, Vu N.
Schlumberger
Montrouge, FRANCE

Durkee, Robin K.
EG&G
Santa Barbara, CA

Dwyer, Priscilla Anne
U.S. NRC
Washington, DC

Ehntholt, Daniel J.
A. D. Little
Cambridge, MA

Eichelberger, John L.
GRQ, Inc.
King of Prussia, PA

Elberston, Frank
FAA Technical Center
Atlantic City, NJ

Elzufon, Eugene E.
Applied Ordnance Technology
Arlington, VA

Eng, Yukwei Sarah
U.S. ARDEC
Picatinny Arsenal, NJ

Ettenhofer, Kurt L.
Environmental Technology Group, Inc.
Baltimore, MD

Fabry, David
FAA Technical Center
Atlantic City, NJ

Falconer, David G.
SRI International
Menlo Park, CA

Fetterrolf, Dean D.
FBI
Quantico, VA

Fine, David H.
Thermedics, Inc.
Woburn, MA

Flynn, Cathal L.
SAIC
San Diego, CA

Foote, Vicki L.
IRT Corp.
San Diego, CA

Fox, S. G.
Ai Cambridge
Cambridge, ENGLAND

Fraim, Freeman W.
Thermedics, Inc.
Woburn, MA

Frey, Manfred E.
MF Physics Corp.
Colorado Springs, CO

Gallucci, John C.
Analytical Instruments
Cambridge, ENGLAND

Gardner, Philip L.
Triumf
Vancouver, BC - CANADA

Gardner, Samuel Dean
Los Alamos National Lab
Los Alamos, NM

Garner, David Wesley
SAIC
McLean, VA

Garroway, Allen N.
Naval Research Laboratory
Washington, DC

Gatto, Joe
FAA Technical Center
Atlantic City, NJ

Giam, C.S.
Texas A&M University
Galveston, TX

Giboni, Karl-Ludwig
Schlumberger
Montrouge, FRANCE

Glish, Gary L.
Oak Ridge National Laboratory
Oak Ridge, TN

Glockmann, Walter F.
Security Defense Systems
Stirling, NJ

Goldsmith, Paul F.
Millitech Corp.
South Deerfield, MA

Gomberg, Henry Jacob
PENETRON, Inc.
Ann Arbor, MI

Gossard, James L.
Westinghouse Electric
Baltimore, MD

Gozani, Tsahi
SAIC
Santa Clara, CA

Grand, Pierre
Amparo
Santa Fe, NM

Grassie, Richard
Techmark Security
Hanover, MA

Grassie, Richard Paul
Barringer Instruments
S. Plainfield, NJ

Gray, Gary
U.S. Navy
Indian Head, MD

Greenlee, Donald R.
SAIC
Falls Church, VA

Greenspan, E.
SAIC
Santa Clara, CA

Grodzins, Lee
MIT
Cambridge, MA

Grow, Ann E.
Sparta, Inc.
San Diego, CA

Guenther, Heinz
Federal Criminal Police Office
Wiesbaden, GERMANY

Hacker, Ken
FAA Technical Center
Atlantic City, NJ

Hadar, Giora
FAA Headquarters
Washington, DC

Haley, Lawrence
CPAO Holdings, Ltd.
Nepean, Ontario - CANADA

Hamm, Robert W.
AccSys Technology, Inc.
Pleasanton, CA

Hammer, William N.
Grumman Aerospace
Bethpage, NY

Hannum, David W.
Sandia National Lab
Albuquerque, NM

Harrington, Kevin
CSIRO
Clayton, AUSTRALIA

Harris, Dan
FAA Technical Center
Atlantic City, NJ

Hay, J. Edmund
US Bureau of Mines
Pittsburgh, PA

Head, Lynne
Home Office PSDB
St Albans, ENGLAND

Henderson, Don O.
Fisk University
Nashville, TN

Hendren, Charles H.
U.S. NRC
Washington, DC

Hentz, Wayne S.
CIA Headquarters
Washington, DC

Hethall, Eric Robert
ASEC
Burlington, MA

Hett, Walter D.
Walter Hett & Associates
Stow, MA

Hill, D. Chandler
Thermedetec, Inc.
Alexandria, VA

Hintz, M. Marx
Scientech, Inc.
Idaho Falls, ID

Hirsh, Isreal
Government of Isreal
New York, NY

Hobbs, John R.
U.S. Department of Transportation
Cambridge, MA

Hodges, Edwin C.
Q-Systems International
Arlington, TX

Hoffland, Lynn D.
U.S. Army CRDEC
Aberdeen, MD

Hogan, Walton
Statcom, Inc.
McLean, VA

Hoglund, David
U.S. Customs Service
Washington, DC

Holsinger, Ronald
Intermagnetics General Corp.
Acton, MA

Hoopengardner, Roger Lyn
SAIC
McLean, VA

Hopler, Robert B.
Ireco, Inc.
Salt Lake City, UT

Hupays, Michel
DGAC
Paris, FRANCE

Huriet, Jean R.
SODERN
Limeil - Brevannes, FRANCE

Hurwitz, Michael
Gamma-Metrics
San Diego, CA

Hussein, Waleed
International Airports Projects
Leesburg, VA

Iatrou, George
International Airports Projects
Jeddah, SAUDI ARABIA

Jackson, Rudy G.
Department of State
Washington, DC

Jacobi, Jonah
Science Research Laboratory, Inc.
Somerville, MA

Jadamec, Joseph Richard
U.S. Coast Guard
Groton, CT

Jankowski, Paul
FAA Technical Center
Atlantic City, NJ

Jenkins, Anthony
Ion Track Instruments, Inc.
Wilmington, MA

Jensen, David B.
Canadian Aircraft Products
Vancouver, BC - CANADA

Jernigan, David
FBI
Newark, N.J.

Johnson, Andrew J.
ASEC
Alexandria, VA

Johnson, Dick
FAA Technical Center
Atlantic City, NJ

Karp, Sherman
Mayo Foundation
Potomac, MD

Keehan, Daniel
U.S. Army CRDEC
Aberdeen, MD

Kelly, Robert J.
Port Authority of NY & NJ
New York, NY

Kenna, Bernard T.
Sandia National Lab
Albuquerque, NM

Khan, Siraj M.
FAA Technical Center
Atlantic City, NJ

Kim, Jung Hyoun
NC A&T State University
Greensboro, NC

King, J. Derwin
Southwest Research Institute
San Antonio, TX

Kleinfelder, John M.
Hughes Aircraft
Eatontown, NJ

Klement, Robert
Dutch National Police Force
Schipol Airport, NETHERLANDS

Klinkowstein, R.E.
Science Research Laboratory
Somerville, MD

Knize, Duane Joseph
SAIC
San Diego, CA

Kolla, Peter
BKA
Wiesbaden, GERMANY

Koo, Lok
FAA Technical Center
Atlantic City, NJ

Koos, Frank S.
SEMCOR, Inc.
Moorestown, NJ

Koren, Baruch
Safeguards Technology
Hackensack, NJ

Kosker, Frank
FAA Technical Center
Atlantic City, NJ

Kotowski, Adreas Felix
Kotowski and Associates
Rancho Palos Verdes, CA

Kraus, Samuel
Government of Israel
New York, NY

Krauss, Ron
FAA Technical Center
Atlantic City, NJ

Krug, Kris D.
Vivid Technologies, Inc.
Waltham, MA

Krutz, Ron
Carnegie Mellon Research Institute
Pittsburgh, PA

Krutz, Ronald
CMRI/Computer Engineering Center
Pittsburg, PA

Kurtz, Alex G.
Deptartment of the Air Force
Wright-Patterson AFB, OH

Kushner, Brian
BDM International, Inc.
Arlington, VA

Kusterbeck, Anne W.
Naval Research Lab
Falls Church, VA

Labaj, Leo E.
CIA
Reston, VA

Lacey, Richard John
Home Office PSDB
St Albans Herts, ENGLAND

Lacy, John K.
Software Corp of America
Pleasentville, NJ

Lanham, Penny Katherine
U.S. Navy
Indian Head, MD

Lannon, Joseph A.
U.S. DARDEC
Picatinny Arsenal, NJ

Lannon, Joseph A.
U.S. Army ARDEC
Picatinny Arsenal, NJ

Lanza, Dick
MIT
Cambridge, MA

Latyn, Michael
FAA Technical Center
Atlantic City, NJ

Lauterstein, Kenneth M.
FAA Security
Herndon, VA

Lavin, Milton
Jet Propulsion Laboratory/NASA
Pasadena, CA

Leach, Eugene R.
Battelle
Columbus, OH

Lee, Edgar
Brigham Young University
Provo, UT

Lee, Milton L.
Brigham Young University
Provo, UT

Lee, Willis
SAIC
Santa Clara, CA

Leek, Bobby J.
Naval Investigative Service
Washington, DC

Leginus, Joseph Michael
Westinghouse
Baltimore, MD

Lempiainen, Errki
Finnish Institute for Int'l Trade
New York, NY

Leonelli, Joseph
SRI International
Menlo Park, CA

Leung, V.
SAIC
Santa Clara, CA

Leupold, Richard A.
U.S. Army, ETDL
Ft. Monmouth, NJ

Lim, Teong C.
Amerasia Technology, Inc.
Westlake Village, CA

Lindmar, Victor
U.S. Army, ARDEC
Picatinny Arsenal, NJ

Lister, Daniel B.
EMR Photoelectric
Princeton, NJ

Lorne, Elias
National Research Council
Ottawa, Ontario - CANADA

Loveman, Robert
SAIC
Santa Clara, CA

Lovett, Stan
Defense Research Agency
Sevenales, ENGLAND

Lukens, Herbert Richard
Diametrix Corp.
San Diego, CA

MacDonald, Stephen J.
Thermedics, Inc.
Woburn, MA

Mahdavi, Mehrzad
EMR Photoelectronic
Princeton, NJ

Mala, Gerard
Schulmberger Industries
Rungis, FRANCE

Malotky, Lyle
FAA Security
Washington, DC

Mancini, Albert
FAA Technical Center
Atlantic City, NJ

Mangano, Joseph
Science Research Laboratory
Arlington, VA

Marino, Robert A.
Hunter College of CUNY
New York, NY

Mason, Patrick H.
Home Office PSDB
St Albans, ENGLAND

Mason, Roy
FAA Technical Center
Atlantic City, NJ

Masonis, Joseph A.
U.S. Secret Service
Washington, DC

Matthews, Edward K.
Scan Tech Security
Nothvale, NJ

Mayer Jr., Robert
Consultant
Dallas, TX

Mayo, William E.
Rutgers University
Piscataway, NJ

McCluskey, Leo F.
McCloskey & Associates
Marshfield, MA

McDaniel, Floyd D.
University of North Texas
Denton, TX

McGann, William
Ion Track Instruments
Wilmington, MA

McGowan, Raymond C.
U.S. Army ETDL
Ft. Monmouth, NJ

McKay, Dale R.
Quantum Magnetics
San Diego, CA

Mercado, Al
FAA Technical Center
Atlantic City, NJ

Meurrens, Bernie E.
EG&G Rocky Flats
Golden, CO

Micheletti, Claude
Cofrexport S.A.
Paris, FRANCE

Michienzi, Barbara H.
Naval Ordnance Station
Indian Head, MD

Middleton, Juliette
Statcom, Inc.
McLean, VA

Middleton, Paul Beadle
Statcom, Inc.
McLean, VA

Mileikowsky, Curt
Scanditronix AB
Uppsala, SWEDEN

Miller, Norman E.
Scan-Tech Security
Northvale, NJ

Miller, Roger
U.S. Technical Security Division
Washington, DC

Miller, Thomas G.
General Research Corp.
Huntsville, AL

Minhas, Khal
FAA Technical Center
Atlantic City, NJ

Mitchener, Bob
Scintrex
Concord, Ontario - CANADA

Moler, Robert Byron
System Support, Inc.
Catharpin, VA

Monetti, Robert G.
Victims of PAN AM 103
Cherry Hill, NJ

Morgado, Richard E.
Los Alamos National Lab
Los Alamos, NM

Morvan, Pascal
Air France
Paris, FRANCE

Muller, Michael G.
U.S. Marshals Service
Arlington, VA

Murnane, Jim
Millitech Corporation
South Deerfield, MA

Myers, Lawrence J.
Institute for Biological Detection Sys
Auburn University, AZ

Nacson, Sabatino
Scintrex Limited
Concord, Ontario - CANADA

Nanni, Clare
FAA Technical Center
Atlantic City, NJ

Nardi, Vittorio M.
Stevens Institute of Technology
Hoboken, NJ

Navvaro, Joseph A.
JAN Associates, Inc.
Bethesda, MD

Nelson, Arthur
EDO Corp
College Point, NY

Nesterok, David
FAA Technical Center
Atlantic City, NJ

Nicholls, Colin
SWRI
San Antonio, TX

Nicolaides, Paris
Thermedics
Woburn, MA

Novakoff, Ken
FAA Technical Center
Atlantic City, NJ

Nusshardt, Rudolf
Ottobrunn, GERMANY

O'Leary, David Edward
U.S. Department of Defense
Ft. Meade, MD

Oppendal, Paul W.
EG&G Rocky Flats
Golden, CO

Orphan, Victor John
SAIC
San Diego, CA

Orrell, Stanley A.
EG&G
Albuquerque, NM

Oxley, Jimmie C.
New Mexico Institute of Mining
Socorro, NM

Parsons, David Victor
Atomic Energy of Canada
Chalk River, Ontario - CANADA

Patel, Divyakant Lallubhai
U.S. Army, Countermine Systems
Ft. Belvoir, VA

Perkins, Thomas Gibson
Link
Silver Spring, MA

Perlea, Caroline
Carnegie Mellon
Pittsburg, PA

Peters, Ricky L.
Department of the Air Force
Wright-Patterson AFB, OH

Petrousky, James A.
Naval EOD Technology Ctr.
Indian Head, MD

Philip, Horbert R.
Bureau of ATF
Washington, DC

Pilon, P.
Government of Canada
Ottawa, Ontario - CANADA

Pirri, Anthony N.
Physical Sciences, Inc.
Andover, MA

Pocaro, Vic J.
U.S. Customs Service
Washington, DC

Pocratsky, Carl A.
U.S. Department of Energy
Washington, DC

Poindexter, Edward
U.S. Army Lab Command
Fort Monmouth, NJ

Polichar, R.
SAIC
San Diego, CA

Polski, Paul
FAA Technical Center
Atlantic City, NJ

Pongratz, Hans Wolfgang
DASA - MBB
Munich, GERMANY

Potdevin, Jean Marc
Schlumberger Security
Rungis, FRANCE

Powell, Charles William
Stevens Institute of Technology
Hoboken, NJ

Powell, Tom
FAA Technical Center
Atlantic City, NJ

Powers, James Joseph
U.S. Nuclear Regulatory Commission
Washington, DC

Prestrude, A.M.
Virginia Polytechnic Institute
Blacksburg, VA

Prime, Arlene
FAA Technical Center
Atlantic City, NJ

Proudfoot, Gary
AEA Technology
Oxfordshire, ENGLAND

Puglielli, Vincent G.
Battelle
Columbus, OH

Ramsey, John Michael
Oak Ridge National Lab
Oak Ridge, TN

Rathmell, Robert D.
National Electrostatics Corp.
Middleton, WI

Ray, Surenda Nath
Software Corporation of America
Lanham, MD

Redman, Richard
FBI Bomb Data Center
Washington, DC

Reilly, Jr., William
FAA Technical Center
Atlantic City, NJ

Remer, James
FAA Technical Center
Atlantic City, NJ

Ricard, Steven Alan
Analysis and Technology, Inc.
New London, CT

Ries, Herman
Heimann GmbH
Wiesbaden, GERMANY

Robbins, Clyde E.
U.S. Dept. of Transportation
Washington, DC

Robinson, M.
Nottingham Polytechnic
Nottingham, ENGLAND

Rodacy, Phil J.
Sandia National Lab
Albuquerque, NM

Roder, Frederick L.
Imatron Federal Systems
Burke, VA

Roehl, Joseph Ellery
Environmental Technologies Group
Baltimore, MD

Rogers, John Douglas
Rolls-Royce
Bristol, ENGLAND

Rolnick, Abe
Scintrex
Concord, Ontario - Canada

Rose, Peter H.
Consultant
Seattle, WA

Rounbehler, David P.
Thermedics
Woburn, MA

Roussel, Michel
DGAC
Leclerc, FRANCE

Rudolf, Terry L.
FBI
Quantico, VA

Ryan, John P.
FAA
Washington, DC

Ryge, Peter
SAIC
Santa Clara, CA

Safeer, Harvey
FAA Technical Center
Atlantic City, NJ

Sahagian, Armen Ara
FAA
Washington, DC

Sakai, Tokiyasu
Maritime Safety Agency
Tokyo, JAPAN

Sawa, Zdizislaw P.
SAIC
Santa Clara, CA

Scarlet, Richard
EG&G
Waltham, MA

Schafer, David A.
American Science and Engineering
Cambridge, MA

Schleinzer, Karl
Vienna International Airport
Vienna, AUSTRIA

Schmor, Paul W.
Triumf
Vancouver, BC - CANADA

Schulte, Robert L.
Grumman Corporation
Bethpage, NY

Scott, William R.
SCIEX
Thornhill, Ontario - CANADA

Scotti, Vince
Hughes Aircraft
Rancho Santa Margarita, CA

Scudiere, John D.
Oxford Superconducting Technology
Carteret, NJ

Sebban, Emmanual
Cofrexport S.A.
Paris, FRANCE

Seher, Chris
FAA Technical Center
Atlantic City, NJ

Seitz, Martin George
Computer Systems Development Corp.
Chantilly, VA

Sentell, Ronald J.
Westinghouse Hanford Co.
Richland, WA

Seward, Dewitt C.
Spatial Dynamics Applications
Action, MA

Shea, Patrick
SAIC
Santa Clara, CA

Shefer, Ruth E.
Science Research Laboratory, Inc.
Somerville, MA

Sheldon, Timothy George
Home Office PSDB
St Albans ENGLAND

Shoop, Doris
FAA Technical Center
Atlantic City, N.J.

Shull, Douglas S.
SAIC
Aiken, SC

Siegel, Melvin W.
Carnegie Mellon University
Pittsburgh, PA

Silberman, Enrique
Fisk University
Nashville, TN

Singh, H.
U.S. Army Labcom
Fort Monmouth, NJ

Sinha, Mahadeva P.
California Institute of Technology
Pasedena, CA

Sipila, Heikki Johannes
Outokumpu Electronics
Espoo, FINLAND

Smith, G. Dan
U.S. Department of Energy
Washington, DC

Smith, Michael Claude
SAIC
McLean, VA

Smith, Richard C.
Kaman Science Corp.
Colorado Springs, CO

Smith, Russ
FAA Technical Center
Atlantic City, NJ

Smith, Stephen R.
Lawrencville, NJ

Smith, Steven W.
IRT Corp.
San Diego, CA

Snyder, Fred
FAA Technical Center
Atlantic City, NJ

Speitel, Louise
FAA Technical Center
Atlantic City, NJ

Spence, Robert G
FAA
Arlington, VA

Staples, Jr., Edward Jerome
Amerasia Technology, Inc.
Westlake Village, CA

Starley, Steve
FAA Technical Center
Atlantic City, NJ

Stein, Jay A.
Vivid Technologies, Inc.
Waltham, MA

Steinfeld, Jeffrey I.
MIT
Cambridge, MA

Steinfield, Jerry
FAA Technical Center
Atlantic City, NJ

Stott, William R.
SCIEX
Thornhill, Ontario - CANADA

Straw, David C.
W. J. Schafer Associates
Arlington, VA

Su, Chih-Wu
USCG R&D Center
Groton, CT

Sundquist, Mark L.
National Electrostatics Corp.
Middleton, WI

Swank, Roy Gregory
Westinghouse Hanford Co.
Richland, WA

Syler, Ronald P.
Sandia National Lab
Albuquerque, NM

Syme, Duncan Brian
Harwell Instruments
Oxon, ENGLAND

Tarshis, Bernard
IBM Latin America
North Tarrytown, NY

Ternes, J.W.
Philadelphia VA Medical Center
Philadelphia, PA

Thai, Tan
Sandia National Lab
Albuquerque, NM

Thompson, Michael
University of Toronto
Toronto, Ontario - CANADA

Thompson, Mike
Outokumpu Electronics
Langhorne, PA

Timm, Ed
FAA Technical Center
Atlantic City, NJ

Todd, A.M.M.
Grumman Space Systems
Princeton, NJ

Toms, Darryl B
U.S. Department of Energy
Washington, DC

Trakimas, Richard S.
W. R. Grace and Co.
Lexington, MA

Trivedi, Mohan M.
University of Tennesse
Knoxville, TN

Trower, W. Peter
Virginia Tech
Blacksburg, VA

Twilt, Hans
Dutch National Police
Amsterdam, NETHERLANDS

Udell, Gillman G.
U.S. Capitol Police
Washington, DC

Ullo, John J.
Schlumberger
Austin, TX

Van Meter, Steven Duane
NASA
Kennedy Space Center, FL

VanDoorm, Bert
Amsterdam Airport Schiphol
Amsterdam, NETHERLANDS

Vernon, Dennis Lee
U.S. Department of Energy
Washington, DC

Vincent, Bille H.
Aerospace Services International
Herndon, VA

Vinh, Paul
U.S. Army - ARDEC
Picatinny Arsenal, NJ

Virca, Nick
Diametrix
San Diego, CA

Vourvopoulos, George
Western Kentucky University
Bowling Green, KY

Walbert, Calvin K.
FAA
Washington, DC

Walker, James J.
Amparo Corp.
Santa Fe, NM

Wallner, Richard A.
SAIC
San Diego, CA

Wang, T. R.
EG&G
Long Beach, CA

Warren, Sandra D.
Adsystech, Inc.
Silver Springs, MD

Warren, Thomas J.
U.S. Department of State
Washington, DC

Wasserzug, Louis Steven
Naval EOD Technology Center
Indian Head, MD

Waters, David Douglas
Bio-Imaging Research Inc.
Lincolnshire, IL

Watson, Gary Wayne
Amerasia Technology, Inc.
Westlake Village, CA

Watt, William S.
W. J. Schafer Associates, Inc.
Arlington, VA

Watters, David Gray
SRI International
Menlo Park, CA

Weinstein, Curt David
NeuroCommunication Research Labs
Danbury, CT

Weinstein, Sidney
NeuroCommunication Research Labs
Danbury, CT

Weissenberger, Stein
Lawrence Livermore National Lab
Livermore, CA

Westerdahl, Carolyn
U.S. ARDEC
Picatinny Arsenal, NJ

Whelan, James P.
GeoCenters, Inc.
Fort Washington, MD

Whilden, Leon
FAA Technical Center
Atlantic City, NJ

Whitehurst, Frederick William
FBI
Washington, DC

Wilkinson, Christer Jonathon
International Airport Projects
Leesburg, VA

Williams, Colin Brian
Gamma-Metrics
San Diego, CA

Wilson, Donald E.
Transport Canada
Ottawa, Ontario - CANADA

Winchester, Leonard W.
Science and Technology Corporation
Hampton, VA

Winsor, Harry V.
Westinghouse
Baltimore, MD

Wittstruck, Richard Harold
U.S. Army ETDL
Ft. Monmouth, NJ

Wolff, Steve H.
Imatron Industrial Products
Foster City, CA

Wolfson, Lennard J.
U.S. Department of Defense
Washington, DC

Wood, Kenneth S.
Barringer Instruments, Inc.
South Plainfield, NJ

Wright, Maryanne
FAA Technical Center
Atlantic City, NJ

Wueest, Werner H.
Zurich State Police
Zurich, SWITZERLAND

Yim, Suk J.
U.S. Army Armament R&D
Picatinny Arsenal, NJ

Yoshida, Dawn E.
Westinghouse Idaho Nuclear Co.
Idaho Falls, ID

Yost, Al
FAA Technical Center
Atlantic City, NJ

APPENDIX B

List of Acronyms Used in Explosive Detection Technology

ADC	Analog to Digital Converter
AI	Artificial Intelligence
ANS	Artificial Neural Systems
API	Atmospheric Pressure Ionization
ART	Algebraic Reconstruction Technique
ASGDI	Atmospheric Sampling Glow Discharge Ionization
ATR	Attenuated Total Reflectance
BEP	Back Error Propagation
BGO	Bismuth Germanate ($Bi_4Ge_3O_{12}$)
BIA	Bioluminescent Immunoassay
BSA	Bovine Serum Albumin
C4	91% RDX + 9% Plastic Binder
CAD	Computer Aided Design
CAMAC	Computer Automated Measurement and Control
CAT	Computed Axial Tomography
CDD	Component Detection Device
CFD	Constant Fraction Discriminator
CHN	Continuous Hopfield Network
CI	Chemical Ionization
CL	Chemiluminescence
CLD	Chemiluminescence Detector
CPU	Central Processing Unit
CT	Computed Tomography
CW	Continuous Wave
DAC	Digital to Analog Converter
DDNP	Diazodinitrophenol
DHN	Discrete Hopfield Network
DNP	Dinitrotoluene
DNP	Dynamic Nuclear Polarization
DRIFT	Diffuse Reflectance Infrared Fourier Transform
DSC	Differential Scanning Calorimetry
DSP	Digital Signal Processing
DVDE	Dual View Dual Energy
EC	Electron Capture
ECD	Electron Capture Detector
EDD	Explosive Detection Device
EDS	Explosive Detection System
EGDN	Ethyleneglycol Dinitrate
EGS4	Electron Gamma Shower, version 4 (simulation code)
EI	Electron Impact
EOG	Electro-Olfactogram
EMI	Electromagnetic Interference

ENG	Electron Neutron Generator
ESCA	Electron Spectroscopy for Chemical Analysis
ESR	Electron Spin Resonance
EVD	Explosive Vapor Detector
FET	Field Effect Transistor
FFT	Fast Fourier Transform
FID	Flame Ionization Detector
FID	Free Induction Decay
FNA	Fast Neutron Analysis
FOIA	Fiber Optic Immunoassay
FOM	Figure of Merit
FPA	Focal Plane Array
FT-ICR	Fourier Transform Ion Cyclotron Resonance
FTIR	Fourier Transform Infrared Spectroscopy
FWHM	Full Width at Half Maximum
GC	Gas Chromatography
GC/CLD	Gas Chromatography/Chemiluminescence Detector
GC/ECD	Gas Chromatography/Electron Capture Detector
GC/MS	Gas Chromatography/Mass Spectrometry
HE	High Explosive
HEBT	High Energy Beam Transport
HECD	Hall Electrolytic Conductivity Detector
HHN	Hybrid Hopfield Network
HMT	Hexamethylenetetramine
HMX	Tetranitramine
HPGe	High Purity Germanium
HPLC	High Performance Liquid Chromatography
HSGC	High Speed Gas Chromatography
IC	Integrated Circuit
IDL	Instrument Detection Limit
IFB	Immunochemical Film Badge
IMS	Ion Mobility Spectroscopy
IR	Infrared
IRRAS	Infrared Reflection-Absorption Spectroscopy
ITD	Ion Trap Detector
LCD	Liquid Crystal Display
LDI	Laser Desorption Ionization
LEBT	Low Energy Beam Transport
LED	Light Emitting Diode
LET	Linear Energy Transfer
LLD	Lower Limit of Detection

LLD	Lower-Level Discriminator
LOD	Limit of Detection
LOQ	Limit of Quantification
MCA	Multi-Channel Analyzer
MCNP	Monte Carlo Neutron Gamma (simulation code)
MDL	Method of Detection Limit
MDT	Mean Down Time
MMW	Milli-Meter Wave
MNT	Mononitrotoluene
MPD	Maximum Permissible Dose
MRI	Magnetic Resonance Imaging
MS	Mass Spectroscopy
MTBF	Mean Tine Between Failure
NAA	Neutron Activation Analysis
NDE	Non-Destructive Evaluation
NEA	Negative Ion Affinity
NES	Neutron Elastic Scatter
NG	Nitroglycerin
NICI	Negative Ion Chemical Ionization
NIM	Nuclear Instrument Module
NMR	Nuclear Magnetic Resonance
NN	Neural Networks
NPD	Nitrogen Phosphorus Detector
NQR	Nuclear Quadrupole Resonance
NRA	Neutron Resonance Attenuation
NRA	Nuclear Resonance Absorption
OD	Optical Density or Outer Diameter
OI	Operator Interface
PD	Probability of Detection
PET	Positron Emission Tomography
PETN	Pentaerythritol Tetranitrate
PFA	Probability of False Alarm
PFNA	Pulse Fast Neutron Analysis
PGNAA	Prompt Gamma Neutron Activation Analysis
PM	Photomultiplier
PMT	Photomultiplier Tube
PSD	Position Sensitive Detector
PSD	Pulse Shape Discrimination
PSND	Position Sensitive Neutron Detector
PWG	Pulse Width Generator
QT	Quadrupole Time-of-Flight

RAIRS	Reflection-Absorption Infrared Spectroscopy
RAM	Random Access Memory
RAM	Reliability, Availability, and Maintainability
RBE	Relative Biological Effectiveness
RDX	Cyclonite or Hexogen (1,3,5-trinitro-1,3,5-triazacyclohexane)
READ	Reverse Electron Attachment Detector
RF	Radio Frequency
RFI	Radio Frequency Interference
RFQ	Radio Frequency Quadrupole
SAW	Surface Acoustic Waves
SCI	Self Chemical Ionization
SNM	Special Nuclear Material
SNR	Signal-to-Noise Ratio, also S/N
SQUID	Superconducting Quantum Interference Device
SRIA	Surface Reflectance Immunoassay
TA	Trace Analysis
TAC	Time-to-Amplitude Convertor
TATP	Tricycloacetone Peroxide
TC	Thermocouple
TCD	Thermal Conductivity Detector
TDC	Time-to-Digital Convertor
TEA	Thermal Energy Analyzer
TLD	Thermoluminescent Dosimeter
TNA	Thermal Neutron Analysis
TNT	Trinitrotoluene
TOF	Time-of-Flight
TOFMS	Time-of-Flight Mass Spectrometer
ULD	Upper Level Discriminator
UV	Ultraviolet
VOI	Voxels of Interest
ZT	Backscatter Tomography (Z refers to atomic number)

APPENDIX C

Bibliography of Explosive Detection Technology

1. Nuclear and Atomic Methods of Mine Detection
(Technical Report)
Moler, R. B.
Army Belvoir Research Development and Engineering Center, Fort Belvoir, VA.
1 Nov 91 40p

2. Detection of Explosives by Nuclear Quadrupole Resonance
(Patent Application)
Beuss, M. L. ; Garroway, A. N.
Department of the Navy, Washington, DC.
Report No.: PAT-APPL-7-704 744
Filed 23 May 91 25p
This Government-owned invention available for U.S. licensing and, possibly, for foreign licensing. Copy of application available from NTIS.

3. Advances in the Location and Identification of Hidden Explosive Munitions
McFee, J. E. ; Das, Y.
Defence Research Establishment, Suffield, Ralston (Alberta).
Report No.: DRES-SR-548
Feb 91 96p

4. Technical Transfer Report on a TNT Enzyluminescent Vapor Detection System
(Final technical report)
Jappinga, E. M. ; Patel, D. L.
Army Belvoir Research Development and Engineering Center, Fort Belvoir, VA.
Report No.: BRDEC-TR-2499
Feb 91 104p

5. Fermilab Industrial Affiliates Roundtable on Applications of Accelerators
Carrigan, R. A.
Fermi National Accelerator Laboratory, Batavia, IL.
Sponsor: Department of Energy, Washington, DC.
May 89 188p
Annual meeting (9th) held in Batavia, IL. on May 26-27, 1989.
Sponsored by Department of Energy, Washington, DC.

6. Proceedings of the U.S. Nuclear Regulatory Commission Security Training Symposium 'Meeting the Challenge-Firearms and Explosives Recognition and Detection'. Held in Bethesda, Maryland on November 28-30, 1989.
Nuclear Regulatory Commission, Washington, DC; Office of Nuclear Material Safety and Safeguards.
Sep 90 297p
Also available from Supt. of Docs.

7. Evaluation of a Field Kit for Detection of TNT in Water and Soils
(Special report)
Jenkins, T. F. ; Schumacher, P. W.
Cold Regions Research and Engineering Laboratory, Hanover, NH.
Report No.: CRREL-SR-90-20; CETHA-TE-CR-90056
Jun 90 21p

8. Immunoassay Procedures for Fiber Optic Sensors
(Final report)
Ligler, F. S.
Naval Research Laboratory, Washington, DC.
30 Apr 88 28p

9. Evaluation of One-Sided Nuclear Magnetic Resonance for Remote Detection of Explosives (Final report)
Burnett, L. J. ; Fineman, M. A.
San Diego State University Foundation, San Diego, CA.
Sponsor: Naval Ocean Systems Center, San Diego, CA.
Report No.: NOSC-TD-1169
Oct 87 112p

10. Proceedings of the Australian Explosives Safety Seminar Held in Canberra, Australia on 18-20 November 1985 (1st)
Australian Ordnance Council, Canberra, Australia.
16 Dec 85 306p

11. Hawthorne Army Ammunition Plant, New Bomb Open Burning/Open Detonation Grounds EOD (Explosive Ordnance Disposal) Surface Sweep - A Project Overview
Douthat, C. D.
Corps of Engineers, Huntsville, AL.
Aug 86 12p
This article is from 'Minutes of the Explosives Safety Seminar (22nd) Held in Anaheim, CA on 26-28 August, 1986. Volume 2,' AD-A181 275, p1223-1236.

12. Assessment of the Feasibility of Performing Infield Nondestructive Evaluation to Determine the Presence of Explosives Materials within Cased Munitions
Gryting, H. J.
Southwest Research Institute, San Antonio, TX.
Aug 86 37p
This article is from 'Minutes of the Explosives Safety Seminar (22nd) Held in Anaheim, CA on 26-28 August 1986. Volume 2,' AD-A181 275, p1185-1221.

13. Chemical and Electromagnetic Methods for High Explosive/Ordnance Detection. Volume 2
Geo-Centers, Inc., Newton Upper Falls, MA.
Report No.: GC-TR-86-1536-VOL-2
Nov 86 133p

14. Chemical and Electromagnetic Methods for High Explosive/Ordnance Detection. Volume 1
Geo-Centers, Inc., Newton Upper Falls, MA.
Report No.: GC-TR-86-1536-VOL-1
Nov 86 250p

15. Workshop Report: Nuclear Techniques for Mine Detection Research, July 22-25, 1985, Lake Luzerne, New York
Moler, Robert B.
Army Belvoir Research and Development Center, Fort Belvoir, VA.
Jul 85 74p

16. Indicator Tubes for the Detection of Explosives
(Final report, Jun 80-Sep 84)
Erickson, E.D. ; Knight, D.J. ; Burdick, D.J. ; Greni, S.R.
Naval Weapons Center, China Lake, CA.
Sponsor: Shared Bibliographic Input.
Report No.: NWC-TP-6569; SBI-AD-E900 428
Nov 84 35p

17. Proposal to Develop a Method for the Detection of HE Employing Chemiluminescence Reactions. Summary of Activities and Accomplishments, February 1 to April 30, 1979.
Neary, M.P.
Los Alamos National Laboratory, NM.
Sponsors: Nuclear Regulatory Commission, Washington DC., Office of Nuclear Regulatory Research; Department of Energy, Washington, DC.
Report No.: LA-8593-PR
Nov 80 10p
See also NUREG/CR-1794-V3.

18. EPR Spectroscopy of Thermally Initiated Free Radicals in RDX
(Memorandum report)
Pace, M. D. ; Farrar, D. R. ; Britt, A. D. ; Moniz, W. B.
Naval Research Laboratory, Washington, DC.
Report No.: NRL-MR-5212
27 Oct 83 13p

19. MERADCOM (Mobility Equipment Research and Development Command) in vitro Biosensor Program
(Report for 1974-1981)
Egghart, Heinrich C.
Army Mobility Equipment Research and Development Command, Fort Belvoir, VA.
Report No.: MERADCOM-2364
Jun 82 73p

20. Numerical Parametric Study of Electromagnetic Wave Scattering by Buried Dielectric Land Mines
(Final report)
Mei, Kenneth K. ; Kvam, Terry M.
Geo Electromagnetics, Inc., Berkeley, CA.
1983 95p

21. Investigation of Behaviorally Modified Rats for Use in Explosives Detection Systems
(Report for FY76-FY81)
Nolan, Raymond V.
Army Mobility Equipment Research and Development Command, Fort Belvoir, VA.
Report No.: MERADCOM-2343
Dec 81 197p

22. Effectiveness of the Civil Aviation Security Program
(Semi-annual report no. 13, 1 Jul-31 Dec 80)
Federal Aviation Administration, Washington, DC.; Office of Civil Aviation Security.
Report No.: FAA-ACS-82-13
15 Apr 81 43p
Report to Congress.

23. Effectiveness of the Civil Aviation Security Program
(Semi-annual report no. 12, 1 Jan-30 Jun 80)
Federal Aviation Administration, Washington, DC; Office of Civil Aviation Security.
Report No.: FAA-ACS-82-12
14 Oct 80 42p
Report to Congress.

24. Effectiveness of the Civil Aviation Security Program
(Semi-annual report no. 4, 1 Jan-30 Jun 76)
Federal Aviation Administration, Washington, DC; Office of Civil Aviation Security.
Report No.: FAA-ACS-82-4
20 Sep 76 39p
Report to Congress.

25. Effectiveness of the Civil Aviation Security Program
(Semiannual report no. 2, 1 Jan-30 Jun 75)
Federal Aviation Administration, Washington, DC; Office of Civil Aviation Security.
Report No.: FAA-ACS-82-2
6 Oct 75 26p
Report to Congress.

26. Effectiveness of the Civil Aviation Security Program
(Semiannual report no. 1, 1973-1974)
Federal Aviation Administration, Washington, DC; Office of Civil Aviation Security.
Report No.: FAA-ACS-82-1
17 Apr 75 21p
Report to Congress.

27. Development of Microencapsulated Perfluorocarbon Materials for Predetonation Detection of Explosives
(Final report, 1 Nov 78-30 Nov 79)
Hart, R. L. ; Davis, D. A.
Capulated Systems, Inc., Yellow Springs, OH.
Sponsor: Aerospace Corp., Washington, DC.
Dec 79 125p

28. The Continuously Operating Perfluorocarbon Sniffer (COPS) for the Detection of Clandestine Tagged Explosives
(Informal report)
Dietz, Russell N. ; Goodrich, Robert W.
Brookhaven National Laboratory, Upton, NY.
Sponsors: Department of Energy, Washington, DC.;
Bureau of Alcohol, Tobacco and Firearms, Washington, DC.
Report No.: BNL-28114
May 80 25p

29. Microencapsulated Vapor Taggants for Predetonation Detection of Explosives
(Final report)
Reyes, Z. ; Smith, J. H. ; McCarthy, E. ; Comas, M.
SRI International, Menlo Park, CA.
Sponsor: Aerospace Corp., Washington, DC.
Sep 79 65p

30. An Evaluation of Potential Taggant-Polymer Combinations for Detection Tagging of Blasting Caps
(Final report)
Toy, M. S. ; Stringham, R. S. ; Toy, S. M.
Science Applications, Inc., Sunnyvale, CA.
Sponsors: Bureau of Alcohol, Tobacco and Firearms, Washington, DC.;
Aerospace Corp., Washington, DC.
Report No.: SAI-78-508-SV
12 May 78 91p

31. Summary of Activities and Accomplishments - Final Report:
A Proposal to Develop a Method for the Detection of HE Employing Chemiluminescence Reactions
(Progress report (Final))
Neary, Michael P.
Los Alamos Scientific Laboratory, Los Alamos, NM.
Sponsors: Nuclear Regulatory Commission, Washington, DC.; Division of Safeguards, Fuel Cycle and Environmental Research; Department of Energy, Washington, DC.
Report No.: LA-8596-PR
Jan 81 57p

32. Spectroscopic Investigations of Energetic Materials and Associated Impurities
(Interim report, 1 Sep 77-31 Aug 78)
Bartolo, B. Di ; Pacheco, D. P. ; Shultz, M. J.
Boston College, Chestnut Hill, MA; Department of Physics.
Report No.: NAVEODFAC-TR-211
Jun 79 144p

33. Array I Photo Imagery Analysis
(Technical report, Jul-Aug 79)
Lopez, Manuel
Environmental Research Institute of Michigan, Ann Arbor; Radar and Optics Division.
Report No.: ERIM-138300-55-T
Jun 80 35p

34. Automatic Analyzers and Signal Indicators of Toxic and Dangerously Explosive Substances in Air
Iovenko, E. N.
Foreign Technology Division, Wright-Patterson AFB, OH
Report No.: FTD-ID(RS)T-1801-79
9 Jan 80 397p
Unedited machine trans. of mono. Avtomaticheskiye Analizatory i Signalizatory Toksichnykh i Vzryvoopasnykh Veshchestv v Vozdukhe (USSR)
p1-186 1972.

35. Neurophysiological Procedures for the Detection of Explosives
(Final report)
Weinstein, Sidney ; Weinstein, Curt ; Drozdenko, Ronald
Neurocommunication Research Laboratories, Inc., Danbury, CT.
Mar 80 31p

36. Characterization of the Component Enzymes of the TNT Detection System-Physical and Chemical Studies
(Final technical report)
Donovan, K. ; Gawronski, T. ; Scott, B.
Beckman Instruments, Inc., Carlsbad, CA; Microbics Operations.
Jun 79 53p

37. Detection of Explosive Vapors by Enzymatic Methods
(Final report)
Strickler, A. ; Brawner, C.
Beckman Instruments, Inc., Anaheim CA; Advanced Technology Operations
Report No.: FR-2711-101
May 79 20p

38. Use of Canines for Explosives Detection in the Personnel Access Control Function at a Nuclear Facility
Smith, J. C.
Allied-General Nuclear Services, Barnwell, SC.
Sponsor: Department of Energy, Washington, DC.
Report No.: CONF-7810115-3
1978 14p
New concepts symposium and workshop on detection and identification of explosives, Reston, VA, USA, 30 Oct 1978.

39. Technology for the Prevention of Airliner Hijacking and Bombing
Henry, James H. ; Cutchis, Pythagoras ; Marder, Stanley; Schnitzler, Alvin D. ; Sheldon, Donald R.
Institute for Defense Analyses, Arlington, VA; Science and Technology Division
Report No.: P-817; IDA/HQ-72-13992
Feb 72 175p
Update and expansion of Report no. S-332 dated Dec 68, AD-500 586L. See also Report no. P-806.

40. Bomb Detection System Study
(Final report)
Dravnieks, Andrew ; Weber, H.
IIT Research Institute, Chicago, IL
Report No.: IITRI-C6026-13; FAA-ADS-34
Jan 65 84p

41. Bomb Detection System Implementation Analysis
(Final report)
Brinton, George M. ; Passell, Thomas O.
Stanford Research Institute, South Pasadena CA; Southern California Labs
Apr 64 108p

42. Bomb Detection System Study
(Technical report)
Dravnieks, A.
IIT Research Institute, Chicago, IL
Report No.: FAA-ADS-81
Oct 66 182p

43. Protection of Public Figures. Symposium Proceedings, May 16-18, 1972
Army Mobility Equipment Research and Development Command, Fort Belvoir, Va
1972 280p
Document Type: Conference proceedings

44. Detection of Explosive Vapors by Enzymatic Methods
-- Laboratory Validation and Systems Analysis
(Final report, Oct 76-Nov 77)
Donovan, K. ; Gawronski, T. ; Greene, M. ; Brawner, C. ; Strickler, A.
Beckman Instruments, Inc., Anaheim CA; Advanced Technology Operations
Report No.: FR-2696-101
Jan 78 31p

45. Mine-Detecting Canines
(Summary report, 1975-1976)
Nolan, R. V. ; Gravitte, D. L.
Army Mobility Equipment Research and Development Command, Fort Belvoir, Va
Report No.: MERADCOM-2217
Sep 77 83p

46. Survey of Bioluminescence Research Pertinent to Explosives Detection
(Technical report, Jun 70-Jun 75)
Kemp, Maryland D.
Army Mobility Equipment Research and Development Command, Fort Belvoir, Va
Report No.: MERADCOM-2196
Nov 76 66p

47. Development of a Simple Portable Detection Kit for Selected Explosives
(Final report, 19 Jun 75-31 Dec 76)
Wyant, Robert E.
Battelle Columbus Laboratories, Ohio
Report No.: NAVEODFAC-TR-185
Sep 77 66p

48. Trace Gas Field Instrumentation Van and Explosive Detection Research
(Final report)
Lawless, P. A.
Research Triangle Institute, Research Triangle Park, NC
Mar 77 192p

49. The Determination of Tetryl and 2,3-, 2,4-, 2,5-, 2,6-,3,4- and 3,5- Dinitrotoluene Using High Performance Liquid Chromatography
(Final report, Sep-Dec 76)
Stanford, Jr, T. B.
Battelle Columbus Laboratories, Ohio
31 Jan 77 14p

50. Study of Conventional Preconcentration Techniques for Explosive Vapors
(Final report, 23 Mar-15 Aug 73)
Hrubesh, Lawrence W. ; Morrison, Robert L. ; Ryon, Richard
W. ; Walter, Edward G. ; Fulk, Marion M.
University of California; Lawrence Livermore Laboratory, Livermore, CA.
Report No.: UCID-16766; NAVEODFAC-TR-170
Feb 76 25p

51. Determining the Potential of Radiofrequency Resonance Absorption Detection of Explosives Hidden in Airline Baggage
(Final report)
Rollwitz, William L. ; King, J. Derwin ; Shaw, Stanley D.
Southwest Research Institute, San Antonio, TX
Sponsor: Federal Aviation Administration, Washington, D.C.; Systems Research and Development Service.
Report No.: SWRI-15-4225-F; FAA/RD-76-29
Oct 75 103p

52. Theory and Application of X-Ray and Gamma-Ray Backscatter to Landmine Detection
(Research report, 1968-1973)
Roder, Fredrick L. ; Van Konynenburg, Richard A.
Army Mobility Equipment Research and Development Center, Fort Belvoir, Va
Report No.: USAMERDC-2134
Mar 75 153p

53. Aerosol Explosive Indicator Kit
(Final report)
Sweeney, F. T. ; Mitchell, P. W. D.
Franklin Institute Research Laboratories, Philadelphia, PA
Sponsor: Army Land Warfare Laboratory, Aberdeen Proving Ground, MD.
Report No.: FIRL-F-C3776-02; LWL-CR-24C74
Jun 74 19p

54. Narcotic-Explosive Detector Dogs
(Final report)
Southwest Research Institute, San Antonio, TX
Report No.: LWL-CR-20B72
Jan 73 17p

55. Explosives Detecting Dogs
Krauss, Max
Mississippi University, Mississippi
Report No.: LWL-TR-71-11
Sept 71 11p
Sponsored in part by the Law Enforcement Assistance Administration, Washington, DC.

APPENDIX D

Author Index

Achter, E.K., 427, 559
Ahmed, M.S., 687
Akery, A.K., 663
Alajajian, S.H., 571
Altshuler, E., 840
Anderson, O.A., 184
Annis, M., 269
Ark, W.F., 739
Atwell, T.A., 388
Autera, J., 739

Bar-Nir, I.M., 396, 409, 415
Bartko, J., 56
Becker, D.A., 347
Bendahan, J., 70, 151, 787, 840
Benetti, R., 825
Beyerle, A., 160
Bjorkholm, P.J., 309
Boubli, B.B., 13
Boumsellek, S., 571
Bromberg, E.A., 552
Brown, G.V., 903
Buchmann, L., 197
Buchsbaum, S., 70
Buess, M.L., 435
Burnett, L.J., 454, 465

Campbell, C., 739, 741
Carroll, A.L., 552, 559
Chen, T.H., 737, 739, 741
Cheung, S., 850
Chou, E., 825
Chutjian, A., 571
Clark, T.D., 689
Clifford, J.R., 237
Cole, R.L., 415, 903
Conrad, F.J., 510
Curby, W.A., 505

Dale, J.M., 637
Danylewych-May, L.L., 672
Davidson, W.R., 663
Derrickson, j., 687
Dolan, K.W., 252
Doney, R.H., 19
Drozdenko, R., 759
Durkee, R., 160

Elias, E., 840
Eng, S., 734
Evans, P., 232

Falconer, D.G., 486
Feinstein, L., 70
Fetterolf, D.D., 689
Fine, D.H., 505, 703
Fraim, F.W., 427, 552, 559

Garroway, A.N., 435
Gerardi, G.J., 493
Giam, C.S., 687
Glish, G.L., 642
Goldberg, S., 309
Gomberg, H.J., 123
Gozani, T., 27, 82, 151, 787, 840
Grant, B.C., 642
Greenlee, D.R., 376
Greenspan, E., 787
Grodzins, L., 201
Guzman, A.M., 873

Habiger, K.W., 237
Hacker, M., 269
Hainsworth, E., 427, 559
Hamm, R.W., 175
Hannum, D.W., 510
Hansen, B.L., 634
Heath, R.L., 634
Henderson, D.O., 604
Hintze, M.M., 634
Hobbs, J.R., 427
Hoopengardner, R.L., 880
Horton, W., 589
Hsiung, D., 911
Hurley, J.P., 160
Hurwitz, M.J., 381, 388

James, G.D., 66
Jenkins, A., 518, 532

Kaufman, W.M., 873
Kehayias, J., 104
Kenna, B.T., 347, 510
Khan, S.M., 1
Kim, J.H., 850
King, J.D., 333, 478
Kirshenbaum, M.S., 739
Knize, D., 70
Kolla, P., 723
Kossack, C.F., 347
Kushner, B.G., 123
Kusterbeck, A.W., 770
Krug, K.D., 282

Lacey, R.J., 368
Lannon, J.A., 734
Lee, E.D., 619
Lee, H.G., 619
Lee, M.L., 619
Lee, W., 151
Legrady, O., 714
Leung, K.N., 184
Leung, V., 311
Leupold, H.A., 493
Lieb, D.P., 552, 703
Ligler, F.S., 770
Liu, F., 311
Lovett, S., 774
Lukens, H.R., 753

MacDonald, S.J., 584, 703
Magnuson, E.E., 454
Mahood, D.B., 151
Martz Jr., H.E., 252
McCullough, W.F., 237
McDaniel, F., 333
McGann, W., 518, 532
McKay, D.R., 454
McKown, H.S., 642
McLuckey, S.A., 642
Miller, J.B., 435
Miller, R.B., 237
Miskolczy, G., 427
Mitchner, B., 714
Moeller, C.R., 454
Morvan, P., 23
Murray, N.C., 368

Nacson, S., 714
Nargolwalla, S., 714
Navarro, J.A., 347
Nicholls, C.I., 333, 478
Noronha, W.P., 381, 388
Ntuen, C., 850

Orphan, V., 285

Park, E.H., 850
Patel, A., 825
Pierre, J., 840
Poindexter, E.H., 493
Policher, R., 285
Polski, P.A., 5
Pongratz, H.W., 319
Paulson, C.C., 184

Ramsey, J.M., 637
Rathke, J.W., 184
Reed, R.A., 739, 741
Redman, R., 21
Reusch, M.F., 184
Ribeiro, K., 518, 532
Rikard, R.D., 252
Robbins, C.E., 9
Robinson, M., 232
Roder, F.L., 297
Rollwitz, W.L., 478
Rounbehler, D.P., 505, 584, 703
Ruddy, F.H., 56
Ryge, P., 151, 396, 409, 825
Ryon, R.W., 252

Safeer, H., 3
Sawa, Z.P., 82
Sanders, J.P., 465
Santos, A.D., 478
Scarlet, R., 309
Schafer, D., 269
Schirato, R., 285
Schmor, P.W., 197
Schneberk, D.J., 252
Schultz, F.J., 104
Seward, D.C., 441
Shea, P., 70, 311, 777, 911
Sheldon, T.G., 368
Shreve, D.C., 285
Silberman, E., 604
Sivakumar, M., 311, 911
Smith, G.M., 368
Smith, S.W., 261
Staples, E., 589
Stein, J.A., 282
Snyder, F.W., 604
Sumi, D., 415
Syme, D.B., 66

Ternes, J. W., 891
Thai, T.Q., 860
Todd, A.M., 184
Trower, W.P., 116
Tunnell, L., 160

Vourvopoulos, G., 104

Wang, T.R., 309
Watters, D.G., 486
Watson, G., 589
Weinstein, C., 759
Weinstein, S., 759
Weller, R.R., 687
Westerdahl, C., 734
Whelan, J.P., 770
Whitten, W.B., 637
Wiegand, D.A., 739
Wittstruck, R.H., 493
Wolff, S., 810

Yukl, T., 441